

MRI Bioeffects, Safety, and Patient Management: Second Edition

Frank G. Shellock, Ph.D. - Editor

Director of MRI Safety

USC Stevens Neuroimaging and Informatics Institute

Adjunct Clinical Professor of Radiology and Medicine

Keck School of Medicine, University of Southern California

Los Angeles, CA

President, Shellock R & D Services, Inc.

Playa Del Rey, CA

John V. Crues, III, M.D. - Editor

Medical Director

Radnet, Inc.

Los Angeles, CA

Professor of Radiology

University of California, San Diego

Alexandra M. Karacozoff, M.P.H. - Associate Editor

Sacramento, California

Biomedical Research Publishing Group

Los Angeles, CA

© 2022 by Biomedical Research Publishing Group and Shellock R & D Services, Inc., Los Angeles, CA. All rights are reserved. This book is protected by copyright. No part of it may be reproduced, stored in a retrieval system, or transmitted, in any form or by any means, electronic, mechanical, photocopying, recording, or otherwise, without the written permission of the Biomedical Research Publishing Group and Shellock R & D Services, Inc.

Made in the United States of America

Library of Congress Cataloging-in-Publication Data

Frank G. Shellock and John V. Crues, III

MRI Bioeffects, Safety, and Patient Management: Second Edition

p. cm.

Includes bibliographical references and index.

ISBN-13 978-0-9891632-8-6

ISBN-10 0-9891632-8-8

-
1. Magnetic resonance imaging. 2. Magnetic resonance imaging—safety measures. 3. Magnetic resonance imaging—Health aspects. 4. Magnetic resonance imaging—Complications. I. Shellock, Frank G. II. Crues, John V. III. Title.
-

Great care has been taken to assure the accuracy of the information contained in this textbook that is intended for educational and informational purposes, only. Neither the publisher nor the authors assume responsibility for errors or for any consequences arising from the use of the information contained herein.

Disclaimer

This textbook was designed to provide a reference for radiologists, MRI technologists, facility managers, MRI physicists, MRI researchers, engineers, and others. The information is current through the publication date of this textbook. The content of this book is designed for general informational purposes only and is not intended to be nor should it be construed to be technical or medical advice or opinion on any specific facts or circumstances.

The authors and publisher of this work disclaim any liability for the acts of any physician, individual, group, or entity acting independently or on behalf of any organization that utilizes information for a medical procedure, activity, service, or other situation through the use of this textbook. The content of this textbook makes no representations or warranties of any kind, expressed or implied, as to the information content, materials or products, included in this textbook. The authors and publisher assume no responsibilities for errors or omissions that may include technical or other inaccuracies, or typographical errors. The authors and publisher of this work specifically disclaim all representations and warranties of any kind, expressed or implied, as to the information, content, materials, or products included or referenced in this textbook.

The authors and publisher disclaim responsibility for any injury and/or damage to persons or property from any of the methods, products, instructions, or ideas contained in this publication. The authors and publisher disclaim liability for any damages of any kind arising from the use of the book, including but not limited to direct, indirect, incidental, punitive and/or consequential damages.

The information and comments provided in this book are not intended to be technical or medical recommendations or advice for individuals or patients. The information and comments provided herein are of a general nature and should not be considered specific to an individual or patient, whether or not a specific patient is referenced by a physician, technologist, individual, group, or other entity seeking information.

The authors and publisher assume no responsibility for the accuracy or validity of the information contained in this book nor the claims or statements of any manufacturer or website that is referenced. Manufacturers' product specifications are subject to change without notice. Always read the product labeling, instructions and warning statements thoroughly before using any medical product or similar device.

Preface

Since its introduction into clinical practice in the early 1980s, magnetic resonance imaging (MRI) has exhibited exceptional growth and created a paradigm shift in medicine. Not only has this imaging modality markedly expanded the roles of imaging in medical diagnoses, opening up vistas in neurological, musculoskeletal, oncological, cardiovascular and a variety of other diseases not accessible to prior imaging techniques, but it has also had a profound impact on our basic understanding of the pathophysiologic mechanisms of abnormal conditions and disease processes.

The continuous growth of MRI has led to an explosion in the number of patients, health-care professionals, and other individuals exposed to the powerful static magnetic fields, rapidly changing magnetic fields, and intense radiofrequency fields used during the procedures. Numerous investigations have been performed during the past 35+ years in an effort to characterize the bioeffects and safety aspects of MRI. However, the interactions of the MRI-related electromagnetic fields with biologic tissues are still incompletely understood and safety issues persist despite best efforts to implement preventive practices. Unfortunately, this has led to many adverse consequences, including injuries to patients and health-care workers, as well as several patient deaths.

The transformative impact of MRI on medicine continues to progress and advances in technology continue unabated. Whereas the highest magnetic field used in routine clinical imaging was 1.5-Tesla during most of the 1990s, 3-Tesla is currently the standard. Presently, a 7-Tesla scanner is approved for clinical use and research is routinely performed at 9.4-Tesla, 10.5- and an 11.7-Tesla MR system recently came on line to scan human subjects. In addition to the high static magnetic fields, both the speed of magnetic field gradient switching and the levels of radiofrequency field exposures are pushing limits well beyond what was possible just a few years before. Therefore, we strongly believe that, for progress to continue in this field, appropriate safeguards must be in place to protect all human subjects exposed to MRI, which includes both patients and healthcare workers, alike. This is best accomplished by conducting careful research directed towards studying the effects of the electromagnetic fields used in clinical and research MRI settings and implementing cautionary measures based on the knowledge acquired during the last three and a half decades.

Ultimately, MRI safety must begin with understanding the interactions of the electromagnetic fields used in MRI with biologic tissues. The issues concerning human safety in the MRI environment led us to enlist leading physicians and scientists around the world to collaborate on the first edition of this textbook, published in 2014, which organized and reviewed the scientific literature on the safety aspects of MRI. Since then, there have been thousands of new articles published in the scientific literature detailing MRI safety issues from every conceivable approach. Thus, the first edition of this textbook rapidly became outdated. Accordingly, we once again brought together an internationally respected group

of experts who are directly involved in all areas of MRI bioeffects, safety, and patient management to update this important book. Notably, several new chapters were added to this second edition, with the intent of covering advanced or emerging topics for the MRI community. The unique collective expertise of these physicians (radiologists, cardiologists, internists, etc.), scientists, engineers, and other professionals has once again resulted in vital contributions to this resource of essential scientific knowledge that covers all of the critical topics of interest to physicians, MRI technologists and radiographers, physicists, scientists, healthcare professionals, imaging center managers, bioengineers, regulatory affairs professionals, and laypersons. The ambitious purpose of this textbook is to provide actionable information that will be used to ensure that the MRI environment is as safe as possible under all circumstances. We hope that we have accomplished this important goal and that the MRI community will benefit from the indispensable contents of this textbook.

Frank G. Shellock

John V. Crues, III

The Editors

Frank G. Shellock, Ph.D. is a physiologist with more than 35 years of experience conducting laboratory and clinical investigations in the field of magnetic resonance imaging (MRI). He is the Director of MRI Safety at the USC Steven Neuroimaging and Informatics Institute which utilizes research and clinical 3-Tesla and 7-Tesla scanners, and an Adjunct Clinical Professor of Radiology and Medicine at the Keck School of Medicine, University of Southern California. As a commitment to the field of MRI safety, bio-effects, and patient management, he created and maintains the internationally popular website, www.MRIsafety.com.



Dr. Shellock has authored or co-authored more than 260 publications in the peer-reviewed literature. His memberships in professional societies include the American College of Radiology, the International Society for Magnetic Resonance in Medicine (ISMRM), the Radiological Society of North America, and the Hawaiian Radiological Society. He is a member and Fellow of the American College of Radiology, the International Society for Magnetic Resonance in Medicine, the American College of Cardiology, and the American College of Sportsmedicine.

Dr. Shellock is a member of the Sub-Committee on MRI safety issues for the American Society for Testing and Materials (ASTM) International. Additionally, he serves in advisory roles to government, industry, and other policy-making organizations. Over the years, he has been involved with the MRI Safety Committees for the American College of Radiology, the International Society for Magnetic Resonance in Medicine, and the International Society for MR Radiographers and Technologists. The Joint Commission appointed Dr. Shellock to the Diagnostic Ionizing Radiation and Magnetic Resonance Expert Panel, where he served from 2012 to 2015. He is a Deputy Editor for the *Journal of Magnetic Resonance Imaging* and a Reviewing Editor for several medical and scientific journals including *Radiology*, *Investigative Radiology*, *Magnetic Resonance in Medicine*, *Magnetic Resonance Imaging*, the *American Journal of Roentgenology*, the *Journal of Cardiovascular Magnetic Resonance*, *Circulation*, *Neuroradiology*, the *European Heart Journal*, *Neurosurgery*, and the *Journal of the American College of Cardiology*.

In 1994, Dr. Shellock received the *Kressel and Crues Educational Award* for exceptional educational contributions to the Section for Magnetic Resonance Technologists (SMRT). The American College of Radiology awarded him a Distinguished Committee Service

Award for years of dedicated service to the *Practice Guidelines and Technical Standards Committee – Body MRI*.

Dr. Shellock is a recipient of a National Research Service Award from the National Institutes of Health, National Heart, Lung, and Blood Institute and has received numerous grants from governmental agencies, private organizations, and medical device companies. He participates in research to define safety for implants and devices including cardiac pacemakers, implantable cardioverter defibrillators, neuromodulation systems, and other electronically-activated devices.

Dr. Shellock has lectured both nationally and internationally and has provided plenary lectures to numerous organizations including the Radiological Society of North America, the International Society for Magnetic Resonance in Medicine, the American College of Radiology, the American Roentgen Ray Society, the American Society of Neuroradiology, the Environmental Protection Agency, the Oklahoma Heart Institute, the Head and Neck Radiology Society, the Center for Devices and Radiological Health (FDA), the Magnetic Resonance Managers Society, the American Heart Association, the American College of Cardiology, the American Society of Neuroimaging, the Society for Cardiovascular Magnetic Resonance, the Heart Rhythm Society, the Association for Medical Imaging Management, the Radiology Business Management Association, Association for Radiologic and Imaging Nursing, the Finnish Radiological Society, the International Congress of Radiology, the Japanese Society of Neuroradiology, the British Chapter of the International Society for Magnetic Resonance in Medicine, the Royal Australian and New Zealand College of Radiologists, the Institute of Physics and Engineering in Medicine, the Karolinska Institute, Cape Peninsula University of Technology and the University of Johannesburg in South Africa.

Dr. Shellock's company, Shellock R & D Services, Inc./Magnetic Resonance Safety Testing Services, specializes in the assessment of MRI issues for implants and devices, as well as the evaluation of electromagnetic field-related bioeffects.

John V. Crues, III, M.D., M.S. is a radiologist with more than 30 years experience in magnetic resonance imaging (MRI). He is the Medical Director and former MRI Fellowship Director for Radnet, Inc., the largest owner and operator of outpatient imaging centers in the United States. His undergraduate degree was in physics at Harvard University and he obtained a masters degree in solid-state physics (MR spectroscopy) with Professor Charles Slichter at the University of Illinois before attending Harvard Medical School.

Dr. Crues has authored more than 100 papers in the medical literature, 13 textbooks and CDs, 27 book chapters, and over 100 abstracts. He is a member of numerous professional societies, including being a past President of the International Society for Magnetic Resonance in Medicine (ISMRM) and a previous Chairperson of the Subcommittee on Magnetic Resonance Biological Effects of the Commission on Neuroradiology and Magnetic Resonance of the American College of Radiology (ACR). Contributions towards the development of clinical magnetic resonance led to his selection as a Fellow of both the ISMRM and the ACR. Dr. Crues has also served on the ACR's MRI Accreditation Committee, the Board of the Intersocietal Commission for the Accreditation of Magnetic Resonance Imaging Laboratories, and the Diagnostic Ionizing Radiation and Magnetic Resonance Expert Panel for The Joint Commission. For six years he represented the ACR on the American Registry of Radiological Technologists, MRI Examination Committee.



Dr. Crues has presented over 2,000 invited lectures on five continents, including plenary lectures for the Society of Nuclear Medicine, Society of Magnetic Resonance in Medicine, Radiologic Society of North America, Colorado Radiologic Society, National Academy of Sciences Second Annual Symposium on Frontiers of Science, American Roentgen Ray Society, Society of Magnetic Resonance Imaging, MR '93 Internationales Kernspintomographic Symposium, German Orthopaedic Society, Austral-Asian Radiological Society, Scandinavian Congress of Radiology, International Skeletal Society, American Society of Emergency Radiology, Brasilian Radiologic Society, Swedish Society of Medical Radiology, International Society for Extremity MRI in Rheumatology, Society of Radiology Physician Extenders, and the Professional Hockey Athletic Trainers Association. As a Visiting Professor, he has been hosted by more than twenty academic institutions world-wide.

Contributors

Louai Al-Dayeh, M.D., Ph.D.

Research and Development Fellow
Boston Scientific Neuromodulation Corporation
Valencia, CA

Gregory Brown, Ph.D., FSMRT

Lecturer in Medical Radiations
Allied Health & Human Performance
University of South Australia
Adelaide, Australia

Giovanni Calcagnini, Ph.D., EEng.

Lead Researcher
Department of Cardiovascular, Endocrine-metabolic Diseases and Aging
Italian National Institute of Health
Rome, Italy

Frederica Censi, Ph.D., EEng.

Lead Researcher
Department of Cardiovascular, Endocrine-metabolic Diseases and Aging
Italian National Institute of Health
Rome, Italy

Patrick M. Colletti, M.D.

Professor of Radiology
Professor of Medicine
Professor of Biokinesiology
Professor of Pharmacology and Pharmaceutical Sciences
Division Chief, Nuclear Medicine
Keck School of Medicine of USC
Los Angeles, CA

John V. Crues, III, M.D., FACR

Medical Director
Radnet, Inc.
Los Angeles, CA
and
Professor of Radiology
University of California, San Diego
San Diego, CA

Heidi A. Edmonson, Ph.D.

Medical Physicist
Department of Radiology
Mayo Clinic
Rochester, MN

Laura Foster, J.D., M.P.H.

Senior Vice President, Compliance and Regulatory Affairs
Radnet, Inc.
Los Angeles, CA

Janice Fairhurst, B.S., R.T. (R)(MR)

Lead MRI Technologist
Radiology Department
Brigham and Women's Hospital
Harvard Medical School
Boston, MA

Trina Gulay, R.T. (R) (MR)

MRI Supervisor
Nanaimo Regional General Hospital
Vancouver Island Health Authority

Vancouver, British Columbia
Canada

Christine Harris, R.T. (R)(MR), MRSO

Corporate Director, Medical Imaging
Jefferson Health System, New Jersey
Cherry Hill, New Jersey

Henry Halperin, M.D., M.A., FHRA, FAHA

David J. Carver Professor of Medicine
Professor of Biomedical Engineering and Radiology
Johns Hopkins Hospital
Baltimore, MD

Bernd Ittermann, Ph.D.

Head of Biomedical Magnetic Resonance Department
Physikalisch-Technische Bundesanstalt (PTB)
Braunschweig und Berlin
Germany

Daniel F. Kacher, M.S.

Clinical Engineer
Biomedical Engineering Department
Brigham and Women's Hospital
Harvard Medical School
Boston, MA

Wolfgang Kainz, Ph.D.

Research Biomedical Engineer
Division of Biomedical Physics
Office of Science and Engineering Laboratories
Center for Devices and Radiological Health
Food and Drug Administration
Silver Spring, MD

Alayar Kangarlu, Ph.D.

Director of MRI Physics
Columbia University
New York, NY

Alexandra M. Karacozoff, MPH

Associate Editor
Biomedical Research Publishing Group
Sacramento, CA

Mark N. Keene, Ph.D.

Chief Technology Officer
Metrasens, Ltd.
Worcestershire
United Kingdom

Stephen F. Keevil, Ph.D.

Head of Medical Physics
Department of Medical Physics
Guy's and St Thomas' NHS Foundation Trust
London, England
United Kingdom
and
Professor of Medical Physics
School of Biomedical Engineering and Imaging Sciences
King's College London
London, England
United Kingdom

Oliver Kraff, Ph.D.
Erwin L. Hahn Institute for MR Imaging
University of Duisburg-Essen
Essen, Germany

Bruno Madore, Ph.D.
Department of Radiology
Brigham and Women's Hospital
Harvard Medical School
Boston, MA

Eugenio Mattei, Ph.D., MedEng.
Researcher
Department of Cardiovascular, Endocrine-metabolic Diseases and
Aging
Italian National Institute of Health
Rome, Italy

Mark McJury, Ph.D.
Consultant Clinical Scientist
Imaging Centre of Excellence
Queen Elizabeth University Hospital Campus
Glasgow, Scotland
United Kingdom

Donald W. McRobbie, Ph.D.
Associate Professor, Discipline of Medical Physics
School of Physical Sciences
University of Adelaide
Adelaide, Australia

Srinivasan Mukundan, Jr. M.D., Ph.D.
Radiology Department
Brigham and Women's Hospital
Harvard Medical School
Boston, MA

Manuel Murbach, Ph.D.
Head of MRI Programs
ZMT Zurich MedTech AG
Zurich, Switzerland

Saman Nazarian, M.D., Ph.D., FHRS, FACC
Associate Professor of Medicine
Cardiac Electrophysiology
Perelman School of Medicine
University of Pennsylvania
Philadelphia, PA

Moriel NessAiver, Ph.D.
President
Simply Physics
Baltimore, MD

John Nyenhuis, Ph.D.
Professor Emeritus of Electrical and Computer Engineering
School of Electrical and Computer Engineering
Purdue University
West Lafayette, IN

Lawrence P. Panych, Ph.D.
 Schulich School of Medicine and Dentistry
 Department of Medical Imaging
 University of Western Ontario
 Ontario, Canada

Sumit Patel, M.D.
 Cardiology Fellow
 Division of Cardiovascular Medicine, Cardiovascular and Thoracic
 Institute
 Keck School of Medicine, University of Southern California
 Los Angeles, CA

John Posh, R.T. (R)(MR)
Lead MRI Technologist
Robert Wood Johnson University Hospital
New Brunswick, NJ

Harald H. Quick, Ph.D.
Erwin L. Hahn Institute for MR Imaging
University of Duisburg-Essen
Essen, Germany
and
High-Field and Hybrid MR Imaging
University Hospital Essen
Essen, Germany

Mizan Rahman, Ph.D.
Electrical Engineering Fellow
Boston Scientific Neuromodulation Corporation
Valencia, CA

Ashok K. Saraswat, M.S., B.Ed., R.T. (R)(MR)
Emeritus MRI Educational Program Director
Ohio State University
Wexner Medical Center
Columbus, OH

Anne Marie Sawyer, B.S., R.T. (R)(MR), FSMRT
Instructor
Magnetic Resonance Imaging Department
Health & Wellness Division
Greenville Technical College
Charleston, SC

Daniel J. Schaefer, Ph.D.
Visiting Professor
Department of Electrical and Computer Engineering
Duke University
Durham, NC

Frank G. Shellock, Ph.D., FACR, FACC, FISMRM
Director of MRI Safety
USC Stevens Neuroimaging and Informatics Institute
Adjunct Clinical Professor of Radiology and Medicine
Keck School of Medicine, University of Southern California
Los Angeles, CA

Jerold S. Shinbane, M.D., FACC, FHRS, FSCCT
Professor of Clinical Medicine
Director, USC Arrhythmia Center
Director, Cardiovascular Computed Tomography
Division of Cardiovascular Medicine, Cardiovascular and Thoracic
Institute
Keck School of Medicine, University of Southern California
Los Angeles, CA

Frank Siebert, Ph.D.
Head of MR Technology Group
Physikalisch-Technische Bundesanstalt (PTB)
Braunschweig und Berlin
Germany

Mark A. Smith M.S., ABMP, R.T. (R)(MR)
MRI Physicist
Nationwide Children's Hospital
Clinical Instructor, Adjunct Faculty
Ohio State University
Wexner Medical Center
Columbus, OH

Alberto Spinazzi, M.D.
Chief Medical and Regulatory Officer
Bracco Group
Monroe, NJ

John Summers, M.D., FACC

Medical Director, Cardiac Electrophysiology and
Watchman Champion
SSM Health Saint Anthony Hospital
Oklahoma City, OK

Lawrence N. Tanenbaum, M.D., FACR

Chief Technology Officer
Radnet, Inc.
New York, NY

Clare M. Tempany-Afdhal, M.D.

Radiology Department
Brigham and Women's Hospital
Harvard Medical School
Boston, MA

Joshua C. Vacanti, M.D.

Anesthesiology Department
Brigham and Women's Hospital
Harvard Medical School
Boston, MA

Johan van den Brink, Ph.D.

Principle Scientist and Architect
Magnetic Resonance
Philips Medical Systems
Best, The Netherlands

Laura Vasquez, Ph.D., RT (R), (MR), (ARRT), MRSO

Chairperson of the Department of Medical Imaging Sciences
College of Health Science
Rush University
Chicago, IL

Ross Venook, Ph.D.

Research and Development Fellow
Boston Scientific Neuromodulation Corporation
Valencia, CA

Robert E. Watson, Jr. M.D., Ph.D.

Neuroradiologist
Division of Neuroradiology
Department of Radiology
Mayo Clinic
Rochester, MN

Lukas Winter, Ph.D.

MR Technology Scientist
Physikalisch-Technische Bundesanstalt (PTB)
Braunschweig und Berlin
Germany

Eunice Yang, M.D.

Postdoctoral Clinical Fellow
Cardiac Electrophysiology
Johns Hopkins Hospital
Baltimore, MD

Luca Zilberti, Ph.D.

Researcher
Istituto Nazionale di Ricerca Metrologica
Torino, Italy

Dedications

This textbook is dedicated to my dear wife, Jaana, for her never ending understanding, support, and devotion that allowed me to expend considerable time on this meaningful undertaking.

Frank G. Shellock, Ph.D.

I dedicate this textbook to my wife, Melinda, whose support has been instrumental in allowing me to dedicate my time to this important effort. I also dedicate this project to Rad-net, a company whose environment has provided me with tolerance and support for time spent in this important endeavor and my involvement in MRI practice, teaching, and research.

John V. Crues, M.D., III

Acknowledgments

We are indebted to Alexandra M. Karacozoff, the Associate Editor, for her exceptional editing and proofreading abilities, as well as her other important contributions to this textbook. We are grateful to Crystal Newton and Anastasios Karatopis for their amazing artistic talents that resulted in the creation of an extraordinary cover. Special thanks to Mark Bass for his extensive experience and great efforts that helped make this textbook possible by taking care of the overall production of this project and providing careful attention to an incredible list of details.

Table of Contents

Disclaimer	iv
Preface	v
The Editors	vii
Contributors.....	x
Dedications.....	xiii
Acknowledgments.....	xiv
CHAPTER 1	
Basic MRI Physics: Implications for MRI Safety	
Moriel NessAiver, Ph.D.	1
CHAPTER 2	
Principals of MRI Safety Physics	
Lawrence Panych, Ph.D.	
Bruno Madore, Ph.D.	34
CHAPTER 3	
MRI Physics and Safety at 7 Tesla	
Oliver Kraff, Ph.D.	
Harald H. Quick, Ph.D.	71
CHAPTER 4	
Bioeffects of Static Magnetic Fields	
Allayar Kangarlu, Ph.D.	96
CHAPTER 5	
Bioeffects of Gradient Magnetic Fields	
Donald W. McRobbie, Ph.D.	132
CHAPTER 6	
Acoustic Noise and MRI Procedures	
Mark McGury, Ph.D.	157
CHAPTER 7	
Bioeffects of Radiofrequency Power Deposition	
Daniel J. Schaefer, Ph.D.	208

CHAPTER 8**Radiofrequency-Energy Induced Heating During MRI: Laboratory and Clinical Experiences**

Frank G. Shellock, Ph.D.233

CHAPTER 9**Thermal Effects Associated with RF Exposures During Clinical MRI**

Johan van den Brink, Ph.D.254

CHAPTER 10**Claustrophobia, Anxiety, and Emotional Distress in the MRI Environment**

Laura Vasquez, Ph.D.284

CHAPTER 11**MRI Procedures and Pregnancy**

Patrick M. Colletti, M.D.306

CHAPTER 12**Identification and Management of Acute Reactions to Gadolinium-Based****Contrast Agents**

Alberto Spinazzi, M.D.333

CHAPTER 13**MRI Contrast Agents and Nephrogenic Systemic Fibrosis**

Alberto Spinazzi, M.D.351

CHAPTER 14**Gadolinium Retention in Brain and Body Tissues: Safety Considerations**

Alberto Spinazzi, M.D.365

CHAPTER 15**MRI Screening for Patients and Individuals**

Ashok K. Saraswat, M.S., B.Ed., R.T. (R)(MR)

Mark A. Smith M.S., ABMP, R.T. (R)(MR)379

CHAPTER 16**Using Ferromagnetic Detection Systems in the MRI Environment**

Mark N. Keene, Ph.D.400

CHAPTER 17**Physiological Monitoring of Patients During MRI**

Frank G. Shellock, Ph.D.435

CHAPTER 18**MRI Issues for Implants and Devices**

Frank G. Shellock, Ph.D.462

CHAPTER 19**Active Implanted Medical Devices: An Overview of MRI Safety Considerations**

Robert E. Watson, Jr., M.D., Ph.D.

Heidi Edmonson, Ph.D.498

CHAPTER 20	
MRI-Related Heating of Implants and Devices	
Lukas Winter, Ph.D.	
Frank Seifert, Ph.D.	
Luca Zilberti, Ph.D.	
Manual Murbach, Ph.D.	
Bernd Ittermann, Ph.D.	514
CHAPTER 21	
MRI Test Methods for MR Conditional Active Implantable Medical Devices	
Louai Al-Dayeh, M.D., Ph.D.	
Ross Venook, Ph.D.	
Mizah Rahman, Ph.D.	552
CHAPTER 22	
Using MRI Simulations and Measurements to Evaluate Heating of Active Implants by Radiofrequency Fields and Gradient Magnetic Fields	
John Nyenhuis, Ph.D.	574
CHAPTER 23	
The Role of Numerical Modeling and Simulations to Evaluate Implantable Leads: Implications for MRI Safety	
Eugenio Mattei, Ph.D.	
Federica Censi, Ph.D., EEng.	
Giovanni Calcagnini, Ph.D., Eng.	611
CHAPTER 24	
Performing MRI In Patients with Conventional (Non-MR Conditional) Cardiac Devices	
Eunice Yang, M.D.	
Saman Nazarian, M.D., Ph.D., FHRS, FACC	
Henry Halperin, M.D., M.A., FHRA, FAHA	656
CHAPTER 25	
MRI and Patients with Cardiac Implantable Electronic Devices	
Sumit Patel, M.D.	
John Summers, M.D., FACC	
Jerold S. Shinbane, M.D., FACC, FHRS, FSCCT	674
CHAPTER 26	
Neuromodulation Systems: MRI Safety Issues	
Mizan Rahman, Ph.D.	
Frank G. Shellock, Ph.D.	710
CHAPTER 27	
MRI Safety Policies and Procedures for a Hospital or Medical Center Setting	
John Posh, R.T. (R)(MR)	749

CHAPTER 28	
MRI Safety Policies and Procedures for an Outpatient Facility	
Laura Foster, J.D., M.P.H.	
Lawrence N. Tanenbaum, M.D.	
John V. Crues, III, M.D.	765
CHAPTER 29	
MRI Safety Policies and Procedures for a Children's Hospital	
Christine Harris, R.T. (MR), MRSO	781
CHAPTER 30	
MRI Safety Policies and Procedures for a Research Facility	
Anne Marie Sawyer, B.S., R.T. (R)(MR), FSMRT	797
CHAPTER 31	
Safety Issues for Interventional MR Systems	
Daniel F. Kacher, M.S.	
Janice Fairhurst, B.S., R.T. (R)(MR)	
Joshua C. Vacanti, M.D.	
Clare M. Tempany-Afdhal, M.D.	
Srinivasan Mukundan Jr. M.D., Ph.D.	833
CHAPTER 32	
Occupational Exposure During MRI	
Donald W. McRobbie, Ph.D.	869
CHAPTER 33	
MRI Standards and Guidance Documents from the United States, Food and Drug Administration	
Wolfgang Kainz, Ph.D.	893
CHAPTER 34	
MRI Standards and Safety Guidelines in Europe	
Stephen F. Keevil, Ph.D.....	911
CHAPTER 35	
MRI Standards and Safety Guidelines in Canada	
Trina Gulay, R.T. (R) (MR)	925
CHAPTER 36	
MRI Standards and Safety Guidelines in Australia	
Gregory Brown, Ph.D., FSMRT	973
Index	996

Chapter 1 Basic MRI Physics: Implications for MRI Safety

MORIEL NESSAIVER, PH.D.

Simply Physics
Baltimore, MD

INTRODUCTION

Most medical professionals today are well aware of the fact that magnetic resonance imaging (MRI) technology uses systems with powerful magnets that make considerable amounts of noise and that you generally cannot bring ferromagnetic objects or patients with certain implants into the scanner room. However, these individuals may not be aware that MR systems use relatively safe radiofrequency (RF) radiation instead of ionizing radiation (e.g., X-rays, gamma rays, etc.) to create images and they may not understand just how powerful the magnets are, why they may always be “on” and why they make so much noise. This chapter provides simple explanations for these matters by presenting information pertaining to basic MRI physics.

MRI has at its root the chemical technique known as nuclear magnetic resonance or NMR (1, 2). As every chemist knows, the use of the word “nuclear” has nothing to do with radioactivity, but since the general population is not composed of mostly chemists, the medical community has dropped that emotionally laden word to become, simply, MRI. For most MRI examinations, the word “nuclear” has to do with the nucleus of the hydrogen atom, which consists of a single proton. The content of this chapter will begin by examining the magnetic properties of protons and then continue with an explanation of the MRI signal, some basic tissue properties, spin echo formation, and conclude with a brief discussion of MRI hardware issues. Much of the information in this chapter is adapted from *All You Really Need to Know About MRI Physics* (3). Several other textbooks also cover this introductory material (4-7).

Note: Throughout this chapter, “Key Definitions” are designated in bold print.

2 Basic MRI Physics: Implications for MRI Safety

MAGNETIC PROPERTIES OF PROTONS

Spinning Protons Act Like Little Magnets

A moving electric charge, be it positive or negative, produces a magnetic field. The faster a charge moves or the larger the charge, the larger the magnetic field it produces. Think back to when you were a child and would make a crude electromagnet by wrapping wire around a nail and connecting it to a battery. The larger the voltage of the battery, the larger the current and the stronger the magnet.

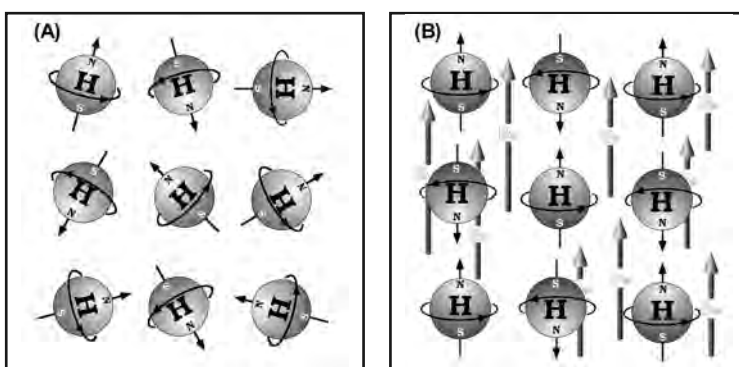
Some of the basic properties of a simple proton include mass, a positive electric charge and spin. Granted, a proton does not have a very large electric charge, but it does spin very fast and, therefore, does produce a very small, yet significant, magnetic field. Water is the largest source of hydrogen protons in the body, followed by fat. Normally, the direction that these tiny magnets point in is randomly distributed (**Figure 1A**).

Key Definition: Spinning protons are little magnets which are frequently referred to as “spins”.

Key Definition: Tesla (T) – A unit of magnetic field strength. $1\text{ T} = 10,000\text{ Gauss}$ (another unit of magnetic field). The earth’s magnetic field is roughly 0.5 Gauss.

Just as a compass aligns with the Earth’s magnetic field, a spinning proton placed near (or within) a large external magnetic field (called \mathbf{B}_0) will align with the external field. Unfortunately, it is not quite so simple. At the atomic level, some of the protons align with the field and some align against the field, cancelling each other out. A slight excess will align with the field so that the net result is an alignment with the external field. **Figure 1B** depicts nine protons, four of which have aligned *against* \mathbf{B}_0 and five have aligned *with* \mathbf{B}_0 resulting in an excess of one proton. (Note that this diagram showing the protons aligning perfectly with or against \mathbf{B}_0 is not completely accurate. This will be addressed further with **Figure 3**.)

Figure 1. (A) Protons that are randomly oriented in the absence of an external magnetic field. **(B)** Protons aligned either with (slight majority) or against (slight minority) an external magnetic field.

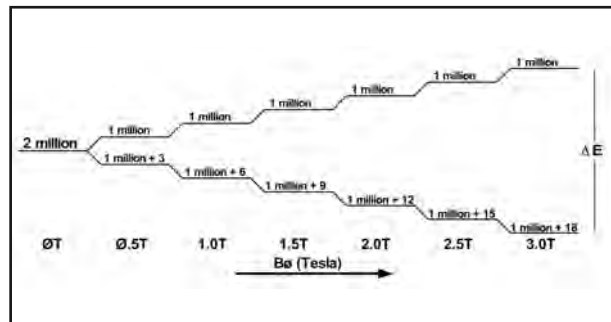


Some Quantum Physics

A complete explanation of why the protons align both with and against the external magnetic field would require a study of quantum mechanics. Suffice it to say that both alignments are possible but the one **with** the field is at a lower energy state. The protons are con-

tinually oscillating back and forth between the two states but at any given instant, and with a large enough sample, there will be a very slight majority aligned with the field. The larger the external static magnetic field, the greater the difference in energy levels and the larger the excess number aligned with the field. **Figure 2** demonstrates this for a sample of two million protons. At 1 T there are just six extra protons. At 1.5 T, there are only nine extra protons for every two million. At 3 T there are 18 and at 7 T, the highest field strength used in the clinical setting, there are 42 excess protons for every two million. The number of excess protons is directly proportional to the strength of the static magnetic field.

Figure 2. The number of excess protons aligned with the B_0 field is directly proportional to the strength of the static magnetic field. At 1.5 T, for every two million protons there are nine more protons aligned with the field than there are aligned against the field. At 3 T, there are 18 excess protons.



As will be discussed more fully later in this chapter, the MR signal comes from just these excess protons. With only nine out of two million protons (at 1.5 T) in excess, one might ask how can we even detect such a small signal? We shall answer that question by first asking a different question: how many excess protons are there in a single imaging voxel? (A voxel is a three-dimensional or volume pixel.) Without going into the math in great detail, assume a voxel dimension of 1-mm x 1-mm x 5-mm = 0.005-cm³ or 0.005-ml. Using Avogadro's Number, we can calculate that there are a total of 3.4×10^{20} water protons in a 0.005-ml voxel. If nine out of every two million protons are in excess, then there are a total of 1.5×10^{15} protons in every voxel that will contribute to the MR signal (or, on the order of a million billion protons). The important lesson here is that even though a spinning proton is a very poor magnet, the number of excess protons that align with the field is so large that we can basically ignore quantum mechanics and focus on the classical mechanics description.

Key Definition: The total magnetic field of the excess protons is defined as M_0 .

While it was stated above that, due to the large number of excess protons, we can pretty much ignore quantum physics, there is still one issue that is best discussed using quantum physics terminology. The relationship between the energy (E) of a photon or a unit of electromagnetic radiation and its frequency (ν) (the Greek symbol ‘nu’) is described by the Planck’s equation:

$$E = h \nu \quad (1)$$

4 Basic MRI Physics: Implications for MRI Safety

Where \hbar is known as Planck's constant. In simple words, the energy of electromagnetic radiation goes up directly with the frequency of the radiation. **Table 1** lists the approximate frequency ranges for different types of electromagnetic radiation. As will be discussed in detail shortly, MRI uses radio waves with frequencies around 10^7 -Hz (cycles per second). Most other radiology imaging techniques (e.g., X-ray, computed tomography, and nuclear medicine) use ionizing radiation with frequencies in the 10^{18} - to 10^{19} -Hz range or roughly 10^{12} larger than those used in MRI. Accordingly, X-rays are roughly a trillion times more "energetic" (and potentially damaging) than radio waves. MRI is able to provide such great images not because of the high energy involved (like computed tomography) but because of the large number of protons found in the body, primarily in water and fat.

Table 1. Frequencies associated with different types of electromagnetic radiation.

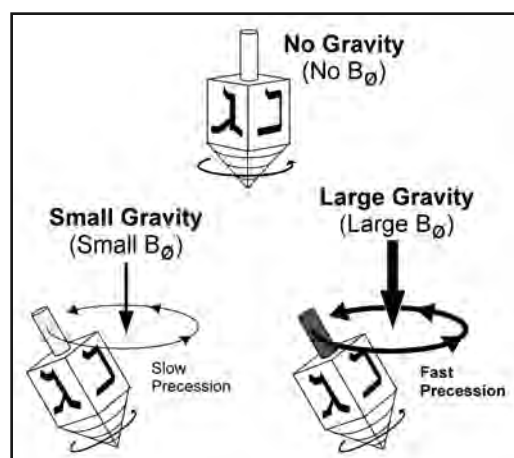
Types of Radiation	Approximate Frequency in Hz
Radio Waves	10^7
Visible Light	10^{14}
Ultraviolet	10^{16}
X-Rays	10^{18}
Gamma Rays	$>10^{19}$

MAGNETIC RESONANCE

Spinning Protons Act Like Dreidels

Three spinning dreidels (i.e., a toy top traditionally used during Chanukah) are shown in **Figure 3**. Imagine the first one is spinning on the international space station. In the absence of gravity, it behaves just like a gyroscope and spins without wobbling. Imagine the second one is spinning on the moon. In the low gravity of the moon, the Dreidle will wobble rather slowly. The third dreidel is spinning on the Earth and wobbles faster than the dreidel on the moon. Imagine a fourth dreidel somewhere on Jupiter (if you could find a solid surface, that is). That dreidel would be wobbling the fastest yet.

Figure 3. Dreidels (toy tops) rapidly spin about their axis while at the same time they wobble or "precess" at a rate that depends on the strength of the gravity field.



Previously, a spinning proton was described as being a very tiny magnet. Just as a spinning dreidel wobbles about its axis, so do spinning protons wobble, or precess, about the axis of the external B_θ field. The frequency of the precession is directly proportional to the strength of the magnetic field and is defined by the Larmor Equation:

Memorize this! $\omega_\theta = \gamma B_\theta$ (2)

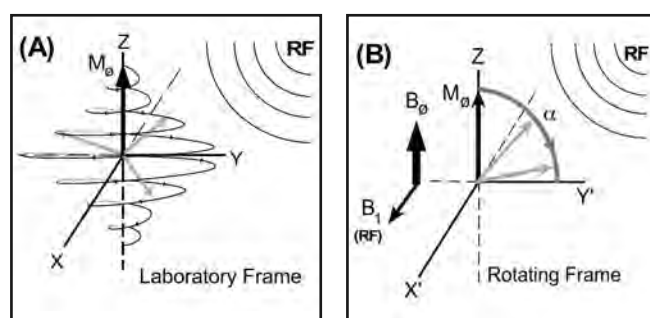
Where, ω_θ is known as either the precessional, Larmor or resonance frequency and γ (gamma) is the gyromagnetic ratio and is a constant unique to every atom. For a simple proton, $\gamma = 42.56\text{-MHz/T}$. As before, B_θ represents the externally applied static magnetic field. At the magnetic field strengths used in clinical MR systems, 0.2 to 7 T, the resonance frequency of hydrogen ranges from 8.5-MHz to 298-MHz ($8.5 \times 10^6\text{-Hz}$ to $2.98 \times 10^8\text{-Hz}$). In **Table 1**, it is shown that this range is in the radiofrequency (RF) portion of the electromagnetic spectrum.

As such, it is now apparent how **Figure 1B** was slightly inaccurate. The spins do align roughly with (or against) the static magnetic field but, if you could take a freeze frame snapshot of all of the protons in a voxel, you would see that each individual proton is slightly tilted. However, remember that the protons are each precessing at faster than ten million times per second, so if you take the average position of the vectors over even a very short amount of time, they will each be aligned either perfectly with, or perfectly against, the main magnetic field.

APPLY AN RF EXCITATION PULSE

If an electromagnetic radiofrequency (RF) pulse is applied at the resonance (Larmor, precession, wobble) frequency, then the protons can absorb that energy. At the quantum level, a single proton “jumps” to a higher energy state. At the macro or classical level, to an observer in the external or laboratory frame of reference, the magnetization vector, M_θ , (roughly a million billion protons) spirals down towards the XY plane (**Figure 4A**). If you could somehow jump aboard M_θ , just like onto a merry-go-round, the laboratory would be seem to be rotating around you. In this rotating frame of reference, M_θ would seem to smoothly tip down (**Figure 4B**). The tip angle is a function of the strength and duration of the RF pulse. The absorption of the energy from the applied RF excitation pulse can be

Figure 4. Radiofrequency (RF) energy is absorbed. (A) An observer in the surrounding laboratory will see M_θ spiral down to the XY-plane (or even down to the negative Z-axis.) (B) An observer riding on the M_θ vector sees the external world rotating about him. The M_θ vector tips α° (alpha degrees) towards the Y'-axis.



6 Basic MRI Physics: Implications for MRI Safety

roughly compared to shining a light onto phosphorescent paint. The stronger the light or the longer it is applied, the more energy is absorbed (up to a point, that is).

Key Definition: Laboratory Frame. The viewpoint of an observer in the laboratory. The laboratory is stationary, the protons are spinning.

Key Definition: Rotating Frame. The viewpoint of an observer riding along on the protons. The protons appear stationary, the laboratory is rotating.

Key Definition: M_z . The component of the net magnetization vector that points in the Z or B_0 direction.

Key Definition: M_{xy} . The component of the net magnetization vector that resides in or projects onto the XY-plane.

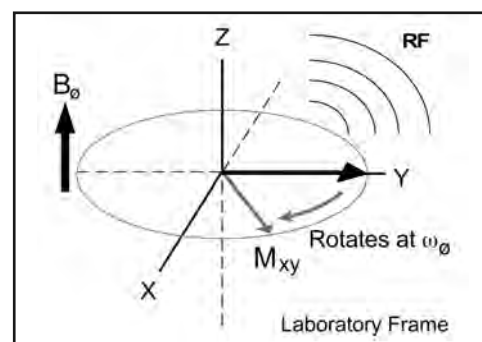
TURN OFF THE TRANSMITTER – WHAT HAPPENS?

Once the RF transmitter is turned off, three things begin to happen simultaneously: (1) the absorbed RF energy is re-transmitted (at the resonance frequency), (2) the excited spins begin to return to the original M_z orientation (i.e., T_1 recovery to thermal equilibrium) and (3) initially in-phase, the excited protons begin to dephase (i.e., T_2 and T_2^* relaxation).

RF Energy Is Re-Transmitted

Continuing the analogy of phosphorescent paint, when the light is turned off the paint will re-emit the absorbed energy and “glow”. Once M_0 has been tipped away from the Z-axis and the RF transmitter is turned off, the vector will continue to precess around the external B_0 field at the resonance frequency, ω_0 (**Figure 5**). Any rotating magnetic field produces electromagnetic radiation. Since ω_0 is in the radiofrequency portion of the electromagnetic spectrum, the rotating vector is said to give off RF waves. These re-emitted RF waves are the MRI signal.

Figure 5. With the RF transmitter turned off, the M_{xy} vector continues to rotate about the Z-axis (B_0) emitting RF energy at the resonance frequency ω_0 .



M_z Recovers Via T_1 Relaxation

The rotating M_{xy} vector shown in **Figure 5** will continue to give off RF waves as long as it continues to rotate. However, to give off energy it has to come from somewhere. The process of giving off RF energy occurs as the spins drop from a high energy state to a low energy state, realigning with B_0 and releasing a photon (**Figure 6**). The RF emission is the

net result of the **Z** component (M_Z) of the magnetization recovering back to M_θ while the M_{XY} component gets smaller and smaller (**Figure 7**).

Figure 6. When a proton flips from aligning *against* B_θ (high energy state) to aligning *with* B_θ (low energy state) it emits a photon at the resonance frequency, ω_θ .

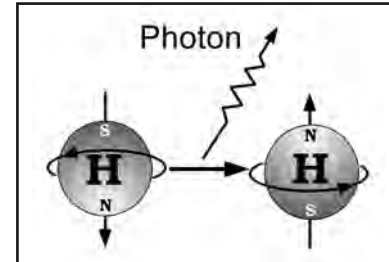
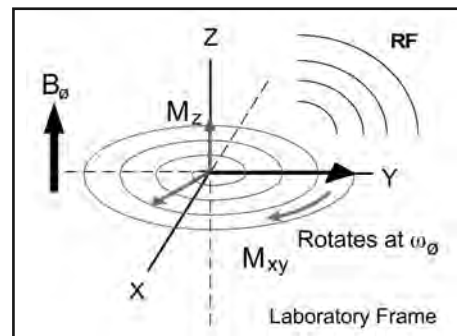


Figure 7. As the M_{XY} vector rotates about the Z-axis it gets steadily smaller, spiraling inwards, as RF energy is released. At the same time an M_Z component starts to recover. This is the exact reverse of the process depicted in **Figure 4A**.



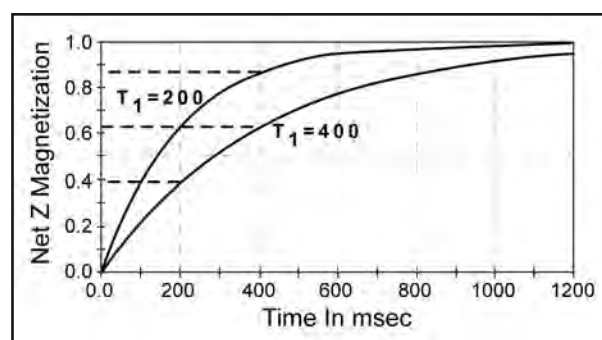
Not all of the energy given off is detectable as an RF signal. Some of the energy is re-absorbed by nearby protons. Most of the energy actually goes to heating up the surrounding tissue, referred to as the lattice. In a global, or rather, universal sense, this system can be divided into the spins, and the rest of the universe, or a very large lattice. This type of spin-lattice interaction is the result of the excited system returning to thermal equilibrium.

Key Definition: Spin-Lattice Relaxation. The process whereby energy absorbed by the excited protons or spins is released back into the surrounding lattice re-establishing thermal equilibrium. In general, T_1 values are longer at higher field strengths.

The time course whereby the system returns to thermal equilibrium, or M_Z grows to M_θ , is mathematically described by an exponential curve [Equation (3)] (**Figure 8**).

$$M_Z = M_\theta \cdot (1 - e^{-t/T_1}) \quad (3)$$

Figure 8. Recovery of Z-magnetization of tissues with two different T_1 time constants. Roughly 63% of Z-magnetization recovers during one T_1 time period.



8 Basic MRI Physics: Implications for MRI Safety

This recovery rate is characterized by the time constant T_1 , which is unique to every tissue. This uniqueness in M_Z recovery rates is one of the mechanisms that enables MRI to differentiate between different types of tissue. At a time $t = T_1$ after the excitation pulse, 63.2% of the magnetization has recovered alignment with B_0 . Full recovery of M_Z to M_0 is considered to occur at a time $\geq 5 T_1$ (**Table 2**).

Table 2. M_Z recovery fractions at different multiples of T_1 times.

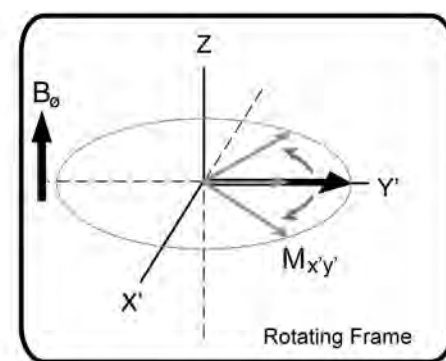
t/T_1	M_Z
-1	0.6321
-2	0.8646
-3	0.9502
-4	0.9816
-5	0.9932

Key Definition: T_1 Relaxation: Spin-Lattice relaxation. The exponential recovery of longitudinal (aligned with B_0) magnetization. M_Z returns to M_0 .

M_{XY} Diminishes Via T_2 Dephasing

When the spins are first tilted down to the XY-plane, they are all in-phase. Think of a playground with a million swings. If all of the children are going up and down together, at exactly the same rate, then they are swinging in-phase. Assuming that all the children are pumping their legs with the same force and frequency, then they will stay in-phase. But if one child stops pumping for a few seconds and another child pumps a little harder or a little faster, then they will start to get out of sync with everyone else. The same type of thing happens to the spins. For reasons that will be described later, some protons spin a little faster while others spin a little slower (**Figure 9**). Very quickly, they get out of phase relative to some reference (usually the spins at the center of the magnet).

Figure 9. Immediately after the M_0 vector is tipped to the XY-plane all of the million, billion or so spins that make up the vector start to spread out.



As another analogy, think of a room filled with a million (or a million billion) people, all of them whispering “Mary had a little lamb”. As long as they are all speaking in-phase with each other, you hear a very loud “**MARY HAD A LITTLE LAMB**”. But what usually happens in a room full of people where those at one end of the room can’t hear those at the

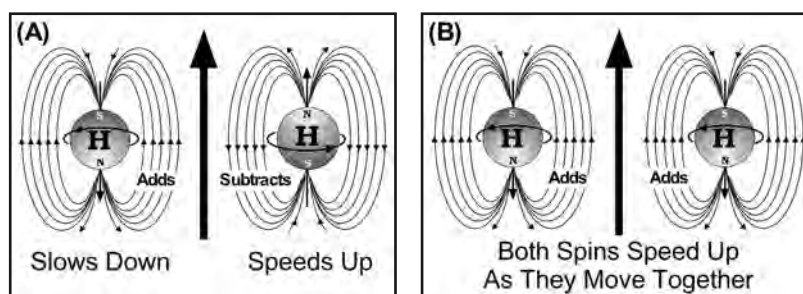
other, some people start speaking a little faster and others a little slower. Soon the words start to become harder to make out until eventually all you hear is some low, background noise (**Figure 10**). The same happens to the spins and the resulting MRI signal.

Figure 10. With a room full of people whispering “**MARY HAD A LITTLE LAMB**” they may all start at the same time and an outside observer can clearly hear the phrase. But what usually happens is that those at one end of the room can’t hear those at the other end, so some people start speaking a little faster and others a little slower. Soon the words start to become harder to make out until eventually all that is heard is some low, background noise. The same happens to the spins and the resulting MRI signal.



How fast a proton wobbles or precesses depends on the magnetic field that it experiences. An isolated proton, far from any other proton (or electron), is only affected by the main magnetic field, B_0 . As protons (or spins) move together (e.g., due to random motion), their magnetic fields begin to interact. If the field from one proton increases the field that the second proton feels, while the field from the second proton reduces the field that the first proton feels, then the second proton will precess at a slightly faster rate, while the first proton will precess slightly slower (**Figure 11A**). If the fields from both protons add to the main field, then both protons will precess more rapidly (**Figure 11B**). As soon as the spins move farther apart, their fields no longer interact and they both return to the original frequency but at different phases. This type of interaction is called spin-spin interaction. These temporary, random interactions cause a cumulative loss of phase across the excited spins resulting in an overall loss of signal.

Figure 11. As two spins (or protons) approach each other, the magnetic fields produced by each will either add to or subtract from the main external field (B_0) causing the other to precess either faster or slower. **(A)** The case where one proton is aligned against the main field while the other is aligned with the main field. **(B)** The case where both spins are aligned against the main field.



10 Basic MRI Physics: Implications for MRI Safety

Key Definition: Spin-Spin Relaxation. The temporary and random interaction between two spins that causes a cumulative loss in-phase resulting in an overall loss of signal, also known as transverse or T_2 relaxation.

Similar to T_1 relaxation, the signal decay resulting from transverse or spin-spin relaxation is described mathematically by an exponential curve, identical in concept to radioactive decay with a half-life measured in tens of milliseconds [Equation (4)] (Figure 12).

$$M_{xy} = M_\theta \cdot e^{-t/T_2} \quad (4)$$

The value T_2 is the time after excitation when the signal amplitude has been reduced to 36.8% of its original value or has lost 63.2%. This is the opposite of T_1 where 63.2% of M_z is recovered in one T_1 period. By three times T_2 there is less than 5% of the original signal remaining (Table 3). The value of T_2 is unique for every kind of tissue and is determined primarily by its chemical environment with little relation to field strength. This uniqueness in T_2 decay rates is one of the other mechanisms that enables MRI to differentiate between different types of tissue.

Figure 12. Graphs depicting the exponential loss of signal from two different tissues with T_2 time constants. Similar to the T_1 recovery curve (Figure 8) where 63% of magnetization is recovered in one T_1 time period, here 63% of magnetization is dephased or lost during one T_2 time period.

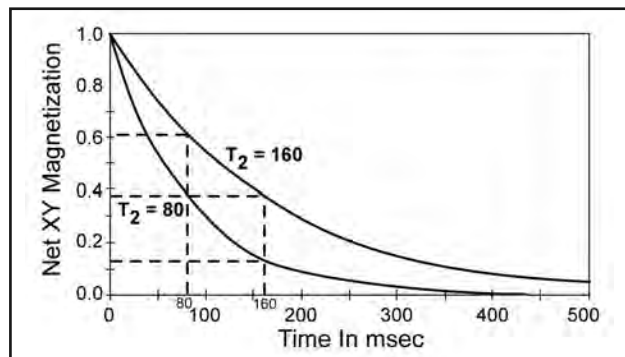


Table 3. M_{xy} residual fractions at different multiples of T_2 times.

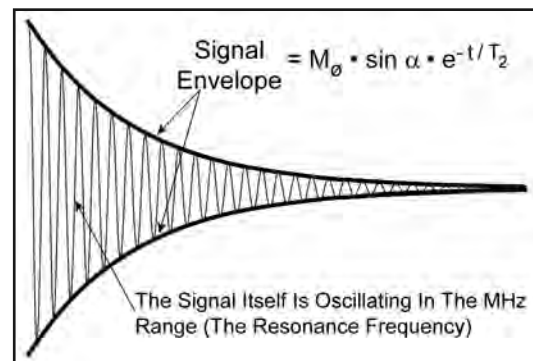
t/T_2	M_{xy}
-0.5	0.6065
-1	0.3679
-2	0.1354
-3	0.0498
-4	0.0184

Key Definition: T_2 Decay. The exponential loss of signal resulting from purely random spin-spin interactions in the transverse or XY-plane. In general, T_2 values are unrelated to field strengths (unlike T_1 values).

FREE INDUCTION DECAY (FID) AND SPIN ECHO FORMATION

To summarize what has been covered so far, after the RF transmitter is turned off, the protons immediately begin to re-radiate the absorbed energy. If nothing is affecting the homogeneity of the magnetic field, all of the protons will spin at the same resonance frequency. The initial amplitude of the signal is determined by the portion of the magnetization vector (\mathbf{M}_0) that has been tipped onto the XY-plane. This, in turn, is determined by the sine of the flip angle, α . The maximum signal is obtained when the flip angle is 90°. [Note: sine (0°) = 0, sine (90°) = 1.0] The signal unaffected by any gradient is known as a Free Induction Decay (FID) (Figure 13). The time constant that determines the rate of decay is called T_2 .

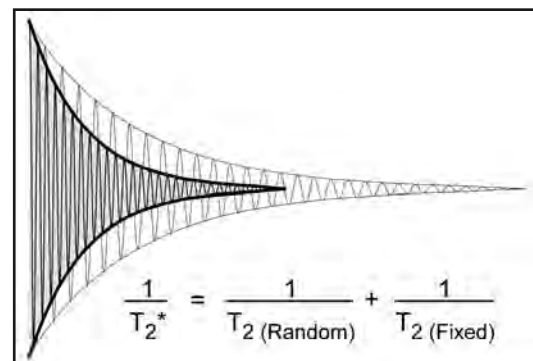
Figure 13. A graph depicting how, while the MR signal oscillates rapidly at the resonance frequency, ω_0 , the amplitude or signal envelope decays at a rate dependent on the T_2 time constant. This type of signal is known as Free Induction Decay or FID.



Key Definition: Free Induction Decay (FID). An MR signal in the absence of any magnetic gradients. The decay curve is the signal envelope. The actual signal is oscillating at the resonance frequency which is in the MHz range.

In the real world, the MR signal decays faster than T_2 would predict. Pure T_2 decay is a function of completely random interactions between spins. The assumption is that the main external \mathbf{B}_0 field is absolutely homogeneous. In reality, there are many factors creating imperfections in the homogeneity of a magnetic field. The main magnet itself will have flaws related to the manufacturing process. Every tissue has a different magnetic susceptibility which distorts the field at tissue borders, particularly at air/tissue interfaces. Additionally, patients may have some type of metallic implants (e.g., clips, staples, heart valves, etc.) which cause disruptions of the magnetic field. The sum total of all of these random and fixed effects is called T_2^* (pronounced “T-two star”) (Figure 14).

Figure 14. The graph of Figure 13 represents the ideal case. In the real world, the FID decays much more rapidly with a time constant of T_2^* (T_2 -star).



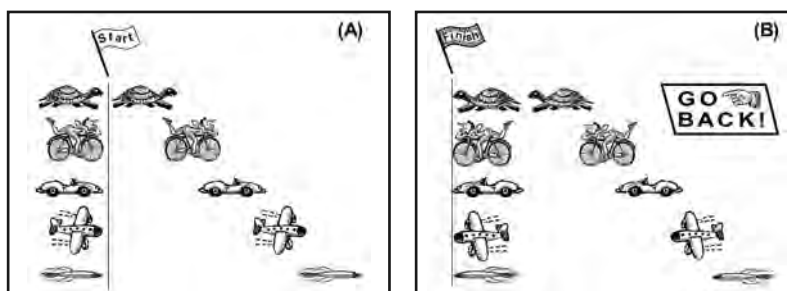
12 Basic MRI Physics: Implications for MRI Safety

Thus, T_2 relaxation comes from random causes while T_2^* comes from a combination of both random and fixed causes. There is nothing that can be done to prevent or compensate for random losses in-phase, but what about the fixed effects? Can anything be done about these losses? The answer is yes.

Consider the following race (**Figure 15A**). The contestants are a turtle, a bicyclist, a pace car, an airplane, and a rocket. At the start of the race, everyone is together (in-phase). Once the race starts (at $t = 0$), the contestants all move out, each at their fastest pace. Soon, there is a noticeable distance between them.

After some time, let's call it $TE/2$, a signal is given for everyone to turn around and go back. Assuming that everyone is still going at the same rate as before, then after an additional time, $TE/2$, they all arrive at the starting/finish line together (**Figure 15B**). In terms of MRI, at the time TE ($TE/2 + TE/2$), all the spins are back in-phase, producing a large signal. This large signal is called a spin echo and the time TE is called the echo time (8).

Figure 15. Excited spins can be compared to contestants in a race. The car in the middle represents the pace car or spins at exactly the resonance frequency. Some spins are at a lower frequency (the bicyclist and the turtle) while others are at a higher frequency (the plane and the rocket.) **(A)** Immediately after the start of the race, the contestants spread out. **(B)** After some sort of signal (Go Back), the contestants turn around and head back to the Start/Finish line, ending in a tie.



Key Definition: Echo. The reflection (mirror image) of a signal caused by some sort of reversal of direction. (e.g., the sound bouncing off of a cliff). In MRI, there are spin echoes and gradient echoes.

The principle of spin echo formation in the rotating frame is presented in **Figure 16**: **(A)** At time $t = 0$, immediately after a 90° RF pulse, \mathbf{M}_0 points along the Y'-axis. **(B)** A time of $TE/2$ is allowed to elapse while the spins dephase (T_2^* mechanisms). At $t = TE/2$, a 180° RF pulse is given which flips the dephased vectors about the X'-axis. **(C)** Another $TE/2$ time is allowed to pass while the vectors rephase. **(D)** At $t = TE$, the vectors have rephased and an echo of opposite sign forms. (The astute observer will note that the arrows drawn to represent the 180° rotation about the X'-axis go above the X'Y'-plane, not below it. This is true only if a negative 180° pulse is what is actually used. Whether a positive or negative 180° is used, or one that rotates about the Y'-axis instead of the X'-axis, the end result is the same.)

As described above, a 180° pulse can be used to reverse the T_2^* dephasing process and, thereby, produce a spin echo. As soon as the spins all come back into phase at the echo time, they immediately start to go out of phase again. A second 180° pulse will generate a second echo. This process can be repeated many times, producing many echoes, as long as the pure T_2 decay mechanisms have left some signal to work with (Figure 17). This repeating echo train can be used to produce multiple images or can be used to greatly speed up the acquisition time using a method known as fast or turbo spin echo imaging.

Figure 16. Spin echo formation. (A) M_0 is flipped down onto the $X'Y'$ plane. (B) Spins dephase (T_2^*) followed by a 180° RF pulse, flipping them to the other side of the X' axis. (C) The spins continue moving at their individual frequencies resulting in them moving back together. (D) Forming the re-phased spin echo.

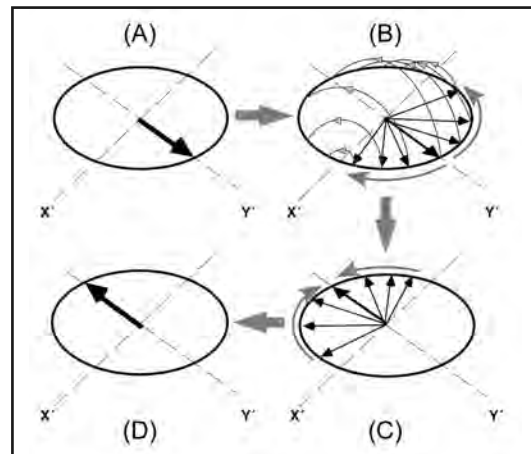
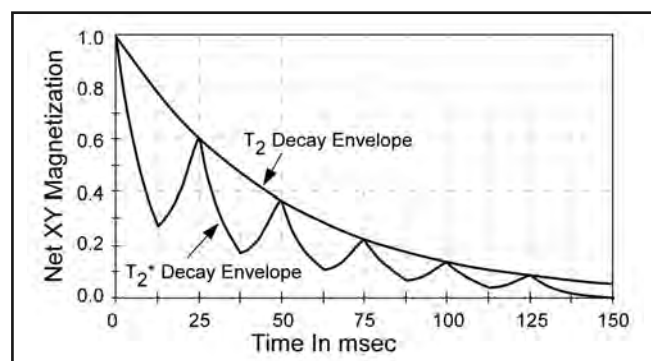


Figure 17. Application of multiple 180° RF pulses will create multiple spin echoes, the amplitude of which is limited by the T_2 decay envelope.



MRI HARDWARE

In order to perform MRI, the patient must be placed inside of some sort of magnet. There are many factors that go into the design of a magnet used in an MR system. As stated above, the higher the strength of the static magnetic field, the larger the number of excess protons there are to produce the MR signal (which usually means better quality images). Also, in order to reduce T_2^* signal dephasing the magnetic field in the imaging volume should be as homogeneous as possible over as large a volume as possible.

A third issue that has not been discussed, nor will it be possible to discuss in any great detail, is the need to be able to change the magnetic field at will. Equation (2) states that the resonance frequency is directly proportional to the strength of the magnetic field. By changing the strength of the magnetic field in some sort of known or predictable fashion,

14 Basic MRI Physics: Implications for MRI Safety

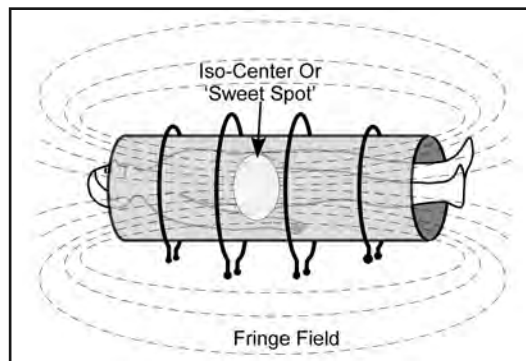
different resonance frequencies can be assigned to different locations in the magnet. This is accomplished using what are known as the X-, Y- and Z-gradients.

The Magnet and the Fringe Field

Horizontal field magnets produce magnetic field lines that go out one end of the magnet, loop around and go back the other end. Areas with the highest density of field lines have the highest strength. However, it is the areas that have the most rapidly changing density of field lines (i.e., the largest spatial gradients) that produce the greatest forces that can act on ferromagnetic materials. In other words, it is these areas that represent the greatest danger for items to become projectiles. Examples of projectiles that occurred in the MRI environment may be seen at www.simplyphysics.com (9).

The vast majority of high field strength MR scanners use superconducting electromagnets to produce the main magnetic field. [Note that some low field MR systems use permanent magnets, which in the past have been limited to fields ≤ 0.35 T (10). More recently, a few vendors have released permanent magnets of 0.4 and 0.5 T (11).] A simple four-loop design of such a magnet used in an MR system is depicted in **Figure 18**. The two central loops produce the majority of the field and the two outer loops help to shape it, to make it more homogeneous. Note that the center of the magnet is where the field lines are most closely packed meaning this is where the highest field strength is. The area marked as “isocenter” is also referred to as the “sweet spot”, the region with the greatest magnetic field uniformity.

Figure 18. The static magnet field for most MR systems is produced using large electromagnets. The main working field is concentrated in the center and the fringe field can extend far outside the imaging region.

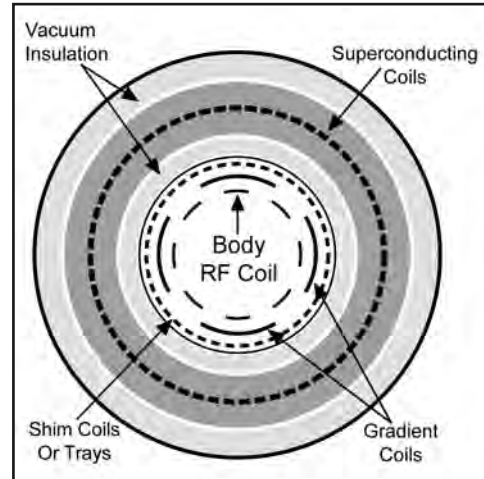


A current running through a loop of wire wrapped around a nail and attached to a battery produces a small magnetic field. (Actually the nail isn't needed, it just acts to intensify the field.) The larger the current flowing, the greater the magnetic field produced. This type of magnet is called a resistive electromagnet because the wire resists the flow of electrons. This resistance to the current flow also produces heat. While larger currents can generate higher magnetic fields, they will also produce considerable heat.

Similar to resistive magnets, the field from a superconducting magnet is produced by current flowing in multiple loops of wires. The wires are made out of niobium-titanium which, when cooled to 9.5°K (9.5° above absolute zero), lose all resistance to current flow. The coils are surrounded by liquid helium which boils at 4.2° K (**Figure 19**). When the scanner is first installed, a power supply is utilized to slowly build up the current and, thus,

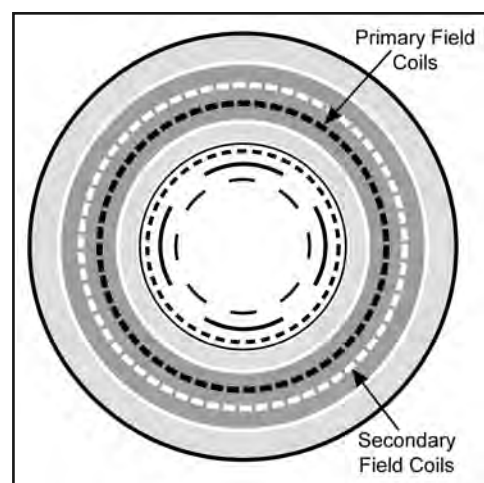
the magnetic field. This can take several hours to accomplish. Once it is up to its full field strength, the power supply is disconnected and the current will continue virtually for centuries (as long as it's kept cold, of course). This is why you will typically see signs outside MR system rooms that state, "Danger! This Magnet is Always On!"

Figure 19. A cross-section through a typical superconducting, high field strength MR scanner.



The magnetic field lines depicted in **Figure 18** that extend outside of the magnet are known as the fringe field. It is this fringe field that can cause problems with ferromagnetic objects. In general, the five gauss line is the demarcation between what is considered safe or a danger for certain objects. Modern-day MR systems use what is known as "active shielding". An actively-shielded magnet has an inner or primary set of field coils that produces more than the desired field with an outer or secondary set of field coils with a lower current going in the opposite direction (**Figure 20**). The smaller opposite field partially cancels the field at the center of the magnet but cancels a much larger portion on the outside. For example, the primary set coils might produce a positive 2 T field while the secondary coils produce a negative 0.5 T, resulting in a net 1.5 T field at the center of the magnet but, because the secondary coils are closer to the outside, they create a greater amount of cancellation.

Figure 20. A cross section through a superconducting, high field strength MR system with active shielding. The current in the secondary field coils flow in the opposite direction from the current in the primary field coils.



16 Basic MRI Physics: Implications for MRI Safety

The advantage of modern actively-shielded magnets is that the five gauss line can be restricted relatively close to the magnet. However, this also means that as one moves closer to the bore of the magnet, the field strength rises rapidly over a relatively short distance (i.e., a high spatial gradient magnetic field is present). Understandably, a relatively high spatial gradient magnetic field can produce substantial issues for ferromagnetic objects. By way of example, **Figure 21** shows a hospital bed lifted completely off the ground and stuck to the front of a 3 T MR system.

Figure 21. A hospital bed stuck to the front of a 3 T MR system. (Photograph provided courtesy of Simply Physics.)



Time-Varying Gradient Magnetic Fields

The main magnetic field, \mathbf{B}_0 , discussed above is also known as the static magnetic field, meaning that it never changes over time. In order to actually produce MR images, it is necessary to apply a magnetic field that changes over time and space in a predictable fashion. What is needed is to be able to produce a change that is linear moving away from the magnet center, with positive changes in one direction and negative changes in the other. (Note, the field at the center of the magnet never changes.) The field produced by a current in a single loop of wire reaches a peak at the center of the coil and drops off non-linearly as it moves out (**Figure 22A**). Obviously, this won't suffice for MRI.

However, if a second coil with a current flowing in the opposite direction is placed one coil diameter away from the first, the fields from each coil totally cancel each other at the point midway between them (**Figure 22B**). The fields interact in such a way that they produce an almost perfectly linear change in the area midway between them. The field change then drops off as you move outside of the coils. This linear change (also known as a gradient) is not only along the centerline between the two coils but remains linear for about half of the center volume. If properly designed, this region of reasonable linearity corresponds with the “sweet spot” or most homogeneous portion of the magnet. Note that the locations with the greatest offset from the field at the center of the magnet are located near the center of each loop. This is also the location of the greatest change in magnetic field per unit time, $d\mathbf{B}/dt$, during an imaging sequence.

Every MR system has three orthogonal (perpendicular) sets of gradient coils (i.e., X-, Y-, and Z-gradient coils) that are mounted on what is referred to as the “gradient tube” (12)

Figure 22. (A) The magnetic field produced by a current in a simple loop of wire is at a maximum at the center of the loop and drops off rapidly (and non-linearly) as you move away. (B) Using two loops of wire separated by roughly the diameter of the coil and with currents flowing in opposite direction results in a region in-between where the strength or amplitude of the magnet field varies in a linear fashion.

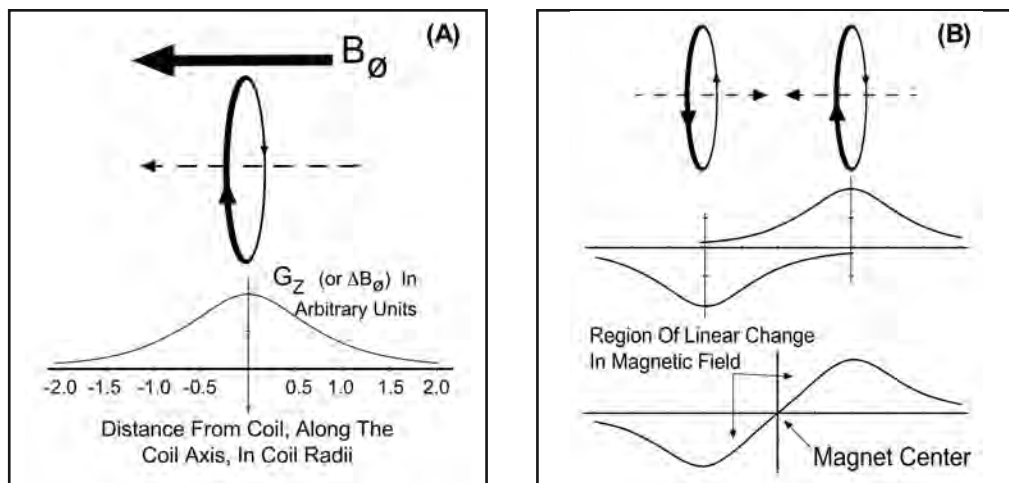
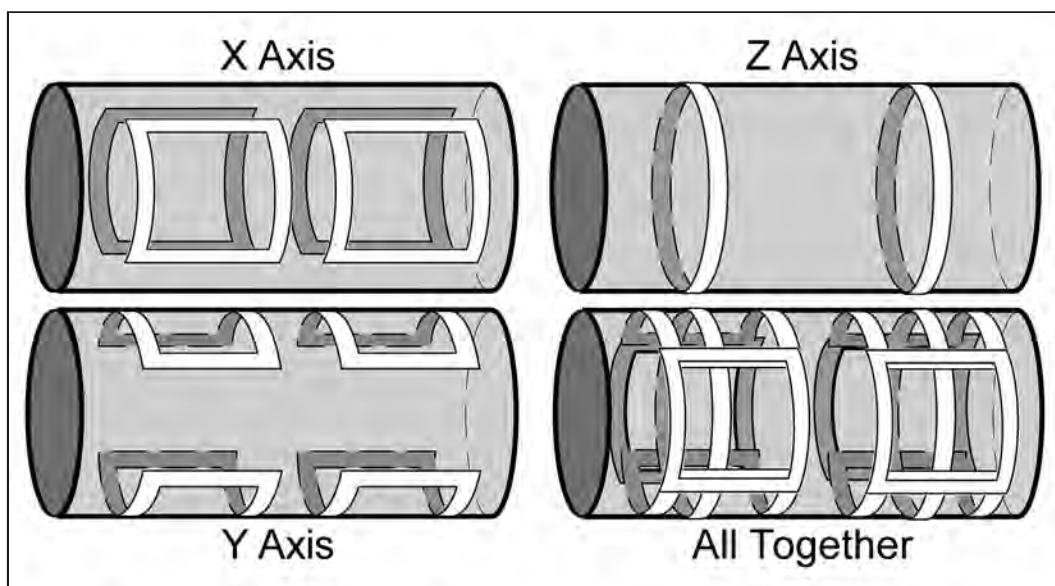


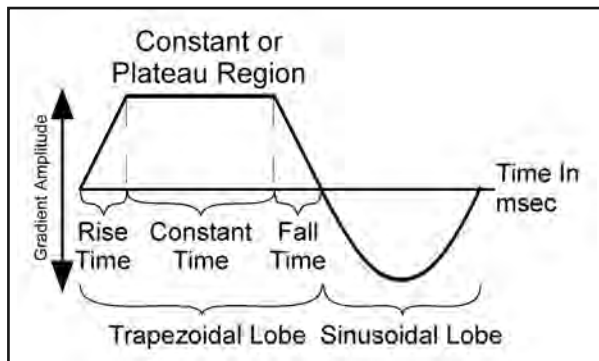
Figure 23. X-, Y- and Z-gradient coils mounted on the gradient tube of an MR system.



18 Basic MRI Physics: Implications for MRI Safety

(Figure 23). Current passing through these coils is rapidly turned on and off during the imaging process and are referred to as time-varying gradient magnetic fields. A diagram depicting the gradient activity during an MRI sequence showing how the gradient is turned on and off, is known as a “pulse profile” (Figure 24). A typical imaging sequence diagram will use pulse profiles to show the temporal relationship between each “gradient channel”, X-, Y-, Z- and the RF transmitter/receiver (Figures 25 to 28).

Figure 24. A pulse profile is a diagram that depicts gradient (or RF) activity during an MRI pulse sequence.



Every gradient system is characterized by two parameters: the peak gradient amplitude, which primarily effects how small the field of view (FOV) may be, and the peak slew rate, which is how fast the gradients can be turned on and off, which affects things like minimum echo and/or repetition times. Between the two, a fast slew rate is usually better from an MR imaging consideration than a high peak amplitude, however, faster slew rates cause more safety-related issues, as will be discussed below.

From the standpoint of MRI safety, these time-varying gradients raise two primary areas of concern. The first is acoustic noise that is associated with the gradient magnetic fields (13-15). An MR system can be compared to a giant speaker system. In a typical stereo speaker, there is a small permanent magnet with loops of wire wrapped around it and the magnet is attached to the center of a diaphragm. When an oscillating current is applied through the wire, it creates a time-varying gradient magnetic field that pushes and pulls on the permanent magnet, causing the supporting speaker diaphragm to vibrate.

The static B_0 magnet of the MR system is like the speaker’s permanent magnet. The imaging gradients are like the loop of wire wrapped around the permanent magnet. The gradient tube is like the diaphragm. During the imaging process, the imaging gradient can be turned on and off in as little as 1-msec (corresponding to 1000-Hz) or as much as 20-msec (corresponding to 50-Hz). This causes the imaging gradients to push and pull against the main magnetic field, and the physical supporting structures, resulting in vibrations that occur in the typical audio range. The higher the magnetic field, B_0 , and the faster the imaging sequence (higher slew rates), the louder the noise is that will be produced. The resulting acoustic noise can be at levels that may cause hearing damage if hearing protection is not used in the MR system room. As shown in the pulse profile of Figure 24, imaging gradients can be turned on and off rather abruptly (i.e., the trapezoidal lobe) or more gradually (i.e., the sinusoidal lobe). There are always trade-offs when designing an imaging se-

quence (see below), but using the lowest amplitude and lowest slew rates possible helps to minimize acoustic noise.

One of the important properties of electromagnetism is that just as an electric current creates a magnetic field, a time-varying gradient magnetic field can produce an electric current in any nearby conductor. This brings us to the other issue that is associated with time-varying gradient magnetic fields. The human body is an electrical conductor. If a patient undergoing MRI has crossed-arms or crossed-legs, these may create a closed loop for current to flow under certain imaging conditions. The rapidly changing imaging gradients can induce current to flow across the body and peripheral nerve stimulation may occur (16). The area near the center of the coils in **Figure 22B** is the location of the largest dB/dt, so it is at this location where the greatest danger of induced currents exists with respect to peripheral nerve stimulation. Note that at the center of the magnet, the gradients do not produce any change in the magnetic field, so this is where the potential for nerve stimulation is the least.

To summarize, the potential problems caused by time-varying gradient magnetic fields are, as follows: (1) acoustic noise and (2) peripheral nerve stimulation. The more rapidly the gradients change and the higher the amplitude, the greater the risks. Importantly, for patients with electronically-activated devices, the location of the greatest risk is not at the center of the MR system but at the outer edges of the gradient coils where the absolute changes in the magnetic fields per unit time (i.e., dB/dt) is the highest.

RF Coils and RF Power Deposition

As discussed above, MRI requires the use of a radio transmitter to provide the RF excitation pulses. Every scanner has a built in body RF coil (**Figure 19**) which is used for many of the imaging sequences. Alternatively, the RF excitation pulses can be applied by a smaller transmit RF coil, most commonly designed for imaging either the patient's head or a knee. While some of the applied RF energy that is absorbed ends up producing the MRI signal, most of it actually results in tissue heating of the patient (17). The amount of RF power absorbed by the body increases approximately with the square of the field strength. Accordingly, at higher static magnetic fields, there can be an inherent danger of over-heating the patient (17). The mass normalized rate at which RF energy is coupled to biological tissue is characterized by the specific absorption rate (SAR) and is reported in W/kg relative to the use of a particular pulse sequence and the body weight of the patient.

The built in transmit body RF coil deposits RF energy over a relatively large area of the patient. Even if only a small amount of tissue is actually being imaged, a large amount of tissue will absorb much of the transmitted energy. By comparison, smaller transmit/receive RF coils have a limited volume of coverage and result in greatly reduced RF power deposition. Additionally, a class of RF coils known as quadrature (quadrature is an engineering term that has nothing to do with the number four) coils result in less power deposition than comparably-sized linear coils. Notably, this information has implications for scanning patients with certain types of biomedical implants insofar as it may be necessary to prevent substantial implant heating by limiting the MRI examination to the use of a transmit/receive head RF coil only, versus performing the MRI procedure using a transmit body RF coil and a receive-only head coil (e.g., certain neurostimulation systems used for spinal cord stimulation have these particular conditions specified in the MRI labeling).

20 Basic MRI Physics: Implications for MRI Safety

Imaging Sequences

While there are many different types of imaging sequences used for MRI, most have three basic steps in common which are: (1) Exciting a slice or slab of tissue by using a slice select gradient combined with one or more RF excitation pulses. In an axial image, the Z-gradient is the slice select gradient. (2) Applying one (2D) or two (3D) spatial encoding gradients known as phase encoding pulses. The details of how this works are beyond the scope of this chapter. In an axial plane 2D image, the phase encoding direction can be in either the X-direction (i.e., left/right) or the Y-direction (i.e., anterior/posterior). For the moment, let's assume it is in the Y-direction. For a three dimensional image, there will also be a phase encode pulse in the Z or slice select direction. (3) Reading out the MRI signal while applying a third spatial encoding gradient known as the frequency encoding gradient.

The pulse diagrams of two of the simplest imaging sequences, a basic gradient echo (GRE) (18), also known as a field echo (FE) and a basic spin echo (SE) are shown in **Figure 25** and **Figure 26**, respectively (8). As was previously discussed (**Figure 16**), a SE sequence requires two RF pulses while, as shown in **Figure 25**, a GRE sequence uses a single RF pulse. The SE pulse sequence is most commonly used for T1-weighted imaging incorporating a 90°/180° pair of RF pulses. The GRE pulse sequence can use virtually any flip angle, which then impacts the type of image-weighting that results, in part, by the combination of the flip angle, echo time (TE) and repetition time (TR). Typically, flip angles from 20° to 40° are used for T₂*-weighting and flip angles from 70° to 90° are used for T₁-weighting. The key point here is that, with only one RF pulse, the RF power deposition, or SAR, is substantially lower with GRE sequences than with SE sequences. This is particularly important on MRI examinations using MR systems operating at 3 T or higher.

Figure 25. This diagram shows the temporal relationship between activity on the X-, Y-, and Z-gradients as well as the RF transmitter and receiver during a simple gradient echo pulse sequence. E.A.O.S., Equal Area Opposite Sign.

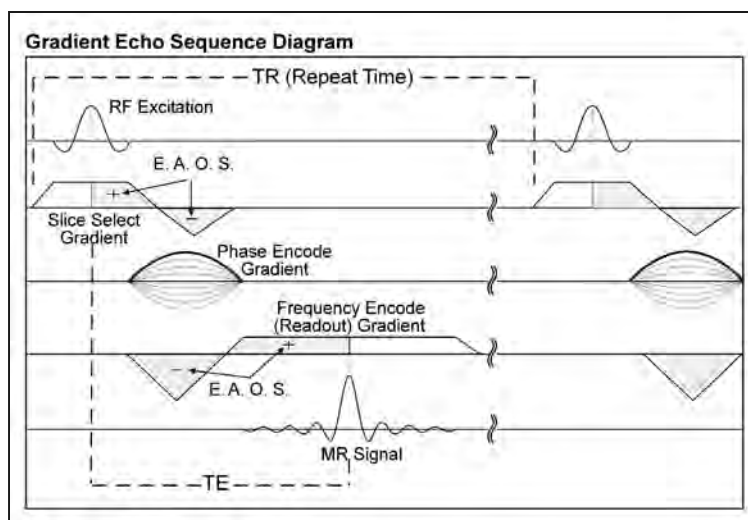


Figure 26. The same diagram as shown in **Figure 25** except for a simple spin echo pulse sequence.

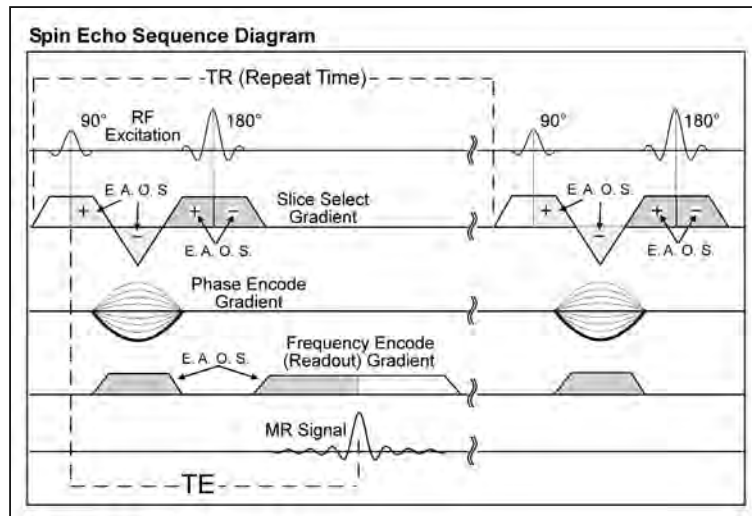
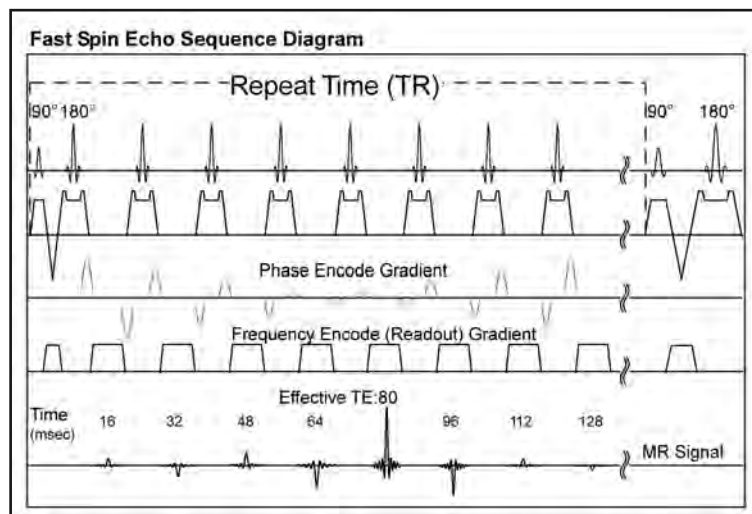


Figure 17 illustrates how it is possible to obtain multiple spin echoes using a train of 180° RF pulses. **Figure 27** shows how a train of eight 180° RF pulses, combined with appropriate slice select, phase encode and frequency encode gradients, comprise what is known as a fast spin echo (FSE) pulse sequence (19) (also known as turbo spin echo, or TSE). This type of sequence can have an echo train length (ETL) as short as two to four for T₁-weighted or proton density-weighting, or moderate echo train lengths of eight to 32 for T₂-weighted imaging, or as long as 128 to 256 for MRI procedures such as single shot myelograms or cholangiograms (20, 21). The advantage of using a FSE pulse sequence is the decreased acquisition time that is due to acquiring multiple echoes or lines of data during one repetition time (TR) interval.

Figure 27. The same diagram as shown in **Figure 26** except for a fast spin echo pulse sequence.

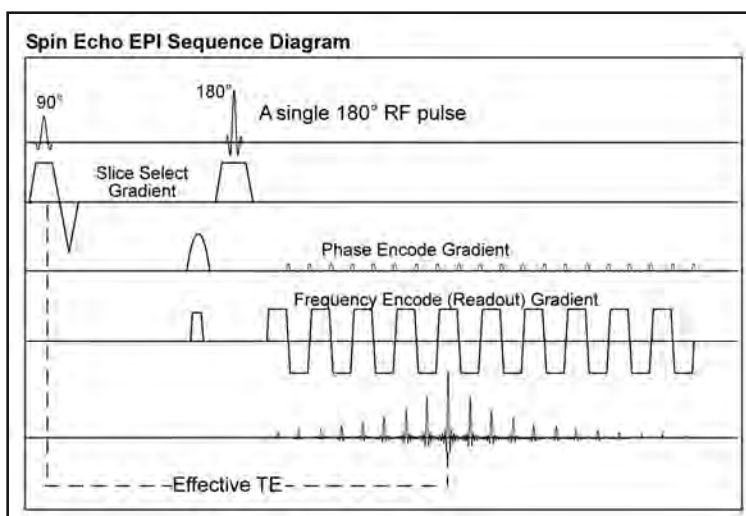


22 Basic MRI Physics: Implications for MRI Safety

With all of the associated gradient activity, a FSE pulse sequence may suffer from the consequences of time-varying gradient magnetic fields discussed earlier. More importantly, particularly at 1.5-T and higher fields, all of the 180° RF pulses significantly increase the specific absorption rate (SAR) level. Accordingly, the MR system reported SAR may exceed the recommended FDA limits for specific absorption rate. When this happens, there are five possible options: (1) Increase the repetition time (TR) so that the average power per unit time goes down. (2) Decrease the total number of slices acquired per TR (3, 17), as half the number of slices means half the RF power. (3) Use the technique known as Half-Fourier imaging (22). This takes advantage of the symmetry in MRI raw data to reduce the number of lines of data required (and the associated acquisition time and RF power) by roughly one half. The disadvantage to this is that it reduces the signal-to-noise ratio (SNR) by the square root of two. (4) Use refocusing RF pulses less than 180°. The amount of RF energy per RF pulse of a given duration is proportional to the square of the flip angle so a 180° RF pulse deposits four times as much as a 90° pulse of the same length. Reduce the flip angle of a large number of RF pulses and the total SAR will be decreased. (5) Use “low SAR” RF pulses. The amount of RF energy per RF pulse of given amplitude is proportional to the duration of the pulse. Instead of doubling the amplitude of the 90° RF pulse to obtain a 180° flip, you can double the duration. This will reduce the specific absorption rate in half but will also result in much longer time between echoes reducing the number of echoes possible per repetition time (TR) thereby increasing the total scan time.

Reducing the flip angle of the refocusing pulse does reduce the SAR, but with all things in MRI, there are tradeoffs. In terms of refocusing spins that are going out of phase due to T_2^* affects (Figure 16), a 180° pulse is optimal. Reducing the refocusing flip angle from 180° to 140° for a single echo will reduce the effectiveness by about 12%. The effect on the signal-to-noise (SNR) when using multiple refocusing pulses becomes very complicated but suffice to say that the SNR is maximum with 180° pulses and goes down from there. While RF power deposition is mainly a problem at higher static magnetic field strengths,

Figure 28. The same as shown in Figure 26 except for a spin echo sequence with an echo planar imaging (EPI) readout.



higher fields have higher SNR starting points so they can better afford some loss in SNR in order to minimize the SAR.

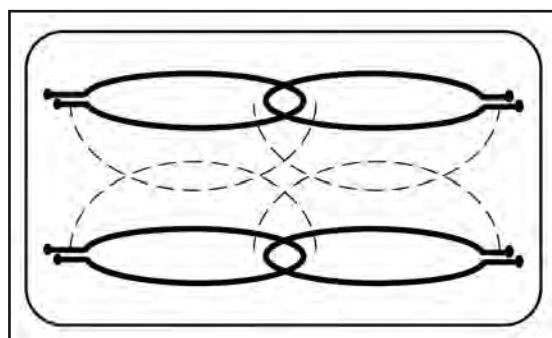
Figure 28 depicts the last imaging sequence to be discussed in this chapter, a spin echo-planar imaging (SE-EPI) pulse sequence (23). This type of sequence is most commonly used for diffusion-weighted imaging (DTI) or functional MRI (fMRI). The RF excitation utilizes a single 90°/180° pair so the SAR levels associated with these pulse sequences are usually not a problem. However, these sequences use the absolute fastest changing gradients so they have the greatest potential for creating the possible problems related to the time-varying gradient magnetic fields discussed above.

Parallel Imaging Reconstruction

The goal of most clinical MRI examinations is to achieve the best quality that is possible in the shortest acquisition time. Over the years, gradient slew rates have increased dramatically, improving the imaging speed of many techniques (such as FSE and EPI discussed above). However, there is still a physical limit as to how fast gradients can be turned on and off as well as the practical limit that exists to prevent problems such as peripheral nerve stimulation. The main purpose of the imaging gradients is to impart spatial information to the MRI signal. One might ask is there any other way of obtaining at least some of the spatial information?

As discussed earlier, with the exception of transmit/received RF coils such as those used for the knee or head, most MRI procedures use the body RF coil for excitation and passive receive-only coils to detect the MRI signal. Modern-day MR systems use multi-channel phased-array (PA) RF coils that are designed for specific, limited anatomical coverage. These PA coils consist of multiple small coils (anywhere from two to 64) where each coil is sensitive to signal from only a portion of the FOV. A very simple four channel configuration typical of early torso phase-array coils is shown in **Figure 29**. In this case, four images are produced, one from the signal obtained from each coil, which are then combined to make a single composite image. Roughly speaking, the SNR of the final image obtained with a PA coil increases by the square root of the number of channels used (24).

Figure 29. A diagram showing a four-channel phased array coil. This is typical configuration for a torso phased-array coil.



Without going into the mathematical details which are beyond the scope of this chapter, specialized techniques such as SENSE, SMASH, GRAPPA (25-27), which are all members

24 Basic MRI Physics: Implications for MRI Safety

of a class of parallel imaging reconstruction methods, utilize the known or measured sensitivity profile of each individual coil to impart some spatial information. This makes it possible to reduce the number of phase encoding (PE) steps that are required for virtually any imaging technique. As the number of PE steps goes down, so does the total SAR. If the acquisition time is reduced by a factor of two, then the SAR is cut in half. If the acquisition time is reduced by a factor of four, then the SAR is cut to one-fourth. Theoretically, while it is possible to “speed up” a scan by a factor equal to the number of different coil elements, in practice the speed up factors are usually less than four. The main reason for this limitation is that while the acquisition time may be faster, the SNR of the final image is proportional to the square root of the number of actual phase encoding views used. If the scan is speeded up by a factor of four, the SNR is cut in half. Therefore, while high field strength MR systems have an initially high SNR, there is a limit as to how much SNR can be “thrown away”.

One final cautionary note about parallel imaging techniques: some MRI centers may decide to use “speed up” factors of two or three but then are unhappy with the SNR of the final images. Therefore, these MRI facilities use two or three signal averages for the pulse sequence. Of course, that just takes the acquisition time back to what it would have been without the use of parallel imaging. In fact, parallel imaging reconstruction can actually add artifacts to the image, particularly if the patient moves. Thus, parallel imaging should only be used with one signal average. If better SNR is desired, it is best to not use parallel imaging.

IS THERE AN OPTIMAL FIELD STRENGTH?

As of 2020 there are at least 16 different companies that manufacture and sell FDA approved MR systems in the United States with static magnetic field strengths ranging from 0.2 T to 7 T (11). An obvious question to ask is, is there an optimal field strength for MRI? The simple answer is, no. A better question is, what are the various tradeoffs at different field strengths? In this final section, many considerations including safety issues when selecting a magnetic field strength for a clinical MR scanner will be presented. A more thorough discussion of the physics of MRI safety is presented in another chapter in this textbook.

Cost

As a general rule of thumb, the cost of an MR scanner is around \$1M per Tesla (28). The cost will also go up with the number of RF coils and the number of channels the system can handle. Furthermore, higher field magnets are usually larger and heavier and have more expensive siting requirements. Choosing an MR system requires a careful examination of the cost-to-benefit ratio.

Signal-To-Noise

As was illustrated in **Figure 2**, the number of excess protons that align with the static magnetic field goes up linearly with field strength. It is these excess protons that are used to produce the MR image. Therefore, the signal strength goes up with the field strength. While there are many other issues that affect SNR, such as the differences of RF penetration and sources of RF noise at different field strengths, as well RF coil design, the number of

channels, differences in relaxation time constants and details of the imaging sequences, in general, the SNR goes up linearly with the field strength (29-31).

This extra SNR can be utilized to obtain higher resolution images in the same scan time or to keep the overall resolution constant but with shorter scans, meaning potentially higher patient throughput. Because the SNR of a scan is proportional to the square root of the scan time, to get the same SNR of a four minute scan at 1.5 T would only require a one minute scan at 3 T. (Of course what usually happens at 3 T is that a higher resolution scan is obtained at some slightly shorter scan time.) At higher static magnetic fields it is also possible to perform techniques that inherently have low SNR such as diffusion tensor imaging (DTI) and functional MRI (fMRI) (32-33). However, for these techniques there are still tradeoffs. For example, scanning at 3 T may be roughly four times faster than at 1.5 T, but problems with image distortion also go up proportional to field strength.

In addition to the inherent higher SNR at higher field strengths, most high and ultra-high field scanners utilize phased array coils with a high number of channels, typically between 8 and 32 channels or even as high as 64. As was stated above, the SNR increases, roughly, with the square root of the number of channels providing more opportunities for faster and/or higher resolution scans. Of course, the greater the number of channels, the higher the monetary cost.

Tissue Heating (SAR)

The International Electrotechnical Commission (IEC) has set guidelines for the specific absorption rate (SAR) during a clinical MRI examination (**Table 4**). It is important to note that these guidelines are independent of the strength of the static magnetic field. Because the RF power deposited in the body increases roughly with the square of the magnetic field (17, 31, 34-36) higher field strength scanners are more likely to bump up against these limits, (1.5 T occasionally, 3 T and up quite frequently).

Table 4. International Electrotechnical Commission (IEC) guidelines on SAR.

Operating Mode	Whole-Body SAR (W/kg)	Head SAR (W/kg)
Normal Operating Mode	2	3.2
First Level Controlled Operating Mode	4	3.2
Second Level Controlled Operating Mode	4	>3.2

There are a number of approaches to reducing SAR and/or its impact on the patient but most of them have noticeable drawbacks. Just a few of the approaches presented by Allison and Yansak are, as follows (36):

26 Basic MRI Physics: Implications for MRI Safety

- Increase the TR, which can lead to longer scan times
- Reduce the flip angles (for fast spin echo sequences use 60 to 130° refocusing pulses rather than 180° pulses), which can alter image contrast-to-noise or signal-to-noise ratios
- Reduce the number of slices per repeat time, which can lead to longer scan times for a fixed number of slices
- Reduce the number of echoes in multi-echo sequences, which can lead to longer scan times
- Take breaks between high SAR acquisitions or interleave high and low SAR acquisitions to allow for patient cooling, which can lead to longer scanning times.

Acoustic Noise

One of the most commonly asked questions about an MR scanner is, why is it so noisy? As was discussed above in the section on time-varying gradient magnetic fields, an MRI system is comparable to a stereo speaker. The force that causes the vibrations is known as the Lorentz force and is described for a single charged particle moving through a magnetic field as (34):

$$\mathbf{F}_L = q(\mathbf{v} \times \mathbf{B}) \quad (5)$$

Where q is the charge of a particle, \mathbf{v} is the velocity of the charge and \mathbf{F}_L is the Lorentz force. If we change q , the charge of a single particle, to Q , the total charge going through a wire, then the product $Q\mathbf{v}$ is effectively the current in the wire which determines the strength of the applied gradient. We see from this that the relevant forces that result in the acoustic noise go up with both the magnetic field and the amplitude of the imaging gradients. Typically, low field magnets have low amplitude gradients with low slew rates and high field magnets have higher amplitudes with higher slew rates.

Price, et al. (34) reported typical acoustic noise levels of approximately 83 dB(A) on a 0.23 T low field open MR system and over 118 dB(A) on a 3 T scanner. These investigators found that pulse sequence parameters (particularly FOV and TR) had a greater effect on the acoustic noise level than did the field strength. However, it should be noted that high field systems typically utilize smaller FOVs and faster scans, inherently resulting in greater acoustic noise.

Flying Objects (Projectiles)

It is well known that ferromagnetic objects are attracted to magnets and, thus, they should not be brought near an MR scanner lest the object become a projectile. Does the danger go up with the field strength? Not necessarily! The translational force exerted on a ferromagnetic object as it is moved near a magnet is not dependent on the strength of the

magnet but, rather, it is dependent on the rate of change or spatial gradient of the magnetic field (35). At the magnet isocenter, where the field is fairly homogenous, there is almost no translational force regardless of the field strength. However, consider the case of two whole body magnets, a 1.5 T and 3 T. Typically, the 5 gauss line is somewhere just past the foot of the patient table or maybe near the scan room door. Between the 5 gauss line and the center of the magnet there is a region where the magnetic field changes fairly rapidly. If the design of the two magnets are similar, then the maximum spatial gradient of the 3 T scanner will be roughly twice that of the 1.5 T scanner. However, you could have one design where most of the change of the 1.5 T field occurs over a shorter distance, say 0.5 meter while a 3 T magnet may be designed to have most of the change occur over a 1.0 meter distance. The spatial gradient magnetic fields would be similar. That being said, the higher the static magnetic field, the greater the likelihood is that it will have a higher spatial gradient and a greater danger of projectile-related incidence objects.

Artifacts

Another consideration for image quality is the presence of imaging artifacts. In general, higher field strengths are more prone to motion artifacts (37). While it is easier to do fat suppression at higher fields, they can also suffer from chemical shift artifacts (38). Susceptibility artifacts also increase with magnetic field strength and may be very problematic in the presence of metallic implants (38, 39). One of the biggest sources of artifacts at high field strengths, and the last topic for this chapter, is the dielectric effect.

RF Penetration and the Dielectric Effect

With all imaging sequences, image contrast depends greatly on the type of RF pulse(s) used. The assumption is that all of the protons in the field of view (FOV) experience roughly the same levels of RF during the imaging sequence. In other words, we assume that the RF field (also known as the B_1 field) is fairly uniform across the FOV. With a well-designed transmit RF coil, at 1.5 T and lower, this is a reasonable assumption. However, at higher field strengths than 1.5 T, dielectric effects can cause substantial variation in the B_1 field across the FOV which, in turn, can cause significant variations in signal amplitude and/or contrast in an image (35, 40-42).

The dielectric constant, ϵ_r , of water (which predominates in the human body) is approximately 80 (in a vacuum it is 1.0). The wavelength of radio waves moving through a medium other than a vacuum is reduced by the square root of ϵ_r , or in this case roughly a factor of 9. At 3 T, with a resonance frequency of 128 MHz, the wavelength in a vacuum is 235 cm but in the human body it is approximately 26 cm. This is on the same order as the dimensions of the human body, particularly of the torso. As a result, “standing waves” can form inside of the body resulting in peaks and troughs of different effective RF strength or flip angles. At 7 T the wavelength drops to around 11 cm and you get substantial dielectric effects in the brain, as well.

When using simple gradient echo (GRE) pulse sequences to image a uniform phantom, the signal amplitude is determined by the amount of spins tipped onto the XY plane and is proportional to the sine of the flip angle (ignoring T1, T2, TR and TE). **Figure 30** depicts a series of images obtained on a Siemens 1.5 T Aera and a Siemens 3 T Skyra using a GRE

28 Basic MRI Physics: Implications for MRI Safety

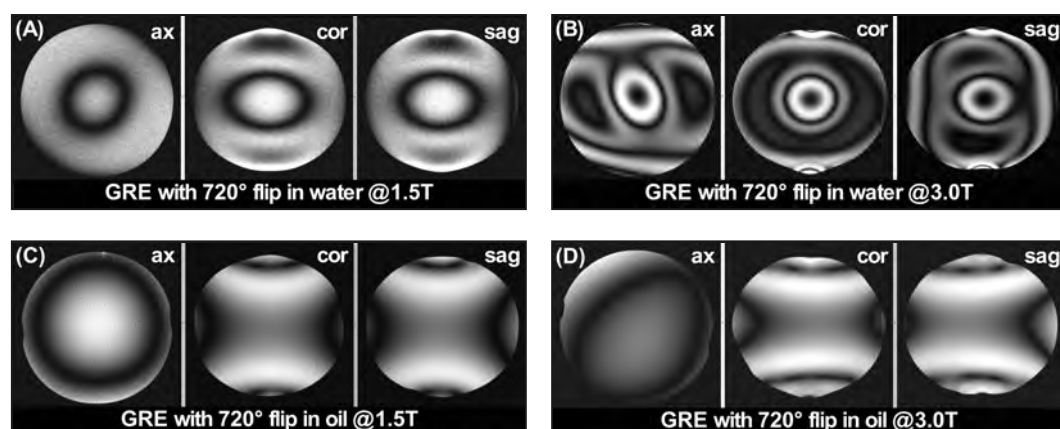
pulse sequence with a flip angle of 720° . Since the sine of $720^\circ = \emptyset$ (as are the sine of 0° , 180° , 360° and 540°) any spins that experience a full 720° flip angle should produce little to no signal.

Figure 30A shows axial, coronal, and sagittal MR images acquired using a water filled phantom on a 1.5 T scanner. The dark ring in each image shows where in the phantom the spins were all tipped the full 720° . The brighter regions show where spins experience either a little more RF or a little less. (Remember, most MR images are magnitude images. If they had been “real” or “complex”, then any spins experiencing more than 720° would have a positive signal and less than 720° would have a negative signal.) Unfortunately, with this single GRE sequence, it is not possible to tell exactly how much more or less than 720° the other spins experienced. The important thing to note about these images is that the signal distribution is rather simple, moderately uniform, and with good circular symmetry.

Figure 30B shows the same water filled phantom imaged on the 3 T MR system. These images are much more complicated, with multiple bands or regions of bright and dark signal. The dark signal occurs everywhere a spin experiences a flip angle that is close to a multiple of 180° , most likely either 540° or 720° . The brightest regions occur where the flip angle is a multiple of $180^\circ \pm 90^\circ$, most likely 630° , with the grey signal somewhere in between. The situation is actually still more complex. Not only does the RF have to penetrate the phantom and excite the spins, the signals from these spins have to make it back out to the RF coil, further complicating the interpretation of these images.

At 3 T and higher, many phantoms used to perform QA testing are filled with some sort of oil (42). General Electric uses poly(dimethylsiloxane) or silicone based oils which have a dielectric constant less than 3. This translates into a wavelength of 136 cm (at 3 T), which is long enough to avoid the same problems that plague water filled phantoms. **Figures 30C**

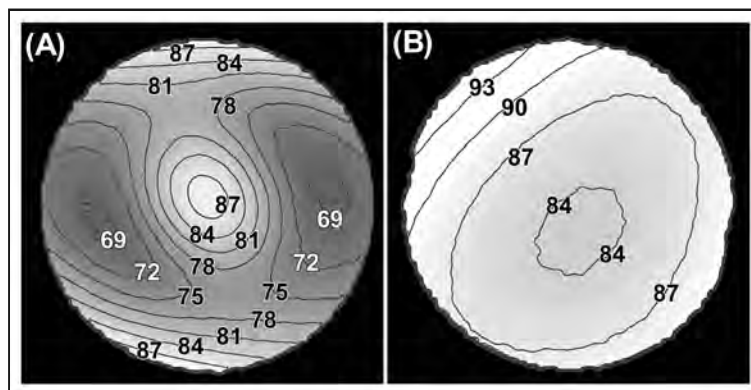
Figure 30. Imaging the RF field in three planes through the magnet isocenter of a Siemens 1.5 T Aera and a Siemens 3 T Skyra MR system using 32 cm spherical phantoms and a GRE pulse sequence with a 720° flip angle. Wherever the actual flip angle is 720° (or 540°) there should be little to no signal. The signal should be brightest where the actual flip angle is 630° . **(A)** Water filled phantom at 1.5 T. **(B)** Water filled phantom at 3 T. Note the very rapid fluctuation of the signal due to dielectric effects. **(C)** Oil filled phantom at 1.5 T. **(D)** Oil filled phantom at 3 T.



and D show the same set of GRE sequences at 1.5 T and 3 T using a silicone oil filled phantom. Note how little difference there is between the 1.5 T and 3 T MR images.

While the images in **Figure 30** help to visualize the problem of the dielectric effect they lack detailed quantitative information. There are many approaches to provide better maps of the B_1 distribution (43-48) the details of which are beyond the scope of this chapter. Siemens provides in their standard service protocol library a sequence, (rf_map), where the amplitude of each pixel in the phase image is directly proportional to the effective flip angle at that pixel assuming that a nominal 90° RF pulse is applied. **Figure 31** shows two 3 T axial B_1 field maps obtained with this sequence. A contour map has been super-imposed on the phase images with the actual flip angles. **Figure 31A** was obtained using the water filled phantom and **Figure 31B** the oil filled phantom. Note that the contours agree with the axial images in **Figures 30B** and **D**. The actual flip angles in the water phantom show extensive spatial fluctuation and range from a low of 69° on the left and right ‘wings’ to a high of 90° at the exact center. The average flip angle is $77.1^\circ \pm 5.3^\circ$. In contrast, the oil filled phantom smoothly changes from about 83° at the center to 93° in the upper left corner with a mean of $87.2^\circ \pm 2.5^\circ$. While not shown, at 1.5 T, both phantoms yielded a mean flip angle of about $87^\circ \pm 2^\circ$. This shows that an oil filled phantom can be used to evaluate the performance of an RF coil without the complication of the dielectric effects.

Figure 31. Quantitative B_1 field maps in the axial plane through the magnet isocenter using the Siemens RF mapping sequence on a 3 T Skyra MR system. (A) Water filled phantom. (B) Oil filled phantom.



The final question is, how does this affect clinical MR images? This is not an easy question to answer because it depends on the type of pulse sequence being used. The greater the number of RF pulses used, the greater the effect. For this discussion, let's only consider a few simple pulse sequences. In each case, we shall call the excitation RF pulse alpha (α) and any refocusing pulse(s), 2α .

Gradient Echo: This is the simplest sequence with only a single α RF pulse. If you have a long TR so that all of the spins have full Mz recovery, then the signal amplitude is proportional to $\sin(\alpha)$. Since $\sin(90^\circ) = 1.0$, the maximum signal is obtained with a 90° flip

30 Basic MRI Physics: Implications for MRI Safety

angle. The average flip angle in the water filled phantom of **Figure 30B** was 77.1° and $\sin(77.1) = 0.975$, so there is less than a 3% decrease in signal. Where the flip angle is 69° (the minimum value shown in **Figure 30B**) there is a 7% loss in signal. However, because the spins are *not* flipped all the way down to the XY plane, they don't take as long to recover back to $M_z = \emptyset$, so T_1 contrast can be reduced.

Spin Echo: This is the next level up in complexity. An ideal spin echo has a 90° excitation pulse and a 180° refocusing pulse. However, any two RF pulses will generate what is known as a Hahn Echo (8) and the signal amplitude is proportional to the product $\sin(\alpha_1) \cdot \sin^2(\alpha_2/2)$, ignoring T_1 recovery. In our case $\alpha_2 = 2\alpha_1$ so the product becomes $\sin(\alpha_1) \cdot \sin^2(\alpha_1) = \sin^3(\alpha)$. If $\alpha = 90^\circ$, then the product equals 1.0. If $\alpha = 77.1$, then the product equals 0.93, a loss of 7%. At $\alpha = 69^\circ$, the product equals 0.81, so a loss of 19%. If the TR is short as for a T_1 -weighted image, then things become complicated. If we assume that the TE is short relative to the T_2 decay rate, then most of the spins effectively experience an $\alpha + 2\alpha = 3\alpha$ flip angle. When $\alpha = 90^\circ$, then that is 270° or completely on the XY plane ($M_z = \emptyset$). However, if $\alpha = 70^\circ$ then this becomes 210° or just 30° past 180° meaning that most of the spins are much closer to the $-M_z$ axis than they are the XY plane and, therefore, will take longer to recover resulting in greater T_1 contrast.

Fast Spin Echo: One would expect that each additional non-optimal refocusing pulse would further reduce the MR signal. However, this is not the case. While the first echo in the echo train is just like the spin echo discussed above and is reduced by $\sin^2(\alpha_2/2)$ (49, 50), the longer echo train drives the magnetization into a pseudo-steady state with a signal that is reduced by only $\sin(\alpha_2/2)$. Again, since $\alpha_2 = 2\alpha_1$ the net signal is proportional to $\sin^2(\alpha)$, (squared instead of cubed). If $\alpha = 90^\circ$, then the product equals 1.0. If $\alpha = 77.1$, then the product equals 0.95, a loss of 5%. At $\alpha = 69^\circ$, the product equals 0.87, so a loss of 13%.

The analysis of other types of imaging pulse sequences is beyond the scope of this text. Suffice to say that the non-uniformities in the B_1 field at higher static magnetic field strengths caused by dielectric effects seriously complicate image contrast. However, there has been much work done to reduce these effects such as the use of dielectric pads (51-54) or multi-channel, transmit RF coils (51-58).

CONCLUSIONS

This chapter presented information on the basic MRI physics that are involved in creating exquisite images of human anatomy. The same physics helps us to understand the potential risks and problems associated with MRI technology and guides us in how to deal with those issues. There is no one optimal static magnetic field strength to use, instead there are a long list of tradeoffs which must be carefully considered. MRI is a safe and effective imaging modality as long as careful attention is given to established safety policies and procedures (59). The other chapters in this textbook provide comprehensive details related to the bioeffects, safety, and patient management aspects of MRI.

REFERENCES

- Block F, Hanson WW, Packard ME. Nuclear induction. Phys Rev 1946;69:127-138.

MRI Bioeffects, Safety, and Patient Management **31**

2. Purcell EM, Torrey HC, Round RV. Resonance absorption by nuclear magnetic moments in solid. *Phys Rev* 1946;69:37.
3. NessAiver MS. All You Really Need to Know About MRI Physics. Chapters 2 and 3. Baltimore: Simply Physics; 1997.
4. Abragam A. The Principles of Nuclear Magnetism. Oxford: Oxford University Press, 1978.
5. Mansfield P, Morris PG. NMR Imaging in Biomedicine. New York: Academic Press; 1982.
6. Stark D, Bradley WG. Magnetic Resonance Imaging. St. Louis: Mosby Year Book; 1992.
7. McRobbie DW, Moore EA, Graves MJ, Prince MR. MRI From Picture to Proton. Second Edition, Cambridge: Cambridge University Press; 2007.
8. Hahn EL. Spin echoes. *Phys Rev* 1950;20:580.
9. NessAiver MS. "Flying Objects" slide show. Available at: http://www.simplyphysics.com/flying_objects.html Accessed 2021.
10. Cosmus TC, Pairzh M. Advances in whole-body MRI magnets. *IEEE Trans Applied Superconductivity* 2011;21:2014-2019.
11. Brands of Scanners. In: Questions and Answers in MRI. Available at <http://mr/questions.com/brands-of-scanners.html>. Accessed 2021.
12. Turner R. Gradient coil design, a review of methods. *Magn Reson Imaging* 1993;11:903-920.
13. Cho ZH, Park SH, Kim JH, et al. Analysis of acoustic noise in MRI. *Magn Reson Imaging* 1997;15:815-22.
14. Price DL, De Wilde JP, Papadaki AM, Curren JS, Kitney RI. Investigation of acoustic noise on 15 MRI scanners from 0.2T to 3 T. *J Magn Reson Imaging* 2001;13:288-93.
15. Cho ZH, Chung SC, Lim DW, Wong IK. Effects of the acoustic noise of the gradient systems on fMRI: A study on auditory, motor, and visual cortices. *Magn Reson Med* 1998;39:331-5.
16. Ham CL, Engels JM, van de Wiel GT, Machielsen A. Peripheral nerve stimulation during MRI: Effects of high gradient amplitudes and switching rates. *J Magn Reson Imaging* 1997;7:933-7.
17. Bottomley PA. Turning up the heat on MRI. *J Am Coll Radiol* 2008;5:853-855.
18. Meulen PD, Groen JP, Cuppen JM. Very fast MR imaging by field echoes and small angle excitation. *Magn Reson Imaging* 1985;3:297-299.
19. Hennig J, Nanert A, Friedburg H. RARE imaging, a fast imaging method for clinical MR. *Magn Reson in Med* 1986;3:823-833.
20. Aggarwal A, Azad R, Ahmad A, Arora P, Gupta P. Additional merits of two-dimensional single thick-slice magnetic resonance myelography in spinal imaging. *J Clin Imaging Sci* 2012;2:84.
21. Van Epps K, Regan F. MR cholangiopancreatography using HASTE sequences. *Clin Radiol* 1999;54:588-94.
22. Runge VM, Wood ML. Half-Fourier MR imaging of CNS disease. *Am J Neuroradiol* 1990;175:77-82.
23. Mansfield P. Real time echo planar imaging by NMR. *Br Med Bull* 1984;40:187-90.
24. Constantinides CD, Atalar E, McVeigh E. Signal-to-noise measurements in magnitude images from NMR phased arrays. *Magn Reson Med* 1997;38: 852-857.
25. Pruessmann KP, Weiger M, Scheidegger MB, Boesiger P. SENSE: Sensitivity encoding for fast MRI. *Magn Reson Med* 1999;42:952-962.
26. Sodickson DK, Manning WJ. Simultaneous acquisition of spatial harmonics (SMASH): Fast imaging with radiofrequency coil arrays. *Mag Reson Med* 1997;38:591-603.
27. Griswold MA, Jakob PM, Heidemann RM, et al. Generalized autocalibrating partially parallel acquisitions (GRAPPA). *Magn Reson Med* 2002;47:1202-1210.
28. Sarracaine M, LaPierre CD, Salameh N, et al. Low-cost high performance MRI. *Sci Rep* 2015;5:15177.

32 Basic MRI Physics: Implications for MRI Safety

29. Edelstein WA, Glover GH, Hardy CJ, Redington RW. The intrinsic signal-to-noise ratio in NMR imaging. *Magn Reson Med* 1986;604-618.
30. Maubon AJ, Ferru JM, Berger V, et al. Effect of field strength on MR images: Comparison of the same subject at 0.5, 1.0 and 1.5 T. *RadioGraphics* 1999;19:1057-1067.
31. Collins CM, Smith MB. Signal-to-noise ratio and absorbed power as functions of main magnetic field strength, and definition of “90°” RF pulse for the head in the birdcage coil. *Magn Reson Med* 2001;45:684-691.
32. Alexander AL, Lee JE, Lazar JE, Field AS. Diffusion tensor imaging of the brain. *Neurotherapeutics* 2007;4:316-329.
33. Glover GH. Overview of functional magnetic resonance imaging. *Neurosurg Clin N Am.* 2011;22:133-vii.
34. Price DL, De Wilde JP, Papadaki AM, Curran JS, Kitney RI. Investigation of acoustic noise on 15 MRI scanners from 0.2T to 3 T. *J Magn Reson* 2001;13:288-293.
35. Panych LP, Bruno M. The physics of MRI safety. *J Magn Reson Imaging* 2018 ;47:28-43.
36. Allison J, Yanasak N. What MRI sequences produce the highest specific absorption rate (SAR), and is there something we should be doing to reduce the SAR during standard examinations? *Amer J Roentgenol* 2015;205:W140.
37. Havsteen I, Ohlhues A, Madsen KH, et al. Are movement artifacts in magnetic resonance imaging a real problem – A narrative review. *Front Neurol* 2017;8:232.
38. Graves MJ, Mitchell DG. Body MRI artifacts in clinical practice: A physicist’s and radiologist’s perspective. *J Magn Reson Imaging* 2013;38:269-287.
39. Budrys TB, Veikutis V, Lukosevicius S, et al. Artifacts in magnetic resonance imaging: How it can really affect diagnostic image quality and confuse clinical diagnosis? *J Vibroengineering* 2018; 20:1202-1213.
40. Norris DG. High field human imaging. *J Magn Reson Imaging* 2003;18:519-529.
41. Bradley WG. Pros and cons of 3 Tesla MRI. *J Am Coll Radiol* 2008;5:871-878.
42. Skloss T. Phantom fluids for high field MR imaging. *Proc Intl Soc Magn Reson Med* 2004;11:1635.
43. Murphy-Boesch J, So GJ, James TL. Precision mapping of the B_1 field using the rotating-frame experiment. *J Magn Reson* 1987;73:293-303.
44. Oh C, Hilal S, Cho Z, Mun I. Radio frequency field intensity mapping using a composite spin-echo sequence. *Magn Reson Imaging* 1990;8:21-25.
45. Insko EK, Bolinger L. Mapping of the radiofrequency field. *J Magn Reson* 1993;103:82-85.
46. Yarnykh VL. Actual flip-angle imaging in the pulsed steady state: A method for rapid three-dimensional mapping of the transmitted radiofrequency field. *Magn Reson Med* 2007;57:192-200.
47. Morrell GR. A phase-sensitive method of flip angle mapping. *Magn Reson Med* 2008; 60:889-894.
48. Sacolick LI, Wiesinger F, Hancu I, Vogel MW. B_1 mapping by Bloch-Siegert shift. *Magn Reson Med* 2010;63:1315-1322.
49. Hennig J. Multiecho imaging sequences with low refocusing flip angles. *J Magn Reson* 1988;78:397-407.
50. Alsop DC. The sensitivity of low flip angle RARE imaging. *Magn Reson Med* 1997;37:176–184.
51. Sled JG, Pike GB. Standing-wave and RF penetration artifacts caused by elliptic geometry: An electrodynamic analysis of MRI. *IEEE Trans Med Imag* 1998;17:653-662.
52. Webb AG. Dielectric materials in magnetic resonance. *Concepts Magn Reson* 2011;38A:148-184.
53. Yang QX, Mao W, Wang J, et al. Manipulation of image intensity distribution at 7.0 T: Passive RF shimming and focusing with dielectric materials. *J Magn Reson Imaging* 2006;24:197-202.
54. Yang QX, Wang J, Wang J, et al. Reducing SAR and enhancing cerebral signal-to-noise ratio with high permittivity padding at 3 T. *Magn Reson Med* 2011;65:358-362.
55. Brink WM, Gulani V, Webb AG. Clinical applications of dual-channel transmit MRI: A review. *J Magn Reson Imaging* 2015;42:855-869.

MRI Bioeffects, Safety, and Patient Management 33

56. Grissom WA, Sacolick L, Vogel MW. Improving high-field MRI using parallel excitation. *Imaging Med* 2010;2:675-693.
57. Katscher U. Basic and tailored RF shimming in a multi-transmit whole body MR system. *PIERS online* 2008;4:781-784.
58. Webb AG, Collins CM. Parallel transmit and receive technology in high-field magnetic resonance neuroimaging. *Int J Imaging Syst Technol* 2010;20:2-13.
59. Shellock, FG. Reference Manual for Magnetic Resonance Safety, Implants and Devices, 2020 Edition. Los Angeles: Biomedical Research Publishing Group; 2020.

Chapter 2 Principles of MRI Safety Physics

LAWRENCE P. PANYCH, PH.D.

Schulich School of Medicine and Dentistry
Department of Medical Imaging
University of Western Ontario
Ontario, Canada

BRUNO MADORE, PH.D.

Department of Radiology
Brigham and Women's Hospital
Harvard Medical School
Boston, MA

INTRODUCTION: MAIN SOURCES OF RISK IN MRI

The Standard Model of physics requires 61 fundamental particles to describe the world we live in: 24 for matter and for antimatter, and 13 for interactions between them. Thankfully this chapter is mostly about just one, the electron. Some of the fundamental particles truly have superhero powers: Neutrinos can fly through the Earth as if it were not even there; about 65 billion solar neutrinos do so every second for every square centimeter of Earth's surface facing the Sun. The Higgs boson can give mass and inertia to objects. Quarks and anti-quarks can mix and match into hundreds of wildly different composite particles, some as mundane as neutrons and protons and others as exotic as pentaquarks or Upsilon mesons. Fortunately, this chapter is only about electrons.

A magnetic resonance MR system or scanner in operation can be thought of as a dance of electrons. A torrent of them goes around and around in the coils of the main magnet, while jets of them streak back and forth in the wires that form the gradient and radiofrequency (RF) coils. Each electron generates a field around itself, to inform the Universe about how everything with electrical charge should get attracted or repelled by it. When an electron moves, it sends a new field, an updated version of the old one. These updates travel outward at the speed of light, broadcasting an electromagnetic wave. As electrons dance, they coax nuclear spins into a dance of their own and the MRI signal is created. This chapter is about this dance of electrons and how individuals may be injured when it goes wrong.

As the term “magnetic” in the name announces, an MR system is very much about magnetism, and fields generated by electrons flowing in three main types of coils are involved in creating images. First there is the so-called ‘main magnet’, which produces the large static magnetic field. This is most often a superconducting electromagnet but it could also be a permanent magnet. Added to this are coils to generate the radiofrequency electromagnetic field, referred to as “RF coils”. Lastly, the “gradient coils” are responsible for creating linearly-varying magnetic fields, for spatial encoding purposes. While these coils and the manner in which the fields they generate interact with matter can lead to useful images, they can also cause serious threats to human subjects (1-11).

The main risks associated with MRI have been extensively reported and studied. For example, everyday objects may turn into projectiles, RF energy deposition can cause burns, time-varying gradient magnetic fields can induce nerve stimulation and loud noises can lead to auditory loss. These various risks are associated with the three types of coils discussed above: main magnet, RF coils, and gradient coils, and will be discussed in turn, below. A number of reviews and exposés on related topics can be recommended as supplemental reading (12-23). For those who wish to go even deeper into the physics, excellent basic textbooks exist on electromagnetism (24, 25) and the magnetic properties of materials (26). Good intuition on the interactions between electromagnetic fields and materials can be obtained through numerical simulation of Maxwell’s equations (27), the fundamental equations that govern these interactions. For this we recommend an excellent textbook by Elsherbeni and Demir (28) that comes complete with well-documented Matlab code.

The present chapter is focused toward providing intuition about the physical mechanisms that give rise to MRI-related risks. In the process, several equations will be presented, including the Lorentz force equation and two of Maxwell’s equations that provide the mathematical basis for the physical interactions considered. All others, along with their application in several detailed sample calculations, are meant to assist the reader gain intuition about these interactions, in particular, with respect to size and degree. How strong is the magnetic force? How much will the RF field heat the tissues? How much current will be induced in a conductor? In this chapter, we intend to provide an understanding of the degree to which a particular interaction might represent a hazard, and in this sense, we hope that this information will be useful to the reader.

RISKS ASSOCIATED WITH THE MAIN MAGNET

The main magnet of a commercial MRI system is the most distinguishing feature of the device, and also the greatest source of risk. The field it generates, approximately 1.5 to 3.0 Tesla (T) for the most widely used high field strength scanners, is much stronger than magnetic fields casually encountered in everyday life. For example, it is roughly 30,000 to 60,000 times stronger than the earth’s magnetic field at the surface and is roughly 300 to 600 times greater than the field of a common refrigerator magnet. While the universe can certainly create much stronger magnets (e.g., the field generated by some neutron stars may reach 100 billion Tesla), magnets used for MRI are among the strongest that exist on Earth. Because MRI involves field strengths much higher than the typical everyday experience, regular objects may behave in a non-intuitive manner near scanners. How objects behave in such conditions greatly depends on what they are made of, and for this reason we will

36 Principles of MRI Safety Physics

begin by looking at the magnetic properties of materials. For objects most affected by magnetic fields, we will consider the translational and rotational forces acting on them. We will also look at the effect of the scanner's static magnetic field on biological processes and the effects of motion in such an environment.

Susceptibility and the Magnetic Properties of Materials

When a given material is placed in an external magnetic field, it becomes magnetized. Permanent magnets are always magnetized regardless of whether an external field is present or not, but permanent magnets are rare in nature and more mundane everyday objects require the coaxing of an external field to become so. The 'volume magnetic susceptibility', commonly represented by the symbol X_v , or more simply X , expresses how easily a given material becomes magnetized. While some material such as crystals may require X to take the form of a tensor, more typically X is just a number and it relates the degree of the induced magnetism to the strength of an externally applied field. **Table 1** below gives the susceptibility of some common materials. More generally, values of X for elements of the periodic table have been tabulated and are readily available from online sources such as www.periodictable.com.

Table 1. Magnetic susceptibility and density of common materials.

Material	Volume Susceptibility	Density (kg/m ³)
Water	-9.0 x 10 ⁻⁶	1000
PVC	-1.1 x 10 ⁻⁵	1400
Copper	-9.6 x 10 ⁻⁶	9000
Titanium	1.8 x 10 ⁻⁴	4500
Nickel	600	8900
Iron	200,000	7900

In terms of magnetic properties there are three main types of materials: those with a value for X that is large and positive, or small and positive, or small and negative. The first category, large and positive, represents ferromagnetic materials and is the only category causing safety concerns in the presence of B_o , the MR system's large static magnetic field. At room temperature only a few elements such as iron, nickel and cobalt exhibit ferromagnetic properties. Of these, iron is most widespread, and for this reason iron-containing objects are typically the culprits for projectile incidents at MRI sites. While all materials are to some extent magnetized when subjected to a large magnetic field, ferromagnetic materials are distinguished in that the magnetic dipoles of every molecule in the material can possibly come into alignment, resulting in a very large magnetization. In such case the object is said to be 'saturated' as further increasing the external field could no longer increase the object's magnetization.

Most everyday objects that do not contain iron would fit in the latter category, having small and negative magnetic susceptibility. Such materials are called diamagnetic and include common materials such as water, wood, many types of plastics, and essentially all biological tissues. The negative sign associated with their magnetic susceptibility means

that such materials are (ever so slightly) repelled by a magnet. A slightly-frivolous yet most dramatic demonstration of this fact was achieved by levitating frogs (29). (Example I presents a calculation for the conditions to levitate a frog along with a rough estimate for what it would take to get a human subject off the ground!)

The third type of material, with small and positive magnetic susceptibility, is referred to as paramagnetic. Although not particularly common in everyday life, paramagnetic materials such as gadolinium and manganese play an important role in the design of chemical contrast agents in MRI. Furthermore, the paramagnetism of deoxyhemoglobin is central to the endogenous blood oxygenation level dependent (BOLD) contrast exploited in functional MRI. Chemical contrast agents and their safety is a topic deserving of consideration on its own, beyond the scope of the present chapter.

In the following subsections, we will look at the translational and torsional forces exerted on ferromagnetic objects due to an external magnetic field. Paramagnetic and diamagnetic materials will not be considered any further, as forces in these materials are generally too small to be of any practical relevance to safety. Because iron is such a prevalent metal, it might be easy at times to develop the impression that all metallic objects must be ferromagnetic. However, in reality, metals such as copper and many types of stainless steel are essentially non-magnetic. Assuming they are pure enough, objects made of these non-magnetic metals do not cause any projectile risk in an MRI environment. That said, and given the prevalence of iron in everyday objects, suspicion toward all metals and testing with a hand-held magnet remains a healthy reflex.

The computation of forces and torques can be very complicated because they depend on the strength of the magnetic field and of its spatial gradient, as well as the exact composition and geometry of the object submitted to it. While a more thorough discussion of this topic can be found elsewhere (18), the text below aims at providing intuition about the forces at play.

Translational Forces Due to Interaction with a Static Magnetic Field

Ferromagnetic objects are attracted to magnets, so logically, the closer one such object gets to an MR scanner the stronger the attraction should grow, should it not? Actually, no, in fact a ferromagnetic object at the center of the bore would feel no attraction at all, and maximum force would instead be felt somewhere outside the scanner. This is one example of non-intuitive behavior, further explained below.

The magnetic field generated by the main magnet is referred to as B_o . It is a vector field meaning that B_o has a magnitude and an orientation at every point in space. The spatial gradient of the main field is simply the change in the field's magnitude, B_o , with respect to position or distance. In general, the spatial gradients of a given quantity are obtained by applying the ‘grad’ operator, denoted as ‘ ∇ ’. Accordingly, ∇B_o represents the spatial gradient of the main field of the MRI; at every point in space the magnitude of ∇B_o represents how steeply B_o is changing around this point, and the orientation of ∇B_o points in the direction of steepest change. The units for ∇B_o are Tesla per meter (T/m), or alternately, Gauss per centimeter (G/cm). While the Tesla is the official unit for magnetic fields according to the International System of Units (SI) the Gauss still remains frequently used. One Tesla is

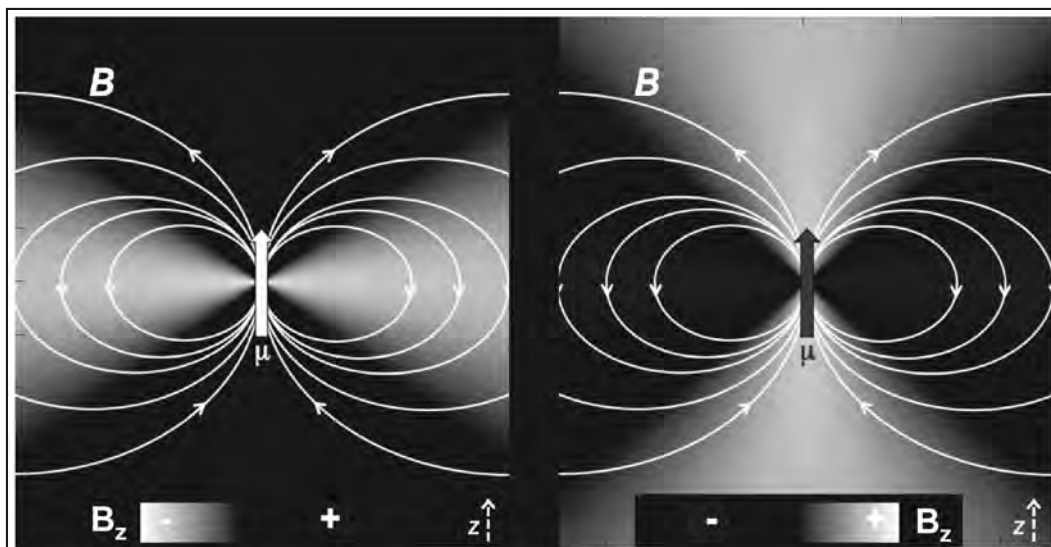
38 Principles of MRI Safety Physics

equal to 10,000 G, one meter is of course equal to 100 cm, and as such 1 T/m is equal to 100 G/cm.

In addition to the spatial gradient of the main field (above), another key quantity in determining the force exerted on an object is the magnetization of this object: a strongly magnetized object will interact strongly with \mathbf{B}_o while a non-magnetized object will not. The magnetization of an object, \mathbf{M} , its magnetic dipole, μ_m , and its internal flux density, \mathbf{B}_m , are closely-related concepts. The internal flux density may be simply equal to $X\mathbf{B}_o$, although complicating factors such as saturation and object shape will be considered below. The magnetization differs from \mathbf{B}_m through a constant of nature, the permeability of free space, so that $\mathbf{B}_m = \mu_0 \mathbf{M}$. The magnetic dipole, μ_m , represents the whole object while \mathbf{M} is expressed per unit of volume, so that $\mu_m = VM$ where V is the volume of the object. **Figure 1** shows a schematic representation of an idealized magnetic dipole and its associated magnetic field lines; the magnetic dipole can be thought of as a current loop enclosing some small region, thus explaining its units of measure, amperes times meters-squared (Am^2). While the dipole itself has no actual spatial extent, it does create a magnetic field in the space around it equivalent to that generated by such a current loop.

An expression for the translational magnetic force, \mathbf{F}_{trans} , which can transform everyday objects into projectiles, can be obtained by calculating the Lorentz force due to \mathbf{B}_o acting on the current loop that is assumed to generate the magnetic dipole (30). More specifically, \mathbf{F}_{trans} depends on the magnetic dipole and spatial variations in the field (26, 30, 31):

Figure 1. This figure shows schematic representations of the \mathbf{B} field lines for a single magnetic dipole, μ_m . (Right) In the bright shaded region, the B_z component of the dipole field is in the positive z -direction. (Left) In the bright shaded region, the B_z component of the dipole field is in the negative z -direction (opposite the dipole orientation).



$$\mathbf{F}_{trans} = \nabla(\mu_m \cdot \mathbf{B}_o) = \mu_m \nabla B_o \quad (1)$$

The dot product of two vectors as used in Equation (1) is a scalar with a magnitude equal to the product of the lengths (magnitudes) of the two vectors times the cosine of the angle between them. If we assume that μ_m and \mathbf{B}_o point in the same direction, then the angle between them is zero, the cosine of that angle is 1, and the middle term in Equation (1) becomes the simpler term on the right, $\mu_m \nabla B_o$, where μ_m represents the magnitude of μ_m . Note that \mathbf{F}_{trans} is also a vector that points in the same direction as ∇B_o . For the remainder of this chapter, however, we will be dealing only with the magnitude of the force, $F_{trans} = \mu_m |\nabla B_o|$.

In terms of MRI safety, values for F_{trans} are not necessarily very telling by themselves. For example, while the strength of one person's arm might be more than enough to throw a hammer in dangerous fashion, the same arm is unlikely to get a large file cabinet to budge in any real way. As a rule of thumb, whenever magnetic forces are significantly less than the gravitational pull on the object then the magnetic forces should pose no major safety concern (32, 33), as weight and friction should prevent the object from turning into a projectile. Therefore, in Equation (2) below, the magnitude of F_{trans} from Equation (1) is placed in relation to the gravitational force, F_g , on the same object:

$$\frac{F_{trans}}{F_g} = CX B_o |\nabla B_o|, \quad C = \frac{1}{(\mu_0 g) \rho} \quad (2)$$

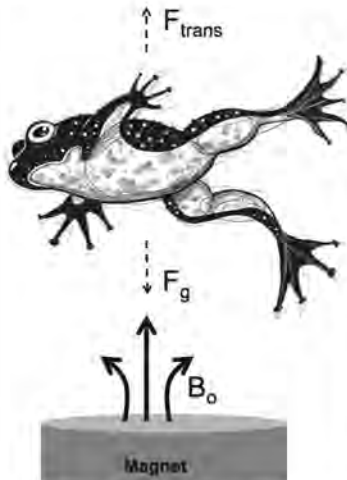
In Equation (2), the relationships $\mu_m = VB_m/\mu_0$, $B_m = X B_o$, $F_g = mg$ and $\rho = m/V$ were also employed, where g is the gravitational acceleration constant, ρ is the material density and $|\nabla B_o|$ at any given point is the length of the vector ∇B_o at that point. The numerical value of the constant C , in ferromagnetic metals, is about 10 m/T^2 , a number that will be used in examples later in the text. Note that F_{trans}/F_g depends on $B_o |\nabla B_o|$, often referred to as the spatial gradient product (SGP). Equation (2) is independent of how much material there is; while a larger object would lead to a stronger magnetic force it would also be heavier, leaving F_{trans}/F_g unchanged. This "relative magnetic force", F_{trans}/F_g , will prove useful in estimating the degree to which a magnetic field can pull on or attract objects.

Relative Magnetic Force Acting on Ferromagnetic Objects

Equation (2) is not always applicable, as saturation and the shape of the object also play a role, as further detailed below. While the term $X B_o$ in Equation (2) represents the strength of the magnetic flux as created within the object, such flux could not grow to arbitrarily large levels even if the magnitude of the applied field, B_o were to grow arbitrarily large. Instead, it would plateau once a maximum value is reached. This maximum is the saturation flux density, B_s . For a given ferromagnetic material, the internal magnetic flux cannot grow beyond B_s regardless of how large B_o might become. For this reason, Equation (2) is only

40 Principles of MRI Safety Physics

Example I(a): Magnetic levitation



Consider the conditions, specifically the spatial gradient product (SGP), required to levitate a small animal such as a frog. Biological tissues have a negative susceptibility ($X < 0$), therefore the magnetic force on the frog will push the frog opposite to the direction of the spatial gradient and away from the magnet (upwards in the figure).

We require from Eq. 2 that:

$$\frac{F_{\text{trans}}}{F_g} = 1 = \frac{1}{(\mu_0 g) \rho} X B_0 |\nabla B_0| ; \quad B_0 |\nabla B_0| = (\mu_0 g) \rho / X$$

The magnetic susceptibility and density values for tissues are similar to those of water: $X = -8.8 \times 10^{-6}$, $\rho = 10^3 \text{ kg/m}^3$

Furthermore, $g = 9.8 \text{ m/s}^2$ and $\mu_0 = 4\pi \times 10^{-7}$. Then:

$$SGP = B_0 |\nabla B_0| = \frac{(4\pi \times 10^{-7}) 9.8 (10^3)}{-8.8 \times 10^{-6}} = -1400 \text{ T}^2/\text{m}$$

The condition for levitating the frog, regardless of its weight, is that it be placed in a magnetic field where the spatial gradient product, SGP , is 1400 T^2/m .

Example I(b): A magnet suitable for levitation

Consider the magnetic field from the simple single coil loop shown in the figure below. Relations are given for B_0 and $B(z)$, the field at the center of the coil and at other locations along the vertical z-axis, respectively. The plots below are of $B(z)$, the spatial gradient, and the SGP , all normalized to B_0 . The z-axis locations are in relation to the loop radius, R . Since the SGP is the relevant variable governing the force delivered by the magnet, we want to place the frog at the relative location of the highest SGP , which in the plot is at $z/R = 0.37$. Reading from the plots, we have:

$$\frac{B(z)}{B_0} = 0.825; \frac{dB_r(z)}{dz_r} = \frac{d(B(z)/B_0)}{d(z/R)} = -0.81; \frac{B(z)}{B_0} \frac{d(B(z)/B_0)}{d(z/R)} = \frac{R}{B_0^2} B(z) \frac{dB(z)}{dz} = \frac{R}{B_0^2} SGP = -0.825 \times 0.81$$

$$SGP = -0.825 \times 0.81 \times \frac{B_0^2}{R}, \quad B_0 = \sqrt{\frac{R \times (-1400)}{-0.825 \times 0.81}} = \sqrt{2095 R}$$

For something the size of a frog, we want the SGP at z around 5 cm. Since the relative location of the greatest SGP for the coils is 0.37, thus,

$$R = 5/0.37 = 13.5 \text{ cm}, \quad B_0 = \sqrt{2095 \times 0.135} = 16.8 \text{ T}$$

****Note that this is very close to the field strength of 16.5 T used in actual frog levitation experiments [29].**

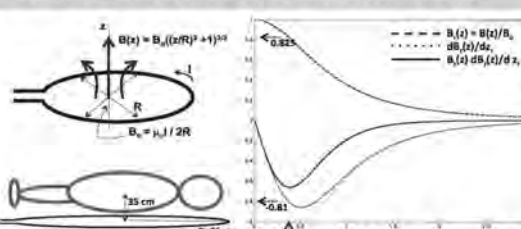
Human body levitation

The parameters for human tissue are effectively the same as for the frog, thus, the same requirement of $SGP = 1400 \text{ T/m}^2$ applies for levitating a human being. However, it is much more difficult to produce this SGP in a magnet big enough to support a human being. To levitate

something the size of a human body, we would want the z distance to be at least 35 cm (with body lying on above the coil as shown). Thus: $R = 35/0.37 = 94.5 \text{ cm}$, $B_0 = \sqrt{2095 \times 0.945} = 44.5 \text{ T}$

As a single loop, it would require a current of almost 67 million amps to produce a B_0 of 44.5 T. Even a coil of 10,000 turns requires thousands of amps to produce a field of this strength.

Conclusion: Human magnetic levitation is not likely to happen any time soon!



valid wherever $X B_o$ is less than B_s , which tends to be true for all realistic values of B_o as far as diamagnetic and paramagnetic materials are concerned, but not so for ferromagnetic materials. For example, in nickel, X is around 600 and B_s is 0.64 T, thus, Equation (2) is only appropriate wherever B_o remains below 1.1 mT. Wherever the material is saturated, Equation (2) should therefore be modified as follows:

$$\frac{F_m}{F_g} = C B_s |\nabla B_o|, \text{ (saturated ferromagnetic objects)} \quad (3)$$

B_s in ferromagnetic objects may range from about 0.25 to 2.5 T, with nickel at about 0.64 T and iron at up to around 2.5 T.

Based on Equation (3), one can estimate how strongly a scanner may attract ferromagnetic objects in its vicinity. The maximum spatial gradient (MSG) on some modern MR systems can exceed 10 T/m and accordingly, from Equation (3), with $C \approx 10 \text{ m/T}^2$, magnetic forces on objects made of nickel or iron can readily reach 60 or 250 times their weight, respectively. Even for a modest one-pound iron object, one can appreciate how magnetic forces can readily become superhuman in nature, and that no amount of ‘holding on tight’ to an object might come close to matching them. Such a force is enough, for example, to accelerate an iron object to a speed of 200 km/hr in less than 25 milliseconds.

Demagnetization Factors

Magnetization in ferromagnetic objects very much depends on their shape, a fact that Equation (2) does not take into account. As the microscopic domains of ferromagnetic materials become aligned with the applied field, their strong magnetic dipole fields overlap so as to partly cancel each other, effectively reducing the magnitude of X . Alternatively, one may think of the induced magnetic field of the material as having a component that opposes the applied field, referred to as the demagnetizing field (26). The demagnetizing field undermines the work of the externally applied field as it tries to magnetize the material, effectively reducing the susceptibility.

Figure 1 may help to visualize the idea of the demagnetizing field. The field lines of a single dipole oriented in the z -direction are shown schematically in the figure (see white lines with arrows). Locations where the z -component of the dipole field is positive are highlighted in the drawing on the right. Magnetic material in the highlighted region will be encouraged to align in the same direction as the dipole, i.e., to become magnetized. In contrast, wherever the z -component of the dipole field is negative, as highlighted in the drawing on the left, magnetic materials tend to align opposite the dipole, i.e., to become de-magnetized. A flat object with almost no extent in the z -direction would have a large demagnetizing field, while a slender object aligned along z might be associated with a negligible demagnetizing field. In general, for arbitrarily-shaped ferromagnetic objects, determining the details of this demagnetizing field can be very complex and requires the use of numerical methods.

42 Principles of MRI Safety Physics

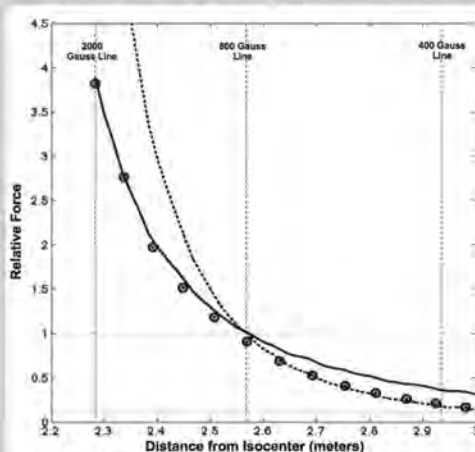
For some simple object geometries, a shape-dependent factor, D , can be introduced to account for the effects of the demagnetizing field. In this case, Equation (2) is modified by replacing X with $X / (1+DX)$:

$$\frac{F_{trans}}{F_g} = C \frac{X}{(1+DX)} B_o |\nabla B_o|, \text{(non saturated ferromagnetic objects)} \quad (4)$$

where the demagnetization factor, D , takes on values between 0 and 1. Strictly speaking, Equation (4) assumes the object to be an ellipsoid of revolution (i.e., created by rotating an ellipse about one of its two axes), with the axis of revolution aligned along B_o (see expression for F_z in (18) with $\theta=0$). For very long and slender needle-like objects, D approaches 0 and $X / (1+DX) \approx X$, meaning that Equation (4) becomes equivalent to Equation (2). However, for strongly magnetic materials where $X \gg 1$, $X / (1+DX) \approx 1/D$, a number much smaller than X . Let's go through a few more examples involving simply-shaped, strongly-magnetic objects oriented in particular ways with respect to the direction of B_o : For a sphere, D equals $1/3$ and therefore the effective susceptibility is just 3, irrespective of the magnitude of X . With a long needle-like object oriented perpendicular to B_o , then D equals $1/2$ and the effective susceptibility is 2. Likewise, for a thin plate or film parallel to B_o , D is equal to 0, but if the plate is perpendicular to B_o , then D is equal to 1.

Overall, for ferromagnetic objects one should use Equation (4) up until the magnitude of the applied field, B_o , reaches a value equal to DB_s , where Equation (4) becomes the same as Equation (3). From this point onward, as B_o increases further, the object remains fully saturated and one should use Equation (3). When one approaches a clinical MR system,

Example II: Effects of demagnetization and saturation



Relative force measurements were made on a small cylindrical piece of iron in a 7T MRI [34]. The saturation flux density, B_s , of the sample was found to be around 0.55 T (5500 Gauss) and, based on the length-to-width ratio of the sample, D was calculated to be $1/7$. The dark circles in the figure show the results of the experimental measurements. The solid line plot shows the expected relative force at different locations along the magnet axis assuming that the sample is magnetically saturated at every location so that Eq.3 was used for the estimates (setting $B_s = 0.55$ T). The dashed line plot shows the relative force assuming that the sample never saturates so that Eq.4 was used

(setting $X/(1+DX) \approx 1/D = 7$). Note that, as one approaches the scanner, Eq.4 should remain valid (no saturation) up until $B_o = DB_s = (1/7) \times 5500 = 786$ Gauss, then Eq.3 should apply as the field gets stronger. Indeed, we see that the experimental measurements (dark circles) follow the dashed line (no saturation) until around 800 Gauss and then the solid line (representing saturation) for greater field strengths.

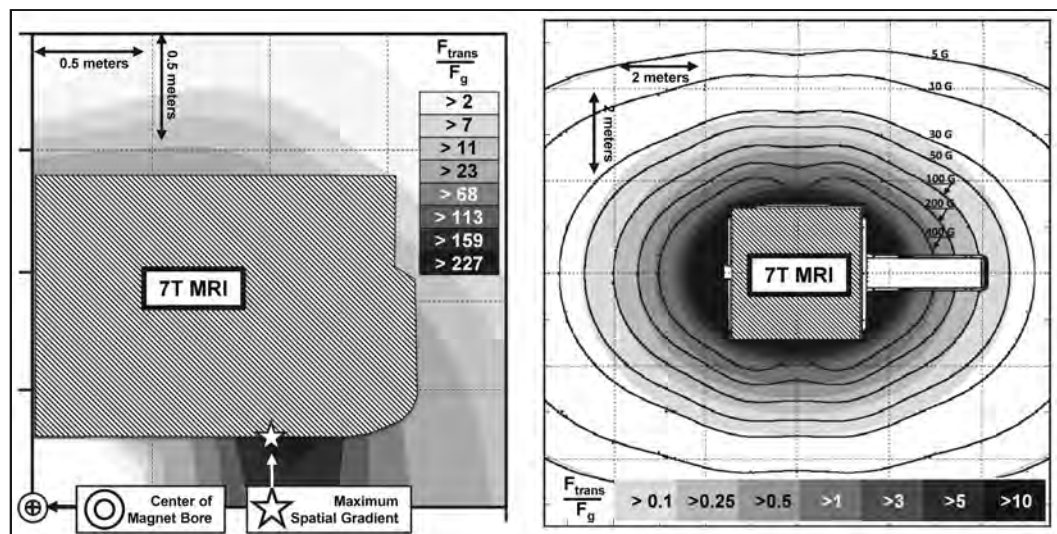
ferromagnetic objects of any shape will become saturated and Equation (3) will apply. Note that Equation (3) does not involve D and shape, meaning that once close enough to a scanner, shape would have little effect on translational pull.

Variation of Magnetic Forces Within the MRI Scan Room

Figure 2 shows two relative force maps (F_{trans}/F_g) derived using manufacturer supplied magnetic field and spatial gradient data for a commercial 7T MR system where it is assumed that some brave (and/or foolish) soul clutches on to an iron object ($B_s = 2.2$ T) as he or she approaches the magnet. From the map on the left, which shows one quadrant of the MRI magnet and the region just outside the bore, it can be clearly seen that maximal translational forces occur near the bore entry (which is where spatial gradients $|\nabla B_o|$ tend to be the greatest) and in some regions the translational forces can reach hundreds of times the object's weight. Active shielding in modern scanners allows the field to be better contained and scanners to be sited in smaller rooms, but they also tend to make $|\nabla B_o|$ much larger, as the field must transition from nearly zero to full strength in a shorter distance. As a result, dynamic shielding actually makes scanners more dangerous by increasing the magnetic translational forces involved. It can also be seen from the figure that inside the bore, as one gets close to isocenter, F_{trans} approaches zero. This is because the field becomes very uniform there meaning that $|\nabla B_o|$ becomes very small.

The right side of Figure 2 shows the force ratio, F_{trans}/F_g , for a larger region around the scanner. It should be noted how, in less than a meter in some places, the ratio may grow from less than 1.0, which may not be dangerous, to above 10 where the situation can rapidly

Figure 2. Relative force maps (F_{trans}/F_g) for a commercial 7 Tesla MR scanner where it is assumed an iron object enters the fringe field. (Left) One quadrant of the 7 Tesla, MR system's magnet and the region just outside the bore. Location of the center of the magnet bore and the location of the maximum spatial gradient magnetic are indicated. (Right) Relative force maps for a large region around the magnet. Locations of the 5, 10, 30, 50, 100, 200 and 400 Gauss lines are shown.



44 Principles of MRI Safety Physics

Table 2. Force index of common objects.

	Paper Clip	Nail Clippers	Kelly Clamp (magnetic stainless steel)	Cell Phone	Piece of Iron	Permanent Magnet	Strongly Ferromagnetic Piece of Iron
Force Index	10.0	11.3	10.2	0.63	6.0	4.31	22.7

become unmanageable and all bets are off. Note that the region roughly between the 50 and 200 Gauss lines comes across as a zone where anyone bearing a ferromagnetic object might want to do some deep thinking about the wisdom of advancing further. In (34) we introduced the ‘force index’, a quantity that can be used to characterize an object according to the degree of relative magnetic force that it would be subjected to if placed in a magnetic field. The force index is equal to $C B_s$ in Equation (4) so that one can determine the magnetic force at any location in the magnetic field (relative to its weight) simply by multiplying the force index by the magnitude of the spatial gradient at that location (assuming the object is already saturated as was assumed when constructing the maps in **Figure 2**). **Table 2** gives the force index as measured for several common objects along with a hypothetical strongly ferromagnetic piece of iron.

Torque Due to Interaction with a Static Magnetic Field

In addition to the translational force that moves ferromagnetic objects along the spatial gradient of the magnetic field, there can also be significant torque applied to objects with highly asymmetric shapes such as long cylinders or ellipsoids. Mathematically, the torque on a dipole μ_m in a magnetic field B_o is equal to the vector product of μ_m and B_o (26):

$$\mathbf{T} = \mu_m \times \mathbf{B}_o \quad (5)$$

where \mathbf{T} is the torque. The vector product of two vectors, also known as a cross product, is also a vector: its orientation is orthogonal to the original two, and its magnitude is equal to the product of their lengths times the sine of the angle between them.

Note how \mathbf{T} in Equation (5) differs from F_{trans} in Equation (1) in the sense that it depends on the strength of the B_o field as opposed to its spatial gradients. For this reason, maximum torque typically occurs inside the MRI’s bore where the field can be very large. For small asymmetrically shaped ferromagnetic objects implanted in the body, the torqueing force may be the dominant safety issue (rather than the translational force) (18), as discussed below.

Let us define a force, F_{torque} , as the restraining force one would have to apply to the two ends of a ferromagnetic, elongated object (e.g., an ellipsoid of revolution with the length several times the width) to prevent it from rotating and lining up with the field. To make

this more intuitive, we put the force in relation with the translational force, F_{trans} , on the same object (18). More specifically, the ratio between the maximal values of both of these forces is given below. Of course, the maximal values of these forces do not occur at the same location in/around the scanner as F_{torque}^{max} occurs near the isocenter while F_{trans}^{max} occurs near the entry to the bore. Even so, the ratio between the two forces can help one understand the importance of torqueing as a safety issue, particularly for small implants. We find that,

$$\frac{F_{torque}^{max}}{F_{trans}^{max}} = \frac{(B_o)_{max}}{L(|\nabla B_o|)_{max}}, \text{ (saturated elongated object)} \quad (6)$$

where L is the length of the object. As an example, taking typical values for a 3T shielded MRI system with a maximum spatial gradient of 10 T/m, and assuming $L = 1$ cm, we find from Equation (6) that the force one needs to apply to the ends of the object to prevent torqueing in the magnetic field can reach 30 times the maximum translational force. Thus, especially in the case of an elongated object implanted into the body, potential damage from torqueing can readily become a greater source of concern than translational forces.

It may seem at first somewhat counterintuitive that for an object of greater length (larger L in Equation (6) the relative importance of F_{torque}^{max} is reduced compared to F_{trans}^{max} . As an object becomes longer/bigger the torque on it would increase, but so would the translational force and both effects cancel out in the ratio in Equation (6). The remaining $1/L$ dependency in Equation (6) is a consequence of our definition of F_{torque} as the force needed at the ends of the object to prevent rotation: a smaller force is required at the ends of a longer object to oppose rotation, for the same reason as loosening a bolt with a long-handled wrench can be much easier than with a short-handled one.

Direct Interactions between the Static Magnetic Field and Living Tissue

For currently available clinical MR systems, magnetic translational forces and torques on diamagnetic and paramagnetic tissues have been estimated and shown to be much too small to be of any safety concern. For example, the tendency of iron-containing red blood cells to separate from plasma due to the differential translational force (ΔF_{trans}) based on the susceptibility difference of the tissues (ΔX) can be calculated. If one assumes a relatively high but realistic SGP of 25 T²/m and in Equation (2) replaces X with ΔX and ρ with $\Delta\rho$, the difference in density between red blood cells and plasma, then ΔF_{trans} is found to be less than 9% of the difference in gravitational pull (ΔF_g) on the tissues (18). Although, for the SPG of 1400 T²/m that was sufficient to levitate frogs (which admittedly is not a very realistic SPG for a practical human-sized MRI), the ΔF_{trans} would be more than 400% of ΔF_g . Accordingly, assuming a suitable magnet were available to a human who was willing to share in the frog's exhilarating experience of magnetic levitation, there might also be a partial separation of their red blood cells from plasma in the process, with unknown health effects.

More immediate concerns regarding the interaction of living tissues with the magnetic fields of actual MR systems in use today involve vertigo and nausea, two well-documented and unpleasant effects on the vestibular system caused by motion in the static magnetic

46 Principles of MRI Safety Physics

field. Whether these vestibular symptoms may be caused by magnetic forces, for example, those resulting from anisotropic susceptibility or from the magnetohydrodynamic effect, or whether they may be related to induced currents associated with motion in the magnetic field, still remains unclear (20).

Another potential force effect comes from current-carrying tissue structures being physically pulled one way or another by the Lorentz force. As charged particles move in a magnetic field, a force emerges that is perpendicular to both the direction of motion and the field:

$$\mathbf{F}_L = q (\mathbf{v} \times \mathbf{B}_o) \quad (7)$$

where q is the charge of the particle, \mathbf{v} is its velocity, and \mathbf{F}_L is the Lorentz force. Note that $\mathbf{v} \times \mathbf{B}_o$ is equivalent to an electric field, \mathbf{E}_L , acting on the particle. The magnitude of the Lorentz force on current-carrying metallic conductors can be significant as will be discussed in the section on gradients. However, currents in biological tissues such as nerves are generally found to be too small to be of any practical concern even at field strengths as high as 20 Tesla (35).

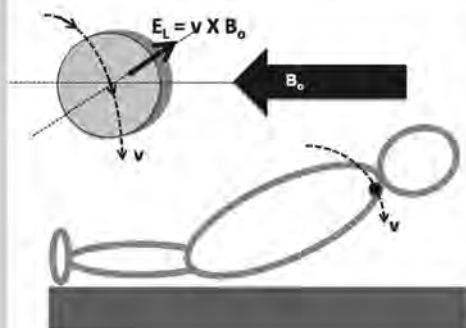
The Lorentz force acts on all charged particles in motion, and these particles may sometimes take the form of ions (i.e., charged molecules) in a flowing liquid. Such interactions fall under the general category of magnetohydrodynamics and the effects in the body have been studied extensively (36-38). Blood flowing in a direction orthogonal to a magnetic field experiences a reverse pressure impeding the flow but this is expected to result in an insignificant increase in blood pressure even in a high field MRI (36, 37). Of greater practical concern is that positive and negative ions in blood are pushed in opposite directions by the Lorentz force, causing a charge separation and an electric field that corrupts electrocardiograms and complicates the task of performing cardiac-gated MRI (39-41).

Effects of Movement in a Strong Static Magnetic Field

It is well known that movement in a magnetic field can induce a voltage (due to Faraday's law of induction to be discussed in more detail later) in electrically conductive materials including biological tissues, especially when the motion is through regions of space where the magnetic field changes steeply. For example, near the entry to the bore of a 3T MRI where $|\nabla B_o|$ tends to be greatest, it can be shown that current densities over 0.1 A/m^2 may be produced in conductive tissues due to the voltage induced by normal movement (42, 43). This is more than twice the 0.04 A/m^2 (low frequency) limit for exposure of workers recommended by the International Commission for Non-Ionizing Radiation Protection (ICNIRP) (44). While there is controversy regarding whether the ICNIRP limit might be too conservative, currents induced in tissue deserve serious attention as a potential MRI safety concern especially when new high-field MR systems are introduced. Furthermore, because the magnitude of the induced current is proportional to conductivity, significant current densities may also be generated in metals used in implants. For example, currents induced in metallic heart valves have been studied over such concerns (45).

Example III: Voltage induced by movement in a magnetic field

Assume a patient has an implanted device (thickness $D = 1 \text{ cm}$) that includes a control unit made of metal. When the patient lies down at the entry to the magnet bore, as shown in the figure, the control unit passes rapidly (at the rate of 2 m/s) through the magnetic field, B_o . An electric field, $E_L = v \times B_o$, is induced across



the device in a direction orthogonal to the direction of motion and the B_o field. Assume that at the entry to the bore, the magnitude of the B_o field is 1.5 Tesla and the direction of motion is almost vertical (and therefore perpendicular to the direction of the B_o field). From the Lorentz force equation we have that the induced voltage or EMF across the device is:

$$\text{EMF} = E_L D = (v B_o)D = (2 \times 1.5) \times .01 = 30 \text{ mV.}$$

While an induced voltage across the device of 30 mV is small, it is not insignificant, and could in principle be harmful to some devices.

RISKS ASSOCIATED WITH THE RF FIELD

To generate RF fields, electrons in the wires of the radiofrequency (RF) coil are coaxed into changing their motion rapidly and repeatedly, at the Larmor frequency, which is equal to γB_o , (where γ is 42.577 MHz/T for hydrogen). Electrons always move of course: only the unreachable depths of an absolute zero temperature could still them, but this motion is coherent and shared as opposed to random and individual. The magnetic field generated by the RF coil excites nuclear spins to produce MRI signals. Compared to the magnitude of the main B_o field, which is strong and static, the magnitude of the magnetic field component of the transmitted RF field (often referred to as B_1) is weak and oscillates at the Larmor frequency, which is about 128 MHz at 3T. The maximum strength of B_1 is only a few microteslas (μT), an order of magnitude lower than the earth's magnetic field at the surface and many orders of magnitude smaller than B_o . However, even though the RF field is small in magnitude, its high frequency leads to safety concerns.

RF Heating of Biological Tissue

The field produced by the RF coil deposits energy into the body in the form of heat: currents are induced in the electrically conductive biological tissues, and heating occurs due to resistance to the current. The problem of heating due to the use of the RF coil can be acute when metallic implants are present, as will be discussed in a later subsection.

The Maxwell-Faraday equation is directly relevant when considering interactions with the RF field. It is written as follows:

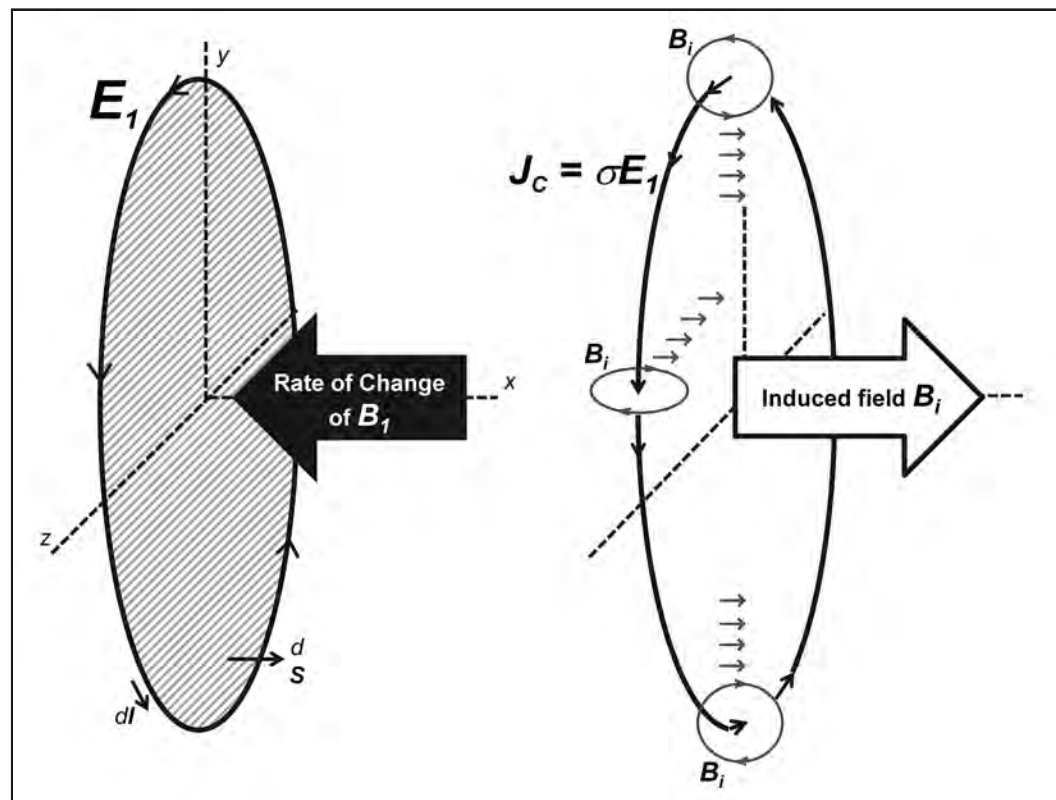
$$\oint_c \mathbf{E} \cdot d\mathbf{l} = - \iint_S \frac{\partial \mathbf{B}}{\partial t} \cdot d\mathbf{s} \quad (8)$$

48 Principles of MRI Safety Physics

where the field \mathbf{B} considered here is the magnetic field generated by the RF coil, \mathbf{B}_1 . Equation (8) expresses the fact that an electric field is generated such that the electromotive force or voltage around a closed loop (integral of \mathbf{E}) is equal to (the negative of) the time rate of change of the magnetic flux integrated over the surface enclosed by the loop. This is shown schematically by the drawing on the left of **Figure 3**.

Note that, as shown in **Figure 3**, $d\mathbf{l}$ is a unit vector tangent to the contour at any point along its length and $d\mathbf{S}$ is a unit vector normal to the enclosed surface at any point on the surface. The plane of orientation of the generated electric field (and therefore the plane of circulation of eddy currents generated in a conductive medium) is perpendicular to the direction of \mathbf{B}_1 , for example, it would be in a sagittal plane if \mathbf{B}_1 were oriented left-right in the scanner. This is nicely demonstrated by the results of a simulation shown in the drawing in **Figure 4**. The \mathbf{E} field vector plots are in the sagittal plane ($y-z$) due to a uniform \mathbf{B}_1 excitation in the x direction. The field calculations for the plots were based on a finite-time finite-difference simulation in a uniform conductive cylinder of a material with electrical and magnetic properties similar to biological tissues ($\sigma = 0.5 \text{ S/m}$, $\epsilon_r = 80$, $\mu_r = 1$). The frequency

Figure 3. (Left) Schematic demonstrating Faraday's law whereby an electric field is generated such that the electromotive force or voltage around a closed loop or contour is proportional to the time rate of change of the magnetic flux integrated over the enclosed surface. (Right) Schematic demonstrating the effect of Ampere's law, whereby a magnetic field, \mathbf{B}_i , is induced by currents, including by the eddy currents generated by Faraday induction.



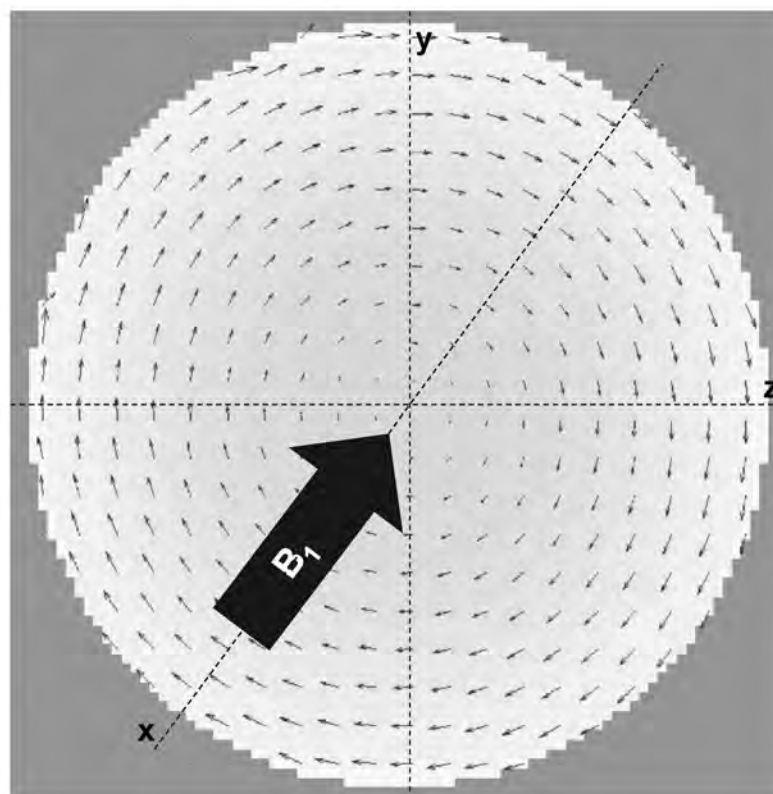
of excitation was 8.52 MHz, the Larmor frequency for a low-field, 0.2 T scanner. Note that, moving towards the center of the cylinder, the \mathbf{E} field vectors become progressively shorter due to the fact that the enclosed areas become smaller.

In the case of heating, it is not directly the transmitted \mathbf{B}_1 that causes problems, but rather the associated electric field. In a conductive medium, \mathbf{E}_1 drives a conduction current density equal to $\sigma\mathbf{E}_1$, where σ is the conductivity of the medium. The instantaneous rate of energy dissipated per unit volume (power density) due to resistance to this current is $\sigma |\mathbf{E}_1|^2$ Watts/m³. Dividing by the mass density of the medium gives the power deposition per kg, which is referred to as the specific absorption rate (or SAR):

$$\text{SAR} = \sigma E_p^2 / 2\rho \text{ (Watts/kg)} \quad (9)$$

where ρ is the mass density (1.06×10^3 kg/m³ in muscle) and E_p is the peak amplitude of the time-varying (and sinusoidal) \mathbf{E}_1 , which oscillates at the Larmor frequency. Using $E_p^2/2$ in Equation (9), as opposed to $|\mathbf{E}_1|^2$, comes from performing a time integral to essentially brush over the nanosecond-scale variations in $|\mathbf{E}_1|^2$, which are of little practical interest

Figure 4. The vector field \mathbf{E} is plotted in the sagittal plane (y - z) due to a uniform 8.52 MHz, \mathbf{B}_1 excitation in the x direction.



50 Principles of MRI Safety Physics

here. Dividing the SAR in Equation (9) by the heat capacity of tissue, which is around 4200 J/kg/°C, one obtains the rate at which tissue is expected to heat if it had no independent way of cooling itself. For example, a SAR of 4.2 Watts/kg will heat tissues at a rate of 10^{-3} °C per second. A volume of tissue subjected to this energy deposition will be heated 1°C (the FDA exposure limit) in 1000 seconds, or about 17 minutes, again assuming there is no cooling during this period.

In order to meet regulatory requirements, it is necessary to measure or calculate the SAR for MRI pulse sequences. A rough estimate of the SAR at the surface of the body may be obtained using a simple loop model (13). Based on the Maxwell-Faraday equation (i.e., Equation (8)), in a surface ring of tissue of radius, R , exposed to a uniform RF field, an electric field would be generated in the loop with peak magnitude as follows:

$$E_P = \pi f B_P R \quad (10)$$

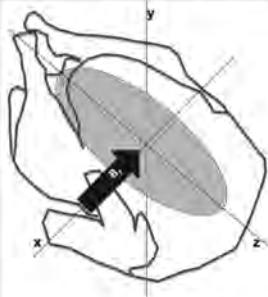
where f is the Larmor frequency (in Hz) and B_P is the peak amplitude of the magnetic field component of the electromagnetic field produced by the RF coil. Equation (10) predicts the behavior of the E field as seen in **Figure 4**, in the sense that the length of the arrows in **Figure 4** increases linearly with R , the distance from the center of the phantom. More specifically, in **Figure 4**, R would be the size of a circle, centered with the simulated phantom, where a time-varying B field generates an E field. Combining Equations (9) and (10),

$$\text{SAR} = \frac{\sigma}{2\rho} (\pi f B_P R)^2 \quad (11)$$

Equation (11) is the usual expression for SAR, as widely published and employed. Although simplistic in some ways detailed below, the equation is useful in the sense that it shows some important trends such as SAR increasing with the square of both f and B_P .

Overall, the assumption that Equation (10) gives the true value of E_P (and thus Equation (11) gives the true SAR) is reasonably accurate for low frequency excitations (e.g., below 10 MHz). Simulations reveal, however, that even at a frequency of 42.58 MHz, the Larmor frequency at 1 T, the estimate of the magnitude of the electric field based on Equation (10) is not accurate. Why is this?

Looking back at **Figure 3** we are reminded that the oscillating B_1 field generated by the RF coil induces an electric field E_1 and, in a conducting medium, a circulating conduction current density equal to σE_1 . This induced current in turn generates a new magnetic field as seen from another of Maxwell's equations, Ampere's law, which further connects E and B as follows:

Example IV: Cooking with MRI

We examine here the potential for MRI to overheat tissue. As an example, consider a raw turkey that, because it is not living tissue, has no capacity to cool from circulating blood. We further assume that the turkey is perfectly insulated (perhaps in an 'ideal' Styrofoam block) so that there is zero heat loss from its surface. The turkey is placed in 3T MRI and subjected to irradiation from a RF train comprised of 90° RF hard pulses of duration $T = 0.5$ msec and peak amplitude $= B_p \mu\text{T}$. Since the frequency due to the RF excitation is equal to $42.58 \times B_p$ cycles per second (with B_p expressed in μT), and a 90° pulse represents 1/4 of a cycle:

$$\frac{0.25}{42.58 \times B_p} = T, \quad B_p = \frac{0.25}{42.58 \times T} = \frac{0.25}{42.58 \times (0.5 \times 10^{-3})} = 11.75 \mu\text{T}.$$

Assuming the radius, R , of the turkey in the sagittal plane is 15 cm, from Eq.11 we obtain:

$$\text{SAR} = \frac{0.5}{2 \times 1000} (\pi 127.7 \times 11.75 \times 0.15)^2 = 125 \text{ W/kg}.$$

This maximum SAR would occur at the surface, where $R = 15$ cm, and it is assumed here that the whole-turkey SAR would be only 40% of the peak SAR. Furthermore, with a duty cycle of 1/2 (i.e. one pulse every 1 msec), which reduces the SAR by a factor of 2, the rate of heating, H_r , would be:

$$H_r = \frac{(0.5 \times 0.4) \times \text{SAR}}{s} = \frac{0.5 \times 0.4 \times 125}{4200} = 0.006 \text{ }^\circ\text{C/s} = 21.4 \text{ }^\circ\text{C/hour}$$

where a specific heat, s , of 4200 Joules/ $^\circ\text{C/s}$ is used. Assuming the turkey is cold (10 $^\circ\text{C}$) when entering the MRI and is cooked once it reaches 75 $^\circ\text{C}$, then it would take just over 3 hours to cook, similar to the time taken to cook in an oven.

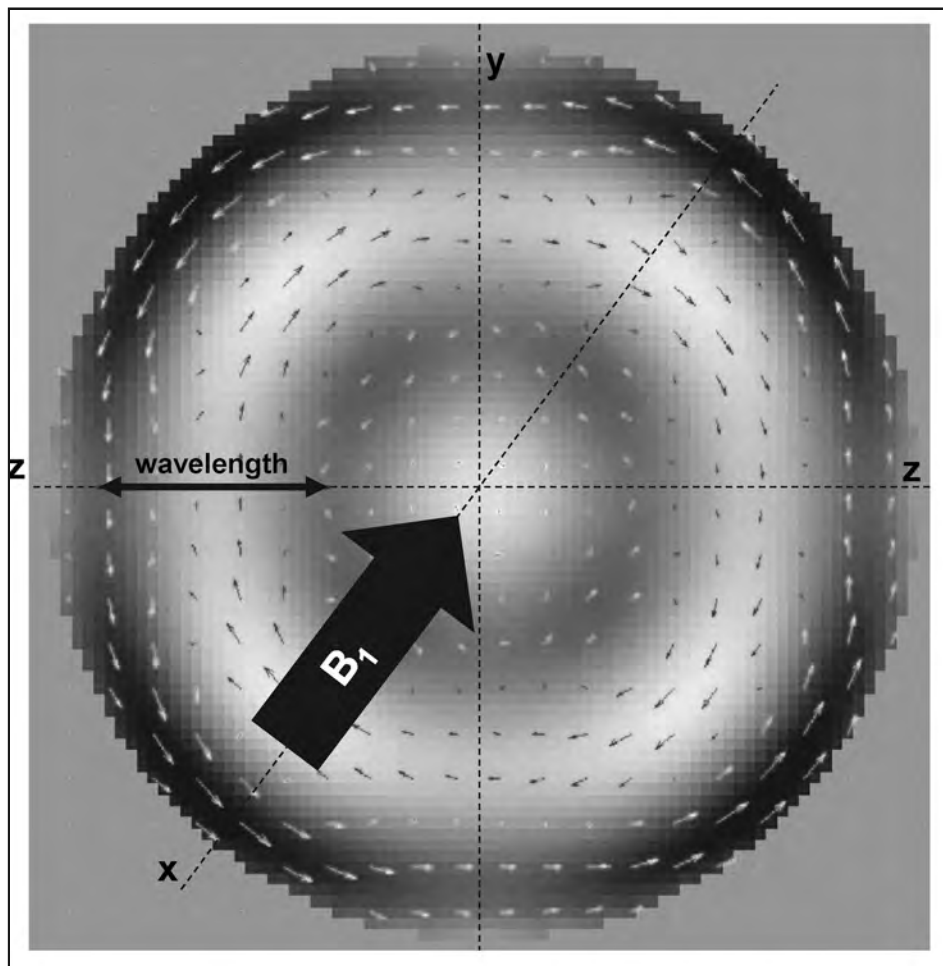
In reality, it would be very difficult to prevent heat loss, and unfortunate dinner guests would likely be presented with a somewhat raw turkey. But this example is meant to help realize that the amount of energy involved in SAR deposition during MRI is far from negligible, and that associated dangers are real.

$$\oint_c \mathbf{B} \cdot d\mathbf{l} = \iint_S \mu \mathbf{J} \cdot d\mathbf{S}, \quad \mathbf{J} = \mathbf{J}_C + \mathbf{J}_D = \sigma \mathbf{E} + \varepsilon \frac{\partial \mathbf{E}}{\partial t} \quad (12)$$

where \mathbf{J}_C and \mathbf{J}_D are the conduction and displacement current densities respectively. Equation (12) expresses the fact that a magnetic field is generated around a closed loop equal to the sum of the total current passing through the surface enclosed by the loop. Ampere's law applies to all currents and, as shown schematically by the drawing on the right side of **Figure 3**, this also includes those eddy currents generated through Faraday induction that were discussed above. Thus, there is a new induced \mathbf{B}_i field that combines with the original source RF field and, because of this, the magnitude of the generated electric field no longer has a simple dependence on the transmitted field, B_p . The importance of the induced magnetic field component increases with increasing frequency. This is demonstrated in the simulation result shown in **Figure 5**, which differs from the simulation result presented in **Figure 4** only in terms of the frequency of the simulated \mathbf{B}_i excitation. In the case shown in **Figure 4**, a relatively low frequency of 8.52 MHz led to a visually-simple vector field, \mathbf{E} , well captured by Equation (10). In contrast, at a higher frequency of 300 MHz (the

52 Principles of MRI Safety Physics

Figure 5. The vector field E is plotted in the sagittal plane ($y-z$) due to a uniform 300 MHz, B_1 excitation in the x direction. The thick solid line shows the wavelength of the excitation for the tissue-like medium.



Larmor frequency at 7T), the vector field E in **Figure 5** is more complicated and does not follow the simple linear relationship with R found in **Equation (10)**. The magnitude of the total \mathbf{B} field, which includes both the exciting field and the induced reverse field, is represented by the gray level images underlying the plots of the vector fields. The \mathbf{B} magnitude image is uniform for the low frequency excitation (**Figure 4**) but is quite non-uniform due to significant wavelength effects for the high frequency, 300 MHz excitation (**Figure 5**). Note that the thick line in **Figure 5** shows the wavelength in the medium (i.e., approximately 11 cm).

The complicated patterns including the phase reversals of the E vectors seen in **Figure 5** can only be explained by the wave equations that result from combining both Maxwell equations. It is possible to combine both Maxwell equations and solve them analytically to obtain more accurate E field and SAR values (12), however, this can only be done for homogeneous media in simple geometries such as spheres and cylinders and with an ideal dis-

tribution of RF irradiation. While solutions involving these simple models may be useful in elucidating the basic behavior of electromagnetic waves in conductive tissue, they are limited when it comes to obtaining direct answers as to what SAR can be expected for a human MRI exam. For this, numerical methods, which are not constrained to solving for simple geometries in homogeneous media, are typically employed (46). A good general discussion of the use of numerical field calculations for MRI safety applications can be found in (47-49) and with respect to the RF field specifically in (50).

Obtaining accurate SAR estimates *in vivo* is especially complicated by the fact that the human body has a complex geometry and is not uniform in terms of its electrical properties (51). Conductivities, for example, can vary by as much as an order of magnitude between tissue types. Attempts have been made to develop human body models that, when used with numerical simulation techniques, may give accurate estimates of SAR (52-61). A more direct and potentially more accurate approach to estimate SAR is to use actual MR images, for example, obtaining B_1 maps that may then be used to estimate the E field and derive the SAR distribution (62-65), although it has been shown that significant changes in SAR and heating distributions are not necessarily reflected in B_1 changes (51). Thermo-acoustic imaging has also been investigated as a method for direct SAR mapping (66).

It is important to note that, for the purposes of safety monitoring, SAR is merely used as a surrogate measure for the potential to cause tissue damage. The real problem is heating. Numerical models that use SAR, not as the endpoint, but as input to estimate resultant temperature changes in the body via, for example, the Pennes bioheat transfer equation, have been employed to this end (67-72). An even more direct means of determining the likelihood of tissue damage is to obtain *in vivo* temperature maps through MR-based temperature mapping using the fact that the water resonant frequency is temperature dependent (73-78).

RF Interaction with Metallic Objects Forming Loops

As long as the MR system is functioning properly and limits regarding SAR are respected, no dangerous heating (or cooking of turkeys) should occur during routine MRI as a result of RF irradiation. It is still possible, however, to cause serious tissue damage when conductive metallic objects are present in patients. Currents generated by the RF field in these objects do not significantly affect global SAR, but they can focus energy deposition in small volumes and create localized tissue damage.

Let us consider a copper loop placed perpendicular to the RF field orientation and examine Equation (11), which was used when estimating the SAR of a ring of tissue. The conductivity of copper is about 8 orders of magnitude higher than that of biological tissues, and its density is close to 10 times that of tissue. Accordingly, from Equation (11), the SAR of the metal would be around 10 million times greater than in tissue and one would expect enormous heating. The fact is, however, that there is actually very little heating of the metallic object (79). How can this discrepancy be explained?

As detailed in the previous section, Equation (11) is only an approximation, and it cannot be applied to situations where currents are large (whether due to high f , or the presence of highly conductive metal). The heating predicted by Equation (11) does not happen because Equation (12), again, comes into play. The current in the loop will itself generate a

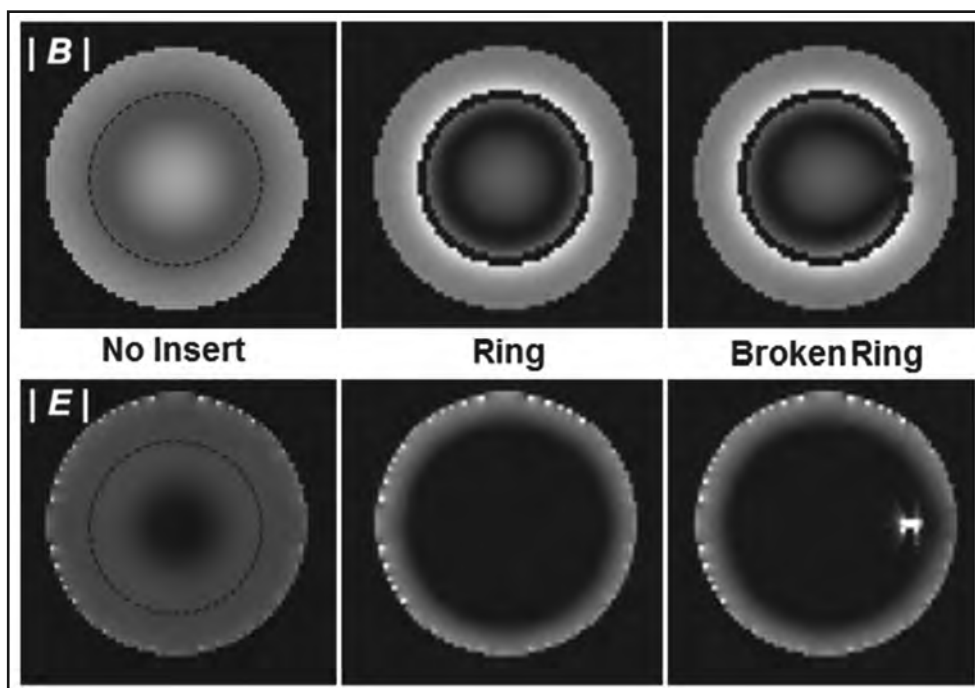
54 Principles of MRI Safety Physics

magnetic field that will counter the driving B_1 field. If the current induced in the loop grows large enough to generate a field that exactly cancels B_1 , then no more current can be induced. **Figure 6**, which shows the total \mathbf{B} and \mathbf{E} fields under different simulated situations, illustrates this fact. The \mathbf{E} field is shown on the bottom left of **Figure 6**, for a section of conductive tissue-like material irradiated by a uniform 128 MHz B_1 field oriented perpendicular to the section. The \mathbf{E} field for the most part shows a radial dependence on intensity, as predicted by Equation (10). Note that the total \mathbf{B} field is no longer uniform due to the contribution from the field generated by the circulating currents.

In the middle column of **Figure 6**, the total \mathbf{B} and \mathbf{E} fields are shown for the case where a simulated conductive metallic ring was placed inside the tissue. Both the \mathbf{E} and \mathbf{B} field inside the ring almost completely vanished as a result. Not only is there minimal SAR within the metallic ring itself (and thus no risk of dangerous heating) but the ring essentially acts as a shield to limit SAR for tissues within it.

Before wrongly concluding that loops of metal pose no risk in MRI, let's consider the case where a small break is present in the loop, as illustrated on the right side of **Figure 6**. Note that the \mathbf{B} field remains mostly unchanged by the presence of a break in the loop, but

Figure 6. Simulated magnitude of \mathbf{E} and \mathbf{B} fields in the sagittal plane ($y-z$) due to a 128 MHz uniform B_1 excitation in the x direction. Images in the left column involve only tissues, no metallic implant. The dashed circle shows the location where a metallic ring was introduced. Simulation results after introduction of a metallic ring are shown in the middle column. The right column shows simulation results when a small gap was introduced into the metallic ring.

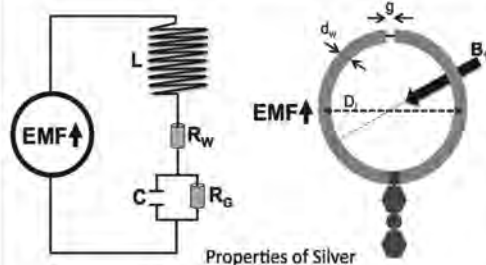


the situation is much different for the E field and the resultant SAR in the region of the ring gap. The SAR is greatly elevated over the level seen in the rest of the tissue, with potential for significant local tissue damage. The importance of avoiding loops containing metal was shown by Bennet, et al. (80), who demonstrated significant heating in a metallic radiosurgery head frame at the tips of screws that clamp the frame to the head. Loops of cables that come in contact with the body also have the potential to cause burns and should be avoided.

Although a less likely scenario, there is also the potential that a loop-containing implanted device might act as a circuit in resonance (79, 81, 82), in which case large amounts of energy may be transferred, possibly resulting in destruction of the device and damage to surrounding tissues. An un-blanked receive coil would be an example (83).

Example V: Heating of a silver earring in the RF field

Consider the potential heating of an earring made from thick silver wire (diameter, d_w) forming a loop (diameter, D) and oriented perpendicular to the RF field direction of a 3T MRI scanner. The figure shows the earring along with a circuit representation of the induction of EMF in the loop by the B_1 RF field.



Properties of Silver

Conductivity, σ :	6.3×10^7 Siemens/m
Density, ρ :	1.05×10^4 kg/m ³
Specific Heat, s :	2.4×10^2 Joules/kg°C

The EMF induced in the loop by the B_1 field generates a current that will itself generate a magnetic field that counters the driving field. A measure of the loop's resistance to the change of current is its inductance, L . The magnitude of this resistance (or impedance) is linearly dependent on frequency and equal to $2\pi fL$, where f is the frequency of the B_1 field. An empirical relation for inductance of a single coil wire loop is as follows:

$$L = \mu_0 \frac{D}{2} [\ln(8 \frac{D}{d_w}) - 1.75],$$

where D is the diameter of the loop and d_w is the diameter of the wire. L for a ring with loop diameter of 25 mm and 'wire' diameter of 2.5 mm is 4.13×10^{-8} Henry. The impedance, Z , due to this inductance is:

$$2\pi fL = 2 \times \pi \times 127.7 \times 10^6 \times 4.13 \times 10^{-8} = 33.1 \Omega.$$

This should be compared to the impedance (resistance) of the silver ring (where the length around the ring's circumference = $2\pi D$ and the cross-sectional area of the ring's band = $\pi(d/2)^2$):

$$\frac{\pi D}{\sigma_{(\text{silver})} \pi(d/2)^2} = \frac{\pi \times 2.5 \times 10^{-2}}{6.3 \times 10^7 \times \pi(1.25 \times 10^{-3})^2} = 0.000254 \Omega.$$

Clearly, the magnitude of the impedance due to the inductance (33.1Ω) is much greater than the electrical resistance of the silver (0.000254Ω) and should therefore be used to determine the heating.

Rate of heating in an unbroken loop of silver:

$$H_s = \frac{EMF^2}{2|Z|}/(\rho V_{ol} s) = \frac{1^2}{2(33.1)} / ((1.05 \times 10^4) \pi (1.25 \times 10^{-3})^2 \pi (2.5 \times 10^{-2}) (2.4 \times 10^2)) = 0.015 ^\circ\text{C/s},$$

where V_{ol} is the volume of the ring = $\pi D \times \pi(d/2)^2$ and the EMF is assumed to be 1 Volt (B_1 of $2.5 \mu\text{T}$).

Though we find a relatively low rate of heating in this earring compared to what would be calculated based only on the resistance of the silver, it should be noted that the heating rate is still 15 times greater than tissue heating with a maximum allowable SAR of 4 W/kg.

56 Principles of MRI Safety Physics

The Antenna Effect

The mechanism for RF heating discussed to this point has only involved the generation of current via induction in conductive loops. Straight wires (not bent into loops) can also pose a significant hazard and serious injury has resulted when they come in contact with the RF field and are subjected to the so-called antenna effect.

From antenna theory, it is known that currents can be induced in a conductive wire when excited by an incident E field oriented parallel to the direction of the wire. This theory has been invoked when explaining the observation that significant heating may be produced at the tips of wires exposed to the RF field in MRI. This is a resonant phenomenon in the sense that the length of the wire must be such as to support the formation of standing waves. Typically, wire lengths of a half wavelength are most likely to result in the maximum heating. The speed of light in void is 3×10^8 m/s, meaning that a wave with $f=127.7$ million oscillations per second would cover 2.35 meters per oscillation, which gives about 1.17 meters for a half wavelength. However, RF waves in MRI do not travel in void and one must take into account the relative permittivity of tissue, $\epsilon_r=80$. The half wavelength in tissue is reduced compared to its value in the void by $\sqrt{\epsilon_r}$ down to about 13 cm here. The conductivity of tissues also comes into play and brings the half wavelength value even further down, for example, close to 12 cm if one assumes a conductivity of 0.5 S/m. Thus, in a 3T scanner ($f=127.7$ MHz), an implanted metallic wire in the range of 12 cm in length should be especially worrisome although, given variability in the electrical properties of different tissues and uncertainty in estimation of wavelengths, one should not assume there will be no heating based on the length of the wire alone. Other factors, such as how the wire is terminated, were also shown to have importance in this regard (84, 85).

The plot in **Figure 7** demonstrates the significant effect of wire length on heating in the RF field. The results of simulations with conductive wires embedded in tissue-like material show that SAR at the ends of the wires is maximized at a length of 12 cm, the half wavelength at $f=127.7$ MHz. The SAR image in **Figure 7** illustrates a highly localized energy deposition in the conductive medium near the ends of the 12 cm wires, where electric field variations are largest.

Localized SAR amplification has been predicted by simulation (86) and extrapolated from experiment (87) to 10,000-fold or more. Thus, even with relatively low RF input power, temperatures can rise rapidly. Indeed, significant temperature increases from 20 to 60°C have been recorded in experiments with a variety of devices that include implanted wires; deep brain stimulation systems (88, 89), vagus nerve stimulation systems (90), cardiac pacemakers (84, 91, 92), guidewires (93, 94), EEG electrodes (95), implanted planar electrodes (96), and implanted stereo-electrodes (97). Temperatures exceeding 60°C were recorded in copper wires of resonant length at 1.5T (79). An incident ascribed to action of the antenna effect in an ECG lead resulted in a fire in 1.5T system and patient burns (98). At high field strengths such as 7T, resonant lengths are much shorter and heating due to the antenna effect can occur in devices such as aneurysm clips that are otherwise too short to be a big concern at lower field strengths (99, 100).

In addition to wire length and terminal conditions, the position and orientation of the wire also have importance (101). This is demonstrated by simulation results shown in

Figure 7. Results of simulations with thin (insulated) wires placed in a uniform B_1 field oscillating at 128 MHz. The field calculations were based on a finite-time finite-difference simulation in a uniform conductive cylinder of a material with electrical properties similar to biological tissues ($\sigma = 0.5 \text{ S/m}$, $\epsilon_r = 80$, $\mu_r = 1$). The plot on the left shows the estimated SAR for wires of varying length. As expected, the peak SAR occurred at 12 cm, the half wavelength value. The center image is the estimated SAR with 12 cm wires placed in the cylinder at four different positions. The position of the four 12 cm wires is indicated by dashed white lines in the images on the right.

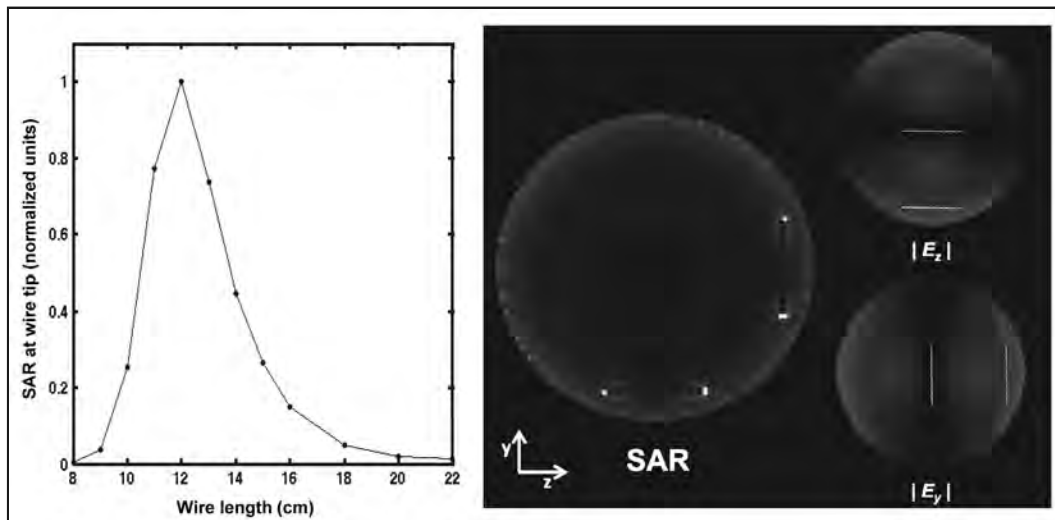


Figure 7 where half-wavelength wires (12 cm) were placed as indicated by the dashed white lines. Two wires oriented in the z -direction were placed as shown, yet only the wire near the edge of the phantom caused any sizeable energy deposition, that is, there is no evidence of elevated SAR near the wire placed at the center of the phantom. This is because there is no significant z -component of E at the center, see image of $|E_z|$ in Figure 7. Similarly, for wires oriented in the y -direction, only the wire at the edge of the phantom caused a sizeable elevation in SAR, because this is where the E field had a sizeable y -component.

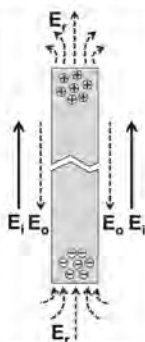
A common intuitive explanation for the antenna effect is that an incident E field of appropriate wavelength and oriented along the length of the wire forces current back and forth coherently along the conductive metallic wire. The wire may then re-radiate energy as, for example, a dipole antenna. More in-depth analysis proceeds by direct application of Maxwell's equations, yielding Hallen's or Pocklington's integral equations whose solution, given the incident field, allows for the calculation of the current distribution on the wire and (more importantly for a SAR estimation) the radiated field pattern (94, 102-104). Other approaches such as treating wires as transmission lines using a lumped-element model have been employed to estimate the current distribution along the wire (106-108). Experimental approaches to measure the transfer function for heating given the incident electric field have also been developed (109-111). Furthermore, MRI has been used to estimate the induced currents by measuring their effect on the B_1 field (112-116) or to directly estimate SAR via MRI-based temperature mapping (117-118) or by thermo-acoustic ultrasound (119). Direct measurement of induced currents with special sensors has also been employed (120-122).

58 Principles of MRI Safety Physics

RISKS ASSOCIATED WITH THE GRADIENT FIELDS

Electrons in the wires of the gradient coils are coaxed into moving in ways that momentarily add to the much larger static B_0 field. Gradient coils in MR systems are used to encode spatial information by adding a relatively small component to the B_0 field that varies linearly with position, thus introducing a small spatially-dependent variation in the Larmor frequency. In today's systems, spatial gradients of around 40 mT/m (or 4 G/cm) are common, and higher-performance systems may reach 80 mT/m. Assuming an imaging field-of-view (FOV) of 50 cm, a 40 mT/m gradient set produces a maximum magnetic field strength of ± 10 mT (± 100 G) at the edges of the FOV. The magnitude of the fields produced by the gradient coils is about three orders of magnitude stronger than magnitude of the fields produced by RF coils, but between two and three orders of magnitude less than the static magnetic field. With slew rates of 200 T/m/s, the orientation of these fields can be reversed in less than one millisecond. Compared to the main magnet and the RF field, the gradient fields are intermediate both in terms of their strength and of the frequency of their temporal variations.

Example VI: Heating due to the antenna effect



Assume a wire of length d is oriented in the same direction as an incident electric field, E_i , and the wire is of half-wavelength, $\lambda/2$, so that it can support the formation of a standing wave. Current is driven along the wire due to E_i and, for simplicity, we assume the current to be zero at both ends of the wire and that positive and negative charge collect at the ends. More specifically, enough charges collect at the ends to create an electric field, E_r , that cancels out E_i (see Figure), at which point charges stop migrating to the ends of the wire. The field E_o at the midpoint on the wire is the sum of the field created by the charge $+Q$ a distance $\lambda/4$ away in one direction and that of the charge $-Q$ a distance $\lambda/4$ away in the other direction, from Coulomb's law:

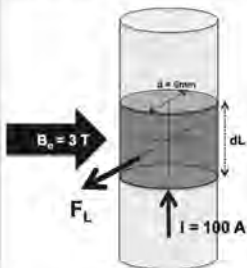
$$E_o = 2 \times \frac{k Q}{(\lambda/4)^2}; \quad Q = \frac{E_o \lambda^2}{32 k}; \quad k = \frac{1}{4 \pi \epsilon_0}.$$

We wish to estimate E_r near the tips of the wire, more specifically a short distance r away from the tips and into the tissues, where intense heating is known to occur. To do this we simply take the charge Q found above and use Coulomb's law again. Of course the entire charge Q could not be entirely concentrated right at the tip, and to get a rough approximation of SAR only a portion of the charge Q equal to $r/(d/2) = 4r/\lambda$ is assumed to contribute to E_r :

$$E_r(r) = \frac{k}{r^2} \left(\frac{E_o \lambda^2}{32 k} \right) \left(\frac{4r}{\lambda} \right) = \frac{E_o}{8} \left(\frac{\lambda}{r} \right); \quad SAR = \frac{\sigma E_r(r)^2}{2 \rho} = \left(\frac{\sigma E_o}{2 \rho} \right) \left(\frac{\lambda}{8 r} \right)^2,$$

where Eq. 9 was used to convert E_r into a measurement of SAR. As usual, σ is the conductivity of tissues and ρ is its density. As seen in the figure, the magnitude of E_o at a given moment is roughly equal to the incident field, E_i , and roughly cancels it out. If the wire were not present, it is the incident field E_i that would be used in Eq. 9 to calculate SAR. Instead, from the equation above, in the presence of the wire the SAR was amplified near the tip by a factor $A = (\lambda/8r)^2$. In [86], the theoretical SAR amplification was computed at the tip of a wire of resonant length, $\lambda = 18$ cm and radius $r = 0.25$ mm and a value of about 7000 was found. Using the same parameters and the approximate approach derived above, a similar SAR amplification factor is obtained:

$$A = (0.18/(8 \times 0.00025))^2 = 8100.$$

Example VII: Force on current carrying wire

We have a copper wire of diameter $d = 6\text{ mm}$, in a scanner with $B_o = 3\text{ T}$. The wire, which is carrying 100 Amps of current, is oriented perpendicular to the direction of the B_o field as shown in the figure. The force on a short length, dL , of the wire can be calculated from the Lorentz equation as follows:

$$F_L = I dL B_o = 300 dL,$$

where dL is in meters and F_L in Newtons. We are interested in the relative force on the wire element with respect to the gravitational force, F_g , on the same piece of wire (of volume, V , and density, ρ).

The gravitation force on the wise is: $F_g = mg = \rho V g = \rho dL \pi (d/2)^2 g$. The relative force, F_R , is:

$$F_R = \frac{F_L}{F_g} = \frac{300}{\rho \pi \left(\frac{d}{2}\right)^2 g} = \frac{300}{(8.96 \times 10^3) \pi (3 \times 10^{-3})^2 \times 9.8} = 120.8$$

We can expect this level of force on current carrying elements of the gradient coils. The rapid reversal of currents in these elements results in rapid force reversals, causing vibration and possibly ear-damaging noise.

While forces due to the magnetic field were the key source of risk for the static magnetic field, and the generation of currents via magnetic induction was the key source of risk of the RF field, both forces *and* magnetic induction come into play when considering the safety of the gradient fields. How these issues are manifested, however, is quite different in the case of the gradients.

The problem of magnetic forces with reference to gradient coils is not one of keeping ferromagnetic objects away from the fields. Indeed, applying Equation (3) for a saturated iron object ($B_s = 2.5\text{ T}$), $C \approx 10\text{ m/T}^2$ and assuming a maximum imaging gradient field of 40 mT/m gives a force ratio of 1, about two orders of magnitude lower than force ratios associated with the main magnet (Section 1). For the gradients, the problem instead is the potential for ear-damaging acoustic noise caused by physical movement of the current-carrying conductors of the gradient coils as they interact with the static magnetic field via the Lorentz force.

The problem of the induction of eddy currents is not the associated direct heating of tissue as it is with the RF field (although heating of metallic objects via gradient induced currents can be theoretically important). When Equation (11) is applied to calculate the SAR at the periphery of a body 20 cm in radius, where the maximum gradient fields strength would be $\pm 4\text{ mT}$ (assuming 40 mT/m gradients), we obtain an SAR due to gradient switching (at 1 kHz) of only 0.003 W/kg , compared to the 6.5 W/kg calculated for the RF field strength of $2\text{ }\mu\text{T}$. Instead of direct tissue heating, for gradients, the major concern is nerve, muscle and other sensitive tissue stimulation that may result from the electric fields associated with the induced currents. These issues are discussed in more detail below.

It was noted in an earlier section that charges moving through a magnetic field experience a force, the Lorentz force, proportional to velocity and the strength of the field (Equation (7)). The Lorentz force acting on current-carrying conductors can be very large even for moderate currents. Hundreds of amperes may flow through gradient coils, resulting in enormous forces on the coil elements. This is comparable to the force ratio we found for

60 Principles of MRI Safety Physics

ferromagnetic objects when in the region of the maximum spatial gradient of the MRI field. Therefore, it is easy to see how it is that the rapid switching of such large currents and the accompanying rapid reversal of the direction of the large Lorentz forces may result in loud sounds (123, 124), the levels of which can easily exceed 130db in modern MR systems (125, 126). Temporary hearing loss was reported in early studies even with relatively low-field systems (127) and guidelines have been established in the intervening years to protect exposed persons from permanent hearing damage (126). Today, hearing protection is considered mandatory during any MRI procedure in order to reduce acoustic noise to safe levels.

Nerve and cardiac tissue stimulation, due to rapidly switching gradients, represent yet another source of concern (128-130). The mechanism by which stimulation occurs has been studied extensively (17, 21, 128). As discussed in previous sections, according to Faraday's law, time-varying magnetic fields induce an EMF around a closed circuit proportional to the time rate of change of the total magnetic flux through the surface enclosed by the circuit. Given the rate of change in the gradient field, dB/dt , with the maximum occurring at the periphery of an FOV of radius, R , the maximum induced field, E is given by $R/2 \cdot dB/dt$ (i.e., this result is obtained from Equation (10) if one substitutes dB/dt for $2\pi f B_p$ assuming a sinusoidal variation of the gradient field with B_p being the peak magnitude). In order to achieve nerve stimulation, there is a threshold electric field strength, E_s , which is equal to $E_r(1+\tau_c/\tau_d)$, where τ_d is the duration of the stimulation, E_r (called the rheobase) is the minimum E_s necessary to cause stimulation, and τ_c (called the chronaxie) is a reference stimulation time.

Values for both the rheobase and the chronaxie are obtained through fits performed on experimental data (129). From simple assumptions about the geometry of the subject, a curve of dB/dt versus stimulus duration (gradient ramp time) can be obtained to determine whether specific ramp durations are likely to cause nerve stimulation. Furthermore, by combining complex body models with electro-magnetic simulations and neuro-dynamic models, accurate prediction of thresholds for stimulation of specific nerves has been shown (131). Peripheral nerve stimulation (PNS) is well within the capability of modern MR systems and has been reported since the first echo-planar capable scanners became available (130). While uncomfortable and possibly painful, PNS does not represent a serious threat. Cardiac stimulation, however, could have serious consequences and must therefore be considered. Fortunately, even with the current maximum dB/dt of 100 T/m, and maximum gradient amplitude of 80 mT/m on the newest commercial MR systems, ramp times to reach peak are well below threshold values to cause cardiac stimulation (17). However, cardiac stimulation remains theoretically possible on some research systems outfitted with 300 mT/m gradients (132), and, thus, special care must be exercised in such a setting.

In addition to the effects of switching gradient fields discussed above, interaction with implanted devices containing metals must also be carefully considered (133). In cardiac pacemakers, gradient field switching could possibly induce currents that might create competitive pacing, with the potential of causing life-threatening arrhythmias (134-136). Unintended electrical stimulation of tissue due to induction of currents on the leads of other active implants such as neurological stimulators could be another concern (137,138). Induced currents from gradient switching may also cause heating of devices containing metal-

lic components (139, 140) although the significance of this heating has not been generally appreciated (141, 142). Gradient-induced currents may also generate a significant magnetic moment and cause vibration of devices as gradients are switched (143, 144). Although less of a safety concern than interactions with the B_o or RF fields, the switching of gradient fields should nevertheless be considered when evaluating devices for potential damaging interactions.

SUMMARY AND CONCLUSIONS

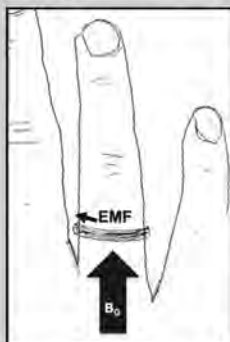
In this chapter, it was explained how electromagnetic fields associated with MRI interact with human tissues and artificial objects. We also provided realistic numerical examples regarding some of the main sources of risks in and around MR systems. With regard to all potential interactions with biological systems, the present text, of course, only scratched the surface. We have mostly limited ourselves to those interactions that are known to represent potentially serious safety hazards in the context of today's MRI setting.

In focusing exclusively on the major hazards associated with MRI we have taken the chance of creating the impression that there is little that can be done about any of it. Fortunately, one constant rule about technological development is that, once a problem is identified, it may be only a matter of time before either a solution or a work-around can be found, and so it is also with MRI. The problem of heating due to the RF field, especially in regard to the interaction with implanted devices, is a good case in point. For example, a variety of techniques have been developed to defeat the antenna effect, by engineering wires and cables to be safer (145-151), or making changes to the RF transmission system (152-157). More general solutions to the SAR problem have involved pulse sequence and RF pulse modifications (158), the use of dual and parallel RF transmitters (159-168), and the strategic use of high-permittivity materials (169-171). Engineering solutions have also been developed to address other safety-related issues such as reducing or buffering the acoustic noise produced by the gradient magnetic fields (172, 173). There is not much that can be done to mitigate the danger inherent in the main magnetic field but there has been progress in developing detection systems to help keep ferromagnetic objects out of the MR system room (174-176). With appropriate evaluation based on a solid understanding of the physical principles underlying interactions of materials with the MRI-related electromagnetic fields, it is possible to scan patients with implanted devices where it was once considered an absolute contraindication by following specific conditions (177, 178).

The central components of the MR system are the subsystems that generate the electromagnetic fields essential to the production of MR images. Enormous energies go into producing these fields, hence the potential dangers to life within them. MRI is known as a safe imaging modality because it does not require the use of ionizing radiation and, with proper care and management, the exquisite MR images we have come to expect can indeed be obtained safely. Understanding the physics underlying the risks in MRI is a key component for proper care and management, and it is with this goal in mind that we offer this work.

62 Principles of MRI Safety Physics

Example VIII: Heating of a Silver Ring in the Gradient field



Consider the heating of a ring made from thick silver wire (diameter, $d = 2.5 \text{ mm}$) that forms an unbroken loop (diameter, $D = 2.5 \text{ cm}$) and is oriented perpendicular to the B_0 field direction of a 3T MRI scanner. The figure shows a drawing of the ring with respect to the direction of the z-gradient field, B_G . Assume that the imaging gradient system has a maximum slew rate of 200 T/m/s and maximum gradient amplitude of 80 mT/m. During the switching of the gradient, the induced electric field, E_G , and the EMF due to the change in magnetic flux through the ring is obtained directly from Faraday's law (Eq. 8):

$$\text{EMF} = -\left(\frac{\pi D^2}{4}\right) \frac{dB_G}{dt},$$

where factor dB_G/dt was obtained from the slew rate of the gradient coil. Assuming the distance between the ring and the isocenter of the scanner is $d_g = 0.3 \text{ m}$, then $dB_G/dt = 200 \times 0.3 = 60 \text{ T/s}$. Thus the (absolute value) of the EMF is:

$$\text{EMF} = \frac{\pi (2.5 \times 10^{-2})^2}{4} \times 60 = 0.0295 \text{ V}.$$

This EMF drives a current that causes the ring to heat up. The parameters ρ and s for silver, as well as the diameter, thickness, resistance and inductance of the ring are the same as in Example V, the RF heating of a silver earring. Because the frequency of the induction field is different, however, we need to recalculate the impedance. Assuming a gradient oscillating at the angular frequency ω :

$$B_G(t) = A \sin(\omega t), \quad \frac{dB_G}{dt}_{\text{max}} = \omega A.$$

Given the maximum gradient amplitude of 80 mT/m and the location of the ring at $d_g = 0.3 \text{ m}$ from isocenter:

$$A = .08 \times 0.3 = .024 \text{ T}, \quad \omega = (dB/dt)/A = 60/.024 = 2500 \text{ rad/s}.$$

The impedance due to the inductance of the loop can be calculated:

$$i\omega L = 2500 \times 4.13 \times 10^{-8} i = 1.034 \times 10^{-4} i \Omega,$$

and by inserting $Z = R_s + i\omega L$ as the total impedance of the loop, the rate of heating, H_s , is found:

$$H_s = \frac{\text{EMF}^2}{2|Z|} / (\rho V_{ol} s) = 1.63 \text{ C/s}$$

In this example, the ring exposed to the imaging gradient experiences a much greater rate of heating than the similar case of the earring in the RF field. Of course, this only applies while the gradient is ramping. Nevertheless, this result shows that gradient-induced heating can be a significant source of risk.

ACKNOWLEDGMENTS

The authors wish to thank Dr. Denis Michaud for useful discussions and a special thank you to Ken MacDonald who provided us with the superb drawing of a levitating frog.

REFERENCES

1. Saunders RD, Smith H. Safety aspects of NMR clinical imaging. Br Med Bull 1984;40:148-154.
2. Gangarosa RE, Minnis JE, Nobbe J, Praschan D, Genberg RW. Operational safety issues in MRI. Magn Reson Imaging 1987;5:287-292.
3. Kanal E, Shellock FG, Talagala L. Safety considerations in MR imaging. Radiology 1990;176:593-606.

MRI Bioeffects, Safety, and Patient Management 63

4. Shellock FG. Radiofrequency energy-induced heating during MR procedures: A review. *J Magn Reson Imaging* 2000;12:30-36.
5. Ahmed S, Shellock FG. Magnetic resonance imaging safety: Implications for cardiovascular patients. *J Cardiovasc Magn Reson* 2001;3:171-182.
6. Shellock FG, Crues JV. MR procedures: Biologic effects, safety, and patient care. *Radiology* 2004;232:635-652.
7. Stecco A, Saponaro A, Carriero A. Patient safety issues in magnetic resonance imaging: State of the art. *Radiol Med* 2007;112:491-508.
8. Durbridge G. Magnetic resonance imaging: Fundamental safety issues. *J Orthop Sports Phys Ther* 2011;41:820-828.
9. Kathiravan S, Kanakaraj J. A review on potential issues and challenges in MR imaging. *ScientificWorld Journal* 2013;2013:783715.
10. Tsai LL, Grant AK, Mortele KJ, Kung JW, Smith MP. A practical guide to MR imaging safety: What radiologists need to know. *Radiographics* 2015;35:1722-1737.
11. Kim SJ, Kim KA. Safety issues and updates under MR environments. *Eur J Radiol* 2017;89:7-13.
12. Bottomley PA, Andrew ER. RF magnetic field penetration, phase shift and power dissipation in biological tissue: Implications for NMR imaging. *Phys Med Biol* 1978;23:630-643.
13. Bottomley PA, Edelstein WA. Power deposition in whole-body NMR imaging. *Med Phys* 1981;8:510-512.
14. Schenck JF. The role of magnetic susceptibility in magnetic resonance imaging: MRI magnetic compatibility of the first and second kinds. *Med Phys* 1996;23:815-850.
15. Schaefer DJ. Safety aspects of radiofrequency power deposition in magnetic resonance. *Magn Reson Imaging Clin N Am* 1998;6:775-789.
16. Price RR. The AAPM/RSNA physics tutorial for residents. MR imaging safety considerations. *Radiographics* 1999;19:1641-1651.
17. Schaefer DJ, Bourland JD, Nyenhuis JA. Review of patient safety in time-varying gradient fields. *J Magn Reson Imaging* 2000;12:20-29.
18. Schenck JF. Safety of strong, static magnetic fields. *J Magn Reson Imaging* 2000;12:2-19.
19. Formica D, Silvestri S. Biological effects of exposure to magnetic resonance imaging: An overview. *Bio-med Eng Online* 2004;3:11.
20. Schenck JF. Physical interactions of static magnetic fields with living tissues. *Prog Biophys Mol Biol* 2005;87:185-204.
21. Glover PM. Interaction of MRI field gradients with the human body. *Phys Med Biol* 2009;54:R99-R115.
22. Kraff O, Quick HH. 7T: Physics, safety, and potential clinical applications. *J Magn Reson Imaging* 2017;46:1573-1589.
23. Panych LP, Madore B. The physics of MRI safety. *J Magn Reson Imaging* 2018;47:28-43.
24. Lorrain P, Corson DR, Lorrain F. Electromagnetic fields and waves, 3rd edition. W.H. Freeman and Company. New York, NY; 1988.
25. Hayt WH, Buck JA. Engineering electromagnetics. 8th Edition. New York: McGraw Hill; 2012.
26. Coey JMD. Magnetism and magnetic materials. Cambridge, UK: Cambridge University Press; 2013.
27. Kabil J, Belguerras L, Trattnig S, et al. A review of numerical simulation and analytical modeling for medical devices safety in MRI. *Yearb Med Inform* 2016;10:152-158.
28. Elsherbeni A, Demir V. The finite-difference time-domain method for electromagnetics with Matlab simulations. Raleigh, NC: SciTech Publishing Inc.; 2009.
29. Berry MV, Geim AK. Of flying frogs and levitrons. *Eur J Phys* 1997;18:307-313.
30. Force and Torque on a Small Magnetic Dipole. http://www.physicsinsights.org/force_on_dipole_1.html. Accessed October 2, 2019.

64 Principles of MRI Safety Physics

31. Chapter 11, section 11.8: Forces on microscopic electric and magnetic dipoles. http://web.mit.edu/6.013_book/www/book.html. Accessed March, 2020.
32. ASTM International, ASTM F2052: Standard test method for measurement of magnetically induced displacement force on medical devices in the magnetic resonance environment. American Society for Testing and Materials (ASTM) International.
33. ASTM International, ASTM F2213: Standard test method for measurement of magnetically induced torque on medical devices in the magnetic resonance environment. American Society for Testing and Materials (ASTM) International.
34. Panych LP, Kimbrell VK, Mukundan S Jr, Madore B. Relative magnetic force measures and their potential role in MRI safety practice. *J Magn Reson Imaging J Magn Reson Imaging*. 2020;51:1260-1271.
35. Budinger TD, Bird MD, Frydman L, et al. Toward 20 T magnetic resonance for human brain studies: Opportunities for discovery and neuroscience rationale. *MAGMA* 2016;29:617-639.
36. Keltner JR, Roos MS, Brakeman PR, Budinger TF. Magnetohydrodynamics of blood flow. *Magn Reson Med* 1990;16:139-149.
37. Kinouchi Y, Yamaguchi H, Tenforde TS. Theoretical analysis of magnetic field interactions with aortic blood flow. *Bioelectromagnetics* 1996;17:21-32.
38. Martin V, Drochon A, Gerbeau JF. Magnetohemodynamics in the aorta and electrocardiograms. *Phys Med Biol* 2012;57:3177-3195.
39. Laudon MK, Webster JG, Frayne R, Grist TM. Minimizing interference from magnetic resonance imagers during electrocardiography. *IEEE Trans Biomed Eng* 1998;45:160-164.
40. Park H, Park Y, Cho S, Jang B, Lee K. New cardiac MRI gating method using event-synchronous adaptive digital filter. *Ann Biomed Eng* 2009;37:2170-2187.
41. Buchenberg WB, Mader W, Hoppe G, et al. *In vitro* study to simulate the intracardiac magnetohydrodynamic effect. *Magn Reson Med* 2015;74:850-857.
42. Crozier S, Trakic A, Wang H, Liu F. Numerical study of currents in workers induced by body-motion around high-ultrahigh field MRI magnets. *J Magn Reson Imaging* 2007;26:1261-1277.
43. Wang H, Takic A, Liu F, Crozier S. Numerical field evaluation of healthcare workers when bending towards high-field MRI magnets. *Magn Reson Med* 2008;59:410-422.
44. International Commission on Non-Ionizing Radiation Protection. ICNIRP Guidelines for limiting exposure to time-varying electric, magnetic and electromagnetic fields (up to 300GHz). *Health Physics* 1998;74:494-522.
45. Condon B, Hadley DM. Potential MR hazard to patients with metallic heart valves: The Lenz effect. *J Magn Reson Imaging* 2000;12:171-176.
46. Hand JW. Modelling the interaction of electromagnetic fields (10 MHz-10 GHz) with the human body: Methods and applications. *Phys Med Biol* 2008;53:R243-286.
47. Collins CM. Numerical field calculations considering the human subject for engineering and safety assurance in MRI. *NMR Biomed* 2009;22:919-926.
48. Hartwig V, Vanello N, Giovannetti G, et al. A novel tool for estimation of magnetic resonance occupational exposure to spatially varying magnetic fields. *MAGMA* 2011;24:323-330.
49. Hartwig V. Engineering for safety assurance in MRI: Analytical, numerical and experimental dosimetry. *Magn Reson Imaging*;33:681-689.
50. Collins CM, Wang Z. Calculation of radiofrequency electromagnetic fields and their effects in MRI of human subjects. *Magn Reson Med* 2011;65:1470-1482.
51. Alon L, Deniz CM, Carluccio G, et al. Effects of anatomical differences on electromagnetic fields, SAR, and temperature change. *Concepts Magn Reson Part B Magn Reson Eng* 2016;46:8-18.
52. Collins CM, Li S, Smith MB. SAR and B1 field distributions in a heterogeneous human head model within a birdcage coil. Specific energy absorption rate. *Magn Reson Med* 1998;40:847-856.

MRI Bioeffects, Safety, and Patient Management **65**

53. Gandhi OP, Chen XB. Specific absorption rates and induced current densities for an anatomy-based model of the human for exposure to time-varying magnetic fields of MRI. *Magn Reson Med* 1999;41:816-823.
54. Collins CM, Smith MB. Calculations of B(1) distribution, SNR, and SAR for a surface coil adjacent to an anatomically-accurate human body model. *Magn Reson Med* 2001;45:692-699.
55. Collins CM, Smith MB. Spatial resolution of numerical models of man and calculated specific absorption rate using the FDTD method: A study at 64 MHz in a magnetic resonance imaging coil. *J Magn Reson Imaging* 2003;18:383-388.
56. Stuchly MA, Abrishamkar H, Strydom ML. Numerical evaluation of radio frequency power deposition in human models during MRI. *Conf Proc IEEE Eng Med Biol Soc* 2006;1:272-275.
57. Murbach M, Cabot E, Neufeld E, et al. Local SAR enhancements in anatomically correct children and adult models as a function of position within 1.5 T MR body coil. *Prog Biophys Mol Biol* 2011;107:428-433.
58. Murbach M, Cabot E, Neufeld E, et al. Whole-body and local RF absorption in human models as a function of anatomy and position within 1.5T MR body coil. *Magn Reson Med* 2014;71:839-845.
59. Gosselin MC, Neufeld E, Moser H, et al. Development of a new generation of high-resolution anatomical models for medical device evaluation: The Virtual Population 3.0. *Phys Med Biol* 2014;59:5287-5303.
60. Li X, Rispoli JV. Toward 7T breast MRI clinical study: Safety assessment using simulation of heterogeneous breast models in RF exposure. *Magn Reson Med* 2019;81:1307-1321.
61. Meliàdò EF, van den Berg CAT, Luijten PR, Raaijmakers AJE. Intersubject specific absorption rate variability analysis through construction of 23 realistic body models for prostate imaging at 7T. *Magn Reson Med* 2019;81:2106-2119.
62. Katscher U, Voigt T, Findeklee C, et al. Determination of electric conductivity and local SAR via B1 mapping. *IEEE Trans Med Imaging* 2009;28:1365-1374.
63. Zhang X, Zhu S, He B. Imaging electric properties of biological tissues by RF field mapping in MRI. *IEEE Trans Med Imaging* 2010;29:474-481.
64. Zhang X, Van de Moortele PF, Liu J, Schmitter S, He B. Quantitative prediction of radio frequency induced local heating derived from measured magnetic field maps in magnetic resonance imaging: A phantom validation at 7T. *Appl Phys Lett* 2014;105:244101.
65. Tiberi G, Costagli M, Biagi L, et al. SAR prediction in adults and children by combining measured B1+ maps and simulations at 7.0 Tesla. *J Magn Reson Imaging* 2016;44:1048-1055.
66. Winkler SA, Picot PA, Thornton MM, Rutt BK. Direct SAR mapping by thermoacoustic imaging: A feasibility study. *Magn Reson Med* 2017;78:1599-1606.
67. Yeung CJ, Atalar E. A Green's function approach to local RF heating in interventional MRI. *Med Phys* 2001;28:826-832.
68. Brix G, Seebass M, Hellwig G, Griebel J. Estimation of heat transfer and temperature rise in partial-body regions during MR procedures: An analytical approach with respect to safety considerations. *Magn Reson Imaging* 2002;20:65-76.
69. Collins CM, Liu W, Wang J, et al. Temperature and SAR calculations for a human head within volume and surface coils at 64 and 300 MHz. *J Magn Reson Imaging* 2004;19:650-656.
70. Wang Z, Lin JC, Vaughan JT, Collins CM. Consideration of physiological response in numerical models of temperature during MRI of the human head. *J Magn Reson Imaging* 2008;28:1303-1308.
71. Wang Z, Collins CM. Effect of RF pulse sequence on temperature elevation for a given time-average SAR. *Concepts Magn Reson Part B Magn Reson Eng* 2010;37B:215-219.
72. van Lier AL, Kotte AN, Raaymakers BW, Lagendijk JJ, van den Berg CA. Radiofrequency heating induced by 7T head MRI: Thermal assessment using discrete vasculature or Pennes' bioheat equation. *J Magn Reson Imaging* 2012;35:795-803.

66 Principles of MRI Safety Physics

73. Ishihara Y, Watanabe H, Okamoto K, Kanamatsu T, Tsukada Y. Temperature monitoring of internal body heating induced by decoupling pulses in animal (13)C-MRS experiments. *Magn Reson Med* 2000;43:796-803.
74. Shapiro EM, Borthakur A, Shapiro MJ, Reddy R, Leigh JS. Fast MRI of RF heating via phase difference mapping. *Magn Reson Med* 2002;47:492-498.
75. Cline H, Mallozzi R, Li Z, McKinnon G, Barber W. Radiofrequency power deposition utilizing thermal imaging. *Magn Reson Med* 2004;51:1129-1137.
76. Wimmer R, Wider G. Real-time imaging of the spatial distribution of RF-heating in NMR samples during broadband decoupling. *J Magn Reson* 2007;187:184-192.
77. Cao Z, Oh S, Otazo R, et al. Complex difference constrained compressed sensing reconstruction for accelerated PRF thermometry with application to MRI-induced RF heating. *Magn Reson Med* 2015;73:1420-1431.
78. Simonis FF, Raaijmakers AJ, Lagendijk JJ, van den Berg CA. Validating subject-specific RF and thermal simulations in the calf muscle using MR-based temperature measurements. *Magn Reson Med* 2017;77:1691-1700.
79. Dempsey MF, Condon B, Hadley DM. Investigation of the factors responsible for burns during MRI. *J Magn Reson Imaging* 2001;13:627-631.
80. Bennett MC, Wiant DB, Gersh JA, et al. Mechanisms and prevention of thermal injury from gamma radiosurgery headframes during 3T MR imaging. *J Appl Clin Med Phys* 2012;13:3613.
81. Busch MH, Vollmann W, Grönemeyer DH. Finite volume analysis of temperature effects induced by active MRI implants: 2. Defects on active MRI implants causing hot spots. *Biomed Eng Online* 2006;5:35.
82. Ballweg V, Eibofner F, Graf H. RF tissue-heating near metallic implants during magnetic resonance examinations: An approach in the ac limit. *Med Phys* 2011;38:5522-5529.
83. Buchli R, Saner M, Meier D, Boskamp EB, Boesiger P. Increased RF power absorption in MR imaging due to RF coupling between body coil and surface coil. *Magn Reson Med* 1989;9:105-112.
84. Langman DA, Goldberg IB, Finn JP, Ennis DB. Pacemaker lead tip heating in abandoned and pacemaker-attached leads at 1.5 Tesla MRI. *J Magn Reson Imaging* 2011;33:426-431.
85. Mattei E, Gentili G, Censi F, Triventi M, Calcagnini G. Impact of capped and uncapped abandoned leads on the heating of an MR-conditional pacemaker implant. *Magn Reson Med* 2015;73:390-400.
86. Yeung CJ, Susil RC, Atalar E. RF safety of wires in interventional MRI: Using a safety index. *Magn Reson Med* 2002;47:187-193.
87. Mattei E, Triventi M, Calcagnini G, et al. Complexity of MRI induced heating on metallic leads: Experimental measurements of 374 configurations. *Biomed Eng Online* 2008;7:11.
88. Rezai AR, Finelli D, Nyenhuis JA, et al. Neurostimulation systems for deep brain stimulation: *In vitro* evaluation of magnetic resonance imaging-related heating at 1.5 Tesla. *J Magn Reson Imaging* 2002;15:241-250.
89. Shrivastava D, Abosch A, Hanson T, et al. Effect of the extracranial deep brain stimulation lead on radiofrequency heating at 9.4 Tesla (400.2 MHz). *J Magn Reson Imaging* 2010;32:600-607.
90. Shellock FG, Begnaud J, Inman DM. Vagus nerve stimulation therapy system: *In vitro* evaluation of magnetic resonance imaging-related heating and function at 1.5 and 3 Tesla. *Neuromodulation* 2006;9:204-213.
91. Sommer T, Vahlhaus C, Lauck G, et al. MR imaging and cardiac pacemakers: In-vitro evaluation and in-vivo studies in 51 patients at 0.5 T. *Radiology* 2000;215:869-879.
92. Nordbeck P, Fidler F, Friedrich MT, et al. Reducing RF-related heating of cardiac pacemaker leads in MRI: Implementation and experimental verification of practical design changes. *Magn Reson Med* 2012;68:1963-1972.
93. Konings MK, Bartels LW, Smits HF, Bakker CJ. Heating around intravascular guidewires by resonating RF waves. *J Magn Reson Imaging* 2000;12:79-85.

MRI Bioeffects, Safety, and Patient Management **67**

94. Armenean C, Perrin E, Armenean M, Beuf O, Pilleul F, Saint-Jalmes H. RF-induced temperature elevation along metallic wires in clinical magnetic resonance imaging: Influence of diameter and length. *Magn Reson Med* 2004;52:1200-1206.
95. Balasubramanian M, Wells WM, Ives JR, et al. RF heating of gold cup and conductive plastic electrodes during simultaneous EEG and MRI. *The Neurodiagnostic Journal* 2017;57:69-83.
96. Erhardt JB, Lottner T, Martinez J, et al. Bock M. It's the little things: On the complexity of planar electrode heating in MRI. *Neuroimage* 2019;195:272-284.
97. Bhusal B, Bhattacharyya P, Baig T, Jones S, Martens M. Measurements and simulation of RF heating of implanted stereo-electroencephalography electrodes during MR scans. *Magn Reson Med* 2018;80:1676-1685.
98. Kugel H, Bremer C, Püschel M, et al. Hazardous situation in the MR bore: Induction in ECG leads causes fire. *Eur Radiol* 2003;13:690-694.
99. Noureddine Y, Kraff O, Ladd ME, et al. *In vitro* and *in silico* assessment of RF-induced heating around intracranial aneurysm clips at 7 Tesla. *Magn Reson Med* 2018;79:568-581.
100. Noureddine Y, Kraff O, Ladd ME, et al. Radiofrequency induced heating around aneurysm clips using a generic birdcage head coil at 7 Tesla under consideration of the minimum distance to decouple multiple aneurysm clips. *Magn Reson Med* 2019;82:1859-1875.
101. Nordbeck P, Fidler F, Weiss I, et al. Spatial distribution of RF-induced E-fields and implant heating in MRI. *Magn Reson Med* 2008;60:312-319.
102. Pictet JI, Meuli R, Wicky S, van der Klink JJ. Radiofrequency heating effects around resonant lengths of wire in MRI. *Phys Med Biol* 2002;47:2973-2985.
103. Rawle WD. A numerical technique for wire antenna design. *High frequency electronics* 2006:42-47.
104. Park SM, Kamondetdacha R, Nyenhuis JA. Calculation of MRI-induced heating of an implanted medical lead wire with an electric field transfer function. *J Magn Reson Imaging* 2007;26:1278-1285.
105. Bayjja M, Boussouis M, Amar Toiuhami N, Zeljami K. Comparison between solution of Pocklington's and Hallen's integral equations for thin wire antennas using method of moments and Haar wavelet. *Int J Innovation Appl Studies* 2015;12:931-942.
106. Nitz WR, Oppelt A, Renz W, et al. On the heating of linear conductive structures as guide wires and catheters in interventional MRI. *J Magn Reson Imaging* 2001;13:105-114.
107. Acikel V, Atalar E. Modeling of radio-frequency induced currents on lead wires during MR imaging using a modified transmission line method. *Med Phys* 2011;38:6623-6632.
108. Özen AC, Lottner T, Bock M. Safety of active catheters in MRI: Termination impedance versus RF-induced heating. *Magn Reson Med* 2019;81:1412-1423.
109. Missoffe A, Aissani S. Experimental setup for transfer function measurement to assess RF heating of medical leads in MRI: Validation in the case of a single wire. *Magn Reson Med* 2018;79:1766-1772.
110. Tokaya JP, Raaijmakers AJE, Luijten PR, Bakker JF, van den Berg CAT. MRI-based transfer function determination for the assessment of implant safety. *Magn Reson Med* 2017;78:2449-2459.
111. Tokaya JP, Raaijmakers AJE, Luijten PR, van den Berg CAT. MRI-based, wireless determination of the transfer function of a linear implant: Introduction of the transfer matrix. *Magn Reson Med* 2018;80:2771-2784.
112. van den Bosch MR, Moerland MA, Lagendijk JJ, Bartels LW, van den Berg CA. New method to monitor RF safety in MRI-guided interventions based on RF induced image artefacts. *Med Phys* 2010;37:814-821.
113. Overall WR, Pauly JM, Stang PP, Scott GC. Ensuring safety of implanted devices under MRI using reversed RF polarization. *Magn Reson Med* 2010;64:823-833.
114. Griffin GH, Anderson KJ, Celik H, Wright GA. Safely assessing radiofrequency heating potential of conductive devices using image-based current measurements. *Magn Reson Med* 2015;73:427-441.
115. Griffin GH, Ramanan V, Barry J, Wright GA. Toward *in vivo* quantification of induced RF currents on long thin conductors. *Magn Reson Med* 2018;80:1922-1934.

68 Principles of MRI Safety Physics

116. Eryaman Y, Kobayashi N, Moen S, et al. A simple geometric analysis method for measuring and mitigating RF induced currents on Deep Brain Stimulation leads by multichannel transmission/reception. *Neuroimage* 2019;184:658-668.
117. Ehses P, Fidler F, Nordbeck P, et al. MRI thermometry: Fast mapping of RF-induced heating along conductive wires. *Magn Reson Med* 2008;60:457-461.
118. Gensler D, Fidler F, Ehses P, et al. MR safety: Fast T₁ thermometry of the RF-induced heating of medical devices. *Magn Reson Med* 2012;68:1593-1599.
119. Dixit N, Stang PP, Pauly JM, Scott GC. Thermo-acoustic ultrasound for detection of RF-induced device lead heating in MRI. *IEEE Trans Med Imaging* 2018;37:536-546.
120. Nordbeck P, Weiss I, Ehses P, et al. Measuring RF-induced currents inside implants: Impact of device configuration on MRI safety of cardiac pacemaker leads. *Magn Reson Med* 2009;61:570-578.
121. Zanchi MG, Venook R, Pauly JM, Scott GC. An optically coupled system for quantitative monitoring of MRI-induced RF currents into long conductors. *IEEE Trans Med Imaging* 2010;29:169-178.
122. Barbier T, Aissani S, Weber N, Pasquier C, Felblinger J. A novel MR-compatible sensor to assess active medical device safety: Stimulation monitoring, rectified radio frequency pulses, and gradient-induced voltage measurements. *MAGMA* 2018;31:677-688.
123. McJury MJ. Acoustic noise levels generated during high field MR imaging. *Clin Radiol* 1995;50:331-334.
124. Counter SA, Olofsson A, Grahn HF, Borg E. MRI acoustic noise: Sound pressure and frequency analysis. *J Magn Reson Imaging* 1997;7:606-611.
125. Ravicz ME, Melcher JR, Kiang NY. Acoustic noise during functional magnetic resonance imaging. *J Acoust Soc Am* 2000;108:1683-1696.
126. Foster JR, Hall DA, Summerfield AQ, Palmer AR, Bowtell RW. Sound-level measurements and calculations of safe noise dosage during EPI at 3 T. *J Magn Reson Imaging* 2000;12:157-163.
127. Brummett RE, Talbot JM, Charuhas P. Potential hearing loss resulting from MR imaging. *Radiology* 1988;169:539-540.
128. Irnich W, Schmitt F. Magnetostimulation in MRI. *Magn Reson Med* 1995;33:619-623.
129. Recoskie BJ, Scholl TJ, Zinke-Allmang M, Chronik BA. Sensory and motor stimulation thresholds of the ulnar nerve from electric and magnetic field stimuli: Implications to gradient coil operation. *Magn Reson Med* 2010;64:1567-1579.
130. Cohen MS, Weisskoff RM, Rzedzian RR, Kantor HL. Sensory stimulation by time-varying magnetic fields. *Magn Reson Med* 1990;14:409-414.
131. Davids M, Guérin B, Vom Endt A, Schad LR, Wald LL. Prediction of peripheral nerve stimulation thresholds of MRI gradient coils using coupled electromagnetic and neurodynamic simulations. *Magn Reson Med* 2019;81:686-701.
132. McNab JA, Edlow BL, Witzel T, et al. The human connectome project and beyond: Initial applications of 300 mT/m gradients. *Neuroimage* 201;80:234-245.
133. Buechler DN, Durney CH, Christensen DA. Calculation of electric fields induced near metal implants by magnetic resonance imaging switched-gradient magnetic fields. *Magn Reson Imaging* 1997;15:1157-1166.
134. Irnich W, Irnich B, Bartsch C, et al. Do we need pacemakers resistant to magnetic resonance imaging? *Eurropace* 2005;7:353-365.
135. Tandri H, Zviman MM, Wedan SR, et al. Determinants of gradient field-induced current in a pacemaker lead system in a magnetic resonance imaging environment. *Heart Rhythm* 2008;5:462-468.
136. Jung W, Zvereva V, Hajredini B, Jäckle S. Initial experience with magnetic resonance imaging-safe pacemakers: A review. *J Interv Card Electrophysiol* 2011;32:213-219.
137. Bassen HI, Angelone LM. Evaluation of unintended electrical stimulation from MR gradient fields. *Front Biosci (Elite Ed)* 2012;4:1731-1742.

MRI Bioeffects, Safety, and Patient Management **69**

138. Aissani S, Laistler E, Felblinger J. MR safety assessment of active implantable medical devices. *Radiologe* 2019;59(Suppl 1):40-45.
139. Graf H, Steidle G, Schick F. Heating of metallic implants and instruments induced by gradient switching in a 1.5-Tesla whole-body unit. *J Magn Reson Imaging* 2007;26:1328-1333.
140. El Bannan K, Handler W, Chronik B, Salisbury SP. Heating of metallic rods induced by time-varying gradient fields in MRI. *J Magn Reson Imaging* 2013;38:411-416.
141. Brühl R, Ihlenfeld A, Ittermann B. Gradient heating of bulk metallic implants can be a safety concern in MRI. *Magn Reson Med* 2017;77:1739-1740.
142. Zilberti L, Arduino A, Bottauscio O, Chiampi M. The underestimated role of gradient coils in MRI safety. *Magn Reson Med* 2017;77:13-15.
143. Graf H, Lauer UA, Schick F. Eddy-current induction in extended metallic parts as a source of considerable torsional moment. *J Magn Reson Imaging* 2006;23:585-590.
144. Fuhrer E, Jouda M, Klein CO, Wilhelm M, Korvink JG. Gradient-induced mechanical vibration of neural interfaces during MRI. *IEEE Trans Biomed Eng* 2020;67:915-923.
145. Bottomley PA, Kumar A, Edelstein WA, Allen JM, Karmarkar PV. Designing passive MRI-safe implantable conducting leads with electrodes. *Med Phys* 2010;37:3828-3843.
146. Ladd ME, Quick HH. Reduction of resonant RF heating in intravascular catheters using coaxial chokes. *Magn Reson Med* 2000;43:615-619.
147. Gray RW, Bibens WT, Shellock FG. Simple design changes to wires to substantially reduce MRI-induced heating at 1.5 T: Implications for implanted leads. *Magn Reson Imaging* 2005;23:887-891.
148. Weiss S, Vernickel P, Schaeffter T, Schulz V, Gleich B. Transmission line for improved RF safety of interventional devices. *Magn Reson Med* 2005;54:182-189.
149. Negishi M, Abildgaard M, Laufer I, Nixon T, Constable RT. An EEG (electroencephalogram) recording system with carbon wire electrodes for simultaneous EEG-fMRI (functional magnetic resonance imaging) recording. *J Neurosci Methods* 2008;173:99-107.
150. Golestanirad L, Angelone LM, Iacono MI, et al. Local SAR near deep brain stimulation (DBS) electrodes at 64 and 127 MHz: A simulation study of the effect of extracranial loops. *Magn Reson Med* 2017;78:1558-1565.
151. Griffin GH, Anderson KJ, Wright GA. Miniaturizing floating traps to increase RF safety of magnetic-resonance-guided percutaneous procedures. *IEEE Trans Biomed Eng* 2017;64:329-340.
152. Eryaman Y, Akin B, Atalar E. Reduction of implant RF heating through modification of transmit coil electric field. *Magn Reson Med* 2011;65:1305-1313.
153. Etezadi-Amoli M, Stang P, Kerr A, Pauly J, Scott G. Controlling radiofrequency-induced currents in guidewires using parallel transmit. *Magn Reson Med* 2015;74:1790-1802.
154. Gudino N, Sonmez M, Yao Z, et al. Parallel transmit excitation at 1.5 T based on the minimization of a driving function for device heating. *Med Phys* 2015;42:359-371.
155. Golestanirad L, Keil B, Angelone LM, et al. Feasibility of using linearly polarized rotating birdcage transmitters and close-fitting receive arrays in MRI to reduce SAR in the vicinity of deep brain simulation implants. *Magn Reson Med* 2017;77:1701-1712.
156. Golestanirad L, Kazemivalipour E, Keil B, et al. Reconfigurable MRI coil technology can substantially reduce RF heating of deep brain stimulation implants: First *in-vitro* study of RF heating reduction in bilateral DBS leads at 1.5 T. *PLoS One* 2019;14:e0220043.
157. Kazemivalipour E, Keil B, Vali A, et al. Reconfigurable MRI technology for low-SAR imaging of deep brain stimulation at 3T: Application in bilateral leads, fully-implanted systems, and surgically modified lead trajectories. *Neuroimage* 2019;199:18-29.
158. Choli M, Blaimer M, Breuer FA, et al. Combined acquisition technique (CAT) for high-field neuroimaging with reduced RF power. *MAGMA* 2013;26:411-418.

70 Principles of MRI Safety Physics

159. Brunner DO, Pruessmann KP. Optimal design of multiple-channel RF pulses under strict power and SAR constraints. *Magn Reson Med* 2010;63:1280-1291.
160. Wu X, Akgün C, Vaughan JT, et al. Adapted RF pulse design for SAR reduction in parallel excitation with experimental verification at 9.4 T. *J Magn Reson* 2010;205:161-170.
161. Sbrizzi A, Hoogduin H, Lagendijk JJ, et al. Fast design of local N-gram-specific absorption rate-optimized radiofrequency pulses for parallel transmit systems. *Magn Reson Med* 2012;67:824-834.
162. Boulant N, Wu X, Adriany G, et al. Direct control of the temperature rise in parallel transmission by means of temperature virtual observation points: Simulations at 10.5 Tesla. *Magn Reson Med* 2016;75:249-256.
163. Deniz CM, Alon L, Brown R, Zhu Y. Subject- and resource-specific monitoring and proactive management of parallel radiofrequency transmission. *Magn Reson Med* 2016;76:20-31.
164. Destruel A, Fuentes M, Weber E, et al. A numerical and experimental study of RF shimming in the presence of hip prostheses using adaptive SAR at 3 T. *Magn Reson Med* 2019;81:3826-3839.
165. Destruel A, O'Brien K, Jin J, et al. Adaptive SAR mass-averaging framework to improve predictions of local RF heating near a hip implant for parallel transmit at 7 T. *Magn Reson Med* 2019;81:615-627.
166. McElcheran CE, Yang B, Anderson KJT, Golestanirad L, Graham SJ. Parallel radiofrequency transmission at 3 Tesla to improve safety in bilateral implanted wires in a heterogeneous model. *Magn Reson Med* 2017;78:2406-2415.
167. Córcoles J, Zastrow E, Kuster N. Convex optimization of MRI exposure for mitigation of RF-heating from active medical implants. *Phys Med Biol* 2015;60:7293-7308.
168. Guerin B, Angelone LM, Dougherty D, Wald LL. Parallel transmission to reduce absorbed power around deep brain stimulation devices in MRI: Impact of number and arrangement of transmit channels. *Magn Reson Med* 2020;83:299-311.
169. Yu Z, Xin X, Collins CM. Potential for high-permittivity materials to reduce local SAR at a pacemaker lead tip during MRI of the head with a body transmit coil at 3 T. *Magn Reson Med* 2017;78:383-386.
170. Brink WM, van den Brink JS, Webb AG. The effect of high-permittivity pads on specific absorption rate in radiofrequency-shimmed dual-transmit cardiovascular magnetic resonance at 3T. *J Cardiovasc Magn Reson* 2015;17:82.
171. Kordzadeh A, De Zanche N. Optimal-permittivity dielectric liners for a 4.7T transceiver array. *Magn Reson Imaging* 2018;48:89-95.
172. McJury M, Stewart RW, Crawford D, Toma E. The use of active noise control (ANC) to reduce acoustic noise generated during MRI scanning: Some initial results. *Magn Reson Imaging* 1997;15:319-322.
173. Alibek S, Vogel M, Sun W, et al. Acoustic noise reduction in MRI using silent scan: An initial experience. *Diagn Interv Radiol* 2014;20:360-363.
174. Shellock FG, Karacozoff AM. Detection of implants and other objects using a ferromagnetic detection system: Implications for patient screening before MRI. *Am J Roentgenol* 2013;201:720-725.
175. Gianesin B, Zefiro D, Paparo F, et al. Characterization of ferromagnetic or conductive properties of metallic foreign objects embedded within the human body with magnetic iron detector (MID): Screening patients for MRI. *Magn Reson Med* 2015;73:2030-2037.
176. Watson RE, Walsh SM, Felmlee JP, Friedman PA, Keene MN. Augmenting MRI safety screening processes: Reliable identification of cardiac implantable electronic devices by a ferromagnetic detector system. *J Magn Reson Imaging* 2019;49:e297-e299.
177. Kalb B, Indik JH, Ott P, Martin DR. MRI of patients with implanted cardiac devices. *J Magn Reson Imaging* 2018;47:595-603.
178. Shellock FG. Reference Manual for Magnetic Resonance Safety, Implants, and Devices: 2020 Edition. Biomedical Research Publishing Group, Los Angeles, CA, 2020.

Chapter 3 MRI Physics and Safety at 7 Tesla

OLIVER KRAFF, PH.D.

Erwin L. Hahn Institute for MR Imaging
University of Duisburg-Essen
Essen, Germany

HARALD H. QUICK, PH.D.

Erwin L. Hahn Institute for MR Imaging
University of Duisburg-Essen
Essen, Germany
and
High-Field and Hybrid MR Imaging
University Hospital Essen
Essen, Germany

INTRODUCTION

Magnetic resonance imaging (MRI) is one of the most flexible tools in diagnostic imaging as well as a highly active field of medical and methodological research (1). In 2015, approximately 37.8 million MRI examinations were performed in the United States (U.S.) alone, with an annual growth rate of around 4% since 2011 (2). However, despite many advances in technology in recent decades, the low sensitivity of MRI remains a limiting factor. Noise in the MRI measurement is not only determined by the underlying hardware, but predominantly by the body to be examined. Consequently, a stronger spin polarization of the body is pursued by using stronger static magnetic fields (B_0). While early work demonstrated that the signal-to-noise ratio (SNR) increases linearly with B_0 , at ultra-high fields (UHF) above 3 T the complete Maxwell equations must be considered, which leads to a more than linear increase in SNR with field strength. Pohmann, et al. (3) experimentally described a supralinear increase ($\text{SNR} \sim B_0^{1.65}$) between 3 and 9.4 T. In a numerical simulation study, Guerin, et al. (4) found a field-strength dependence that varies with the position within the sample. For voxels near the surface of the sample, the SNR increases roughly linearly, while for deeper-lying voxels, the increase can even be quadratic. Since the relationship between SNR and B_0 applies not only to the hydrogen nuclei, but also to all “MR-

72 MRI Physics and Safety at 7 Tesla

“active” nuclei with a resulting non-zero nuclear spin, the increased sensitivity of UHF MR systems also opens up the potential for MR tomography and spectroscopy (MRS) with other nuclei such as ^{19}F , ^{23}Na and ^{31}P . These so-called X-nuclei are used in UHF MRI to gain new insights into pathophysiological processes (5). Furthermore, the SNR increase is also dependent on the parallel imaging acceleration factor. The advantage of higher field strengths is larger at higher acceleration factors compared to non-accelerated imaging (4).

With the introduction of the first 3 T MR systems at the end of the 1990s, this magnetic field strength was regarded as high field, whereby at the turn of the millennium 7 T started to claim the UHF regime. In the meantime, there are research devices with even higher magnetic field strengths. In addition to 9.4 T devices in Tübingen, Germany and Maastricht, the Netherlands, there is already a 10.5 T whole-body MR system in operation at the University of Minnesota. A 130-ton 11.7 T whole-body magnet was delivered to the NeuroSpin Research Center in Paris-Saclay, France in May 2017. Another 11.7 T magnet, in this case a smaller diameter head-only system, is currently being installed at the National Institutes of Health in the U.S.. Furthermore, there are efforts to increase the limit of the magnetic field strength for human use to 14 T or even 20 T in the U.S., Korea, and Europe (6, 7). However, to date, most of the approximately 80 UHF MR systems worldwide operate at 7 T. Of these systems, the majority are first- and second-generation 7 T scanners for investigational use only. Since 2017, the latest (third) generation of 7 T MR systems have been approved by the Food and Drug Administration (FDA) as medical devices for diagnostic imaging of the head, legs, and arms (8). The reason for these anatomical restrictions is due to the unsolved physical challenges at UHF, which have been expertly summarized in several review articles (1, 5). The following sections will provide a brief overview of the differences between 3 T and 7 T scanners, as well as on the technical demands and safety aspects at UHF.

PHYSICS

Key Challenges

A prerequisite for a diagnostically useful MR image is good image quality, which requires homogeneous contrast throughout the imaging volume. At 1.5 or 3 T, a transmit radiofrequency (RF) body coil integrated in the scanner is typically used to provide homogeneous excitation of the spins within the sample volume. A homogeneous RF transmission field, B_1^+ , guarantees that the contrast in the image is only determined by the tissue properties and does not depend on the B_1^+ field distribution of the RF transmission coil. When moving from 1.5 to 3 T, the Larmor resonance frequency increases from 64 MHz to 128 MHz. At the same time, the wavelength of the transmit RF field in tissue decreases from approximately 52 cm at 1.5 T to about 11 cm at 7 T. Constructive and destructive interference of the RF waves can occur as soon as the dimensions of the imaging sample are no longer negligible relative to the wavelength. While such B_1^+ inhomogeneities occur in the abdomen at 3 T, a central brightening and associated inhomogeneities are already observed in the head at 7 T (9). In addition to the field strength dependence of the Larmor frequency, the distribution of different tissue types (fat, muscle, fluids) and their frequency-dependent dielectric properties (conductivity, permittivity) determine how strong the artifacts due to RF inhomogeneities are pronounced.

When exposed to RF fields, energy is absorbed in the lossy human body tissue, which can lead to tissue heating. The amount of energy deposition is expressed by the specific absorption rate (SAR) in units of watts per kilogram (W/kg). Especially at UHF, it is much more likely that foci of RF heating will occur due to the shorter wavelength, representing a significant restriction for many pulse sequences, particularly those relying on large flip angles. In addition, RF coil design and transmit RF strategies in general trying to homogenize the B_1^+ field must also be optimized for a low SAR load.

The third key challenge of UHF MRI refers to the topic of implant safety, which will be discussed in other chapters in this textbook. Both for a clinically indicated MRI scan and for a research study, the user is often confronted with the issue of implant safety since few biomedical implants have been evaluated for exposure to 7 T MRI.

Differences Between 3 T and 7 T

Similar to 1.5 or 3 T, a UHF MR system comprises three main components. A superconducting magnet generates a homogeneous static magnetic field for spin polarization. During imaging, radio waves are switched for spin excitation via a transmit RF coil. For spatial encoding, a set of gradient coils generates magnetic gradient fields, which are switched in the kHz range. The amendment of the International Electrotechnical Commission (IEC) standard 60601-2-33 from 2015 increased the First Level Operating Mode limit for the static magnetic field of the MR system from 4 T to 8 T (10). This is in line with the FDA declaration from 2003 that MRI up to 8 T constitutes a non-significant risk for adults, children, and infants of 1 month and older (11). Similarly, a report from the International Commission on Non-Ionizing Radiation Protection (ICNIRP) from 2009 (12) as well as other peer-reviewed scientific literature indicated no serious health effects resulting from acute exposure to static magnetic fields up to 8 T (13-15). Safety aspects at UHF have been expertly summarized in several review articles (1, 16, 17) and will be discussed in detail in a dedicated section of this chapter.

Superconducting Magnets

There are currently five different 7 T magnets for human MRI applications. The first magnet generation consisted of whole-body systems with passive shielding by installing approximately 400 tons of steel in the MR system room. In the second generation, after the year 2010, actively shielded magnets were introduced, both as whole-body and as head-only systems. All three magnet types were built by Magnex Scientific (now Agilent Technologies LDA, UK), but are no longer manufactured or offered. Since 2017, Siemens Healthcare has been offering a new, actively-shielded 7 T whole-body magnet from its own production, which is also part of the medical device MAGNETOM Terra (Siemens Healthcare GmbH, Erlangen, Germany) (18). In addition, the British magnet manufacturer Tesla Engineering Ltd. has announced to provide a 7 T whole-body MR system together with GE Healthcare in the future (19).

From a safety consideration, the attractive force on magnetizable objects is the number one risk factor in the MRI environment. The force on a paramagnetic or (non-saturated) ferromagnetic device is a product of magnetic field (B_0) and spatial gradient magnetic field ((dB_0 / dx)). The type of magnet shielding has an influence on the spatial magnetic field gra-

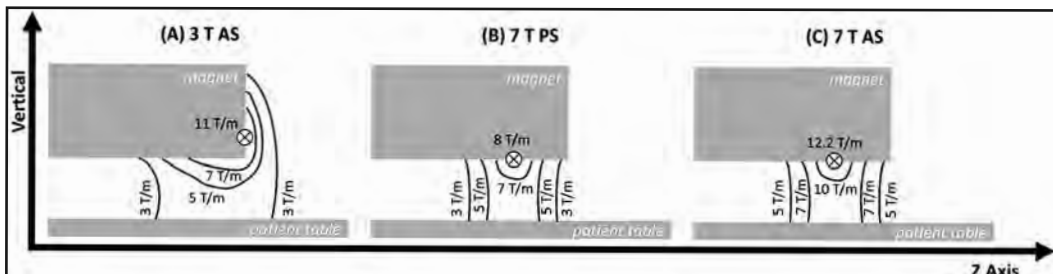
74 MRI Physics and Safety at 7 Tesla

dients, which are much steeper with active shielding than with passive shielding of the magnet. Similarly, a more compact design of the magnet affects the magnetic fringe field. **Figure 1** shows a schematic comparison of different magnet types. It can be seen that the distribution of the spatial gradient magnetic field of an actively-shielded 3 T magnet is very similar to that of a passively-shielded 7 T magnet. With actively-shielded 7 T magnets, slightly higher spatial magnetic field gradients occur with 5 to 10 T/m compared to passively-shielded 7 T or actively-shielded 3 T magnets (3 to 7 T/m). Overall, the attractive force at 7 T can be up to 2.3 times stronger than at 3 T. Since for “MR Safe” and “3 T MR Conditional” certified implants the maximum allowable forces tends to be less than the gravitational force, at least slightly paramagnetic objects made of titanium or aluminum will, therefore, not experience significant translational deflections or force even at 7 T. However, the true problem lies in the description of the implant information in accordance with the applicable ASTM International standard F2503 (20). As already described by Kanal, et al. (21) the implant labeling information does not specify the measured deflection angle. Consequently, one does not know if at 3 T a deflection angle just below the maximum allowed angle of 45° (say, 44°) was measured, or a much lower (i.e., 2°), which even with appropriate scaling to the exposure at 7 T would still be below 45°.

Gradient Coils

The gradient coils used in 7 T and UHF systems are not different from those of current 1.5 T or 3 T MR scanners. For example, the gradient strength amounts to about 80 mT/m with a slew rate of 200 T/m/s. The risk of peripheral nerve stimulation (PNS) in the patient or subject due to gradient switching, thus, remains the same across static magnetic field strengths. In large metallic implants, especially those that form closed loops, the rapidly switched gradient fields can induce electric fields and, thus, eddy currents. In various stud-

Figure 1. Side view of various magnet types (front quadrant, patient end) and a comparison of their respective, exemplary distributions of the spatial gradient magnetic fields. Part (A) shows a MAGNETOM Skyra 3 T actively-shielded (AS) magnet compared to a passively-shielded (PS) 7 T (first generation) magnet in (B), and an actively-shielded 7 T magnet of type MAGNETOM Terra shown in (C). The values displayed were obtained from the respective compatibility data sheets with the permission of Siemens Healthcare GmbH. The plots were schematically drawn and do not reflect the exact courses or distributions. Marked (cross inside of a circle) are the positions where the force on a magnetically saturated ferromagnetic object is greatest. Modified from Reference 94. Kraff O, Quick HH. Safety of implants in high field and ultrahigh field MRI. Radioloe 2019;59:898-905 with permission from Springer Nature.

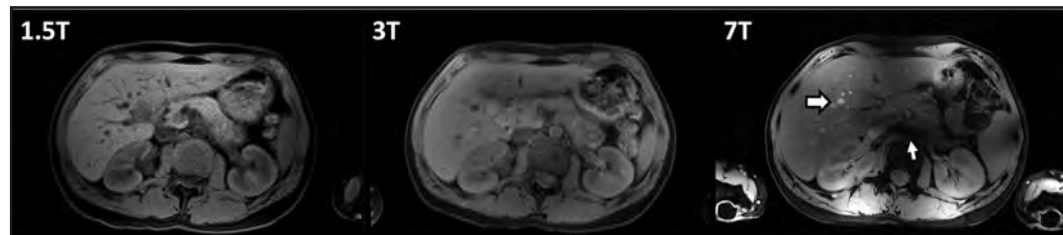


ies, gradient-induced heating of the implant and, hence, of the surrounding tissue, has been reported as an often disregarded safety concern with larger implants, such as total hip prostheses (22). However, as in the case of PNS, the risk would not increase with increasing static magnetic field strengths. It rather depends on the pulse sequence and the performance and design of the gradient coil, only. On the other hand, it should be noted that Lorentz forces might act on the implant via the induced currents in the static magnetic field, which can then put the implant into rapid vibration, which may be an unpleasant or disconcerting sensation for the patient. The Lorentz forces and magnitude of the vibration would be larger at 7 T due to the higher static magnetic field compared to 3 T. Similarly, currents in the gradient coils impose Lorentz forces, which lead to physical vibrations of the magnet structure of the MR system and, thus, cause acoustic noise. In theory, one would expect higher acoustic noise levels for higher static magnetic fields. However, with improved insulation against sound and vibration, sound pressure levels in practice are only slightly higher at 7 T compared to 3 T.

RF Coils

While 1.5 or 3 T MR systems nearly exclusively use an transmit RF birdcage (BC) coil integrated in the scanner for spin excitation and additional sets of local RF receive coils for reception, UHF systems use local RF coils only, which therefore must have both transmit RF and receive capabilities. The reason is that the B_1^+ inhomogeneities at 7 T due to reduced RF excitation wavelength are so severe in the body (**Figure 2**), that a standard volume body coil with only one transmit RF channel does not make sense at 7 T and, therefore, it is not integrated in current UHF MR systems. Compared to 1.5 T and 3 T where RF coils only need to provide RF receive capabilities, the availability of commercially available transmit/receive RF coils at 7 T is rather small. The major manufacturers offer local transmit RF/receive coils for the head and extremities. Smaller spin-offs from universities provide 7 T RF arrays for body applications, but most 7 T transmit/receive RF coils remain custom-built prototypes developed at different institutions. A detailed overview of this topic can be found in our 2019 publication (23). However, it must be noted that for clinical scanning at

Figure 2. Static magnetic field strength comparison in abdominal MR imaging using a gradient echo pulse sequence of similar acquisition time and spatial coverage at 1.5 T (left), at 3 T (center), and 7 T (right) in the same subject. Note the inherently bright vasculature signal (black outlined, white arrow) at 7 T, but also the strong signal void medially (white arrow) due to B_1^+ inhomogeneities. The 7 T acquisition was performed using a local 8-channel transmit/receive body RF coil driven in the first circularly polarized mode, which was also used for the system-integrated transmit/receive body RF coils at 1.5 T and 3 T, respectively.



76 MRI Physics and Safety at 7 Tesla

7 T, only head and extremity scans with certified RF coils are allowed and currently labeled. The most widely used 7 T RF coil is a 1-channel BC transmit / 32-channel receive head coil (Nova Medical, Wilmington, MA, USA) (24), which is also approved for clinical use on the new 7 T MR systems. Also approved for scans in the clinical mode of operation are a dual-tuned 1-channel ^1H / ^{23}Na transmit / 32-channel ^{23}Na receive head coil (Rapid Biomedical GmbH, Würzburg, Germany) and the transmit RF knee coil with integrated 28 receive coils (Quality Electrodynamics, Mayfield Village, OH, USA) (25) shown in **Figure 3**. No other RF coil or multichannel excitation scenario can be used in the clinical setting. Investigational RF coils are only permitted for use when scanning in the research mode on the new 7 T MR systems.

The research mode allows use of multi-channel transmit RF coil arrays that emit the RF waves from several independent coil elements in parallel, similar to radar technology. If one adjusts the amplitude and phase of the RF pulse at the individual spatially distributed coil elements (or even varies the RF pulse itself), B_1^+ inhomogeneities can be successfully reduced or shifted out of the field of view. Here, the number of coil elements (to be considered as a number of setscrews) is crucial, so that most RF coils for UHF MRI provide at least eight independent transmitting elements. The adjustment of amplitude and phase of

Figure 3. Examples of commercially-available RF coils that can be used for imaging in the clinical mode using the MAGNETOM Terra 7 T MR system (Siemens Healthcare GmbH, Erlangen, Germany). Both RF coils in the top row are head coils. Part (A) shows a single channel transmit / 32-channel receive head coil (Nova Medical, Wilmington, MA) for proton imaging, while (B) shows a head coil composed of a double-tuned transmit birdcage and integrated ^{23}Na 32-channel receive array (RAPID Biomedical, Germany) for X-nuclei MR imaging. The bottom row shows RF coils for imaging the extremities. A single channel transmit / 28-channel receive knee coil (Quality Electrodynamics, Mayfield Village, OH) is shown in (C). In (D), a birdcage transmit and 16-channel receive coil for wrist MR imaging is shown.

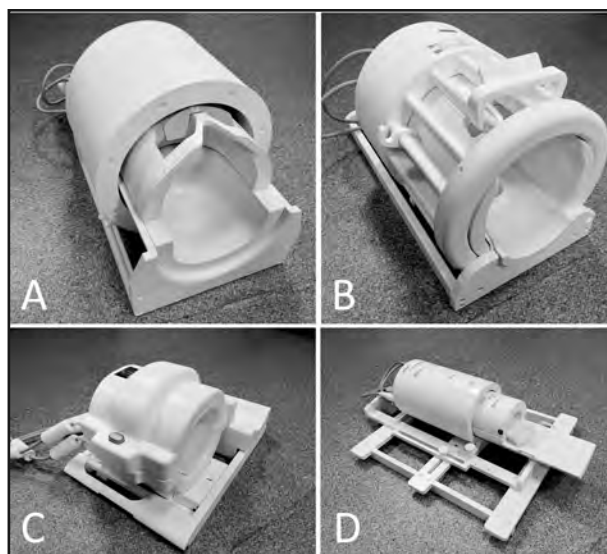
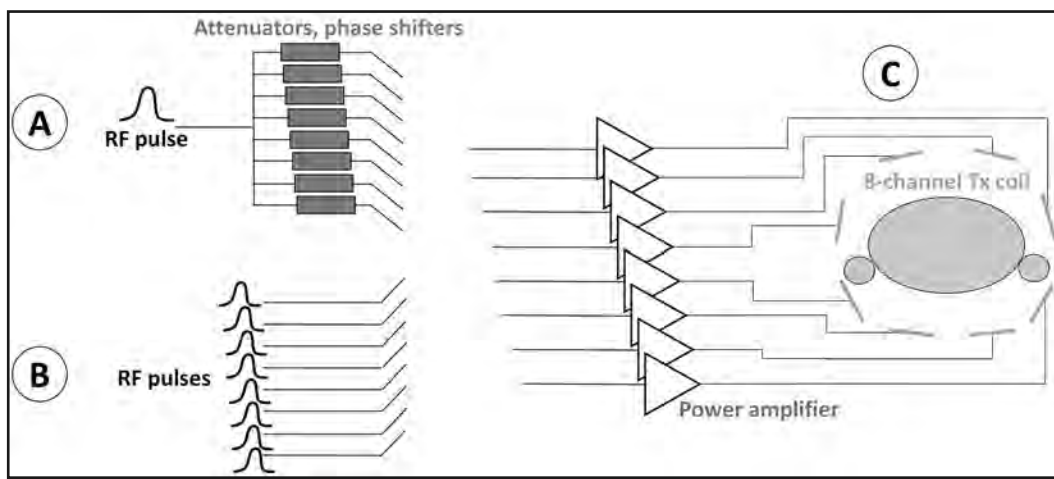


Figure 4. System architectures for RF excitation strategies to minimize B_1^+ inhomogeneities. In RF shimming, a single RF pulse is modulated in amplitude and phase (A) separately for each individual transmit RF coil channel (C). The pulse form, however, remains identical to all channels. In most cases, phase-only RF shimming is applied since amplitude modulation, (i.e., attenuation) also results in a loss in transmit efficiency. For full parallel transmit capability, multiple individual excitors are used (B). This allows the use of different RF pulse forms for each transmit channel (C), which provides maximum control of the resulting transmit field, but also increases the complexity of the system architecture.

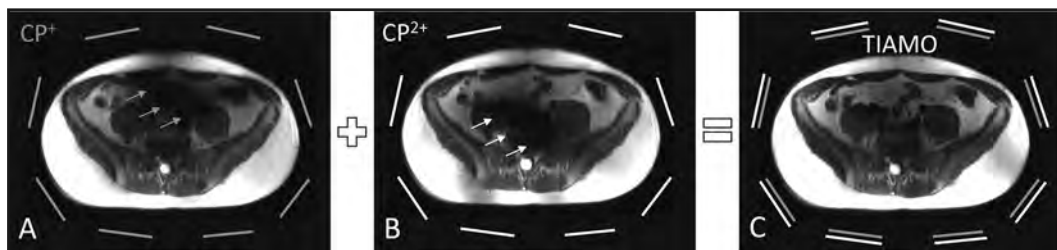


the pulses is referred to as RF shimming (**Figure 4**) (26), and is analogous to shimming the static magnetic field B_0 .

A successful further development of RF shimming at 7 T is the so-called Time-Interleaved Acquisition of Modes or TIAMO technique (27, 28), in which two (or more) inherently inhomogeneous but orthogonal excitations are combined, so that in sum, a homogeneous image is formed (**Figure 5**). Due to the doubling of the measurement time by playing two excitation modes, parallel imaging techniques should be used on the receive side to keep the measurement time short. The advantage here is that the individual excitation modes form virtual elements, which benefit parallel imaging accelerations.

In addition to the aforementioned static RF shimming, where only the relative amplitudes and phases are varied, different RF pulse shapes can also be played out with each coil element. This approach is called “parallel transmit” or transmit SENSE (“SENSitivity Encoding”) (29) and offers the possibility of realizing multidimensional RF pulses either for homogenization of the excitation or for spatially selective excitation. However, these systems are much more complex, not only due to the necessary synchronization of the RF, but also in the RF monitoring to rule out excessive tissue heating. This method also heavily depends on the acquisition of B_1^+ maps of the entire 3D region with sufficient coverage, which can be time-consuming (30). A recent study has investigated the use of “universal pulses” for brain imaging that were designed based on the B_1^+ maps of a few subjects (31). Subsequently, the universal pulses were successfully applied in more subjects without acquiring

Figure 5. Pelvic T2-weighted, single-shot turbo spin echo images of a human volunteer subject demonstrating the TIAMO technique. Both acquisitions used circularly-polarized modes, CP⁺ (A) and CP²⁺ (B), yielding substantial signal voids (arrows). Note that the areas of signal losses appear at different locations depending on the applied excitation mode. Hence, by combining two orthogonal modes with the TIAMO technique (sum of squares algorithm), a nearly homogeneous image can be obtained (C). Due to the different excitation modes, the receive profiles of each RF coil element will change, so that for the combined TIAMO reconstruction, twice the number of physical receive RF coil elements will be available as virtual elements. Thus, the two-fold accelerated, parallel imaging encoding minimizes the scan time penalty and delivers only moderately less SNR than a conventional acquisition with a single excitation mode and full encoding.



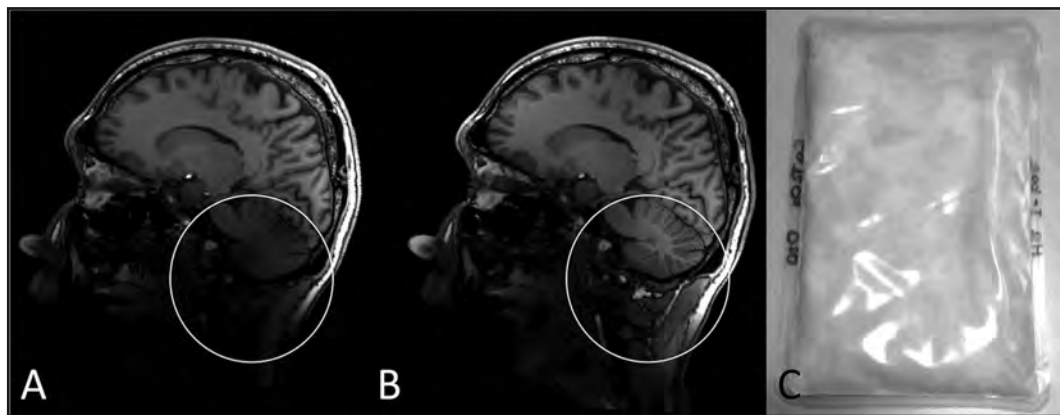
additional calibration data. This approach has the high potential for clinical brain UHF imaging because it substantially reduces the time for calibration, does not require online RF pulse design, and allows a pre-calculation of the expected SAR load. However, for applications in other, more challenging body parts, a successful demonstration of the technique is pending.

A simple and much cheaper way of B_1^+ field homogenization is dielectric shimming (**Figure 6**) (32, 33). With the help of pads containing a material of very high permittivity (e.g., calcium or barium titanate) and deuterium oxide (D_2O , with properties such as water, but not visible in the MR image), the RF field distribution of a RF coil can be influenced so that locally in the vicinity of the pads a higher B_1^+ field is present. Successful applications have been found especially in studies of the cerebellum (33) and inner ear (34), as well as for knee imaging at 7 T (35). On the other hand, proper placement of pads is important, and different pad sizes (and fillings) are often needed to obtain an improvement in B_1^+ , making the technique unsuitable for some applications (36). In addition, with regards to MRI safety, it should be noted that dielectric pads influence the transmit RF field and, thus, may not be allowed for scans in the clinical mode (37, 38).

Pulse Sequences

The relaxation times, T1 and T2, are a function of the strength of the static magnetic field. As a general rule, when the field strength increases from 3 to 7 T, only a slight shortening of the T2 relaxation times occurs, whereas the T1 relaxation time increases depending on the tissue type. For example, the T1 of the gray matter increases from $T1 = 1,197 \pm 134$ ms at 1.5 T, to $1,605 \pm 112$ ms at 3 T, and finally to $1,939 \pm 149$ ms at 7 T (39). Hence, to obtain the same T1-weighted contrast at 1.5 T, the measurement time would have to be in-

Figure 6. RF shimming with high permittivity pads. A sagittal plane MPRAGE MR image is shown in (A). The circle indicates a region of low signal resulting from transmit inefficiency in the cerebellar region of the commercially-available 1-channel transmit/32-channel receive head coil (Nova Medical, Wilmington, MA, USA). However, signal can be successfully regained (B) by placing pads with high permittivity material (C), calcium titanate and deuterium oxide in this case, around the subject's head. Typically, three thin pads are used. Two pads are placed at either side of the subject's head, while the third pad is placed underneath the head in the RF coil. Notably, even a single pad placed underneath the head can improve imaging of the cerebellum. In some subjects with large head sizes, the relatively narrow RF head coil does not allow room to place additional pads.



creased at 7 T. In addition, standard multi-slice, turbo spin echo imaging (TSE), considered the “workhorse” pulse sequence in 1.5 and 3 T clinical imaging protocols, is heavily impaired by B_1^+ inhomogeneities and RF power deposition at 7 T. One way to address these challenges is to replace standard TSE sequences by magnetization-prepared, rapid gradient echo (MPRAGE) sequences that produce an excellent T1-weighted contrast and come with a low SAR profile (**Figure 7**). Optimized versions have been proposed with adiabatic pulses for magnetization preparation to counteract caudal image contrast inversion and signal inhomogeneity (40), typically observed in head RF coils with limited efficiency in the z-direction. On the other hand, the extension of the T1 time of the stationary tissue leads to a marked improvement in image quality, (e.g., in time-of-flight (TOF) angiographies), as the background tissue is better suppressed during the entire measurement because of the lower T1 relaxation at short repetition times (41).

Contrast Agents

The relaxivity of contrast agents is field strength dependent. It is known that, at higher field strengths, the relaxivity of gadolinium chelates increases. This leads to a relative signal increase in T1-weighted sequences, which should at least theoretically lead to an improved contrast-to-noise ratio (CNR). However, these processes are not proportional to each other. Basically, it can be assumed that the CNR between lesion and surrounding tissue improves with appropriately optimized T1-weighted sequences. At the present time, however, there is insufficient experience to generally recommend a reduction in contrast agent dose in UHF

Figure 7. Static magnetic strength comparison of a T1-weighted, MPRAGE pulse sequence at 1.5 T (A), 3 T (B) and 7 T (C). In particular, the transition to 7 T shows clear contrast differences, as in the hyperintense arterial vessel signal (black outlined, white arrow). In addition, artifacts are more obvious at 7 T, such as susceptibility artifacts near the sinuses (white arrow). A caudal signal decreased caused by the local RF transmit and receive coil of limited spatial coverage is also visible at 7 T. At 1.5 and 3 T, an integrated whole-body transmit RF coil was used along with a head and neck coil for RF signal reception.



studies, which of course from a commercial point of view, as well as regarding current discussions on gadolinium deposition in the brain and the risk factors for the development of nephrogenic systemic fibrosis, are highly desirable (42). For this reason, the standard contrast agent dose used at 1.5 T is still predominantly used at 7 T. However, studies have already discussed the possibility of reducing the contrast agent dose down to the complete omission of a contrast-enhanced MRA at 7 T (43). In the case of intracranial MR angiography, the inherently hyperintense arterial vascular signal in gradient echo pulse sequences and excellent time-of-flight (TOF) MRA capabilities allow for a wider range of non-contrast enhanced angiographic sequences at 7 T than at 1.5 T or 3 T (44, 45).

Susceptibility and Chemical Displacement

With increasing field strength, MR imaging becomes much more prone to susceptibility effects, which can cause substantial problems for example in the visualization of tissue near air-filled areas such as the sinuses (**Figure 7**) or intestines at UHF. A given susceptibility difference causes larger magnetic field differences at 7 T than at 3 T or 1.5 T. The resulting faster spin dephasing can be described as shortened T_2^* time. This is an advantage in the visualization of venous architecture or microbleeds with SWI (susceptibility weighted imaging) (46, 47), as well as for functional imaging (BOLD contrast) (48).

The frequency difference between protons in water and in fat molecules is about 3.4 ppm of the resonance frequency. In absolute units, this is about 217 Hz at 1.5 T, and almost five-fold at 7 T with it being 1.01 kHz. For a fixed bandwidth of the pulse sequence, the shift of the fat versus the water protons, and accordingly the chemical-shift artifact, is almost five times as large. Such large water-fat shifts can significantly affect image quality. In addition to increasing the bandwidth, which, however, causes a loss of SNR, the application

of fat suppression techniques may be helpful to reduce or eliminate chemical-shift artifacts. Frequency-selective fat saturation techniques are of considerable importance in high-field imaging but require good B_0 field homogenization by powerful shimming techniques. They have the disadvantage of increasing the RF heat input into the tissue through the additionally required high-frequency pulses. In addition, these RF pulses prolong the overall acquisition time.

Table 1 provides a brief overview of properties that change with increasing static magnetic field strength.

Table 1. Properties that change with increasing static magnetic field strength.

SNR	The supralinear increase in SNR allows the acquisition of much higher spatial resolution at UHF compared to lower static magnetic field strengths. Investing SNR for shorter acquisition times, however, is often prohibited by SAR constraints at UHF.
Sensitivity	The gain in SNR makes X-nuclei MR applications possible at UHF. In particular, ^{23}Na and ^{31}P have shown clinical values at 7 T, but also other nuclei have been successfully imaged.
Artifacts	Not only the SNR, but also the artifact-to-noise ratio increases with increasing static magnetic fields, leading to more pronounced artifacts at UHF. In particular, susceptibility artifacts near air-filled cavities and chemical-shift artifacts introduce challenges.
Susceptibility	Stronger susceptibility changes result in stronger artifacts due to faster dephasing and greater distortion. On the other hand, they are diagnostically beneficial in depicting venous architecture or microbleeds, as well as for functional MRI.
Relaxation Times	The increase in T1 time causes longer acquisition times, but also improves the background saturation in time-of-flight MR angiography. The T2 and T2* times are slightly shortened, which is beneficial for susceptibility imaging and BOLD imaging, but detrimental for diffusion weighted imaging due to long echo times.
Contrast Agents	The higher relaxivity of Gadolinium has generally not led to a reduction in the dosage at UHF MR imaging. The hyperintense arterial vasculature in native gradient echo sequences, however, may allow for complete elimination of contrast-enhanced MR angiography at UHF in selected vascular regions.
Chemical Displacement	The fat-water shift increases with increasing static magnetic fields, resulting in better spectral resolution and fat saturation, but also enhances chemical shift artifacts.
RF Homogeneity	The shortened wavelength causes constructive and destructive interference, which leads to strong flip angle variations and contrast jumps. This must be compensated by new RF transmission strategies.

SAFETY

Physiological Effects

Exposure to UHF MR systems obviously raises the concern of increased physiologic effects since the interaction between biologic tissue (and fluids) and a strong magnetic field will lead to Lorentz forces and induced currents in a human body. Although these effects will be transient and are considered to be harmless, they can be perceived as unpleasant by the subject. The Lorentz force on the ionic fluid inside the semicircular ducts, for example, can lead to nystagmus and the mild perception of rotation, which may persist for a short period even after the motion through the magnetic field has stopped (49). Vestibular activation has been shown to last for at least 2:30 min after a half-an-hour exposure to 7 T (50). A recent 10.5 T study showed significantly increased nystagmus at isocenter of the MR system (15).

Similarly, the blood pressure might be elevated since the Lorentz force will lead to additional efforts to transport the electrically conductive blood through the static magnetic field. However, a measured increase of only 3.6 mm Hg in systolic blood pressure at 8 T (51), as well as findings of a recent animal study at 10.5 T, showing an average increase of only 4.5 mm Hg in diastolic blood pressure (52), are far below elevations produced by changing postural position and, therefore, are not of clinical concern.

Currents are induced in tissue when the human body moves through an inhomogeneous magnetic field. These induced currents have been linked to the occurrence of magnetic phosphenes and to unpleasant sensations of vertigo and nausea. This is the case for both, a subject being brought into the scanner on the patient table, and for the MR system operator who occasionally bends into the bore opening for cleaning purposes, to plug in RF coils, or to set up auxiliary equipment like back-projection screens for visual stimulation in functional MRI (fMRI) studies. Although physiologic effects are higher at UHF compared to lower static magnetic fields, a multi-center study reported that only 0.9%, (i.e., 31/3,404) participants said that they would not undergo a subsequent UHF MRI study for any reason (14). In other words, 99% of all participants undergoing an UHF MRI study would be willing to undergo another UHF MRI study for research or clinical purposes. In more detail, complained causes of discomfort in these studies were examination duration, followed by acoustic noise and lying still, which are all not directly related to the exposure to a strong static magnetic field. Regarding occupational exposure, in the European Union (EU), minimum standards have been set for electromagnetic (em) exposure of workers across all economic sectors (53). Standards apply for time-varying RF fields over a large frequency range applied during MR imaging, but also for the static magnetic field. Latter is not only the most significant change at UHF, it is also the electromagnetic fields that all workers from different divisions will be exposed to at the MR system, that is MRI technologists or radiographers, nurses supporting a patient, physicians, custodial personnel, service engineers, and others. While 8 T is the limit for localized exposure of the extremities, exposure of the head above 2 T should be avoided in workers. In the case of MRI-related work procedures, the EU em field directive states a derogation rule that permits exceeding the limits, if particular prerequisites are fulfilled. Hence, for the aforementioned tasks that require bending into the bore opening of a UHF MR system, the limit of 2 T for normal working conditions

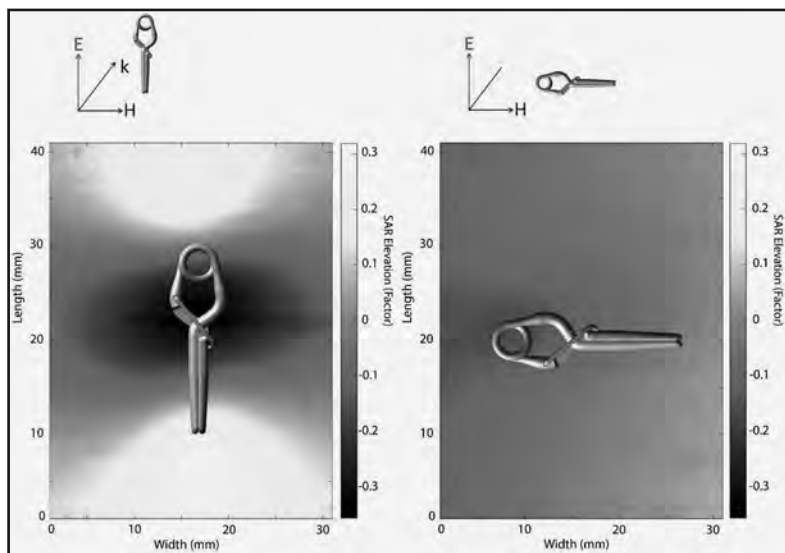
is easily exceeded, which requires special training and documentation to avoid overexposure.

Safety Aspects in Relation to the RF Field

In addition to the projectile effect, the interaction between the emitted transmit RF fields and the human body poses the greatest security risk during an MRI exam. Since there is no integrated standard transmit RF body coil incorporated into UHF MR systems, the variety of local multi-channel transmit RF coils increases the complexity of this safety aspect significantly. During the RF exposure, energy is absorbed in lossy human body tissue causing a heat deposition in the tissue. The degree of heat deposition is described by the associated SAR in units of W/kg. The standard IEC 60601-2-33 sets different limits for a time-averaged SAR in different body parts (10). The SAR limits are the same for all static magnetic field strengths. With increasing excitation frequency, however, the SAR limits are more restricting to pulse sequences and protocols, which require workarounds such as prolonging the repetition time, increasing the RF pulses in time, or reducing the flip angle. In contradiction to the traditionally cited quadratic dependency of SAR with B_0 , studies have shown a flattening of the SAR distribution, which adheres closely to a linear increase with magnetic field strengths above 3 T (54, 55). In particular, this was shown in combination with parallel RF transmission techniques (56). Furthermore, while global SAR values, (i.e., whole-body or partial-body-averaged SAR), are mostly limiting for 1.5 T (64 MHz) and 3 T (128 MHz) MR exams, the local SAR averaged over 10-grams of tissue mass is the most critical aspect at higher excitation frequencies (7 T, 298 MHz). Hence, the safety supervision during 7 T MRI examinations becomes more complex, especially for multichannel RF arrays. For parallel RF transmission operation, SAR becomes a function of the complex RF voltages (amplitude and phase) applied to each individual transmit element of the multichannel RF arrays. However, it has been shown that even volume transmit RF coils at 3 T do not expose uniformly, as assumed, but local limits are also exceeded (57). When going to higher static magnetic fields or higher excitation frequencies, it should be noted that the general characteristic of the RF field profoundly changes. Up to approximately 80 MHz, the quasi-static regime applies, whereas at higher frequencies the electromagnetic regime applies. The latter allows waves to separate from the source and travel in space. At 7 T/298 MHz, the wavelength of the emitted RF is small enough compared to the bore diameter of the conductive magnetic cryostat, so that the lower limit frequency of the lowest waveguide mode is just exceeded and so-called “traveling waves” can propagate within the MR system’s bore (58). Consequently, the RF energy may be absorbed by the body further away from the transmit RF source or interact with distant metallic objects. This crucial aspect must be taken into account in the safety-related discussion of implants and the application of local transmit RF coils. Furthermore, the RF field characteristic changes with increasing frequency to the extent that the coupling in the human body changes due to the frequency-dependent tissue properties. At 7 T, the current density distributions are significantly more complex compared to lower field strengths. Besides polarization effects, local SAR elevations now appear much deeper in the tissue. As shown in several studies, the orientation of the implant to the electric field component of the incidental RF wave determines how much surface currents are induced on the implant (59, 60). The surface currents, in turn, cause electrical field elevations at the ends or edges of the implant, which eventually lead to SAR elevations. **Figure 8** exemplifies the differences between an intracranial aneurysm clip (18.8 mm in length) with

84 MRI Physics and Safety at 7 Tesla

Figure 8. Simulation of an intracranial aneurysm clip for two exposure scenarios. On the left is the case of parallel alignment of the implant relative to the electric field component of the incident RF wave, resulting in an approximately 30% SAR elevation at the ends of the clip. On the right, however, is the case of orthogonal alignment of the clip to the electric field component, which has little effect on the SAR distribution. Adapted from Reference 60. Noureddine Y, Kraff O, Ladd ME, et al. In vitro and in silico assessment of RF-induced heating around intracranial aneurysm clips at 7 Tesla. Magn Reson Med 2018;79:568-581.



parallel alignment to the incident electric field component, which causes a 30% increase in SAR at the ends of the clip, and an orthogonal orientation, which has virtually no influence on the SAR distribution (60). Of note is that, in contrast to temperature, there is no direct correlation between SAR and possible tissue damage. Furthermore, in the vicinity of metallic parts with small dimensions, safety tests based on SAR can yield unreliable results (61). An averaging mass of 10 or even 1-gram is a large volume of tissue with respect to rapidly changing fields from the implant, which may conceal high SAR values and potentially high temperature increases. Therefore, it is important to pay particular attention not to SAR, but to temperature increases in implant safety assessments.

Passive Implants With Safety Evaluation at 7 T

So far, relatively few implants have undergone testing that resulted in being labeled MR Conditional at 7 T by the implant manufacturers. These are mostly very small, non-ferromagnetic implants, such as a pin-sized stents for controlling eye pressure (62), or those with lengths up to 10 mm, as used in otologic applications for ventilation, as well as for a tympanic or stapes prosthesis (63-65). Slightly larger are upper eyelid implants made of platinum-iridium with a length of up to 20 mm (65) and titanium tracheal support implants with a length of 35 mm that have undergone testing (66). The referenced implants can be safely examined in the direct RF exposure volume at 7 T with the MR system operating in

the Normal Operating Mode according to the respective implant manufacturer. The critical implant length for resonance effects and the presence of standing waves typically occurs at half of the wavelength (or integer multiples thereof) of the excitation frequency (67). However, this serves only as a rough guide, since studies have shown that resonance effects can occur even at a quarter of the wavelength (68).

While the critical lengths at 1.5 T correspond to approximately 26 cm and approximately 13 cm at 3 T, several studies have shown temperature increases at an implant length of approximately 5 cm at 7 T. For example, Wezel, et al. (69) studied dental retainer wires of different lengths in intensive numerical simulations and direct temperature measurements. A temperature increase of 1.6°C was measured for a 5 cm long retainer (69). In another work, Oriso, et al. (70) investigated various dental implants, such as crowns, supports and implants of different lengths, which are implanted in the mandible or maxilla. Here, again, the 5 cm long implant showed an experimentally measured temperature increase of 1.6°C. At the 7 T MR system facility in Essen, Germany, more than 100 subjects with retainer wires and almost 300 with general dental implants haven been safely imaged, to date (71, 72). It may be concluded that normal dental implants at 7 T are not an exclusion criterion. However, caution or possible exclusion applies, of course, even at 3 T in the case of large-scale braces or magnetic dental attachments (70). The latter could be demagnetized solely by the exposure to the static magnetic field and would not be able to hold the prosthesis afterwards. Likewise, programmable cerebral spinal fluid (CSF) shunt valves that contain small permanent magnets have been tested for their functionality after exposure to a 7 T magnetic field (73). After insertion into the isocenter of a 7 T MR system, the two programmable shunt valves tested, proGAV 2.0 (Miethke GmbH, Germany) and Codman CERTAS Plus (Codman & Shurtleff, Inc., MA, USA), both lost their functionality of reprogramming and exhibited reverse polarized permanent magnets. While the proGAV 2.0 Shunt Valve maintained its pressure setting, the pressure setting of the Codman CERTAS Plus Shunt Valve changed. The latter also exhibited a deflection angle of 43° on the passively shielded 7 T whole body magnet using the ASTM International deflection angle test (74).

Implants utilized for the fixation of the cranial bone after craniotomy, such as osteosynthesis plates and titanium clips have been tested regarding RF-induced heating in scientific publications (59, 75, 76). Subsequently, Chen, et al. (75) showed in a pre- and postoperative comparison that the image quality is hardly affected by titanium implants at 7 T and that the artifacts are comparable to 3 T (75).

Intracranial aneurysm clips represent a group of implants that may pose a contraindication for patients undergoing MRI examinations, even at 1.5 and 3 T. Some aneurysm clips made from titanium or other non-ferromagnetic materials have been tested and labeled "MR Conditional" for use at 1.5 and/or 3 T. One manufacturer of intracranial aneurysm clips has already identified a product as MR Conditional at 7 T (Sugita Titanium 2 Clip, Mizuho America Inc., CA) (77). In addition, extensive numerical simulations of possible RF induced tissue heating have been published in scientific articles (60, 78). Noureddine, et al. (60) investigated in a first study the previously mentioned dependence on the orientation of the clips relative to the incident electric field. In addition, different implant lengths were studied, with the result that maximum temperature rise occurred at a clip length of about 4 to 5 cm. Since the exact orientation of the clip to the electrical field component during an MRI ex-

86 MRI Physics and Safety at 7 Tesla

amination remains unknown, as well as maybe even the clip length, the authors have calculated a conservative power of 4.6 W for an 8-channel transmit/receive RF head coil. Although this is a reduction of the maximum allowable input power by almost a factor of eight for the specific transmit RF coil, it would still allow application of pulse sequences such as T1-weighted, three-dimensional gradient echo (MPRAGE: magnetization-prepared rapid gradient echo) and susceptibility-weighted imaging (SWI) at 7 T (79). In the case of a known clip length of 18.8 mm or shorter, which is usually the case in practice, the conservative power increases to about 17 W, which is not at all a limitation for common neurological imaging protocols at 7 T. In a second work, Noureddine, et al. (78) studied the effect of multiple aneurysm clips, and in this case using the commercially available 1-channel transmit / 32-channel receive head coil (Nova Medical, Wilmington, MA, USA), which is also approved for clinical use on the new 7 T MR systems. For a minimum distance of 35 mm from one aneurysm clip to another, multiple clips can be considered as independent and not coupled to each other. The conservative input power for the RF coil was calculated to be 3.3 W (possibly limitations in the MPRAGE, no restrictions for SWI), or in the case of a known clip length of 18.8 mm or shorter, a value of 13 W. The authors also showed the influence of different thermoregulation models in the temperature simulations on the maximum permissible power in each exposure case. It should be noted that, not only the choice of the respective model, but the input parameters and other factors, plus the lack of an existing test standard, impacts the results of the various studies.

Further individual safety considerations of implants at 7 T may be found in the peer-reviewed literature. Coronary artery stents were examined for their interaction with the RF field at 7 T. Santoro, et al. (80) reported using numerical simulations and experimental temperature measurements obtained in a phantom within the MR system that a coronary artery stent with a length of 4 cm had no significant increase in temperature when the current IEC limits for local and global SAR were used for the experiment. However, the results correspond to an experimental transmit RF head coil with a diameter of 20 cm, which would never be used in this form for patient imaging. In a follow-up study, Winter, et al. (81) provided an analytical approach that allows the determination of the implant-induced increase in a one gram averaged local SAR for stents of any length and arbitrary RF coil configuration and, thus, estimates a conservative power-limiting factor.

A study on subcutaneously implanted port catheters, which are not located within the transmit RF head coil but still close to its housing and, thus, within the RF exposure volume, showed no relevant temperature increases, either in numerical simulations, nor in experimental measurements. **Table 2** gives an overview of safety assessments of passive implants at 7 T (82).

The aforementioned examples of scientific studies on the safety of biomedical implants revealed that the evaluations were only conducted with regard to specific aspects (e.g., only RF-induced heating) and partly using custom-built RF coils, which renders a generalization or extrapolation to other exposure scenarios problematic. In addition, the necessary safety considerations are the subject of current discussions, since even for 3 T MR systems, the commonly used ASTM International test standard, F2182 (83) used for the determination of RF-induced heating of passive implants has recently undergone substantial revisions. In some of the investigations, this was addressed by new approaches with intensive numerical

Table 2. Overview of various implants that have been tested under certain conditions in association with 7 T MR systems. Readers are advised to always consult the original reference and critically question how the reported results can be extrapolated for a given study subject or patient. Test methods vary, and, most importantly, the utilized transmit RF coil from the safety test in respective references may be different from the one of the individual set-up. Translated and modified from Reference 94. Kraff O, Quick HH. Safety of implants in high field and ultrahigh field MRI. Radiologe 2019;59:898-905 with permission from Springer Nature.

Implant Type	Tests	Result	Reference
Cranial Fixation Plates	RF	No significant heating for up to three implants on a circle of ≥ 6 cm in diameter.	59, 75, 91
Programmable CSF Shunt Valves	B ₀	Reverse polarization of permanent magnets. Partial pressure setting changed.	73
Intracranial Aneurysm Clips	RF, B ₀	Only one product certified by vendor; RF simulation studies permit 7 T imaging with reduced RF power (SAR) settings; high caution generally advised.	60, 77, 78
Middle Ear Implants	RF, B ₀	Many implants MR Conditional at 7 T. However, some ventilation tubes were already labeled MR Unsafe at 1.5 T.	63-65
Upper Eyelid Wire	RF, B ₀	7 T MR Conditional	65
Intraocular Lenses	RF, B ₀	No significant heating for a 6-cm diameter transmit/receive RF surface coil. No significant deflection angles (force) measured at 7 T.	88
Eye Pressure Stent	RF, B ₀	7 T MR Conditional	62
Tantalum Eye Markers	RF	Slight SAR and temperature increases estimated via numerical modeling.	89
Dental Implants	RF, B ₀	Nonmagnetic implants < 4 cm in uncritical length at 7 T, no significant heating.	69, 70
Tracheal Stents	RF	7 T MR Conditional	66
Vascular Port Catheter	RF	No temperature increase measured for ports outside the transmit RF head coil.	82
Coronary Artery Stents	RF	SAR increased estimated via formula.	80, 81
Peripheral Stent Grafts	RF, B ₀	No significant temperature increases measured within a custom-built, transmit RF breast coil and deflection angles were below 33°.	92
Intrauterine Devices	RF, B ₀	No significant heating measured and no significant deflection angles at 7 T.	93
Vascular & Orthopedic Implants, Biopsy Markers	RF, B ₀	Large collection and variety of implants, partly 7 T MR Conditional, partly MR Unsafe.	90

88 MRI Physics and Safety at 7 Tesla

temperature simulations. However, it is important that the reader recognizes differences in the quality of the published publications. Likewise, the transferability of the published results to the respective patient case with regard to the variety of local RF coils and transmission strategies at 7 T must always be critically questioned.

Passive Implants Without Safety Evaluation at 7 T

The majority of implants will certainly not receive a dedicated safety evaluation for 7 T from the implant manufacturers. Likewise, many of these implants will not be in the direct exposure volume of the local transmit RF coil. Thus, using a well-considered, risk versus benefit analysis, the already known advantages of 7 T MRI in neurological and musculoskeletal diagnostic imaging should not be denied to the patient despite the presence of a passive implant, which is labeled MR Conditional at 3 T. However, even in scientific studies, where there is no diagnostic benefit for the subject, the investigator is often confronted with the implant problem. Studies that tend to be the most impacted by the presence on an implant in the patient are those that include many or even exclusively older study subjects. Practically speaking, these investigations cannot be performed with a conservative exclusion rule of “all subjects with implants”, regardless of implant size, type and site of implantation.

In January 2016, the national network German Ultrahigh Field Imaging (GUFI) published a consensus recommendation on the inclusion of study subjects at 7 T and UHF MRI, which was signed by all 13 participating sites (84). The recommendation states that the use of local transmit/receive RF coils has the advantage that the transmit RF exposure volume is substantially lower compared to the large exposure volume of built-in transmit RF coils that are used by 1.5 and 3 T MR systems. Consequently, the power density outside of local transmit RF coils decreases rapidly. For study subjects with passive implants that are labeled MR Conditional at 3 T, that do not contain magnetizable components, and that are located at a certain distance from the transmit RF coil, an overly conservative exclusion would no longer be warranted, as previously required by many ethics committees (84). A flowchart of the decision tree as suggested by the GUFI network is given in **Figure 9**. However, the minimum distance between the implant and the local transmit RF coil depends on both components and must always be discussed individually, on a case-by-case basis. In particular, the aforementioned “traveling wave” effects (58) are to be taken into account, primarily with implants of complex geometry or forming conducting loops, with a dimension of integral multiples of half a wavelength, or partially implanted metallic objects.

Figure 10 shows schematically the inclusion criterion from the UHF site in Essen, Germany (72). The minimum allowable distance between the housing of the transmit RF coil and the implant is 30 cm. Of note is that this value has not been precisely determined by numerical simulations of various exposure scenarios, but rather represents a conservative guideline value for the implants to be discussed in each case. However, the minimum distance seems quite plausible if compared to the SAR distribution in the male human body model Duke (i.e., a member of the Virtual Population, which is a high-resolution, accurate, whole-body anatomical virtual human model of an adult man) using a local 8-channel head coil (**Figure 10 B**). The 10-gram-averaged local SAR is reduced in the chest by -20 dB to the reference value in the head (0 dB), which corresponds to an attenuation by a factor of 100. Less attenuation (-10 dB corresponding to a factor of 10) is observed in the arms

Figure 9. Recommended procedure by the German Ultrahigh Field Imaging (GUFI) network for management of subjects for MR imaging at ultrahigh-field MRI in suspected cases of metallic implants. Adapted from Reference 84. German Ultrahigh Field Imaging (GUFI) Network. Approval of subjects for measurements at ultra-high-field MRI. 2016.

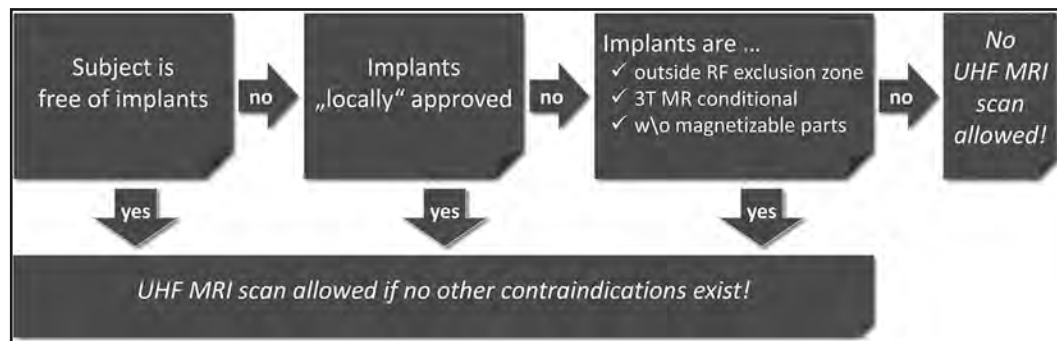
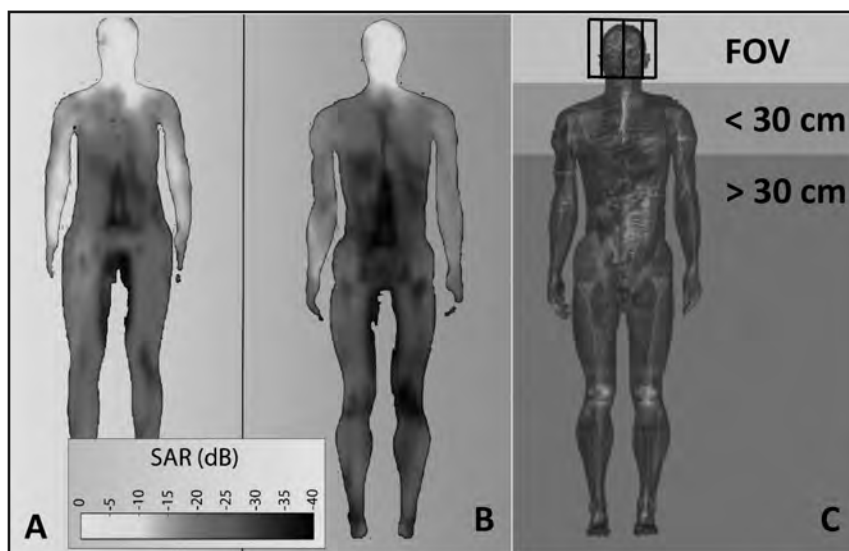


Figure 10. 10-gram-averaged local SAR distributions in the female (A) and male (B) body models for exposure using a local RF head coil at 7 T. On the right (C), the inclusion criterion for subjects with passive implants is exemplarily presented for the 7 T site in Essen, Germany. From a minimum distance of 30 cm to the local transmit RF coil, subjects with 3 T MR Conditional passive implants may be examined at 7 T. However, please note that especially for the female model (A) at the same distance from the RF coil less attenuation can be observed in the arms (-10 dB) compared to the chest region (-20 dB). Therefore, each subject should be managed on a case-by-case in Essen, Germany. Adapted from Reference 72. Noureddine Y, Bitz AK, Ladd ME, et al. Experience with magnetic resonance imaging of human subjects with passive implants and tattoos at 7 T: A retrospective study. Magn Reson Mater Phy 2015;28:577-590.



90 MRI Physics and Safety at 7 Tesla

(**Figure 10 A**), which should be treated more carefully. By way of example, in a retrospective study on the 7 T MR system in Essen, nearly 400 subjects were imaged with implants until April 2018 (71, 72). Large implants such as hip and knee prostheses were also cleared for examinations when using a head coil for RF transmission (71, 85). In over 260 cases in Essen, the implant was in the direct exposure volume of the transmit RF coil (71, 72). Similar to the case of intracranial aneurysm clips, for which conservative RF input powers have been calculated, it is often possible to provide access to MRI exams performed at 7 T by implementing a conservative power limitation without severely restricting the imaging protocol, especially when using predominantly low SAR, gradient echo pulse sequences.

Active Implants

An active implant, according to the definition, contains electrical circuits and/or a power supply. Examples for frequent active implants are cardiac pacemakers, implantable cardioverter defibrillators (ICD), loop recorders, cochlear implants (CI), neuromodulation systems, and implantable drug infusion pumps. Most active implants in the past were labeled “MR Unsafe” and were contraindicated for MRI regardless of the strength of the static magnetic field. Over the last 15 years, however, new active implants (e.g., cardiac pacemakers, ICD, CI, neuromodulation systems, etc.) have been specially designed and tested in the MRI setting, resulting in them being designated as “MR Conditional”, with labeling indicating the acceptable strength of the static magnetic field and specific absorption rate to ensure patient safety. Over the years, countless studies have been conducted at 1.5 and 3 T and guidelines and workflow recommendations have been published regarding the management of patients with active implants. This development from strict contraindication to the availability of MR Conditional, active implants has enabled numerous patients to undergo diagnostic MRI examinations at 1.5 and 3 T.

At the level of 7 T and other UHF MRI, active implants, without exception, have to be considered “MR Unsafe”. Notably, to date, no active implant has been tested and labeled MR Conditional at 7 T. The potential safety risks are high and manifold (magnetic field interactions, RF heating, induced currents, device malfunction, etc.) and there is no diagnostic justification to conduct an MRI exam at 7 T. In other words, if an MRI procedure for a patient with an active implant is potentially indicated, it would have to be conducted at 1.5 or 3 T according to the current labels and conditions specified by the implant manufacturer.

CONCLUSION

Ultra-high field MRI has come a long way since the first installation of a 7 T MR system at the turn of the millennium. Today, the latest generation of the 7 T MR system has been FDA approved as medical device for diagnostic imaging of the head and the extremities. Besides hazards due to the magnetic force that can be up to 2.3 times stronger at 7 T compared to 3 T, increased risks of RF-induced tissue heating are the most critical aspects. The resonant length of an implant at 7 T is approximately 5 cm. Other than at 3 T, MR systems operating at 7 T are less standardized. Especially with regard to the transmit RF coil and transmission methods used. At 7T, considering the inherent technology, substantial differences need to be expected. Hence, it is important to critically question published safety assessments of implants and to have a thorough discussion about how this relates to the

individual patient or study subject exposure scenario. For nonmagnetic implants without a dedicated 7 T safety evaluation, but which are labeled MR Conditional at 3 T and have a certain minimum distance to the transmit RF coil, a consensus recommendation for managing human subjects from the national network German Ultrahigh Field Imaging (GUFI) may be helpful. However, each patient case should be discussed individually and the value of minimum distance should be understood as an approximate guide rather than a fixed landmark, after which everything will be safe. This would certainly be a false interpretation or assumption. It is the responsibility of the institution and MR system operator to ensure the safety of volunteers and patients during the entire exposure to the UHF MRI environment.

Acknowledgement

Portions of this chapter have been translated and modified from Reference 94. Kraff O, Quick HH. Safety of implants in high field and ultrahigh field MRI. Radioloe 2019;59:898-905 with permission from Springer Nature.

REFERENCES

1. Kraff O, Quick HH. 7T: Physics, safety, and potential clinical applications. *J Magn Reson Imaging* 2017;46:1573-1589.
2. IMV. MR Market Outlook Report 2015. Available from: <http://www.imvinfo.com/index.aspx?sec=mri&sub=dis&itemid=200085>.
3. Pohmann R, Speck O, Scheffler K. Signal-to-noise ratio and MR tissue parameters in human brain imaging at 3, 7, and 9.4 Tesla using current receive coil arrays. *Magn Reson Med* 2016;75:801-809.
4. Guerin B, Villena JF, Polimeridis AG, et al. The ultimate signal-to-noise ratio in realistic body models. *Magn Reson Med* 2017;78:1969-1980.
5. Ladd ME, Bachert P, Meyerspeer M, et al. Pros and cons of ultra-high-field MRI/MRS for human application. *Progress Nuc Magn Reson Spectr* 2018;109:1-50.
6. Budinger TF, Bird MD, Frydman L, et al. Toward 20 T magnetic resonance for human brain studies: opportunities for discovery and neuroscience rationale. *Magn Reson Mater Phy* 2016;29:617-639.
7. Wissenschaftsrat. Bericht zur wissenschaftsgeleiteten Bewertung umfangreicher Forschungsinfrastrukturvorhaben für die Nationale Roadmap; Kapitel IV.3 Nationale Biomedizinische Bildgebungseinrichtung (NIF). 2017. Available from: <https://www.wissenschaftsrat.de/download/archiv/6410-17.pdf>. (Accessed 2021).
8. U.S. Food and Drug Administration. FDA clears first 7T magnetic resonance imaging device. October 12, 2017. Available from: <https://www.fda.gov/NewsEvents/Newsroom/PressAnnouncements/ucm580154.htm>. (Accessed 2021).
9. Van de Moortele PF, Akgun C, Adriany G, et al. B(1) destructive interferences and spatial phase patterns at 7 T with a head transceiver array coil. *Magn Reson Med* 2005;54:1503-1518.
10. International Electrotechnical Commission. Medical electrical equipment - Part 2-33: Particular requirements for the safety of magnetic resonance diagnostic devices. IEC 60601-2-33. 3.2 Edition, 2015.
11. United States Food and Drug Administration. Guidance for industry and FDA staff: Criteria for significant risk investigations of magnetic resonance diagnostic devices. 2018.
12. International Commission on Non-Ionizing Radiation Protection. Amendment to the ICNIRP statement on medical magnetic resonance (MR) procedures: Protection of patients. Volume 97: Health Physics. 2009.
13. Groebner J, Umathum R, Bock M, et al. MR safety: Simultaneous B_0 , $d\Phi/dt$, and dB/dt measurements on MR-workers up to 7 T. *Magn Reson Mater Phy* 2011;24:315-322.

92 MRI Physics and Safety at 7 Tesla

14. Rauschenberg J, Nagel AM, Ladd SC, et al. Multicenter study of subjective acceptance during magnetic resonance imaging at 7 and 9.4 T. *Invest Radiol* 2014;49:249-259.
15. Grant AN, Kulesa J, He X, et al. Safety evaluation of human exposure to a 10.5T whole body magnet: Protocol design and preliminary results. In: *Proceedings Intl Soc Magn Reson Med*; 2019. pp. 797.
16. van Osch JP, Webb AG. Safety of ultra-high field MRI: What are the specific risks? *Curr Radiol Rep* 2014;2:8.
17. Hoff MN, McKinney A, Shellock FG, et al. Safety considerations of 7-T MRI in clinical practice. *Radiology* 2019;292:509-518.
18. Siemens Healthcare GmbH. New 7 Tesla MRI research system ready for future clinical use. 2015 Available from: [http://www.siemens.com/press/en/pressrelease/?press=/en/pressrelease/2015/healthcare/pr2015060231hcen.htm&content\[\]](http://www.siemens.com/press/en/pressrelease/?press=/en/pressrelease/2015/healthcare/pr2015060231hcen.htm&content[])=HC. (Accessed 2021)
19. Tesla Engineering Ltd, Magnet Devision. GE Healthcare collaborates with Tesla Engineering Ltd. to produce Ultra High-Field 7.0T MRI systems for research institutions. Available from <http://www.tesla.co.uk/magnet/tesla-engineering-magnet-division-superconducting-magnets/tesla-engineering-magnet-division-mri-magnets.html>. (Accessed 2021).
20. American Society for Testing and Materials (ASTM) International. F2503. Standard Practice for Marking Medical Devices and Other Items for Safety in the Magnetic Resonance Environment. West Conshohocken, PA
21. Kanal E, Froelich J, Barkovich AJ, et al. Standardized MR terminology and reporting of implants and devices as recommended by the American College of Radiology Subcommittee on MR Safety. *Radiology* 2015;274:866-870.
22. Bruhl R, Ihlenfeld A, Ittermann B. Gradient heating of bulk metallic implants can be a safety concern in MRI. *Magn Reson Med* 2017;77:1739-1740.
23. Kraff O, Quick HH. Radiofrequency coils for 7 Tesla MRI. *Topics Magn Reson Imaging* 2019;28:145-158.
24. Ledden PJ, Mareyam A, Wang S, van Gelderen P, Duyn JH. 32 channel receive-only SENSE array for brain imaging at 7T. In: *Proceedings Intl Soc Magn Reson Med Berlin, Germany*; 2007. p. 242.
25. Finnerty M, Yang X, Zheng T, et al. A 7-Tesla high density transmit with 28-channel receive-only array knee coil. In: *Proceedings Intl Soc Magn Reson Med Stockholm, Sweden*; 2010. p. 642.
26. Hoult DI, Phil D. Sensitivity and power deposition in a high-field imaging experiment. *J Magn Reson Imaging* 2000;12:46-67.
27. Orzada S, Maderwald S, Poser BA, et al. RF excitation using time interleaved acquisition of modes (TIAMO) to address B1 inhomogeneity in high-field MRI. *Magn Reson Med* 2010;64:327-333.
28. Orzada S, Maderwald S, Poser BA, et al. Time-interleaved acquisition of modes: An analysis of SAR and image contrast implications. *Magn Reson Med* 2012;67:1033-1041.
29. Zhu Y. Parallel excitation with an array of transmit coils. *Magn Reson Med* 2004;51:775-784.
30. Brunheim S, Gratz M, Johst S, et al. Fast and accurate multi-channel B1+ mapping based on the TIAMO technique for 7T UHF body MRI. *Magn Reson Med* 2018;79:2652-2664.
31. Gras V, Vignaud A, Amadon A, Le Bihan D, Boulant N. Universal pulses: A new concept for calibration-free parallel transmission. *Magn Reson Med* 2017;77:635-643.
32. O'Reilly TP, Webb AG, Brink WM. Practical improvements in the design of high permittivity pads for dielectric shimming in neuroimaging at 7T. *J Magn Reson* 2016;270:108-114.
33. Teeuwisse WM, Brink WM, Webb AG. Quantitative assessment of the effects of high-permittivity pads in 7 Tesla MRI of the brain. *Magn Reson Med* 2012;67:1285-1293.
34. Brink WM, van der Jagt AM, Versluis MJ, Verbist BM, Webb AG. High permittivity dielectric pads improve high spatial resolution magnetic resonance imaging of the inner ear at 7 T. *Invest Radiol* 2014;49:271-277.

MRI Bioeffects, Safety, and Patient Management **93**

35. Fagan A, Amrami K, Frick M, et al. Use of passive B_1^+ shimming via dielectric pads for uniformity improvements in 7T clinical knee imaging. In: Proceedings Intl Soc Mag Reson Med Montréal, QC, Canada; 2019. p. 1430.
36. Kraff O, Lazik-Palm A, Brink W, et al. Evaluation of potential improvements from high permittivity pads for imaging upper extremities at 7 Tesla. In: Proceedings Intl Soc Mag Reson Med Singapore; 2016. p. 3542.
37. Brink WM, van den Brink JS, Webb AG. The effect of high-permittivity pads on specific absorption rate in radiofrequency-shimmed dual-transmit cardiovascular magnetic resonance at 3T. *J Cardiovasc Magn Reson* 2015;17:82.
38. Bitz AK, Kraff O, Orzada S, et al. RF safety evaluation of different configurations of high-permittivity pads used to improve imaging of the cerebellum at 7 Tesla. In: Proceedings Intl Soc Mag Reson Med Milan, Italy; 2014. p. 4892.
39. Wright PJ, Mougin OE, Totman JJ, et al. Water proton T1 measurements in brain tissue at 7, 3, and 1.5 T using IR-EPI, IR-TSE, and MPRAGE: Results and optimization. *Magn Reson Mater Phy* 2008;21:121-130.
40. Wrede KH, Johst S, Dammann P, et al. Caudal image contrast inversion in MPRAGE at 7 Tesla: Problem and solution. *Acad Radiol* 2012;19:172-178.
41. Matsushige T, Kraemer M, Schlamann M, et al. Ventricular Microaneurysms in Moyamoya Angiopathy Visualized with 7T MR Angiography. *Am J Neuroradiol* 2016;37:1669-1672.
42. Fraum TJ, Ludwig DR, Bashir MR, Fowler KJ. Gadolinium-based contrast agents: A comprehensive risk assessment. *J Magn Reson Imaging* 2017;46:338-353.
43. Beiderwellen K, Kraff O, Laader A, et al. Contrast enhanced renal MR angiography at 7 Tesla: How much gadolinium do we need? *Eur J Radiol* 2017;86:76-82.
44. Wrede KH, Matsushige T, Goericke SL, et al. Non-enhanced magnetic resonance imaging of unruptured intracranial aneurysms at 7 Tesla: Comparison with digital subtraction angiography. *Eur Radiol* 2017;27S:354-364.
45. Mattern H, Sciarra A, Godenschweger F, et al. Prospective motion correction enables highest resolution time-of-flight angiography at 7T. *Magn Reson Med* 2018;80:248-258.
46. Moenninghoff C, Kraff O, Maderwald S, et al. Diffuse axonal injury at ultra-high field MRI. *PloS one* 2015;10:e0122329.
47. Dammann P, Wrede KH, Maderwald S, et al. The venous angioarchitecture of sporadic cerebral cavernous malformations: A susceptibility weighted imaging study at 7 T MRI. *J Neurol Neurosurg Psychiatry* 2013;84:194-200.
48. Ugurbil K. Imaging at ultrahigh magnetic fields: History, challenges, and solutions. *Neuroimage* 2018;168:7-32.
49. Mian OS, Li Y, Antunes A, Glover PM, Day BL. On the vertigo due to static magnetic fields. *PloS one* 2013;8:e78748.
50. Theysohn JM, Kraff O, Eilers K, et al. Vestibular effects of a 7 Tesla MRI examination compared to 1.5 T and 0 T in healthy volunteers. *PloS one* 2014;9:e92104.
51. Chakeres DW, Kangarlu A, Boudoulas H, Young DC. Effect of static magnetic field exposure of up to 8 Tesla on sequential human vital sign measurements. *J Magn Reson Imaging* 2003;18:346-352.
52. Eryaman Y, Zhang P, Utecht L, et al. Investigating the physiological effects of 10.5 Tesla static field exposure on anesthetized swine. *Magn Reson Med* 2018;79:511-514.
53. The European Parliament and the European Council, Directive 2007/47/EC amending Council Directive 90/385/EEC on the approximation of the laws of the Member States relating to active implantable medical devices, Council Directive 93/42/EEC concerning medical devices and Directive 98/8/EC concerning the placing of biocidal products on the market. *J Europ Union* 2007(L247): p. 21-55.

94 MRI Physics and Safety at 7 Tesla

54. Collins CM, Smith MB. Signal-to-noise ratio and absorbed power as functions of main magnetic field strength, and definition of “90 degrees” RF pulse for the head in the birdcage coil. *Magn Reson Med* 2001;45:684-691.
55. Lattanzi R, Sodickson DK, Grant AK, Zhu Y. Electrodynamic constraints on homogeneity and radiofrequency power deposition in multiple coil excitations. *Magn Reson Med* 2009;61:315-334.
56. Deniz CM, Vaidya MV, Sodickson DK, Lattanzi R. Radiofrequency energy deposition and radiofrequency power requirements in parallel transmission with increasing distance from the coil to the sample. *Magn Reson Med* 2016;75:423-432.
57. Murbach M, Cabot E, Neufeld E, et al. Local SAR enhancements in anatomically correct children and adult models as a function of position within 1.5 T MR body coil. *Prog Biophys Mol Biol* 2011;107:428-433.
58. Brunner DO, De Zanche N, Frohlich J, Paska J, Pruessmann KP. Travelling-wave nuclear magnetic resonance. *Nature* 2009;457:994-998.
59. Kraff O, Wrede KH, Schoemberg T, et al. MR safety assessment of potential RF heating from cranial fixation plates at 7 T. *Med Phys* 2013;4:042302.
60. Noureddine Y, Kraff O, Ladd ME, et al. *In vitro* and *in silico* assessment of RF-induced heating around intracranial aneurysm clips at 7 Tesla. *Magn Reson Med* 2018;79:568-581.
61. Virtanen H, Keshvari J, Lappalainen R. Interaction of radio frequency electromagnetic fields and passive metallic implants--a brief review. *Bioelectromagnetics* 2006;27:431-439.
62. Glaukos Corporation, iStent Trabecular Micro-Bypass Stent Instructions for Use. Available from: <https://www.glaukos.com>. (Accessed 2021).
63. Thelen A, Bauknecht HC, Asbach P, Schrom T. Behavior of metal implants used in ENT surgery in 7 Tesla magnetic resonance imaging. *Europ Arch Otorhinolaryngol* 2006;263:900-905.
64. Grace Medical Inc., Magnetic Resonance Imaging (MRI) Information for Grace Medical Otologic Implants. Available from: http://www.gracemedical.com/sites/488/uploaded/files/Grace_Medical_MRI_Letter_November_2014.pdf 2014. (Accessed 2021).
65. Kurz Medical Inc., MR Information, Available from: http://www.kurzmed.de/medien/pdf/MR_Information_en_Rev_06.pdf, (Accessed 2021).
66. Novatech SA, Novatech TTS MRI Safety Information. Available from: <https://www.novatech.fr/en/home/>. (Accessed 2021).
67. Nyenhuis JA, Park SM, Kamondetdacha R, et al. MRI and implanted medical devices: Basic interactions with an emphasis on heating. *IEEE Transactions on Device and Materials Reliability* 2005;5:467-480.
68. Yeung CJ, Karmarkar P, McVeigh ER. Minimizing RF heating of conducting wires in MRI. *Magn Reson Med* 2007;58:1028-1034.
69. Wezel J, Kooij BJ, Webb AG. Assessing the MR compatibility of dental retainer wires at 7 Tesla. *Magn Reson Med* 2014;72:1191-1198.
70. Oriso K, Kobayashi T, Sasaki M, et al. Impact of the static and radiofrequency magnetic fields produced by a 7T MR imager on metallic dental materials. *Magn Reson Med Sci* 2016;15:26-33.
71. Kraff O, Berghs RM, Noureddine Y, Ladd ME, Quick HH. Experience with 7 Tesla MRI of human subjects with passive implants and tattoos: An update. In: Proceedings Intl Soc Mag Reson Med Paris, France; 2018. p. 4059.
72. Noureddine Y, Bitz AK, Ladd ME, et al. Experience with magnetic resonance imaging of human subjects with passive implants and tattoos at 7 T: A retrospective study. *Magn Reson Mater Phy* 2015;28:577-590.
73. Wrede KH, Chen B, Sure U, Quick HH, Kraff O. Safety and function of programmable ventriculo-peritoneal shunt valves: An *in vitro* 7 Tesla magnetic resonance imaging study. In: Proceedings Intl Soc Mag Reson Med Honolulu, HI, USA; 2017. p. 5584.

MRI Bioeffects, Safety, and Patient Management **95**

74. American Society for Testing and Materials (ASTM) International. ASTM F2052. Standard test method for measurement of magnetically induced displacement force on medical devices in the magnetic resonance environment. West Conshohocken, PA.
75. Chen B, Schoemberg T, Kraff O, et al. Cranial fixation plates in cerebral magnetic resonance imaging: A 3 and 7 Tesla *in vivo* image quality study. *Magn Reson Mater Phy* 2016;2:389-398.
76. Sammet CL, Yang X, Wassenaar PA, et al. RF-related heating assessment of extracranial neurosurgical implants at 7T. *Magn Reson Imaging* 2013;31:1029-1034.
77. Mizuho America Inc., Sugita Titanium 2 Aneurysm Clips and Appliers. Available from http://www.mizuho.com/wp-content/uploads/2014/05/9-T2-Full-Brochure_6_20_2018.pdf. (Accessed 2021).
78. Noureddine Y, Kraff O, Ladd ME, et al. Radiofrequency induced heating around aneurysm clips using a generic birdcage head coil at 7 Tesla under consideration of the minimum distance to decouple multiple aneurysm clips. *Magn Reson Med* 2019; 82:1859-1875.
79. Kraff O, Hüning BM, Deistung A, et al. On the SAR load of typical head protocols at 7T. In: Proceedings Intl Soc Mag Reson Med Honolulu, HI, USA; 2017. p. 2648.
80. Santoro D, Winter L, Muller A, et al. Detailing radio frequency heating induced by coronary stents: A 7.0 Tesla magnetic resonance study. *PloS one* 2012;7:e49963.
81. Winter L, Oberacker E, Ozerdem C, et al. On the RF heating of coronary stents at 7.0 Tesla MRI. *Magn Reson Med* 2015;74:999-1010.
82. Kraff O, Noureddine Y, Frerk E, et al. RF safety of an implanted port catheter in direct vicinity of a 7T transmit head coil. In: Proceedings Intl Soc Mag Reson Med Honolulu, HI, USA; 2017. p. 5452.
83. American Society for Testing and Materials (ASTM) International. F2182. Standard test method for measurement of radio frequency induced heating on or near passive implants during magnetic resonance imaging. West Conshohocken, PA.
84. German Ultrahigh Field Imaging (GUFI) Network, 2016. Approval of subjects for measurements at ultrahigh-field MRI. Available from http://www.mr-gufi.de/images/documents/Approval_of_subjects_for_measurements_at_UHF.pdf. (Accessed 2021).
85. Barisano G, Culo B, Shellock FG, et al. 7-Tesla MRI of the brain in a research subject with bilateral, total knee replacement implants: Case report and proposed safety guidelines. *Magn Reson Imaging* 2019;57:313-316.
86. Nordbeck P, Ertl G, Ritter O. Magnetic resonance imaging safety in pacemaker and implantable cardioverter defibrillator patients: How far have we come? *Eur Heart J* 2015;36:1505-1511.
87. Sommer T, Luechinger R, Barkhausen J, et al. German Roentgen Society statement on MR imaging of patients with cardiac pacemakers. *RoFo Fortschr Roentgenstr* 2015; 187: 777-787.
88. van Rijn GA, Mourik JE, Teeuwisse WM, Luyten GP, Webb AG. Magnetic resonance compatibility of intraocular lenses measured at 7 Tesla. *Invest Ophthalmol Vis Sci* 2012;53:3449-3453.
89. Oberacker E, Paul K, Huelnhagen T, et al. Magnetic resonance safety and compatibility of tantalum markers used in proton beam therapy for intraocular tumors: A 7.0 Tesla study. *Magn Reson Med* 2017;78:1533-1546.
90. Dula AN, Virostko J, Shellock FG. Assessment of MRI issues at 7 T for 28 implants and other objects. *Am J Roentgenol* 2014;202:401-405.
91. Rauschenberg J, Groebner J, Nagel A, et al. Safety measurements of intracranial fixation devices at 7T. In: Proceedings Intl Soc Mag Reson Med Stockholm, Sweden; 2010. p. 778.
92. Ansems J, van der Kolk A, Kroese H, et al. MR imaging of patients with stents is safe at 7.0 Tesla. In: Proceedings Intl Soc Mag Reson Med Melbourne, Australia; 2012. p. 2764.
93. Sammet S, Koch R, Murrey D, Knopp M. MR-safety and compatibility of intrauterine devices at 3T and 7T. In: Proceedings Intl Soc Mag Reson Med Berlin, Germany; 2007. p. 1075.
94. Kraff O, Quick HH. Safety of implants in high field and ultrahigh field MRI. *Radiologe* 2019;59:898-905.

Chapter 4 Bioeffects of Static Magnetic Fields

ALAYAR KANGARLU, PH.D.

Director of MRI Physics
Columbia University
New York, NY

INTRODUCTION

Among the three different electromagnetic fields associated with magnetic resonance imaging (MRI), the static magnetic field has always been a primary focus of safety considerations. The need for intermittent exposure to the powerful static magnetic field of the MR system is at the base of safety concerns, from the pioneers working on developing nuclear magnetic resonance (NMR), to the diagnostic imaging technique that is currently used today, as MRI. Since the early 1970s, when Raymond Damadian's pioneering work on animal tumor imaging and Paul Lauterbur's application of gradient magnetic fields in combination with a strong magnetic field to generate images marked the birth of MRI (1, 2), the safety implications for human subjects have been a constant preoccupation of practitioners (1, 2). This is the case even though there have been no unpreventable safety incidents for patients and others in the MRI environment (3). The safety record of scanning hundreds of millions of human subjects imaged in MR systems worldwide indicates a relative lack of inherent risk associated with MRI.

Although the static magnetic field (B_0) is not the only source of safety concern, the other two, that is, the gradient magnetic fields (dB/dt) and the radiofrequency (RF) fields (B_1), warrant their own safety evaluations. Considering that all three of these electromagnetic fields act simultaneously on the human body during MRI, understanding their interactions constitutes the first order of business in quantifying safety implications. In so doing, in the present chapter, there will be an exclusive focus on the task of understanding the interactions of static magnetic fields with the human body. The other two, radiofrequency fields and gradient magnetic fields, are easier to quantify since a large part of their interactions is a manifestation of Faraday's Law of Induction. These effects are functions of easily controlled characteristics of transmit RF coils and the gradient magnetic fields, such as amplitude and frequency. It is inherently easier to build a transmit RF coil operating at high frequencies greater than 300-MHz and gradients operating at greater than 50-mT/m with slew rates of higher than 200-T/m/s than to build a whole-body magnet operating at greater

than 7-Tesla (T). Furthermore, computations of specific absorption rate (SAR) and concomitant RF-induced tissue heating or gradient field-induced voltage and associated neurostimulation are readily carried out. By comparison, the limiting physiological effects of static magnetic fields on biological tissues have not been sufficiently quantified because the observable effects on tissues are relatively small and it is difficult to estimate the static magnetic field strengths at which these may become substantial hazards (**Table 1**) (3).

However, since the development and manufacturing of powerful magnets, scientists have begun to understand the mechanisms of interactions with biological tissues at different levels. To date, the strongest of these effects is the attractive force on ferromagnetic materials which demonstrates the most ominous of all safety risks to the life and wellbeing of patients and other individuals (4, 5). Notably, this effect, also known as the projectile or missile effect, is a secondary effect meaning that it is easily avoidable and is not inherent to the interaction of the static magnetic field with the human body. As far as the hazards associated with intrinsic interactions, the scientific community has yet to establish an upper limit for the static magnetic field designed for exposure of human subjects. Considering the difficulty of building whole-body magnets operating at field strengths much higher than currently recommended by the United States Food and Drug Administration (FDA), presently standing at 8-Tesla (5), it is conceivable that there would be many opportunities and available hardware to characterize such effects. Proliferation of 7-T whole-body magnets (subsequent to the success of the 8-T scanner, designed by the team at the Ohio State University in 1998) has offered a fertile ground to study the interactions of static magnetic fields with biological tissues using all available techniques, in addition to the imaging capabilities that such scanners afford the scientists and clinicians. The safe operation of the more than eighty 7-T research and clinical MR systems around the world has encouraged scientists to dream of even higher field strengths. NeuroSpin in Orsay, France, and the National Institutes of Health (NIH) now have 11.7-T, whole-body MR systems. The successful move to the ultra-high-field (UHF), 11.7-T scanner was undoubtedly the result of the invaluable information that was gained from the exposure of thousands of human subjects to 7-, 8-, 9.4-, and 10.5-T static magnetic fields since 1998. To date, numerous safety investigations have been conducted on UHF MR systems (5-10). Importantly, as the number of high-field (HF) scanners (i.e., less than 3-T) increases in clinical settings and the number of UHF MR systems (higher than 4-T) increases in research and clinical facilities, the opportunity is created for more

Table 1. Comparison of the physical effects of the various fields applied to patients during MRI.

Type of Field	Physical Limitation on Human Exposure
Static Magnetic Fields	Unknown
Gradient Magnetic Fields	Peripheral Nerve Stimulation ^{1,2}
Radiofrequency Fields	Tissue Heating ¹

¹ The origin of both effects can be attributed to the electric field that accompanies all time-dependent magnetic fields and not the static magnetic field, itself.

² Both the rate of change of the field and the duration of the change must be above threshold values for stimulation to occur.

98 Bioeffects of Static Magnetic Fields

complex safety studies to investigate the interactions of powerful magnets with matter at molecular, cellular, tissue, and systems levels.

HISTORICAL PERSPECTIVE

Over more than a century of recorded research on the effect of static magnetic fields on human subjects, there have been many publications (11-98). These works have shown that no verifiable harmful effect can be attributed to exposure to strong static magnetic fields. This is predominantly attributed to the diamagnetic nature of human tissues and the small number of paramagnetic elements present in the human body. Nevertheless, the fact that, following the introduction of MRI as a dominant medical imaging device, an even larger segment of the human population is being exposed to powerful magnetic fields each year, warranting additional research in this field. It is conceivable that, as MRI becomes available to more developing countries, there will come a time that most human beings will be exposed to strong magnetic fields at some point in their lives.

There have been few reports of deaths associated with the MRI environment (99-101). A close examination of these fatalities reveals that they were all caused by controllable factors and involved implanted or other extraneous devices that interacted strongly with the MR system's static magnetic field. Knowing that life on our planet is formed in the magnetic field of about 0.5-Gauss indicates that the probable interaction of molecules building life with the magnetic field at this field strength is incorporated into the structure and function of biological tissues. Although the earth's magnetic field is relatively weak, it is sufficient to put a proton of hydrogen into a precession of approximately 2-kHz. Thus, the Larmor precession that takes into account the torque imparted on nuclear spins and formulates their rotational motion will allow the use of the gyromagnetic ratio (γ) of a hydrogen proton to yield its frequency of rotation. This magnetic effect is the basis of the mechanism of signal generation in MRI.

Attraction by natural magnets had been discovered and cited in many ancient treatises (11). Chinese, Greek, and Persian scientists discovered the unique properties of magnets and offered various treatments for diseases more than a thousand years ago (102, 103). However, since natural ores can produce magnets with a field strength of less than 0.5-T, these materials do not have very high magnetic polarization. Furthermore, the field distributions of natural magnets are inhomogeneous, producing a strong field in small regions unsuitable for observation of any effects that would otherwise require establishing strong fields in larger areas. This is why magnets were not used in many tools before the 19th century. Electromagnets provided the opportunity of manufacturing magnets stronger than 1-T, but the resistive heat in these magnets placed an upper limit on their applications.

At the present time, the most powerful electromagnet in the world generates a continuous magnetic field of 35-T, which is a Bitter magnet located at the U.S. National High Magnetic Field Laboratory in Tallahassee, Florida. Such magnets allow scientists to study exotic effects exhibited by matter only under extreme conditions. The possibility that metallic hydrogen may be a superconductor at room temperature was put forward in 1968, and its potential technological applications initiated interest in even stronger magnets. Because compact high field magnets made of high temperature superconductors may offer highly

efficient transportation systems and quantum leaps in the computational power of computers, research on the health implications of strong magnets go well beyond their application to MR scanners. Today, the magnets used for MR systems utilize special Niobium-Titanium alloys, which are capable of producing magnetic fields up to approximately 10-Tesla at liquid helium temperatures (104). These so-called type II superconductors are only one class of alloys that reveal superconductivity at cryogenic temperatures. Other materials, such as bismuth alloys, have been used to construct test coils that can achieve 32-Tesla. While strong magnets have been built for research in charged particle accelerators and in electromagnetic ore extraction, their use has not produced a widespread exposure of human subjects to such magnetic fields. The introduction of MRI as the standard of medical diagnosis started the era of pervasive human exposure to strong magnetic fields in the early 1980s.

From the time of magnetotherapy, when magnets were used for therapeutic purposes, some scientists believed in the treatment capability of magnetic effects on the body. Centuries ago, magnets were used for their presumed effectiveness in remedying headache, pain, and other conditions (105). However, in consideration of the diamagnetic property of human tissues, the interaction with magnetic fields is negligible for most tissues. Because of its iron content and different susceptibility state between oxyhemoglobin and deoxyhemoglobin, there is a slight magnetic interaction with hemoglobin. However, this effect has not been large enough for bulk measurement other than its effect on functional MR images, or fMRI. The need for a high static magnetic field and high homogeneity in MR systems requires that these magnets be much larger to simply produce a given field strength. MR scanner magnets are designed to produce a field homogeneity on the order of 10 parts per million (ppm) over the diameter of spherical volumes (DSV) of 50-cm. Producing a highly homogeneous DSV50 with a solenoid magnet is the primary requirement of MR systems.

Cylindrical superconducting geometries are the most abundant form of “closed” scanners, while permanent and hybrid magnets are often used for “open” MR systems. An account of the dates when MR systems with various magnetic fields were debuted is listed in **Table 2** (106-115). In this table, the timing of major increases in field strength has been presented but it is not meant to be a catalogue of improvement in all aspects of magnet technology.

In assimilation of new MRI technology, three factors have dominated the introduction of new scanners: engineering innovation, safety, and an advantage in clinical diagnostics. The complexity of scientific, financial, and technical factors involved in justifying, funding, and manufacturing whole-body scanners with ever higher field strengths is indicated by the eleven years that were required from the installation of the first 4-T human scanners to the introduction of the first 8-T whole-body MR system (98).

Currently, a 9.4-T whole-body MR system is located at the University of Illinois and a 10.5-T whole-body scanner exists at the University of Minnesota. The most powerful MR systems in the world, which operate at 11.7-T, have been installed at the National Institutes of Health and at NeuroSpin in Orsay, France. Thus, the increasing the range of proton frequency for the use of MR scanners in human subjects has moved towards 500-MHz. The economics of magnet technology and the scientific capabilities and image resolution of MR systems are on the opposite sides of the trend toward higher field strengths. In one analysis

100 Bioeffects of Static Magnetic Fields

Table 2. Historical development of MRI-related static magnetic field strengths (Data adapted from references 63, 65, 76, 77, 93-101).

Field Strength (Tesla)	Date of Introduction	Institution	Type	Comments
0.05 to 0.10	1977	State University of New York, Brooklyn	Superconducting	This MR system produced an early image of the human thorax.
0.7	1977	University of Nottingham	Iron core electromagnet	This machine, with a 13-cm gap, produced an early wrist image.
0.04	1980	Aberdeen	Air core electromagnet	This machine was used for the first clinical MRI studies.
0.35	1981	Hammersmith, Diasonics	Whole-body, superconducting	These MR systems were the first whole-body superconducting scanners.
1.5	1982	General Electric	Whole-body, superconducting	Whole-body MR systems at 1.5-T have been in widespread clinical use since the mid-1980s.
3.0, 4.0	1987	Siemens, General Electric, Philips	Whole-body, superconducting	During the late 1990s 3-T and 4-T scanners became widely available at research institutions.
8	1998	Ohio State University	Whole-body, superconducting	MR system was used for UHF safety studies.
9.4	2004	University of Illinois	Whole-body, superconducting	MR system used for research.
10.5	2018	University of Minnesota	Whole-body, superconducting	MR system used for research.
11.7	2020	National Institutes of Health, Bethesda, MD and NeuroSpin, Orsay, France	Whole-body, superconducting	MR system used for research.

published in 2002 that was based on sales activity at that time, it was predicted that 3-T would displace 1.5-T MR systems and become the dominant field strength by 2012 (115). This prediction has only been realized to a certain degree, as approximately one-quarter of new installations in 2012 were at 3-T. By the same token, UHF units are being installed in more research facilities and, as their technological challenges are met, they will provide the

incentive for pushing field strength beyond 3-T for clinical applications during the next decade.

At this point, it is worth remembering the prediction of early MRI pioneers that declared MRI a safe modality for scanning humans. That no major, unavoidable incidents have occurred in association with MRI is a testimony to the sound basis of analyzing the interactions of static magnetic fields with human subjects (35-37). Similar studies have been conducted at UHF ranges, indicating that the magnetic interactions with biological tissues are safe up to and including 8-T (98). However, it should be noted that the consequence of taking ferromagnetic materials into the fringe fields of a UHF MR system will create more serious problems than predicted by many authors (57, 62, 63, 66, 83). Similar facts are at work regarding medical implants in patients within fringe fields of MR scanners.

INTERACTIONS WITH HUMAN TISSUE

The mechanisms of interactions between static magnetic fields and biological tissues can be used as the basis for assessing the potential damage in human subjects. Understanding these mechanisms will allow the use of the benefits of MRI while avoiding the possible hazards of exposure to strong magnetic fields. The major effects that have been researched to date are described below.

Magnetic Forces

High magnetic fields will exert an attractive force on tissues with permanent magnetic dipoles. Tissues with higher magnetic susceptibilities than water will repel diamagnetic materials (116-117). High field regions are centers of attraction and this is a way for separating tissues with higher paramagnetic susceptibilities. But, this effect is too weak for practical use in living tissues even in high static magnetic fields. The absence of permanently magnetized tissues in the human body makes this force of lesser concern in assessing the safety of these fields, except where materials with permanent magnetic properties are present (e.g., ferromagnetic foreign bodies), because they may experience displacement forces in regions of the spatial gradient magnetic fields.

Magnetic forces can produce torque on permanently magnetized materials with an elongated shape that will tend to rotate them to align their magnetic moment with the direction of the magnetic field. As such, magnetic torque will rotate magnetic materials to make the long axis of the object parallel to the applied field. Foreign bodies that are ferromagnetic may experience sizable torque, posing even a greater potential hazard than the translational forces on such materials. For materials with different paramagnetic susceptibilities in different directions with respect to the magnetizing field, the anisotropic susceptibility will lead to torque on the axis of the most positive susceptibility, tending to align it with the magnetic field. Diamagnetic susceptibility anisotropy (DSA) observed in some materials has the effect of rotating them to align the axis of least negative susceptibility with the field. Observation of DSA can only be made *in vitro* because the effect is too weak *in vivo* for quantitative measurement.

102 Bioeffects of Static Magnetic Fields

Flow and Its Consequences

In the human body, electric fields are normally produced by processes such as the depolarization of the heart tissue that produces current flow, which is the basis of the electrocardiogram (ECG). In addition to the normal static field currents producing the ECG, any motion by the tissue will produce an additional term in the expression for the current density, $\mathbf{J} = \sigma (\mathbf{E} + \mathbf{v} \times \mathbf{B})$ where \mathbf{v} is the velocity of the moving tissue relative to the static magnetic field. The term, $\mathbf{v} \times \mathbf{B}$, is the consequence of motion and can be viewed as a motion-induced electric field.

Motion of conductive tissues within a magnetic field will produce a force perpendicular to the direction of motion. There are many different types of motions by internal organs in the human body, including those associated with the respiration, peristalsis, the beating heart, and blood flow. The currents produced by blood flow in the presence of powerful magnetic fields are large enough that their effects on body surface potentials have been proposed to be used for a flow meter (118-119).

The electromotive force (emf) induced as a result of blood flow in the heart produces a large signal during the T-wave phase of the cardiac cycle. In the 1960s, it was shown that electrocardiograms of monkey hearts in strong magnetic fields displayed a field-induced amplified T-wave (44). Subsequent studies have shown this T-wave amplification is the result of blood flow and not from a direct magnetic field effect on cardiac muscle (120-121). This effect is easily demonstrated in patients in clinical, high-field MR systems and contributes to the difficulty in obtaining acceptable electrocardiograms during MRI procedures.

Dependence of the induced emf on the velocity of blood flow and the strength of the static magnetic has been visualized in humans at field strengths as high as 8-Tesla (98). Importantly, there is no evidence of flow-induced nerve or muscle stimulation for fields as high as 9.4-T because the induced emf is below the threshold levels required for such stimulations to occur (122). As the magnetic field strengths of MR scanners increase, the flow-induced currents near blood vessels could eventually reach levels capable of inducing nerve stimulation, and this may determine the upper limit of human tolerance for exposure to extremely high static magnetic fields (87-88). However, all currently planned research and clinical MR systems operate well below these levels.

Interactions with Metabolic Reactions

Chemical reactions are at the core of the metabolic function of tissues. The massive number of chemical reactions required for normal function indicates that any external factor, such as an applied static magnetic field capable of altering the rate of these reactions, could affect their equilibrium positions (123-130). This condition prevails, for example, in those chemical reactions in which the products are more paramagnetic than the reactants. Such reactions will respond to the presence of a magnetic field by shifting the reaction equilibrium towards an increase in the concentration of the products, thus, displacing the equilibrium position of the reaction.

The presence of molecules of different magnetic properties on opposite sides of a reaction is among the class of reactions that will be affected by magnetic fields. For example,

the dissociation of oxygen from hemoglobin as oxyhemoglobin is diamagnetic, and both oxygen and hemoglobin are paramagnetic. However, although the applied field will lower the energy barrier for the dissociation of diamagnetic molecules to paramagnetic molecules, calculations show that the free energy barrier to dissociation of oxyhemoglobin (approximately 64,000-J/mol) will only be changed by about 1-J/mol at a field strength of 4-T. Such disturbances of oxygen dissociation are comparable to a temperature change of only 0.01°C, making it unable to significantly modify the reaction equilibrium (87).

Another possible magnetic field effect on a chemical reaction involves the dissociation of a binary molecule, AB (124-130). If the bond between A and B is nonmagnetic (electron-pair bond) but the dissociated radicals A and B have unpaired electrons, then the magnetic field will favor dissociation of the bound state, as the two electrons in the bond will have opposite spins and a total spin of zero, while the free spins of individual radicals will be nonzero. Precession of the A and B spins subsequent to dissociation will limit to some extent the tendency toward re-bonding. However, no significant effects on reactions of biochemical significance have been reported from this effect.

Ferromagnetic Tissue Components

The magnitude of interaction of materials with magnetic fields is directly proportional to their magnetic susceptibility (35). The human body is diamagnetic which makes its interaction with external magnetic fields inherently weak. However, there are small amounts of tissue components that are paramagnetic, which allows them to couple more strongly with magnetic fields (131-136). There is about 3.7-grams of iron in the body of a 70-kg adult human. Fortunately, the iron in the human body is in weak paramagnetic form incorporated in various chemical compounds such as hemoglobin, ferritin and hemosiderin that are spread throughout the body, preventing strong interactions with applied fields. The small concentration of these paramagnetic substances is insufficient to make the overall susceptibility of the tissues, including blood, paramagnetic (90). Obviously, exogenous paramagnetic materials can enter the human body, causing interaction with a magnetic field. For example, studies involving coal miners exposed to rock dust have detected small amounts of particulate magnetite in their lungs (132). Other forms of the deliberate addition of iron oxide-based compounds applied to the body, such as in tattooing involving iron oxide-based pigments, will similarly increase the possibility of magnetic interactions.

The presence of particles of iron oxides less than 500-angstroms in diameter has been reported in the human brain and other tissues using electron microscopy in autopsy studies (136). The source and function of such particles are unclear and determination of their origin requires further investigations. The small size of these particles makes their artifacts on MR images too small to be detected at the range of field strengths used for human MR imaging. Perhaps at higher field strengths, susceptibility enhanced pulse sequences would permit visualization of these particles. However, such “artifacts” will most likely induce sub-voxel signal dropout and require rigorous quantification methods to measure their interactions with magnetic fields.

MRI examinations performed in patients with tattoos or permanent eye makeup using iron oxide-based pigments have shown artifacts around those regions as well as local edema in some cases. This effect does not appear to be caused by the static magnetic field but,

104 Bioeffects of Static Magnetic Fields

rather, results from interactions with the RF fields used during MRI (65, 68, 70-72). However, it may be possible that irregularly shaped, iron oxide particles in the implanted pigments experience torque in the magnetic field that rotates them, making their long axis move parallel to the direction of the static magnetic field. The image artifact is caused by the magnetic fields of these particles resulting in signal losses or voids, while the torque that forces their alignment with that static magnetic field may be the cause of tissue irritation, resulting in localized edema. Such tissue irritation could be exacerbated by patient movement inside the static magnetic field of the MR system (i.e., if the patient moves his/her head side-to-side).

Magnetoresistance

The magnitude of electrical resistance of a material will change when it is placed in an external magnetic field. This phenomenon, called magnetoresistance, is caused by the forces exerted on ions in solutions moving through strong magnetic fields. Depolarizing currents associated with the propagation of nerve and muscle action potentials could be modified by such a field-dependent effect. However, since electrical resistance is a function of dynamics of current-carrying particles, the mean free path (MFP) of these carriers and the time between their collisions plays an important role in determining the size of the magnetoresistance effect.

For a sufficiently long MFP, an electric field perpendicular to the direction of current will be established, increasing the effective resistivity of the conductors when they are placed in a magnetic field. This phenomenon is called the Hall Effect and, in nerve and muscle tissues, could modify the transmission of currents. However, ions whose flow determines the action potentials of nerve and muscle tissue have an extremely short mean MFP ($\sim 1\text{-angstrom}$) and collision times (10^{-12}-seconds), drastically reducing the effect of magnetoresistance on the associated action potentials (60). Interestingly, neurocognitive studies inside magnetic fields of up to 8-T have not detected a decrease in the performance of motor, sensory, and cognitive tasks (10).

Magnetohydrodynamics (MHD)

Currents flowing in tissues experience a body force. The resulting pressures and forces are transmitted to the tissues. These forces can be substantial in flowing liquid metals such as mercury. However, flowing physiological fluids such as blood have much lower electrical conductivities than mercury, and MHD forces on flowing blood are relatively small compared to the naturally occurring hemodynamic forces in the vascular system. Therefore, contrary to early speculations, there is no requirement for increased heart activity to maintain the cardiac output in the presence of a strong static magnetic field. On the other hand, it may be that very small MHD forces operating on the endolymphatic tissues of the inner ear are the source of sensations of nausea and vertigo sometimes reported by human subjects in the presence of higher static magnetic fields (86, 87). Recently, the feasibility of using MHD effects at 7-T for synchronization of MRI with the cardiac cycle has been reported (137).

Magnetostriction

A substantial force acting on an object can change its size and shape. Among the three types of magnetic properties, ferromagnetism produces by far the largest magnetostrictive forces. Therefore, in consideration of the range of susceptibility of biological tissues, their size and shape change only slightly when exposed to strong magnetic fields (138, 139). Since human tissues do not normally contain ferromagnetic materials, magnetostriction is negligible. Furthermore, compared to the naturally occurring forces (i.e., thermal expansion and mechanical stresses), any effect in human tissue would be insignificant.

CALCULATION OF STATIC MAGNETIC FIELD EFFECTS

Magnetic susceptibility is the term used to define the quantification of the effect of static magnetic fields on matter. Analysis of the magnetic response of tissues through the concept of magnetic susceptibility is a simple method that will be discussed in this section. This analysis will show that the large differences between the magnetic properties of biological tissues and those of ferromagnetic materials govern their different responses to magnetic fields. This difference is so profound that, in many cases, it makes their response to applied magnetic fields qualitatively different. This is why extrapolation of our daily experiences with ferromagnetic materials has been the source of the many concerns with the safety of powerful static magnetic fields in predicting the response of tissues to such fields. In this section, the concept of magnetic susceptibility is discussed and the calculations of magnetic forces and torque are presented. The quantitative response of tissues to applied magnetic fields will then be formulated in these terms.

Magnetic Susceptibility

Magnetic susceptibility is a quantity that describes the response of materials that are not permanently magnetized to applied magnetic fields (90). The discussion will not consider permanent magnets, such as bar magnets, because their strong interaction with magnetic fields makes them extremely hazardous in the MRI environment. Thus, except in rare situations, permanent magnets are not allowed in the MR system room. Biological tissues have very small magnetic susceptibilities, so they do not interact strongly with applied magnetic fields. This fact is supported by noting the high quality of MR images due to the highly uniform magnetic field inside the human body, as it is situated within the MR scanner (i.e., due to the slight variation in susceptibility in biological tissues).

Polarization of materials in an applied magnetic field is measured by a quantity called the magnetization, defined as the magnetic dipole moment per unit volume. To provide a quantitative account of the response to magnetic fields in terms of magnetization, System International (SI) units are used along with the standard mathematical convention of using bold face symbols to designate vector quantities. If matter of susceptibility, χ , is placed in magnetic field \mathbf{H} , it will develop a magnetization \mathbf{M} given by the equation $\mathbf{M} = \chi \mathbf{H}$. The susceptibility, χ , is a dimensionless quantity as both \mathbf{M} and \mathbf{H} represent the strength of magnetic fields, \mathbf{H} for the external field and \mathbf{M} for the induced field. \mathbf{B} , the magnetic flux density is given by $\mathbf{B} = \mu_0 (\mathbf{H} + \mathbf{M})$. The induced field is a property of the magnetized object, while the applied field only modulates that property. Interaction between them is best managed if

106 Bioeffects of Static Magnetic Fields

we designate the total field with \mathbf{B} and the applied field with the symbol $\mathbf{B}_o = \mu_r \mu_0 \mathbf{H}$, where μ_r is called the relative permeability.

In an isotropic material, χ is a scalar quantity, meaning that it has the same value in all directions. This is the case in most materials. In isotropic materials, the induced magnetization \mathbf{M} is parallel to \mathbf{H} , which makes \mathbf{M} , \mathbf{B} , and \mathbf{H} all parallel to each other. If matter has a preferred direction in which it magnetizes more easily than in other directions, the resultant magnetization is not necessarily parallel to the magnetic field. Such materials are represented by an anisotropic χ in the form of a symmetric tensor.

Aside from discussing the weak torque formed in certain biological crystals, the analysis is limited to isotropic materials. For materials with large susceptibilities, magnetization is found by taking into account the induced and applied field effects in a self-consistent way. This is due to the fact that in the definition of χ , \mathbf{H} is the sum of the applied and induced fields. The example of ellipsoidal objects using demagnetizing coefficients is worked out in this section to demonstrate such calculations. For biological tissues with very low susceptibility, however, the fields induced by the magnetization are much smaller than the applied field, which makes them negligible. For such material, the magnetization is determined entirely by the applied field, and the more complex self-consistent method is not necessary for their calculations.

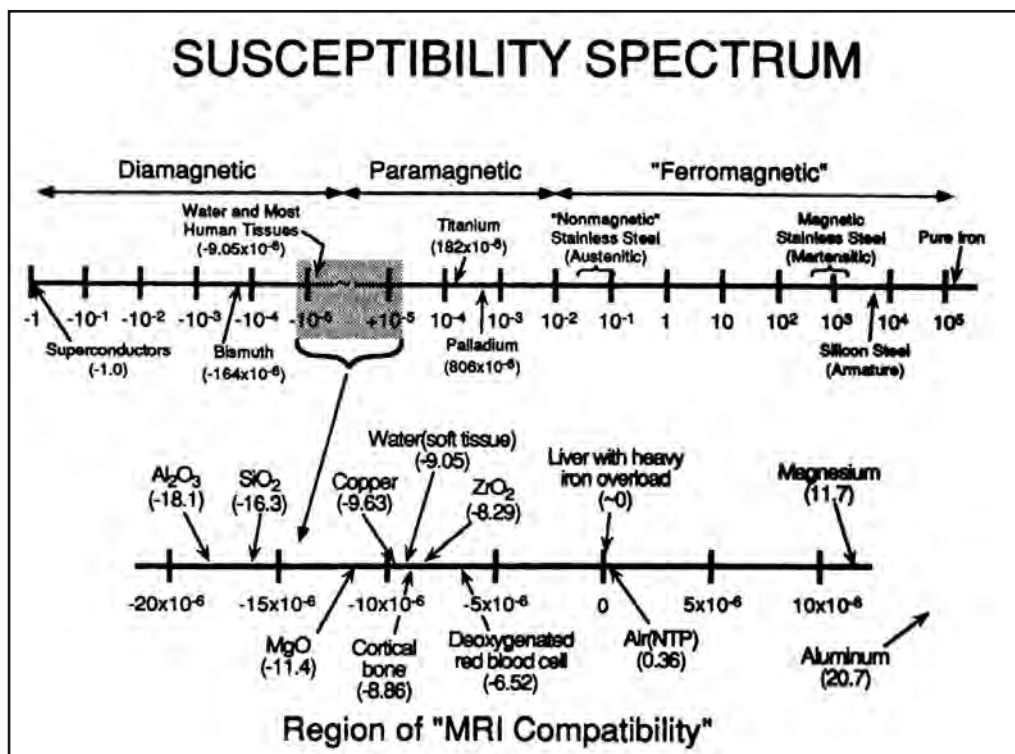
In isotropic material, \mathbf{M} , \mathbf{H} , and \mathbf{B} are parallel and, as shown in the following discussion, no torque will be formed to align the object with local fields. In reality, the negligible magnitude of torque due to the applied field compared to other biological forces acting on the tissue component allows us to ignore it in our calculations.

The magnitude and sign of χ determines the extent of the interaction with the applied field. In this regard, materials are classified into three large groups: diamagnetic, paramagnetic and ferromagnetic. Conservation of energy requires that only χ with values > -1 are possible (140). Diamagnetic materials have negative susceptibilities (i.e., $-1.0 < \chi < 0$). This property causes them to be magnetized in the opposite direction of the applied magnetic field, causing them to be repelled from regions of strong magnetic fields. All materials have diamagnetic properties if they do not possess components, such as the magnetic ions in transition elements, which make a larger positive contribution to χ . Paramagnetic materials have positive χ that makes them attracted to regions of strong magnetic fields. Materials with $|\chi| < 0.01$ do not respond to weak sources of magnetic fields such as handheld magnets and are therefore classified as nonmagnetic. Most common materials including all living beings, with the exception of magnetotactic bacteria, are in this group.

Ferromagnetic materials with $|\chi| \geq 0.01$ constitute the third group of materials to which we will refer as ferromagnetic or magnetic. These materials exhibit a strong response to an applied magnetic field, and the large attractive force induced on them poses the biggest danger if taken into the vicinity of an MR system. Some ferromagnetic materials do not appear magnetic until they are exposed to an external field. They are called “soft magnets” to distinguish them from permanent magnets or “hard” magnetic materials.

The enormous range of susceptibility values of all matter in nature is shown in **Figure 1** (90). As is seen in this figure, the vast majority of materials have susceptibility values

Figure 1. Spectrum of magnetic susceptibilities. The upper diagram uses a logarithmic scale to indicate the full range of observed magnetic susceptibility values: it extends from $\chi = -1.0$ for superconductors to $\chi > 100,000$ for soft ferromagnetic materials. The bottom diagram uses a linear scale (in ppm) to indicate the properties of some materials with $|\chi| < 20$ ppm. The susceptibilities of most human tissues are in the range from -7.0 to -11.0 ppm (Adapted from Reference 90).



much less than 0.001, making the magnetic forces on such materials very weak and, therefore, not easily observable. Relevant to this discussion are the vast majority of biological tissues with susceptibilities very close to the susceptibility of water, $\chi_{\text{H}_2\text{O}} = -9.05 \times 10^{-6}$ in SI units. In fact, χ of most biological tissues differs from that of water by about $\pm 20\%$. This narrow range of variation of χ is the primary reason why exquisite MR images are acquired from biological tissues. In regions of the human body where large variation in susceptibility is present (e.g., the air/tissue interfaces between the sinuses and the orbitofrontal regions of the brain), high field MRI causes large position-dependent variations in the Larmor frequency that results in severe signal losses.

Because of diamagnetism, small forces act on the patients as they are inserted into MR systems. This force is so small that it cannot be perceived. Normal magnetic materials, on the other hand, have susceptibility values much larger than those of diamagnetic materials, usually a factor of 1000 or more, that lead to much stronger responses in the presence of magnetic fields. The large variation in the magnitude of susceptibility causes qualitatively

108 Bioeffects of Static Magnetic Fields

differing responses by ferromagnetic and diamagnetic materials to applied fields, as discussed later in this section.

A demonstration of the existence of repulsive diamagnetic forces exerted on living beings by strong magnets has been made by suspending small frogs and other diamagnetic objects in midair in the vertical bore of a magnet operating at 16-T (116, 117). In achieving such suspension, the diamagnetic force counters the weight of the frog. It is worth noting that even in the presence of very high magnetic fields, no harm was done to the frog.

Magnetic Energy

The force of the magnetic field on matter could cause two types of motion, translational and rotational. An object, like a ferromagnetic aneurysm clip with a long blade, if placed in a strong magnetic field, experiences a magnetic force that could cause measurable translational and rotational motions. In the human body, depending on its shape, the object could experience translational attraction and torque that could cause it to move and rotate with respect to the direction of the static magnetic field. The size of the translational forces and/or torque depends on the applied field strength, the susceptibility, and the shape of the material. This could vary from no observable effect to forces large enough to produce serious injury or even lethal consequences. Typically, to understand whether these translational forces and torque will be at a level to significantly alter the structure or function of tissues, we need to develop rigorous mathematical expressions based on the physical properties of the material.

The work required to move magnetic dipoles within a magnetic field is independent of its path. Therefore, a magnetic potential energy function, U , can be defined that depends on the field strength (position), magnetic dipole moment of the object, the relative angle between the direction of the field and the dipole orientation, and the magnetic properties of the medium (139-142). For magnetization, \mathbf{M} , the total dipole moment of a volume, V , for a uniformly magnetized object is $\mathbf{m} = \mathbf{M} V$. The energy required to bring an object with permanent dipole moment, \mathbf{m} , to a point within a magnetic field \mathbf{B}_0 is $U = \mathbf{m} \bullet \mathbf{B}_0$. To assess the energy of a non-permanently magnetized object, as is the case for the human body in an MR system, we have to take into account the fact that biological tissues within a static magnetic field acquire a magnetic moment that is proportional to the applied field. If biological tissues are brought within a magnetic field, \mathbf{B}_0 , they acquire an induced moment,

\mathbf{m} , and an energy $U = \frac{1}{2} \mathbf{m} \bullet \mathbf{B}_0$. The reason for the presence of the factor 1/2 for the sec-

ond case, with all other variables held constant, is that when biological tissues with no permanent magnetic dipole (the second case) are brought into the magnetic field, their magnetic moment increases from zero (where the magnetic field is zero) to \mathbf{m} (where the magnetic field is \mathbf{B}_0). This is in contrast with the case of permanently magnetized objects, in which magnetization is \mathbf{m} all along the path. The magnetic field energy increases through the work of forces and torque on objects introduced in them. Magnetic forces attract paramagnetic materials and repel diamagnetic ones. Also, if \mathbf{m} is not aligned with \mathbf{B}_0 , the magnetic field will produce torque on it to make it parallel to \mathbf{B}_0 . Therefore, using the expression for the

force, $\mathbf{F} = \nabla U$ and torque $\boldsymbol{\tau} = \frac{\partial U}{\partial \theta} \mathbf{u} = \mathbf{M} \times \mathbf{B}_0$, where \mathbf{u} is the unit vector perpendicular

to the plane of \mathbf{M} and \mathbf{B} and θ is the angle between \mathbf{M} and \mathbf{B}_0 , the expression for energy for an object of volume V and susceptibility χ is then found to be

$$\mathbf{m} = \mathbf{MV} = \chi V \mathbf{H}_0 = \frac{\chi}{\mu_0} V \mathbf{B}_0 \quad \text{and} \quad U = \frac{1}{2} \mathbf{M} \cdot \mathbf{B}_0 = \frac{1}{2} \frac{\chi V}{\mu_0} B_0^2. \quad \text{This expression ap-}$$

pplies to situations where the magnitude of the susceptibility is much less than one and \mathbf{B}_0 is uniform over the volume of the object. The square dependence of energy on \mathbf{B}_0 has implications on both energy deposition and the magnitude of the attractive or repulsive force that magnetic fields exert on diamagnetic objects within them.

Demagnetizing Factor

This chapter is concerned with the effect of magnetic fields on biological tissues, which do not have fixed dipole moments. For these materials, the evaluation of the translational attraction and torque must take into account the fact that magnetization is induced by the applied field. This makes it necessary to determine the field-induced dipole moment that must be inserted back into the above formulas to find translational force and torque. In general, this is a complex mathematical process. However, for certain simple shapes, such as ellipsoids, the math is simple. Once results for ellipsoids, such as spheres, cylinders, and flat plates are calculated, they offer a good estimate of this effect for more objects with a more complex shape. A simple analysis for ellipsoids is presented below.

If an ellipsoid object with isotropic susceptibility is placed in a field along its principal axis, an internal field parallel to the applied field will be induced in the object. This field, called the demagnetization field, \mathbf{H}_{dm} , is given by $\mathbf{H}_{dm} = -D \mathbf{M}$ where the demagnetizing factor, D , is a number that depends on the shape of the object, and it varies between zero and one (90-138). In general, the sum of the three demagnetizing factors along all axes of an object is equal to one. Spherical objects for which the three principal axes of a sphere are equivalent, making the demagnetizing factor for any direction equal to one-third constitutes the simplest case. In contrast, ellipsoids have three distinct principal axes. For a cylinder placed in a magnetic field so that its long axis is parallel to this field, $D = 0$. However, if the long axis is perpendicular to the applied field, $D = 1/2$. To find the total internal field \mathbf{H} the demagnetizing field, \mathbf{H}_{dm} must be added to the applied field, $\mathbf{H}_0 = \mathbf{B}_0/\mu_0$. Replacing the expression for magnetization, $\mathbf{M} = \chi \mathbf{H}$, in the formula for magnetic flux, $\mathbf{B} = \mu_0 (\mathbf{H} + \mathbf{M})$, the total internal fields can be found in terms of the applied field \mathbf{B}_0 , as follows:

$$\begin{aligned}\mathbf{B} &= \mu_0 \mathbf{H} (1 + \chi), \\ \mathbf{H} &= \mathbf{H}_0 + \mathbf{H}_{dm} = \mathbf{H}_0 - D \mathbf{M} = \mathbf{H}_0 - D \chi \mathbf{H}, \\ \mathbf{H}_0 &= \mathbf{H} + D \chi \mathbf{H} = \mathbf{H} (1 + D\chi), \\ \mathbf{H} &= \mathbf{H}_0 / (1 + D\chi), \\ \mathbf{B} &= \mu_0 \mathbf{H} (1 + \chi) = \mathbf{B}_0 (1 + \chi) / (1 + D\chi), \\ \mu_0 \mathbf{H} &= \mathbf{B}_0 / (1 + D\chi), \\ \mu_0 \mathbf{M} &= \mathbf{B}_0 \chi / (1 + D\chi).\end{aligned}$$

110 Bioeffects of Static Magnetic Fields

To derive these results, D is assumed to be the demagnetizing factor for the principal axes parallel to \mathbf{B}_0 . This result can be extended to cases where \mathbf{B}_0 is not along a principal axis by resolving it into components along these axes to find the resulting field, which is the sum of the fields along each axis. These expressions for the magnetic response of the object to an applied field work well because they take into account the interaction of \mathbf{B}_0 with both the shape of an object, as is represented by D , and the magnetic properties, as is represented by χ .

Ellipsoids of revolution, with two equivalent axes and two identical demagnetization factors, are a simpler form of the more general ellipsoids that have three independent principal axes and three different demagnetizing factors. For most cases, it is adequate to consider only ellipsoids of revolution. Deduction of important trends for the behavior of non-isotropic objects in a magnetic field is evidence to the utility of the above results. For example, it can be stated that for strongly magnetic materials with $\chi > 1$, to the first order, the internal field \mathbf{B} and the magnetization are independent of the susceptibility and only depend on the shape of the object, D . However, for materials with $|\chi| \ll 1$, magnetization $\mathbf{M} = \chi \mathbf{B}_0 / \mu_o$, which makes it parallel to the applied field and independent of the shape of the ellipsoid. Thus, translational forces and torque acting on ferromagnetic objects in a magnetic field critically depend on the object's shape. For biological tissues with tiny susceptibilities, these same equations predict that the force and torque associated with the magnetic field will be independent of the shape of the tissues.

Quantification of Forces

If a magnetic force induces magnetization in a direction, say along the z-axis, an isotropic object's magnitude will be given by $F_z = \frac{\partial U}{\partial z} = \frac{\chi V}{\mu_o} B \frac{\partial B}{\partial z}$. For paramagnetic materials with positive χ , the force will be in the direction of increasing \mathbf{B}_0 and for diamagnetic material with negative χ , force will be in the direction of decreasing \mathbf{B}_0 . This means that in MR systems, paramagnetic materials are pushed towards the center of the magnet where the field is most homogenous, while diamagnetic materials are pushed out of the magnet. This effect could have implications on the signal-to-noise ratio for a functional MRI (fMRI) examination in which the signal is largely determined by the replacement of paramagnetic deoxyhemoglobin with diamagnetic oxyhemoglobin. This force will have an impeding effect on the direction of flow for both oxyhemoglobin into the brain and deoxyhemoglobin out of the brain, thereby reducing the fMRI signal. For medical implants, such as ferromagnetic aneurysm clips that have high magnetic susceptibility,

$$F_z = \frac{V}{2\alpha\mu_o} B_z \frac{\partial B_z}{\partial z} \text{ and for weakly magnetic objects } F_z = \frac{V}{2\mu_o} \chi B_z \frac{\partial B_z}{\partial z}.$$

Torque, τ , is given by $\tau = \mathbf{M} \times \mathbf{B}_o$ or, if the y-axis is perpendicular to \mathbf{B}_o and \mathbf{M} , $\tau_y = \frac{\partial U}{\partial \theta} = MB_o \sin \theta$, where, θ , is the angle between \mathbf{M} and \mathbf{B}_o .

Risks Posed By Translational Forces And Torques

Since ellipsoids of revolution illustrate most of the important features of magnetic interaction with matter, a summary of the expressions for the quantities derived in this chapter including magnetic energy, force and torque are listed in **Table 3**. Also, the asymptotic limits of these expressions for extreme values of the susceptibility predict behaviors that are qualitatively different from one other. Designating the demagnetizing factor along the axis of symmetry of the object as D_a and the radial demagnetizing factor in the transverse direction as D_r from the earlier discussion, we have $D_a + 2D_r = 1$. The relative values of D_a and D_r offer simple results with powerful implications. For needle-like ellipsoids with one very long axis of symmetry and isotropic radial directions, $D_a \rightarrow 0$ and $D_r \rightarrow \frac{1}{2}$. For a sphere, $D_a = D_r = 1/3$. For flat ellipsoids, $D_a \rightarrow 1$ and $D_r \rightarrow 0$. These case examples are useful to

Table 3. Magnetic properties of ellipsoids of revolution.

Qty	Full Expression	Soft Magnetic Materials $\chi D_a, \chi D_r \gg 1$	“Non-Magnetic” Materials $ \chi \ll 1$
U	$\frac{\chi VB_o^2}{2\mu_o} \left[\frac{\cos^2 \theta}{1 + \chi D_a} + \frac{\sin^2 \theta}{1 + \chi D_r} \right]$	$\frac{VB_o^2}{2\mu_o} \frac{\cos^2 \theta}{D_a} + \frac{\sin^2 \theta}{D_r}$	$\frac{\chi VB_o^2}{2\mu_o}$
F_z	$\frac{\chi V}{\mu_o} B_o \frac{\partial B_o}{\partial z} \left[\frac{\cos^2 \theta}{1 + \chi D_a} + \frac{\sin^2 \theta}{1 + \chi D_r} \right]$	$\frac{V}{\mu_o} B_o \frac{\partial B_o}{\partial z} \left[\frac{\cos^2 \theta}{D_a} + \frac{\sin^2 \theta}{D_r} \right]$	$\frac{\chi V}{\mu_o} B_o \frac{\partial B_o}{\partial z}$
M_x	$\frac{\chi B_o}{\mu_o} \left[\frac{D_r - D_a}{(1 + \chi D_a)(1 + \chi D_r)} \right] \cos \theta \sin \theta$	$\frac{B_o}{\mu_o} \frac{D_r - D_a}{D_a D_r} \cos \theta \sin \theta$	$\frac{\chi^2 B_o}{\mu_o} (D_r - D_a) \cos \theta \sin \theta$
M_z	$\frac{\chi B_o}{\mu_o} \left[\frac{\cos^2 \theta}{1 + \chi D_a} + \frac{\sin^2 \theta}{1 + \chi D_r} \right]$	$\frac{B_o}{\mu_o} \left[\frac{\cos^2 \theta}{D_a} + \frac{\sin^2 \theta}{D_r} \right]$	$\frac{\chi B_o}{\mu_o}$
τ_y	$\frac{\chi^2 V B_o^2}{\mu_o} \frac{D_a - D_r}{(1 + \chi D_a)(1 + \chi D_r)} \cos \theta \sin \theta$	$\frac{V B_o^2}{\mu_o} \frac{D_a - D_r}{D_a D_r} \cos \theta \sin \theta$	$\frac{\chi^2 V B_o^2}{\mu_o} (D_a - D_r) \cos \theta \sin \theta$

The first column gives the complete expression for the magnetic potential energy (U), force (F_z), magnetization (M_x and M_z) and torque (τ_y) for an ellipsoid of revolution in a magnetic field along the z -axis. The symmetry axis is in the x -direction and θ is the angle between this axis and the magnetic field. The second column gives approximations appropriate for soft magnetic materials and the third column gives approximations appropriate to materials, such as biological tissues, with very small susceptibilities. For objects inside a medium of uniform susceptibility, such as water or tissue with $\chi = \chi_{H_2O}$, χ should be replaced by

$\Delta\chi = \chi - \chi_{H_2O}$. It is assumed that B_z is the only non-zero component of \mathbf{B}_o at the location of the object and

that the spatial derivatives of the transverse components, $\frac{fB_x}{fx}, \frac{fB_y}{fx}$, etc. are all zero. This is the case

along the central axis of the magnets commonly used in MRI. At other points in the field, there may be non-zero force components in addition to F_z , but the qualitative physical principles are unchanged.

112 Bioeffects of Static Magnetic Fields

provide an insight in the behavior of biological tissues in magnetic fields. Expressions for demagnetization factors for a broad range of ellipsoids of revolution are available in the published literature (90).

Certain metallic implants have magnetic properties that could put the patient at risk from translational force and torque in association with exposure to the powerful static magnetic field of an MR system. If the combination of the geometrical and magnetic properties produces substantial translational force, then the object could move in the presence of a strong static magnetic field. If the same combination results in torque, then the object could be rotated into alignment with the direction of the static magnetic field. The factors determining the relative strength of these two effects are magnetic susceptibility and the shape of the object as well as its position in the magnetic field that determines the magnitude and the field's spatial gradient magnetic field. Notice that the force does not just depend on the field strength but the product of field's spatial gradient by field strength, $B \partial B / \partial z$. Therefore, in the regions of a homogeneous magnetic field where $\partial B / \partial z \sim 0$, the translational forces are negligible. This does not mean that such metallic devices are safe, because the patient has to pass through the entry region of the MR system where $B \partial B / \partial z$ is large and the object could experience a large translational force during this time. As expressions for torque reveal, even for metallic devices with low translational force, torque could pose a greater hazard than the translational force in some cases. A discussion of such cases is warranted here.

A cylindrical magnet, such as that often used in a high-field MR scanner, offers an opportunity to look in more detail at the analysis of magnetic forces because regions near its central axis have a uniform magnetic field and small field spatial gradients. For spherically symmetrical objects, there is no torque acting on the object. So, the translational forces are caused by the induced magnetization, which is parallel to the applied magnetic field. In the cases of non-isotropic objects like long, thin needles or thin and flat plates, large torque may be formed on these objects. The forces will rotate elongated objects, to make the long axis of the object parallel to the direction of the magnetic field. On a flat object, however, the magnetic field will exert torque, turning it parallel to the field lines of the magnet. The following quantitative analysis is meant to support these predictions.

The large disparity between demagnetizing factors along axial (a) and radial (r) axes of a needle-like object ($D_r \gg D_a$) when placed in the magnet, with the long axis of the object parallel to the z -axis of the magnet, produces the maximum translational force when the

needle is aligned with the field ($\theta = 0$) and at a location where the product $B_z \frac{\partial B_z}{\partial z}$ is maximum. Regions at the isocenter of MR system's magnet (i.e., where MR imaging occurs)

have a very homogenous magnetic field ($\frac{\partial B_z}{\partial z} = 0$), although the magnitude of the magnetic field in these regions is highest. No translational forces will form on the objects in the central, homogenous regions of the magnet where $B_z \frac{\partial B_z}{\partial z}$ is zero. These conditions are created by the geometry of the magnet and the orientation of the object.

ated in two distinct regions, one outside and far from the magnet where $B = 0$ and, another,

in the central regions where $\frac{\partial B_z}{\partial z} = 0$. The product of the magnetic field with the spatial gra-

dient magnetic field decreases to zero at the center of the magnet and regions far outside the magnet, and goes through a maximum near the openings (i.e., front and back) of the MR system's bore, at z_{\max} . These conditions cause the attractive translational force to reach a maximum value at z_{\max} .

A plot of $B_z \frac{\partial B_z}{\partial z}$ for an 8-Tesla MR system with a 90-cm bore diameter and 3.4-meter

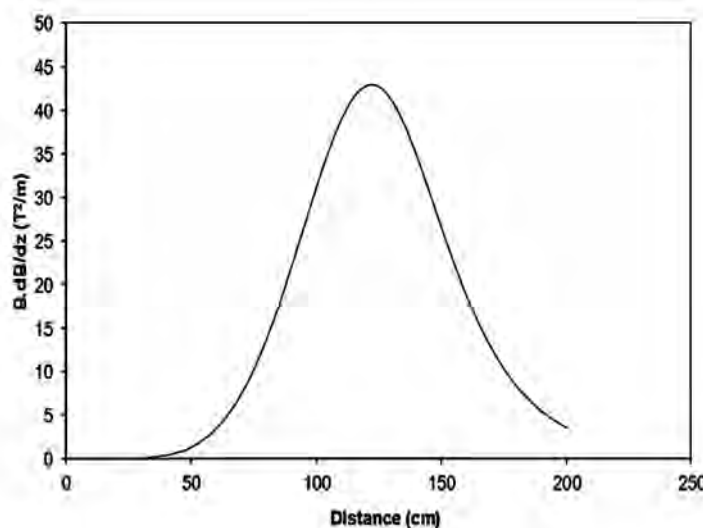
length is shown in **Figure 2**. If magnetic objects get pulled into the magnet of the MR system, they will be lodged at the center of the magnet, where the force drops to zero. To dislodge such objects, the maximum force needs to be overcome, which could be enormous depending on the magnitude of the variables determining the force. The maximum value of

the quantity $\left[B_z \frac{\partial B_z}{\partial z} \right]_{\max}$ determines the maximum value of the translational force for

a needle-like object when it resides on the axis of the magnet and is given by

$$F_{trans}^{\max} = \frac{V}{\mu_o D_a} \left[B_z \frac{\partial B_z}{\partial z} \right]_{\max}. \text{ To determine the torque on the same object, the strength}$$

Figure 2. Force by magnetic field spatial gradient. The product of the spatial gradient of the magnetic and the magnetic field ($B_d B/d_z$) produces a large force that rises to a maximum value around the entry point on either end of the magnet of the MR system. A plot of $B_d B/d_z$ for the 8-T whole-body magnetic field is shown here. The origin corresponds to the center of the magnet.



114 Bioeffects of Static Magnetic Fields

of the force couple applied to both ends of the symmetry axis, say F_{torque} , can be defined as the force necessary to prevent the ellipsoid from being twisted and aligned with \mathbf{B}_0 . The maximum torque along the main axis of the magnet (z -axis) will occur at the isocenter,

when the angle between the long axis of the ellipsoid and the magnet is $\theta = \frac{\pi}{4}$. If the total

length of the ellipsoid is $2 L$, then the absolute value of the forces creating the torque is

$$F_{torque}^{\max} \approx \frac{V}{2\mu_o LD_a} B_z^2 \Big|_{\max}. \text{ Therefore, the rotational force and translation force will be}$$

$$\frac{F_{torque}^{\max}}{F_{trans}^{\max}} = \frac{1}{2L} B_z^2 \Big|_{\max} \sqrt{\left[B_z \frac{\partial B_z}{\partial z} \right]_{\max}}. \text{ For the 8-T whole-body MR system (5) these values}$$

$$\text{are } B_z^{\max} = 8 \text{ T and } \left[B_z \frac{\partial B_z}{\partial z} \right]_{\max} = 42.6 \text{ T}^2/\text{m}. \text{ The ratio (R) of } B_z^2 \Big|_{\max} / \left[B_z \frac{\partial B_z}{\partial z} \right]_{\max}$$

for this magnet was $1.5/\text{m}$, while for most superconducting cylindrical magnets, regardless of their field strengths, this ratio will be comparable to that of the 8-T scanner. For an ellip-

soid of length $L = 1\text{-cm}$ in this magnet the $\frac{F_{torque}^{\max}}{F_{trans}^{\max}} = 75$. Since the 8-T magnet was un-

shielded, for shielded magnets, the ratio, R, would be smaller because the value

$$\left[B_z \frac{\partial B_z}{\partial z} \right]_{\max} \text{ is larger for such magnets. The large ratio of rotational and translational}$$

force indicates that elongated ferromagnetic implants must be tightly anchored to or retained in the patient's tissues because a much larger force is required to prevent rotation as opposed to translational attraction. This is particularly true for implants such as a ferromagnetic aneurysm clip with one dimension longer than the other (i.e., an aneurysm clip with a long blade). These calculations indicate that the possibility of patient injury from aneurysm clips in magnetic fields is much higher due to rotational force than by translational motion. This is notable, because estimations of the effect of magnetic fields have traditionally been focused on translational forces.

Hairpins or paper clips are occasionally lodged inside the MR system. Since the clip is being pulled out of the magnet, the small attractive translational force is at a maximum near the opening of the magnet (i.e., the opening of the bore the scanner) where the patient is inserted for the MRI exam. Torque, however, has a different positional dependence and a maximum value occurs near the center of the magnet, where the axis of the paper clip is at a direction of 45-degrees with respect to the z -axis of the magnetic field.

A close examination of the behavior of biological tissues, with $|\chi| \ll 1$ by using the expressions listed in **Table 3**, demonstrates that the magnitude of the torque acting on these tissues is proportional to χ^2 . Due to the opposite signs of the susceptibilities of diamagnetic and paramagnetic materials, they are expected to point in opposite directions when lined

up in a uniform magnetic field. However, the χ^2 -dependence of torque means that the direction of alignment would be the same for both types of materials. A more important consequence of the χ^2 -dependence of torque is that, for very small values of χ , the alignment torque that is caused by the shape-dependence is negligible. As shown by the above analysis, materials with high susceptibility and those of very low susceptibilities show qualitatively different responses to magnetic fields. Thus, powerful fmagnetic fields apply strong forces on flat ferromagnetic objects, such as magnetic washers, that could align their “face” parallel to the field. Since red blood cells basically have the same geometry as washers, they were expected to experience torque large enough to align them with their flat side parallel to the magnetic field. But, due to the small magnitude of their susceptibility, $\chi^2 \approx 10^{-10}$, the torque acting on red blood cells is exceedingly low and unable to cause any measurable, shape-dependent effect.

Diamagnetic Susceptibility Anisotropy

The shape-dependence of torque due to field inhomogeneity and demagnetizing factors has been demonstrated to be negligible for biological materials due to χ^2 -dependence of the torque expression. However, another mechanism through which magnetic fields can interact with biological tissues is referred to as diamagnetic susceptibility anisotropy (DSA). This effect has been observed in the assembly of large numbers of macromolecules when they are bound together in a crystalline structure. This effect is present when all the molecules in a crystal are twisted in the same orientation by the applied magnetic field. Such conditions allow the torque on individual elements in all the molecules or cells in a volume V to add up to a measurable level. If susceptibility is anisotropic in a tissue, then we can designate its magnitude in one direction of this tissue as χ_1 and the angle between this direction and the applied field as θ . For tissues in which susceptibility in both orthogonal directions is the same and equal to χ_2 , we can assume that for diamagnetic tissues $|\chi_1|, |\chi_2| \ll 1$. For such

tissues, the magnetic energy is given by $U = \frac{1}{2}V\mathbf{M} \bullet \mathbf{B}_o = \frac{VB_o^2}{2\mu_o} [\chi_1 \cos^2 \theta + \chi_2 \sin^2 \theta]$

and the expression of torque will be $T = \frac{\partial U}{\partial \theta} = \frac{VB_o^2}{\mu_o} (\chi_2 - \chi_1) \sin \theta \cos \theta$.

Biological materials usually have negative χ_1 and χ_2 of the order of -10^{-5} that in magnetic fields will experience torque that tends to rotate the object in a direction that aligns the axis with the least negative value of χ with the field. The difference of susceptibility between the two axes is $\Delta\chi = \chi_1 - \chi_2$ that is approximately 1% to 10% of the average susceptibility, $(\chi_1 + 2\chi_2)/3$. For biological tissues, $\Delta\chi$ is of the range of 10^{-7} to 10^{-6} , which is much larger than the shape-dependent torque that has an order of magnitude of 10^{-10} . Prediction of the analysis presented here (i.e., the four order of magnitude larger value of anisotropy-dependent torque than shape-dependent torque) is confirmed by observation in biological materials (143). Another important factor governing the size of torque in the expressions derived in this chapter is the volume, V , of the tissue, which indicates that aggregation of anisotropic molecules to form larger assemblies will increase the torque that can, in turn, enhance the effect of the magnetic field on these tissues.

116 Bioeffects of Static Magnetic Fields

Among biological tissues, red blood cells of sickle cell anemia patients have received much attention, as they have been shown that they align in a field of 0.5-T, *in vitro* (45, 46). The lack of observation of alignment of the hemoglobin molecules in normal red blood cells is due to the fact that they are free in solution and randomly oriented. However, the hemoglobin S molecules in sickle cell red blood cells have a tendency to “stick” together. This binding tendency makes them aggregate, polymerize, form fibers and gel-like structures that are made up of similarly oriented hemoglobin molecules that are bound together. The anisotropic molecules in these structures and their binding in an aligned formation increase the anisotropy of the overall structure that have revealed anisotropy-dependent orientation in these studies (45, 46). However, this effect has only been reported based on laboratory studies. Unlike the conditions *in vitro*, where there is no force competing with magnetic force, the forces experienced by red blood cells in flowing blood are much larger than the magnetic forces of orientation (61, 74, 77, 85). Experiments allowing the observation of magnetic orientation in the presence of flow, however slow, would shed light on the necessary conditions for red blood cell orientation, *in vivo*.

Other structures, such as retinal rod cells, nucleic acid solutions, and fibrin gels have revealed similar orientation effects, *in vitro* (144-149). Similar to red blood cells, we are unaware of a report of magnetic orientation effects by these structures, *in vivo*, for the same reason that flow forces overwhelm the magnetic orientation forces preventing alignment. The size of the magnetic torque, however, as is shown by our equations, depends on B_o^2 . This fact points to a rapidly growing orientation torque as the magnetic field strength increases. Since the trend in MRI is relentlessly pushing for higher static magnetic fields, studies of orientation effects at these higher field strengths are warranted to reveal them, *in vivo*, and to incorporate them into plans for safe exposure of human subjects to such high static magnetic fields. In fact, experiments have already been performed in which 16-T magnets were used to demonstrate that cleavage planes of developing frog embryos orient in powerful magnetic fields (150). Anisotropy-dependent alignment of tubulin molecules has been presented as the cause of this observation (151). Independent confirmation of these effects would validate the effect and the explanation, because many magnetic field effects on biological tissues have proven difficult to reproduce.

Alignment of Water Molecules

We need to be aware of the magnetic field strength required to align water molecules, *in vivo*. Although not reported, the far-reaching consequence of such effect on life justifies the vigilance. The possibility of aligning of water molecules in magnetic fields and its ability to alter the biological and physiological processes in tissues are already proposed as a rationale for magnetotherapy, a commercial venture with some success in convincing its followers of its therapeutic efficacy. This is in consideration of the fact that physics allows us to estimate the extent of alignment of water molecules inside magnetic fields. The random orientation of water molecules is the cause of its small magnetic susceptibility of $\chi = -9.05 \times 10^{-6}$. A variation of about one-percent in χ along the principal axes of the molecule is caused by the asymmetry of the water molecule (152). As previously discussed, susceptibility anisotropy is the basis of the development of magnetic torque. Therefore, we need to calculate the magnetic alignment energy of a water molecule. Here, we will present such calculations for an applied field of 10-Tesla as is presently close to the upper range of

field strengths of research scanners to which human subjects have been exposed. Inserting the susceptibility of water and field strength of $B = 10\text{-T}$ in the expression for magnetization

yields $M = \chi H = \frac{\chi}{\mu_0} B = -72 \text{ A/m}$. This is the magnetization, which is the sum of magnetic dipole moments of 3.34×10^{28} water molecules per cubic meter. The average dipole moment per water molecule in a field of 10-Tesla is calculated to be $m = -2.16 \times 10^{-27} \text{ J/T}$.

The implication of 1% anisotropy of the molecular magnetization is that a maximum magnetic energy change due to change in molecular orientation is calculated to be $\Delta E = 2.16 \times 10^{-29} \text{ J}$. To compare this magnetic energy with thermal energy of the human body at 38°C

yields $kT = 4.28 \times 10^{-21} \text{ J}$ and a ratio of $\frac{\Delta E}{kT} = 5.0 \times 10^{-9}$ for a 10-T magnet. This indicates that the magnetic energy is 200 million times smaller than thermal energy at 10-Tesla.

Such minimal energy is unlikely to cause significant biological or physiological changes in water molecules, *in vivo*.

These results indicate that for a 0.01% deviation from random orientation of water molecules, a static magnetic field strength of 450-Tesla is needed. This is in spite of the B^2 -dependence of the magnetic energy. By comparison, the expected alignment within the fields of even ultra-high-field-strength MR systems is negligible. To our knowledge, to date, no observation of magnetic field-induced alignment of water molecules has been reported at the static magnetic field strengths used for research or clinical scanners. This is in agreement with the model presented above for magnetic alignment of diamagnetic molecules in strong magnetic fields.

Translational Forces

Injury can be caused by the application of forces on tissues. For tissue components with large differences in magnetic properties, such forces could develop in nonuniform magnetic fields. As it was shown earlier, diamagnetic tissue components tend to move toward lower fields and paramagnetic tissue components will be forced to higher field regions. The formation of such opposing forces on components of the same tissue could interfere with the physiological function of the tissue and lead to injury. It is conceivable that under normal circumstances, biological structures have greater internal forces, such as electric forces involved in chemical reactions, than magnetic forces due to susceptibility variations (34, 87). Furthermore, gravitational forces and forces produced by acceleration and other motions during routine activities produce considerable forces on tissue components. The evolution of life under the gravitational action of Earth and routine life activities must have resulted in development of the “means” to incorporate these forces in the inner workings of living beings. These “means” will be unable to identify the source of the force and end up preventing tissue function from being substantially affected by magnetic forces.

As it was shown in the examples above for UHF magnets, for magnetic torque acting on water molecules, the differential magnetic forces can be much smaller than differential gravitational forces. This is important since even the larger differential gravitational forces are too small to disturb physiological processes. Here, too, red blood cells can be used to

118 Bioeffects of Static Magnetic Fields

as a quantitative analysis of the role of magnetic translational forces. Behavior of red blood cells in the blood is affected by its higher density than plasma, making them sink in the blood in the absence of larger hemodynamic forces. This effect, called erythrocyte sedimentation rate (ESR), is used in the laboratory to test for abnormalities of blood proteins. While gravitational forces are useful for separation of blood ingredients in test tubes, they are too small to make red blood cells sink, *in vivo*.

The molecule, hemoglobin, has four iron atoms in each molecule that reduce the diamagnetic properties of red blood cells, making it slightly less than that of surrounding plasma. This pushes red blood cells toward regions of strong magnetic fields relative to the plasma. Using the expression for magnetic force from **Table 3**, the magnitude of this

differential force is given by $\frac{(\chi_{rbc} - \chi_{plasma})V_{rbc}}{\mu_o} B_o \frac{\partial B_o}{\partial z}$. Working this example for the

8-T whole body scanner, the maximum value of $B_o \frac{\partial B_o}{\partial z}$ is 42.6-T²/m. To find the sus-

ceptibility of deoxygenated hemoglobin, participation of four iron atoms per molecule is taken into account to get $\chi_{rbc} = -6.53 \times 10^{-6}$. Take the susceptibility of plasma to be the same as water, -9.05×10^{-6} . In addition, the mass densities of red blood cells and plasma are given by $\rho_{rbc} = 1.093 \text{ g/cc}$ and $\rho_{plasma} = 1.027 \text{-g/cc}$. Inserting these quantities in the equation will give the ratio of the magnetic and gravitational forces at 8-T to be

$$\frac{F_m}{F_g} = \frac{1}{\mu_o g} B \frac{\partial B}{\partial z} \frac{\chi_{rbc} - \chi_{plasma}}{\rho_{rbc} - \rho_{plasma}} = 0.13 \text{ where gravitational acceleration is taken to be}$$

$g = 9.8 \text{-m/s}^2$. As is seen from these calculations, even at the highest static magnetic field strength available for MRI research, the maximum magnetic force capable of separating the red blood cells from the plasma is about 13 percent of the gravitational forces. Considering that gravitational forces have negligible effects, *in vivo*, the effect of magnetic forces is even smaller by almost an order of magnitude for static magnetic fields of up to 8-T.

Discussions and calculations in this section show that, while finite magnetic effects act on tissues in magnetic fields, their magnitude for field strengths available for MRI examinations in human subjects is relatively small when compared to other known forces, such as gravitational and routine physical activities, and these forces are clearly incapable of causing injury to biological tissues. Importantly, forces maintaining the integrity of molecular and cellular structures of biological tissues appear to be orders of magnitude larger than the forces that magnetic fields can exert on living beings.

SENSORY EFFECTS OF STATIC MAGNETIC FIELDS

Static magnetic effects acting on stationary tissues were presented in previous sections. Here, we will analyze the interaction of sensory tissues with magnetic fields. Research in this area has revealed that motion in strong magnetic fields could induce mild sensory effects that are transient and not harmful (44, 48, 80, 86). These reports rely on a subjective description of sensory stimulations and, as such, their effects have to be interpreted with great

caution because the number of studies of these effects is limited. On the issue of subjectivity of this effect, reports have documented static magnetic field-induced sensory effects experienced by staff members working around superconducting magnets, even during the time when the magnets were “off” (89). Nevertheless, comparisons of incidents at different field strengths show that human subjects exposed to higher fields (e.g., 9.4-Tesla) reported higher rates of sensory stimulation than those subjected to a 0.5-Tesla field (5, 86, 153). Field-dependence of sensory effects has been both expected and reported by workers on high field strength scanners. Particularly, sensations of nausea, vertigo, and metallic taste related to exposures to static magnetic fields operating at 4-, 8-, and 9.4-Tesla have been reported (5, 86, 153). However, effects such as headache, tinnitus, vomiting, hiccups, and numbness that have sometimes been attributed to static magnetic field exposures have not been consistently observed for the same field strengths.

Magnetophosphenes, sensations of light flashing when the eyes are moved rapidly while inside the magnetic field in a dark room, have been reported at static magnetic field strengths of up to 9.4-Tesla. Computational results have confirmed the factors involved in the observation of magnetophosphenes and have provided quantitative models for this phenomenon (154).

Sensory experiences in static magnetic fields from 0.5- to 9.4-Tesla have been reported and shown that avoiding rapid body movements inside these magnetic fields may reduce these sensations. In addition, lower field strengths are associated with reduced sensations of peripheral nerve stimulation. However, there is substantial evidence that magnetic field-induced sensory effects are caused by activation of highly excitable sensory systems by weak electrical currents that can be induced by moving certain body parts inside magnetic fields (154-156). Sensations such as nausea have been reported, which are probably caused by magnetic forces exciting motion sensors in the semicircular canals of the inner ear (98). This specific effect may be created due to a conflict in the position information supplied by the visual systems and vestibular position-sensing system. A possible source of vertigo could be magnetic forces caused by diamagnetic anisotropy of the inner ear receptors. Small amounts of torque acting on these receptors could induce a small level of sensory effects. Notably, the slow movement of the patient inside or around a very strong magnetic field drastically reduces sensory stimulations and provides comfort in association with the performance of an MRI examination using a UHF MR system. For this reason, the 7-Tesla MR system that is approved for clinical use (Terra, Siemens Healthineers) has a table that moves the patient slowly into the scanner, thus, avoiding the afore-mentioned issues related to rapid movements in a powerful static magnetic field.

HEATING EFFECTS

Studies using laboratory animals have reported the effect of static magnetic fields on body and skin temperatures (157-162). However, these investigations do not offer an unequivocal conclusion about this issue. One report indicated that exposure to static magnetic fields can change body temperature depending on the orientation of the animal with respect to the magnetic field (157). Another report presented measurements performed on small animals and made specific comments about their mechanism of action (161). Still other

120 Bioeffects of Static Magnetic Fields

studies of mammals, including those involving human subjects, reported the absence of an effect of static magnetic fields on skin and body temperatures (158-160).

Most reports of temperature changes related to static magnetic fields have not proposed a plausible mechanism for these observations. The choice of animals as well as the temperature measuring devices could affect the results of such studies because, in some of the reports of static magnetic field-induced temperature changes, the investigations used temperature-labile mammals or problematic instrumentation. Also, the possibility of the strong static magnetic fields causing erroneous readings on the temperature recording devices was not addressed.

Various investigations performed using laboratory animals and human subjects exposed to high static magnetic fields have reported that there are no changes in skin or body temperatures (6, 158-160). Utilizing a fluoroptic thermometry system known to be impervious to strong magnetic fields to record temperatures in laboratory animals and human studies ensures that accurate temperature readings are achieved inside the bore of the MR system. In consideration of the above, to date, exposure to static magnetic fields is not believed to alter human body temperatures.

SAFETY REGULATIONS

The safety of human exposure to MR systems is the responsibility of the Food and Drug Administration (FDA) in the United States (U.S.) and other similar agencies outside of the U.S. The FDA provides guidelines for the limits of safe exposures to static magnetic fields as well as the other electromagnetic fields used for MRI (i.e., gradient magnetic fields and radiofrequency power deposition). The FDA's assessment of the health risks associated with exposure to static magnetic fields was last updated in 2014, with the upper limit set at 8-Tesla (4). The World Health Organization (WHO) also established health criteria for static magnetic fields within the Environmental Health Criteria Program (163). The International Commission on Non-Ionizing Radiation Protection (ICNIRP) reports, along with other similar documents, offers insight and regulatory guidelines pertaining to the biological effects of exposure to static magnetic fields (163-176). The regulatory body in the United Kingdom for medical device safety is the National Radiological Protection Board (NRPB) and in the European Union, this task is carried out by the International Electrotechnical Commission (IEC). All of these regulatory bodies evaluate the available scientific databases and develop the rationale for updated guidelines as new data and technology become available (169-179).

The Medical Devices Act passed by the U.S. Congress in 1977 required MRI to demonstrate its viability as an imaging modality and safety for the first time. Subsequent to the discovery of MRI as an important medical imaging device, major manufacturers introduced their products and applied for FDA approval. Rapid success in demonstrating its safe operation led to the 1987 FDA designation of a static magnetic field strength of 2-T as the limit below which MR systems will pose a non-significant risk to human subjects. Proliferation of MR scanners and research systems helped to support an increase in the non-significant field strength risk to 4-T in 1996 and 8-T in 2003 (note, this document was updated in 2014)(4). Accordingly, since 2003, exposure of research subjects to static magnetic fields

above 8-T in the U.S. requires approval of the research protocol by an Institutional Review Board (IRB) with informed consent of the subjects.

Occupational Exposure

Exposure to strong magnetic fields is often greater from a time consideration for workers involved with manufacturing and testing magnet-based instruments and devices than it is for patients. In addition to workers involved in the manufacturing process for MR systems, MRI researchers, MRI technologists/radiographers working in research, medical center, and out-patient settings, as well as experimental high-energy physicists are among the populations with chronic exposures to strong static magnetic fields. To regulate chronic exposures, guidelines have been developed by certain countries. Proposed in Europe, a time-weighted-average field exposure of 0.20-T/8-hour would limit the workers to 0.2-T field for an eight-hour day or 8-T for 12-minutes. A higher limit of 2-T/8-hour limit was proposed for the extremities by these guidelines. The lack of confirmed evidence for harmful cumulative effects of exposures to static magnetic fields has made these limits less consequential than the limit on the highest static magnetic field strength applied to human subjects. This is especially true as the fields outside the magnets are highly inhomogeneous. The strong spatial variation of the magnetic fields is not usually specified for MR systems, and because of this (i.e., the fringe field), workers are not constantly exposed to the magnetic field, making it difficult to measure the effect over a workday period. For these workers, the most ominous potential hazard remains to be the inadvertent introduction of ferromagnetic tools or other objects into areas with high fringe fields.

Researchers are continuing to investigate the chronic effects of any mechanism of tissue injury at the static magnetic field strengths currently available for human magnets (i.e., whole-body MR scanners). Expanding the number of controlled studies that involve long-term exposures of animals and human subjects to strong magnetic fields may offer valuable insight into the safety of chronic magnetic field exposures. Furthermore, the collection of safety data from MR system manufacturers, researchers, and medical staff will be helpful for the analysis of the effects of static magnetic fields on human subjects.

CONCLUSIONS

According to health data published by the Organization for Economic Co-operation and Development (OECD) in 2009, the average number of MRI examinations performed per 1,000-population per year for the thirty countries of the OECD was forty-one. Considering the population of the OECD to be 1.2 billion means that approximately 54 million MRI exams were performed in the thirty OECD countries each year (180). In the United States, 91.2 MRI procedures per 1,000-population equates to about 28 million examinations annually. Nevertheless, no unpreventable harm to the patients from exposure to the static magnetic field has been reported. As previously indicated, all serious accidents associated with MR systems, to date, have been caused by the involuntary introduction of ferromagnetic materials or medical devices into the magnetic field. In addition to clinical scanners, research scanners operating at fields of up to 11.7-Tesla for human subjects and over 20-T for animals have shown no major safety incidents, which has laid the foundation for clinical scanners to be designed for operation at higher field strengths. There is still considerable fertile

122 Bioeffects of Static Magnetic Fields

ground for research in studying the interaction of biological tissues with stronger magnetic fields, regardless of how safe the record of operation at high static magnetic fields is at the present time.

Keeping in mind that the spatial gradient magnetic field will be larger for higher field strength magnets, more stringent measures to exclude the presence of ferromagnetic objects from MRI suites will be needed. In spite of the existence of more than eighty 7-T research and clinical MR systems around the world, a number of technological issues such as RF inhomogeneity, susceptibility artifacts, and RF power deposition (i.e., SAR) issues will continue to present challenges (178). Nevertheless, the relentless drive for higher fields is achieving new milestones, such as the 21.1-T, 105-mm magnet located at the National High Magnetic Field Laboratory in Tallahassee, Florida (which currently is the strongest MR system in the world used for small animal imaging). Nuclear magnetic resonance (NMR) devices operating at 23.5-T with a hydrogen proton Larmor frequency of 1-GHz and a bore size of 54-mm are now commercially available. This trend will continue and the safety investigations involving small animals will add valuable information for our understanding of the interactions of these fields with living beings.

Research on the effect of strong magnetic fields on tissues, cells, and molecules has not produced evidence for its harm to human life. The magnetic forces analyzed in many publications have proven to be insignificant compared to the natural forces that maintain the structural integrity of the tissues and the routine forces to which the human body is exposed to during everyday activities.

Regulatory bodies have justifiably taken the attitude of requiring verification of any claim of adverse effects to static magnetic fields before limits are incorporated into safety guidelines. This is a reasonable approach that has demonstrated attention to scientific findings, while preventing unnecessary impediments to research and exploration of benefits of magnetic fields for the good of society.

Fortunately, the physics of such interactions are straightforward and simple calculations provide insight into the order of magnitude of magnetic field effects. To date, such calculations have indicated that forces exerted on diamagnetic materials, of which biological tissue are overwhelmingly made, are insignificant compared to other forces involved in maintaining their structure and function. It seems that all of the major revisions in the FDA guidelines for assessing non-significant risk involved in the exposure of human subjects to static magnetic fields have followed this course of action. The present FDA guidelines recommend 8-T as the strongest magnetic field with non-significant risk. As the field strengths are increasing for whole body scanners, it is conceivable that sensory effects such as vertigo, metallic taste, magnetophosphenes, and possibly other responses may become more prevalent. However, no permanent harm from these effects has been presented. Transient effects caused by movement inside the magnetic field can be minimized through MRI operator training. Notably, the long-term, cumulative effect of exposures to static magnetic fields is a topic requiring additional research.

As the field strength of MR systems increases, it is conceivable that eventually, one of the forces of interaction will become large enough to require limiting its effect on human life. Diamagnetic susceptibility is unlikely to be the limiting factor. However, the effect of

field inhomogeneity and the magnetic effect on blood flow could limit the persistent drive towards higher fields. For now, even research magnets seem to be far from that limit and we are fortunate to be able to safely explore the benefits of higher static magnetic fields in order to visualize the structure and function of the human body. If more complex safety studies continue to confirm that there are no substantial adverse effects, then much higher magnetic fields could become available for human MR imaging to continuously enhance our ability to observe otherwise opaque biological structures and functions. Such observations may lead to better healthcare for future generations and offer an understanding of the mysteries of life.

(Portions this chapter were excerpted from Kangarlu A, Schenck JF. Chapter 2, Biological Effects of Static Magnetic Fields. In: Shellock FG, Crues JV, Editors. Bioeffects, Safety, and Patient Management. Biomedical Research Publishing Group, Los Angeles, CA, 2014.)

REFERENCES

1. Damadian R. Tumor detection by nuclear magnetic resonance. *Science* 1971;171:1151-1153.
2. Lauterbur PC. Image formation by induced local interactions: Examples employing nuclear magnetic resonance. *Nature* 1973;242:190 -191.
3. McRobbie DW. Occupational exposure in MRI. *Br J Radiol* 2012;85:293-312.
4. U.S. Department of Health and Human Services, Food and Drug Administration, Center for Devices and Radiological Health. Criteria for Significant Risk Investigations of Magnetic Resonance Diagnostic Devices - Guidance for MRI Industry and FDA Staff. Issued June 20, 2014.
5. Kangarlu A, Robitaille PML. Biological effects and health implications in magnetic resonance imaging. *Concepts in Magnetic Resonance* 2000;12:321–359.
6. Kangarlu A, Shellock FG, Chakeres DW. 8.0-Tesla human MR system: Temperature changes associated with radiofrequency-induced heating of a head phantom. *J Magn Reson Imaging* 2003;17:220-6.
7. Kangarlu A, Shellock FG. Aneurysm clips: Evaluation of magnetic field interactions with an 8.0 T MR system. *J Magn Reson Imaging* 2000;12:107-11.
8. Heinrich A, Szostek A, Meyer P, et al. Cognition and sensation in very high static magnetic fields: A randomized case-crossover study with different field strengths. *Radiology* 2013;266:236-45.
9. Chakeres DW, Kangarlu A, Boudoulas H, Young DC. Effect of static magnetic field exposure of up to 8 Tesla on sequential human vital sign measurements. *J Magn Reson Imaging* 2003;18:346-52.
10. Chakeres DW, Bornstein R, Kangarlu A. Randomized comparison of cognitive function in humans at 0 and 8 Tesla. *J Magn Reson Imag* 2003;18:342-5.
11. Mottelay PF. *Bibliographical History of Electricity and Magnetism Chronologically Arranged*. London: Charles Griffin & Co.; 1922.
12. Davis LD, Pappajohn K, Plavnieks IM, Spiegler PE, Jacobius AJ. Bibliography of the biological effects of magnetic fields. *Fed Proc Suppl* 1962;2:1-38.
13. Gross L. Bibliography of the Biological Effects of Static Magnetic Fields. In: Barnothy MF, Editor. *Biological Effects of Magnetic Fields*. New York: Plenum Press; 1964. pp. 297-311.
14. Gartrell RG. *Electricity, Magnetism, and Animal Magnetism: A Checklist of Printed Sources, 1600-1850*. Wilmington, DE: Scholarly Resources, Inc.; 1975.
15. Mourino MR. From Thales to Lauterbur, or from the lodestone to MR imaging: Magnetism and medicine. *Radiology* 1991;180:593-612.

124 Bioeffects of Static Magnetic Fields

16. Binet A, Fétré C. *Animal Magnetism*. Kegan Paul, Editor. London: 1887. Reprinted, New York: Gryphon Editions; 1993.
17. Barnothy MF. *Editor, Biological Effects of Magnetic Fields*. New York: Plenum Press; 1964.
18. Kholodov YA. *The effect of electromagnetic and magnetic fields on the central nervous system*. NASA Technical Translation F-465, Clearing House for Federal Scientific and Technical Information, Springfield, VA: 1967.
19. Barnothy MF. *Editor, Biological Effects of Magnetic Fields. Volume 2*. New York: Plenum Press; 1969.
20. Pressman AS. *Electromagnetic Fields and Life*. Sinclair FL, Brown FA Jr, Translators. New York: Plenum Press; 1970.
21. Kholodov YA. *Editor, Influence of Magnetic Fields on Biological Objects*. Springfield, VA: JPRS 63038, National Technical Information Service; 1974.
22. Llaurodo JG, Sances A, Battocletti AJH, Editors. *Biologic and Clinical Effects of Low-Frequency Magnetic and Electric fields*. Springfield, IL: Thomas; 1974.
23. Buranelli V. *The Wizard from Vienna: Franz Anton Mesmer*. New York: Coward, McCann and Geohagen; 1975.
24. Tenforde TS. *Editor. Magnetic Field Effect on Biological Systems*. New York: Plenum Press; 1979.
25. Herlach F. Editors, *Strong and Ultrastrong Magnetic Fields and Their Applications*. Berlin: Springer-Verlag; 1985.
26. Maret G, Boccara N, Kiepenheuer J, Editors. *Biophysical Effects of Steady Magnetic Fields*. Berlin: Springer-Verlag; 1986.
27. Polk C, Postow E. *Handbook of Biological Effects of Electromagnetic Fields*. Boca Raton, FL: CRC Press; 1986.
28. Crabtree A. *From Mesmer to Freud: Magnetic Sleep and the Roots of Psychological Healing*. New Haven: Yale University Press; 1993.
29. Shellock FG, Kanal E, *Magnetic Resonance: Bioeffects, Patient Safety, and Patient Management*. Second Edition. Philadelphia, PA: Lippincott-Raven; 1996.
30. Whitaker J, Adderly B. *The Pain Relief Breakthrough: The Power of Magnets to Relieve Backaches, Arthritis, Menstrual Cramps, Carpal Tunnel Syndrome, Sports Injuries and More*, Boston: Little Brown; 1998.
31. Quinan JR. *The use of the magnet in medicine: A historical study*. Maryland Med J 1886;14:460-465.
32. Schaefer DJ. *Safety Aspects of Magnetic Resonance Imaging*. In: Wehrli FW, Shaw D, Kneeland JB, Editors. *Biomedical Magnetic Resonance Imaging: Principles, Methodology and Applications*. Weinheim: VCH Verlagsgesellschaft; 1988. pp. 553-578.
33. Shellock FG, Kanal E, Moscatel M. *Bioeffects and Safety Considerations*. In: Atlas SW, Editor. *Magnetic Resonance Imaging of the Brain and Spine*. Second Edition. Philadelphia, PA: Lippincott-Raven; 1996. pp. 109-148.
34. Schenck JF. *MR Safety at High Magnetic Field Strengths*. In: Kanal E. Editor. *Magnetic Resonance Imaging Clinics of North America: MR Safety*. Volume 6. Philadelphia, PA: Saunders; 1998. pp. 715-730.
35. Hermann L. *Hat das magnetische Feld directe physiologische Wirkungen?* Pflügers Arch Gesammte Physiol Menschen Thiere 1888;43:217-234.
36. Peterson F, Kennelly AE. *Some physiological experiments with magnets at the Edison Laboratory*. NY Med J 1892;56:729-734.
37. Drinker CK, Thomson RM. *Does the magnetic field constitute an industrial hazard?* J Ind Hyg 1921;3:117-129.
38. American Medical Association. *Theronoid and vitrona: The magic horse collar campaign continues*. JAMA 931;96:1718-1719.

MRI Bioeffects, Safety, and Patient Management 125

39. Barnothy MF, Barnothy JM, Boszormenyi-Nagy I. Influence of magnetic field upon the leucocytes of the mouse. *Nature* 1956;177: 577-578.
40. Barnothy MF, Barnothy JM. Biological effect of a magnetic field and the radiation syndrome. *Nature* 1958;181:1785-1786.
41. Freeman MW, Arrott A, Watson JHL. Magnetism in medicine. *J Appl Phys* 1960;31:404S-405S.
42. Eiselein TE, Boutell HM, Biggs MW. Biological effects of magnetic fields – negative results. *Aerospace Medicine* 1961;32:383-386.
43. Beischer DE. Human tolerance to magnetic fields. *Astronautics* 1962;7:24-25.
44. Beischer DE, Knepton Jr JC. Influence of strong magnetic fields on the electrocardiogram of squirrel monkeys (*Saimiri sciureus*). *Aerospace Medicine* 1964;35: 939-944.
45. Murayama M. Orientation of sickled erythrocytes in a magnetic field. *Nature* 1965;206:420-422.
46. Murayama M. Molecular mechanism of red cell “sickling”. *Science* 1966;153:145-149.
47. Malinin GI, Gregory WD, Morelli L, Sharma VK, Houck JC. Evidence of morphological and physiological transformation of mammalian cells by strong magnetic fields. *Science* 1976;194:844-846.
48. St. Lorant SJ. Biomagnetism: A Review. In: SLAC Publication, 1984. Stanford, CA: Stanford Linear Accelerator; 1977. pp. 1-9.
49. Ketchen EE, Porter WE, Bolton NE. The biological effects of magnetic fields on man. *Am Ind Hyg Assoc J* 1978;39:1-11.
50. Budinger TF. Threshold for physiological effects due to RF and magnetic fields used in NMR imaging. *IEEE Trans Nucl Sci* 1979;NS-26:2821-2825.
51. Saunders RD. Biological Hazards of NMR. In: Witcofski RL, Karstaedt N, Partain CL, Editors. *Proceedings of an International Symposium on Nuclear Magnetic Resonance Imaging*. Winston-Salem, NC: Bowman Gray School of Medicine; 1981. pp. 65-71.
52. Battocletti JH, Salles-Cunha S, Halbach RE, et al. Exposure of rhesus monkeys to 20000 G steady magnetic field: Effect on blood parameters. *Med Phys* 1981;8:115-118.
53. Budinger TF. Nuclear magnetic resonance (NMR) *in vitro* studies: Known thresholds for health effects. *J Comput Assisted Tomog* 1981;5:800-811.
54. Hong C-Z, Lin JC, Bender LF, et al. Magnetic necklace: Its therapeutic effectiveness on neck and shoulder pain. *Arch Phys Med Rehabil* 1982;63:462-466.
55. Budinger TF. Hazards from DC and AC Magnetic Fields. In: Book of Abstracts. Berkeley, CA: Society of Magnetic Resonance in Medicine; 1982. pp. 29-30.
56. Milham S. Mortality from leukemia in workers exposed to electrical and magnetic fields (Letter). *N Engl J Med* 1982;307:249.
57. New PF, Rosen BR, Brady TJ, et al. Potential hazards and artifacts of ferromagnetic and nonferromagnetic surgical and dental materials and devices in nuclear magnetic resonance imaging. *Radiology* 1983;147:139-148.
58. Saunders RD, Smith H. Safety aspects of NMR clinical imaging. *Br Med Bull* 1984;40:148-154.
59. Budinger TF, Bristol KS, Yen CK, Wong P. Biological Effects of Static Magnetic Fields. In: Book of Abstracts. Berkeley, CA: Society of Magnetic Resonance in Medicine; 1984. pp. 113-114.
60. Budinger TF, Cullander C. Health Effects of *In Vivo* Nuclear Magnetic Resonance. In: Biomedical Magnetic Resonance. James CE, Margulis A. Editors. San Francisco: Radiology Research and Education Foundation; 1984. pp. 421-441.
61. Brody AS, Sorette MP, Gooding CA, et al. Induced alignment of flowing sickle erythrocytes in a magnetic field: A preliminary report. *Invest Radiol* 1985;20:560-566.
62. Kelly WM, Paglen PG, Pearson JA, San Diego AG, Soloman MA. Ferromagnetism of intraocular foreign body causes unilateral blindness after MR study. *Am J Roentgenol* 1986;7:243-245.

126 Bioeffects of Static Magnetic Fields

63. Gleick J. Man hurt as medical magnet attracts forklift. New York Times 1986;A21.
64. von Klitzing L. Do static magnetic fields of NMR influence biological signals? *Clin Phys Physiol Meas* 1986;7:157-160.
65. Lund G, Nelson JD, Wirtschafter JD, et al. Tattooing of eyelids: Magnetic resonance imaging artifacts. *Ophthalmic Surg* 1986;17:550-553.
66. Fowler JR, Ter Penning B, Syverud SA, Levy RC. Magnetic field hazard (Letter). *N Engl J Med* 1986;314:1517.
67. Miller G. Exposure guidelines for magnetic fields. *Am Ind Hyg Assoc J* 1987;48:957-968.
68. Weiss RA, et al. Mascara and eye-lining tattoos: MRI artifacts. *Ann Ophthalmology* 1989;21:129-131.
69. Budinger TF. Magnetohydrodynamic Retarding Effect on Blood Flow Velocity at 4.7 Tesla Found to be Insignificant. In: Book of Abstracts. Berkeley, CA: Society of Magnetic Resonance in Medicine; 1987. pp.183.
70. Tope WD, Shellock FG. Magnetic resonance imaging and permanent cosmetics (tattoos): Survey of complications and adverse events. *J Magn Reson Imag* 2002;15:180-184.
71. Sacco DC, Steiger DA, Bellon EM, et al. Artifacts caused by cosmetics in MR imaging of the head. *Am J Roentgenol* 1987;148:1001-1004.
72. Wolfley DE, Flynn KJ, Cartwright J. Eyelid pigment implantation: Early and late histopathology. *Plast Reconstr Surg* 1988;82:770-774.
73. Schenck JF, Dumoulin CL, Mueller OM, et al. Proton Imaging of Humans at 4.0 Tesla. In: Book of Abstracts. Berkeley, CA: Society of Magnetic Resonance in Medicine; 1988. pp. 153.
74. Brody AS, Embury SH, Mentzer WC, Winkler M, Gooding CA. Preservation of sickle cell bloodflow patterns during MR imaging: An *in vivo* study. *Am J Roentgenol* 1988;151:139-141.
75. Redington RW, Dumoulin CL, Schenck JF, et al. MR Imaging and Bio-effects in a Whole-Body 4.0 Tesla Imaging System. In: Book of Abstracts. Berkeley, CA: Society of Magnetic Resonance in Medicine; 1988. pp. 20.
76. Wahlund L-O, Agartz, I, Almqvist, O, et al. The brain in healthy aged individuals. *Radiology* 1990;174:674-679.
77. Mankad VN, Williams JP, Harpen MD, et al. Magnetic resonance imaging of bone marrow in sickle cell disease: clinical, hematological, and pathologic correlations. *Blood* 1990;75:274-283.
78. Hong C-Z, Shellock F. Short term exposure to a 1.5 Tesla static magnetic field does not affect somatosensory-evoked potentials in man. *Magn Reson Imaging* 1990;8:65-69.
79. Muller S, Hotz M. Human brainstem auditory evoked potentials (BAEP) before and after MR examinations. *Magn Reson Med* 1990;16:476-480.
80. Schenck JF, Dumoulin CL, Souza SP. Health and Physiological effects of human exposure to whole-body 4 Tesla magnetic fields during magnetic resonance scanning. In: Book of Abstracts. Berkeley, CA: Society of Magnetic Resonance in Medicine; 1990. pp. 277.
81. Keltner JR, Roos MS, Brakeman PR, Budinger TF. Magnetohydrodynamics of blood flow. *Magn Reson Med* 1990;16:139-149.
82. Phillips ME. Industrial hygiene investigation of static magnetic fields in nuclear magnetic resonance facilities. *Appl Occup Environ Hyg* 1990;5:353-358.
83. Kelsey CA, King JN, Keck GM, et al. Ocular hazard of metallic fragments during MR imaging at 0.06 T. *Radiology* 1991;180:282-283.
84. Buettner UW. Human Interactions with Ultra High Fields. In: Magin RL, Liburdy RP, Persson B, Editors. *Biological and Safety Aspects of Nuclear Magnetic Resonance Imaging and Spectroscopy*. Annals of the New York Academy of Sciences, Volume 649. New York: New York Academy of Sciences; 1992. pp. 59-66.

MRI Bioeffects, Safety, and Patient Management 127

85. Schenck JF. Quantitative Assessment of the magnetic forces and torques in red blood cells: Implications for patients with sickle cell anemia. In: Book of Abstracts. Berkeley, CA: Society of Magnetic Resonance in Medicine; 1992. pp. 3405.
86. Schenck JF, Dumoulin CL, Redington RW, et al. Human exposure to 4.0-Tesla magnetic fields in a whole-body scanner. *Med Phys* 1992;19:1089-1098.
87. Schenck JF. Health and Physiological Effects of Human Exposure to Whole-Body Four-Tesla Magnetic Fields During MRI. In: Magain RL, Liburdy RP, Persson B. Editors. *Biological and Safety Aspects of Nuclear Magnetic Resonance Imaging and Spectroscopy*. Annals of the New York Academy of Sciences, Volume 649. New York: New York Academy of Sciences; 1992. pp 285-301.
88. Macklis RM. Magnetic healing, quackery, and the debate about the health effects of electromagnetic fields. *Ann Int Med* 1993;118:376-383.
89. Erhard P, Chen W, Lee J-H, Ugurbil K. A study of effects reported by subjects at high magnetic fields. In: Book of Abstracts. Berkeley, CA: Society of Magnetic Resonance in Medicine; 1995. pp. 1219.
90. Schenck JF. The role of magnetic susceptibility in magnetic resonance imaging: Magnetic field compatibility of the first and second kinds. *Med Phys* 1996;23:815-850.
91. Shermer M, Salas C, Salas D. Testing the claims of mesmerism: Commissioned by King Louis XVI: Designed, conducted and written by Benjamin Franklin, Antoine Lavoisier and others. Translation of the 1784 report of the commissioners charged by the King to examine animal magnetism. *Skeptic* 1996;4:66-83.
92. Minczykowski A, Włodzimierz P, Smielecki J, et al. Effects of magnetic resonance imaging on polymorphonuclear neutrophil functions. *Acad Radiol* 1996;3:97-102.
93. Vallbona C, Hazlewood CF, Jurida G. Response of pain to static magnetic fields in postpolio patients: A double-blind pilot study. *Arch Phys Med Rehabil* 1997;78:1200-1203.
94. Horstman J. Explorations: Magnets. *Arthritis Today* 1988;12:48-51.
95. Ramey DW. Magnetic and electromagnetic therapy. *Sci Rev Alt Med* 1998;2:13-19.
96. Kinouchi Y, Yamaguchi H, Tenforde TS. Theoretical analysis of magnetic field interactions with aortic blood flow. *Bioelectromagnetics* 1996;17:21-32.
97. Feingold L. Magnet therapy. *Sci Rev Alt Med* 1999;3:26-33.
98. Kangarlu A, Burgess RE, Zhu H, et al. Cognitive, cardiac, and physiological safety studies in ultra high field magnetic resonance imaging. *Magn Reson Imaging* 1990;17:1407-1416.
99. Klucznik RP, Carrier DA, Pyka R, et al. Placement of a ferromagnetic intracerebral aneurysm clip with a fatal outcome. *Radiology* 1993;187:587-599.
100. Kanal E, Shellock FG. MR imaging of patients with intracranial aneurysm clips. *Radiology* 1993;187:612-614.
101. Gimbel JR, Johnson D, Levine PA, et al. Safe performance of magnetic resonance imaging on five patients with permanent cardiac pacemakers. *Pacing Clin Electrophysiol* 1996;19:913-919.
102. Becker RO. *Cross Currents. The Promise of Electromedicine, the Perils of Electropollution*. Torcher. Los Angeles: 1990.
103. Davis AR, Rawls WC. *Magnetism and Its Effects on the Living System*. Smithtown, NY: Exposition Press; 1975.
104. Wilson MN. *Superconducting Magnets*. Oxford: Clarendon Press; 1983.
105. Vallbona C, Richards T. Evolution of magnetic therapy from alternative to traditional medicine. *Phys Med Rehabil Clin N Am* 1999;10:729-54.
106. Hinshaw WS, Bottomley PA, Holland GN. Radiographic thin-section image of the human wrist by nuclear magnetic resonance. *Nature* 1977;270:722-723.
107. Hinshaw WS, Andrew ER, Bottomley PA, et al. Display of cross sectional anatomy by nuclear magnetic resonance imaging. *Br J Radiol* 1978;51:273-280.

128 Bioeffects of Static Magnetic Fields

108. Damadian R, Minkoff L, Goldsmith M. Field-focusing nuclear magnetic resonance (FONAR). *Naturwissenschaften* 1978;65:250-252.
109. Edelstein WA, Hutchison JMS, Johnson G, et al. Spin warp NMR imaging and applications to human whole-body imaging. *Phys Med Biol* 1980;25:751-756.
110. Vetter J, Siebold H, Söldner L. A 4 -T Superconducting Whole-Body Magnet for MR-Imaging and Spectroscopy. In: Book of Abstracts. Berkeley, CA: Society of Magnetic Resonance in Medicine; 1987. pp. 181.
111. Vetter J, Ries G, Reichert T. A 4-Tesla superconducting whole-body magnet for MR imaging and spectroscopy. *IEEE Trans Magn* 1988;24:1285-1287.
112. Barfuss H, Fischer H, Hentschel D, et al. Whole-body MR imaging and spectroscopy with a 4-T system. *Radiology* 1988;169: 811-816.
113. Barfuss H, Fischer H, Hentschel D, et al. *In vivo* magnetic resonance imaging and spectroscopy of humans with a 4T whole-body magnet. *NMR in Biomed* 1990;3:31-45.
114. Chu SC. The development of a 4T whole body system for clinical research. *Jap J Magn Reson Med* 1990;10:63-64.
115. Bell RA. Economics of MRI technology. *J Magn Reson Imaging* 1996;6:10-25.
116. Berry MV, Geim AK. Of flying frogs and levitrons. *Eur J Phys* 1997;18:307-313.
117. Geim AK, Simon MD, Boamfa MI, Heflinger LO. Magnet levitation at your fingertips. *Nature* 1999;400:323-324.
118. Kolin A. Improved apparatus and technique for electromagnetic determination of blood flow. *Rev Sci Instr* 1952;23:235-242.
119. Kanai H, Yamano E, Nakayama K, Kawamura N, Furuhata H. Transcutaneous blood flow measurement by electromagnetic induction. *IEEE Trans Biomed Eng* 1974;21:144-151.
120. Togawa T, Okai O, Ohima M. Observation of blood flow e.m.f. in externally applied strong magnetic fields by surface electrodes. *Med Biol Engineer* 1967;5:169-170.
121. Tenforde TS, Gaffey CT, Moyer BR, Budinger TF. Cardiovascular alterations in Macaca monkeys exposed to stationary magnetic fields: Experimental observations and theoretical analysis. *Bioelectromagnetics* 1983;4:1-9.
122. Winfrey AT. The electrical thresholds of ventricular myocardium. *J Cardiovascular Physiol* 1990;1:393-410.
123. Haberditzl W. Enzyme activity in high magnetic fields. *Nature* 1967;213:72-73.
124. Atkins PW. Magnetic field effects. *Chem Brit* 1976;12:214-218.
125. Atkins PW, Lambert TP. The effect of a magnetic field on chemical reactions. *Ann Rep Prog Chem* 1976;A72:67-88.
126. Brocklehurst B. Spin correlation in the geminate recombination of radical ions in hydrocarbons. Part I - theory of the magnetic field effect. *J Chem Soc Faraday Trans* 1976;72:1869-1864.
127. McLauchlan KA. The effects of magnetic fields on chemical reactions. *Sci Prog (Oxford)* 1981;67:509-529.
128. Turro NJ. Influence of nuclear spin on chemical reactions: Magnetic isotope and magnetic field effects (a review). *Proc Natl Acad Sci* 1983;80:609-621.
129. Gould IR, Turro NJ, Zimmt MB. Magnetic Field and Magnetic Isotope Effects on the Products of Organic Reactions. In: Gold V, Bethel D, Editors. *Advances in Physical Organic Chemistry*, Volume 20. New York: Academic Press; 1984.
130. Steiner UE, Ulrich T. Magnetic field effects in chemical kinetics and related phenomena. *Chem Rev* 1989;89:51-147.
131. Cohen C. Ferromagnetic contamination in the lungs and other organs of the body. *Science* 1973;180:745-748.

MRI Bioeffects, Safety, and Patient Management 129

132. Freedman AP, Robinson SE, Johnston RJ. Non-invasive magnetopneumographic estimation of lung dust loads and distribution in bituminous coal workers. *J Occupational Med* 1980;22:613-618.
133. Cohen D, Nemoto I. Ferrimagnetic particles in the lung part 1: The magnetizing process. *IEEE Trans Biomed Engineer* 1984;31:261-273.
134. Cohen D, Nemoto I, Kaufman L, et al. Ferrimagnetic particles in the lung part II: The relaxation process. *IEEE Trans Biomed Engineer* 1984;31:274-284.
135. Moatamed F, Johnson FB. Identification and significance of magnetite in human tissues. *Arch Pathol Lab Med* 1986;110:618-621.
136. Kirschvink JL, Kobayashi-Kirschvink A, Woodford BJ. Magnetite biominerilization in the human brain. *Proc Natl Acad Sci* 1992;89:7683-7687.
137. Frauenrath T, Fuchs K, Dieringer MA, et al. Detailing the use of magnetohydrodynamic effects for synchronization of MRI with the cardiac cycle: A feasibility study. *J Magn Reson Imaging* 2012;36:364-72.
138. Bozorth RM. Ferromagnetism. New York: Van Nostrand; 1951. Reprinted, Piscataway, NJ: IEEE; 1993. pp. 627-699.
139. Scott WT. The Physics of Electricity and Magnetism. Second Edition. New York: Wiley; 1966. pp. 323-368.
140. Landau LD, Lifshitz EM, Pitaevskii LP. Electrodynamics of Continuous Media, Second Edition, Oxford: Pergamon Press; 1984. pp. 105-128; 217-222.
141. Bleaney BI, Bleaney B. Electricity and Magnetism. Third Edition. Oxford: Oxford University Press; 1976. pp. 101-107.
142. Jackson JD. Classical Electrodynamics. Third Edition. New York: Wiley; 1999. pp. 214.
143. Hong FT. Magnetic anisotropy of the visual pigment rhodopsin. *Biophysical Journal* 1980;29:343-346.
144. Torbet J, Freyssinet J-M, Hudry-Clergeon G. Oriented fibrin gels formed by polymerization in strong magnetic fields. *Nature* 1981;289:91-93.
145. Maret G, von Schickfus M, Mayer A, Dransfeld K. Orientation of nucleic acids in high magnetic fields. *Phys Rev Lett* 1975;35:397-400.
146. Worcester DL. Structural origins of diamagnetic anisotropy in proteins. *Proc Natl Acad Sci* 1978;75: 5475-547.
147. Hong FT. Photoelectric and magneto-orientation effects in pigmented biological membranes. *J Colloid Interface Sci* 1977;58:471-497.
148. Geacintov NE, Van Nostrand F, Becker JF, Tinkel JB. Magnetic field orientation of photosynthetic systems. *Biochem Biophys Acta* 1972;267:65-79.
149. Hong FT, Mauzerall D, Mauro A. Magnetic anisotropy and the orientation of retinal rods in a homogeneous magnetic field. *Proc Natl Acad Sci* 1971;68:1283-1285.
150. Denegre JM, Valles JM, Lin K, Jordan WB, Mowry KL. Cleavage planes in frog eggs altered by strong magnetic fields. *Proc Natl Acad Sci* 1998;95:14729-14732.
151. Bras W, Diakun GP, Diaz JF, et al. The susceptibility of pure tubulin to high magnetic fields: A magnetic birefringence and x-ray fiber diffraction study. *Biophys J* 1998;74:1509-1521.
152. Kern CW, Karplus M. The Water Molecule. In: Franks F, Editor. *Water: A Comprehensive Treatise*. Volume 1. The Physics and Physical Chemistry of Water. New York: Plenum Press; 1972. pp. 21-91.
153. Patel M, Williamson RA, Dorevitch S, Buchanan S. Pilot study investigating the effect of the static magnetic field from a 9.4-T MRI on the vestibular system. *J Occup Environ Med* 2008;50:576-83.
154. Laakso I, Hirata A. Computational analysis of thresholds for magnetophosphenes. *Phys Med Biol* 2012;57:6147-6165.
155. Jokela K, Saunders RD. Physiologic and dosimetric considerations for limiting electric fields induced in the body by movement in a static magnetic field. *Health Phys* 2011;100:641-653.

130 Bioeffects of Static Magnetic Fields

156. Hirata A, Takano Y, Fujiwara O, Dovan T, Kavet R. An electric field induced in the retina and brain at threshold magnetic flux density causing magnetophosphenes. *Phys Med Biol* 2011;6:4091-4101.
157. Gemmel H, Wendhausen H, Wunsch F. Biologische effekte statischer magnetfelder bei NMR-tomographie am menschen. *Radiologische Klinik Wiss Mitt Univ Kiel*: 1983.
158. Shellock F, Schaefer D, Crues JV. Exposure to a 1.5 T static magnetic fields does not alter body and skin temperatures in man. *Magn Reson Med* 1989;11:371-375.
159. Shellock F, Schaefer D, Gordon C. Effect of a 1.5-T static magnetic field on body temperature of man. *Magn Reson Med* 1986;3:644-647.
160. Tenforde T, Levy L. Thermoregulation in rodents exposed to homogeneous (7.55 Tesla and gradient (60 Tesla per second) DC magnetic fields. Proceedings of the Bioelectromagnetics Society. Seventh Annual Meeting Abstract: 1985. pp. 7.
161. László JF, Hernádi L. Whole body static magnetic field exposure increases thermal nociceptive threshold in the snail, *Helix pomatia*. *Acta Biol Hung* 2012;63:441-452.
162. Yan Y, Shen G, Xie K, et al. Wavelet analysis of acute effects of static magnetic field on resting skin blood flow at the nail wall in young men. *Microvasc Res* 2011;82:277-83.
163. Environmental Health Criteria, Static fields, Geneva: World Health Organization, Monograph, Vol. 232: 2006.
164. Noble D, McKinlay A, Repacholi M. Effects of static magnetic fields relevant to human health. *Prog Biophys Mol Biol* 2005;87:171-372.
165. McKinlay AF, Allen SG, Cox R, et al. Review of the scientific evidence for limiting exposure to electromagnetic fields (0–300 GHz). Chilton: National Radiological Protection Board (NRPB) 15;2004.
166. Goyan JE. Medical devices. Procedures for investigational device exemptions. *Fed Regist* 1980;45:3732-3759.
167. National Radiological Protection Board (NRPB). Exposure to nuclear magnetic resonance clinical imaging. *Radiography* 1980;47:258-260.
168. Gundaker WE. Guidelines for Evaluating Electromagnetic Risk for Trials of Clinical NMR Systems. Rockville, MD: U.S. Food and Drug Administration; 1982.
169. National Radiological Protection Board (NRPB). Revised guidance on acceptable limits of exposure during nuclear magnetic resonance clinical imaging. *Br J Radiology* 1982;56:974-977.
170. Villforth JC. Guidelines for Evaluating Electromagnetic Exposure Risk for Trials of Clinical NMR Systems. Rockville, MD: U.S. Food and Drug Administration; 1982.
171. Medicine and Healthcare Products Medical Agency (MHRA) Safety Guidelines for Magnetic Resonance Imaging Equipment in Clinical Use, DB2007 (03): 2007.
172. U.S. Food and Drug Administration. Magnetic resonance diagnostic device. Panel recommendation and report on petitions for MR reclassification. *Fed Regist* 1988;53:7575-7579.
173. International Commission on Non-Ionizing Radiation Protection. ICNIRP statement on medical magnetic resonance procedures: Protection of Patients. *Health Physics* 2004;87:197-216.
174. International Commission on Non-Ionizing Radiation Protection. ICNIRP guidelines on limits of exposure to static magnetic fields. *Health Physics* 2009;96:504-519.
175. National Health and Medical Research Council, Safety Guidelines for Magnetic Resonance Diagnostic Facilities: Radiation Health Series, Number 34. Canberra: Australian Government Publishing Service; 1991.
176. International Electrotechnical Commission: IEC 60601-2-33 Medical electrical equipment – Part 2-33: Particular requirements for the basic safety and essential performance of magnetic resonance equipment for medical diagnosis, Edition 3.2, 2015.
177. Normile D. Race for stronger magnets turns into marathon. *Science* 1998;281:164-165.

MRI Bioeffects, Safety, and Patient Management 131

178. Kraff O, Quick HH. 7T: Physics, safety, and potential clinical applications. *J Magn Reson Imag* 2017;46:1573–1589.
179. Budinger TF, Bird MD. MRI and MRS of the human brain at magnetic fields of 14T to 20T: Technical feasibility, safety, and neuroscience horizons. *Neuroimage* 2018;168:509–531.
180. Organization for Economic Cooperation and Development, Total Population. In: *OECD Factbook 2010 Economic, Environmental and Social Statistics*. OECD Publishing, 2010.

Chapter 5 Bioeffects of Gradient Magnetic Fields

DONALD W. MCROBBIE, PH.D.

Associate Professor, Discipline of Medical Physics
School of Physical Sciences
University of Adelaide
Adelaide, Australia

INTRODUCTION

During magnetic resonance imaging (MRI), the patient is exposed to the static magnetic field, which produces the nuclear magnetization in tissues, radiofrequency (RF) pulses, which manipulate the magnetization in order to detect an MRI signal, and low frequency pulsed magnetic field gradients, which are used for localization of the signal in image formation. This chapter concerns the physiological effects of exposure to time-varying magnetic fields from the imaging gradients, hereafter simply referred to as the “gradients” or “gradient magnetic fields”.

The principal known biological effect from exposure to gradient magnetic fields is peripheral nerve stimulation (PNS). Other types of magnetically-induced stimulation (e.g., of the heart, retina or brain) do not occur at exposure levels currently encountered during MRI but will be considered briefly. Another important effect of the gradients is the generation of acoustic noise resulting from the Lorentz force. This is considered elsewhere in this textbook. In this chapter, the basic physical and physiological processes of magnetic stimulation, the properties of magnetic stimulation, human PNS associated with MRI, models of induced electric fields, and the relevant patient exposure limits will be considered.

BASIC PHYSICS AND PHYSIOLOGY

Imaging Gradients

The imaging gradients are defined as linear spatial variations in the z-component of the static magnetic field B_z , that is, along the axis of the MR system’s bore, as follows:

$$G_x = \frac{dB_z}{dx}; \quad G_y = \frac{dB_z}{dy}; \quad G_z = \frac{dB_z}{dz} \quad (1)$$

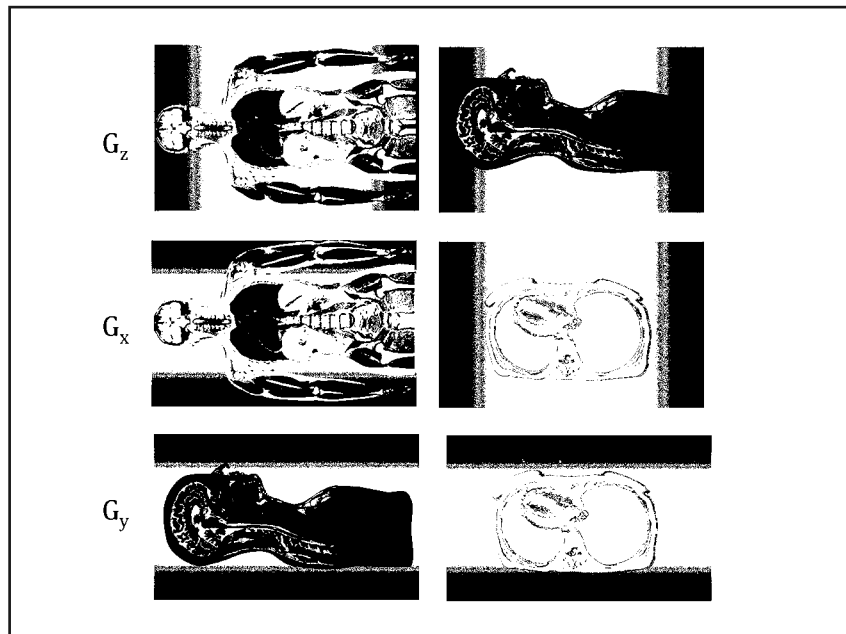
and are specified in millitesla per meter (mT/m). Within the imaging field-of-view (FOV), the gradients produce static magnetic fields whose z-axis components are additive to B_0 :

$$B_z(x,y,z) = B_0 + x G_x + y G_y + z G_z \quad (2)$$

The gradients alter the Larmor frequency of the MR signal depending upon its source location. For example, with $G_x = 10\text{-mT/m}$ at 0.2-m along the x-axis from the isocenter, the additional field from the x-gradient is 2-mT. The maximum field experienced by the patient will depend upon the patient's size and the linearity of the gradients. **Figure 1** illustrates how the magnitude of the gradient fields varies across the patient in the scanner's field-of-view (FOV). Note that the gradient field will be negative over half the FOV.

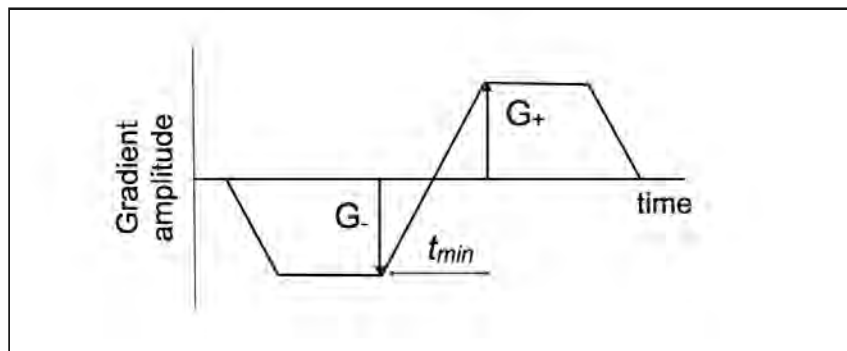
Gradient pulses are commonly applied as trapezoidal waveforms with durations of a few milliseconds, ramp times of typically 0.1- to 1.0-ms and amplitudes of up to, and in excess of, 50-mT/m (**Figure 2**). The gradient slew rate (SR), defined in T/m/s, is given by

Figure 1. The variation in the B -field magnitude from each gradient axis relative to patient position: z is head-foot, y is anterior-posterior, x is left-right. The field magnitude is shown by the shading.



134 Bioeffects of Gradient Magnetic Fields

Figure 2. Typical gradient waveform, showing amplitude and minimum ramp time. Slew rate is defined as $(G_+ + G_-)/t_{min}$.



$$SR = (G_+ + G_-) / t_{min} \quad (3)$$

where G_+ and G_- are the maximum and minimum amplitudes and t_{min} is the minimum time to switch between them. In modern scanners SR may reach 200-T/m/s. In the example above, if the slew rate is 100-T/m/s, the minimum ramp time for one gradient lobe is 0.1-ms and the rate of change of field (dB/dt) is 20-T/s. The rate of change of field dB/dt , for example, at any point along the z-axis from G_z is given by

$$\frac{dB}{dt} = zG_z/\Delta t \quad (4)$$

where Δt is the duration of the change in B or the rise (or fall) time of the gradient waveform. However, the peak exposure may exceed the maximum specified value within the imaging FOV, or the specification volume because only the most linear portion of the gradient field is utilized during MRI (Figure 3).

In order to acquire an image, the gradient and RF pulses are arranged as a pulse sequence that is repeated with the repetition time TR (Figure 4). In the pulse sequence, the gradient pulses are denoted by their function in the image formation process (i.e., slice selection, phase or frequency encoding). Depending on the anatomical orientation of the image section location, these may or may not correspond to the magnet axes x, y, and z, and thus, frequently the patient may be exposed to the simultaneous action of all three physical gradients G_x , G_y , G_z .

Figure 3. The field generated by a gradient coil exceeds the linear portion that defines the MR system's field-of-view.

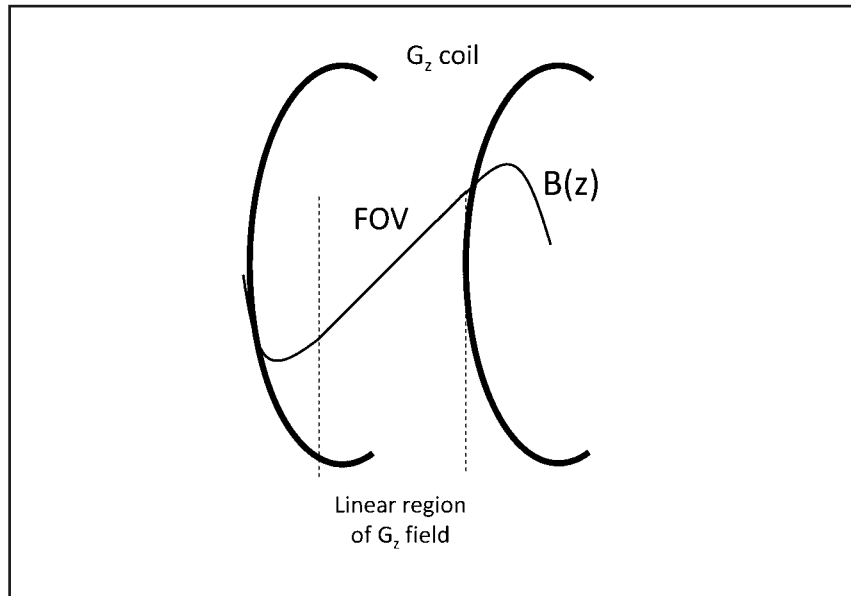
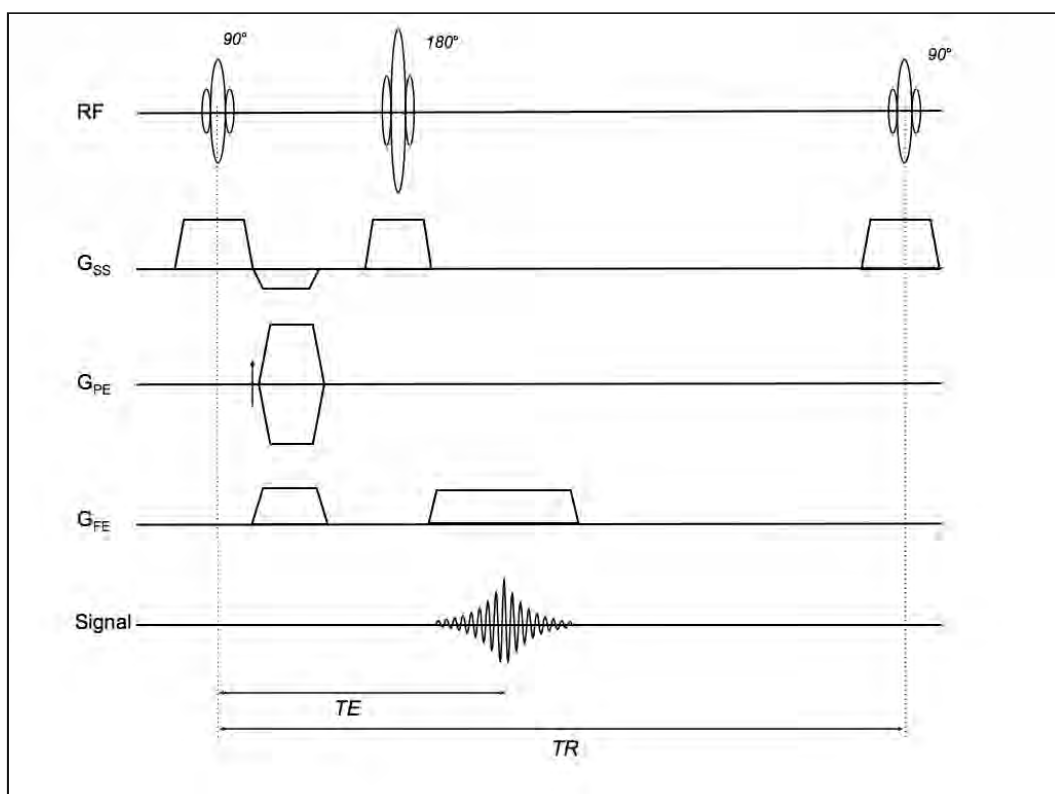


Figure 4. Example of a basic spin echo pulse sequence, consisting of gradients (G_{SS} , G_{PE} , G_{FE}) and RF pulses with echo time (TE) and repetition time (TR).



136 Bioeffects of Gradient Magnetic Fields

Complications Associated with Gradient Magnetic Fields. Simple linear gradient fields with only a B_z component cannot exist in actuality. This is a consequence of Maxwell's equations. So-called concomitant fields (1) in the x and y directions must exist such that

$$\mathbf{B}(x, y, z) = ax \mathbf{G}_x \hat{\mathbf{i}} + by \mathbf{G}_y \hat{\mathbf{j}} + z \mathbf{G}_z \hat{\mathbf{k}} \quad (5)$$

$\hat{\mathbf{i}}$, $\hat{\mathbf{j}}$, $\hat{\mathbf{k}}$ are unit vectors with a magnitude equal to 1, pointing along the x, y and z directions. For a Maxwell pair coil used, for example, as a simple z-gradient coil $a=b=-0.5$. Each gradient coil produces B_x and B_y components. These do not affect imaging much because the tissue magnetization is sensitised in the z-axis, however they affect the magnitude of B and dB/dt exposure. For example, the amplitude of the x-gradient field is:

$$|\mathbf{B}| = G_x \sqrt{x^2 + z^2} \quad (6)$$

The gradient field has zero z-dependence only in the plane of the isocenter. This results in a patient exposure greater than can be considered from the simple calculations considered above.

Faraday's Law of Induction

Faraday's law of induction forms the basis of the generation of induced fields in tissue:

$$\oint \mathbf{E} \cdot d\mathbf{l} = -\frac{d}{dt} \int_s \mathbf{B} \cdot d\mathbf{S} \quad (7)$$

where E is the induced electric field around a closed path and $d\mathbf{S}$ is the differential area vector normal to the applied field. For a circular loop of radius r, in a uniform medium normal to the applied field (**Figure 5**) this simplifies to (2):

$$E = \frac{r}{2} \frac{dB}{dt} \quad (8)$$

Thus, the largest induced electric field will occur in the patient's superficial tissues, and larger patients will experience higher induced fields. The induced electric field generates a current density J (A/m^2) in tissue:

$$J = \sigma E = \frac{r}{2} \sigma \frac{dB}{dt} \quad (9)$$

where σ is the electrical conductivity of the tissue (S/m). Values in the range 0.1 to 0.2-S/m are often used for average body conductivity at low frequencies. The induced E and J from a trapezoidal gradient pulse consist of two opposed polarity rectangular pulses separated by the gradient pulse plateau length (**Figure 5**). The induced current direction will therefore reverse as the gradient waveform returns to zero.

For an elliptical body cross-section perpendicular to the magnetic field, the maximum current density is (3):

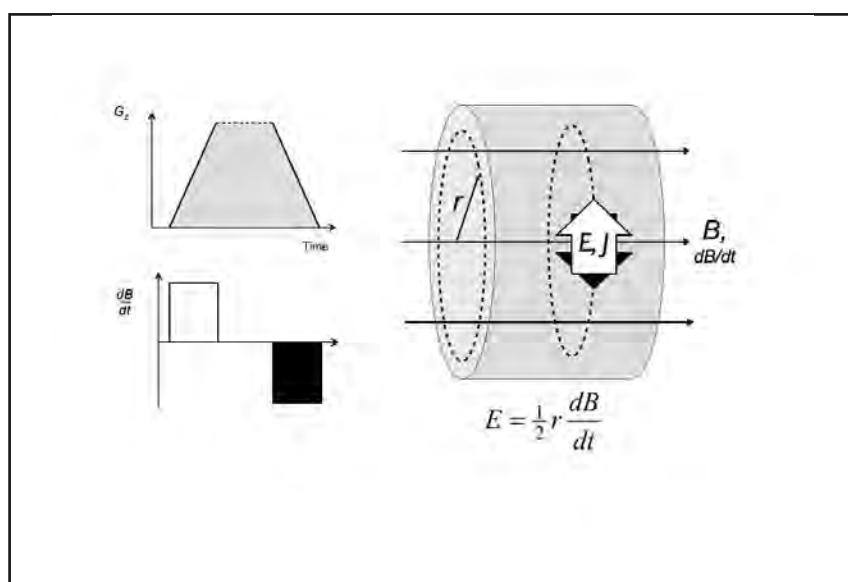
$$J_{\max} = \frac{a^2 b}{a^2 + b^2} \sigma \frac{dB}{dt} \quad (10)$$

where a is the semi-major axial length and b is the semi-minor. As the gradients produce time-varying components of B_z , the orientation of the induced field and current will be generally orthogonal to the magnet axis but their distribution will depend upon the orientation of the applied gradient pulses.

The above simple model only applies for the z-gradient. A simplified E-field solution for a cylinder of radius r_0 has been stated as (4)

$$E_x = \frac{xy}{2} \frac{dG_x}{dt} + \frac{r_0^2 - x^2 + y^2}{4} \frac{dG_y}{dt} + \frac{xz}{2} \frac{dG_z}{dt} \quad (11a)$$

Figure 5. Induced electric field E, and current density J in a homogeneous medium arising from dB/dt from a typical gradient waveform.



138 Bioeffects of Gradient Magnetic Fields

$$E_y = \frac{-xy}{2} \frac{dG_y}{dt} - \frac{r_0^2 - x^2 + y^2}{4} \frac{dG_x}{dt} - \frac{xz}{2} \frac{dG_z}{dt} \quad (11b)$$

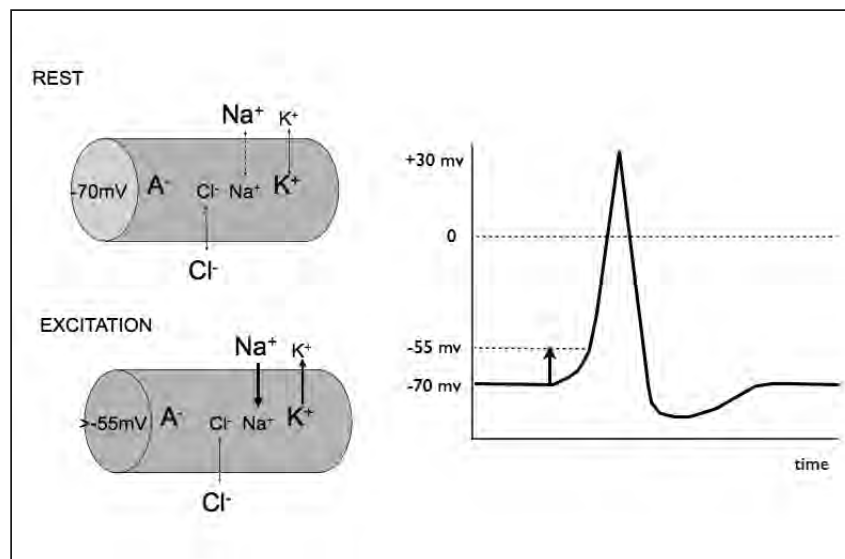
$$E_z = -yz \frac{dG_x}{dt} + xy \frac{dG_z}{dt} \quad (11c)$$

Human anatomy, with irregular shapes and differing tissue conductivities, exhibits much more complex behaviour, with E-field lines and current loops altered by tissue boundaries and electrostatic charges induced on these boundaries.

Physiology

Peripheral nerves are the portion of a spinal nerve distal to the root and plexus. They consist of bundles of nerve fibers of varying diameter from 0.3 to around 20- μm . The larger fibers convey motor, touch and proprioceptive impulses, while the smaller ones convey pain, temperature and autonomic impulses. The nerve fiber consists of the long axon surrounded by a myelin sheath that has periodic breaks, or Nodes of Ranvier. The axon electric potential is maintained, at rest, at around -70mV by the intra-extra cellular balance of sodium, potassium and chloride ions (**Figure 6**). A change in the axon potential of approximately +15-mV will result in the nerve firing, with the sodium channels opening to allow ingress of positive sodium ions, thus elevating the potential further, until the channels close. At this point the potassium channels open allowing egress of positive potassium ions until

Figure 6. Ionic balance (sodium Na^+ , potassium K^+ , chlorine Cl^-) and action potential for a peripheral nerve at rest and during excitation.



the resting potential of -70-mV is restored. Once stimulated, the impulse will be transmitted along the nerve. A refractory period inhibits further firing. Rapid repetitive stimulation may lead to accommodation, or a decrease in the magnitude of the response.

Strength-Duration Curve

The physiology of electrical stimulation of nerves has been known for a long time and is characterized by the strength-duration (SD) curve. Two basic forms of SD curves have been used: the earliest is the hyperbolic form of Weiss (5):

$$I_{\text{thresh}}(t) = I_{\text{Rb}} \left[1 + \frac{c}{t} \right] \quad (12)$$

where I_{thresh} is the threshold generator current (applied via electrodes) to cause stimulation and t is the stimulus duration (for a rectangular pulse). The constant c is the chronaxie and is the stimulus duration required to double the threshold from its minimum value. This minimum value I_{Rb} is known as the rheobase and is asymptotic for long stimulus durations. The SD curve may also be described in terms of the more physiologically relevant electric field E in tissue or, in magnetic stimulation, by dB/dt (see dashed line in **Figure 7**).

The other common form of the SD curve is the exponential or Lapicque form (6):

$$I_{\text{thresh}}(t) = I_{\text{Rb}} / (1 - e^{-t/\tau}) \quad (13)$$

where τ is the tissue time constant, shown for dB/dt as the solid line in **Figure 7**.

Electrophysiologists currently do not agree on the more appropriate form of the SD curve and magnetic stimulation studies provide evidence for both forms. One theoretical advantage of the exponential form is that it produces the predicted response of a simple equivalent circuit of the nerve under the action of a rectangular current stimulus (**Figure 8**). Moreover, the tissue time constants can be theoretically derived from the fiber diameters (7). Time constants vary according to tissue type. Peripheral motor nerves have time constants of the order of 0.1-ms, while cardiac muscle has τ in the region 2- to 3-ms and synapses up to 25-ms. Based upon this equivalent circuit, the Spatially Extended Non-linear Node (SENN) model has been used extensively in electro-stimulation studies, and forms the theoretical basis for some patient exposure limits during MRI (8).

The specific agent of stimulation is usually considered to be the spatial gradient of the induced electric field. Nerve discontinuities such as bends or synaptic terminations (e.g., in muscle) effectively produce E-field spatial gradients, rendering them common stimulation sites. In magnetic stimulation, the stimulus is usually considered to be dB/dt , which is directly proportional to the induced E in tissue. However, just as for electrical stimulation where the SD curve can be derived in terms of electrical charge Q ($I = dQ/dt$), one can con-

140 Bioeffects of Gradient Magnetic Fields

Figure 7. PNS strength-duration curve for magnetic stimulation redrawn from McRobbie and Foster (19). The dashed line is a fit to the hyperbolic SD curve, for which rheobase and chronaxie are shown. The solid line is a fit to the exponential form, resulting in a higher estimated rheobase. It is difficult to stimulate peripheral nerves for long pulse durations.

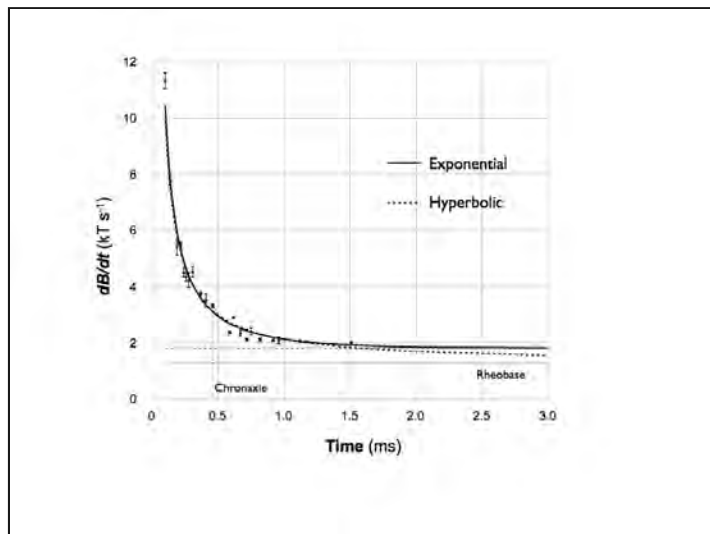
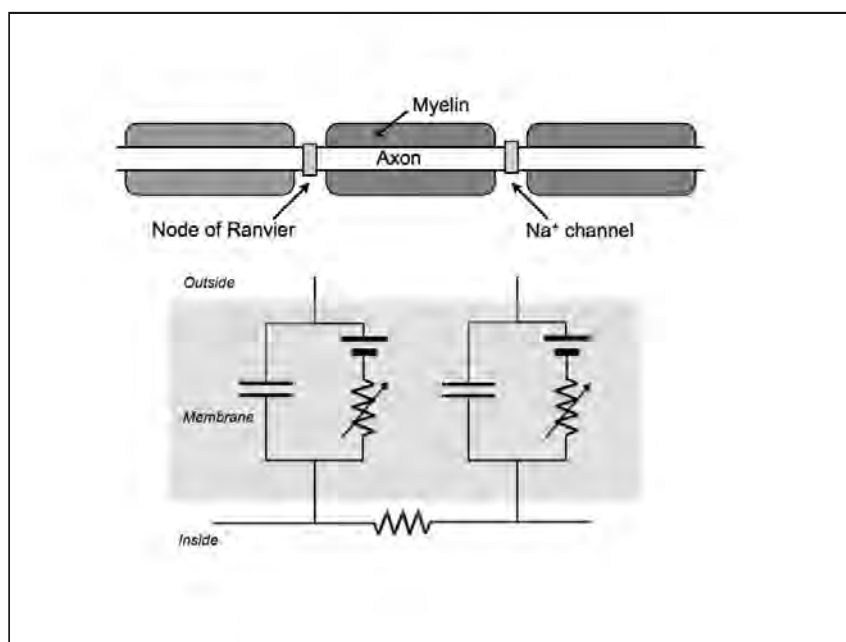


Figure 8. Simple electrical circuit representation of a myelinated nerve used in the SENN model (References 7, 8).



sider the step change in magnetic field ΔB as the stimulus (9). The SD curve, now assuming its hyperbolic form, becomes linear for ΔB :

$$\Delta B_{\text{thresh}} = \Delta B_{\min} \left[1 + \frac{\Delta t}{c} \right] \quad (14)$$

where ΔB_{\min} is the minimum change in magnetic field for an infinitely short stimulus, that is, an infinite dB/dt . Although not obviously intuitive, this latter formulation is instructive for comparing diverse physiological effects and stimuli. Glover (10) has also commented upon the role of ΔB for static field effects such as metallic taste and vertigo.

MAGNETIC STIMULATION

One of the most sensitive and earliest observed forms of magnetic stimulation was that of magnetophosphenes, as reported in 1896 by d'Arsonval (11) (**Figure 9**), perceived by the subject as faint flashes of light, and which are thought to originate from stimulation of the retina or the optic nerve. Kavet, et al. (12) provided a review of the magnetophosphene literature, but from these only two or three publications present sufficient dosimetric information to deduce accurate thresholds and frequency response. Losvund (13) conducted the most extensive of these studies, reporting a minimum threshold of 12-mT root mean square (RMS) in the frequency range 20- to 45-Hz, depending upon the ambient light conditions and dark-adaption of the subjects. **Figure 10** summarizes the available quantitative data on magnetophosphenes.

Direct magnetic stimulation of nerves was first demonstrated *in vitro* by Oberg (14) in 1973, resulting in a measurable twitch of the gastrocnemius muscle of the frog suspended in Ringer's solution. In 1982, Polson, et al. (15) were the first to demonstrate human peripheral nerve stimulation *in vivo* using a small diameter topical solenoidal coil powered by a capacitance discharge system. They estimated an induced current density of 20-A/m² and demonstrated the stimulus-response curve from threshold to supra-maximal (when all the fibers in the bundle have been recruited). The topical magnetic stimulation technique was subsequently applied by Barker, et al. (16) to the motor cortex of the brain, and forms the basis of transcranial magnetic stimulation (TMS). TMS is a common tool in neuroscience research and therapy used in the treatment of depression and psychiatric conditions (17,18).

Properties of Magnetic Stimulation

McRobbie and Foster (19) first demonstrated the strength-duration curve from topical stimulation of the median nerve in 1984 using electromyography (EMG) to determine reproducible thresholds (**Figure 7**). They fitted an exponential form of the SD curve with a time constant of 0.47-ms and an estimated J rheobase of 3.6-A/m², corresponding to an estimated E_{Rb} of 12-V/m. They also demonstrated that, contrary to expectations of the SENN, the biphasic damped sinusoidal pulse produced by their capacitance discharge system was a more effective stimulus than mono-phasic pulses (**Figure 11**). This is supported by further evidence from the TMS literature (20, 21) and the recent ultra-high slew rate studies (22).

142 Bioeffects of Gradient Magnetic Fields

Figure 9. Magnetophosphene experiments of Arsene d'Asonval, Paris 1896 (Reference 11).

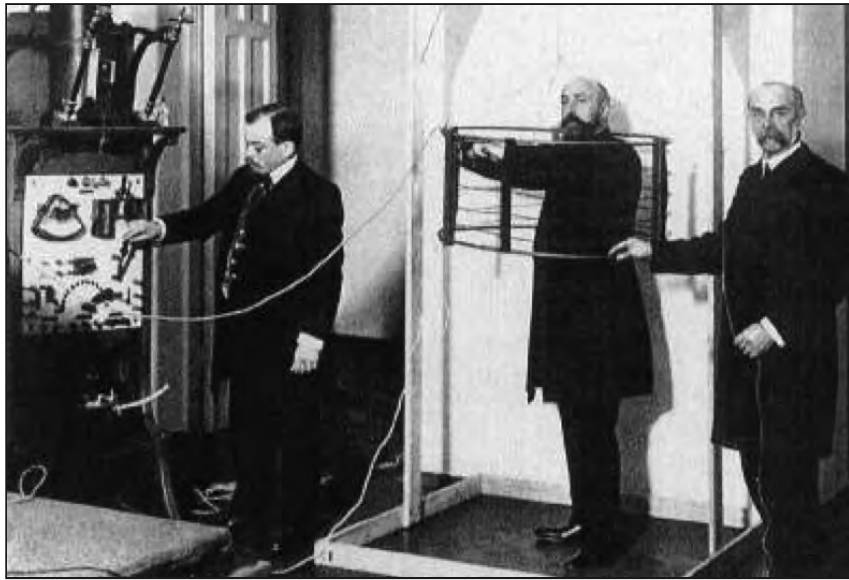
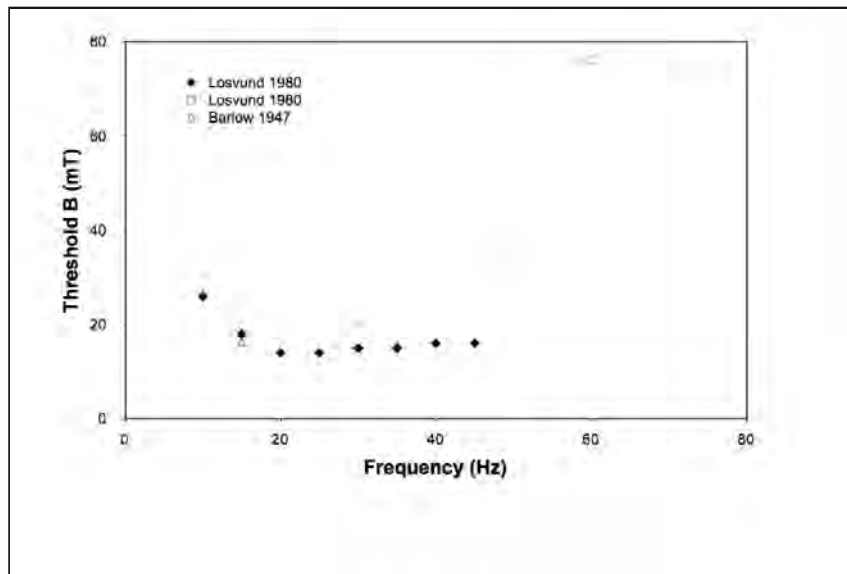
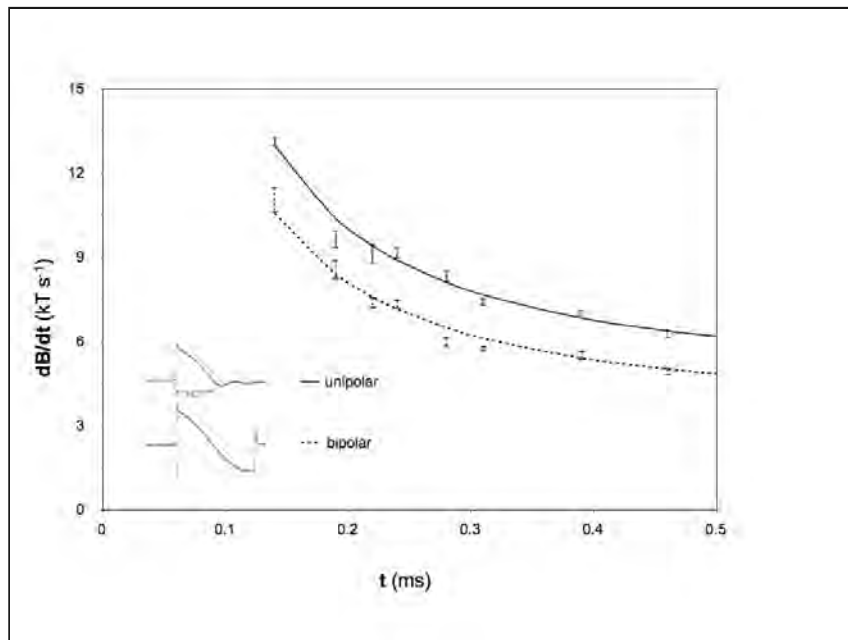


Figure 10. Magnetophosphene thresholds from the literature, derived from Kavet, et al. (12). The data from Barlow were assumed to be peak to peak. All stimuli were sinusoidal waveforms with results shown as rms.



The reason for the lower thresholds of biphasic pulses may be offered by the ΔB linear SD formulation, in which a biphasic pulse will have a greater ΔB excursion than a monophasic pulse, and therefore lower dB/dt thresholds.

Figure 11. Pulse shape dependence. Bipolar damped sinusoidal pulses are shown to have lower dB/dt thresholds than unipolar pulses with a similar waveform. Adapted from reference 19.



In the SENN model, a 20- μm nerve fiber is predicted to have a theoretical time constant of 0.12-ms (7). Despite SENN apologists' appeal to magnetic stimulation for validation of the theory (8), most magnetic stimulation results contradict the predictions of the SENN model. In carefully devised experiments, Rescoskie, et al. (23, 24) demonstrated large discrepancies in chronaxies from electrical and topical magnetic stimulation of the ulnar nerve for both perception and EMG thresholds. Perception chronaxies were 0.024 ± 0.02 -ms for electrical stimulation, against 0.67 ± 0.18 -ms for magnetic stimulation. A confounding factor is the huge variation (i.e., thirty times) in reported electrical stimulation chronaxies. This raises issues about the validity of applying electrical stimulation data to formulate limits for time-varying magnetic fields.

Weinberg, et al. (22) investigated ultra-high dB/dt, high frequency (> 100 kHz) pulses, using a topical coil, and reported a significantly reduced probability for stimulation at these frequencies (Figure 12). They concluded that ultra-short pulses (were the technology available) in whole-body gradient systems are unlikely to cause PNS despite very high dB/dt. Using results from Magnetic Particle Imaging (25) and MRI studies (26), a modified SD curve has been proposed (27). Shown in Figure 13, the threshold is seen to rise for very short (< 20 μs) stimuli above 25 kHz. Also shown are SENN predictions.

Magnetic Stimulation and Different Organs

Magnetic stimulation of the phrenic nerve in humans resulting in respiratory disruption has been reported by Mouchtar, et al. (28) using a damped sinusoidal pulse from a topical

144 Bioeffects of Gradient Magnetic Fields

Figure 12. Probability of PNS sensation at various frequencies, at magnitude 0.4-T. Error bars correspond to exact confidence intervals with 95% power. Data points are labeled with frequency values. Reproduced with permission from Reference 22.

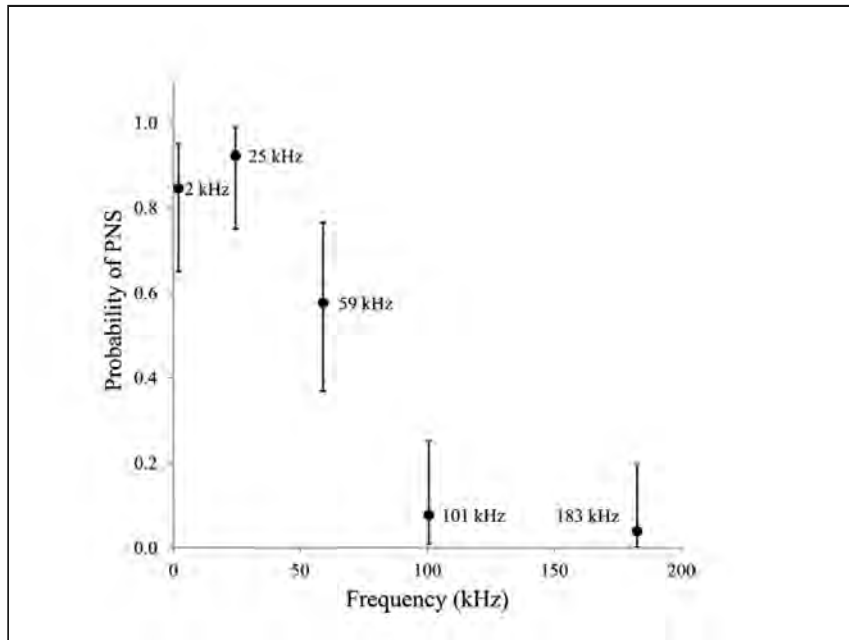
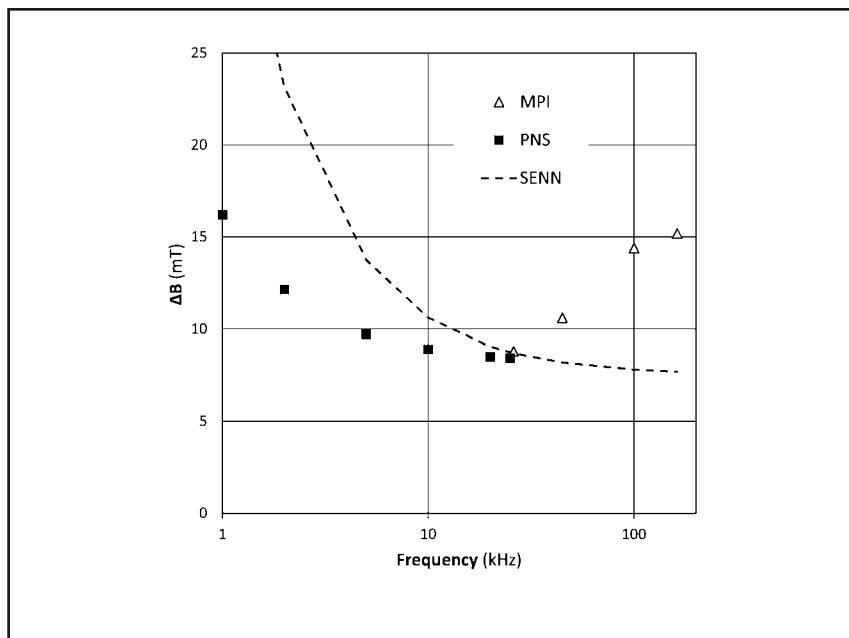


Figure 13. A strength-duration curve (ΔB formulation) for PNS compiled from MRI and MPI results showing the increase in threshold at frequencies above 25 kHz (References 25-27).



coil with a frequency of 853-Hz. In later work, the median canine respiration threshold for a 0.53-ms pulse was shown to be around 900-T/s.

Direct cardiac stimulation is more difficult to achieve due to the longer time constants of cardiac muscle and the smaller induction paths around the organ. Early attempts with small coil systems produced violent muscular contractions and estimated current densities in the range 5 to 20-A/m² but without any detected cardiac arrhythmias in rats (29, 30). Nevertheless, Bourland, et al. (31) achieved trans-chest magnetic simulation of the dog heart, producing ectopic beats but not ventricular fibrillation, with an estimated induced electric field of 50-V/m and a median threshold dB/dt of 2,700-T/s. for a 0.53-ms pulse. Using a tissue time constant of 3-ms, a rheobase of 400-T/s can be extrapolated. Yamaguchi, et al. (32) showed similar results with an estimated E_{Rb} of 55- to 340-V/m. Cohen, et al. (33) did not detect any changes in the electrocardiogram (ECG) of canines exposed to up to 66-T/s. using a human whole-body gradient system. The cardiac stimulation dB/dt rheobase for the most sensitive percentile of the population has been theoretically estimated as 62-T/s. (34). It is thought that at least 50 times the electrical stimulus for cardiac stimulation is required to cause ventricular fibrillation (35).

Interestingly, exposure of pregnant mice to dB/dt of up to 3,600-T/sec. at 2.2-kHz caused significant muscular contractions but showed no effect on the litter size or teratogenicity (3).

PERIPHERAL NERVE STIMULATION FROM THE MRI-RELATED GRADIENT MAGNETIC FIELDS

PNS associated with MRI-related gradient magnetic fields was first reported by Cohen, et al. (33) and Budinger, et al. (36). Initially, the possibility of PNS was limited to high slew rate specialist gradient systems, based upon capacitance discharge technology, for echo planar imaging (EPI). The advent of improved linear amplifiers for the MRI-related gradients has resulted in a much greater likelihood of patients experiencing stimulation. For example, Vogt, et al. (37) exposed 210 patients to gradient slew rates of 120% of the International Electrotechnical Commission (IEC) limit for PNS (38) using a rapid gradient echo (FLASH) sequence. For this study group, 16.7% reported PNS with 2.9% reporting very uncomfortable stimulation.

The Purdue University group (39, 40) has published extensive studies of MRI-related gradient stimulation using y- (anatomically aligned anterior-posterior) and z-gradient coil systems external to the bore of the MR system. **Figure 14** shows SD curves for an individual subject's subjective reporting of three levels of stimulation (1 = threshold, 5 = uncomfortable, 10 = intolerable) fitted to the hyperbolic form. The subjects ($n = 84$) reported uncomfortable stimulation at about 50% higher exposure than for the threshold, and about 100% higher than threshold for intolerable. Pooling these data, one can calculate a stimulus or dose response curve and a population SD curve (**Figure 15**). For perception, the median dB/dt rheobases were 15-T/s for the y-gradient and 26-T/s for x with similar chronaxies (0.37-ms, 0.38-ms). The stimulus was a train of 64 trapezoidal gradient lobes, resulting in 128 rectangular dB/dt pulses of duration 0.05 to 1.0-ms. Using dB/dt pulse lengths of 0.2- and 0.5-ms, there was no correlation between subject height, sex or age on stimulation

146 Bioeffects of Gradient Magnetic Fields

Figure 14. Individual SD curves from y- and z-gradients showing perception (score = 1), discomfort (score = 5) and intolerable stimulation (score = 10) from Nyenhuis, et al. (40). In this experiment the y-axis refers to the AP direction. The solid lines are fitted to the hyperbolic SD curve. Reproduced with permission.

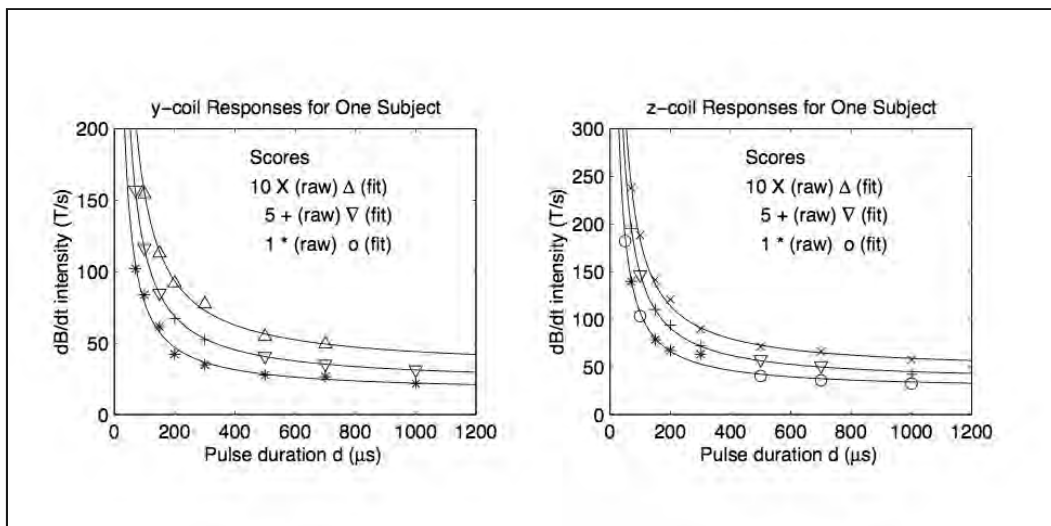


Figure 15. Pooled results from a human PNS experiment (Nyenhuis, et al.). *Top.* The group stimulus-response curves for perception, discomfort and intolerable stimulation. *Bottom.* From the above, the median population SD curves may be derived, fitted to a hyperbolic SD curve. Reproduced with permission.

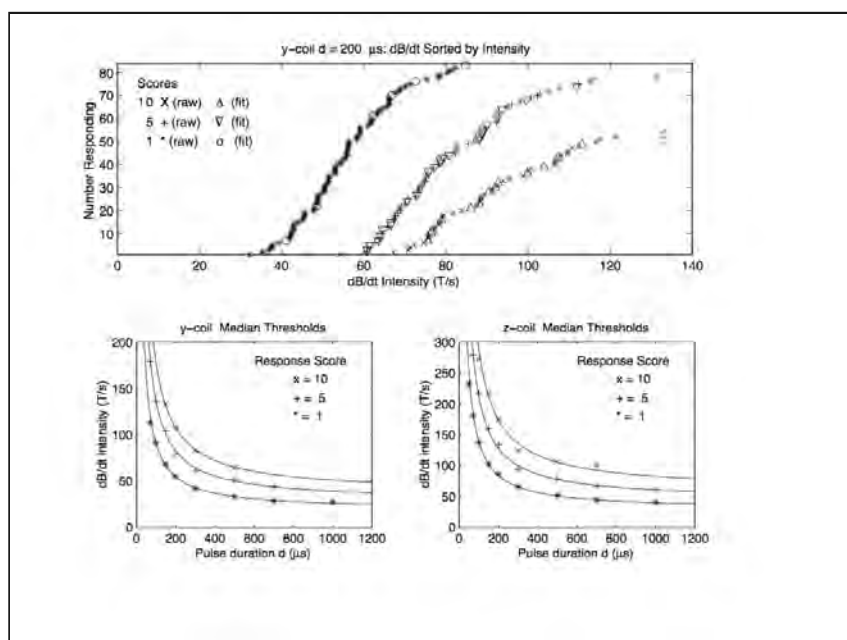


Table 1. Literature results for gradient coil PNS perception thresholds and chronaxies using the hyperbolic formulation of the SD curve. The mean values are weighted for the number of subjects, N. The column, ΔB , is calculated from Equation (14).

	Reference	Waveform	N	Axis	dB/dt (T/s)	ΔB (mT)	c (ms)
Irnich and Schmitt	9	Sinusoid	1	Z	18.0	9.9	0.55
Bourland	39	Trap 128	84	Y	14.9	5.4	0.37
			84	Z	26.2	9.9	0.38
Den Boer, et al.	42	Trap	153	Y	18.8	6.8	0.36
Hebrank, et al.	43	Trap 128	65	Y	16.3	8.6	0.52
			65	XY	18.6	8.7	0.47
			65	XYZ	20.1	10.2	0.51
Zhang, et al.	44	Trap 64	20	XY	24.7	11.1	0.53
Mean Value					19.4	8.1	0.42

threshold. Limited correlation of girth and threshold for the z-gradient coil was observed but not evaluated statistically. Abart, et al. (41) also noted lack of correlation of stimulus threshold with age, body surface, and sex.

Many other authors have investigated PNS perception thresholds for various combinations of axes on whole-body, MRI-related gradient systems (9, 39, 42-44). Rheobases and chronaxies from these studies are shown in **Table 1**. Given the range of combinations of waveforms, axes and coil designs, there is a striking consistency across these results. Taking the weighted mean from these studies, we arrive at an average dB/dt rheobase of 19.4-T/s. and a chronaxie of 0.42-ms - in agreement with topical stimulation studies (19, 22-24). Using Equations (9), (10) and (14) with $a=0.4\text{-m}$, $b=0.2\text{-m}$ and $\sigma=0.2\text{-S/m}$ one can deduce the rheobase for E, and J to be in the region of 3.1-V/m and 0.62-A/m² with a ΔB_{\min} of 8.1-mT.

Chronik and Rutt (45) derived the law of stimulation in terms of the MRI-related gradient parameters:

$$\Delta G(\Delta t) = SR_{\min} c + \Delta G_{\min} \quad (15)$$

where SR_{\min} is the smallest stimulating slew rate for infinitely long pulse durations, ΔG_{\min} is the smallest stimulating gradient excursion for infinitely short pulse durations, and c is the chronaxie. This can be represented diagrammatically (**Figure 16**) where the gradient

148 Bioeffects of Gradient Magnetic Fields

Table 2. Literature results for gradient coil PNS perception thresholds and chronaxies using the Chronik and Rutt formulation of the SD curve as in Equation (15). The results of Feldman, et al. (49) were for planar coils and are excluded from the weighted mean calculation. N is the number of subjects. The results for Zhang, et al. (44) were for 48¹, 40² and 35³ cm defined spherical volume (DSV) coils.

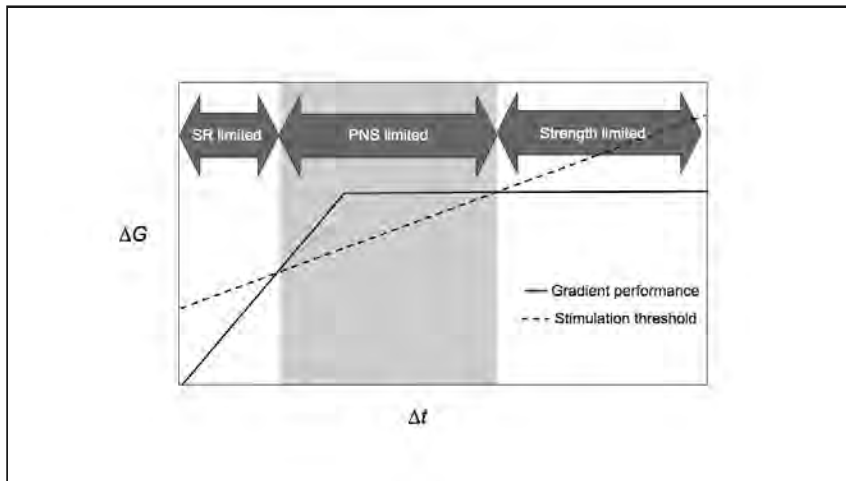
	Reference	Waveform	N	Axis	SR _{min} (T/m/s)	G _{min} (T/m)	c (ms)
Ham, et al.	46	Sinusoid	4	Z	41.5	34	0.81
Zhang, et al.	44	Trap 64	20	XY ¹	66.8	24.7	0.37
			20	XY ²	75.4	34.0	0.45
			20	XY ³	77.0	40.5	0.53
Hoffman, et al.	50	Trap	14	Y	26.0	20.8	1.03
Chronik, et al.	47	Trap	20	XY	62.2	44.4	0.77
Chronik, et al.	48	Trap	18	XY	50.1	48.5	1.054
Feldman, et al.	49	Trap	14	X	252	218	0.87
			14	Y	222	147	0.66
			14	Z	210	133	0.63
Mean Value					59.3	35.4	0.69

coil technical performance is shown in terms of its slew rate limitation and its amplitude limitation. The PNS threshold has a linear form and can easily be used to predict the PNS-limited region of the gradient's operation.

Table 2 shows a summary of PNS studies using this alternative gradient formulation of the SD curve (44, 46-50). Excluding the results from Feldman, et al. (49) who used planar coils, the weighted average minimum stimulating slew rate was 59.3-T/m/s, the minimum gradient amplitude (at infinite slew rate) for stimulation was 35.4-mT/m with a mean chronaxie of 0.69-ms. A notable observation is that there appears to be a dependence of the chronaxie on the coil dimension (44). The results from Feldman, et al. (49) show that significant increases in gradient coil performance without causing PNS are achievable, and secondly, that the chronaxie appears to have some dependence upon the coil design, and not just physiologic factors. As with earlier experiments, the linear SD formulation found no convincing correlation with anatomical measurements, including weight, height, girth, and average body fat percentage (48) although a weak correlation between ΔG_{\min} and the effective radius was reported (**Figure 17**).

Hoffman, et al. (50) used EMG to determine responses to gradient stimulation. They concluded that EMG thresholds and perception thresholds were equally reproducible with

Figure 16. Gradient performance and PNS limitations redrawn from Chronik and Rutt (47). The shaded region is where peripheral nerve stimulation is likely to occur.



standard deviations of 2.1- and 2.0-mT/m, respectively, and a difference of only 0.45-mT/m, the subjective threshold being the lower.

MODELING OF INDUCED CURRENT DENSITIES

The simple expressions [Equations (8) to (11)] for the induced E field and current are only useful in idealized, but unrealistic geometries, or to provide an understanding of the basic principles of induction. Computational modeling of the field interactions using realistic anatomical models and gradient coil specifications have shown that the induced E-field and current densities are highly inhomogeneous for various body geometries. Both quasi-static finite difference or finite integration numerical techniques have been applied (51-54). **Figure 18** shows the pattern of induced E-field arising from a planar y-gradient coil with dB/dt of 100-T/m/s. So, et al. (53) used actual PNS experimental data from y- and z-gradient coils with theoretical calculation of induced electric fields in subcutaneous fat and skin, estimating the stimulation thresholds in the range 3.6 to 5.8-V/m, close the SENN model predicted value of 6.2-V/m. Strong correlations between peak induced electric field in a human model in a head/neck gradient coil and subjects' reported stimulation sites, predominantly in the front of the head, in the vicinity of the sinuses, forehead, and teeth, has been demonstrated (55). Peak induced E-fields were estimated as 40-V/m.

There are a number of technical limitations to electromagnetic field modeling such as the proprietary details of commercially available gradient coil geometries, the use of a single sinusoidal gradient waveform, the requirement for computation time-saving strategies such as frequency scaling, the spatial resolution of the model, and partial volume effects where tissues are mixed within a voxel. Notwithstanding these issues, computational modeling has provided various insights into the induced electric fields and current densities and their role in peripheral nerve stimulation.

150 Bioeffects of Gradient Magnetic Fields

Figure 17. Experimental values of ΔG_{\min} and effective loop radius R_{ax} plotted for 37 subjects fitted to a power law function. Reproduced with permission from Reference 48.

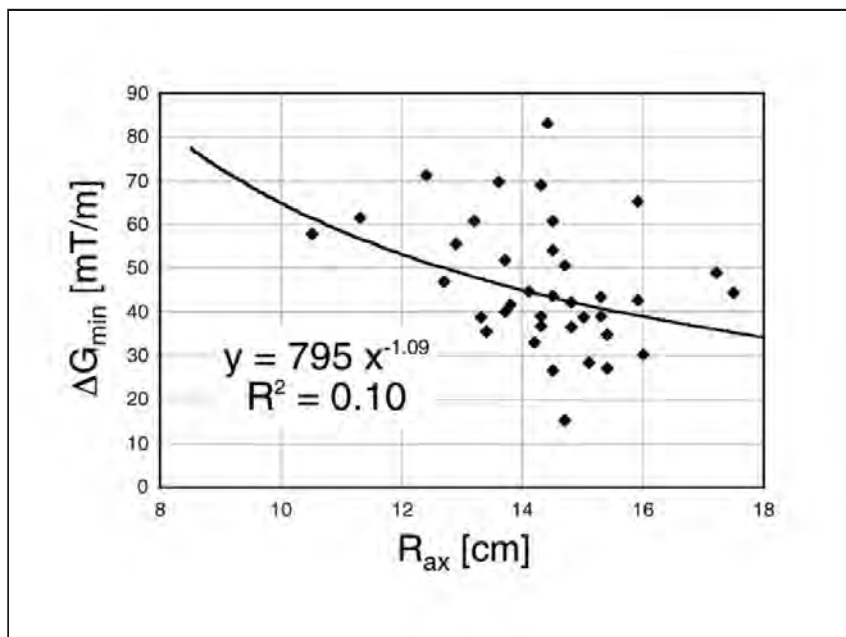
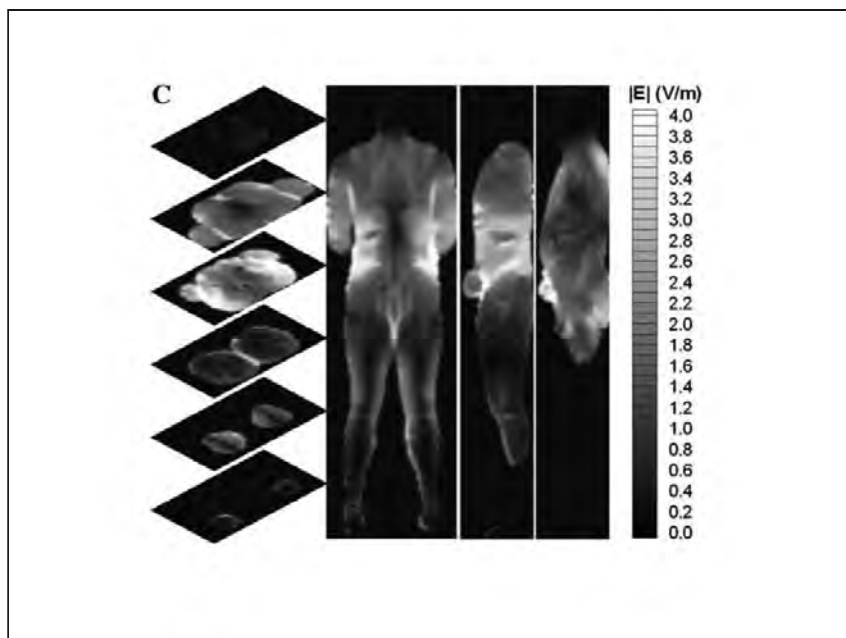


Figure 18. Results of computer simulation of the induced electric fields from whole body magnetic field gradients. Calculation of the induced electric fields inside the human whole-body model excited by a typical planar gradient y-coil with a slew rate of $dG/dt=100-T/m/s$, at a frequency of 1 kHz. Reproduced with permission from reference 52.



EXPOSURE LIMITS

Most standards for patient exposure during MRI utilize PNS SD data derived theoretically or from direct measurement in volunteers according to a defined protocol (38, 56, 57). The Normal Operating Mode for the MR system's gradient magnetic fields is defined as 80% of the median perception threshold for PNS. The First Level Controlled Operating Mode is defined as 100% of the median perception threshold. Where MR system-specific experimental data is unavailable, theoretical data may be used. The International Electrotechnical Commission (IEC) standard 60601-2-33 3rd Edition uses a theoretical dB/dt rheobase (rb) of 20-T/s, with a chronaxie of 0.36-ms for PNS, giving its three operational mode limits:

- *Normal Operating Mode*: 80% of the median perception threshold of the population either from direct measurement or from:

$$L_{01} = 0.8 \text{ Rb} \left(1 + \frac{0.36}{t_{\text{eff}}}\right) \quad (16a)$$

- *First Level Controlled Operating Mode (L1)*: 100% of the median perception threshold or from

$$L_{12} = 1.0 \text{ Rb} \left(1 + \frac{0.36}{t_{\text{eff}}}\right) \quad (16b)$$

- *Second Level Controlled Operating Mode (L2)*: Up to 120% of the median perception

$$L_{02} = 1.2 \text{ Rb} \left(1 + \frac{0.36}{t_{\text{eff}}}\right) \quad (16c)$$

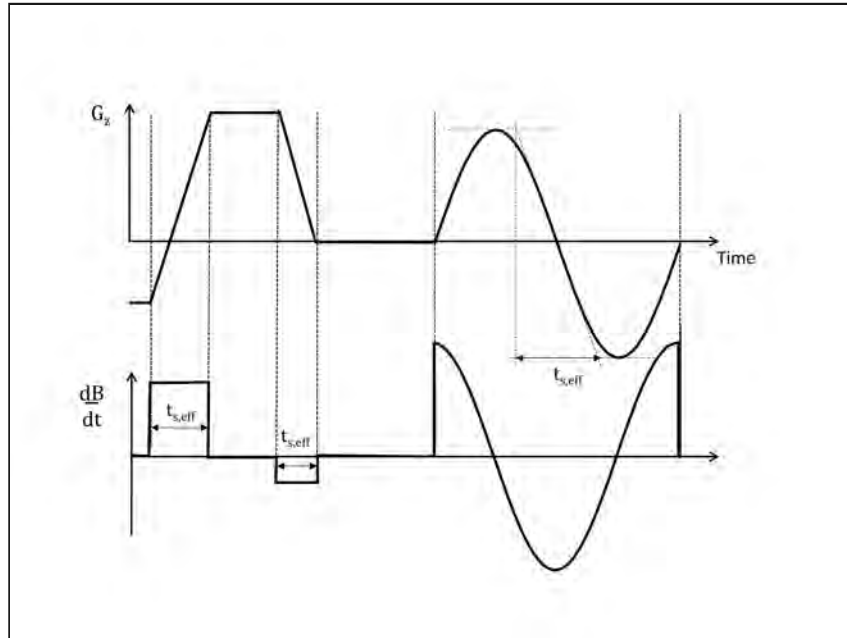
where t_{eff} is the duration of the dB/dt pulse (**Figure 19**). Alternatively, an E-field rheobase of 2.2-V/m may be used.

Of note is that the Second Level Controlled Operating Mode is only accessible as a research mode, subject to Institutional Review Board (IRB) or ethics committee approval. The International Commission on Non-Ionizing Radiation Protection (ICNIRP) defines the operational modes in a similar manner with identical limits (57).

Gradient weighting-factors are applied to the scanner's stimulation prediction monitor to account for the different sensitivities of each axis: $W_{\text{AP}} = 1.0$, $W_{\text{LR}} = 0.8$, $W_{\text{HF}} = 0.7$ where AP, HF, and LR are the anatomical orientations of the gradient axes. This results in a modified limiting SD curve:

152 Bioeffects of Gradient Magnetic Fields

Figure 19. Definition of stimulus duration t_{eff} for gradient waveforms from IEC 60601-2-33 (Reference 38).



$$\sqrt{\left(\sum_i w_i (dB/dt)_i\right)^2} < 20(1 + 0.36/t_{\text{eff}}) \quad (17)$$

The IEC cardiac limit uses the exponential version of the SD curve:

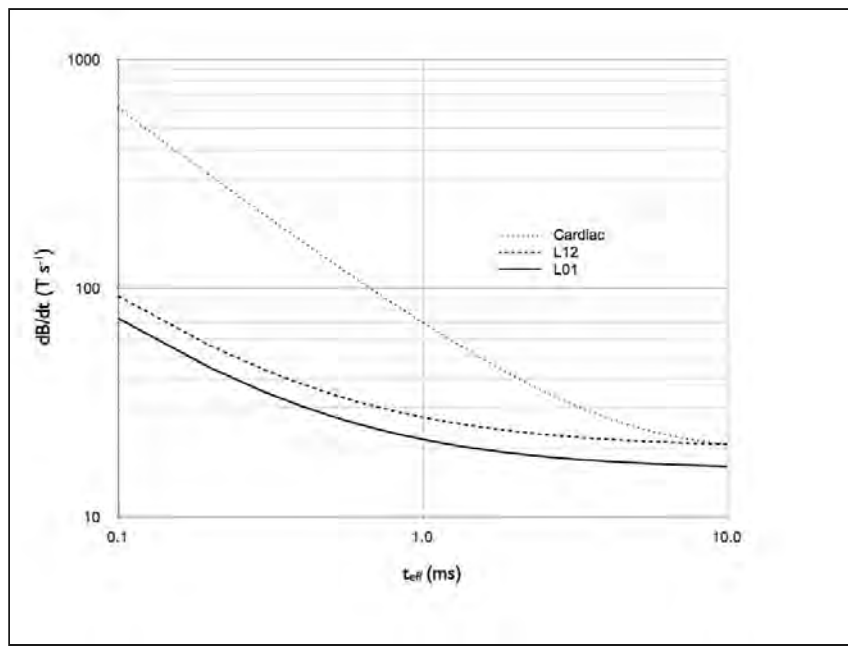
$$\frac{dB}{dt} < 20/(1 - e^{-\frac{t_{\text{eff}}}{3}}) \quad (18)$$

or in terms of induced electric field

$$E < 2/(1 - e^{-\frac{t_{\text{eff}}}{3}}) \quad (19)$$

The IEC limits are shown in **Figure 20**. In the United States (U.S.) IEC 60601-2-33 is adopted as a voluntary standard. The Food and Drug Administration (FDA) does not specify numerical limits in its *Criteria for Significant Risk Investigations of Magnetic Resonance Devices*, but advocates that uncomfortable or painful PNS be avoided (58).

Figure 20. IEC (38) limits for cardiac stimulation and Normal Operating Mode (L01) and First Level Controlled Operating Mode (L12) for peripheral nerve stimulation, and the cardiac limit. t_{eff} is the effective duration of the field change as defined in **Figure 19**.



AVOIDING PERIPHERAL NERVE STIMULATION (PNS) DURING MRI

Although PNS is not harmful, and rarely intolerable, its avoidance is desirable for maximum patient cooperation and comfort. The strength duration behaviour in MR systems is well categorized and hence the scanner's software is able to predict the likely onset of stimulation. This is related to the type of pulse sequence. Sequences with high dB/dt include echo planar imaging (EPI) and balanced steady state free precession (SSFP) gradient echo (e.g., TruFISP, b-FFE, FIESTA). Echo planar imaging has the additional feature of the rapid train of opposed polarity readout lobes, resulting in a longer stimulus duration and greater ΔB , which is more likely to cause PNS. Notably, PNS tends to occur in the following instances:

- During the use of rapid pulse sequences, such as EPI (echo planar imaging);
- When the y-gradient has the greatest gradient activity (e.g., if used for frequency-encoding during EPI);
- During diffusion-weighted MR imaging, where stronger gradient amplitudes are used;
- When obtaining high resolution images, which require higher gradient amplitudes; and
- When obtaining oblique section locations.

CONCLUSIONS

There is sufficient data from well-conducted human exposure studies with whole-body, MRI-related gradient systems, to have a high degree of confidence in the stimulation pre-

154 Bioeffects of Gradient Magnetic Fields

diction algorithms of clinical MR systems. These studies consistently show dB/dt rheobases for perception of around 20-T/s, with a ΔB_{\min} of around 8-mT. The y-gradient (anterior-posterior) is the most effective for stimulation with a rheobase in the range 15 to 19-T/s and measured chronaxies are remarkably similar across many different experiments. The threshold for discomfort or pain from PNS is approximately 50 to 100% higher than the perception threshold, and not generally achievable using clinical MR systems. The longer time constant for cardiac muscle and the smaller conduction loops around the heart make direct cardiac stimulation extremely unlikely.

ACKNOWLEDGEMENTS

Special thanks to John Nyenhuis, Joe Bourland and Alexander Kildishev of Purdue University, Lafayette, IN and Daniel (Joe) Schaefer of Duke University, Durham, NC for assistance with certain figures used in this chapter.

REFERENCES

1. Norris DG, Hutchison JMS. Concomitant magnetic field gradients and their effects on imaging at low magnetic field strengths. *Magn Reson Imag* 1990;8:33-37.
2. Budinger TF. Thresholds for physiological effects due to RF and magnetic fields used in NMR imaging. *IEEE Trans Nucl Sci* 1979;NS-26:2821-2825.
3. McRobbie D, Foster MA. Pulsed magnetic field exposure during pregnancy and implications for NMR foetal imaging: A study with mice. *Magn Reson Imag* 1985;3:231-234.
4. Turk EA, Kopanoglu E, Guney S, et al. A simple expression for the gradient induced potential on active implants during MRI. *IEEE Trans Biomed Eng* 2012;59:2845-2851.
5. Weiss G. Sur la possibility de rendre comparables entre eux les appareils servant à l'excitation électrique. *Arch Ital Biol* 1901;35:413-446.
6. Lapicque L. Recherches quantitatifs sur l'excitation électrique des nerfs traité comme un polarisation. *J Physiol Paris* 1907;9:622-635.
7. Reilly JP. Peripheral nerve stimulation by induced electric current: Exposure to time-varying magnetic fields. *Med Bio Eng Comput* 1989;27:101-110.
8. Reilly JP, Diamant AM. Electrostimulation: Theory, Applications, and Computational Model. Norwood, MA USA: Artech House; 2011.
9. Irnich W, Schmitt F. Magnetostimulation in MRI. *Magn Reson Med* 1995;33:619-623.
10. Glover PM. Interaction of MRI field gradients with the human body. *Phys Med Biol* 2009;54:R99-R115.
11. D'Arsonval A. Dispositifs pour la mesure des courants alternatifs de toutes fréquences. *Compt Rend Soc Biol* 1896;3:450-451.
12. Kavet R, Hailey WH, Bracken TD, Patterson RM. Recent advances in research relevant to electric and magnetic field exposure guidelines. *Bioelectromagnetics* 2008;29:499-525.
13. Lovsund P, Oberg PA, Nilsson SEG. Magnetophosphenes: A quantitative analysis of thresholds. *Med Biol Eng Comput* 1980;18:326-334.
14. Oberg PA. Magnetic stimulation of nerve tissue. *Med Biol Eng Comput* 1973;55-64.
15. Polson MJ, Barker AT, Freeston IL. Stimulation of nerve trunks with time-varying magnetic fields. *Med Biol Eng Comput* 1982;20:243-244.
16. Barker AT, Freeston IL, Jalinous R, Jarratt JA. Magnetic stimulation of human brain and peripheral nervous system: An introduction and the results of an initial clinical evaluation. *Neurosurgery* 1987;20:100-109.

MRI Bioeffects, Safety, and Patient Management 155

17. Conolly KR, Helmer A, Cristancho MA, et al. Effectiveness of transcranial magnetic stimulation in clinical practice post-FDA approval in the United States: Results observed with the first 100 cases of depression at an academic clinical center. *J Clin Psychiatry* 2012;73:e567-e573.
18. Klomjai W, Katz R, Lackmy-Vallee A. Basic principles of transcranial magnetic stimulation (TMS) and repetitive TMS (rTMS). *Ann Phys Rehab Med* 2015;58:208-213.
19. McRobbie D, Foster MA. Thresholds for biological effects of magnetic fields. *Clin Phys Physiol Meas* 1984;5:67-78.
20. Maccabee PJ, Amassian VE, Cracco RQ, Cadwell JA. An analysis of peripheral motor nerve stimulation in humans using the magnetic coil. *Electroencephalogr Clin Neurophysiol* 1988;70:524-533.
21. Claus D, Murray NM, Spitzer A, Flugel D. The influence of stimulus type on the magnetic excitation of nerve structures. *Electroencephalogr Clin Neurophysiol* 1990;75:342-349.
22. Weinberg IN, Stepanov PY, Fricke S, et al. Increasing the oscillation frequency of strong magnetic fields above 101 kHz significantly raises peripheral nerve excitation thresholds. *Med Phys* 2012;39:2578-2583.
23. Recoskie BJ, Scholl TJ, Chronik BA. The discrepancy between human peripheral nerve chronaxie times as measured using magnetic and electric field stimuli: The relevance to MRI-related gradient coil safety. *Phys Med Biol* 2009;54:5965-79.
24. Recoskie BJ, Scholl TJ, Zinke-Allmang M, Chronik BA. Sensory and motor stimulation thresholds of the ulnar nerve from electrical and magnetic field stimuli: Implications to gradient coil operation. *Magn Reson Med* 2010;64:1567-79.
25. Schmale I, Gleich B, Rahmer J, et al. Patient safety in future magnetic particle imaging: First experimental study of PNS thresholds. *Safety in MRI: Guidelines, Rationale & Challenges*, Washington DC, 2014. Berkeley: International Society for Magnetic Resonance in Medicine.
26. McRobbie DW. Bioeffects of gradient magnetic fields. In: *MRI Bioeffects, Safety, and Patient Management*. F.G. Shellock FD and J.V. Crues JV III, Editors. 2014; pp. 256-281. Los Angeles, CA: Biomedical Research Publishing Group.
27. McRobbie DW. Does trans-membrane stimulation occur in peripheral nerve stimulation: Why the SENN does not fit the data? *Proceedings of the 24th Annual Scientific Meeting of the International Society for Magnetic Resonance in Medicine*. Berkeley, CA: 2015. p.24.
28. Mouchawar G, Bourland JD, Voorhees WD, Geddes LA. Stimulation of inspiratory motor nerves with a pulsed magnetic field. *Med Biol Eng Comput* 1990;28:613.
29. McRobbie D, Foster MA Cardiac response to pulsed magnetic fields with regard to safety in NMR imaging. *Phys Med Biol* 1985;30:695-702.
30. Polson MJR, Barker AT, Gardner S. The effect of rapid rise-time magnetic fields on the ECG of the rat. *Clin Phys Physiol Meas* 1982;3:231-234.
31. Bourland JD, Mouchawar, Geddes LA, et al. Trans chest magnetic (eddy current) stimulation of the dog heart. *Med Biol Eng Comput* 1990;28:196-198.
32. Yamaguchi M, Andoh T, Goto T, et al. Effects of strong pulsed magnetic field on the cardiac activity of an open chest dog. *IEEE Trans BioMed Eng* 1994;41:1188-1191.
33. Cohen MS, Weisskopf MR, Rzedian RR, et al. Sensory stimulation by time varying magnetic field. *Magn Reson Med* 1990;14:409-414.
34. Reilly JP. Peripheral nerve and cardiac excitation by time-varying magnetic fields: A comparison of thresholds. *NY Acad of Sci* 1992;649:96-117.
35. Reilly JP. Neuroelectric mechanisms applied to low frequency electric and magnetic field exposure guidelines – part 1: Sinusoidal waveforms. *Health Physics* 2002;83:341-355.
36. Budinger TF, Fischer H, Hentschel D, et al. Physiologic effects of fast oscillating magnetic field gradients. *J Comput Assist Tomogr* 1991;15:609-614.
37. Vogt FM, Ladd ME, Hunold P, et al. Increased time rate of change of gradient fields: Effect on peripheral nerve stimulation at clinical MR imaging. *Radiology* 2004;233:548-554.

156 Bioeffects of Gradient Magnetic Fields

38. International Electrotechnical Commission. Medical Electrical Equipment – Part 2-33: Particular Requirements for the Safety of Magnetic Resonance Equipment for Medical Diagnosis. IEC 60601-2-33 3rd Edition. Geneva: IEC, 2015.
39. Bourland JD, Nyenhuis JA, Schaefer DJ. Physiologic effects of intense MR imaging gradient fields. *Neuroimaging Clin N Am* 1999;9:363-377.
40. Nyenhuis JA, Bourland JD, Kildishev AV. Health Effects and Safety of Intense MRI Gradient Magnetic Fields. In: Shellock FG, Editor. *Magnetic Resonance Procedures: Health Effects and Safety*. Boca Raton, USA: CRC Press, 2001.
41. Abart J, Eberhardt K, Fischer H, et al. Peripherial nerve stimulation by time-varying magnetic fields. *J Comput Assist Tomogr* 1997;21:523-538.
42. Den Boer JA, Bourland JD, Nyenhuis JA, et al. Comparison of the threshold for peripheral nerve stimulation during gradient switching in whole body MR systems. *J Magn Reson Imaging* 2002;15:520-525.
43. Hebrank FX, Gebhardt M. SAFE-Model – a new method for predicting peripheral nerve stimulation in MRI. In: Proceedings of the Joint Annual Meeting of the International Society for Magnetic Resonance in Medicine and the European Society for Magnetic Resonance in Medicine and Biology, Berkeley CA, USA: 2007.
44. Zhang B, Yen YF, Chronik BA, et al. Peripheral nerve stimulation properties of head and body gradient coils of various sizes. *Magn Reson Med* 2003;50:50-58.
45. Chronik BA, Rutt BK. Simple linear formulation for magnetostimulation specific to MRI-related gradient coils. *Magn Reson Med* 2001;45:916-919.
46. Ham CL, Engels JM, van de Wiel GT, Machielsen A. Peripheral nerve stimulation during MRI: Effects of high gradient amplitudes and switching rates. *J Magn Reson Imag* 1997;7:933-937.
47. Chronik BA, Rutt BK. A comparison between human magnetostimulation thresholds in whole-body and head/neck gradient coils. *Magn Reson Med* 2001;46:386-394.
48. Chronik BA, Ramachandran MJ. Simple anatomical measurements do not correlate significantly to individual peripheral nerve stimulation thresholds as measured in MRI-related gradient coils. *Magn Reson Imag* 2003;17:716-721.
49. Feldman RE, Hardy CJ, Aksel B, Schenck J, Chronik BA. Experimental determination of human peripheral nerve stimulation thresholds in a 3-axis planar gradient system. *Magn Reson Med* 2009;62:763-770.
50. Hoffmann A, Faber SC, Werhahn KJ, Jager L, Reiser M. Electromyography in MRI - first recordings of peripheral nerve stimulation caused by fast magnetic field gradients. *Magn Reson Med* 2000;43:534-539.
51. Zhao H, Crozier S, Lui F. Finite difference time domain (FDTD) method for modeling the effect of switched gradients on the human body in MRI. *Magn Reson Med* 2002;48:1037-1042.
52. Liu F, Crozier S. A distributed equivalent magnetic current based FDTD method for the calculation of E-fields induced by gradient coils. *J Magn Reson Imag* 2004;169:323-327.
53. So PP, Stuchly MA, Nyenhuis JA. Peripheral nerve stimulation by gradient switching fields in magnetic resonance imaging. *IEEE Trans Biomed Eng* 2004;51:1907-1914.
54. Neufeld E, Vogiatzis Oikonomidis I, Ida Iacono M, et al. Investigation of assumptions underlying current safety guidelines on EM-induced nerve stimulation. *Phys Med Biol* 2016;61:4466-4478.
55. Feldman RE, Odenggaard J, Handler WR, Chronik BA. Simulation of head-gradient-coil induced electric fields in a human model. *Magn Reson Med* 2012;68:1973-82.
56. Health Protection Agency. Protection of patients and volunteers undergoing MRI procedures. Documents of the Health Protection Agency RCE-7, Chilton, UK: Health Protection Agency, 2008.
57. International Commission on Non-Ionizing Radiation Protection. Medical magnetic resonance (MR) procedures: Protection of patients. *Health Phys* 2004;87:197-216.
58. Food and Drugs Administration. Criteria for significant risk investigations of magnetic resonance diagnostic devices. Rockville, MD: Center for Devices and Radiological Health, U.S. Food and Drug Administration, 2014.

Chapter 6 Acoustic Noise Associated With MRI Procedures

MARK MCJURY, PH.D.

Imaging Centre of Excellence
Queen Elizabeth University Hospital Campus
Glasgow, Scotland
United Kingdom

INTRODUCTION

During the operation of the magnetic resonance (MR) system, various types of acoustic noises are produced. The problems associated with acoustic noise for patients and healthcare workers are wide ranging, from simple annoyance and difficulties in verbal communication between staff and patients, to heightened anxiety or discomfort, and even potentially permanent hearing impairment (1-9). Acoustic noise may pose a particular problem for specific patient groups that may be at increased risk. For example, patients with head injuries or psychiatric disorders, the elderly, young children, and infants may be confused or suffer from heightened anxiety during MRI procedures (2). Patients taking medications may experience increased hearing sensitivity (3). Additionally, neonates with immature anatomical development may be at increased risk for adverse effects associated with acoustic noise. For example, significant fluctuations in vital signs of newborns have been reported during magnetic resonance imaging (MRI) examinations, which may partly be attributable to acoustic noise (4). High levels of acoustic noise may also impact the quality of the MRI procedure by causing distress in the patient.

Due to several of the issues listed above and the more specific issues discussed below, acoustic noise levels also pose a significant problem for one particular area of MRI: the increasing amount of research in functional MRI (fMRI) studies of brain activation. Typically, patients and volunteer subjects will be provided earplugs to wear during fMRI. However, these may impair vocal communication with staff members and also the perception of study stimuli. The acoustic noise associated with fMRI procedures can often be comparatively loud, as the use of fast acquisition sequences (e.g., echo planar imaging, EPI) are normally used. Acoustic noise can often lead to motion-related artifacts and degraded image quality. Furthermore, acoustic noise has been reported to interfere with auditory functional studies,

158 Acoustic Noise Associated With MRI Procedures

and more broadly, with cross modal neural activity (10-14). A summary of the potential issues related to the acoustic noise that is associated with fMRI is shown in **Table 1**.

MR system-related acoustic noise will interfere with the communication of activation task instructions that often must be provided during scanning. One area of particular interest is the study of auditory and language function (13). In this work, the response to pure tone stimuli is analyzed. Therefore, any background levels of unwanted or uncontrolled acoustic noise can interfere with the delivery of these sound stimuli and affect experimental integrity. Solutions specific to controlling acoustic noise exposure during fMRI are generally sequence-related and a full discussion of this topic is presented later in this chapter.

Acoustic noise levels during echo planar imaging have been reported to significantly increase pure tone hearing thresholds in the optimal frequency hearing range (0- to 8-kHz) (15). These effects vary across the frequency range and the threshold changes depend on the characteristics of the sequence-generated acoustic noise. It may be possible to take into account, or adjust for, the MR system-induced auditory activation by using a control series

Table 1. A summary of potential issues with unwanted acoustic noise in fMRI (14). Reproduced by permission, Wiley - John Wiley and Son Publishers, NY

Mechanism		Characteristics
Direct confounding	Intra-acquisition response	Activation by scanner noise within same volume acquisition. Primarily interfering with auditory fMRI.
	Inter-acquisition response	Activation by scanner noise of preceding volume acquisition. Primarily interfering with auditory fMRI.
Indirect confounding	Attention	Increased activation in attention-related cortical areas.
	Distraction	Decreased activation in cortical areas by (inter-modal) distraction.
	Habituation	Slowly developing adaption-related loss of attention. May be advantageous in noisy environments.
	Motion artifacts	Not substantially related to scanner noise.
	Masking	Overlap of spectral components of scanner noise and auditory stimuli. Confined to auditory fMRI.
	Stapedial muscle reflex	Changes in cochlear perception of auditory stimuli (intensity and frequency). Confined to auditory fMRI.
	Temporary hearing loss	Changes in cochlear perception of auditory stimuli (intensity and frequency). Confined to auditory fMRI.

of scans during task paradigms. Results have been reported on mapping auditory activation induced by MR system-induced acoustic noise (16).

The problem of acoustic noise may also have implications for the operational costs of an MRI facility. Notably, there can be a potential decrease in image quality due to patient movement resulting from the patient being startled or uncomfortable in association with acoustic noise. This may add to the need to repeat scans or to interrupt studies that can adversely impact the efficiency of an MRI facility. For all the above reasons, it is important that the MRI-related acoustic noise is quantified and characterized as part of a safety and quality assurance program. Furthermore, any exposure to acoustic noise that is excessive must be controlled or alleviated.

Acoustic noise experienced during routine clinical MRI examinations can generally be confined to levels within permissible limits with relatively little effort by using passive hearing protection (e.g., disposable earplugs). Several more sophisticated methods are also under investigation by researchers, offering more comprehensive and elegant solutions without the disadvantages of passive methods. This chapter will discuss acoustic noise and hearing, describe the common characteristics of MRI-related acoustic noise, explain the current permissible levels for acoustic noise, and present the main methods used for measurement and control of this potential hazard.

ACOUSTIC NOISE AND HEARING

The ear is a highly sensitive wide-band receiver, with the typical frequency range of 2-Hz to 20-kHz for normal hearing (17). The arrival of sound waves at the ear sets up a fluctuating pressure just outside the entrance to the external auditory canal. These fluctuations are then transmitted as pressure waves along the auditory canal. Normally under slight tension, the eardrum, or tympanic membrane, is physically moved by these pressure waves.

On the other side of the membrane, three tiny bones known as the ossicles, transmit this movement across the middle ear cavity to another membrane, the oval window, which forms the end of the spiral-shaped, fluid-filled cochlea. The vibration of the membrane and hair cells in the cochlea is transformed, via the auditory nerve, to give a sense of hearing. **Figure 1** shows the main components of the hearing mechanism.

At high sound intensities, the muscles that control the motion of the ossicles alter their tension creating the acoustic reflex to protect the ear from damage. However, this reflex occurs approximately 0.5-milliseconds after the insult, such that the ear is particularly vulnerable to impact noise of high intensity. The human ear does not tend to discern sound powers in absolute terms, but assesses how much greater one power is than another. Reflecting the very wide range of powers that exist, the logarithmic decibel scale, dB, is used when referring to sound power.

The sound level that is measured depends not only on the source, but also the environment (e.g., the proximity of surfaces that may reflect sound). Thus, sound levels are usually quoted in terms of sound pressure level (SPL), which accounts for the environment of the measurement. **Table 2** displays a range of sound pressure levels for some typical sources of acoustic noise.

160 Acoustic Noise Associated With MRI Procedures

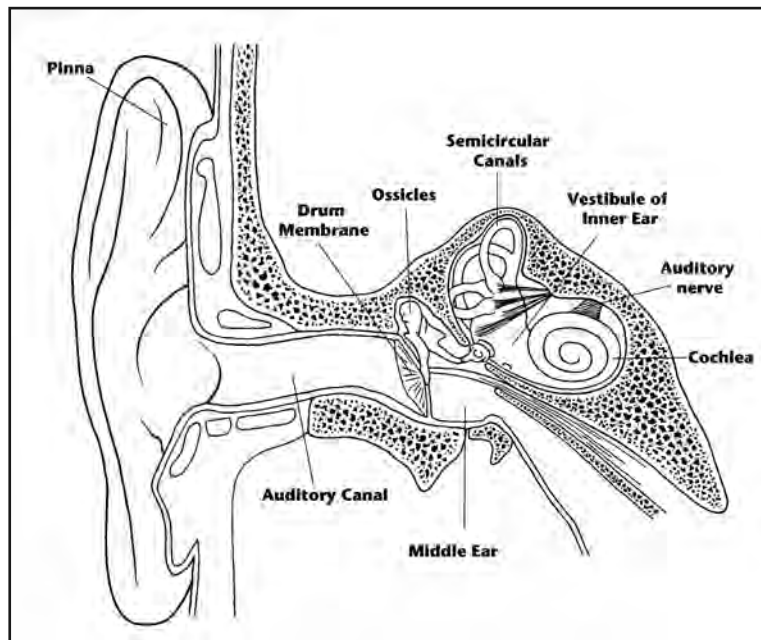
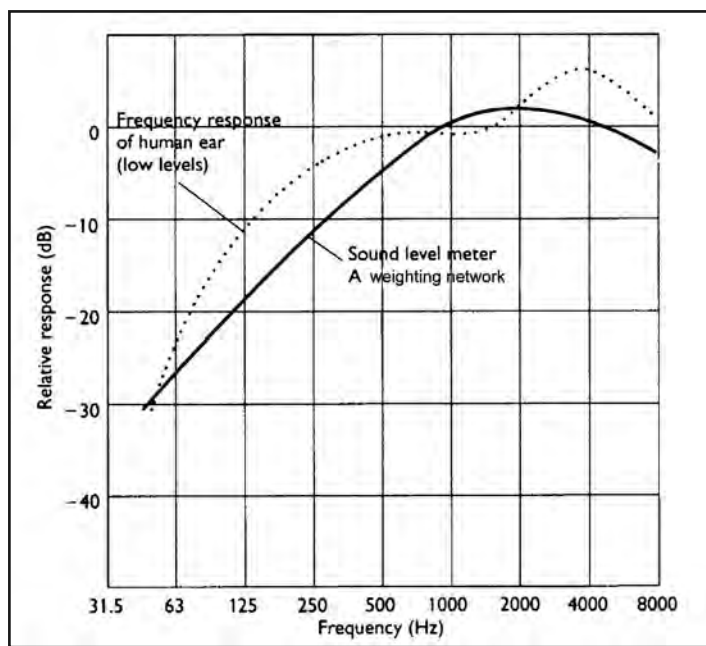
Figure 1. The main components of the human hearing mechanism.**Figure 2.** The frequency response of the human ear. The dashed line shows the relative frequency response of the human ear and the solid line shows the A-weighted filter approximation to this response (18). Reproduced by permission through the HMSO Open Government License.

Table 2. Sound pressure level for some typical sources of acoustic noise.

Sound Pressure Level (dB)	Typical Sound Sources
140	Threshold of pain
130	Pneumatic drill
120	Chainsaw
110 - 120	Car horn at 1-meter
80 - 90	Inside a bus
70 - 80	Traffic at street corner
60 - 70	Normal voice
50 - 60	Typical office
30	Whisper
0	Threshold of hearing

The sensitivity of the ear is also frequency dependent, as shown in **Figure 2** (18). Peak hearing sensitivity occurs in the region of 4-kHz. This is also the region where potential maximum hearing loss will occur, with damage spreading into neighboring frequencies. Since the ear is not equally sensitive to all frequencies, measured data may be weighted using the dBA measurement or “A-weighted” scale, which biases the meter to respond similarly to the human ear. The quality, or efficiency of hearing, is defined by the audible threshold, which is the SPL at which one can just begin to detect a sound. This is normally defined as 0 (zero)-dB.

Acoustic noise is defined in terms of frequency spectrum (measured and indicated in Hz), intensity (indicated in decibels or dB), and duration (or time). Additionally, noise may be steady state, intermittent, impulsive, or explosive. Time-varying noise is reported in terms of L_{eq} , which is defined as the continuous SPL that contains the same sound energy as the time-varying sound over the measurement period. This can be considered as the average noise level. Stimulation of the ear by acoustic noise has three potential effects: 1) Adaptation, 2) Temporary threshold shift (TTS) (post-stimulation fatigue), and 3) Permanent threshold shift (PTS) (permanent impairment).

In hearing adaption, loud sounds cause a small muscle attached to one of the bones of the inner ear to contract. This attenuates the transmission of sound vibration to the inner ear, which is a protective mechanism that does not work well for short duration, very intense sounds. Transient hearing loss may occur following loud noise (>100-dBA), resulting in a temporary threshold shift (i.e., a shift in audible threshold). With a TTS, subjects may experience a dulling in hearing at the end of the noise and tinnitus in some cases. Recovery typically occurs quickly (1). However, full recovery can take up to several weeks if the noise insult is particularly severe. Intense impulsive noises at 650-Hz with cut-offs at 300- and 1-kHz have also been shown to generate substantial TTS (19). Noise above 100-dBA can cause disturbances of the microcirculation in the cortical organ and short impulsive noise at levels of 120- to 130-dBA can lead to mechanical damage in this organ.

If the noise is sufficiently severe, this may result in a permanent threshold shift at specific frequencies (20, 21). Hearing damage from steady-state noise usually takes the form

162 Acoustic Noise Associated With MRI Procedures

of inner ear damage. That is, destruction of the hair cells that convert acoustic energy to electrical impulses transmitted via the nervous system to the brain. These cells cannot regenerate and, therefore, the damage is irreversible. This damage is similar to age-related hearing loss (presbycusis) in that it progresses slowly, with the affected hearing threshold rising. Mean hearing loss is a function of noise frequency and duration (20). Permanent damage is primarily a risk for prolonged daily exposure to loud (>85-dB) occupational noise or short impulsive noise around 140-dB. Excessive noise is known to be one of the most common causes of hearing loss (20). The risk of hearing damage increases with the noise level, duration of the noise, the number of exposures to the noise, and the susceptibility of the individual (20, 21). Along with sensitive groups, children have a lower threshold for hearing damage and, therefore, restricting exposure levels to around 120-dB or lower is recommended (22). It is generally accepted that exposure to noise levels up to a maximum of 75-dBA will not result in PTS irrespective of the duration of exposure (22). Over the years, several instances of noise-related incidents have been reported in the literature (see below).

Noise That Is Not Perceived By the Ear Canal

The ear canal is not the only path for transmission of sound to the cochlea. Sound may be conducted via air and bone conduction, through the ear canal, head, and body. Protection of the ear canal via earplugs will, thus, never lead to silence, due to the remaining sound conduction via the other paths. Sound can be conducted directly to the cochlea, to the middle ear and then to the cochlea, or through the walls of the middle ear, along the ear canal to the middle ear, and then to the cochlea (23). When the ear canal is relatively unprotected, this path will be the dominant one for perception of sound. However, as noise is attenuated along the ear canal, the other paths become increasingly dominant and further hearing protection measures will have little effect on the residual noise. Using a helmet in addition to conventional earplugs and “defenders”, Ravicz and Melcher, (24) studied the impact of isolating the head and ear canal from sound. Isolating the head enabled the original noise attenuation of 39- to 41-dB to increase to 55- to 63-dB.

Prenatal and Neonatal Hearing and Acoustic Noise

By around the twentieth week of gestation, the outer, middle, and inner ear of the fetus appear to be fully formed. The fetus can then begin to detect sounds (25). Indeed, Hepper and Shahidullah, (26) reported that the responsiveness of the fetus to audio stimuli occurs between 19 to 35 weeks, with initial responses being to sounds at low frequencies. They measured an initial response at 20 weeks to a 500-Hz pure tone. As the pregnancy progressed, there was a significant reduction (20- to 30-dB) in the intensity of sound required to elicit a response. Studies report that maternal tissues and fluid surrounding the fetal head act as efficient low-pass filters for sound (27-31).

Acoustic noise is known to be a concern for neonates who generally have sensitive hearing. Aside from artifacts introduced from involuntary motion related to startle reflexes, the noise can provoke adverse responses such as autonomic instability (32-36). Neonatal intensive care unit guidelines often suggest minimizing the risk of physiological stress by adhering to a limit for exposure to acoustic noise (see below).

CHARACTERISTICS OF MRI-RELATED ACOUSTIC NOISE

Early measurements of MRI-related acoustic noise offered little more than an assessment of intensity levels. Over time, researchers began to investigate the noise in more detail and to characterize it in terms of frequency components, variability with pulse sequences, and the contribution of individual gradients.

The gradient magnetic field of the MR system is the primary source of acoustic noise associated with MRI. This noise occurs during the rapid alterations of currents within the gradient coils. These currents, in the presence of the strong static magnetic field of the MR system, produce significant (Lorentz) forces that act upon the gradient coils. From basic physics, a conductor element dl carrying a current $I = I \hat{i}$ placed into a magnetic uniform field $\mathbf{B} = B \hat{k}$, will experience a Lorentz force F per unit length given by,

$$\mathbf{F} = \mathbf{I} \times \mathbf{B} = jBI \sin \theta \quad (1)$$

where θ is the angle between the conductor and the field direction and \hat{i} , \hat{j} , \hat{k} are unit vectors along the conductor, force, and magnetic field direction, respectively. Therefore, simplistically we would expect acoustic noise to be theoretically linear with the static magnetic field of the MR system (37). In fact, Moelker, et al. (38) reported on a measured non-linearity, with noise levels measured at high field being lower than that expected with a linear dependence. The noise from these mechanical forces is then transferred into airborne acoustic noise or sound pressure, due to an acoustic noise transfer function (38).

Acoustic noise, manifested as loud tapping, knocking, and other sounds is produced when the forces cause motion or vibration of the gradient coils as they impact against their mountings, which then also flex and vibrate. All structures have intrinsic resonance frequencies and these frequencies have their own modal shapes. In fact, there are several pathways of noise generation associated with MRI (40).

If the gradient coil modal shape due to deformation corresponds to the shape of the exciting Lorentz force distribution, then large gradient coil displacements occur and result in the generation of significant acoustic noise. Current designs of gradient coils are often manufactured to have a high stiffness, which minimizes coil motion and, thus, the structural resonances of the coils.

Various factors have been shown to affect the acoustic noise generated during MRI, including the strength of the static magnetic field (mentioned above) and alteration of the gradient output (i.e., rise time and amplitude). Interestingly, Price, et al. (39) reported that there is greater impact on acoustic noise levels generated from imaging parameters than the field strength. Acoustic noise is enhanced by decreases in section thickness, field of view, repetition time, and echo time. The physical features of the MR system and its environment as well as the material and construction of the gradient coils and support structures also affect the transmission of the acoustic noise and its perception by the patient and MR system operators.

164 Acoustic Noise Associated With MRI Procedures

Gradient magnetic field-induced noise levels have been measured during a variety of pulse sequences for clinical and research MR systems with static magnetic field strengths ranging from 0.35- to 4-T, with acoustic noise levels of over 130-dB reported (39-54). Obviously, since the gradient magnetic field is primarily responsible for acoustic noise, the ability of the MR system to produce noise is dependent upon the specifications for the gradients (amplitudes and slew rates) as well as the types of imaging parameters that are available on the scanner.

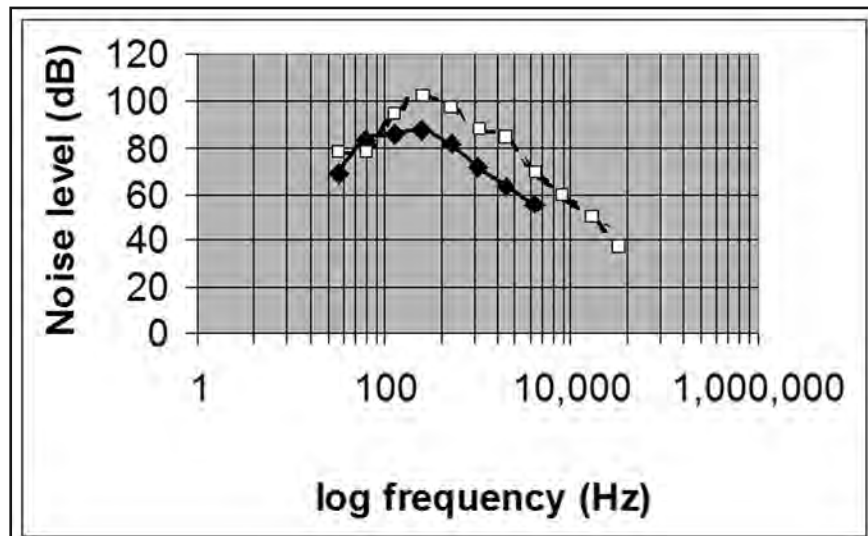
Not surprisingly, fast gradient echo pulse sequences produce, comparatively, louder noise during MRI than spin echo sequences. Three-dimensional and diffusion MR pulse sequences, where multiple gradients are applied simultaneously, are among the loudest. Many studies have focused on assessing the maximum MR system acoustic noise, which is usually related to using EPI methods, due to the associated high gradient performance inherent in these ultrafast sequences. Echo planar sequences, in collecting a complete image in one radiofrequency (RF) excitation of the spin system, require extremely fast gradient switching times and high gradient amplitudes. The increased interest in diffusion imaging and fMRI has meant a heightened interest in using high field strength MR systems (i.e., mostly 3-, 4-, and 7-T) with fast gradient capability (switching rates and high amplitudes) to acquire multi-slice, EPI images of high quality (see below for more on high field issues).

Shellock, et al. (43) reported relatively high levels of acoustic noise, up to 102- to 103-dBA on the two 1.5-T MR systems tested when running EPI sequences with parameters selected to represent a “worst-case” protocol. Nevertheless, these acoustic noise levels were within current permissible limits for MR systems. Miyati, et al. (50) conducted an extensive survey of EPI sequences performed on eleven MR systems. The results of the sound level measurements reported to be at levels within permissible limits.

Price, et al. (39) surveyed fifteen MR scanners, with static magnetic field strengths from 0.2-T to 3-T, reporting worst case noise levels in the range 82.5- to 118.3-dBA, but for two-dimensional MRI techniques, only. They reported the lowest noise levels for the lowest static field strength scanner and the highest noise recorded for the highest field strength scanner, but noted low levels of acoustic noise recorded for a 1.5-T scanner fitted with vacuum-encased gradient coils. Higher acoustic noise levels have been reported by Ravicz, et al. (52) (up to 138-dB for 3-T) and More, et al. (53) (130-dB for 4-T).

Foster, et al. (54) reported EPI-related acoustic noise levels of 123- to 132-dBA for a 3-T research scanner. Since EPI sequences are significantly shorter in duration than conventional sequences, in terms of acoustic noise exposure, higher sound exposure levels are possible for the shorter times involved. However, these levels, when converted to eight hour equivalent values ($L_{eq} = 108$ -dBA), are higher than the limits for occupational acoustic noise exposure used in the United Kingdom (UK) and in the United States (U.S.). Therefore, hearing protection must be used for patients undergoing MRI procedures under these circumstances. Conventional EPI sequences generally comprise constant readout gradients and a train of very short high level trapezoidal phase encode gradient ‘blips’. It is not surprising that the blipped gradient contributes the larger proportion of the sequence-related acoustic noise (55). As the gradient blips are at higher frequency than the readout gradient, the resultant acoustic noise will have a larger proportion of high frequencies.

Figure 3. Octave band spectra for two MR systems: 1-T Siemens Impact (black squares) and a 1.5-T Siemens Magnetom (open squares). Measurements obtained on these MR systems show that the peaks in noise intensity are at approximately 200-Hz (45).



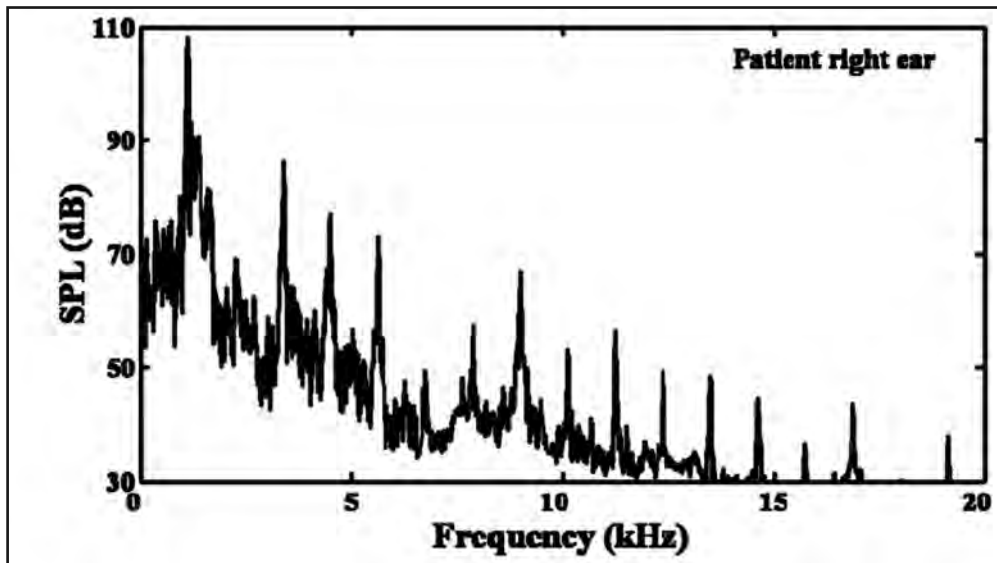
Measurements of sound pressure levels offer a limited amount of information with regard to the quality of the noise and its impact on hearing. In addition to measurements of noise level, several groups have recorded and analyzed the acoustic noise. Similar noise levels and characteristics are found when comparing different clinical MR systems. Frequency analysis of the noise shows that noise is pseudo-periodic, with variations in the degree of periodicity depending on the pulse sequence used and the vibrational characteristics of the gradient coils (46).

For conventional pulse sequences used for MRI, peak noise levels are found at the low frequency region of the spectra. **Figure 3** shows an example of the octave band spectra for a 1.0-T and 1.5-T MR systems (44, 45). Spectral peaks in the sound levels were found in the range of 0.2- to 1.5-kHz (22). Cho, et al. (48) have also reported that pre-scan noise generated high levels (100-dB, C-weighted scale) across a wide spectral range up to 4-kHz with peaks around 2.4-kHz.

More, et al. (53) noted that repetition time (TR) had a minimal impact on overall SPL, while increasing the echo time (TE) increased attenuation, in agreement with Price, et al. (39). Unlike the use of conventional sequences, EPI-related sound levels have been reported to contain a larger fraction of high frequency noise (around 4-kHz) with most noise comprising the fundamental frequency and harmonics in the frequency range of 0.5- to 4-kHz (52). For EPI sequences, More, et al. (53) also noted considerable non-harmonic noise flanking the harmonics. The acoustic noise was also noted to contain a higher proportion of broad frequency spectrum noise (**Figure 4**). For their pulse sequence, More, et al. (53) found the even harmonics to be associated with the phase-encoding gradient, the frequency encoding gradient generated the odd harmonics and non-harmonic acoustic noise, while the slice-selective gradients generated the broad spectrum noise (**Figure 5**).

166 Acoustic Noise Associated With MRI Procedures

Figure 4. Measured acoustic noise for an echo planar imaging (EPI) pulse sequence. Acoustic noise spectrum at the right ear (53). Reproduced by permission, Wiley - John Wiley and Son Publishers, NY.



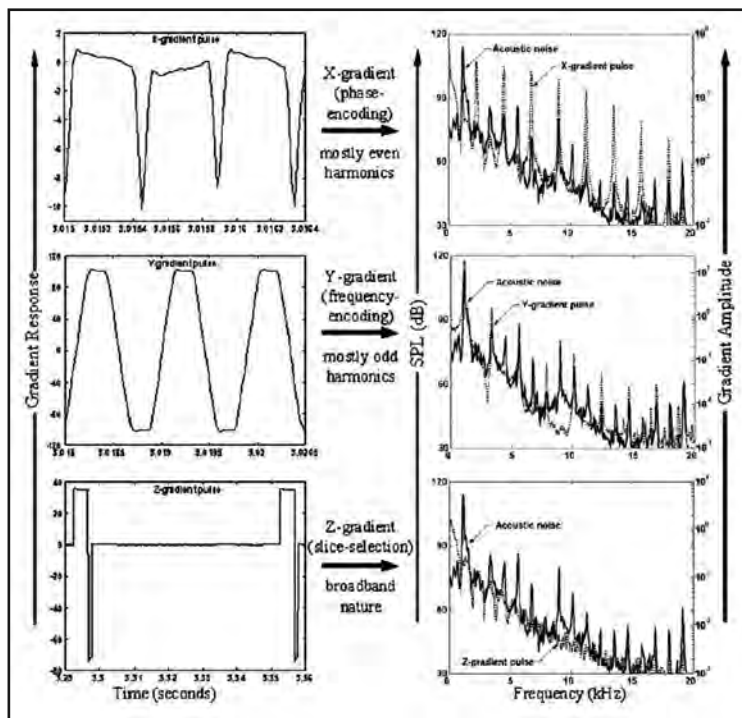
In addition to the dependence on pulse sequence parameters, MR system hardware and construction, acoustic noise is dependent on the immediate environment. Spatially, the acoustic noise will vary along the bore of the scanner. However, how it varies will depend on the MR system's structure and design. Price, et al. (39) presents acoustic noise measurements across a range of scanner geometries and designs, systems ranging from static magnetic field strengths of 0.2 to 3-T. Reports providing values of acoustic noise tend to disagree because of differences related to whether the maximum acoustic noise levels were measured at the isocenter of the bore or not (39, 47, 49). The noise distributions along radial and axial directions are also likely to be asymmetric, due to standing wave effects in the scanner's bore (53).

Furthermore, noise levels have been found to vary by as much as 10-dB as a function of the patient's position inside the MR system (47) such that the presence and size of the patient affects the level of acoustic noise. For example, an increase of 1- to 3-dB has been measured with a patient present inside of the MR system (47), which may be due to pressure doubling (i.e., the increase in sound pressure close to a solid object, caused when sound waves reflect and undergo in-phase enhancement).

Acoustic Noise and Ultra-High-Field MRI

Technical developments enable a continuing increase in available research and clinical static magnetic field strengths, with scanners operating at 7-T or above typically referred to as ultra-high-field (UHF) systems. Interestingly, research is on-going for possible human scanning using MR systems operating up to 20-T (56). As mentioned above, knowing that there is a strong (non-linear) dependence between the acoustic noise levels that are generated and the strength of the static magnetic field (38), we might expect acoustic noise levels to

Figure 5. Relationship between the operating acoustic noise at the left ear and gradient pulse waveform for an EPI pulse sequence. Data is shown for each separate gradient and the associated noise spectral peaks (53). Reproduced by permission, Wiley - John Wiley and Son Publishers, NY.



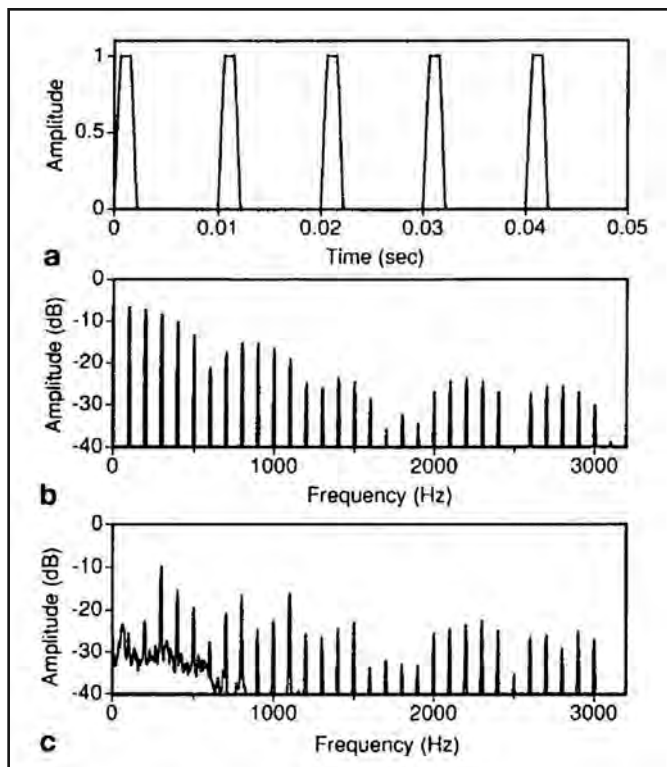
increase significantly for UHF scanners. When increasing the static magnetic field strength from 1.5-T to 11.7-T, a simple linear model predicts an increase in the acoustic noise level by approximately 22-dB. But, in fact, in line with earlier results (38), this has not been observed in practice (57). Applying a logarithmic scale, changing from 7-T to 20-T, a 9-dB increase in acoustic noise level would be predicted. However, building in additional effects such as Lorentz damping (58), results in increases in acoustic noise levels that are actually lower than expected, and in some cases very similar to reported noise levels at 3-T (59-60).

Notably, one practical difference (61) is that head coils at 7-T are generally more tightly fitting than those used at 3-T because they are comprise of a multi-channel insert. This makes using double passive hearing protection (earplugs and earmuffs) impractical and, thus, the acoustic noise is only attenuated by earplugs alone.

Presently, findings obtained at 7-T remain sparse (61-64). Costagli, et al. (62) reported acoustic noise levels of 89.9 +/- 0.7-dBA for conventional T₁-weighted, fast spoiled gradient recalled (FSPGR) pulse sequences at 7-T. Speck, et al. (64) reported acoustic noise levels of 101-dBA for a standard EPI sequence, also at 7-T. Importantly, these levels are considerably lower than early measurements recorded on 3- and 4-T scanners. Therefore, there

168 Acoustic Noise Associated With MRI Procedures

Figure 6. Gradient trapezoidal current excitation and acoustic noise response. (a) Trapezoidal current waveform time series. The signal consisted of a series of simple trapezoidal gradient pulses. (b) Fourier transform of trapezoidal time series, and (c) measured acoustic response (47). Reproduced by permission, Wiley - John Wiley and Son Publishers, NY.



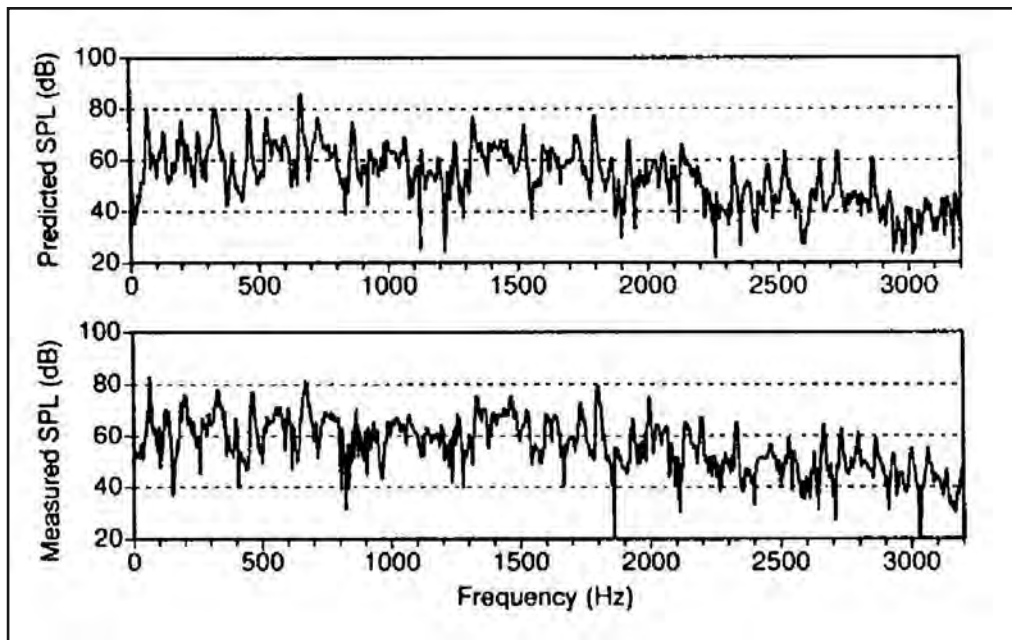
appears to be little concern for substantial increases in risks for acoustic noise-related issues associated with the currently used UHF MR systems.

Analysis, Simulation and Modeling of MR System Acoustic Noise

Hedeen and Edelstein (47) demonstrated the similarity between the gradient pulse spectrum and the acquired noise spectrum, which are affected by additional system acoustic resonances (**Figure 6**). There was a good qualitative match between the input signal and resulting acoustic noise spectrum. Hedeen and Edelstein (47) derived an acoustic transfer function that is independent of input, and which once determined, may be applied to any input impulse function and will then predict the generated acoustic noise.

Defining the scanner's frequency response function (FRF) as $H(f)$, the input signal represented in the frequency domain as $G(f)$, and the resulting acoustic noise, $P(f)$, the following may be expressed,

Figure 7. Predicted (top) and measured (bottom) acoustic noise spectrums, SPL, for a fast spin echo (FSE) pulse sequence. Overall predicted and measured levels were 93.1- and 92.7-dB respectively. Good agreement over a broad spectral range is evident (47). Reproduced by permission, Wiley - John Wiley and Son Publishers, NY.



$$P(f) = H(f) \cdot G(f) \quad (2)$$

Hedeen and Edelstein (47) applied this analysis to a fast spin echo (FSE) pulse sequence and achieved an agreement between measured and predicted acoustic noise level to within 0.4-dB (**Figure 7**). Other authors, such as More, et al. (53) and Rizzo-Sierra, et al. (65) have used similar approaches in deriving simple acoustic transfer or impulse response functions with considerable success in predicting the acoustic noise associated with the MR system's gradient behavior.

Interestingly, Hamaguchi, et al. (66) applied an acoustic transfer function approach to compare the acoustic noise characteristics of several clinical MR systems. This group assessed 10 scanners, finding results (higher acoustic response at high frequency) that contradict those reported by others (22, 44, 45).

A number of investigators reported detailed acoustic analysis and modeling of the acoustic noise from commercial and purpose-built gradient coil systems. Researchers have made a significant contribution to this field, reporting on a number of approaches to gradient modeling as well as conducting evaluations and testing on noise reduction techniques (67-

170 Acoustic Noise Associated With MRI Procedures

74). In 2002, Mechefske, et al. (67) developed the simulation of a cylindrical whole-body gradient coil housed in a 4-T MR scanner and driven by triangular and trapezoidal gradient pulses. The simulation was based on finite element (FE) analysis. Acoustic frequency responses predicted by the simulation were compared to experimental measures, showing broad agreement. Further reports investigated experiments and simulation of purpose-built gradient coils, including vibration and acoustic noise measurements (68, 69). In their finite element model, Lorentz forces were used as the system load, with acoustic radiation modeled using the Kirchhoff-Helmholtz equation. These researchers performed the analysis for a small head geometry gradient coil and achieved reasonable agreement of theory and experiment (68, 69).

Further work in this field has been conducted by Kuijpers, et al. (75), who created a mathematical model of acoustic noise radiation in finite ducts. Shao and Mechefske (70) reported on the development of a predictive analytical model, allowing for inclusion of acoustic liners inside the gradient coil inner wall. They also compared analytic and boundary element models. The analytical model was comparative in terms of results, but computationally more efficient. Additional papers investigated the dynamic behavior of gradient coils of varying wall thickness (71-74) and by applying shell theory (76). Investigators have also investigated the coupling of gradient coils to other associated structures, reporting on structural analyses (77). Recently (and mentioned above), Winkler, et al. (57, 58) utilized a vibroacoustic FE approach to predict acoustic noise levels for UHF scanning that included the effects of Lorentz damping.

ACOUSTIC NOISE LEVELS AND PERMISSIBLE LIMITS

Several of the available guidance documents discussed below adopt a similar framework, referring back to the same source for action levels and permissible limits. Much of the international guidance is based on occupational exposure limits that assume chronic exposures. These are not entirely satisfactory for application to patient exposures associated with MRI, which can be short but with potentially intense noise, causing discomfort. When time-averaged, these types of exposures can fall below action levels but still present a hazard. For normal individuals, the typical threshold for discomfort related to acoustic noise is approximately 120-dB in the 1- to 5-kHz range (78), however, those with particular sensitivity can experience discomfort at much lower acoustic noise levels (79).

For acoustic noise exposure involving *staff members*, the current UK occupational guidelines are based on the Control of Noise at Work legislation, published in 2005 (80). This document sets out the responsibilities of the employer and makes a number of recommendations based on a small set of action levels. Acoustic noise is graded to that which is below 80-dBA, a lower action level at 80-dBA daily or weekly exposure (peak 135-dBC), and upper action level at 85-dBA daily or weekly exposure (peak 135-dBC). It should be noted that values for lower and upper action levels have been reduced by 5-dBA, compared to previous Noise at Work action levels published in 1989. This document also recommends that hearing protection should be available for all staff members, and that its use be mandatory for noise above the upper action level. For MRI healthcare workers, there is generally little need to be in the MR system room during scanning. Because the acoustic noise levels that exist outside the scanner's bore are relatively low, the risks are similarly low.

Table 3. Occupational noise action values and limits (adapted from reference 80). Reproduced by permission, HMSO (Open Government License).

Action Level	Daily or Weekly Personal Exposure dB(A) (average value)	Peak Sound Pressure, dB
Lower exposure value	80	135
Upper exposure value	85	137
Exposure limit values	87	140

The management of exposure to acoustic noise for the **general public** is covered by the Management of Health and Safety at Work (1999) (81), but, since the general public does not have access to the controlled area or MR system room, again, the risks are low. European guidance is published as directive 2013/35/EU (82) and has similar limits and action levels to those in the UK.

In the United States (U.S.), occupational limits are mandated by the Occupational Safety and Health Authority (OSHA) (83) and have also been adopted by the Food and Drug Administration (FDA) (84). OSHA guidance is geared towards traditional ‘heavy’ industries where there are very noisy environments and medium-to-high risk to hearing. Their list of affected industries does not include MRI/Healthcare. Now somewhat outdated, the OSHA guidelines apply to a slightly raised action level of 90-dBA (daily or eight-hour average) in line with the older UK guidance (85).

Current UK guidance on noise exposure limits for MRI **patients and volunteer subjects** (including staff members) is presented in the MHRA guidelines (86). For patients and volunteer subjects, it suggests hearing protection should always be offered unless noise levels are proven to be below 80-dBA. Hearing protection should reduce levels at the ear to below 85-dBA. The recommended action levels are based on the noise at work regulations (72) and are shown in **Table 3**. The International Commission on Non-Ionizing Radiation Protection (ICNIRP) (87, 88) notes the range of guidance from the International Electrotechnical Commission (IEC) (89), but accepts the need for a conservative approach to protect vulnerable patient groups, also recommending the MHRA action levels. The MHRA document shows the relationship between the acoustic noise level and time necessary to reach the daily action level (86) (**Table 3**). Recommendations for acoustic noise and hearing protection are, as follows (86):

- The use of hearing protection is highly recommended. Protection should be available and all patients and volunteers should be encouraged to use it. Protection should always be worn by vulnerable patients.
- Protection should reduce noise level at the ear to below 85 dBA. For the noisiest circumstances, earplugs and muffs can be used together.
- Staff should be trained in the selection and fitting of hearing protection. Protection should be selected to match the noise frequency spectrum of the scanner. Implicitly, this must, therefore, be known.

172 Acoustic Noise Associated With MRI Procedures

- Staff should be offered hearing protection if acoustic noise levels are above the lower action level and use is mandatory for noise at the upper action level.
- Particular care should be taken with vulnerable patient groups, such as pediatric and unconscious patients.
- Pregnant staff members are advised not to remain in the MR system room during scanning. Sites should undertake a risk assessment to evaluate staff time and motion around the scanner in order to minimize exposure to the MRI setting.

In the U.S., various patient exposure guidelines related to the MRI environment were initially recommended in a document issued by the American College of Radiology in 2002 (90) and this was updated in 2013 (91). The ACR document makes little mention of the risks associated with acoustic noise, however, it does recommend that all patients should be offered hearing protection and that this is mandatory for those undergoing MRI procedures using research pulse sequences.

While the acoustic noise levels suggested for patients exposed during MRI examinations on an infrequent and short-term temporal basis are considered to be highly conservative, they may not be appropriate for individuals with underlying health problems who may be sensitive to noise at certain levels or at particular frequencies.

Overall, the acoustic noise produced during MRI on a modern-day scanner should represent a minimal risk to patients if good quality hearing protection is used. However, the possibility exists that substantial gradient magnetic field-induced noise may represent a heightened risk in certain patients who are particularly susceptible to the damaging effects of loud noises or for those with poorly fitting hearing protection. In fact, there have been unconfirmed claims of permanent hearing loss associated with MRI examinations (9). Therefore, vigilance and care is essential when controlling noise levels associated with MR procedures.

Limits During Pregnancy and Neonatal Imaging

Due to lack of data and a full understanding of response, UK guidance (86) suggests a cautious approach to scanning the fetus and pregnant patients. Scanning during the first trimester is discouraged unless justified by a critical risk assessment. Because acoustic noise is known to be a concern for neonates who have sensitive hearing, neonatal intensive care unit (NICU) guidelines suggest minimizing the risk of physiological stress by adhering to a limit for noise exposure to 65-dBA (92).

Fetal MRI has become increasingly important, particularly in diagnosis of fetal abnormalities and for the management of the mother. Although discouraged, if necessary MRI procedures may be performed during the first trimester of pregnancy. In a survey conducted by De Wilde, et al. (93), 83% of the clinics that responded suggested that they would scan patients during the first trimester in cases of clinical need. While the mother may wear hearing protection, the fetus is protected only by the attenuation provided by the intra-uterine fluid and the maternal abdomen. Thus acoustic noise has the ability to impact the fetus (94). To minimize motion-related artifacts, fast imaging techniques are required for fetal MRI examinations, which results in the potential for exposures to comparatively high levels of acoustic noise. Glover, et al. (95) investigated acoustic noise absorption through the ab-

domen using a hydrophone in the stomach of a (male) volunteer. For scans performed at 0.5-T, these researchers reported a reduction of approximately 30-dB in acoustic noise levels. However, this study was a very limited approximation to scanning a pregnant patient and the associated sound absorption. The strength of the static magnetic field of the MR system, which directly affects acoustic noise levels generated, was also low (0.5-T) compared to the majority of clinical scanners in current use. Certain research has reported high frequency hearing loss, shortened gestation, and decreased birth weight following exposure to high levels of acoustic noise (>99-dBA) (96).

To investigate this particular safety issue, there have been a number of follow-up studies (97-106). For example, Reeves, et al. (97) investigated the rates of cochlear impairment for a cohort of second and third trimester neonates who had been exposed to acoustic noise during 1.5-T MRI examinations. Their data showed no association between exposure to noise and an increased risk of hearing impairment. General guidelines for managing exposure to acoustic noise produced by the United Kingdom (UK), Medicines and Healthcare products Regulatory Agency (MHRA) (86) and based on evidence in several reports (98-100) suggest that the data on the effects of noise on the health of the fetus is inconclusive.

Bouissant-Kobar, et al. (101) followed-up (i.e., at approximately 24 months) on a cohort of 72 pre-school children scanned at 1.5-T during their mothers' pregnancies (mean gestational age at scanning, 30 weeks). All children were born at term and achieved age-appropriate scores in the Vineland Adaptive Behaviour Scale (VABS) tests. In addition, all study subjects passed their new-born otoacoustic tests and demonstrated normal hearing at pre-school age. These findings confirmed a lack of MRI-related impact on functional outcomes or hearing impairment at pre-school age. De vita, et al. (102) and Jaimes, et al. (103) investigated the effects of higher field strength scanning on pre-terms (4.7-T and 3-T, respectiv). Both groups noted no increase in risks in moving to a higher field strength MR system. Clements, et al. (104) report similar normal findings, in this case for a smaller cohort (20 cases) whose mothers had been exposed to echo planar imaging (EPI) at 0.5-T four times between 20 weeks and term. Thus, the current data appears to provide general reassurance in that there is low risk present when applying MRI in prenatal and neonatal patients (101-106). An optimized solution for neonatal imaging with clear benefits was reported by Tkach, et al. (107, 108). This group scanned 15 non-sedated neonates in an adapted small-bore (diameter 22- cm) 1.5 -T orthopedic MR system. Although the scanner has approximately twice the gradient strength (70-mT/m) and slew rate (300-mT/m/s) of conventional full-size MR systems, the gradient coil was smaller and shorter, leading to lower levels of acoustic noise or equivalent pulse sequences (107). Using specifically designed hearing protection,, high quality images were obtained for and all MRI examinations that were completed successfully, suggesting minimal impact of the acoustic noise. Of further note is that De Vita, et al. (102) reported successful imaging of nine ventilated neonates at 4.7-T without any acute adverse effects.

Overall, the use of a combination of hearing protection (e.g., earplugs and earmuffs or headphones) and the additional attenuation of having the neonate placed inside the transmit RF coil, mean that the acoustic noise at the ear is likely to be lower for neonates than for adults, which may explain why no adverse effects have been reported, to date. The anatom-

174 Acoustic Noise Associated With MRI Procedures

ical attenuation afforded to fetuses also seems to be sufficiently effective to enable safe scanning with current clinical static magnetic field strengths and protocols.

Adverse Incidents Associated with Exposure to MRI-Related Acoustic Noise

(A) Temporary Threshold Shifts (TTS)

As mentioned above, short-term exposure to intense noise (>100-dBA) can induce a temporary shift in the hearing threshold. Brummett, et al. (1) reported temporary shifts in hearing thresholds in 43% of the patients scanned without hearing protection or with improperly fitted earplugs. Normal hearing returned after 15-minutes. Notably, noise levels during scanning were not measured as part of their study. However, Hurwitz, et al. (42) made measurements using the same scanner, reporting values for gradient echo sequences (likely to be some of the loudest sequences on this system) of around 93-dBA. Of the 14 patients scanned without hearing protection in their study, six suffered TTS with threshold loss greater than 15-dB. For those using hearing protection, only one experienced a TTS. It should be noted that these data were associated with scans performed on a comparatively low field strength MR system (0.35-T). A study by Wagner, et al. (109), found conflicting results.

Ulmer, et al. (16) measured changes in pure tone thresholds in volunteer subjects wearing hearing protection exposed to EPI pulse sequences. Intense impulse noise at 0.65-kHz with cut-offs at 0.3-kHz and 1.0-kHz were also shown to generate substantial hearing threshold shifts. In 2011, Govindaraju, et al. (110) reported a possible incidence of TTS for a man scanned while wearing earplugs on a 3-T scanner. The patient experienced unilateral hearing loss and tinnitus immediately following the MRI examination. The hearing loss resolved completely within 24-hours but the tinnitus persisted. Acoustic noise levels were checked for the conventional sequences that were performed and found to be in the range of L_{eq} 101- to 112-dBA (L_{peak} 115- to 124-dB).

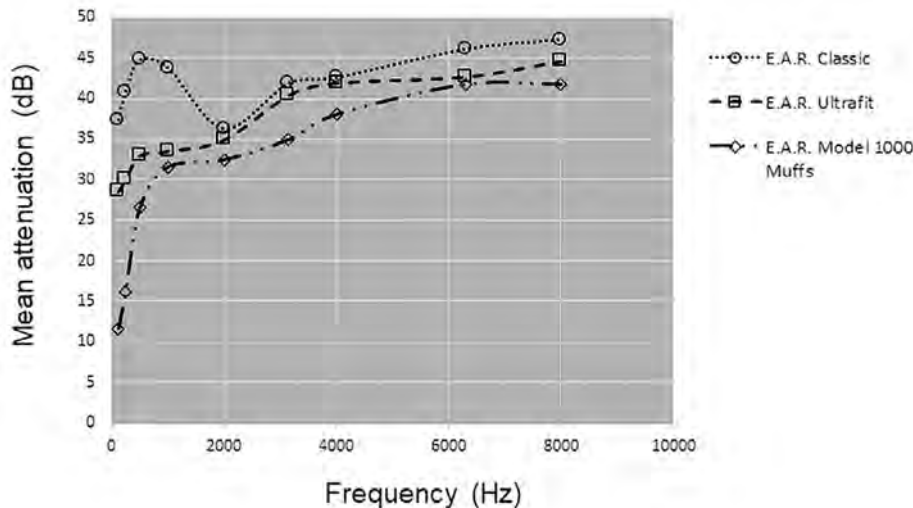
(B) Permanent Threshold Shifts (PTS)

If the noise exposure at intense levels is prolonged, or repeated in close time intervals, threshold shifts can be permanent. The threshold for permanent hearing damage is approximately 140-dB for short impulsive noise and around 85-dB for chronic exposure. Commercial MR systems that are designed to be compliant with IEC standards are not able to generate noise in excess of 140-dB (89). De Wilde, et al. (9) reported one case of excessive acoustic noise that occurred in the United Kingdom. The patient reported severe headaches, dizziness, and ear pain following the MRI examination. Importantly, this patient was not provided hearing protection because the manager of the MRI site was confident that the noise levels generated by the 0.5-T MR system were not at a level of concern.

ACOUSTIC NOISE CONTROL TECHNIQUES

Controlling acoustic noise is generally accomplished in one of three simple ways: control of noise at the receiver (e.g., using earplugs, or anti-noise interference), control along the path of the noise, or control of the noise at the source (e.g., redesigned gradients, or

Figure 8. Noise attenuation for several commercial earplugs and ear defenders. Note the significant variability in attenuation at low frequencies. Reproduced by permission, the 3M™ Company. E.A.R. Classic™ and E.A.R. Ultrafit™ are trademarks of the 3M™ Company.



pulse sequences). Once acoustic energy has been generated in the air, it can be difficult to control, so the control of noise at the source is considered to be the preferred method.

Passive Hearing Protection

The simplest, most convenient, and least expensive means of preventing problems associated with acoustic noise during MRI procedures is to use disposable earplugs and/or headphones. Earplugs, when properly fitted can abate noise by 10- to 30-dB (depending on the frequency), which is usually an adequate amount of sound attenuation for the MRI environment. **Figure 8** shows examples of the octave band spectra of some commercially available earplugs and other hearing protection devices, demonstrating typical noise attenuation values. The use of earmuffs, headphones, or disposable earplugs has been shown to provide a sufficient decrease in acoustic noise that, in turn, would be capable of preventing the potential temporary hearing loss associated with MRI procedures (1).

The level and frequency range of noise attenuation will vary with the type and design of hearing protection that is utilized. If data is unavailable for the noise abatement device, the protector should be tested. Since the designs of hearing protectors do vary, care should be taken when offering these to patients. Additionally, proper fitting instructions must be provided. A patient who may be confused, young, or have difficulty in correctly fitting the hearing protection may need additional assistance to prevent poorly fitting the device and having compromised noise attenuation. If using earmuffs or headphones, these should be

176 Acoustic Noise Associated With MRI Procedures

regularly assessed for wear to the seals and replaced, as needed. Current guidelines suggest staff members should have training in the selection and fitting of hearing protection (86).

Unfortunately, earplugs, earmuffs, and headphones suffer from a number of problems. These devices tend to hamper verbal communication with the patient during the operation of the MR system. In certain circumstances, these devices can also create discomfort or impair immobilization of the patient's head, which is problematic when optimal immobilization is required for certain studies that are particularly sensitive to patient movement (e.g., diffusion and phase-sensitive studies).

Standard foam-based earplugs are often too large for the ear canal of infants. Some small sizes are available from certain MRI accessory companies, although snug fit is essential if acoustic noise is to be efficiently attenuated. Neonates present a particular challenge when trying to use conventional earplugs or other similar devices. Nordell, et al. (111) reported on a patient-independent device constructed from absorbent padding, which can be placed over the neonate during the MRI examination. Reductions in peak noise levels of 16- to 22-dBA averaged over the hearing spectrum of 4- to 13-dBA were reported. Specially-designed small earplugs or earmuffs (e.g. MiniMuffs Neonatal Noise Attenuators, Natus Newborn Care, www.newborncare.natus.com) can be used in these cases.

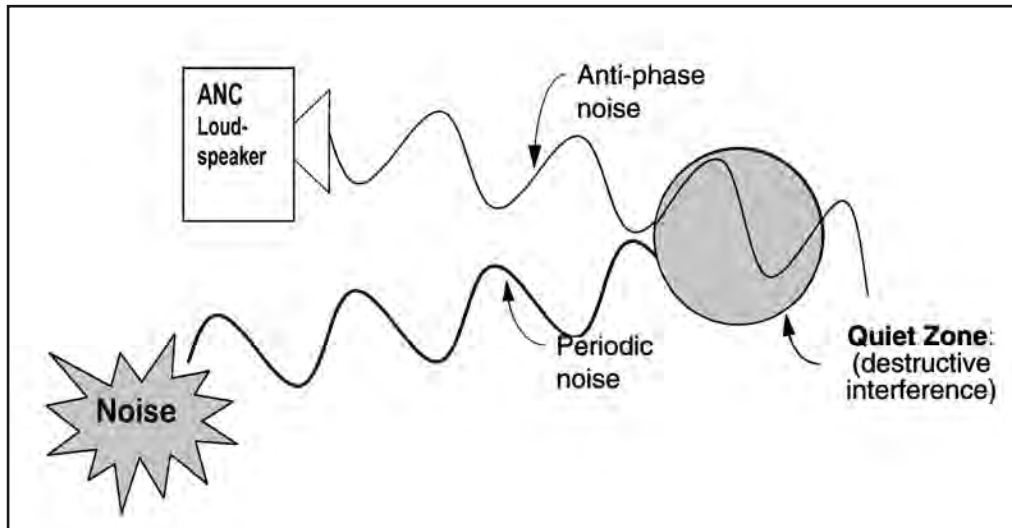
Passive devices used for hearing protection may attenuate noise non-uniformly over the hearing range. While high frequency sound may be well attenuated, attenuation can be poor at low frequency. This is unfortunate because the low frequency range is also where the peak in MRI-related acoustic noise is often generated, however, this may be balanced by the lower hearing sensitivity also in this frequency range (**Figure 2**).

Passive protection devices will also offer poor attenuation of noise transmitted to the patient through bone conduction (112). The effect of vibration being conducted during MRI and affecting noise has been reported by Glover, et al. (95). The presence of an insulating foam mattress on the patient couch has been found to reduce vibrational coupling to the patient and noise levels by around 10-dB. This underlying bone conduction transmission path puts a practical attenuation limit for passive protection at around 40-dB (113). As previously indicated, Ravicz and Melcher (24) studied the potential for isolating the body from the MR system using a helmet to minimize acoustic noise transmission via bone conduction. They used passive hearing protection in combination with the helmet system. Adding protection, they reported a total noise attenuation of 55- to 63-dB, by using a combination of earplugs (25- to 28-dB alone), ear defenders (i.e., headphones) (39- to 41-dB alone), and an isolating helmet. While the use of a helmet may suit research studies with volunteer subjects, it may not be clinically acceptable for use in patients. However, in general, earplugs and ear defenders can also be used effectively, offering added hearing protection for patients undergoing MRI examinations.

Methods Using Anti-Phase Noise: Active Noise Control

A significant reduction in the level of acoustic noise caused by MRI procedures has been accomplished by implementing the use of a noise cancellation, or "anti-phase" noise technique (41, 114, 115). Unlike many other noise control solutions that result in compromised performance of the MRI examination or hardware, this technique should have no im-

Figure 9. Principle of sound attenuation using anti-phase noise to create a zone of quiet. This diagram shows a noise (periodic) source and synthesized anti-phase noise interfering destructively in a specific region to produce a zone of quiet.



pact on the performance of the MR system. The principle is simply to generate noise, which will interfere destructively with the scanner noise incident at the patient's ear.

The loudspeaker producing this anti-phase noise can be built into the scanner bore or built into a pair of headphones for the patient (thus, harnessing passive protection as well). A major disadvantage of this technique is that, if it performs poorly at certain frequencies or in some spatial regions, noise levels may be enhanced rather than attenuated by the superposition of the additional anti-noise.

Controlling acoustic noise from a particular source by introducing anti-phase noise to interfere destructively with the noise source is by no means a new idea (116, 117) (Figure 9). For use in the MRI environment, conventional active-noise control (ANC) systems require some modification. Notably, loudspeakers and microphones designed to be utilized in the MRI setting must be used to acquire scanner noise and to transmit control anti-noise and, secondly, the ANC controller must be optimized and synchronized to the scanner.

The initial results for the use of anti-noise applied to MRI achieved only modest noise attenuation. Goldman, et al. (41) acquired MR system noise with a microphone, performed a Fourier transform (FT) of the noise, and generated control noise by inverting the phase of the major components of the FT, and then transmitted this anti-noise through a loudspeaker built into a set of headphones (i.e., a combination active-passive system), achieving an average noise reduction of around 14-dB. The performance of this system was not much better than that of some standard passive headphones, alone, in the low frequency region of the hearing range. The control sound was delivered using long tubes, introducing a time delay, which limited control efficiency.

178 Acoustic Noise Associated With MRI Procedures

Advances in digital signal processing (DSP) technology permit efficient modern ANC systems to be realized at a modest cost (118). The essence of an anti-noise system involves either a continuous feed-forward or feedback loop with continuous sampling of the sounds in the noise environment so that the gradient magnetic field-induced noise is attenuated. Thus, it is possible to attenuate the pseudo-periodic MR system-related noise while allowing the transmission of vocal communication or music to be maintained. The feedback loop uses a sampling microphone placed close to the ear, where noise reduction is required. It will attempt to attenuate all noise propagating into the ear. A feed-forward algorithm uses a sampling microphone close to the problematic noise source, offering a potentially more selective cancellation of noise source. Frequently, time limitations in anti-noise getting from the loudspeaker to the subject as well as stability requirements set a practical upper frequency limit for ANC systems. This problem of poorer high frequency attenuation performance is mitigated by building the systems into complementary passive ear defenders, resulting in a better broad frequency noise reduction.

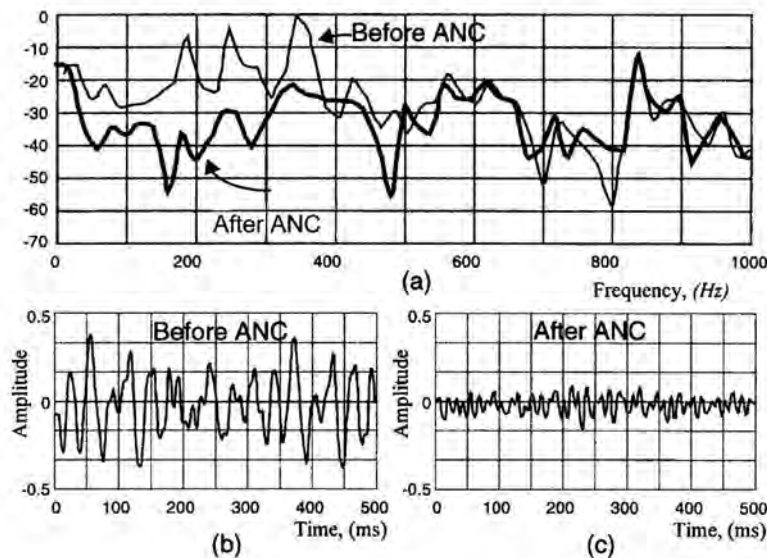
Similar to Goldman, et al. (41), commercial manufacturers have offered ANC systems based on delivering anti-noise to patient headphones (42), however, the long tubing imposes a time delay in getting noise to the ear, limiting the performance of such a system. In 1995, Pla, et al. (119) reported improved results using a system based on an x-filtered least mean squares (LMS) algorithm, driving piezoelectric speakers near the patient's ears. These researchers achieved noise attenuation up to 25-dB for frequencies below 1.2-kHz and for the first few harmonics only. In 1997, McJury, et al. (114) reported on the performance of a multichannel filtered U-least mean squares algorithm for acoustic noise control. Acoustic noise was recorded digitally from a series of typical clinical MRI protocols performed on a 1.0-T Siemens Impact. This noise was then replayed through a bench-top adaptive real-time DSP ANC system (Motorola DSP 56001). A typical peak sound attenuation of approximately 30-dB was achieved over the frequency range from 0- to 700-Hz (**Figure 10**).

In 1999, Chen, et al. (115) published results using an ANC system based on a modified feedback method with a second order cascaded neural network architecture, with loudspeaker mounted in a headset. For acoustic noise up to 3-kHz, they achieved an average attenuation of 19-dB. This study was also based on recorded scanner noise attenuated with a lab-based ANC system.

More recently, Chambers, et al. (120) demonstrated improved results over a wide frequency range using an ANC system that was based on an LMS feed-forward algorithm and built into a set of ear defenders (i.e., headphones). From 600-Hz to 4-kHz, peak attenuation of around 40-dB was measured for scanner noise. Importantly, the use of feed-forward methodology allows cancellation of scanner noise with less attenuation of any noise stimuli introduced during the use of fMRI protocols. However, this system did not acquire its reference noise in real-time, but required a recording phase to obtain reference data.

To date, some of the most successful solutions for acoustic noise reductions were the results from Li, et al. (121) and Lee, et al. (122). Li, et al. (121) reported results with a patented, ANC system based on a feed-forward, x-LMS algorithm that uses multiple reference signals. The ANC system was built into a headset to also benefit from the passive attenuation of noise at higher frequencies. Impressive acoustic noise reductions of up to 55-dB

Figure 10. Results of noise cancellation for a typical clinical spin echo pulse sequence. Noise level spectra before (dotted line) and after cancellation (solid line) are shown for time and frequency domain spectra. A major disadvantage of this technique is that, if performed below optimal efficiency, at certain frequencies or in some spatial regions, noise levels may be enhanced rather than attenuated by the superposition of the additional anti-noise control (ANC) (114). Reproduced by permission, Elsevier, Philadelphia, PA.



at a harmonic frequency were achieved, with an average of 21-dB (30-dBA) over the entire spectrum. As for passive noise control, bone conduction remains a residual issue, limiting noise control. Lee, et al. (122) achieved improved results on a 3-T MR system for standard spin echo and gradient echo pulse sequences. They reported approximately 35-dB attenuation over the frequency range 80- to 160-Hz.

Active Vibration Control (AVC)

Aeronautical engineers, amongst others, have an interest in noise reduction inside cylindrical shells. In their case, the cylindrical models represent airplane cabins. Results from their studies show that a significant amount of low frequency noise is associated with shell vibration (123, 124), which is directly applicable to an MR system with a similar cylindrical geometry. Their methods of using active vibration control are also transferrable, however, until more recently (40, 125), they received little attention from the MRI community. These methods aim for global control of the entire gradient loudspeaker, not just the noise impacting on the ear canal, and would also control noise from bone conduction.

Qiu and Tani, (126) devised an AVC system for use with a typical MRI-clamped, cylindrical gradient coil, which is based on distributed piezoelectric actuators. These attempt to suppress a limited set of vibrational modes of the gradient coil over a set frequency range. Their system, similarly to other aeronautical models, tries to reduce mainly low frequency

180 Acoustic Noise Associated With MRI Procedures

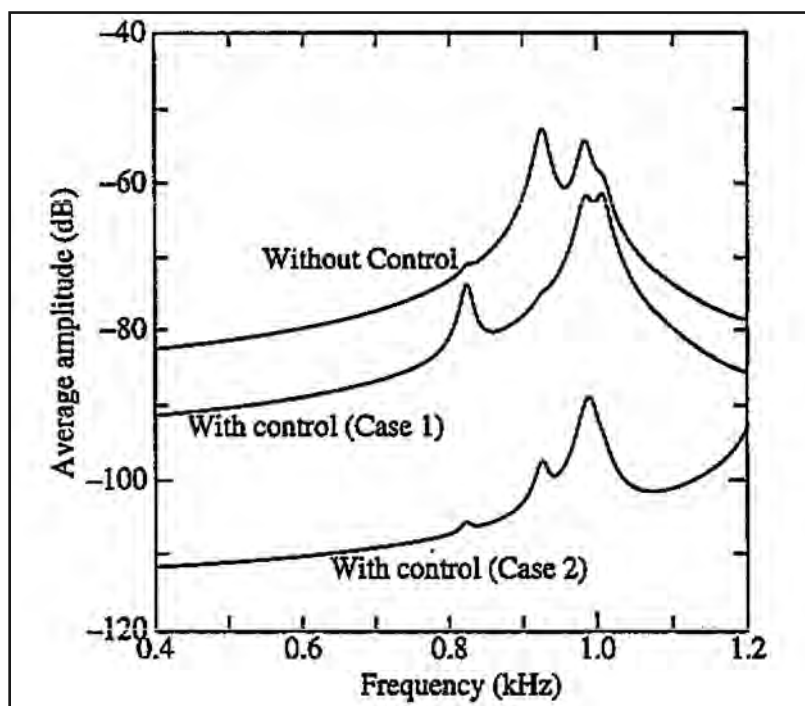
(<1.2-kHz) noise, where passive hearing protection performs poorly. They achieved an average reduction in vibrational amplitudes of 20-dB with an optimized system (**Figure 11**). Roozen, et al. (40) also designed an AVC system based on seismic mass piezoelectric actuators. However, for a gradient coil driven by FE-EPI, their system comprising only four actuators achieved a more modest averaged vibrational amplitude reduction of 3-dB over the frequency range 0.5- to 1.5-kHz. Recently, Oeisi and Nestorovic (127) reported on methods for vibration suppression based on a combination of uncertainty modelling and robust controller design.

Optimizing MRI Pulse Sequences

Using a software-based approach to minimize acoustic noise may be the least expensive and most easily implemented technique that could be applied to current scanners. However, it may also be the least efficient because, simplistically, it involves individually optimizing each pulse sequence that is to be used on a given patient. Considering the fact that most clinical MR systems offer literally hundreds of scanning sequences, this would seem an unattractive approach.

Since concerns about acoustic noise levels tend to be restricted to a subset of sequences and applications that require high levels of gradient activity (those used for fMRI, diffusion-weighted MR, fast gradient echo, ultrafast MR, etc.), there is a good argument to avoid compromising the entire system with hardware changes that might negatively impact gradient performance when only very specific sequences are problematic. Importantly, this ap-

Figure 11. Reduction in vibrational amplitudes with active vibration control (AVC). Results are shown for no control, case 1 (non-optimized control), and case 2 (optimized control)(126). Reproduced by permission, Institute of Physics Publishing.



proach has been highly successful with some solutions creating sequences that are almost “silent”.

(A) Basic Reductions in Gradient Activity to Reduce Acoustic Noise

Minimizing Conventional Gradient Levels

Because the dominant effect of acoustic noise levels is associated with the signal details of a particular MRI protocol rather than the structure of the MR system (47), it follows that it should be possible to reduce the noise level by optimizing the choice of pulse sequence parameters. Simply using a spin echo (SE) sequence rather than a gradient echo (GE) pulse sequence and running the sequence with reduced gradient parameters (i.e., rise-time and amplitude) can significantly reduce the levels of acoustic noise. Skare, et al. (128) designed so-called “quiet” sequences in this way and defined a simple “quietness factor” (*QF*) as,

$$QF = \frac{RT_m}{RT_s} \quad (3)$$

where the RT_m is the rise-time of the modified sequence and RT_s , the original/default rise-time. On a 1.5-T MR system, a *QF* of six resulted in a noise attenuation of 20-dB. This procedure, however, lengthens the echo time (TE), reduces the number of acquisition slices, and results in a longer examination time.

(B) Minimizing the Number of Gradient Echoes

A reduction of acoustic noise levels may also be achieved by reducing the level of gradient pulsing in a pulse sequence (129, 130). A rapid, single-shot, multi-slice imaging technique (i.e., STEAM-Burst) is based on stimulated-echoes without the rapid gradient switching necessary in other single-shot techniques such as echo planar (130). The STEAM-Burst sequence uses a combination of the “Burst” technique (131), involving the application of multiple RF pulses under a constant gradient and subsequent refocusing of the resultant set of echoes, and the STEAM-stimulated echo acquisition mode (132). Limited data on acoustic noise measurements shows peak noise attenuation of 15-dB compared with a similar EPI sequence (130).

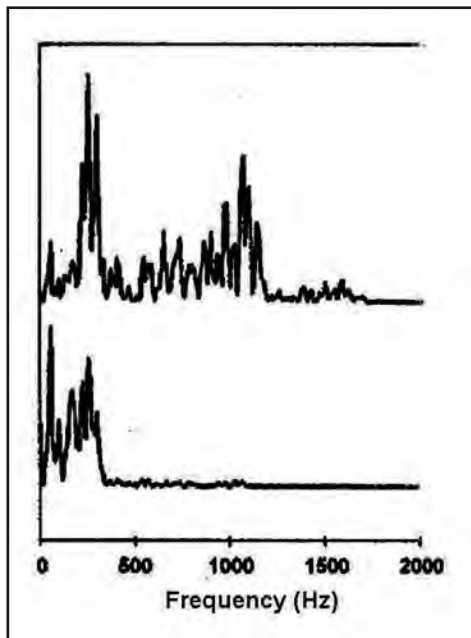
This pulse sequence offers the potential for rapid acquisition of MR images, but it is sensitive to artifacts due to static magnetic field inhomogeneities while generating reduced levels of acoustic noise. The sequence suffers from two main problems. First, the signal-to-noise ratio (SNR) is low compared with other rapid imaging techniques. Second, the images acquired at 3-T have an SNR of approximately of 20:1. Thus, these pulse sequences remain more suited to specific research applications than routine use in the clinical MRI setting.

(C) Re-Shaping and Re-Sampling

An obvious optimization of the pulse sequence is to “smooth” or “soften” gradient waveforms to lower activity and acoustic noise. This is one of the most popular techniques

182 Acoustic Noise Associated With MRI Procedures

Figure 12. The efficiency of soft gradient pulses. Magnitude spectra are shown (with an arbitrary linear scale) for the sound generated by the readout gradient of a FLASH (i.e., fast gradient echo) pulse sequence. Data was acquired with a linear ramp, 0.5-msec duration (top plot) and sinusoidal ramp duration 4-msec (lower plot). With the sinusoidal ramping, high frequency acoustic components above 500-Hz are severely attenuated (133). Reproduced by permission, Wiley - John Wiley and Son Publishers, NY.



used in modern reduced acoustic noise sequence optimization and was first suggested by Hennel, (133). Notably, this technique may be applied to minimize the acoustic noise generated by a range of conventional MRI pulse sequences. As mentioned above, it has been shown that the acoustic response of the gradient system to current pulses is linear (47). Thus, the sound generated by a gradient waveform can be derived from a product of the FT of the source input and the frequency response function (FRF) of the gradient system (see Equation 2). If gradient pulses are designed such that their current waveforms contain no frequencies for which the amplitude of the FRF is high, then resultant acoustic noise levels should be minimized (133). The FRF of the gradient system in a 3-T MR system was measured and a very low response noted at low frequencies (below 200-Hz). Frequency components below this threshold should be attenuated in the acoustic spectrum of any pulse sequences.

In minimizing high frequency components in the gradient pulses, it is possible to avoid or reduce sharp transitions, such as step functions in the waveform, and to replace these with more slowly varying sinusoidal transitions. This may be accomplished by following three simple rules:

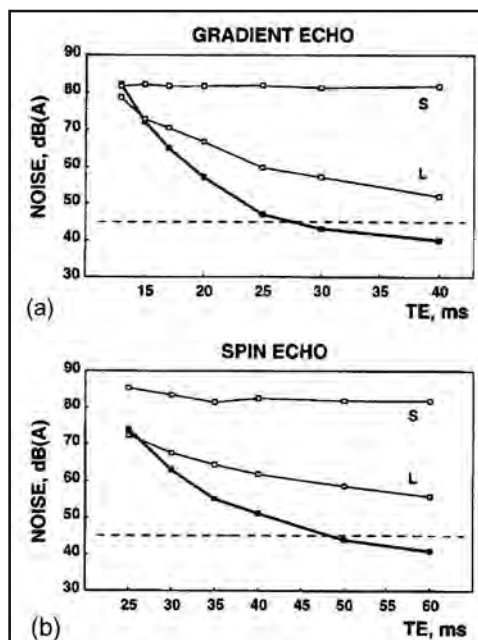
- (1) Use sinusoidal ramping rather than trapezoidal ramping.
- (2) Maximize ramp duration (keeps cut-off frequency low for efficient band limiting).

- (3) Minimize the number of ramps (merge consecutive gradients on the same channel).

The use and efficiency of soft pulses are shown in **Figure 12**. With the sinusoidal ramping, high frequency acoustic components above 500-Hz are severely attenuated. Acoustic noise levels, averaged over 1-second, were measured for spin echo and gradient echo sequences as a function of echo time (**Figure 13**). Good quality MR images may be acquired with sound levels dropping as echo time (TE) increases. At echo times of 30- to 50-msec, good quality images are still possible and acoustic noise levels are below the ambient room noise (i.e., with the air-conditioning running, room sound levels approach 45-dBA). Three main limitations were identified with the initial implementation of this technique, as follows: 1) there was an increased sensitivity of the pulse sequences to vascular flow, 2) the high-speed MRI pulse sequences tended to be unsuitable for clinical applications, and 3) increased voltages by factor of two were needed to produce sinusoidal ramps instead of linear ramps.

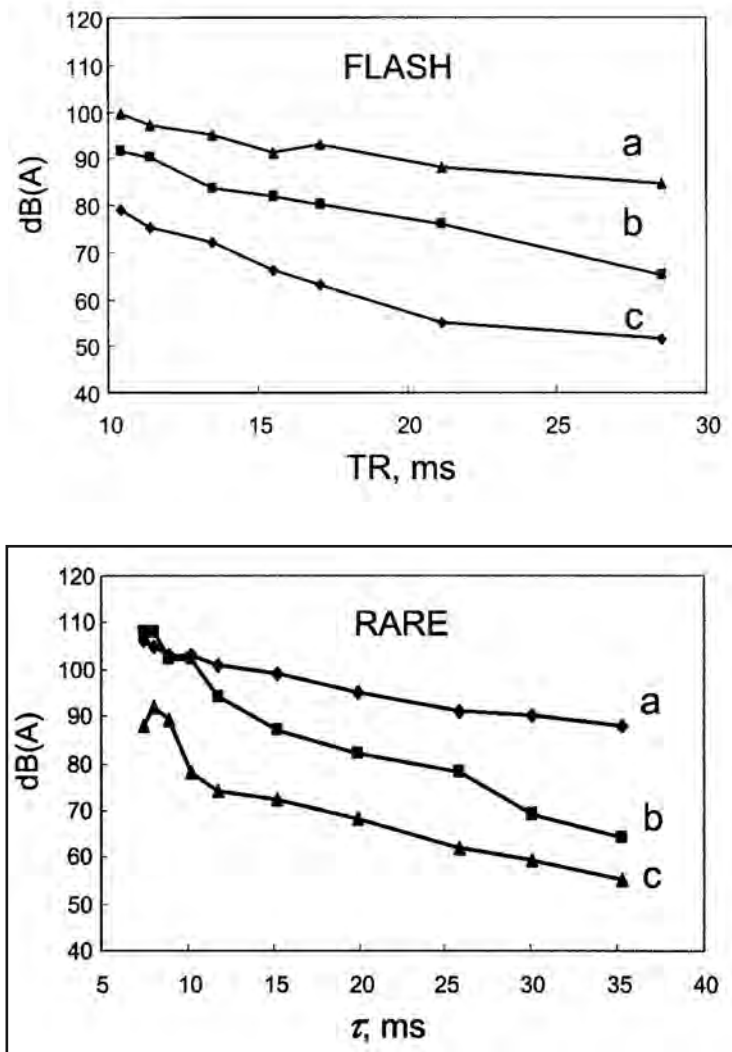
The pulse sequence strategy was extended to fast imaging sequences (FLASH and RARE) in 2001 (134). Noise reductions of 20- to 40-dBA were reported compared to standard sequences (**Figure 14**). However, acquisition time remained at around one second per slice, which is unsuitable for an fMRI examination. Loenneker, et al. (135) also extended the technique, by integrating into a T_2^* pulse sequence, and improving the volume coverage

Figure 13. Acoustic noise levels for gradient-echo (a) and spin-echo (b) pulse sequences measured as a function of echo time (TE, milliseconds) at 3-T. The top lines in the graphs correspond to sequences using soft (S) gradient pulses. The middle lines in the graphs show sequences with linear (L) ramps of maximum duration. The bottom lines in the graphs show standard sequence default settings. The dashed line is the level of ambient room noise from the air-conditioning system (133). Reproduced by permission, Wiley - John Wiley and Son Publishers, NY.



184 Acoustic Noise Associated With MRI Procedures

Figure 14. Optimized use of soft gradient pulses for two fast imaging sequences: (Top) FLASH sequence, (Bottom) RARE sequence. In each case, three types of gradient waveform are compared: (a) hard trapezoidal, (b) older style soft waveforms designed according to (133), and (c) new soft waveforms designed according to (134). Reproduced by permission, Wiley - John Wiley and Son Publishers, NY.



by using simultaneous multi-slice excitation with SIMEX (i.e., a modern statistical technique that estimates bias by tracking measurement error as a function of added noise) pulses. This enabled the technique to be applied to fMRI. Oesterle, et al. (136) also reported on an improved technique utilizing “soft” gradient pulses. In this case, the limitation due to long acquisition times was minimized using interleaved spiral gradient, read-out trajectories. Using

this pulse sequence with optimized sampling scheme on a 2-T MR system, an average noise reduction of 22-dBA was achieved. The use of sinusoidal gradient waveforms continues to be common (137 - 139).

An algorithmic approach to sequence optimization involving gradient reshaping has been reported by Heismann, et al. (140). Here, gradient waveforms are smoothed (spline interpolation) and optimized, with the algorithm adapting some sections of the pulse sequence, and leaving others unchanged. This can be successfully applied to conventional imaging sequences (141).

Rather than re-shaping the waveform, a further method is to revise the sampling of k-space. Spiral scanning was used successfully to substantially reduce acoustic noise (136). Initially, this was used to counteract the long acquisition times resulting from increased (and lower) gradient durations to reduce acoustic noise. Later, this method has been incorporated into highly successful “silent” ultrashort TE methods, and techniques for diffusion-weighted MRI (see below).

(D) Using Parallel Imaging

Similar to the slew rate reduction associated with a soft gradient pulse technique, De Zwart, et al. (142) used SENSE parallel imaging techniques to obtain significant reductions in gradient slew rates and achieved reductions in acoustic noise. The use of sensitivity encoding in combination with multi-channel detector arrays allows reduced gradient switching through reduced k-space sampling. Using another type of MRI sequence (i.e., SENSE), a gradient slew rate reduction was achieved at constant image acquisition time and image spatial resolution. For two-fold SENSE under sampling, the gradient amplitude was reduced to 50% (13-mT/m), and ramp time doubled (360-microseconds), resulting in a slew rate of 37-T/m/sec (a 4-fold reduction in the maximum slew rate). SPL reductions for two scanners were reported: 14-dBA (1.5-T) and 12-dB (3-T).

Moelker, et al. (143) reported an interesting variant of this approach. This group built a manual controller to reduce gradient slew rates and the associated acoustic noise for use during interventional MRI, where acoustic noise may be particularly unpleasant for staff members, while small degradations to image quality can be tolerated. Their controller allowed a 16-fold reduction in slew rate, with acoustic noise reduced by up to 21-dBA.

In several more recent optimized sequences, parallel imaging forms a part of the optimization, especially in challenging areas such as fast imaging and diffusion-weighted MR imaging (139, 144).

(E) Minimizing the MR System Acoustic Response Function

For each separate gradient (x-, y-, and z-gradient), Tomasi, et al. (145) compared the current waveforms and resulting vibrational response. This group demonstrated, that by altering the read-out frequency of the EPI gradient (and, hence, the bandwidth) to avoid known vibrational resonances, significant reductions in acoustic noise could be achieved. Altering the read-out frequency from 720-Hz to 920-Hz resulted in a noise reduction of 12-dB.

186 Acoustic Noise Associated With MRI Procedures

A similar approach was reported by Schmitter, et al. in 2008 (138). These researchers devised the so-called “sEPI” technique, which is a low noise EPI pulse sequence for use with fMRI. This sequence produces a narrow acoustic frequency spectrum by using a sinusoidal read-out gradient waveform with smooth ramps and constant phase encode gradient. By varying the switching frequency of the read-out gradient, this narrow band can be shifted in frequency to match the minima of the scanner frequency response function, avoiding major resonance modes and minimizing acoustic noise. These researchers reported that the average SPL of the standard EPI, 82.5-dBA, was reduced to 61.7-dBA. This sequence did not include optimization of the slice selection gradient, and so this work was extended in 2010 with the introduction of noise-optimized “VERSE” pulses, and a parallel imaging approach.(139). Zapp, et al. (139) further expanded sEPI with the use of parallel imaging. Segbers, et al. (146) and Ott, et al. (147) have also used a combination of methodologies, including frequency-shifting, to avoid acoustic noise resonance modes.

(F) Ultrashort and Zero TE methods

In recent years, imaging tissues with very short T2 (for example cortical bone or lung) has been improved by the emergence of ultrashort TE (UTE) or zero TE sequences (ZTE) (148, 149). UTE sequences offer effective TE reductions of 10-200 times that offered by more conventional sequences. In ZTE sequences, the readout gradient starts simultaneously with signal excitation (ramping up prior to the excitation pulse), producing an effective TE of zero. Measurement times are short, but acquisition is inherently three dimensional.

Both these techniques generally involve (non-Cartesian) radial imaging of k-space. TRs are also very short, so there is no need to switch off gradients between excitations, and this lowering of gradient activity results in almost silent sequences. ZTE methods require high-bandwidth excitation, so the specific absorption ratio (SAR) can become an issue, particularly at high field. The wide bandwidth excitation can be achieved either using short hard RF pulses, or by sweeping the frequency of an arbitrary length pulse, the so-called SWIFT technique (150, 151).

These methods are highly successful in reducing acoustic noise, producing almost silent MR sequences, with sequence noise at the level of ambient levels. Hence, they have generated significant commercial interest, and form the basis of solutions implemented by GE and Siemens.

GE were early implementers of UTE methods, basing their Silenz™ product on the RUFIS sequence (152). A prototype Silenz implementation on a 3-T scanner and running neuro sequences, produced acoustic noise levels which were similar to room ambient noise (68.8-dB) (153). Ohlmann-Knauf, et al. (154) reported on a comparison of the image quality of Silenz T₁-w and T₂-w scans versus non-Silenz versions at 3-T for neuro patients. The Silenz scan quality compared well, with the main drawback being the significantly longer scan times for the T₁-w sequences. Others reported on UTE variants for quiet MR, for fast imaging applications (155, 156).

Due to the acquisition of signal from free induction decays (FIDs) rather echoes, UTE/ZTE methods are less sensitive to motion. The long readout time can also cause image blurring. Holdsworth, et al. (157) compared Silenz-based and conventional MR angiography

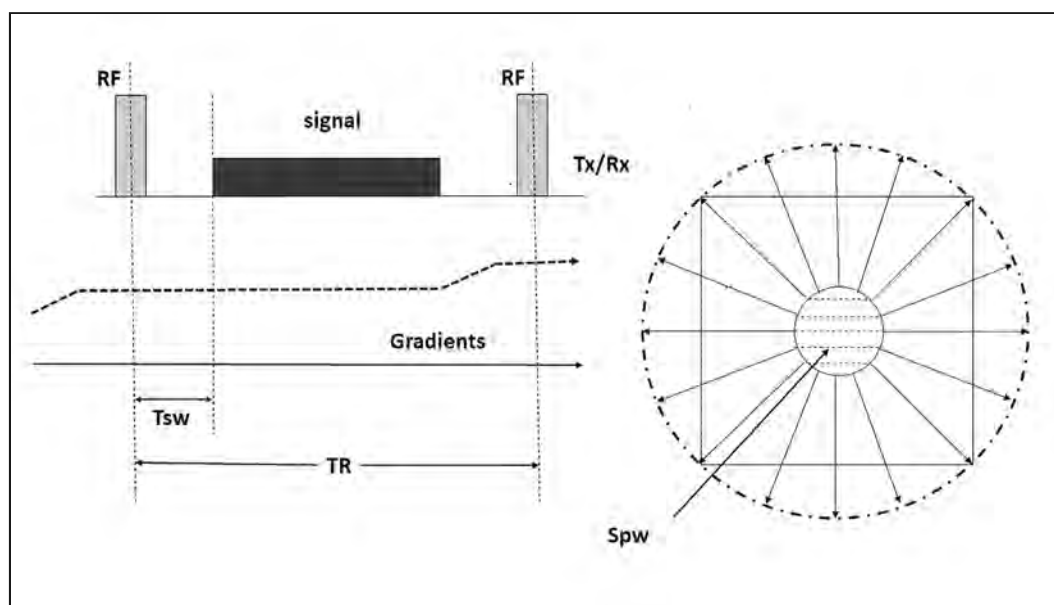
(MRA) sequences. Silenz-based sequences scored poorly, with only 40% being rated as diagnostic quality.

A further variant of these methods, is pointwise encoding time reduction with radial acquisition (PETRA) (**Figure 15**)⁽¹⁵⁸⁾. This forms the basis of sequences in the Quiet Suite™ product from Siemens. Reports have assessed silent PETRA sequences for neurological (159) and pediatric applications (160).

(G) Using Gradient Cancellation Pulses

Some researchers proposed a technique involving additional “follow-up” gradient pulses, to cancel the initial pulses that would generate unwanted acoustic noise. This is effectively a type of an anti-noise approach, using anti-phase gradients instead of anti-phase acoustic noise (161, 162). There is, in effect, a change to the gradient input function, such that initial impulsive forces generated by the gradients are cancelled by subsequent counter impulsive forces, minimizing the potential for the generation of acoustic noise. These ideas can be seen as an extension of the initial observations of the acoustic noise characteristics of trapezoidal gradient pulses as reported by Wu, et al. (163). Shou, et al. (162) demonstrated that follow-on trapezoidal gradient pulses can cancel two frequencies and their harmonics. The initial studies from this group showed that a significant noise reduction was possible (around 13-dB) when cancelling at least three of the dominant acoustic noise spectral peaks.

Figure 15. Left: Pulse sequence diagram for one repetition of the radial part of the PETRA sequence. Gradients are held constant during almost an entire repetition time (TR) period and altered only slightly at the end of each repetition without being ramped down. This very low gradient activity leads to minimal acoustic noise. Tsw is the time required to switch from transmission mode to receive mode. Right: During Tsw, a spherical volume of data, Spw is missed, and that data is collected separately, point-wise. Redrawn from Ida, et al. (159).



188 Acoustic Noise Associated With MRI Procedures

Segbers, et al. (146) took a hybrid approach to optimizing the gradient pulse sequence, based on using soft gradient pulses, cancellation pulses, and frequency shifting to avoid resonance modes. These researchers ran versions of EPI and turbo spin echo sequences with optimized gradient pulse sequences on a 3-T MR system. The gradient coil had a maximum gradient strength of 21-mT/m and slew rate of 200-mT/m/ms. Using a combination of single and double follow-on trapezoidal gradient pulses, Segbers, et al. (146) managed to suppress several of the main acoustic noise spectral frequencies and achieved a maximum noise reduction of 12-dB.

(H) Application-Specific Methods

1) fMRI Methods. As mentioned above, MRI-related acoustic noise can interfere with the presentation and processing of functional stimuli and generate blood oxygen level dependent (BOLD)-related contrast in the auditory cortex. Passive hearing protection may not offer sufficiently quiet conditions for psychological studies of hearing (164). Unfortunately, residual noise can often be loud enough to mask the perception of experimental sound stimuli (11). Due the inherent requirement for ultrafast image acquisition, quiet MRI sequences employing shallow gradient ramps or soft gradient pulses frequently cannot easily be applied to fMRI without compromising data quality. Marcar, et al. (165) modified a fMRI acquisition using soft gradient pulses (133) at 2-T. In achieving a silent sequence, the time penalty results in a 24 sec acquisition time for a set of 4 slices. Rather than using the approach of Hennel, et al. (133), using sinusoidal readout gradient switching and continuous phase gradients is popular and effective (139, 166). It is common to manage these issues using different types of sequence-related solutions: (1) sparse imaging (167-169) and (2) using event-related strategies (170).

i) Modified Block Designs for fMRI. These sequences (also called clustered volume acquisition, flat car design, sparse, and behavior interleaved gradients), involve using a TR that is longer than the acquisition time, allowing time for interleaving short (1- to 4-seconds) silent gaps within fMRI sequences. In the brain, the peak hemodynamic response to noise occurs after a time delay of around 5-seconds following stimulation. Knowing this, it is possible to present stimuli in these silent gaps where the scanner is silent and then to acquire the subsequent images when the peak response will occur. This cycle is then repeated for the entire block. The duration of the gap is dependent on the number of slices acquired and the repetition time (TR) used. Therefore, care is needed to avoid extending the sequence length, which can have penalties in terms of patient motion and image quality. An underlying assumption is also made with simple modified block designs, that any BOLD response to scanner noise during acquisition will apply equally when stimulus is on and when it is off. Optimization of the block design involves two additional criteria. If the silent gap is extended to 9- to 10-seconds, enough time will have elapsed to allow any hemodynamic response produced by the previous acquisition to return to baseline. Sampling of any BOLD signal relating to acoustic noise from the previous acquisition will then be minimized. Lastly, keeping the acquisition time under 2-seconds will prevent measurement of any hemodynamic response (HR) from the current acquisition.

Interleaved silent steady-state imaging (ISSS) (171) is a popular variation of sparse imaging. This sequence uses continuous excitation pulses (which maintain a steady state longitudinal magnetization) and variable readout gradients. Like sparse imaging, stimuli are presented in the quiet gaps, but longer data acquisition is used for multiple volumes, improving the sequence temporal resolution. As the data sampling rate is not consistent, it can be challenging to analyze ISSS data. Andoh, et al. (172) reported encouraging results with a comparison of a resting-state version of ISSS and conventional resting-state fMRI (rs-fMRI).

ii) Event-Related Designs for fMRI. This method involves sampling the peak of the stimulus HR, followed by a waiting period to avoid acquisition during scanner noise HR. When scanner HR has dissipated, baseline sampling then occurs. The speed of data collection directly determines study data quality and the repetition time should be kept to a minimum. This type of sequence typically allows one measurement every 20-seconds (173).

Peele, et al. (166) reported on a comparison of four differing fMRI acquisitions: (1) **STD** - standard EPI, and versions based on (2) **Sparse** – sparse-based sequence, (3) **Quiet** - sinusoidal readout and continuous phase gradients (137). Aside from gradient changes, the Quiet sequence also differs from STD in having a longer TE and narrower bandwidth. To separate out these confounding issues, an additional sequence was also generated, 4) **Matched** - which is a version of (1) with the bandwidth matching (3). They noted the Quiet sequence had the highest SNR (27% greater, $p < 0.001$), which was balanced by a reduction BOLD sensitivity.

2) Ultrafast and Diffusion MRI Methods. Some applications, including fMRI, and diffusion MR (dMRI), inherently require high levels of gradient activity. EPI variants are usually the sequence of choice to acquire images quickly, with high gradient slew rates. Due to their inherent demand for high levels of gradient activity, many of the above approaches (e.g. gradient smoothing) work much less well for these applications. Originally, hardware-based solutions were often used with EPI (174).

As mentioned above, early work includes Schmitter, et al. (138) who replaced trapezoidal gradient waveforms with sinusoidal readout and a constant phase encode gradient. They further avoided acoustic resonance modes, by varying the frequency of the readout gradient. Zapp, et al. (139) successfully combined sinusoidal gradients with parallel imaging for fMRI. As mentioned above, Tomasi, et al. (145) achieved 12-dB noise reduction by increasing the readout gradient frequency to avoid acoustic resonance modes.

Hutter, et al. (175) more recently investigated methods of acoustic noise reduction for diffusion applications. They also extended the basic sinusoidal read and constant phase gradients, to include multiband acceleration (176), and the effect of CAIPRINHA shift gradient blips (177), and optimization of diffusion gradient crushers. Tested on adults and fetal subjects at 3-T, they succeeded in maintaining diffusion MR image quality whilst reducing acoustic noise by 12-dB.

190 Acoustic Noise Associated With MRI Procedures

Liebig, et al. (178) also recently reported on similar EPI-modified solutions. They have modified k-space sampling, including acceleration with parallel imaging via reconstructing with Cartesian (179) and non-Cartesian (180) methods. Rather than reporting acoustic noise levels, they report on modest gains in efficiency for some sequences.

Ott, et al. (147) used a conventional approach for dMRI, comprising lower gradient levels, reduced slew rates, and frequency adjustment to avoid acoustic noise resonance modes. They implemented solutions on 1.5-T and 3-T scanners, achieving noise reductions of up to 20-dBA.

Methods Involving Hardware Design and Optimization

Arguably the best, if not the most technically challenging, solution to minimize acoustic noise is to eliminate the noise at the source by designing a “quiet” gradient coil which generates no acoustic noise or vibration. Acoustic noise and vibration arises due to physical buckling and resonance of the gradient coil (and former), as well as coupling to other structures. Noise control may be achieved by special designs taking into consideration the construction and materials of the gradient coil formers, coupling with other structures, use of noise insulation materials, and finally the design of the coil windings themselves. This however, represents (for existing scanners) probably the most inconvenient and expensive solution. This section discusses each of these aspects in more detail.

(A) Passive Insulation, Materials, and Structure

Stiffness and Damping. As suggested above, greater gradient coil stiffness should reduce mechanical vibration and associated noise. Stiffness is dependent on material properties and geometrical factors. Altering gradient coil dimensions or materials to increase Young’s modulus will help reduce acoustic noise due to vibration. Lin, et al. (181) reported on the use of a variety of reinforcements to increase the gradient coil stiffness, reduce vibration, and the associated acoustic noise. These investigators found that increasing the stiffness of the gradient coil former reduced the amplitude of the forced vibration response of the gradient coil at low frequencies and the noise generated by the coil. In addition, the gradient coil demonstrated a reduced number of resonance modes in the low and medium frequency ranges, in turn, reducing the chance of the system being excited into resonance and generating high levels of acoustic noise.

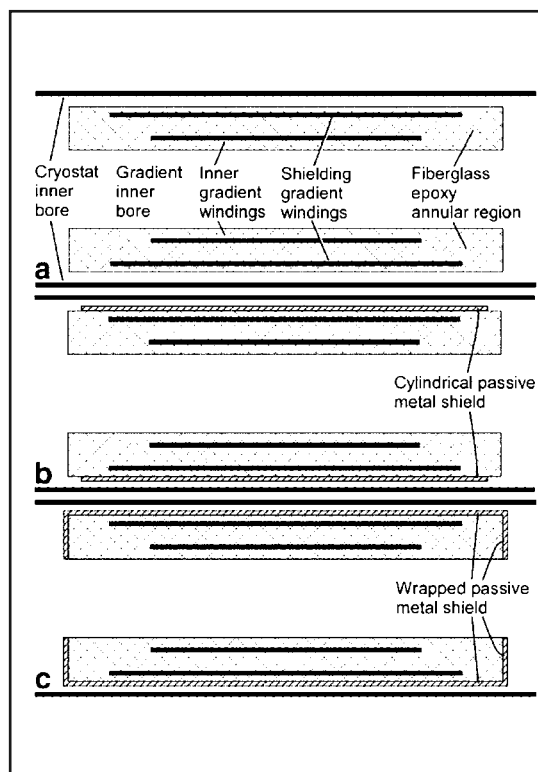
Damping the gradient coil may also attenuate the mechanical vibration. This can be achieved by using particular materials for construction or by mounting the coil in such a way that an acoustic absorber surrounds it. Damping is most efficient at or near resonance and, unfortunately, will reduce the overall stiffness of the coil structure. Several commercial manufacturers use damping techniques for their gradient coil systems (46, 51). A reduction of around 3-dBA due to the use of acoustically damped commercial gradient systems have been reported (46). Mechemske, et al. (182) reported improved results by mounting an acoustic liner inside the bore of a 4-Tesla research scanner, with damping material applied to the back. The bore of this MR system was also fitted with an “endcap”. Running an EPI sequence, acoustic attenuation of around 20-dB was possible, however the scanner did not

have a body RF coil, *in situ*, at the time of the experiments, and the liner may be difficult to use in a commercial scanner.

In 2005, Shao, et al. (70) reported on the development of an analytic model that predicted the acoustic noise generated by an MRI gradient coil with finite acoustic impedance, which was based on initial work by Kuijpers, et al. (75). This group modeled the use of an absorptive liner inside the gradient coils and tested predictions with measurements made in a 4-Tesla MR system. They found that an acoustic noise reduction of the order of 10-dB at the low frequency end of the spectrum was possible, but the practicality of using thick materials in limited space is doubtful.

Isolation/Evacuation/Enclosure. Some groups tried to isolate the gradient coil to prevent the transmission of vibrations to other structures (183-5). As acoustic waves can only travel in a medium, mounting or encasing the gradient coil in a vacuum should avoid transmission of any generated noise (183-186). Edelstein, et al. (185) controlled acoustic noise by using a combination of evacuating the gradient coil structure and using a magnet with a non-conducting inner cryostat bore. They achieved total reduction in acoustic noise of around 20-dB (peak). Their results showed that eddy currents caused by gradient shielding leakage can generate significant Lorentz forces on the inner cryostat bore. These forces contribute a significant level of the total scanner acoustic noise. Edelstein, et al. (185) reported that is

Figure 16. Examples of design configurations for active-passive gradient shielding systems (187). Reproduced by permission, Wiley - John Wiley and Son Publishers, NY.



192 Acoustic Noise Associated With MRI Procedures

it important to provide electromagnetic isolation. In 2005, based on finite element modeling, they redesigned standard active gradient shielding to include an additional passive copper layer (187). This added passive shield prevented power deposition in the warm bore, which resulted in an efficient hybrid active-passive shielding system. **Figure 16** shows examples of typical configurations for such a strategy. The modeled power reductions associated with the system predicted a reduction in acoustic noise of approximately 25-dB.

Tkach, et al. (108) reported on the acoustic noise levels generated by a purpose-designed neonatal 1.5-T MR system. One of the design features was a cantilevered patient couch. The couch effectively suspends the patient inside the scanner bore, isolating or decoupling the patient from vibration from the gradient coils and bore panels. For a range of 6 clinical sequences, they recorded noise levels of 77.3- to 88.0-dB, representing an average reduction of 11-dB for this system compared to typical adult scanners running similar clinical sequences.

Katsunuma, et al. (183), evacuated the area surrounding the gradient coil system so that insulation would prevent propagation of sound and a separate mount (i.e., floor mounting the gradient coil former) that prevented transmission of vibration from other structures. Acoustic noise reduction levels of around 30-dB (peak) were possible, but this is an expensive solution and not suited for retrofit. “Enclosure” is a traditional technique used in noise control, which involves enclosing the noise source in an airtight skin, damping the source side of the enclosure, and decoupling the enclosure from the source (51).

Perforating a noise-generating surface has been found to significantly reduce the levels of acoustic noise generated (188). Systems involving the use of micro-perforated panels (MPPs), first suggested by Maa (189), are typically used with an air-filled backing cavity and rigid back wall. These methods can also be difficult to implement efficiently in MR systems due to additional space requirements. More recently, Li and Mecheske (190) investigated the implementation of an MPP system for use in MRI. Their basic expansion modeling showed that the MPP systems can be particularly efficient at low frequencies. However, optimized parameters also allow good efficiency over a wider band. As with poorly designed ANC systems, noise levels have been found to increase with poorly designed perforation systems (190).

Insulation has also been successful in increasing noise attenuation when applied to transmit RF coils. For example Ireland, et al. (191) reported on the results of additional insulation built into a head RF coil (18-cm inner diameter) for neonatal imaging. The insulation achieved an average additional attenuation of 9-dBA across a range of six different clinical imaging sequences at 1.5-T, resulting in noise levels of approximately 82-dBA, that were then further attenuated with passive hearing protection.

(B) Design of Gradient Coil Windings: Force-Balanced Coils (Active Acoustic Shielding)

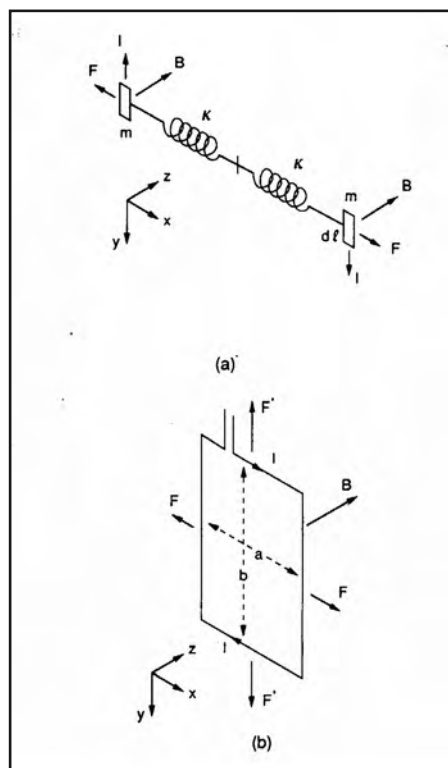
In theory, it is possible to design gradient coil windings such that all Lorentz forces generated by current pulsing are balanced (i.e., each force is effectively cancelled by one of equal magnitude at a conjugate position relative to the coil center) (37, 192-195). This is, in essence, similar to using anti-phase noise to cancel a noise source. For example, ac-

tively-shielded gradient coils are intrinsically force-balanced to a degree. They are designed to have a secondary coil operate in opposition to the main primary to minimize Lorentz forces on the primary. The combination of coil design and a consideration of construction methods and materials are essential for efficient results.

Rather than trying to mount a vibrating gradient coil to a heavy and immovable former or somehow damp the coil, if the coil is considered as a harmonic oscillator and coupled to another, back-to-back, and if masses and spring constants are equal, the center of mass of the system will be constant without the need for a heavy mount (192, 193). This is the principle of active force balancing which may be applied to gradient coil design (**Figure 17**).

All solids have visco-elastic properties and this will result in residual movement of the conductors, limiting the ideal noise cancellation suggested above. These movements will result in compression waves propagating through the material with velocity,

Figure 17. (a) Diagram representing two coupled line elements of conductor, dl , of equal mass, m , carrying equal and opposite currents. The center of mass of the system remains fixed if the spring constants, K , are equal. The system is placed in a magnetic field \mathbf{B} , which gives rise to the forces, F , causing displacements. (b) Rectangular conductor loop carrying a current, I , placed in a magnetic field \mathbf{B} , such that the loop plane is normal \mathbf{B} . All forces F and F' are balanced, provided the plane of the coil is oriented perpendicular to the magnetic field direction. If these coils are coupled to similar others via non-compressive struts, then all forces in the system are balanced. If non-compressive materials are used, the conductors cannot move and no sound is generated (192). Reproduced by permission, Institute of Physics Publishing.



194 Acoustic Noise Associated With MRI Procedures

$$v = \left(\frac{E}{\rho} \right)^{\frac{1}{2}} \quad (4)$$

Where, E , is Young's modulus and ρ is the density of the material. Knowing that wave velocity and frequency are related by $v = f\lambda$, a slow wave velocity will result in low frequency, above which progressive phase effects will be expected which will interfere with noise cancellation.

For optimal acoustic noise cancellation, strut material should have a large value for E and small value for ρ , resulting in a high compressional wave velocity. Thus, a light coupling structure of high strength may perform as well as a heavier structure. Composite materials have been tested and found to perform well with a frequency response up to 20-kHz (single loop coil of dimensions 30-cm x 20-cm) (125). Using a bench-top prototype 2-coil system (a square coil design measuring 40-cm along each size, powered by a 10-A sinusoidal current), the reported noise attenuation, when powered in balanced mode, was approximately 40-dB at 100-Hz, dropping to 0-dB at 3.5-Hz (**Figure 18**). The results of attenuation levels agree reasonably well with a theoretical prediction (curve D) (192).

Designs have also been extended and tailored to include the capability of current balancing, acoustic screening and magnetic field screening in one coil (195). A head gradient coil has been designed analytically using co-axial return paths to minimize localized Lorentz forces and acoustic noise. When performing EPI (3-mm slice thickness, gradient switching frequency 830-Hz, current 207-A) in a 3-T MR system, noise levels of 102-dB (root mean square) have been reported (192).

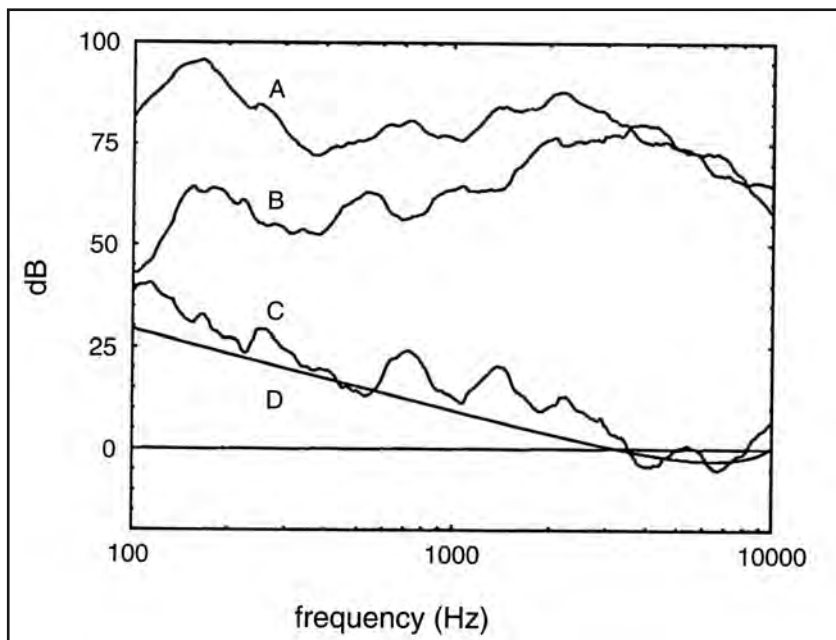
The implications for gradient coil characteristics of the acoustic screening design mean a loss of gradient strength and an increase in coil inductance, thus, reducing high-speed performance. Estimates of the increase in inductance for a three-cylinder coil system (i.e., fully force shielded as well as acoustically and magnetically shielded) over a gradient coil with only active magnetic shielding is a factor of approximately eight.

To counteract this in keeping performance constant, an increase in driver current of the square root of 8 is required that will, in turn, increase the acoustic noise output of the coil. Throughout the data on sound generation in relatively simple gradient structures (37), the highest sound pressure levels were noted to come from spurious resonances, thought to be due to bending and buckling of the coil structures (Chladni resonances). Designing coil systems that completely cancel acoustic noise including contributions from these sources is a considerable challenge.

(C) Other Gradient Design Methods

Researchers have devised an analytical approach to the design of quiet gradient coils (196-198). This work, which is a form of target field approach, uses an inverse method for designing winding paths, explicitly accounting for finite coil length. It treats the Biot-Savart law as a first kind integral equation for the current density on the gradient coil, once the magnetic field has been specified, and uses Tikhonov regularization to handle the inherent

Figure 18. A plot showing SPL and attenuation A dB versus f for a test coil. Curve **A** corresponds to the radiated sound received when one coil only is powered. Curve **B** is the reduced level when two coils are powered in balanced mode. Curve **C** is the resultant sound attenuation (the difference between **A** and **B**) and curve **D** is the theoretical prediction. The results of attenuation levels agree reasonably well with a theoretical prediction (curve **D**)(192). Reproduced by permission, Institute of Physics Publishing.



non-unique aspect of the design problem. Researchers using this approach achieved very modest acoustic attenuation levels.

Reduced acoustic noise levels have been reported for asymmetric gradient coils (199-200). To address the impact of claustrophobia associated with standard cylindrical scanner geometry, one solution is to move the imaging isocenter towards one end of the scanner (201). This involves asymmetric magnet design, and associated changes to hardware such as the gradient coils (202, 203). Wang, et al. (199) implemented an asymmetric gradient coil, and found improvements in efficiency, lower inductance and resistance. They also reported lower levels of acoustic noise, however they don't report absolute noise levels or comparisons to similar conventional systems.

The development of MRI-guided linear accelerator (MRI-LINAC) technology has driven a variety of changes, one of which is gradient coils with split designs (199). Split designs allow for asymmetric acoustic design solutions and there have been several studies in this area assessing the benefits of designs incorporating asymmetric acoustic tunnels, as well as liners (204-207). Studies also include the optimization of the structure of the scanner bore exit, to act as an acoustic horn and potentially redirect acoustic noise away from the patient (208-210). Nan, et al. (211) report on a split gradient design methodology using these ideas, intended for the design of MRI-LINAC system gradient coils that have a central

196 Acoustic Noise Associated With MRI Procedures

gap region where the patients will be accommodated. In the gap region, using FE analysis, their asymmetric designs incorporating bore-end optimization, resulted in acoustic noise attenuation levels of up to 7.4-dB.

OTHER SOURCES OF MR SYSTEM-RELATED ACOUSTIC NOISE

Auditory Perception of Radiofrequency (RF) Electromagnetic Fields

When the human head is subjected to pulsed RF radiation at certain frequencies, an audible sound perceived as a click or knocking noise may be heard (212-214). This acoustic phenomenon is referred to as “RF hearing”, “RF sound” or “microwave hearing”. Thermo-elastic expansion is believed to be the mechanism responsible for the production of RF hearing, whereby there is absorption of RF energy that produces a minute temperature elevation (i.e., approximately 1×10^{-6} °C) over a brief time period (i.e., approximately 10-microseconds) in the tissue of the head (212-214). Subsequently, a pressure wave is induced that is sensed by the hair cells of the cochlea via bone conduction. In this manner, the pulse of RF energy is transferred into an acoustic wave within the human head and sensed by the hearing organs.

The sounds that occur with RF hearing appear to originate from within or near the back of the human head, regardless of the orientation of the head in the RF field. The actual type of noise that is heard varies with the RF pulse width and repetition rate. The relative loudness is dependent on the total energy per pulse. RF energy-related acoustic noise has been observed at frequencies ranging from 216 to 7500-MHz (212-214).

RF hearing is mathematically predictable from classical physics and has been studied and characterized in laboratory animals and human subjects. Individuals involved with the use of microwaves in industrial and military settings commonly experience RF hearing. With specific reference to the operation of MR systems, RF hearing has been found to be associated with frequencies ranging from 2.4- to 170-MHz (212).

The gradient magnetic field-induced acoustic noise that occurs during MRI procedures is significantly louder than the sounds associated with RF hearing. Therefore, noises produced by the RF auditory phenomenon are effectively masked and not perceived by patients or MR system operators (212). Furthermore, there is no evidence of any detrimental health effects related to the presence of RF hearing. However, Roschmann, et al. (212) recommends an upper level limit of 30-kW applied peak pulse power of RF energy for head coils and 6-kW for surface coils used during MR imaging or spectroscopy to avoid RF-evoked sound pressure levels in the head increasing above the discomfort threshold of 110-dB.

Noise from Subsidiary Systems

Room air conditioners, fans for patient comfort, and cryogen reclamation systems associated with superconducting magnets are the main sources of ambient acoustic noise found in the MRI environment. Cryogen reclamation systems are devices that are effectively used to minimize the loss of cryogens and function on a continuous basis, producing sounds that are considerably less than those associated with the activation of the gradient magnetic fields during MRI procedures. Therefore, this acoustic noise may, at the very most, be a

mild annoyance to patients or MR system operators in the MRI environment. Some authors reported ambient room noise levels to be 60- to 70-dB (52, 146).

SUMMARY AND CONCLUSIONS

MRI procedures can generate significant levels of acoustic noise under certain conditions (41, 54). This noise can be an annoyance, hinder communication with staff members and, at high levels, presents a potential safety hazard to patients that must be managed and controlled.

Many groups have measured and analyzed the acoustic noise associated with MRI. Acoustic noise levels increase with changes in imaging parameters including a decrease in section thickness, field-of-view, gradient ramp time, and an increase in the gradient amplitude. The environment, hardware design, and the presence of the patient in the MR system will also affect noise levels.

Although many options are available for noise control, the use of simple passive protection in the form of earplugs is generally sufficient to decrease noise to levels within permissible limits for the great majority of patients. However, care must be taken to ensure passive protection is properly fitted and in good condition (1). Noise measurements or data for the scanner should also be acquired and checked in association with the attenuation of the passive protection to ensure resultant noise levels at the ear will be within safe limits.

Current documents regarding permissible limits vary, but a general consensus appears to set a permissible average noise level at the patient's ear of 85-dBA (80, 88, 96). Noise levels outside the MR system's bore are lower and present reduced risks for an MRI healthcare worker present during the MRI examination.

Of course, passive methods have limitations and more elegant and effective solutions are possible. These methods range from optimizing the MRI pulse sequences in terms of minimizing gradient activity, to the utilization of active noise control and active vibration control systems, or entirely redesigning the gradient coils.

As with many aspects of MRI, the specifications for achieving high noise attenuation often run counter to fast acquisition of high quality diagnostic images and compromises must be made. Optimizing procedures to lengthen gradient ramp times, lower amplitudes, or minimize pulsing can result in sequences with reduced performance (133-135). Designing gradient coils that are force-balanced to minimize acoustic resonances will compromise performance in terms of increasing inductance and loss of gradient strength (37, 192-195).

A solution that presents a minimal impact on the performance of the MR system is active noise control using anti-noise (114-122). This is a promising technique but an optimal system has yet to be fully implemented on clinical scanners.

Over the last decade, the most effective solutions reported, are those involving sequence optimization. UTE-type sequences which incorporate spiral k-space trajectory acquisition, and very low gradient activity produce almost silent MR scanning (148-160). Gradient fil-

198 Acoustic Noise Associated With MRI Procedures

tering or re-shaping has also been proven to be very effective. It is no coincidence that two commercial solutions (SilenzTM, and Quiet SuiteTM) are based on these approaches.

These solutions (UTE methods in particular) have not been applied to every MR sequence, and are not suited to certain applications, such as ultrafast MR. However, given the comparative low cost and ease of install for these acoustic noise solutions, coupled with their efficiency, it seems likely that ongoing research in these directions will prove fruitful and silent MR sequences will multiply on clinical scanners over time.

Current trends in MRI include increasing static magnetic field strengths and improved gradient performance for rapid clinical imaging applications. The need for ultrafast sequences for fMRI and other advanced techniques continues. These developments will result in increases in MRI-generated acoustic noise levels. This will mean a continuing interest and evolution in acoustic noise control methods that warrant continued investigation, development, and commercial implementation of these techniques.

REFERENCES

1. Brummett RE, Talbot JM, Charuhas P. Potential hearing loss resulting from MR imaging. *Radiology* 1988;169:539-540.
2. Quirk ME, Letendre AJ, Ciottone RA, Lingley JF. Anxiety in patients undergoing MR imaging. *Radiology* 1989;170:463-466.
3. Laurell G. The combined effect of noise and cisplatin. *Ann Otol Rhinol Laryngol* 1992;100:969-976.
4. Philbin MK, Taber KH, Hayman LA. Preliminary report: Changes in vital signs of term newborns during MR. *Am J Neurorad* 1996;17:1033-1036.
5. Kanal E, Shellock FG, Talagala L. Safety considerations in MR imaging. *Radiology* 1990;176:593-606.
6. Shellock FG, Kanal E. Policies, guidelines, and recommendations for MR imaging safety and patient management. *J Magn Reson Imaging* 1991;1:97-101.
7. Shellock FG, Litwer CA, Kanal E. Magnetic resonance imaging: Bioeffects, safety, and patient management. *Magn Reson Q* 1992;4:21-63.
8. Kanal E, Shellock FG, Sonnenblick D. MRI clinical site safety survey: Phase I results and preliminary data. *Magn Reson Imaging* 1988;7:106.
9. De Wilde JP, Grainger D, Price DL, Renaud C. Magnetic resonance imaging safety issues including an analysis of recorded incidents within the UK. *Prog Nucl Magn Reson Spectr* 2007;51:37-48.
10. Zhang N, Zhu XH, Chen W. Influence of gradient acoustic noise on fMRI response in the human visual cortex. *Magn Reson Med* 2005;54:258-283.
11. Shah NJ, Jancke L, Grosse-Rukken ML, Muller-Gartner HW. Influence of acoustic masking noise in fMRI of the auditory cortex during phonetic discrimination. *J Magn Reson Imaging* 1999;9:19-25.
12. Ravicz ME, Melcher JR, Kiang NY. Acoustic noise during functional magnetic resonance imaging. *J Acoust Soc Am* 2001;108:1683-1696.
13. Hall DA, Haggard MP, et al. Functional magnetic resonance imaging measurements of sound-level encoding in the absence of background scanner noise. *Acoust Soc Am* 2000;109:1559-1570.
14. Moelker A, Pattynama MT. Acoustic noise concerns in functional magnetic resonance imaging. *Human Brain Mapping* 2003;20:123-141.
15. Strainer JC, Ulmer JL, et al. Functional MR of the primary auditory cortex: An analysis of pure tone activation and tone discrimination. *Am J Neuroradiol* 1997;18:601-610.

MRI Bioeffects, Safety, and Patient Management 199

16. Ulmer JL, Biswal BB, et al. Acoustic echo-planar scanner noise and pure tone hearing thresholds: The effects of sequence repetition times and acoustic noise rates. *J Comp Assist Tomog* 1998;22:480-486.
17. Bess FH, Humes LE. *Audiology: The Fundamentals*. 4th Edition. Baltimore: Williams and Wilkins;1995.
18. Department of Health. *Acoustics: design considerations*, HTM 2045. London: HMSO;1996.
19. Hetu R, Laroche C, Quoc HT, LePage B, St Vincent J. The Spectrum of Impulse Noise and the Human Ear Response. In: Dancer AL, Henderson D, Salvi RJ, Hamernik RP, Editors. *Noise-Induced Hearing Loss*. St. Louis: Mosby Press;1992. pp. 361.
20. Alberti P. Noise and the Ear. In: Stephens D, Editor. *Adult Audiology*. UK: Butterworths;1987.
21. Mills JH. Effects of Noise on Auditory Sensitivity, Psychophysical Tuning Curves and Suppression. In: Hamernik RP, Henderson D, Salvi R, Editors. *New Perspectives on Noise Induced Hearing Loss*. New York: Raven Press;1982.
22. Prasher D. Estimation of Hearing Damage From Noise Exposure. Report From the Technical Meeting on Exposure-Response Relationships of Noise on Health, Bonn, Germany. Geneva: World Health Organization; 2003. pp. 82-97.
23. Khanna SM, Tonndorf J, Queller J. Mechanical parameters of hearing by bone conduction. *J Acoust Soc Am* 1976;60:139-154.
24. Ravicz ME, Melcher JR. Isolating the auditory system from acoustic noise during fMRI: noise conduction through the ear canal, head and body. *J Acoust Soc Am* 2001;1:216-231.
25. Pujol R, Lavigne-Rebillard M, Uziel A. Physiological correlates of development of the human cochlea. *Semin Perinatol* 1990;14:275-280.
26. Shepper PG, Shahidullah BS. Development of fetal hearing. *Arch Dis Child* 1994;71:81-87.
27. Richards DS, Frenzen B, Gerhardt KJ, McCann ME, Abrams RM. Sound levels in the human uterus. *Obster Gynecol* 1992;80:186-190.
28. Shepper PG, Shahidullah BS. Noise and the fetus: A critical review of the literature. Sudbury: HSE Books;1994.
29. Gerhardt KJ, Abrams RM. Fetal hearing: characterization of the stimulus and response *Semin Perinatol* 1996;20:11-20.
30. Gerhardt KJ, Abrams RM. Fetal exposures to sound and vibroacoustic stimulation. *J Perinatol* 2000;20:S21-S30.
31. Lecanuet JP, Gautheron B, et al. What sounds reach fetuses: Biological and non-biological modeling of the transmission of pure tones. *Dev Psychobiol* 1998;33:203-219.
32. Philbin MK, Taber KH, Hayman LA. Preliminary report: Changes in vital signs of term newborns during MR. *Am J Neuroradiol* 1996;17:1033-1036.
33. Lasky R, Williams A. The development of the auditory system from conception to term. *Neo Reviews* 2005;6:141-152.
34. Graven SN, Browne JV. Auditory development in the fetus and infant. *Newborn Infant Nurs Rev* 2008;8:187-193.
35. Graven SN. Early neurosensory visual development of the fetus and newborn. *Clin Perinatol* 2004; 31:199-216.
36. Graven SN, Browne JV. Sensory development in the fetus, neonate, and infant. *Newborn Infant Nurs Rev* 2008;8:169-172.
37. Mansfield P, Glover PM, Beaumont J. Sound generation in gradient coil structures for MRI. *Magn Reson Ned* 1998;39:539-550.
38. Moelker A, Wielopolski PA, Pattynama PMT. Relationship between magnetic field strength and magnetic resonance-related acoustic noise. *Magn Reson Mater Phys Biol* 2003;16:52-55.
39. Price DL, De Wilde JP, Papadaki AM, Curran JS, Kitney RI. Investigation of acoustic noise on 15 MRI scanners from 0.2 to 3 T. *J Magn Reson Imaging* 2001;13:288-293.

200 Acoustic Noise Associated With MRI Procedures

40. Roozen NB, Koevoets AH, den Hamer AJ. Active vibration control of gradient coils to reduce acoustic noise of MRI systems. *IEEE Trans Mechatronics* 2008;13:325-334.
41. Goldman AM, Gossman WE, Friedlander PC. Reduction of sound levels with antinoise in MR imaging. *Radiology* 1989;173:549-550.
42. Hurwitz R, Lane SR, Bell RA, Brant-Zawadzki MN. Acoustic analysis of gradient-coil noise in MR imaging. *Radiology* 1989;173:545-48.
43. Shellock FG, Morisoli SM, Ziarati M. Measurement of acoustic noise during MR imaging: Evaluation of six “worst-case” pulse sequences. *Radiology* 1994;191:91-93.
44. McJury M, Blug A, Joerger C, Condon B, Wyper D. Acoustic noise levels during magnetic resonance imaging scanning at 1.5 T. *Brit J Radiol* 1994;64:413-5.
45. McJury MJ. Acoustic noise levels generated during high field MR imaging. *Clin Radiol* 1995;50:331-333.
46. Counter SA, Olfsson A, Grahn HF, Borg E. MRI acoustic noise: Sound pressure and frequency analysis. *J Magn Reson Imaging* 1997;7:606-611.
47. Hedeen RA, Edelstein WA. Characteristics and prediction of gradient acoustic noise in MR imagers. *Magn Reson Med* 1997;37:7-10.
48. Cho ZH, Park SH, Kim JH, et al. Analysis of acoustic noise in MRI. *Magn Reson Imaging* 1997;15:815-822.
49. Shellock FG, Ziarati M, Atkinson D, Chen DY. Determination of gradient magnetic field-induced acoustic noise associated with the use of echo planar and three-dimensional fast spin echo techniques. *J Magn Reson Imaging* 1998;8:1154-7.
50. Miyati T, Banno T, Fujita H, et al. Acoustic noise analysis in echo planar imaging: multi-center trial and comparison with other pulse sequences. *IEEE Trans Med Imaging* 1999;18:773-6.
51. Sellers MB, Pavlids JD, Carlberger T. MRI acoustic noise. *Int J Neuroradiol* 1996;2:549.
52. Ravicz ME, Melcher JR, Kiang NYS. Acoustic noise during functional MRI. *J Acoust Soc Am* 2000;108:1683-96.
53. More SR, Lim TC, Li M, Holland CK, Boyce SE, Lee JH. Acoustic noise characteristics of a 4T MRI scanner. *J Magn Reson Imaging* 2006;23:388-397.
54. Foster JR, Hall DA, Summerfield AQ, Palmer AR, Bowtell RW. Sound level measurements and calculations of safe noise dosage during EPI at 3 T. *J Magn Reson Imaging* 2000;12:157-163.
55. Schmitter S. Entwicklung von geräuscharmen Bildgebungstechniken für die funktionelle Magnetresonanztomographie. Doctoral thesis. 2008.
56. Budinger TF, Bird MD. MRI and MRS of the human brain at magnetic fields of 14 T to 20 T: Technical feasibility, safety, and neuroscience horizons. *NeuroImage* 2018;168:509–531.
57. Winkler SA, Schmitt F, Landes H, et al. Gradient and shim technologies for ultra high field MRI. *NeuroImage* 2018;168:59–70.
58. Winkler SA, Alejski A, Wade T, McKenzie C, Rutt, BK. Lorentz damping and the field dependence of gradient coil vibroacoustics. *Proceedings of the International Society of Magnetic Resonance in Medicine*. 2015;1020.
59. Capstick M, McRobbie D, Hand J, et al. An investigation into occupational exposure to electromagnetic fields for personnel working with and around medical magnetic resonance imaging equipment. 2008. Project Report VT/2007/017. <https://itis.swiss/news-events/news/publications/2008/an-investigation-into-occupational-exposure-to-electromagnetic-fields-for-personnel-working-with-and-around-medical-magnetic-resonance-imaging-equipment/> Accessed March, 2020.
60. Schmitter S, Mueller M, Semmler W, Bock M. Maximum sound pressure levels at 7 Tesla—What's all this fuss about? *Proceedings of the International Society of Magnetic Resonance in Medicine*. 2014;3029.
61. van Osch MJP, Webb AG. Safety of ultra-high-field MRI: What are the specific risks? *Curr Radiol Rep* 2014;2:1-8.

MRI Bioeffects, Safety, and Patient Management 201

62. Costagli M, Symms MR, Angeli L, et al. Assessment of Silent T₁-weighted head imaging at 7 T. *Eur Radiol* 2016;26:1879–1888.
63. Hoff MN, McKinney IV A, Shellock FG, et al. Safety considerations of 7-T MRI in Clinical Practice. *Radiology* 2019;00:1–10.
64. Speck O, Stadler J, Zaitsev M. High resolution single-shot EPI at 7T. *Magn Reson Mater Phys* 2008;21:73–86.
65. Rizzo-Sierra CV, Verslius MJ, Hoogduin JM, Duifhuis H. Acoustic fMRI noise: Linear time-invariant system model. *IEEE Trans Biomed Eng* 2008;55:2115–2123.
66. Hamaguchi T, Miyati T, Ohno N, et al. Acoustic noise transfer function in clinical MRI: A multicenter analysis. *Acad Radiol* 2011;18:101–106.
67. Mechefske CK, Wu Y, Rutt BK. Characterization of acoustic noise and magnetic field fluctuations in a 4 T whole-body MRI scanner. *Mech Systems and Sign Proceedings* 2002;16:459–473.
68. Yao GZ, Mechefske CK, Rutt BK. Characterization of vibration and acoustic noise in a gradient coil insert. *MAGMA* 2004;17:12–27.
69. Yao GZ, Mechefske CK, Rutt BK. Acoustic noise simulation and measurement of a gradient insert in a 4T MRI. *Appl Acoust* 2005;66:957–973.
70. Shao W, Mechefske CK. Acoustic analysis of a gradient coil winding in an MRI scanner. *Concepts in Magn Reson Part B* 2004;24B:15–27.
71. Wang F, Mechefske CK. Modal analysis and testing of a thin-walled gradient coil cylinder model. *Concepts in Magn Reson Part B* 2004;27B:34–50.
72. Mechefske CK, Wang F. Theoretical, numerical, and experimental modal analysis of a single-winding gradient coil insert cylinder. *Magn Reson Mater Phys Biol* 2006;19:152–166.
73. Wang F, Mechefske CK. Modal analysis of a multilayered gradient coil insert in a 4T MRI scanner. *Concepts in Magn Reson Part B* 2007;31B:237–254.
74. Wang FL. Dynamic modeling of gradient coils in an MRI scanner. Queen's University, Kingston, Ontario, Canada. Doctoral Thesis. 2006.
75. Kuijpers AHW, Rienstra SW, Verbeek G, Verheeij JW. The acoustic radiation of baffled finite ducts with vibrating walls. *J Sound and Vibr* 1998;216:461–493.
76. Sodell W. *Vibrations of Shells and Plates*. 3rd Edition. New York: Dekker; 2004.
77. Li G, Mechefske CK. Structural-acoustic modal analysis of cylindrical shells: application to MRI scanner systems. *Magn Reson Mater Phys Biol* 2009;22:353–364.
78. Findell IH. Fundamentals of Human Response to Sound. In: Fahy FJ Walker JG, Editors. *Fundamentals of Noise and Vibration*. London: 1998. pp.145.
79. Anari M, Axelsson A, Eliasson A, Magnusson L. Hypersensitivity to sound- questionnaire data, audimetry, and classification. *Scand Audiol* 1999;28:219–230.
80. Control of Noise at Work. London: HMSO; 2005.
81. The Management of Health and Safety at Work Regulations. Statutory Instrument No. 3242; 1999.
82. Directive of the European Parliament and Council, 2013/35/EU.
83. Occupational Safety and Health Administration (OSHA). Occupational noise exposure. 29 C.F.R. 1988.
84. U.S. Food and Drug Administration. Criteria for significant risk investigations of magnetic resonance diagnostic devices. guidance for industry and food and drug administration staff. Rockville, MD: Food and Drug Administration Center for Devices and Radiological Health. 2014.
85. Department of Health, Guidelines for Magnetic Resonance Diagnostic Equipment in Clinical Use. London: HMSO; 1993.
86. Medicines and Healthcare Products Regulatory Authority (MHRA). Safety Guidelines for Magnetic Resonance Imaging Equipment in Clinical Use. 2015.

202 Acoustic Noise Associated With MRI Procedures

87. International Commission on Non-Ionizing Radiation (ICNIRP). Guidelines on limits of static magnetic fields. *Health Physics* 1994;66:100-106.
88. International Commission on Non-Ionizing Radiation (ICNIRP). Statement on MR procedures: Protection of patients. *Health Physics* 2004;87:197-216.
89. International Electrotechnical Commission (IEC). Particular requirements for the safety of magnetic resonance equipment for medical diagnosis. Geneva: IEC;60601-2-33;2001.
90. Kanal E, Borgstede JP, Barkovich AJ, et al. American College of Radiology white paper on MR Safety. *AJR Am J Roentgenol* 2002;178:1335-1347.
91. Kanal E, Barkovich AJ, Bell C, et al. ACR Guidance document on MR safe practices: 2013. *J Magn Reson Imaging* 2013;37:501-530.
92. White RD, Smith JA, Shepley MM. Recommended standards for newborn ICU design. *J Perinatol* 2013;33:S2-S16.
93. De Wilde JP, Rivers AW, Price DL. A review of the current use of magnetic resonance imaging in pregnancy and safety implications for the fetus. *Progr Biophys and Mol Biol* 2005;87:335-353.
94. Brezinka C, Lechner T, Stephens K. The fetus and noise. *Gynal-geburt Runds* 1997;37:119-129.
95. Glover P, Hykin J, Gowland P, Wright J, Johnson J, Mansfield PM. An assessment of the intrauterine sound intensity level during obstetric echo-planar magnetic resonance imaging. *Brit J Rad* 1995;68:1090-4.
96. Etzel RA, Balk SJ, Bearer CF, et al. Noise: a hazard for the fetus and newborn. *Paediatrics* 1997;100:724-727.
97. Reeves MJ, Brandreth M, Whity EH, et al. Neonatal cochlear function: Measurement after exposure to acoustic noise during *in utero* MR imaging. *Radiology* 2010;257:802-809.
98. Health and Safety Executive. Noise and the Fetus: A Critical Review of the Literature. Sudbury: HSE Books; 1994.
99. Health and Safety Executive. Non-Auditory Effects of Noise at Work: A Critical Review of the Literature Post 1998. Sudbury: HSE Books; 1999.
100. American Academy of Paediatrics: Committee on environmental health. Noise: A hazard for the fetus and newborn. *Paediatrics* 1997;100:724-727.
101. Bouyssi-Kobar M, du Plessis AJ, Robertson RL, Limperopoulos C. Fetal magnetic resonance imaging: Exposure times and functional outcomes at preschool age. *Pediatr Radiol* 2015;45:1823-1830.
102. De Vita E, Bainbridge A, Cheong JLY, et al. Magnetic resonance imaging of neonatal encephalopathy at 4.7 Tesla: Initial experiences. *Pediatrics* 2006;118:e1812-e1821.
103. Jaimes C, Delgado J, Cunnane MB, et al. Does 3-T fetal MRI induce adverse acoustic effects in the neonate? A preliminary study comparing postnatal auditory test performance of fetuses scanned at 1.5 and 3 T. *Pediatr Radiol* 2019;49:37-45.
104. Clements H, Duncan KR, Fielding K, et al. Infants exposed to MRI *in utero* have a normal paediatric assessment at 9 months of age. *Brit J Radiol* 2000;73:190-194.
105. Koka RD, de Vries MM, Heerschap A, van den Berg PP. Absence of harmful effects of magnetic resonance exposure at 1.5 T *in utero* during the third trimester of pregnancy: A follow-up study. *Magn Reson Imaging* 2004;22:851-854.
106. Strizek B, Jani JC, Mucyo E, et al. Safety of MR imaging at 1.5 T in fetuses: A retrospective case-control study of birth weights and the effects of acoustic noise. *Radiology* 2015;275:530-537.
107. Tkach JA, Merhar SL, Kline-Fath BM, et al. MRI in the neonatal ICU: Initial experience using a small-footprint 1.5-T system. *AJR Am J Roentgenol* 2013;202:W95-W105.
108. Tkach JA, Li Y, Pratt RG, et al. Characterization of acoustic noise in a neonatal intensive care unit MRI system. *Pediatr Radiol* 2014;44:1011-1019.

MRI Bioeffects, Safety, and Patient Management 203

109. Wagner W, Staud I, Frank G, et al. Noise in magnetic resonance imaging: No risk for sensorineural function but increased amplitude variability of otoacoustic emissions. *Laryngoscope* 2003;113:1216-23.
110. Govindaraju R, Omar R, Rajagopalan R, Norlisah R, Kwan-Hoong N. Hearing loss after noise exposure. *Auris Nasus Larynx* 2011;38:319-322.
111. Nordell A, Lundh M, Horsch S, et al. The acoustic hood: A patient-independent device for improving acoustic noise protection during neonatal magnetic resonance imaging. *Acta Paed* 2009;98:1278-1283.
112. Naughton RF. The Measurement of Hearing by Bone Conduction. In: Jerger J, Editor. *Modern Developments in Audiology*. New York: Academic Press; 1963.
113. Berger EH. Hearing protection: surpassing the limitations to attenuation imposed by the bone conduction pathways. *J Acoust Soc Am* 2003;114:1955-67.
114. McJury M, Stewart RW, Crawford D, Toma E. The use of active noise control (ANC) to reduce acoustic noise generated during MRI scanning: Some initial results. *Magn Reson Imaging* 1997;15:319-322.
115. Chen CK, Chiueh TD, Chen JH. Active cancellation system of acoustic noise in MR imaging. *IEEE Trans Biomed Eng* 1999;46:186-191.
116. Lueg P. Process of silencing sound oscillations. U.S. Patent;2043416,1936.
117. Chaplain GBB. Anti-noise: the Essex breakthrough. *Chart Mech Eng* 1983;30:41-47.
118. Elliott SJ, Nelson PA. The acoustic control of sound. *IEEE Sign Proc Magn* 1993;10:12-35.
119. Pla FG, Sommerfeldt SD, Heden RA. Active noise control in magnetic resonance imaging. *Proc of Active 95* 2005;573-582.
120. Chambers J, Akeroyd MA, Sumerfield Q, Palmer AR. Active control of the volume acquisition noise in functional magnetic resonance imaging: Method and psychoacoustical evaluation. *J Acoust Soc Am* 2001;110:3014-54.
121. Li M, Rudd B, Lim TC, Lee JH. *In situ* active control of noise in a 4T MRI scanner. *J Magn Reson Imaging* 2011;34:662-669.
122. Lee N, Park Y, Lee GW. Frequency-domain active noise control for magnetic resonance imaging acoustic noise. *Appl Acoust* 2017;118:30-38.
123. Fuller CR. Noise control characteristics of synchrophasing: Part 1. *Am Inst Aeron Astron J* 1986;24:1063-8.
124. Jones JD, Fuller CR. Noise control characteristics of synchrophasing: Part 2. *Am Inst Aeron Astron J* 1986;24:1271-6.
125. Nestorovic-Trajkov T, Koppe H, Gabbert U. Active vibration control using optimal LQ tracking system with additional elements. *Int J Control* 2005;78:1182-1197.
126. Qiu J, Tani J. Vibration control of a cylindrical shell used in MRI equipment. *Smart Mater Struct* 1995;4:A75-A81.
127. Oveisi A, Nestorović T. MU-Synthesis based active robust vibration control of an MRI inlet. *Mech Eng* 2016;14:37-53.
128. Skare S, Nordell B, et al. An incubator and “quiet” pulse sequences for MRI examination of premature neonates. *Proceedings of the International Society of Magnetic Resonance Imaging* 1996;1727.
129. Jakob P, Schlaug MG, Griswold M, et al. Functional burst imaging. *Magn Reson Med* 1998;40:614-621.
130. Cremillieux Y, Wheeler-Kingshott CA, Briguet A, Doran SJ. STEAM-BURST: a single-shot multi-slice imaging sequence without rapid gradient switching. *Magn Reson Med* 1997;38:645-652.
131. Hennig J, Hodapp M. Burst imaging. *MAGMA* 1993;1:39-48.
132. Frahm J, Merboldt K, Hanicke W, Haase A. Stimulated echo imaging. *J Magn Reson Imaging* 1985;64:81-93.
133. Hennel F, Giard F, Loenneker T. Silent MRI with soft gradient pulses. *Magn Reson Med* 1999;42:6-10.

204 Acoustic Noise Associated With MRI Procedures

134. Hennel F. Fast spin echo and fast gradient echo MRI with low acoustic noise. *J Magn Reson Imaging* 2001;13:960-966.
135. Loenneker T, Hennel F, Ludwig U, Hennig J. Silent BOLD imaging. *Magn Reson Mater Phys Biol Med* 2001;13:76-81.
136. Osterle C, Hennel F, Hennig J. Quiet imaging with interleaved spiral read-out. *Magn Reson Imaging* 2001;19:1333-1337.
137. Schmitter S, Diesch E, Amann M, et al. Silent echo-planar imaging for auditory fMRI. *Magn Reson Mater Phys* 2008;21:317-325.
138. Schmitter S, Bock M. Acoustic noise-optimized VERSE pulses. *Magn Reson in Med* 2010;64:1447-1453.
139. Zapp J, Schmitter S, Schad LR. Sinusoidal echo-planar imaging with parallel acquisition technique for reduced acoustic noise in auditory fMRI. *J Magn Reson Imaging* 2012;36:581-588.
140. Heismann B, Ott M, Grodzki D. Sequence-based acoustic noise reduction of clinical MRI scans. *Magn Reson Med* 2015;73:1104-1109.
141. Fischer S, Grodzki DM, Domschke M, K, et al. Quiet MR sequences in clinical routine: Initial experience in abdominal imaging. *Radiol Med* 2017;122:194-203.
142. de Zwart JA, Van Gelderen P, Kellman P, Duyn JH. Reduction of gradient acoustic noise in MRI using SENSE-EPI. *Neuroimage* 2001;16:1151-1155.
143. Moelker A, Vogel MW, Pattynama PMT. Real-time modulation of acoustic gradient noise in interventional MRI. *Concepts in Magn Reson Part B* 2003;20B:34-39.
144. Pierre EY, Grodzki D, Heismann B, et al. Making MRI scanning quieter: Optimized TSE sequences with parallel imaging. *Magnetom Flash* 2013;5:30-34.
145. Tomasi DG, Ernst T. Echo planar imaging at 4 Tesla with minimum acoustic noise. *J Magn Reson Imaging* 2003;18:128-130.
146. Segbers M, Rizzo-Sierra CV, Duifhuis H, Hoogduin JM. Shaping and timing gradient pulses to reduce MRI acoustic noise. *Magn Reson Med* 2010;64:546-553.
147. Ott M, Blaimer M, Grodzki DM, et al. Acoustic-noise-optimized-diffusion-weighted imaging. *Magn Reson Mater Phy* 2015;28:511-521.
148. Gatehouse PD, Bydder GM. Magnetic resonance imaging of short T_2 components in tissue. *Clin Radiol* 2003;58:1-19.
149. Weiger M, Brunner DO, Dietrich BE, Meuller CF, Pruessmann KP. ZTE imaging in humans. *Magn Reson Med* 2013;70:328-332.
150. Idiyatullin D, Corum C, Park J-Y, Garwood M. Fast and quiet MRI using a swept radiofrequency. *J Magn Reson Imaging* 2006;181:342-349.
151. Weiger M, Pruessmann KP, Hennel F. MRI with zero echo time: Hard versus sweep pulse excitation. *Magn Reson Med* 2011;66:379-389.
152. Madio DP, Lowe IJ. Ultra-fast imaging using low flip angles and FIDs. *Magn Reson Med* 1995;34:525-529.
153. Alibek S, Vogel M, Sun W, et al. Acoustic noise reduction in MRI using Silent Scan: An initial experience. *Diagn Interv Radiol* 2014;20:360-363.
154. Ohlmann-Knafo S, Morlo M, Tarnoki DL, et al. Comparison of image quality characteristics on Silent MR versus conventional MR imaging of brain lesions at 3 Tesla. *Br J Radiol* 2016;89:20150801.
155. Solana AB, Menini A, Sacolick LI, Hehn N, Wiesinger F. Quiet and distortion-free, whole brain BOLD fMRI using T_2 -prepared RUFIS. *Magn Reson Med* 2016;75:1402-1412.
156. Wiesinger F, Menini A, Solana AB. Looping star. *Magn Reson Med* 2019;81:57-68.
157. Holdsworth SJ, Macpherson SJ, Yeom KW, Wintermark M, Zaharchuk G. Clinical evaluation of silent T_1 -weighted MRI and silent MR angiography of the brain. *Am J Radiol* 2018;210:404-411.

MRI Bioeffects, Safety, and Patient Management 205

158. Grodzki DM, Jakob PM, Heismann B. Ultrashort echo time imaging using pointwise encoding time reduction with radial acquisition (PETRA). *Magn Reson Med* 2012;67:510–518.
159. Ida M, Wakayama T, Nielsen ML, Abe T, Grodzki DM. Quiet T1-weighted imaging using PETRA: Initial clinical evaluation in intracranial tumor patients. *J Magn Reson Imaging* 2015;41:447–453.
160. Aida N, Niwa T, Fujii Y, et al. Quiet T1-weighted pointwise encoding time reduction with radial acquisition for assessing myelination in the pediatric brain. *Am J Neuroradiol* 2016;37:1528–34.
161. Eagan T, Baig TN, Derakhshan JJ, Duerk JL, Brown RW. Acoustic noise suppression: Gradient self-help? *Proceedings of the International Society of Magnetic Resonance Imaging* 2007;1101.
162. Shou X, Chen X, Derakhshan J, et al. The suppression of selected acoustic frequencies in MRI. *Appl Acoustics* 2010;71:191–200.
163. Wu Y, Chronik BA, Bowen C, Mechefske CK, Rutt BK. Gradient-induced acoustic and magnetic field fluctuations a 4-T whole-body MR imager. *Magn Reson Med* 2000;44:532–536.
164. Savoy RL, Ravicz ME, Gollub R. The Psychological Laboratory in the Magnet: Stimulus Delivery, Response Recording and Safety. In: Moonen C, Bandettini P, Editors. *Medical Radiology, Diagnostic Imaging and Radiation Oncology: Functional MRI*. Berlin: Springer; 1999. pp. 347–365.
165. Marcar VL, Girard F, Rinkel Y, Schneider JF, Martin E. Inaudible functional MRI using a truly mute gradient echo sequence. *Neuroradiology* 2002;44:893–899.
166. Peelle JE, Eason RJ, Schmitter S, Schwarzbauer C, Davis MH. Evaluating an acoustically quiet EPI sequence for use in fMRI studies of speech and auditory processing. *NeuroImage* 2010;52:1410–1419.
167. Scheffler K, Bileen D, Schmid N, Tschopp K, Seelig J. Auditory cortical responses to hearing subjects and unilateral deaf patients as detected by functional magnetic resonance imaging. *Cereb Cortex* 1998;8:156–163.
168. Hall DA, Haggard MP, Akeroyd MA, et al. “Sparse” temporal sampling in auditory fMRI. *Human Brain Mapping* 1999;7:213–223.
169. Melcher JR, Talavage TM, Harms MP. Functional MRI of the Auditory System. In: Moonen C, Bandettini P, Editors. *Medical Radiology, Diagnostic Imaging and Radiation Oncology: Functional MRI*. Berlin: Springer; 1999. pp. 393–406.
170. Amaro E, Williams SCR, Shergill SS, et al. Acoustic noise and functional MRI: current strategies and future prospects. *J Magn Reson Imaging* 2002;16:497–510.
171. Schwarzbauer C, Davis MH, Rodd JM, Johnsrude I. Interleaved silent steady state (ISSS) imaging: a new sparse imaging method applied to auditory fMRI. *NeuroImage* 2006;29:774–782.
172. Andoh J, Ferreira M, Leppert IR, et al. How restful is it with all that noise? Comparison of Interleaved silent steady state (ISSS) and conventional imaging in resting-state fMRI. *NeuroImage* 2017;147:726–735.
173. Yang Y, Engelien A, Engelien W, et al. A silent event-related functional MRI technique for brain activation without interference of scanner acoustic noise. *Magn Reson Med* 2000;43:185–190.
174. Mansfield P. Multi-planar image formation using NMR spin echoes. *J Phys C Solid State Phys* 1977;10:L55–8.
175. Hutter J, Price AN, Cordero-Grande L, et al. Quiet echo planar imaging for functional and diffusion MRI. *Magn Reson Med* 2018;79:1447–1459.
176. Larkman DJ, Hajnal JV, Herlihy AH, et al. Use of multicoil arrays for separation of signal from multiple slices simultaneously excited. *J Magn Reson Imaging* 2001;13:313–317.
177. Breuer FA, Blaimer M, Mueller MF, et al. Controlled Aliasing in Volumetric Parallel Imaging (2D CAIPIRINHA). *Magn Reson Med* 2006;55:549–556.
178. Liebig P, Heidemann RM, Hensel B, Porter DA. Accelerated silent echo-planar imaging. *Magn Reson Imaging* 2019;55:81–85.
179. Griswold MA, Jacob PM, Heidemann RM, et al. Generalized autocalibrating partially parallel acquisitions (GRAPPA). *Magn Reson Med* 2002;47:1202–10.

206 Acoustic Noise Associated With MRI Procedures

180. Uecker M, Lia P, Murphy MJ, et al. ESPIRiT—an eigenvalue approach to autocalibrating parallel MRI: Where SENSE meets GRAPPA. *Magn Reson Med* 2014;71:990–1001.
181. Lin TR, O’Shea P, Mechefske CK. Reducing MRI gradient coil vibration with rib stiffeners. *Concepts in Magn Reson Part B* 2009;35B:198–209.
182. Mechefske CK, Geris R, Gati JS, Rutt BK. Acoustic noise reduction in a 4T MRI scanner. *Magn Reson Mater Phys Med Biol* 2002;13:172–176.
183. Katsunuma A, Takamori H, Sakakura Y, et al. Quiet MRI with novel acoustic noise reduction. *Magn Reson Mater Phys Med Biol* 2002;13:139–144.
184. Toshiba KK. MRI system having mechanically decoupled field generators to reduce ambient acoustic noise. U.S. Patent;6043653,2000.
185. Edelstein WA, Hedeon RA, Mallozzi RP, et al. Making MR quieter. *Magn Reson Imaging* 2002;20:155–161.
186. Yoshida T, Takamori H, Katsunuma HA. EXCELART MRI system with revolutionary Pianissimo noise reduction technology. *Medical Review* 2000;71.
187. Edelstein WA, Kidane TK, Eagan TP, et al. Active-passive gradient shielding for MRI acoustic noise reduction. *Magn Reson Med* 2005;53:1013–1017.
188. Mulholland KA. Noise Control. In: Tempest W, Editor. *The Noise Handbook*. New York: Academic Press; 1985. pp. 282.
189. Maa DY. Theory and design of microperforated panel sound absorbing constructions. *Sci Sin* 1975;18:155–170.
190. Li G, Mechefske CK. A comprehensive experimental study of micro-perforated panel acoustic absorbers in MRI scanners. *Magn Reson Mater Phys Biol Med* 2010;23:177–185.
191. Ireland CM, Giaquinto RO, Loew W, et al. A novel acoustically quiet coil for neonatal MRI system. *Concepts in Magn Reson Part B* 2015;45B:107–114.
192. Mansfield P, Glover PM, Bowtell RW. Active acoustic screening: Design principles for quiet gradient coils in MRI. *Meas Sci Technol* 1994;5:1021–25.
193. Mansfield P, Chapman BL, Bowtell R, et al. Active acoustic screening: Reduction of noise in gradient coils by Lorentz forces balancing. *Magn Reson Med* 1995;33:276–281.
194. Bowtell RW, Mansfield PM. Quiet transverse gradient coils: Lorentz force balancing designs using geometric similitude. *Magn Reson Med* 1995;34:494–7.
195. Bowtell RW, Peters A. Analytic approach to the design of transverse gradient coils with co-axial return paths. *Magn Reson Med* 1999;41:600–608.
196. Jackson JM, Brideson MA, Forbes LK, Crozier S. Tikhonov regularization approach for acoustic noise reduction in an asymmetric, self-shielded MRI gradient coil. *Concepts in Magn Reson* 2010;37B:167–179.
197. Forbes LK, Brideson MA, Crozier S, While PT. An analytical approach to the design of quiet cylindrical asymmetric gradient coils in MRI. *Concepts in Magn Reson Part B* 2007;31B:218–236.
198. Forbes LK, Crozier S. Novel target field method for designing shielded bi-planar shim and gradient coils. *IEEE Trans on Magnetics* 2004;40:1929–1938.
199. Wang Y, Liu F, Weber E, et al. Acoustic analysis for a split MRI system using FE method. *Concepts in Magn Reson Part B* 2015;45B:85–96.
200. Tan ET, Hardy CJ, Shu Y, et al. Reduced acoustic noise in diffusion tensor imaging on a compact MRI system. *Magn Reson Med* 2018;79:2902–2911.
201. DeMeester G, Morich M, Byrne A, et al. Challenges of short magnet design. *MAGMA* 2002;13:193–198.
202. Liu F, Wei R, Crozier S. Open-bore magnet for use in magnetic resonance imaging. U.S. Patent;20120258862A1,2012.

MRI Bioeffects, Safety, and Patient Management 207

203. Zhao H, Crozier S, Doddrell DM. Asymmetric MRI magnet design using a hybrid numerical method. *J Magn Reson Imaging* 1999;141:340–346.
204. Rim M, Kim YH. Narrowband noise attenuation characteristics of in-duct acoustic screens. *J Sound Vibr* 2000;234:737–759.
205. Selamet A, Ji ZL. Acoustic attenuation performance of circular expansion chambers with extended inlet/outlet. *J Sound Vibr* 1999;223:197–212.
206. Lipstein NJ. Acoustic duct with asymmetric acoustical treatment. *J Acoust Soc Am* 1982;71:1309.
207. Selamet A, Ji ZL. Circular asymmetric Helmholtz resonators. *J Acoust Soc Am* 2000;107:2360–2369.
208. Bangtsson E, Noreland D, Berggren M. Shape optimization of an acoustic horn. *Comp Methods App Mech Eng* 2003;192:1533–1571.
209. Udawalpola R, Berggren M. Optimization of an acoustic horn with respect to efficiency and directivity. *Int J Numerical Methods Eng* 2008;73:1571–1606.
210. Winkler SA, Alejski A, Wade T, McKenzie C, Rutt BK. A traveling-wave approach to acoustic noise reduction in MR gradient coils. *Proceedings of the International Society of Magnetic Resonance Imaging* 2014;4852.
211. Nan J, Zong N, Chen Q, et al. A structure design method for reduction of MRI acoustic noise. *Comput Math Methods Med* 2017;2017:6253428.
212. Roschmann P. Human auditory system responses to radio frequency energy in RF coils for magnetic resonance at 2.4 to 170 MHz. *Magn Reson Med* 1991;21:197–215.
213. Elder JA. Special senses. In: *Biological Effects of Radio Frequency Radiation*. United States Environmental Protection Agency, Health Effects Research Laboratory, EPA-600/8-83-026F, Research Triangle Park 1984. pp. 570.
214. Postow E, Swicord ML. Modulated fields and “window” effects. In: Polk C, Postow E, Editors. *CRC Handbook of Biological Effects of Electromagnetic Fields*. Boca Raton: CRC Press Inc.;1989. pp. 425.

Chapter 7 Bioeffects of Radiofrequency Power Deposition Associated With MRI

DANIEL J. SCHAEFER, PH.D.

Visiting Professor
Department of Electrical and Computer Engineering
Duke University
Durham, NC

INTRODUCTION

Radiofrequency (RF) energy is defined as nonionizing electromagnetic radiation in the frequency range of 3-kHz to 300-GHz, as distinguished from the very high photon energies and frequencies associated with ionizing electromagnetic radiation (e.g., gamma and X-rays). The RF spectrum includes radar, ultra-high frequency (UHF), and very high frequency (VHF) television, AM and FM radio, and microwave communication frequencies. Resonant radiofrequency (RF) magnetic fields are used in magnetic resonance (MR) for imaging and spectroscopy procedures (1).

This chapter will present and discuss various important aspects of RF power deposition associated with magnetic resonance imaging (MRI) procedures with an emphasis on non-clinical, physical factors, calculations, and measurements used to characterize this electromagnetic field.

RADIO FREQUENCY MAGNETIC FIELDS AND MRI PROCEDURES

During an MRI procedure, the patient absorbs a portion of the transmitted RF energy, which may result in tissue heating (2-16). Thus, whole-body and localized heating are the primary safety concerns associated with the absorption of RF energy. Notably, the elevation of core body temperatures to sufficiently high levels may be life-threatening (2, 17, 18). With local transmit RF coils, the primary safety concern is to prevent burns by limiting localized heating.

The specific absorption rate, or SAR, is the RF power absorbed per unit mass of tissue and is the metric for RF power deposition typically reported in W/kg. SAR is believed to serve as a crude measure of heating potential. It is essential for patient safety to limit whole-

body-averaged and localized temperatures to appropriate SAR levels (2, 18-23). Therefore, national and international safety standards (2, 19-21) appropriately limit or recommend SAR levels for clinical MRI examinations. Heating experienced by the patient during an MRI examination depends on the RF power deposited per unit mass (or SAR), ambient temperature, relative humidity, airflow rate, blood flow, sweating rate, and patient insulation.

Resonant frequency scales with the static magnetic field strength and nuclei of interest. For hydrogen protons, the resonant RF frequency is 42-MHz/Tesla (1). The tip angle is proportional to the area under the envelope of the RF waveform. Typically, the amplitude of the RF pulse (i.e., the tip angle) is adjusted to maximize the received signal. For a given waveform, RF energy is proportional to the square of the tip angle. Only the magnetic component of the RF field is useful in MRI. Designs usually reduce electric field coupling to patients. Since RF power deposition is mostly through magnetic induction, the distribution of the RF power deposition associated with an MRI procedure tends to be mostly peripheral or on the surface of the subject's body (9-11). Plane wave exposures (in non-MRI applications) may lead to higher heating at greater depths (18, 24).

The average RF power (and SAR) is proportional to the number of images per unit time and peak RF power. Peak RF power depends on patient dimensions, the RF waveform, flip angle, and whether the MR system's transmit RF coil is operating in a linear or quadrature (i.e., has a circularly polarized magnetic field vector) mode during the transmission of RF energy. Notably, quadrature excitation lowers RF peak power requirements and SAR by a factor of two and "stirs" any field inhomogeneities (10). For a given static magnetic field strength and RF waveform, SAR is independent of the type of nucleus.

MR SAFETY STANDARDS

The United States, Food and Drug Administration (FDA) published "Non-Significant Risk Criteria" for MR systems (22). These criteria state that clinical MRI examinations need Investigational Device Exemption (IDE) if the SAR exceeds the following levels:

- (1) 4-W/kg (averaged over the whole body over any 15-min. period) or
- (2) 3.2-W/kg (averaged over the head over in any 10-min. period).

Notably, the FDA's significant risk criteria also include limits that are unrelated to RF power deposition.

The International Electrotechnical Commission (IEC) developed the international MRI safety standard IEC 60601-2-33 (23). The IEC MRI safety standard is three-tiered. The first tier is referred to as the *Normal Operating Mode* and is for routine scanning of patients. The second tier is designated as the *First Level Controlled Operating Mode*. The MR system operator must take a deliberate action (usually using an "accept" button on the MR system console) to enter the *First Level Controlled Operating Mode*. This mode provides higher MR system performance, but requires the MRI healthcare worker to closely monitor the patient during the MRI examination. Finally, the third tier is the *Second Level Controlled Operating Mode*, which is used only for research purposes under limits controlled by an Investigational Review Board (IRB).

210 Bioeffects of Radiofrequency Power Deposition

When the environmental temperature is $\leq 25^{\circ}\text{C}$, the current IEC MRI safety standard for RF energy during an MRI procedure permits (assuming SAR averaged over any 10-second period ≤ 2 times the 6-min. average SAR limit) the following limits for volume transmit RF coils:

- a) Whole-body SAR (averaged over any 6-min period):
 - 1) The Normal Operating Mode - SAR $\leq 2\text{-W/kg}$;
 - 2) The First Level Controlled Operating Mode - SAR $\leq 4\text{-W/kg}$;
 - 3) The Second Level Controlled Operating Mode - SAR < IRB limit.
- b) Partial Body SAR (averaged over any 6-min. period):
 - 1) The Normal Operating Mode - SAR $\leq 10\text{ W/kg} - (8\text{-W/kg} * \text{exposed patient mass} / \text{patient mass})$;
 - 2) The First Level Controlled Operating Mode - SAR $\leq 10\text{-W/kg} - (6\text{-W/kg} * \text{exposed patient mass} / \text{patient mass})$;
 - 3) The Second Level Controlled Operating Mode - SAR < IRB limit.
- c) Head SAR (averaged over any 6-min. period):
 - 1) The Normal Operating Mode - SAR $\leq 3.2\text{-W/kg}$;
 - 2) The First Level Controlled Operating Mode - SAR $\leq 3.2\text{-W/kg}$;
 - 3) The Second Level Controlled Operating Mode - SAR < IRB limit.

The maximum energy limit is to be determined by the risk management file (note, previously this was equivalent to 4-W/kg for one hour). Whole-body SAR limits are de-rated by 0.25-W/kg for each degree C that the environmental temperature exceeds 25°C for the First Level Controlled Operating Mode, only.

For local transmit RF coils, local SAR limits (averaged over the worst-case 10-grams for 6- min.) are:

- a) The Normal Operating Mode
 - 1) SAR $\leq 10\text{-W/kg}$ in the head or trunk (provided local temperature rise in the orbits is limited to a 1°C).
 - 2) SAR $\leq 20\text{-W/kg}$ in the extremities;
- b) The First Level Controlled Operating Mode- SAR $\leq 3.2\text{-W/kg}$;
 - 1) SAR $\leq 20\text{-W/kg}$ in the head or trunk (provided local temperature rise in the orbits is limited to a 1°C).
 - 2) SAR $\leq 40\text{-W/kg}$ in the extremities;
- c) The Second Level Controlled Operating Mode - SAR < IRB limit.

Note that the third edition of IEC 60601-2-33 is current as this is written. Work is continuing on improving the scientific basis for local SAR limits or some equivalent criterion.

The IEC 60601-2-33 does not require local SAR limits for volume transmit RF coils, but does require local SAR limits for local transmit RF coils that may produce inhomogeneous RF electromagnetic fields. For 3-Tesla MR systems and higher, MR image “shading” can be a concern. This issue is apparently associated with the standing waves interfering at field strengths where electrical lengths in the body that approach, or are less than, the dimensions of the body. There are now efforts (known as dual drive, parallel transmit, elliptical drive, or RF shimming; parallel transmit will be used here to represent these techniques) to minimize shading by adjusting excitations on two or more RF channels to improve the quadrature uniformity in the body (not necessarily in air) for a particular field of view. These techniques are intended to improve quadrature uniformity in the body and reduce or

at least not increase the local SAR over that caused by conventional quadrature (in air) excitation. The local SAR level could increase if the excitation is not properly controlled. Since there is a long safety record associated with conventional quadrature excitation, there generally is no concern provided that parallel transmit does not generate a local SAR higher than conventional quadrature imaging for similar tissues. However, the scientific basis for local SAR limits (i.e., RF power averaged over the worst case 10 grams) is currently unclear.

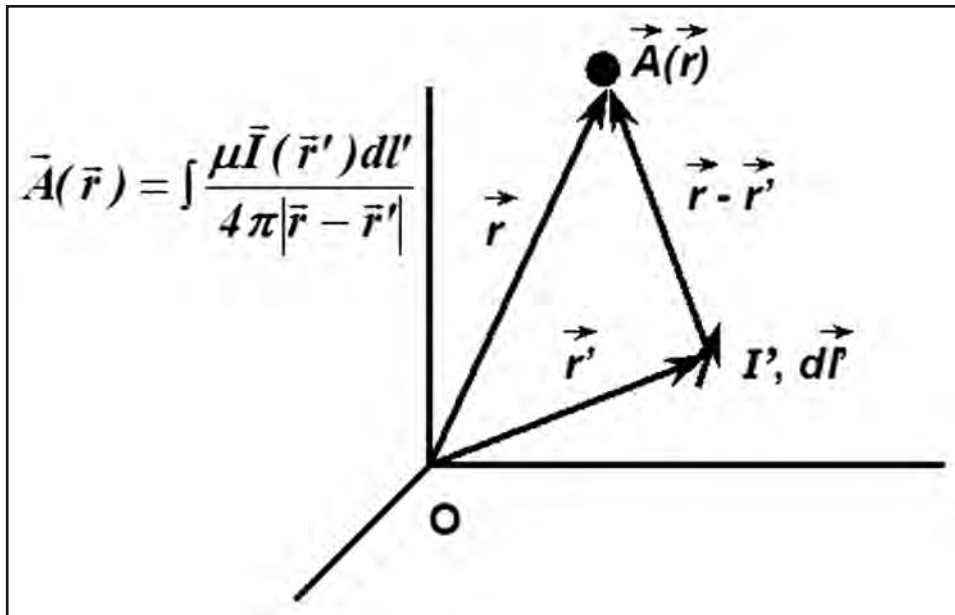
Moritz and Henriques (25, 26) found that the thresholds for local thermal damage to skin depended non-linearly on local tissue temperature and its duration. Comparisons of the effectiveness of microwave hyperthermia protocols for cancer therapy with various temperature-time courses have been modeled in terms of the equivalent cumulative exposure minutes at 43 degrees C (27). These values are known as CEM43. A proposal has been made to use CEM43-derived limits to replace existing SAR safety limits (28). The proposed CEM43 estimates tissue viability through Arrhenius equations based on temperature due to local SAR from numerical simulations, duration, mass blood flow, and most sensitive exposed tissue type (29, 30). It is not yet certain whether approximations made in deriving CEM43 limits to determine thermal safety for MRI and spectroscopy are accurate. Safety based on whole-body, head, and local SAR limits has been effective for the approximately 35-year history of MRI (30, 31). In addition, a vast array of implants and devices potentially used in patients undergoing MRI examinations are classified as “MR Conditional” meaning that they are safe for patients as long as certain specified conditions are followed, which typically include a particular whole-body-averaged SAR level (32). It is of interest that in 2011 the Health Council of the Netherlands decided there was no need to change their electromagnetic field exposure limits from SAR to time-temperature (33). Perhaps CEM43 or something similar might find at least indirect use in studying appropriate RF safety limits for local SAR values.

Another IEC safety standard, IEC 60601-1, establishes additional safety criteria for medical devices including electrical, mechanical, and thermal safety (34). Surface contact temperatures are limited to 41.0°C (34). Note that during an MRI examination using a high SAR, the average skin temperature of a human subject approaches 37.0°C (for a 4.0°C margin for temperature rise). During an MRI examination using very low SAR, the average skin temperature is typically 33.0°C (for a temperature rise margin of 8.0°C).

In 2013, the American College of Radiology published a useful paper for MRI safety guidance (35). This paper is not a regulatory document but, instead, it has various recommendations and suggestions for safety procedures for MRI facilities, some of which pertain to the topic of this chapter.

The Technical Specification, ISO/TS 10974:2011 (36), is a trial standard available for active medical implants to aid in determining whether they are MR Conditional devices. MR Conditional devices are acceptable for patients undergoing MRI examinations only if certain conditions apply. There are also several American Society for Testing and Materials (ASTM) International test standards used to determine safe conditions for use for MR Conditional implants and devices (32, 37-41). Note that the ASTM International heating test implicitly assumes quadrature excitation for the RF energy. Importantly, parallel transmit excitation might produce different heating results.

212 Bioeffects of Radiofrequency Power Deposition

Figure 1. Calculation of the magnetic vector potential, A.

CALCULATION OF MAGNETIC AND ELECTRIC FIELDS ASSOCIATED WITH THE SPECIFIC ABSORPTION RATE (SAR)

The patient's RF power absorption during an MRI procedure can be approximated from quasi static analysis for homogeneous objects, assuming that electric field coupling to the patient can be neglected as well as the RF phase (42, 43). In practice, quasi-static approximations for whole-body SAR in homogeneous spheres appear to be adequate for MR systems operating up to 1.5-T/64-MHz. Calculation of actual SAR levels at 3-T/128-MHz and above, and for local SAR at all static magnetic field strengths and frequencies, requires numerical techniques. Many commercially available software packages exist at this time. Quasi-static methods will usually overestimate whole-body and local SARs (under homogeneous conditions and for certain shapes) when conductor dimensions approach a wavelength.

Assume a line segment of length, dl , carries current, I , and is located a vector, r' , from the origin, O, (Figure 1). The magnetic vector potential, A , at a point located a vector r (x_2 , y_2 , z_2) from the origin may be expressed as (24, 43, 44):

$$\vec{A}(\vec{r}) = \int \frac{\mu \vec{I}(\vec{r}') \bullet d\vec{l}'}{4\pi |\vec{r} - \vec{r}'|} \quad (1)$$

The radiofrequency magnetic field, B_1 , may then be found from the magnetic vector potential:

$$\vec{B}_1 = \nabla \times \vec{A}$$

$$\Rightarrow B_{1x} = \frac{\partial A_z}{\partial y} - \frac{\partial A_y}{\partial z}, B_{1y} = \frac{\partial A_x}{\partial z} - \frac{\partial A_z}{\partial x}, \text{ and } B_{1z} = \frac{\partial A_y}{\partial x} - \frac{\partial A_x}{\partial y}. \quad (2)$$

Note that B_1 scales with current. Coil current is scaled until the desired B_1 is produced at the appropriate site. Usually, the 180-degree pulse centers on the site resulting in the greatest total return signal. The signal distribution, $S(x, y, z)$, might be approximated as:

$$S(x, y, z) = \left(\sin \left(\frac{\pi B_1(x, y, z)}{2B_{1\max}} \right) \right)^3 \quad (3)$$

The total signal is the sum of the signal from all locations. Magnetic vector components are scaled by the coil current required to produce the 180-degree (or whatever is desired) flip angle.

Let ω be the radian frequency and let Φ be the electrostatic potential due to electric charges at electrical conductivity discontinuities. Neglecting currents induced from capacitive coupling, the electric field, E , may be expressed as:

$$E = -\frac{\partial A}{\partial t} - \nabla \Phi = -\omega A - \nabla \Phi \quad (4)$$

While it is generally necessary to use numerical techniques to find the electrostatic potential, for certain ideal geometries such as conductive spheres the electrostatic potential term vanishes.

QUASI-STATIC ESTIMATION OF WHOLE-BODY SAR

The specific absorption rate, SAR, is defined above as the power absorbed per unit mass. Let DC be the ratio of average to peak power over the pulse repetition period. Let σ be the electrical conductivity and ρ be the density of the surrounding tissue. SAR at a point in a sphere may be expressed as:

$$SAR = \frac{\sigma DC |E|^2}{2\rho} = \frac{\sigma DC |\omega A|^2}{2\rho} \quad (5)$$

For RF coils that produce homogeneous B_1 fields, it is possible to investigate the whole-body averaged and peak SARs theoretically for certain object shapes. The patient's RF

214 Bioeffects of Radiofrequency Power Deposition

power absorption during an MRI examination can be approximated from quasi static analysis assuming electric field coupling to patients can be neglected (15, 43, 44). Consider a homogeneous, tissue sphere of radius R . Assume that this sphere is placed in a uniform RF electromagnetic field of strength B_1 . The total average RF power, P_{total} , deposited in the sphere may be expressed as:

$$P_{\text{total}} = \frac{\sigma DC\pi\omega^2 B_1^2 R^5}{15} \quad (6)$$

The average Specific Absorption Rate, SAR_{ave} , may be expressed as:

$$\text{SAR} = \frac{P_{\text{total}}}{\rho \left(\frac{4}{3}\pi R^3 \right)} = \frac{\sigma DC\omega^2 B_1^2 R^2}{20\rho} \quad (7)$$

The highest spatial peak SAR, SAR_{peak} , for a homogeneous sphere may be found, as follows:

$$\text{SAR}_{\text{peak}} = \frac{\sigma DC\omega^2 B_1^2 R^2}{8\rho} = 2.5 \text{ SAR}_{\text{ave}} \quad (8)$$

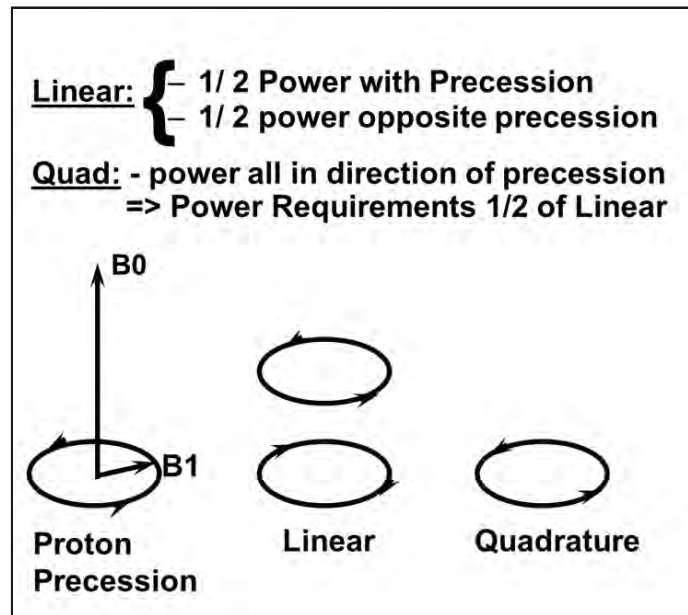
RF energy-induced heating during an MRI procedure is by magnetic induction. Power deposition in homogeneous spheres immersed in uniform RF electromagnetic fields, increases with the fifth power of the radius, R [see Equation (6)]. Because heating is largely peripheral and little deep body heating occurs in a human subject, the body may more easily dissipate the additional heat load. The RF power, P , deposited between a smaller radius, $r = \alpha * R$ (where $\alpha < 1$), and the outer radius, R , normalized to the total power deposited is n :

$$n = \frac{P(R) - P(r)}{P(R)} = \frac{R^5 - r^5}{R^5} = 1 - \alpha^5 \quad (9)$$

Equation (8) shows that peak power deposition for homogeneous spheres is 2.5 times the average (15), consistent with the peripheral nature of RF deposition during the MRI examination. From Equation (9) it is clear that, at least for homogeneous spheres, 87% of the total RF power deposition is in the outer third of the sphere.

RF pulses are used in MRI examinations to flip the macroscopic magnetization vectors through desired angles. Recall that nuclei with magnetic moments precess about the static magnetic field vector in accordance with the right hand rule. Linearly polarized waves may

Figure 2. Comparison of quadrature and linear RF excitation of spins. Note that linear excitation wastes half the applied power.



be treated as the superposition of left and right handed circularly polarized waves. Only that portion of the RF that is circularly polarized in the same sense as the nuclear precession influences the nuclei (**Figure 2**). The other RF component contributes noise and increases RF power requirements. During the MRI examination, transmit RF coils may be driven linearly (linearly polarized RF electromagnetic vector) or they may be driven in quadrature (circularly polarized RF electromagnetic vector). Quadrature RF transmit systems reduce patient heating during the MRI procedure by a factor of two, and spatially stir any RF “hot-spots” (9).

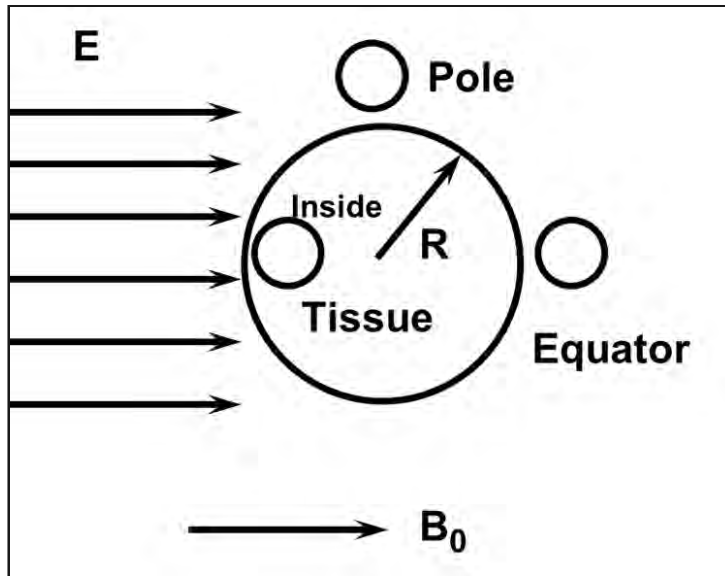
Let γ be the magnetogyric ratio for a given type of nucleus. Note that the energy, W , deposited per pulse depends on the square of the RF tip angle, θ , the square of the static field strength, B_0 , and inversely on RF pulse width, τ , and a waveform factor, η :

$$\theta = \int \omega dt = \eta \gamma B_{1p} \tau \quad \Rightarrow \quad SAR \propto W \propto \tau \omega^2 B_{1p}^2 = \frac{\gamma^2 B_0^2 \theta^2 \tau}{(\eta \gamma \tau)^2} = \frac{B_0^2 \theta^2}{\eta^2 \tau} \quad (10)$$

It is important to note that, for a given field strength and RF waveform, SAR is independent of the nucleus species.

216 Bioeffects of Radiofrequency Power Deposition

Figure 3. Effect of inhomogeneities on RF power deposition. To model the effect, a small, homogeneous sphere is placed either inside a larger tissue sphere or at the pole or equator of the larger tissue sphere (with respect to the RF electric field vector).



SAR "HOT-SPOTS"

Next, consider localized regions of RF power deposition that might lead to heating, commonly referred to as SAR "hot spots". Inhomogeneities in the electrical properties of tissue may result in high local SAR levels. RF-induced biological effects appear to depend upon temperature rather than on RF power deposition. A region of high local SAR may not be a region of high temperature due to blood flow or diffusion or other cooling mechanisms. The distinction between temperature hot spots and SAR hot spots is often ignored or misunderstood.

What effect do inhomogeneities have on the distribution of RF power deposition? Using spherical models, Schenck and Hussain (45) demonstrated that production of power deposition "hot spots" depends upon both the dielectric constants and the conductivities of the media. The model was later reformulated and used to investigate several problems involving worst-case conditions and magnitudes of local power deposition (10). Assume that there is a small, homogeneous sphere (sphere 1) with permittivity ϵ_1 and conductivity σ_1 (Figure 3). Let sphere 2 be a much larger, homogeneous sphere of "standard tissue" representing the body. Sphere 2 has a permittivity ϵ_2 and conductivity σ_2 . Sphere 1 may be placed outside sphere 2 at the pole (tangential electric field location) or at the equator (normal electric field location). In addition, sphere 1 may be placed inside sphere 2. When sphere 1 is placed near the pole of sphere 2, the local power deposition is amplified by a factor, A_p , which may be expressed as:

$$A_p = \frac{9(\sigma_1^2 + \omega^2 \epsilon_1^2)}{(\sigma_1 + 2\sigma_2)^2 + \omega^2(\epsilon_1 + 2\epsilon_2)^2} \quad (11)$$

When sphere 1 is placed near the equator of sphere 2, the local power deposition amplification factor, A_e , may be expressed as:

$$A_e = \frac{9(\sigma_2^2 + \omega^2 \epsilon_2^2)}{(\sigma_1 + 2\sigma_2)^2 + \omega^2(\epsilon_1 + 2\epsilon_2)^2}. \quad (12)$$

Finally, if sphere 1 is placed inside sphere 2, the local power deposition amplification factor, A_s , may be represented as:

$$A_s = \frac{9\sigma_1(\sigma_2^2 + \omega^2 \epsilon_2^2)}{\sigma_2((\sigma_1 + 2\sigma_2)^2 + \omega^2(\epsilon_1 + 2\epsilon_2)^2)} = \left(\frac{\sigma_1}{\sigma_2}\right) A_e \quad (13)$$

All the terms in equations (11), (12), and (13) are positive. The electrical properties of sphere 1 are treated as variables so conditions for maximum amplification of local power deposition may be determined.

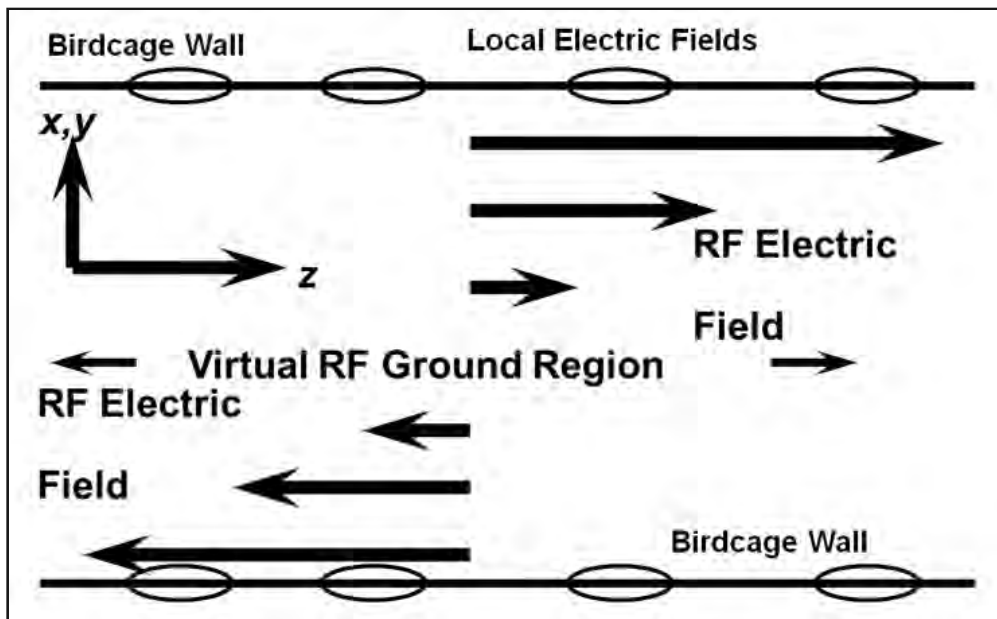
When sphere 1 is near the pole, amplification of local power deposition, A_p , is greatest when sphere 1 is a perfect conductor ($\sigma_1 \approx \infty$). A perfectly conducting small sphere at the pole will result in a local amplification factor of $A_p = 9$. Recall that the spatial peak SAR in a homogeneous sphere is already 2.5 times average SAR for the sphere. Combining these results, the peak SAR at the pole is = 22.5 times the SAR averaged over sphere 2. Conductive leads (e.g., used with electrocardiogram monitoring equipment) placed in contact with the skin of patients may simulate this situation. Note that there is almost no amplification of local power deposition if sphere 1 is a radius or more from sphere 2. Spacing conductors well away from patients can dramatically reduce the local heating potential.

Assume sphere 1 is placed near the equator of sphere 2. Then the greatest amplification of local power deposition takes place when sphere 1 electrical properties are minimal; i.e., $\sigma_1 = 0$ and $\epsilon_1 = \epsilon_0$ (free space value). So for a void, such as an air bubble, $A_e = 2.25$. Fat or bone at the equator produces slightly smaller amplifications (10, 37). When a low conductivity sphere is located near the outer edge of the equator of a larger (conductive) sphere, the local SAR is highest and is limited to 5.625 times the average SAR.

Finally, assume sphere 1 is placed inside the large sphere. This situation may simulate an implanted prostheses. While local SAR is amplified the most when $\sigma_1 = 2\sigma_2$ and $\epsilon_1 = 2\epsilon_2$ (not a likely situation), the amplification factor is only $A_s = 1.125$. The highest local SAR works out to 2.8125 times the local average SAR.

218 Bioeffects of Radiofrequency Power Deposition

Figure 4. Electric fields inside a low-pass, RF birdcage coil. Note that the electric fields reach their maximum magnitude at the coil and fall to zero along the coil axis. Capacitors along the coil wall may also give rise to high electric fields, locally. Any conductors should be routed along regions of the low electric field or orthogonal to the electric field to prevent problems or issues.



The analyses above assume linearly polarized RF magnetic fields. Notably, if the transmit RF coil produces quadrature excitation, then the amplification of local power deposition is reduced. The reduction in local power deposition results from rotating eddy current loops during quadrature excitation. Sphere 1 alternates between the equator and the pole of the larger sphere during quadrature excitation. So, worst-case quadrature local SAR amplification (assuming inhomogeneous biology) is $0.5 * (2.5 + 2.8125) = 2.66$. For maximum SAR amplification at the equator, the electrical properties of sphere 1 approach those of a void.

Similarly, for an infinitely conducting sphere 1, during quadrature RF excitation, the worst-case local power deposition amplification would be $0.5 * (2.5 + 22.5) = 12.5$. However, the presence of a conductor may complicate the production of a perfect quadrature RF field by setting up difficult boundary conditions.

Currently, many useful electromagnetic simulation packages are commercially available that can calculate whole-body average, head average, partial body average, and local SAR (averaged over the worst-case contiguous 10-grams). As mentioned under the MRI safety standards section above, it turns out that, in the transmit body RF coil, the ratio of peak local SAR to the whole-body average SAR may be high (as high as about 13 times) (38).

Transmit RF body coils induce electric fields in patients during MRI procedures. RF-induced electric fields are largest near RF coil conductors (**Figure 4**). Transmit RF coils may have high electric fields near capacitors on the coil as well. During high SAR MRI examinations, placing patients well away from transmit body RF coil conductors may reduce

Figure 5. Receive-only RF surface coil with blocking network. During body RF coil transmission, the blocking network, Z, becomes a high impedance to prevent high-induced currents from flowing in the coil. Such currents could lead to extremely high, local SAR levels. During surface RF coil reception, the blocking network becomes a very low impedance to improve the image signal-to-noise ratio.

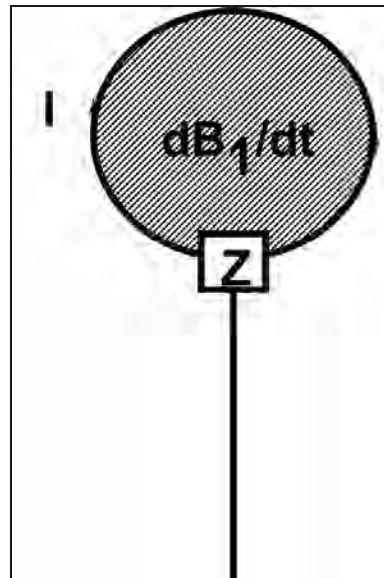
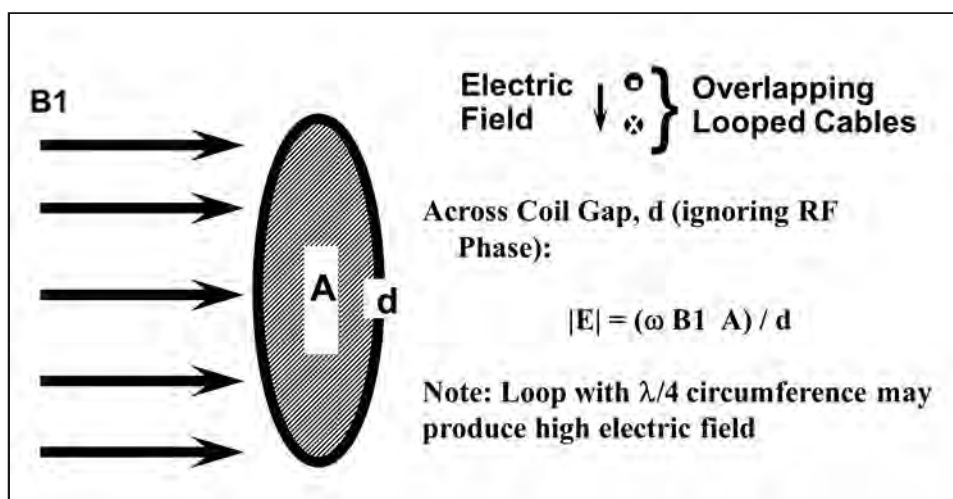
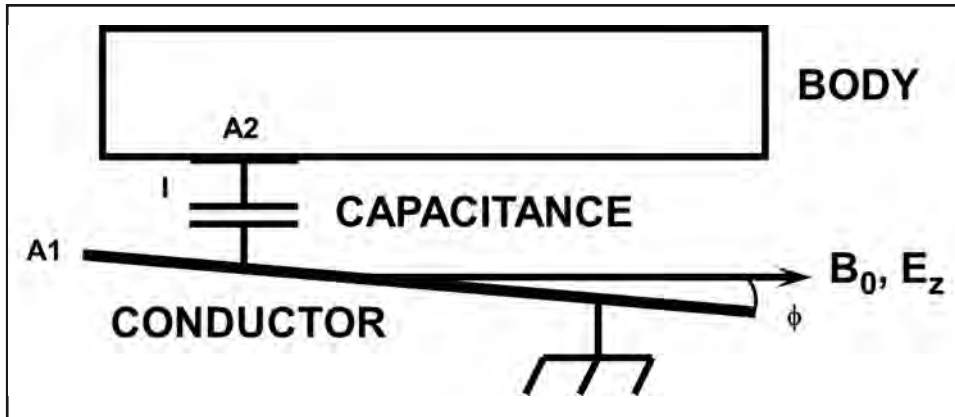


Figure 6. Any loop whose axis is parallel to the RF electromagnetic field may produce high currents and voltages by Faraday induction. Conductive loops of a relatively large size should be avoided in the MR system.



220 Bioeffects of Radiofrequency Power Deposition

Figure 7. Even straight conductors may act as antennas and couple to the RF electric field (which is highest near the wall of the body RF coil). Loops may also short out a mode of quadrature coils, resulting in linear excitation.



local power deposition and heating. The axis of birdcage RF coils is nearly a virtual ground. Conductors that must be introduced into the bore will minimally affect local SAR if they are placed along this virtual ground.

Receive-only RF coils, including most surface coils, typically use transmit body RF coils to transmit RF excitation pulses. Receive-only coils are resonant during RF reception. However, if these RF coils were resonant during transmission of RF energy, then large currents may be produced in the receive-only coils. These large currents would, by Lenz's law, induce opposing RF magnetic fields. Flip angle profiles could be altered by the opposing RF magnetic fields, degrading image quality. The opposing RF magnetic fields may induce large electric fields in the body leading to large local SAR levels. Manufacturers use high impedance blocking networks to detune surface coils and limit surface coil current during body coil transmit (**Figure 5**).

If conductive loops (e.g., associated with the use of monitoring equipment or even a coiled transmission line) are introduced into the MR system, high local SAR levels may result (39, 40) (**Figure 6**). Even straight conductors may increase local SAR significantly (41-44) (**Figure 7**). Therefore, for patient safety, fiber optic-based devices should be used instead of conductors, when possible.

Local temperature rise typically does not correlate well with local power deposition in a human subject. Thermal diffusion, blood flow, thermal radiation, sweating, and airflow may influence the local temperature rise. Consider a region with a small mass, m , cooled by blood flowing from a cooler, more massive region. Under steady-state conditions, the SAR that is dumped to the more massive region depends upon an energy constant, K , the specific heat, C , the temperature difference between the massive and small region, ΔT , and the mass rate of blood flow, dM/dt , and may be expressed as:

Table 1. Maximum local SAR level for local temperature rise of 1°Celsius for various perfused organs (data calculated from Reference 60).

Organ	Mass (kg)	Blood Flow (ml/kg/min)	Maximum SAR (W/kg)*	Maximum ΔT (°C)**
Brain	1.4	540	31	0.13
Heart (Muscle)	0.3	840	48.3	0.08
Liver	2.6	577	33.4	0.12
Kidneys	0.3	4200	243.2	0.02
Skin (normal)	3.6	128	7.4	0.54
Skin (vasodilation)	3.6	1500	86.9	0.05

*Maximum local SAR level which would cause a local temperature rise of 1°C, ignoring vasodilatation and changes in cardiac output.

**Maximum local temperature rise for local SAR exposures of 4.0-W/Kg, assuming no vasodilatation and no change in cardiac output.

$$SAR = \frac{K C \Delta T}{m} \left(\frac{dM}{dt} \right) \quad (14)$$

The SAR required for a 1°C temperature rise in various organs may be estimated using Equation (14). Blood flow rates per unit mass vary from 128-ml/kg/min for the cutaneous circulation to 4200-ml/kg/min for the kidneys. **Table 1** lists local SAR levels required to produce a local temperature rise of one degree C for various organs (23). **Table 1** demonstrates the homogenizing property of blood flow to limit temperature "hot-spots" in the body. Resulting steady-state (maximum) temperature rises for each organ exposed locally to 4-W/kg is also presented in **Table 1**. Athey (53) has shown similar theoretical results demonstrating that significant thermal "hot spots" are not probable for typical head exposures.

RF POWER DEPOSITION IN BIRDCAGE COILS AND NEAR CONDUCTORS

Ideally, birdcage coils would produce uniform B_1 fields. Perfectly uniform B_1 requires an infinitely long birdcage coil (or a spherical current density). Components of A (and thus E) must be parallel to the current density on the conductors that produced them. The B_1 field is related to magnetic vector potential:

$$B_1 = \nabla \times A = \hat{a}_x \left[\left(\frac{\partial A_z}{\partial y} \right) - \left(\frac{\partial A_y}{\partial z} \right) \right] + \hat{a}_y \left[\left(\frac{\partial A_x}{\partial z} \right) - \left(\frac{\partial A_z}{\partial x} \right) \right] + \hat{a}_z \left[\left(\frac{\partial A_y}{\partial x} \right) - \left(\frac{\partial A_x}{\partial y} \right) \right] \quad (15)$$

222 Bioeffects of Radiofrequency Power Deposition

Assume that (at the moment of time we look) $B_I = B_{Ix}$ ($B_{Iy} = B_{Iz} = 0$). Assume that RF coil conductors lie only along the z direction, then $A_y = A_x = 0$ (remember that B_I is constant).

Let "a" be the radius of the birdcage coil. Without significant coupling, equation (16) becomes:

$$\vec{B}_{Ix} = \frac{\partial \vec{A}_z}{\partial y}; \Rightarrow \vec{A}_z = \vec{B}_I y; \Rightarrow \vec{E}_z = -\omega \vec{B}_I y \quad (16)$$

$$E_{max} = -\omega B_I a \quad (\text{at } (0, a, 0)) \quad (17)$$

Note that the z-component of the RF electric field inside an ideal birdcage coil depends linearly on the radial position. Suppose, for example, that at $\omega = 2\pi$ (63.86-MHz), $a = 0.3$ -m, and $B_I = 14.7\text{-}\mu\text{T}$, then $E_z = (-5898\text{-v/m}^2)y$ and $E_{max} = 1,769\text{-v/m}$.

Equation (16) predicts that the electric fields (and currents) in a birdcage coil of radius, a , need to be sinusoidal to produce a uniform magnetic field:

$$E_z(\theta) = -\omega B_I a \sin(\theta) \quad (18)$$

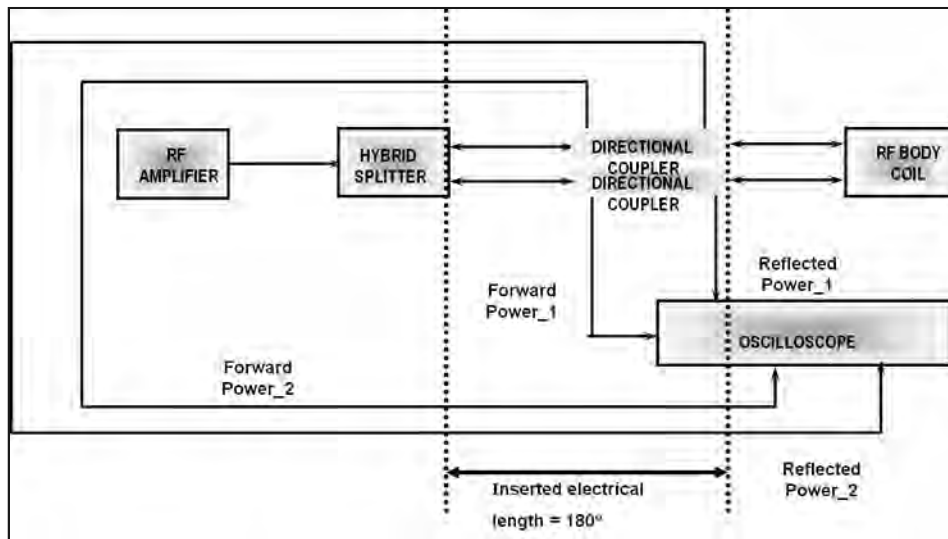
Assume that the "duty cycle" (ratio of average to peak RF power), DC , is 5%. Assume the RF coil length, h , is 0.6-m. Then a conductor of length, L , (where $L \leq h$) making an angle ϕ with the z -axis, will (ignoring RF electrical length and matching issues) experience a voltage, V , induced on it in the birdcage coil:

$$V = -\omega B_I y L \cos(\phi) \quad (19)$$

If the conductor, whose impedance is Z , contacts a patient through a cross section of area, α , the current density, J , may be expressed as:

$$J = \frac{V}{\alpha Z} = \frac{-\omega B_I L \cos(\phi)}{\alpha Z} \quad (20)$$

Figure 8. Experimental measurement of the whole-body-averaged specific absorption rate (SAR).



If the patient conductivity is σ , then the local electric field, E' , in the patient (at the point of conductor contact) is $E' = J/\sigma$. Assume the patient density is ρ . Then the local SAR at the point of contact may be written as:

$$SAR = \frac{\sigma DC|E'|^2}{2\rho} = \frac{DC|\omega B_1 L \cos(\phi)|^2}{2\sigma\rho\alpha^2 Z^2} \quad (21)$$

Therefore, the SAR from conductors in the bore of an MR system may be limited by making the impedance to the body large ($Z = \infty$). SAR from conductors may also be limited by keeping conductors very short ($L = 0$). Additionally, the SAR from conductors may be minimized by routing the conductors down the center of the bore ($y = 0$) or by routing them along $\phi = \pi/2$. Note that the analysis above was for a linear coil in the homogeneous region (away from coil conductors) for simplicity.

WHOLE-BODY SAR MEASUREMENTS

By measuring the RF peak forward, reflected, and (possibly) dummy load power levels required for 180-degree pulses (Figure 8) with a known waveform, it is possible to measure the energy absorbed per pulse by the patient. Note that these measurements may be made while exposing human subjects to very low SAR levels. This information may be used to calculate whole-body SAR for any pulse with that patient in the same location. Details are in a National Electrical Manufacturers Association (NEMA) Standard (54).

224 Bioeffects of Radiofrequency Power Deposition

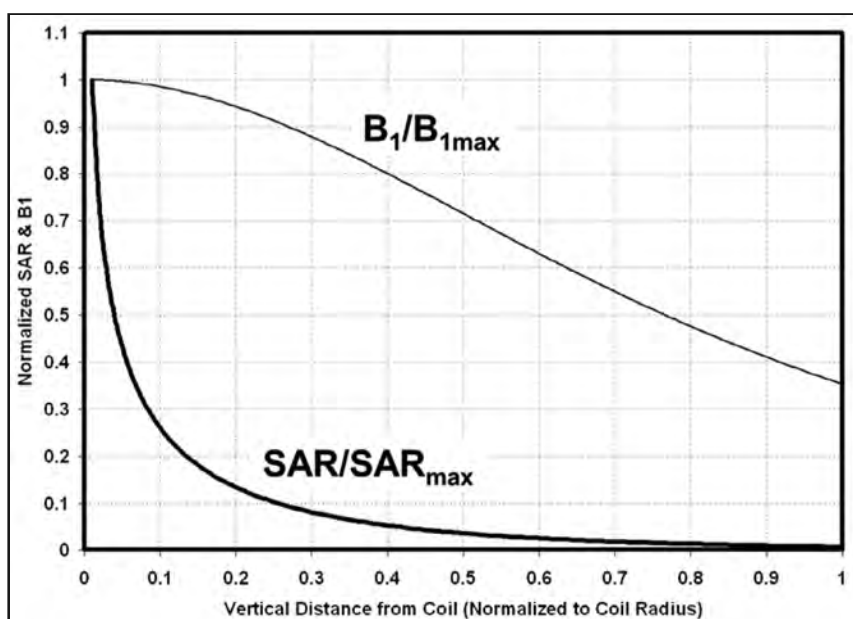
TRANSMIT/RECEIVE SURFACE COILS AND LOCAL SAR

Planar, surface transmit RF coils are often used in MR spectroscopy studies. The primary safety concern with transmit/receive surface coils involves local SAR issues. While it is straightforward to calculate local RF power deposition in volume transmit RF coils, estimation of spatial peak specific absorption rate (SAR) for planar transmit surface coils is complex. To prevent excessive local RF power deposition, it is imperative to at least estimate an upper bound for the local SAR. The local SAR is highest near the coil conductors. For such cases, simplifying assumptions may be made to calculate appropriate design limits (55). Assume there is an anti-parallel pair of infinitely long conductors of width, d , with a return a distance $2 * a_1$ apart. Schenck, et al. (56) showed that the in-plane magnetic vector potential at a distance r from one conductor for the case where $d \ll a_1$ (and where quasi-static conditions apply) may be expressed as:

$$A_z = \frac{\mu_0 I}{4\pi d} \left[4\pi(a_1 - r) + 4r \tan^{-1}\left(\frac{2r}{d}\right) - 4(2a_1 - r) \tan^{-1}\left(\frac{2(2a_1 - r)}{d}\right) + d \ln\left(\frac{4(2a_1 - r)^2 + d^2}{4r^2 + d^2}\right) \right] \quad (22)$$

The local SAR may be calculated by inserting A_z from Equation (22) into Equation (5). It is necessary to scale current to levels that produce the desired B_1 at the desired location. Equations (2) and (22) may be used to find B_1 :

Figure 9. Normalized local SAR and B_1 versus distance for a circular RF coil. B_1 is calculated along the coil axis. The local SAR is calculated from under the coil conductor.



$$B_i = \frac{-\mu I}{\pi d} \left[\tan^{-1} \left(\frac{-2(dr+2a_1-r)}{r^2+d^2-2a_1 r} \right) - \pi \right] \quad (23)$$

Note that the local SAR falls off much faster than B_i (or signal) with distance to the patient. In **Figure 9**, normalized B_i and normalized local SAR are plotted against the normalized distance from a planar, circular coil. A seven-fold reduction in local SAR may be achieved at the expense of a 5% reduction in B_i . Equations (5), (22), and (23) should permit coil designers to theoretically estimate the local SAR. Quasi-static calculations could also be done using Equations (1) through (5).

MEASUREMENT OF LOCAL SAR IN PHANTOMS

It is possible to experimentally measure local SAR in phantoms using materials with electrical properties and density similar to muscle (24, 57-59). To accomplish this, it is useful to use fiber-optic (non-conductive) temperature probes under the transmit RF coil conductors in contact with the tissue-phantom and thermally isolated from the RF coil. The local SAR may be calculated from the early (linear) portion of the heating curve:

$$SAR = C \frac{dT}{dt} \quad (24)$$

In the equation above, C is the specific heat of the tissue and T is the temperature. Equation (24) is expressed in MKS units. Other loss mechanisms (convection, radiation, and conduction) must be minimized during the experiment. Convection may be limited by using a gel-filled phantom (49). Conduction losses may be minimized by keeping materials insulated and by starting with the coil and the “tissue/phantom” at room temperature.

SAFETY CONSIDERATION OF RECEIVE-ONLY RF SURFACE COILS

Exceptionally large surface coil currents may flow if receive-only RF surface coils were resonant while RF excitation pulses are played out on the transmit body RF coil (59-61). These currents may result in extremely high local SAR levels near the surface coil. In addition, the surface coil reaction currents would destroy B_i homogeneity, by generating opposing magnetic fields. To prevent such problems, a blocking network in the surface coil presents a high impedance to limit surface coil currents during RF excitation (**Figure 5**). The blocking impedance required depends on the area of the RF coil, frequency, and how large an opposing field is to be allowed. Typical blocking impedances are a few hundred ohms. Note that in the case of phased array receive coils, special care must be exercised to avoid the development of high local electric fields from differential voltages on adjacent conductors.

226 Bioeffects of Radiofrequency Power Deposition

Unfortunately, surface coil blocking networks may become warm. IEC 60601-1 sets a surface temperature limit ($T_{limit} = 41^\circ\text{C}$) for objects that may touch human subjects (34). Skin temperature under normal, non-MRI or low SAR conditions is approximately 33.0°C . However, during an MRI procedure involving a high SAR level, skin blood vessels dilate, the cutaneous circulation increases, and skin temperatures may approach the level of the core temperature. In tests with phantoms initially at ambient temperature, a 4.0°C rise should be the limit for systems capable of high SAR. For low SAR systems, the surface coil temperature rise may be limited to 8.0°C above ambient temperature.

POTENTIAL MECHANISMS FOR RF BIOEFFECTS

Thermal effects arise from the temperature dependence of most biological functions. Chemical reaction rates approximately double with each 10°C rise in temperature (62). Protein denaturation takes place at temperatures of approximately 45°C (18). The fluidity of cell membranes is also affected by temperature. Thermal effects may be caused by whole body heating of the organism or by localized heating of tissues. During an MRI examination, while only the body parts inside of the transmit RF coil are exposed to RF power deposition, the entire body may be affected by thermal reactions.

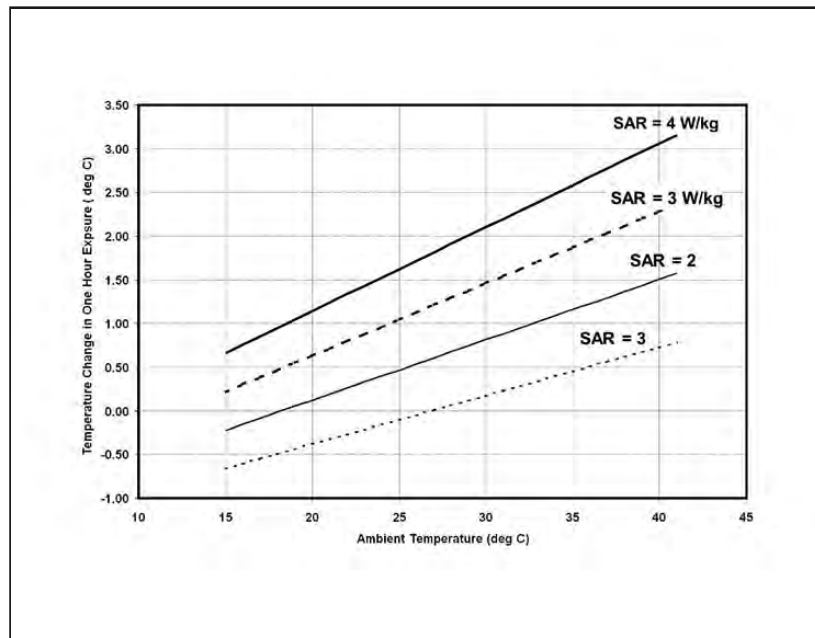
The mechanisms behind non thermal effects are unclear. The energy of a single photon at 85-MHz or 2-Tesla is 5.304×10^{26} Joules (63). The energy of chemical bonds is much larger. In fact, even relatively weak hydrogen bonds between groups in protein structures have energies of 3.125×10^{20} Joules (62). Notably, thermal energy at body temperature is 4.28×10^{21} Joules, five orders of magnitude greater than the energy of RF photons at 2-Tesla (85-MHz).

LITERATURE REVIEW: THERMAL PHYSICS AND PHYSIOLOGY

RF fields are too high in frequency to electrically stimulate excitable tissues (64). Thus, as previously mentioned, the only well-established mechanism for RF energy-related bio-effects is heating (18). Guy, et al. (65) showed that the SAR threshold for cataractogenesis is 100-W/kg. The highest safe core temperature for workers is considered to be 39.4°C (24, 66, 67). The threshold core temperature for teratogenic effects in pregnant women is 38.9°C (60). During the day, core temperature fluctuates approximately 1°C or more (17, 68). Skin temperature fluctuates over a range of 15°C (17). The skin pain threshold is 43°C (69). Finally, the resting metabolic rate is 1.3-W/kg, while during vigorous exercise, in highly trained athletes, may be as high as 18-W/kg (24).

Consider an insulated tissue section. In one hour, the insulated tissue will, when exposed to an SAR of 1.0-W/kg, rise approximately 1.0°C . Insulated tissue would rise to infinite temperature in infinite time at any finite SAR. In use, physiologic heat dissipation mechanisms of the human body limit temperature rise to a steady-state value. A body, whose outer surface temperature, T_{sk} , is warmer than the ambient temperature, T_a , will radiate to the surroundings (17). When exposed to RF power deposition, the body temperature will increase until steady-state conditions prevail. In a steady state, the body dissipates energy to the environment at the same rate that it gains energy from RF power deposition. Temperature in-

Figure 10. Effects of specific absorption rate (SAR, W/kg) and ambient temperature on human core temperature during 60-minute MRI procedures (i.e., based on Adair thermal model assuming a relative humidity of 50%, clothing = 0.2 clo, and a 40% impairment of blood flow at various SAR levels and ambient temperatures).



creases initially, and then asymptotically approaches the final steady state value. The temperature time course may be expressed as:

$$\Delta T = \Delta T_0 (1 - \exp(-\frac{t}{\tau})) \quad (25)$$

In equation (25), τ is a constant, ΔT , is the temperature rise at any time, t , and ΔT_0 , is the steady state temperature rise. Note that an infinite duration RF exposure results in a finite, non-linear temperature rise. If σ_s is taken as the Stefan-Boltzmann constant, and A is the surface area of the body, then the radiated power, P , may be expressed as:

$$P = \sigma_s A (T_{sk}^4 - T_a^4) \approx 4 \sigma_s A T_a^3 \Delta T \quad (26)$$

Consider a hypothetical, uninsulated human subject (70-kg) who is constrained to lose energy to the environment only by radiation. Assume that the ambient temperature is 25°C

228 Bioeffects of Radiofrequency Power Deposition

and the thermal neutral (steady state) temperature of the skin is 33 °C. In a steady state, the hypothetical human would radiate about 1.4-W/kg, which is replaced by his own metabolic energy at the same rate. The result is no change in deep body or core temperature.

Next consider the same hypothetical human, but this time the skin temperature has risen to 38°C (vasodilatation of skin blood vessels may permit the skin to reach core temperature). Now the hypothetical human radiates energy at a rate of 2.4-W/kg, 1-W/kg above his metabolic rate. This hypothetical human might experience a 1.0°C rise in temperature in one hour when exposed to 2-W/kg, demonstrating the importance of ambient temperature to the core temperature rise.

Adair and Berglund (70, 71) utilized a mathematical thermal model of the body, based on the Gagge model (72), to predict the effects of SAR, ambient temperature, impairment of blood flow, relative humidity, clothing, and scan time on core temperature rise. Their summarized results can be approximated with a simple program (71). The Adair program was used to predict the effect of ambient temperature on core temperature rise (10) (**Figure 10**). For the plot, it was assumed that clothing = 0.2 clo, relative humidity was 50%, blood flow impairment was 40%, and the scan duration was 60 minutes. A 40% reduction in cardiac output is life threatening (73). From the plot, it is evident that an exposure to 4-W/kg for an hour should result in only a 1°C core temperature rise when $T_a = 19^\circ\text{C}$. However, if $T_a = 25^\circ\text{C}$, then 3-W/kg is needed. A one hour exposure to 1 W/kg even at $T_a = 27^\circ\text{C}$ should result in no temperature rise. Of course, ambient temperature plays an important role in core temperature rise.

SUMMARY AND CONCLUSIONS

A variety of physical factors affect the manner in which the RF fields used for MRI examinations impact patients. Both whole body and localized depositions of RF energy may result in tissue heating. In consideration of this primary safety concern, regulatory agencies have provided guidelines based on whole-body-averaged and/or peak SARs to ensure the safe operation of MR systems. In this chapter, various techniques of calculating and estimating SARs associated with MRI procedures have been described. Additionally, there has been a discussion of the possible mechanisms responsible for observed RF bioeffects and a review of the thermal physics and mathematical models used to predict human thermal responses to absorption of RF energy. This work served as the basis for characterizing the RF fields used during MRI examinations and helps to estimate the thermophysiological alterations in patients.

REFERENCES

1. Mansfield P, Morris PG. Advances in Magnetic Resonance. In: Waugh JS, Editor. NMR Imaging in Biomedicine. Academic Press, New York, 1982. pp. 310-314.
2. Athey TW. Current FDA guidance for MR patient exposure and considerations for the future. Ann New York Acad Sci 1992;649:242-257.
3. Bernhardt JH. Non-ionizing radiation safety: Radio-frequency radiation, electric and magnetic fields. Phys Med Biol 1992;4:807-844.

MRI Bioeffects, Safety, and Patient Management 229

4. Budinger TF, Cullander C. Health Effects of In vivo Nuclear Magnetic Resonance. In: Margulis AR, Higgins CB, Kaufman L, Crooks LE, Editors. Clinical Magnetic Resonance Imaging. Radiological Research and Education Foundation, San Francisco, 1983.
5. Budinger TF. Emerging nuclear magnetic resonance technologies: Health and safety. Ann New York Acad Sci 1992;649:1-18.
6. Kanal E. An overview of electromagnetic safety considerations associated with magnetic resonance imaging. Ann New York Acad Sci 1992;649:204-224.
7. Persson BRR, Stahlberg F. Seminars on Biomedical Applications of Nuclear Magnetic Resonance. In: Potential Health Hazards and Safety Aspects of Clinical NMR Examinations. Sweden: Radiation Physics Department. 1984.
8. Saunders RD, Smith H. Safety aspects of NMR clinical imaging. Br Med Bull 1984;40:148-154.
9. Schaefer DJ. Safety aspects of magnetic resonance imaging. In: Wehrli FW, Shaw D, Kneeland JB, Editors. Biomedical Magnetic Resonance Imaging: Principles, Methodology and Applications. VCH Publishers, New York. 1988. pp. 553-578.
10. Schaefer DJ. Dosimetry and effects of MR exposure to RF and switched magnetic fields. Ann New York Acad Sci 1992;649:225-236.
11. Schaefer DJ. Bioeffects of MRI and patient safety. Amer Assoc Phys Med 1993;649:607-647.
12. Shellock FG. Biological effects and safety aspects of magnetic resonance imaging. Magn Reson Quarterly 1989;5:243-261.
13. Tenforde TS, Budinger TF. Biological Effects and Physical Safety Aspects of NMR Imaging and In-Vivo Spectroscopy. In: Thomas SR, Dixon RL, Editors. NMR in Medicine: Instrumentation and Clinical Applications, Medical Monograph. No. 14. Amer Assoc Phys Med; 1986. pp. 493-548.
14. Schaefer DJ. Safety aspects of radio frequency power deposition in magnetic resonance. Magn Reson Imaging Clin N Am 1998;6:775-789.
15. Bottomley PA, Andrew ER. RF electromagnetic field penetration, phase shift and power dissipation in biological tissue: Implications for NMR imaging. Phys Med Biol 1978;23:630-643.
16. Shellock FG, Kanal E. Bioeffects of Radiofrequency Electromagnetic Fields. In: Magnetic Resonance: Bioeffects, Safety, and Patient Management. 2nd Edition. Lippincott-Raven Press, New York, 1996. pp. 25-48.
17. Carlson LD, Hsieh ACL. Control of Energy Exchange. Macmillan, London. 1982.
18. Elder JE. Special Senses. In: Elder JE, Cahill DF, Editors. Biological Effects of Radio-Frequency Radiation. North Carolina: US Environmental Protection Agency; 1984. pp. 64-78.
19. U.S. Department of Health and Human Services, Food and Drug Administration. Magnetic resonance diagnostic device. Panel recommendation and report on petitions for MR reclassification. Fed Reg 1988;53:7575-7579.
20. U.S. Department of Health and Human Services, Food and Drug Administration. Recommendation and report on petitions for magnetic resonance reclassification and codification of reclassification, final rule, 21 CFR Part 892. Fed Reg 1989;54:5077-5088.
21. U.S. Department of Health and Human Services, Food and Drug Administration, Center for Devices and Radiological Health, Radiological Devices Branch, Division of Reproductive, Abdominal, and Radiological Devices, Office of Device Evaluation, Guidance for Industry and FDA Staff: Criteria for Significant Risk Investigations of Magnetic Resonance Diagnostic Devices. Issued July 14, 2003.
22. U.S. Department of Health and Human Services, Food and Drug Administration. Criteria for Significant Risk Investigations of Magnetic Resonance Diagnostic Devices Guidance for Industry and Food and Drug Administration Staff. Issued June 13, 2014
23. IEC 60601-2-33, Medical electrical equipment - Part 2: Particular requirements for the safety of magnetic resonance equipment for medical diagnosis. International Electrotechnical Commission (IEC), 2015.

230 Bioeffects of Radiofrequency Power Deposition

24. Durney CH, Johnson CC, Barber PW, et al. Radiofrequency Radiation Dosimetry Handbook. 2nd Edition. 1978; pp. 8-126.
25. Henriques, FC, and Moritz, AR. Studies of thermal injury. I. The conduction of heat to and through skin and the temperatures attained therein. A theoretical and an experimental investigation. *Am J Pathol* 1947; 23:1-549.
26. Moritz AR, Henriques FC. Studies of thermal Injury. II. The relative importance of time and surface temperature in the causation of cutaneous burns. *Am J Pathol* 1947;23:695-720.
27. Sapareto, DA and Dewey, WC, Thermal dose determinations in cancer therapy, *International Journal of Radiation Oncology* 1984;10:87-800.
28. Van Rhoon GC, Samaras T, Yarmolenko PS, Dewhirst MW, Neufeld E, Kuster N. CEM43°C thermal dose thresholds: A potential guide for magnetic resonance radiofrequency exposure levels? *Eur Radiol* 2013;22:215-27.
29. Pennes HH. Analysis of tissue and arterial blood temperatures in the resting human forearm. 1948, *J Appl Physiol* (1985). 1998;85:5-34.
30. Van den Brink JS. Thermal effects associated with RF exposures in diagnostic MRI: Overview of existing and emerging concepts of protection. *Concepts in Magnetic Resonance* 2019;1-17
31. Sienkiewicz Z, Van Rongen E, Croft R, Ziegelberger G, Veyret B. A closer look at the thresholds of thermal damage: Workshop Report by an ICNIRP Task Group. *Health Phys* 2016;111:300-306.
32. American Society for Testing and Materials (ASTM) International, F2503 Practice for marking medical devices and other items for safety in the magnetic resonance environment. West Conshohocken, PA.
33. Van Rhoon GC, Aleman A, Kelfkens G, et al. No need to change from SAR to time-temperature relation in electromagnetic fields exposure limits, *International Journal of Hyperthermia*. 2011;27:399-404.
34. IEC 60601-1-1, Medical electrical equipment - Part 1: General requirements for safety; safety requirements for medical electrical systems, 2005-12, International Electrotechnical Commission (IEC), 2005.
35. Kanal E, Barkovich AJ, Bell C, et al. ACR guidance document on MR safe practices: 2013. *J Magn Reson Imaging* 2013;37:501-530.
36. ISO/TS 10974:2011, Assessment of the safety of magnetic resonance imaging for patients with an active implantable medical device. ISO, Case postale 56 CH-1211 Geneva 20, 2011.
37. American Society for Testing and Materials (ASTM) International, F1542 Specification for the requirements and disclosure of self-closing aneurysm clips. West Conshohocken, PA.
38. American Society for Testing and Materials (ASTM) International, F2052 Test method for measurement of magnetically induced displacement force on medical devices in the magnetic resonance environment. West Conshohocken, PA.
39. American Society for Testing and Materials (ASTM) International, F2119 Test method for evaluation of MR image artifacts from passive implants. West Conshohocken, PA.
40. American Society for Testing and Materials (ASTM) International, F2182 Measurement of radio frequency induced heating near passive implants during magnetic resonance imaging. West Conshohocken, PA.
41. American Society for Testing and Materials (ASTM) International, F2213 Measurement of Magnetically Induced Torque on Medical Devices in the Magnetic Resonance Environment. West Conshohocken, PA.
42. Bottomley PA, Roemer PB. Homogeneous tissue model estimates of RF power deposition in human NMR studies. Local elevations predicted in surface coil decoupling. *Ann N Y Acad Sci* 1992;649:144-59.
43. Ramo S, Whinnery JR, Van Duzer T. Fields and Waves in Communication Electronics. 3rd Edition. New York: J Wiley & Sons; 1965. pp. 108-124.
44. Plonus MA. Applied Electromagnetics. New York: McGraw-Hill; 1984. pp. 290-299, 453.
45. Schenck JF, Hussain MA. Power deposition during magnetic resonance: The effects of local electrical inhomogeneities and field exclusion. General Electric Corporate Research and Development Labs. 1984.

MRI Bioeffects, Safety, and Patient Management 231

46. Collins CM, Mao W, Liu W, Smith MB. Calculated local and average SAR in comparison with regulatory limits. *Proc Intl So Mag Reson Med* 2006;14:2044.
47. Davis PL, Crooks L, Arakawa M, et al. Potential hazards in NMR imaging: heating effects of changing magnetic fields and RF fields on small metallic implants. *Am J Roentgenol* 1981;137:857-860.
48. Chou CK, McDougall JA, Chan KW. RF heating of implanted spinal fusion stimulator during magnetic resonance imaging. *IEEE Trans Biomed Eng* 1997;44:367-373.
49. Lemieux L, Allen PJ, Franconi F, et al. Recording of EEG during fMRI experiments: Patient safety. *Magn Reson Med* 1997;38:943-952.
50. Hofman MB, de Cock CC, van der Linden JC, et al. Transesophageal cardiac pacing during magnetic resonance imaging: Feasibility and safety considerations. *Magn Reson Med* 1996;35:413-422.
51. Hess T, Stepanow B, Knopp MV. Safety of intrauterine contraceptive devices during MR imaging. *Eur Radiol* 1996;6:66-68.
52. Shellock FG. Reference Manual for Magnetic Resonance Safety, Implants, and Devices: 2020 Edition. Biomedical Research Publishing Group, Los Angeles, CA, 2020.
53. Athey TW. A model of the temperature rise in the head due to magnetic resonance imaging procedures. *Magn Reson Med* 1989;177-184.
54. NEMA MS 8-1993. Characterization of the specific absorption rate for magnetic resonance imaging systems. National Electrical Manufacturers Association, 2008.
55. Schaefer DJ. Estimation of current limits for RF power deposition from planar, transmit surface coils. New York: Abstracts of the Society of Magnetic Resonance Imaging; 1996. pp. 1446.
56. Schenck JF, Boskamp EB, Schaefer DJ, Barber WD, Vander Heiden RH. Estimating local SAR produced by RF transmitter coils: examples using the birdcage coil. Berkeley: Abstracts of the International Society of Magnetic Resonance in Medicine; 1998. pp. 649.
57. Chou CK, Chen GW, Guy AW, Luk KH. Formulas for preparing phantom muscle tissue at various radiofrequencies. *Bioelectromagnetics* 1984;5:435-441.
58. Gandhi OP, Chien, JY. Absorption and distribution patterns of RF fields. *Ann New York Acad Sci* 1992;649:131-143.
59. Grandolfo M, Polichetti A, Vecchia P, Gandhi OP. Spatial distribution of RF power in critical organs during magnetic resonance imaging. *Ann New York Acad Sci* 1992;649:178.
60. Buchli R, Saner M, Meier D, Boskamp EB, Boesiger P. Increased RF power absorption in MR imaging due to RF coupling between body coil and surface coil. *Magn Reson Med* 1989;9:105-112.
61. Boesiger P, Buchli R, Saner M, Meier D. An overview of electromagnetic safety considerations associated with magnetic resonance imaging. *Ann New York Acad Sci* 1992;649:160-165.
62. Lehninger AL. Biochemistry. New York: Worth; 1972.
63. Halliday D, Resnick R. Physics. New York: John Wiley; 1966.
64. Kennelly AE, Alexanderson EFW. The physiological tolerance of alternating current strengths up to frequencies of 100,000 cycles per second. *Electrical World* 1910;56:154 156.
65. Guy AW, Lin JC, Kramer PO, Emery AF. Effect of 2450 MHz radiation on the rabbit eye. *IEEE Trans Microwave Theory Tech* 1975;23:492 498.
66. Goldman RF, Green EB, Iampietro PF. Tolerance of hot wet environments by resting men. *J Appl Physiol* 1965;20:271 277.
67. Smith DA, Clarren SK, Harvey MAS. Hyperthermia as a possible teratogenic agent. *Pediatrics* 1978;92:878-883.
68. Ganong WF. Review of Medical Physiology. 6th Edition. Los Altos: Lange Medical Publications; 1973. pp. 193-197, pp. 474-476.
69. Benjamin FB. Pain reaction to locally applied heat. *J Appl Physiol* 1952;52:250-263.

232 Bioeffects of Radiofrequency Power Deposition

70. Adair ER, Berglund LG. On the thermoregulatory consequences of NMR imaging. Magn Reson Imaging 1986;4:321-333.
71. Adair ER, Berglund LG. Thermoregulatory consequences of cardiovascular impairment during NMR imaging in warm/humid environments. Magn Reson Imaging 1989;7:25-35.
72. Gagge AP. The New Effective Temperature (ET) An Index of Human Adaptation to Warm Environments. In: Horvath S, Yousef M, Editors. Environmental Physiology: Aging, Heat, and Altitude. 1980. pp. 9 77.
73. Hurst J, Willis ED. The Heart. McGraw-Hill, New York, 1978.

Chapter 8 Radiofrequency-Energy Induced Heating During MRI: Laboratory and Clinical Experiences

FRANK G. SHELLOCK, PH.D.

Director of MRI Safety
USC Stevens Neuroimaging and Informatics Institute

Adjunct Clinical Professor of Radiology and Medicine
Keck School of Medicine, University of Southern California
Los Angeles, CA

INTRODUCTION

Radiofrequency (RF) energy is nonionizing, electromagnetic radiation in the frequency range of 20-kHz to 3,000-GHz (1-7). The RF spectrum includes radar, ultra high frequency (UHF), and very high frequency (VHF) television, AM and FM radio, and microwave communication frequencies. During magnetic resonance imaging (MRI), most of the transmitted radiofrequency (RF) power is transformed into heat within the patient's tissue as a result the induction of eddy currents due to the nonzero conductivity of tissue via Faraday's law. Not surprisingly, the primary health effects and safety concerns associated with RF energy-induced heating are directly related to the thermogenic qualities of this electromagnetic field (1-58). The deposition of thermalizing energy in the human body by exposure to RF fields provides a unique exception to the energy flows normally encountered by human subjects.

Research investigations conducted over the last several decades have indicated that exposure to RF radiation may produce a variety of physiologic effects including those associated with alterations in visual, auditory, endocrine, neural, cardiovascular, immune, reproductive, and developmental function (1-50). In general, these biological changes occur due to RF-induced heating. Exposure to RF energy may also cause athermal, field-specific changes in biological systems that are produced without an increase in temperature (59-62). However, athermal effects associated with RF radiation are not well understood and, to date, have not been systematically studied with respect to MRI.

234 Radiofrequency-Energy Induced Heating During MRI

Prior to 1985, there were no published reports pertaining to the effects of exposing human subjects to RF energy during MRI examinations. In fact, there was a general paucity of quantitative data on thermal and other physiological responses of human subjects exposed to RF radiation from any source. The previous investigations that were conducted on this topic typically examined responses to therapeutic applications of diathermy or thermal sensations related to exposure to RF radiation (38-45). Because localized or limited exposures to RF energy were unlike the conditions that occur during MRI, the information gained from the prior studies could not be used to derive an understanding or prediction of what to expect with respect to the use of MRI technology. Therefore, to properly characterize the thermophysiological aspects of RF energy, investigations were conducted using laboratory animals, volunteer subjects, and patients (8, 9, 12-19, 24, 25, 27-37, 51-54). The resulting research yielded extremely useful and important data with regard to thermoregulatory responses to RF radiation-induced heating associated with MRI.

This chapter will review and discuss the various aspects of RF energy-induced heating during MRI with an emphasis on the studies performed in human subjects to assess thermal and other physiologic responses. For additional information on this important topic, readers are referred to the chapter in this textbook by Johan van den Brink, Ph.D., **Thermal Effects Associated with RF Exposures During Clinical MRI**.

MRI PROCEDURES AND SPECIFIC ABSORPTION RATE

The thermoregulatory and other physiologic changes that a laboratory animal or human subject exhibits in response to exposure to RF radiation are directly dependent on the amount of energy that is absorbed (1-7, 22-26, 29, 31, 37, 49). The basic dosimetric term used to describe the absorption of RF radiation is the specific absorption rate, or SAR. The SAR is the mass normalized rate at which RF power is coupled to biological tissue and is typically indicated in units of watts per kilogram (W/kg).

The relative amount of RF radiation that an organism encounters during an MRI examination is usually characterized with respect to the whole-body averaged and peak SAR levels (i.e., the SAR averaged in one-gram of tissue). In some instances, other values may also be reported by the MR system, including the “local” body SAR. Importantly, SAR information is used by regulatory agencies with regard to safety guidelines for the exposure to RF energy during MRI and has particular relevance with respect to scanning patients with medical implants.

Notably, measurements or estimates of SAR are not trivial, particularly in human subjects (1-3, 6, 10, 49, 63). Several methods exist to determine this parameter for the purpose of RF energy dosimetry in association with the use of MRI. The SAR that is produced during MRI is a complex function of numerous variables including the frequency (i.e., determined by the strength of the static magnetic field, with resonant frequencies producing the greatest effects), the type of RF pulse used (e.g., 90° vs. 180° pulse), the repetition time, the type of transmit RF coil used (e.g., linear vs. circularly-polarized or quadrature transmission, transmit whole body vs. local RF coil, etc.), the volume of tissue contained within the RF coil, the shape of the anatomical region exposed, the orientation of the body to the field vectors, as well as other factors (1-3, 6, 10, 49, 63). Therefore, SAR, being a critical parameter that

is used to ensure the safety aspects of exposure to RF energy, is difficult to calculate or estimate precisely for MRI examinations. Interestingly, MR system manufacturers appear to apply various safety or modeling factors to the SAR values reported by their scanners. Thus, manufacturers err on the side of safety when estimating SAR values for clinical MRI (10, 49).

RF ENERGY-INDUCED HEATING AND MRI: EVALUATION OF LABORATORY ANIMALS

Although there have been several studies performed using laboratory animals to assess thermoregulatory reactions to tissue heating associated with exposure to RF radiation, these experiments do not directly apply to the specific conditions that occur with MRI. Furthermore, the results of these investigations cannot be easily extrapolated to provide useful information for human subjects (1-5, 38, 47, 64). For example, the pattern of RF coupling and resulting absorption of RF energy to biological tissues is primarily dependent on the organism's size, anatomical features, the duration of exposure, the sensitivity of the involved tissues, and a myriad of other variables (1-5, 38, 47, 64).

Importantly, it is well known that there is no laboratory animal that sufficiently mimics or simulates the thermoregulatory responses with respect to the dimensions, anatomical features, and specific responses that occur in human subjects. Therefore, experimental results obtained in laboratory animals cannot be simply "scaled" or extrapolated to predict thermoregulatory or other physiologic changes in human subjects exposed to RF radiation-induced heating during MRI. Nevertheless, experiments have been conducted in the MRI environment using laboratory animals as an initial step to determine the effects of RF energy-induced heating associated with exposures to high SAR levels (19, 27, 51-54).

Shuman, et al. (19) studied laboratory dogs undergoing MRI at relatively high levels of RF energy. Superficial- and deep-tissue temperatures were measured in five animals before, during, and after exposure to RF energy determine whether significant temperature changes could be produced in association with operation of a 1.5-T/64-MHz MR system (19). The RF power output that was applied in this investigation was 6.3 times that required for routine MRI exams, with calculated SARs that averaged 7.9-W/kg (19). Shuman, et al. (19) reported that there was a linear temperature increase of several degrees, with a maximal average temperature rise of 4.6°C that was measured in the urinary bladder (i.e., a "deep" body site). Overall, the temperature elevations were slightly greater in deeper tissues compared to those recorded in superficial tissues. Shuman, et al. (19) stated that these findings suggested continued caution in the design and operation of MR systems that were capable of depositing high SAR levels, particularly when the scanners were used to image infants or patients with altered thermoregulatory capabilities.

While the results of Shuman, et al. (19) are intriguing, it should be noted that this study was conducted in anesthetized laboratory animals. As such, the findings do not pertain to conscious, adult human subjects because of the previously discussed factors related to the physical dimensions of the animals and the fact that anesthetic agents substantially impact thermoregulation (65, 66). Additionally, the thermoregulatory systems of these two species are quite dissimilar (e.g., the dog pants to dissipate heat while human subjects sweat). Nev-

236 Radiofrequency-Energy Induced Heating During MRI

ertheless, data obtained by Shuman, et al. (19) may have implications for the use of MRI in pediatric patients because this patient population is typically sedated or anesthetized and the physical dimensions of the laboratory dog are somewhat comparable to a pediatric patient.

Barber, et al. (27) also conducted a study to determine the effects of heating related to MRI. The objective of their investigation was to provide a worst-case estimate of the thermal effects of MRI by subjecting anesthetized, unshorn sheep to RF power deposition at SAR levels well above approved standards for periods of time in excess of normal clinical imaging protocols (27). The sheep underwent MRI using a 1.5-Tesla, 64-MHz MR system. A control period with no RF power was followed by experiments using 20- to 105-minutes of RF power applications. Afterward, there was a 20-minute or longer recovery period with no RF energy applied to the sheep. Eight sheep were scanned at whole-body averaged SARs that ranged from 1.5- to 4.0-W/kg while rectal and skin temperatures were monitored. In addition to the whole-body RF exposures, Barber, et al. (27) subjected four sheep to MRI exams involving the head to determine the effects of RF energy-induced heating of the brain. The average scan time was 75-minutes and temperatures of the cornea, vitreous humor, scalp skin, jugular vein, and rectum were measured during the experiment.

In the whole-body exposure experiments, elevation of rectal temperature was correlated with RF energy deposition. Deep body temperature rises in excess of 2°C were attained for the whole-body averaged SAR level of 4.0-W/kg during exposure periods greater than 82-minutes. In the head scanning experiments, skin and eye temperatures increased approximately 1.5°C. Additionally, jugular vein temperature increased a maximum of 0.4°C after an average exposure time of 75-minutes. Sheep exposed for 40-minutes to an SAR of 4.0-W/kg in either the transmit body RF coil (three sheep) or transmit head RF coil (two sheep) were recovered and observed to be in good health after 10 weeks. Importantly, no cataracts were found in the sheep (27). Thus, using this animal model, Barber, et al. (27) concluded that RF power deposition at SAR levels well above typical clinical MRI protocols caused various tissue temperatures to increase. Furthermore, for exposure periods in excess of standard clinical MRI protocols, the temperature increases were insufficient to cause adverse thermal effects (27).

Shrivastava, et al. (51) investigated RF field-induced heating of the head at 9.4-Tesla in anesthetized swine. Temperatures were measured at three depths: inside the brain, in the rectum, and at the scalp skin of the swine. A 400-MHz, continuous wave RF power was deposited to the head using a volume coil. The whole-head averaged SAR values were varied between 2.7- to 5.8-W/kg. The RF power exposure durations were varied between 1.4 to 3.7 hours. In order to differentiate the temperature response caused by the RF energy from that associated with the anesthesia, temperatures were recorded in four “unheated” swine. The findings demonstrated that *in vivo* brain temperatures correlated well with the average SAR values. Furthermore, the skin temperature changes were not the maximum temperature alterations that were recorded, the RF energy heating caused an inhomogeneous brain temperature distribution, and the maximum temperature occurred inside the brain (51). While interesting, these findings only have relevance to MRI-related heating at 9.4-Tesla/400-MHz.

In another study by Shrivastava, et al. (52) that was also conducted in swine at 9.4-Tesla/400-MHz, temperatures were measured in the scalp skin, brain, and rectum. “Sham RF” was delivered to three swine to understand the thermal effects of anesthesia. Continuous wave RF energy was delivered to six animals for 2.5 to 3.4 hours. The whole-head averaged SAR varied between 2.71-W/kg and 3.20-W/kg. Anesthesia caused the brain and rectal temperatures to decrease in a linear manner. Altered thermoregulatory responses were detected by comparing the differences in the temperature slopes before and after the delivery of RF energy. RF-induced heating significantly altered the rate of cooling down of the animal. The temperature slope changes correlated well with the RF energy per unit head weight and the duration of heating, as well as the maximum rectal temperature change during heating. Again, these results apply only to MRI-related heating at 9.4-Tesla/400-MHz.

Shrivastava, et al. (53) also investigated RF heating in a porcine model at 7-Tesla/298-MHz. Temperatures were measured in the scalp skin, brain, and rectum in four pigs exposed to continuous wave RF. The RF power was delivered to the pig’s head for approximately 3 hours at a whole-head averaged SAR of approximately 3-W/kg. Simple bioheat transfer models were used to simulate the RF power induced temperature changes. The results indicated that the RF power produced uniform temperature changes in the heads of the pigs with no plateau achieved during heating. The researchers concluded that validated bioheat models may predict accurate temperature changes related to RF energy-induced heating of the head. Since 7-Tesla MR systems are presently used in research and clinical settings, this information is of interest to the MRI community.

CHARACTERISTICS OF RF ENERGY-INDUCED HEATING: IMPLICATIONS FOR HUMAN SUBJECTS

The physical dimensions and anatomic configurations of biologic tissues in relation to the incident wavelength are important factors that determine the relative amount and pattern of RF energy that is absorbed by the human body (1-5, 38, 47, 64). For example, if the size of the tissue is large in relation to the incident wavelength, RF energy is predominantly absorbed on the surface. If it is small relative to the wavelength, there is little absorption of RF power and, thus, the effects of heating are minimized (1-5, 38, 47, 64).

As previously mentioned, tissue heating that results from the RF energy used during MRI is primarily caused by magnetic induction, with a negligible contribution from the electric fields (10, 49). Because of the RF frequencies used for MRI, this ohmic tissue heating is greatest at the surface or periphery and minimal at the center of a human subject’s body. Predictive calculations and measurements obtained in phantoms, laboratory animals, and human subjects exposed to various MRI conditions support this pattern of temperature distribution (14-36, 50, 51).

The actual increase in tissue temperature caused by exposure to RF energy is dependent on a variety of factors related to the thermoregulatory system of the individual and the surrounding environment (1-5, 8-38, 44-55). In regards to the thermoregulatory system, when subjected to a thermal challenge, the human body loses heat by means of convection, conduction, radiation, and evaporation (38, 67-70). Each mechanism is responsible to a varying degree for heat dissipation, as the body attempts to maintain thermal homeostasis. If the

238 Radiofrequency-Energy Induced Heating During MRI

thermoregulatory effectors are not capable of totally dissipating the heat load, heat accumulates and is stored, resulting in an elevation in local and/or overall tissue temperatures (38, 67-70).

Underlying health conditions may seriously impact an individual's ability to tolerate a thermal challenge. These conditions include cardiovascular disease, hypertension, diabetes, spinal cord injuries, fever, old age, and obesity (71-78). Various medications (e.g., diuretics, beta-blockers, calcium blockers, vasodilators, amphetamines, muscle relaxers, sedatives, anesthetic agents, etc.) can also greatly alter thermoregulatory responses to a heat load (65, 66). In fact, certain medications may have a synergistic effect with respect to tissue heating if the thermal load is specifically caused by exposure to RF radiation (65).

The environmental conditions that exist in and around the MR system will also affect temperature elevations associated with RF energy-induced heating. Thus, during MRI, the amount of tissue heating that occurs is dependent upon environmental factors that include the ambient temperature, relative humidity, and airflow within and through the bore of the scanner.

With further regard to the environmental conditions of the MR system, it has been proposed that, in order to counterbalance excessive tissue heating that may occur during exposure to high levels of RF energy, patients should be "pre-cooled" before their MRI exams. However, the subjective perception to the environmental temperature depends on the gradient of temperature that is sensed by the individual's peripheral thermoreceptors such as those located throughout the skin and superficial tissues. Therefore, a patient going from a cooler (i.e., using a "pre-cooled" room) to a warmer environment (i.e., the MR system) would very likely be uncomfortable.

IMPORTANT CONSIDERATIONS FOR THE EVALUATION OF PHYSIOLOGICAL CHANGES DURING RF ENERGY-INDUCED HEATING

Acquiring measurements of temperature and other physiologic parameters in human subjects within the harsh electromagnetic environment of the MR system is not a simple task. The static magnetic field of the MR system can easily create missiles out of conventional monitoring devices because they usually contain ferromagnetic components (79-82). Furthermore, the static, time-varying gradient, and RF electromagnetic fields may adversely interfere with the proper operation of monitoring equipment. In turn, the measurement devices may produce subtle or substantial artifacts by generating electromagnetic interference that can impact the quality of the MR images. Therefore, temperature recording devices and physiologic monitors must be specially designed or modified and then rigorously tested prior to use in the MRI setting. Otherwise, the data pertaining to thermal and other physiologic responses may be erroneous and misleading. Another solution to this important matter is to simply use MR Conditional monitoring equipment that has been thoroughly tested and demonstrated to work appropriately in the MR system room.

Currently, MR Conditional temperature recording devices and physiologic monitors, as well as other patient support devices are commercially available for use in the MRI environment. Every physiologic parameter that is typically recorded in the critical care area

or operating room setting may be obtained during MRI, including heart rate, oxygen saturation, end-tidal carbon dioxide, respiratory rate, blood pressure, cutaneous blood flow and, most importantly, body and skin temperatures (79-83).

For the assessment of thermal responses during MRI, volunteer subjects and patients have been monitored throughout the experimental procedures using several different types of devices (9, 12, 13, 16, 17, 24-36, 79-84). For example, sublingual pocket or tympanic membrane temperatures have been obtained immediately before and after MRI using sensitive electronic thermometry or infrared devices. Notably, there is a good relationship between temperatures measured in the sublingual pocket or tympanic membrane and esophageal temperature, which is an indicator of core or “deep” temperature.

Skin temperatures have been measured immediately before and after MRI examinations using highly sensitive and accurate infrared thermometry or digital thermographic equipment (9, 12, 13, 16, 17, 24, 25, 31). Body and skin temperatures measured at multiple sites have been recorded before, during, and after MRI using a fluoroptic (i.e., fiber-optic) thermometry system that is unperturbed by electromagnetic radiation of all types, including static magnetic fields of up to 9.0-Tesla (9, 12, 13, 16, 17, 24, 25, 31, 83). Heart rate, oxygen saturation, blood pressure, respiratory rate, and cutaneous blood flow, which are important physiological variables that change in human subjects in response to a thermal load, have been monitored before, during, and after MRI to assess the reaction of the thermoregulatory system to exposures to RF energy-induced heating. All of these parameters may be assessed using devices that have been extensively tested and demonstrated to provide sensitive and accurate data in the MRI environment.

RF ENERGY-INDUCED HEATING AND MRI: ASSESSMENT OF VOLUNTEER SUBJECTS AND PATIENTS

As previously described in this chapter, the increase in tissue temperature caused by exposure to RF energy during MRI depends on multiple physical, physiological, and environmental factors. These include the rate at which RF energy is deposited, the status of the patient’s thermoregulatory system, the presence of an underlying health condition or medications, and the ambient conditions within the MR system.

Although the main cause of tissue heating associated with MRI is attributed to RF radiation, reports have suggested that exposure to powerful static magnetic fields may also cause temperature changes (85, 86). However, the mechanism responsible for such an effect remains unclear. Nevertheless, the results of these previously published studies warranted investigations in human subjects to determine the possible contribution of the static magnetic field to temperature changes that may be observed during MRI (87-89).

Studies have been performed in human subjects exposed to a 1.5-Tesla static magnetic field to evaluate thermal alterations produced in body and/or skin temperatures (87, 88). The data revealed that there were no statistically significant alterations in any of the recorded tissue temperature or other physiologic parameter. Chakeres, et al. (89) evaluated human subjects exposed to an 8-Tesla static magnetic field and reported no significant change in body temperature. Furthermore, Tenforde (90) examined this phenomenon in laboratory ro-

240 Radiofrequency-Energy Induced Heating During MRI

dents exposed to static magnetic fields of as high as 7.55-Tesla and also reported no thermal effect. Accordingly, static magnetic fields used for clinical and research applications do not cause an elevation in body temperature. As far as the potential for the production of heat by time-varying gradient magnetic fields is concerned, an elevation in tissue temperature is not believed to occur due to MRI (15, 19, 20, 22).

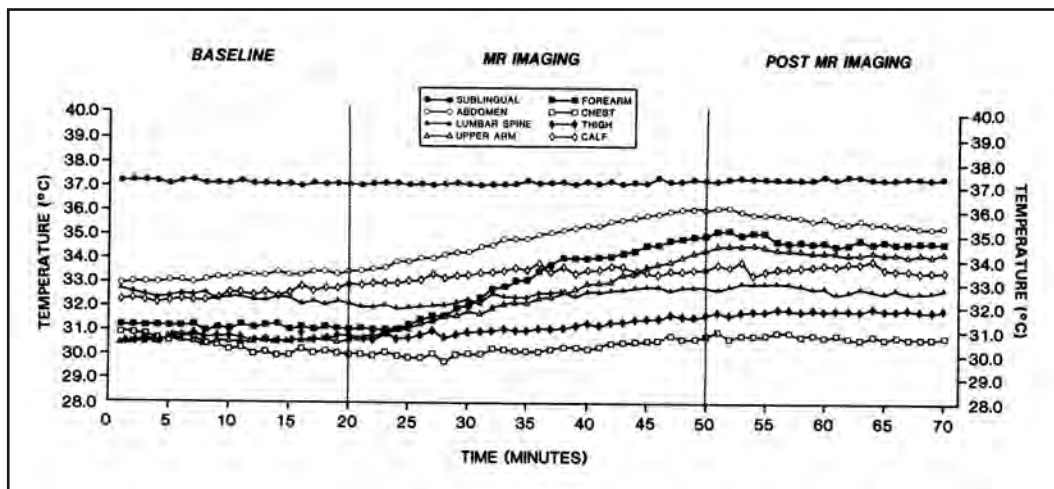
With respect to the effects of RF energy-induced heating, Schaefer, et al. (8) conducted the first study of human thermal responses associated with MRI in 1985. It should be realized that, during this time, the whole-body averaged SAR recommended by the United Kingdom, National Radiological Protection Board and the United States, Food and Drug Administration for clinical MRI was 0.4-W/kg (91, 92), which is an order of magnitude lower than what it is today (93, 94). Temperature changes and other physiologic parameters were assessed in volunteer subjects exposed to relatively high, whole-body averaged SAR levels (approximately 4.0-W/kg). The findings indicated that there were no excessive temperature elevations or other deleterious physiologic consequences related to exposure to RF radiation (8).

Several studies were subsequently conducted involving volunteer subjects and patients undergoing MRI at 1.5-Tesla/64-MHz with the intent of obtaining information that would be applicable to the patient population typically encountered in the MRI setting (12, 13, 15-18, 24, 25, 28, 30-36). The whole-body averaged SAR levels ranged from approximately 0.05-W/kg (e.g., for MRI exams involving the use of a transmit/receive head RF coil) to 6.0-W/kg (e.g., for MRI exams involving the spine or abdomen with a transmit/receive body RF coil), which greatly exceeds the limit for the whole-body averaged SAR of 4.0-W/kg (12, 13, 15-18, 24, 25, 28, 30-36, 93, 94). By way of example, **Figure 1** shows the body and skin temperature changes related to MRI performed at 1.5-Tesla/64-MHz and a whole-body averaged SAR of 2.8-W/kg.

Boss, et al. (32) conducted one of the few investigations that addressed heating at 3-Tesla/128-MHz in human subjects. Eighteen volunteers were divided into three groups: those that underwent MRI of the (1) head, (2) pelvis, or (3) knee. MRI was performed up to the First Level Controlled Operating Mode, allowing RF radiation up to the legal limit for the whole-body averaged SAR (i.e., 4.0-W/kg). Temperature changes were measured using a fiber-optic thermometer and an infrared camera. Temperature rises were highest for the scans involving the pelvis compared to the head and knee. There were no significant changes in heart rate or blood pressure. The authors concluded that MRI at 3-Tesla/128-MHz resulted in measurable and perceptible thermal energy deposition. However, under the conditions of the study, the physiological changes were regarded as safe concerning thermoregulatory and cardiovascular stress.

Isaacson, et al. (33) determined core body temperature (i.e., temporal artery temperature) variations in a large group of pediatric patients ($N = 400$) that underwent MRI on 1.5-Tesla or 3-Tesla scanners, with and without propofol sedation. For patients with complete pre- and post-MRI temperature data, mean temperatures did not significantly change. However, temperature changes differed significantly between propofol-sedated and non-sedated patients (i.e., non-sedated patients had slightly higher temperatures). Patients scanned at 3-Tesla had statistically higher temperature changes compared to those scanned at 1.5-Tesla.

Figure 1. Body (sublingual pocket) and multiple skin temperatures measured at one-minute intervals using a fluoroptic thermometry system before (baseline), during (MRI), and after (post-MRI) MRI performed at a whole-body averaged SAR of 2.8-W/kg. Note that there were little or no changes in body temperature, whereas there were slight to moderate changes in skin temperatures depending on the site of measurement during MRI. After MRI, some skin temperatures returned to the baseline level, whereas others remained elevated during the 20-min post-MRI evaluation period.



In another investigation involving pediatric patients imaged at 3-Tesla, Cawley, et al. (34) recorded rectal temperatures in 25 neonates that underwent MRI of the brain and reported no significant “hyperthermic threat”.

Fumagalli, et al. (36) evaluated the effects of MRI of the brain at 3-Tesla in 49 newborns (i.e., born preterm and at term). Rectal and skin temperatures, oxygen saturation and heart rate were recorded before, during, and after the scans. There was a statistically significant increase in skin temperature, while there was no significant change in rectal temperature, heart rate or oxygen saturation. The investigators concluded that core temperature, heart rate, and oxygen saturation in newborns were not affected by 3-T MRI of the brain.

Kim, et al. (35) investigated the relationship between the increase in body temperature and the RF power deposited during routine clinical MRI exams of the head at 1.5-Tesla and 3-Tesla. Tympanic membrane temperature was recorded in 69 patients immediately before and after MRI. The findings indicated a link between increasing age and body temperature, as well as an influence on the field strength of the MRI exam. Thus, a higher increase in body temperature was observed in older patients after a 3-Tesla MRI procedure compared to a 1.5-Tesla scan.

To date, the studies performed in human subjects demonstrated that changes in body temperatures were physiologically inconsequential (i.e., less than 1.0°C). While there was a tendency for statistically significant increases in skin temperatures to occur, these were not physiologically deleterious or otherwise problematic. Furthermore, there were no sub-

242 Radiofrequency-Energy Induced Heating During MRI

stantial alterations in the hemodynamic parameters that were assessed during these investigations (i.e., heart rate, blood pressure, and cutaneous blood flow).

Interestingly, research has indicated that there is a poor correlation between changes in body and skin temperatures versus whole-body averaged SARs for clinical MRI exams (**Figure 2**). This finding is not surprising considering the previously mentioned myriad of variables that may alter thermal responses in a patient population. Therefore, the thermal responses to a given whole-body averaged SAR may be extremely variable depending on the individual's thermoregulatory system and the presence of one or more underlying condition(s) that can alter or impair the ability to dissipate heat, as well as the environmental conditions of the MR system room.

Presently, the highest level of exposure to RF energy that has been reported for human subjects undergoing MRI is a whole-body averaged SAR of 6.0-W/kg (31). In this investigation, Shellock, et al. (31) conducted experiments involving volunteer subjects to characterize thermal and other physiologic responses to this high level of RF energy. The motivation for this study coincided with the advent of pulse sequences that had relatively high SAR levels associated with their use.

The temperature of the tympanic membrane (i.e., an index of deep body temperature) and seven different skin temperatures were monitored along with blood pressure, heart rate, oxygen saturation, and cutaneous blood flow (**Figure 3**)(31). Measurements were obtained immediately before, during, and after exposure to RF energy. Statistically significant increases in the temperatures of the tympanic membrane and the skin of the chest, abdomen, upper arm, hand, and thigh occurred. In addition, there were statistically significant increases in heart rate and cutaneous blood flow associated with exposure to the high SAR level. Importantly, the tissue temperature increases were within acceptable, safe levels and none of the other physiological changes were considered to be deleterious to human subjects. Of particular note is that these data indicated that an MRI exam performed at a whole-body averaged SAR of 6.0-W/kg can be tolerated by an individual with normal thermoregulatory function (31).

While the data obtained so far are encouraging regarding the lack of substantial health effects from exposure to high SAR levels associated with MRI, it must be remembered that patients may have compromised thermoregulatory systems that could substantially alter their ability to handle a heat load (65, 66, 72-78). Certainly, thermal stress is likely to pose a problem for some patient groups exposed to relatively high whole-body averaged SAR levels. Therefore, additional investigations are warranted to specifically address this important safety issue.

RF ENERGY INDUCED-HEATING AND THERMAL-SENSITIVE ORGANS

The testes and eyes of human subjects have reduced capabilities for heat dissipation and may be injured or damaged by elevated temperatures (1-7, 14, 17, 22, 23, 28, 30, 39-41). Therefore, the testes and eyes are primary sites of potential harmful effects if exposure to RF radiation during MRI is excessive (1-7, 14, 17, 22, 23, 28, 30, 39-41).

Figure 2. (A) Changes in body temperatures versus whole-body averaged SARs during clinical MRI examinations. Note that there is a poor correlation between these two variables.

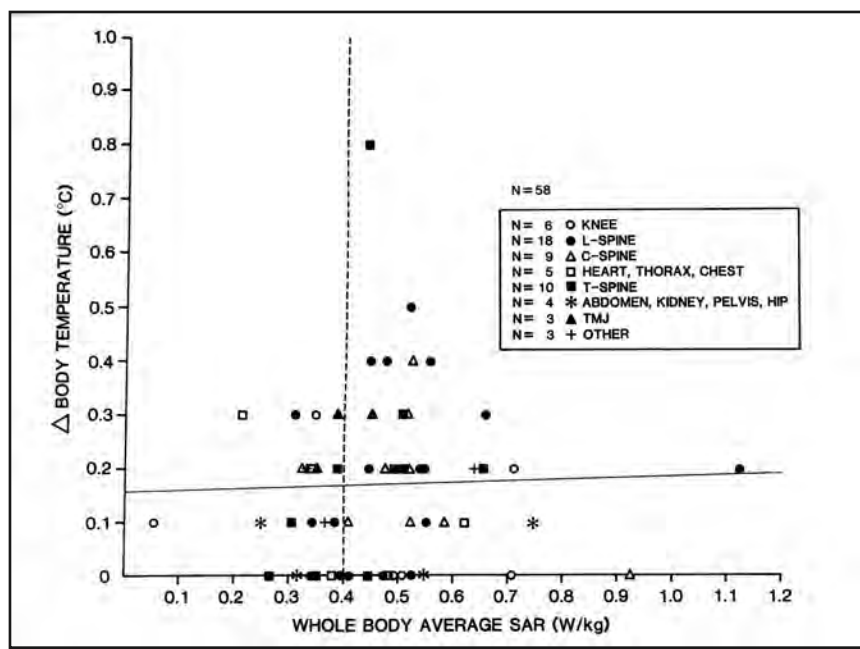
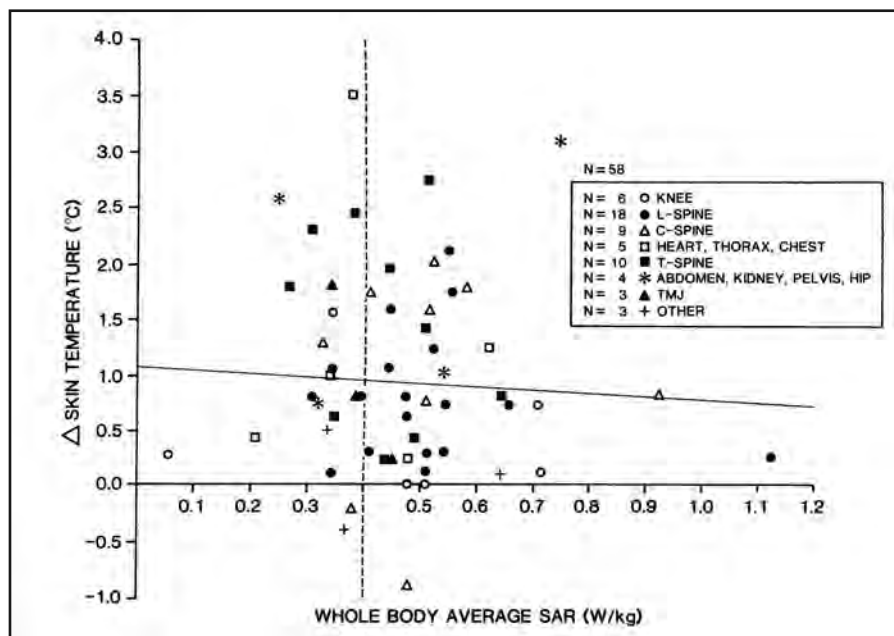
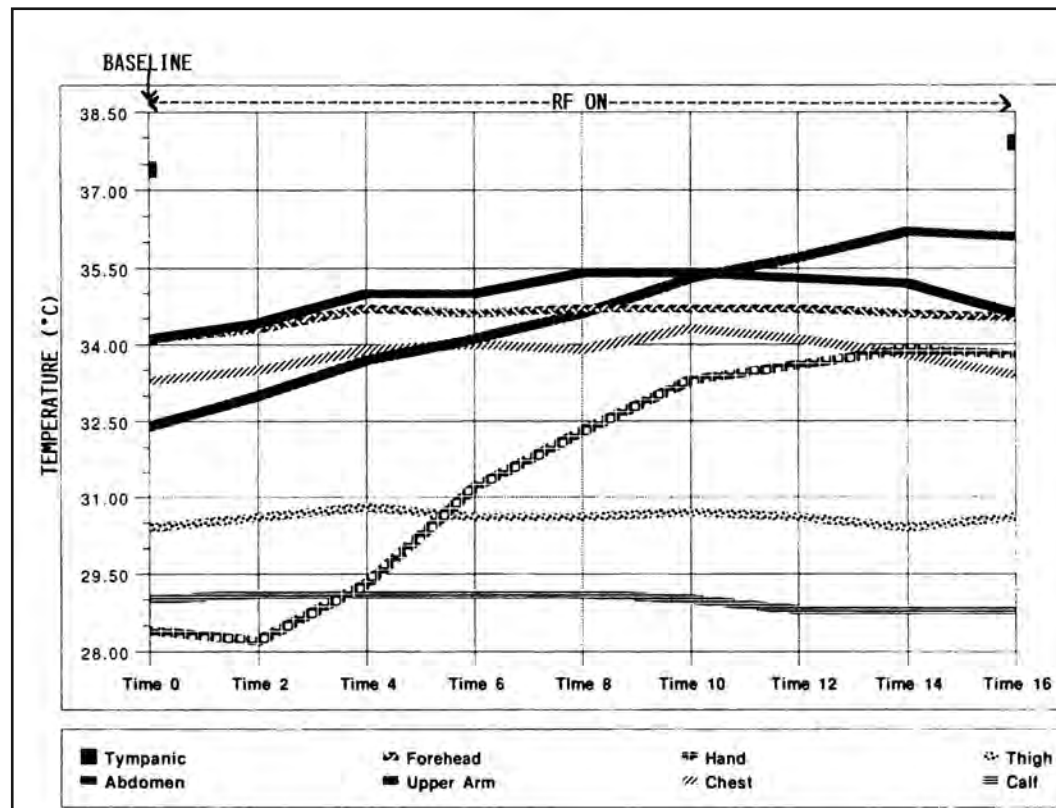


Figure 2. (B) Changes in skin temperatures versus whole-body averaged SARs during clinical MRI procedures. A poor correlation also exists between these two variables. This is not surprising considering the many factors that impact body and skin temperatures in a patient population.



244 Radiofrequency-Energy Induced Heating During MRI

Figure 3. Tympanic membrane and skin temperatures recorded in a subject immediately before, at 2-minute intervals for 16 minutes during, and immediately after MRI performed at a whole-body averaged SAR of 6.0-W/kg which, to date, is the highest level of exposure to RF energy that has been studied in human subjects. Tympanic membrane temperature increased 0.5°C. Skin temperatures showed variable responses depending on the measurement site with hand skin temperature increasing the most followed by forehead, and abdomen skin temperatures, respectively.



The Testes

Laboratory investigations have demonstrated that RF energy-induced heating may have detrimental effects on testicular function. The temperature of the testes correlates directly with the temperature of the scrotal skin (96). This temperature level exists because the scrotum has little or no subcutaneous fat or connective tissue and, as such, there is no tissue mediated temperature gradient present. If the exposure level to RF energy increases scrotal and/or testicular temperatures to between 38°C to 42°C (41), this heating can cause a reduction or cessation of spermatogenesis, impaired sperm motility, degeneration of seminiferous tubules, as well as other abnormal conditions (41, 96). Notably, there is a direct relationship between temperature and sperm motility and viability.

In 1990, Shellock, et al. (28) conducted an investigation to examine the thermal effects of MRI performed at 1.5-Tesla on the scrotum to determine if excessive heating of this body part occurred. A non-contact infrared thermometer was used to measure scrotal skin tem-

perature (i.e., an indicator of testicular temperature) immediately before and after MRI performed at relatively high SAR levels (28). A statistically significant increase in scrotal skin temperature was associated with MRI. The highest temperature that was recorded was 34.2°C (28), which is well below the threshold known to alter or adversely affect the function of the testes (41, 96).

Excessive heating of the scrotum associated with MRI could exacerbate a pre-existing disorder associated with increased testicular temperature (e.g., febrile illnesses, varicocele, etc.) in patients who are already oligospermic, leading to temporary or permanent sterility. Therefore, additional investigations designed to investigate this issue with regard to the testes are warranted, particularly if patients are subjected to MRI using RF energy levels that are greater than those previously evaluated. This scenario is entirely possible considering the widespread use of pulse sequences that utilize high levels of RF energy (e.g., fast or turbo spin echo sequences) and MR systems operating at higher static magnetic field strengths, including clinical 3-Tesla and 7-Tesla scanners that inherently use higher whole-body averaged specific absorption rates.

The Eye

Dissipation of heat from the eye is a slow and inefficient process due to its relative lack of vascularization (39, 95). Exposure to RF energy has been reported to cause a variety of ocular effects, primarily cataracts but also effects on the retina, cornea, and other ocular systems (39, 94). Cataracts have been observed in experimental animals when one eye was exposed to a localized, very high RF field and the other eye was the unexposed control. In the rabbit eye, cataracts developed secondary to RF exposures that generated temperatures greater than or equal to 41°C (39, 95). However, cataracts were not observed in the monkey eye subjected to similar exposure conditions, reflecting the different patterns of energy absorption due to anatomical differences (39, 95). Nevertheless, it is reasonable to assume that an SAR level that would induce temperatures of 41°C or higher in or near the lens in the human eye could produce cataracts by the same mechanism (i.e., heating) that caused cataracts in the rabbit lens (39, 95).

Other ocular effects including corneal lesions, retinal effects, and changes in vascular permeability have been observed after localized exposure of the eyes of laboratory animals to both continuous wave and pulsed wave exposures of RF energy, but the inconsistencies in these results, the failure to independently confirm corneal lesions after continuous wave exposure, the failure to independently confirm retinal effects after pulsed wave exposure, and the absence of functional changes in vision are reasons why these ocular effects are not useful in defining a particular adverse effect level for RF energy (95). The results from long term studies involving nonhuman primates support the conclusion that clinically significant ocular effects, including cataracts, have not been confirmed in human subjects exposed to low level RF energy (95).

An investigation conducted by Sacks, et al. (14) in 1986 which utilized a spectrometer operating at 2.7-Tesla/29-MHz revealed that there were no discernible effects on the eyes of laboratory rats at RF energy and exposure levels (6 hours) that far exceeded levels used in the clinical MRI setting. However, as previously indicated, when it comes to the effects of RF radiation, it is unacceptable to extrapolate data from laboratory animals to human

246 Radiofrequency-Energy Induced Heating During MRI

subjects because, in this case, the coupling of RF radiation to the eye of a rat is markedly different compared to a human subject (i.e., with respect to size, shape, and anatomic position).

Shellock, et al. (17, 30) performed two clinical studies to evaluate the thermal effects of RF energy-induced heating of the eye associated with MRI. In both investigations, corneal temperatures were measured using a non-contact infrared thermometer immediately before and after MRI. Notably, corneal temperature is a representative site of the average temperature of the human eye (97).

In the first study, corneal temperatures were measured in patients undergoing MRI of the brain using a transmit/receive head RF coil at peak SARs ranged from 2.5- to 3.1-W/kg (17). The greatest change in corneal temperature change was 1.8°C and the highest temperature measured was 34.4°C. The second study examined corneal temperatures in patients with suspected ocular pathology who underwent MRI using the transmit body RF coil and a special eye coil for RF reception (30). Fast spin echo pulse sequences were used to examine the eye. The peak SARs for these sequences ranged from 3.3- to 8.4-W/kg. The greatest temperature change was 1.8°C and the highest corneal temperature measured was 35.1°C (30).

Therefore, the findings from these two clinical investigations indicated that corneal temperatures did not exceed the upper limit of normal for the human cornea, which is 36°C (95, 97). Thus, it does not appear that clinical MRI under the conditions studied has the potential to cause thermal damage to ocular tissue. However, with higher RF energy used for research and clinical MRI applications, such as those involving ultra-high-field scanners, the thermal effects on ocular tissue requires further assessment.

MRI AND “HOT SPOTS”

Theoretically, during exposure to RF energy, “hot spots” (i.e., an excessive concentration of RF energy) may develop due to an uneven distribution of RF power in human subjects in association with restrictive conductive patterns (3, 5, 8, 9). Obviously, an unwanted result of RF energy-induced hot spots would be thermal hot spots, or localized elevations in tissue temperature.

Because RF radiation is mainly absorbed by peripheral tissues during MRI, surface thermography was used to study the heating pattern in volunteer subjects exposed to relatively high whole-body averaged SARs at 1.5-Tesla/64-MHz (8, 9). The findings of this research demonstrated that there was no evidence of surface thermal “hot spots” (8, 9). Apparently, the thermoregulatory system responds to any RF radiation-related “hot spot” by evenly distributing the thermal load via cutaneous circulation.

There is the possibility that thermal “hot spots” may develop internally during MRI. For example, Shuman, et al. (19) reported that significant temperature increases occurred in the internal organs of laboratory dogs as a result of MRI performed at high SAR levels. These findings suggested that internal thermal “hot spots” may occur in association with MRI. Therefore, the presence of possible internal “hot spots” needs to be thoroughly examined in human subjects undergoing MRI, with the addition of investigations performed

using higher field strengths, clinical scanners operating 3-Tesla/128-MHz and 7-Tesla/298-MHz. This could be accomplished noninvasively using MRI thermometry, which is based on temperature-sensitive MRI parameters such as the proton resonance frequency, the diffusion coefficient, T1 and T2 relaxation times, magnetization transfer, as well as temperature-sensitive contrast agents (98, 99).

CONCLUSIONS

The characteristics of RF energy-induced heating associated with MRI have been presented with an emphasis on research pertaining to laboratory animals and human subjects. These investigations began in the mid-1980s and continue to the present day. Of note is that the majority of the studies were conducted at 1.5-Tesla/64-MHz. Many of the investigations performed after the mid-1990s involved attempts to predict or study the heating aspects of RF energy by using modeling-based investigations, temperatures obtained in phantoms or, in a few instances, temperatures recorded in laboratory animals (40-54, 100-121). Without validation in human subjects, including patient populations, the safety of exposures to high levels of RF energy remains unknown.

Because MR systems operating at higher field strengths and frequencies are used for research and clinical applications (3-, 4-, 7-, 9.4-, 10.5-Tesla) (51-55, 100, 101, 122, 123), and there are new clinical applications (e.g., advanced pulse sequences, specialized transmit RF coils, etc.) with associated greater levels of RF radiation, additional investigations are necessary to assess the effects of heating. Importantly, studies are particularly needed to evaluate patients with conditions that impair heat dissipation.

REFERENCES

1. National Council on Radiation Protection and Measurements. Biological effects and exposure criteria for radiofrequency electromagnetic fields. Report No. 86. National Council on Radiation Protection and Measurements. Bethesda, MD; 1986.
2. United States Environmental Protection Agency, Health Effects Research Laboratory, Biological Effects of Radiofrequency Radiation, EPA-600/8-83-026A. Research Triangle Park, NC. 1984.
3. Michaelson SM, Lin JC. Biological Effects and Health Implications of Radiofrequency Radiation. New York: Plenum; 1987.
4. Hardell L, Sage C. Biological effects from electromagnetic field exposure and public exposure standards. *Biomed Pharmacother* 2008;62:104-109.
5. Habash RWY, Elwood JM, Krewski D, et al. Recent advances in research on radiofrequency fields and health: 2004-2007. *J Toxicol Environ Health B Crit Rev* 2009;12:250-88.
6. Institute of Electrical and Electronics Engineers (IEEE), C95.1-2019 - IEEE Standard for Safety Levels with Respect to Human Exposure to Electric, Magnetic, and Electromagnetic Fields, 0 Hz to 300 GHz, 2019.
7. International Commission on Non-Ionizing Radiation Protection (ICNIRP). Guidelines for limiting exposure to electromagnetic fields (100 kHz to 300 GHz). *Health Phys* 2010;99:818-36.
8. Schaefer DJ, Barber BJ, Gordon CJ, et al. Thermal effects of magnetic resonance imaging. In: Book of Abstracts, Society for Magnetic Resonance in Medicine. Berkeley, CA: Society for Magnetic Resonance in Medicine. Abstract. 1985;2:925.

248 Radiofrequency-Energy Induced Heating During MRI

9. Schaefer DJ, Shellock FG, Crues JV, Gordon CJ. Infrared thermographic studies of human surface temperature in magnetic resonance imaging. In: Proceedings of the Bioelectromagnetics Society, Eighth Annual Meeting. Abstract. 1986; p. 68.
10. Bottomley PA, Redington RW, Edelstein WA, et al. Estimating radiofrequency power deposition in body NMR imaging. *Magn Reson Med* 1985;2:336-349.
11. Adair ER, Berglund LG. On the thermoregulatory consequences of NMR imaging. *Magn Reson Imaging* 1986;4:321-333.
12. Shellock FG, Schaefer DJ, Grundfest W, et al. Thermal effects of high-field (1.5 Tesla) magnetic resonance imaging of the spine: clinical experience above a specific absorption rate of 0.4 W/kg. *Acta Radiol Suppl* 1986;369:514-516.
13. Shellock FG, Gordon CJ, Schaefer DJ. Thermoregulatory response to clinical magnetic resonance imaging of the head at 1.5 Tesla: Lack of evidence for direct effects on the hypothalamus. *Acta Radiol Suppl* 1986;369:512-513.
14. Sacks E, Worgul BV, Merriam GR. The effects of nuclear magnetic resonance imaging on ocular tissues. *Arch Ophthalmol* 1986;104:890-893.
15. Kido DK, Morris TW, Erickson JL, et al. Physiologic changes during high-field strength MR imaging. *Am J Neuroradiol* 1987;8:263-266.
16. Shellock FG, Crues JV. Temperature, heart rate, and blood pressure changes associated with clinical MR imaging at 1.5-T. *Radiology* 1987;163:259-262.
17. Shellock FG, Crues JV. Corneal temperature changes associated with high-field MR imaging using a head coil. *Radiology* 1988;167:809-811.61.
18. Vogl T, Krimmel K, Fuchs A, et al. Influence of magnetic resonance imaging of human body core and intravascular temperature. *Med Phys* 1988;15:562-566.
19. Shuman WP, Haynor DR, Guy AW, et al. Superficial and deep-tissue increases in anesthetized dogs during exposure to high specific absorption rates in a 1.5-T MR imager. *Radiology* 1988;167:551-554.
20. Athey TW. A model of the temperature rise in the head due to magnetic resonance imaging procedures. *Magn Res Med* 1989;9:177-184.
21. Adair ER, Berglund LG. Thermoregulatory consequences of cardiovascular impairment during NMR imaging in warm/humid environments. *Magn Res Imaging* 1989;7:25-37.
22. Persson BRR, Stahlberg F. Health and Safety of Clinical NMR Examinations. Boca Raton, Florida: CRC Press; 1989.
23. Shellock FG. Biological effects and safety aspects of magnetic resonance imaging. *Magn Res Q* 1989;5:243-261.
24. Shellock FG, Schaefer DJ, Crues JV. Evaluation of skin blood flow, body and skin temperatures in man during MR imaging at high levels of RF energy. *Magn Res Imaging* 1989;7:335.
25. Shellock FG, Schaefer DJ, Crues JV. Alterations in body and skin temperatures caused by MR imaging: Is the recommended exposure for radiofrequency radiation too conservative? *Br J Radiol* 1989;62:904-909.
26. Wang J. Issues with radiofrequency heating in MRI. *J Appl Clin Med Phys* 2014;15:5064.
27. Barber BJ, Schaefer DJ, Gordon CJ, Zawieja DC, Hecker J. Thermal effects of MR imaging: worst-case studies on sheep. *Am J Roentgenol* 1990;155:1105-1110.
28. Shellock FG, Rothman B, Sarti D. Heating of the scrotum by high-field-strength MR imaging. *Am J Roentgenol* 1990;154:1229-1232.
29. Shellock FG. Thermal responses in human subjects exposed to magnetic resonance imaging. *Annals of the New York Academy of Sciences* 1992;649:260-272.
30. Shellock FG, Schatz CJ. Increases in corneal temperature caused by MR imaging of the eye with a dedicated local coil. *Radiology* 1992;185:697-699.

MRI Bioeffects, Safety, and Patient Management 249

31. Shellock FG, Schaefer DJ, Kanal E. Physiologic responses to MR imaging performed at an SAR level of 6.0 W/kg. *Radiology* 1994;192:865-868.
32. Boss A, Graf H, Berger A, et al. Tissue warming and regulatory responses induced by radio frequency energy deposition on a whole-body averaged 3-Tesla magnetic resonance imager. *J Magn Reson Imaging* 2007;26:1334-1339.
33. Isaacson DL, Yanosky DJ, Jones RA, Dennehy N, Spandorfer P, Baxter AL. Effect of MRI strength and propofol sedation on pediatric core temperature change. *J Magn Reson Imaging* 2011;33:950-956.
34. Cawley P, Few K, Greenwood R, et al. Does magnetic resonance brain scanning at 3.0 Tesla pose a hyperthermic challenge to term neonates? *J Pediatr* 2016;175:228-230.
35. Kim MS. Investigation of factors affecting body temperature changes during routine clinical head magnetic resonance imaging. *Iran J Radiol* 2016;13:e34016.
36. Fumagalli M, Cinnante CM, Calloni SF, et al. Clinical safety of 3-T brain magnetic resonance imaging in newborns. *Pediatr Radiol* 2018;48:992-998.
37. van den Brink JS. Thermal effects associated with RF exposures in diagnostic MRI: Overview of existing and emerging concepts of protection. *Concepts Magn Reson Part B Magn Reson Eng* 2019;2019:1-17.
38. Gordon CJ. Thermal Physiology. In: *Biological Effects of Radiofrequency Radiation*, EPA-600/8-83-026A. Research Triangle Park, NC. 1984. pp. 4-1 to 4-27.
39. Elder JA. Special Senses. In: *Biological Effects of Radiofrequency Radiation*. *Biological Effects of Radiofrequency Radiation*, EPA-600/8-83-026A. Research Triangle Park, NC. 1984. pp. 5-64 to 5-78.
40. Adibzadeh F, van Rhoon GC, Verduin GM, Naus-Postema NC, Paulides MM. Absence of acute ocular damage in humans after prolonged exposure to intense RF EMF. *Phys Med Biol* 2016;61:488-503.
41. Berman E. Reproductive effects. In: *Biological Effects of Radiofrequency Radiation*, EPA-600/8-83-026A. Research Triangle Park, NC. 1984. pp. 5-13 to 5-41.
42. O'Conner ME. Mammalian teratogenesis and radio-frequency fields. *Proceed IEEE* 1980;68:56-60.
43. Lary JM, Conover DL. Teratogenic effects of radiofrequency radiation. *IEEE Engineering in Medicine and Biology* 1987;44:42-46.
44. Coulter S, Osbourne SL. Short wave diathermy in heating of human tissues. *Arch Phys Ther* 1936;17:679-687.
45. Gersten JW, Wakim KG, Herrick JF, Krusen FH. The effect of microwave diathermy on the peripheral circulation and on tissue temperature in man. *Arch Phys Med* 1949;30:7-25.
46. Persson BRR, Stahlberg F. *Health and Safety of Clinical NMR Examinations*. Boca Raton, Florida: CRC Press; 1989.
47. Shellock FG. Biological effects and safety aspects of magnetic resonance imaging. *Magn Res Q* 1989;5:243-261.
48. Morvan D, Leroy-Willig A, Jehenson P, Cuenod CA, Syrota A. Temperature changes induced in human muscle by radiofrequency H-1 coupling: Measurement with an MR imaging diffusion technique. *Radiology* 1992;185:871-874.
49. Bottomley PA. Turning up the heat on MRI. *J Am Coll Radiol* 2008;5:853-5.
50. Kangarlu A, Shellock FG, Chakeres D. 8.0-Tesla MR system: Temperature changes associated with radiofrequency-induced heating of a head phantom. *J Magn Reson Imaging* 2003;17:220-226.
51. Shrivastava D, Hanson T, Schlentz R, et al. Radiofrequency heating at 9.4T: *In vivo* temperature measurement results in swine. *Magn Reson Med* 2008;59:73-78.
52. Shrivastava D, Hanson T, Kulesa J, et al. Radio frequency heating at 9.4T (400.2 MHz): *In vivo* thermoregulatory temperature response in swine. *Magn Reson Med* 2009;62:888-895.
53. Shrivastava D, Hanson T, Kulesa J, et al. Radiofrequency heating in porcine models with a "large" 32 cm internal diameter, 7 T (296 MHz) head coil. *Magn Reson Med* 2011;66:255-263.

250 Radiofrequency-Energy Induced Heating During MRI

54. Shrivastava D, Utecht L, Tian J, et al. *In vivo* radiofrequency heating in swine in a 3T (123.2-MHz) birdcage whole body coil. *Magn Reson Med* 2014;72:1141-50.
55. Hoff M, McKinney A, Shellock FG, et al. Safety concerns of 7-T MRI in clinical practice. *Radiology* 2019;292:509-518.
56. International Commission on Non-Ionizing Radiation Protection (ICNIRP) statement, medical magnetic resonance procedures: Protection of patients. *Health Physics* 2004;87:197-216.
57. Israel M, Zaryabova V, Ivanova M. Electromagnetic field occupational exposure: Non-thermal vs. thermal effects. *Electromagn Biol Med* 2013;32:145-54.
58. Panych LP, Madore B. The physics of MRI safety. *J Magn Reson Imaging* 2018;47:28-43.
59. Food and Drug Administration. Review of published literature between 2008 and 2018 of relevance to radiofrequency radiation and cancer. Available at <https://www.fda.gov/media/135043/download>. Accessed August, 2021.
60. Wust P, Kortüm B, Strauss U, et al. Non-thermal effects of radiofrequency electromagnetic fields. *Sci Rep* 2020;10:13488.
61. Giuliani L, Soffritti M. Editors. Non-Thermal Effects and Mechanisms of Action Between Electromagnetic Fields and Living Matter. An ICEMS Monograph, National Institute for the Study and Control of Cancer and Environmental Diseases. Bologna, Italy, 2010.
62. U.S. Environmental Protection Agency. Evaluation of potential electromagnetic carcinogenicity. Office of Health and Environmental Assessment. U.S. Environmental Protection Agency, EPA-600/6 90 005A, 1990.
63. Baker KB, Tkach JA, Nyenhuis JA, et al. Evaluation of specific absorption rate as a dosimeter of MRI-related implant heating. *J Magn Reson Imaging* 2004;20:315-320.
64. Gordon CJ. Normalizing the thermal effects of radiofrequency radiation: Body mass versus total body surface area. *Bioelectromagnetics* 1987;8:111-118.
65. Jauchem JR. Effects of drugs on thermal responses to microwaves. *Gen Pharmacol* 1985;16:307-310.
66. Cuddy MLS. The effects of drugs on thermoregulation. *AACN Clin Issues* 2004;15:238-53
67. Kiayatkin EA. Brain temperature homeostasis: Physiological fluctuations and pathological shifts. *Front Biosci* 2010;15:73-92.
68. Tansey EA, Johnson CD. Recent advances in thermoregulation. *Adv Physiol Educ* 2015;39:139-148.
69. Morrison SF, Nakamura K. Central mechanisms for thermoregulation. *Annu Rev Physiol* 2019;81:285-308.
70. Katic K, Li R, Zeiler W. Thermophysiological models and their applications: A review. *Building and Environment* 2016;106:286-300.
71. Rowell LB. Cardiovascular aspects of human thermoregulation. *Circ Res* 1983;52:367-379.
72. Donaldson GC, Keatinge WR, Saunders RD. Cardiovascular responses to heat stress and their adverse consequences in healthy and vulnerable human populations. *Int J Hyperthermia* 2003;19:225-235.
73. Cheshire Jr WP. Thermoregulatory disorders and illness related to heat and cold stress. *Auton Neurosci* 2016;196:91-104.
74. Skelton F. Impaired Thermoregulation. Available at American Academy of Physical Medicine and Rehabilitation, <https://now.aapmr.org/impaired-thermoregulation/> Accessed August, 2021.
75. Drinkwater BL, Horvath SM. Heat tolerance and aging. *Med Sci Sport Exer* 1979;11:49-55.
76. Fennel WH, Moore RE. Responses of aged men to passive heating. *Amer J Physiol* 1969;67:118-119.
77. Kenny WL. Physiological correlates of heat intolerance. *Sports Med* 1985;2:279-286.
78. Buskirk EF, Lundergren H, Magnussen L. Heat acclimation patterns in obese and lean individuals. *Ann NY Acad Sci* 1965;131:637-653.

MRI Bioeffects, Safety, and Patient Management 251

79. Shellock FG, Myers SM, Kimble K. Monitoring heart rate and oxygen saturation during MRI with a fiber-optic pulse oximeter. *Amer J Roentgenol* 1992;158:663-664.
80. Shellock FG. Monitoring during MRI: An evaluation of the effect of high-field MRI on various patient monitors. *Med Electron* 1986;93-97.
81. Holshouser B, Hinshaw DB, Shellock FG. Sedation, anesthesia, and physiologic monitoring during MRI. *J Magn Res Imaging* 1993;3:553-8.
82. Kanal E, Shellock FG. Patient monitoring during clinical MR imaging. *Radiology* 1992;85:623-629.
83. Wickersheim KA, Sun MH. Fluoroptic thermometry. *Med Electron* 1987;84-91.
84. Shellock FG, Rubin SA, Everest CE. Surface temperature measurement by IR. *Med Electron* 1986;86:81-83.
85. Sperber D, Oldenbourg R, Dransfeld K. Magnetic field induced temperature change in mice. *Naturwissenschaften* 1984;71:100-101.
86. Gremmel H, Wendhausen H, Wunsch F. Biologische effekte statischer magnetfelder bei NMR-tomographic am menschen. *Wiss Mitt Univ Kiel Radiol Klinik* 1983.
87. Shellock FG, Schaefer DJ, Gordon CJ. Effect of a 1.5 Tesla static magnetic field on body temperature of man. *Magn Reson Med* 1986;3:644-647.
88. Shellock FG, Schaefer DJ, Crues JV. Exposure to a 1.5-T static magnetic field does not alter body and skin temperatures in man. *Magn Reson Med* 1989;10:371-375.
89. Chakeres DW, de Vocht F. Static magnetic field effects on human subjects related to magnetic resonance imaging systems. *Prog Biophys Mol Biol* 2005;87:255-265.
90. Tenforde TS. Thermoregulation in rodents exposed to high intensity stationary magnetic fields. *Bioelectromagnetics* 1986;7:341-346.
91. Advice on acceptable limits of exposure to nuclear magnetic resonance clinical imaging. National Radiological Protection Board. *Radiography* 1984;50:220.
92. Food and Drug Administration. Magnetic resonance diagnostic device: panel recommendation and report on petitions for MR reclassification. *Fed Reg* 1988;53:7575-7579.
93. U.S. Department of Health and Human Services, Food and Drug Administration, Center for Devices and Radiological Health, Criteria for Significant Risk Investigations of Magnetic Resonance Diagnostic Devices, Guidance for Industry and Food and Drug Administration Staff, 2014.
94. International Electrotechnical Commission, IEC 60601-2-33 Edition 3 Amendment 2. Medical electrical equipment - Part 2-33: Particular requirements for the basic safety and essential performance of magnetic resonance equipment for medical diagnosis. Available at <https://webstore.iec.ch/publication/22705>. Accessed August, 2021.
95. Elder JA. Ocular effects of radiofrequency energy. *Bioelectromagnetics* 2003;6:S148-S161.
96. Kurz KR, Goldstein M. Scrotal temperature reflects intratesticular temperature and is lowered by shaving. *J Urol* 1986;135:290-292.
97. Mapstone R. Measurement of corneal temperature. *Exp Eye Res* 1968;7:233-243.
98. Ludemann L, Włodarczyk W, Nadobny J, et al. Non-invasive magnetic resonance thermography during regional hyperthermia. *Hyperthermia*. 2010;26:273-282.
99. Rieke V, Butts Pauly K. MR thermometry. *J Magn Reson Imaging* 2008;27:376-390.
100. Eryaman Y, Zhang P, Utecht L, et al. Investigating the physiological effects of 10.5 Tesla static field exposure on anesthetized swine. *Magn Reson Med* 2018;79:511-514
101. Sadeghi-Tarakameh A, DelaBarre L, Lagore RL, et al. *In vivo* human head MRI at 10.5T: A radiofrequency safety study and preliminary imaging results. *Magn Reson Med* 2020;84:484-496.
102. Collins CM. Numerical field calculations considering the human subject for engineering and safety assurance in MRI. *NMR Biomed* 2009;22:919-26.

252 Radiofrequency-Energy Induced Heating During MRI

103. Collins CM, Wang Z. Calculation of radiofrequency electromagnetic fields and their effects in MRI of human subjects. *Magn Reson Med* 2011;65:1470-82.
104. de Greef M, Ipek O, Raaijmakers AJ, et al. Specific absorption rate inter-subject variability in 7-T parallel transmit MRI of the head. *Magn Reson Med* 2013;69:1476-85.
105. Kangarlu A, Ibrahim TS, Shellock FG. Effects of coil dimensions and field polarization on RF heating inside a head phantom. *Magn Reson Imaging* 2005;23:53-60.
106. Massire A, Cloos MA, Luong M, et al. Thermal simulations in the human head for high field MRI using parallel transmission. *J Magn Reson Imaging* 2012 35:1312–1321.
107. Le Garrec M, Gras V, Hang M-F, et al. Probabilistic analysis of the specific absorption rate intersubject variability safety factor in parallel transmission MRI. *Magn Reson Med* 2017;78:1217–1223.
108. Meliàdò EF, van den Berg CAT, Luijten PR, et al. Intersubject specific absorption rate variability analysis through construction of 23 realistic body models for prostate imaging at 7 T. *Magn Reson Med* 2019;81:2106–2119
109. van Lier AL, Kotte AN, Raaymakers BW, Lagendijk JJ, van den Berg CA. Radiofrequency heating induced by 7 T head MRI: Thermal assessment using discrete vasculature or Pennes' bioheat equation. *J Magn Reson Imaging* 2012 35:795–803.
110. Fiedler TM, Ladd ME, Bitz AK. SAR simulations and safety. *Neuroimage* 2018;168:33–58.
111. Nadobny J, Szmitenings M, Diehl D, et al. Evaluation of MR-induced hot spots for different temporal SAR modes using a time-dependent finite difference method with explicit temperature gradient treatment. *IEEE Trans Biomed Eng* 2007;54:1837–1849.
112. Wang Z, Lin JC, Vaughan JT, Collins CM. Consideration of physiological response in numerical models of temperature during MRI of the human head. *J Magn Reson Imaging* 2008;28:1303–1308.
113. Wang Z, Lin JC, Mao W, et al. SAR and temperature: Simulations and comparison to regulatory limits for MRI. *J Magn Reson Imaging* 2007;26:437–441.
114. Wang Z, Collins CM. Effect of RF pulse sequence on temperature elevation for a given time-average SAR. *Concepts Magn Reson Part B Magn Reson Eng* 2010;37B:215–219.
115. Murbach M, Cabot E, Neufeld E, et al. Local SAR enhancements in anatomically correct children and adult models as a function of position within 1.5 T MR body coil. *Prog Biophys Mol Biol* 2011;107:428–433.
116. Murbach M, Neufeld E, Capstick M, et al. Thermal tissue damage model analyzed for different whole-body averaged SAR and scan durations for standard MR body coils. *Magn Reson Med* 2014;71:421–431.
117. Murbach M, Neufeld E, Kainz W, Pruessmann KP, Kuster N. Whole-body and local RF absorption in human models as a function of anatomy and position within 1.5 T MR body coil. *Magn Reson Med* 2014;71:839–845.
118. Murbach M, Neufeld E, Cabot E, et al. Virtual population-based assessment of the impact of 3 Tesla radiofrequency shimming and thermoregulation on safety and B_1^+ uniformity. *Magn Reson Med* 2016;76:986–997.
119. Murbach M, Neufeld E, Samaras T, et al. Pregnant women models analyzed for RF exposure and temperature increase in 3 T RF shimmed birdcages. *Magn Reson Med* 2017;77:2048–2056.
120. Jin J, Liu F, Weber E, Crozier S. Improving SAR estimations in MRI using subject-specific models. *Phys Med Biol* 2012;57:8153–71.
121. Wolf S, Diehl D, Gebhardt M, et al. SAR simulations for high-field MRI: How much detail, effort, and accuracy is needed? *Magn Reson Med* 2013;69:1157–6.
122. Barisano G, Culo B, Shellock FG, Sepehrband F, Wang DJ, Toga AW, Law M. 7-Tesla MRI of the brain in a patient with total knee replacement implants: Case report and proposed safety guidelines. *Magnetic Reson Imaging* 2019;57:313–316.

MRI Bioeffects, Safety, and Patient Management 253

123. Thulborn KR, Ma C, Sun C, Atkinson IC, et al. SERIAL transmit - parallel receive (ST(x)PR(x)) MR imaging produces acceptable proton image uniformity without compromising field of view or SAR guidelines for human neuroimaging at 9.4 Tesla. Magn Reson Med 2018;293:145-153.

Chapter 9 Thermal Effects Associated with RF Exposures During Clinical MRI

JOHAN VAN DEN BRINK, PH.D.

Principle Scientist and Architect
Magnetic Resonance
Philips Medical Systems
Best, The Netherlands

INTRODUCTION

Magnetic resonance imaging (MRI) is itself one of the best examples that electromagnetic fields interact with biological tissue, providing a wide variety of soft-tissue contrasts that can be generated by the subtle interplay between radiofrequency (RF) pulse amplitudes and timing. Unfortunately, RF energy not only subtly disturbs the Boltzmann equilibrium of the nuclear spins, it also produces heat as it drives rapid molecular reorientation in cells and induces currents in the human body. Strain and friction might not functionally impair cellular and enzymatic processes, but will definitely lead to dissipation and local, non-uniform tissue heating. Such thermal effects are used therapeutically to kill tumors (i.e., RF field-induced hyperthermia) and applied in the food processing industry to sterilize at relatively low temperatures (50 to 60°C).

The aim of this chapter is to present an overview of experimental data and modeling studies for core and local tissue temperature rises in clinical MRI, which mostly operates at 1.5 T (64 MHz) or 3 T (128 MHz). Safe temperatures must be maintained at all times during the MRI examination. Health effects related to mild hyperthermia will be used to explain necessary restrictions for temperature increase and thermal dose, expressed as temperature exposure of tissue at cumulative equivalent minutes at 43°C (CEM43) (1), and the derived exposure limits for whole-body averaged and head RF power deposition, expressed as specific absorption rate (SAR in W/kg) in the MRI product safety standard from the International Electrotechnical Commission, IEC 60601-2-33 (2). A simplified version of the applicable limits is shown in **Table 1**.

Table 1. Limits to RF exposure in MRI equipment (2). For global exposure or protection from systemic thermal effects, 6 minutes-averaged whole-body SAR and head SAR must be controlled. Additional limits apply to control local exposure, for example, from small transmit RF coils or inhomogeneous RF fields. This table contains only a subset of requirements. Refer to (2) for detailed specifications including partial body SAR, short-term SAR, and specific absorption (limits not shown).

Global Exposure				
	Local Exposure			
	Whole Body SAR	Head SAR	Local Torso 10g SAR	Local Extremity 10g SAR
Normal Operating Mode	2 W/kg	3.2 W/kg	10 W/kg	20 W/kg
First Level Controlled Operating Mode	4 W/kg	3.2 W/kg	20 W/kg	40 W/kg

Basic restrictions for temperature and thermal dose apply equally at ultra-high field MRI (7 T and higher), but SAR management requirements may be different due to the more localized exposure to RF energy from parallel-transmit arrays (3). Considerations related to partial-body and localized exposures using such arrays, and analyses of RF field-related implant heating are beyond the scope of this chapter.

POTENTIAL HEALTH EFFECTS FROM RF EXPOSURE

Potential risks associated with exposure to RF fields are actively monitored by the World Health Organization (WHO), the European Scientific Committee on Emerging and Newly Identified Health Risks (SCENIHR), the International Commission on Non-Ionizing Radiation Protection (ICNIRP) (4) and the International Committee on Electromagnetic Safety (ICES, part of IEEE) (5). After decades of research related to RF exposures in wireless communication, the general consensus of these scientific expert groups is that prevention of adverse health effects from exposure to RF fields can be based on avoidance of acute thermal effects (during or within minutes after exposure). It should be noted, however, that a few recent, well-designed studies comparing RF and non-RF field-induced hyperthermia in food safety (6) and humans (7) indicate that induced cross-membrane electric fields enhance thermal damage at moderately elevated temperatures.

While the energy of RF photons is too low to dissociate chemical bonds, for example in DNA, coupling to vibrational modes in proteins may alter reaction kinetics. Reported proliferation effects in cell lines, *in vitro* and in animals, caused the International Agency of Research of Cancer (8) to classify RF radiation in 2011 as “possibly carcinogenic to humans” (Group 2B). The Food and Drug Administration (FDA) recently reviewed evidence for tumorigenesis and concluded that “a lack of clear dose response relationship, a lack of consistent findings or specificity, and a lack of biological mechanistic plausibility” (9). Ad-

256 Thermal Effects Associated with RF Exposures During Clinical MRI

ditional studies published in 2018 by the U.S. National Toxicology Program (NTP) and from Italy (10) indicated that the risk may increase in laboratory animals as a result of prolonged exposure at high SAR levels. Potential biochemical mechanisms relate to thermal vulnerability of routine DNA repair pathways: exposure to heat (stress) leads to accumulation of DNA double-strand break (DSB) recognition proteins such as γ H2AX and micro-nucleation (11) and references cited therein (12, 13). The latter paper shows that heat stress affects the DNA integrity in a cell cycle phase-dependent manner (i.e., DSBs in G1/G2 phase) and stalling DNA replication forks in synthesis (S) phase (14). Additionally, Takahashi A, et al. (15) reported that γ H2AX foci formation is rapid and shows similar Arrhenius kinetics as cell killing by temperature.

Notably, no epidemiological indications exist from over 35 years of the use of MRI, with more than 150 million examinations being performed annually, to suggest an increased cancer incidence. Alleged excess DNA damage caused by MRI was excluded in a well-designed study (16). Similarly, no oncological concerns are known for the (local) thermal burden in diagnostic ultrasound (17-20), taking into account that clinical practice guidelines nevertheless strongly recommend “as low as reasonably possible” thermal exposure levels. Exposure to RF fields during MRI examinations can also lead to substantial thermal load, and only slightly-higher power levels are used in RF field-induced hyperthermia or focused ultrasound to ablate tumors (1, 21).

Thermal Thresholds and Basic Restrictions

The recent update of RF exposure guidelines by ICNIRP (4) defines the concepts for establishing exposure restrictions to prevent harmful effects to human health. This committee has performed an extensive literature review (see Appendix B of their guidelines) to identify substantiated effects with adequate scientific evidence. This includes independent reproduction of reported effects and adequate study design and dosimetry, but allows for inclusion of known biological mechanisms from which adverse effects can reasonably be hypothesized. A relevant discussion topic, which has not been closed to satisfaction, is whether excessive sweating and strong recruitment of thermoregulation would constitute adverse health effects, at least in some groups of human subjects. For now, it is assumed that this is not the case.

Thresholds for health effects were determined from the RF field exposure literature or from other sources (e.g., burns, hyperthermia, etc.). The latter are called “operational thresholds”. The ICNIRP applies reduction factors to derive the restriction values. These reduction factors are chosen to account for biological variation, variation of the baseline physiological and environmental conditions, and dosimetric uncertainty. The threshold value combined with the reduction factor results in the “basic restrictions”. Relative to earlier publications, three notable changes were introduced in the 2020 Guidelines:

- (1) The averaging time for whole-body averaged SAR (4 W/kg) has been increased from 6 minutes to 30 minutes, which is the assumed time to reach steady-state temperature in the adult. For reference, metabolic rates are approximately 1 W/kg at rest (22), 2 W/kg standing, and 12 W/kg when running (23, 24). Note that the local SAR averaging time is retained at 6 minutes, based on numerical simulations in the GHz range (25). The basic restrictions also remain unchanged at 10 W/kg and 20 W/kg for 10 gram averaged local

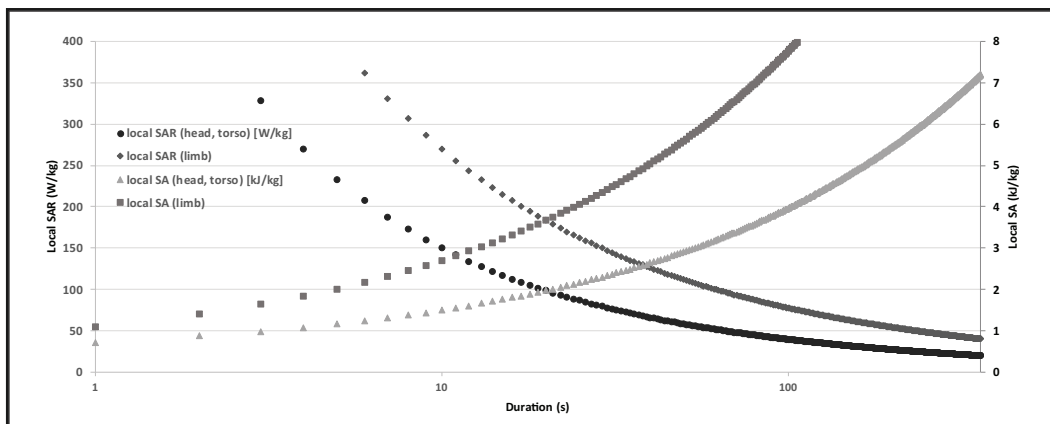
SAR in head/torso and limb, respectively. The 10 gram averaging volume is based on the insight that heat diffusion is rapid and equilibrates temperature at these length scales (26).

- (2) Using CEM43 to assess thermal burden and potential harm was evaluated and explicitly discarded as (operational) threshold. Rather, two “tissue types” have been introduced with maximum-allowed temperature increases:
 - a) “Type-1” tissue includes all tissues in the upper arm, forearm, hand, thigh, leg, foot, pinna and the cornea, anterior chamber and iris of the eye, epidermal, dermal, fat, muscle, and bone. Normothermal temperature for Type-1 tissue is typically < 33 to 36°C, and allowed temperature increase is set to 5°C.
 - b) “Type-2” tissue includes all tissues in the head, eye, abdomen, back, thorax, and pelvis, excluding those defined as Type-1 tissue. Its normothermal temperature is <38.5°C, and allowed temperature increase is set to 2°C. Note that this includes the fetus, but does not provide a clear understanding how peripheral nerves in muscle and bone should be treated.

The use of specific absorption (SA) in any 10g of cubic mass as restriction at frequencies > 400 MHz (a somewhat arbitrary cut-off value based on RF penetration depth arguments.) The newly introduced formula leads to (not explicitly disclosed) allowance for short-term high local SAR. **Figure 1** provides an overview of the time dependence of this restriction, where the exposure of groups of pulses must satisfy the restrictions at all time scales.

The ICNIRP’s methodological approach provides a concise overview of the available evidence for health effects to identify adverse health effects and their thresholds. A similarly structured review concerning thermal effects associated with RF exposures in diagnostic MRI is available in (27). In clinical settings, a benefit to risk assessment may justify application of higher exposure levels than those applicable in daily life. IEC 60601-2-33 therefore adopted local SAR restrictions of 20 W/kg and 40 W/kg for 10 gram (10g) averaged local SAR in head/torso and limb, respectively. Extensive simulations have since been performed

Figure 1. Restrictions for local SA (10 g) as defined by the ICNIRP for frequencies > 400 MHz, and derived (i.e., short-term) local SAR values. Note that these values cannot be directly applied to the frequencies of clinical MR systems, but indicate that short-term considerations may allow for burst SAR.



258 Thermal Effects Associated with RF Exposures During Clinical MRI

(28-32) to evaluate if higher allowed exposures can be justified based on CEM43 analyses and their allowable safe values (20, 33).

No thermal risk is assumed to result if the Basic Safety Restriction for thermal dose is set to the lowest CEM43 level, at which no apoptotic (i.e., the process of programmed cell death) effects have been reported. The diagnostic ultrasound community has evaluated the usefulness of CEM43 to provide user feedback on potential thermal risks (17, 18) and has established that 1 CEM43 is a conservative safety threshold for fetal, neonatal and adult exposure (19, 20). Higher thresholds have been proposed for MRI (33), taking into consideration the type of tissue and patient's health status, with 2 CEM43 proposed as a conservative safety threshold for MRI examinations under all conditions. In addition to this proposal, higher allowable local SAR values have been proposed based on a limited set of RF field-induced hyperthermia exposures and reported complaints (34).

Derivation of temperature-based local SAR limits needs to account for whole-body averaged RF deposition, equilibration of core temperature towards the legs, thermoregulatory responses and capabilities, and patient variability. Temperature effects from MRI exposures were established in the late 1980s using animal and human volunteer experiments (35), and thermophysiological modeling. The allowed maximum temperature increases postulated by the ICNIRP include such global and systemic effects, but (reversely) cannot be directly related to the temperature increase from the local SAR, alone: especially in whole-body averaged MRI, effects of the whole-body averaged specific absorption must be included when controlling RF power deposition.

This chapter will first addresses the available systemic temperature data from MRI exposures, both experimental and simulated. It then presents an analysis of health effects to determine thermal thresholds, corroborating those presented by the ICNIRP. The potential role of CEM43 as a control measure will also be discussed in relation to local SAR simulations and their accuracy, reproducibility and representativeness.

TEMPERATURE DATA FROM MRI EXPOSURES: SYSTEMIC BURDEN

MR systems intentionally expose patients to high RF power, generally for a single episode (examination) of short duration, typically less than one hour. RF deposition is expressed as SAR in W/kg and accumulated as specific absorption in J/kg. First generation MR scanners operated at relatively low SARs and initially exposed the head with local transmit RF coils. Such exposures are nowadays common for 7 T MR systems (localized, small coverage transmit RF coils) and deposit relatively little energy in the body of adult patients. With the advent of whole-body averaged transmit (quadrature birdcage) RF coils for 1.5 T systems, increases in SAR levels to 2 to 4 W/kg were deemed necessary to ensure adequate image quality and scan efficiency for spine and body imaging, with total exposure durations of 20 to 40 minutes. In current clinical practice, even longer examinations with continuous high-SAR scanning are not uncommon.

The generally-accepted upper limit to the whole-body averaged SAR is 4 W/kg (36), established from observed behavioral changes in animal studies. Such exposures are reported to induce strong heat sensations in healthy human subjects. A reduced whole-body

averaged SAR of 2 W/kg already falls within the normal temperature variation due to metabolic activity and exercise: the average metabolic rate, as a conversion of chemical into mechanical and thermal energy in the human body, is estimated to be 80 W at rest and 270 W for moderate physical activity (24). Thus, 2 W/kg for a 100 kg person represents a situation of homeostasis without undue stress, and is chosen as an acceptable exposure for the Normal Operating Mode for MR systems, which all individuals, regardless of health status, should be able to tolerate.

Several investigations have evaluated the physiological implications of such exposures on healthy volunteers and patients, studying heart rate, blood pressure, sweating and skin or core temperature. Profound sweating and mild cardiovascular challenge at a higher SA have not been considered a potential reason for concern. **Table 2** provides an overview of identified reports of temperature increase related to MRI exposures, including an example

Table 2. Overview of experimental data for core temperature rise in relation to RF energy exposure in association with MRI.

Reference and Year of Publication	Number of Subjects	Exposure Type	Dosimetry	SAR and Duration	Max Core Temperature Increase	Mean Core Temperature Increase
(137) (1986)	25 Patients	ambient temperature 20 to 24°C whole body	No	0.5 to 1.3 W/kg per sequence 40 to 90 min	0.6°C	-
(140) 1986	15 Patients	ambient temperature 20 to 24°C head	No	0.8 to 1.2 W/kg	0.2°C	0.4 °C
(46) (1987)	50 Patients	ambient temperature 20 to 24°C whole body	No	0.6 to 1 W/kg per sequence	0.5°C	0.2 °C
(141) 1988	35 Patients	head	No	0.1 to 0.9	0.1°C	0.0°C
(38) (1989)	6 Volunteers	whole body	Partial	3 to 4 W/kg 30 min	-	0 °C
(47) (1994)	6 Volunteers	ambient temperature 21 to 23°C whole body	Yes	6 W/kg 16 min	> 1°C	0.5 °C
(138) (2011)	400 Children	whole body, head	No	Unknown	> 1°C (2%)	-
(139) (2016)	25 Neonates	Body	No	Unknown	-	0 °C
(142) (2016)	69 Patients	Head	No	Unknown < 30 min	> 1°C	0.8 °C

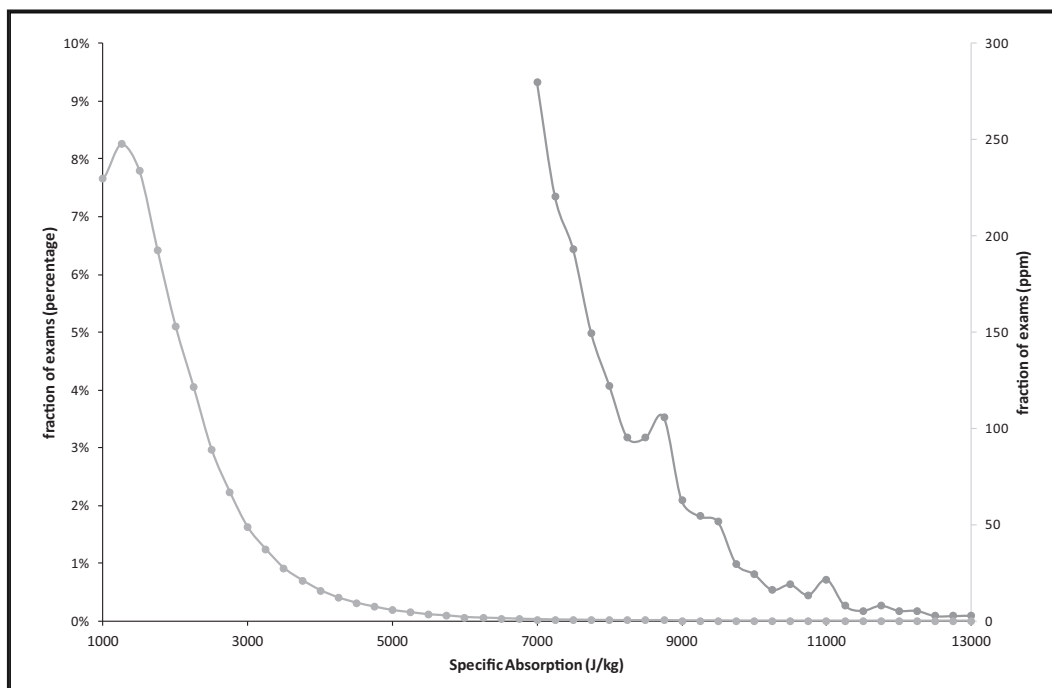
260 Thermal Effects Associated with RF Exposures During Clinical MRI

of a large whole-body averaged study on RF field-induced hyperthermia. Unfortunately, most identified studies lack appropriate dosimetric information to confirm SAR and SA values. This may explain the anomaly of the reported mean temperature increase in (37), although measurement approach and volunteer characteristics may explain a low core temperature increase. Notably, however, a recent investigation of 15 volunteers in an MRI setup without RF exposure showed (repeatable) increasing and decreasing temperatures (ranging from +0.5 °C to -0.5 °C; Nicolas Boulant, Caroline Le Ster and Alexandre Vignaud, *private communication*). This casts additional doubt on the quality of the data used as reference for the core temperature predictions as discussed in the next section. The high temperature increase reported by Wust, et al. (38) indicates that patients may experience a higher core temperature elevation than normal volunteers. A confounding factor may be that thermal insulation is applied in the hyperthermia setup and, thus, thermoregulation may be compromised while high SAR levels are applied. In previous assessments, reported mean core temperature increases were used to argue that effects are marginal. A more appropriate parameter to consider when establishing exposure limit values is the maximum reported core temperature increase, for which esophageal measurements are the most accurate, but tympanic membrane temperatures can also provide representative data (39-44).

Total energy absorbed, or SA, provides an easy estimate for systemic thermal burden. Actual temperatures reached depend on many factors such as initial temperature distribution in the body, thermoregulatory capability, and dissipation options (clothing and blankets), see (44) and the section in this chapter discussing core temperature predictions from simulation models. An additional confounding factor not accounted for in these studies is the psychological response to the MRI exposure: are people feeling at rest or stressed? A careful analysis of sham exposure has also not been performed but recent data suggests significant inter-subject variability. Irrespective, the data suggests that an SA of approximately 4 kJ/kg is sufficient to raise core temperature by 1 °C, which corresponds to a continuous high whole-body averaged SAR (> 3 W/kg) applied for 15 to 20 minutes.

Predicted SA values in the tens of millions of MRI examinations performed annually can be assessed from scanner utilization data. **Figure 2** shows a representative distribution obtained from 367,000 examinations at 1.5 T systems. Resulting core temperature values of examinations with (predicted) SA values > 7 kJ/kg are not known, and will depend on the length of the examination (long term RF duty cycle) and the thermoregulatory and heat loss capabilities of the patient. In general, high SA levels can be expected, and have been reported as being uncomfortable, and MRI scanner manufacturers recommend not to exceed the value of 7 kJ/kg unless a clinical benefit-risk assessment is made and patient surveillance is in place. On the other hand, no evidence exists that the 0.01% of examinations with SA > 10 kJ/kg correlate significantly with adverse events. The lack of large-scale data for core temperature increase in patients associated with MRI examinations warrants additional and well-controlled measurements in routine clinical settings. Such data should include tympanic membrane (pre and post) temperature, patient weight, gender, age, body part examined, ambient temperature, and appropriate dosimetry for SA and SAR values. Beyond core temperature, several studies report rapidly-developing profound sweating, whereas heart rate and blood pressure effects were generally negligible (45, 46). Significant but highly variable skin temperature increases have also been reported (37, 46-50) (**Table 2**), but that data is not considered to constitute an indicator of potential health concerns.

Figure 2. Typical distribution of predicted specific absorption (SA, in bins of 250 J/kg) observed in clinical use of 1.5 T MRI examinations for all body parts at multiple hospitals. The curve to the left side/axis shows the percentage of examinations as a function of exposure. Less than 10% of the examinations is performed with SA > 3 kJ/kg. Use of much higher SA values is, however, not uncommon, see the curve to the right side/axis, showing the fraction of examinations in ppm: approximately 1% of patients are exposed to > 7 kJ/kg, and 0.1% to > 10 kJ/kg. (Reproduced with permission, copyright © 2019 Johan S. van den Brink.)



Core Temperature Predictions

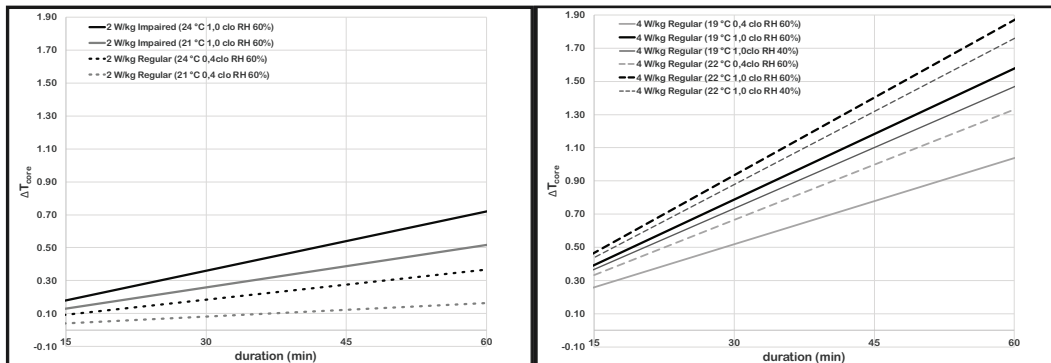
Thermophysiological models can be used to estimate RF-induced core temperature increase as function of SAR and exposure duration. Heat accumulation in the human body mostly depends on ambient temperature and insulation (clothing), as well as thermoregulatory capabilities. In their pioneering work, Adair and Berglund (48, 49, 51) used a two-node model (70 kg man) based on the Stolwijk approach to evaluate core temperature increase as a function of whole-body averaged SAR, skin blood flow impairment, ambient temperature, relative humidity, and insulation. Predicted core temperature increases correlate well with experimental data, and a sensitivity analysis provided strong indications that the ambient temperature should not exceed 21°C, air humidity should be kept around 50%, and only light clothing can be tolerated (i.e., avoid the use of blankets). Under these circumstances, and limiting SA to 10 kJ/kg, moderate cardiovascular impairment effects will not seriously enhance core temperature elevations to levels > 1°C. Adair and Berglund also recommended keeping the SAR to < 3 W/kg, and to limit examination time to 20 min. Their modeling showed that cool down and recovery time is at least 30 minutes under optimal patient health conditions.

The Stolwijk approach used by Adair and Berglund has been superseded by advanced multi-node human models in the context of heat exposure in buildings, cars, and under (occupational) activity (52, 53). Application of such advanced models to the context of MRI (i.e., the supine patient in an enclosed space) may be of future interest, once more experimental data is available for core temperature and dosimetry over a large number of patients, including analysis of sham exposures.

In the current situation, the rationale for exposure limits and guidance relies on the Adair and Berglund model. This can be done with confidence, since more recent and more detailed RF exposure modeling studies have confirmed their thermal predictions (54-59). These studies indicated that the effect of aging requires additional conservativeness when establishing exposure limits, but pediatric exposure is of lesser concern. Children have a greater surface-to-volume ratio than adults, and can tolerate approximately 30% higher whole-body averaged SAR than adults for the same core temperature increase (60).

A simplified parametric approach is suggested by Adair, et al. (48) to enable a sensitivity analysis of core temperature increase as a function of SAR, skin blood flow impairment, clothing/insulation, ambient temperature and air humidity. Temperature rise correlates with total deposited energy (SA) and restriction of the allowable SA value was suggested by Barber, et al. (61). Some scenarios of this linearized parametric approach are provided in **Figure 3** to illustrate the relative importance of the model parameters. For further detailed analyses, refer to the work by Adair, et al. (48-49). Notably, the effect of room humidity is not a major

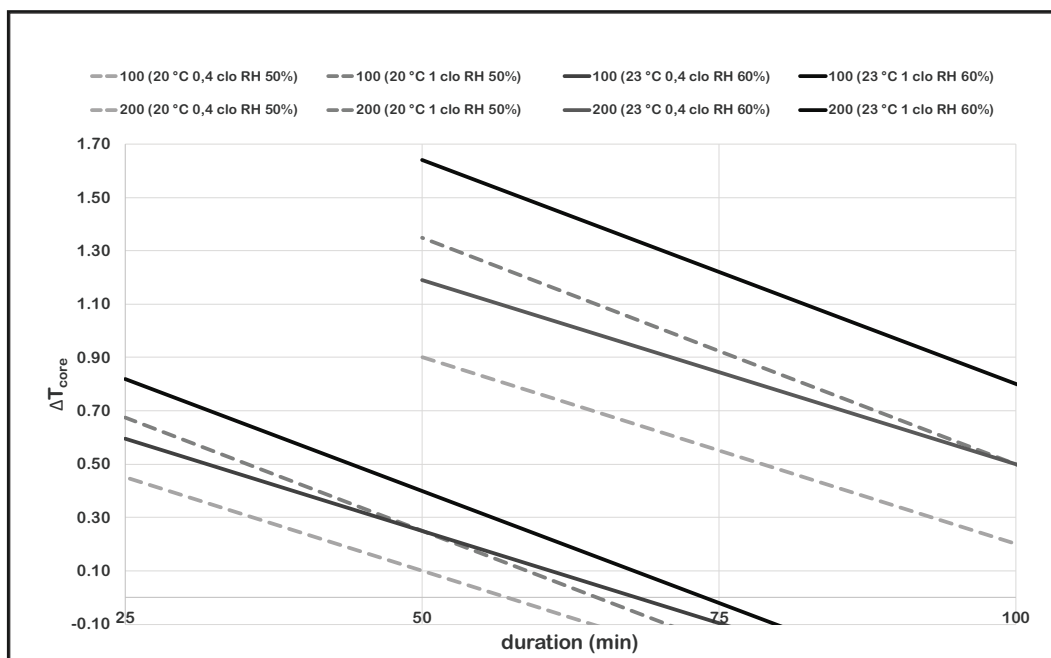
Figures 3a (left) and 3b (right). Estimated core temperature increase for a 70kg human using the simplified assessment proposed by Adair, et al. (49) to demonstrate sensitivity on several model parameters. The grey and black lines in (a) show the significant dependence on room temperature (solid lines), clothing (dotted versus solid lines), and the thermoregulatory health of the patient. These predictions are at relatively high room temperature but with the MR system operating in the Normal Operating Mode. The light-grey and mid-grey lines in (b) were derived at the upper limit of the First Level Controlled Operating Mode (continuous 4 W/kg) but at lower ambient temperatures than those used in (a). No data is shown for thermoregulatory impaired patients, which should never be exposed to high SAR values. Light clothing is a determining factor for managing core temperature. Room humidity is a less important parameter to control, even at high RF power deposition (4 W/kg).



factor in addressing systemic heat load concerns whereas room temperature must be kept low, especially when the MR scanner operates in the First Level Controlled Operating Mode (whole-body averaged SARs between 2 and 4 W/kg). Covering blankets should be avoided, but patients may come into the MR system room feeling cold. A good recommendation may be to take away any blankets after 10 to 15 minutes of scanning or when the SA level reaches 2 to 3 kJ/kg.

Figure 4 analyzes thermal effects for several scan room conditions, clothing, and selected SAR level. Thermal insulation that is comfortable for an individual at rest, where the relative humidity is < 50% and the air movement is 6 m/min, is equal to one clo unit (1.0 clo). Colloquially, this equates to a man wearing a three-piece suit with light underclothes (62). Several representative exposure scenarios are provided for unimpaired (**a**) and severely impaired (**b**) skin blood flow. Three SA levels are evaluated to estimate core temperature rise ($100 \text{ W} \cdot \text{min}/\text{kg} = 6 \text{ kJ}/\text{kg}$ and $200 \text{ W} \cdot \text{min}/\text{kg} = 12 \text{ kJ}/\text{kg}$). Individual lines represent:

Figure 4a. Estimated core temperature increase for a 70kg human with normal thermoregulation from Adair, et al. (49), at different environmental conditions, and for three levels of Specific Absorption (SA) (100 and 200 W.min/kg), up to an SAR level of 4 W/kg. Each graph represents an iso-SA line, and the corresponding SA value (e.g., 200 W.min/kg for the lowest dashed blue line) divided by the scan or examination duration provides the whole-body average SAR. For example, a duration of 50 min and SA = 100 W.min/kg correspond to an average SAR of 2 W/kg and a predicted core temperature rise of approx. 0.3°C. Similarly, a duration of 25 min on the same line corresponds to an average SAR of 4 W/kg and a predicted temperature increase of 0.7°C. Notably, the predictions for SA of 100 W.min/kg correspond reasonably well with the data in **Table 2** (estimated 1 clo, room temperature not specified but likely close to 23°C).



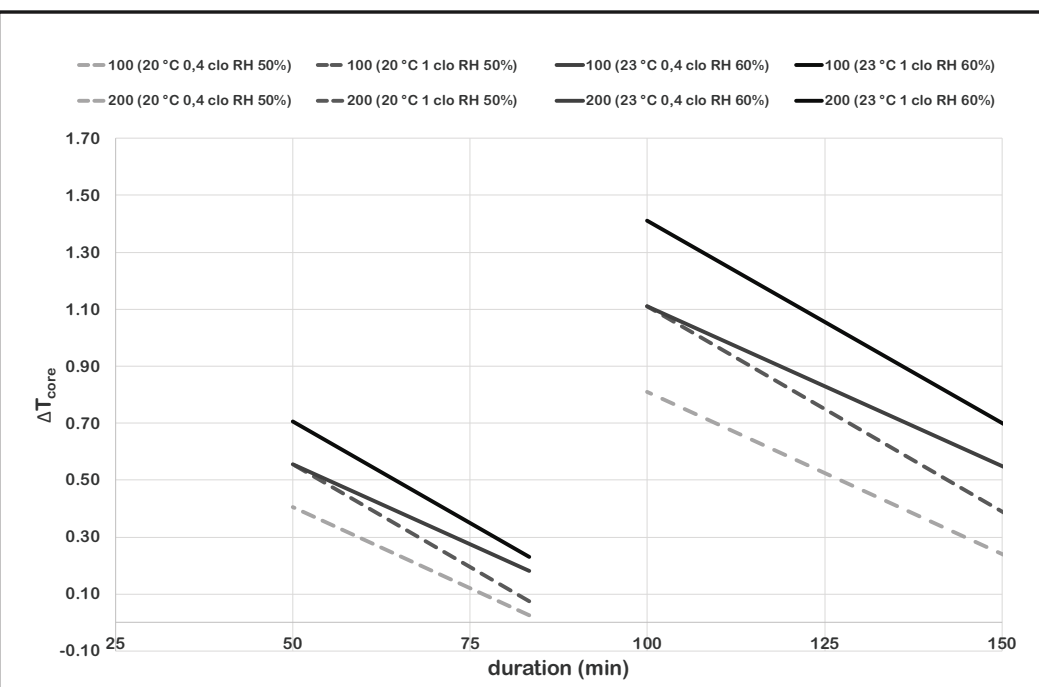
264 Thermal Effects Associated with RF Exposures During Clinical MRI

- ambient temperatures of 20°C and 23°C,
- light clothing (hospital gown, 0.4 clo) and additional blankets or large surface coils (1.0 clo), and
- relative humidity of 50% at 20°C and 60% at 23°C.

The whole-body averaged SAR at each point of the iso-SA line can be calculated as the SA value divided by the time in minutes. The upper left endpoint of each line in **Figure 4a** corresponds to 4 W/kg, a highly unlikely long-term average exposure during an MRI examination. Examples of clinically relevant worst-case examinations with high whole-body averaged SARs and 45 to 60 min scan durations are continuous turbo spin echo (TSE) scans for the thoracic and lumbar spine, with an average SAR value of > 3 W/kg. The graphs in **Figure 3** show that the core temperature increase in individuals with a normal thermoregulatory system could readily exceed the postulated threshold of 1°C, and reach up to or exceed 1.4°C. When thermoregulation is severely compromised, such as in a patient with a condition that compromises the thermoregulatory system (35), a far higher temperature increase can be expected.

It should be noted that various health conditions may affect an individual's ability to tolerate a thermal challenge including cardiovascular disease, hypertension, diabetes, fever, old age, and obesity. In addition, medications including diuretics, beta-blockers, calcium

Figure 4b. Representative estimates of core temperature increase for a 70kg human with impaired thermoregulation, at different environmental conditions, and for three levels of Specific Absorption (100 and 200 W.min/kg), up to an SAR level of 2 W/kg. The predicted core temperature increases for very long examinations (approximately 2 hours) are unlikely to be observed since no continuous scanning will occur.



blockers, amphetamines, and sedatives can alter thermoregulatory responses to a heat load. Patients presenting with such conditions should only be scanned in the Normal Operating Mode (i.e., whole-body averaged SAR up to 2 W/kg). IEC 60601-2-33 (2) postulates that the core temperature increase should not exceed 0.5°C in that case. TSE scans of the spine at a whole-body averaged SAR of 2 W/kg will take considerably longer and SA levels of 120 to 160 W·min/kg may not be uncommon, corresponding to potential temperature increases of 0.6 to 0.8°C. See **Figure 4b**, where the top left of the iso-SA curves corresponds with 2 W/kg.

The next section will review thermal thresholds in consideration of the observed discrepancy between anticipated core temperature increases in actual use in current (i.e., safe) MRI practice, and restrictions postulated in IEC 60601-2-33.

Thermal Thresholds for Core, Brain and Eyes

This section provides an overview of the global thermal thresholds for sensitive internal organs, especially the brain and the eyes. The temperatures in these organs relate directly to blood temperature, and are part of the assessment of systemic burden. Basic restrictions in RF field-related safety standards and guidelines (4, 36) aim to prevent the occurrence of high core temperature rises (i.e., average blood temperature) (63-65), primarily to prevent functional changes and structural damage in the brain (including the eye) and to avoid a potential overload of thermoregulation capacity, such as stress to cardiovascular function (42). Maintenance of core temperature and protection against thermal insults at cellular and organ levels rely on intricate mechanisms of neuronal and biochemical signaling. For a recent review, see the work by Morrison and Nakamura (66).

Induced thermal stress results in a rapid increase in cutaneous blood flow, coupled to an increase in sweat rate, an increased cardiac output, and a potential decrease in arterial blood pressure (49, 67, 68). Precise levels for core temperatures at which biophysical control mechanisms are activated or may fail are not well established, and may vary as function of age, pregnancy, obesity and hypertension, or additional stress factors (e.g., diuretics, tranquilizers and sedatives, vasodilators and other drugs, chemotherapy, or radiotherapy) (35, 69, 70).

Core Temperature Considerations

Healthy human subjects can tolerate core temperature increases $> 1^{\circ}\text{C}$ for a few hours, but longer exposure at slightly higher temperatures can lead to serious adverse effects (e.g., heat stroke, often associated with severe dehydration). The ICNIRP has adopted and reconfirmed the use of 1°C as a conservative limit for a core temperature rise, or “operational adverse health effect threshold,” in occupational settings (4). Higher values can be allowed in a controlled setting when appropriate training is provided for workers with normal health conditions. Since RF exposures during MRI examinations may cause a temperature increase $> 1^{\circ}\text{C}$ in certain patients, further evaluation of this safety criterion is needed.

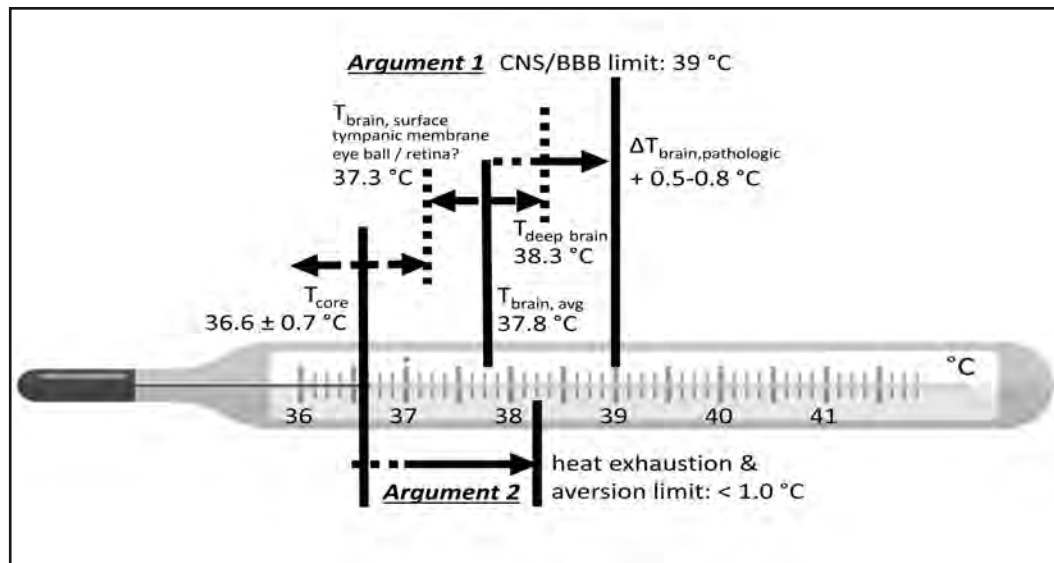
Normal core temperature for humans is commonly postulated to be 37°C (40) with variations up to 0.5°C (mean 0.25°C) associated with the diurnal cycle. Additional temperature variation up to 0.5°C (mean 0.25°C) is associated with the menstrual cycle (71). A critical

266 Thermal Effects Associated with RF Exposures During Clinical MRI

review of thermometer technology and the site of measurement reported that the mean value for core temperature is 0.2 to 0.5°C lower than 37°C (40). A diverse cohort study of 35,488 patients (mean age 52.9 years, 64% women, 41% non-white race) with 243,506 temperature measurements reported a mean temperature of 36.6°C (95% range 35.7 to 37.3°C, 99% range 35.3 to 37.7°C) (72). This range includes effects of the circadian cycle, and will be used in this section to assess if additional margin can be allowed for the commonly adopted limit of 1°C for core temperature increase for MRI exposures.

Preventing harm from core temperature elevations relies on two arguments (36, 42, 63): (1) effects on the central nervous system (CNS) and induced permeability of the blood-brain barrier (BBB), and (2) heat exhaustion and behavioral aversion. **Figure 5** summarizes human core and brain temperatures and the variations concerning these guiding principles. In the subsequent paragraphs, both arguments are discussed in greater detail.

Figure 5. Overview of body temperature data for adults and their relation to an allowable temperature increase from RF exposure.



Argument 1

Limits to core or blood temperature intend to prevent indirect (additional) heating of internal organs, especially the brain. Note the presence of an approximate 1°C temperature gradient in the brain, where the surface temperature (e.g., at the tympanic membrane) equals core (blood) temperature (73). The average and deep brain temperatures are 0.5 to 1.0°C higher than core temperature due to the intense metabolic activity in gray matter. Activation of the visual cortex is reported to locally increase its temperature by 0.7°C (73). Arterial blood and cerebral spinal fluid (CSF) provide the necessary cooling capacity to maintain homeostasis. Notably, even higher temperatures can be caused by certain drugs or neurologic diseases (43, 74).

Physiological Stress. MR systems intentionally expose patients to high RF amplitude and dose, generally for a short duration (i.e., less than 1 hour). Such exposures must be controlled to avoid “physiological stress”, defined as occurrence of effects beyond modest discomfort. Control mechanisms include considerations of transient effects (75-78) and local effects (see the section on Thermal Dose). The requirement that diagnostic imaging procedures shall not invoke undue stress is different from limits based on risk versus benefit considerations which are used in treatments like RF field-induced hyperthermia, where occasional side effects could be acceptable when treating a known serious health risk (38, 79-81). The onset of sweating and the additional load of the cardiovascular system related to the thermoregulatory response may, however, need to be avoided in certain patient groups (35, 49, 67, 68). The whole-body averaged SAR limit for the Normal Operating Mode in IEC 60601-2-33 (2) is, therefore, set to 2 W/kg. Simulations indicate that no special provisions are needed for elderly people, since the estimated effect of aging is less than variations in the increase in core temperature associated with other factors (54, 57).

Blood-Brain Barrier. The ICNIRP proposes to limit the temperature increase for the brain (including the eye) conservatively to 2°C for occupational settings (4). Such temperature increases, however, cannot be justified in cases of brain injury, such as stroke or traumatic brain injury (TBI), where modest temperature increases have been reported to adversely affect outcomes (43, 82, 83). Similar caution is needed for cerebral disease or drug regimens where brain temperatures are elevated (71, 74).

Limited experimental data from animal models indicates that functional abnormalities of the CNS, and BBB disruption are initiated at temperatures of 39 to 39.5°C (74, 84). Effects on brain function and tissue seem reversible in the case of a short duration temperature elevation, and an upper limit of 39.5°C for maximum (deep) brain temperature seems sufficiently conservative. Taking into account the temperature allowance necessary to account for possibly unknown pathologic brain conditions, and at maximum core temperature levels, deep brain temperature without exposure to RF energy may reach 38.8°C. Consequently, an increase of 0.6 to 0.7°C is deemed acceptable for vulnerable patients.

IEC 60601-2-33 requires scanning such patients in the Normal Operating Mode, with reduced RF energy output and clinical observation. **Figure 2b** indicates that under such conditions, the temperature increase will not exceed these limits. Temperature in patients with normal thermoregulation will be considerably (at least 0.7°C) lower than 38.8°C, and a 1.3 to 1.4°C core temperature increase can be considered acceptable. This value is predicted in **Figure 2a** for long duration examinations performed at high SAR levels (i.e., with the MR system operating in the First Level Controlled Operating Mode), and is consistent with the history of the safe use of MRI.

The Eye. Thermal sensitivity of the eye is inherently linked to thermal limits for systemic protection, because the temperature of the eye is largely determined by arterial blood temperature. Corneal temperature is approximately 3°C lower than core temperature (85, 86). Cataract formation is reported in rabbits (albeit, a poor model due to the lateralized position of the eyes compared to human subjects) for 20 to 40 W/kg local SAR at the eye. The absence of such effects at these SAR levels in monkeys is attributed to differences in skull and eye anatomy (87).

268 Thermal Effects Associated with RF Exposures During Clinical MRI

Lesions have also been detected in isolated bovine eyes for incidental exposure to temperatures $> 39^{\circ}\text{C}$ (88). Damage of the bovine lenses was recoverable when exposed for one hour to 39.5°C , but remained in the lens epithelial cells. Experimental data reported temperature increases of the cornea $< 1.8^{\circ}\text{C}$ in 33 patients at RF field exposures of 3 W/kg for the head SAR (89), which is of no concern considering the low basal temperature of the lens (85). Such an increase is consistent with numerical simulation results predicting a temperature increase $> 1^{\circ}\text{C}$ in the eye when applying 3.2 W/kg head SAR for 30 minutes (90, 91). The local-to-head SAR ratio in quadrature RF excitations is approximately 4 W/kg (77, 92), and 3.2 W/kg head SAR corresponds to a local SAR exposure of 10 to 13 W/kg, or $< 1^{\circ}\text{C}$ temperature increase in brain tissue (93, 94). Note that 3.2 W/kg head SAR applies to both the Normal Operating Mode and the First Level Controlled Mode in IEC60601-2-33, and is inconsistent with different local SAR limits for those modes (10 and 20 W/kg, respectively).

The local SAR hotspot for quadrature-excitation does not coincide with the eye and, in that case, no temperature concerns are present. Of course, this would be different for parallel transmit, RF-shimmed excitations (91). Specific attention is needed to prevent an excessive temperature increase in the eye for localized transmit or parallel transmit scenarios where RF energy is focused in the ocular area (93). Steering of local SAR by RF pulse design and averaging of RF power deposition by multiple shimmed RF pulses can be used to mitigate such high local SAR hotspots, especially at ultra-high static magnetic fields and using multi-channel parallel transmit RF systems (93). Notably, exposure to higher levels of local SAR (20 W/kg, 0.56 CEM43) in the context of RF field-induced hyperthermia in oncology patients did not reveal cataract formation (95).

Argument 2

Thermally-induced task aversion resulting from 4 W/kg RF exposure has been reported in animals (36). Similarly, humans will adapt their behavior in warm environments to avoid heat stroke. Studies in healthy volunteer subjects have shown significant adverse effects when exposed to core temperatures approaching 39°C as associated with severe exercise (36, 44, 96). Effects of temperature and dehydration cannot be separated in such studies. There is a broad consensus that avoidance of undue heat stress in healthy humans requires core temperature to stay below 38.5°C , as measured at the tympanic membrane, and should likely be less in vulnerable human subjects. This value is consistent with an allowable increase of 1.3 to 1.4°C beyond the highest reported core temperature in non-febrile patients, that is, 37.3°C (72).

Thermal Protection of the Fetus

Episodes of high temperature in the embryonic stage can be teratogenic or can result in developmental defects (97). A retrospective review supported concerns for a potential negative health impact associated with first trimester fever in human subjects (98). To the contrary, a subsequent large-scale prospective study by the same investigators concluded that there was no evidence that maternal fever during pregnancy induced congenital defects (99). The latter finding corroborates reports that (non-contrast enhanced) MRI during pregnancy does not negatively impact childhood outcomes (100, 101).

MR imaging was likely performed using the Normal Operating Mode (2 W/kg whole-body averaged SAR), as required by IEC 60601-2-33 in the case of pregnancy. Additional information on this topic is presented by Hand, et al. (102). Alternatively, a level of 1.5 W/kg for up to one hour of scanning is suggested as the limit for second and third trimester patients by Ziskin and Morissey (97). Guidelines for obstetricians also suggest deferring MRI, if any, to after the first trimester (103). This is in line with consensus guidelines for fetal ultrasound (19, 20) which aim for As Low As Reasonable Achievable (ALARA) risk by limiting thermal dose to the fetus to 1 CEM43 (see below).

Fetal temperature is 0.3 to 0.5°C above maternal core temperature (32, 104, 105), and heat exchange depends almost completely on the umbilical cord and placental heat exchange. Numerical simulations of 80 MHz plane wave exposure show that the average fetal temperature increase may exceed that of the mother (28), with values of 0.4 to 0.8°C for one hour at 2 to 4 W/kg whole-body averaged SAR in the mother. Similar values have been reported by various researchers for one hour MRI exposures in the Normal Operating Mode (1.5 to 2 W/kg) (32, 102, 104). These predicted increases will keep the average temperature in the fetus below 38°C.

High-resolution numerical modeling indicates the existence of local thermal hotspots in the fetus and the placenta (32), similar to inhomogeneous local SAR and temperature distributions in adults (28-31, 75, 77, 106). Hotspots in the fetus may be particularly enhanced in case of unfavorable RF shimming conditions at 3 T (32), where image quality optimization (B_1^+ homogenization) in the mother may unduly increase the RF load in the fetus. Safe use of RF shimming is possible when the MR system software takes into account appropriate constraints on the allowed shim conditions (107). Otherwise, the use of the circularly-polarized (CP) mode is recommended, at the expense of uniform flip angle distribution. Note that frequent fetal movements are expected to reduce the severity of local SAR and temperature hotspots in the fetus, but not in the placenta. Short duration, low SAR, CP mode scanning should remain the guidance for the utilization of MRI in pregnant patients.

Thermal Dose and its Proposed Used in MRI

Globally uniform RF transmit fields, such as CP in birdcage volume transmit coils, lead to a highly non-uniform local SAR distribution in the human body (108). Early attempts aimed to reflect this effect by using partial-body SAR instead of whole-body averaged SAR, but simulations have shown that this approach allows for higher RF duty cycles and thereby even higher local SAR (109, 110). Local SAR hotspots may cause a local temperature rise, which may, at least in patients with sufficient thermoregulatory response, be moderated by thermal diffusion and (increasing) blood flow.

An overview of the biophysical aspects connecting SAR and local temperature is provided in the work by Szasz, et al. (111), where it is argued that vasodilation may not be effective for localized exposures. Numerical electromagnetic simulations provide local SAR values which can be used in combination with Pennes' Bioheat Equation (PBE) to derive temperature distributions with an acclaimed accuracy of 10 to 15% (28-31, 75, 77, 93, 106, 112). A more advanced model, the Generic Bioheat Transfer Model, was proposed to better fit data obtained in anesthetized swine (113), and addresses issues related to the assumption of constant blood temperature in PBE. The lack of experimental data in human subjects,

270 Thermal Effects Associated with RF Exposures During Clinical MRI

and variability of human anatomy and physiology, make it virtually impossible to decide which model is more appropriate. The required accuracy for the local SAR and temperature simulations with respect to averaging volume: 1g versus 10g (114, 115), averaging scheme (4, 94, 116), and the number of required tissue types is discussed by Homann, et al. (114).

The use of steady state approaches clearly overestimates the initial thermal response (15 minutes), since energy deposition can, under normal circumstances, first be redistributed in the peripheral body parts (111). A critical review of the merits and implications of the use of PBE concludes that it is adequate in the context of RF field-induced heating simulations (117). This modeling approach has been validated with measurements in RF field-induced hyperthermia (118), for local exposure at 7 T (119), and in anesthetized swine where severe muscle damage was observed for > 4 W/kg and SA of 8 to 15 kJ/kg (120). The observed damage in the work by Nadobny, et al. (120) points to the usefulness of applying the thermal dose concept, or CEM43, from hyperthermia to assess potential risks associated with long-term, high-SAR MRI examinations.

Cumulative Equivalent Minutes at 43°C as a Basic Restriction

CEM43, or Cumulative Equivalent Minutes at 43°C is a local thermal dose “iso-effect” metric (1), representing the duration of exposure at a reference temperature of 43°C, associated with the magnitude of a thermally-induced bio-effect observed or predicted to occur at a different temperature, T , for duration, t_{exam} . The actual temperature, T , may vary as a function of time. In this context, 10 CEM43 represents 10 min of exposure at 43°C. The CEM43 model approximates the non-linear relationship of tissue damage by using two log-linear relationships with a break point at 43°C:

$$CEM43 = \int_0^{t_{exam}} R^{k(T(\tau)-43)} d\tau \quad (1)$$

where

- k = $(1^{\circ}\text{C})^{-1}$, a constant to render the exponent dimensionless
- $T(\tau)$ = temperature during time course τ of an MRI examination
- τ = time
- t_{exam} = duration of the MRI examination, including additional integration time after the last RF exposure to account for temperature normalization
- R = exponential constant, 0.25 for $T < 43^{\circ}\text{C}$ and 0.5 for $T \geq 43^{\circ}\text{C}$

Validity of CEM43 as a metric to assess treatment effects and risk to damage surrounding tissue is generally accepted for temperatures in the range of 39°C to 57°C (121). Note, however, that CEM43 is based on Arrhenius plot for counted death cells, while the onset of detectable death cells is not immediate. A more accurate parameter to describe the absence of risk would be the fraction of living cells, which involves higher-order biochemical feedback paths (122). CEM43 is considered to over-predict tissue damage risk at moderate tem-

perature elevations (17), which can be considered adequate to establish safety in association with MRI because it adds conservativeness in protection against damage. The delay of observable damage (122) may, however, indicate a risk of unnoticed thermal overburden related to an MRI examination.

The exponential constant, R, is determined from cell cultures and animal models (121). Human data is scarce but indicates that the R-values in human tissue may reflect a higher thermal tolerance. Using the established R-values of 0.25 and 0.5 provides a more conservative accumulation of CEM43, and thresholds for basic restrictions have also been derived based on these values for R (121, 122). Thresholds vary by more than two orders of magnitude with animal species and tissue type, and an analysis of the lowest value with reported damage, and the highest value with no reported damage is provided by van Rhoon, et al. (33). A conservative threshold of 2 CEM43 is proposed for all tissues and all patients. Higher values (i.e., 9 CEM43 and 15 CEM43) are suggested to be safe for skin, muscle, fat and bone. The ultrasound community has used the same information to derive a limit value of 1 CEM43, but acknowledges that 2 CEM43 would also be acceptable (20, 97). This threshold will protect nerves, both in the spinal cord and embedded in muscle. Peripheral nerves are reported to be particularly vulnerable in sensitive patient classes, such as those with diabetes or multiple sclerosis, and those undergoing chemo- or radiotherapy (123, 124).

Local SAR Modeling and Model Variability

CEM43 can easily be calculated from local SAR values obtained from numerical modeling (i.e., peak 10g averaged specific absorption rate, psSAR10g) (125). The use of 10 g versus 1g averaging for local SAR has been evaluated in several studies (114, 115), with the consensus being that a cubic averaging mass of 10g is appropriate when considering thermal effects. For additional information, refer to the ICNIRP document and references cited, therein (4). The use of smaller volumes does not reflect the typical heat diffusion length and time scales, although some studies suggested that higher resolution might point to the high local E-fields and locations at risk of skin-to-skin burns (126, 127). Different approaches to spatial averaging have been shown to correspond to a factor of two difference in estimated values (128). This is of course already potentially problematic when considering that the difference in the exposure limits for the Normal Operating Mode and the First Level Controlled Operating Mode differ by just a factor of two.

Inhomogeneous local SAR and distributions have been studied using high-resolution models for adults and children at different landmarks and poses (28-31, 75, 77, 106). Interpretation of the results remains a challenge for several reasons: in the real-world exposure scenario, the transmit RF coil is tuned for an average load which, together with the design details of the resonator, are difficult to represent in multiple setups. When appropriate caution is taken, the results from the modeling packages, Remcon XFDTD and Sim4Life, match extremely well (Private communication, Z. Zhang, 2021). Posing the model and avoiding undue artifactual hotspots requires careful model setup and evaluation. Another parameter to choose is the distance to shift the model through the transmit RF body coil when assessing exposure scenarios. The difference in observed psSAR10g for actual simulation at a shift of 2.5 cm or when interpolating from data simulated at 10 cm shifts is in the order of 2% with outliers up to 10% (Private communication, Z. Zhang, 2021). This gives confidence

272 Thermal Effects Associated with RF Exposures During Clinical MRI

that a limited set of exposure scenarios is sufficient to characterize the SAR behavior. In addition, segmentation of tissues and assignment of boundaries for different conductivities further contributes to uncertainty in simulated local SAR values. Early studies showed that 5 mm resolution is sufficient to obtain robust estimates of psSAR10g (129, 130), and a reduction to three tissue types (muscle, fat, and lung) does not alter the overall reliability of psSAR10g averages in the Visible Human Male and Female (114).

A similar study was performed on the Chinese Adult Male and Female models and for a comparable Chinese individual (deformable) model, reporting agreement to within 10% for simulated psSAR10g between multi-tissue and reduced tissue-type simulations (131). This approach using a limited set of tissue types was further advanced by the introduction of the so-called Q-matrix formalism, which allowed for a rapid patient-individualized SAR determination to control RF shimming at 3 T (106, 132). B_1^+ optimization while also controlling local SAR in the arms was shown to provide a far (up to four times) lower local SAR in both the torso and in the extremities than when the arms were not taken into consideration. This suggests that individualized SAR assessment is a valuable asset for reducing variability of actually delivered SAR across subjects. Evaluation of psSAR10g for 7 T, local transmit RF coils in the brain (133) and in the prostate/pelvis using four-tissue segmented data from 23 subjects indicated that a safety margin of one-half to two-times is necessary if no explicit assessment of inter-subject variability is taken into account (134). RF shimming simultaneously improves the B_1 uniformity and lowers psSAR10g relative to regular quadrature-excitation (i.e., circularly-polarized).

Additional studies focused on the effects of RF shimming in fetal imaging (32) and the intra-subject and mother's posture differences in maternal and fetal SAR (135). The observed variability in psSAR10g, especially in whole-body averaged exposure scenarios, indicates that appropriate model choice and selection of additional safety margin is not trivial. Irrespectively, the data in by Homann, et al. (114) shows that the Visible Human Male provides a reasonable worst-case human model for assessment of whole-body averaged SAR and for psSAR10g in torso and extremities. An additional safety margin of 10 to 20% for extremity SAR may be needed to ensure coverage of different poses of the arms across humans.

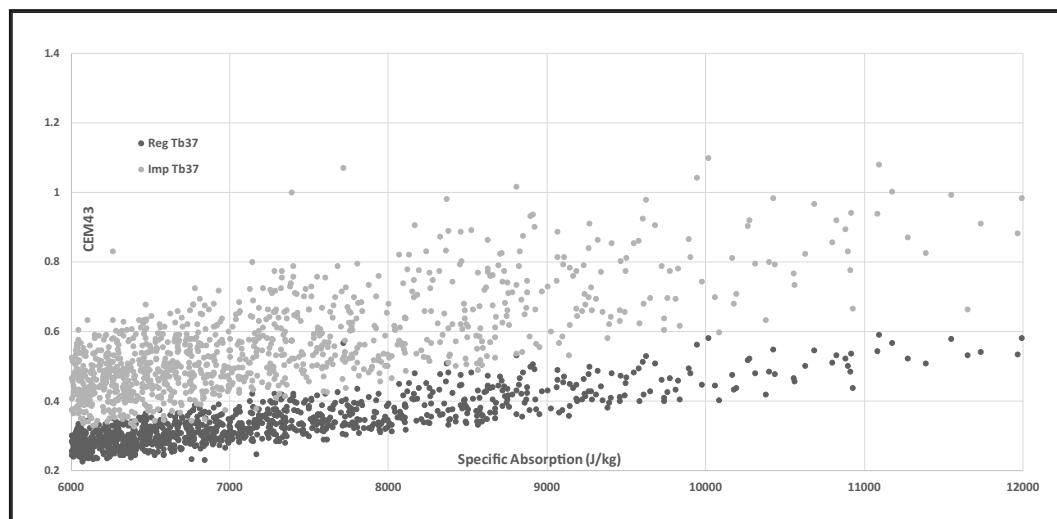
Real-World Evidence for CEM43 Values in MRI Examinations

Peak temperature increases and thermal time constants were obtained for six numerical human models at different imaging positions at 1.5 T and 3 T (28-30), under the conditions of thermoregulation, and for basal perfusion. Extension to impaired thermoregulation is presented in the work by Murbach, et al. (31), with an update of the parameters to be used in the model. Temperature increase is calculated as a function of the value of psSAR10g for the voxel where local SAR is highest (125). Using an estimated baseline body temperature (e.g., 36.8°C or 38°C), a worst-case estimate for CEM43 is obtained, albeit those effects of core temperature increase are not accounted for. A re-evaluation of the results by Neufeld, et al. (125) seems warranted since the core temperature increase could add 20 to 25% to the temperature increase caused by local SAR. Another necessary extension relates to local exposure scenarios (125), using detachable transmit RF coils for head and knee im-

aging, as well as for cardiac and prostate imaging at 7 T. Specific parameters are needed to derive the temperature increase from the maximum local SAR in such cases.

Worst-case CEM43 values were calculated for the exposure scenario where local SAR limits from IEC 60601-2-33 are applied to a whole-body averaged RF excitation (125). The calculated thermal dose values are based on predicted local SAR values from the Philips MR system software (Philips Medical Systems, Best, The Netherlands). **Figure 6** shows a correlation of calculated CEM43 and predicted specific absorption for 6,500 body/torso exams with SA between 4 and 11 kJ/kg (subset of data used for **Figure 2**), using a baseline temperature of 37°C and assuming that either all patients have fully-regulated perfusion or all patients present with severely impaired thermoregulation. High SA levels will only be reached for landmarks between the neck and groin (whole-body averaged SAR is lower for other landmarks). Considering that local torso SAR is limited to 20 W/kg, the thermal dose will not exceed 1 CEM43 in examinations of the torso. In other words, high SA does not directly correlate with the high local thermal dose.

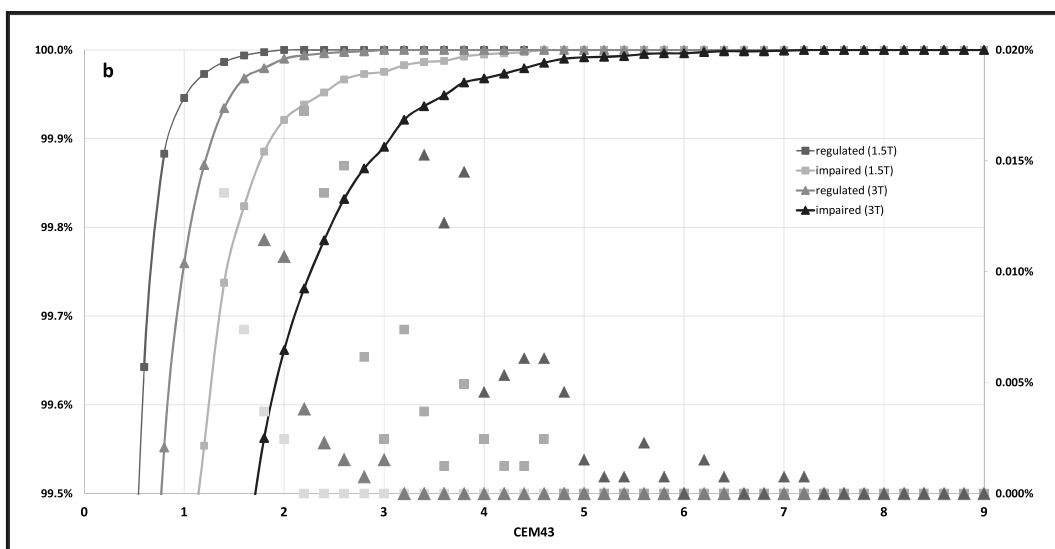
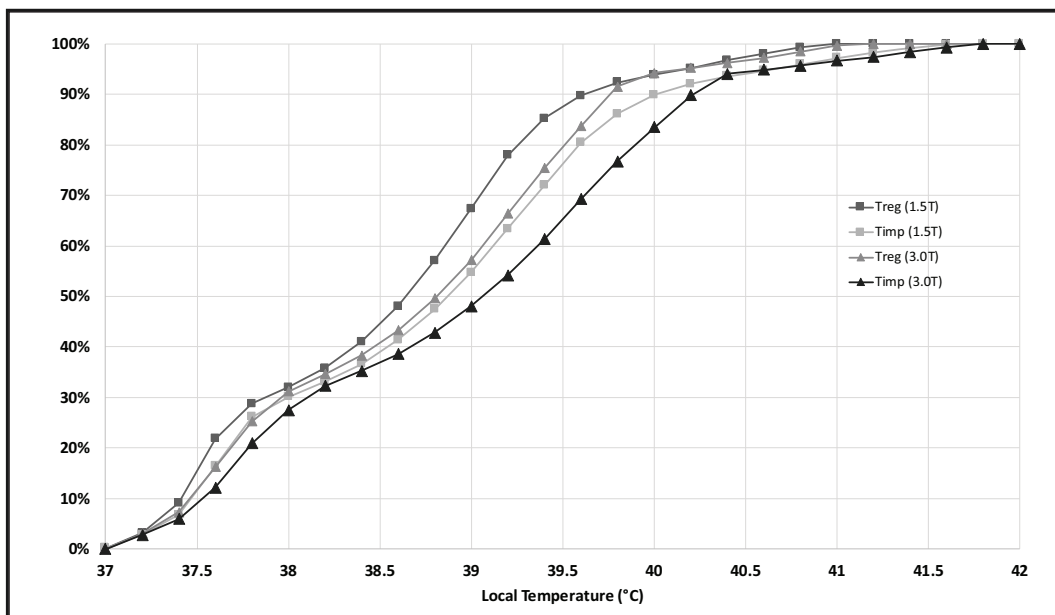
Figure 6. Scatter plot of CEM43 and Specific Absorption (SA) for 6,500 examinations at 1.5 T (out of 367,000 examinations shown in **Figure 2**), with SAR limited to a local torso level of 20 W/kg (4).



Higher CEM43 values may be reached for landmarks where the ratio of local SAR to whole-body averaged SAR is higher. **Figure 7** provides an overview of 210,000 examinations at 1.5 T and 3 T to assess the predicted temperature distribution and the resulting likelihood of high CEM43 values, under conditions of normal and compromised thermoregulation. Under the assumptions used in the work by Neufeld, et al. (125) (i.e., heavy patient, worst-case hotspot, basal temperature of 37°C at any tissue), it can be inferred that less than one in 10,000 patients would be exposed to a thermal dose > 2 CEM43. Note that this predicted thermal dose value will over-estimate thermal dose in most patients due to assumptions presented by Neufeld, et al. (125). The values shown in **Figure 5** cannot be used to establish limits based on “history of safe use” arguments. Validation of temper-

274 Thermal Effects Associated with RF Exposures During Clinical MRI

Figures 7a (top) and 7b (bottom). Typical distribution of (a) predicted hotspot temperature and (b) CEM43 (in bins of 0.2) observed in clinical use of 210,000 examinations at MRI performed at 1.5 T and 3 T MRI for all body parts at multiple hospitals. The curves represent normal and impaired thermoregulation starting from a basal temperature of 37°C (125), and show the percentage of examinations where a certain CEM43 is calculated. The fraction of high CEM43 values for each bin and each condition are represented as unconnected data points with values shown at the right-side axis. Note that assumed impaired thermoregulation shifts the curves to higher CEM43 values, but such values for thermoregulatory impaired conditions may be a significant overestimate due to model assumptions. (Reproduced with permission, copyright © 2019 Johan S. van den Brink.)



atures and thermal dose values require further investigation before safe thresholds can be established.

High local thermal dose is delivered on purpose in RF field-induced hyperthermia, where acute adverse effects (e.g., pain and RF burns) are reported for high local SAR values (100 W/kg and higher) (38, 81). Where Wust, et al. (38) uses their observation that 1% of (700) patients in 3,000 treatment sessions showed burns to propose safe local SAR limits for MRI at 20 W/kg for head, neck and torso, and 30 W/kg for the extremities, the results from Adibzadeh, et al. (81) and other data in the peer-reviewed literature (121) are used by Adibzadeh, et al. (136) to derive the lowest thermal dose (TD) required to induce acute local tissue damage, and to calculate the corresponding TD-functional SAR limits (SAR_{TDFL}) for a 10 minute and a 60 minute steady-state exposure.

CEM43 restrictions can be realized by applying appropriate SAR_{TDFL} limits to whole-body transmit RF coils, in conjunction with limits for whole-body averaged SAR or head SAR values. Using the thermal damage threshold for muscle (60 CEM43) (136) suggests that a SAR_{TDFL} of 200 to 300 W/kg could be tolerable. Current local SAR limits in IEC 60601-2-33 are 5 to 10 times lower (20 W/kg in the trunk and 40 W/kg in the extremities). These reduced limits seem justified given the uncertainties in modeling and across the population. Care must be taken, however, to not apply the uncertainty in both defining the limits and when applying modeling approaches to demonstrate compliance with the limits. Preliminary analysis of CEM43 “big data” indicates that 2 CEM43 corresponds with current limit values for local SAR in IEC 60601-2-33 (Figure 7), but that higher values could occasionally occur. Such higher values have been previously suggested to be safe based on an extensive review of CEM43 data (33), but evidence is insufficient to adopt thermal dose thresholds > 2 CEM43. Further studies are necessary to establish the appropriate model to evaluate CEM43 and conservative values for CEM43 limits in the brain and lower extremities, especially when using detachable transmit head or knee RF coils at 7 T. These use scenarios are insufficiently covered by Neufeld, et al. (125), but their methodology can be used to assess potential thermal risks in such designs.

SUMMARY

Protecting patients undergoing MRI examinations from adverse thermal effects necessitates considering both systemic and local temperature increases, as well as the thermal dose. Prolonged duration, high-SAR MRI examinations can cause a core temperature increase $> 1^{\circ}\text{C}$, which is generally not problematic considering normal body temperatures, thermoregulatory capabilities, and the allowable brain temperature. To prevent an excessive core temperature increase ($> 1.3^{\circ}\text{C}$), the temperature in the MR system room should be maintained at or below 22°C , the use of blankets should be avoided or blankets should be removed from patients after a few initial scans, and the actual-delivered, specific absorption should not exceed 4 kJ/kg. If higher SA levels are necessary, active cooling of the patient by airflow and medical intervention may be warranted to prevent serious discomfort. Lower whole-body averaged SAR (< 2 W/kg) values and short duration examinations should be considered in vulnerable patient groups, including pregnant women. Local SAR control (< 20 W/kg) for torso and spine MRI examinations is in most cases sufficient to prevent exceeding 2 CEM43 if the increase in core temperature is not considered. Further studies are

276 Thermal Effects Associated with RF Exposures During Clinical MRI

needed to account for core temperature increases when calculating CEM43, and to establish appropriate CEM43 limits and evaluation models for exposure of the brain and lower extremities, especially when using detachable transmit RF coils.

ACKNOWLEDGMENTS

This work was funded by the EUREKA cluster programme, ITEA3 project STARLIT (16016) and PENTA project DISPERSE (16012).

REFERENCES

1. Sapareto DA, Dewey WC. Thermal dose determinations in cancer therapy. *Int J Radiat Oncol* 1984;10:787–800.
2. International Electrotechnical Commission, IEC 60601-2-33 Edition 3 Amendment 2. Medical electrical equipment - Part 2-33: Particular requirements for the basic safety and essential performance of magnetic resonance equipment for medical diagnosis. Available at <https://webstore.iec.ch/publication/22705>. Accessed June, 2021.
3. Deniz CM. Parallel transmission for ultrahigh field MRI. *Top Magn Reson Imaging* 2019; 28:159–171.
4. International Commission on Non-Ionizing Radiation Protection (ICNIRP). Guidelines for limiting exposure to electromagnetic fields (100 kHz to 300 GHz). *Health Phys* 2020;118:483-524.
5. Institute of Electrical and Electronics Engineers (IEEE), C95.1-2019 - IEEE Standard for Safety Levels with Respect to Human Exposure to Electric, Magnetic, and Electromagnetic Fields, 0 Hz to 300 GHz, 2019.
6. Kou X, Li R, Hou L, Zhang L, Wang S. Identifying possible non-thermal effects of radio frequency energy on inactivating food microorganisms. *Int J Food Microbiol* 2018;269:89-97.
7. Wust P, Kortüm B, Strauss U, et al. Non-thermal effects of radiofrequency electromagnetic fields. *Sci Rep* 2020;10:13488.
8. IARC Working Group on the Evaluation of Carcinogenic Risks to Humans. Non-Ionizing Radiation, Part 2: Radiofrequency Electromagnetic Fields. Lyon (FR): International Agency for Research on Cancer; 2013.
9. Food & Drug Administration. Review of published literature between 2008 and 2018 of relevance to radiofrequency radiation and cancer. 2020. Available at <https://www.fda.gov/media/135043/download>. Accessed June, 2021.
10. Falcioni L, Bua L, Tibaldi E, et al. Report of final results regarding brain and heart tumors in Sprague-Dawley rats exposed from prenatal life until natural death to mobile phone radiofrequency field representative of a 1.8GHz GSM base station environmental emission. *Environ Res* 2018;165:496-503.
11. Takahashi A, Mori E, Ohnishi T. The foci of DNA double strand break-recognition proteins localize with gammaH2AX after heat treatment. *J Radiat Res* 2010;51:91-95.
12. Velichko A, Petrova NV, Kantidze OL, Razin SV. Dual effect of heat shock on DNA replication and genome integrity. *Mol Biol Cell* 2012;23:3450-3460.
13. Kantidze OL, Velichko AK, Luzhin AV, Razin SV. Heat stress-induced DNA damage. *Acta Naturae* 2016;8:75-78.
14. Balajee AS, Geard CR. Replication protein A and gamma-H2AX foci assembly is triggered by cellular response to DNA double-strand breaks. *Expt Cell Res* 2004;300:320-334.
15. Takahashi A, Matsumoto H, Nagayama K, et al. Evidence for the involvement of double-strand breaks in heat-induced cell killing. *Cancer Res* 2004;64:8839-8845.

MRI Bioeffects, Safety, and Patient Management 277

16. Fasshauer M, Krüwel T, Zapf A, et al. Absence of DNA double-strand breaks in human peripheral blood mononuclear cells after 3 Tesla magnetic resonance imaging assessed by γ H2AX flow cytometry. *Eur Radiol* 2018;28:149–156.
17. O'Brien Jr WD, Deng CX, Harris GR, et al. The risk of exposure to diagnostic ultrasound in postnatal subjects: Thermal effects. *J Ultrasound Med* 2008;27:517–535.
18. IEC TR 62799. Models for evaluation of thermal hazard in medical diagnostic ultrasonic fields. Available at <https://standards.iteh.ai/catalog/standards/iec/f5b1d7bf-3304-4d59-8c79-efee1c8f92d6/iec-tr-62799-2013>. Accessed June, 2021.
19. Ziskin MC. The thermal dose index. *J Ultrasound Med* 2010;29:1475–1479.
20. Harris GR, Church GC, Dalecki D, Ziskin MC, Bagley JE. Comparison of thermal safety practice guidelines for diagnostic ultrasound exposures. *Ultrasound Med Biol* 2016;42:345–357.
21. Kok HP, Cressman ENK, Ceelen W, et al. Heating technology for malignant tumors: A review. *Int Journal Hyperthermia* 2020;37:711–741.
22. Weyand PG, Smith BR, Sandell RF. Assessing the metabolic cost of walking: The influence of baseline subtractions. *Annu Int Conf IEEE Eng Med Biol Soc* 2009;2009:6878–81.
23. Teunissen LP, Grabowski A, Kram R. Effects of independently altering body weight and body mass on the metabolic cost of running. *J Experimental Biol* 2007;210:4418–4427.
24. ASHRAE. Chapter 9: Thermal Comfort. Available at http://courses.washington.edu/me333afe/ASHRAE_Comfort.pdf. Accessed June, 2021.
25. Morimoto R, Hirata A, Laakso I, Ziskin M, Foster R. Time constants for elevation in human models exposed to dipole antenna and beams in the frequency range from 1 to 30 GHz. *Phys Med Biol* 2017;62:1676–1699.
26. Hirata A, Fujiwara O. The correlation between mass-averaged SAR and temperature elevation in the human head model exposed to RF near-fields from 1 to 6GHz. *Phys Med Biol* 2009;54:7171–7182.
27. van den Brink, JS. Thermal effects associated with RF exposures in diagnostic MRI: Overview of existing and emerging concepts of protection. *Concepts Magn Reson Part B Magn Reson Eng* 2019;2019:1–17.
28. Murbach M, Cabot E, Neufeld E, et al. Local SAR enhancements in anatomically correct children and adult models as a function of position within 1.5 T MR body coil. *Prog Biophys Mol Biol* 2011;107:428–433.
29. Murbach M, Neufeld E, Capstick M, et al. Thermal tissue damage model analyzed for different whole-body averaged SAR and scan durations for standard MR body coils. *Magn Reson Med* 2014;71:421–431.
30. Murbach M, Neufeld E, Kainz W, Pruessmann KP, Kuster N. Whole-body and local RF absorption in human models as a function of anatomy and position within 1.5 T MR body coil. *Magn Reson Med* 2014;71:839–845.
31. Murbach M, Neufeld E, Cabot E, et al. Virtual population-based assessment of the impact of 3 Tesla radiofrequency shimming and thermoregulation on safety and B_1^+ uniformity. *Magn Reson Med* 2016;76:986–997.
32. Murbach M, Neufeld E, Samaras T, et al. Pregnant women models analyzed for RF exposure and temperature increase in 3 T RF shimmed birdcages. *Magn Reson Med* 2017;77:2048–2056.
33. van Rhoon GC, Samaras T, Yarmolenko PS, et al. CEM43°C thermal dose thresholds: A potential guide for magnetic resonance radiofrequency exposure levels? *Eur Radiol* 2013;23:2215–2227.
34. Adibzadeh F, Paulides MM, van Rhoon GC. SAR thresholds for electromagnetic exposure using functional thermal dose limits. *Int J Hyperthermia* 2018;18:1–7.
35. Shellock FG. Chapter 6. Radiofrequency-Energy Induced Heating During MRI: Laboratory and Clinical Experiences. In: Shellock FG, Crues JV, Editors. *MRI Bioeffects, Safety, and Patient Management*. Los Angeles: Biomedical Publications; 2014. pp. 155–170

278 Thermal Effects Associated with RF Exposures During Clinical MRI

36. IEEE Standard C95.1-2005. IEEE standard for safety levels with respect to human exposure to radio frequency electromagnetic fields, 3 kHz to 300 GHz. Available at https://standards.ieee.org/standard/C95_1-2005.html. Accessed June, 2021
37. Shellock FG, Schaefer DJ, Crues JV. Alterations in body and skin temperatures caused by magnetic resonance imaging: Is the recommended exposure for radio frequency radiation too conservative? *Br J Radiol* 1989;62:902–909.
38. Wust P, Nadobny J, Szmitenings M, Stetter E, Gellermann J. Implications of clinical RF hyperthermia on protection limits in the RF range. *Health Physics* 2007;92:565–573.
39. Del Bene VE. Temperature. In: Walker HK, Hall WD, Hurst JW, Editors. *Clinical Methods: The History, Physical, and Laboratory Examinations*, Third Edition. Boston: Butterworths; 1990; pp. 990–993.
40. Kelly G. Body temperature variability (Part 1): A review of the history of body temperature and its variability due to site selection, biological rhythms, fitness, and aging. *Altern Med Rev* 2006;11:278–293.
41. Mcilvoy L. Comparison of brain temperature to core temperature: A review of the literature. *J Neurosci Nurs* 2004;36:23–31.
42. Cheshire Jr WP. Thermoregulatory disorders and illness related to heat and cold stress. *Auton Neurosci* 2016;196:91–104.
43. Childs C, Lunn, KW. Clinical review: Brain-body temperature differences in adults with severe traumatic brain injury. *Critical Care* 2013;17:222.
44. Lim CL, Byrne C, Lee JK. Human thermoregulation and measurement of body temperature in exercise and clinical settings. *Ann Acad Med Singapore* 2008;37:347–353.
45. Shellock FG, Crues, JV. Temperature, heart rate and blood pressure changes associated with clinical imaging at 1.5 T. *Radiology* 1987;163:259–262.
46. Shellock FG, Schaefer DJ, Kanal E. Physiologic responses to an MR imaging procedure performed at a specific absorption rate of 6.0 W/kg. *Radiology* 1994;192:865–868.
47. Adair ER, Blick DW, Allen SJ, et al. Thermophysiological responses of human volunteers to whole-body RF exposure at 220 MHz. *Bioelectromagnetics* 2005;26:448–461.
48. Adair ER, Berglund LG. Thermoregulatory consequences of cardiovascular impairment during NMR imaging in warm/humid environments. *Magn Reson Imaging* 1989;7:25–37.
49. Adair ER, Berglund LG. Predicted Thermophysiological Responses of Humans to MRI Fields. In: Magin RI, Liburdy RP, Persson B, Editors. *Biological Effects and Safety Aspects of Nuclear Magnetic Resonance Imaging and Spectroscopy*. Annals of the New York Academy of Sciences. 1992. pp. 188–200.
50. Boss A, Graf H, Berger A, et al. Tissue warming and regulatory responses induced by radio frequency energy deposition on a whole-body averaged 3-Tesla magnetic resonance imager. *J Magn Reson Imaging* 2007;26:1334–1339.
51. Adair ER, Berglund LG. On the thermoregulatory consequences of NMR imaging. *Magn Reson Imaging* 1986;4:321–333.
52. Katic K, Li R, Zeiler W. Thermophysiological models and their applications: A review. *Building and Environment* 2016;106:286–300.
53. Fu M, Weng W, Chen W, Luo N. Review on modeling heat transfer and thermoregulatory responses in human body. *Journal of Thermal Biology* 2016;62:189–200.
54. Nomura T, Laakso I, Hirata A. FDTD computation of temperature elevation in the elderly for far-field RF exposures. *Radiat Prot Dosimetry* 2014;58:497–500.
55. Hirata A, Laakso I, Oizumi T, et al. The relationship between specific absorption rate and temperature elevation in anatomically based human body models for plane wave exposure from 30 MHz to 6 GHz. *Phys Med Biol* 2013;58:903–921.
56. Nelson DA, Curran AR, Nyberg HA, et al. High-resolution simulations of the thermophysiological effects of human exposure to 100 MHz RF energy. *Phys Med Biol* 2013;58:1947–1968.

MRI Bioeffects, Safety, and Patient Management 279

57. Laakso I, Hirata A. Dominant factors affecting temperature rise in simulations of human thermoregulation during RF exposure. *Phys Med Biol* 2011;56:7449–7471.
58. Hirata A, Sugiyama H, Fujiwara O. Estimation of core temperature elevation in humans and animals for whole-body averaged averaged SAR. *Progr in Electromagn Research* 2009;99:53–70.
59. Moore SM, McIntosh RL, Iskra S, Lajevardipour A, Wood AW. Effect of adverse environmental conditions and protective clothing on temperature rise in a human body exposed to radiofrequency electromagnetic fields. *Bioelectromagnetics* 2017;38:356–363.
60. Hirata A, Asano T, Fujiwara O. FDTD analysis of human body-core temperature elevation due to RF far-field energy prescribed in the ICNIRP guidelines. *Phys Med Biol* 2007;52:5013–5023.
61. Barber BJ, Schaefer DJ, Gordon CJ, Zawieja DC, Hecker, J. Thermal effects of MR imaging: Worst-case studies on sheep. *AJR Am J Roentgenol* 1990;155:1105–1110.
62. Clo unit definition. Oxford Reference. Available at <https://www.oxfordreference.com/view/10.1093/oi/authority.20110803095619345>. Accessed June, 2021.
63. D'Andrea JA, Ziriax JM, Adair ER. Radio frequency electromagnetic fields: Mild hyperthermia and safety standards. *Prog Brain Res* 2007;162:107–135.
64. Kheifets L, Repacholi M, Saunders R. Thermal stress and radiation protection principles. *Int J Hyperthermia* 2003;19: 215–224.
65. Saunders RD, Croft RJ, Van Rongen E. Biological effects and health consequences of ELF and RF fields. *Comprehensive Biomedical Physics* 2014;7:323–353.
66. Morrison SF, Nakamura K. Central mechanisms for thermoregulation. *Annu Rev Physiol* 2019;81:285–308.
67. Donaldson GC, Keatinge WR, Saunders RD. Cardiovascular responses to heat stress and their adverse consequences in healthy and vulnerable human populations. *Int J Hyperthermia* 2003;19:225–235.
68. Adair ER, Kelleher SA, Mack GW, Morocco TS. Thermophysiological responses of human volunteers during controlled whole-body averaged radio frequency exposure at 450 MHz. *Bioelectromagnetics* 1998;19:232–245.
69. Skelton F. Impaired thermoregulation. Available at AAPMR. <https://now.aapmr.org/impaired-thermoregulation/>. Accessed June, 2021.
70. Adams SC, Schondorf R, Benoit J, Kilgour RD. Impact of cancer and chemotherapy on autonomic nervous system function and cardiovascular reactivity in young adults with cancer: A case-controlled feasibility study. *BMC Cancer* 2015;15:414.
71. Kräuchi K, Konieczka K, Roescheisen-Weich C, et al. Diurnal and menstrual cycles in body temperature are regulated differently: A 28-day ambulatory study in healthy women with thermal discomfort of cold extremities and controls. *Chronobiol Int* 2014;31:102–113.
72. Obermeyer Z, Samra JK, Mullainathan S. Individual differences in normal body temperature: longitudinal big data analysis of patient records. *BMJ* 2017;359:j5468.
73. Wang H, Wang B, Normoyle KP, et al. Brain temperature and its fundamental properties: A review for clinical neuroscientists. *Frontiers in Neuroscience* 2014;8:1–17.
74. Kiyatkin EA. Brain temperature homeostasis: Physiological fluctuations and pathological shifts. *Frontiers in Bioscience* 2010;15:73–92.
75. Nadobny J, Szmitenings M, Diehl D, et al. Evaluation of MR-induced hot spots for different temporal SAR modes using a time-dependent finite difference method with explicit temperature gradient treatment. *IEEE Trans Biomed Eng* 2007;54:1837–1849.
76. Wang Z, Lin JC, Vaughan JT, Collins CM. Consideration of physiological response in numerical models of temperature during MRI of the human head. *J Magn Reson Imaging* 2008;28:1303–1308.
77. Wang Z, Lin JC, Mao W, et al. SAR and temperature: Simulations and comparison to regulatory limits for MRI. *J Magn Reson Imaging* 2007;26:437–441.

280 Thermal Effects Associated with RF Exposures During Clinical MRI

78. Wang Z, Collins, CM. Effect of RF pulse sequence on temperature elevation for a given time-average SAR. *Concepts Magn Reson Part B Magn Reson Eng* 2010;37B:215–219.
79. Wust P, Stahl H, Löeffel J, et al. Clinical, physiological and anatomical determinants for radiofrequency hyperthermia. *Int J Hyperthermia* 1995;11:151–167.
80. van Rhoon GC. Is CEM43 still a relevant thermal dose parameter for hyperthermia treatment monitoring? *Int J Hyperthermia* 2016;32:50–62.
81. Adibzadeh F, Verhaart RF, Verduijn GM, et al. Association of acute adverse effects with high local SAR induced in the brain from prolonged RF head and neck hyperthermia. *Phys Med Biol* 2015;60:995–1006.
82. Soukup J, Zauner A, Doppenberg EMR, et al. The importance of brain temperature in patients after severe head injury: Relationship to intracranial pressure, cerebral perfusion pressure, cerebral blood flow, and outcome. *J Neurotrauma* 2002;19:559–571.
83. Dietrich WD, Bramlett HM. Hyperthermia and central nervous system injury. *Progress in Brain Research* 2007;62:201–217.
84. Kiyatkin EA, Sharma HS. Permeability of the blood-brain barrier depends on brain temperature. *Neuroscience* 2009;161:926–939.
85. Kessel L, Johnson L, Arvidsson H, Larsen M. The relationship between body and ambient temperature and corneal temperature. *IOVS* 2010;51:6593–6597.
86. Dixon JM, Blackwood L. Thermal variations of the human eye. *Trans Am Ophthalmol Soc* 1991;89:183–193.
87. Elder JA. Ocular effects of radiofrequency energy. *Bioelectromagnetics* 2003;6:S148–S161.
88. Sharon N, Bar-Yoseph PZ, Bormusov E, Dovrat A. Simulation of heat exposure and damage to the eye lens in a neighborhood bakery. *Experimental Eye Research* 2008;87:49–55.
89. Shellock FG, Crues JV. Corneal temperature changes induced by high-field-strength MR imaging with a head coil. *Radiology* 1988;167:809–811.
90. Athey TW. A model of the temperature rise in the head due to magnetic resonance imaging procedures. *Magn Reson Med* 1989;9:177–184.
91. Massire A, Cloos MA, Luong M, et al. Thermal simulations in the human head for high field MRI using parallel transmission. *J Magn Reson Imaging* 2012 35:1312–1321.
92. van Lier AL, Kotte AN, Raaymakers BW, Lagendijk JJ, van den Berg CA. Radiofrequency heating induced by 7 T head MRI: Thermal assessment using discrete vasculature or Pennes' bioheat equation. *J Magn Reson Imaging* 2012 35:795–803.
93. Fiedler TM, Ladd ME, Bitz AK. SAR simulations & safety. *Neuroimage* 2018;168:33–58.
94. Kodera S, Gomez-Tames J, Hirata A. Temperature elevation in the human brain and skin with thermoregulation during exposure to RF energy. *BioMed Eng OnLine* 2018;17:1.
95. Adibzadeh F, van Rhoon GC, Verduijn GM, Naus-Postema NC, Paulides MM. Absence of acute ocular damage in humans after prolonged exposure to intense RF EMF. *Phys Med Biol* 2016;61:488–503.
96. Cheung SS, Lee JK, Oksa J. Thermal stress, human performance, and physical employment standards. *Appl Physiol Nutr Metab* 2016;41:S148–S164.
97. Ziskin MC, Morrissey J. Thermal thresholds for teratogenicity, reproduction, and development. *Int J Hyperthermia* 2011;27:374–387.
98. Dreier JW, Nybo Andersen AM, Berg-Beckhoff G. Systematic review and meta-analyses: Fever in pregnancy and health impacts in the offspring. *Pediatrics* 2014;133:e674–e688.
99. Sass L, Urhoj SK, Kjærgaard J, et al. Fever in pregnancy and the risk of congenital malformations: A cohort study. *BMC Pregnancy and Childbirth* 2017;17:413–422.
100. Choi JS, Ahn HK, Han JY, et al. A case series of 15 women inadvertently exposed to magnetic resonance imaging in the first trimester of pregnancy. *J Obstet Gynaecol* 2015;35:871–872.

MRI Bioeffects, Safety, and Patient Management 281

101. Ray JG, Vermeulen MJ, Bharatha A, Montanera WJ, Park AL. Association between MRI exposure during pregnancy and fetal and childhood outcomes. *JAMA* 2016;316:952–961.
102. Hand JW, Li Y, Hajnal JV. Numerical study of RF exposure and the resulting temperature rise in the foetus during a magnetic resonance procedure. *Phys Med Biol* 2010;55:913–930.
103. Eskandar OS, Eckford SD, Watkinson T. Safety of diagnostic imaging in pregnancy. Part 2: Magnetic resonance imaging, ultrasound scanning and Doppler assessment. *The Obstetrician & Gynaecologist* 2010;12:171–177.
104. Gowland PA, De Wilde J. Temperature increase in the fetus due to radio frequency exposure during magnetic resonance scanning. *Phys Med Biol* 2008;53:L15–L18.
105. Hirata A, Ishii Y, Nomura T, Laakso I. Computation of temperature elevation in fetus due to radio-frequency exposure with a new thermal modeling. *Conf Proc IEEE Eng Med Biol Soc* 2013;2013:3753–3756.
106. Voigt T, Homann H, Katscher U, Doessel O. Patient-individual local SAR determination: *In vivo* measurements and numerical validation. *Mag Reson Med* 2012;68:1176–1126.
107. Possanzini C, Zhai Z, Harvey PR. 3 T RF simulations of pregnant women and MR system behavior. *International Society for Magnetic Resonance in Medicine* 2020:4190.
108. Gordon CJ. Local and global thermoregulatory response to MRI electromagnetic fields. *Ann N Y Acad Sci* 1992;649:273–84.
109. Brix G, Seebass M, Hellwig G, Griebel J. Estimation of heat transfer and temperature rise in partial-body regions during MR procedures: An analytical approach with respect to safety considerations. *Magn Reson Imaging* 2002;20:65–76.
110. Wang Z, Lin JC. Partial-body SAR calculations in magnetic–resonance image (MRI) scanning systems. *IEEE Antennas and Propagation Magazine* 2012;54:230–237.
111. Szasz O, Szigeti G, Szasz A. Connections between the specific absorption rate and the local temperature. *Open Journal of Biophysics* 2016;6:53–74.
112. Yeo DTB, Wang Z, Loew W, Vogel MW, Hancu I. Local specific absorption rate in high-pass birdcage and transverse electromagnetic body coils for multiple human body models in clinical landmark positions at 3 T. *J Magn Reson Imaging* 2011;33:1209–1217.
113. Shrivastava D, Utecht L, Tian J, Hughes J, Vaughan JT. *In vivo* radiofrequency heating in swine in a 3 T (123.2-MHz) birdcage whole-body coil. *Magn Reson Med* 2014;72:1141–1150.
114. Homann H, Boernert P, Eggers H, et al. Toward individualized SAR models and *in vivo* validation. *Magn Reson Med* 2011;66:1767–1776.
115. Wolf S, Diehl D, Gebhardt M, Mallow J, Speck O. SAR simulations for high-field MRI: How much detail, effort, and accuracy is needed. *Magn Reson Med* 2013;69:1157–1168.
116. Roy CR, Martin LJ. A comparison of important international and national standards for limiting exposure to EMF including the scientific rationale. *Health Phys* 2007;92:635–641.
117. Foster KR, Ziskin MC, Balzano Q, Bit-Babik G. Modeling tissue heating from exposure to radiofrequency energy and relevance of tissue heating to exposure limits: Heating factor. *Health Phys* 2018;115:295–307.
118. Verhaart RF, Verdijnen GM, Fortunati V, et al. Accurate 3D temperature dosimetry during hyperthermia therapy by combining invasive measurements and patient-specific simulations. *Int J Hyperthermia* 2015;31:686–692.
119. Simonis FF, Raaijmakers AJ, Lagendijk JJ, van den Berg CA. Validating subject-specific RF and thermal simulations in the calf muscle using MR-based temperature measurements. *Magn Reson Med* 2017;77:1691–1700.
120. Nadobny J, Klopffleisch R, Brinker G, Stoltenburg-Didinger G. Experimental investigation and histopathological identification of acute thermal damage in skeletal porcine muscle in relation to whole-body averaged SAR, maximum temperature, and CEM43 °C due to RF irradiation in an MR body coil of birdcage type at 123 MHz. *Int J Hyperthermia* 2015;31:409–420.

282 Thermal Effects Associated with RF Exposures During Clinical MRI

121. Yarmolenko PS, Moon EJ, Landon C, et al. Thresholds for thermal damage to normal tissues: An update. *Int J Hyperthermia* 2011;27:320–343.
122. Pearce JA. Comparative analysis of mathematical models of cell death and thermal damage processes. *Int J Hyperthermia* 2013;29:262–280.
123. Haveman J, van der Zee J, Wondergem J, Hoogeveen JF, Hulshof MCCM. Effects of hyperthermia on the peripheral nervous system: A review. *Int J Hyperthermia* 2004;20:371–391.
124. Hoogeveen JF, van der Kracht AHW, Wondergem J, Haveman J. Effects of local hyperthermia on the sensitivity of rat sciatic nerve from diabetic rats. *Neurosci Research Comm* 1993;12:63–70.
125. Neufeld E, Fuetterer M, Murbach M, Kuster N. Rapid method for thermal dose-based safety supervision during MR scans. *Bioelectromagnetics* 2015;36:398–407.
126. Jin J, Liu F, Weber E, Crozier S. Improving SAR estimations in MRI using subject-specific models. *Phys Med Biol* 2012;57:8153–71.
127. Tang M, Okamoto K, Haruyama T, Yamamoto T. Electromagnetic simulation of RF burn injuries occurring at skin-skin and skin-bore wall contact points in an MRI scanner with a birdcage coil. *Phys Med* 2021;82:219–227.
128. Hirata A, Fujimoto M, Asano T, et al. Correlation between maximum temperature increase and peak SAR with different average schemes and masses. *IEEE Trans Electromagn Compat* 2006;48:569–578.
129. Mason PA, Hurt WD, Walters TJ, et al. Effects of frequency, permittivity, and voxel size on predicted specific absorption rate values in biological tissue during electromagnetic-field exposure. *IEEE Trans Microwave Theory Tech* 2000;48:2050–2058.
130. Collins CM, Smith MB. Spatial resolution of numerical models of man and calculated specific absorption rate using the FDTD method: A study at 64 MHz in a magnetic resonance imaging coil. *J Magn Reson Imaging* 2003;18:383–388.
131. Liu W, Wang H, Zhang P, et al. Statistical evaluation of radiofrequency exposure during magnetic resonant imaging: Application of whole-body averaged individual human model and body motion in the coil. *Int J Environ Res Public Health* 2019;16:1069.
132. H Homann, I Graesslin, H Eggers, et al. Local SAR management by RF shimming: A simulation study with multiple human body models, *Magn Reson Mater* 2012;25:193–204.
133. Le Garrec M, Gras V, Hang M-F, et al. Probabilistic analysis of the specific absorption rate intersubject variability safety factor in parallel transmission MRI. *Magn Reson Med* 2017;78:1217–1223.
134. Meliadò EF, van den Berg CAT, Luijten PR, et al. Intersubject specific absorption rate variability analysis through construction of 23 realistic body models for prostate imaging at 7 T. *Magn Reson Med* 2019;81:2106–2119.
135. Abaci Turk E, Yetisir F, Adalsteinsson E, et al. Individual variation in simulated fetal SAR assessed in multiple body models. *Magn Reson Med* 2020;83:1418–1428.
136. Adibzadeh F, Paulides MM, van Rhoon GC. SAR thresholds for electromagnetic exposure using functional thermal dose limits. *Int J Hyperthermia* 2018;18:1–7.
137. Shellock FG, Schaefer DJ, Grundfest W, Crues JV. Thermal effects of high-field (1.5 tesla) magnetic resonance imaging of the spine. Clinical experience above a specific absorption rate of 0.4 W/kg. *Acta Radiol Suppl* 1986;369:514–516.
138. Isaacson DL, Yanosky DJ, Jones RA, Dennehy N, Spandorfer P, Baxter AL. Effect of MRI strength and propofol sedation on pediatric core temperature change. *J Magn Reson Imaging* 2011;33:950–956.
139. Cawley P, Few K, Greenwood R, et al. Does magnetic resonance brain scanning at 3.0 Tesla pose a hyperthermic challenge to term neonates? *J Pediatr* 2016;175:228–230.
140. Shellock FG, Gordon CJ, Schaefer DJ. Thermoregulatory responses to clinical magnetic resonance imaging of the head at 1.5 Tesla: Lack of evidence for direct effects on the hypothalamus. *Acta Radiologica, Suppl.* 1986;369:512–513.

MRI Bioeffects, Safety, and Patient Management 283

141. Shellock FG, Crues JV. Temperature changes caused by clinical MR imaging of the brain at 1.5 Tesla using a head coil. *AJNR Am J Neuroradiol* 1988;9:287-291.
142. Shellock FG, Rothman B, Sarti D. Heating of the scrotum by high-field-strength MR imaging. *AJR Am J Roentgenol* 1990;154:1229-1232.
143. Kim MS. Investigation of factors affecting body temperature changes during routine clinical head magnetic resonance imaging. *Iran J Radiol* 2016;13:e34016.

Chapter 10 **Claustrophobia, Anxiety, and Emotional Distress in the MRI Environment**

LAURA VASQUEZ, PH.D., RVT (ARDMS), RT (R), (MR), (ARRT), MRSO (MRSC™)

Chairperson of the Department of Medical Imaging Sciences
Rush University, College of Health Science
Chicago, IL

INTRODUCTION

The increasing availability and capabilities of magnetic resonance imaging (MRI) to improve medical diagnosis and prognosis has dramatically increased the number of MRI procedures performed worldwide. Thus, many more first-time and repeat patients are undergoing these MRI examinations for an ever-widening spectrum of medical indications. Notably, increasing proportions of these procedures are performed on patients suffering from unstable medical and psychological illnesses. For many of the millions of patients who undergo MRI examinations every year, the experience may cause great emotional distress. The referring physicians, radiologists, and technologists are best prepared to manage affected patients if they understand the etiology of the problem and know the appropriate maneuver or intervention to implement for treatment of the condition (1).

This chapter discusses the prevalence of claustrophobia in association with the use of MRI, how emotional distress affects outcomes for the MRI procedure, factors contributing to patient distress, and techniques to help minimize anxiety and distress in patients with claustrophobia while undergoing MR imaging. Recent investigations involving emerging MRI applications are also taken into consideration.

INCIDENCE OF DISTRESS IN THE MRI ENVIRONMENT

Psychological distress in the MRI environment includes all subjectively unpleasant experiences that are directly attributable to MRI. Distress for the patient undergoing an MRI procedure can range from mild anxiety that can be managed simply with minimal reassurance to a full-blown panic attack that requires psychiatric intervention. Severe psychological

distress reactions to MRI examinations, namely severe anxiety and panic attacks, are typically characterized by the rapid onset of at least four of the following clinical signs: fear of losing control or dying, nausea, paresthesias, palpitations, chest pain, faintness, dyspnea, feeling of choking, sweating, trembling, vertigo, or depersonalization (2).

Many symptoms of panic attack mimic over activity of the sympathetic nervous system (3), prompting concern that catecholamine responses may precipitate cardiac arrhythmias and/or ischemia in susceptible patients during the MRI examination (4). However, this has not been reported in a clinical MRI setting or any other similar situation. Nevertheless, it is advisable that, in a medically unstable patient, the use of physiologic monitoring be a routine component of the MRI examination. Pre-emptive efforts to minimize patient distress are the most important factors in preventing or containing a panic attack in susceptible patients.

In the mildest form, distress is the normal amount of anxiety any reasonable person will experience when undergoing a diagnostic procedure. Moderate distress severe enough to be described as a dysphoric psychological reaction has been reported by as many as 65% of the patients examined by MRI (5-8). The most severe forms of psychological distress described by patients are claustrophobia, panic attacks, and anxiety (3, 5-12), the latter of which occurs in moderate to severe forms in up to 37% of patients undergoing MRI (13, 14).

Claustrophobia is a disorder characterized by the marked, persistent and excessive fear of enclosed spaces (2). In such affected individuals, exposure to enclosed spaces such as the MR system, but no other situations or stimuli, almost invariably provokes an immediate anxiety response that in its most extreme form is indistinguishable from a panic attack as described above.

The reported incidence of distress in the MRI setting is highly variable across studies in part reflecting differences in outcome measures used to characterize distress. Some studies indicated that as many as 20% of individuals attempting to undergo MRI can't complete it secondary to serious distress such as claustrophobia or other similar sensation (15, 16). In contrast, others have reported that as few as 0.7% of individuals have incomplete or failed MRI examinations due to distress (8, 17). In a study of over 55,000 patients undergoing MRI, claustrophobia was present in 1.8% of cases, and a review of previous literature indicated that 2.3% of patients experienced claustrophobia requiring sedation or termination of the procedure (18). A reasonable estimate of the number of patients that experience distress that compromises either their own well-being or the diagnostic utility MRI is 3 to 5% of all studies. For patients with pre-existing anxiety or claustrophobia, however, the termination rate can be as high as 39% (19, 20).

Notably, there are no perfect predictors of distress in the MRI environment. In fact, different studies cite opposing results such as which gender has greater difficulty tolerating MRI (17, 18, 21). A cohort study of over 55,000 patients in an outpatient setting in Germany reported that females (2.3%) had a significantly higher rate of claustrophobia than males (1.3%) (18). This is in contrast to an earlier study conducted in Malaysia where the rate of MRI termination was found to be 0.54%, and of those, 67% of the patients who terminated their scans were male (17). Obviously, these differences may reflect cultural, socioeconomic or other influences.

286 Claustrophobia, Anxiety, and Emotional Distress

THE IMPACT OF EMOTIONAL DISTRESS IN THE MRI ENVIRONMENT

Patient distress can contribute to adverse outcomes for the MRI procedure. These adverse outcomes include unintentional exacerbation of patient distress, a compromise in the diagnostic power of the MRI examination due to poor image quality, and decreased efficiency of the imaging facility due to delayed, cancelled or prematurely terminated studies. Patient compliance during MRI, such as the ability to remain in the MR system and hold still long enough to complete the study is of paramount importance to achieving a high quality, diagnostic examination.

If a good quality study can't be obtained, the patient may require an invasive diagnostic examination in place of the safer, less painful and risky MRI exam. Thus, for the distressed patient unable to undergo MRI, there are potential clinical, medico-legal, and economic related considerations implications.

Patient distress due to MRI may also impact regional brain activity as indicated by functional neuroimaging measurements. Elevated endocrine levels have been observed in association with scanning procedures compared to baseline, particularly in stress hormones such as cortisol (22-24). Studies have indicated that elevated salivary cortisol levels are associated with MRI examinations in both adolescents and healthy adults (23, 24). In contrast, Muehlhan, et al. (25) found changes in salivary alpha amylase but not in cortisol prior to MRI. This evidence, while inconclusive, points towards increased activity in the hypothalamic-pituitary-adrenal and the sympatho-adrenal-medullary axes which are, in turn, associated with regionally specific neural activation and deactivation (26, 27). Fluctuating endocrine levels have been implicated in the modulation of regional brain activity, a suggestion that has broad implications for interpreting functional neuroimaging results. Functional MRI (fMRI) is at the forefront of neuroimaging research. Because fMRI is increasingly introduced into clinical practice a variety of critical applications the effects of hormone levels on brain activity related to anxiety and emotional distress could impact this procedure.

Increasing pressure to use scanner time efficiently to cover the costs of this expensive diagnostic imaging equipment puts greater stress on both staff members and patients. The ability of referring physicians, radiologists, and MRI technologists to detect patient distress at the earliest possible time, to discover the source of the distress, and then provide appropriate intervention can greatly improve patient comfort, the quality of the imaging studies, and the efficiency of the MRI facility (1).

Motion artifact disrupting image quality is frequently the result of patient distress. That is, the distressed patient becomes agitated and finds it difficult to remain motionless during MRI. Obviously, motion artifacts can compromise the diagnostic power of an MRI exam. One investigation in 297 first-time outpatients undergoing MRI indicated that approximately 13% of the MRI studies showed motion artifacts (i.e., unrelated to normal body pulsations) and about half of these impaired the diagnostic quality of the examination (8). Subsequent studies have confirmed these estimates (20, 28). One of these investigations reported an even higher proportion of scans with motion artifacts (18%) in a sample of patients with pre-existing anxiety conditions and non-anxious controls (20).

Excessive anxiety with accompanying tremors, trembling, jaw clenching and other related body movements have been presumed to contribute to motion artifacts in MR images. Dantendorfer, et al. (8) attempted to investigate this directly and found that, while specific measures of anxiety do not predict motion artifacts, reported concerns about the scanner did predict motion artifacts. Tournquist, et al. (28) designed an experiment to test whether increased awareness about the procedure prior to initiating the scan would reduce motion related artifacts. The investigators found nearly a three-fold reduction in the number of scans with artifacts in the intervention group (4%) compared to the control condition (15.4%). The patients in the intervention group received additional written information that included details about what the procedure would entail, as well as sensory and temporal information related to the procedure (28). These results support the interpretation that adequate patient education about the MRI procedure is one of the most important aspects of minimizing distress and the associated adverse outcomes.

The emotional distress that comes with claustrophobia and anxiety may lead to a compromise in MR image quality due to motion artifacts related to the patient's inability to remain motionless. While this is undoubtedly crucial to achieving a diagnostically acceptable examination, Klaming L, et al. (66) reported that there was little evidence to support the assumption that anxiety increases patient motion and decreases image quality during MRI. However, the evidence supporting the benefits of patient education prior to MRI still remains relevant and critical to ensuring the best possible outcomes in patients with claustrophobia, anxiety, and emotional distress.

FACTORS THAT CONTRIBUTE TO DISTRESS IN THE MRI ENVIRONMENT

Many factors contribute to distress experienced by certain patients undergoing MRI. Most commonly cited are concerns about the physical environment of the scanner. Also well documented are the anxieties associated with the underlying medical problem necessitating the MRI exam. Notably, certain individuals, such as those with psychiatric illnesses, may be predisposed to suffer greater distress related to the MRI procedure.

The physical environment of the scanner is clearly one important source of distress to patients. Sensations of apprehension, tension, worry, claustrophobia, anxiety, fear, and even panic attacks have been directly attributed to the confining dimensions of the interior of the MR system. For example, for certain types of scanners, the patient's face may be three to ten inches from the inner portion of the scanner, prompting feelings of uncontrolled confinement and detachment (3, 5-12, 15, 16, 29-34). In one study, confinement was reported by 22.9% of patients as the most unpleasant feature of the MRI experience (34). This factor, combined with other physical aspects of the MRI environment may contribute to the high levels of distress observed in patients undergoing MRI.

Similar distressing sensations have been attributed to the other aspects of the MRI setting including the prolonged duration of the MRI examination, the gradient magnetic field-induced acoustic noise, the temperature and humidity within the MR system, and the distress related to the restriction of movement (3-12, 15, 16, 29-33, 35, 36). Other studies have reported stress related to the administration of an intravenous MRI contrast agent (3, 5-7, 9-

288 Claustrophobia, Anxiety, and Emotional Distress

12, 15, 16, 29-33, 35-37). Additionally, the scanner may produce feelings of sensory deprivation, restriction, and suffocation, which are also known to be precursors of severe anxiety states (10, 38). Investigations have indicated that phobias related to specific aspects of the MRI environment can predict claustrophobic fears and psychological outcomes in the scanner (14, 34, 39, 40). Using pre-scan questionnaires, clinicians may be able to identify patients who are at risk for terminating the scan due to claustrophobia (20, 34, 39, 40).

One of the more overwhelming features of the MRI procedure is the acoustic noise generated by the MR system. Gradient magnetic field-induced noise may be sufficiently intense to cause transient hearing threshold shifts in as many as 43% of patients undergoing MRI (41). Obviously, acoustic noise in and of itself can be a source of stress and, thus, particularly troublesome to certain patients in association with MRI. In one study, noise alone was considered the most unpleasant feature of MRI by 19.5% of patients (34). This information suggests that the noise reduction achieved in the new generation of scanners may be an important factor in reducing distress. The use of newer scanners demonstrated up to a 97% reduction in acoustic noise compared to older scanners. Dewey, et al. (18) observed a three-fold reduction in reports of claustrophobia using the newer short- and wide-bore scanners that have noise emission levels below 99-dB compared to conventional, older scanners.

MR systems that have an architecture that utilizes a vertical magnetic field offer a more open design that is presumed to reduce the frequency of distress associated with MRI. The latest versions of these so-called “open” scanners, despite having static magnetic field strengths of 0.35-Tesla or lower have improved technology (i.e., faster gradient fields, optimized surface coils, etc.) that permit acceptable image quality for virtually all types of standard, diagnostic imaging procedures. Also, the latest generation of high-field-strength (1.5-Tesla and 3-Tesla) MR systems have shorter and wider bore configurations such that these newer scanners tend to be more acceptable to patients with feelings of distress related to close confinement.

After the release of the first commercially available open MR systems, Datendorfer, et al. (8) designed a study to compare an open system to a standard scanner. This report indicated that there was no difference between a conventional 1.5-T MR system (Siemens Magnetom SP-65, Siemens Medical Solutions) and a more open 0.5-Tesla scanner (Philips Gyroscan P-5, Philips Medical Systems) with regard to the incidence of adverse reactions (i.e., pre- or post-scan anxiety, claustrophobia, motion artifacts, or aborted exams).

MRI scanner design has been postulated to be a key factor that contributes to patient distress, and it's known that “open” configured scanners with shorter and wider bore configurations have increased examination success rate. However, Enders, et al. (19) reported that there wasn't a substantial difference in claustrophobia experienced by patients undergoing MRI in an open versus a short-bore MR system. A subsequent study by Enders, et al. (75), further examined the use of a high-field open scanner (1.0-Tesla) and a short-bore, high field MR system (1.5-T) used for MRI of the spine. In this randomized controlled comparison of spinal MR imaging with an open versus a short-bore scanner, short-bore MR imaging revealed considerably higher image quality with shorter scanning times. Interestingly, patients reported claustrophobia in both types of MR scanners.

In contrast to the aforementioned investigations, two non-randomized studies of claustrophobic patients demonstrated a decreased rate of claustrophobic events in open MR systems compared to closed scanners (42, 43). Decreases of similar magnitude have been observed in newer generations of short- and wide-bore scanners compared to conventional MR systems (44). In one study of claustrophobic patients who previously failed completing an MRI procedure, Hunt, et al. (44) observed an 89% success rate for patients scanned in a short- and wide-bore 1.5-Tesla MR system compared to their previously unsuccessful procedure in a conventional 1.5-Tesla scanner.

In another study, Dewey, et al. (18) compared the rate of claustrophobia between short- and wide-bore configured 1.5-Tesla MR systems (Magnetom Avanto, Siemens Medical Solutions) and conventional 1.0-Tesla scanners (Magnetom Impact Expert Plus, Siemens Medical Solutions) in an outpatient setting. Data from this study collected over the course of eight years demonstrated significantly lower rates of claustrophobic reactions among patients scanned on newer 1.5-Tesla scanners (0.7%) compared to conventional 1.0-Tesla MR systems (2.1%) (18). Considered together, these data suggest that although the patient-centered design of MR scanners has evolved in the past 20 or so years, even the most state-of-the-art systems do not prevent claustrophobia, indicating that there are other factors besides the physical aspects of the MR system that are related to claustrophobic events.

In the early 1990s, a specially-designed, low-field-strength (0.2-Tesla) MR system (Artoscan, Lunar Corporation/General Electric Medical Systems and Esaote) first became commercially available for MR imaging of extremities. The use of dedicated extremity scanners such as these provides an accurate, reliable, and relatively inexpensive means (i.e., in comparison to the use of a whole-body MR system) of evaluating various types of musculoskeletal abnormalities. Therefore, utilization of the extremity scanner to assess musculoskeletal pathology is a viable and acceptable alternative to the use of whole-body scanners (45). This is particularly the case since the image quality and diagnostic capabilities for the evaluation of the knee and other extremities has been reported to be comparable to mid- or high-field strength MR systems for certain musculoskeletal applications (45).

The architecture of the extremity MR system has no confining features or other aspects that would typically create patient-related problems. This is because only the body part that requires imaging is placed inside the magnet bore during the MR examination. One study reported that 100% of the MRI examinations that were initiated were completed without being interrupted or cancelled for patient-related problems (Shellock FG, Unpublished Data, 2011). The unique design of the extremity scanner likely contributed to the totally successful completion of MRI examinations in the patients of this study. Furthermore, these findings represent a dramatic improvement compared with the published incidence of patient distress that tends to interrupt or prevent the completion of MRI examinations using whole-body MR systems.

Currently, there are no reports available on the topic of “upright” or “standing” MR systems and patients with claustrophobia. Anecdotally, the ability to stand or sit for the MRI exam and, thus, avoid having the scanner in close proximity to the face often proves helpful for individuals who may otherwise experience claustrophobia (**Figures 1a** and **1b**).

290 Claustrophobia, Anxiety, and Emotional Distress

Figure 1. Examples of an “upright” or “standing” MR system. Anecdotally, the ability to stand (**a**) (G-Scan Brio, Esaote, www.esaote.com) or sit (**b**) (Upright MRI Fonar, www.fonar.com) during an MRI exam and avoid having the scanner in close proximity to the face often proves helpful for individuals who may experience claustrophobia.



Adverse psychological reactions are sometimes associated with MRI simply because the examination may be perceived by the patient as a “dramatic” medical test that has an associated uncertainty of outcome, such that there may be a fear of the presence of disease or other abnormality (5, 10). In fact, any type of diagnostic imaging procedure may produce a certain amount of anxiety for the patient (30). For example, Thorp, et al. (16) found that, with the exception of the MR system environment issue (i.e., the confined space), patients undergoing computed tomography compared to those undergoing MRI had similar feelings that the procedure was unpleasant. Patients finding the experience difficult tended to be those with high initial levels of anxiety, little experience with diagnostic procedures, and those that believed they had cancer (16). This study underscores the need for direct professional interaction to prepare and educate the patient prior to any form of diagnostic imaging examination. Improved patient compliance was reported in a study that investigated the impact of more detailed patient education on adverse outcomes from MR mammography, a procedure known to have an atypically high rate of noncompliance (46). Likewise, in a study designed to test the noncompliance rate before and after hospital radiology staff were trained in nonpharmacological analgesia, one multi-site practice observed a significant decrease in noncompliance rates during the period of time following the training. This particular training program involved two components: advanced rapport training and self-hypnotic relaxation, both highlighting the importance of individualized care and interpersonal interactions in patient care (47).

Patients with pre-existing psychiatric disorders may be at greater risk for experiencing distress in the MRI environment. One problem that arises more often in this population is the refusal of the prescribed MRI exam by the patient. Frequently, the cause for refusal is an inadequate understanding of why the procedure was ordered and what the actual procedure involves.

For patients with pre-existing anxiety disorders who agree to undergo MRI, it is prudent for hospital radiology staff to use augmented methods to minimize additional anxiety or distress. Grey, et al. (48) reported the efficacy of an anxiety reduction protocol in patients with moderate to high trait anxiety. Prior to MRI, patients in the intervention group were given detailed information regarding scanning procedures including descriptions of the acoustic noise, equipment and the procedure room, the timing of scans and degree of interaction with the MRI technologist, as well as coping strategies for anxiety in the scanner such as increasing the audio volume and paying attention to a clock on the wall. Patients in the intervention group were significantly less anxious during the procedure and retrospectively when asked about the whole procedure compared to those patients in the control condition, indicating that the extra time and effort spent preparing the patients in the intervention group made a positive impact on patients with pre-existing anxiety (48).

In a small study of older adults with generalized anxiety disorder (GAD) the rate of unsuccessful MRI examinations in patients with pre-existing anxiety was assessed and compared to a control group. In this study, an unsuccessful scan was defined as one in which there was excessive movement or premature termination of the scan. There was no significant difference in the rate of successful MRI outcome in this group of GAD patients and non-anxious controls (20). To date, this study is the only report of the differential frequency of distress or adverse outcomes for MRI exams in such patients compared to non-psychiatrically impaired patients. Although these findings fail to find a difference between cohorts, future studies are still warranted and specific inquiry should be made to identify patients with pre-existing anxiety disorders including claustrophobia, generalized anxiety disorder, post-traumatic stress disorder, and obsessive-compulsive disorder in order to increase anxiety minimizing efforts in these patients.

Patients with other psychiatric illnesses such as depression and any illness complicated by thought disorder such as schizophrenia and manic-depressive disorder may also be at increased risk for distress in the MRI environment. Patients with psychiatric illnesses may, under normal circumstances, be able to tolerate the MRI setting without a problem, as is clear from the thousands who participate in clinical neuroimaging research studies each year (49). However, the increased stress due to their medical illness or fear of medical illness may exacerbate their psychiatric symptoms to such an extent that they may have difficulty complying with MRI procedures. At the very least, patients with psychiatric illnesses may require more time and patience to provide the appropriate level of preparatory information.

TECHNIQUES TO MINIMIZE PATIENT DISTRESS IN THE MRI ENVIRONMENT

There are procedures that may be used to minimize subjective distress for patients undergoing MRI. Certain measures to alleviate distress should be employed for all MRI ex-

292 **Claustrophobia, Anxiety, and Emotional Distress**

Table 1. Recommended techniques for managing patients with claustrophobia or emotional distress related to MRI examinations.

- (1) Prepare and educate the patient concerning specific aspects of the MRI exam (e.g., MR system dimensions, gradient noise, intercom system, etc.).
- (2) Allow an appropriately-screened relative or friend to remain with the patient during the MRI procedure.
- (3) Maintain physical or verbal contact with the patient during the MRI exam.
- (4) Use MR Conditional headphones to provide music to the patient and to minimize gradient magnetic field-induced noise.
- (5) Use an MR Conditional video monitor to provide a visual distraction to the patient.
- (6) Place the patient in a prone position inside the scanner.
- (7) Position the patient feet-first instead of head-first into the MR system.
- (8) Use special mirrors or prism glasses for the patient.
- (9) Use a blindfold so that the patient is not aware of the close surroundings.
- (10) Use bright lights inside and at either end of the scanner.
- (11) Use a fan inside of the MR system to provide adequate air movement.
- (12) Use lemon or vanilla scented oil or other similar aromatherapy so that the patient can comfortably experience olfactory stimulation.
- (13) Use relaxation techniques such as controlled breathing or mental imagery.
- (14) Use systematic desensitization.
- (15) Use medical hypnosis.
- (16) Use a sedative or other similar medication.
- (17) Use foot massage or touch therapy.
- (18) Use a virtual reality system to provide audio and visual distraction for the patient.
- (19) Use a virtual reality app to educate and simulate the experience of undergoing an MRI exam.

aminations. A number of other measures will be required if the patient is experiencing significant distress due to factors as described above. Finally, other distress-alleviation techniques will only be necessary for patients with co-existing psychiatric illness or other special problems. Coordination of these efforts among the referring physician, the radiologist, the MRI technologist and the facility support staff is crucial. Most of these methods have been described in the peer-reviewed literature and are summarized in **Table 1** (3-5, 7, 9, 11, 12, 21, 33, 35, 36, 46, 50-54, 67, 69, 72).

For All Patients Undergoing MRI Procedures

Referring clinicians should take the time to explain the rationale for the MRI examination and what he/she expects to learn from the results with respect to the implications for treatment and prognosis. Importantly, the clinician should schedule time with the patient to communicate the results of the MRI procedure.

The single most important step is to educate the patient about the specific aspects of the MRI examination that are known to be particularly difficult. This includes conveying in terms that are understandable to the patient the internal dimensions of the MR system, the level of gradient magnetic field-induced acoustic noise to expect, and the estimated time duration of the examination.

Studies have documented a decrease in the incidence of premature termination of MRI when patients are provided with more detailed information regarding the examination (46-48, 67, 68, 72). This may be effectively accomplished by means of providing the patient time to view an educational videotape or written brochure supplemented by a question and

answer session with an MRI-trained healthcare worker prior to MRI. An investigation by Tazegul G, et al. (72) also supports the use of information and communication as a method for preventing and reducing anxiety in patients, encouraging the continued use of this method by radiology technologists.

Some authors have proposed adding a pre-scan “fear assessment” to help predict patients who will experience psychological problems related to MRI (15, 20, 29, 30, 34, 39, 40). Such a brief questionnaire could be used to help elicit questions and concerns from patients and to provide guidance to staff about which distress minimization strategies are most likely to be effective for the patient.

One study on anxiety and MRI exams conducted by Van Minde, et al. (76) specifically looked at patients who were highly anxious before MRI. The study measured stress and anxiety throughout the exam by monitoring the patient’s heart rate. The data showed that patient anxiety levels were highest at the very beginning of the procedure, particularly when the MRI table was moving into the scanner. However, anxiety and stress decreased over the course of the examination. This information not only proves helpful to radiology professionals working with patients but may also aid in the development of more effective anxiety-reduction strategies in the future.

Upon entering the MRI facility, patients who are treated with respect and are welcomed into a calm environment will report less distress. Many details of patient positioning in the MR system can increase comfort and minimize distress. Taking time to ensure comfortable positioning with adequate padding and blankets to alleviate undue discomfort or pain from positioning is also important. Adequate hearing protection should be provided routinely to decrease acoustic noise generated by the MR system. Demonstration of the two-way intercom system to reassure to patients that the MRI staff members can hear them when they speak and can speak to them during the examination can also be reassuring.

For Mildly to Moderately Distressed Patients

If a patient that continues to experience distress after the afore-mentioned measures are implemented, additional interventions are required. Frequently, all that is necessary to successfully complete an MRI examination is to allow an appropriately-screened relative or friend to remain with the patient during the procedure. A familiar person in the MR system room often helps the patient who is anxious to develop an increased sense of security (12, 35). If a supportive companion is not present, then simply having an MRI staff member maintain verbal contact via the intercom system or physical contact by having a staff person remain in the MR system room with the patient during the examination will frequently decrease psychological distress (7, 12, 35).

Placing the patient in a prone position inside the MR system so that the patient can visualize the opening of the bore provides a sensation of being inside a device that is more spacious and alleviates the “closed-in” feeling associated with the supine position (35, 55, 67). Prone positioning of the patient may not be a practical alternative if MRI requires the use of certain types of radiofrequency (RF) coils or if the patient has underlying medical conditions (e.g., shortness of breath, the presence of chest tubes, etc.) that preclude lying in

294 Claustrophobia, Anxiety, and Emotional Distress

this position. Another method of positioning the patient that may help is to place the individual feet-first instead of head-first into the scanner.

An MR system, head-coil mounted mirror (**Figure 2**) or prism glasses (**Figure 3**) can be used to permit the patient to maintain a vertical view of the outside of the scanner in order to minimize claustrophobic responses. Using a blindfold so that the patient is not aware of the close surroundings has also been suggested to be an effective technique for enabling anxious patients to successfully undergo MRI (12, 35).

The internal environment of the MR system may be changed to optimize the management of apprehensive patients (12). For example, the presence of higher lighting levels tends to make most individuals feel less anxious. Therefore, the use of bright lights at either end and inside of the MR system can produce a less imposing environment for the patient. In addition, using a fan inside of the scanner to provide more air movement will help reduce the sensation of confinement and lessen any tissue heating that may result when high levels of RF power absorption are used for MRI (12). Some MRI staff members have reported that placing a cotton pad moistened with a few drops of lemon, vanilla, cucumber oil or other similar form of aromatherapy in the MR system for the patient to receive olfactory stimulation can also reduce distress. Reports by Munn, et al. (67, 68) found that cognitive behavioral strategies, MRI design features, team training, fragrance administration, information, and prone positioning all have a positive impact on outcomes in reducing fear, anxiety, and claustrophobia. Not only do these measures increase patient comfort, but they also reduce the need for sedation.

Figure 2. Example of an MR system, head-coil mounted mirror that permits the patient to have a vertical view of the outside of the scanner to help minimize claustrophobia.



Figure 3. Example of prism glasses that permits the patient to have a vertical view of the outside of the scanner to help minimize claustrophobia.



Figure 4. Example of audio device specially designed for use in the MR system room. MR Conditional audio devices that transmit music and/or provide audio communication through headphones have been developed for use with scanners and are available from several vendors.



296 Claustrophobia, Anxiety, and Emotional Distress

Audio devices that transmit music and/or provide audio communication through headphones have been developed specifically for use with MR systems (51, 52, 56, 57). These MR Conditional music/audio systems may be acquired from commercial vendors. This equipment can be used to provide calming music to the patient and, with the proper design, help to minimize exposure to gradient magnetic field-induced acoustic noise (**Figure 4**). Reports have indicated that the use of these devices has been successful in reducing symptoms of anxiety in patients during MRI (52, 56, 58). Furthermore, one study suggested that having a live musician play music that matches the rhythm of the gradient magnetic fields improves patient perceptions of the MRI examination (58). This improved perception may also be due in part to the perceived increase in the social interaction that the patient has during MRI. Obviously, that particular means of helping an anxious patient to get through a clinical MRI exam tends to be impractical.

Another technique investigated for reducing anxiety during MRI exams is foot massage or touch therapy, both of which may be beneficial due to the increase in social interaction during the procedure. Not only was foot massage or touch therapy found acceptable and feasible by both patients and MRI technologists, Parmar, et al. (69) reported that these interventions were associated with lower levels of anxiety during MRI.

It is also possible to provide visual stimulation to the patient via special goggles or a headset (57). Use of visual stimuli to distract patients may also reduce distress. Finally, a specialized system has been developed to provide a virtual reality environment for the patient that may likewise serve as an acceptable means of audio and visual distraction from the MRI exam (**Figures 5a** and **5b**). A case study of two patients with claustrophobia demonstrated that virtual reality distraction decreased subjective anxiety ratings when compared to no distraction (59).

The use of a virtual reality tool that simulates the MRI experience may also be effective at helping to prepare patients with claustrophobia and anxiety for MRI exams. Previous studies have shown that desensitization therapy via the use of virtual reality (VR) offers an effective method of treating anxiety (74, 77). A VR app has been developed that helps to educate the patient about the MRI exam by simulating the experience (**Figure 6**). The app incorporates both visual and auditory sensations normally encountered by patients during MRI. Developers believe that this tool has potential similar to desensitization therapy, reducing patient anxiety prior to MRI and lowering the incidence of claustrophobia-related issues. Importantly, when used in pediatric patients, this VR app reduces the need for the use of sedation or anesthesia (80).

For Severely Distressed or Claustrophobic Patients

Patients who are at high risk for severe distress in the MRI setting and can be identified as such by their referring clinician or by the scheduling MRI staff could be offered the opportunity to have pre-MRI behavioral therapy. MRI examinations that were conducted in patients that previously refused or were unable to tolerate the MRI environment have been reported to be successful as a result of treatment with relaxation techniques (9, 54), systematic desensitization (11), and medical hypnosis (33, 36, 53). Quirk, et al. (9) reported that psychological preparation that included information about MRI and the use of relaxation strategies (i.e., breathing relaxation techniques, visualization of pleasant images, perform-

Figure 5. (a) CinemaVision (Resonance Technology Inc.) is an MR Conditional audiovisual system that uses wireless technology allowing transmission of the audio and video signals from the control room to the MR system room.



Figure 5. (b) The headphones and headset both fit easily into all standard head RF coils. The digital audio headset system blocks 30-dB of acoustic noise, permitting two-way communication between the patient and the MRI technologists.



298 **Claustrophobia, Anxiety, and Emotional Distress**

ance of mental exercises, etc.) was more effective for reducing anxiety in patients compared to providing information alone.

Klonoff, et al. (11) provided a detailed example of one successful systematic desensitization protocol. This was conducted prior to MRI and involved having the patient lie on the floor at home with her head in a box. The size of the box was incrementally decreased until it approximated the internal dimensions of the MR system. Additionally, the patient was required to gradually increase the amount of time that she could tolerate spending time with the box over her head, until it equaled 50 to 60 minutes, to approximate the maximum time needed for MRI. The patient also wore prism glasses that permitted her to have a direct view in the vertical plane during MRI. After four treatment sessions, the patient was able to successfully undergo MRI (11). Notably, because of the time involved with systematic desensitization, this technique of preparing the distressed patient for MRI is impractical for clinical MRI facilities.

Medical hypnosis has been demonstrated to be a successful means of treating phobias (50) and, not surprisingly, has been used as an effective intervention to enable a claustrophobic or anxious patient to complete MRI (33, 36, 53). Successful hypnotherapy requires a trained medical hypnotist and a willing, trance-susceptible patient. Therefore, identifying the appropriate patient that would benefit from being hypnotized before and during MRI and having a hypnosis therapist available for treatment are prerequisites for instituting this technique of patient management. There is a secondary effect of using hypnosis for patients with psychological disorders undergoing MRI insofar as patients have reported feeling a general reduction in anxiety in their everyday lives after undergoing hypnosis (33).

In the majority of MRI facilities, patients that are severely affected by claustrophobia, anxiety, or panic attacks in response to MRI are usually pharmacologically sedated when other attempts to counteract their distress fail. Using short-acting sedatives such as lorazepam, diazepam, alprazolam, or intranasal midazolam or one of the other anxiolytic medications may be the only means of managing patients with a high degree of anxiety related to MRI. Published reports of the rate of pharmacological sedation for patients undergoing MRI range from 2 to 14% (8, 21).

A study conducted by Avrahami (3) in patients with panic attacks who were unable to undergo MRI reported that treatment with intravenous diazepam caused the symptoms to disappear rapidly and permitted completion of the examination in every case. However, the use of sedatives in patients prior to and during MRI may not be required in all instances nor is it always practical (1).

Of special note is that anxious patients with a history of substance abuse who are in recovery programs may not be willing to take mind-altering medications because this is typically contraindicated during their treatment. These patients should be referred for behavioral therapy before MRI. In all cases, one or more of the recommended, non-medication-related techniques indicated in **Table 1** should be attempted for these patients before electing to use a sedative.

Performing sedation for the patient in the MRI environment is not a totally benign procedure. Confusion and respiratory compromise as well as other untoward reactions have

Figure 6. Free virtual reality app that prepares patients for MRI by providing a 360-degree, virtual reality video of the entire MRI procedure. This app when used with a virtual reality headset and a smart phone or tablet, allows patients to feel as though they are inside an MR system. For pediatric patients, this app reduces the need for the use of sedation or anesthesia. (Virtual Reality MRI. App for iOS version: <https://apps.apple.com/us/app/virtual-reality-mri/id1263101285>. App for Android version, https://play.google.com/store/apps/details?id=net.belfasttrust.vrmri&hl=en_US)



been reported in response to relatively modest doses of commonly employed sedatives (6, 9). If a sedative or other similar drug is used in a patient in preparation for MRI, it should be understood that the use of this medication involves several important patient management considerations (31). For example, the time when the patient should be administered the medication for optimal effect prior to the examination should be considered along with the possibility that there may be an adverse reaction to the drug (31). The use of proper physiologic monitoring equipment during the MRI examination is essential. Additionally, provisions should be available for an area to permit adequate recovery of the patient after MRI

300 **Claustrophobia, Anxiety, and Emotional Distress**

and the patient should have someone available to provide transportation from the MRI facility after receiving a sedative.

According to Rotunda (70), patients with post-traumatic stress disorder (PTSD) and who may also have severe claustrophobia frequently are unable to successfully complete MRI exams, which may greatly affect their health outcomes. Research studies comparing the brains of patients with PTSD versus people who do not have PTSD have shown diffuse decreases in white and gray matter in patients who developed PTSD after various traumas. The areas in which these types of white and gray matter changes occur might provide some insight into the anatomical and physiological reasons for PTSD symptoms (71). For health-care professionals, it is important to be aware of the potential differences in the brain of a patient with PTSD and the effects that these differences may have on behavior. Therefore, educated MRI technologists who can adapt to the specific needs of their patients, such as those with PTSD, are more likely to provide the best experiences which leads to better patient outcomes. This includes being proactive with respect to preparing and managing patients with PTSD for MRI exams.

For Pediatric Patients

Careful consideration of methods for reducing distress in pediatric patients is extremely important as the implications of imaging procedures have both short- and long-term effects in this population. In addition to the short-term effects of distress, anxiety and pain, resulting in crying and lack of cooperation, there may be long-term psychological effects into adulthood such as medical fears, less perceived control over health, and in some cases, post-traumatic stress responses and claustrophobic feelings (60, 61). Some of the methods for minimizing distress and discomfort in the scanner are similar to those used in adults, however, important differences should be highlighted. Similar to adults, pediatric patients can also benefit from preparation prior to the procedure, hypnosis, music and sedation. Other pediatric specific methods such as visual and audio distraction, positive reinforcement and parental involvement have also been shown to be effective (60).

Parental involvement can be a particularly useful technique as it engages the parents, which in turn reduces the parents' own anxiety and ensures that the child is in close proximity to them. Techniques with parental involvement include comforting and distracting the child while holding the child in a comforting position, educating and preparing the child for the procedure, and providing positive reinforcement. Parents must be careful in these interactions with their children, as any anxiety or stress they express can induce anxiety and stress in the child (60).

Educational materials and procedural preparation can be helpful for both the parents and the child. Parents and pediatric patients can watch educational videos together, practice positioning for the procedure, and observe other children modeling various coping skills. With the assistance of radiology staff members, parents can help their children practice breathing techniques and engage in positive imagery (60).

Some radiology teams also employ child-life specialists who are specifically trained to teach pediatric patients and their parents various coping skills that they can employ during MRI. These skills include visual, auditory and tactile distraction and breathing exercises

(60). In addition to reducing stress and anxiety in pediatric patients, child-life specialists have been shown to contribute to the reduction of sedation rates associated with pediatric MRI procedures (62).

Just as there are risks associated with using sedatives in adult patients, there are risks for sedating pediatric patients. Unlike for adult patients, however, the process of inducing sedation can be equally as traumatizing to the child as the MRI exam, itself. Under certain circumstances, sedation is the only way to achieve the quality of scans required for diagnosis, particularly in young children under the age of eight (63). In this case, radiology teams should follow established sedation programs that are safe and effective (64).

ROLES AND RESPONSIBILITIES

With the increasing proportion of patients taking greater responsibility for their own health, there is a rise in the number of patients using these web-based portals for information on their own health as well as information about the procedures they will undergo. With more than 60% of patients using web-based systems (65) such as Medline Plus, WebMD, and other online sources to find healthcare information, it is important for hospital radiology teams to provide their patients with specific and up-to-date information regarding their procedures. An increased focus on patient-centered medicine and improved patient education has prompted hospitals and other medical imaging facilities to provide detailed information to patients and their families.

From the referring physicians and radiologists to the technologists and support staff, each member of the team has a specific role in providing care for their patients. Primary care physicians and specialists who order the procedures have a responsibility to engage their patients in the medical process and explain the rationale for the MRI procedure. The healthcare support staff that schedule, greet, and provide the patients with pamphlets of information are an extremely valuable resource for the patients as they are the most visible members of the team.

The radiology technologists who perform the diagnostic procedures have the most direct impact on the care of the patients during potentially distressing procedures. They are highly trained professionals who not only conduct a wide range of diagnostic tests but also provide educational information and prepare patients for the procedures prior to conducting tests. As always, the radiologists and physicians who interpret the results of the tests and discuss the diagnoses with their patients have the responsibility of establishing good lines of communication with the patients and understanding their mental state following potentially distressing procedures.

CONCLUSIONS

The advances in MRI technology combined with the advances in clinical applications to aid in the diagnosis and management of an ever-increasing number of medical conditions will ensure that the number of patients undergoing MRI will continue to increase every year. Thus, the number of patients at risk for experiencing claustrophobia, anxiety, or emotional distress may likewise increase. As such, the implementation of techniques to

302 Claustrophobia, Anxiety, and Emotional Distress

minimize patient distress continues to be critical in reducing the incidence of prematurely terminated or canceled MRI exams.

Simple and effective strategies for reducing and perhaps eliminating this distress for patients have been presented in this chapter. Patient education and preparation pertaining to MRI is perhaps the single most important measure to reduce distress and the associated adverse outcomes. Importantly, adherence to the outlined measures will greatly improve patient comfort, reduce the need for sedation and, thereby, greatly decrease the number of repeat or nondiagnostic MRI exams.

(Portions of this chapter were excerpted from Spaeth RB, Gollub RL. Chapter 8, Claustrophobia, Anxiety, and Emotional Distress in the MRI Environment. Shellock FG, Crues JV, Editors. In, Bioeffects, Safety, and Patient Management. Biomedical Research Publishing Group, Los Angeles, CA, 2014.)

REFERENCES

1. Shellock, FG. Claustrophobia, Anxiety, and Panic Disorders Associated with MR Procedures. In: Shellock FG, Kanal E, Editors. Magnetic Resonance: Bioeffects, Safety, and Patient Management. New York: Lippincott-Raven Press; 1996. pp. 65.
2. Diagnostic and Statistical Manual of Mental Disorders, 4th Edition. Washington, DC: American Psychiatric Press; 1994.
3. Avrahami E. Panic attacks during MR imaging: Treatment with IV diazepam. Am J Neuroradiol 1990;11:833-835.
4. Brennan SC, Redd WH, Jacobsen PB, et al. Anxiety and panic during magnetic resonance scans. Lancet 1988;2:512.
5. Granet RB, Gelber LJ. Claustrophobia during MR imaging. New Jersey Medicine 1990;87:479-482.
6. Quirk ME, Letendre AJ, Ciottone RA, et al. Anxiety in patients undergoing MR imaging. Radiology 1989;170:463-466.
7. Shellock FG, Kanal E. Policies, guidelines, and recommendations for MR imaging and patient management. J Magn Reson Imaging 1991;1:97-101.
8. Dantendorfer K, Amering M, Bankier A, et al. A study of the effect of patient anxiety, perception and equipment on motion artifacts in magnetic resonance imaging. Magn Reson Imaging 1997;15:301-306.
9. Quirk ME, Letendre AJ, Ciottone RA, et al. Evaluation of three psychological interventions to reduce anxiety during MR imaging. Radiology 1989;173:759-762.
10. Flaherty JA, Hoskinson K. Emotional distress during magnetic resonance imaging. N Eng J Med 1989;320:467-468.
11. Klonoff EA, Janata JW, Kaufman B. The use of systematic desensitization to overcome resistance to magnetic resonance imaging (MRI) scanning. J Behav Ther Exp Psych 1986;17:189-192.
12. Weinreb J, Maravilla KR, Peshock R, et al. Magnetic resonance imaging: Improving patient tolerance and safety. AJR Am J Roentgenol 1984;143:1285-1287.
13. Katz RC, Wilson L, Frazer N. Anxiety and its determinants in patients undergoing magnetic-resonance-imaging. J Behav Ther Exp Psychiatry 1994;25:131-134.
14. McIsaac HM, Thordarson DS, Shafrazi R, Rachman S, Poole G. Claustrophobia and the magnetic resonance imaging procedure. J Behav Med 1998;21:255-268.

MRI Bioeffects, Safety, and Patient Management 303

15. Melendez C, McCrank E. Anxiety-related reactions associated with magnetic resonance imaging examinations. *JAMA* 1993;270:745-747.
16. Thorp D, Owens RG, Whitehouse G, et al. Subjective experiences of magnetic resonance imaging. *Clin Radiol* 1990;41:276-278.
17. Sarji SA, Abdullah BJ, Kumar G, Tan AH, Narayanan P. Failed magnetic resonance imaging examinations due to claustrophobia. *Australas Radiol* 1998;42:293-295.
18. Dewey M, Schink T, Dewey CF. Claustrophobia during magnetic resonance imaging: Cohort study in over 55,000 patients. *J Magn Reson Imag* 2007;26:1322-1327.
19. Enders J, Zimmermann E, Rief M, et al. Reduction of claustrophobia with short-bore versus open magnetic resonance imaging: A randomized controlled trial. *PLoS One* 2011;6:1-10.
20. Mohlman J, Eldreth DA, Price RB, Chazin D, Glover DA. Predictors of unsuccessful magnetic resonance imaging scanning in older generalized anxiety disorder patients and controls. *J Behav Med* 2012;35:19-26.
21. Murphy KJ, Brunberg JA. Adult claustrophobia, anxiety and sedation in MRI. *Magn Reson Imag* 1997;15:51-54.
22. Peters S, Cleare AJ, Papadopoulos A, Fu CHY. Cortisol responses to serial MRI scans in healthy adults and in depression. *Psychoneuroendocrinology* 2011;36:737-741.
23. Eatough EM, Shirtcliff EA, Hanson JL, Pollak SD. Hormonal reactivity to MRI scanning in adolescents. *Psychoneuroendocrinology* 2009;34:1242-1246.
24. Tessner KD, Walker EF, Hochman K, Hamann S. Cortisol responses of healthy volunteers undergoing magnetic resonance imaging. *Hum Brain Mapp* 2006;27:889-895.
25. Muehlhan M, Lueken U, Wittchen HU, Kirschbaum C. The scanner as a stressor: Evidence from subjective and neuroendocrine stress parameters in the time course of a functional magnetic resonance imaging session. *Int J Psychophysiol* 2011;79:118-126.
26. van Stegeren AH, Wolf OT, Everaerd W, et al. Endogenous cortisol level interacts with noradrenergic activation in the human amygdala. *Neurobiol Learn Mem* 2007;87:57-66.
27. Pruessner JC, Dedovic K, Khalili-Mahani N, et al. Deactivation of the limbic system during acute psychosocial stress: Evidence from positron emission tomography and functional magnetic resonance imaging studies. *Biol Psychiatry* 2008;63:234-240.
28. Tornqvist E, Mansson A, Larsson EM, Hallstrom I. Impact of extended written information on patient anxiety and image motion artifacts during magnetic resonance Imaging. *Acta Radiol* 2006;47:474-480.
29. Kilborn LC, Labbe EE. Magnetic resonance imaging scanning procedures: Development of phobic response during scan and at one-month follow-up. *J Behav Med* 1990;13:391-401.
30. MacKenzie R, Sims C, Owens RG, et al. Patient's perceptions of magnetic resonance imaging. *Clin Radiol* 1995;50:137-143.
31. Moss ML, Boungiorno PA, Clancy VA. Intranasal midazolam for claustrophobia in MRI. *J Comp Assist Tomo* 1993;17:991-992.
32. Deluca SA, Castronovo FP. Hazards of magnetic resonance imaging. *Am Fam Phys* 1990;41:145-146.
33. Friday PJ, Kubal WS. Magnetic resonance imaging: Improved patient tolerance utilizing medical hypnosis. *Am J Clin Hypnosis* 1990;33:80-84.
34. Harris LM, Cumming SR, Menzies RG. Predicting anxiety in magnetic resonance imaging scans. *Int J Beh Med* 2004;11:1-7.
35. Hricak H, Amparo EG. Body MRI: Alleviation of claustrophobia by prone positioning. *Radiology* 1984;152:819.
36. Phelps LA. MRI and claustrophobia. *Am Fam Phys* 1991;42:930.
37. Thomsen HS. Frequency of acute adverse events to a non-ionic low-osmolar contrast medium: The effect of verbal interview. *Pharmacol and Toxicol* 1997;80:108-110.

304 Claustrophobia, Anxiety, and Emotional Distress

38. Rachman S, Taylor S. Analyses of claustrophobia. *J Anxiety Disord* 1993;7:281-291.
39. Thorpe S, Salkovskis PM, Dittner A. Claustrophobia in MRI: The role of cognitions. *Magn Reson Imag* 2008;26:1081-1088.
40. Harris LM, Robinson J, Menzies RG. Predictors of panic symptoms during magnetic resonance imaging scans. *Int J Behav Med* 2001;8:80-87.
41. Brummett RE, Talbot JM, Charuhas P. Potential hearing loss resulting from MR imaging. *Radiology* 1988;169:539-540.
42. Bangard C, Paszek J, Berg F, et al. MR imaging of claustrophobic patients in an open 1.0T scanner: Motion artifacts and patient acceptability compared with closed bore magnets. *Eur J Radiol* 2007;64:152-157.
43. Spouse E, Gedroyc WM. MRI of the claustrophobic patient: Interventionally configured magnets. *Br J Radiol* 2000;73:146-151.
44. Hunt CH, Wood CP, Lane JI, et al. Wide, short bore magnetic resonance at 1.5 T. *Clin Neuroradiol* 2011;21:141-144.
45. Shellock FG, Stone KR, Resnick D, et al. Subjective perceptions of MRI examinations performed using an extremity MR system. *Signals* 2000;32:16-31.
46. Youssefzadeh S, Eibenberger K, Helbich T, et al. Reduction of adverse events in MRI of the breast by personal patient care. *Clin Radiol* 1997;52:862-864.
47. Lang EV, Ward C, Laser E. Effect of team training on patients' ability to complete MRI examinations. *Acad Radiol* 2010;17:18-23.
48. Grey SJ, Price G, Mathews A. Reduction of anxiety during MR imaging: A controlled trial. *Magn Reson Imaging* 2000;18:351-355.
49. Rauch SL, Renshaw PF. Clinical neuroimaging in psychiatry. *Harv Rev Psychiatry* 1995;2:297-312.
50. McGuinness TP. Hypnosis in the treatment of phobias: A review of the literature. *Am J Clin Hypnosis* 1984;26:261-272.
51. Axel L. Simpler music/audio system for patients having MR imaging. *Am J Roentgenol* 1988;151:1080.
52. Miyamoto AT, Kasson RT. Simple music/audio system for patients having MR imaging. *Am J Roentgenol* 1988;151:1060.
53. Simon EP. Hypnosis using a communication device to increase magnetic resonance imaging tolerance with a claustrophobic patient. *Mil Med* 1999;164:71-72.
54. Lukins R, Davan IG, Drummond PD. A cognitive behavioural approach to preventing anxiety during magnetic resonance imaging. *J Behav Ther Exper Psych* 1997;28:97-104.
55. Eshed I, Althoff CE, Hamm B, Hermann KGA. Claustrophobia and premature termination of magnetic resonance imaging examinations. *J Magn Reson Imaging* 2007;26:401-404.
56. Slifer KJ, Penn-Jones K, Cataldo MF, et al. Music enhances patient's comfort during MR imaging. *AJR Am J Roentgenol* 1991;156:403.
57. Savoy RL, Ravicz ME, Gollub R. The Psychophysiological Laboratory in the Magnet: Stimulus Delivery, Response Recording, and Safety. In: Moonen CTW, Bandettini PA, Editors. *Functional MRI*. Berlin: Springer; 1999. pp. 347.
58. Walworth DD. Effect of live music therapy for patients undergoing magnetic resonance imaging. *J Music Ther* 2010;47:335-350.
59. Garcia-Palacios A, Hoffman HG, Richards TR, Seibel EJ, Sharar SR. Use of virtual reality distraction to reduce claustrophobia symptoms during a mock magnetic resonance imaging brain scan: A case report. *Cyberpsychol Behav* 2007;10:485-488.
60. Alexander M. Managing patient stress in pediatric radiology. *Radiol Technol* 2012;83:549-560.
61. Wood BS, McGlynn FD. Research on posttreatment return of claustrophobic fear, arousal, and avoidance using mock diagnostic imaging. *Behav Modif* 2000;24:379-394.

MRI Bioeffects, Safety, and Patient Management 305

62. Khan JJ, Donnelly LF, Koch BL, et al. A program to decrease the need for pediatric sedation for CT and MRI. *Applied Radiology* 2007;36:30-33.
63. Hallowell LM, Stewart SE, Silva C, Ditchfield MR. Reviewing the process of preparing children for MRI. *Pediatr Radiol* 2008;38:271-279.
64. Keengwe IN, Hegde S, Dearlove O, et al. Structured sedation program for magnetic resonance imaging examination in children. *Anaesthesia* 1999;54:1069-1072.
65. D'Auria JP. In search of quality health information. *J Pediatr Health Care* 2010;24:137-140.
66. Klaming L, van Minde D, Weda H, Nielsen T, Duijm LE. The relation between anticipatory anxiety and movement during an MR examination. *Acad Radiol* 2015;22:1571-8.
67. Munn Z, Jordan Z. Interventions to reduce anxiety, distress and the need for sedation in adult patients undergoing magnetic resonance imaging: A systematic review. *Int J Evid Based Healthcare* 2013;11:265-74.
68. Munn Z, Moola S, Lisy K, et al. Claustrophobia in magnetic resonance imaging: A systematic review and meta-analysis. *Radiography* 2015;21:e59-e63.
69. Parmar R, Brewer BB, Szalacha LA. Foot massage, touch, and presence in decreasing anxiety during a magnetic resonance imaging: A feasibility study. *J Altern Complement Med* 2018;24:268-275.
70. Rotunda TJ. Reducing occurrences of MR-related claustrophobia in patients with PTSD. *Radiol Technol* 2017;89:97-99.
71. Germino JC, Rapp EJ, Hippe DS, et al. Assessing and optimizing imaging of patients with posttraumatic stress disorder. *J Am Coll Radiol* 2014;11:629-31.
72. Tazegul G, Erciooglu E, Yildiz F, Yildiz R, Tuney D. Can MRI related patient anxiety be prevented? *Magn Reson Imaging* 2015;33:180-3.
73. Viggiano MP, Giganti F, Rossi A, et al. Impact of psychological interventions on reducing anxiety, fear and the need for sedation in children undergoing magnetic resonance imaging. *Pediatr Rep* 2015;7:5682.
74. Brown R, Brown RKJ, Petty S, O'Malley S, et al. Virtual reality tool simulates MRI experience. *Tomography* 2018;4:95-98.
75. Enders J, Rief M, Zimmermann E. High-field open versus short-bore magnetic resonance imaging of the spine: A randomized controlled comparison of image quality. *PLoS One* 2013;8:e83427.
76. Van Minde D, Klaming L, Weda H. Pinpointing moments of high anxiety during an MRI examination. *International Journal of Behavioral Medicine* 2014;21:487-495.
77. Ashmore J, Di Pietro J, Williams K, et al. A free virtual reality experience to prepare pediatric patients for magnetic resonance imaging: Cross-sectional questionnaire study. *JMIR Pediatr Parent* 2019;2:e11684.

Chapter 11 MRI Procedures and Pregnancy

PATRICK M. COLLETTI, M.D. FACNM, FSNMMI

Professor of Radiology
Professor of Medicine
Professor of Biokinesiology
Professor of Pharmacology and Pharmaceutical Sciences
Division Chief, Nuclear Medicine
Keck School of Medicine of USC
Los Angeles, CA

INTRODUCTION

Medical imaging remains a common requirement in pregnant patients. Because of the increased scrutiny for possible radiation effects associated with pregnancy (1-4), it is not surprising that the question of whether a patient should undergo a magnetic resonance imaging (MRI) examination during pregnancy frequently arises. While a 1988 survey by Kanal, et al. (5) showed that 36% of sites did not perform MRI procedures in pregnant patients, a subsequent publication by De Wilde, et al. (6) indicated that 91% of 352 MRI facilities in the United Kingdom performed MRI examinations in second and third trimester patients, and 8% had protocols for selective fetal imaging (6). Of further note is that Kwan, et al. (7) reported that “magnetic resonance imaging rates increased steadily from 1.0/1,000 pregnancies in 1996 to 11.9/1,000 pregnancies in 2016 in the United States and from 0.5/1,000 pregnancies in 1996 to 9.8/1,000 pregnancies in 2016 in Ontario, surpassing CT rates in 2013 in the United States and in 2007 in Ontario.”

Although advice from regulatory agencies such as the United States Food and Drug Administration (FDA) is limited, the International Society for Magnetic Resonance Imaging (ISMRM), the American College of Radiology (ACR), and other organizations have provided useful clarifications, as follows (8-13):

- 1989, FDA: “The safety of MRI when used to image fetuses and infants has not been established” (8).
- 1991, Safety Committee for the Society of Magnetic Resonance Imaging (SMRI): “MR imaging may be used in pregnant women if other non-ionizing forms of diagnostic imaging are inadequate or if the examination provides impor-

MRI Bioeffects, Safety, and Patient Management 307

tant information that would otherwise require exposure to ionizing radiation...”, and there is “... no indication that the use of clinical MR imaging during pregnancy has produce deleterious effects” (9). This policy adopted by the American College of Radiology was considered a “standard of care” with reference to pregnant patients (10).

- 2002, the American College of Radiology (ACR) White Paper on MR Safety: “Pregnant patients can ... undergo MR scans at any stage of pregnancy if, in the determination of a Level Two MR Personnel-designated attending radiologist, the risk–benefit ratio to the patient warrants that the study be performed” (11).
- 2007, the ACR Guidance Document for Safe MR Practices: “Present data have not conclusively documented any deleterious effects of MR imaging exposure on the developing fetus”, and; “... no special consideration is recommended for the first, versus any other, trimester in pregnancy” (12). It is, therefore, “prudent” to document pregnancy and consult with the patient and her physician regarding the clinical urgency for immediate MRI versus waiting for MRI until after delivery.
- 2013, the ACR updated the information for the use of MRI in pregnancy, as follows: “Present data have not conclusively documented any deleterious effects of MR imaging exposure on the developing fetus. Therefore, no special consideration is recommended for the first, versus any other, trimester in pregnancy. Nevertheless, as with all interventions during pregnancy, it is prudent to screen females of reproductive age for pregnancy before permitting them access to MR imaging environments. If pregnancy is established consideration should be given to reassessing the potential risks versus benefits of the pending study in determining whether the requested MR examination could safely wait to the end of the pregnancy before being performed.
 - A. Pregnant patients can be accepted to undergo MR scans at any stage of pregnancy if, in the determination of a Level 2 MR Personnel-designated attending radiologist, the risk–benefit ratio to the patient warrants that the study be performed. The radiologist should confer with the referring physician and document the following in the radiology report or the patient’s medical record:
 1. The information requested from the MR study cannot be acquired by means of nonionizing means (e.g., ultrasonography).
 2. The data is needed to potentially affect the care of the patient or fetus during the pregnancy.
 3. The referring physician believes that it is not prudent to wait until the patient is no longer pregnant to obtain this data.
 - B. MR contrast agents should not be routinely provided to pregnant patients. This decision too, is one that must be made on a case-by-case basis by the covering Level 2 MR Personnel-designated attending radiologist who will assess the risk–benefit ratio for that particular patient.” Notably, the 2013 document from the ACR does not indicate that there is a need for informed consent for the use of MRI in pregnant patients (13).

308 MRI Procedures and Pregnancy

- 2018, the ACR Manual On Contrast Media Version 10.3 states that if GBCAs are to be given to a pregnant patient: “It is recommended that informed consent be obtained from the patient after discussion with the referring physician (14).”

SAFETY

Basic Research and Animal Studies

MRI exposes the patient and fetus to a powerful static magnetic field, rapidly changing, gradient magnetic fields, acoustic noise, and radiofrequency (RF) radiation. The effects of these electromagnetic fields on the human fetus are not easily determined. Consider the following:

- The strength of the static magnetic field is well known (e.g., 1.5-Tesla, 3-Tesla, etc.).
- The gradient amplitude (e.g., 20-mT/m) and slew rate, dB/dt (i.e., 3-T/s) can be determined at the location of the fetus for a given pulse sequence.
- RF energy power deposition or the specific absorption rate (SAR) level (e.g., whole body averaged SAR, 2.0-W/kg with the MR system operating in the Normal Operating Mode) will vary considerably with the type of transmit RF coil that is used and system configuration, as well as the pulse sequences that are selected for the procedure. Popular sequences for fast fetal imaging, such as fast spin echo, employ multiple rapid RF pulses, and would be expected to deposit more RF energy compared to gradient echo techniques.
- Using computer modeling, Murbach, et al. (15) described the potential risks associated with the use of two-port radiofrequency (RF) shimming when examining a pregnant woman at 3-T. They stated: “Although RF shimmed configurations may lower the local RF exposure for the mother, they can increase the thermal load on the fetus. In worst-case configurations, whole-body exposure and local peak temperatures-up to 40.8°C-are equal in fetus and mother”. Of course, this finding has not been verified in human subjects undergoing MRI and there are well-known issues when using modeling to predict temperature elevations in patients in association with MRI.
- RF power deposition varies considerably with the body part undergoing MRI. While Schaefer (16) concluded that approximately 87% of the RF energy would likely be deposited in the outer 1/3 of the body (16), Hand, et al. (17) predicted that the fetus would be exposed to a peak of approximately 40 to 60% of the maternal peak value at 64-MHz (1.5-Tesla), increasing to approximately 50 to 70% at 128-MHz (3-Tesla). Thus, in most instances, the embryo or fetus would receive relatively small RF exposures (18-20).
- Heating is the only well-established mechanism for bioeffects related to RF energy (21). Interestingly, the fetus may be heat energy tolerant due to a large fetal surface area-to-volume ratio. In addition, amniotic fluid, with its relatively high heat capacity, would be expected to sufficiently absorb heat transferred by convection. Kikuchi, et al. (22) used a thermal model to predict that 40-minutes of

Table 1. Spontaneous adverse outcomes of pregnancy.

Period	Risk	Spontaneous Occurrence Rate
Day 1 to 10	Reabsorption	30%
Day 10 to 50	Abnormal Organogenesis	4 to 6%
>Day 50	Intra-uterine Growth Retardation	4%

Table 2. Safety of MRI in pregnancy: Non-adverse outcomes in animals.

Study	Findings
McRobbie and Foster (24) 1985	No change in litter number or growth rate in mice exposed to gradients ranging from 3.5- to 12-kT/s.
Teskey, et al. (25) 1987	No change in stress reactivity or survivability in rats repeatedly exposed in-utero.
Heinrichs, et al. (26) 1988	No embryo toxicity or teratogenesis with prolonged exposure (BLB/c mice, midgestational, 0.35-T).
Kay, et al. (27) 1988	No adverse effects (<i>Xenopus laevis</i> embryo, long-term exposure, 1.5-T).
Tyndall (28) 1990	MRI exposure does not add to low level x-ray irradiation induced teratogenesis in C57B1/6J mice at 1.5-T.
Murkami, et al. (29) 1992	No change in pregnancy outcomes for mice exposed to 6.3-T for 1-hour per day from day 7 to 14.
Malko, et al. (30) 1994	No change in cell density (yeast cells grown at 1.5-T).
Yip, et al. (31) 1994 and Yip, et al. (32) 1995	No change in survival, migration, and proliferation and no effect on axonal growth in chick embryos exposed to simulated imaging conditions at 1.5-T.
Tablado, et al. (33) 2000	No testicular abnormalities in mice continually exposed in-utero from day 7 to birth at 0.7-T.
Ruckhaberle E, et al. (34) 2008	No significant amniotic fluid temperature or acoustic noise changes in pregnant ewes at 1.5-T. Intrauterine peak acoustic levels did not exceed 100.0-dB.

scanning at a whole-body averaged SAR of 2-W/kg may increase fetal temperature more than the 0.5°C, as recommended by the International Commission on Non-Ionizing Radiation Protection, but less than the proposed teratogenic cutoff value of 1.5 °C (22).

- The anatomically “deep” position of the fetus and the surrounding amniotic fluid could reduce the effects of gradient field-related, acoustic noise.
- While the stage of pregnancy may be important with regard to the potential risk to the embryo or fetus, it should be noted that spontaneous adverse outcomes are common (23) (**Table 1**).

A number of biological studies have assessed the effects of MRI in pregnancy. Most of these studies show no evidence for fetal harm (24-40) (**Tables 2 and 3**). However, there

310 MRI Procedures and Pregnancy

Table 3. Safety of MRI in pregnancy: Adverse outcomes in animals and human cell cultures.

Study	Findings
Tyndall and Sulik (35) 1991	At least two-fold increased incidence of eye malformations (C57B16J mice, 10% spontaneous eye malformations, gestational day 7, 1.5-T for 36-minutes).
Tyndall (36) 1993	Increased teratogenicity with reduced crown-rump length and craniofacial size in C57B1/6J mice exposed to clinically realistic MRI at 1.5-T.
Yip, et al. (37) 1994	“trend toward higher abnormality and mortality rates..” in chick embryos exposed simulated imaging conditions at 1.5-T.
Carnes, et al. (38) 1996	Fetal weight reduction (11%) in mice exposed to 8 hours in midgestation at 4.7-T
Narra, et al. (39) 1996	Reduced spermatogenesis and embryogenesis in Webster mice exposed in-utero to 1.5-T for 30-minutes.
Lee, et al. (40) 2011	3-T MRI induces genotoxic effects (significant increase in the frequency of micronuclei and single-strand DNA breaks) in cultured human lymphocytes proportional to exposure time.

Table 4. Safety of MRI in pregnancy: Non-adverse outcomes in humans.

Study	Findings
Johnson, et al. (41) 1990	No change in fetal heart rate or Doppler-determined umbilical artery blood flow (humans, 10 to 20 weeks, 0.5-T).
Kanal, et al. (42) 1993	No increase in adverse reproductive outcomes (280 pregnant female MR imaging workers).
Baker, et al. (43) 1994	No increase in disease or disability, no hearing loss in 20 children at 3 years after in-utero exposure to echo-planar MRI at 0.5-T.
Myers, et al. (44) 1998	No significant decrease vs. matched controls in fetal growth in 74 volunteers exposed in-utero to echo-planar MRI up to 5 times at 0.5-T.
Vadeyar, et al. (45) 2000	No change in fetal heart rate in human volunteers at term (37 to 41 weeks), echo-planar MRI at 0.5-T.
Kok, et al. (46) 2004	No harmful effects of prenatal 1.5-T MR exposure in the third trimester of pregnancy were detected in 35 children at 1 to 3 years and in 9 children at 8-9 years.
Reeves, et al. (47) 2010	Second and third trimester fetal exposure to 1.5-T MR imaging is not associated with an increased risk of substantial neonatal hearing impairment.
Bouyssi-Kobar, et al. (48) 2015	Second and third trimester fetal exposure to 1.5-T MR imaging is not associated with disturbances in functional outcomes or hearing impairment at preschool age. N = 72.
Strizek, et al. (49) 2015	No adverse effects of exposure to 1.5-T MR imaging in utero on neonatal hearing function or birth weight percentiles. N = 751.
Jaimes, et al. (50) 2019	The increase in noise associated with 3-T does not increase the rate of clinically detectable hearing abnormalities when compared to in utero exposure to 1.5-T. N = 62 in each group, p = 0.8.
Chartier, et al. (51) 2019	No adverse effects regarding neonatal hearing or fetal growth in healthy neonates who were variably exposed to 3-T MR in utero for clinical maternal or fetal indications at any gestational age. N = 81.

Table 5. Currently approved MRI contrast agents.

Agent	Molecular Weight	Charge	Relative Stability	Excess Free Ligand in Formulation
Gadolinium-based contrast agents				
Gadopentetate dimeglumine (Magnevist, Bayer Healthcare, Wayne, NJ) (56)	938	Linear-ionic	Moderate	0.4-mg/ml
Gadobenate (MultiHance, Gd-BOPTA, Bracco, Milan, Italy) (57)	1058	Linear-ionic	Moderate	0.4-mg/ml
Gadodiamide (Omniscan, Nycomed Amersham, Princeton, NJ) (58)	574	Linear-nonionic	Low	12-mg/ml
Gadovesetamide (OptiMARK, Mallinkrodt, St. Louis) (59)	661	Linear-nonionic	Low	28.4-mg/ml
Gadoteridol (ProHance, Bracco, Princeton, NJ) (60)	559	Macro-cyclic-nonionic	High	Not applicable
Gadobutrol Gd-BT-DO3A (Gadovist, Bayer Schering Pharma, Berlin, Germany) (61)	605	Macro-cyclic-nonionic	High	Not applicable
Gadoterate Gd-DOTA (Dotarem, Guerbet, Roissy, France) (62)	558	Macro-cyclic-nonionic	High	Not applicable
Gadofosveset trisodium (Ablavar, Lantheus Pharmaceuticals, Boston, MA) (63)	976	Linear-ionic; binds reversibly to serum albumin	High	Not applicable
Gadoxetic acid (Eovist, Bayer Healthcare, Wayne, NJ; Primovist, Bayer Healthcare, Berlin, Germany) (64)	725	Linear-ionic	High	Not applicable
Non-gadolinium-based contrast agents				
*FDA approved or discontinued				
Mangafodipar (Teslascan, Nycomed Amersham, Princeton, NJ) (65)	757	Manganese		fodipir, 0.25-mg/ml
Ferumoxide (Feridex IV, Berlex, Wayne, NJ) (66)	83, in 80 to 160-nm particles	Super-paramagnetic oxide particles		mannitol 61.3-mg, dextran 5.6– to 9.1-mg/ml

has been little clinical follow-up for humans exposed to MRI, *in-utero* (41-52) (**Table 4**). A survey of reproductive health among 280 pregnant MRI healthcare workers performed by Kanal, et al. (42), showed no substantial increase in common adverse reproductive outcomes. Baker, et al. (43) showed no demonstrable increase in disease, disabilities, or hearing loss in 20 children examined *in-utero* with echo-planar MRI performed to assess suspected

312 MRI Procedures and Pregnancy

Table 6. Safety of gadolinium-based MRI contrast agents in pregnancy*.

Retarded development without congenital abnormalities in rats (Magnevist, 2.5 to 12.5 times human dose) and in rabbits (Magnevist, 7.5 to 12.5 times human dose for 12 days) (56).
Teratogenic in rabbits; microphthalmia/small eye and/or focal retinal fold in 3 fetuses from 3 litters (MultiHance, 6 times human dose during organogenesis, days 6 to 18) (57).
Increased intrauterine deaths in rabbits (MultiHance, 10 times human dose) (57).
No teratogenic effects or systemic toxicity or abnormal peri or post-natal birth, survival, growth, development or F1 generation fertility in rats (MultiHance, 3 times human dose) (57).
Skeletal and visceral abnormalities in rabbits (Omniscan, 5 times human dose) (58).
Reduced dam body weight and fetal “flexed” appendages and skeletal malformations (OmniScan, 0.6 times human dose for 13 days) (58).
No adverse effects in rats (OmniScan, 1.3 times human dose for 10 days) (58).
Maternal toxicity and reduced mean fetal weight, abnormal liver lobulation, delayed sternal ossification, and delayed behavioral development (startle reflex and air rights reflex) in rats (OptiMARK, 10 times human dose; gestation days 7 to 17). These effects were not observed at 1 times human dose (59).
Forelimb flexures in rabbits (OptiMARK, 1 times human dose, gestation days 6 to 18) (59).
Malformed thoracic arteries, septal defect, and abnormal ventricle in rabbits (OptiMARK, 4 times human dose, gestation days 6 through 18) (59).
Postimplantation fetal loss doubled in rats (ProHance, 33 times human dose for 12 days) (60).
Increased spontaneous locomotor activity in rats (ProHance, 33 times human dose for 12 days) (60).
Increased spontaneous abortion and early delivery in rabbits (ProHance, 20 times human dose for 13 days) (60).
Radioactively labeled gadobutrol was detected in rabbit fetuses but not in rat fetuses (61).
No teratogenicity in rats, rabbits or cynomolgus monkeys (Gadovist, repeated doses) (61).
Delayed embryonal development in rats and rabbits and increased embryolethality in rats, rabbits and monkeys (Gadovist, repeated doses of 25 to 50 times human dose) (61).
Fetal plasma level was 5% of maternal level in rats (Dotarem, gestation day 18) (62).
No evidence of embryotoxicity or teratogenicity in rats and rabbits (Dotarem, at 1.3 times (rats) or 2.4 times (rabbits) the human dose) (62).
Increased post-implantation loss, resorption, fetal death and maternal toxicity without fetal anomalies in rats and rabbits (Ablavar, at 11 times (rats) and 21.5 times (rabbits) the human dose) (63).
Embryotoxicity with increased post implantation loss and absorption and decreased litter size in rabbits (EOVIST, 26 times human dose) (64).
Maternal toxicity without teratogenicity in rats (EOVIST, 32 times human dose) (64).
Increased preimplantation loss in rats (EOVIST, 3.2 times human dose) (64).

* Data from package inserts of Magnevist, MultiHance, Omniscan, OptiMARK, ProHance, Gadovist, Dotarem, Ablavar, and EOVIST.

fetal compromise. Myers, et al. (44) showed no significant reduction in fetal growth vs. matched controls in 74 volunteers exposed *in-utero* to echo-planar MRI at 0.5-Tesla.

Table 7. Safety of non-gadolinium-based MRI contrast agents in pregnancy (data from package inserts of Feridex and Teslascan).

Animal studies have shown that ^{54}Mn manganese crosses the placenta and locates in fetal liver and bones (65).
Increased skeletal malformations and decreased fetal body weight in rats (Teslascan, 2 to 8 times human dose gestation days 6 to 17 of gestation). No effects seen at 1 times human dose (65).
Increased post-implantation losses and resorption, and decreased fetal viability in rabbits, (Teslascan, 8 to 10 times human dose days 6 to 18 of gestation). No effects seen at 4 times human dose (65).
Teratogenicity in rabbits (Feridex, I.V, 6 times human dose) (66).

Use of MRI Contrast Agents in Pregnancy

Bird, et al. (52) have “identified 1.2 gadolinium-based contrast agent (GBCA) exposures per 1,000 live births, or one exposure for every 860 pregnancies especially during the first few weeks of pregnancy compared with the later weeks of pregnancy, suggesting inadvertent exposure to GBCAs might occur before pregnancy is recognized (52).”

While some moieties are transferred across the placenta by active transporters located on both the fetal and maternal side of the trophoblast layer, most substances administered during pregnancy will, to a certain degree, traverse the placenta and enter the fetus via passive diffusion. Transplacental passive diffusion is affected by molecular properties such as molecular weight, the acid dissociation constant (pKa), lipid solubility, and plasma protein binding (53, 54). Polar molecules with a molecular weight of less than 500-D are more likely to traverse the placenta. Significant plasma protein binding favors maternal blood pool compartmentalization and placental blood pool localization without transplacental diffusion.

Most currently approved gadolinium-based MRI contrast agents have a relatively low molecular weight and, thus, would be expected to readily cross the placental barrier (52-72) (**Table 5**). Massive doses of these agents have been shown to cause post-implantation fetal loss, delayed development, increased locomotive activity, and skeletal as well as visceral abnormalities in experimental animals [(56-66) (**Table 6**) and (56-64) (**Table 7**)]. Thus, the Food and Drug Administration (FDA) generally lists MRI contrast agents as “PREGNANCY CATEGORY C”. Statements such as “adequate and controlled studies in pregnant woman have not been conducted” and *this agent* “should only be used during pregnancy if the potential benefit justifies the potential risk to the fetus” are typically noted in the package inserts for these products (56-66).

Because some of the effects described in animal experiments may be caused by a generic contrast agent, transmetallated gadolinium, or disassociated ligand moieties, for the purpose of this presentation, specific product names are presented rather than a generic contrast agent component, but only for the adverse effects presented in **Table 6** and **Table 7**.

After intravenous administration of a gadolinium-based contrast agent, a portion of this substance will localize in the placental blood pool (67-72) (**Figure 1**). From there, a small portion will reach the fetus. If the fetal kidneys are developed (i.e., beyond seven weeks), the gadolinium chelate will be excreted into the fetal bladder (**Figure 2**), where it would be

314 MRI Procedures and Pregnancy

Figure 1. Dynamic contrast enhancement of the placenta (arrows) in a 28-year-old pregnant woman at 30 weeks. Note the rapid, heterogeneous enhancement.

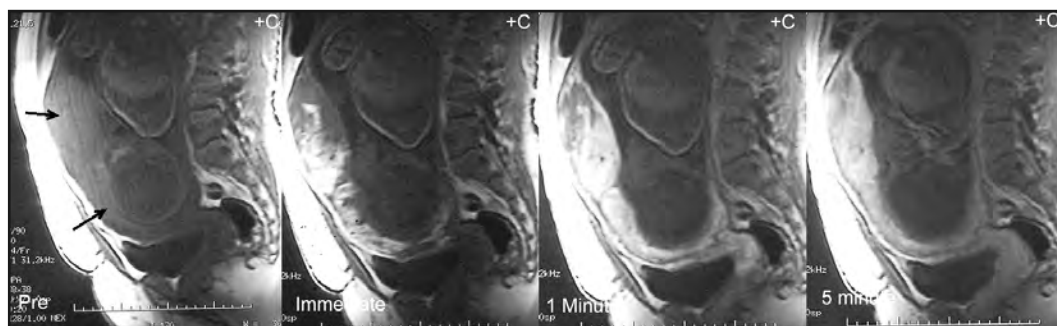
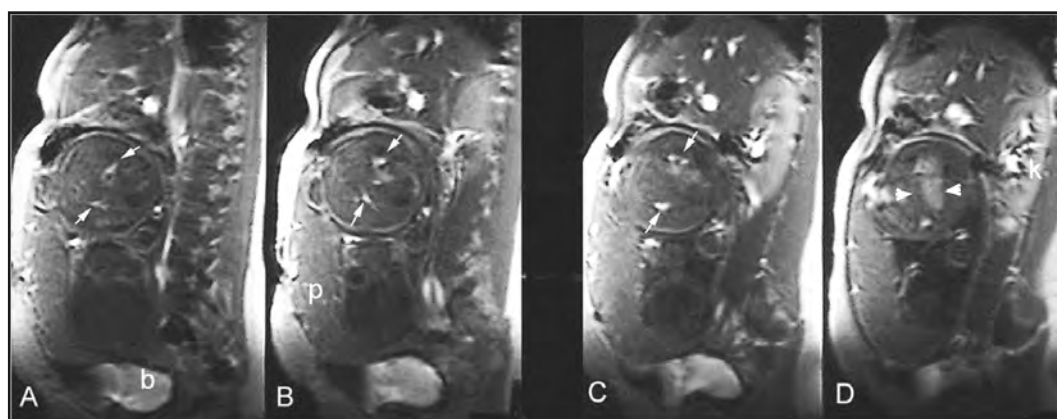


Figure 2. Contrast enhanced spoiled gradient echo MRI of the fetus at 32 weeks shows fetal renal enhancement, (arrows) (A, B, C) and fetal bladder (arrowheads) (D). Maternal kidney (k), bladder (b), placenta (p).



voided into the amniotic fluid. From there, the fetus would swallow some of the contrast material and it would pass through the fetal gut, eventually reentering the amniotic fluid (67-72). Based on postnatal animal studies that demonstrated less than 1% intestinal gadolinium chelate absorption (72-76), significant fetal intestinal absorption of gadolinium-based contrast agents might not be expected. Conversely, fetal amniotic circulation may participate unpredictably in the breakdown and absorption of intact contrast agents and free gadolinium. Excess chelating ligand may be absorbed with potential fetotoxic effects as shown in **Table 6**. It is predictable that the dissociation of the gadolinium chelate bond will be greater with thermodynamically less stable MRI contrast agents (e.g., OmniScan, OptiMARK, and Magnevist) as compared to more stable agents (e.g., ProHance, Gadovist, and Dotarem) and, thus, the latter three would be better choices for use when required in pregnant patients (77-78).

Ray, et al. (79) demonstrated that “of 1,424,105 deliveries the MRI rate was 3.97 per 1,000 pregnancies.” Comparing gadolinium MRI ($n = 397$) with no MRI ($n = 1,418,451$),

the hazard ratio for NSF-like outcomes was not statistically significant, though the data may have been underpowered for this distinction.

Rheumatological, inflammatory, or infiltrative skin condition were noted in 123 vs. 384,180 births (adjusted HR, 1.36; 95%CI, 1.09 to 1.69) for an adjusted risk difference of 45.3 per 1,000 person-years (95%CI, 11.3 to 86.8). “Stillbirths and neonatal deaths occurred in 7 MRI-exposed vs 9,844 unexposed pregnancies (adjusted RR, 3.70; 95%CI, 1.55 to 8.85) for an adjusted risk difference of 47.5 per 1,000 pregnancies (95%CI, 9.7 to 138.2) (79).”

Ray, et al. (79) concluded “Gadolinium MRI at any time during pregnancy was associated with an increased risk of a broad set of rheumatological, inflammatory, or infiltrative skin conditions and for stillbirth or neonatal death”.

CLINICAL APPLICATIONS OF MRI PROCEDURES IN PREGNANT PATIENTS

Non-Pelvic Imaging The pregnant patient is subject to most of the same brain, spine, body, and musculoskeletal conditions as the non-pregnant patient (80). In addition, abnormalities associated with pregnancy, such as toxemia and sagittal sinus thrombosis can occur. Furthermore, pituitary adenomas may show growth during pregnancy. Therefore, diagnostic imaging is frequently required with these conditions. Because MRI used nonionizing radiation, it is particularly suited as an alternative to computed tomography (CT) in situations where ultrasound is either unsatisfactory or inappropriate.

Brain Imaging

Besides the specific brain conditions associated with pregnancy, other common cerebral abnormalities such as tumor, infarction, hemorrhage (**Figure 3**), demyelination, arteriovenous malformation, and aneurysm may occur during pregnancy (81). These are also best evaluated using MRI. MRI contrast agents should be reserved for patients in whom diagnosis (i.e., metastasis) or therapy (i.e., brain tumor therapy prior to surgery) is urgently needed (**Figures 4 and 5**). Diffusion-weighted MR imaging is useful if acute cerebral infarction is suspected. MR angiography is helpful to screen for cerebral aneurysm in the pregnant patient with a family history of aneurysm in preparation for the stress of vaginal delivery.

Spine Imaging

MRI should be reserved for specific cases of suspected disc extrusion in which surgery would be performed during the pregnancy. MRI is also appropriate for the evaluation of spinal tumor, unstable fracture, infection (82), syrinx (**Figure 4**), or vascular malformation, all of which may affect immediate therapy or mode of delivery (Caesarean section vs. vaginal).

Musculoskeletal Imaging

MRI is particularly useful in the evaluation of musculoskeletal abnormalities in selected patients in whom intervention is required during pregnancy. Routine knee and shoulder

316 MRI Procedures and Pregnancy

Figure 3. A 23-year-old woman presents with severe headache and lethargy at 18 weeks of pregnancy. Axial T1 (A), T2 (B), FLAIR (C), and diffusion-weighted MR images (D) show a prominent left sided subdural hematoma (arrows) with midline shift. The subdural hematoma was evacuated and the patient improved. Non-traumatic subdural hematoma.

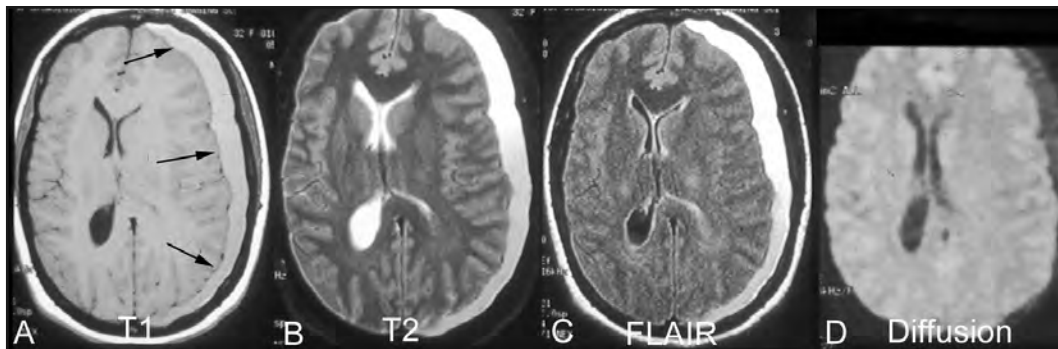
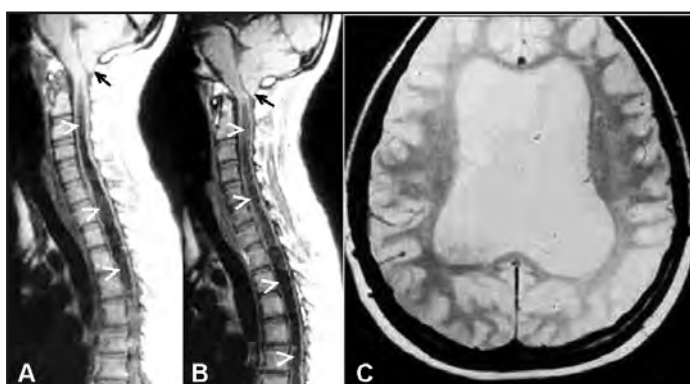


Figure 4. A 19-year-old woman presents at 30 weeks of pregnancy with the history of Chiari II congenital malformation. Sagittal TR-600, TE-20 images (A, B) demonstrate tonsillar herniation (arrows) and hydromyelia (arrowheads). Axial brain MRI (TR-2000, Effective TE-100) demonstrates hydrocephalus (C). Chiari II malformation.



examinations can often be delayed until after delivery, but the evaluation of suspected infection or neoplasm must often be performed immediately (82).

Head and Neck Imaging

MRI of the head and neck may be advantageous compared to CT because of its lack of ionizing radiation and lesser need for the use of contrast agents.

Chest and Cardiovascular Imaging

Hilar and mediastinal nodes can be shown easily with MRI without the use of ionizing radiation or contrast agents. Additionally, whole torso MRI examinations may be used to

Figure 5. This 24-year-old woman presents at 27 weeks of pregnancy with a right neck mass. Biopsy revealed low-grade lymphoma. Whole body single-shot fast spin-echo MRI shows extensive mediastinal adenopathy (arrows). No evidence of abdominal or pelvic disease. Gallstones and the fetus are seen. Lymphoma.

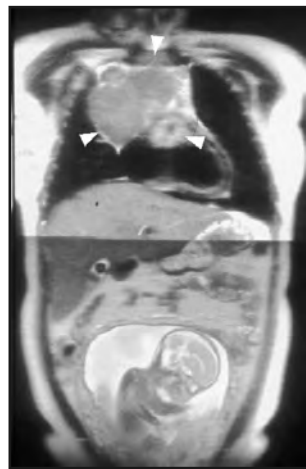
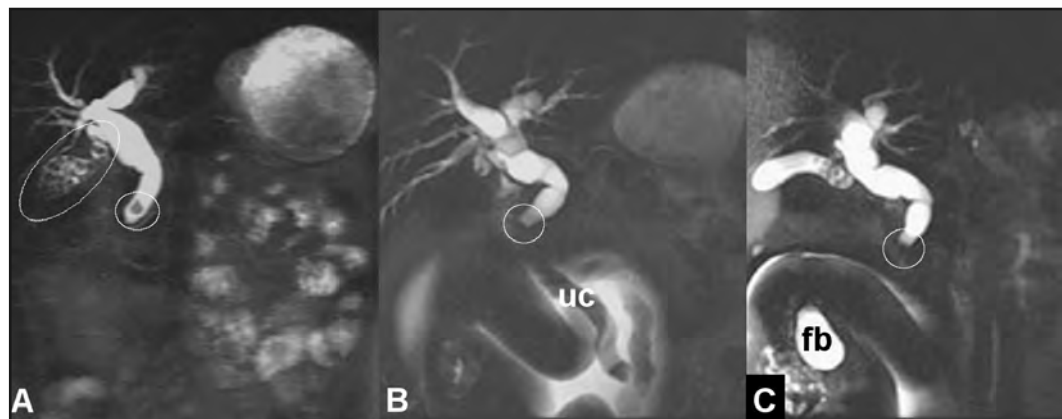


Figure 6. This 32-year-old woman presents with abdominal pain and elevated bilirubin at 12 weeks of pregnancy. Anterior and oblique MRCP projections (A to C) demonstrate innumerable gallstones (oval) and markedly dilated bile ducts, with one large obstruction common bile duct stone (circle). Incidentally noted are the fetal kidney and bladder (fb) and umbilical cord (uc). Choledocholithiasis.



evaluate neoplasm staging during pregnancy (**Figure 5**). While echocardiography remains the standard non-invasive cardiac imaging modality of choice, particularly in the pregnant patient, MRI is ideal to demonstrate and confirm cardiovascular abnormalities such as coarctation of the aorta, aortitis, aortic dissection, and atrial myxoma (83-84). MRI may also be an alternative to CT pulmonary angiography for suspected pulmonary emboli in pregnancy (84).

318 MRI Procedures and Pregnancy

Figure 7. This 27-year-old woman presented with right lower abdominal pain at 17 weeks of pregnancy. Coronal (A) single-shot fast spin-echo and sagittal (B) T2-weighted MR images demonstrate a dilated, fluid filled appendix with a thickened wall (arrows). The thickened, fluid filled appendix with surrounding inflammation (circled) is confirmed on axial FSPGR (C) and T2-weighted, FIESTA images (D). Acute appendicitis.

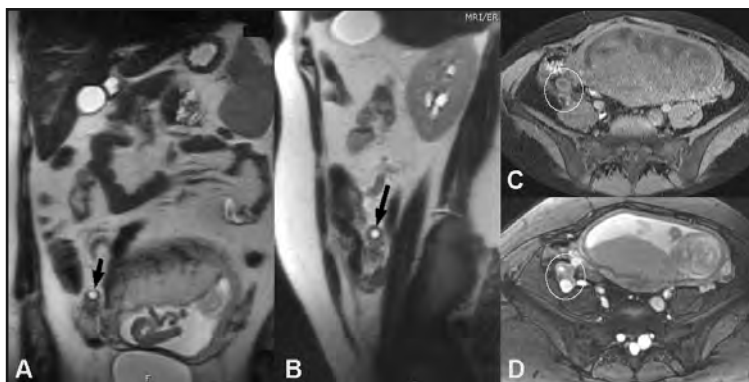


Figure 8. This 30-year-old woman presents at 6 weeks pregnancy with right lower abdominal pain and tenderness. Axial T2 single-shot fast spin-echo image demonstrates fluid within an intrauterine gestational sac (gs) and a fluid filled adjacent right lower quadrant appendiceal abscess (aa). Appendiceal abscess.



Abdominal Imaging

Although sonography is the diagnostic examination of choice for abdominal imaging in the pregnant patient, there has been considerable interest in the use of MRI for abdominal applications as an alternative to CT (85-95). The absence of ionizing radiation gives MRI an inherent advantage over CT, particularly to evaluate the liver, pancreas and retroperitoneum. Large lesions such as tumors, pseudocysts, and abscesses are well shown with MRI. Fatty liver in pregnancy may also be evaluated with an MRI examination.

Figure 9. This 34-year-old woman presented as “large for dates” at 12 weeks of pregnancy. Ultrasound showed a right mid abdominal complex mass. Coronal T1-weighted MR image demonstrates a relatively low signal pedunculated mass (*) connected to the gravid uterus (arrowheads) by a relatively narrow connection (arrows). Pedunculated leiomyoma.



Masselli, et al. (91) demonstrated no significant difference between 61 MRI exams and 44 CT exams in comparable pregnant patients with acute abdominal symptoms (sensitivity 91% vs. 88%, specificity 85% vs. 90%, positive predictive value 81% vs. 91%, negative predictive value 94% vs. 85%, and diagnostic accuracy 88% vs. 88%, respectively) (91).

Specifically, MRI may be used effectively to evaluate the maternal urinary tract, biliary system (**Figure 6**), and appendix for suspected acute conditions including urinary obstruction, biliary obstruction, cholecystitis, and appendicitis (85-93) (**Figures 7 and 8**).

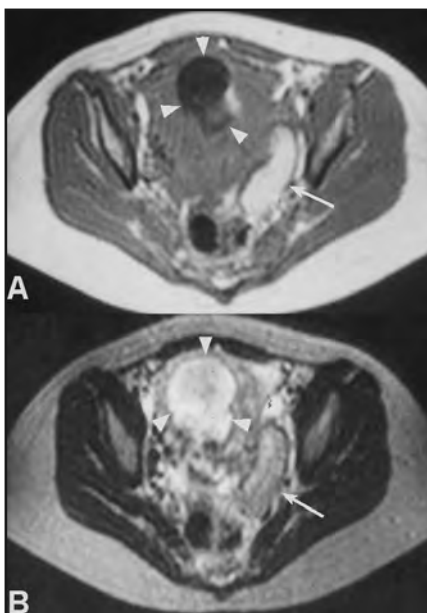
Pelvic Imaging

Pregnancy can accelerate the growth of benign and malignant pelvic masses. A common diagnostic differential decision involves the separation of uterine abnormalities such as leiomyoma (**Figure 9**) from adnexal lesions, including ovarian cysts and neoplasms (**Figure 10**). Occasionally, ultrasound has difficulty with this distinction, particularly when larger lesions are present. MRI may better delineate and characterize these abnormalities (94, 95). Breath-held images with relative T1- and T2-weighting are useful to localize and characterize lesions on MRI examinations.

MR angiography may be used to demonstrate pelvic arterial and venous vessels in the pregnant patient. An enlarged uterus may cause markedly reduced flow in the inferior vena

320 MRI Procedures and Pregnancy

Figure 10. Pelvic ultrasound of this 25-year-old woman at 9 weeks of pregnancy demonstrated a 6 x 3 x 2-cm left adnexal mass. Axial TR-400, TE-20 (A) and TR-2200, TE-80 (B) images demonstrate a left adnexal mass (arrows) with fat signal on T1- and T2-weighted sequences. The gestational sac is noted (arrowheads). Dermoid.



cava and iliac veins with extensive collateral vessel formation during the third trimester. Two-dimensional, time-of-flight MR angiography with superior saturation shows these vessels exceptionally well. Normal fetal vessels may also be visualized with this technique.

Additionally, MRI may be useful to demonstrate pelvic abnormalities related specifically to pregnancy such as placenta previa, placenta acreta, abruptio placentae, chorioangioma, ectopic pregnancy, and abdominal pregnancy. MR-pelvimetry may be used as an alternative to radiographic or CT pelvimetry (96, 97).

MRI of the Fetus

There have been a number of institutional review board approved, MRI investigations of fetal abnormalities (41, 98-142). Fetal sedation is no longer considered necessary to obtain good fetal MR images. While gross fetal motion may cause image degradation (Figure 11), much of the difficulty in performing fetal MRI is due to maternal respiration. Current imaging strategies generally utilize breath-held MRI with single-shot, fast spin echo techniques (ssFSE) (Figure 12 and Figure 13) along with fast gradient refocused echo or fast spoiled gradient echo MRI techniques (110-142). Echo planar imaging (EPI) pulse sequences have also shown considerable success in fetal MRI (43).

Because an abnormal fetus often has reduced fat due to growth retardation, MR images obtained in these fetuses may show relatively poor detail. Brain myelination *in-utero* may be demonstrated using T1- and T2-weighted MR images. Normal fetal structures such as

Figure 11. Thirty-two-week fetus in a 22-year-old woman demonstrates gross fetal motion with marked positional changes seen in a repeat breath-held single-shot fast spin-echo coronal view at 30 minutes. Fetal movement.

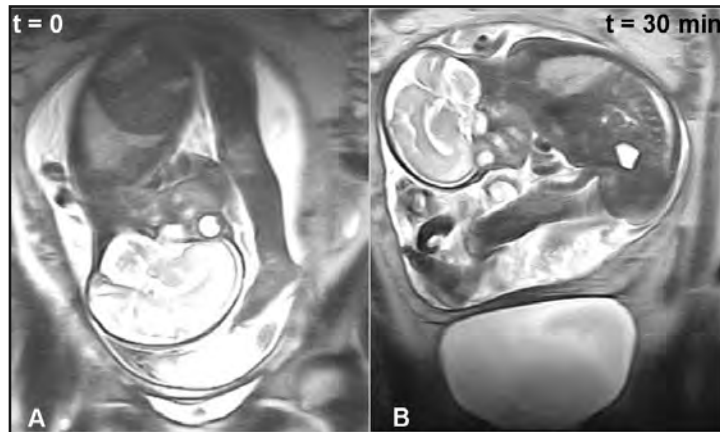
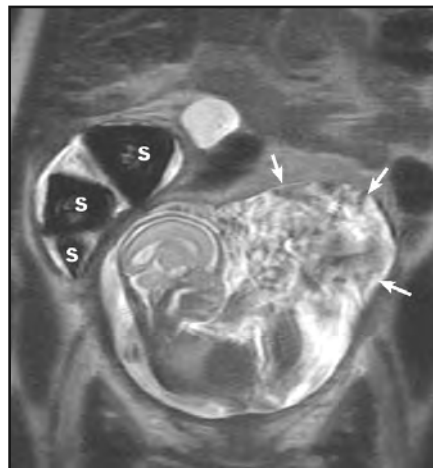


Figure 12. Twenty-week twin gestation in a 30-year-old woman. Breath-held, 11-second single-shot fast spin-echo sagittal view shows demise of one twin with marked deformity (arrows). Incidentally noted are very large gallstones. Twins with demise of one fetus.



the brain, face, spine, heart, liver, stomach, intestines, and bladder are seen routinely on MRI examinations. Frequently, the fetal genitalia are identified on MR images (**Figure 14**). Obviously, these structures are easier to evaluate in later pregnancy, although with higher quality, faster techniques, reasonable detail can be obtained by the mid-second trimester.

MRI can confirm most sonographically detected gross fetal abnormalities such as hydrocephalus, schizencephaly (**Figure 15**), anencephaly, meningocele, omphalocele, gas-

322 MRI Procedures and Pregnancy

Figure 13. Axial breath-held 12-second single-shot fast spin-echo views show normal fetal anatomy at 28 weeks. Images at the level of the fetal midbrain (A), and pons (B) are seen.

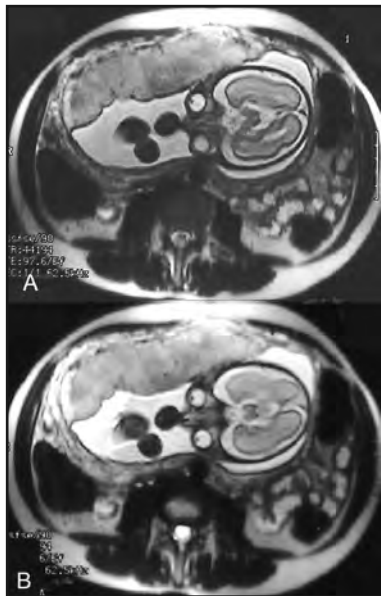


Figure 14. Fetal anatomy. Axial T1 weighted image (A) demonstrates the fetal heart; intraventricular septum (arrow), descending aorta (arrowhead), and right atrium (open arrow). Axial T1 weighted image (B) shows the fetal bladder (b) and high signal meconium filled rectum (r). Oblique reformatted single-shot fast spin-echo image (C) demonstrates low signal fetal liver and high signal meconium in the colon (c). Axial T2 FSE image demonstrates fetal testes and phallus (arrow).

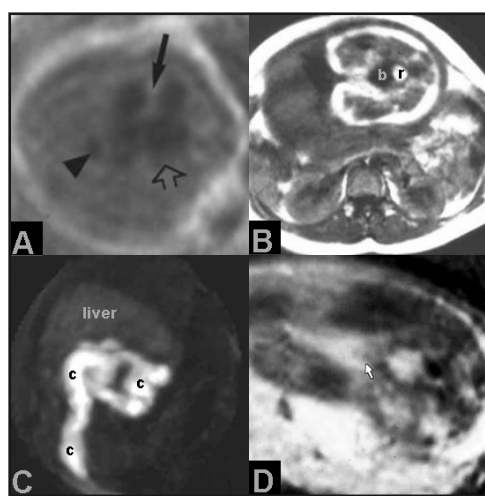
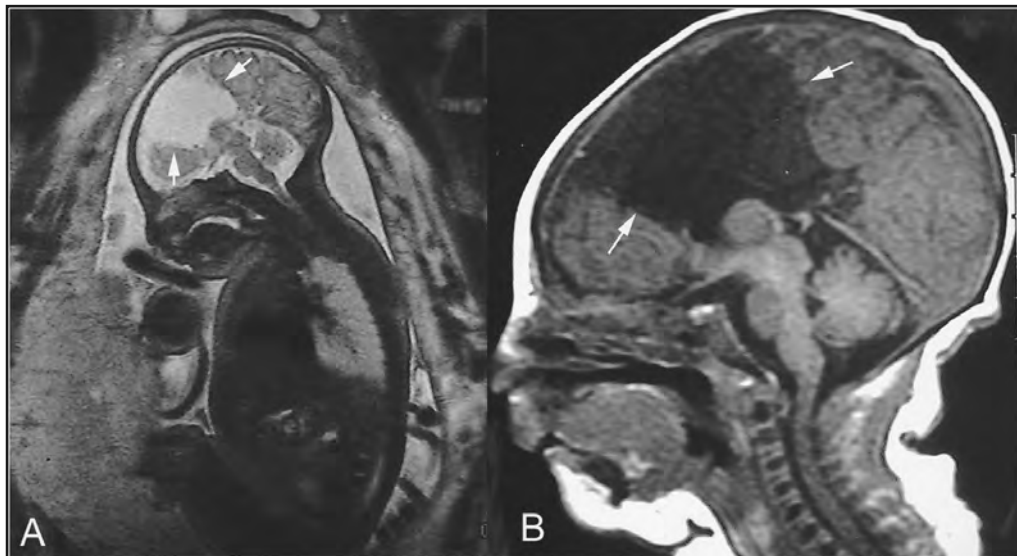


Figure 15. A coronal breath-held, 11-second ssFSE view (A, inverted for display) at 32 weeks of pregnancy shows agenesis of the corpus callosum and a large midline cleft (arrows). A sagittal TR-400, TE-18 MR image of the newborn on day three confirms these findings (B).



troschisis, congenital hiatal hernia (**Figure 16**) and teratoma (**Figure 17**). Subtle anomalies, such as limb abnormalities are more difficult to detect, but even these are demonstrated occasionally with current imaging techniques. MRI provides information that is not readily apparent on sonography in approximately 10% of cases. This is most often seen in examination of the fetal brain but, again, with current techniques, occasionally fetal lungs, fetal diaphragm, fetal liver, and fetal kidneys may be better visualized using MRI.

It is particularly important to consider the added stress perceived by pregnant women undergoing MRI for the evaluation of possible fetal abnormalities. Ideally, comfortable positioning of pregnant patients should be individualized during the MRI examination. Noise protection should be optimized and rapid, efficient scanning should be carefully planned (143).

QUESTIONS TO CONSIDER PRIOR TO USING MRI IN A PREGNANT PATIENT

The decision to utilize MRI in the pregnant patient referred for diagnostic imaging typically involves answering a series of questions as part of the assessment of risk vs. benefit for a given patient, including, the following (76):

- Is imaging required?
- Is the patient pregnant?
- Is sonography satisfactory for diagnosis?

324 MRI Procedures and Pregnancy

Figure 16. Congenital diaphragmatic hernia (arrows). Image provided courtesy of Teresa Victoria M.D., Ph.D., Children's Hospital of Philadelphia, Philadelphia, PA.

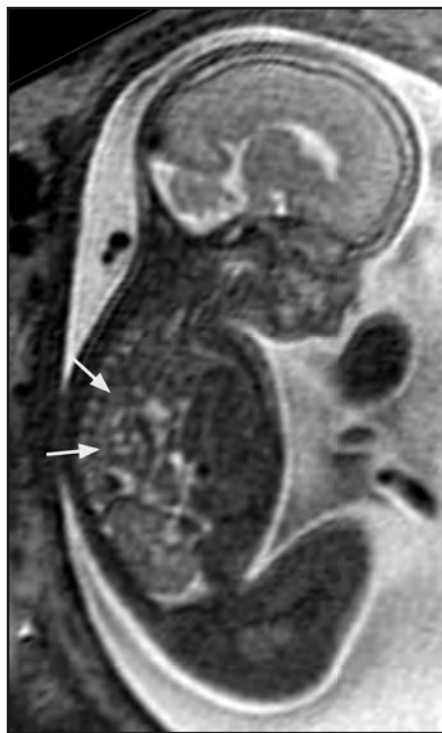
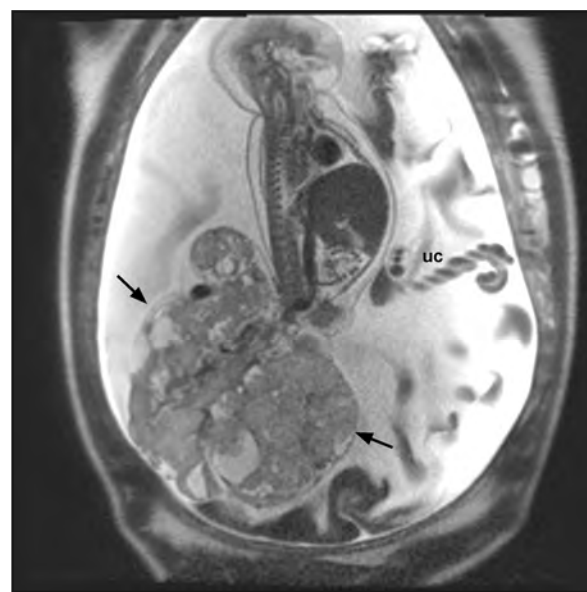


Figure 17. Sacral Teratoma (arrows). Umbilical cord (uc). Image provided courtesy of Teresa Victoria M.D., Ph.D., Children's Hospital of Philadelphia, Philadelphia, PA



- Is MRI appropriate to address the clinical question?
- Can MRI be delayed until after delivery?
- Is obstetrical intervention prior to scanning a possibility?
- Is termination of pregnancy a consideration?
- Is early delivery a consideration?
- Is the use of an MRI contrast agent essential to diagnosis and treatment?

PREGNANT HEALTHCARE WORKERS IN THE MRI ENVIRONMENT

Pregnant healthcare workers may need to perform duties in the scanner room during the performance of an MRI examination. Generally, there is little or no exposure to the time-varying and RF electromagnetic fields associated with MRI. The main exposure of the pregnant healthcare worker is to the powerful static magnetic field, with time and distance from the magnet being the major variations. For example, a pregnant MRI technologist might be within a static magnetic field of several hundred gauss or higher during each working day for prolonged periods of time. Although Kanal, et al. (42) reported that there is no increase in adverse outcomes of pregnancies in MRI workers, it may be reasonable to limit the amount of time spent by the pregnant worker within the MR system room. Thus, the pregnant physician or nurse anesthetist probably would be advised against monitoring the patient from within the scanner room or inside of the bore of the MR system during image acquisition. Particularly with field strengths of 3-Tesla or greater, MRI healthcare workers may experience vertigo-like sensations (144), especially when passing rapidly through spatial gradient magnetic fields near the magnet. While no evidence for injury has been demonstrated, it is reasonable to minimize such activities during pregnancy in consideration of taking a cautious approach to such situations.

Therefore, a policy is recommended that permits a pregnant MRI technologist and other healthcare worker to perform MRI, as well as to enter the MR system room, and attend to the patient, regardless of the trimester of the pregnancy. Importantly, MRI technologists and healthcare workers should not remain within the bore of the scanner during its operation. This later recommendation is especially important for those healthcare workers involved in patient management or interventional MRI procedures, since it may be necessary for them to be directly exposed to the scanner's electromagnetic fields at levels similar to those used for patients. These recommendations are not based on indications of adverse effects, but rather, from a conservative point of view and the fact that there are insufficient data pertaining to the effects of the other electromagnetic fields of the MR system to support or allow unnecessary exposures (13, 42).

SUMMARY AND CONCLUSIONS

MRI examinations should not be withheld from pregnant patients with the following conditions (145):

- With active brain or spine signs and symptoms requiring diagnostic imaging.
- With cancer requiring diagnostic imaging.

326 MRI Procedures and Pregnancy

- With chest, abdomen, and pelvic signs and symptoms of active disease when sonography is non-diagnostic.
- In specific cases of suspected fetal anomaly, MRI may be helpful.

With regard to pregnant healthcare workers working in the MRI environment, especially the MR system room:

- These individuals have not been shown to be at increased risk of adverse outcomes from occupational exposures to static magnetic fields.
- The time in the scanner room should be minimized.

REFERENCES

- Williams PM, Fletcher S. Health effects of prenatal radiation exposure. *Am Fam Physician* 2010;82:488–493.
- Patel SJ, Reede DL, Katz DS, Subramaniam R, Amorosa JK. Imaging the pregnant patient for nonobstetric conditions: Algorithms and radiation dose considerations. *RadioGraphics* 2007;27:1705–1722.
- McCollough CH, Schueler BA, Atwell TD, et al. Radiation exposure and pregnancy: When should we be concerned? *RadioGraphics* 2007;27:909–917.
- American College of Radiology. ACR practice guideline for imaging pregnant or potentially pregnant adolescents and women with ionizing radiation. Reston, VA: American College of Radiology, 2008.
- Kanal E, Shellock FG, Sonnenblick D. MRI clinical site safety: Phase I results and preliminary data. *Magn Reson Imaging* 1988;1:106.
- De Wilde JP, Rivers AW, Price DL. A review of the current use of magnetic resonance imaging in pregnancy and safety implications for the fetus. *Prog Biophys Mol Biol* 2005;87:335–353.
- Kwan ML, Miglioretti DL, Marlow EC, et al. Trends in medical imaging during pregnancy in the United States and Ontario, Canada, 1996 to 2016. *JAMA Network Open*. 2019;2:e197249.
- United States, Food and Drug Administration. Guidelines for Evaluating Electromagnetic Exposure Risk Trials of Clinical NMR Systems. Rockville, MD, Bureau of Radiological Health 1982.
- Shellock FG, Kanal E. Policies, guidelines, and recommendations for MR imaging safety and patient management. *J Magn Reson Imaging* 1991;1:97–101.
- Shellock FG, Kanal E. Magnetic Resonance Procedures and Pregnancy. In: *Magnetic Resonance Bioeffects, Safety, and Patient Management*, Second Edition. Philadelphia, New York: Lippincott-Raven; 1996. Chapter 4.
- Kanal E, Borgstede JP, Barkovich JA, et al. American College of Radiology white paper on MR safety. *Amer J of Roentgenol* 2002;178:1335–1347.
- Kanal E, Barkovich JA, Bell C, et al. ACR guidance document for safe MR practices: 2007. *Amer J of Roentgenol* 2007;188:1447–1474.
- Kanal E, Barkovich AJ, Bell C, et al. ACR guidance document on MR safe practices: 2013. *J Magn Reson Imaging* 2013;37:501–530.
- American College of Radiology. ACR manual on contrast media. Version 10.3. Reston (VA): ACR; 2017. Available at: <https://www.acr.org/~media/37D84428BF1D4E1B9A3A2918DA9E27A3.pdf>. Retrieved September 16, 2019.
- Murbach M, Neufeld E, Samaras T, et al. Pregnant women models analyzed for RF exposure and temperature increase in 3T RF shimmed birdcages. *Magn Reson Med* 2017;77:2048–2056.

MRI Bioeffects, Safety, and Patient Management 327

16. Schaefer DJ. Safety aspects of radiofrequency power deposition in magnetic resonance. *MRI Clin N Am* 1998;6:775-789.
17. Hand JW, Li Y, Thomas EL, Rutherford MA, Hajnal JV. Numerical study of RF exposure and the resulting temperature rise in the foetus during a magnetic resonance procedure. *Phys Med Biol* 2010;55:913-930.
18. Nagaoka T, Togashi T, Saito K, et al. An anatomically realistic whole-body pregnant-woman model and specific absorption rates for pregnant-woman exposure to electromagnetic plane waves from 10 MHz to 2 GHz. *Phys Med Biol* 2007;52:6731-6745.
19. Dimbylow PJ, Nagaoka T, Xu XG. A comparison of foetal SAR in three sets of pregnant female models. *Phys Med Biol* 2009;54:2755-2767.
20. Hand JW, Li Y, Hajnal JV. Numerical study of RF exposure and the resulting temperature rise in the foetus during a magnetic resonance procedure. *Phys Med Biol* 2010;55:913-930.
21. Elder JE. Special senses. In: Elder JE, Cahill DP, Editors. *Biological effects of radio-frequency radiation*, 2nd Edition. US EPA, 1984. pp. 64-78.
22. Kikuchi S, Saito K, Takahashi M, Ito K. Temperature elevation in the fetus from electromagnetic exposure during magnetic resonance imaging. *Phys Med Biol* 2010;55:2411-2426.
23. Wilcox A, Weinberg C, O'Connor J, et al. Incidence of early loss of pregnancy. *New Engl J Med* 1988;319:189-194.
24. McRobbie D, Foster MA. Pulsed magnetic field exposure during pregnancy and implications for NMR foetal imaging: A study with mice. *Magn Reson Imaging* 1985;3:231-234.
25. Tesky GC, Ossenkopp KP, Prato FS, Sestini E. Survivability and long-term stress reactivity levels following repeated exposure to nuclear magnetic resonance imaging procedures in rats. *Physiol Chem Phys Med NMR* 1987;19:43-49.
26. Heinrichs WL, Fong P, Flannery M, et al. Midgestational exposure of pregnant BALB/c mice to magnetic resonance imaging conditions. *Magn Reson Imaging* 1988;6:305-313.
27. Kay HH, Herfkens RJ, Kay BK. Effect of magnetic resonance imaging on *Xenopus laevis* embryogenesis. *Magn Reson Imaging* 1988;6:501-506.
28. Tyndall DA. MRI effects on the teratogenicity of x-irradiation in the C57BL/6J mouse. *Magn Reson Imaging* 1990;8:423-433.
29. Murakami J, Torii Y, Masuda K. Fetal development of mice following intrauterine exposure to a static magnetic field of 6.3T. *Magn Reson Imaging* 1992;10:433-437.
30. Malko JA, Constatinidis I, Dillehay D, et al. Search for influence of 1.5T magnetic field on growth of yeast cells. *Bioelectromagnetics* 1987;15:495-501.
31. Yip YP, Capriotti C, Talagala SL, Yip JW. Effects of MR exposure at 1.5 T on early embryonic development of the chick. *J Magn Reson Imaging* 1994;4:742-748.
32. Yip YP, Capriotti C, Yip JW. Effects of MR exposure on axonal outgrowth in the sympathetic nervous system of the chick. *J Magn Reson Imaging* 1995;4:457-462.
33. Tablado L, Soler C, Nunez M, et al. Development of mouse testis and epididymis following intrauterine exposure to a static magnetic field. *Bioelectromagnetics* 2000;21:19-24.
34. Ruckhäberle E, Nekolla SG, Ganter C, et al. *In vivo* intrauterine sound pressure and temperature measurements during magnetic resonance imaging (1.5 T) in pregnant ewes. *Fetal Diagn Ther* 2008;24:203-210.
35. Tyndall RJ, Sulik KK. Effects of magnetic resonance imaging on eye development in the C57BL/6J mouse. *Teratology* 1991;43:263-275.
36. Tyndall DA. MRI effects on craniofacial size and crown-rump length in C57BL/6J mice in 1.5T fields. *Oral Surg Oral Med Oral Pathol* 1993;76:655-660.
37. Yip YP, Capriotti C, Norbush SG, Talagala SL, Yip JW. Effects of MR exposure on cell proliferation and migration of chick motor neurons. *J Magn Reson Imaging* 1994;4:799-804.

328 MRI Procedures and Pregnancy

38. Carnes KI, Magin RL. Effects of in utero exposure to 4.7T MR imaging conditions on fetal growth and testicular development in the mouse. *Magn Reson Imaging* 1996;14:263-274.
39. Nara VR, Howell RW, Goddu SM, et al. Effects of a 1.5T static magnetic field on spermatogenesis and embryogenesis in mice. *Invest Radiol* 1996;31:586-590.
40. Lee JW, Kim MS, Kim YJ, et al. Genotoxic effects of 3 T magnetic resonance imaging in cultured human lymphocytes. *Bioelectromagnetics* 2011;32:535-542.
41. Johnson IR, Stehling MK, Blamire A, et al. Study of the internal structure of the human fetus in utero by echo-planar magnetic resonance imaging. *Am J Obstet Gynecol* 1990;163:601-607.
42. Kanal E, Gillen J, Evans JA, et al. Survey of reproductive health among female MR workers. *Radiology* 1993;187:395-399.
43. Baker PN, Johnson IR, Harvey PR, et al. A three-year follow-up of children imaged in utero with echo-planar magnetic resonance. *Am J Obstet Gynecol* 1994;170:32-33.
44. Myers C, Duncan KR, Gowland PA, et al. Failure to detect intrauterine growth restriction following in utero exposure to MRI. *Br J Radiol* 1998;71:549-551.
45. Vadeyar SH, Moore RJ, Strachan BK, et al. Effect of fetal magnetic resonance imaging on fetal heart rate patterns. *Am J Obstet Gynecol* 2000;182:666-669.
46. Kok RD, de Vries MM, Heerschap A, van den Berg PP. Absence of harmful effects of magnetic resonance exposure at 1.5 T in utero during the third trimester of pregnancy: A follow-up study. *Magn Reson Imaging* 2004;22:851-854.
47. Reeves MJ, Brandreth M, Whitby EH, et al. Neonatal cochlear function: measurement after exposure to acoustic noise during in utero MR imaging. *Radiology* 2010;257:802-809.
48. Bouyssi-Kobar M, du Plessis AJ, Robertson RL, Limperopoulos C. Fetal magnetic resonance imaging: Exposure times and functional outcomes at preschool age. *Pediatr Radiol* 2015;45:1823-1830.
49. Strizek B, Jani JC, Mucyo E, et al. Safety of MR imaging at 1.5 T in fetuses: A retrospective case-control study of birth weights and the effects of acoustic noise. *Radiology* 2015;275:530-537.
50. Jaimes C, Delgado J, Cunnane MB, et al. Does 3-T fetal MRI induce adverse acoustic effects in the neonate? A preliminary study comparing postnatal auditory test performance of fetuses scanned at 1.5 and 3 T. *Pediatr Radiol* 2019;49:37-45.
51. Chartier AL, Bouvier MJ, McPherson DR, et al. The safety of maternal and fetal MRI at 3T. *AJR Am J Roentgenol* 2019;213:1-4.
52. Bird ST, Gelperin K, Sahin L, et al. First-trimester exposure to Gadolinium-based contrast agents: A utilization study of 4.6 million U.S. pregnancies. *Radiology* 2019;293:193-200.
53. Syme MR, Paxton JW, Keelan JA. Drug transfer and metabolism by the human placenta. *Clin Pharmacokinet* 2004;43:487-514.
54. Pacifici GM, Nottoli R. Placental transfer of drugs administered to the mother. *Clin Pharmacokinet* 1995;28:235-269.
55. Ni Z, Mao Q. ATP-binding cassette efflux transporters in human placenta. *Curr Pharm Biotechnol* 2011;12:674-685.
56. Magnevist package insert: http://labeling.bayerhealthcare.com/html/products/pi/MagnevistPBP_PI.pdf
57. MultiHance package insert: http://www.multihanceusa.com/Shared%20Documents/MultiHance_Combined_PI.pdf
58. OmniScan package insert: <http://www.fda.gov/downloads/AdvisoryCommittees/CommitteesMeetingMaterials/Drugs/DrugSafetyandRiskManagementAdvisoryCommittee/UCM192009.pdf>
59. OptiMARK package insert: <http://www.mallinckrodt.com/webforms/threecolumn.aspx?id=497&view=faq>
60. ProHance package insert: http://www.multihanceusa.com/Shared%20Documents/ProHance_Combined_PI.pdf
61. Gadovist package insert: <http://www.bayerresources.com.au/resources/uploads/PI/file9345.pdf>

MRI Bioeffects, Safety, and Patient Management 329

62. Dotarem package insert: <http://www.medicines.org.au/files/aspdotar.pdf>
63. ABLAVAR package insert: [http://www.ablavavar.com/docs/PI_ABLAVAR_US_515952-0211_\(8.5x11\)_v6_11Apr11.pdf](http://www.ablavavar.com/docs/PI_ABLAVAR_US_515952-0211_(8.5x11)_v6_11Apr11.pdf)
64. EOVIST package insert: http://labeling.bayerhealthcare.com/html/products/pi/Eovist_PI.pdf
65. Teslascan package insert: <http://md.gehealthcare.com/shared/pdfs/pi/teslascan.pdf>
66. Feridex IV package insert: <http://www.drugs.com/pro/feridex.html>
67. Salomon LJ, Siauve N, Balvay D, et al. Placental perfusion MR imaging with contrast agents in a mouse model. *Radiology* 2005;235:73–80.
68. Taillieu F, Salomon LJ, Siauve N, et al. Placental perfusion and permeability: simultaneous assessment with dual-echo contrast-enhanced MR imaging in mice. *Radiology* 2006;241:737–745.
69. Marcos HB, Semelka RC, Worawattanakul S. Normal placenta: gadolinium-enhanced dynamic MR imaging. *Radiology* 1997;205:493–496.
70. Tanaka YO, Sohda S, Shigemitsu S, Niitsu M, Itai Y. High temporal resolution dynamic contrast MRI in a high risk group for placenta accreta. *Magn Reson Imaging* 2001;19:635–642.
71. Novak Z, Thurmond AS, Ross PL, Jones MK, Thornburg KL, Katzberg RW. Gadolinium-DTPA transplacental transfer and distribution in fetal tissue in rabbits. *Invest Radiol* 1993;28:828–830.
72. Muhler MR, Clément O, Salomon LJ, et al. Maternofetal pharmacokinetics of a gadolinium chelate contrast agent in mice. *Radiology* 2011;258:455–460.
73. Weinmann HJ, Brasch RC, Press WR, Wesbey GE. Characteristics of gadolinium-DTPA complex: a potential NMR contrast agent. *AJR Am J Roentgenol* 1984;142:619–624.
74. Okazaki O, Murayama N, Masubuchi N, Nomura H, Hakusui H. Placental transfer and milk secretion of gadodiamide injection in rats. *Arzneimittelforschung* 1996;46:83–86.
75. Hylton NM. Suspension of breast-feeding following gadopentetate dimeglumine administration. *Radiology* 2000;216:325–326.
76. Junkermann H. Indications and contraindications for contrast-enhanced MRI and CT during pregnancy. *Radiology* 2007;47:774–777.
77. Garcia-Bournissen F, Shrim A, Koren G. Safety of gadolinium during pregnancy. *Can Fam Physician* 2006;52:309–310.
78. Webb JA, Thomsen HS, Morcos SK, et al. The use of iodinated and gadolinium contrast media during pregnancy and lactation. *Eur Radiol* 2005;15:1234–1240.
79. Ray JG, Vermeulen MJ, Bharatha A, et al. Association between MRI exposure during pregnancy and fetal and childhood outcomes. *JAMA* 2016;316:952–961.
80. Colletti PM, Sylvestre PB. Magnetic resonance imaging in pregnancy. *MRI Clin N Am* 1994;2: 291–307.
81. Semere LG, McElrath TF, Klein AM. Neuroimaging in pregnancy: A review of clinical indications and obstetric outcomes. *J Matern Fetal Neonatal Med* 2013;26:1371–1379.
82. Wilbur AC, Langer BG, Spigos DG. Diagnosis of sacroiliac joint infection in pregnancy by magnetic resonance imaging. *Magn Reson Imaging* 1988;6:341–343.
83. Ain DL, Narula J, Sengupta PP. Cardiovascular imaging and diagnostic procedures in pregnancy. *Cardiol Clin* 2012;30:331–341.
84. Colletti PM, Lee KH, Elkayam U. Cardiovascular imaging of the pregnant patient. *AJR Am J Roentgenol* 2013;200:1–7.
85. Birchard KR, Brown MA, Hyslop WB, et al. MRI of acute abdominal and pelvic pain in pregnant patients. *AJR Am J Roentgenol* 2005;184:452–458.
86. Pedrosa I, Levine D, Eyvazzadeh AD, et al. MR imaging evaluation of acute appendicitis in pregnancy. *Radiology* 2006;238:891–899.

330 MRI Procedures and Pregnancy

87. Oto A. MR imaging evaluation of acute abdominal pain during pregnancy. *Magn Reson Imaging Clin N Am* 2006;14:489-501.
88. Singh A, Danrad R, Hahn PF, Blake MA, et al. MR imaging of the acute abdomen and pelvis: Acute appendicitis and beyond. *Radiographics* 2007;27:1419-1431.
89. Oto A, Ernst RD, Ghulmiyyah LM, Nishino TK, et al. MR imaging in the triage of pregnant patients with acute abdominal and pelvic pain. *Abdom Imaging* 2009;34:243-250.
90. Singh AK, Desai H, Novelline RA. Emergency MRI of acute pelvic pain: MR protocol with no oral contrast. *Emerg Radio*. 2009;16:133-141.
91. Masselli G, Brunelli R, Casciani E, et al. Acute abdominal and pelvic pain in pregnancy: MR imaging as a valuable adjunct to ultrasound? *Abdom Imaging* 2011;36:596-603.
92. Long SS, Long C, Lai H, Macura KJ. Imaging strategies for right lower quadrant pain in pregnancy. *AJR Am J Roentgenol* 2011;196:4-12.
93. Baron KT, Arleo EK, Robinson C, Sanelli PC. Comparing the diagnostic performance of MRI versus CT in the evaluation of acute nontraumatic abdominal pain during pregnancy. *Emerg Radiol* 2012;19:519-25.
94. Weinreb JC, Brown CE, Lowe TW, et al. Pelvic masses in pregnant patients: MR and US imaging. *Radiology* 1986;159:717-724.
95. McCarthy SM, Stark DD, Filly RA, et al. Uterine neoplasms: MR imaging. *Radiology* 1989;170:125-128.
96. Stark DD, McCarthy SM, Filly RA, et al. Pelvimetry by magnetic resonance imaging. *AJR Am J Roentgenol* 1985;144:947-950.
97. Michel SC, Rake A, Götzmann L, et al. Pelvimetry and patient acceptability compared between open 0.5-T and closed 1.5-T MR systems. *Eur Radiol* 2002;12:2898-2905.
98. Angtuaco TL, Shah HR, Mattison DR, et al. MR imaging in high-risk obstetric patients: A valuable complement to US. *Radiographics* 1992;12:91-109.
99. Benson RC, Colletti PM, Platt LD, et al. MR imaging of fetal anomalies. *AJR Am J Roentgenol* 1991;156:1205-1207.
100. Brown CEL, Weinreb JC. Magnetic resonance imaging appearance of growth retardation in a twin pregnancy. *Obstet Gynecol* 1988;71:987.
101. Carswell H. Fast MRI of fetus yields considerable anatomic detail. *Diag Imaging* 1988;11:12.
102. Catizone FA, Gesmundo G, Montemagno R, et al. The non-invasive methods of prenatal diagnosis: the role of ultrasound and MRI. *J Perinat Med* 1991;19:42-49.
103. Colletti PM, Platt LD. When to use MRI in obstetrics. *Diag Imaging* 1989;11:84-88.
104. De Clyn K, Degryse H, Slanger T, et al. MRI in the prenatal diagnosis of bilateral renal agenesis. *Fortschr Rontgenstr Ger* 1989;150:104-105.
105. Deans HE, Smith FW, Lloyd DJ, et al. Fetal fat measurement by magnetic resonance imaging. *Br J Radiol* 1989;62:603-607.
106. Dinh DH, Wright RM, Hanigan WC. The use of magnetic resonance imaging for the diagnosis of fetal intracranial anomalies. *Child Nerv Syst* 1990;6:212-215.
107. Dunn RS, Weiner SN. Antenatal diagnosis of sacrococcygeal teratoma facilitated by combined use of Doppler sonography and MR imaging. *AJR* 1991;156:1115-1116.
108. Fitamorris-Glass R, Mattrey RF, Cantrell CJ. Magnetic resonance imaging as an adjunct to ultrasound in oligohydramnios. *J Ultrasound Med* 1989;8:159-162.
109. Fraser R. Magnetic resonance imaging of the fetus: Initial experience [letter]. *Gynecol Obstet Invest* 1990;29:255-258.
110. Gardens AS, Weindling AM, Griffiths RD, et al. Fast-scan magnetic resonance imagin of fetal anomalies. *Br J Obstet Gynecol* 1991;98:1217-1222.

MRI Bioeffects, Safety, and Patient Management 331

111. Hill MC, Lande IM, Larsen JW Jr. Prenatal diagnosis of fetal anomalies using ultrasound and MRI. *Radiol Clin North Am* 1988;26:287-307.
112. Horvath L, Seeds JW. Temporary arrest of fetal movement with pancuronium bromide to enable antenatal magnetic resonance imagin of holosencephaly. *AJR Am J Roentgenol* 1989;6:418-420.
113. Lenke RR, Persutte WH, Nemes JM. Use of pancuronium bromide to inhibit fetal movement during magnetic resonance imaging. *J Reprod Med* 1989;34:315-317.
114. Mansfield P, Stehling MK, Ordidge RJ, et al. Study of internal structure of the human fetus in utero at 0.5T. *Br J Radiol* 1990;13:314-318.
115. Mattison DR, Angtuaco T, Miller FC, et al. Magnetic resonance imaging in maternal and fetal medicine. *J Perinatol* 1989;9:411-419.
116. Mattison DR, Angtuaco T. Magnetic resonance imaging in pernatal diagnosis. *Clin Obstet Gynecol* 1988;31:353-389.
117. Mattison DR, Kay HH, Miller RK, et al. Magnetic resonance imaging: A noninvasive tool for fetal and placental physiology. *Biol Reprod* 1988;38:39-49.
118. McCarthy SM, Filly RA, Stark DD, et al. Magnetic resonance imaging of fetal anomalies in utero: Early experience. *AJR Am J Roentgenol* 1985;145:677-682.
119. McCarthy SM, Filly RA, Stark DD, et al. Obstetrical magnetic resonance imaging: Fetal anatomy. *Radiology* 1985;154:427-432.
120. Powell MC, Worthington BS, Buckley JM, et al. Magnetic resonance imaging (MRI) in obstetrics II. Fetal anatomy. *Br J Obstet Gynaecol* 1988;95:38-46.
121. Smith FW. Magnetic resonance tomography of the pelvis. *Cardiovasc Intervent Radiol* 1986;8:367-376.
122. Smith FW, Kent C, Abramovich DR, et al. Nuclear magnetic resonance imaging – A new look at the fetus. *Br J Gynaecol* 1985;92:1024-1033.
123. Smith FW, Sutherland HW. Magnetic resonance imaging: The use of the inversion recovery sequence to display fetal morphology. *Br J Radiol* 1988;61:338-341.
124. Stehling MK, Mansfield P, Ordidge RJ, et al. Echoplanar magnetic resonance imaging in abnormal pregnancies. *Lancet* 1989;157. 1989;2(8655):157.
125. Toma P, Lucigrai G, Dodero P, et al. Prenatal detection of an abdominal mass by MR imaging performed while the fetus is immobilized with pancuronium bromide. *AJR Am J Roentgenol* 1990;154:1049-1050.
126. Toma P, Lucigrai G, Ravegnai M, et al. Hydrocephalus and porencephaly: Prenatal diagnosis by ultrasonography and MR imaging. *JCAT* 1990;14:843-845.
127. Turner RJ, Hankins GVD, Weinreb JC, et al. Magnetic resonance imaging and ultrasonography in antenatal evaluation of cojoined twins. *Am J Obstet Gynecol* 1986;77:529-532.
128. Vila-Coro AA, Dominguez R. Intrauterine diagnosis of hydroencephaly by magnetic resonance imaging. *Magn Reson Imaging* 1989;7:105-107.
129. Weinreb JC, Lowe T, Cohen JM, et al. Human fetal anatomy: MR imaging. *Radiology* 1985;157:715-720.
130. Weinreb JC, Lowe T, Santos-Ramos R, et al. Magnetic resonance imaging in obstetric diagnosis. *Radiology* 1985;154:157-161.
131. Wenstrom KD, Williamson RA, Weiner CP, et al. Magnetic resonance imaging of fetuses with intracranial defects. *Obstet Gynecol* 1991;77:529-532.
132. Williamson RA, Weiner CP, Yuh WTC, et al. Magnetic resonance imaging of anomalous fetuses. *Obstet Gynecol* 1988;71:952-956.
133. Levine D, Hatabu H, Gan J, et al. Fetal anatomy revealed with fast MR sequences. *AJR Am J Roentgenol* 1996;167:905-908.
134. Garden AS, Griffiths RD, Weindling AM, et al. Fast-scan magnetic resonance imaging in fetal visualization. *Am J Obstet Gynecol* 1991;164:1190-1196.

332 MRI Procedures and Pregnancy

135. Amin RS, Nikolaids P, Kawashima A, et al. Normal anatomy of the fetus at MR imaging. *Radiographics* 1999;19:S201-214.
136. Huppert BJ, Brandt KR, Ramin KD, et al. Single-shot fast spin-echo MR imaging of the fetus: a pictorial essay. *Radiographics* 1999;19:S215-227.
137. Levine D, Barnes PD, Sher S, et al. Fetal fast MR imaging: reproducibility, technical quality, and conspicuity of anatomy. *Radiology* 1998;206:549-554.
138. Levine D, Barnes PD, Edelman RR. Obstetric MR imaging. *Radiology* 1999;211:609-617.
139. Yanashita Y, Namimoto T, Abe Y, et al. MR imaging of the fetus by HASTE sequence. *AJR Am J Roentgenol* 1997;168:513-519.
140. Colletti PM. Computer-assisted imaging of the fetus with magnetic resonance imaging. *Comput Med Imaging Graph* 1996;20:491-496.
141. Levine D. Obstetric MRI. *J Magn Reson Imaging* 2006;24:1-15.
142. Tsuchiya K, Katase S, Seki T, et al. Short communication: MR imaging of fetal brain abnormalities using HASTE sequence. *Br J Radiol* 1996;69:668-670.
143. Leithner K, Pornbacher S, Assem-Hilger E, et al. Psychological reactions in women undergoing fetal magnetic resonance imaging. *Obstet Gynecol* 2008;111:396-402.
144. Glover PM, Cavin I, Qian W, Bowtell R, Gowland PA. Magnetic-field-induced vertigo: a theoretical and experimental investigation. *Bioelectromagnetics* 2007;28:349-361.
145. Mervak BM, Altun E, McGinty KA, Hyslop WB, Semelka RC, Burke LM. MRI in pregnancy: Indications and practical considerations. *J Magn Reson Imaging* 2019;49:621-631.

Chapter 12 Identification and Management of Acute Reactions to Gadolinium-Based Contrast Agents

ALBERTO SPINAZZI, M.D.

Chief Medical and Regulatory Officer
Bracco Group
Monroe, NJ

INTRODUCTION

Gadolinium-based contrast agents (GBCAs) have been used in clinical practice since the 1980s. Over the years, nine GBCAs have been approved for intravenous or intra-articular use in various countries throughout the world: Ablavar (gadofosveset), Dotarem (gadoterate meglumine), Eovist/Primovist (gadoxetate disodium), Gadavist/Gadovist (gadobutrol), Magnevist (gadopentetate dimeglumine), MultiHance (gadobenate dimeglumine), ProHance (gadoteridol), Omnipaque (gadodiamide), and OptiMARK (gadoversetamide).

“Adverse reactions” are defined by all regulatory authorities as noxious and unintended responses to a medicinal product (1). The phrase “responses to a medicinal product” means that a causal relationship between exposure to a medicinal product and an untoward medical occurrence is at least a reasonable possibility. All medicinal products can produce an adverse reaction in someone who has been exposed to them. GBCAs, though generally safe and well tolerated, are no exception: adverse reactions can occur after their administration, particularly in patients with underlying risk factors.

“Acute adverse reactions” to GBCAs are defined as undesirable side effects that occur within the first 60 minutes after administration of a GBCA (2). According to the approved prescribing information of the GBCAs that are currently commercially available in the United States (U.S.), the most frequent acute reactions to these imaging agents are headache, nausea with or without vomiting, injection site reactions, dizziness, localized rash, and pruritus (incidence rate, 1 to 5%) (3-7). Importantly, reactions like coldness, warmth, or pain at the injection site or headache probably depend on the physicochemical characteristics of the GBCAs, while all other types of immediate reactions fall into the category of hypersensitivity reactions and are either allergic or pseudoallergic (allergy-like) in nature (8, 9).

334 Acute Reactions to Gadolinium-Based Contrast Agents

These latter two reactions are clinically indistinguishable due to their symptomatic similarities. However, they vastly differ mechanistically. Allergy-like reactions lack immunological specificity and do not require previous exposure to the triggering antigen to elicit a response (10). Conversely, allergic reactions are characterized by immunological specificity and transferability. In cases of an allergic reaction, the patient's immune system is able to recognize and mount an immune response against an antigen, particularly due to subsequent exposures to the same antigen (10). Allergy-like reactions are not associated with immunological specificity but with direct release of histamine and other mediators from activated mast cells and circulating basophils and eosinophils, activation of the contact and complement systems, conversion of L-arginine into nitric oxide, and activation of the XII clotting system leading to the production of bradykinin (11). Current clinical evidence shows that most acute reactions to GBCAs are allergy-like in nature (8). However, cases of true allergic reactions to GBCAs have been reported (9, 12-14).

The severity of immediate GBCA reactions can range from non-serious and mild in intensity (i.e., transient and self-resolving symptoms), to life-threatening events, as shown in **Table 1**. Most acute reactions to GBCAs are mild, self-limiting, and do not require specific treatment. However, serious immediate reactions, such as anaphylactic or anaphylactic-like

Table 1. Type and severity of acute adverse reactions to gadolinium-based contrast agents (adapted from Reference 15).

Mild (self-limited, nonprogressive)

- Altered taste
- Pallor, flushing, warmth, chills, sweats
- Scattered and/or transient urticaria/Itching
- Cough
- Nasal congestion, rhinorrhea, sneezing, conjunctivitis
- Headache, dizziness
- Mild and transient nausea/vomiting
- Mild and transient hypertension or hypotension
- Short-lasting and self-limited vasovagal reaction
- Mild and limited tachycardia/bradycardia

Moderate (requires medical treatment, may progress if untreated)

- Protracted nausea/vomiting
- Diffuse urticaria/itching
- Diffuse erythema, stable vital signs
- Bronchospasm, dyspnea
- Facial/laryngeal edema without dyspnea
- Moderate and protracted tachycardia
- Hypertension/hypotension/vasovagal reaction that requires and responds to treatment
- Isolated chest pain, no electrocardiographic changes

Severe (life-threatening, may result in inpatient hospitalization, prolongation of hospitalization, permanent morbidity or death)

- Hypotensive shock
- Respiratory arrest
- Cardiac arrest
- Vasovagal reaction resistant to treatment
- Convulsions/seizures
- Unresponsiveness
- Severe or rapidly progressing laryngeal edema with stridor and/or hypoxia
- Severe bronchospasm with significant hypoxia
- Diffuse erythema with hypotension
- Hypertensive emergency
- Clinically manifested arrhythmias

events, may rarely occur (less than 1 in every 10,000 administered doses) (15-25). Serious adverse reactions may result in patient hospitalizations, prolongation of hospitalization, permanent morbidity, or even have a fatal outcome, especially if they are not promptly recognized and properly managed (15, 26).

This chapter aims to provide information on the following: (1) how to identify patients who may be at risk for developing serious acute reactions; (2) how to properly assess the risks and benefits of using GBCAs in individual patients; (3) the preventative measures that should be adopted; (4) when and how to promptly recognize the type of acute reaction; and (5) the treatments that are recommended for patients experiencing serious adverse reactions. These recommendations are based on guidance documents developed and published by leading scientific societies (2, 15, 27).

WHAT TO DO BEFORE THE EXAM

To prevent or minimize the risk of complications following administration of GBCAs, the following five steps should be adhered to before any contrast-enhanced magnetic resonance imaging (MRI) exam: (1) be aware of possible complications; (2) know your patient; (3) assess risk/benefit of GBCA administration; (4) adopt preventative measures, if and when necessary; and (5) be prepared to manage any adverse reaction.

(1) Be Aware of Possible Complications

Before proceeding with a contrast-enhanced MRI exam, all personnel should be familiar with all of the possible risk factors and be knowledgeable about the entire spectrum of adverse events that may occur after the administration of the GBCA to be used. This can be achieved by carefully reading the prescribing information, being fluent with the relevant literature and, if needed, requesting specific safety information from the manufacturer. Documentation of continuing medical education of all involved healthcare professionals related to the use of GBCAs should be maintained.

Also, healthcare professionals should be aware of the potential for acute reactions to drugs administered concomitantly for the sake of the MRI procedure, such as drugs used to reduce anxiety, to sedate the patient, for analgesia or anesthesia, antihistamines, or pharmacologic stressors.

(2) Know Your Patient

Risk factors associated with the development of immediate hypersensitivity reactions to GBCAs are well known. However, the occurrence of acute adverse reactions is substantially unpredictable, and allergic or allergy-like acute reactions, including serious ones, are frequently observed in the absence of risk factors.

Patients at risk for developing acute reactions include those who have experienced prior reactions to a GBCA (2, 15, 20, 27, 28). These patients are eight times more likely to experience subsequent reactions, the severity of which may be greater than that of previous reactions (29). Patients with underlying asthma or allergic diathesis, including hypersensitivity to food, chemicals, or other medications, are also considered to be at increased risk. Al-

336 Acute Reactions to Gadolinium-Based Contrast Agents

though there is no cross-reactivity, patients with known hypersensitivity to other types of medical imaging agents (e.g., radiocontrast iodinated agents) should be considered at higher risk for the development of hypersensitivity reactions to GBCAs (2, 15, 20, 28).

Patients receiving treatment with beta-adrenergic blockers have been reported to be at increased risk for experiencing hypersensitivity reactions to iodinated agents due to an increase in the release of mediators involved in anaphylaxis (30). Importantly, in the event that a severe hypersensitivity reaction occurs, beta-blocking agents may decrease the cardiovascular compensatory changes to the anaphylactic shock, and epinephrine (adrenaline) may be ineffective or promote paradoxical reflex vagotonic effects when used to resolve the reaction (31-34).

Therefore, before administering a GBCA, the healthcare professionals responsible for the procedure should be aware of the patient's pre-existing conditions, including the main known or suspected diseases and any potential co-morbidities, identify any possible risk factors, and ensure all medications the patient is taking have been identified. It is recommended to use a questionnaire to in order to ensure possible risk factors are identified and to best assess the risk of GBCA use in individual patients. Finally, attention should be also given to the emotional state of patients. Anxiety may cause panic attacks with symptoms that may mimic hypersensitivity reactions. Also, under high stress situations, vasovagal reactions may occur as well and it may be difficult to distinguish them from real hypersensitivity reactions. Severe acute reactions to GBCAs can be mitigated at least in part by having a calm, relaxing atmosphere, and experienced personnel familiar with the GBCAs being utilized and able to reduce anxiety (28).

(3) Assess Risk-Benefit of GBCA Administration

Patient risk versus potential benefit of the GBCA-enhanced MRI examination should be evaluated and possibly documented on an individual basis by the referring physician and the radiologist for each patient. The radiologist should also consider the risk-benefit ratio of imaging alternatives. If a GBCA-enhanced exam is based on a valid clinical indication, patients should be properly informed about its risks and benefits and provided written informed consent.

(4) Adopt Preventative Measures, If And When Necessary

There are no widely accepted policies for dealing with patients who have experienced prior reactions to GBCAs and the need for subsequent exposure to the same or other GBCAs. However, even in the absence of supportive evidence, it is suggested that in the case of a patient who experiences an acute reaction to a GBCA and requires a future contrast-enhanced MRI, every effort should be made to determine if a GBCA is absolutely necessary, and if so, identify the specific GBCA that elicited the initial reaction so that a different agent may be selected for use (2, 15, 27).

Premedication with corticosteroids and antihistamines is recommended for patients with a history of previous hypersensitivity reactions to GBCAs, allergies or known hypersensitivity to drugs or chemicals (2, 15). Two premedication regimens (**Table 2**) have been recommended (15, 35, 36), of which the adults dosing regimens are summarized as follows:

MRI Bioeffects, Safety, and Patient Management 337

- a) Prednisone-based: 50-mg prednisone by mouth at 13 hours, seven hours, and one hour before GBCA administration, plus 50-mg diphenhydramine intravenously, intramuscularly, or by mouth one hour before GBCA administration, or
- b) Methylprednisolone-based: 32-mg methylprednisolone by mouth 12 hours and two hours before GBCA administration; 50-mg diphenhydramine may be added as in the prednisone-based option.

It is important to note that such regimens may reduce the frequency or severity of reactions but are not always effective as breakthrough reactions, including life-threatening

Table 2. Suitable premedication regimens (adapted from Reference 15).

Regimen	Drug and Timing	Adult Dose	Pediatric Dose
Option 1	Prednisone given at 13, 7, and 1 hour before GBCA, plus	50-mg PO	0.5 to 0.7-mg/kg PO (up to 50-mg)
	Diphenhydramine one hour before GBCA	50-mg PO	1.25-mg/kg PO (up to 50-mg)
Option 2	Methylprednisolone 12 and two hours before GBCA, plus	32-mg PO	N/A
	Diphenhydramine one hour before GBCA (optional)	50-mg PO	N/A

GBCA = gadolinium-based contrast agent; N/A = not applicable; PO = orally

Note: Suitable intravenous doses may be substituted for patients unable to take medication orally.

events, have been observed after GBCA administration in pre-medicated patients, and radiology teams must be prepared to treat breakthrough reactions when they occur (37-42).

Oral corticosteroids should be used with caution in patients with uncontrolled hypertension, diabetes, active tuberculosis, systemic fungal infections, active peptic ulcer, or diverticulitis. Antihistamines may cause drowsiness and should not be taken shortly before operating a vehicle. Some patients have experienced allergies to the individual medications used in premedication (15). Also, premedication may cause a delay in diagnosis imparted by the multi-hour duration of premedication, increase hospital length of stay, increase time to imaging exam, increase hospital-acquired infection risk, and increase costs compared to non-premedicated controls (43). The indirect harms of premedication likely overshadow the benefits of premedication in some vulnerable populations (15).

Pretreatment may create a false sense of security, so that healthcare providers may neglect appropriate measures to monitor patients and to treat adverse reactions. It is important to note that no premedication strategy is a substitute for preparedness to treat adverse reactions.

338 Acute Reactions to Gadolinium-Based Contrast Agents

(5) Be Prepared to Manage Any Adverse Reaction

Prerequisites to managing acute reactions include properly trained personnel and well-designed treatment plans. Personnel should be periodically and effectively trained to rapidly recognize and assess acute adverse reactions and take all the necessary steps to initiate appropriate treatment, with properly documented review sessions and assessments. Periodic training of onsite health care providers in cardiopulmonary resuscitation techniques, including basic life support or advanced cardiac life support, is recommended. Staff should be also aware of how to activate the emergency response system to elevate the level of care if needed in extreme cases. The contact phone number of the cardiopulmonary arrest emergency response team (i.e., the Code Blue team) should be clearly posted within or near any room in which a GBCA is to be injected.

All MRI facilities should have readily available, basic equipment and medications needed to assess and treat acute reactions. As shown in **Table 3**, this list includes but is not limited to equipment to assess a patient, such as stethoscope, blood pressure and pulse monitor, pulse oximeter, as well as medications and equipment needed to treat a patient, such as sterile saline for intravenous injection, epinephrine, atropine, diphenhydramine, beta-agonist inhalers, oxygen, intubation equipment, and a cardiac defibrillator (2, 15). MRI facilities should institute periodic monitoring programs to ensure functionality of equipment and confirm all medications are within expiration date limits (2, 15). The equipment to assess and treat acute reactions must be readily available and within or nearby any room in which a GBCA is to be injected. The number and distribution of carts designed to treat acute adverse reactions should be tailored to the size of the imaging facility.

Table 3. Equipment and medications supply list for patient examination room or emergency carts (adapted from references 2 and 15).

Equipment	Medications
Oxygen	Epinephrine 1:1,000 (1-mL for SC/IM injection) or IM auto-injector
Suction (wall-mounted or portable), tubing and catheters	Epinephrine 1:10,000 (10-mL preloaded syringe for IV injection)
Oral airways	Atropine
“Ambu”-type bag	Beta-agonist metered dose inhaler
Endotracheal tubes	Diphenhydramine
Stethoscope, sphygmomanometer, tourniquets, tongue depressor	Nitroglycerin
One-way mouth breather apparatus	Aspirin
IV fluids (normal saline or Ringer’s solution)	Anti-convulsive drugs
Tourniquets, syringes and needles of varying sizes	
Tracheostomy set, cut-down trays with sterile instruments	
On Emergency Cart or Immediately Available	
Defibrillator	Blood pressure/pulse monitor
Electrocardiogram	Pulse oximeter (optional)

IM = intramuscular; IV = intravenous; SC = subcutaneous

Finally, at-risk patients should be scheduled during daytime hours when more personnel are available to assist in the event of an adverse reaction, preferably at a hospital-based MRI facility, wherein a code team is readily available to help manage life-threatening reactions.

WHAT TO DO DURING THE MRI EXAM

(1) Monitor Patients During the Procedure

The vast majority of patients undergoing a contrast-enhanced MR exam do not experience any adverse event. However, even if rare, serious complications may occur. Therefore, it is imperative that practitioners monitor all patients receiving a GBCA closely during the procedure and remain in the immediate vicinity for at least 30 to 45 minutes following the contrast injection. If there is an increased risk of an adverse reaction, venous access should be left in place (8). Some patients are quick to report minor symptoms, while others may wait until symptoms are more severe before alerting health care personnel. Thus, patients should be instructed to call for help as soon as they experience any symptoms.

Patients with concomitant impaired vision or hearing, neurologic disease, psychiatric illness, such as depression, substance abuse, autism spectrum disorder, attention deficit hyperactivity disorder, or cognitive disorders, may have diminished awareness of hypersensitivity triggers and symptoms. At any age, concurrent use of central nervous system-active medications such as sedatives, hypnotics, antidepressants, and first generation sedating H1-antihistamines can interfere with the recognition of symptoms and with the patient's ability to describe symptoms.

Most severe reactions (94 to 100%) occur within 20 minutes of the GBCA injection; therefore, it is imperative that equipment and medications be immediately available, but positioned for use outside the MR system room (8). Patients requiring treatment should be quickly moved from the scanner room to a safe area away from the influence of the powerful static magnetic, using an MR Conditional transport stretcher or other suitable device so that none of the resuscitative equipment becomes a projectile hazard (15). Assessment of reaction severity is somewhat subjective and, thus, it is difficult to succinctly describe all possible degrees of reaction severity. Sound clinical judgment should be used to determine when and how aggressively an acute reaction should be treated (15).

Mild reactions are usually self-limiting and do not require treatment (2, 15). Patients who experience mild reactions should be monitored for at least 30 minutes after the first symptoms are reported and longer, if necessary, to ensure there is no progression to a more severe event (15).

Moderate reactions can be more pronounced and persistent, requiring specific treatment, and may progress if left untreated. Patients experiencing a moderate reaction should have their vital signs closely monitored to make certain that progression to a more serious event is avoided.

Severe reactions are rare but of utmost concern since they may be life-threatening. While they rarely occur, immediate recognition and treatment is necessary. In many cases,

340 Acute Reactions to Gadolinium-Based Contrast Agents

life-threatening events begin with mild signs and symptoms, and then rapidly evolve to a severe reaction. As a result, it is imperative that practitioners monitor all patients experiencing minor or moderate adverse reactions until their complete resolution.

(2) Prompt Recognition of the Type and Severity of Adverse Reactions

In the event of acute reactions, assessment of airway, breathing, circulation, and mentation are necessary before proceeding to management steps. The American College of Radiology (ACR) Manual on Contrast Media recommends that the following assessments be immediately made (15):

- (1) How does the patient look?
- (2) Can the patient speak?
- (3) How does the patient's voice sound?
- (4) How is the patient's breathing?
- (5) What is the patient's pulse strength and rate?
- (6) What is the patient's blood pressure?

The level of consciousness, appearance of the skin, quality of phonation, lung auscultation, blood pressure and heart rate assessment will allow the responding physician to quickly determine not only the severity of a reaction but also allow for the proper diagnosis of the reaction (15). Once the type and severity of a reaction have been identified, the appropriate treatment should be initiated. In cases of severe reactions, such as cardiopulmonary arrest, it may be necessary to seek additional assistance to obtain access to specialized life-support equipment and the expertise of appropriately trained personnel. The ACR and the European Society of Urogenital Radiology (ESUR) both publish guidelines for practitioners to use as references. These guidelines, summarized in **Table 4** and **Table 5**, include information concerning the latest approaches to treatment for various signs and symptoms of acute reactions (2, 15). Patients should be monitored continuously to facilitate prompt detection of any clinical changes or progression to more severe symptoms.

Distinguishing Vasovagal Episodes From Hypersensitivity Reactions. Distinguishing between vagal reactions and hypersensitivity reactions is critical since the approach to treatment is markedly different. Also known as neurally-mediated syncope, vasovagal reactions are characterized by abrupt peripheral vasodilation and hypotension, along with bradycardia. Patients can also experience pallor, nausea, vomiting, and loss of consciousness, but no cutaneous rash, bronchospasm, tachycardia, or angioedema are observed. The exact cause of vagal reactions is unknown, but triggers such as anxiety and fear are known to elicit the response (44, 45).

In anaphylactic or anaphylactic-like reactions, the most common areas affected include the skin (flushing, itching, urticaria, angioedema in 80 to 90% of cases), respiratory tract (throat itching and tightness, dysphonia, hoarseness, stridor, dry staccato cough, wheezing/bronchospasm in 70% of cases), gastrointestinal tract (abdominal pain, nausea, vomiting, diarrhea in 30 to 45% of cases), heart and vasculature (hypotension, tachycardia, bradycardia, cardiac arrest in 10 to 45% of cases), and central nervous system (altered mental status, dizziness, confusion, loss of consciousness in 10 to 15% of cases) (46).

Table 4. Management of acute reactions to gadolinium-based contrast agents in adult patients (adapted from references 2 and 15).**Nausea/Vomiting**

1. Transient: Supportive treatment.
2. Severe, protracted: Appropriate antiemetic drugs should be considered.

Urticaria

1. Discontinue injection if not completed.
2. No treatment necessary in most cases.
3. ACR guidelines:
 - Administer H₁-receptor blocker: Diphenhydramine PO/IM/IV 25 to 50-mg.
 - If severe or widely disseminated: Give α-agonist (arteriolar and venous constriction): epinephrine SC (1:1,000) 0.1- to 0.3-mL (0.1- to 0.3-mg) (if no cardiac contraindications).
4. ESUR guidelines:
 - Scattered, transient: Supportive treatment including observation.
 - Scattered, protracted: H₁-receptor blocker IM or IV should be considered.
 - Generalized: H₁-receptor blocker IM or IV. Consider epinephrine IM (1:1,000) 0.1- to 0.3-mL (0.1- to 0.3-mg). Repeat as needed.

Facial or Laryngeal Edema

1. Administer oxygen 6- to 10-L/min via mask
2. ACR guidelines:
 - Administer alpha-agonist (arteriolar and venous constriction): Epinephrine SC or IM (1:1,000) 0.1- to 0.3-mL (0.1- to 0.3-mg) or, especially if hypotension is evident, epinephrine (1:10,000) slowly IV – 3-mL (0.1- to 0.3-mg)
 - Repeat as needed to a maximum of 1-mg
 - If not responsive to therapy or if there is no obvious acute laryngeal edema, seek appropriate assistance (cardiopulmonary arrest response team).
3. ESUR guidelines (laryngeal edema):
 - Epinephrine IM (1:1,000) 0.5-mL (0.5-mg). Repeat as needed.

Bronchospasm

1. Administer O₂, 6 to 10-L/min via mask. Monitor: Electrocardiogram, O₂ saturation, and blood pressure.
2. Administer beta-agonist inhalers (bronchiolar dilators such as metaproterenol, terbutaline, or albuterol) two to three puffs; repeat as necessary. If unresponsive to inhalers, use SC, IM, or IV epinephrine.
3. ACR guidelines:
 - Administer epinephrine SC or IM (1:1,000) 0.1- to 0.3-mL (0.1- to 0.3-mg) or, especially if hypotension is evident, epinephrine (1:10,000) slowly IV, 1- to 3 mL (0.1- to 0.3-mg).
 - Repeat as needed to a maximum of 1-mg.
 - Call for assistance (cardiopulmonary arrest response team) if severe bronchospasm or if O₂ saturation <88% persists.
4. ESUR guidelines:
 - Normal blood pressure: Epinephrine IM (1:1,000) 0.1 to 0.3-mL (0.1- to 0.3-mg). Use smaller doses in patients with CAD or if elderly.
 - Decreased blood pressure: Epinephrine IM (1:1,000) 0.5-mL (0.5-mg).

Hypotension with Tachycardia

1. Legs elevated 60-degrees or more (preferred) or Trendelenburg position.
2. Monitor: Electrocardiogram, pulse oximeter, blood pressure.
3. Administer O₂, 6 to 10-L/min (via mask).
4. Rapid IV administration of large volumes of Ringer's lactate or normal saline.
5. ACR guidelines:

342 Acute Reactions to Gadolinium-Based Contrast Agents

- If poorly responsive: Epinephrine (1:10,000) slowly IV 1-mL (0.1-mg).
 - Repeat as needed to a maximum of 1-mg.
 - If still poorly responsive seek appropriate assistance (cardiopulmonary arrest response team).
6. ESUR guidelines (isolated hypotension):
- If unresponsive: Epinephrine IM (1:1,000) 0.5-mL (0.5-mg). Repeat as needed.

Hypotension with Bradycardia (Vagal Reaction)

1. Secure airway: give O₂, 6 to 10-L/min (via mask).
2. Monitor vital signs.
3. Legs elevated 60-degrees or more (preferred) or Trendelenburg position.
4. Secure IV access: Rapid IV administration of Ringer's lactate or normal saline.
5. Administer atropine 0.6 to 1-mg IV slowly if patient does not respond quickly to steps 2 to 4.
6. Repeat atropine up to a total dose of 0.04-mg/kg (2 to 3-mg) in adult.
7. Ensure complete resolution of hypotension and bradycardia prior to discharge.

Hypertension, severe

1. Administer O₂, 6 to 10-L/min via mask
2. Monitor: Electrocardiogram, pulse oximeter, blood pressure.
3. Administer nitroglycerine 0.4-mg tablet, sublingual (may repeat x 3); or, topical 2% ointment, apply 1-inch strip.
4. If no response, consider labetalol 20-mg IV, then 20 to 80-mg IV every 10 minutes up to 300-mg.
5. Transfer to intensive care unit or emergency department.
6. For pheochromocytoma: Phentolamine 5-mg IV (may use labetalol if phentolamine is not available)

Seizures or Convulsions

1. Administer O₂, 6 to 10-L/min via mask.
2. Consider diazepam 5-mg IV (or more, as appropriate) or midazolam 0.5 to 1-mg IV.
3. If longer effect needed, obtain consultation; consider phenytoin infusion 15 to 18-mg/kg at 50-mg/min.
4. Careful monitoring of vital signs required, particularly of pO₂ because of risk to respiratory depression with benzodiazepine administration.
5. Consider using cardiopulmonary arrest response team for intubation if needed.

Pulmonary Edema

1. Administer O₂, 6 to 10-L/min via mask.
2. Elevate torso.
3. Give diuretics: Furosemide 20 to 40-mg IV, slow push.
4. Consider giving morphine (1 to 3-mg IV).
5. Transfer to intensive care unit or emergency department.

Generalized Anaphylactoid Reaction

1. Call for resuscitation team.
2. Suction airway as needed.
3. Elevate legs if hypotensive.
4. Oxygen by mask, 6 to 10-L/min.
5. Epinephrine IM (1:1,000) 0.5 mL (0.5-mg). Repeat as needed.
6. Intravenous fluids (e.g., normal saline, Ringer's solution).
7. H₁-blocker, e.g., diphenhydramine 25 to 50-mg intravenously.

ACR = American College of Radiology; CAD = coronary artery disease; ESUR = European Society of Urogenital Radiology; IM = intramuscular; IV = intravenous; PO = orally; SC = subcutaneous

Table 5. Management of acute reactions to gadolinium-based contrast agents in pediatric patients (adapted from references 2 and 15).**Urticaria**

1. No treatment necessary in most cases.
2. For moderate itching, consider H₁-receptor blocker: Diphenhydramine PO/IM or slow IV 1 to 2-mg/kg, up to 50-mg.
3. ACR guidelines:
 - If severe or widely disseminated: consider α-agonist: epinephrine IV (1:10,000) 0.1-mL/kg slow push over 2 to 5 minutes, up to 3 mL.
4. ESUR guidelines:
 - Epinephrine IM (1:1,000):
 - 6 to 12 year old - 50% of adult dose.
 - <6 years of age - 25% of adult dose.
 - Repeat as needed.

Facial Edema

1. Secure airway and administer O₂, 6 to 10-L/min (via mask, face tent, or blow-by stream). Monitor: electrocardiogram, O₂ saturation, and blood pressure.
2. Administer α-agonist: Epinephrine IV (1:10,000) 0.1-mL/kg slow push over 2 to 5 minutes, up to 3-mL/dose. Repeat in 5 to 30 minutes as needed.
3. Consider H₁-receptor blocker: Diphenhydramine IM or slow IV push 1 to 2-mg/kg, up to 50-mg.
4. Note: If facial edema is mild and there is no reaction progression, observation alone may be appropriate
 - If not responsive to therapy, seek appropriate assistance (e.g., cardiopulmonary arrest response team).

Bronchospasm

1. Secure airway and administer oxygen 6 to 10-L/min (via mask, face tent, or blow-by stream). Monitor: electrocardiogram, O₂ saturation, and blood pressure.
2. Administer beta-agonist (bronchiolar dilator such as albuterol) 2 to 3 puffs from metered dose inhaler; repeat as necessary.
3. ACR guidelines:
 - If bronchospasm progresses, administer epinephrine (1:10,000) IV 0.1-mL/kg slow push over 2 to 5 minutes, up to 3-mL/dose. Repeat in 5 to 30 minutes as needed.
 - If not responsive to therapy, call for assistance (e.g., cardiopulmonary arrest response team) for severe bronchospasm or if O₂ saturation <88% persists.
4. ESUR guidelines:
 - Epinephrine IM (1:1,000) when patient has normal blood pressure:
 - 6 to 12 year old – 50% of adult dose.
 - <6 years of age – 25% of adult dose.
 - Repeat as needed.
 - Epinephrine IM (1:1,000) when patient has decreased blood pressure:
 - 6 to 12 year old – 0.3-mL (0.3-mg).
 - <6 years of age – 0.15-mL (0.15-mg).

Laryngeal Edema

1. Secure airway and administer oxygen 6 to 10-L/min (via mask, face tent, or blow-by stream). Monitor: electrocardiogram, O₂ saturation, and blood pressure.
2. ACR guidelines:
 - Administer epinephrine (1:10,000) IV 0.1-mL/kg slow push over 2 to 5 minutes, up to 3-mL/dose. Repeat in 5 to 30 minutes as needed.
 - If not promptly responsive to initial therapy, call for assistance (e.g., cardiopulmonary arrest response team).
3. ESUR guidelines:

344 Acute Reactions to Gadolinium-Based Contrast Agents

- Epinephrine IM (1:1,000):
 - 6 to 12 years old – 0.3-mL (0.3-mg).
 - <6 years of age – 0.15-mL (0.15-mg).

Pulmonary Edema

1. Secure airway and administer oxygen 6 to 10-L/min (via mask, face tent, or blow-by stream). Monitor: electrocardiogram, O₂ saturation, and blood pressure.
2. Administer diuretic: Furosemide IV 1 to 2-mg/kg
 - If not responsive to therapy, call for assistance (e.g., cardiopulmonary arrest response team).

Hypotension with Tachycardia (Anaphylactic Shock)

1. Secure airway and administer oxygen 6 to 10-L/min (via mask). Monitor: Electrocardiogram, O₂ saturation, and blood pressure.
2. Legs elevated 60-degrees or more (preferred) or Trendelenburg position.
3. Keep patient warm.
4. Give rapid infusion of IV or IO normal saline or Ringer's lactate.
5. ACR guidelines:
 - If severe, give α -agonist: Epinephrine IV (1:10,000) 0.1-mL/kg slow push over 2 to 5 minutes, up to 3-mL/dose. Repeat as needed 5 to 30 minutes as needed.
 - If not responsive to therapy, seek appropriate assistance (e.g., cardiopulmonary arrest response team).
6. ESUR guidelines (isolated hypotension):
 - Epinephrine IM (1:1,000):
 - 6 to 12 year old – 0.3-mL (0.3-mg).
 - <6 years of age – 0.15-mL (0.15-mg).

Hypotension with Bradycardia (Vagal Reaction)

1. Secure airway and give oxygen 6 to 10-L/min (via mask). Monitor: Electrocardiogram, O₂ saturation, and blood pressure.
2. Legs elevated 60-degrees or more (preferred) or Trendelenburg position.
3. Keep patient warm.
4. Rapid administration of IV or IO normal saline or Ringer's lactate. Caution should be used to avoid hypervolemia in children with myocardial dysfunction.
5. Administer atropine IV 0.02-mg/kg if patient does not respond quickly to steps 2 to 4. Minimum initial dose of 0.1-mg.
 - ACR guidelines: Maximum initial dose of 0.5-mg (infant/child), 1.0-mg (adolescent). May repeat every 3 to 5 minutes up to a maximum dose of 1.0-mg (infant/child), 2.0-mg (adolescent). If not responsive to therapy, seek appropriate assistance (e.g., cardiopulmonary arrest response team).
 - ESUR guidelines: Maximum dose of 0.6-mg. Repeat if necessary to 2-mg total.

Generalized Anaphylactoid Reaction

1. Call for resuscitation team.
2. Suction airway as needed.
3. Elevate legs if hypotensive.
4. Oxygen by mask, 6 to 10-L/min.
5. Epinephrine IM (1:1,000)
 - 6 to 12 year old - 0.3-mL (0.3-mg).
 - <6 years of age - 0.15-mL (0.15-mg).
6. Intravenous fluids (e.g., normal saline, Ringer's solution).
7. H₁-blocker, eg, diphenhydramine 25 to 50-mg intravenously.

ACR = American College of Radiology; ESUR = European Society of Urogenital Radiology; IM= intramuscular; IO = intraosseous; IV = intravenous; PO = orally

Distinguishing Anxiety or Panic Attacks From Hypersensitivity Reactions. An anxiety or panic attack can cause diagnostic confusion because a sense of impending doom, breathlessness, flushing, tachycardia, and gastrointestinal symptoms can occur in both anxiety/panic attacks and in hypersensitivity events. However, urticaria, angioedema, wheezing, and hypotension are unlikely to occur during an anxiety/panic attack (45, 46).

Be aware of possible difficulties in timely detection of hypersensitivity reactions. In patients with concomitant medical conditions, for example, asthma, chronic obstructive pulmonary disease, congestive heart failure, pulmonary embolism, or pre-existing myocardial infarction, signs and symptoms of these diseases can cause confusion in the differential diagnosis of anaphylactic or anaphylactic-type reactions (46).

(3) Timely and Appropriate Treatment of the Adverse Reaction

The vast majority of patients with moderate-to-severe reactions recover if they are treated quickly and appropriately.

Treatment of Vasovagal Reactions. The pathophysiology of vasovagal syncope is characterized by an activation of the parasympathetic nervous system triggering a rapid decrease in heartbeat (bradycardia), accompanied by an acute loss of sympathetic stimulation causing a reduction of vascular tone and drop of blood pressure (hypotension) (47). Vasovagal reactions are effectively treated by elevating the patient's legs, increasing intravascular fluid volume, and administering atropine to reverse bradycardia (2, 15).

Epinephrine is the treatment of choice for severe hypersensitivity reactions. Anaphylactic and anaphylactic-like reactions are rapid onset, multisystem, and potentially lethal events that develop very quickly as a result of mast cells and basophils systemically and abruptly releasing mediators of inflammation. Different from vagal reactions, anaphylactic and anaphylactic-like reactions are most effectively treated with rapid infusion of large volumes of fluids, along with epinephrine (2, 15, 48-50). If administered properly and promptly, epinephrine can prevent or reverse the life-threatening symptoms of anaphylactic shock. Patients are at risk for death in as little as five minutes following exposure to GBCAs. Epinephrine is life-saving because it is a mixed alpha-and beta-adrenergic receptor agonist with rapid onset of action (48, 49). The alpha-adrenergic vasoconstricting effect reverses vasodilation, thus alleviating hypotension and reducing erythema, urticaria, and angioedema (49-50). Beta-adrenergic receptor agonist activity acts to dilate bronchial airways, increase the force of myocardial muscle contraction (inotropy) and heart rate (chronotropy), which increases cardiac output, and attenuates the severity of histamine-induced symptoms via beta-2 receptors on mast cells (48-52). Fatality studies provide the most compelling evidence for prompt epinephrine injection (53-56).

While epinephrine is recommended as first-line therapy, antihistamines and corticosteroids can be considered as adjunctive therapies and may be tried after epinephrine is administered to help control cutaneous and cardiovascular manifestations such as itching, flushing, urticaria, angioedema, and nasal and eye symptoms, as well as to prevent secondary reactions. There is no evidence that either antihistamines or corticosteroids provide life-saving treatment (i.e., they do not prevent or relieve upper airway obstruction, hypotension, or shock) (49). Besides, antihistamines, such as diphenhydramine, have a significantly

346 Acute Reactions to Gadolinium-Based Contrast Agents

longer onset of action and longer time to peak activity compared with epinephrine (57). Similarly, corticosteroids have the potential to prevent recurrent or protracted episodes, but should not be used in place of, or prior to, epinephrine, as they are not helpful for acute symptoms (49). Of note, administering one or more second-line medications potentially delays prompt injection of epinephrine, the first-line treatment (58-60).

Issues Related to the Use of Epinephrine in the Management of Serious Hypersensitivity. Despite the knowledge that epinephrine can save lives, it may be underused by physicians, health care professionals, and even emergency medical services. Rates of epinephrine use in the emergency department (ED) as first-line treatment of anaphylaxis are generally low, even in patients who have been clearly diagnosed with anaphylaxis (60). In a small 2013 cross-sectional survey of emergency medical health professionals ($N = 207$) in EDs in the United States, only 42% of healthcare professionals reported using epinephrine for most anaphylactic episodes (61). In a retrospective study analyzing anaphylaxis-related International Classification of Diseases, Ninth Revision (ICD-9) codes in a large health maintenance organization from 2008 to 2012 ($N > 150,000$), epinephrine was only used in 16.2% of total anaphylaxis cases (62). In a study of pediatric patients treated in the emergency department for anaphylaxis, high proportions were inappropriately treated with antihistamines (92%) or corticosteroids (78%), while only 54% of patients in this study received epinephrine initially to treat the event (63).

No use, use of inadequate doses, or delayed use of epinephrine is associated with poor outcomes: fatality, encephalopathy because of hypoxia and/or ischemia, and protracted or biphasic reactions (that is, reactions lasting several hours or a second phase occurring an hour or more after the onset of the first phase, respectively) (60). A patient may still experience serious complications or die in the instance of using epinephrine that has passed its expiration date (48).

If a patient does not respond to timely and appropriate treatment with epinephrine, positioning on the back with the lower extremities elevated, supplemental oxygen, intravenous fluid resuscitation, and rapid transfer to the care of a team specialized in emergency medicine, critical care medicine, or anesthesiology is recommended (46). Even if it is critical for effectively resolving anaphylactic or anaphylactic-like reactions, the use of epinephrine is not devoid of risk and, therefore, caution should be exercised when using it.

Common side effects that occur at recommended doses of epinephrine via any route of administration include agitation, anxiety, tremulousness, headache, dizziness, pallor, or palpitations (48). Rarely, and usually associated with overdosage or overly rapid rate of intravenous infusion, epinephrine administration might contribute to or cause myocardial ischemia, pulmonary edema, prolonged ventricular repolarization and arrhythmias, accelerated hypertension, and intracranial hemorrhage in adults and children alike (48). Particularly vulnerable populations are those individuals at the extremes of age and those with hypertension, peripheral vascular disease, ischemic heart disease, or untreated hyperthyroidism (i.e., due to an increased number of beta-adrenergic receptors in the vasculature of these individuals, rendering the myocardium more sensitive to the beta-adrenergic effects of epinephrine) (48).

Concomitant use of beta-adrenergic blockers decreases the effectiveness of exogenously administered epinephrine. Angiotensin-converting enzyme inhibitors and possibly angiotensin II receptor blockers may interfere with intrinsic compensatory responses to hypotension. Tricyclic antidepressants and monoamine oxidase inhibitors may impede epinephrine metabolism and lead to increased plasma and tissue concentrations. Cocaine and amphetamines sensitize the myocardium to the effects of epinephrine, thus increasing the risk of toxicity (48).

WHAT TO DO AFTER THE MRI EXAM

If no adverse reaction occurred during the MRI exam, it is advisable to observe patients for 30 minutes after the GBCA administration and those at risk for hypersensitivity reactions may be kept under monitoring for a longer period of time (2, 15). Patients experiencing non-life-threatening hypersensitivity reactions may be observed for four to six hours after successful treatment and then discharged. Patients who experience serious acute reactions (with cardiovascular and/or severe respiratory symptoms) should be admitted or treated and observed for a longer time period in the ED or an observation area.

FINAL RECOMMENDATIONS

GBCAs are, in general, very safe. Serious adverse reactions to GBCAs are fortunately uncommon and fatal reactions are extremely rare. Proper patient evaluation and adequate prophylactic measures can prevent some of these complications. Knowledge, training, and preparation are crucial for appropriate and effective management of these events. Prompt recognition and treatment are invaluable in attenuating an adverse reaction of a patient to GBCAs, and may prevent a reaction from becoming severe or even life threatening.

REFERENCES

1. International Conference on Harmonisation of Technical Requirements for Registration of Pharmaceuticals for Human Use. ICH Harmonised Tripartite Guideline 2003. Post-Approval Safety Data Management: Definitions and Standards For Expedited Reporting E2D. Available at https://www.ich.org/fileadmin/Public_Web_Site/ICH_Products/Guidelines/Efficacy/E2D/Step4/E2D_Guideline.pdf. Accessed March, 2021.
2. European Society of Urogenital Radiology (ESUR). ESUR Guidelines on Contrast Media. Version 10.0. 2019: A1. Acute Adverse Reactions. Available at http://www.esur-cm.org/index.php/a-general-adverse-reactions-2#A_1_1. Accessed March, 2021.
3. Dotarem (gadoterate meglumine) Injection. U.S. Prescribing information. Available via https://www.accessdata.fda.gov/drugsatfda_docs/label/2018/204781s008lbl.pdf. Accessed March, 2021.
4. Eovist (gadoxetate disodium) Injection. U.S. Prescribing information. Available via http://labeling.bayer-healthcare.com/html/products/pi/Eovist_PI.pdf. Accessed March, 2021.
5. Gadavist (gadobutrol) Injection. U.S. Prescribing information. Available via http://labeling.bayerhealthcare.com/html/products/pi/gadavist_PI.pdf. Accessed March, 2021.
6. MultiHance (gadobenate dimeglumine) Injection. U.S. Prescribing Information. Available via https://imaging.bracco.com/sites/braccoimaging.com/files/technica_sheet_pdf/us-en-2019-01-16-spc-medication-guide-multihance.pdf. Accessed March, 2021.

348 Acute Reactions to Gadolinium-Based Contrast Agents

7. Omniscan (gadodiamide) Injection. U.S. Prescribing Information. Available via <https://www.gehealthcare.com/-/media/a3f25c3ec97642599ad91266a2364685.pdf?la=en-us>. Accessed March, 2021.
8. Thomsen HS. How to manage (treat) immediate-type adverse reactions to GBCA. *Top Magn Reson Imaging* 2016;25:269-274.
9. Carr TF. Pathophysiology of immediate reactions to injectable gadolinium-based contrast agents. *Top Magn Reson Imaging* 2016;25:265-268.
10. Joint Task Force on Practice Parameters; American Academy of Allergy, Asthma and Immunology. American College of Allergy, Asthma and Immunology. Joint Council of Allergy, Asthma and Immunology. Drug allergy: An updated practice parameter. *Ann Allergy Asthma Immunol* 2010;105:259-273.
11. Fok JS, Smith WB. Hypersensitivity reactions to gadolinium-based contrast agents. *Curr Opin Allergy Clin Immunol* 2017;17:241-246.
12. Schiavino D, Murzilli F, Del Ninno M, et al. Demonstration of an IgE-mediated immunological pathogenesis of a severe reaction to gadopentetate dimeglumine. *J Invest Allergol Clin Immunol* 2003;13:140-142.
13. Galera C, Pur Ozyigit L, Cavigioli S, Bousquet PJ, Demoly P. Gadoteridol-induced anaphylaxis: Not a class allergy. *Allergy* 2010;65:132-134.
14. Hasdenteufel F, Luyasu S, Renaudin JM, et al. Anaphylactic shock after first exposure to gadoterate meglumine: Two case reports documented by positive allergy assessment. *J Allergy Clin Immunol* 2008;121:527-528.
15. ACR Committee on Drugs and Contrast Media. In: ACR Manual on Contrast Media. American College of Radiology (2021). Available via https://www.acr.org/-/media/ACR/Files/Clinical-Resources/Contrast_Media.pdf. Accessed March, 2021.
16. Abujudeh HH, Kosaraju VK, Kaewlai R. Acute adverse reactions to gadopentetate dimeglumine and gadobenate dimeglumine: Experience with 21,659 injections. *AJR Am J Roentgentol* 2010;194:430-434.
17. Bruder O, Schneider S, Nothnagel D, et al. Acute adverse reactions to gadolinium-based contrast agents in CMR: Multicenter experience with 17,767 patients from the EuroCMR Registry. *JACC Cardiovasc Imaging* 2011;4:1171-1176.
18. Dillman JR, Ellis JH, Cohan RH, Strouse PJ, Jan SC. Frequency and severity of acute allergic-like reactions to gadolinium-containing i.v. contrast media in children and adults. *AJR Am J Roentgenol* 2007;189:1533-1538.
19. Hunt CH, Hartman RP, Hesley GK. Frequency and severity of adverse effects of iodinated and gadolinium contrast materials: Retrospective review of 456,930 doses. *AJR Am J Roentgenol* 2009;193:1124-1127.
20. Jung JW, Kang HR, Kim MH, et al. Immediate hypersensitivity reaction to gadolinium-based MR contrast media. *Radiology* 2012;264:414-422.
21. Li A, Wong CS, Wong MK, Lee CM, Au Yeung MC. Acute adverse reactions to magnetic resonance contrast media--gadolinium chelates. *Br J Radiol* 2006;79:368-371.
22. Murphy KP, Szopinski KT, Cohal RH, Mermilliod B, Ellis JH. Occurrence of adverse reactions to gadolinium-based contrast material and management of patients at increased risk: A survey of the American Society of Neuroradiology Fellowship Directors. *Acad Radiol* 1999;6:656-664.
23. Prince MR, Zhang H, Zou Z, Staron RB, Brill PW. Incidence of immediate gadolinium contrast media reactions. *AJR Am J Roentgenol* 2011;196:W138-143.
24. Behzadi AH, Zhao Y, Farooq Z, Prince MR. Immediate allergic reactions to gadolinium-based contrast agents: A systematic review and meta-analysis. *Radiology* 2018;286:471-482.
25. McDonald JS, Hunt CH, Kolbe AB, et al. Acute adverse events following gadolinium-based contrast agent administration: A single-center retrospective study of 281 945 injections. *Radiology* 2019;292:620-627.
26. Murphy KP, Szopinski KT, Cohal RH, Mermilliod B, Ellis JH. Occurrence of adverse reactions to gadolinium-based contrast material and management of patients at increased risk: A survey of the American Society of Neuroradiology Fellowship Directors. *Acad Radiol* 1999;6:656-664.

MRI Bioeffects, Safety, and Patient Management 349

27. Expert Panel on MR Safety, Kanal E, Barkovich AJ, et al. ACR guidance document on MR safe practices: 2013. *J Magn Reson Imaging* 2013;37:501-530.
28. Heshmatzadeh Behzadi A, Prince MR. Preventing allergic reactions to gadolinium-based contrast agents. *Top Magn Reson Imaging* 2016; 25:275-279.
29. Nelson KL, Gifford LM, Lauber-Huber C, Gross CA, Lasser TA. Clinical safety of gadopentetate dimeglumine. *Radiology* 1995;196:439-443.
30. Lang DM, Alpern MB, Visintainer PF, Smith ST. Elevated risk of anaphylactoid reaction from radiographic contrast media is associated with both beta-blocker exposure and cardiovascular disorders. *Arch Intern Med* 1993;153:2033-2040.
31. Javeed N, Javeed H, Javeed S, et al. Refractory anaphylactoid shock potentiated by beta-blockers. *Cathet Cardiovasc Diagn* 1996;39:383-384.
32. Lang DM. Anaphylactoid and anaphylactic reactions. Hazards of beta-blockers. *Drug Safety* 1995;12:299-304.
33. Lang DM, Alpern MB, Visintainer PF, Smith ST. Increased risk for anaphylactoid reaction from contrast media in patients on beta-adrenergic blockers or with asthma. *Ann Intern Med* 1991;115:270-276.
34. Greenberger PA, Meyers SN, Kramer BL, Kramer BL. Effects of beta-adrenergic and calcium antagonists on the development of anaphylactoid reactions from radiographic contrast media during cardiac angiography. *J Allergy Clin Immunol* 1987;80:698-702.
35. Lasser EC, Berry CC, Talner LB, et al. Pretreatment with corticosteroids to alleviate reactions to intravenous contrast material. *N Engl J Med* 1987;317:845-849.
36. Greenberger PA, Patterson R. The prevention of immediate generalized reactions to radiocontrast media in high-risk patients. *J Allergy Clin Immunol* 1991;87:867-872.
37. Dillman JR, Ellis JH, Cohan RH, Strouse PJ, Jan SC. Allergic-like breakthrough reactions to gadolinium contrast agents after corticosteroid and antihistamine premedication. *AJR Am J Roentgenol* 2008;190:187-190.
38. Jingu A, Fukuda J, Taketomi-Takahashi A, Tsushima Y. Breakthrough reactions of iodinated and gadolinium contrast media after oral steroid premedication protocol. *BMC Med Imaging* 2014;6:14-34.
39. Power S, Talbot N, Kucharczyk W, Mandell DM. Allergic-like reactions to the MR imaging contrast agent gadobutrol: A prospective study of 32,991 consecutive injections. *Radiology* 2016; 281:72-77.
40. Davenport MS, Cohan RH. The evidence for and against corticosteroid prophylaxis in at-risk patients. *Radiol Clin North Am* 2017;55:413-421.
41. Bhatti ZS, Mervak BM, Dillman JR, Davenport MS. Breakthrough reactions to gadobenate dimeglumine. *Invest Radiol* 2018;53:551-554.
42. Walker D, Chakraborty S, Schieda N. Single-center retrospective analysis of breakthrough allergic-like reactions to gadobutrol. *Invest Radiol* 2019;54:448-451.
43. Davenport MS, Mervak BM, Ellis JH, et al. Indirect cost and harm attributable to oral 13- hour inpatient corticosteroid prophylaxis before contrast-enhanced CT. *Radiology* 2016;279:492-501.
44. Bush WH, Swanson DP. Acute reactions to intravascular contrast media: Types, risk factors, recognition, and specific treatment. *AJR Am J Roentgenol* 1991;157:1153-1161.
45. Simons FE. Anaphylaxis. *J Allergy Clin Immunol* 2010;125:S161-S181. Erratum in: *J Allergy Clin Immunol* 2010;126:885.
46. Simons FE, World Allergy Organization. World Allergy Organization survey on global availability of essentials for the assessment and management of anaphylaxis by allergy-immunology specialists in health care settings. *Ann Allergy Asthma Immunol* 2010;104:405-412.
47. Aydin MA, Salukhe TV, Wilke I, Willems S. Management and therapy of vasovagal syncope: A review. *World J Cardiol* 2010;2:308-315.

350 Acute Reactions to Gadolinium-Based Contrast Agents

48. Kemp SF, Lockey RF, Simons FE, World Allergy Organization ad hoc Committee on Epinephrine in Anaphylaxis. Epinephrine: The drug of choice for anaphylaxis. A statement of the World Allergy Organization. *Allergy* 2008;63:1061-1070.
49. Wood PJ, Traub SJ, Lipinski C. Safety of epinephrine for anaphylaxis in the emergency setting. *World J Emerg Med* 2013;4:245-251.
50. McLean-Tooke AP, Bethune CA, et al. Adrenaline in the treatment of anaphylaxis: What is the evidence? *BMJ* 2003;327:1332-1335.
51. Masch WR, Wang CL, Davenport MS. Severe allergic-like contrast reactions: Epidemiology and appropriate treatment. *Abdom Radiol (NY)* 2016;41:1632-1639.
52. Kay LJ, Peachell PT. Mast cell beta₂-adrenoceptors. *Chem Immunol Allergy* 2005;87:145-153.
53. Bock SA, Munoz-Furlong A, Sampson HA. Further fatalities caused by anaphylactic reactions to food, 2001-2006. *J Allergy Clin Immunol* 2007;119:1016-1018.
54. Pumphrey RS, Gowland MH. Further fatal allergic reactions to food in the United Kingdom, 1999-2006. *J Allergy Clin Immunol* 2007;119:1018-1019.
55. Greenberger PA, Rotskoff BD, Lifschultz B. Fatal anaphylaxis: Postmortem findings and associated comorbid diseases. *Ann Allergy Asthma Immunol* 2007;98:252-257.
56. Pumphrey RS. Lessons for management of anaphylaxis from a study of fatal reactions. *Clin Exp Allergy* 2000;30:1144-1150.
57. Jones DH, Romero FA, Casale TB. Time-dependent inhibition of histamine-induced cutaneous responses by oral and intramuscular diphenhydramine and oral fexofenadine. *Ann Allergy Asthma Immunol* 2008;100:452-456.
58. Simons FE, World Allergy Organization. World Allergy Organization survey on global availability of essentials for the assessment and management of anaphylaxis by allergy-immunology specialists in health care settings. *Ann Allergy Asthma Immunol* 2010;104:405-412.
59. Simons KJ, Simons FE. Epinephrine and its use in anaphylaxis: Current issues. *Curr Opin Allergy Clin Immunol* 2010;10:354-361.
60. Greenberger PA, Wallace DV, Lieberman PL, Gregory SM. Contemporary issues in anaphylaxis and the evolution of epinephrine autoinjectors: What will the future bring? *Ann Allergy Asthma Immunol* 2017;119:333-338.
61. Russell WS, Farrar JR, Nowak R, et al. Evaluating the management of anaphylaxis in US emergency departments: Guidelines vs. practice. *World J Emerg Med* 2013;4:98-106.
62. Pourang D, Batech M, Sheikh J, Samant S, Kaplan M. Anaphylaxis in a health maintenance organization: International Classification of Diseases coding and epinephrine auto-injector prescribing. *Ann Allergy Asthma Immunol* 2017;118:186-190.
63. Russell S, Monroe K, Losek JD. Anaphylaxis management in the pediatric emergency department: opportunities for improvement. *Pediatr Emerg Care* 2010;26:71-76.

Chapter 13 MRI Contrast Agents and Nephrogenic Systemic Fibrosis

ALBERTO SPINAZZI, M.D.

Senior Vice President
Chief Medical and Regulatory Officer
Bracco Group
Monroe, NJ

INTRODUCTION

Nephrogenic systemic fibrosis (NSF) is a rare, systemic fibrosing disorder reminiscent, but distinct from scleroderma or scleromyxedema. Its most prominent and visible effects are observed in the skin, which led to the disease originally being named “nephrogenic fibrosing dermopathy”, or NFD (1). The first cases of NSF were identified in 1997 and the first published report of 14 cases appeared in 2000 (2). “Nephrogenic” does not mean that the disease is caused by factors originating in the kidney, but that NSF has been observed only in patients with acute or chronic severe renal insufficiency (estimated glomerular filtration rate, eGFR <30 mL/min/1.73 m²), end-stage renal disease, or with acute renal insufficiency of any severity due to hepatorenal syndrome or in the perioperative liver transplantation period. “Systemic Fibrosis” emphasizes the systemic nature of this fibrosing disorder. Along with thickening and hardening of the skin, it may involve nerves and skeletal muscles, and it has also been linked with myocardial, pericardial, and pleural fibrosis (2, 3, 4, 5).

In some patients, NSF may be fatal; however, the disease by itself is not a cause of death. Rather, NSF may contribute to death by restricting effective ventilation, or by restricting mobility to the point of causing an accidental fall that may lead to fractures and clotting complications (4).

Epidemiology

Two extensive, systematic literature reviews provided information on the epidemiology of NSF. The first systematic review was conducted in 2013 and focused on 815 distinct

352 MRI Contrast Agents and Nephrogenic Systemic Fibrosis

cases of NSF with clinical and/or histological confirmation of the condition reported in 200 articles in peer-reviewed literature from 2000 until December 2012 (6). These 200 papers were obtained by performing a literature search of the PubMed database using the following key words: “*nephrogenic systemic fibrosis*”, “*nephrogenic fibrosing dermopathy*”, “*scleromyxedema-like*”, and “*scleroderma and gadolinium*”. The second and more recent literature review was based on a search of the same database (PubMed) using the terms “*nephrogenic systemic fibrosis*,” “*nephrogenic fibrosing dermopathy*,” and “*NSF*” from January 2000 until February 2019 and was able to detect 639 distinct cases of NSF in 173 peer-reviewed articles (7). Differently from the previous systematic review, cases without histological confirmation were discarded. Cases from abstracts, letters-to-the-editor, or other correspondence were not included in either of the two systematic reviews if they lacked sufficient information, and duplicates were removed. In several cases, authors were contacted in order to obtain additional information or confirm information reported in the article.

Results of both systematic reviews showed that NSF affected males and females in approximately equal numbers and was identified in patients from a large variety of ethnic backgrounds and from North America, Europe, and Asia. The disease tends to affect middle-aged adults most commonly (6, 7). No cases of NSF were reported in neonates or toddlers; however, NSF has been confirmed in pediatric patients and elderly adults, with 6 years as the youngest age reported (6), and 87 years the oldest (6, 7).

In both reviews, almost all the cases of NSF were observed in patients with severe acute or chronic renal insufficiency (estimated glomerular filtration rate, eGFR below 30 mL/min/1.73 m²), with acute renal insufficiency due to hepatorenal syndrome, or in the perioperative liver transplantation period (6, 7). The vast majority of patients with NSF (>75%) were on dialysis (6, 7). The few reports of patients developing NSF with eGFR values greater than 29 mL/min/1.73 m² were actually cases of acute renal failure resulting in eGFR overestimation or errors in the proper estimation of GFR (6).

In summary, systematic reviews of published reports of NSF indicate that NSF is a rare disease that may occur in patients of either gender and any age or race with severe chronic or acute renal insufficiency or, mostly, end-stage renal disease.

Etiology

Despite considerable effort, no case of NSF could be identified before 1997 (8). This truly new disease entity should therefore have resulted from exposure of patients with advanced renal failure to one or more new exogenous agents—that is, a new medication, toxin, or infectious agent—or to new ways of using previously existing medications (9). The first suspect was high-dose erythropoietin (8-10) in the presence of co-factors such as hypercoagulable states, various forms of vascular injury, vascular surgical procedures, and liver failure (in particular, hepatorenal syndrome and liver transplantation) (11). Erythropoietin is the principal therapy for anemia in both dialysis and pre-dialysis patients. Its use and doses dramatically increased after the publication of the Dialysis Outcomes Quality Initiative guidelines for anemia management in 1997, i.e., in the same year that the first case of nephrogenic fibrosing dermopathy was reported.

In 2006 Grobner, et al. (12) reported 5 cases of NSF in patients previously exposed to high doses of a GBCA (OmniscanTM, active ingredient: gadodiamide) and suggested a possible association between exposure to GBCAs and the development of the condition in patients with severe impairment of renal function. Since that report, GBCAs have been the prime suspect, even though GBCAs had already been widely available for clinical use since the late 1980's, i.e., at least 10 years before the first cases of NSF were identified.

NSF cases have been observed weeks, months or even years after the administration of certain GBCAs (13). It has been suggested that cumulative lifetime GBCA exposure increases the risk of NSF (4). However, GBCA exposure and renal insufficiency cannot be the sole effectors of NSF. The vast majority of patients with end-stage renal disease on chronic dialysis do not acquire the disease, even following multiple exposures to the GBCAs that have been associated with the highest number of NSF cases. Also, cases of NSF have been reported in patients with no history of GBCA exposure (7, 14-16).

As for the pathogenesis of NSF, the working hypothesis is that Gd complexes may stay for weeks, months or even years within the skin and other tissues. In the skin of susceptible patients with advanced renal failure, the retained Gd complexes may potentially attract and/or activate circulating fibrocytes, bone marrow-derived cells that participate in normal wound healing and fibrosis. These activated fibroblasts are believed to underlie the aberrant fibrosis seen in NSF (4, 17). These cells are distinct from other fibrocytes in that they have a specific immunophenotype, i.e., the CD34-/ procollagen I dual positive profile (4, 18). Histology of the skin of patients with NSF reveals increased cellularity, with CD34- and procollagen I-expressing spindle cells, occasional histiocytes, and factor XIIIa+ dendritic cells. Higher levels of retained Gd have been observed in areas of increased cellularity (4, 17). As of today, however, the pathogenesis of NSF is largely unknown, as well as the role that GBCAs might play. (5, 18)

NSF cases occurring after the sole administration of one GBCA are defined as "single-agent" or "unconfounded." If a case of NSF follows the administration of two or more GBCAs, it is impossible to determine which agent is associated with the development of the disorder, and the case is reported as "multiple-agent" or "confounded" (4).

Almost all unconfounded NSF cases occurred after single or repeated exposure to three GBCAs: gadopentetate dimeglumine (Magnevist[®] and generic equivalents), gadoverse-tamide (OptiMark[®]), and gadodiamide (OmniscanTM) (18). No or very few unconfounded cases were reported following exposure to any of the other GBCAs, i.e., gadobenate dimeglumine (MultiHance[®]), gadobutrol (Gadovist[®]/Gadavist[®]), gadoterate meglumine (Dotarem and generic equivalents), gadoteridol (ProHance), gadoxetate disodium (Primovist/Eovist) (18).

Regulatory Authority intervention, culminating in 2009-2010 with the contraindication of these three GBCAs for use in patients with an eGFR <30 mL/min/1.73 m² due to chronic kidney disease or an acute deterioration of the renal function, dramatically reduced the risk of NSF. The estimated rate of NSF per million exposures up to 2008 (2.07; 95% confidence interval: 1.90, 2.26) fell significantly (p<0.001) to only 0.028 (95% confidence interval: 0.012, 0.060) after 2008. (5, 18)

354 MRI Contrast Agents and Nephrogenic Systemic Fibrosis

Of note, monitoring of NSF based on spontaneous reporting of adverse drug reactions and literature case reports may lead to underreporting of NSF cases. Missing or inconclusive information in spontaneously reported cases is also a limitation of NSF monitoring (19), as for some reports it may not be possible to confirm or exclude a diagnosis of NSF using the clinicopathological criteria developed by Girardi et al (20). On the other hand, clinical data from large-scale studies of individual GBCAs in high-risk patients, with prolonged and extensive follow-up and systematic collection of all the clinical and pathology information needed for a reliable, accurate diagnosis of NSF, may provide better, more precise information on NSF risk deriving from exposure to individual GBCAs, assuming the patient population is large enough to draw meaningful conclusions.

A recent systematic review and meta-analysis by Woolen et al (21) looked at 16 unique studies published between May 2008 and April 2019 that involved 4931 patients with stage 4 or 5 CKD (eGFR, <30 mL/min/1.73m²) and/or receiving dialysis who underwent MRI with one of four low-risk GBCAs (gadobenate dimeglumine, gadoterate meglumine, gadobutrol, gadoteridol). The outcome measure required for inclusion was assessment of unconfounded incidence of NSF. The pooled incidence of NSF across these 4931 patients was 0 (0%; upper boundary of 95% CI, 0.07%). The upper bounds of the 95% CIs varied on a study-specific basis owing to differences in study-specific eligible sample sizes. Nevertheless, the greatest safety margin (i.e., largest sample size) was for gadobenate dimeglumine (upper bound 95% CI, 0.12% [0 of 3167]), followed by gadoterate meglumine (0.31% [0 of 1204]) gadobutrol (1.11% [0 of 330]), and gadoteridol (1.59% [0 of 230]). Consistent with these findings, recent updates to the guidelines released by the American College of Radiology, ACR (3), the European Society of Urogenital Radiology (22), and the Canadian Association of Radiologists (23) support use of indicated low-risk GBCAs in patients with eGFR<30 mL/min/1.73m². These conclusions have been echoed in a consensus statement from the ACR and National Kidney Foundation (24). The findings reported by Woolen, et al. (21) have since been substantiated in a recent systematic review by Lunyera, et al (25). Recent results from a retrospective study also showed no cases of NSF following administration of gadoxetic acid (Primovist/Eovist) to 153 patients with severely impaired renal function (26).

Although the risk of NSF from administration of low-risk GBCAs in patients with severely impaired renal function is very low, likely less than 0.07%, it is important to note that there have been rare reports of clinically and histologically confirmed cases of NSF following exposure to these safer agents. Therefore, guidelines aimed at minimizing risk should nevertheless still be followed.

DIAGNOSIS

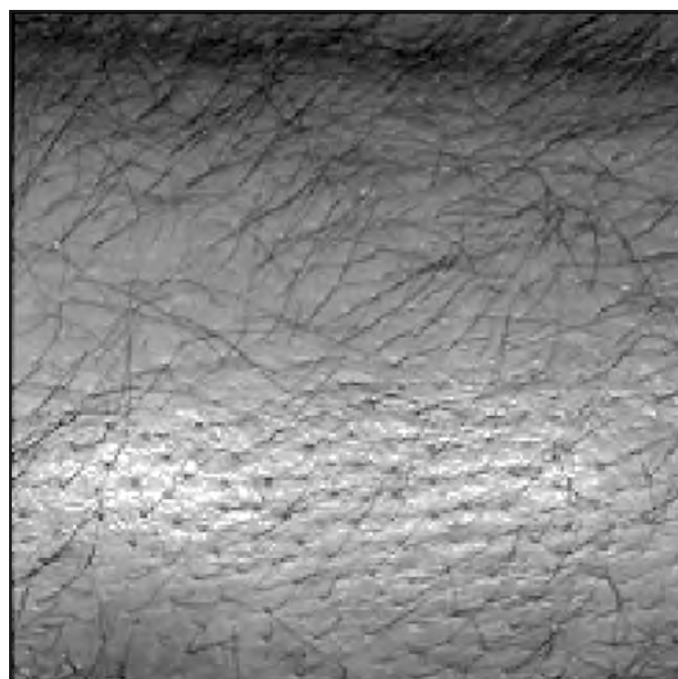
NSF is different from adverse events usually encountered by radiologists because it does not occur at the time of the imaging study. Instead, NSF typically occurs days to months later. Individually, the clinical and pathological features of NSF are not unique to that disease, so that no single test or other finding can be relied on to be 100% sensitive and specific for the diagnosis of NSF (20, 27). A confident diagnosis may be reached only through the combination of clinical history, a physical examination, and compelling histologic features of a biopsy specimen of involved skin (20, 27). A clinicopathological defini-

tion of NSF developed by a multidisciplinary team of highly experienced clinicians and dermatopathologists is the universally accepted reference to diagnose NSF (20). This definition relies upon a combination of clinical and pathological findings derived from the study of numerous patients, the relevant medical literature, and histological slides and data contained within the Yale NSF Registry to create a reproducible diagnostic and workup scheme for putative cases of NSF. As mentioned previously, to date, NSF has been observed only in patients either with acute or chronic renal insufficiency or, mostly end-stage renal disease. Therefore, the main elements that should guide physicians in the diagnostic process are clinical presentation and confirmatory cutaneous histopathologic findings in the setting of decreased or absent glomerular filtration, either acutely or chronically (4, 20, 27).

Physical Examination

The skin changes caused by NSF can mimic progressive systemic sclerosis with a predilection for extremity involvement that can extend to the torso (4, 14, 20, 21). Unlike scleroderma, NSF usually spares the face (4, 20, 27). Skin lesions typically begin with swelling, progressing to erythematous papules and coalescing violaceous to hyperpigmented, brawny plaques with follicular dimpling (*peau d'orange*) changes (Figure 1) (4, 20, 27, 28). Peripheral irregular fingerlike or ameboid projections may be present along with islands of sparing (Figure 2) (20, 28, 29). The involved skin and subcutis can become markedly thickened and hardened, unpinchable, with a wooden consistency to palpation (Figure 3) (4, 20, 26, 27). The indurations characteristically involve the distal extremities first, gradually proceeding to involve the proximal extremities to the level of the mid-thigh and mid upper arms where they may show a pattern of bumpiness ("cobblestoning") (Figure 4) (4, 20, 26, 27). Involvement of the skin and subcutaneous tissues overlying joints can cause a decrease in function of the hands and feet first and then of more proximal joints in

Figure 1. Affected areas showing follicular dimpling (*peau d'orange*) changes (major clinical criterion), usually present on the lower extremity above the knee, or upper extremity (1).



356 MRI Contrast Agents and Nephrogenic Systemic Fibrosis

Figure 2. Red to violaceous, thin, fixed plaques showing polygonal, reticular, or “amoeboid” morphologies (patterned plaques, major clinical criterion) (1).

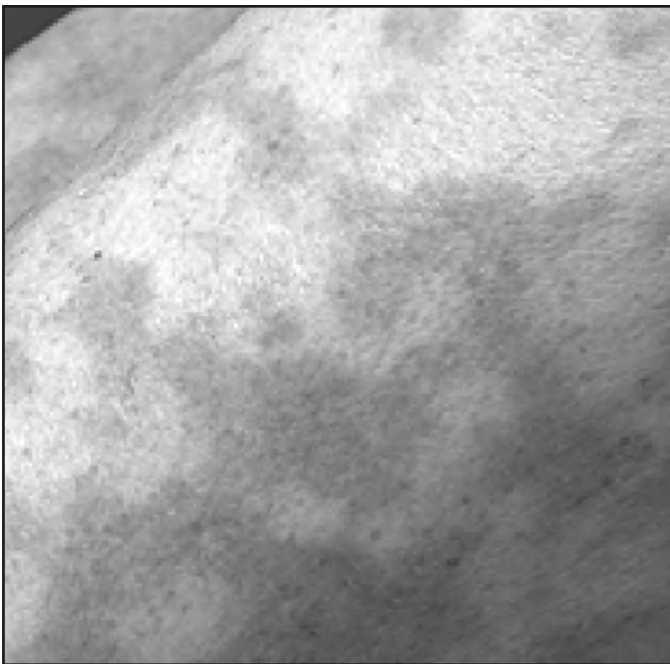


Figure 3. Unpinchable, firm, shiny, often hyperpigmented, bound-down skin over the extremities (marked induration, major clinical criterion) (1).

the affected extremities, often leaving patients wheelchair-dependent (4, 20, 26). Joint contractures may be accompanied by edema of the fingers, wrists, toes, and ankles (**Figure 5**). In **Table 1**, more (major) and less (minor) frequent clinical findings are listed (20).

Patients with NSF may complain of itching and sharp pain that may be localized in the affected areas, in the rib cage, or the hips. Loss of appetite, paresthesia, and muscle weakness are also described (4, 20, 26). If these symptoms and these or other skin lesions are observed

Figure 4. Bumpy, “pseudo-cellulite” pattern, formed by deep induration of the upper arms and/or thighs (“cobblestoning”, major clinical criterion) (1).

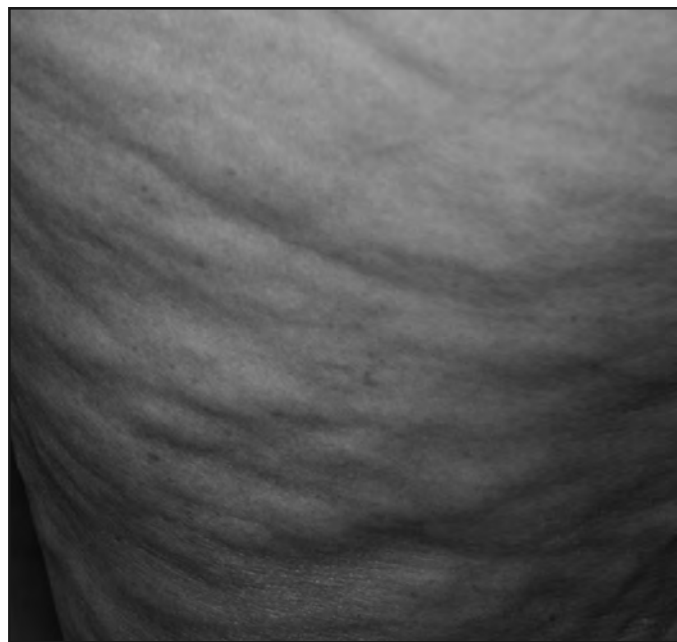


Figure 5. Edema of the fingers and wrists, with loss of range of motion of fingers and wrists (1).

in a patient with reduced renal function and history of exposure to one or more GBCAs, a full-body skin examination should be performed on the patient by a dermatologist or rheumatologist who is familiar, not only with the clinical findings of NSF, but also with those of the other conditions within the differential diagnosis (4, 20). Of note, some patients (estimated at < 5%) develop rapidly progressive, fulminant NSF associated with an accelerated loss of mobility and severe pain (4).

Histopathological Evaluation

If the signs and symptoms noted are observed in patients with severe renal insufficiency, a biopsy should be performed to obtain specimens of involved skin (20, 27, 28). A deep punch biopsy of at least 4-mm in size and extending to the subcutaneous fat may reveal

358 MRI Contrast Agents and Nephrogenic Systemic Fibrosis

Table 1. Clinical findings for the diagnosis of nephrogenic systemic fibrosis.

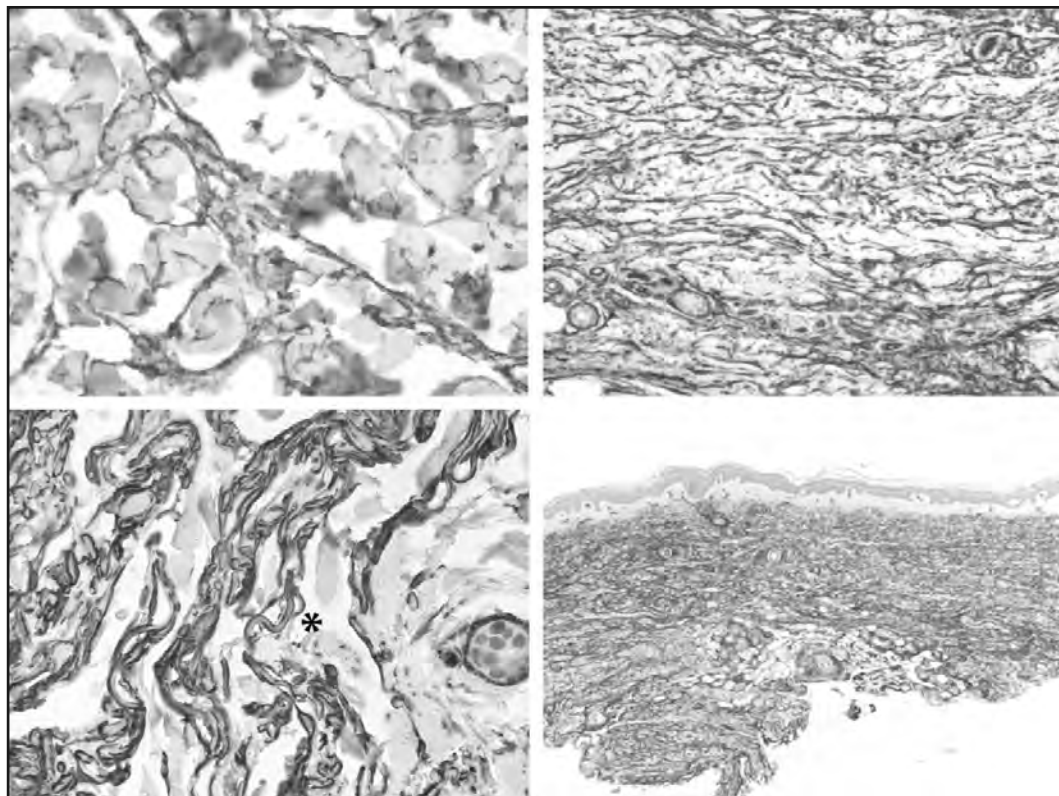
- Skin lesions
 - Lesion distribution: mostly upper and lower extremities with involvement of trunk in a minority of cases. Face is involved in approximately 3% of cases.
 - Lesion morphology: fixed plaques (polygonal, reticular, or amoeboid; red to violaceous to hyperpigmented); induration (unpinchable firm skin over the extremities with a wooden consistency to palpation and a pattern of bumpiness over the upper arms or thighs); papules, nodules, erythema, and swelling may be also present
- Major criteria for diagnosis
 - Patterned plaques
 - Joint contractures
 - “Cobblestoning”
 - Marked induration / Peau d’orange
- Minor criteria for diagnosis
 - Puckering/linear banding
 - Superficial plaque/patch
 - Dermal papules
 - Scleral plaques (age below 45 years old)

sufficient findings to make a more confident diagnosis in cases of superficial lesions. However, it is always better to obtain deeper biopsy specimens because the disease characteristically extends along fibrous septa into subcutaneous fat and fascia and sometimes into underlying skeletal muscle (20). For lesions of differing morphologies and/or locations, multiple cutaneous biopsy specimens are recommended (20). Histologically, NSF is characterized by dermal fibrosis and may be indistinguishable from scleromyxedema (20, 27, 28). Preserved elastic tissue is a finding that allows dermatopathologists to distinguish NSF from morphea and scleroderma (20). In NSF, there is always an increased number of fibrocytes that are CD34-positive and procollagen I-positive when stained immunohistochemically (**Figure 6**). This dual positivity is characteristic of so-called “circulating fibrocytes,” mesenchymal stem cells of bone marrow origin that participate in wound repair (29). Other features that, if present, help make a more confident diagnosis of NSF are: increased numbers of spindled and/or epithelioid cells (i.e., activated macrophages resembling epithelial cells) with few other inflammatory cells in the dermis; thin, especially in early lesions, and thick collagen bundles that generally maintain clefts of separation between their neighbors; involvement of subcutaneous septa which are markedly widened and collagenized as described above; osseous metaplasia, with foci of osteoid deposition, or calcified bone spicules around elastic fibers, which are considered a highly specific feature of NSF (20, 27, 28, 30).

Scoring and Reporting

The same multidisciplinary team of clinicians and dermatopathologists that completed the clinicopathological definition of NSF also proposed a schematic and scoring system to assess putative cases of NSF (20). However, those same NSF experts also warned healthcare professionals that accurate diagnosis of NSF requires judgment and interpretation, qualities that rely heavily on experience (20). If the signs and symptoms suggestive of NSF are observed in patients with severe renal insufficiency previously exposed to one or more GBCA,

Figure 6. CD34+ spindle or epithelioid cells in a reticular or parallel arrangement with “tram-tracking” (CD34+ dendritic processes on either side of elastic fibers *) (1).



a physical examination of those patients should be performed by experienced dermatologists or rheumatologists, and biopsy specimens should be examined by experienced dermatopathologists, bearing in mind that even experienced clinicians or pathologists may have personally examined only a limited number of patients with NSF (20).

HOW TO MINIMIZE THE RISK OF NSF

Because there is no consistently effective treatment for NSF, prevention is important. A prevention strategy implies sequential steps aimed at defining and identifying the population at risk in routine clinical practice, and at minimizing risk to that susceptible population.

Step 1. Identify Patients at Risk

Patients at risk of developing NSF are those with severe acute or chronic renal insufficiency (estimated glomerular filtration rate, eGFR below 30 mL/min/1.73 m²), with acute renal insufficiency due to hepatorenal syndrome, or in the perioperative liver transplantation period (6, 7).

360 MRI Contrast Agents and Nephrogenic Systemic Fibrosis

Many people with chronically impaired renal function do not feel any symptoms (31). The following factors and conditions are more frequently associated with chronic kidney disease and may warrant serum creatinine testing and calculation of the level of eGFR (3, 31-33):

- Age over 60;
- Family history of chronic kidney disease;
- Personal history of renal disease, including:
 - Glomerulonephritis,
 - Proteinuria,
 - Inherited diseases, such as polycystic kidney disease,
 - Recurrent urinary infections,
 - Kidney cancer,
 - Dialysis,
 - Kidney surgery,
 - Single kidney,
 - Renal transplant;
- Hypertension requiring medical therapy,
- History of diabetes mellitus, gout, and/or lupus and other autoimmune diseases; and
- History of recent exposure to nephrotoxic drugs (e.g., amphotericin B, cyclosporine, cisplatin, acyclovir, methotrexate, aminoglycoside antibiotics, iodinated contrast media, etc.).

The risk of NSF from administration of the safer GBCAs gadobenate dimeglumine, gadoteridol, gadobutrol, and gadoterate meglumine in patients with severely impaired renal function is very low, likely less than 0.07%. Therefore, the identification of patients at risk using a questionnaire or laboratory testing prior to exposure to these agents can be considered optional (3). On the contrary, it is highly recommended before intravenous administration of any other GBCA.

Clinical laboratories now routinely report eGFR based on filtration markers. The most common filtration marker used is creatinine, for which laboratory assays have been standardized since 2003 (33). The preferred estimating equation in the United States and much of the world is the CKD-EPI 2009 creatinine equation, which is more accurate than the earlier MDRD equation, particularly for eGFR values greater than 60 mL/min/1.73 m² (33). Anyway, neither equation is suitable if renal function is in an unstable condition, that is, in patients with acute renal failure or on dialysis. Results may also deviate from true values in patients with exceptional dietary intake (e.g., vegetarian diet, high protein diet, creatine supplements), extremes of body composition (e.g., very lean, obese, paraplegia), or severe liver disease. In view of this latter limitation, patients with hepatorenal syndrome and those with reduced renal function who have had or are awaiting liver transplantation should be considered at risk of NSF if they have any level of GFR below 60-mL/min/1.73 m².

In situations requiring additional accuracy and precision, cystatin C can be used with creatinine in the CKD-EPI 2012 creatinine-cystatin C equation (34). Adding cystatin C may be particularly useful for individuals with altered creatinine production and/or metabolism, e.g., extremely high or low body size or muscle mass, limb amputation, high-protein diet, use of creatinine supplements, or use of drugs affecting tubular secretion of creatinine) (35).

There is no evidence to guide the time interval within which eGFR should be obtained prior to GBCA injection to patients identified by screening to have one or more risk factor for compromised renal function. However, it is recommended to measure renal function within two to seven days before the date of the contrast-enhanced procedure.

A single normal eGFR measurement usually does not rule out acute renal insufficiency since there is a delay between a change in renal function and the corresponding change in serum creatinine (4). The patient's clinical condition should, therefore, also be assessed close to the time of the procedure and, if factors that could cause acute renal failure are detected, the renal function should be measured again before the GBCA is given (4). In practice all patients with suspected acute renal failure should be considered at risk of developing NSF, regardless of measured serum creatinine or calculated GFR values (4).

Step 2. Assess Risk–Benefit of Contrast-Enhanced MRI in Patients at Risk

A patient at risk of NSF should receive a GBCA only when no suitable diagnostic alternatives are available and a thorough risk–benefit assessment for that patient indicates that the benefit clearly outweighs the potential risk of NSF (3, 4, 22, 23). The risk–benefit evaluation should be made by the radiologist in conjunction with the referring physician and should be properly and prospectively documented. History of previous exposures to GBCAs, especially if recent, or if other factors that are thought to act as possible co-triggers of the disease, such as metabolic acidosis, vascular surgery, thrombotic events, and so on, should be taken into account during the risk–benefit assessment of each individual at-risk patient. Patients or parents or guardians (in the case of minors) should be properly informed of the benefits, risks, and diagnostic alternatives based on all the information available at that time and should provide their consent in writing (3, 4, 22, 23).

Step 3. Perform Any Unenhanced MRI Sequence That May be Helpful Before Injecting the MRI Contrast Agent

Even after the decision is made to perform a contrast-enhanced MR examination, and the patient has consented to receive a GBCA, the prescribing information for individual GBCAs all indicate that the use of GBCAs should be avoided unless the diagnostic information from the use of contrast is essential and not available with unenhanced MRI. Therefore, all unenhanced MRI pulse sequences that may help to make a diagnosis should be performed and the MR images should be evaluated by an experienced radiologist to ensure that the administration of a GBCA is still deemed necessary.

Step 4. Choice of the GBCA and Dose

To minimize risk of NSF development, no GBCA containing gadodiamide, gadoversetamide, or gadopentetate dimeglumine should ever be used in patients with severely impaired renal function. Any of the low-risk GBCAs (gadobenate dimeglumine, gadoxetate

362 MRI Contrast Agents and Nephrogenic Systemic Fibrosis

disodium, gadoteridol, gadobutrol, gadoterate meglumine) can be used instead when clinically indicated (3, 22, 23).

The recommendations for use in at-risk patients are to use the lowest dose of a low-risk GBCA required to obtain the needed clinical information and to not exceed the recommended single dose. Moreover, a sufficient period of time is required to allow elimination of the drug from the body prior to re-administration. Note that the lowest diagnostic dose has not been thoroughly investigated for many indications or all the low-risk GBCAs and therefore, caution should be exercised so as not to administer a dose that is too low to provide the diagnostic information sought from the examination.

Step 5. What to Do After the MRI Examination

The GBCA and dose used should be accurately recorded. Patients at risk of NSF should be followed up for at least twelve months following the contrast-enhanced MRI examination in order to detect any sign or symptom suggestive of the disease. It is recommended to notify the local regulatory authorities immediately of any putative case of NSF and to keep them informed until the diagnosis of NSF is confirmed or ruled out.

The usefulness of hemodialysis in the prevention of NSF is unknown. However, it is recommended that elective GBCA-enhanced MRI examinations be performed as closely before hemodialysis as is possible, as prompt postprocedural hemodialysis, although unproven to date, may reduce the likelihood that NSF will develop (3). Because it may be difficult for a dialysis center to alter dialysis schedules at the request of imaging departments, it may be more feasible for elective imaging studies to be timed to precede a scheduled dialysis session. Some experts recommend multiple dialysis sessions following GBCA administration, with use of prolonged dialysis times and increased flow rates and volumes to facilitate GBCA clearance, but the incremental benefits remain speculative (3). It has been estimated that three consecutive hemodialysis treatments over a six-day period would be needed to remove 97% of the administered extracellular GBCA (36). Peritoneal dialysis probably provides less potential NSF risk reduction compared to hemodialysis and should not be considered protective (4).

CONCLUSIONS

NSF is a rare, serious, systemic, fibrosing disorder observed almost only in patients with acute or chronic severe renal insufficiency ($\text{GFR} < 30\text{-mL/min/1.73-m}^2$), or with acute renal insufficiency of any severity due to hepatorenal syndrome, or in the perioperative liver transplantation period. Most patients with NSF had a $\text{GFR} < 15\text{- mL/min/1.73-m}^2$ and were undergoing (or had undergone) either hemodialysis or peritoneal dialysis or both.

It is unclear if GBCAs can trigger NSF. Nevertheless, it is appropriate to assume that a potential association might exist for all GBCAs. Use of the preventive measures discussed in this chapter may minimize the risk of developing NSF.

Notably, altered patterns of use of GBCAs in susceptible populations in response to restrictive measures taken by regulatory authorities for some GBCAs and guidelines released

by professional societies to minimize risk have resulted in the incidence of NSF dropping close to zero (5, 18, 24).

REFERENCES

1. Galan A, Cowper SE, Bucala R. Nephrogenic systemic fibrosis (nephrogenic fibrosing dermopathy). *Curr Opin Rheumatol* 2006;18:614-17.
2. Cowper SE, Robin HS, Steinberg SM, et al. Scleromyxedema-like cutaneous diseases in renal-dialysis patients. *Lancet* 2000;356:1000-1.
3. ACR Committee on Drugs and Contrast Media. ACR manual on contrast media, version 2021. https://www.acr.org/-/media/ACR/Files/Clinical-Resources/Contrast_Media.pdf. Chapter 16. Nephrogenic Systemic Fibrosis. Pages 83-91. Published January 2021. Accessed July, 2021.
4. Shellock FG, Spinazzi A. MRI safety update 2008: Part 1, MRI contrast agents and nephrogenic systemic fibrosis. *AJR Am J Roentgenol* 2008;191:1129-39.
5. Mathur M, Jones JR, Weinreb JC. Gadolinium Deposition and Nephrogenic Systemic Fibrosis: A Radiologist's Primer. *Radiographics* 2020;40:153-62.
6. Spinazzi A. MRI Contrast Agents and Nephrogenic Systemic Fibrosis. In: Shellock FG, Crues III JV, Karacozoff AM. *MRI Bioeffects, Safety and Patient Management*. 2014, pp: 256-81. Biomedical Research Publishing Group, Los Angeles, CA.
7. Attari H, Cao Y, Elmholdt TR et al. A systematic review of 639 patients with biopsy-confirmed nephrogenic systemic fibrosis. *Radiology* 2019; 292:376-86.
8. Cowper SE, Bucala R, Leboit PE. Nephrogenic fibrosing dermopathy/nephrogenic systemic fibrosis: setting the record straight. *Semin Arthritis Rheum* 2006;35:208-10.
9. Galan A, Cowper SE, Bucala R. Nephrogenic systemic fibrosis (nephrogenic fibrosing dermopathy). *Curr Opin Rheumatol* 2006;18:614-17.
10. Swaminathan S, Ahmed I, McCarthy JT, et al. Nephrogenic fibrosing dermopathy and high-dose erythropoietin therapy. *Ann Intern Med*. 2006;145:234-35.
11. Goveia M, Chan BP, Patel PR. Evaluating the role of recombinant erythropoietin in nephrogenic systemic fibrosis. *J Am Acad Dermatol* 2007;57:725-27.
12. Grobner T. Gadolinium - a specific trigger for the development of nephrogenic fibrosing dermopathy and nephrogenic systemic fibrosis? *Nephrol Dial Transplant* 2006;21:1104-1108.
13. Othersen JB, Maize JC, Woolson RF, Budisavljevic MN. Nephrogenic systemic fibrosis after exposure to gadolinium in patients with renal failure. *Nephrol Dial Transplant* 2007;22:3179-85.
14. Wahba IM, Simpson EL, White K. Gadolinium is not the only trigger for nephrogenic systemic fibrosis: insights from two cases and review of the recent literature. *Am J Transplant* 2007;7:2425-32.
15. Anavekar NS, Chong AH, Norris R, Dowling J, Goodman D. Nephrogenic systemic fibrosis in a gadolinium-naive renal transplant recipient. *Australas J Dermatol* 2008;49:44-47.
16. Lemy AA, del Marmol V, Kolivras A, et al. Revisiting nephrogenic systemic fibrosis in 6 kidney transplant recipients: a single-center experience. *J Am Acad Dermatol* 2010;63:389-99.
17. Wagner B, Drel V, Gorin Y. Pathophysiology of gadolinium-associated systemic fibrosis. *Am J Physiol Renal Physiol* 2016;311:F1-F11.
18. Shamam YM, De Jesus O. Nephrogenic Systemic Fibrosis. Last update April 7, 2021. In: StatPearls (Internet) Treasure Island (FL): StatPearls Publishing; 2021 Jan. <https://www.ncbi.nlm.nih.gov/books/NBK567754/>. Accessed July, 2021.
19. Spinazzi A, Kirchin MA, Pirovano G. Nephrogenic systemic fibrosis: The need for accurate case reporting. *J Magn Reson Imaging* 2009;29:1240.

364 MRI Contrast Agents and Nephrogenic Systemic Fibrosis

20. Girardi M, Kay J, Elston DM, et al. Nephrogenic systemic fibrosis: Clinicopathological definition and workup recommendations. *J Am Acad Dermatol* 2011;65:1095-1106.
21. Woolen SA, Shankar PR, Gagnier JJ, et al. Risk of nephrogenic systemic fibrosis in patients with stage 4 or 5 chronic kidney disease receiving a group II gadolinium-based contrast agent: A systematic review and meta-analysis. *JAMA Intern Med* 2020;180:223-30.
22. European Society of Urogenital Radiology. ESUR guidelines on contrast agents, version 10.0. <http://www.esur-cm.org/index.php/a-general-adverse-reactions-2>, 2018. Accessed July, 2021.
23. Schieda N, Maralani PJ, Hurrell C, Tsampalieros AK, Hiremath S. Updated clinical practice guideline on use of gadolinium-based contrast agents in kidney disease issued by the Canadian Association of Radiologists. *Can Assoc Radiol J* 2019;70:226-32.
24. Weinreb JC, Rodby RA, Yee J, et al. Use of intravenous gadolinium-based contrast media in patients with kidney disease: Consensus statements from the American College of Radiology and the National Kidney Foundation. *Radiology* 2021;298:28-35.
25. Lunyera J, Mohottige D, Alexopoulos AS, et al. Risk for nephrogenic systemic fibrosis after exposure to newer gadolinium agents: A systematic review. *Ann Intern Med* 2020;173:110-19.
26. Starekova J, Bruce RJ, Sadowski EA, Reeder SB. No cases of nephrogenic systemic fibrosis after administration of gadoxetic acid. *Radiology* 2020;297:556-62.
27. Cowper SE, Rabach M, Girardi M. Clinical and histological findings in nephrogenic systemic fibrosis. *Eur J Radiol* 2008;66:191-99.
28. Knobler R, Moinzadeh P, Hunzelmann N, et al. European dermatology forum S1-guideline on the diagnosis and treatment of sclerosing diseases of the skin, Part 2: Scleromyxedema, scleredema and nephrogenic systemic fibrosis. *J Eur Acad Dermatol Venereol* 2017;31:1581-94.
29. Bucala R. Circulating fibrocytes: Cellular basis for NSF. *J Am Coll Radiol* 2008;5:36-39.
30. Bhawan J, Swick BL, Koff AB, Stone MS. Sclerotic bodies in nephrogenic systemic fibrosis: A new histopathologic finding. *J Cutan Pathol* 2009;36:548-52.
31. Thomsen HS, Morcos SK, Almén T, et al. Nephrogenic systemic fibrosis and gadolinium-based contrast media: Updated ESUR Contrast Medium Safety Committee guidelines. *Eur Radiol* 2013;23:307-18.
32. Webster AC, Nagler EV, Morton RL, Masson P. Chronic kidney disease. *Lancet* 2017;389:1238-52.
33. Chen TK, Knically DH, Grams ME. Chronic kidney disease diagnosis and management: A Review. *JAMA* 2019;322:1294-1304.
34. Inker LA, Schmid CH, Tighiouart H, et al.; CKD-EPI Investigators. Estimating glomerular filtration rate from serum creatinine and cystatin C. *N Engl J Med* 2012;367: 20-29.
35. Levey AS, Becker C, Inker LA. Glomerular filtration rate and albuminuria for detection and staging of acute and chronic kidney disease in adults: a systematic review. *JAMA* 2015; 313: 837-46.
36. Collidge TA, Thomson PC, Mark PB, et al. Gadolinium-enhanced MR imaging and nephrogenic systemic fibrosis: retrospective study of a renal replacement therapy cohort. *Radiology* 2007;245:168-75.

Chapter 14 Gadolinium Retention in Brain and Body Tissues - Safety Considerations

ALBERTO SPINAZZI, M.D.

Senior Vice President
Chief Medical and Regulatory Officer
Bracco Group
Monroe, NJ

INTRODUCTION

More than 8 years after the first report of nephrogenic systemic fibrosis (NSF), incidental retention of gadolinium (Gd) was reported to occur in the brain following exposure to gadolinium-based contrast agents (GBCAs) (1). The main finding was increased T1-weighted signal intensity (SI) on unenhanced T1-weighted magnetic resonance (MR) images in certain portions of the brain (e.g., dentate nuclei and globi pallidi), particularly in instances where patients had undergone multiple contrast-enhanced MRI examinations. Following studies also implied Gd retention in brain tissues by determining change in SI or R1 relaxation rate on unenhanced MR images of the brain (2,3). Confirmation that those imaging findings were indeed related to retention of Gd in the brain required direct determination of Gd presence by means of analytical chemistry methods, such as inductively coupled plasma combined with mass spectrometry (ICP-MS). ICP-MS is a highly sensitive but destructive technique that reports only on the elemental composition and not on form of the Gd, i.e., whether it is still present as intact contrast agent molecule or other chemical forms (3). A large body of studies has clearly shown that indeed traces of Gd remain in the brain following exposure to GBCAs including in people with normal kidney function (3). The magnitude of observed retention is always in the order of few micrograms per gram of wet tissue. In animal studies, the highest levels of retained Gd have been observed after intravenous administration of gadodiamide (OmniscanTM), followed by gadopentetate dimeglumine (Magnevist[®] and generic equivalents). Lower levels have been reported after administration gadobenate dimeglumine (MultiHance[®]) and gadoxetate disodium (Primovist[®]/Eovist[®]). The lowest levels were found after exposure to gadobutrol (Gadovist[®]/Gadavist[®]), gadoterate meglumine (Dotarem[®] and generic equivalents, e.g., ClariscanTM), and gadoteridol (ProHance[®]).

366 Gadolinium Retention in Brain and Body Tissues – Safety Considerations

Although it had been known for decades that Gd is retained in other tissues, such as in skin, bone and liver tissues, and Gd retention is lower in the brain than in other organs (2, 3), the discovery of possible Gd retention in brain tissues raised a number of questions related to the safety of GBCAs, that is, chronic retention of traces of residual Gd species from GBCAs associated with damage of involved tissues? Is there evidence of clinically relevant harm to patients? Does the available evidence change the benefit/risk balance of GBCAs? This chapter is aimed at providing evidence to address these fundamental questions.

Long-term Gd retention in the brain: any evidence of chronic neurotoxicity?

Data in the context of possible neurotoxicity after exposure of cells and tissues to Gd exist within a hierarchy that is not always acknowledged and considered throughout experimentation, discussion of results and especially when drawing conclusions. At the bottom of the hierarchy are data obtained *in vitro* under extreme experimental conditions, which usually do not occur *in vivo* in any biological system. For instance, several *in vitro* experiments aimed at assessing the potential for neurotoxic effects of GBCAs investigated the effect of direct and prolonged exposure of Purkinje cells, astrocytes, or cortical neurons to Gd ions from the dissociation of Gd chloride (GdCl_3) (4-6). However, free Gd ions cannot survive in biological fluids or tissues because they have a high affinity for abundantly present anions like phosphates, carbonates and citrates, and, to a lesser extent, macromolecules. As a matter of fact, preliminary speciation analysis showed that Gd appears to be retained in insoluble forms (most likely bound to anions), soluble high-molecular-weight complexes (Gd bound to macromolecules), or low-molecular-weight molecules (most likely intact GBCA molecules) (7, 8). Therefore, the concept of direct toxicity of Gd ions, acting as calcium antagonists and blocking voltage-gated calcium channels in the human brain and other tissues following the release of the metal from GBCAs is a pure myth, which, however, appears pretty difficult to debunk.

Data more predictive of possible neurotoxic effects in humans may be provided by *in vivo* studies in animals. Several studies in different animal species have confirmed long-term brain retention of traces of Gd-containing species following doses of GBCAs exceeding clinical doses by several orders of magnitude but always failed to demonstrate any evidence of injury to neurons, glial cells, or the brain interstitium from retained Gd (3, 8-11). Some of these studies also found no adverse effects of long-term retention of the metal on cognitive or motor function in neonatal, juvenile and adult animals (12-14). These results are consistent with those of a recent investigation aimed at assessing the adverse central nervous system effect of Gd deposition by using a rotarod performance test (15). The authors concluded that Gd deposition did not lead to alterations in locomotor abilities in healthy mice, although their mouse model was obtained by long-term (90 weeks) oral administration of GdCl_3 .

Some evidence of potential neurotoxicity was reported by Khairinisa, et al. (16) in pregnant BALB/c mice. Prenatal exposure (embryonic days 15 to 19) to intravenous gadoterate meglumine (Dotarem®) or gadodiamide (Omniscan™) was associated with abnormal behaviors and decreased muscle strength of offspring. Of note, the sponsor Bracco had already conducted two perinatal/postnatal studies the effects of the macrocyclic GBCA gadoteridol (ProHance®) and of the linear GBCA gadobenate dimeglumine (MultiHance®) on the off-

spring of female mice exposed to intravenous bolus injections up to 4 times the clinical dose for 12 consecutive days during gestation (17,18). The evaluation went from implantation throughout the fetal period and continued through sexual maturity of the offspring until day 70 postpartum. Among the observations performed during the two studies, the Functional Observational Battery (FOB) included sensorimotor responses to visual, acoustic, tactile and painful stimuli (reactivity and sensitivity). These two studies did not show any effect of the two GBCAs on the cognitive or motor function of the offspring, nor decreased muscle strength. Anyway, the study by Khairinisa, et al. (16) drew the attention to a possible effect of exposure to GBCAs during pregnancy on brain development of the fetus, despite existing data and even if the transferability to humans of the results from the mouse model used in that small animal study could not be properly assessed due to significant limitations of the study. That led the United States Food and Drug Administration (FDA) to request all marketing authorization holders to carry out additional, large juvenile and perinatal/postnatal mice studies with all the GBCAs in clinical use. As expected, the preliminary results of these regulatory safety animal studies do not confirm the findings reported by Khairinisa, et al. (16).

In conclusion, *in vivo* studies in several animal species have not yet provided evidence of chronic toxicity arising from retained Gd in brain tissues.

At the pinnacle of the hierarchy of scientific evidence are data obtained from human subjects. Several post-mortem studies assessed potential signs of neurotoxicity using structural histopathology assessments and transmission electron microscopy and energy-dispersive X-ray spectroscopy (TEM-EDX) to identify possible ultrastructural changes (18-23). Histologic examination of brain tissues did not show gross histologic changes between contrast and control groups in hematoxylin-eosin-stained tissue samples examined with visual light microscopy. In one study of pediatric patients, dentate tissue from two patients, one with pontine glioma and one with neuroblastoma who received high cumulative doses of gadodiamide (OmniscanTM), had mildly to severely gliotic regions with prominent axonal spheroids (22). It is likely, however, that these changes were associated with prior external beam radiation therapy. TEM-EDX DID not show ultrastructural abnormalities.

In vivo studies in humans also showed a substantial absence of clinical neurological and neuropsychological worsening related to cumulative GBCA doses. Cao, et al. (24) conducted a retrospective study aimed at comparing brain T1 signal changes in patients exposed to GBCAs while on chronic hemodialysis to matched control patients with near-normal renal function (eGFR >60 mL/min per 1.73 m²). Because dialysis patients were regularly evaluated by nurses and physicians, typically 3 times per week, there was also an opportunity to search for patterns of clinical events that might be occurring after each exposure to GBCAs in these patients. An electronic medical records search of 2 large medical centers identified 25 patients who received linear GBCAs while on hemodialysis and had unenhanced T1-weighted images of the brain before and after. T1-weighted SI analysis was performed to detect abnormal T1 shortening in the dentate nucleus (DN) and globus pallidus (GP) in the patients on hemodialysis compared with 25 age/sex/GBCA exposure-matched control patients with normal or near-normal renal function (estimated glomerular filtration rate >60 mL/min per 1.73m²). Two additional control groups included 13 patients on hemodialysis without GBCA exposure and 13 age/sex-matched patients with estimated

368 Gadolinium Retention in Brain and Body Tissues – Safety Considerations

glomerular filtration rate greater than 60 mL/min per 1.73 m². The 25 dialysis patients received 44 administrations of linear GBCAs. A greater T1 SI change in the dentate nucleus (but not in the globus pallidus) was observed in dialysis patients receiving GBCA compared to matched patients with normal or near-normal renal function. Despite evidence of abnormal T1 shortening and Gd retention, there was no increase or unique pattern of clinical events occurring within 30 days after any of the 44 GBCA exposures in this cohort. In particular, 7 neurological issues described during the 30 days following GBCA doses (migraine headache, loss of consciousness, memory loss, falling, lightheadedness, and ataxia) were also present before GBCA exposure.

Welk, et al. (25) conducted a population-based study to assess the association between Gd exposure and parkinsonism using multiple and linked administrative databases from Ontario, Canada. Patients who were exposed to GBCA-enhanced MRIs, modeled as a time-varying, cumulative count variable, were compared with patients who received unenhanced MRIs and were never exposed to GBCAs. The primary outcome was a new diagnosis of parkinsonism based on a validated definition (sensitivity, 81.7%; specificity, 99.7%; positive predictive value, 78.0%; negative predictive value, 99.8%; accuracy, 99.5%; and disease prevalence, 1.4%) using diagnosis codes from hospital admissions and physician visits or a dispensed Parkinson disease-specific medication (24). Since medication coverage is provided in Ontario, Canada for those older than 65 years, only patients of 66 years of age or older were included in the study. At the same time, to avoid confounding factors, patients who underwent MRI of the central nervous system (CNS), neurosurgery or had pre-existing Parkinson's disease or parkinsonism were excluded. Of the 246,557 patients undergoing at least 1 non-CNS MRI during the study period, 146,818 (59.5%) underwent 1 or more unenhanced MRI and 99,739 (40.5%) received at least 1 GBCA dose. Among patients who underwent contrast-enhanced MRIs, 81,827 (81.5%) were exposed to a single GBCA injection, 11,278 (15.8%) to 2-3 injections, and 6,634 to 4 or more injections. Incident parkinsonism developed in 1.16% of unexposed patients and in 1.17% of those exposed to GBCAs. In adjusted analysis, there was no significantly increased hazard of parkinsonism among patients with cumulative exposure to GBCAs compared with those never exposed to the agents. Of note, the incidence rate of parkinsonism was lower (0.70%) in the cohort of patients exposed 4 or more times to GBCAs.

McDonald, et al. (27, 28) reported findings from the Mayo Clinic Study of Aging (MCSA), a large study of the incidence and natural history of normal and abnormal (mild cognitive impairment and dementia) cognitive decline over time. While this study was not initially conceived to identify the neurologic effects of GBCA exposure, it remained an ideal dataset for such an investigation as it was a prospectively enrolled, population-based cohort with unique linkage to demographic, clinical and vital records data provided from the Rochester Epidemiology Project (REP), a large population-based study of human health (29). The MCSA continuously enrolled patients in a prospective manner since study initiation on October 1, 2004. After enrolment, all patients underwent extensive longitudinal clinical (neurologic evaluation, neuropsychological testing) and imaging (unenhanced MRI and PET/CT) assessment at baseline and 15-month follow-up intervals. After searching the electronic medical record and REP data, patients were segregated into those with no history of prior GBCA exposure (control group) and those who underwent prior GBCA-enhanced MRI examinations. The linear GBCA gadodiamide (Omniscan™) was used in all the con-

trast-enhanced MRI procedures. Of note, GBCA exposure was independent of MCSA participation and, as a result of MCSA inclusion and exclusion criteria, was not related to an underlying neuropathologic process that could confound the results of the analysis. All study subjects underwent a large battery of neurologic and neurocognitive tests. Among 4261 cognitively normal study participants aged 50-89 (mean age at enrolment: 72 years), 1092 patients (25.6%) received one or more GBCA doses (range: 1-28 doses) unrelated to their participation in the MCSA. The GBCA exposed group was followed prospectively for a total of 7,104 person years and had a total of 83,119 person-years of retrospective clinical data available from the REP. Similarly, the control group was followed prospectively for a total of 16,078 person years with a total of 236,384 person years of retrospective clinical data available from the REP. After adjusting for over 20 demographic and clinical variables including age, sex, education level, baseline neurocognitive performance, Charlson comorbidity index, and ApoE4 status, exposure to the least stable GBCA, gadodiamide (OmniscanTM), did not turn out to be a significant predictor of excess decline in cognitive function or motor performance. A total of 670 (16%) of the 4261 participants who were initially cognitively normal at the time of enrolment progressed to mild cognitive impairment during the study timeframe. The incidence of progression to cognitive decline in the GBCA-exposed group, standardized by age, sex, and education level to the Olmsted County population, was 29.1 per 1,000 person-years (95% CI: 25.7-31.2) while the control group was 27.6 per 1,000 person-years (95% CI: 24.9-30.4). After adjusting for age, sex, education level, and other covariates, neither GBCA exposure nor cumulative lifetime GBCA dose was associated with significant excess risk of conversion to cognitive impairment in the study population.

The previous studies, showing no effect of exposure to GBCAs on cognitive function or motor skills in special and vulnerable populations, such as elderly subjects and patients with impaired renal function, specifically excluded patients with diseases of the central and peripheral nervous system, to avoid any confounding bias. So, what about possible additional neurological damage in patients with neurological disorders, especially those requiring multiple GBCA-enhanced MRI exams? Forslin, et al. (30) conducted a retrospective, longitudinal cohort study aimed at investigating the relationship of multiple GBCA administrations with SI increase in the DN and GP, and any possible effect on cognitive function in 23 patients with multiple sclerosis (MS) who had undergone physical disability assessments and neurological and neuropsychological evaluations at 3 time points during 18-years of follow-up. A cohort of 23 healthy, age-/gender-matched subjects were used as single time-point controls. All control subjects underwent one unenhanced MRI scan. An increase in SI in the dentate nucleus was observed in the MS cohort and was associated with lower verbal fluency scores, which remained significant after correction for several aspects of disease severity. The same group reported cross-sectional cohort study of 85 patients with MS and 23 age- and sex-matched healthy controls without exposure to GBCAs (31). Single time-point physical disability assessments and neurological and neuropsychological evaluations were carried out in MS patients and controls. Longitudinal (T1) and transversal (T2) relaxation rates relaxometry of dentate nucleus, globus pallidus, caudate nucleus, and thalamus was used to assess possible Gd retention in those brain areas. Higher relaxation was associated with lower information-processing speed (dentate nucleus, thalamus) and verbal fluency (caudate nucleus, thalamus). No associations were found with physical disability

370 Gadolinium Retention in Brain and Body Tissues – Safety Considerations

or fatigue. Because a decrease in verbal fluency and information-processing speed are the cognitive domains most commonly affected in MS, and the controls in both studies were just matched for age and sex, the authors of these two studies were not able to separate the effects of the disease itself from a possible toxicity of the GBCAs. A more recent retrospective study of 74 relapsing-remitting MS patients investigated the relationship between changes in the expanded disability status scale, T1-weighted hyperintensity and higher longitudinal relaxation rate in the dentate nucleus and (R1) maps, and confirmed the absence of association between imaging findings suggestive of Gd retention and progression of physical disability (32). Another retrospective study evaluated the association between lifetime cumulative doses of the least stable, linear agent gadodiamide (OmniscanTM), increased SI within the dentate nucleus, globus pallidus, and thalamus, and disease progression in patients with early MS (33). A total of 203 patients with MS (107) with baseline and follow-up MRI assessments and 262 age- and sex-matched controls were included in this study. Patients with MS had disease duration <2 years at baseline and received exclusively gadodiamide (OmniscanTM) at all MRI time points. The mean follow-up time was 55.4 months, and the mean number of gadolinium-based contrast agents administrations was 9.2. No significant association was observed between imaging signs of Gd retention and outcomes of disease severity, i.e., accumulation of lesion burden, development of brain atrophy, occurrence of relapses, or increase in disability over the years of follow-up. Finally, two studies assessed possible structural damage to the dentate nuclei in patients with MS exposed to multiple administrations of either linear or macrocyclic GBCAs. Despite visible, abnormal T1 hyperintensity, interpreted as a sign of Gd retention, either diffusion-weighted MRI or sodium (²³Na) MRI at 3T indicated no changes of tissue integrity of the dentate nuclei in any the MS patients in the two studies (34, 35).

In conclusion, although there is data that all GBCAs leave trace amounts of residual Gd in brain tissues after intravenous GBCA administration, there is no convincing evidence indicating chronic neurotoxicity arising from long-term Gd retention, harmful effects, and potential interaction with neurological disease processes. (36).

Long-term Gd retention in non-CNS tissue: any clinically meaningful effects?

It is clear that Gd retention in a number of non-CNS tissues, including bone, skin, and liver, may occur with all types of GBCAs (3). While most *in vivo* studies in different animal species and models focused on Gd retention in tissues, a few reports describe the results of histologic assessment of potential toxicity of retained Gd, with emphasis on the skin, to assess the possible association of exposure to GBCAs with the development of nephrogenic systemic fibrosis (NSF). In healthy rat, histologic evidence of skin lesions was observed only in animals administered the linear GBCAs associated with the highest levels of Gd retention, i.e., gadodiamide (OmniscanTM) and gadoversetamide (OptiMARK[®]) (37-41). Similar findings were reported using animal models of renal impairment (42-44). Fretellier, et al. (44) demonstrated that hyperphosphatemia induced in partially nephrectomized rats by a high phosphate diet increased the frequency and severity of gadodiamide-induced skin lesions. The observed skin changes were characterized by dermal fibrosis and infiltration of different cells, including mononuclear cells and CD34-positive cells (43, 45). One study (41) showed elevation of several proinflammatory cytokines in the serum of gadodiamide-treated rats, suggesting the involvement of inflammatory pathways in the pathogenesis of

skin damage. However, the skin lesions observed in rats following exposure to gadodiamide (Omniscan™) were not completely consistent with histopathology of NSF in humans. Some of the difference between the cutaneous changes described in the gadodiamide (Omniscan™)-treated rats and human NSF are possibly due to anatomical differences, such as the presence of the panniculus carnosus in rats, a structure that separates the dermis from the subcutis and explains the fact that the observed skin lesions were restricted to the dermis in this animal species (46). All in all, these results of studies in animals might provide clues about the possible pathogenesis of NSF in humans. However, it should be noted that signs of possible toxicity in skin tissues from retained Gd were only observed following exposure to gadodiamide (Omniscan™) and gadoversetamide (OptiMARK™, not available for clinical use). Also, one study showed that marked skin lesions, characterized by epidermal hyperplasia and hyperkeratosis, crusting and ulceration, and dermal infiltration by acute and chronic inflammatory cells, mast cells and mineralization, were observed after exposure to the active ingredient of Omniscan™, gadodiamide, and not after exposure to another GBCA or even to Gd salts, showing a possible role of the intact GBCA and not of retained Gd (47).

NSF is a serious clinical syndrome associated with Gd retention in body tissues. It has been observed only in patients with acute or chronic severe renal insufficiency (eGFR <30 mL/min/1.73 m²), end-stage renal disease, or with acute renal insufficiency of any severity due to hepatorenal syndrome or in the perioperative liver transplantation period (48). NSF cases occurring after the sole administration of one GBCA are defined as “single-agent” or “unconfounded.” If a case of NSF follows the administration of two or more GBCAs, it is impossible to determine which agent is associated with the development of the disorder, and the case is reported as “multiple-agent” or “confounded” (48). Almost all unconfounded NSF cases occurred after single or repeated exposure to three GBCAs: gadopentetate dimeglumine (Magnevist® and generic equivalents), gadoversetamide (OptiMark®), and gadodiamide (Omniscan™) (49). No or very few unconfounded cases were reported following exposure to any of the other GBCAs available for clinical use, that is, gadoterate meglumine (Dotarem® and generic equivalents(Dotarem® and generic equivalents, e.g., Clariscan™), gadoteridol (ProHance®), gadoxetate disodium (Primovist® /Eovist®) (49). The available evidence on NSF with the individual GBCAs is provided and discussed in Chapter 13 of this book.

Other entities that have been reported as possibly associated with residual Gd following exposure to GBCAs are the “gadolinium-associated plaques” and the “gadolinium deposition disease”. “Gadolinium-associated plaques” is the proposed name of a condition observed in a total of 4 cases between the first report in 2013 and the last in 2019 (50-52). Three patients presented with 0.5-2.5 cm plaques that resembled dermal infiltrative processes such as granuloma annulare or cutaneous sarcoidosis in two cases (51); in one case, it was an accidental finding in excisional specimens obtained during surgical removal of squamous cell carcinoma (50). One patient showed ill-defined, hyperpigmented and violaceous macules coalescing into ill-defined nummular patches with fine scale on the upper back, right forearm and right lower leg (52). Eosinophilic, collagenous, round, or ovoid sclerotic bodies in various stages of calcification were the pathognomonic histopathologic feature of the condition. Renal function was impaired in three patients and normal in the remaining one. In one case, the patient could not recall exposure to any GBCA (52). Two cases have been reported after administration of gadodiamide (Omniscan™, total cumulative

372 Gadolinium Retention in Brain and Body Tissues – Safety Considerations

volume: 90 mL in one case, 100 mL in the other), one following exposure to an unknown dose of an unknown GBCA (50, 51). When exposure to GBCAs was ascertained, the interval between last exposure and onset of the skin lesions ranged between 3.5 and 5 years. Plaques were asymptomatic in three cases, and pruritic and burning in one. The association between the observed skin lesions and exposure to GBCAs was suggested because sclerotic bodies and osseous metaplasia have been described as a late finding in the course of NSF, and the observed plaques were seen in two patients exposed to a GBCA (gadodiamide, Omniscan), a GBCA known to be associated with NSF. The diagnosis of NSF was always ruled out, however, as no other clinical or pathological sign of the disease was observed.

First reported by Semelka, et al. in 2016 (53, 54), “gadolinium deposition disease” (GDD) is still only a proposed disease process with no clear proof of its true existence. GDD describes a condition in which a patient with normal or near-normal kidney function develops long-lasting symptoms reportedly after exposure to one or more GBCAs, assuming that alternative conditions and causes have been excluded (55). All the publications about GDD cases came from the same small group of investigators, who very recently acknowledged that this entity had been met with skepticism among physicians because their papers describing the disease had been criticized for flaws in their methodology (55). Over the years, those investigators provided several definitions of GDD. The most recent definition (55) indicates that a diagnosis of GDD requires that: i) the patient has to be exposed to a GBCA in the last month prior to onset of symptoms; ii) the symptoms should be new to the patient, i.e., not reflecting any pre-existing disease or symptoms observed before exposure to GBCAs; iii) symptoms include brain fog, pins and needles sensations, glove and stocking distribution of symptomatology, skin discoloration, pain (including bone pain and a burning sensation), and/or subcutaneous tissue thickening; iv) whenever possible, evidence should be obtained that Gd remained in the patient’s system for more than 30 days after exposure to GBCAs; v) the patient should have had normal or near-normal renal function at the time of the exposure to GBCAs. Symptoms reportedly may arise within the first 24 hours after exposure to any of the GBCAs in clinical use and may last for weeks, months or even years (55). The group of investigators reporting these cases indicated that GDD is a rare encounter, and that this presumed disease process might initially resemble an acute hypersensitivity reaction to the GBCAs; therefore it may not be related to Gd deposition but rather involve the immune system in the presence of host factors such as genetic susceptibility and/or adaptive immune response (53-55). However, possible predisposing conditions or risk factors were never reported. The same group of investigators also reported that chelation therapy with Ca-diethylenetriaminepentaacetic acid increased urine Gd content and serum levels of some cytokines in patients with presumed GDD and caused an exacerbation of symptoms (flare) within the first 24 hours (56-57). All in all, the published literature to date failed to validate the existence of a novel condition characterized by the development of long-lasting symptoms following exposure to GBCAs and possibly maintained by Gd retained in tissues. The very few reports always came from the same group of investigators, showed significant selection bias, lacked clinical information to exclude alternative medical diagnoses and/or to substantiate findings, and sample sizes were always so small to render the results difficult to interpret. In the absence of evidence from well-designed clinical studies that could validate the existence of GDD and its pathogenesis, the use of chelation therapy in patients

with no clear evidence-based indication potentially increases the risk of clinically significant harm from the well-known adverse effects of chelation (58).

In September 2017, during a meeting of the Medical Imaging Drugs Advisory Committee (MIDAC), the FDA presented a series of patients reporting symptoms potentially related to GBCA exposure. A total of 132 case reports were identified, with various symptoms often centering around pain; most were self-reported and lacked significant and validated clinical information. The MIDAC concluded that no association between exposure to GBCAs, Gd retention and patient symptoms could be established (59). From January 1, 2010 and December 31, 2020, Bracco, the marketing authorization holder of two GBCAs, gadobenate dimeglumine (MultiHance®) and gadoteridol (ProHance®) received a total number of 14 cases of symptoms (7 with gadobenate dimeglumine and 7 with gadoteridol) persisting for more than 4 weeks, with or without evidence of Gd retention in hair or urine. The majority (10) of these cases were not confirmed by any healthcare professional. Also, most of them reportedly followed exposure to multiple GBCAs. The interval between last exposure to a GBCA and onset of symptoms ranged from 2 hours to years. In one case, symptoms were pre-existing the exposure to gadobenate dimeglumine. Overall, the reporting rate of patients with persisting symptoms was lower than 1 case over more than 238,000 exposures to GBCAs. Overall, the reports received by Bracco referred to heterogeneous clusters of symptoms, without any common suggestive clinical pattern. Relatedness of the reported symptoms to GBCAs could not be established due to the scarce quality of the available information, together with the multifactorial nature of the reported events and/or the presence of underlying co-morbidities which could explain the reported symptoms (60).

In conclusion, besides NSF, there is no evidence suggesting that retention of Gd in non-CNS tissues may be associated with harmful effects and potential interaction with disease processes.

Does the available evidence on Gd retention in tissues change the benefit-risk balance of GBCAs?

While the effectiveness and benefit provided by GBCAs has been properly demonstrated before and after their approval by all regulatory authorities in the world, there is no evidence of new, additional risk resulting from Gd retention in brain and body tissues. To date, NSF is the most significant clinical syndrome associated with retention of Gd in body tissues, and important and effective risk minimization measures for NSF have been introduced since 2010, virtually eradicating the disease.

CONCLUSIONS

By enhancing the quality of MR images and improving the diagnostic performance of MRI and MR angiography, the use of GBCAs has been part of standard clinical practice to provide treatment guidance for more than three decades. In many instances, GBCA-enhanced MRI or MRA provide diagnostic information that would otherwise be unavailable. As such, their use is routine and a crucial component in the diagnosis and follow-up of patients with serious medical conditions, including cancer, vascular pathology, and infection. While GBCAs provide crucial, life-saving medical information, each time an individual

374 Gadolinium Retention in Brain and Body Tissues – Safety Considerations

GBCA-enhanced MRI or MRA study is considered, it is important to consider its clinical benefit against the potential risk deriving from its use.

Known risks associated with exposure to GBCAs include the possible occurrence of immediate-type reactions and nephrogenic systemic fibrosis (NSF). Immediate-type adverse reactions are those occurring within 1 hour of injection of a GBCA, and most of them are hypersensitivity reactions and are unpredictable. Patients at risk for acute hypersensitivity reactions are those with a history of a previous acute reaction to a GBCA, asthma, or other allergic disorders. To minimize the occurrence and severity of hypersensitivity reactions, warnings and precautions specifically related to the risk of serious hypersensitivity reactions are given in the prescribing information of all approved GBCAs (please see Chapter 10 of this book for more detailed information on how to minimize the risk of immediate-type reactions to GBCAs).

NSF is the most serious clinical syndrome associated with Gd retention in body tissues to date. It has been observed only in patients with acute or chronic severe renal insufficiency (eGFR <30 mL/min/1.73 m²), end-stage renal disease, or with acute renal insufficiency of any severity due to hepatorenal syndrome or in the perioperative liver transplantation period (“high-risk patients”). Notably, important and effective risk minimization measures for NSF have been introduced since 2010, virtually eradicating the disease (please see Chapter 13 of this book for more detailed information on how to minimize the risk of NSF).

Although it had been known for decades that Gd is retained in other tissues, such as in skin, bone and liver tissues, the observation of traces of residual Gd in brain tissues of patients exposed to GBCAs raised a number of questions related to the safety of GBCAs. However, besides NSF, the available evidence failed to demonstrate an association between Gd retention in brain or body tissues and harm to patients. Notably, following extensive assessments, all regulatory authorities around the world agreed on the absence of evidence of any harmful effect of Gd retention in humans following exposure to any of the approved GBCAs; however, even if based on the same amount of preclinical and clinical evidence available in adults and children, regulatory authorities used different approaches resulting in different actions and decisions regarding the labeling and market authorizations of individual GBCAs (61).

Of note, lack of evidence is not conclusive evidence of absence. If Gd retention is associated with clinical harm, the harm is likely rare or occult for the vast majority of exposed patients. Future studies should be appropriately powered to enable detection of rare or subtle adverse effects; however, it should be recognized that it is not possible to scientifically prove the absence of harm, and that the specific signs, symptoms, and diseases to investigate are unclear (3).

Until new evidence may become available, the most practical approach may be to treat GBCAs like ionizing radiation, i.e., to follow an ALARA (as low as reasonably achievable) approach (2). Exposure to GBCAs should be minimized as much as is reasonable while remembering that the diagnostic benefits generally still greatly exceed the risks for indicated contrast-enhanced MR examinations. GBCAs should not be administered freely regardless of medical appropriateness, but instead should be used when clinically indicated, like any other medication. To this purpose, the prescribing information for all GBCAs has been up-

dated to contain clear, unambiguous wording to make the health care professionals utilizing the products aware of Gd retention and minimize exposure (61).

REFERENCES

1. Kanda T, Ishii K, Kawaguchi H, et al. High signal intensity in the dentate nucleus and globus pallidus on unenhanced T1-weighted MR images: relationship with increasing cumulative dose of a gadolinium-based contrast material. *Radiology* 2014; 270: 834-41
2. Dillman JR, Davenport MS. Gadolinium retention – 5 years later.... *Pediatr Radiol* 2020; 50: 166–67
3. McDonald RJ, Levine D, Weinreb J, et al. Gadolinium Retention: A Research Roadmap from the 2018 NIH/ACR/RSSNA Workshop on Gadolinium Chelates. *Radiology* 2018; 289: 517-34
4. Sharonova IN, Dvorzhak AY, Vorobjov VS. Gadolinium blocks proton-activated currents in isolated Purkinje cells. *Bull Exp Biol Med* 2008; 145: 307–11
5. Feng X, Xia Q, Yuan L, Yang X, Wang K (2010) Impaired mitochondrial function and oxidative stress in rat cortical neurons: implications for gadolinium-induced neurotoxicity. *Neurotoxicology* 2010; 31: 391–8
6. Xia Q, Feng X, Huang H, du L, Yang X, Wang K. Gadolinium-induced oxidative stress triggers endoplasmic reticulum stress in rat cortical neurons. *J Neurochem* 2011; 117: 38–46
7. Rasschaert M, Weller RO, Schroeder JA, Brochhausen C, Idée JM. Retention of Gadolinium in Brain Parenchyma: Pathways for Speciation, Access, and Distribution. A Critical Review. *J Magn Reson Imaging* 2020; 52: 1293-1305
8. Strzeminska I, Factor C, Robert P, Szpunar J, Corot C, Lobinski R. Speciation Analysis of Gadolinium in the Water-Insoluble Rat Brain Fraction After Administration of Gadolinium-Based Contrast Agents. *Invest Radiol* 2021; 56: 535-44
9. Smith APL, Marino M, Roberts J, Crowder JM, Castle J, Lowery L, Morton C, Hibberd MG, Evans PM. Clearance of gadolinium from the brain with no pathologic effect after repeated administration of gadodiamide in healthy rats: an analytical and histologic study. *Radiology* 2017; 282:743–51
10. Lohrke J, Frisk AL, Frenzel T, Schöckel L, Rosenbruch M, Jost G, Lenhard DC, Sieber MA, Nischwitz V, Küppers A, Pietsch H. Histology and gadolinium distribution in the rodent brain after the administration of cumulative high doses of linear and macrocyclic gadolinium-based contrast agents. *Invest Radiol* 2017; 52:324–33
11. El Hamrani D, Vives V, Buchholz R, et al. (2019) Effect of long-term retention of gadolinium on metabolism of deep cerebellar nuclei after repeated injections of gadodiamide in rats. *Investig Radiol* 2019; 55:120–8
12. Bussi S, Penard L, Bonafè R, Botteron C, Celeste R, Coppo A, Queliti R, Kirchin MA, Tedoldi F, Maisano F. Non-clinical assessment of safety and gadolinium deposition after cumulative administration of gadobenate dimeglumine (MultiHance®) to neonatal and juvenile rats. *Regul Toxicol Pharmacol* 2018; 92: 268-77
13. Giorgi H, Ammerman J, Briffaux JP, Fretellier N, Corot C, Bourrinet P. Non-clinical safety assessment of gadoterate meglumine (Dotarem®) in neonatal and juvenile rats. *Regul Toxicol Pharmacol* 2015; 73: 960-70
14. Akai H, Miyagawa K, Takahashi K, Mochida-Saito A, Kurokawa K, Takeda H, Tsuji M, Sugawara H, Yasaka K, Kunimatsu A, Inoue Y, Abe O, Ohtomo K, Kiryu S. Effects of Gadolinium Deposition in the Brain on Motor or Behavioral Function: A Mouse Model. *Radiology* 2021 Aug 31:210892. doi: 10.1148/radiol.2021210892. Epub ahead of print.
15. Nörenberg D, Schmidt F, Schinke K, et al. Investigation of potential adverse central nervous system effects after long term oral administration of gadolinium in mice. *PLoS One* 2020; 15(4):e0231495
16. Khairnisa MA, Takatsuru Y, Amano I, et al. The effect of perinatal gadolinium-based contrast agents on adult mice behavior. *Invest Radiol* 2018; 53:110–18

376 Gadolinium Retention in Brain and Body Tissues – Safety Considerations

17. Bracco Study No. 20173083. A Developmental and Perinatal/Postnatal Reproduction Study of ProHance® by Intravenous (Bolus) Injection in Mice, Including a Postnatal Behavioral/Functional Evaluation. Data on file.
18. Bracco Study No. 20173081. A Developmental and Perinatal/Postnatal Reproduction Study of Multi-Hance® by Intravenous (Bolus) Injection in Mice, Including a Postnatal Behavioral/Functional Evaluation. Data on file.
19. McDonald RJ, McDonald JS, Kallmes DF, et al. Intracranial gadolinium deposition after contrast-enhanced MR imaging. *Radiology* 2015; 275:772–82
20. Murata N, Murata K, Gonzalez-Cuyar LF, Maravilla KR. Gadolinium tissue deposition in brain and bone. *Magn Reson Imaging* 2016; 34: 1359–65
21. McDonald RJ, McDonald JS, Kallmes DF, Jentoft ME, Paolini MA, Murray DL, Williamson EE, Eckel LJ. Gadolinium Deposition in Human Brain Tissues after Contrast-enhanced MR Imaging in Adult Patients without Intracranial Abnormalities. *Radiology*. 2017 Nov;285(2):546-554
22. McDonald JS, McDonald RJ, Jentoft ME, Paolini MA, Murray DL, Kallmes DF, Eckel LJ. Intracranial Gadolinium Deposition Following Gadodiamide-Enhanced Magnetic Resonance Imaging in Pediatric Patients: A Case-Control Study. *JAMA Pediatr* 2017; 171: 705-7
23. Fingerhut S, Sperling M, Holling M, Niederstadt T, Allkemper T, Radbruch A, Heindel W, Paulus W, Jeibmann A, Karst U. Gadolinium-based contrast agents induce gadolinium deposits in cerebral vessel walls, while the neuropil is not affected: an autopsy study. *Acta Neuropathol* 2018; 136:127–31
24. Cao Y, Zhang Y, Shih G, Zhang Y, Bohmert A, Hecht EM, Prince MR. Effect of renal function on gadolinium-related signal increases on unenhanced T1-weighted brain magnetic resonance imaging. *Invest Radiol* 2016; 51: 677-82
25. Welk B, McArthur E, Morrow SA, et al. Association between gadolinium contrast exposure and the risk of parkinsonism. *JAMA* 2016; 316: 96–8
26. Butt DA, Tu K, Young J, Green D, Wang M, Ivers N, et al. A validation study of administrative data algorithms to identify patients with parkinsonism with prevalence and incidence trends. *Neuroepidemiology* 2014; 43: 28-37
27. McDonald, et al., in PRAC (Pharmacovigilance Risk Assessment Committee) Rapporteur Re-examination Assessment Report (28 June 2017). Referral under Article 31 of Directive 2001/83/EC, EMEA/H/A-31/1437. Pages 46-52
28. McDonald RJ (2017) No evidence gadolinium causes neurologic harm. RSNA 2017 Daily Bulletin. Accessed on January 14, 2020.
29. Melton LJ 3rd. History of the Rochester Epidemiology Project. *Mayo Clin Proc* 1996; 71: 266-74
30. Forslin Y, Shams S, Hashim F, Aspelin P, Bergendal G, Martola J, et al. Retention of gadolinium-based contrast agents in multiple sclerosis: Retrospective analysis of an 18-year longitudinal study. *AJNR Am J Neuroradiol* 2017; 38: 1311-16
31. Forslin Y, Martola J, Bergendal Å, Fredrikson S, Wiberg MK, Granberg T (2019) Gadolinium retention in the brain: an MRI relaxometry study of linear and macrocyclic gadolinium-based contrast agents in multiple sclerosis. *Am J Neuroradiol* 2019; 40:1265–73
32. Cocozza S, Pontillo G, Lanzillo R, Russo C, Petracca M, et al. MRI features suggestive of gadolinium retention do not correlate with expanded disability status scale worsening in multiple sclerosis. *Neuroradiology* 2019; 61: 155–62
33. Zivadinov R, Bergsland N, Hagemeier J, Ramasamy DP, et al. (2019) Cumulative gadodiamide administration leads to brain gadolinium deposition in early MS. *Neurology* 2019; 93: e611–e623
34. Eisele P, Konstandin S, Szabo K, Ong M, et al. Schoenberg SO, Gass A (2017) Sodium MRI of T1 high signal intensity in the dentate nucleus due to gadolinium deposition in multiple sclerosis. *J Neuroimaging* 2017; 27: 372-75

MRI Bioeffects, Safety, and Patient Management 377

35. Eisele P, Szabo K, Ebert A, Radbruch A, et al. Diffusion-weighted imaging of the dentate nucleus after repeated application of gadolinium-based contrast agents in multiple sclerosis. *Magn Reson Imaging* 2019; 58: 1-5
36. Mallio CA, Rovira Å, Parizel PM, Quattrocchi CC. Exposure to gadolinium and neurotoxicity: current status of preclinical and clinical studies. *Neuroradiology* 2020; 62: 925-934
37. Sieber MA, Lengsfeld P, Frenzel T, Golfier S, et al. Preclinical investigation to compare different gadolinium-based contrast agents regarding their propensity to release gadolinium in vivo and to trigger nephrogenic systemic fibrosis-like lesions. *Eur Radiol* 2008; 18: 2164-73
38. Sieber M, Pietsch H, Walter J, Haider W, et al. A preclinical study to investigate the development of nephrogenic systemic fibrosis: a possible role for gadolinium-based contrast media. *Invest Radiol* 2008; 43: 65-75
39. Sieber MA, Lengsfeld P, Walter J, Schirmer H, et al. Gadolinium-based contrast agents and their potential role in the pathogenesis of nephrogenic systemic fibrosis: the role of excess ligand. *J Magn Reson Imaging*. 2008; 27: 955-62.
40. Pietsch H, Lengsfeld P, Jost G, Frenzel T, et al. Long-term retention of gadolinium in the skin of rodents following the administration of gadolinium-based contrast agents. *Eur Radiol*. 2009; 19: 1417-24
41. Steger-Hartmann T, Raschke M, Rieke B, Pietsch H, et al. The involvement of pro-inflammatory cytokines in nephrogenic systemic fibrosis – a mechanistic hypothesis based on preclinical results from a rat model treated with gadodiamide. *Exp Toxicol Pathol* 2009; 61: 537-52
42. Pietsch H, Lengsfeld P, Steger-Hartmann T, Löwe A, et al. Impact of renal impairment on long-term retention of gadolinium in the rodent skin following the administration of gadolinium-based contrast agents. *Invest Radiol* 2009; 44: 226-33
43. Sato T, Ito K, Tamada T, Kanki A, et al. Tissue gadolinium deposition in renally impaired rats exposed to different gadolinium-based MRI contrast agents: Evaluation with inductively coupled plasma mass spectrometry (ICP-MS). *Magn Reson Imaging* 2013;31:1412-17
44. Fretellier N, Idée J, Bruneval P, Guerret S, Daubiné F, Jestin G, et al. Hyperphosphataemia sensitizes renally impaired rats to the profibrotic effects of gadodiamide. *Br J Pharmacol* 2012; 165: 1151-62
45. Haylor J, Schroeder J, Wagner B, Nutter F, Jestin G, Idée JM, Morcos S. Skin gadolinium following use of MR contrast agents in a rat model of nephrogenic systemic fibrosis. *Radiology* 2012;263:107-16
46. Sieber MA, Steger-Hartmann T, Lengsfeld P, Pietsch H. Gadolinium-based contrast agents and NSF: evidence from animal experience. *J Magn Reson Imaging*. 2009; 30: 1268-76
47. Grant D, Johnsen H, Juelsrud A, Løvhaug D. Effects of gadolinium contrast agents in naïve and nephrectomized rats: relevance to nephrogenic systemic fibrosis. *Acta Radiol*. 2009; 50: 156-69
48. Shellock FG, Spinazzi A. MRI safety update 2008: Part 1, MRI contrast agents and nephrogenic systemic fibrosis. *AJR Am J Roentgenol*. 2008; 191:1129-39
49. Shamam YM, De Jesus O. Nephrogenic Systemic Fibrosis. 2021 Apr 7. In: StatPearls [Internet]. Treasure Island (FL): StatPearls Publishing; 2021 Jan-. PMID: 33620831
50. Bhawan J, Perez-Chua TA, Goldberg L. Sclerotic bodies beyond nephrogenic systemic fibrosis. *J Cutan Pathol* 2013; 40: 812-7
51. Gathings RM, Reddy R, Santa Cruz D, Brodell RT. Gadolinium-associated plaques: a new, distinctive clinical entity. *JAMA Dermatol* 2015;151: 316-9
52. Olayiwola O, Ronkainen S, Miller D, High W, Farah RS. Image Gallery: A case of gadolinium-associated plaques requiring confirmation with mass spectrometry. *Br J Dermatol* 2019; 180: e66
53. Semelka RC, Commander CW, Jay M, Burke LM, Ramalho M. Presumed gadolinium toxicity in subjects with normal renal function: a report of 4 cases. *Invest Radiol* 2016; 51: 661-65
54. Semelka RC, Ramalho M, AlObaidy M, Ramalho J. Gadolinium in humans: A family of disorders. *AJR Am J Roentgenol* 2016; 207: 229-33

378 Gadolinium Retention in Brain and Body Tissues – Safety Considerations

55. Semelka RC, Ramalho M. Physicians with self-diagnosed gadolinium deposition disease: a case series. *Radiol Bras* 2021; 54: 238-242
56. Maecker HT, Siebert JC, Rosenberg-Hasson Y, Koran LM, Ramalho M, Semelka RC. Acute Chelation Therapy-Associated Changes in Urine Gadolinium, Self-reported Flare Severity, and Serum Cytokines in Gadolinium Deposition Disease. *Invest Radiol* 2021; 56: 374-384
57. Maecker HT, Siebert JC, Rosenberg-Hasson Y, Koran LM, Ramalho M, Semelka RC. Dynamic Serial Cytokine Measurements During Intravenous Ca-DTPA Chelation in Gadolinium Deposition Disease and Gadolinium Storage Condition: A Pilot Study. *Invest Radiol.* 2021 Jun 11. doi: 10.1097/RLI.0000000000000803. Epub ahead of print. PMID: 34120127
58. Layne KA, Wood DM, Dargan PI. Gadolinium-based contrast agents - what is the evidence for 'gadolinium deposition disease' and the use of chelation therapy? *Clin Toxicol (Phila)* 2020; 58: 151-60
59. Food and Drug Administration Center for Drug Evaluation and Research, Medical Imaging Drugs Advisory Committee (MIDAC) . Transcript: Friday, September 8, 2017, 7:30 a.m. to 4:10 p.m., FDA White Oak Campus, White Oak Conference Center, Building 31, The Great Room, Silver Spring, Maryland. <https://www.fda.gov/downloads/AdvisoryCommittees/CommitteesMeetingMaterials/Drugs/MedicalImagingDrugsAdvisoryCommittee/UCM584442.pdf>. Accessed August 31, 2021.
60. Bracco, Pharmacovigilance Assessment Reports on MultiHance® and ProHance®. Data on file.
61. Lancelot E, Desché P. Gadolinium Retention as a Safety Signal: Experience of a Manufacturer. *Invest Radiol* 2020; 55: 20-24

Chapter 15 MRI Screening for Patients and Individuals

ASHOK K. SARASWAT, M.S., B.ED., R.T. (R)(MR)

Emeritus MRI Educational Program Director
Ohio State University
Wexner Medical Center
Columbus, OH

MARK A. SMITH M.S., ABMP, R.T.(R)(MR)

MRI Physicist
Nationwide Children's Hospital
Clinical Instructor, Adjunct Faculty
Ohio State University
Wexner Medical Center
Columbus, OH

INTRODUCTION

The clinical applications of magnetic resonance imaging (MRI) have expanded rapidly in recent years, resulting in a greater percentage of the patient population undergoing diagnostic imaging using this modality. In addition, the number of patients and individuals possessing implantable devices continues to grow, as does the variation and complexity of these devices. Non-medical implants and materials such as body piercings, tattoos, and permanent cosmetics (e.g., eyeliner) have also increased in popularity. This progressive array of implanted patients and individuals, combined with the implementation of scanners with higher static magnetic fields (i.e., 3- and 7-Tesla) presents particular challenges for screening in the MRI environment. Indeed, accidents and injuries have increased over the years along with the increased use of MRI. Accordingly, this has captured the attention of various organizations and entities including the United States (U.S.) Food and Drug Administration (FDA), the Joint Commission, and the American College of Radiology (ACR). Public awareness of MRI-related hazards has heightened as well, particularly due to the fatality of a young boy in 2001. The majority of accidents and injuries that have occurred in the MRI setting have been the result of insufficient or no screening procedures. Unfortunately, considerable subjectivity remains among the policies and procedures implemented by MRI fa-

380 MRI Screening for Patients and Individuals

cilities, despite screening recommendations presented as far back as 1987 and periodically revised and updated to the present day (1-23).

This chapter presents the purpose of comprehensive MRI screening concepts and discusses proper procedures. The recommended written screening forms to be used for individuals and patients are displayed and reviewed. Each section of these forms is explained, and justifications are given for the questions asked. Verbal MRI screening procedures are also reviewed, and the use of ferromagnetic detection systems as part of the screening process is discussed. Finally, secondary purposes and advantages of MRI screening are presented.

MRI SCREENING PROCEDURES

All patients undergoing MRI examinations must be screened prior to entering the MRI environment. Any other individual that needs to enter the MRI environment for any reason, even if just momentarily, must also be screened. This would include family members, friends, staff, visitors, field engineers, and emergency or security personnel such as firemen, police, and first responders. The screening process must include the completion of an MRI screening form by the patient or individual, followed by verbal MRI screening procedure conducted by the MRI technologist or other MRI safety-trained healthcare worker. Currently, many healthcare facilities have moved to electronic records that include MRI screening forms, while others still use paper forms. All MRI facilities (clinical or research) should embrace a specific MRI screening process that is both consistent and thorough. This should be part of the MRI center's formal written policy, to be followed without exception. To stay current, MRI facilities need to revise and update the screening protocol, on an ongoing and consistent basis.

SCREENING FORM AND PROCEDURES FOR PATIENTS

A variety of MRI screening forms are available from different sources, however, all variations of screening forms strive to achieve the same goal of 100% safety. A standard, two-page MRI screening form for patients developed by Frank G. Shellock, Ph.D. and available on www.MRIsafety.com is presented in **Figure 1** and **Figure 2** (the Spanish and Arabic language versions are shown in **Figures 3 to 6**). The ACR (American College of Radiology, www.ACR.org) also offers an MRI screening form (13, 15, 23). Before each MRI examination, proper MRI screening must be conducted for each patient. By way of example, this chapter will focus on the written screening forms provided on www.MRIsafety.com, which are in widespread use.

SAFETY QUESTIONS AND INFORMATION

The upper section on the first page of the screening form (**Figure 1**) asks for patient identification (ID) and demographics. This section must be completed and double checked for correct patient ID and MRI order or request. An incorrect patient or examination problem can easily occur during the fervor of an over-booked clinical schedule. The referring physician's name and telephone number should also be filled out, but this information may

MRI Bioeffects, Safety, and Patient Management 381

also be available at different information systems and may be different than the “ordering” physician. The rest of the first page of the screening form lists various medical and surgical history questions for the patient (note: certain questions pertain to female patients, only). Explanations of the questions and their importance to MRI screening are provided below.

Question #1 asks about previous surgeries or procedures. Many patient safety concerns in MRI are impacted by the response to this question, so it cannot be left unanswered. If the answer to Question #1 is “yes”, additional information must be given on types and dates of all surgeries and/or related procedures. Accuracy is paramount here, since information on potential implants, devices, and materials can be discovered. If the patient is a minor or is not fully aware of this information, a parent, guardian or other knowledgeable caregiver must assist in providing and verifying this information. Further review of the patient’s chart or medical records may be necessary. If previous surgery or other procedural information is not available at the time of the MRI examination, as with an outpatient who has arrived with a limited history, MRI must be postponed or rescheduled until this information can be captured and verified.

Question #2 asks about previous diagnostic imaging studies (MRI, computed tomography or CT, X-ray, ultrasound, nuclear medicine, etc.). The results of these examinations can help verify the patient’s surgical or other procedural history and assist in identifying the presence of an implant, device, or foreign body that may be of concern.

Question #3 asks the patient about problems related to a prior MRI examination. If the answer to this question is “yes”, the patient is asked to describe the problem, prompting the MRI technologist to investigate and otherwise consider this matter further. Notably, if the answer to this question is “no”, the patient cannot simply bypass the MRI screening process. A written screening form must still be completed, in case the patient that had a previous MRI exam performed had the placement of an implant, device, material, or encountered a foreign body. Assumptions should not be made that non-incidental; previous MRI examinations permit subsequent incident-free MRI procedures. Factors related to the MRI examination such as the orientation (i.e., vertical versus horizontal) and strength of the static magnetic field, maximum spatial gradient magnetic field, time-varying gradient magnetic fields, type of RF coil used, amount of RF power (specific absorption rate, SAR) and pulse sequence parameters can vary significantly among different MR systems. Careful investigation is required for implants or devices assumed to be “MR Safe” for a previous scanner, because this can change to “MR Conditional” or even “MR Unsafe” based on the MR system-related factors indicated above (15). The MRI technologist or radiologist can refer to the latest version of the *Reference Manual for Magnetic Resonance Safety, Implants, and Devices* (16), or visit the website, www.MRIsafety.com, for specific information pertaining to information for implants and devices. Notably, it may be necessary to consult the manufacturer of the implant or device for more information, especially if an electronically-activated implant is encountered (16).

Questions #4 and #5 ask the patient about personal injury involving a metallic object or foreign body. If the answer to either question is “yes”, further questioning must be conducted as to whether the object was removed entirely, and if not, the location and composition of the object must be investigated further. In the case of injuries involving the eyes,

382 MRI Screening for Patients and Individuals

Figure 1. The MRI Screening Form used to screen patients, page one.

MAGNETIC RESONANCE (MR) PROCEDURE SCREENING FORM FOR PATIENTS					
Date _____ / _____ / _____		Patient Number _____			
Name _____ Last name _____ First name _____		Middle Initial _____	Age _____	Height _____	Weight _____
Date of Birth _____ / _____ / _____		Male <input type="checkbox"/>	Female <input type="checkbox"/>	Body Part to be Examined _____	
Address _____ month day year			Telephone (home) (_____) ____ - _____		
City _____			Telephone (work) (_____) ____ - _____		
State _____		Zip Code _____			
Reason for MRI and/or Symptoms _____					
Referring Physician _____			Telephone (_____) ____ - _____		
1. Have you had prior surgery or an operation (e.g., arthroscopy, endoscopy, etc.) of any kind? <input type="checkbox"/> No <input type="checkbox"/> Yes If yes, please indicate the date and type of surgery: Date _____ / _____ / _____ Type of surgery _____ Date _____ / _____ / _____ Type of surgery _____					
2. Have you had a prior diagnostic imaging study or examination (MRI, CT, Ultrasound, X-ray, etc.)? If yes, please list: Body part _____ Date _____ Facility _____ MRI _____ / _____ / _____ CT/CAT Scan _____ / _____ / _____ X-Ray _____ / _____ / _____ Ultrasound _____ / _____ / _____ Nuclear Medicine _____ / _____ / _____ Other _____ / _____ / _____					
3. Have you experienced any problem related to a previous MRI examination or MR procedure? If yes, please describe: _____ <input type="checkbox"/> No <input type="checkbox"/> Yes					
4. Have you had an injury to the eye involving a metallic object or fragment (e.g., metallic slivers, shavings, foreign body, etc.)? If yes, please describe: _____ <input type="checkbox"/> No <input type="checkbox"/> Yes					
5. Have you ever been injured by a metallic object or foreign body (e.g., BB, bullet, shrapnel, etc.)? If yes, please describe: _____ <input type="checkbox"/> No <input type="checkbox"/> Yes					
6. Are you currently taking or have you recently taken any medication or drug? If yes, please list: _____ <input type="checkbox"/> No <input type="checkbox"/> Yes					
7. Are you allergic to any medication? If yes, please list: _____ <input type="checkbox"/> No <input type="checkbox"/> Yes					
8. Do you have a history of asthma, allergic reaction, respiratory disease, or reaction to a contrast medium or dye used for an MRI, CT, or X-ray examination? <input type="checkbox"/> No <input type="checkbox"/> Yes					
9. Do you have anemia or any disease(s) that affects your blood, a history of renal (kidney) disease, renal (kidney) failure, renal (kidney) transplant, high blood pressure (hypertension), liver (hepatic) disease, a history of diabetes, or seizures? If yes, please describe: _____ <input type="checkbox"/> No <input type="checkbox"/> Yes					
For female patients: 10. Date of last menstrual period: _____ / _____ / _____ Post menopausal? <input type="checkbox"/> No <input type="checkbox"/> Yes 11. Are you pregnant or experiencing a late menstrual period? <input type="checkbox"/> No <input type="checkbox"/> Yes 12. Are you taking oral contraceptives or receiving hormonal treatment? <input type="checkbox"/> No <input type="checkbox"/> Yes 13. Are you taking any type of fertility medication or having fertility treatments? If yes, please describe: _____ <input type="checkbox"/> No <input type="checkbox"/> Yes 14. Are you currently breastfeeding? <input type="checkbox"/> No <input type="checkbox"/> Yes					

MRI Bioeffects, Safety, and Patient Management 383

Figure 2. The MRI Screening Form used to screen patients, page two.

WARNING: Certain implants, devices, or objects may be hazardous to you and/or may interfere with the MR procedure (i.e., MRI, MR angiography, functional MRI, MR spectroscopy). Do not enter the MR system room or MR environment if you have any question or concern regarding an implant, device, or object. Consult the MRI Technologist or Radiologist BEFORE entering the MR system room. The MR system magnet is ALWAYS on.

Please indicate if you have any of the following:

<input type="checkbox"/> Yes	<input type="checkbox"/> No	Aneurysm clip(s)
<input type="checkbox"/> Yes	<input type="checkbox"/> No	Cardiac pacemaker
<input type="checkbox"/> Yes	<input type="checkbox"/> No	Implanted cardioverter defibrillator (ICD)
<input type="checkbox"/> Yes	<input type="checkbox"/> No	Electronic implant or device
<input type="checkbox"/> Yes	<input type="checkbox"/> No	Magnetically-activated implant or device
<input type="checkbox"/> Yes	<input type="checkbox"/> No	Neurostimulation system
<input type="checkbox"/> Yes	<input type="checkbox"/> No	Spinal cord stimulator
<input type="checkbox"/> Yes	<input type="checkbox"/> No	Internal electrodes or wires
<input type="checkbox"/> Yes	<input type="checkbox"/> No	Bone growth/bone fusion stimulator
<input type="checkbox"/> Yes	<input type="checkbox"/> No	Cochlear, otologic, or other ear implant
<input type="checkbox"/> Yes	<input type="checkbox"/> No	Insulin or other infusion pump
<input type="checkbox"/> Yes	<input type="checkbox"/> No	Implanted drug infusion device
<input type="checkbox"/> Yes	<input type="checkbox"/> No	Any type of prosthesis (eye, penile, etc.)
<input type="checkbox"/> Yes	<input type="checkbox"/> No	Heart valve prosthesis
<input type="checkbox"/> Yes	<input type="checkbox"/> No	Eyelid spring or wire
<input type="checkbox"/> Yes	<input type="checkbox"/> No	Artificial or prosthetic limb
<input type="checkbox"/> Yes	<input type="checkbox"/> No	Metallic stent, filter, or coil
<input type="checkbox"/> Yes	<input type="checkbox"/> No	Shunt (spinal or intraventricular)
<input type="checkbox"/> Yes	<input type="checkbox"/> No	Vascular access port and/or catheter
<input type="checkbox"/> Yes	<input type="checkbox"/> No	Radiation seeds or implants
<input type="checkbox"/> Yes	<input type="checkbox"/> No	Swan-Ganz or thermodilution catheter
<input type="checkbox"/> Yes	<input type="checkbox"/> No	Medication patch (Nicotine, Nitroglycerine)
<input type="checkbox"/> Yes	<input type="checkbox"/> No	Any metallic fragment, foreign body
<input type="checkbox"/> Yes	<input type="checkbox"/> No	Wire mesh implant
<input type="checkbox"/> Yes	<input type="checkbox"/> No	Tissue expander (e.g., breast)
<input type="checkbox"/> Yes	<input type="checkbox"/> No	Surgical staples, clips, or metallic sutures
<input type="checkbox"/> Yes	<input type="checkbox"/> No	Joint replacement (hip, knee, etc.)
<input type="checkbox"/> Yes	<input type="checkbox"/> No	Bone/joint pin, screw, nail, wire, plate, etc.
<input type="checkbox"/> Yes	<input type="checkbox"/> No	IUD, diaphragm, or pessary
<input type="checkbox"/> Yes	<input type="checkbox"/> No	Are you here for an MRI examination?
<input type="checkbox"/> Yes	<input type="checkbox"/> No	Dentures or partial plates
<input type="checkbox"/> Yes	<input type="checkbox"/> No	Tattoo or permanent makeup
<input type="checkbox"/> Yes	<input type="checkbox"/> No	Body piercing jewelry
<input type="checkbox"/> Yes	<input type="checkbox"/> No	Hearing aid

(Remove before entering MR system room)

Yes No Other implant _____

Yes No Breathing problem or motion disorder _____

NOTE: You may be advised or required to wear earplugs or other hearing protection during the MR procedure to prevent possible problems or hazards related to acoustic noise.

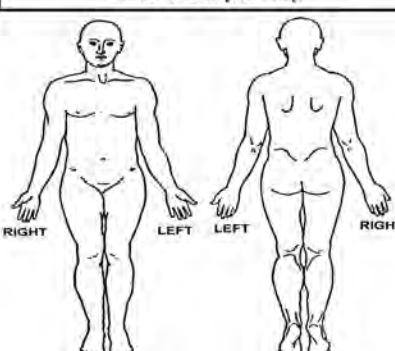
I attest that the above information is correct to the best of my knowledge, I read and understand the contents of this form and had the opportunity to ask questions regarding the information on this form and regarding the MR procedure that I am about to undergo.

Signature of Person Completing Form: _____ Signature: _____ Date: ____ / ____ / ____

Form Completed By: Patient Relative Nurse _____ Print name: _____ Relationship to patient: _____

Form Information Reviewed By: _____ Print name: _____ Signature: _____

MRI Technologist Nurse Radiologist Other _____



IMPORTANT INSTRUCTIONS

Before entering the MR environment or MR system room, you must remove all metallic objects including hearing aids, dentures, partial plates, keys, beeper, cell phone, eyeglasses, hair pins, barrettes, jewelry, body piercing jewelry, watch, safety pins, paperclips, money clip, credit cards, bank cards, magnetic strip cards, coins, pens, pocket knife, nail clipper, tools, clothing with metal fasteners, & clothing with metallic threads.

Please consult the MRI Technologist or Radiologist if you have any question or concern BEFORE you enter the MR system room.

384 MRI Screening for Patients and Individuals

Figure 3. The MRI Screening Form used to screen patients, Spanish language version, page one.

CUESTIONARIO PREVIO A ESTUDIO CON RESONANCIA MAGNÉTICA (MR) PARA PACIENTES																										
Fecha _____ / _____ / _____	Número de paciente _____																									
Nombre _____ Apellido _____	Primer Nombre _____	Segundo Nombre _____	Edad _____	Altura _____	Peso _____																					
Fecha de nacimiento _____ / _____ / _____ examinada _____	Varón <input type="checkbox"/>	Hembra <input type="checkbox"/>	Parte del cuerpo a ser mes _____ día _____ año _____																							
Dirección _____	Teléfono (domicilio) (_____) - _____																									
Ciudad _____	Teléfono (trabajo) (_____) - _____																									
Provincia _____	Código Postal _____																									
Motivo para el estudio de MRI y/o síntomas _____																										
Médico que le refirió _____	Teléfono (_____) - _____																									
1. Anteriormente, ¿le han hecho alguna cirugía u operación (e.g., artroscopia, endoscopía, etc.) de cualquier tipo? <input type="checkbox"/> No <input type="checkbox"/> Sí Si respondió afirmativamente, indique la fecha y que tipo de cirugía: Fecha _____ / _____ / _____ Tipo de cirugía _____ Fecha _____ / _____ / _____ Tipo de cirugía _____																										
2. Anteriormente, ¿le han hecho algún estudio o examen de diagnóstico (MRI, CT, Ultrasonido, Rayos-X, etc.)? <input type="checkbox"/> No <input type="checkbox"/> Sí Si respondió afirmativamente, describalos a continuación: <table style="width: 100%; border-collapse: collapse;"> <thead> <tr> <th style="width: 30%;">Parte del Cuerpo</th> <th style="width: 30%;">Fecha</th> <th style="width: 40%;">Lugar/Institución</th> </tr> </thead> <tbody> <tr> <td>MRJ</td> <td>/ /</td> <td></td> </tr> <tr> <td>CT/CAT</td> <td>/ /</td> <td></td> </tr> <tr> <td>Rayos-X</td> <td>/ /</td> <td></td> </tr> <tr> <td>Ultrasonido</td> <td>/ /</td> <td></td> </tr> <tr> <td>Medicina Nuclear</td> <td>/ /</td> <td></td> </tr> <tr> <td>Otro</td> <td>/ /</td> <td></td> </tr> </tbody> </table>						Parte del Cuerpo	Fecha	Lugar/Institución	MRJ	/ /		CT/CAT	/ /		Rayos-X	/ /		Ultrasonido	/ /		Medicina Nuclear	/ /		Otro	/ /	
Parte del Cuerpo	Fecha	Lugar/Institución																								
MRJ	/ /																									
CT/CAT	/ /																									
Rayos-X	/ /																									
Ultrasonido	/ /																									
Medicina Nuclear	/ /																									
Otro	/ /																									
3. ¿Ha tenido algún problema relacionado con estudios ó procedimientos anteriores con MR? <input type="checkbox"/> No <input type="checkbox"/> Sí Si respondió afirmativamente, describalos: 4. ¿Se ha golpeado el ojo con un objeto ó fragmento metálico (e.g., astillas metálicas, virutas, objeto extraño, etc.)? <input type="checkbox"/> No <input type="checkbox"/> Sí Si respondió afirmativamente, describa el incidente: 5. ¿Ha sido alcanzado alguna vez por un objeto metálico u objeto extraño (e.g., perdigones, bala, metralla, etc.)? <input type="checkbox"/> No <input type="checkbox"/> Sí Si respondió afirmativamente, describa el incidente: 6. ¿Está actualmente tomando ó ha recientemente tomado algún medicamento o droga? <input type="checkbox"/> No <input type="checkbox"/> Sí Si respondió afirmativamente, indique el nombre del medicamento: 7. ¿Es Ud. alérgico/a a algún medicamento? <input type="checkbox"/> No <input type="checkbox"/> Sí Si respondió afirmativamente, indique el nombre del medicamento: 8. ¿Tiene historia de asma, reacción alérgica, enfermedad respiratoria, ó reacción a contrastes ó tinturas usados en MRI, CT, ó Rayos-X? <input type="checkbox"/> No <input type="checkbox"/> Sí																										
9. ¿Tiene anemia u otra enfermedad que afecte su sangre, algún episodio de enfermedad de riñón, fracaso de riñón, un trasplante de riñón, hipertensión, la historia de la diabetes, relativo al hígado ó ataques epilépticos? <input type="checkbox"/> No <input type="checkbox"/> Sí Si respondió afirmativamente, describalos:																										
Para los pacientes femeninos: 10. Fecha de su último período menstrual: _____ / _____ / _____ En la menopausia? <input type="checkbox"/> No <input type="checkbox"/> Sí 11. ¿Está embarazada ó tiene retraso con su período menstrual? <input type="checkbox"/> No <input type="checkbox"/> Sí 12. ¿Está tomando contraceptivos orales ó recibiendo tratamiento hormonal? <input type="checkbox"/> No <input type="checkbox"/> Sí 13. ¿Está tomando algún tipo de medicamento para la fertilidad ó recibiendo tratamientos de fertilidad? <input type="checkbox"/> No <input type="checkbox"/> Sí Si responde afirmativamente, describalos a continuación: 14. ¿Está amamantando a su bebé? <input type="checkbox"/> No <input type="checkbox"/> Sí																										
Translation by Olga Fernández-Flygare, M.S., Brain Mapping Center, UCLA School of Medicine, Los Angeles, CA																										

MRI Bioeffects, Safety, and Patient Management 385

Figure 4. The MRI Screening Form used to screen patients, Spanish language version, page two.

	ADVERTENCIA: Ciertos implantes, dispositivos, u objetos pueden ser peligrosos y/o pueden interferir con el procedimiento de resonancia magnética (es decir, MRI, MR angiografía, MRI funcional, MR espectroscopia). No entre a la sala del escáner de MR o a la zona del laboratorio de MR si tiene alguna pregunta o duda relacionadas con un implante, dispositivo, u objeto. Consulte con el técnico o radiólogo de MRI ANTES de entrar a la sala del escáner de MR. Recuerde que el imán del sistema MR está SIEMPRE encendido.
Por favor indique si tiene alguno de los siguientes:	
<input type="checkbox"/> Sí <input type="checkbox"/> No Pinza(s) de aneurisma <input type="checkbox"/> Sí <input type="checkbox"/> No Marcapasos cardíaco <input type="checkbox"/> Sí <input type="checkbox"/> No Implante con desfibrilador para conversión cardíaca (ICD) <input type="checkbox"/> Sí <input type="checkbox"/> No Implante electrónico ó dispositivo electrónico <input type="checkbox"/> Sí <input type="checkbox"/> No Implante ó dispositivo activado magnéticamente <input type="checkbox"/> Sí <input type="checkbox"/> No Sistema de neuroestimulación <input type="checkbox"/> Sí <input type="checkbox"/> No Estimulador de la médula espinal <input type="checkbox"/> Sí <input type="checkbox"/> No Electrodo(s) ó alambres internos <input type="checkbox"/> Sí <input type="checkbox"/> No Estimulador de crecimiento/fusión del hueso <input type="checkbox"/> Sí <input type="checkbox"/> No Implante coclear, otológico, u otro implante del oído <input type="checkbox"/> Sí <input type="checkbox"/> No Bomba de infusión de insulina ó similar <input type="checkbox"/> Sí <input type="checkbox"/> No Dispositivo implantado para infusión de medicamento <input type="checkbox"/> Sí <input type="checkbox"/> No Cualquier tipo de prótesis (ojo, peneal, etc.) <input type="checkbox"/> Sí <input type="checkbox"/> No Prótesis de válvula cardíaca <input type="checkbox"/> Sí <input type="checkbox"/> No Muelle ó alambre del párpado <input type="checkbox"/> Sí <input type="checkbox"/> No Extremidad artificial ó protésica <input type="checkbox"/> Sí <input type="checkbox"/> No Malla metálica (stent), filtro, ó anillo metálico <input type="checkbox"/> Sí <input type="checkbox"/> No Shunt (espinal ó intraventricular) <input type="checkbox"/> Sí <input type="checkbox"/> No Catéter y/u orificio de acceso vascular <input type="checkbox"/> Sí <input type="checkbox"/> No Semillas ó implantes de radiación <input type="checkbox"/> Sí <input type="checkbox"/> No Catéter de Swan-Ganz ó de termodilución <input type="checkbox"/> Sí <input type="checkbox"/> No Parche de medicamentos (Nicotina, Nitroglicerina) <input type="checkbox"/> Sí <input type="checkbox"/> No Cualquier fragmento metálico ó cuerpo extraño <input type="checkbox"/> Sí <input type="checkbox"/> No Implante tipo malla <input type="checkbox"/> Sí <input type="checkbox"/> No Aumentador de tejidos (e.g. pecho) <input type="checkbox"/> Sí <input type="checkbox"/> No Grapas quirúrgicas, clips, ó suturas metálicas <input type="checkbox"/> Sí <input type="checkbox"/> No Articulaciones artificiales (cadera, rodilla, etc.) <input type="checkbox"/> Sí <input type="checkbox"/> No Varilla de hueso/coyuntura, tornillo, clavo, alambre, chapas, etc. <input type="checkbox"/> Sí <input type="checkbox"/> No Dispositivo intrauterino (IUD), diafragma, ó pessario <input type="checkbox"/> Sí <input type="checkbox"/> No Dentaduras ó placas parciales <input type="checkbox"/> Sí <input type="checkbox"/> No Tatuaje ó maquillaje permanente <input type="checkbox"/> Sí <input type="checkbox"/> No Perforación (piercing) del cuerpo <input type="checkbox"/> Sí <input type="checkbox"/> No Audífono (<i>Quíteselo antes de entrar a la sala del escáner de MR</i>) <input type="checkbox"/> Sí <input type="checkbox"/> No Otro implante _____ <input type="checkbox"/> Sí <input type="checkbox"/> No Problema respiratorio ó desorden del movimiento	
Por favor marque en la imagen de abajo la localización de cualquier implante ó metal en su cuerpo.	
¡AVISO IMPORTANTE!	
<p>Antes de entrar a la zona de MR ó a la sala del escáner de MR, tendrá que quitarse todo objeto metálico incluyendo audífono, dentaduras, placas parciales, llaves, beeper, teléfono celular, lentes, horquillas de pelo, pasadores, todas las joyas (incluyendo "body piercing"), reloj, alfileres, sujetapapeles, clip de billetes, tarjetas de crédito ó de banco, toda tarjeta con banda magnética, monedas, plumas, cuchillos, corta uñas, herramientas, ropa con enganches de metal, y ropa con hilos metálicos.</p>	
<p>Por favor consulte con el Técnico de MRI ó Radiólogo si tiene alguna pregunta o duda ANTES de entrar a la sala de escáner de MR.</p>	
NOTA: Es posible se le pida usar auriculares u otra protección para prevenir problemas ó riesgos asociados al nivel de ruido en la sala de escáner de MRI.	
<p>Atestigüo que la información anterior es correcta según mi mejor entender. Leo y entiendo el contenido de este cuestionario y he tenido la oportunidad de hacer preguntas en relación a la información en el cuestionario y en relación al estudio de MR al que me voy a someter a continuación.</p>	
Firma de la persona llenando este cuestionario: _____ Firma _____ Fecha _____ / _____ / _____	
Cuestionario lleno por: <input type="checkbox"/> Paciente <input type="checkbox"/> Pariente <input type="checkbox"/> Enfermera _____ Firma _____ Nombre en letra de texto _____ Relación con el paciente _____	
Información revisada por: _____ Nombre en letra de texto _____ Relación con el paciente _____	
<input type="checkbox"/> Técnico de MRI <input type="checkbox"/> Enfermera <input type="checkbox"/> Radiólogo <input type="checkbox"/> Otro _____ Firma _____	
<small>Translated by Olga Esmonde-Feijoo, M.S., Brain Mapping Center, UCLA School of Medicine, Los Angeles, CA</small>	

386 MRI Screening for Patients and Individuals

Figure 5. The MRI Screening Form used to screen patients, Arabic language version, page one.

الرنين المغناطيسي (MRI) : نموذج الأسئلة التي يجب أن يجيب عليها المريض قبل فحص التصوير بالرنين									
الاسم	الاسم الأول	الاسم الأب	الجد	العائلة	الطول	الوزن	كغم	رقم ملف المريض	التاريخ
تاريخ الميلاد	يوم	شهر	سنة						
العنوان									
المدينة									
البلد									
الرمز البريدي									
سبب صورة الرنين أو الأعراض									
اسم الطبيب المعالج									
رقم هاتف الطبيب									
(____) - _____	(____) - _____	(____) - _____	(____) - _____	(____) - _____	(____) - _____	(____) - _____	(____) - _____	(____) - _____	(____) - _____
1. هل خضعت سابقاً للجراحة أو أي عمليات طبية (مثل، تقطير المفاصل، المنظار العام، إلخ.) من أي نوع؟ إذا كانت الإجابة نعم، فضلاً رقم بكتابة التاريخ ونوع العملية الجراحية :									
التاريخ	نوع الجراحة								
التاريخ	نوع الجراحة								
2. هل أجريت أي صور طبية أو فحوصات تشخيصية (رنين مغناطيسي، تصوير طبيقي، سونار، أشعة سينية، إلخ.) لا إذا كانت الإجابة نعم ، فضلاً اذكر: عضو الجسم									
الرنين المغناطيسي									
التصوير الطبيقي									
الأشعة السينية									
الموجات الصوتية									
الطب النووي									
آخر									
3. هل واجهت أي مشاكل سابقاً متعلقة بتصوير الرنين المغناطيسي أو إجراءات الرنين المغناطيسي؟ إذا كانت الإجابة نعم ، فضلاً اذكر:									
نعم	لا								
4. هل تعرضت لاصابة سابقاً في العين بجسم معدني أو شظية (مثل، خراطة المعدن، برادة الحديد، إلخ) إذا كانت الإجابة نعم ، فضلاً اذكر:									
نعم	لا								
5. هل تعرضت للإصابة بجسم معدني غريب (مثل، خردق الصيد، رصاص، سطوايا معدنية، إلخ) إذا كانت الإجابة نعم ، فضلاً اذكر:									
نعم	لا								
6. هل تأخذ حالياً أو أخذت مؤخراً أي أدوية أو مستحضرات طبية؟ إذا كانت الإجابة نعم ، فضلاً اذكرها:									
نعم	لا								
7. هل لديك حساسية من أي أدوية؟ إذا كانت الإجابة نعم ، فضلاً اذكرها:									
نعم	لا								
8. هل تعاني من الربو أو الازمة الصدرية ، تحسس ، أمراض تنفسية ، أو تعرضت لردة فعل تحسيسي سبب المادة الملوونة أو سبيكة التصوير المستخدمة في فحوصات الرنين المغناطيسي أو التصوير الطبيقي أو الأشعة السينية؟ إذا كانت الإجابة نعم ، فضلاً اذكرها:									
نعم	لا								
9. هل لديك فقر دم أو أي مرض (أمراض) مؤثرة في الدم ، أو تاريخ مرضي في الكلى ، أو فشل كلوي ، أجريت زراعة كلٍى ، أو تعاني من ارتفاع ضغط الدم ، أو أمراض الكبد ، السكري ، أو ثوبات صرع؟ إذا كانت الإجابة نعم ، فضلاً اذكر:									
نعم	لا								
10. هل جميع الأسئلة السابقة واضحة بالنسبة لكم؟ للسيدات :									
نعم	لا								
11. هل يوجد حمل أو هناك تأخر في موعد الدورة الشهرية؟ هل تتناولين حبوب منع الحمل أو تأخذين علاج هرموني؟									
نعم	لا								
نعم	لا								
نعم	لا								
12. هل تتناولين أي نوع من أدوية الخصوبة أو تأخذين علاج للعقم؟ إذا كانت الإجابة نعم ، فضلاً اذكرها:									
نعم	لا								
13. هل أنت حالياً مرضعة؟									
نعم	لا								

Translated by: Ayman Darwish MRT (MR) (R)

Figure 6. The MRI Screening Form used to screen patients, Arabic language version, page two.

تحذير: بعض الغرستات الجراحية أو الأجهزة الطبية المزروعة داخل الجسم من المحمّل أن تشكّل خطورة عليك أو أن تؤثّر سلباً على فحص الرنين المغناطيسي (صورة الرنين العادي، تصوير الشرايين بالرنين، صورة الرنين الوظيفية، التحليل الطيفي بالرنين المغناطيسي) أو كلاهما معاً. لاتدخل غرفة الرنين المغناطيسي أو الأماكن المخصصة به إذا كان لديك شيك أو قلق حيال جهاز طبي مزروع داخل جسمك أو أي غرسة معنوية. قم بإبتناءه على خصائصي الرنين المغناطيسي أو طبيب الأشعة قبل دخول محيط جهاز الرنين المغناطيسي. المجال المغناطيسي لجهاز الرنين دائمًا في وضع التشغيل	
	
يرجى توضيح ما إذا كان لديك أي مما يلي:	
<input type="checkbox"/> لا <input checked="" type="checkbox"/> نعم مشبك أو مدمج الدم الدماغية (تمدد الأوعية الدموية) <input type="checkbox"/> لا <input checked="" type="checkbox"/> نعم جهاز تنظيم ضربات القلب <input type="checkbox"/> لا <input checked="" type="checkbox"/> نعم مزيل الرفakan الطيفي المغروس <input type="checkbox"/> لا <input checked="" type="checkbox"/> نعم أجهزة الكترونية أو زرارات طيبة داخل الجسم <input type="checkbox"/> لا <input checked="" type="checkbox"/> نعم اجهزه مغناطيسية مزروعة داخل الجسم <input type="checkbox"/> لا <input checked="" type="checkbox"/> نعم جهاز الحفاظ الشوكي <input type="checkbox"/> لا <input checked="" type="checkbox"/> نعم الأقطاب الداخلية أو الأسلاك الطيبة <input type="checkbox"/> لا <input checked="" type="checkbox"/> نعم مخزز نمو الثلمان العظام <input type="checkbox"/> لا <input checked="" type="checkbox"/> نعم زرارات في القوحة، الأنف أو القناة السمعية <input type="checkbox"/> لا <input checked="" type="checkbox"/> نعم مضخة الإنسولين أو أي مضخات أخرى <input type="checkbox"/> لا <input checked="" type="checkbox"/> نعم أجهزة حقن الأدوية المغروسة في الجسم <input type="checkbox"/> لا <input checked="" type="checkbox"/> نعم الأصداء الصناعية في (العين، القصبة، الخ) يمين <input type="checkbox"/> لا <input checked="" type="checkbox"/> نعم صمام القلب الصناعي <input type="checkbox"/> لا <input checked="" type="checkbox"/> نعم نابض أو زنبرك في جفن العين <input type="checkbox"/> لا <input checked="" type="checkbox"/> نعم الأطراف الصناعية <input type="checkbox"/> لا <input checked="" type="checkbox"/> نعم الدعامات المعنوية، فلت، أو لفائف <input type="checkbox"/> لا <input checked="" type="checkbox"/> نعم علوية التحويل من الدماغ أو الحبل الشوكي للبطن <input type="checkbox"/> لا <input checked="" type="checkbox"/> نعم منفذ وصول الأوعية الدموية / أو القسطرة <input type="checkbox"/> لا <input checked="" type="checkbox"/> نعم بذور مشعة في عدة البروستاتا <input type="checkbox"/> لا <input checked="" type="checkbox"/> نعم سوان-غانز أو قسطرةقياس فرق الحرارة <input type="checkbox"/> لا <input checked="" type="checkbox"/> نعم لسقات دوائية (بيكتين، لصفة النيتروزوبيريم) <input type="checkbox"/> لا <input checked="" type="checkbox"/> نعم أي جزء معدني أو غيره داخل الجسم <input type="checkbox"/> لا <input checked="" type="checkbox"/> نعم شبكات معدنية طيبة داخل الجسم <input type="checkbox"/> لا <input checked="" type="checkbox"/> نعم موسوعة الأنسجة (مثل، الثدي، الخ) <input type="checkbox"/> لا <input checked="" type="checkbox"/> نعم دبليوس أو مشبك جراحية أو غرز ، قطب معدنية <input type="checkbox"/> لا <input checked="" type="checkbox"/> نعم مفاصل صناعية (الفخذ، الركبة، الخ) <input type="checkbox"/> لا <input checked="" type="checkbox"/> نعم مسامير ، أسلاك ، صفائح أو برااغي العظام والمفاصل <input type="checkbox"/> لا <input checked="" type="checkbox"/> نعم اللوكيل أو أدوات منع الحمل <input type="checkbox"/> لا <input checked="" type="checkbox"/> نعم أقطم الأسنان أو التركيبات المتحركة <input type="checkbox"/> لا <input checked="" type="checkbox"/> نعم الوشم أو مكياج دائم <input type="checkbox"/> لا <input checked="" type="checkbox"/> نعم الأقراط أو حلقات المعلقة بالجسم <input type="checkbox"/> لا <input checked="" type="checkbox"/> نعم مساعدات السمع (قم ببارتها قبل دخول صورة الرنين) <input type="checkbox"/> لا <input checked="" type="checkbox"/> نعم أي زرارات طيبة أخرى <input type="checkbox"/> لا <input checked="" type="checkbox"/> نعم صعوبة في التنفس أو اضطرابات في الحركة <input type="checkbox"/> لا <input checked="" type="checkbox"/> نعم الخوف من الأماكن الضيقة	
ملاحظة: قد ينصح أو يطلب منك ارتداء سدادات الأنف أو غيرها من وسائل حماية من المشاكل المختلطة أو المخاطر المتعلقة بالضوضاء الصوتية. إجراء الرنين المغناطيسي وذاك للحماية من المشاكل المختلطة أو المخاطر المتعلقة بالضوضاء الصوتية.	
<p>أقر بأن جميع المعلومات المذكورة أعلاه صحيحة على حد علمي. لقد قمت بقراءة وفهم محتويات هذا النموذج وأتيحت لي الفرصة لطرح الأسئلة التوضيحية المتعلقة بالمعلومات المذكورة أعلاه وبها يتعلق بفحص الرنين المغناطيسي الذي سوف أضع له.</p> <p>_____ التاريخ _____</p> <p>توقيع الشخص الذي قام بالإجابة على النموذج: _____</p> <p>تمت تعبئة النموذج بواسطة: <input type="checkbox"/> المريض نفسه <input type="checkbox"/> أحد الأقارب <input type="checkbox"/> التمريض _____</p> <p>صلة القرابة بالمريض _____</p> <p>الاسم _____</p> <p>التوقيع _____</p> <p>تمت مراجعة المعلومات في النموذج بواسطة: _____</p> <p>الاسم _____</p> <p>التوقيع _____</p> <p><input type="checkbox"/> أخصائي الرنين المغناطيسي <input type="checkbox"/> طبيب الأشعة <input type="checkbox"/> شخص آخر</p>	

388 MRI Screening for Patients and Individuals

it is important to negate the presence of any remaining metal. If the patient answers that an orbital metal foreign body (e.g., fragment, sliver, bullet, BB, shrapnel, welding slag, etc.) does remain or is unsure, the MRI exam must be postponed or rescheduled, and the patient is not allowed to enter the MRI environment. If the patient cannot recount with confidence that all metallic foreign bodies within the orbit(s) have been removed, an X-ray is indicated to determine the presence of metal. If the X-ray is unremarkable, and MRI screening is otherwise complete, the examination can be performed. If the X-ray identifies the presence of any non-surgical orbital metal, the MRI examination must be cancelled. Under certain circumstances, the radiologist may allow the MRI procedure to proceed if the X-rays show the metal is of relatively low mass, located in an extra-orbital, non-threatening position, or it has been determined that the metal is non-ferrous.

Questions #6 and #7 ask the patient about current medications and allergies to medications. These questions may not be directly related to MRI safety, but if the patient needs to receive emergency medical attention, such information could be vital. Some patients may complain of problems such as vertigo, headache, or memory loss immediately following MRI, or days after the exam. In such cases, it can be helpful to the radiologist or clinician to check the written screening form for medications the patient listed, as these may help explain the patient's symptoms. Many radiologists can attest to incidents where patients mistakenly associated medical problems with an MRI procedure or other imaging modality.

Question #8 asks about asthma, allergic reaction, or respiratory disease, but also specifically asks about prior reaction to contrast medium used in MRI, CT, or X-ray. It is not uncommon for patients to cite previous episodes of transient flushing, metallic taste, or nausea immediately following an injection. Unpleasant as it is for the patients, such transient symptoms are usually harmless. Notably, adverse reactions to MRI contrast agents can occur, although serious reactions such as anaphylactic responses to a gadolinium-based contrast agent (GBCA) are extremely rare. If the patient indicates a previous reaction to what they perceive as "dye", further questioning will be needed to clarify this matter. The patient may not make the distinction between CT and MRI, nor between GBCAs and iodinated contrast agents used in X-ray and CT. A polite but thorough interview with the patient should be able to determine the severity of a previous adverse event and which contrast agent was administered. If available, a review of the patient's chart or medical records should be done for clarification.

Question #9 asks about anemia or other blood diseases, renal or hepatic disease, diabetes, and seizures. Importantly, MRI contrast agents may be contraindicated for some of these conditions. For example, the use of GBCAs has emerged as an MRI safety concern in patients with renal insufficiency because certain GBCAs have been implicated in causing nephrogenic systemic fibrosis (NSF) and some gadolinium may be retained in the patient's body (16). Hence, the results of a glomerular filtration rate (GFR) test must be obtained prior to a GBCA administration in patients with suspected renal insufficiency. This important topic is discussed in considerable detail in another chapter of this textbook.

Questions #10 through #14 pertain to female patients, asking about possible pregnancy, menstrual cycle, and breastfeeding. Prior to entering the MRI environment, any patient who is unsure about pregnancy must undergo a pregnancy test. If the patient is pregnant, a con-

Figure 7. The MRI Screening Form used to screen individuals (i.e., nonpatients).

MAGNETIC RESONANCE (MR) ENVIRONMENT SCREENING FORM FOR INDIVIDUALS*					
 <p>The MR system has a very strong magnetic field that may be hazardous to individuals entering the MR environment or MR system room if they have certain metallic, electronic, magnetic, or mechanical implants, devices, or objects. Therefore, all individuals are required to fill out this form BEFORE entering the MR environment or MR system room. Be advised, the MR system magnet is ALWAYS on.</p>					
*NOTE: If you are a patient preparing to undergo an MR examination, you are required to fill out a different form.					
Date _____ month / day / year	Name _____ Last Name _____	First Name _____	Middle Initial _____	Age _____	
Address _____			Telephone (home) (_____) ____-_____		
City _____			Telephone (work) (_____) ____-_____		
State _____		Zip Code _____			
1. Have you had prior surgery or an operation (e.g., arthroscopy, endoscopy, etc.) of any kind? <input type="checkbox"/> No <input type="checkbox"/> Yes If yes, please indicate date and type of surgery: Date _____ / _____ / _____ Type of surgery _____ 2. Have you had an injury to the eye involving a metallic object (e.g., metallic slivers, foreign body)? <input type="checkbox"/> No <input type="checkbox"/> Yes If yes, please describe: _____ 3. Have you ever been injured by a metallic object or foreign body (e.g., BB, bullet, shrapnel, etc.)? If yes, please describe: _____ <input type="checkbox"/> No <input type="checkbox"/> Yes 4. Are you pregnant or suspect that you are pregnant? <input type="checkbox"/> No <input type="checkbox"/> Yes					
 <p>WARNING: Certain implants, devices, or objects may be hazardous to you in the MR environment or MR system room. Do not enter the MR environment or MR system room if you have any question or concern regarding an implant, device, or object.</p>					
Please indicate if you have any of the following: <input type="checkbox"/> Yes <input type="checkbox"/> No Aneurysm clip(s) <input type="checkbox"/> Yes <input type="checkbox"/> No Cardiac pacemaker <input type="checkbox"/> Yes <input type="checkbox"/> No Implanted cardioverter defibrillator (ICD) <input type="checkbox"/> Yes <input type="checkbox"/> No Electronic implant or device <input type="checkbox"/> Yes <input type="checkbox"/> No Magnetically-activated implant or device <input type="checkbox"/> Yes <input type="checkbox"/> No Neurostimulation system <input type="checkbox"/> Yes <input type="checkbox"/> No Spinal cord stimulation system <input type="checkbox"/> Yes <input type="checkbox"/> No Cochlear implant or implanted hearing aid <input type="checkbox"/> Yes <input type="checkbox"/> No Insulin or infusion pump <input type="checkbox"/> Yes <input type="checkbox"/> No Implanted drug infusion device <input type="checkbox"/> Yes <input type="checkbox"/> No Any type of prosthesis or implant <input type="checkbox"/> Yes <input type="checkbox"/> No Artificial or prosthetic limb <input type="checkbox"/> Yes <input type="checkbox"/> No Any metallic fragment or foreign body <input type="checkbox"/> Yes <input type="checkbox"/> No Are you going into the MRI system room? <input type="checkbox"/> Yes <input type="checkbox"/> No Any external or internal metallic object <input type="checkbox"/> Yes <input type="checkbox"/> No Hearing aid <i>(Remove before entering the MR system room)</i> <input type="checkbox"/> Yes <input type="checkbox"/> No Other implant					
 <p>IMPORTANT INSTRUCTIONS</p> <p>Remove all metallic objects before entering the MR environment or MR system room including hearing aids, beeper, cell phone, keys, eyeglasses, hair pins, barrettes, jewelry (including body piercing jewelry), watch, safety pins, paperclips, money clip, credit cards, bank cards, magnetic strip cards, coins, pens, pocket knife, nail clipper, steel-toed boots/shoes, and tools. Loose metallic objects are especially prohibited in the MR system room and MR environment.</p> <p>Please consult the MRI Technologist or Radiologist if you have any question or concern BEFORE you enter the MR system room.</p>					
<p>I attest that the above information is correct to the best of my knowledge. I have read and understand the entire contents of this form and have had the opportunity to ask questions regarding the information on this form.</p> <p>Signature of Person Completing Form: _____ Date _____ / _____ / _____ <small>Print name _____ Signature _____</small></p> <p>Form Information Reviewed By: _____ Print name _____ Signature _____</p> <p><input type="checkbox"/> MRI Technologist <input type="checkbox"/> Radiologist <input type="checkbox"/> Other _____</p>					

390 MRI Screening for Patients and Individuals

sultation between the patient, radiologist and referring clinician is required in assessing the risk versus benefit of performing the MRI examination. The ACR recommends the use of MRI in pregnant patients if other non-ionizing imaging modalities are diagnostically inadequate, or ionizing procedures would otherwise have to be performed to answer critical clinical questions about the patient or fetus (15, 23). Furthermore, MRI may be performed without written or verbal informed consent in pregnant patients (15, 23).

Non-pregnant patients should still answer questions #10 through #14 to the best of their ability, especially if they are scheduled for a breast or pelvic MRI. This information can aid the radiologist to interpret the results of the MRI procedure since hormonal changes induced by menstrual cycle, fertility treatments, and breastfeeding can alter tissue contrast on MR images. In particular, hormonal changes directly impact the timing and rate of breast tissue enhancement following the administration of a GBCA. Also, breastfeeding patients (Question #14) will be instructed to refrain from breastfeeding for 24-hours following administration of a GBCA (while continuing to express and discard the breast milk). This will help ensure that suckling infants ingest negligible amounts of gadolinium chelates.

The top of the second page of the screening form for patients is intended to capture the attention of the patient or individual filling out the form (**Figure 2**). A “bold” warning statement is issued that certain implants, devices, or objects may be hazardous, and/or interfere with the MRI procedure. Thus, the patient is instructed not to enter the MRI environment if he or she has any question concerning an implant, device or object, and to consult the radiologist or MRI technologist before entering the MR system room. The patient or individual is also reminded that the “MR system magnet is ALWAYS on!” This warning statement is not intended to frighten patients or individuals who may already be anxious about their ensuing exam, but rather to discourage those who otherwise might wander into restricted areas in the MRI environment.

The middle section of the second page, the screening form lists thirty-five implant or device categories of potential concern. The patient or individual filling out the form is asked to indicate whether he or she possesses any implant or device by checking a “Yes” or “No” box. By doing so, the patient or individual may recall previous forgotten surgeries or procedures that involved the implants or devices listed. If the patient has an implant or device not listed, the patient is asked to write it down at the bottom of the list. If the patient or individual does possess an implant, device, object, or metal on or in the body, he or she is instructed to indicate the location(s) on the diagrams of the human body (anterior and posterior views) provided on the form.

Below the body sketch diagrams, the patient or individual is reminded to remove all metal objects such as hearing aids, dentures, jewelry, eyeglasses, keys, cell phones, belts, and other objects before entering the MR system room. Articles of clothing containing metal such as buttons, zippers and wires should also be removed. Some clothing manufacturers have recently been incorporating anti-microbial silver, copper microfibers, or other metallic components in sportswear and undergarments. These metallic fibers are often not detectable in the fabric and product labeling is often unreliable. The metal in the clothing may be non-ferromagnetic but can still degrade image quality if located proximal to the region being scanned. More importantly, the metallic components found in fabric are conductive and,

thus, may excessively heat during certain MRI conditions, causing burn injuries in patients. As a critical policy, MRI facilities should require patients to remove all clothing and change into a gown or scrubs that have no pockets as part of the screening process. Lockers must be provided to secure the belongings of patients and other individuals. Without harsh interrogation or inappropriate searching, the MRI technologist must always check the patient or individual to verify that all metal of concern has been removed prior to entering the MR system room. Some facilities refer to this second check as the “Full Stop and Final Check” (22, 23).

During the screening process, questions may be asked about breathing problems, movement disorders, or claustrophobia. These questions are used to assess the patient’s general ability to hold still and tolerate the MRI procedure. These issues are not too critical for safety, but may determine whether the patient needs extra attention or sedation, which will dictate scheduling times and different MRI facility staffing needs.

Hearing protection for the patient or individual is also recommended on the MRI screening form, which reflects many early guidelines pertaining to this matter as well as current ACR recommendations (15, 23). In the distribution of hearing protection such as disposable earplugs, the MRI technologist or trained healthcare worker should assist the patient or individual in placement of the disposable earplugs. Some individuals will have difficulty in properly positioning the earplugs, especially if the ear canal is curved. At times, it may be necessary to immobilize the earplugs in place by using hypoallergenic tape to prevent them from loosening during the exam. The ear canals of small infants often will not accommodate conventional foam earplugs, but the earplugs can easily be cut to fit (any cutting with tools such as scissors or knives must of course be done outside the MRI environment) or alternative hearing protection devices can be used in these cases.

The last section on the second page of the MRI screening form provides a place for the person completing the form to sign, print name, and date the form. When signing, the patient attests that the information provided on the form is correct. For a minor, a parent or legal guardian should print their name and sign the form. If the patient is unable to sign the form, an authorized relative or knowledgeable healthcare professional may need to sign (**Figure 8**). The MRI technologist, or other appropriately trained staff who reviewed the form and conducted the verbal interview must also print their name and sign this document (**Figure 9**). If the completed form is handed off to another MRI technologist to perform the MRI examination, care must be taken that the scanning MRI technologist checks the form to be sure that it was reviewed and signed. This final step must be done prior to escorting the patient or individual into the MR system room (**Figure 10**).

In the event that the patient is comatose or for whatever reason unable to verbally communicate, the written screening form should be completed by the most qualified individual (e.g., physician, family member, etc.) that has knowledge about the patient’s medical history and present condition. If the screening information is inadequate, it is advisable to look for surgical scars on the patient and/or to obtain plain films of the skull and/or chest to search for implants that may be particularly hazardous in the MRI environment (e.g., aneurysm clips, cardiac pacemakers, neuromodulation systems, etc.) (15, 16, 23).

392 MRI Screening for Patients and Individuals



Figure 8. Patient in Zone II preparing for MRI exam by filling out the written screening form in the presence of an MRI technologist.

WRITTEN SCREENING FORM AND PROCEDURES FOR INDIVIDUALS

As stated previously, any individual other than the patient that needs to enter the MRI environment for any reason must also complete a written screening form (**Figure 7**). This form is basically an abbreviated version of the patient MRI screening form. Whether the MRI facility is in a hospital, clinic, or free-standing imaging center, a certain amount of employee turnover is inevitable. New physicians or house staff, MRI technologists, nurses, anesthesia staff, medical assistants, students, and other staff members will rotate through the MRI center, some of which will need to enter the MRI environment. MRI screening is also required for caregivers, security personnel, fire fighters, and others. No one is exempt from completing the screening form and going through the screening process prior to entering the MRI environment. For individuals that must frequently enter the MRI environment as part of their duty, such as an MRI technologist, the screening form can be completed initially and kept on file. Any subsequent changes to an individual's medical or physical history such as a surgical procedure with placement of an implant, pregnancy, exposure to shrapnel or other similar matter will void the prior MRI clearance on file. It is the individual's responsibility to make this known so that the re-screening and/or updating of screening history can take place.

Importantly, if for any reason the individual other than the patient, need to enter the MR system itself (e.g., moving partially into the bore of the scanner to help manage the patient) and, thus, become exposed to the electromagnetic fields used for the MRI procedure, this person must be screened prior to entry using the detailed form for patient screening.

VERBAL SCREENING PROCEDURES

Equally important to the completion of the MRI screening forms for both patients and other individuals is the verbal screening procedure or interview (**Figure 9**). Additional information or clarification of information about prior surgeries, procedures, or incidents is often obtained during this time. The interview provides a mechanism for clarification or confirmation of the answers to the questions posed to the patient so that there is no miscommunication regarding important MRI safety issues. In addition, because the patient may not be fully aware of the medical terminology used for a particular implant or device, it is imperative that this particular information on the form be discussed during the verbal interview. Additionally, a patient might be reluctant to indicate a pregnancy or foreign body on the written form in the presence of family or friends, but honesty might prevail in a private interview with the MRI technologist or MRI safety-trained healthcare worker. Due to cultural or religious reasons, some patients may ask for a male or female MRI technologist to conduct the interview. Questions, misconceptions, and fears that the patient might harbor can also be discussed and answered. Both the stress of the patient and the difficulty of the MRI examination can be reduced as a result of a satisfactorily performed, verbal screening procedure.

With the use of any type of written questionnaire, limitations exist related to incomplete or incorrect answers provided by the patient or individual. For example, there may be difficulties associated with patients that are impaired with respect to their vision, language flu-

Figure 9. The MRI technologist conducts a verbal interview and helps the patient prepare for the MRI examination by doing final preparations and checks.



394 MRI Screening for Patients and Individuals

ency, or level of literacy. Therefore, an appropriate accompanying family member or other individual (e.g., referring physician) should be involved in the screening process to verify information that may impact patient safety. Versions of the screening form (**Figures 3 to 6**) should be available in other languages, as needed (i.e., specific to the demographics of the MRI facility).



Figure 10. Following the completion of MRI screening, the MRI technologist escorts the patient through a ferromagnetic detection system in Zone III, and into the Zone IV, the MR system room.



Figure 11. Typical location of a mounted ferromagnetic detection system in Zone III (outside of the MR system room).

THE USE OF FERROMAGNETIC DETECTION SYSTEMS IN MRI SCREENING

The use of conventional metal detectors as a MRI screening tool has not been recommended in the past mainly as a result of false positive and false negative alarms, resulting in “alarm fatigue”. Such detectors have exhibited inconsistent sensitivities, operator error, and the inability to distinguish between ferrous and non-ferrous metals. In recent years, many new designs of ferromagnetic detection systems have emerged that have proven helpful in the screening process. These ferromagnetic detection systems are typically installed prior to the entrance into the scanner room (or Zone III, according to the zone scheme described by the ACR) (**Figure 11**).

Ferromagnetic detection systems may be utilized immediate area outside of the scanner room (i.e., the patient dressing room) to facilitate screening. Notably, the ACR recommends the use of ferromagnetic detection systems, but only as an adjunct to a thorough and competent MRI screening process (15, 23). At least one type of ferromagnetic detection system has been used to identify ferromagnetic implants or foreign bodies (e.g., armor-piercing bullets)(18-20).

PATIENT SAFETY AND SCREENING CONSIDERATIONS FOR 7 -TESLA MRI

In 2017, the U.S. Food and Drug Administration (FDA) approved the first 7-Tesla MR system for clinical imaging. The 7-Tesla MRI environment warrants attention for MRI screening and exposing patients and others to this ultra-high-field setting (21, 23). Some concerns and considerations are, as follows:

Untested Implants and Devices at 7-Tesla

To-date, over 6,500 metallic implant or devices undergone testing for MRI-issues at 1.5- and 3-Tesla static magnetic field strengths. At the writing of this chapter, little more than 300 of implants and devices have been tested under 7-Tesla conditions. Because of this limited information, scanning patients with implants and devices at 7-Tesla is far more challenging. As always, the decision to scan a patient with an untested device or implant should be based on a careful assessment of risk verses benefit which is conducted by the supervising physician.

Implant Heating at 7-Tesla

Implants or devices that may be scanned at 1.5- or 3-Tesla may heat excessively at 7-Tesla (298-MHz). Due to the decreased wavelength of the transmitted RF at 7-T ($\lambda=c/v$), implants 5 to 7 cm in length may be unsafe for patients undergoing MRI due to high temperature increases (21).

Stronger Translational, Rotational, and Lenz's Forces at 7-Tesla

Because the 7-Tesla scanner is substantially stronger than the more common 1.5- or 3-Tesla MR system, translational attraction and rotational (torque) forces become an increased concern. In MRI environment, Faraday's law of induction and related Lenz's law may play an important role for metallic implants, as well. An increase in Lenz's forces at 7-T is worth

396 MRI Screening for Patients and Individuals

noting. A brief explanation is, as follows: when an electrical conductor moves through a changing magnetic field such as the spatial gradient magnetic field at the entrance of the scanner, an electrical current will be generated that induces an additional magnetic field that opposes the spatial gradient magnetic field and the static magnetic field. Thus, the motion of any metallic implant, device, or object (made from ferromagnetic or nonferromagnetic material), will be opposed. This phenomenon may be manifested as a “tugging” sensation that patients with large metallic implants or devices may experience as they move into the bore of the MR system. Although this sensation is transient and harmless, it can be unsettling to patients, compelling them to bring it to the attention of the MRI technologist. Fortunately, Lenz’s forces can be markedly reduced by slowly moving the patient into a 7-T scanner. With further regard to Lenz’s forces at 7-T, it is a good practice to explain to a patient with a larger metallic implant that there is the possibility of a tugging sensation prior to the MRI exam to avoid undue issues (21-23).

SECONDARY PURPOSES AND ADVANTAGES OF MRI SCREENING

Obviously, the primary purpose of MRI screening is safety, but screening serves secondary purposes and advantages, as presented below.

Optimizing the Diagnostic Value of the MRI Examination

Many implants and devices do not pose safety issues, but some can significantly degrade image quality, especially when in or near to the anatomical region of interest. Information gathered during MRI screening regarding the type and location of a metallic implant or foreign body can allow for strategies and/or adjustments in the MRI protocol to minimize signal loss and/or distortion. For example, an adolescent with extensive orthodontic work who is scheduled for a pituitary study might be scanned on a 1.5-Tesla MR system rather than a 3-Tesla or 7-Tesla scanner in an effort to reduce susceptibility artifacts. Alternatively, the optimization of imaging parameters that are known to reduce artifacts related to metallic objects may be necessary in order to maintain the diagnostic aspects of the MRI examination.

Appropriate Patient Management Aided by MRI Screening

A physician ordering a clinical MRI examination must state a “reason for exam”. Based on this information, the attending MRI-trained physician will then select an appropriate protocol (i.e., with consideration given to the type of transmit/receive RF coil to be used, pulse sequences, etc.), which is unique for the desired outcome for that specific patient. Additional communication between the ordering/referring physician and the radiologist may be necessary if this information and justification for the MRI procedure is vague.

If the patient arrives for the MRI appointment with a limited history, and the ordering physician is not available for consultation, the screening information that is obtained may be helpful to the radiologist. For instance, if the reason for the examination simply indicates “headache”, and the screening procedure reveals that the patient has not had a prior MRI procedure, the radiologist may optimize the scan protocol with more diagnostic emphasis. Conversely, if MRI screening reveals previous MRI studies, and the present MRI exam is for surgical planning, the radiologist may optimize the scan protocol with this in mind. Oth-

erwise, the radiologist may simply protocol “repeat prior study” or the MRI protocol may involve performing additional sequences, possibly with an injection of an MRI contrast agent.

INITIAL MRI SCREENING

In the current age of faxing, email, and the use of other electronic media, MRI facilities can readily distribute electronic versions of the written MRI screening forms to referring physician’s offices, clinics, or any service that may order an MRI. Once the physician has seen the patient and has decided that an MRI procedure is indicated, the patient can be given the MRI screening form to fill out, or at a minimum, answer key MRI screening questions. This information can then be returned to the MRI facility prior to the appointment date. Such a practice has multiple purposes and advantages, including:

Early Discovery of Implants, Devices, or Other Objects

Initial MRI screening of a patient can reveal MR Conditional or MR Unsafe implants, devices, or other objects. The MRI facility can then investigate the item ahead of time and decide, under what conditions, the patient can be scanned, if at all. Patients with non-medical objects such as piercings or excessive jewelry can be instructed to remove these items prior to their MRI appointments.

Management of Severe Anxiety or Claustrophobia

If the MRI facility receives early notification that a patient suffers from severe anxiety or claustrophobia, then the patient may be scheduled on an “open” or wide-bore MR system, or the facility staff can prepare to coach or sedate the patient for the MRI exam (16-23).

Patient Body Habitus Management

MR systems typically have weight and/or dimensional limits for patients. If an MRI examination has been ordered on an excessively large patient, the weight and dimensions of the patient should be recorded and relayed to the MRI facility during the initial MRI screening procedure to ensure that the scanner can accommodate the patient. This can save time and embarrassment for all involved.

Anticipation and Preparation of the MRI Facility’s Staffing Needs

Patients who need special assistance, sedation, or high-risk patients who may need general anesthesia require specific and additional staff at the time of the MRI examinations. Furthermore, additional time will likely be needed to complete the MRI procedure and, possibly, to manage the patient after the exam (e.g., in the case of needing to recover a patient after general anesthesia). Initial MRI screening information is particularly beneficial for managing the afore-mentioned patients, because the MRI facility will need to prepare and schedule these patients, accordingly.

398 MRI Screening for Patients and Individuals

“No Show” Rate Reduction

Initial MRI screening (i.e., using verbal or written methods) can help reduce the “no show” rate of an MRI facility. During the initial screening process, certain patients may refuse the MRI examination, despite the physician’s recommendation. Common MRI contraindications and limitations are also exposed during this time. Thus, it may not be possible to schedule such patients right away. Frequently, MRI facilities dedicate a staff member to review the MRI screening information while placing “reminder” telephone calls to patients a few days before their appointments. At the time of the call, the patient may indicate that he or she is unable to honor the appointment, and the appointment will need to be re-scheduled or canceled. In either case, a likely “no show” can be averted by following simple tasks involved in initial MRI screening.

CONCLUSIONS

The process of MRI screening is absolutely critical to avoid MRI-related accidents and injuries, as well as to ensure safety for staff members and others. MRI screening must never be performed in haste, but rather, in a consistent and thorough manner. If a reduction in MRI incidents is to be realized, adhering to comprehensive MRI screening protocols and revising screening criteria must be an integral part of MRI policies and procedures. As emphasized throughout this chapter, MRI screening of patients and individuals must, at a minimum, include completion of an MRI screening form and a subsequent verbal interview, and have the form signed-off by the MRI technologist or other MRI safety-trained healthcare worker. The MRI screening process may start in advance, but only safety-trained personnel should perform the final screening procedure and just before exposing patients or other individuals to the strong electromagnetic fields of the MR system. Beyond MRI safety, screening proves efficacious by providing information that allows proper scheduling of the patient and preparation of the MRI facility to accommodate the patient’s needs for effective customer service standards, improved business, and optimal patient-care outcomes.

REFERENCES

1. Gangarosa RE, Minnis JE, Nobbe J, Praschan D, Genberg RW. Operational safety issues in MRI. Magn Reson Imaging 1987;5:287-92.
2. Shellock FG, Kanal E. Policies, guidelines, and recommendations for MR imaging safety and patient management. J Magn Reson Imaging 1991;1:97-101.
3. Shellock FG, Kanal E. SMRI Report. Policies, guidelines and recommendations for MR imaging safety and patient management. Questionnaire for screening patients before MR procedures. J Magn Reson Imaging 1992;2:247-8.
4. Shellock FG, Kanal E. Guidelines and recommendations for MR imaging safety and patient management. III. Questionnaire for screening patients before MR procedures. The SMRI Safety Committee. J Magn Reson Imaging 1994;4:749-51.
5. Elster AD, Link KM, Carr JJ. Patient screening prior to MR imaging: A practical approach synthesized from protocols at 15 U.S. medical centers. AJR Am J Roentgenol 1994;162:195-9.
6. Shellock FG, Kanal E. Magnetic Resonance: Bioeffects, Safety, and Patient Management. New York: Lippincott-Raven Press: 1996.

MRI Bioeffects, Safety, and Patient Management 399

7. Sawyer-Glover AM, Shellock FG. Pre-MRI procedure screening: Recommendations and safety considerations for biomedical implants and devices. *J Magn Reson Imaging* 2000;12:510-515.
8. Shellock FG. New recommendations for screening patients for suspected orbital foreign bodies. *Signals* 2001;36:8-9.
9. Sawyer-Glover A, Shellock FG. Pre-Magnetic Resonance Procedure Screening. In: *Magnetic Resonance Procedures: Health Effects and Safety*. Shellock FG, Editor. Boca Raton: CRC Press, LLC; 2001.
10. Kanal E, Borgstede JP, Barkovich AJ, et al. American College of Radiology. American College of Radiology white paper on MR safety. *AJR Am J Roentgenol* 2002;178:1335-47.
11. Shellock FG, Crues JV. Commentary. MR safety and the American College of Radiology white paper. *AJR Am J Roentgenol* 2002;178:1349-1352.
12. Shellock FG, Crues JV. MR procedures: Biologic effects, safety, and patient care. *Radiology* 2004;232:635-652.
13. Kanal E, Barkovich AJ, Bell C, et al. ACR Blue Ribbon Panel on MR safety. ACR guidance document for safe MR practices: 2007. *AJR Am J Roentgenol* 2007;188:1447-74.
14. Shellock FG, Spinazzi A. MRI Safety Update: 2008, Part 2, Screening patients for MRI. *AJR Am J Roentgenol* 2008;191:12-21.
15. Expert Panel on MR Safety, Kanal E, Barkovich AJ, Bell C, et al. ACR guidance document on MR safe practices: 2013. *J Magn Reson Imaging* 2013;37:501-30.
16. Shellock FG. Reference Manual for Magnetic Resonance Safety, Implants, and Devices: 2020 Edition. Biomedical Research Publishing Group, Los Angeles, CA, 2020.
17. Boutin RD, Briggs JE, Williamson MR. Injuries associated with MR imaging: Survey of safety records and methods used to screen patients for metallic foreign bodies before imaging. *AJR Am J Roentgenol* 1994;162:189-94.
18. James CA, Karacozoff AM, Shellock FG. Undisclosed and undetected foreign bodies during MRI screening resulting in a potentially serious outcome. *Magn Reson Imaging* 2013;31:630-3.
19. Shellock FG, Karacozoff AM. Detection of implants and other objects using a ferromagnetic detection system: Implications for patient screening prior to MRI. *AJR Am J Roentgenol* 2013;201:720-725.
20. Karacozoff AM, Shellock FG. Armor-piercing bullet: 3-Tesla MRI findings and identification by a ferromagnetic detection system. *Military Medicine* 2013;178:e380-5.
21. Hoff MN, McKinney A, Shellock FG, et al., Safety considerations of 7-T MRI in clinical practice. *Radiology* 2019;292:509-518.
22. ACR Committee on MR Safety: Greenberg TD, Hoff MN, et al. ACR guidance document on MR safe practices: Updates and critical information. *Magn Reson Imaging* 2020;51:331-338.
23. ACR Manual on MR Safety, ACR Committee on MR Safety, Version 1.0, 2020 <https://www.acr.org/Clinical-Resources/Radiology-Safety/MR-Safety>.

Chapter 16 Using Ferromagnetic Detection Systems in the MRI Environment

MARK N. KEENE, PH.D.

Chief Technology Officer
Metrasens, Ltd.
Worcestershire
United Kingdom

INTRODUCTION

Magnetic resonance imaging (MRI) is an important diagnostic modality that utilizes a powerful static magnetic field that may pose serious hazards to patients and other individuals. The potentially violent attraction of ferromagnetic objects into the bore of a magnetic resonance (MR) system is referred to as the missile (or projectile) effect. Magnetic field interactions acting on a highly ferromagnetic object brought too close to the magnet of the scanner can become so substantial as to be unstoppable by human effort. Items such as steel gas cylinders (e.g., an oxygen tank) and fire extinguishers can enter the MR system at 30- to 40-mph, the same speed they would reach if dropped from a 40-foot building to the ground. The kinetic energy gained by a steel cylinder that becomes a missile as it rapidly moves towards the scanner is dissipated on impact. A 15-lb cylinder acting as a projectile can seriously injure an individual and/or severely damage the MR system.

Ferromagnetic detection systems (FMDS) are available for use in the MRI environment. These devices have several uses (note that not all FMDS provide each of the following):

- To mitigate the risk of missile-relateds occurring by warning if ferromagnetic objects are approaching the MR system room (Zone IV).
- To reduce image artifacts and minor missile-related incidents by discovering ferromagnetic objects on patients inadvertently missed by routine patient screening.
- To detect ferromagnetic implants, such as cardiac pacemakers, that were missed by routine patient screening.
- To monitor safety metrics remotely and centrally across a number of MR systems to manage safety processes and procedures.

A ferromagnetic detection (FMD) device may be defined as:

A device that passively detects the presence of a ferromagnetic object by means of the object's naturally surrounding magnetic field, and issues an alert to indicate that the object has been detected.

Various versions of FMDS currently exist. These devices are specially designed to only detect ferromagnetic items. Other materials, such as aluminum and copper, are nonferromagnetic and, therefore, are not detected by an FMD device. There are many ferromagnetic metals but, by far, the most common is martensitic, which is magnetic, steel. An FMD device will detect a steel gas cylinder and indicate a positive alarm, but it will not detect or alarm on an aluminum one. Thus, the FMD device will only alarm on potentially dangerous objects relative to issues related to magnetic field interactions. Utilizing an FMD device in the MRI environment is recommended or required by various influential organizations concerned with MRI safety, including the American College of Radiology (ACR) and The Joint Commission (1-5).

This chapter discusses the missile effect, its causes, and consequences. The unique detection technology utilized by FMDS is then presented. Included in this chapter is a practical guide to working with an FMD device in the MRI environment. The potential application of an FMD device for screening patients to identify ferromagnetic implants and foreign bodies using an FMD device is also discussed, followed by a perspective on the future of these devices.

THE MISSILE EFFECT AND ITS CONSEQUENCES

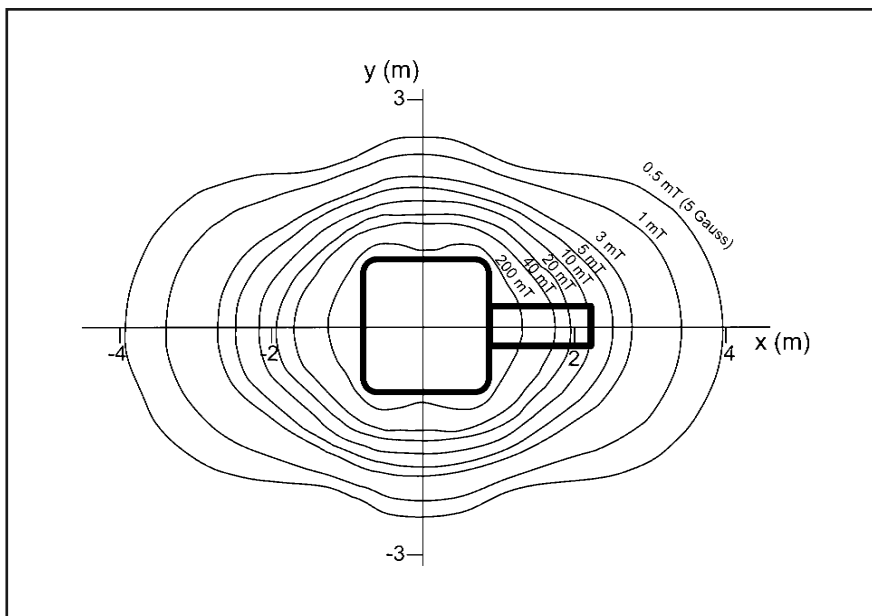
The Fringe Field Associated with an MR System

A properly functioning MR system has a powerful and highly uniform static magnetic field (6). The vast majority of scanners use superconducting electromagnets because these provide substantially higher static magnetic fields and considerably lower power consumption than electromagnets. Superconducting electromagnets have the interesting property such that the massive electrical currents in their coils will flow perpetually without the need for a power supply as long as they are kept cold enough to remain superconducting. A superconducting magnet does need high power to establish the field while the magnet is being “ramped up”. The energy that is used during this time is stored in the magnetic field. This stored energy will only be released when the magnet is “ramped-down” or quenched.

From a safety consideration, it is important to understand that a magnetic field is an “energy store”. An analogy might be a gas cylinder insofar as it requires energy to compress a gas into the cylinder. Once there (and with the valve closed), no power or energy is required to maintain it. The stored energy is only released when the gas is let out. With the gas cylinder, the energy is stored safely within the walls of the cylinder. However, with a magnet used by an MR system, the energy is stored in the magnetic field on the *outside*, through which staff members, patients, and other individuals walk through and work in every day. It is a common misconception that the energy in an MR system’s magnet is stored in the electrical current in the windings, safely within the scanner. However, that is not the case. Inside the bore of the magnet and in the area surrounding the magnet there is an energy

402 Using Ferromagnetic Detection Systems in the MRI Environment

Figure 1. Example of a magnetic field contour plot for the fringe field of a 1.5-T MR system. The contours are of a constant field magnitude (i.e., irrespective of the field orientation). The field value for each contour is as marked.



field that cannot be felt, seen, heard, tasted, or smelled. The only sense of the presence and power of this energy field is when a ferromagnetic object is taken into the area and the forces are felt that are exerted on the object.

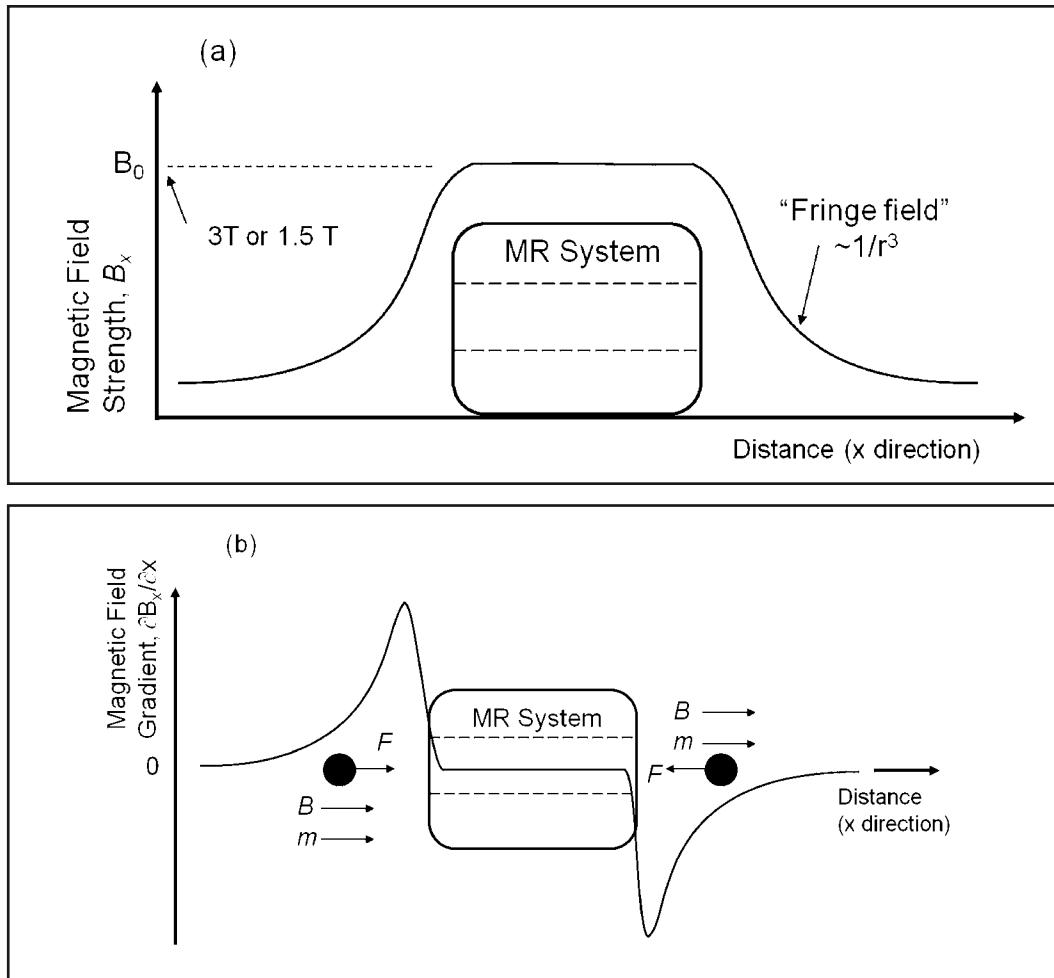
During the planning of an MRI facility, a plot showing the magnetic contours surrounding the MR system is typically provided by the manufacturer, an example of which is shown in **Figure 1**. Normally, MR system rooms are designed such that, where there are walls adjoining areas occupied by individuals, the fringe field is less than 5-Gauss (7). This is considered to be the generally permissible magnetic field level that ensures safety for individuals with electronically-activated devices, such as cardiac pacemakers. Frequently, the 5-Gauss line is contained well within the MRI environment, usually at or within a controlled area.

The fringe field associated with the magnet of the MR system falls away in all directions, getting weaker as the distance increases. The rate of change of the magnetic field with distance is called the spatial gradient magnetic field. If the magnetic field is B , then the gradient is $\partial B / \partial x$ where x is the distance in the x-direction. An illustration of the fringe field and gradient profiles are shown in **Figure 2 (a)** and **Figure 2 (b)**.

How Magnetic Fields Interact with Metallic Objects

There are four primary mechanical effects that a magnetic field could impart on a metallic object: (1) linear force or translational attraction, (2) torque or rotational force, (3) magnetization effects, and (4) motion damping. These mechanical effects are described below.

Figure 2. Illustrations showing examples of the fringe field and spatial gradient magnetic field. (a) The magnetic field amplitude in the x direction is nearly constant within the bore of the MR system and decays rapidly with distance away from the bore. (b) The magnetic field gradient, $\partial B_x / \partial x$, as a function of distance. The direction of the force on a ferromagnetic object is shown in relation to the field and the sign of the gradient.



Linear Force

Linear force is the mechanism that causes the missile or projectile effect. It occurs because an object, having been magnetized by the magnetization effect, or by its previous magnetization state (or both) becomes attracted to the magnet of the scanner. The spatial gradient of the magnetic field is responsible for linear force. The position at which the magnetic field is highly uniform, such as in the middle of the bore of the MR system, the linear force is close to zero. This is discussed in more detail later in this chapter.

404 Using Ferromagnetic Detection Systems in the MRI Environment

Torque

Torque is when a ferromagnetic object, in the presence of a magnetic field, experiences a torque to rotate or align it with respect to the direction of the magnetic field. Once in the preferred direction, there is no further rotation. However, torque will oppose any attempt to orient the object in another direction. This is the principle that magnetic compasses use to indicate the direction of the Earth's magnetic poles. An elongated ferromagnetic object (e.g., a steel oxygen cylinder, pen, etc.) becomes magnetized along its long axis in preference to another direction. Unless the object is spherical, it will usually experience torque.

Magnetization Effects

Magnetization effects only occurs in ferromagnetic objects. The magnetization of a ferromagnetic object increases with the applied magnetic field. This means that the closer a ferromagnetic object approaches to the magnet of the MR system, the more magnetized it becomes.

Motion Damping

Motion damping is the only main effect that all metallic objects experience whether or not they are ferromagnetic. It is a mechanism that is a function of the electrical conductivity of the metallic object and its shape. If a metallic object moves through a magnetic field gradient so that the field it experiences changes with time, then eddy currents are generated within the metal, obeying Faraday's Law of Induction, also known as the dynamo effect. The eddy currents circulate, according to Lenz's Law in a manner that generates their own magnetic field that opposes the movement (i.e., the objects resist motion)(8). The reason this is discussed here is because a ferromagnetic missile accelerating toward the bore of the magnet is slowed down by this effect. Without this effect, missile incidents would be even more damaging.

When an individual approaches the magnetic field of the MR system with a ferromagnetic object, the object will typically first encounter torque as the first effect to be noticed. The linear force acting on the object is often felt closer to the scanner. The motion damping effect is not that noticeable but can be experienced if an aluminum sheet is taken into close to the origin of the magnetic field and moved around. A favorite trick MRI physicists like to display is to take a half-inch thick aluminum object, such as a pizza pan, stand it edgewise on the patient table near the opening of bore of the MR system, and then tip it over. The object falls in a surprisingly slow manner.

The Missile Effect

Although the missile effect is predominantly caused by the linear force acting on a ferromagnetic object, each of the four interactions described above plays a part. Let's begin by considering the linear force in more detail. As a ferromagnetic object approaches the magnet, the force it experiences dramatically increases. Thus, every time the distance to the magnet is reduced by 10%, the force doubles. Therefore, small changes in distance equate to large changes in the force acting on the ferromagnetic object. Decreasing the distance to the magnet by half increases the force by approximately 130 times.

This highly non-linear distance dependence on the force causes problems for individuals carrying ferromagnetic objects close to the MR system. When the forces begin to increase, muscle control typically cannot cope with the non-linearity. Thus, there is a point at which the ferromagnetic object can no longer be restrained. The force is so highly non-linear that it is rare for individuals to experience or encounter similar forces under other circumstances because we are naturally more accustomed to sensations involving constant or linear forces. It is often an unconscious assumption by people who deliberately take ferromagnetic objects into the MR system room that the force will increase more smoothly than it actually does, as the ferromagnetic object gets close to the scanner. This incorrect assumption has led to many missile-related accidents. In various videos posted on the Internet of individuals deliberately demonstrating the missile effect, one can see the sudden attraction of a ferromagnetic object into the bore of the MR system. Additional information on this topic directed towards the interests of the MRI physicist is presented in the comprehensive publication by Bleaney and Bleaney (9).

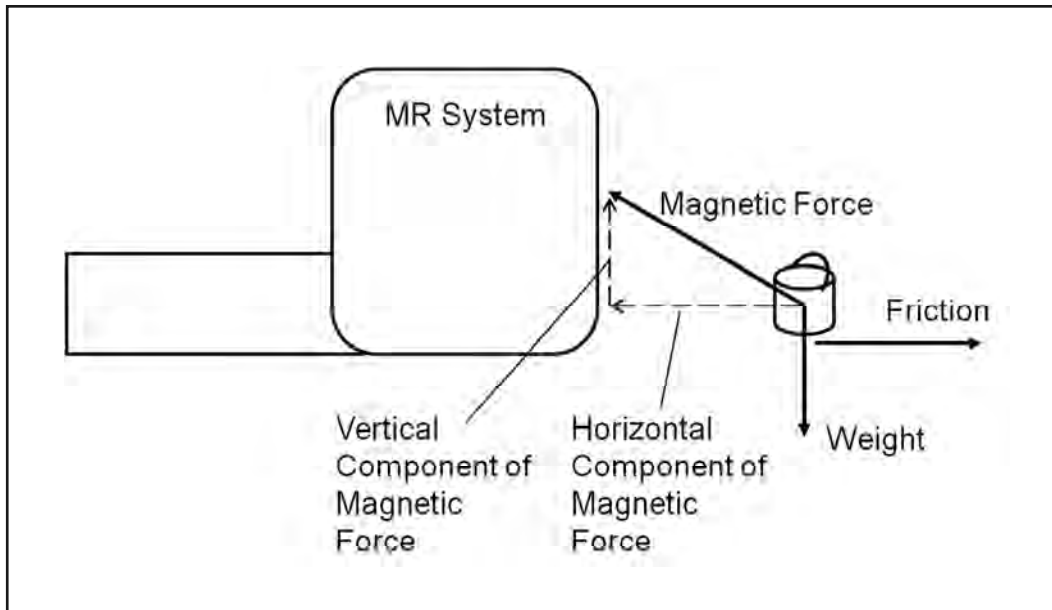
TERMINOLOGY USED FOR IMPLANTS AND DEVICES

Descriptions of the current terminology and classifications used for implants and devices, including patient support equipment, have been presented by Shellock, et al. (10). One important aspect of these classifications is the item's susceptibility to becoming a missile-related hazard. For example, MR Safe items are those defined as, amongst other things, "nonmetallic, nonmagnetic, and nonconducting" objects (10). MR Unsafe items are "known to pose hazards in all MR environments" (10). Objects made from martensitic stainless steel or iron may be MR Unsafe. MR Conditional items have, "been demonstrated to pose no known hazards in a specified MR environment with specified conditions of use. Field conditions that define the MR environment include static magnetic field strength...." (10). As far as missile-related hazards are concerned, this classification refers to items that are either very weakly magnetic or composite items that have small amounts of ferromagnetic materials. For implants, the counterforces present for certain MR Conditional items must be taken into consideration because these can prevent risks related to movement or displacement relative to the use of MRI.

An important area to consider is composite equipment that is classified as MR Conditional, where the majority of the materials that are used are nonferromagnetic but there may be ferromagnetic components, as well. Most MR Conditional gurneys, wheelchairs, and removable MR system patient tables are in this category. The ferromagnetic materials found in composite equipment always experiences forces of attraction in association with scanner, so an interesting question is, when does an object become too magnetic and in danger of becoming a missile? On one level the answer is simple. It is when the attractive force of the magnet overcomes the restraining or counterforce holding the object back. For a piece of patient support equipment, such as a wheelchair, there are two primary forces that can prevent it from becoming a missile: the weight which acts in a downward direction and the friction due to contact with the ground, which acts along the floor in the opposite direction of the force, as illustrated in **Figure 3**. This force of attraction is generally toward the nearest edge of the bore of the MR system. In **Figure 3**, the magnetic force is shown resolved into

406 Using Ferromagnetic Detection Systems in the MRI Environment

Figure 3. An illustration of the forces acting on an object in the fringe field of an MR system's magnet. The magnetic attraction force is shown resolved into vertical and horizontal components that oppose gravity and friction.



its horizontal and vertical components. The forces of gravity and friction are in opposition to these components.

First, consider the friction. This has the property that frictional force increases to exactly match any horizontal force on the object up to a point called F_{max} , beyond which it will begin to slide toward the MR system. A full analysis is complicated because F_{max} is proportional to the object's weight and it also depends on the properties of the two surfaces in contact. For a given object, there will be an area surrounding the MR system's magnet, outside of which the object will remain stationary on the floor, and inside of which it will become a missile, due to horizontal forces. Objects with wheels have intrinsically low F_{max} because that is the point of having wheels in the first place. That is, to allow devices such as wheelchairs and gurneys to move horizontally with very low friction. This means special care must be taken with wheeled items when present in the MR system room so that these devices are not moved closer than allowed based on the approved MR Conditional labeling. For example, certain patient support devices are labeled MR Conditional and the conditions specify use at 500-Gauss or less. Moving the device closer than 500-Gauss may pose a missile-related hazard.

The vertical forces are different in nature. An object of a given weight will remain on the floor until the vertical component of the magnetic force exceeds it. Then, it may become a missile, as it rises off the floor and moves towards the scanner. This cannot be disentangled from the horizontal forces because F_{max} depends on the force pressing the object to the floor, which is the difference between its weight and the opposing vertical magnetic force.

component. Because of this, objects positioned on the floor will tend to first travel along the floor, move near the MR system, and then leap up off the floor into the scanner.

Again, it should be noted that the magnetic force is related to the spatial gradient of the magnetic field and not to the strength of the static magnetic field. While it is generally true that a ferromagnetic object in the presence of a 3-Tesla MR system will tend to be more strongly attracted than in association with a 1.5-Tesla scanner, with the emergence of new “open”, vertical field MR systems it is conceivable that a lower strength magnet can have larger spatial gradients than a higher field strength one. The take home message is that it is always prudent to be cautious when introducing an MR Conditional item into the MR system room for the first time, even if the condition relative to the static magnetic field is met. What is important is the allowable fringe field (e.g., 500-Gauss or less) for which the device is labeled and where that value exists in the specific room where the device is intended for use.

For handheld item, the restraining force is related to the muscular activity of the individual holding the object. Like the frictional force, muscular strength can also restrain a ferromagnetic object up to a point. Beyond this, the object may be snatched away from the person’s grasp and become a missile. Normally, torque acting on the object is experienced prior to this point.

THE CAUSES AND CONSEQUENCES OF MISSILE-RELATED ACCIDENTS

Why Missile-Related Accidents Occur

Human risk factors are fundamentally inherent in the delivery of healthcare associated with medical devices and their applications during medical procedures. Simply stated, we are human and we are imperfect, so accidents will happen. Missile-related accidents occur for many reasons but there tends to be five main causes.

(1) *Faulty safety protocols.* Some MRI facilities have inadequate or outdated safety protocols that have dangerous gaps. Common examples include allowing untrained staff members or maintenance people into the MR system room, inadequate training regimes, lack of a policy regarding the use of certain types of equipment in the MRI environment, and failure to check and follow equipment labeling (11). The solution for this is to have an MRI Safety Officer or other individual responsible for developing and implementing proper safety policies and procedures.

(2) *Ignorance of safety protocols by staff members.* This occurs when staff members have not been properly educated and trained to follow the MRI facility’s safety protocols and, thus, they are ignorant or unaware of them. Common accidents where this is the cause involve cleaning and maintenance staff as well as non-MRI medical professionals and other individuals. The prevention of this problem involves a concerted effort to educate and train all of those involved in the MRI environment.

(3) *Unintentional disregard for safety protocols.* Staff members may unintentionally disregard safety protocols due to lapses in concentration, or making wrong decisions under

408 Using Ferromagnetic Detection Systems in the MRI Environment

high pressure settings, or in emergency situations (12). This can, and often does, occur with highly experienced staff members. Long-term experience and a good previous record will not ensure safety due to this cause. There is no practical mitigation against this, although regular practice of safety policies especially those related to emergency situations may help.

(4) *Deliberate disregard of safety protocols.* This is the “I know better than the MRI Safety Officer” or “it will never happen to me” attitude. Some staff members guilty of such attitudes may decide that some aspects of their safety protocols are unnecessary or incorrect and, thus, they have decided to ignore them. Fundamentally, this is about the personality of the staff member. Strong character traits of arrogance, pride, or an attraction to risk may lead to this problem. Prevention of this issue is difficult, but training and safety inspections help. Disciplinary action should be considered for staff members caught disregarding safety protocols.

(5) *Incorrect or absent information on MR Safe or MR Conditional equipment.* The current MRI labeling was instituted in 2005 (10). Equipment labeling prior to 2005 may not have updated labeling applied. Even now, some equipment labeled MR Safe is not. Thus, the regular review of equipment and application of proper labeling are important procedures for MRI facilities. Additionally, MR Conditional equipment does not always have the conditions for use marked on the devices (13). Furthermore, an MRI facility may have recently upgraded from a 1.5-T to a 3-T MR system, resulting in different conditions that may pose risks. Prevention of this issue involves regular equipment inspections and review, particularly with regard to MRI labeling.

Frequency of Occurrence

It is well known that the majority of missile-related incidents are not reported. This is because, in many instances, missile-related incidents that do not hurt individuals don’t tend to be reported. Also, at least in the U.S., only a small minority of medical incidents of all kinds that result in patient harm are reported (14). For accidents involving the missile effect, estimates vary between 5% and 20% for the proportion of potentially harmful incidents that are actually reported. Despite the unknown scale of the problem, the missile effect is often quoted as one of the most serious hazards in the U.S. healthcare system (5).

Fatalities in the MR setting are extremely rare, but it is estimated that major injuries occur approximately once a year across 20,000 MR systems. For minor injuries, there are no reliable statistics, but these are believed to be far more common. Expensive accidents resulting in damage to the scanner and downtime are thought to be relatively common. However, again, there are no reliable statistics in the public domain pertaining to this matter. Small accidents involving scissors, pens, paper clips, and other similar items that can be removed from MR systems without the need to quench the MR system are very common. Most MRI facilities have several stories of such incidents but there are no known statistics that document how often these problems occur.

Consequences of Missile-Related Accidents

An internet-based search for MRI accidents will reveal many photographs and reports of some of the more serious cases. Floor buffers, gas cylinders, and office chairs are amongst

the most common missiles, although monitoring equipment, ventilators, tools and even handguns may be seen. There are also many links to news reports describing accidents involving victims and near misses.

If a patient or staff member is injured or killed, then there is a high risk of expensive litigation, and a significant loss of reputation for the hospital or the MRI facility. Larger ferromagnetic objects cannot be manually removed from the MR system unless the magnet is quenched, reducing the level of the static magnetic field.

Therefore, it is usual for the manufacturer of the scanner to provide technical support to ramp the magnet down, remove the item, and repair any damage. After that, the magnetic field of the MR system needs to be ramped-up and shimmed. This process can take several days, resulting in a significant loss of imaging time. Estimates for the average cost of a missile-related accident not involving human injury vary between \$20,000 to more than \$200,000. If an injury is involved, the monetary costs can be excessive, not including any commercial damage due to loss of reputation.

FERROMAGNETIC DETECTION SYSTEMS

Introduction To Ferromagnetic Detection Systems

Ferromagnetic Detection Systems (FMDS) designed for the MRI environment appeared in 2002, shortly after the tragic death of Michael Colombini in 2001. Colombini was struck by a steel oxygen tank that was brought into the MR system room while he was in the scanner undergoing a brain MRI (15). Prior to this, conventional archway metal detectors and some forms of magnetometers were tried at MR system room doorways, but these were not found to be useful. Conventional metal detectors “alarm” on all metals, ferromagnetic and non-ferromagnetic and, therefore, may detect many objects that can be legitimately taken into the MR system room which do not pose a missile-related hazard.

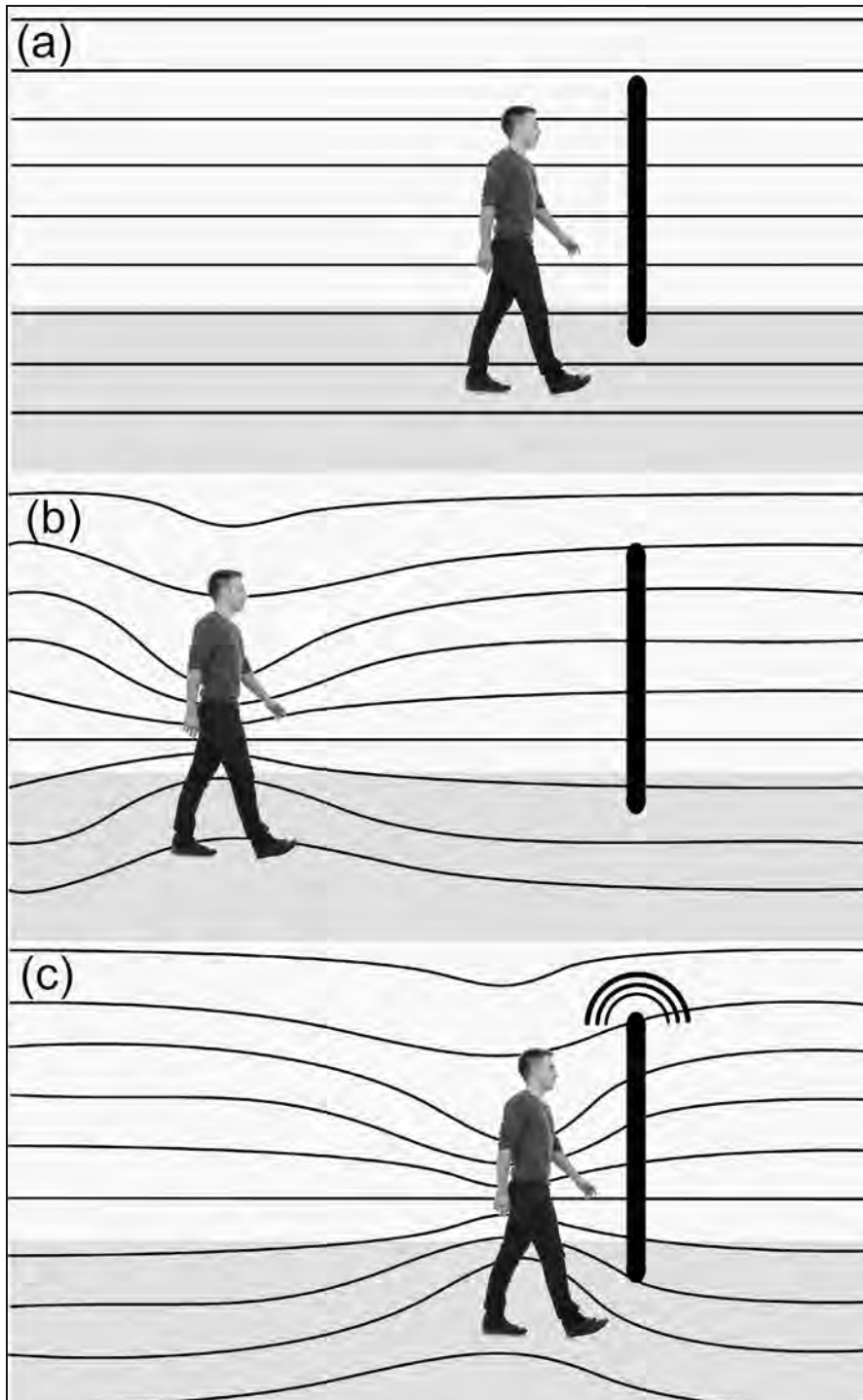
The first example of a modern-day FMD device was installed in the Royal Hospital Haslar in the United Kingdom in November 2002. Since then, several companies specializing in FMDS have supplied these devices commercially (16-18).

As the name suggests, ferromagnetic detection systems selectively detect ferromagnetic objects, ignoring nonferromagnetic objects. Because only ferromagnetic objects pose a missile-related hazard, an FMD device selectively detects threats and operates by monitoring the ambient magnetic field using magnetic sensors. The ambient field is a combination of the fringe field of the magnet and the Earth’s magnetic field plus the contribution from architectural steel and any other stationary steel objects in the immediate vicinity. A ferromagnetic object distorts the ambient field in its vicinity. If it is brought close to an FMD device, the distortion is detected as a changing magnetic field and an alert is triggered. This is illustrated in **Figure 4**, where the ambient field is illustrated as parallel horizontal lines. A person who is not carrying any ferromagnetic material will not modify this field in any way and can walk past the FMD device undetected, as seen in **Figure 4 (a)**.

Figure 4 (b) shows how a ferromagnetic object carried by a person perturbs the ambient magnetic field. Note that the perturbation in the field is local to the object. Because the per-

410 Using Ferromagnetic Detection Systems in the MRI Environment

Figure 4. An example of the operation of an FMD device. **(a)** With no ferromagnetic object present, the ambient field lines are not affected, and as the person passes the FMD device, there is no alarm. **(b)** With a ferromagnetic object present, the ambient field becomes perturbed in the vicinity of the object. **(c)** The changing field caused by the ferromagnetic object is detected by the FMD device, resulting in an alarm.



son is far from the FMD device, the ambient field is unchanged, so the FMD device has not detected the object, as of yet. In **Figure 4 (c)**, the person carrying the ferromagnetic object is now close enough to the FMD device such that the perturbation in the field surrounding the object has caused a change of the ambient field at the FMD device. This change triggers an alarm.

Importantly, an FMD device ignores static magnetic fields (i.e., magnetic fields that do not change with time). In practice, this means that the FMD device is only sensitive to changing magnetic fields or moving ferromagnetic objects. The device is insensitive to a stationary ferromagnetic object, so if an object is placed near to an FMD device it will be detected as it is put in place but thereafter ignored, until it is moved again. The reason for this is that the ambient magnetic fields are very large compared with the magnetic perturbations caused by a ferromagnetic object, and it is difficult to measure tiny changes on a large background field. The large static background is therefore removed by the FMD device by filtering it out, irrespective of whichever components make up that static magnetic field including the magnet of the MR system, the Earth's magnetic field, or a metal cabinet next to the FMDS.

For a handheld FMD device, the object may be stationary but the FMD device is moved, so it is the relative motion that is important when using this type of device. By comparison, a stationary FMD device detects moving ferromagnetic objects only.

Magnetic Sensors

There are several types of magnetic sensors, however, only three types have been used in devices used for FMDS. Each has relative merits and drawbacks. The detailed workings of the sensors have been described previously (19). Therefore, only a brief summary of features relevant to FMDS is provided below.

Fluxgates

These are the most sensitive magnetic sensors used in FMDS. Fluxgates can resolve better than 20×10^{-12} -Tesla in a 1-Hz bandwidth at 1-Hz. Their main drawback is their high price and several are needed in an FMD device. The high sensitivity and high price means that fluxgates are only used in top-end FMDS.

Amorphous Magneto-Resistive (AMR)

These are solid-state devices with a resolution of 350×10^{-12} -Tesla in a 1-Hz bandwidth at 1-Hz and cost one-tenth of the price of fluxgates. Their main limitation is the limited sensitivity, so more of them are required to provide full coverage in an FMD device.

Induction Coils

These sensors are coils of wire wound on ferrite cores. They are intrinsically similar to an AMR sensor in both sensitivity and cost. Induction coil FMDS are used by one company in their hand-held FMD device (17, 18) where they use a magnet within them to boost the ambient field and hence the magnetization of the ferromagnetic objects they seek to detect

412 Using Ferromagnetic Detection Systems in the MRI Environment

(17, 18, 20). This adds to the effective sensitivity close to the FMD device's sensors, but the device should be kept away from electronic implants and the eyes.

Ferromagnetic Detection Systems

A stationary FMD device needs to be highly sensitive in its immediate vicinity but highly immune to large moving ferromagnetic objects further away, such as cars on roads and elevator counterweights. These FMDS consist of magnetic sensors along with the necessary amplifiers and filters to condition the signals. There are methods employed to provide the rejection of unwanted distant moving ferromagnetic objects. Following the signal conditioning is the detection stage. Detection can be done in several ways but the simplest is to rectify the signals so that they are always positive and compare them with a threshold level. If the threshold is exceeded by the magnetic signal, an audible and visual alarm will result. Adjusting the threshold modifies the sensitivity of the system. That is, a higher threshold means that the magnetic signal must be larger to exceed it and vice versa.

There are two uses of FMDS: entryway and patient screening:

Entryway FMDS. The purpose of these is to protect the MR system room and any people within it. Entryway FMDS are systems that are normally mounted at or near to the entrances of the scanner rooms. Their main use is to provide a warning to individuals approaching the scanner room if they are bringing ferromagnetic objects with them, prior to their actual entry. Normally these FMDS are configured to detect objects that can cause serious accidents such as phones, scissors and, in particular, larger ferromagnetic objects.

Patient Screening. These FMDS mounted in or near the patient preparation areas (e.g. the dressing rooms) with the purpose of warning if the patient who is about to be scanned is carrying a ferromagnetic object. This type of an FMD device may be a wall-mounted or a handheld device. They are set to be of higher sensitivity than the entryway systems because they need to detect relatively small objects such as bobby pins that may cause imaging artifacts. This type an FMD device comes in two forms: wall-mounted as a single upright unit, in front of which a patient rotates, or as a handheld device.

For an entryway FMD device, if ferromagnetic objects are moving close to it that are not intended to go into the MR system room, most manufacturers have techniques for suppressing the alarm unless the object is actually passing into the scanner room itself. This reduces the unwanted or nuisance alarms (21). Because doors leading into the MR system room tend to be relatively wide, in order to get good coverage across the width, the FMD device will have sensors on both sides of the door. This may be in the form of two wall-mounted units as illustrated in **Figure 5 (a)**, a frame surrounding the door as shown in **Figure 5 (b)**, or two freestanding units that are upright poles with bases, although these are less common.

It is important to note that the sensors are housed in the upright sections of the FMD device, and the closer these are together the more sensitive the system will be in its least sensitive position, that is, at the midpoint of the uprights. **Figure 6** shows illustratively how the field perturbation from a ferromagnetic object decays with distance as $B \propto 1 / r^3$. An object at position A has a larger field, B_A at the FMD device's sensors than it would if it

Figure 5. Examples of entryway or portal-type (i.e., around the door) ferromagnetic detection systems. (a) Photograph courtesy of Metrasens, Ltd. (b) Photograph courtesy of Kopp Development, Inc.



were at the midpoint, position B, with a lower field B_B . This can more usefully be looked at from the viewpoint of what the signal is measured by the FMD device as a function of the ferromagnetic object's position across the door to the MR system.

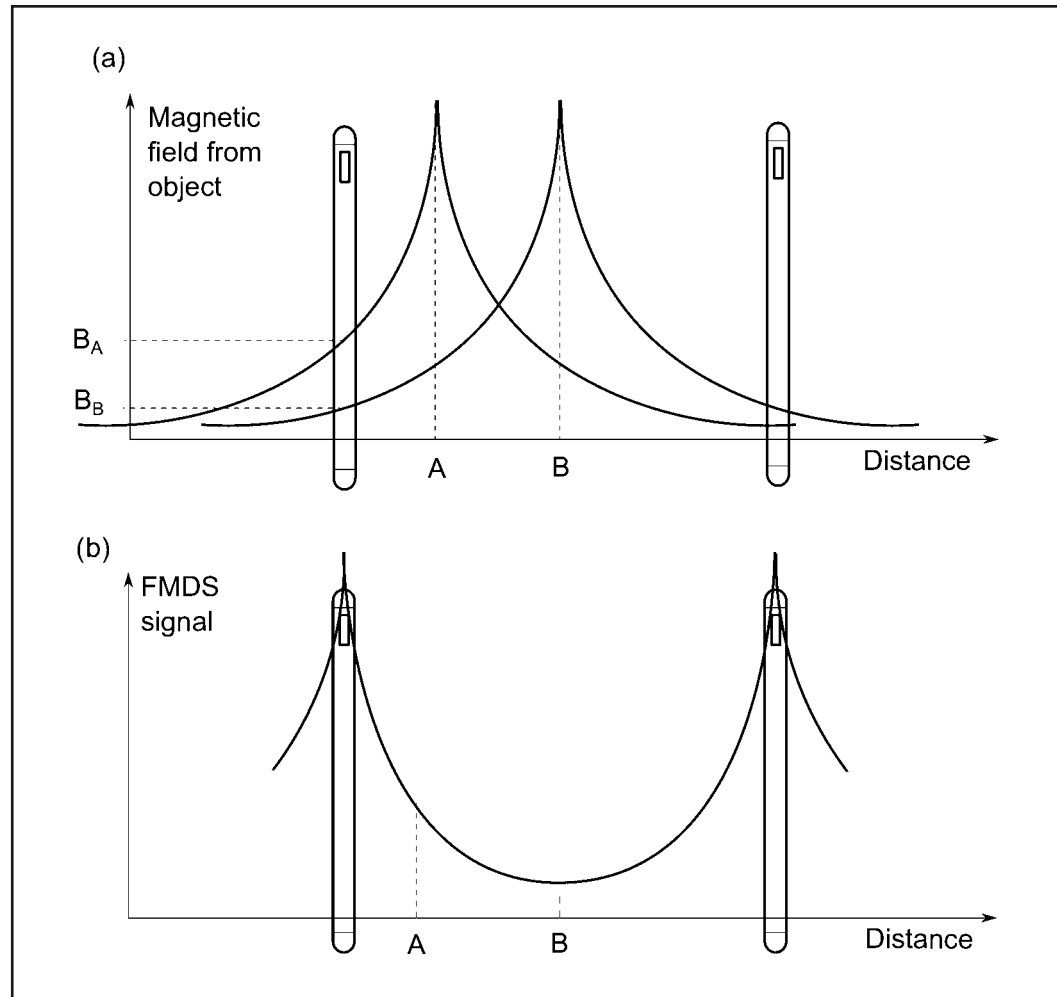
Note that the FMDS response is non-uniform and has a minimum for objects at the midpoint, point B (**Figure 6**). If the FMD device uprights were further apart, the minimum would be lower. At some separation, the minimum will be reduced below the sensitivity threshold of the FMD device. In this case, there will be a gap through which a ferromagnetic object could pass undetected.

Sensitivity and Extraneous Alarms

Sensitivity (or true positive alert rate) in the context of FMDS is the ability for detecting ferromagnetic objects. The higher the sensitivity of the sensors within an FMD device, the smaller the ferromagnetic object it will detect. For a patient screening FMD device, this is extremely important because a more sensitive device can find ferromagnetic objects that a less sensitive one will miss. Not all FMDS are the same. Sensitivity can vary considerably between different manufacturers. The FMD device market is unregulated and most manufacturers claim, without accountability, to have the most sensitive products. When selecting an FMD device it is especially prudent to ask the vendor to provide the evidence supporting

414 Using Ferromagnetic Detection Systems in the MRI Environment

Figure 6. Illustration of the relationship between the position of a ferromagnetic object across the door to the MR system room and the FMD device's signal. (a) This shows how the decaying field from a ferromagnetic object impacts an FMD device when it is to one side, position A, and in the center, position B. The magnetic fields at the FMD device are B_A and B_B , respectively. (b) The resulting signal from the FMD device (i.e., proportional to the measured magnetic field) as a function of the ferromagnetic object's position across the door.



their claims, such as requesting independent test house results or citations from independent peer-reviewed journals.

The level of extraneous, unwanted alarms is also an important factor. FMDS have improved considerably in this regard since their initial introduction. For example, the door to the MR system room is a large moving ferromagnetic object. Some FMDS now have a mechanism for not alarming on the influence of the moving door. There are several other frequently encountered effects in and around the scanner's door that some FMDS now ignore or compensate for. Again, not all FMDS are the same for nuisance alarm rates. The

practicalities of working with different sensitivities and nuisance alarm rates will be discussed later in this chapter.

User Interfaces

To warn an individual approaching an MR system doorway with a ferromagnetic object, entryway FMDS typically incorporate both lights and sound. For entryway systems, the magnetic sensors can detect objects before they get to the threshold. The distance at which they can do this depends on the magnetic susceptibility and size of the object and the sensitivity setting of the detector. Visible lights, normally green for no detection and red or yellow for a detection, are used to indicate approaching ferromagnetic objects. It is incumbent upon the person entering to stop and check themselves prior to entering if a red or amber warning light is observed. FMDS also normally have a light beam or other sensor across the threshold to sense whether a person or object is entering the scanner room rather than passing by. If the beam is broken by an individual and there is a detected ferromagnetic object, then an audible alert will be issued (21). The audible alert is the final warning before the MR system room is entered.

Installation Considerations

The effectiveness of an FMD device depends not only upon the quality of the system itself, but where it is sited and what its environment is. We first consider the entryway FMDS. It is important that an FMD device is sited such that anyone entering the MR system room must pass through it. There may be many different architectural layouts for scanner rooms, however, there are five main entrance types. These are, as follows:

Off an atrium. In this case, the door is in the wall of a room that may have an open control room (or several) or a waiting area. In some facilities, these are highly compact with control room desks and patient transfer equipment in a confined space. Others have large uncluttered areas.

With an anti-chamber. Here, stub walls are built out from both sides of the MR system doorway, usually to a distance of 1.5- to 2-meters. These may be built for a variety of reasons, but most commonly for allowing extra control desk and working areas, or dedicated space for outward opening MR system room doors to swing into. Sometimes these are built specially to accommodate an FMD device.

End of a corridor. Due to being at the end, the last section of the corridor is dedicated to the MR scanner. In this respect, it is similar to the anti-chamber setting. The system control room will often have a door to the side of the corridor shortly before the MR system door, itself.

Side of a corridor. This is a common layout but the least safe. This layout is poor practice from a safety consideration unless the corridor can be a controlled area.

Mobile MRI trailer. This a highly compact setting and a smaller than standard MR system door is usually installed. The control room is in close proximity to the door.

416 Using Ferromagnetic Detection Systems in the MRI Environment

For each of these entrance types, the door may be swing-in or swing-out (although swing-out is rare for a side of a corridor entrance). Usually the FMD device will be installed on the immediate surrounding area of the door itself because there is normally available wall space. It is preferable to use an FMD device that has a door-ignore capability to mount at the door. Otherwise, the system should be offset a distance of 1.5- to 2-meters in front of the door so the person entering has been screened by the FMD device before the door is opened. This can only be practically achieved with anti-chamber or end of corridor layouts.

For swing-out doors that open near an FMD device mounted on the outside of the door, an issue is presented because the FMD device needs to distinguish between the door opening and a person carrying a ferromagnetic object. In both cases, a moving ferromagnetic object is passing through the FMD device, the door is safe and the person is unsafe. Different manufacturers of FMDS have developed different solutions to address this situation. One manufacturer developed a solution that allows the FMD device to be mounted on the outside of a swing-out door and operate normally (22). Another manufacturer elected to install the FMD device on the inside of the MR system room, so that the door swings outwards away from the device, not through it (17). Notably, some MRI users regard this as providing a warning too late, or as being non-compliant with ACR recommendations (2), while others accept it.

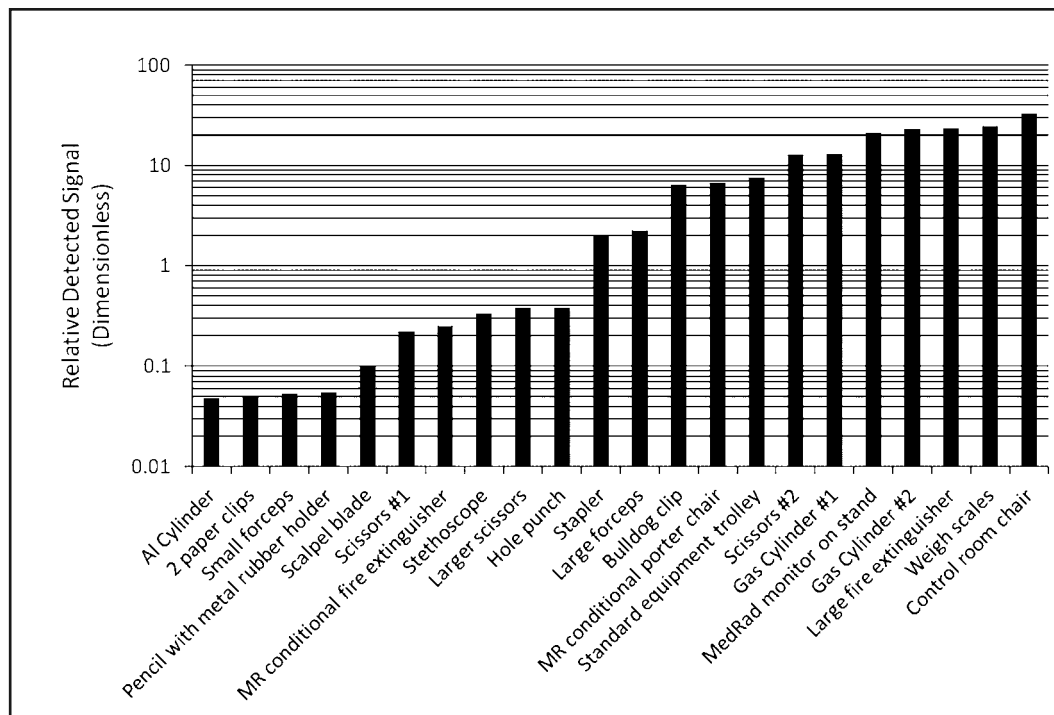
WHAT FMDS WILL AND WILL NOT DETECT: ADVANTAGES AND LIMITATIONS

Magnetic Qualities of Potentially Dangerous Objects

The physics involved with magnetics is not intuitive. There are two common misconceptions that individuals have when they consider using an FMD device in the MRI setting. It is often expected that identical objects will have identical magnetic qualities but, in fact, they can magnetically vary by several orders of magnitude. Another misconception is that larger ferromagnetic objects will be magnetically stronger (and pose a greater risk) than smaller ones. This premise can be true but so can the converse. Probably the most common question asked of the FMD device manufacturers is, *what is the smallest object that can be detected?* It is one of the most difficult questions to answer because a ferromagnetic object's size is not strongly related to its magnetic properties. Furthermore, because of the strong dependence on distance, very small ferromagnetic objects may be detected close to an FMD device sensor, whereas at longer distances to the FMD device, the same or larger objects may not be detected.

As previously mentioned, the magnetic properties of a ferromagnetic object depend primarily on the material's magnetic susceptibility and the shape of the object (23). For objects with different sizes but made of the identical material, there is potential for the larger objects to be more heavily magnetized than the smaller ones. Also, for objects of identical size but made from different materials, there is potential for the objects with higher magnetic permeability to be more heavily magnetic than those with lower magnetic permeability. For example, a "weakly magnetic" pair of scissors made from steel can be magnetized more than a stainless steel pair of the same size and shape.

Figure 7. The magnetic signal strength of objects commonly found in a control room for an MR system, measured at the mid-point of an FMD device in a 1-Gauss magnetic fringe field.

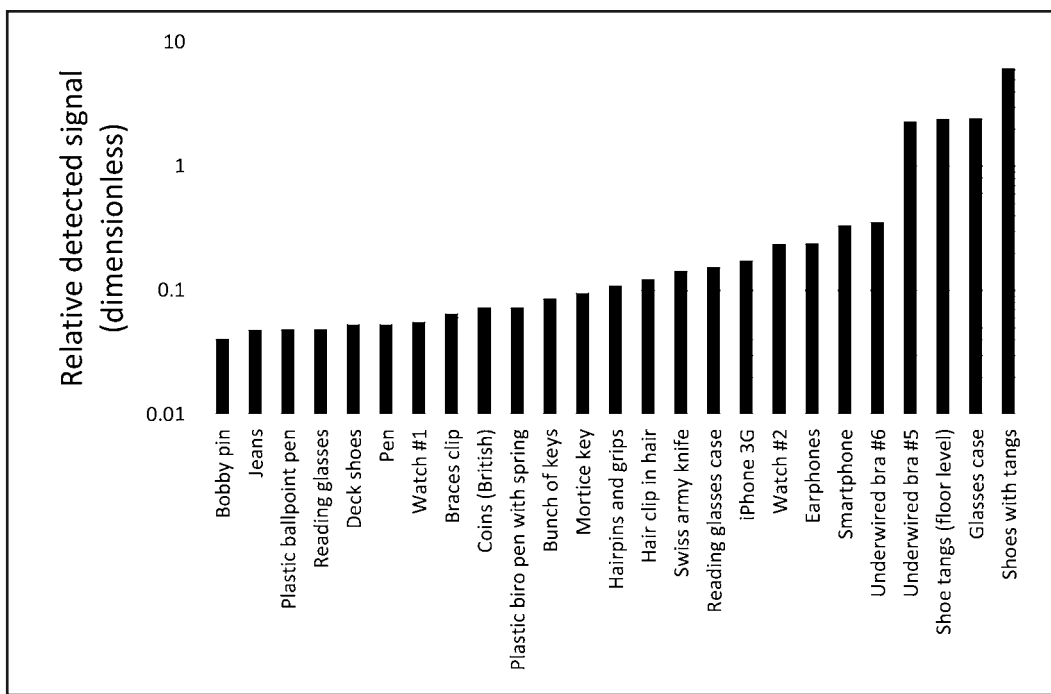


Very small objects have only a limited potential to achieve high magnetic moments. Most magnets associated with MR systems will have relatively minor missile-related occurrences by paper clips, pens, or other small objects. The limited magnetic qualities along with the very light weight of certain objects such as those means that they cannot accumulate enough kinetic energy to do damage or cause much inconvenience (unless the object impacts a particularly delicate area, such as the human eye). There is clearly a grey-scale between this and a missile-related accident with larger objects that will be inevitably serious. Using an FMD device at the MR system door should, at the mid-point of the door, at least detect the latter.

The relative signal strength related to the magnetic qualities of different objects that may be commonly found in the MRI setting has been measured (M.N. Keene, unpublished data) (**Figure 7** and **Figure 8**). These measurements were made in the fringe field, just outside of an MR system room at 1-Gauss and at the mid-point, 75-cm from the uprights of the FMDS. The average of several movements past the FMD device for each object are shown. **Figure 7** shows data for objects commonly found in control rooms and **Figure 8** shows data for personal items. The vertical scale is consistent between **Figure 7** and **Figure 8**. Depending upon the type of sensor used (or brand of the FMD device), the maximum sensitivity that is available is between 0.06 and 0.3 on this scale. Notably, the signals are much higher if the objects are near to the FMD device's uprights.

418 Using Ferromagnetic Detection Systems in the MRI Environment

Figure 8. The magnetic signal strength of personal items measured at the mid-point of an FMD device in a 1-Gauss magnetic fringe field.



PRACTICAL ASPECTS OF MR SYSTEM ENTRYWAY PROTECTION

Working With Entryway FMDS

The ideal FMD device (which does not yet exist) would have the following qualities: (1) no adaptations to workflow would be needed to accommodate the FMD device, (2) the FMD device would never alarm unless there was a ferromagnetic object entering the MR system room and (3) the FMD device would only alarm on loose objects that could become a hazard and not on tethered or restrained ferromagnetic objects (e.g., bra underwires or docking tables associated with scanners).

It is not ideal for MRI technologists or radiographers to have to modify their behavior to accommodate an FMD device. The main concern is opening and entering the door (which is highly magnetic) to the MR system room. At least one system allows the door to be opened and swinging as the MRI technologist enters and is still able to screen them efficiently (16). Others do not and so the door must be open and stationary before anyone can enter. The door is not an issue where an FMD device that is mounted a few feet in front of the door, although this configuration only works with certain facility layouts.

Some unwanted audible alerts may occur when a person not carrying a ferromagnetic object enters the MRI room at a time when there is a large ferromagnetic object moving nearby, such as a control room chair. FMDS are developed to minimize the detection of

moving ferromagnetic objects in Zone III but different systems do this to different degrees. Also, the more compact the Zone III space is, the more likely this will occur.

An FMD device cannot yet distinguish between loose ferromagnetic objects that could become missiles and “fixed” ferromagnetic objects that cannot. For example, the bolts in an MR Conditional gurney or the ferromagnetic components in MR Conditional monitoring equipment become problematic for screening. In these instances, the FMD device detects only the presence of ferromagnetic objects and not whether they are free to move. Therefore, extraneous alarms are inevitable in some circumstances. This will be discussed in more detail in the following section.

Overall, the use of an FMD device is believed to significantly enhance the safety level of MRI facilities, although non-ideal aspects of the current systems can impact the day-to-day activity and workflow of the MRI staff members, especially the MRI technologists. The individuals who are believed to cause most missile-related accidents are non-MRI workers who enter the room. While MRI technologists may not be able to supervise and control access to the scanner room constantly, an FMD device can and, thus, provides a warning to a person entering when the door is unsupervised. If non-technologists cause “alarms”, they should be trained to seek the advice of an MRI technologist before entering the MR system room.

When an FMD device alarms, its purpose is to prompt the MRI technologist to investigate. For example, an MRI technologist pushes an MR Conditional stretcher into the room and the alarm sounds, as always, because the stretcher typically has ferromagnetic components. The correct response of the MRI technologist is to stop and to perform a final check of the patient and the stretcher. Is the stretcher acceptable to use with this particular MR system? Is there a ferromagnetic oxygen cylinder or IV pole present that is MR Unsafe? Is there a ferromagnetic object under the sheets such as a sand bag with metallic shot? The incorrect response is to ignore the alarm because an MR Conditional stretcher will always trigger an alarm. Many accidents have occurred because of ferromagnetic items being placed on top of stretchers or underneath sheets, next to the patient. In this case, the alarm from the FMD device acts as a reminder to do a final check. It must be emphasized that FMDS are an adjunct to all other safe practices established for the MRI environment and should not replace any part of it. An FMD device adds an extra layer of safety.

Extraneous Alarms and False Alarms: Causes and Prevention

There is an important distinction between false alarms and extraneous (nuisance) alarms. A *false alarm* occurs when there is no ferromagnetic material passing through the FMD device but the alarm is activated. This may be due to some external factor causing a magnetic disturbance at the same time as a magnetically “clean” person passes through or by the FMD device. False alarms are rare when the FMD device has been installed and set up properly. The most common cause of false alarms are control room chairs when they are close to the FMD device and the occupant is moving or swiveling on it.

An *extraneous alarm* occurs when ferromagnetic material is deliberately passed through the FMD device because it is known to not present a missile-related hazard. The most common causes of extraneous alarms are, the following: the door to the MR system room mov-

420 Using Ferromagnetic Detection Systems in the MRI Environment

ing as individuals pass through; MR Conditional equipment (e.g., gurneys, wheelchairs, monitoring equipment, equipment tables, etc.) passing by the FMD device, staff clothing and accessories (e.g., underwire bras, watches, shoes with metal supports, etc.); and patient clothing and accessories. Notably, with extraneous alarms, the FMD device is functioning normally and doing its job.

If the frequency of extraneous alarms is excessive, alarm fatigue sets in and staff members soon begin to ignore the FMD device. When this occurs, the FMD device is reduced in effectiveness during the working hours of the MRI facility, although it still remains effective for non-MRI staff members. However, most of the causes of extraneous alarms are preventable and within the power of the MRI technologists to remediate them. Certain solutions exist to prevent extraneous alarms including, the following:

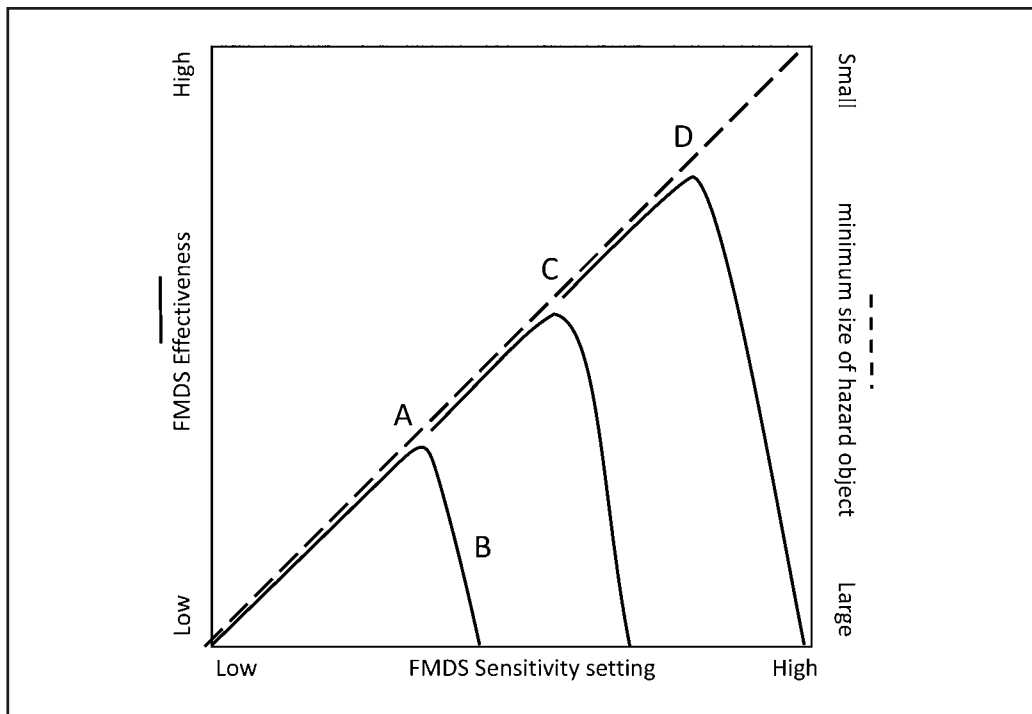
Staff member clothing and accessories. This can be one of the biggest causes of extraneous alarms. One of the most common items is the ferromagnetic underwires in bras. Considering the activities of female MRI technologists, nurses and other personnel, these wires may come into close proximity with the MR system's magnet and, thus, become highly magnetized, for example some underwires can increase in magnetization by 20 times as a result of exposure to an MRI magnet. Other objects such as watches, bracelets, and shoes with tangs or metallic supports can also trigger the FMDS. Alternatives for all such clothing and accessories are readily available. Watches and ferromagnetic jewelry can easily be removed.

MR Conditional equipment. For patient transfer equipment, there are products that are available that are entirely nonferromagnetic and, thus, will not cause extraneous alarms. The use of nonferromagnetic transfer equipment means an FMD device will alarm only on any ferromagnetic materials carried on them. For docking tables associated with scanners, patient monitors, and other equipment there is currently no solution. It is recommended that the extraneous alarm should be used for the purpose of taking the time to check the equipment for objects placed upon them before proceeding into the MR system room.

Patient clothing and accessories. It is always best practice to place patients in pocketless gowns or scrubs in preparation for MRI examinations. Accordingly, any FMD device alarm will be real and not extraneous. Underwire bras, shoes with metal supports, and ferromagnetic jewelry issues are the same as for staff members.

There is a relationship between the effectiveness of an FMD device and its sensitivity level that becomes limited by the extraneous alert rate (24). Referring to **Figure 9**, the 'effectiveness' of an FMD device is its ability to warn users that there are ferromagnetic objects entering the MR system room. When plotted against the sensitivity setting of an FMD device, the effectiveness increases with the sensitivity setting, up to a point (Point A in **Figure 9**). Further increasing the sensitivity results in lowered effectiveness due to alarm fatigue (Point B) caused by watches, shoes, pens, badges, underwires bras, and other items that the staff members may have as they enter the scanner room or pass the FMD device, or due to MR Conditional equipment with ferromagnetic components. Where such things are limited, the extraneous alarm rate may be lowered and a higher sensitivity level can be set, thus, increasing the FMD device's effectiveness (Point C). Some facilities operate a "zero magnetic" working policy (see next section) and with this, the highest effectiveness is achieved

Figure 9. A graphical representation of the relationship between an FMD device's detection sensitivity setting (left axis solid lines) and its effectiveness at detecting potentially hazardous objects. The right axis (dashed line) illustrates the general trend such that the higher the sensitivity, the smaller (magnetically) the object it can detect.



(Point D). Therefore, the sensitivity of an FMD device should be set appropriately for the environment to maximize the effectiveness point.

Zero Magnetic Working In the MRI Environment

While it is unacceptable for patients to enter the MR system room with unnecessary ferromagnetic objects, it is often deemed acceptable (albeit poor practice) for staff members to do, with the exception of those objects are retained in place by counterforces (e.g., watches, underwire bras, belt buckles, etc.). Zero magnetic working in the MRI environment is a method of working whereby staff members adopt the same mantra as patients and have no unnecessary ferromagnetic objects. The purpose is to minimize extraneous alarms on entryway an FMD device so that they can be set to a higher sensitivity level with a low extraneous alert rate (Point D, **Figure 9**) to provide higher levels of safety. In addition, zero magnetic transfer equipment is used so that an alert will register a ferromagnetic object on a non-ambulatory patient being transferred into MR system room.

Obviously, zero magnetic working is challenging to adopt. It requires staff members to use tested products to wear, or to take a small magnet into stores to test clothing items. For example, it will be noted that not all underwires in bras are magnetic. While martensitic stainless steel wires are ferromagnetic, austenitic stainless steel or other nonferromagnetic

422 Using Ferromagnetic Detection Systems in the MRI Environment

materials or nonmetallic materials used for this same application are acceptable for zero magnetic working. Unfortunately, all materials are rarely if ever reported on product labeling for clothing items. Therefore, the only practical approach is to test them with a magnet.

Guidance on the Adoption of FMDS

The effectiveness of an entryway an FMD device for improving safety depends predominantly on the attitude of the MRI facility's managers and MRI technologists. The introduction of an FMD device significantly increases the potential for safety improvements, but this may not be realized due to various factors. To illustrate this, two examples are provided.

MRI Facility A purchased several entryway FMDS to protect their scanner rooms. They adopted a zero magnetic working policy. The patient transfer equipment was replaced with entirely nonferromagnetic equivalents. A culture of "zero tolerance" to unnecessary ferromagnetic materials entering the MR system rooms was introduced. Staff members were required to be entirely nonferromagnetic, adopting the same standard of "magnetic cleanliness" as their patients, and even wore pocketless scrubs to prevent accidental entry of objects. Each patient was gowned and checked with a screening FMD device prior to entry into the MR system room. The doors to the scanner rooms were always kept closed when not in use. The low extraneous alarm rate that resulted from these measures allowed each FMD device to be set at a relatively high sensitivity level, such that it could detect smaller ferromagnetic objects. The staff members had regular MRI safety training and were able to contribute to the evolving safety protocols for the facility.

MRI Facility B also purchased several entryway FMDS to protect their MR system rooms. Unfortunately, the ferromagnetic detection systems were purchased by an inexperienced manager without consultation the MRI technologists. The staff members were unwilling to change the way they clothed, and the managers were unwilling to enforce a clothing policy. They kept their regular MR Conditional transfer equipment. Staff members resisted making any workflow concessions with regard to the doors to the MR system rooms. Patients were not gowned and their family members were allowed into the scanner rooms. A patient screening FMD device was not utilized. Despite being set to a low sensitivity to reduce extraneous alarms, each FMD device alarmed on virtually every entrance and exit occurrence. When this became intolerable each FMD device was turned off.

The examples of *MRI Facility A* and *MRI Facility B* may be regarded as being at opposite ends of a safety spectrum where one facility maximized its safety standard and represented best practice, while the other facility was unchanged from its initial poor practice. For any MRI facility, improving safety with regard to missile-related accidents using an FMD device is a journey. Some facilities choose to make that journey in one leap with a radical culture change to become like *MRI Facility A* in a very short time. Typically, the facility will usually have good reason to do this with the most common reason being an occurrence of a missile-related accident or near miss that shocked the facility. Events like these tend to unite the MRI technologists and the facility management to take all effective measures to prevent a problem from occurring again.

For most facilities, the implementation of an FMD device involves gradual changes. The FMD device may be set to the modest sensitivity initially (e.g., Point A in **Figure 9**). As the MRI technologists improve their protocols, procedures, and their surrounding environmental factors, the sensitivity of the FMD device may be increased accordingly, as time goes by. Well-organized facilities do this as a defined structured plan. It is possible with some entryway FMDS to chart the number of entries into MR system room and the number for which an alert was issued (see *The Entryway FMD Device as a Safety Management Tool* below). Thus, improvements due to new procedures, workflow or environment can be measured. It is much more motivating for MRI technologists to see that changes can result in measurable improvements to safety.

Workflow Aspects of Using an Entryway FMD Device

The FMD device should be sited where workflow is least affected. For an MRI facility that is high on the safety scale where extraneous alarms are low, there is very little impact on workflow. In the case of where there are a substantial number of extraneous alarms and each one is investigated, the impact increases. In many facilities, the workflow is a key priority that will not be compromised. There are two common responses to this situation. One is to ignore the FMD device, which reduces safety levels. The other is to move up the safety scale to reduce the extraneous alarms. Both responses retain the workflow, but one increases safety while the other reduces it. For example, implementing a nonferromagnetic clothing policy tends to make the greatest impact on maintaining workflow in a positive safety direction followed by changing to nonferromagnetic patient transfer equipment.

The Entryway FMD Device as a Safety Management Tool

Recent innovations in entryway FMDS have taken them beyond a warning device at the MR system door. Some entryway systems (16, 17) now have optional cameras that can make a short video recording or take a series of photographs when an alarm is triggered. This may help a facility understand the causes of alarms or to perform a root cause analysis on missile-related events.

The most advanced FMDS can additionally collect data from the scanner doorways and provide access and interpretation of it to be presented on an app or a web browser (16). The data that such an FMD device can measure include the number of times the MR system room (i.e., Zone IV) has been entered, the number of times a ferromagnetic object has entered, the general level of magnetic activity in the area prior to the MR system room (i.e., Zone III), the status of the door (i.e., opened or closed), and the FMD device's self-test results. These data accumulate with time so trends can be observed. The data from each entryway FMD device within the facility can be inspected from an office computer, or on a smart phone or tablet remotely, and at any time by authorized users.

These data can be distilled into information that is useful to a facility manager, the MR safety officer, or the lead MRI technologist. For example, knowing the proportion of entries that cause extraneous alerts may be used to track the progress of process improvements implemented to reduce the entry of ferromagnetic objects. Additionally, the trend over time provides evidence of safety improving or worsening. Because the data from all MR systems owned by a facility are monitored, comparisons can be made between different shifts and

424 Using Ferromagnetic Detection Systems in the MRI Environment

between different scanners. This reveals where attention needs to be given for safety improvements. It is obvious that the fewer unnecessary ferromagnetic objects that enter the MR system room, the lower the probability of missile-related accidents. Thus, to measure and analyze this information will help to manage the improvement processes. Example data that illustrate the above is shown in **Figure 10**. This facility implemented a procedural change during a one-month period that resulted in a lower number of incidents related to ferromagnetic objects.

Figure 10. Illustration of how data from an FMD device can be used to manage safety. Here, it was observed that the ingress of unnecessary ferromagnetic material into the MR system room (Zone IV) required improvement. A process improvement was introduced at the end of February 2017 and the situation measurably improved. (Figure courtesy of Metrasens Ltd.)



Data on the status of the MR system door can also drive safety management decisions. For example, the data may show that MRI A has the door left open on average 10 minutes per hour but is used by individuals passing through only for 2 minutes. By comparison, for MRI B, the door is only opened for people passing in and is closed at all other times. This may suggest for MRI A, that the door is left open unnecessarily, which is a safety weakness whereas MRI B has a good safety practice in this regard.

High levels of magnetic activity outside the MR system door may indicate the presence of ferromagnetic objects that could accidentally and easily be carried into the room because they are in the immediate vicinity. It is not uncommon to find ferromagnetic trash bins, chairs, stools, linen carts, oxygen cylinder carts, and crash carts placed immediately outside the door to the scanner. Having the data to indicate which MR system room has a high level of magnetic activity immediately outside the door may motivate an inspection and lead to improvements.

The collection of these data from across a facility, regardless of whether they are in different buildings or even different cities, allows these aspects of safety to be actively managed, centrally. Improvements can be targeted, and the effect of any changes measured. Safety changes that are evidence-based are often more acceptable than seemingly esoteric changes.

FERROMAGNETIC DETECTION SYSTEMS FOR USE TO SCREEN PATIENTS

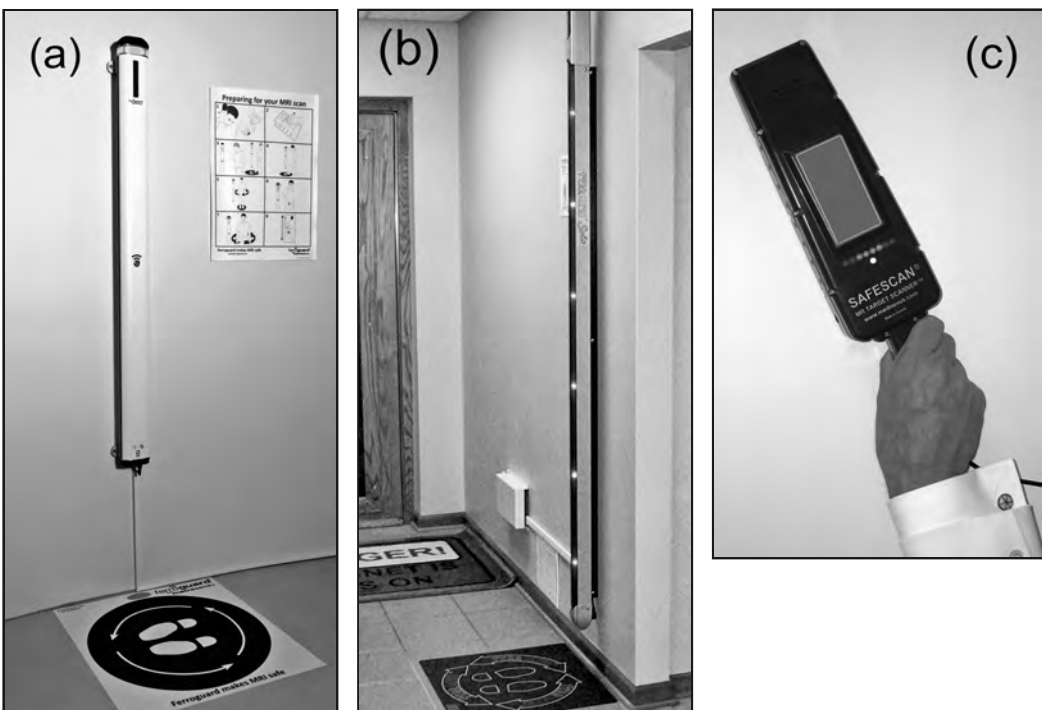
Using an FMD device for patient screening is becoming more common (25-29). The main purpose of this practice is to check patients for ferromagnetic objects just prior to the MRI examination. The utilization of an FMD device will help to prevent potential missile-related incidents from devices a patient may bring into the MR system room and to reduce scanning artifacts due to small and well-hidden ferromagnetic objects such as bobby pins.

A detailed study by the Pennsylvania Patient Safety Authority (30) reveals the range of objects and frequency of reported events for ferromagnetic items that passed conventional screening undetected. This study included events where objects were carried in by staff members. Ferromagnetic screening can significantly reduce the number of unnecessary ferromagnetic objects being carried into the MR system room by patients, as well as staff members if they screen themselves as a safety check.

There are two types of patient screening FMDS available, wall-mounted as shown in **Figures 11 (a)** and **11 (b)** and a handheld device, **Figure 11 (c)**. For a wall-mounted FMD device, the patient approaches the unit and slowly rotates in front of it. This process brings all parts of the surface of the patient within a few inches of the FMD device, which has a twofold purpose: (1) the small distance between a ferromagnetic object and the magnetic sensors permits smaller (i.e., lower magnetic susceptibility) objects to be detected and (2) it provides the necessary motion of the ferromagnetic object relative to the FMD device. By comparison, handheld FMD device is used to methodically scan the surface of the patient.

426 Using Ferromagnetic Detection Systems in the MRI Environment

Figure 11. (a) and (b) Examples of wall-mounted ferromagnetic detection systems used to screen patients that rotate in front of these devices. **(c)** Handheld FMD device that is swept over the patient's body. (Photographs provided courtesy of Metrasens Ltd., Kopp Development Inc., and Mednovus, Inc.)



Performing patient screening using an FMD device does not tend to have extraneous alarms because only the patient is screened and should essentially be free of ferromagnetic objects. Staff members and equipment are not screened this way unless there is a policy for this procedure. However, patient screening using an FMD device is subject to false alarms if there is a moving ferromagnetic object nearby during this screening process. Normally, the MRI technologist can easily identify this situation by observation, and repeat the screening, as needed.

The Patient Screening Process Using an FMD device

Screening the patient using an FMD device is an additional step in the screening process and is the last step before the MRI examination. It is important to note that it is not a replacement for any aspect of the screening procedure but rather it is an supplemental procedure that adds a final objective check prior to performing MRI (29). This type of screening normally takes less than a few minutes to complete provided that there is no positive alarm. It takes somewhat longer to use a handheld FMD device because it has to be manually scanned over the entire surface area of the patient's body. Ideally, there will be a line item at the bottom of the screening questionnaire that records the result FMD device screening and any observations or actions as a result.

If a patient passes the FMD device screening without a detection occurring (i.e., no positive alarm), this should be documented on the screening form and the patient may then proceed with the MRI examination. If an alarm occurs, then the patient must be investigated for the presence of a ferromagnetic object and it should be removed, if possible. Once this has been completed, the patient should be re-screened using the FMD device. If a ferromagnetic object cannot be found, the FMD device screening should be repeated in case the original result was a false positive alarm. With genuine alarms that cannot be resolved, the MRI technologist must then suspect the possibility that the ferromagnetic object is internal, being either an implant or a foreign body (25-29). The patient's history should then be thoroughly checked before proceeding to MRI.

Detection Performance

The earlier discussion concerning the size of ferromagnetic objects that can be detected using entryway FMDS applies to patient screening utilizing an FMD device, as well. However, due to the shorter distance when using a patient screening FMD device, magnetically weaker objects can be more reliably detected. In general, bobby pins, hair barrettes, and other similar items can be reliably detected with the best performing patient screening FMD device. Obviously, this feature is good for artifact reduction and will save time re-scanning individuals in the MRI setting. However, very small ferromagnetic objects are not likely to be detected, such as a small metallic ferromagnetic foreign body in the eye.

Because potentially dangerous objects that are discovered by FMD device screening and removed prior to MRI are not reportable, the efficacy of patient screening using this technique in clinical environments is difficult to accurately measure. Some investigations have been performed and report the performance of using a patient screening FMD device (25, 31, 32), but several are unpublished. A summary of information regarding clinical alert rates is provided in **Table 1**. It is interesting to note that although the patients in each of these published and unpublished studies were gowned, there were a surprising number of positive alarms. These alarms were mainly associated with removable dental implants, eyeglasses, underwire bras, and other objects.

Using a Wall-Mounted Versus Handheld FMD Device

The use of a wall-mounted FMD device provides head-to-toe, whole-body screening that is easy to accomplish and fast to perform for cooperative ambulatory patients. For non-ambulatory patients, the only means of screening with a wall-mounted FMD device is to use a nonferromagnetic gurney or wheelchair and perform a "drive-by" in two directions parallel to the wall, pushed by an MRI technologist that has no ferromagnetic objects. However, this process will not provide the close distance required to detect the smallest objects, but is nonetheless useful for the detection of larger personal items.

The use of a handheld FMD device (17, 18) is somewhat similar to using a handheld metal detector (e.g., the type used at airports), insofar as it must be swept or scanned over the surface of the individual's body at close range, usually within 5-cm of the surface. The sensing area is relatively small (approximately 5-cm x 9-cm) so that care must be taken to ensure that screening occurs with no gaps while maintaining a relatively short, stand-off distance. Due to this being a manual process, the quality and reliability of the screening de-

428 Using Ferromagnetic Detection Systems in the MRI Environment

Table 1. Summary of patient screening studies using FMD device technology. All studies involved patients who were in gowns. Note that the data presented below is for a single type of FMD device (see Ref. 16).

	Hospital 1	Hospital 2	Hospital 3	Hospital 4	Hospital 5	Hospital 6
Number of patients presenting to MRI	75	20	38	91	340	977
Number of screens performed	95	20	26	55	340	1032
Number of alerts raised	27	3	8	5	16	55
Number of alerts/screens	28.4%	15%	30.76%	9.1%	4.7%	5%
[Hospital 1- US out-patient facility (Unpublished), 2- English NHS Trust, (Unpublished), 3-Scottish Health Board Twin Site, (Unpublished), 4-Scottish General Hospital, (Unpublished), 5-University Hospital Jena (25), 6-Princess Elizabeth Hospital, Guernsey (Ref. 31).]						

pends on the person performing the scan using the handheld FMD device. Staff members may be reluctant to screen an intimate patient area, such as the groin, which may result in safety issues as reported by James et al. (26). Notably, the only available handheld FMD device at this time has a strong permanent magnet within it to boost the magnetization of ferromagnetic objects (17, 18). Because of this, this type of handheld FMD device should never be used close the eyes, near cardiac pacemakers, or other similar implanted devices to prevent the magnetic field from posing possible problems. A handheld FMD device can be used for a non-ambulatory patient on an MR Conditional stretcher or wheelchair, as well as nonferromagnetic ones. Using a stretcher, the patient needs to turn over from one side to the other to get full coverage for proper screening. Using a wheelchair, it is more difficult to get full coverage unless the patient can stand in front of the FMD device for a short period of time.

Screening for Ferromagnetic Implants, Devices, and Foreign Bodies

The question surrounding the detection of ferromagnetic implants, devices, and foreign bodies is a current research topic with growing interest (25-29, 31). The use of a patient screening FMD device is not intended to be used for the specific purpose of detecting implanted objects according to the manufacturers of these systems. However, because human flesh is effectively transparent to ferromagnetic detection, the distinction between *ex vivo* and *in vivo* ferromagnetic objects is merely one of range, and it can therefore be expected that ferromagnetic implants can be detected. Investigations on implant and foreign body detection have been conducted (25-29, 30, 32). Recently, a more comprehensive study confined to cardiac pacemakers demonstrated that good detection of such devices is possible with all pacemakers detected in the study group (33 different pacemaker models)(32). Pace-

makers constitute by far the largest proportion, (58% compared to second place 14%), of objects causing adverse screening events in the most systematic study currently available, to date (30). Implanted objects can range from completely nonferromagnetic (e.g., abandoned cardiac pacing leads) to highly ferromagnetic items. The implants that may or may not be reliably detected are, therefore, dependent upon the sensitivity of the FMD device. It is important to note that FMDS are not approved medical devices by the U.S. Food and Drug Administration and, thus, cannot be sold as “implant detectors”. Because of this, there are no standards of performance for the detection of implanted devices. Therefore, it is important to see published evidence in the peer-reviewed literature for performance of different FMDS if patient screening is to be considered for this additional use.

It is important to note that conventional handheld metal detectors are still commonly found in patient screening areas. These handheld devices transmit a fluctuating magnetic field, which, if strong enough, could exceed the safe conditions for certain active implanted devices. However, the manufacturer rarely states the specifications for their device and how it changes with distance. As such, it is difficult to be certain that these are acceptable metal detectors for use on patients intended to detect active implants. Experimental studies have not determined a combination of implantable device and metal detector that may cause an adverse event (33), likewise for the handheld FMD device (17, 18) that contains a strong magnet (17, 18).

Siting Considerations for FMDS

Wall-mounted and handheld patient screening devices have two requirements on their installation or use location. First, this type an FMD device needs to be installed in a convenient position from the point of view of efficient workflow. This will typically be in the patient changing or preparation area, or sometimes in the immediate area prior to the MR system room (Zone III), although this is less ideal due to the activities in this area. The second requirement is that it is located sufficiently far enough awayfrom interfering magnetic sources so that it can be set to maximum sensitivity. Interfering sources may include public corridors, roads, and elevators.

INTERVENTIONAL, INTRAOPERATIVE, HYBRID-MR SYSTEMS, AND 7-T MRI ENVIRONMENTS

There are increasing numbers of hospitals using suites where the MRI is not a stand-alone diagnostic imaging tool. These include interventional, intraoperative, hybrid-MR systems (e.g., PET/MR, radiation therapy MR, etc.), and ultra-high-field systems, each of which present new challenges for patient safety with respect to missile-related events. These suites are intrinsically more at risk from ferromagnetic projectiles than regular clinical MR scanners for two important reasons: (1) there is a more varied mixture of staff members involved with the procedures, so a consistently high standard of safety knowledge and training is very difficult to achieve, and (2) there is a substantially larger number of types of equipment that is needed in the respective scanner.

Interventional. The use of an entryway FMD device at an interventional MR system room entrance is likely to be counter-productive unless it is implemented as part of a broader

430 Using Ferromagnetic Detection Systems in the MRI Environment

safety strategy. The main issue is alarm fatigue because the mixture of different staff members, types equipment that is required for use in this setting, and other factors. Currently, there are two approaches for the use of an entryway FMD device in the interventional MRI environment. The first is to implement a zero magnetic dress code for all staff members working in this area regardless of role or position. Notably, an FMD device patient screener repurposed as a staff screener outside of the suite will enable self-checking. All equipment entering should be inspected for safety and transferred in only by the MRI technologist preferably in advance of the procedure and other staff members arriving. This way, the equipment may be checked by an experienced individual and the FMD device can be ignored or temporarily silenced (a feature that some FMDS have) during this ingress.. With the exception of the patient being transferred to the room on the docking MR system table or MR Conditional gurney, there should be no further extraneous alerts.

The second approach is to use an entryway FMD device in an area some distance in front of the suite's door such that it can be bypassed. Thus, the FMD device can then be used at the discretion of the MRI technologist to check individuals and equipment for which there is some uncertainty. Objects or staff members that the MRI technologist has confidence are safe for the MR system room but that are likely to cause an alert, may bypass the FMD device.

Intraoperative. For entrances between interoperative suites (including the IMRIS Hybrid Operating Suites), the issues and solutions are similar to the interventional suite. However, if there is a door to the scanner room from the control room for the MRI technologist to use and is not in the workflow for patients and the other staff members, then a regular entryway FMD device may be used. Many intraoperative suites have inner sliding doors between the operating room and the MR system, such as that used with the IMRIS Hybrid Operating Suite. It is inadvisable to use an entryway FMD device in this setting because there will always be nuisance alerts related to movement of the table. However, the installation of a '*patient screener*' FMD device near these doors in the OR side is advisable for the use of OR staff to check themselves prior to entering the MR system room. It is the role of the technologist to assess the safety of the docking table with the patient on the table. This may be by visual inspection and also questioning the surgeon about whether any instruments are internal to or attached to the patient.

Linac/MR. Linac (linear accelerator)/MR radiotherapy suites feature very heavy radiation shielded doors that are very slow opening due to the lead and concrete construction in a steel frame. This presents a challenge to install entryway FMDS at the door as regular door-ignoring technology in FMDS struggle to cope with slow moving automated sliding doors. An entryway FMD device may be installed at the doorway, but it is best to wait for it to fully open before entering. Alternatively, they may feature a *maze corridor* leading to a regular MRI door to prevent any line-of-sight for radiation leakage into the hospital. It is advisable to install an entryway an FMD device in this corridor prior to the scanner's entry door.

7-T MRI Environment. The introduction of research and clinical 7-T MR systems presents new challenges for safety. The magnetic fringe fields are generally higher than for 1.5- and 3-T and, thus, the forces acting on ferromagnetic objects will be higher. Much of the

equipment labeled MR Conditional that is familiar for everyday use in scanners with lower static magnetic fields needs to be tested at 7-Tesla. This important task been accomplished by Culo, et al. (34) for many commonly used patient support devices including wheelchairs, IV poles, instrument tables, step stools, and others devices. Entryway and/or patient screening FMDS may be used for 7-T MRI settings similar to how they are used with lower field strength scanners. In 2019, Hoff, et al. (35) presented general safety considerations for the 7-T MRI environment.

REQUIREMENTS AND RECOMMENDATIONS FOR FMDS

In the United States (U.S.), the American College of Radiology (ACR) recommends the use of FMDS in their guidance document on MR safe practices (2). This document is largely regarded as a model for the standard management of patients referred for MRI examinations. The Facilities Guidelines Institute (FGI) requires FMDS for new and retrofitted builds (36). The FGI guidelines have been adopted by The Joint Commission in their Environment of Care Standard EC.02.06.05 and by over 40 states in the U.S. (37).

In the United Kingdom, the Medicines and Healthcare products Regulatory Agency (MHRA) recommends the use of FMDS (38), and Italy is likely to emerge as the first country to have a national requirement (39). There are other international bodies that make similar recommendations based on the ACR's recommendations (2). Therefore, it is advisable for all MRI facility planners and managers to familiarize themselves with the recommendations or requirements from their national regulators with respect to FMDS.

CONCLUSIONS

The safety of patients, staff, equipment, and reputation of an MRI facility should be recognized as a holistic issue, not just about the use of an FMD device, but the entire culture. This culture should be characterized by the adoption of best practice in safety procedures, staff training and education, use of safety-related technology along with a striving for continuous improvements at all levels. Unfortunately, there is a notion that adopting high safety standards often work against the high throughput or efficiency of the MRI facility. This is a dangerous and incorrect perspective.

The availability of an FMD device as a safety technology has substantially increased the potential safety levels that a facility may attain. If these devices are adopted with the view that they are one key element of an overall safety improvement program, they will be most effective. If they are adopted as an excuse to do nothing more on training or safety procedures, they will have a limited positive benefit.

Earlier in this chapter, the ideal FMD device was defined. As the technology continues to develop, systems will move toward this ideal. The main non-ideal issue present with an FMD device relates to extraneous alarms, which are partly a result of the introduction of the FMD device into a setting where unnecessary ferromagnetic objects may be routinely carried into the MR system room and partly due to problematic siting (e.g., in proximity to equipment that transmits “magnetic noise”). Hopefully, technology used for FMDS will evolve to eventually overcome these matters.

432 Using Ferromagnetic Detection Systems in the MRI Environment

FMDS are not currently subjected to regulatory standards so there is no minimum performance standard defined for these devices. When selecting an FMD device, an MRI facility currently has to rely on the manufacturer's claims, whether or not a satisfactory experience occurred during the demonstration of the product, or recommendations from MRI safety experts. Fortunately, articles in the peer-reviewed literature have also helped to support the use of FMDS to prevent incidents and accidents.

At some point, the use of an FMD device may become an essential screening tool for MRI facilities. To date, the statistical impact that these devices have on safety has yet to be investigated and, therefore, it is difficult to know how many accidents or injuries have been avoided. As the recognition of the need to improve MRI safety proliferates and as the use of FMD device technology correspondingly widens, the global MRI community will hopefully become substantially safer.

Entryway FMDS may now have an additional use in the management of safety due to the data they collect at the doorway. This has elevated them from being just a point-of-use device to, additionally, an IoT (Internet of Things) device whereby safety managers may view and act upon data from all of their scanners in order to direct changes and target improvements, as well as to measure improvements. Additionally, these particular devices provide a recorded audit trail. Patient screening FMDS are increasingly being used as a final objective check for a patient before performing MRI. Their ability to discover certain important-to-detect implants and foreign bodies has been realized (26-32).

REFERENCES

1. Kanal E, Barkovich J, Bell C, et al. ACR guidance document for safe MR practices: 2007. American Journal of Roentgenology 2007;188:1447.
2. Kanal E, Barkovich AJ, Bell C, et al. ACR guidance document on MR safe practices: 2013. J Magn Reson Imaging 2013;37:501-530.
3. The Joint Commission. Preventing accidents and injuries in the MRI suite. Sentinel Event Alert, Issue 38, February 14, 2008.
4. United States Department of Veterans Affairs. MRI Design Guide. 2008;2-25 – 2-28.
5. ECRI Institute, Health Devices. 2010 Top 10 Technology Hazards. 2009;38:11:1-10.
6. Shellock FG. Reference Manual for Magnetic Resonance Safety, Implants, and Devices: 2020 Edition. Biomedical Research Publishing Group, Los Angeles, CA, 2020.
7. Karpowicz J, Gryz K. Health risk assessment of occupational exposure to a magnetic field from magnetic resonance imaging devices. International Journal of Occupational Safety and Ergonomics (JOSE) 2006;12:155–167.
8. Duffin WJ. Electricity and magnetism, Third Edition. London: McGraw-Hill; 1980:230-232.
9. Bleaney BI, Bleaney B. Electricity and magnetism. Third edition. Oxford: Oxford University Press; 1978:101-107.
10. Shellock FG, Woods TO, Crues JV. MRI labeling information for implants and devices: Explanation of terminology. Radiology 2009;253:26-30.
11. Kanal E, Borgstede JP, Barkovich AJ. American College of Radiology white paper on MR safety. AJR Am J Roentgenol 2002;178:1335-1347.
12. Kohn LT, Corrigan JM, Donaldson MS, Editors. To err is human: Building a safer health system. Washington, DC: National Academy Press, Institute of Medicine; 1999.

MRI Bioeffects, Safety, and Patient Management 433

13. Riva D. Magnetic Resonance Imaging (MRI) Safety. Introduction to Public Workshop. Public Workshop, Magnetic Resonance Imaging Safety, U.S. Food and Drug Administration, White Oak Campus, Silver Spring, MD, 2011.
14. Levinson DR. Hospital incident reporting systems do not capture most patient harm. Department of Health and Human Services, Office of Inspector General, OEI-06-09-0009, 2012.
15. Chen DW. Boy, 6, dies of skull injury during MRI. New York Times. July 31, 2001:B1-B5.
16. Metrasens Ltd., www.metasens.com.
17. Kopp Development, Inc., www.koppdevelopment.com.
18. Mednovus Inc., www.mednovus.com.
19. Ripka P, Editor. Magnetic Sensors and Magnetometers. Boston: Artech House; 2001.
20. Czippott PV, Kumar S, Wolff S, et al. Magnetic Resonance Imaging Screening Method and Apparatus. 2008; United States Patent. No. U.S. 7,315,166 B2.
21. Keene MN. Ferromagnetic Object Detector. 2006; United States Patent. No. U.S. 7,113,092 B2.
22. Wooliscroft MJ. Apparatus for detecting ferromagnetic objects and a protected doorway assembly. 2012; World Intellectual Property Organization, International Publication Number WO 2012/022971 A2.
23. Jiles DC. Introduction to magnetism and magnetic materials, Second Edition. Florida: Chapman & Hall/CRC Press; 1998.
24. Keene MN, Watson RE. Ferromagnetic detectors for MRI safety: Toy or tool? Current Radiology Reports 2016;4:20:1-20.
25. Heinrich A, Gütter F, Jäger U, Teichgräber U. Can ferromagnetic metal detectors improve MRI safety? Biomed. Tech. 2012;57(Suppl. 1):709.
26. James CA, Karacozoff AM, Shellock FG. Undisclosed and undetected foreign bodies during MRI screening resulting in a potentially serious outcome. Magn Reson Imaging 2013;31:630-633.
27. Keene MN, Shellock FG, Karacozoff AM. Detection of ferromagnetic implants using a ferromagnetic detection system: Implications for patient screening prior to MRI. MR Safety in Practice: Now and In the Future. International Society for Magnetic Resonance in Medicine, Scientific Workshop; Lund, Sweden, 2012.
28. Karacozoff AM, Shellock FG. Armor-piercing bullet: 3-Tesla MRI findings and identification by a ferromagnetic detection system. Military Medicine 2013;178:e380- e385.
29. Shellock FG, Karacozoff AM. Detection of implants and other objects using a ferromagnetic detection system: Implications for patient screening prior to MRI. AJR Am J Roentgenol 2013;201:720-725.
30. Field C. MRI Screening: What's in your pocket? Pennsylvania Patient Safety Advisory 2018;15:1-12.
31. Orchard LJ. Implementation of a ferromagnetic detection system in a clinical MRI setting. Radiography 2015;21:248-253.
32. Watson RE, Walsh SM, Felmlee JP, Friedman PA, Keene MN. Augmenting MRI safety screening processes: Reliable identification of cardiac implantable electronic devices by a ferromagnetic detector system. J Magn Reson Imaging 2019;49:e297-e299.
33. Jilek C, Tzis S, et al. Safety of screening procedures with hand held metal detectors among patients with implanted cardiac rhythm devices: A cross sectional analysis. Annals of Internal Medicine 2011;155:587-592.
34. Culo B, Valencerina S, Law M, Shellock FG. Assessment of metallic patient support devices and other items at 7-Tesla: Findings applied to 46 additional devices. Magn Reson Imaging 2019;57:250-253.
35. Hoff MN, McKinney IV A, Shellock FG, et al. Safety considerations of 7-T MRI in clinical practice. Radiology 2019;292:509-518.
36. Facility Guidelines Institute. <https://www.fgiguidelines.org/>

434 Using Ferromagnetic Detection Systems in the MRI Environment

37. FGI Guidelines for US state adoption. <https://www.fgiguideelines.org/guidelines/state-adoption-fgi-guidelines/> Note: This site updates regularly to reflect current state adoption of FGI guidelines.
38. MHRA: Safety guidelines for magnetic resonance imaging equipment in clinical use. 2015;Section 5.4.11.
39. Gazzetta Ufficiale Della Repubblica Italiana Serie generale - n. 236, 2018;5-34.

Chapter 17 Physiological Monitoring of Patients During MRI

FRANK G. SHELLOCK, PH.D.

Director of MRI Safety
USC Stevens Neuroimaging and Informatics Institute

Adjunct Clinical Professor of Radiology and Medicine
Keck School of Medicine, University of Southern California
Los Angeles, CA

ALEXANDRA KARACOZOFF, MPH

Associate Editor
Biomedical Research Publishing Group
Sacramento, CA

INTRODUCTION

Conventional physiological monitoring equipment and patient support devices were not originally designed to be utilized in the harsh magnetic resonance imaging (MRI) environment where static, time-varying gradient, and radiofrequency (RF) electromagnetic fields can adversely impact (e.g., as a result of missile effects), affect, or alter the operation or use of these devices (1). Fortunately, various monitors and other patient support devices have been specially modified or specifically developed to be utilized safely in the MRI setting (1-32). Thus, commercially available MR Conditional monitors and other devices (note, certain devices are MR Safe if made from nonconducting, non-metallic materials) are readily available and can be used routinely for patients in the MRI environment (1-32).

MRI healthcare professionals must carefully consider the ethical and medicolegal ramifications of providing proper patient care that includes identifying patients who require monitoring in the MRI setting and following a protocol that ensures their safety by using appropriate equipment, devices, and accessories (1, 33-43). The early detection and immediate treatment of complications that may occur in high-risk, critically ill, or anesthetized patients undergoing MRI can prevent relatively minor problems from becoming life-threatening situations.

436 Physiological Monitoring of Patients During MRI

This chapter provides information, recommendations, and guidelines for patient monitoring in the MRI environment. In addition, techniques, equipment, and devices that may be used to monitor and support patients undergoing MRI examinations are described herein.

MONITORING PATIENTS DURING MRI: RECOMMENDATIONS AND GUIDELINES

General Policies and Procedures

In general, monitoring during an MRI examination is indicated whenever a patient requires observations of vital physiological parameters due to an underlying health problem or whenever a patient is unable to respond or alert the MRI technologist or another healthcare professional regarding pain, respiratory or cardiac distress, or other difficulty that might arise during the examination (1-3). In addition, patients should be monitored if there is a greater potential for a change in their physiological status or condition during MRI (1-3). Besides physiological monitoring, various support devices and accessories may be needed for use in high-risk patients to ensure safety (1-32).

With the advent of advanced MRI applications such as MRI-guided interventional or intraoperative procedures, there is an increased need to monitor patients, especially since these individuals are typically anesthetized during the procedures. Additionally, patients (or volunteer subjects) undergoing MRI examinations using experimental MR systems, experimental MRI accessories (e.g., transmit radiofrequency coils), or experimental pulse sequences should be monitored continuously to ensure their safety due to possible problems that may be encountered.

Because of the widespread use of MRI contrast agents and the potential for adverse effects or idiosyncratic reactions to occur, it is prudent to have appropriate monitoring equipment and accessories readily available for the management and support of patients who may experience deleterious side effects (1-3). This is emphasized because adverse events, while extremely rare, may be serious or fatal.

In 1992, the Safety Committee of the Society for Magnetic Resonance Imaging published guidelines and recommendations concerning the monitoring of patients during MRI examinations (2). The information indicated that all patients undergoing MRI should, at the very least, be visually and/or verbally (e.g., intercom system) monitored, and that patients who are sedated, anesthetized, or are unable to communicate should be physiologically monitored and supported by the appropriate means (2).

Severe injuries and fatalities have occurred in association with MRI technology that could have been prevented with the proper use of monitoring equipment and devices (1, 3). Notably, recommendations issued by The Joint Commission state that MRI facilities should proactively plan for the management of critically ill patients who require physiological monitoring and continuous use of life-sustaining drugs while in the MRI suite (33).

Over the years, the American Society of Anesthesiologists Task Force on Anesthetic Care for Magnetic Resonance Imaging has regularly issued practice advisories that include advice on performing physiological monitoring in patients undergoing MRI examinations.

The latest advisory, published in 2015, has the following indicated purposes: (1) to promote patient and staff safety in the MRI environment, (2) to prevent the occurrence of MRI-associated accidents, (3) to promote optimal patient management and reduce adverse patient outcomes associated with MRI, (4) to identify potential equipment-related hazards in the MRI environment, (5) to identify limitations of physiological monitoring capabilities in the MRI setting, and (6) to identify potential health hazards associated with the MRI environment (34). With specific reference to monitoring patients during MRI, the Practice Advisory suggests the use of appropriate equipment (e.g., MR Conditional monitors and other devices) and compliance with standards from the American Society of Anesthesiologists (34).

The American College of Radiology's (ACR) Manual on MR Safety has information and recommendations for physiological monitoring of patients during MRI (35). The ACR's document states that monitoring techniques should be carefully selected primarily because of the risk of thermal injury associated with monitoring equipment in the MRI setting. While not all RF-induced thermal injuries can be detected as they are developing, sedated, anesthetized, or unconscious patients are especially vulnerable to such injuries because they are unable to provide the MR system operator with adequate warning of actively developing thermal injuries. The ACR's Manual on MR Safety also has advice regarding suitable monitoring devices that can be safely utilized to record various physiological parameters in the MRI environment.

Other organizations similarly recommend the need to monitor certain patients using proper equipment and techniques in the MRI setting (36-38). **Table 1** summarizes the types of patients who may require physiological monitoring and support during MRI examinations (1).

Selection of Parameters to Monitor

The proper selection of the specific physiological parameter(s) that should be monitored during MRI is crucial for patient safety. Various factors must be considered including the patient's medical history, present condition, the use of medication and possible associated side effects, as well as the aspects of the MRI procedure to be performed (1-3, 34-39). For example, if the patient is to receive a sedative, it is generally necessary to monitor respiratory

Table 1. Types of patients that may require physiological monitoring and support during MRI examinations.

- Sedated or anesthetized patients.
- Critically ill or high-risk patients.
- Patients that may have a reaction to an MRI contrast agent.
- Neonatal and pediatric patients.
- Patients that have compromised physiological functions.
- Patients that are physically or mentally unstable.
- Patients that are unable to communicate.
- Patients undergoing MRI-guided interventional or intraoperative procedures.
- Patients undergoing MRI examinations using experimental MR systems.
- Patients undergoing MRI examinations using experimental techniques.

438 Physiological Monitoring of Patients During MRI

rate, apnea, and/or oxygen saturation (34-38). If the patient requires general anesthesia during MRI, monitoring multiple physiological parameters is required (1, 3, 34-39).

Policies and procedures for the management of the patient in the MRI environment with respect to monitoring should be comparable to those used in the operating room or critical care setting, especially with respect to monitoring and support requirements. Specific recommendations for physiological monitoring of patients during MRI examinations should be developed in consideration of “standard of care” issues as well as in consultation with anesthesiologists, critical care specialists, and other similar healthcare professionals (1, 3, 11, 28, 29, 34-40).

Personnel Involved in Patient Monitoring

Only healthcare professionals with appropriate training and experience should be permitted to be responsible for monitoring patients during MRI (1, 3, 28, 29, 34-40). This includes several facets of training and experience. The healthcare professional must be well acquainted with the operation of the monitoring equipment and accessories used in the MRI setting and should be able to recognize equipment malfunctions, device problems, and recording artifacts. Furthermore, the healthcare professionals responsible for monitoring the patient should be well versed in screening patients for conditions that may complicate the procedure. For example, patients with asthma, congestive heart failure, obesity, obstructive sleep apnea, and other underlying health conditions are at increased risk for having problems during sedation or anesthesia (29, 34-40). Also, the healthcare professionals must be able to identify and manage adverse events (e.g., respiratory or cardiac arrest) using appropriate equipment and procedures that are applicable for the MRI environment (1, 3, 11, 28, 29, 34-40).

If a sedated patient suddenly exhibits a rapid decline in oxygen saturation during MRI, a healthcare professional must be able to recognize this problem, assess the patient for potential causes, and rapidly determine if intervention is necessary. At the very minimum, the individual should be capable of recognizing and responding quickly to contact an emergency team in the event that an adverse event is experienced by the patient. Additionally, there must be policies and procedures implemented to continue physiological monitoring and support of the patient, as needed, by trained personnel after the MRI examination is performed. This is especially necessary for a patient recovering from the effects of a sedative or general anesthesia.

The monitoring of physiological parameters and management of the patient during MRI may be the responsibility of one or more individuals depending on the level of training for the healthcare worker and in consideration of the condition, medical history, and procedure that is to be performed on the patient. These individuals include anesthesiologists, nurse anesthetists, imaging nurses, and registered nurses (34-40).

Emergency Plan

The development, implementation, and regular practice of an emergency plan that addresses and defines the activities, use of equipment, and other pertinent issues pertaining to a medical emergency are important for patient safety in the MRI environment (1, 3, 29, 35-

38). For example, a plan needs to be developed to immediately remove the patient from the MR system room in order to perform cardiopulmonary resuscitation in the event of cardiac or respiratory arrest. Obviously, taking vital equipment such as a cardiac defibrillator, intubation instruments, “crash cart,” or other similar devices near the MR scanner could pose a substantial hazard to patients and healthcare professionals since these items tend to be unsafe for use in the MRI setting. Appropriately-trained healthcare professionals that are in charge of the emergency or code blue team, maintaining the patient’s airway, administering drugs, recording events, and conducting other emergency-related duties must be identified, trained, and continuously practiced in the performance of these critical activities in the MRI environment. Accordingly, a “mock code” that includes all essential personnel should be scheduled and practiced on a regular basis.

Attempting to manage an emergency in the MR system room is widely considered an unsafe practice and, thus, must be avoided in the interest of safety (1, 3, 28, 29, 34-40). This is primarily because unacceptable equipment may be brought into the area by first responders unaware of the dangers associated with the MRI environment. Therefore, for emergencies, it is important that there is a policy to immediately remove the patient from the MR scanner room and to transfer the patient to a suitable, designated location where the management of the patient may be safely conducted with appropriate equipment and devices that are readily available (1, 3, 28, 29, 34-40).

For outpatient MRI facilities or mobile MR systems, it is usually necessary to have an advanced agreement with outside emergency personnel, such as the local paramedics, and an acute care hospital willing to take care of their patients in the event of emergencies. Typically, MRI facilities not affiliated with or in close proximity to a hospital must contact paramedics to handle medical emergencies and to transport patients to the hospital for additional care. Therefore, personnel responsible for summoning the paramedics, notifying the hospital, and performing other essential activities must be designated beforehand to avoid problems and confusion during an actual emergency event.

TECHNIQUES AND EQUIPMENT FOR PHYSIOLOGICAL MONITORING PATIENT AND SUPPORT

Physiological monitoring and support of patients is not a trivial task in the MRI environment. A variety of potential problems and hazards exist. Furthermore, the types of equipment used for patient monitoring and support must be considered carefully and implemented properly to ensure the safety of both patients and MRI healthcare professionals.

During the early days of MRI, MR Conditional monitoring equipment did not exist. Therefore, it was a common practice to modify or otherwise adapt conventional physiological monitoring equipment in order for it to be utilized on patients undergoing MRI (2-21, 28). Over the years, monitoring equipment was specially designed to be acceptable for use in the MRI setting (i.e., properly tested and labeled MR Conditional) and there are now many commercially available devices that may be used to monitor patients during MRI which include stand-alone individual monitors (e.g., used to record heart rate, blood pressure, oxygen saturation, temperature, etc.) as well as more sophisticated, multi-parameter

440 Physiological Monitoring of Patients During MRI

Table 2. List of manufacturers and suppliers of physiological monitors and support devices for use in the MRI environment.

Company	Products
Airon Corporation (www.aironusa.com)	Ventilators
AliMed (www.alimed.com)	Patient support equipment
Draeger Medical, Inc. (www.draeger.com)	Ventilators
Hamilton Medical (www.hamiltonmedical.com)	Ventilators
IRadimed (www.iradimed.com)	Multi-parameter monitor, infusion pump
Magmedix, Inc. (www.magmedix.com)	Monitors, patient support equipment
Maquet, Inc. (www.maquet.com)	Ventilators
MRIEquip (www.mriequip.com)	Monitors, patient support equipment
MRI Med (www.mrimed.com)	Patient support equipment
Newmatic Medical (www.newmaticmedical.com)	Patient support equipment
Nonin Medical, Inc. (www.nonin.com)	Pulse oximeter
Philips (www.usa.philips.com)	Multi-parameter monitor
Schiller (www.schillerservice.com)	Multi-parameter monitor
Smiths Medical (www.smiths-medical.com)	Ventilators
W.T. Farley (www.wtfarley.com)	Patient support equipment

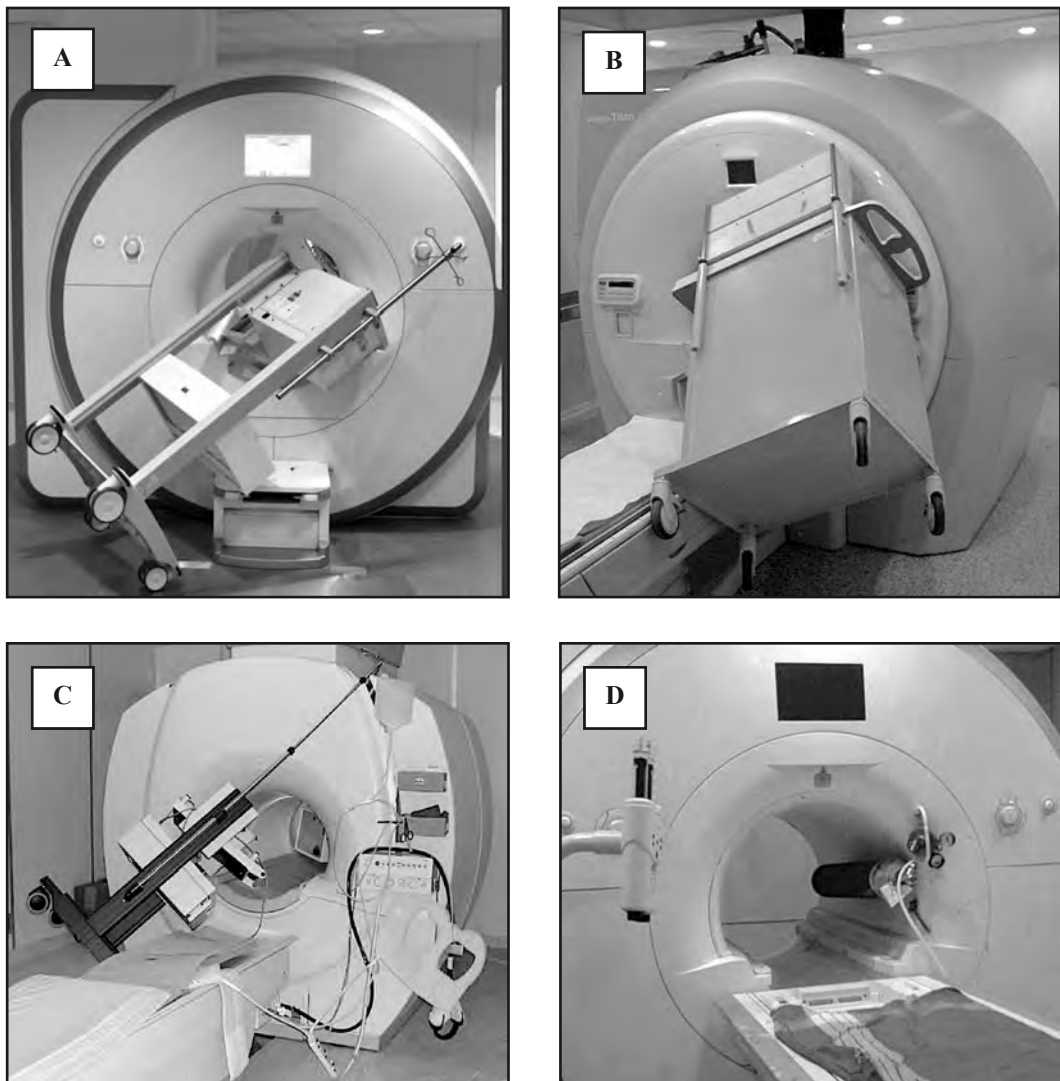
systems that are similar to those found in the operating room or critical care setting (**Table 2**).

Potential Problems and Hazards

Several potential problems and hazards are associated with the performance of patient monitoring and support in the MRI setting. Conventional or even MR Conditional physiological monitors and other accessories that contain ferromagnetic components (e.g., transformers, power supplies, batteries, etc.) may be strongly attracted by the powerful static magnetic field of the MR system, posing a serious missile or projectile hazard to patients and MRI healthcare professionals. **Figure 1** shows various examples of projectile-related accidents, all of which could have been easily prevented if policies and procedures were in place along with proper safety training of all staff members working in the MRI setting. Notably, several serious injuries and at least one fatality have occurred as a result of bringing MR Unsafe gas cylinders (e.g., oxygen tanks) into the MR system room (1, 3, 41-44). In addition to being a tragedy for the involved individuals that could have been avoided, MR scanners can sustain substantial damage as a result of being struck by large ferromagnetic objects. Further expense is incurred if it is necessary to quench a superconducting magnet associated with an MR system in order to remove a large ferromagnetic object (43).

If possible, MR Conditional devices that have specific gauss-level ratings as part of the specified conditions of use (e.g., a device that is labeled to state that it must not be used in a gauss level above 200-gauss) such as monitoring equipment, gas anesthesia machines, and ventilators because of the presence of ferromagnetic materials or operational components that may be damaged by exposure to higher magnetic fields should be permanently fixed to the floor or otherwise “tethered” to prevent them from becoming projectiles. Furthermore, these devices must have prominent warning labels to inform MRI healthcare professionals and others that they should not move this equipment too close to the MR scanner.

Figure 1. Examples of projectile-related accidents. (A, upper left) Cart with infusion pumps and I.V. pole. (B, upper right) Crash cart. (C, lower left) Cart with infusion pump, I.V. pole, and accessories. (D, lower right) Steel oxygen tank.

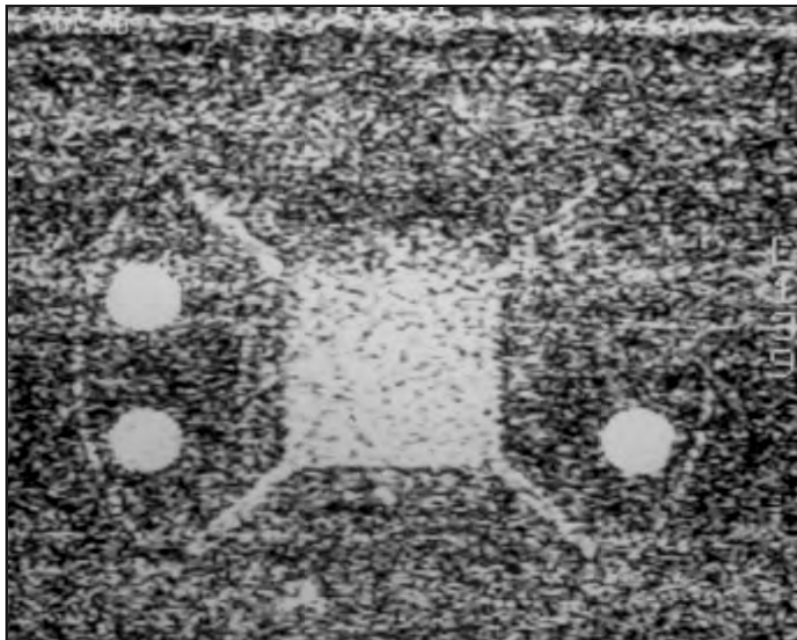


Importantly, all personnel involved with the MRI examinations should be trained and made aware of the importance of the placement and use of the equipment in the MR system room, especially with regard to the hazards of moving portable devices too close to the scanner.

Radiofrequency (RF) fields from the MR system can significantly effect the operation of conventional monitoring equipment, especially those with displays that involve electron beams (i.e., cathode ray tube, CRT) or video display screens, with the exception of those that use a liquid crystal display, LCD. In addition, the monitoring equipment itself may emit

442 Physiological Monitoring of Patients During MRI

Figure 2. T1-weighted, MR image of a fluid-filled phantom showing substantial artifacts related to electromagnetic interference associated with the operation of a monitor in the MR system room.

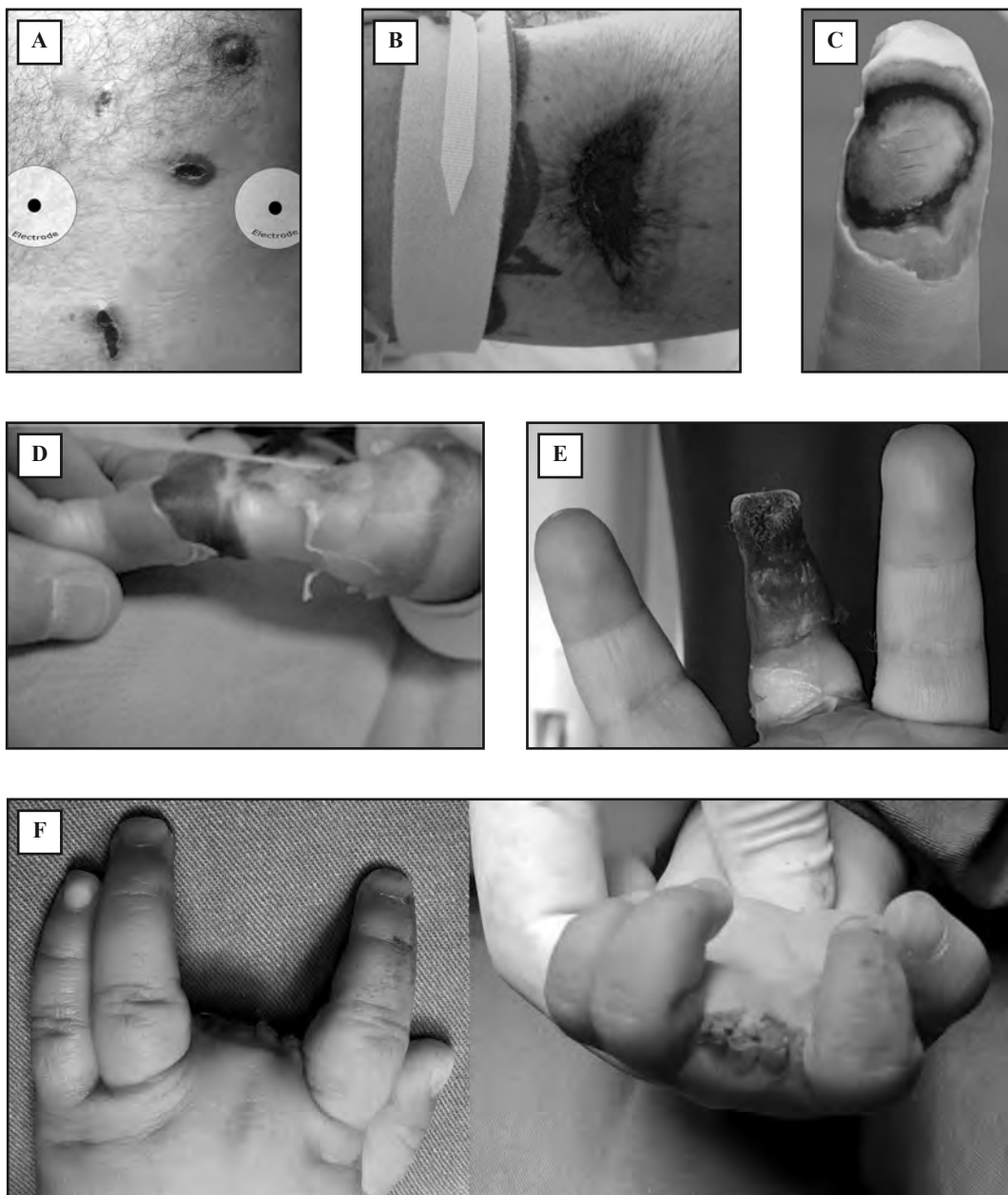


spurious electromagnetic noise that, in turn, produces artifacts on the MR images (**Figure 2**).

Physiological monitors that contain microprocessors or other similar components may “leak” RF, producing electromagnetic interference that can substantially impact MR images (1, 3). To prevent adverse radiofrequency-related interactions with physiological monitors, RF-shielded cables, RF filters, special outer RF-shielded enclosures, and/or fiber-optic techniques can be utilized to prevent image-related or other problems in the MRI setting (1, 3, 28).

During the operation of an MR system, electrical currents may be generated in the conductive materials of monitoring equipment that are used as the interface to the patient (e.g., electrodes, cables, leads, probes, etc.). These currents may be of sufficient magnitude to cause excessive heating and thermal injuries to patients (1-3, 41, 45-62). The primary bio-effect associated with the RF power deposition used during MRI is related to the thermogenic qualities of this electromagnetic field (1). Notably, numerous burns have occurred in association with MRI examinations that were directly attributed to the use of monitoring devices (1, 3, 45-62) (**Figure 3**). These thermal injuries have been associated with the use of electrocardiographic (ECG) leads, ECG electrodes, plethysmographic gating systems, pulse oximeters, intracranial pressure monitoring catheters, and other types of monitoring equipment comprised of wires, cables, and catheters with thermistors or similar components made from conductive materials (1, 3, 45-62). Patient burns related to the use of monitoring

Figure 3. Examples of burns caused by the inappropriate use of monitoring equipment. (A) Multiple burns caused by unconnected ECG electrodes that were permitted to remain on the patient during MRI. (B) Serious burn caused by the cable of an arterial blood pressure monitoring device that was in direct contact with the patient's arm during MRI. (C) Severe burn to the patient's finger caused by the probe from an MR Unsafe pulse oximeter. (D) Severe burn to an infant's arm caused by the probe from an MR Unsafe pulse oximeter. (E) Severe burn to an infant's finger caused by the probe from an MR Unsafe pulse oximeter. (F) For the case shown in (E), the substantial tissue damage from the burn required amputation of the finger.



444 Physiological Monitoring of Patients During MRI

Table 3. Recommendations to prevent excessive heating and possible burns in association with MRI examinations.

- The patient should change into a gown or other appropriate attire that does not contain metallic material.
- Do not permit patients to wear clothing items (e.g., sportswear, underwear, yoga pants, etc.) that have metal-based fibers.
- Prepare the patient for the MRI exam by ensuring that there are no unnecessary metallic objects contacting the patient's skin (e.g., drug delivery patches with metallic components, ECG electrodes, jewelry, necklaces, bracelets, key chains, etc.).
- Prepare the patient for the MRI exam by using insulation material (i.e., appropriate padding) to prevent skin-to-skin contact points and the formation of "closed-loops" from touching body parts.
- Insulating material (minimum recommended thickness, 1-cm) should be placed between the patient's skin and transmit RF coil that is used for the MRI exam. Alternatively, the transmit RF coil itself should be padded. There should be no direct contact between the patient's skin and the transmit RF body coil of the MR system. This may be accomplished by having the patient place his/her arms over his/her head or by using elbow pads or foam padding between the patient's tissue and the transmit RF body coil of the MR system. This is especially important for MRI exams that use the transmit RF body coil or other large RF coils for transmission of RF energy.
- Use only electrically conductive devices, equipment, accessories (e.g., ECG leads, electrodes, etc.), and materials that have been thoroughly tested and determined to be safe or otherwise acceptable for MRI exams.
- Carefully follow the MR Safe or MR Conditional criteria and recommendations for implants and devices made from electrically-conductive materials (e.g., bone fusion stimulators, neuromodulation systems, cardiac devices, cochlear implants, etc.).
- Before using electrical equipment, check the integrity of the insulation and/or housing of all components including surface RF coils, monitoring leads, cables, and wires. Preventive maintenance should be practiced routinely for such equipment.
- Remove all non-essential electrically conductive materials from the MR system prior to the MRI exam (i.e., unused surface RF coils, ECG leads, EEG leads, cables, wires, etc.).
- Keep electrically conductive materials that must remain in the MR system from directly contacting the patient by placing thermal and/or electrical insulation between the conductive material and the patient.
- Keep electrically conductive materials that must remain within the transmit body RF coil or other transmit RF coil from forming conductive loops. Note: The patient's tissue is conductive and, therefore, may be involved in the formation of a conductive loop, which can be circular, U-shaped, or S-shaped.
- Position electrically conductive materials to prevent "cross points". A cross point is the point where a cable crosses another cable, where a cable loops across itself, or where a cable touches either the patient or sides of the transmit RF coil more than once. Even the close proximity of conductive materials with each other should be avoided because cables and RF coils can capacitively-couple (without any contact or crossover) when placed close together.

Table 3. (Continued)

- Position electrically conductive materials (e.g., cables, wires, etc.) to exit down the center of the MR system, *not* along the side of the MR system or close to the transmit RF body coil or other transmit RF coil.
- Do not position electrically conductive materials across an external metallic prosthesis (e.g., external fixation device, cervical fixation device, etc.) or similar device that is in direct contact with the patient.
- Allow only properly trained individuals to operate devices (e.g., monitoring equipment) in the MRI environment.
- Follow all manufacturer instructions for the proper operation and maintenance of physiological monitoring or other similar electronic equipment intended for use during MRI.
- Electrical devices that do not appear to be operating properly during the MRI exam should be removed from the patient immediately.
- RF surface coil decoupling failures can cause localized RF power deposition levels to reach excessive levels. The MR system operator will recognize such a failure as a set of concentric semicircles in the tissue on the associated MR image or as an unusual amount of image non-uniformity related to the position of the transmit RF coil.
- Closely monitor the patient during the MRI exam. If the patient reports sensations of heating or other unusual sensation, discontinue the MRI exam immediately and perform a thorough assessment of the situation.

equipment and other devices or materials are a frequent problem that may be prevented by following the recommendations indicated in **Table 3**.

Monitoring Equipment and Support Devices

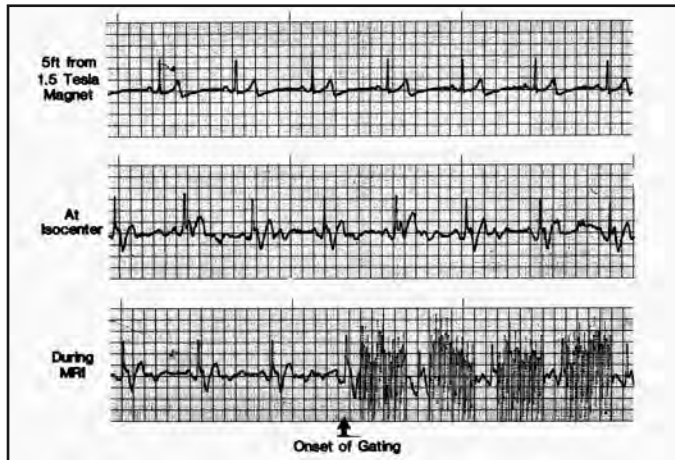
This section describes the physiological parameters that may be assessed in patients during MRI examinations using MR Conditional monitoring equipment. In addition, various devices and accessories that may be utilized to support and manage patients in the MRI setting are presented.

Electrocardiogram and Heart Rate. Monitoring the patient's electrocardiogram (ECG) in the MR system room is particularly challenging because of the inherent distortion of the ECG waveform that occurs (1, 3, 11, 18, 19, 22, 27, 28, 63, 68). This effect is observed as blood, a conductive fluid, flows through the large vascular structures in the presence of the static magnetic field of the MR system (11, 21, 63, 68). The resulting induced biopotential is seen primarily as an augmented T-wave amplitude, although other non-specific waveform changes are also apparent on the ECG (1, 3, 63, 64). Since altered T-waves or ST segments may be associated with cardiac disorders, static magnetic field-induced ECG distortions can be particularly problematic.

Importantly, additional artifacts caused by the static, time-varying gradient, and RF electromagnetic fields can severely distort the ECG, making observation of morphologic

446 Physiological Monitoring of Patients During MRI

Figure 4. Electrocardiogram recorded in a patient in the MR system room: (**Top panel**) Five-feet from a 1.5-Tesla MR system; (**Middle panel**) At isocenter; and (**Bottom panel**) Inside the MR system during MRI. Note the augmented T-wave resulting from the induced flow potential as well as the other nonspecific changes caused by the static magnetic field of the MR system. During MRI, there is severe distortion of the electrocardiographic waveform.



changes and detection of arrhythmias extremely difficult (**Figure 4**). To minimize some of these artifacts, a variety of filtering techniques, including passive and active methods, may be used. Passive techniques include the use of special cable and lead preparation methods along with the proper placement of leads that will minimize the artifacts seen on the ECG in the MRI environment (64, 65). Active techniques involve the use of low pass filters or the electronic suppression of noise that decrease the artifacts from the gradient and RF electromagnetic fields, while maintaining the intrinsic qualities of the ECG.

ECG artifacts that occur in the MRI environment may also be markedly decreased by implementing several simple techniques including (1-3, 11, 18, 21, 22): (1) using ECG electrodes that have minimal metallic components, (2) selecting electrodes and cables that contain no ferromagnetic materials, (3) using leads that are nonmetallic (i.e., fiber-optic leads), (4) placing the limb electrodes in close proximity to one another, (5) positioning the line between the limb electrodes and leg electrodes parallel to the magnetic field flux lines of the scanner, (6) maintaining a relatively small distance between the limb and leg electrodes, (7) placing the anatomic area of the electrodes near or in the center of the MR system, and (8) twisting or braiding the ECG cables.

The use of proper ECG electrodes is required to ensure patient safety and proper recording of the electrocardiogram in the MRI setting (22). Accordingly, this means that only the ECG electrodes recommended or otherwise approved by the manufacturer of the ECG recording equipment (i.e., the MR Conditional monitoring device) should be used in order to protect the patient from potentially hazardous conditions. Similarly, the ECG leads and cables should also be those recommended by the manufacturer and deemed acceptable for use in the MR system room.

As previously indicated, it is well known that the use of standard ECG electrodes, leads, and cables may cause excessive heating that results in patient burns at the electrode sites or where the leads and cables are in direct contact with the patient's tissues. Notably, even MR Conditional, ECG monitoring systems have been responsible for patient burns in association with MRI as the result of improper uses of the devices. As such, whenever using MR Conditional monitoring systems, the *Instructions for Use* should always be followed carefully.

Various techniques have been developed to prevent excessive heating related to the use of ECG recording equipment in the MRI setting, including using fiber-optic technology and/or wireless methods to record the ECG. The use of the fiber-optic technique combined with a wireless method to monitor the ECG during MRI removes the potential for burns associated with hard-wired ECG systems by eliminating the conductive leads and cable, which prevents the "antenna effect" that is typically responsible for excessive heating of these items during MRI. Accordingly, most modern day, MR Conditional ECG monitoring systems employ this technological solution to ensure patient safety.

Heart rate may be monitored in the MR system room using a number of different methods. Besides using the ECG monitor to record heart rate in patients undergoing MRI, this physiological parameter may be determined using MR Conditional devices such as the photoplethysmograph found with a pulse oximeter or a noninvasive, heart rate/blood pressure monitor (see section below) that can also be utilized to obtain intermittent or semi-continuous recordings of heart rate during MRI (1, 3, 11).

Blood Pressure. Several different techniques may be used to monitor blood pressure in patients undergoing MRI (1, 3, 4, 11, 66-69). MR Conditional sphygmomanometers are commercially available to manually measure blood pressure in patients. When using this methodology, it's important to also use an MR Conditional stethoscope.

An MR Conditional blood pressure monitor that uses the oscillometric method can obtain semi-continuous recordings of systolic, diastolic, and mean blood pressures as well as heart rate in patients. Thus, this device can be utilized to record systemic blood pressure in adult, pediatric, and neonatal patients by selecting the appropriate size for the blood pressure cuff based on the type of patient that will be monitored.

It should be noted that the intermittent inflation of the blood pressure cuff from a manual or an automated, noninvasive blood pressure device can disturb lightly-sedated patients, especially pediatric or neonatal patients, causing them to move and disrupt the MRI examination. For this reason, the use of a noninvasive blood pressure monitor may not be the best instrument to perform physiological monitoring in every type of patient.

Arterial blood pressure may also be monitored using a direct hemodynamic monitoring technique, which is considered the most accurate means of assessing blood pressure in patients undergoing MRI. In order to accomplish this, a catheter is inserted into the radial artery and attached by pressure tubing to an MR Conditional pressure transducer, which is then interfaced with an appropriate MR Conditional monitor.

Intravascular, Intracardiac, and Intracranial Pressures. Direct monitoring of intravascular, intracardiac, or intracranial pressures may be performed in patients during MRI using

448 Physiological Monitoring of Patients During MRI

specially designed, fiber-optic pressure transducers, nonferromagnetic, micromanometer-tipped catheters, or by other means. These monitoring devices are unaffected by the electromagnetic fields used for MRI and are capable of invasively recording pressures (6, 9, 11, 45, 46).

Monitoring intracranial pressure (ICP) is essential in the management of severe head injuries and for other conditions. However, it should be noted that, ICP monitoring devices labeled MR Conditional require special positioning of the catheter in order to ensure patient safety (1, 45, 46), otherwise serious patient injuries can occur due to excessive heating of these devices, as reported by Tanaka, et al. (45) and Newcombe, et al. (46).

Respiratory Rate and Apnea. Because respiratory depression and upper airway obstruction are frequent complications associated with the use of sedatives and anesthetics, monitoring techniques that detect a decrease in respiratory rate, hypoxemia, or airway obstruction should be used during the administration of these drugs (1, 3, 29, 34, 36-38, 66-69). Impaired respiratory function due to existing conditions such as tonsillar hypertrophy is also a risk factor (34). This is particularly important in the MRI setting because visual observation of the patient's respiratory effort is often difficult, especially when the patient is entirely inside the bore of an MR system and the direct line of sight is obstructed (34). Other factors impacting direct patient observation during an MRI examination include the typically darkened environment, acoustic noise, and other distractions (34).

Respiratory rate monitoring can be performed effectively during MRI examinations by various techniques. The impedance method that utilizes MR Conditional chest leads and electrodes (similar to those used to record the ECG) can be used to monitor respiratory rate. This method of assessing respiratory rate measures a difference in electrical impedance induced between the leads that correspond to changes in respiratory movements. Unfortunately, the electrical impedance method of determining respiratory rate may be inaccurate in pediatric patients because of the small volumes and associated motions of the relatively small thorax area. Additionally, the leads and electrodes used with impedance-based techniques must be designed to prevent excessive heating, similar to what is done when monitoring the ECG in the MRI setting.

Respiratory rate may also be monitored during MRI examinations using a rubber bellows placed around the patient's thorax or abdomen (i.e., for "chest" or "belly" breathers) (1, 3, 11). The bellows device is attached to a remote pressure transducer that records changes in body movements associated with inspiration and expiration. However, the bellows monitoring technique, like the electrical impedance method, is only capable of recording body movements associated with respiratory efforts. Therefore, these techniques of monitoring respiratory rate do not detect apneic episodes related to upper airway obstruction (i.e., absent airflow despite respiratory effort) and, thus, may not provide sufficient sensitivity for assessing patients undergoing MRI. For this reason, assessment of respiratory rate and detection of apnea should be accomplished using other, more appropriate monitoring methods.

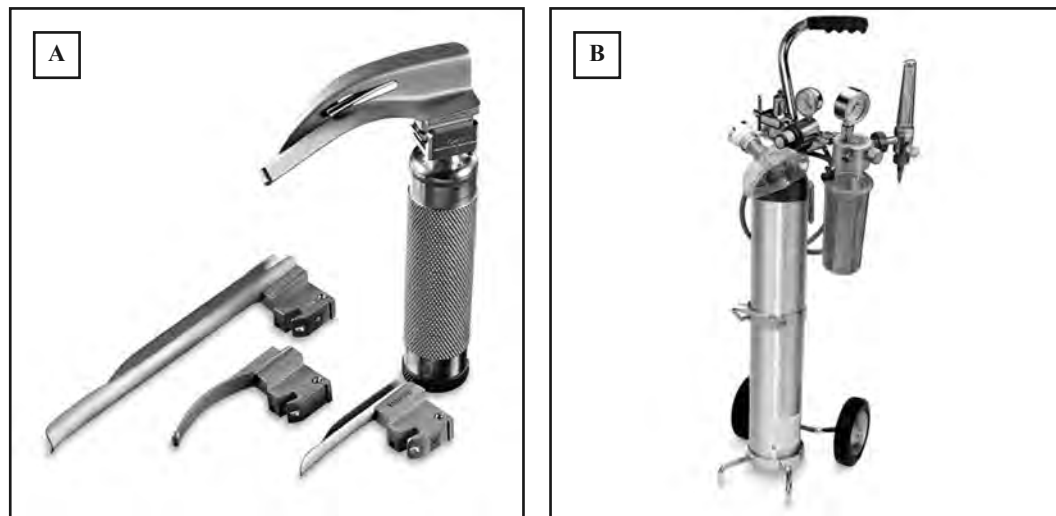
Respiratory rate and apnea may be monitored during MRI using an MR Conditional, end-tidal carbon dioxide monitor or a capnometer. These different devices measure the level of carbon dioxide during the end of the respiratory cycle (i.e., end-tidal carbon dioxide),

when carbon dioxide is at its maximum level. Additionally, capnometers can provide quantitative data with respect to end-tidal carbon dioxide that is important for determining certain aspects of gas exchange in patients. The waveform provided on end-tidal carbon dioxide monitors is also useful for visually determining whether the patient is having difficulties breathing. Importantly, the interface between the patient for the end-tidal carbon dioxide monitor and capnometer is a nasal or oro-nasal cannula that is made out of plastic and, thus, it is MR Safe. Obviously, this type of interface prevents any potential adverse interaction between monitors, which typically must be positioned outside the 200-gauss line associated with the MR scanner, and the patient.

Anesthesiology personnel should have a clear plan of how to deal with patients that experience respiratory distress while undergoing MRI, including how best to utilize airway management equipment and the suction system, both of which should be readily accessible outside the MR system room (i.e., Zone IV) (34) (**Figure 5**).

Oxygen Saturation. Oxygen saturation is a critical variable to measure in high-risk, sedated or anesthetized patients, especially in the MRI setting (1, 3, 11, 14, 24, 29, 34-40, 66-69). This physiological parameter is measured using pulse oximetry, a technique that assesses the oxygenation of tissue, which may be accomplished using an MR Conditional pulse oximeter. Because oxygen-saturated blood absorbs differing quantities of light compared to unsaturated blood, the amount of light that is absorbed by the blood can be utilized to determine the ratio of oxygenated hemoglobin to total hemoglobin and displayed as the oxygen saturation on the monitor. Additionally, the patient's heart rate may be determined using the pulse oximeter by measuring the frequency that pulsations occur as the blood moves through the vascular bed. Thus, the pulse oximeter determines oxygen saturation and heart rate on a continuous basis by measuring the transmission of light through a vas-

Figure 5. (A, left) MR Conditional, laryngoscope showing the handle and different blades. **(B, right)** Portable MR Conditional oxygen tank and suction system. These devices can be used in the MRI setting to manage the patient in the event of respiratory distress.



450 Physiological Monitoring of Patients During MRI

Figure 6. Monitoring the patient's heart rate and oxygen saturation in the MRI setting using an MR Conditional pulse oximeter. Note the waveform on the monitor that is representative of the pulsations that occur as blood moves through the vascular bed. The frequency of the pulsations is used to determine heart rate.



cular measuring site such as the ear lobe, fingertip, or toe (**Figure 6**). Importantly, the use of pulse oximetry is considered by anesthesiologists as the standard practice for monitoring sedated or anesthetized patients (34, 36, 37, 66-69).

Conventional pulse oximeters typically have hard-wire cables that are of great concern and have been responsible for causing serious burns in patients in the MRI environment (1, 3, 24, 47, 53-57). Fortunately, pulse oximeters have been developed that use fiber-optic technology to obtain and transmit the physiological signals from the patient (1, 3, 11, 24) (**Figure 7**). It is physically impossible for a patient to be burned by a fiber-optic pulse oximeter during an MRI procedure because there are no conductive pathways formed by metallic materials directly contacting the patient. Notably, these commercially available, MR Conditional devices operate without interference from the electromagnetic fields used during MRI.

Temperature. In human subjects, “deep” body or core temperature is regulated between 36°C and 38°C by the hypothalamus and continuously fluctuates due to diurnal, internal, and external factors (68, 70). Importantly, the regulation of body temperature is suppressed by anesthesia and generally results in the patients becoming hypothermic (71, 72). Health conditions related to a decrease in body temperature include hypovolemia, myocardial ischemia, cardiac arrhythmia, pulmonary edema, decreased cerebral blood flow, and mortality (i.e., caused by extreme hypothermia) (73). In the MRI setting, besides monitoring body temperature in anesthetized adult patients, it is also important to record temperatures in

Figure 7. MR Conditional pulse oximeter that uses fiber-optic technology to continuously monitor oxygen saturation and heart rate (Nonin Medical, www.nonin.com).



neonates because they have inherent problems retaining body heat, a tendency that is augmented during sedation and anesthesia. Accordingly, body temperature is an important parameter to monitor in various patient groups undergoing MRI.

With further regard to patients who are anesthetized during MRI, some patients may experience malignant hyperthermia, which is a rare life-threatening condition that may be triggered by exposure to certain drugs used for general anesthesia. In susceptible individuals, these drugs can induce a drastic and uncontrolled increase in skeletal muscle oxidative metabolism, which overwhelms the body's capacity to supply oxygen, to remove carbon dioxide, and to regulate body temperature. Malignant hyperthermia can eventually lead to circulatory collapse and death if not quickly identified and treated.

Those responsible for administering anesthesia in the MRI environment, that is, the anesthesiologist or nurse anesthetist, may not be able to adequately visualize or have close access to the patient during MRI due to the design of the scanner. Therefore, it is imperative to continuously monitor body temperature in certain patients, obtaining real-time information for the anesthesia provider. It is also important that the measurement site used to determine body temperature has clinical relevance and a relatively "fast" response time to any substantial fluctuation because the anesthesiologist or nurse anesthetist is unable to readily observe the discoloration of the patient's skin, which is a hallmark sign of a sudden temperature change.

Over the years, the accuracy and efficacy of the measurement of body temperature has been a topic of discussion (70, 74-80). Temperature measurements in human subjects are affected by many factors, including (70, 76, 77): (1) the site of measurement (e.g., skin, oral, esophagus, rectal, pulmonary artery, bladder, tympanic membrane, or axillary area); (2) the environmental conditions (i.e., temperature and humidity); and (3) the measurement

452 Physiological Monitoring of Patients During MRI

technique (e.g., mercury thermometer, electronic thermometer, thermistor probe, thermocouple-based probe, thermography, and the fiber-optic method).

The most accurate deep body temperature is measured at the hypothalamus, but this site is obviously not accessible by any practical means. Therefore, a “deep” body site that directly reflects the temperature “sensed” by the hypothalamus will provide the optimal, clinically relevant information (70). For example, sites that provide high levels of accuracy and correlate well with the deep body temperature are pulmonary artery blood, urinary bladder, the esophagus, and rectum. However, the temporal resolution for each site varies, which can dramatically impact the ability to recognize clinically important changes that may require prompt patient management (71-76).

When monitoring temperature during MRI, the decision on which body site to use should be based on accuracy as well as accessibility. Additionally, there may be limitations on the type of equipment available for temperature measurements in the MR system room. For example, hard-wire thermistor or thermocouple-based sensors are prone to measurement errors due to electromagnetic interference (EMI) and can introduce artifacts in the MR images (1-3, 11). Additionally, wire-based temperature measurement techniques are prone to excessive MRI-related heating and can result in burn injuries to patients. Fiber-optic sensors (i.e., fluoroptic thermometry) are optimally used to record temperatures in the MRI environment because they are unaffected by EMI and are safe (3). Of note is that, similar to other methods used to assess physiological parameters in patients undergoing MRI, the measurement of temperature must employ a suitable technique that is MR Conditional (81-83). Fluoroptic thermometry, which utilizes fiber-optic technology has been successfully used to monitor body and skin temperatures in the clinical MRI setting (81-85).

In the MR system room, anesthesiologists, nurse anesthetists, and clinicians may feel that they are limited to measure “surface” temperatures in patients, such as the temperatures of the skin, axilla, or groin. However, these measurement sites are problematic because they do not properly reflect “deep” body temperature nor do they respond rapidly to quick fluctuations in body temperature. While a so-called “surface” temperature site (i.e., skin, axilla, and groin) has been used to record temperature during MRI mainly because of the ease of obtaining the measurement with currently available equipment, this method does not provide an accurate representation of body temperature and is susceptible to substantial variations and erroneous information relative to the deep body temperature due to the specific site selected for temperature probe placement, patient movement, and environmental conditions (75-77, 79).

Notably, the level of the patient’s perspiration due to RF-induced heating and the use of blankets or air circulation from the fan in the bore of the scanner can greatly influence the recording of skin or other surface temperature during MRI. Additionally, investigations have demonstrated that peripheral vasoconstriction resulting from cooling of the skin decreases the surface temperature without influencing the deep body temperature, resulting in misleading information if the intent was to use a surface site as a surrogate for deep body temperature (79).

Two of the most prevalent core temperature measurement sites used during MRI examinations are the rectum and esophagus. Rectal temperature measurements are highly ac-

curate and within 0.6°C of deep body temperature (72, 75, 76). The main drawback to this measurement site is associated with a lag or delay in the temporal response to a changing body temperature due to the presence of thermal inertia from the intervening tissues (i.e., the tissues between the rectum and hypothalamus). This temporal delay may also be caused by the presence of feces and poor blood supply in the rectum (75, 76, 80). Newsham, et al. (80) reported that rectal temperature substantially lagged when compared to changes in tympanic membrane temperature (which is a well known surrogate for deep body temperature). This delay can present issues when the intent is to identify body temperature excursions that require medical intervention. Of note is that the lack of proper temporal resolution for a temperature recording method can subject the patient to a hypothermic or hyperthermic condition for an extended period without being recognized by the clinician. Also of consideration when using the rectum as the site of temperature measurement is the fact that special care must be taken when placing a rectal temperature probe in a neonatal or pediatric patient in order to prevent perforation or infection (80).

Measurement of esophageal temperature provides a high level of accuracy and good temporal correlation to deep body temperature due to the close proximity to the aorta, a “deep body” site (76). In addition to this accuracy, esophageal temperature is responsive to fluctuations in body temperature and readily tracks changes compared to rectal or surface temperature measurement sites (75, 76). The only caveat is that the accuracy of measuring temperature in the esophagus is directly linked to the proper positioning of the thermometry probe (75, 76). Airflow in the trachea can impact the measured temperature if the probe is not inserted deep enough into the patient’s esophagus. For accurate deep body temperature measurements, the recommended placement of the thermometry probe is in the lower one-third of the esophagus (75, 76).

In consideration of the available temperature measurement sites that may be monitored during MRI, especially with regard to which site provides the most accurate information along with the best temporal resolution, the temperature of the esophagus is considered to be the site of the most acceptable and clinically relevant information. Furthermore, esophageal temperature is insensitive to ambient air circulation and has the added benefit of fast response time to temperature fluctuations in the body compared to the measurement of temperature in the rectum.

The current availability of fiber-optic temperature probes and recording equipment properly designed for use in the MRI setting permits the monitoring of body temperature in the esophagus, which provides physiological information that is vital to patient care. Temperature monitoring capabilities are typically found in association with multi-parameter physiological monitoring equipment that have been properly tested and labeled, MR Conditional.

Multi-Parameter, Physiological Monitoring Systems. In certain cases, it may be necessary to monitor several different physiological parameters simultaneously in patients undergoing MRI (1, 3, 11, 29, 32, 36-40, 66-69). While several different stand-alone units may be combined together to accomplish this task, the most efficient means of recording multiple parameters is by utilizing a monitoring system that permits the measurement of vital physiological functions such as heart rate, respiratory rate, blood pressure, oxygen sat-

454 Physiological Monitoring of Patients During MRI

Figure 8. Example of an MR Conditional, multi-parameter, physiological monitoring system (Model 3880 MRI Patient Monitor, IRadimed, www.iradimed.com) used on a patient being prepared to undergo an MRI examination. Note the MR Conditional infusion pumps (Model 3860+ MRI Infusion Pump) mounted on the I.V. pole.



uration, and temperature (**Figure 8**). Currently, there are several commercially available MR Conditional, multi-parameter patient monitoring systems designed for use in the MRI setting (**Table 2**).

Ventilators. Devices used for mechanical ventilation of patients typically contain mechanical switches, microprocessors, and ferromagnetic components that may be adversely affected by the electromagnetic fields associated with MR systems (1, 3, 8, 11, 15, 75). Ventilators that are activated by high-pressure oxygen and controlled by the use of fluidics (i.e., no requirements for electricity) may still have ferromagnetic parts that can malfunction as a result of interactions with MR scanners.

Fortunately, MR Conditional ventilators have been specially designed for use in the MR system room and can be utilized in adult as well as pediatric and neonatal patients (**Table 2**). These devices are constructed from nonferromagnetic materials and have undergone pre-clinical evaluations to ensure that they operate properly in the MRI environment, without producing artifacts on MR images (**Figure 9**).

Importantly, many ventilators classified as MR Conditional have specific fringe field requirements due to the presence of ferromagnetic parts or functional aspects that may be compromised in association with powerful static magnetic fields. For example, the ventilator may not be used in fields greater than a certain gauss level, such as 300-gauss. Therefore, as always, to prevent accidents and incidents, it is crucial for all healthcare professionals working in the MRI environment to have an understanding of the issues related to the use

Figure 9. Example of an MR Conditional ventilator (pNeuton Pneumatic Ventilator, Airon Corporation, www.aironusa.com). This device is a pneumatic ventilator and was specially designed for use in the MRI setting.



of potentially dangerous equipment, particularly if ferromagnetic objects, such as ventilators, are inadvertently brought into the MR system room (86).

If the ventilator must be maintained at a designated gauss level relative to the MR scanner, this area should be clearly demarcated on the floor of the room and all healthcare personnel must be educated regarding the importance of maintaining the device at or behind this marked area. One way to ensure this would be to attach a tether or restraint strap to the ventilator that provides a mechanism that would “catch” in order to prevent encroachment of the device to an unsafe area. Importantly, the tethering system should only be used to prevent disaster and not relied on as the primary restraint mechanism.

Alternatively, a device called the GaussAlert (Kopp Development, Inc., www.koppdevelopment.com) can be utilized to help maintain an MR Conditional ventilator (or other similar equipment such as infusion pumps, contrast injectors, patient monitors, gas anesthesia machines, etc.) outside of a particular MRI exclusion zone (**Figure 10**). This magnetic field strength alarm system was specifically designed for this task and produces an audio alert when a preset magnetic field strength is exceeded.

Patient Support Devices and Accessories. Patient safety is assured by having clear processes established for patient monitoring, sedation or anesthesia, and management of emergencies (i.e., remove the patient immediately from the MR system room and then proceed with emergency care). In addition, anesthesiologists should be attentive and aware of the potential for emergencies that may arise in the MRI environment and know where all appropriate and safe support devices are located (1, 4, 11, 34-41). A variety of devices and accessories are often necessary for support and management of patients in the MRI setting. MR Safe or MR Conditional gurneys, wheelchairs, oxygen tanks, stethoscopes, suction devices, intubation equipment, infusion pumps, power injectors, gas anesthesia systems, and other similar devices and accessories are commercially available and may be obtained from various manufacturers and distributors (**Figure 11**) (**Table 2**).

456 Physiological Monitoring of Patients During MRI

Figure 10. Example of an MR Conditional ventilator system. This equipment includes a magnetic field strength alarm system (**arrow**) (GaussAlert, Kopp Development Inc., www.koppdevelopment.com) that is designed to help keep MR Conditional equipment outside of a particular MRI exclusion zone (e.g., 300-gauss).

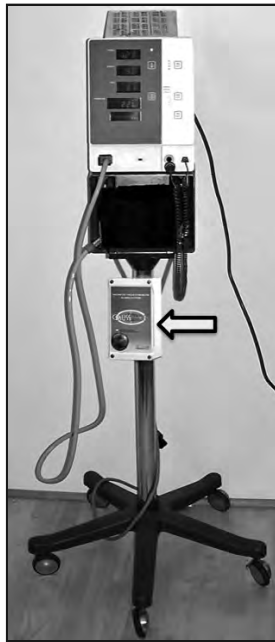


Figure 11. Example of an MR Conditional gas anesthesia machine and related accessories.



In order to prevent the inadvertent entry of an MR Unsafe device into the scanner room, consideration should be given to the installation of a ferromagnetic detection system as an adjunctive tool that supplements the MRI facility's policies, procedures, and annual MRI safety training of its full-time staff members and others who may occasionally work in this setting (1).

CONCLUSIONS

The care and management of high-risk, critically ill, and sedated or anesthetized patients undergoing MRI examinations presents special challenges. These challenges are related to requirements for MR Safe and MR Conditional equipment and devices as well as the need for MRI facilities to implement MRI-specific policies and procedures that ensure patient safety. Safely performing MRI examinations in patients that require physiological monitoring is straightforward as long as there is clear and consistent communication among all staff members, proper labeling of all devices and equipment, and an understanding of the unique aspects of the MRI environment.

REFERENCES

1. Shellock FG. Reference Manual for Magnetic Resonance Safety: 2020 Edition. Los Angeles: Biomedical Research Publishing Group; 2020.
2. Kanal E, Shellock FG. Policies, guidelines, and recommendations for MR imaging safety and patient management. Patient monitoring during MR examinations, *J Magn Reson Imaging* 1992;2:247-8.
3. Shellock FG. Chapter 4. Magnetic Resonance Imaging: Safety and Bioeffects. In: Open MRI. Philadelphia: Lippincott Williams and Wilkins; 1998. pp. 23-38.
4. Barnett GH, Roper AHD, Johnson AK. Physiological support and monitoring of critically ill patients during magnetic resonance imaging. *J Neurosurg* 1988;68:246.
5. Boutros A, Pavlicek W. Anesthesia for magnetic resonance imaging. *Anesth Analg* 1987;66:367.
6. Dell' Italia LJ, Carter B, Millar H, Pohost GM. Development of a micromanometer-tip catheter to record high-fidelity pressures during cine-gated NMR without significant image distortion. *Magn Reson Med* 1991;17:119-25.
7. Fisher DM, Litt W, Cote CJ. Use of oximetry during MR imaging of pediatric patients. *Radiology* 1991;178:891-892.
8. Dunn V, Coffman CE, McGowan JE, Ehrhardt JC. Mechanical ventilation during magnetic resonance imaging. *Magn Reson Imaging* 1985;3:169-72.
9. Roos CF, Carroll FE. Fiber-optic pressure transducer for use near MR magnetic fields. *Radiology* 1985;156:548.
10. Geiger RS, Cascorbi HF. Anesthesia in an NMR scanner. *Anesth Analg* 1984;63:622-3.
11. Holshouser B, Hinshaw DB, Shellock FG. Sedation, anesthesia, and physiological monitoring during MRI. *J Magn Reson Imaging* 1993;3:553-558.
12. Hubbard A, Markowitz R, Kimmel B, Kroger M, Bartko M. Sedation for pediatric patients undergoing CT and MRI. *Journal of Computer Assisted Tomography* 1992;16:3-6.
13. Karlik S, Heatherley T, Pavan F, et al. Patient anesthesia and monitoring at a 1.5 T MRI installation. *Magn Reson Med* 1988;7:210-21.
14. McArdle C, Nicholas D, Richardson C, Amparo E. Monitoring of the neonate undergoing MR imaging: Technical considerations. *Radiology* 1986;159:223-6.

458 Physiological Monitoring of Patients During MRI

15. McGowan JE, Erenberg A. Mechanical ventilation of the neonate during magnetic resonance imaging. *Magn Reson Imaging* 1989;7:145-8.
16. Mirvis SE, Borg U, Belzberg H. MR imaging of ventilator-dependent patients: Preliminary experience. *AJR Am J Roentgenol* 1987;149:845-6.
17. Rejger VS, Cohn BF, Vielvoye GJ, De-Raadt FB. A simple anesthetic and monitoring system for magnetic resonance imaging. *European Journal of Anesthesiology* 1989;6:373-8.
18. Rokey RR, Wendt RE, Johnston DL. Monitoring of acutely ill patients during nuclear magnetic resonance imaging: Use of a time-varying filter electrocardiographic gating device to reduce gradient artifacts. *Magn Reson Med* 1988;6:240-5.
19. Roth JL, Nugent M, Gray JE, et al. Patient monitoring during magnetic resonance imaging. *Anesthesiology* 1985;62:80-3.
20. Selden H, De Chateau P, Ekman G, et al. Circulatory monitoring of children during anesthesia in low-field magnetic resonance imaging. *Acta Anesthesiol* 1990;34:41-3.
21. Shellock FG. Monitoring during MRI. An evaluation of the effect of high-field MRI on various patient monitors. *Med Electron* 1986;17:93-7.
22. Shellock FG. MRI and ECG electrodes. *Signals* 1999;29:10-14.
23. Shellock FG. Monitoring sedated patients during MRI (letter). *Radiology* 1990;177:586.
24. Shellock FG, Myers SM, Kimble K. Monitoring heart rate and oxygen saturation during MRI with a fiber-optic pulse oximeter. *AJR Am J Roentgenology* 1991;158:663-4.
25. Smith DS, Askey P, Young ML, Kressel HY. Anesthetic management of acutely ill patients during magnetic resonance imaging. *Anesthesiology* 1986;65:710-1.
26. Taber K, Layman H. Temperature monitoring during MR imaging: Comparison of fluoroptic and standard thermistors. *J Magn Reson Imaging* 1992;2:99.
27. Wendt RE, Rokey R, Vick GW, Johnston DL. Electrocardiographic gating and monitoring in NMR imaging. *Magn Reson Imaging* 1988;6:89.
28. Kanal E, Shellock FG. Patient monitoring during clinical MR imaging. *Radiology* 1992;185:623-9.
29. Reinking Rothschild, D. Chapter 5. Sedation for Open Magnetic Resonance Imaging. In: Rothschild PA, Rothschild DR, Editors. *Open MRI*. Philadelphia: Lippincott, Williams and Wilkins; 2000. pp. 39-53.
30. Tobin JR, Spurrier EA, Wetzel RC. Anaesthesia for critically ill children during magnetic resonance imaging. *Br J Anaesth* 1992;69:482-6.
31. Szelenyi A, Gasser T, Seifert V. Intraoperative neurophysiological monitoring in an open low-field magnetic resonance imaging system: Clinical experience and technical considerations. *Neurosurgery* 2008;63:268-75.
32. Menon DK, Peden CJ, Hall AS, Sargentoni J, et al. Magnetic resonance for the anesthetist, part II: Anesthesia and monitoring in MR units. *Anesthesia* 1992;47:508-17.
33. The Joint Commission. Sentinel Event Alert. Preventing accidents and injuries in the MRI suite. Issue 38, 2008.
34. Practice Advisory on Anesthetic Care for Magnetic Resonance Imaging: An Updated Report by the American Society of Anesthesiologists Task Force on Anesthetic Care for Magnetic Resonance Imaging. *Anesthesiology* 2015;122:495-520.
35. ACR Manual on MR Safety, American College of Radiology, www.ACR.org, 2020.
36. Guidelines for monitoring and management of pediatric patients during and after sedation for diagnostic and therapeutic procedures: An update. *Pediatrics* 2006;118:2587-2602.
37. American College of Radiology (ACR), Society of Interventional Radiology (SIR) Practice Parameter for Minimal and/or Moderate Sedation/Analgesia. American College of Radiology, www.acr.org, 2020.

MRI Bioeffects, Safety, and Patient Management 459

38. Wilson SR, Shinde S, Boscoe M, et al. Guidelines for the safe provision of anaesthesia in magnetic resonance units 2019: Guidelines from the Association of Anaesthetists and the Neuro Anaesthesia and Critical Care Society of Great Britain and Ireland. *Anaesthesia* 2019;74:638-650.
39. Heinrichs B, Walsh RP. Intraoperative MRI for neurosurgical and general surgical interventions. *Curr Opin Anaesthesiol* 2014;27:448-52.
40. Rotello LC, Radin EJ, Jastremski MS, Craner D, Milewski A. MRI protocol for critically ill patients. *Am J Crit Care* 1994;3:187-90.
41. Shellock FG, Crues, JV. MR procedures: Biologic effects, safety, and patient care. *Radiology* 2004;232:635-52.
42. Chaljub G, Kramer LA, Johnson RF III, Singh H, Crow WN. Projectile cylinder accidents resulting from the presence of ferromagnetic nitrous oxide or oxygen tanks in the MR suite. *AJR Am J Roentgenol* 2001;177:27-30.
43. Colletti PM. Size "H" oxygen cylinder: Accidental MR projectile at 1.5 Tesla. *J Magn Reson Imaging* 2004;19:141-3.
44. ECRI hazard report: Patient death illustrates the importance of adhering to safety precautions in magnetic resonance environments. *Health Devices* 2001;30:311-4.
45. Tanaka R, Yumoto T, Shiba N, et al. Overheated and melted intracranial pressure transducer as cause of thermal brain injury during magnetic resonance imaging. *J Neurosurg* 2012;117:1100-9.
46. Newcombe VF, Hawkes RC, Harding SG, et al. Potential heating caused by intraparenchymal intracranial pressure transducers in a 3-Tesla magnetic resonance imaging system using a body radiofrequency resonator: Assessment of the Codman MicroSensor Transducer. *J Neurosurg* 2008;109:159-64.
47. Shellock FG, Slimp G. Severe burn of the finger caused by using a pulse oximeter during MRI. *AJR Am J Roentgenology* 1989;153:1105.
48. ECRI. A new MRI complication? *Health Devices Alert* 1988;1.
49. ECRI. Thermal injuries and patient monitoring during MRI studies. *Health Devices Alert* 1991;20:362-3.
50. Kanal E, Shellock FG. Burns associated with clinical MR examinations. *Radiology* 1990;175:585.
51. Keens SJ, Laurence AS. Burns caused by ECG monitoring during MRI imaging. *Anesthesiology* 1996;51:1188-9.
52. Brown TR, Goldstein B, Little J. Severe burns resulting from magnetic resonance imaging with cardiopulmonary monitoring. Risks and relevant safety precautions. *Am J Phys Med Rehabil* 1993;72:166-7.
53. Bashein G, Syrory G. Burns associated with pulse oximetry during magnetic resonance imaging. *Anesthesiology* 1991;75:382-3.
54. Haik J, Daniel S, Tessone A, Orenstein A, Winkler E. MRI induced fourth-degree burn in an extremity, leading to amputation. *Burns* 2009;35:294-6.
55. Hall SC, Stevenson GW, Suresh S. Burn associated with temperature monitoring during magnetic resonance imaging. *Anesthesiology* 1992;76:152.
56. Hardy PT, Weil KM. A review of thermal MR injuries. *Radiol Technol* 2010;81:606-9.
57. Delfino JG, Krainak DM, Flesher SA, Miller DL. MRI-related FDA adverse event reports: A 10-yr review. *Med Phys* 2019;46:5562-5571.
58. Jones S, Jaffe W, Alvi R. Burns associated with electrocardiographic monitoring during magnetic resonance imaging. *Burns* 1996;22:420-421.
59. Brix L, Isaksen C, Kristensen BH, Tufa B. Third degree skin burns caused by a MRI conditional electrocardiographic monitoring system. *Journal of Radiology and Imaging* 2016;1:29-32.
60. Karoo RO, Whitaker IS, Garrido A, Sharpe DT. Full-thickness burns following magnetic resonance imaging: A discussion of the dangers and safety suggestions. *Plast Reconstr Surg* 2004;114:1344-1345.
61. Lange S, Nguyen QN. Cables and electrodes can burn patients during MRI. *Nursing* 2006;36:18.

460 Physiological Monitoring of Patients During MRI

62. Ruschulte H, Piepenbrock S, Munte S, Lotz J. Severe burns during magnetic resonance examination. *Eur J Anaesthesiol* 2005;22:319-320.
63. Tenefford TS, Gaffey CT, Moyer BR, Budinger TF. Cardiovascular alterations in Macaca moneys exposed to stationary magnetic fields. Experimental observations and theoretical analysis. *Bioelectromagnetics* 1983;4:1-9.
64. Dimick RN, Hedlund LW, Herfkens RF, et al. Optimizing electrocardiographic electrode placement for cardiac-gated magnetic resonance imaging. *Invest Radiol* 1987;22:17-22.
65. Damji AA, Snyder RE, Ellinger DC, et al. RF interference suppression in a cardiac synchronization system operating in a high magnetic field NMR imaging system. *Magn Reson Imaging* 1988;6:637-640.
66. Berkow LC, et al. Anesthetic management and human factors in the intraoperative MRI environment. *Curr Opin Anaesthesiol* 2016;29:563-7.
67. Gandhe RU, Bhave CP. Intraoperative magnetic resonance imaging for neurosurgery - An anaesthesiologist's challenge. *Indian J Anaesth* 2018;62:411-417.
68. Schroeck H, Welch TL, Rovner MS, et al. Anesthetic challenges and outcomes for procedures in the intraoperative magnetic resonance imaging suite: A systematic review. *J Clin Anesth* 2019;54:89-101.
69. Deen J, Vandevivere Y, Van de Putte P. Challenges in the anesthetic management of ambulatory patients in the MRI suites. *Curr Opin Anaesthesiol* 2017;30:670-675.
70. Shellock FG, Rubin SA. Simplified and highly accurate core temperature measurements. *Med Prog Technol*. 1982;8:187-8.
71. Michiaki Y. Anesthesia and body temperature: Temperature regulation under general anesthesia combined with epidural anesthesia. *Journal of Clinical Anesthesia* 2000;24:1416-1424.
72. Takashi M. Anesthesia and body temperature: General anesthesia and thermoregulation. *Journal of Clinical Anesthesia* 2000; 24:1408-1415.
73. Schubert A. Side effects of mild hypothermia. *Journal of Neurological Anesthesiology* 1995;7:139-147.
74. Lilly JK, Boland JP, Zekan S. Urinary bladder temperature monitoring: A new index of body core temperatures. *Critical Care Medicine* 1980;8:742-744.
75. Lefrant J Y, Muller L, Emmanuel de La Coussaye E, et al. Temperature measurement in intensive care patients: Comparison of urinary bladder, esophageal, rectal, axillary, and inguinal methods versus pulmonary artery core method. *Intensive Care Med* 2003;29:414-418.
76. Robinson J, Charlton J, Seal R, et al. Esophageal, rectal, axillary, tympanic, and pulmonary artery temperatures during cardiac surgery. *Canadian Journal of Anesthesiology* 1998;45:317-323.
77. Takashi A. Anesthesia and body temperature: Interoperative monitoring of body temperature and its significance. *Journal of Clinical Anesthesia*, 2000;24:1432-1443.
78. Gooden CK. Anesthesia for magnetic resonance imaging. *Curr Opin Anaesthesiol*. 2004;17:339-42.
79. Wilson TE, Sauder CL, Kearney ML, et al. Skin surface cooling elicits peripheral and visceral vasoconstriction in humans. *Journal of Applied Physiology* 2007;103:1257-1262.
80. Newsham KR, Saunders JE, Nordin ES. Comparison of rectal and tympanic thermometry during exercise. *Southern Medical Journal* 2002;95:804-810.
81. Shellock FG, Gordon CJ, Schaefer DJ. Thermoregulatory responses to clinical magnetic resonance imaging of the head at 1.5 Tesla: Lack of evidence for direct effects on the hypothalamus. *Acta Radiologica* 1986;Suppl. 369:512-513.
82. Shellock FG, Crues JV. Temperature, heart rate, and blood pressure changes associated with clinical magnetic resonance imaging at 1.5 T. *Radiology* 1987;163:259-262.
83. Shellock FG, Crues JV. Temperature changes caused by clinical MR imaging of the brain at 1.5 Tesla using a head coil. *Am J Neuroradiol* 1988;9:287-291.
84. Shellock FG, Schaefer DJ, Crues JV. Alterations in body and skin temperatures caused by MR imaging: Is the recommended exposure for radiofrequency radiation too conservative? *Brit J Radiol* 1989;62:904-909.

MRI Bioeffects, Safety, and Patient Management 461

85. Shellock FG, Schaefer DJ, Kanal E. Physiologic responses to MR imaging performed at an SAR level of 6.0 W/kg. *Radiology* 1994;192:865-868.
86. Greenberg KL, Weinreb J, Shellock FG. "MR conditional" respiratory ventilator system incident in a 3-T MRI environment. *Magn Reson Imaging* 2011;29:1150-4.

Chapter 18 MRI-Related Issues for Implants and Devices

FRANK G. SHELLOCK, PH.D.

Director of MRI Safety
USC Stevens Neuroimaging and Informatics Institute

Adjunct Clinical Professor of Radiology and Medicine
Keck School of Medicine, University of Southern California
Los Angeles, CA

INTRODUCTION

One of the most critical factors involved in protecting patients from magnetic resonance imaging (MRI)-related injuries involves an understanding of the risks associated with the presence of metallic implants and devices that may cause problems that include serious injuries and fatalities (1-21). The standard of care for managing a patient referred for an MRI examination with an implant or device is to positively identify the particular item and then determine the relative safety of scanning the patient. This is best accomplished by referring to the MRI-specific labeling for the implant or device, which is typically presented in the *Instructions for Use* (IFU). In instances when no labeling exists, the supervising physician (which is typically a radiologist) is responsible for making a decision on whether to scan the patient based on a careful consideration of the risks associated with the metallic object and the benefit of the diagnostic information provided by the MRI examination (1, 4, 5, 12).

This chapter discusses the various MRI-related issues that exist for implants and devices (1-21). Notably, a comprehensive understanding of this essential information is particularly vital when managing patients with unlabeled medical products (1, 4, 5, 12). This chapter will also review information for commonly encountered implants, as well as medical devices that may present challenges with respect to MRI-related labeling.

MRI-RELATED ISSUES FOR IMPLANTS AND DEVICES

It is well known that MRI may be a contraindication for a patient with a metallic implant because of various factors that can result in serious injury or death (1-16). These include movement or dislodgment of a ferromagnetic implant or device, excessive MRI-related heating associated with the time-varying, gradient magnetic fields (i.e., for certain implants) and/or the RF field, induction of currents resulting in unintentional stimulation or other issues, changes in the operational aspects of the device, damage to the function of the device, the difficulty in interpreting MR images due to signal loss and/or distortion, and the misinterpretation of an imaging artifact as an abnormality (1-19).

Implants and devices are typically categorized into two types: passive and active. A passive implant, such as a vascular clip or heart valve prosthesis, is one that serves its function without any source of power other than that generated by the gravity or the human body, while an active implant (often referred to as an active implantable medical device or AIMD), such as a cardiac pacemaker or neuromodulation system, is a medical device that relies on its function from a source of electrical energy or any source of power other than that directly generated by gravity or the human body (1, 9, 21, 22). Because of their complexity, AIMDs inherently pose a greater number MRI-related issues for patients compared to passive implants. The possible MRI-related risks for passive and active implants are summarized in **Table 1** and **Table 2**.

Table 1. Possible MRI-related risks for passive implants.

-
- Translational Attraction/Force
 - Torque
 - Lenz Forces
 - RF-Induced Heating
 - Gradient Magnetic Field-Induced Heating*
 - Artifacts
 - Change in Function or Operation
 - Temporary or Permanent Damage

(*An implant with a relatively large surface area may exhibit measurable gradient magnetic field-induced heating.)

Table 2. Possible MRI-related risks for active implants.

-
- Translational Attraction/Force
 - Torque
 - Lenz Forces
 - RF-Induced Heating
 - Gradient Magnetic Field-Induced Heating*
 - Gradient Magnetic Field-Induced Vibration
 - Unintended Stimulation
 - Artifacts
 - Change in Function or Operation
 - Temporary or Permanent Damage

(*An implant with a relatively large surface area may exhibit measurable gradient magnetic field-induced heating.)

464 MRI-Related Issues for Implants and Devices

Magnetic Field Interactions

Translational Attraction and Torque. With regard to magnetic field interactions and MRI, translational attraction and/or torque may cause movement or dislodgment of a ferromagnetic implant, resulting in an uncomfortable sensation for the patient, an injury, or even a fatality (1-4, 20, 21, 23-58). Therefore, both translational attraction and torque are important to evaluate for implants and devices before patients with metallic objects are allowed to undergo MRI (1, 20-58).

The effect of translational attraction acting on an implanted ferromagnetic object is predominantly responsible for a hazard that may occur in the immediate area of the MR system (1, 3, 8, 10, 12). That is, as one moves closer to the scanner or as the patient is moved into the bore for the MRI examination. The predominant effect of torque (or rotational alignment to the magnetic field) as it acts on a ferromagnetic object occurs in the center of the MR system, where the magnetic field is most homogenous (1, 3, 8, 10, 12). Notably, torque, which is proportional to the strength of the static magnetic field, will greatly influence implants and devices that have an elongated shape. Obviously, both translational attraction and torque combine to impact a ferromagnetic implant or device as the patient with the object moves towards the MR system and then into the center of the bore of the scanner (1, 3, 8, 10, 12).

Various factors influence the risk of performing MRI in a patient with a ferromagnetic object including the strength of the static magnetic field, the level of the spatial gradient magnetic field (discussed below), the magnetic susceptibility of the object, the mass of the object, the geometry of the object, the location and orientation of the object *in situ*, the presence of retentive or anchoring mechanisms (i.e., fibrotic tissue, sutures, etc.), and the length of time the object has been implanted. These factors should be carefully considered before subjecting a patient with a metallic implant or other object to an MRI examination. This is particularly important if the object is located in a potentially dangerous area of the body such as a vital neural, vascular, or soft tissue structure where movement or dislodgment could injure the patient.

With respect to the potential risks associated with a ferromagnetic implant, in addition to the findings for translational attraction and torque, the “intended *in vivo* use” of the implant or device must be considered as well as the mechanisms that may provide retention of the object once it is implanted, as discussed above (e.g., implants or devices held in place by sutures, granulation or ingrowth of tissue, fixation devices, or by other means). Accordingly, sufficient counterforces may exist to retain even a ferromagnetic implant in place, *in situ*.

Numerous studies have assessed magnetic field interactions for implants and other items by measuring translational attraction and torque associated with static magnetic fields of MR systems operating as high as 8-Tesla (1, 23-58). These investigations generally demonstrated that MRI can be performed safely in patients with metallic objects that are nonferromagnetic or “weakly” ferromagnetic (i.e., only minimally attracted by the magnetic field), such that the magnetic field interactions are insufficient to move or dislodge them, *in situ*.

Additionally, patients with certain implants or devices that have relatively strong ferromagnetic qualities may be safely scanned using MRI because the objects are held in place by retentive forces that prevent them from being moved or dislodged with reference to the “intended *in vivo* use” of the object. For example, there is an interference screw (i.e., the Perfix Interference Screw) used for reconstruction of the anterior cruciate ligament that is highly ferromagnetic. However, once this implant is placed in the patient (i.e., screwed into the patient’s bone), this prevents it from being moved, even if the patient is exposed to a high-field MR system. Other medical implants that exhibit substantial ferromagnetic qualities may likewise be safe for patients undergoing MRI as a result of the presence of counterforces that prevent displacement of these objects. Of note is that there are medical implants that actually incorporate magnets as their functional components, such as programmable cerebral spinal fluid (CSF) shunt valves, cochlear implants, and certain orthopedic implants (e.g., the MAGEC System, Nuvasive, www.nuvasive.com). These particular implants are safe for patients undergoing MRI as long as highly specific safety guidelines are followed.

In general, medical implants should undergo testing using *ex vivo* techniques to assess translational attraction and torque before allowing a patient with the object to undergo an MRI exam (1, 20-22). By following this guideline, the magnetic-aspects of an object may be determined so that a competent decision can be made concerning possible risks associated with subjecting the patient to MRI. Because movement or dislodgment of an implanted metallic object is one of the main mechanisms responsible for an injury, this part of implant testing is considered to be of utmost importance and should involve the use of an MR system operating at an appropriate static magnetic field strength. That is, if the intent is to scan the patient with the implant at 3-Tesla, the implant must be tested for magnetic field interactions at that field strength.

Lenz Effect-Related Forces. Forces related to the Lenz Effect are of potential concern in the MRI environment. In 1835, Heinrich Lenz stated the law that an electric current induced by a changing magnetic field will flow such that it will create its own magnetic field that opposes the magnetic field that created it. These opposing fields, which occupy the same space at the same time, result in a pair of forces. The more current that is generated, the greater the force that opposes it. The so-called “Lenz Effect” occurs with electrically conductive materials (i.e. not just ferromagnetic materials) that develop eddy currents in the presence of high-field-strength static magnetic fields, such as those associated with MR systems.

Force associated with the Lenz Effect may restrict movement of large metallic objects (e.g., an aluminum oxygen tank) or potentially compromise the function of certain implants in the MRI setting, such as those with moving metallic parts. Interestingly, this force has been suggested to be of concern for prosthetic heart valves that have leaflets or discs, especially if the cardiac implant is used for mitral valve replacement, where the range of pressures are relatively low (higher pressures are more likely to overcome a substantial Lenz Effect).

Condon and Hadley (59) first reported the theoretical possibility of Lenz Effect-related actions for heart valve prostheses that contain metallic disks or leaflets. In theory, “resistive

466 MRI-Related Issues for Implants and Devices

pressure” may develop with the potential to inhibit both the opening and closing mechanism of a mechanical heart valve prosthesis that has leaflets or disks. In 2012, Golestanirad, et al. (60) conducted a comprehensive analysis of the Lenz Effect due to motion of artificial heart valves during MRI. They concluded that mechanical heart valves with strengthening rings may be considered safe even under ultra-high-field MRI conditions with field intensities as high as 10 Tesla. Edwards, et al. (61) performed an *in vitro* study of the occurrence of Lenz Effect-related forces on various heart valve prostheses at 1.5-Tesla and assessed the risk of the impedance of valve function. The findings provided evidence of the Lenz Effect on certain cardiac valve prostheses exposed to the static magnetic field, which resulted in functional valve impedance and a potentially increased risk of valve regurgitation. While further evaluation of this phenomenon may be warranted, to date, the Lenz Effect has not been observed in association with clinical MRI examinations nor has it posed additional risks for patients with certain heart valve prostheses (i.e. those with metallic leaflets or disks) or any other implant for that matter.

One important scenario of Lenz Effect-related forces involves patients with relatively large metallic implants, like implantable infusion pumps or external fixation systems. Despite the lack of movement or displacement hazards for these implants, rapid motion of the patient (e.g., as the patient enters the scanner’s bore) with a large metallic implant that is oriented perpendicular to direction of the static magnetic field of the scanner can result in forces on the implant opposing the motion that may be detected by the patient. In the event that the patient complains of experiencing forces, such as tugging or pulling on the implant, this might lead to the patient or MRI personnel erroneously concluding that the device has ferromagnetic components, and possibly cancelling the MRI examination (1, 4). Slowly moving a patient with a large metallic implant into and out of the bore of the MR system is essential to mitigate Lenz Effect-related forces that might be induced, decreasing the likelihood of a misunderstanding or unnecessary exam cancellation (1, 4).

Magnetic Field Interactions and Operational Disturbances. In certain cases, there is a possibility of changing the operation or function of a medical implant or device as a result of exposure to the powerful static magnetic field of the MR system. For an implant that has a component that is magnetic (e.g., cochlear implants, programmable CSF shunt valves, magnetic reflux management device, etc.), it is possible to disrupt the function of the device or to demagnetize the magnet, rendering it unacceptable for its intended use (1, 2). Therefore, this important aspect must be evaluated using comprehensive *ex vivo* testing techniques to verify that specific MRI conditions will not alter the device’s function (20-22).

MR systems with very low (0.064-Tesla or less) or very high (10.5-Tesla) static magnetic fields are currently used for clinical and research applications. Considering that most metallic objects evaluated for magnetic field interactions were assessed at 1.5- or 3-Tesla, an appropriate variance or modification of the information provided regarding the safety of performing an MRI procedure in a patient with a metallic object may exist when a scanner with a lower or higher static magnetic field strength was used for testing and labeling. Therefore, it is deemed acceptable to adjust safety recommendations depending on the static magnetic field strength and other considerations of a given scanner. Obviously, performing an MRI procedure using a 0.064-Tesla MR system has different risk implications for a patient with a ferromagnetic implant compared with using a 10.5-Tesla scanner.

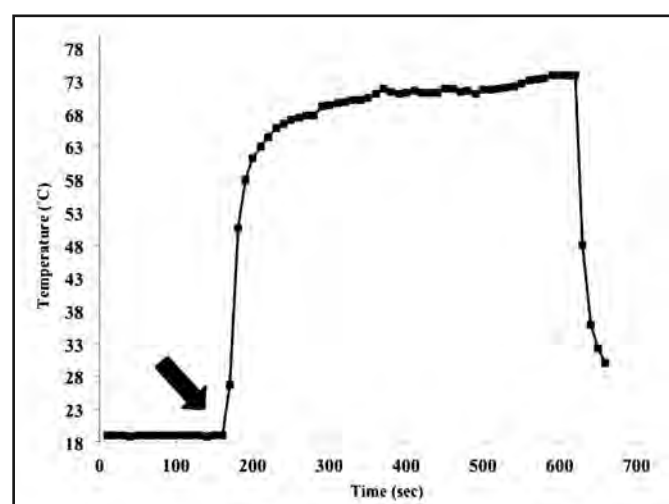
MRI-Related Heating

Temperature increases produced in association with MRI have been studied using *ex vivo* techniques to evaluate various metallic implants, devices, and objects that have a variety of sizes, shapes, and metallic compositions or that are made from other conducting materials (1, 2, 38-82). In general, reports have indicated that only minor temperature changes occur in association with MRI and relatively short or compact metallic objects that are passive implants, including items such as aneurysm clips, hemostatic clips, prosthetic heart valves, vascular access ports, and similar devices. Therefore, heat generated during MRI involving a patient with a relatively small, passive implant does not appear to be a substantial hazard. Notably, to date, there has been no report of a patient being seriously injured as a result of excessive heating of a small passive implant or device.

However, MRI-related heating is potentially problematic for implants that have an elongated shape or those that form a conducting loop of a particular diameter (1, 2, 4, 6-12, 15, 20-22, 62-75). For example, substantial heating resulting in injuries to patients can occur under certain MRI conditions for elongated implants (e.g., leads, wires, etc.) that form resonant antennas or that form resonant conducting loops (Figure 1).

Radiofrequency Field-Related Heating. Radiofrequency (RF) fields associated with MRI can induce electric current in conductors that causes tissue heating primarily due to resistive losses (1, 2, 4, 6, 8-12). Metallic implants and devices have high conductivity and low resistance to electric currents, which results in a minimal amount of implant heating. However, tissues surrounding a metallic implant can heat due to its relatively high electrical resistance (1, 2, 4, 6, 8-12). The evaluation of an implant or device for heating is particularly challenging because of the many factors that effect temperature increases in these items.

Figure 1. Example of excessive MRI-related heating of a medical implant. An abandoned lead from a neuromodulation system was placed in a gelled-saline filled phantom and scanned using a 1.5-Tesla MR system at a whole-body averaged specific absorption rate of 3.8-W/kg. Note the rapid rise in temperature that occurred at the onset of MRI (black arrow) and the substantial heating of the lead that exceeded 73°C.



468 MRI-Related Issues for Implants and Devices

Variables that impact RF field-related heating include: the specific type of implant or device; the electrical characteristics of the materials used for the implant or device; the transmitted RF wavelength of the MR system (e.g., at 1.5-Tesla, 64-MHz; at 3-Tesla, 128-MHz); the type of transmit RF coil that is used (i.e., transmit body RF coil, transmit head RF coil, etc.); the amount of RF energy delivered (i.e., based on the specific absorption rate, SAR or other RF energy-related metric); the technique used to calculate or estimate the SAR that is utilized by the MR system; the landmark position or body part undergoing MRI relative to the transmit RF coil; and the orientation or configuration of the implant or device relative to the source of RF energy (i.e., the transmit RF coil) (1, 2, 4, 6-12, 15, 20-22, 62-75).

One consideration of RF field-related heating of an implant that may not be intuitive is that for a given item, heating can be substantially different depending on the frequency of RF that is applied. For example, evidence from an *ex vivo* study conducted by Shellock, et al. (83) reported that significantly *less* MRI-related heating occurred at 3-Tesla/128-MHz (whole-body-averaged SAR, 3-W/kg) versus 1.5-Tesla/64-MHz (whole-body-averaged SAR, 1.4-W/kg) for a pacemaker lead that was not connected to a pulse generator (same lead length, positioning in the phantom, etc.). This phenomenon whereby less heating was observed at 128-MHz versus 64-MHz has also been observed for external fixation devices, Foley catheters with temperature sensors, neuromodulation systems, relatively long peripheral vascular stents, and other implants. Therefore, it is vital to perform *ex vivo* testing to properly characterize MRI-related heating to identify potentially hazardous medical implants.

Gradient Magnetic Field-Induced Heating. Exposure to gradient magnetic fields utilized during MRI can induce eddy currents on the conductive surface of a metallic implant that is located inside the bore of the MR system (1, 4, 10, 14, 16, 76-78). Thus, this is a potential safety concern for patients that have certain metallic implants. The impact of the gradient magnetic fields is primarily determined by the surface area and thickness of the conductor (i.e., with specific respect to the dimensional aspects of the implant), the electrical conductivity of the metal, the rate of change of the gradient magnetic fields, and the relative orientation of implant to the gradient magnetic fields (1, 4, 10, 14, 16, 76-78).

Because of the typical small planar surface area that exists for most passive implants, gradient magnetic field-induced heating is generally not expected to pose a hazard with respect to tissue damage for passive medical devices (1, 4, 10, 14, 16, 76-78). This is also the case for active implants that may have a relatively small surface area (e.g., leads associated with cardiac pacemakers and neuromodulation systems). However, gradient magnetic field-induced heating can be substantial for patients with certain sizable passive implants such as large cranial plates, acetabular cups used with total hip replacement prostheses, and implantable infusion pumps (1, 4, 10, 14, 16, 76-78). Accordingly, these situations pose a possible safety issue. Importantly, to date (i.e., 35+ years), there has been no report of an injury to a patient that has been attributed to gradient magnetic field-induced heating of a medical implant.

Induced Currents

The potential for MRI examinations to injure patients by inducing electrical currents in implants or devices made from conductive materials such as cardiac pacemakers, neuro-

modulation systems, and other similar items has been previously reported (1, 2, 79-82). Notably, the performance of *ex vivo* testing of implants and devices to assess induced currents is predominantly focused on AIMDs since induced currents have not been described for passive implants (1, 2, 9, 20-22). In general, AIMDs developed to be safe for patients undergoing MRI incorporate special design features to suppress or prevent induced currents from presenting problems (9).

Artifacts

The type and extent of artifacts caused by the presence of metallic implants and devices have been described and tend to be easily recognized on MR images (1, 2, 4, 17-19). Signal loss and/or image distortion associated with metallic objects are predominantly caused by a disruption of the local magnetic field that perturbs the relationship between position and frequency. In some cases, there may be areas of high signal intensity seen along the edge of a signal void or when there is an abrupt change in the shape of the item (e.g., the tip of a biopsy needle). Additionally, artifacts seen on MR images may be caused by gradient switching due to the generation of eddy currents.

The extent of the artifact on an MR image is dependent on the implant's magnetic susceptibility, size, shape, position in the patient's body, the technique used for imaging (i.e., the specific pulse sequence parameters), and the image processing method. Careful selection of pulse sequence parameters decreases the size of artifacts and this is done routinely, especially for patients that undergo MRI with implants that are particularly large, such as total hip or total knee prostheses. Additionally, software-based techniques, such as the metal artifact reduction sequence (MARS), have been described that substantially reduce artifacts associated with metallic objects. **Table 3** presents techniques that may be used to reduce artifacts associated with metallic implants.

TERMINOLOGY FOR IMPLANTS AND DEVICES

With the growing use of MRI in the 1990s, the Food and Drug Administration (FDA) recognized the need for standardized tests to address MRI safety issues for implants and other medical devices. Thus, over the years, test methods have been developed by various

Table 3. Techniques to reduce artifacts associated with metallic implants.

- Use a lower static magnetic field strength
- Select different pulse sequence (e.g., FSE vs. SE; SE vs. GRE)
- Decrease echo time
- Decrease repetition time
- Increase bandwidth
- Increase matrix size
- Decrease section thickness
- Increase the number of excitations
- Swap phase and frequency encoding direction
- Use STIR for fat suppression vs. frequency selective fat suppression
- Use software-based method (e.g., metal artifact reduction sequence, MARS)

(FSE, fast spin echo; SE, spin echo; GRE, gradient echo; STIR, short tau inversion recovery)

470 MRI-Related Issues for Implants and Devices

organizations including the American Society for Testing and Materials (ASTM) International, and the International Organization for Standardization (ISO), with an ongoing commitment to ensure patient safety in the MRI environment (20-22, 84-88).

The FDA is responsible for reviewing the test information submitted to them by the implant or device manufacturer, the MRI terminology, and the labeling assigned to the product. This terminology has evolved to keep pace with advances in MRI technology. Unfortunately, members of the MRI community frequently may not understand the terms that are used and are often confused by the conditions that are specified in “MR Conditional” labeling. This lack of understanding may result in patients with implants being exposed to potentially hazardous MRI conditions or in inappropriately preventing them from undergoing needed examinations. Importantly, the current labeling terminology that exists is associated with expanded labeling information that relates to the conditions that are deemed acceptable to ensure patient safety (21).

Prior to implementing the current terminology, the terms “MR Safe” and “MR Compatible” were used for labeling purposes (89, 90). In time, it became apparent that these terms were somewhat confusing and often used interchangeably or incorrectly. In particular, these terms were frequently used without including the conditions for which the device had been demonstrated to be safe. Therefore, in an effort to develop more appropriate terminology and, more importantly, because the misuse of the terms could result in serious risks for patients and others in the MRI environment, a new set of MRI labeling terms was developed and released in 2005 (91). Thus, this terminology, which is currently recognized by the FDA (as well as notified or regulatory bodies outside the United States) and applied to implants and devices is, as follows (21): (a) *MR Safe* - a medical device that poses no known hazards resulting from exposure to any MR environment. MR Safe medical devices are composed of materials that are electrically nonconductive, nonmetallic, and nonmagnetic. Using this terminology, MR Safe items are non-conducting, non-metallic, and non-magnetic items such as a catheter made from silicone. (b) *MR Conditional* - a medical device with demonstrated safety in the MR environment within defined conditions including conditions for the static magnetic field, the time-varying gradient magnetic fields, and the radiofrequency fields. Conditions that define the MRI environment may include the strength of the static magnetic field value, the spatial gradient magnetic field value, the time-varying magnetic field value, the RF field value, and the specific absorption rate (SAR) level. Additional conditions, including the specific configuration for the item (e.g., the routing of leads used for a neurostimulation system) may be required. Other possible safety issues that may be part of the MR Conditional labeling include but are not limited to thermal injury, induced currents, electromagnetic interference, unintended stimulation, and unwanted interactions among other devices. (c) *MR Unsafe* – a medical device which poses unacceptable risks to the patient, medical staff, or other persons within the MR environment. MR Unsafe items include items such as a pair of ferromagnetic scissors.

Because of the variety of MR systems (e.g., ranging from 0.064- to 7-Tesla) and conditions in clinical use today, the current terminology is intended to help elucidate labeling matters for medical devices and other items that may be used in the MRI environment to ensure the safe use of MRI technology. However, it should be noted that this updated terminology has not been applied retrospectively to the many implants and devices that pre-

viously received FDA approved labeling using the now outdated terms, “MR Safe” or “MR Compatible” (in general, this applies to those objects tested prior to the release of the ASTM International information for labeling in 2005). Therefore, this important point must be understood to avoid undue confusion regarding the matter of the labeling that has been applied to previously tested implants (i.e., those labeled as MR Safe or MR Compatible) versus those that have recently undergone MRI testing and now labeled MR Safe, MR Conditional, or MR Unsafe (89-91). Notably, the specific content of the MRI labeling for an implant or device may take various forms (especially for AIMDs) because the format continues to be refined by the FDA in an ongoing effort to properly communicate this information to MRI healthcare professionals (21).

MR Conditional Labeling Information: Explanation of the Content

In addition to the frequent problems associated with understanding the MRI labeling, the actual content of the label is often misunderstood with respect to the conditions indicated for a given implant that is labeled “MR Conditional”. Therefore, the following is an example of MR Conditional labeling for an implant, *Example Implant*, along with an explanation of the content provided for each aspect of the label (89):

MRI Safety Information

Non-clinical testing has demonstrated the *Example Implant* is MR Conditional. A patient with this implant can be scanned safely under the following conditions:

- Static magnetic field of 1.5- or 3-Tesla

(*Note*: These are static magnetic fields for which the implant gave acceptable test results with respect to the assessments for translational attraction, torque, and MRI-related heating. Therefore, carefully reading and implementing this part of the labeling is advised in order to avoid possible injuries to patients.)

- Spatial gradient magnetic field of 720-gauss/cm or less.

(*Note*: This is a frequently misinterpreted parameter because the MRI healthcare worker sees the term “gradient field” and may presume that it refers to the time-varying or gradient fields used during MRI. However, the term, “spatial gradient magnetic field” for medical device labeling relates to the rate at which the static magnetic field strength changes over space per unit distance and is the position in the MR system used to determine the translational attraction for the implant, according to the test procedure described in ASTM F2052 (84). Thus, indicated as dB/dx or, in this case, as 720-gauss/cm. In certain instances, if the measured deflection is relatively low, that is, 10-degrees or less, a calculation is performed to extrapolate the spatial gradient magnetic field value to a higher value in consideration of the basic acceptance criterion of 45-degrees or less for translational attraction. Therefore, it is not unusual to see labeling for implants or devices that present a spatial gradient magnetic field value of 2,000-gauss/cm or higher.)

- Maximum MR system reported, whole body averaged specific absorption rate (SAR) of 2-W/kg (Normal Operating Mode) for 15-minutes of scanning.

(*Note*: There is frequently confusion with respect to this stated parameter insofar as the term “scanning” is presumed to apply to the entire MRI procedure when, in fact, it typically

472 MRI-Related Issues for Implants and Devices

applies to each particular pulse sequence that is used and, of course, multiple sequences are utilized when performing the MRI examination. Therefore, for passive implants, the “15-minutes of scanning” refers to the maximum time per pulse sequence. By comparison, MRI labeling for active implants may indicate a maximum scanning time along with a “cooling” period.)

- Under the scan conditions defined, the *Example Implant* is expected to produce a maximum temperature rise of 2.8°C after 15-minutes of continuous scanning (i.e., per pulse sequence).

(*Note:* The labeling typically has additional information with respect to the temperature rise that is associated with certain MRI parameters. This information was based on the findings obtained in the MRI-related heating tests that were conducted on the implant according to ASTM F2182 (86). Therefore, in this example, the expected “worst case” temperature rise is 2.8°C during MRI performed at a whole body averaged SAR of 2-W/kg for 15-minutes.)

- Image Artifact

In non-clinical testing, the image artifact caused by the *Example Implant* extends approximately 15-mm from this implant when imaged using a gradient echo pulse sequence and a 3-Tesla MR system.

(*Note:* This is a common statement for many different implants and is based on testing performed according to ASTM F2119 (87). Since the size of the artifact for an implant may impact the diagnostic use of MRI, information is typically provided in the label that characterizes the size and shape of the artifacts associated the gradient echo pulse sequence.)

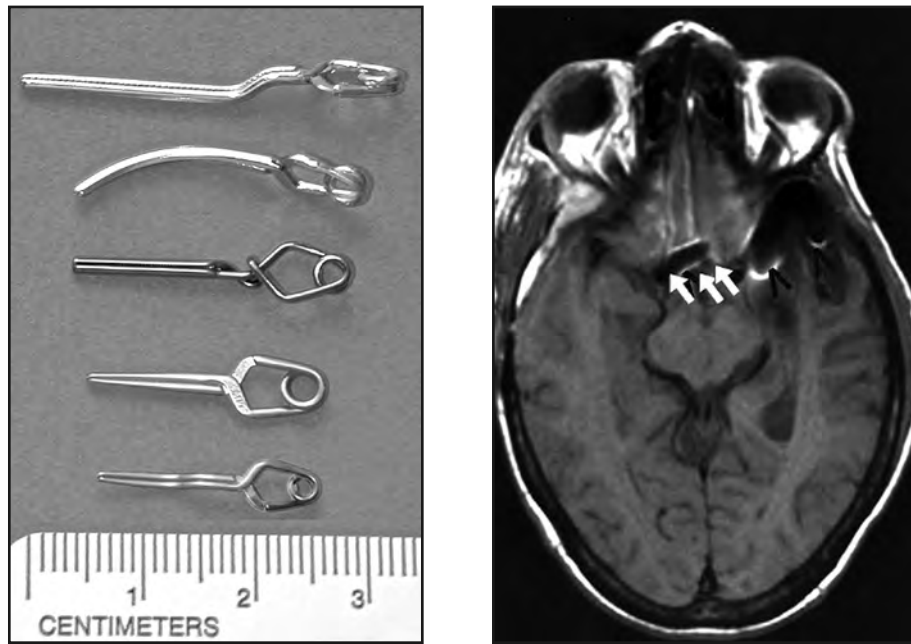
MRI INFORMATION FOR IMPLANTS AND DEVICES

New implants and devices are developed on an ongoing basis, which necessitates continuous endeavors to obtain current documentation for these medical products prior to subjecting patients to MRI examinations. In certain instances, the MRI labeling may change for an implant as a result of new testing that was conducted or a due to a change in materials. Importantly, the labeling that ensures the safe use of MRI is highly specific to the conditions that were utilized to assess the implant or device and any deviation from the defined procedures can lead to deleterious events, severe patient injuries, or fatalities, especially when AIMDs are present (1, 2, 4, 6-10, 79-82). MRI-related information is presented herein for a selection of *passive* implants in an effort to illustrate commonly encountered items as well as unique medical products. Information for many *active* implants, including cardiac devices and neuromodulation systems, is provided in other chapters in this textbook.

Aneurysm Clips

The surgical management of intracranial aneurysms and arteriovenous malformations (AVMs) by the application of an aneurysm clip is a well-established procedure. The presence of an aneurysm clip in a patient referred for an MRI exam represents a situation that requires the utmost consideration because of the associated risks (1, 2, 4, 6, 27-33)(Figure 2). Certain types of intracranial aneurysm clips (e.g., those made from martensitic stainless steels such

Figure 2. (left) Examples of aneurysm clips. (right) MRI of the brain in a patient with multiple, MR Conditional aneurysm clips. The relatively small artifacts (white arrows and black arrow heads) associated with the clips are due to the materials that have low magnetic susceptibilities.



as 17-7PH or 405 stainless steel) are a contraindication to the use of MRI because excessive, magnetically-induced forces can displace these implants and cause serious injury or death. By comparison, aneurysm clips classified as “nonferromagnetic” or “weakly ferromagnetic” are acceptable for patients undergoing MRI. (For the sake of discussion, the term “weakly ferromagnetic” refers to metal that demonstrates extremely low ferromagnetic qualities using highly sensitive instrumentation such as vibrating sample magnetometer or superconducting quantum interference and, thus, may not be technically referred to as being “nonferromagnetic.” All metals possess some degree of magnetism, such that no metal is entirely nonferromagnetic.)

The following guidelines are recommended with regard to performing MRI in a patient or before allowing an individual with an aneurysm clip into the MRI environment (1, 2, 4, 6, 7):

- (1) The specific information (i.e., manufacturer, type or model, material, lot and serial numbers) about the aneurysm clip must be known, especially with respect to the material used to make the clip, so that only patients or individuals with nonferromagnetic or weakly ferromagnetic clips are allowed into the MRI environment. The manufacturer provides this information in the labeling of the aneurysm clip. The implanting surgeon is responsible for properly recording and communicating this information in the patient’s or individual’s records.

474 MRI-Related Issues for Implants and Devices

- (2) An aneurysm clip that is in its original package and made from Phynox, Elgiloy, MP35N, titanium alloy, commercially pure titanium or other material known to be nonferromagnetic or weakly ferromagnetic does not need to be evaluated for ferromagnetism. Aneurysm clips made from nonferromagnetic or “weakly” ferromagnetic materials in original packages do not require testing because the manufacturers ensure the materials used to make the clips and, therefore, are responsible for the accuracy of the labeling.
- (3) If the aneurysm clip is not in its original package and/or properly labeled, it should undergo testing for magnetic field interactions according to appropriate testing procedures to determine if it is safe.
- (4) Consideration must be given to the static magnetic field strength that is to be used for the MRI procedure and the strength of the static magnetic field that was used to test magnetic field interactions for the aneurysm clip in question.
- (5) The radiologist and patient’s surgeon are responsible for evaluating the information pertaining to the aneurysm clip, verifying its accuracy, obtaining written documentation, and deciding to perform MRI after considering the risk versus benefit for a given patient.

Breast Tissue Expanders

Adjustable breast tissue expanders are utilized for breast reconstruction following mastectomy, for the correction of breast and chest-wall deformities as well as underdevelopment, for tissue defect procedures, and for cosmetic augmentation. These devices are typically equipped with either an integrated injection port that is utilized to accept a needle for placement of saline for expansion of the prosthesis intra-operatively and/or postoperatively (47, 55, 58, 92-97).

Breast tissue expanders commonly incorporate magnetic ports to allow for accurate detection of the injection site. These implants are substantially attracted to the static magnetic fields of MR systems and, therefore, may be uncomfortable, injurious, or contraindicated for patients undergoing MRI (47, 55, 58, 92-97). In general, because the magnetic infusion ports incorporated into most breast tissue expanders presumably interact adversely with the electromagnetic fields used for MRI, all such implants are labeled MR Unsafe. Therefore, the consensus practice is to use other imaging techniques when diagnostic exams, such as ultrasound or computed tomography, are needed for patient management (92-95). Another issue over and above safety is that breast tissue expanders with magnetic ports produce extremely large artifacts on MR images and, therefore, assessment of the breast using MRI is problematic (92-95). Of additional importance is that here may be a situation during which a patient is referred for MRI for the determination of breast cancer or an implant rupture, such that the presence of the excessive metallic artifact could obscure the precise location or nature of the abnormality.

Over the years, there has been considerable controversy regarding the safety scanning patients with breast tissue expanders with magnetic ports (47, 55, 58, 92-97). During a period of more than three decades, only two cases reported problems associated with tissue expanders for patients that underwent MRI (96, 97), while a study conducted in a large series of patients where special precautions were taken to mitigate risks revealed no substantial issues (95).

Performing MRI in Patients with Tissue Expanders with Magnetic Ports. For certain indications that include neurological, musculoskeletal, or cardiovascular diagnoses, MRI is the superior diagnostic imaging modality. Considering the preponderance of evidence that exists for tissue expanders with magnetic ports, Dibbs, et al. (55) recommended that it was time to reconsider whether these implants should truly be considered “MR Unsafe” and, thus, a strict contraindication for an admittedly vital diagnostic imaging procedure.

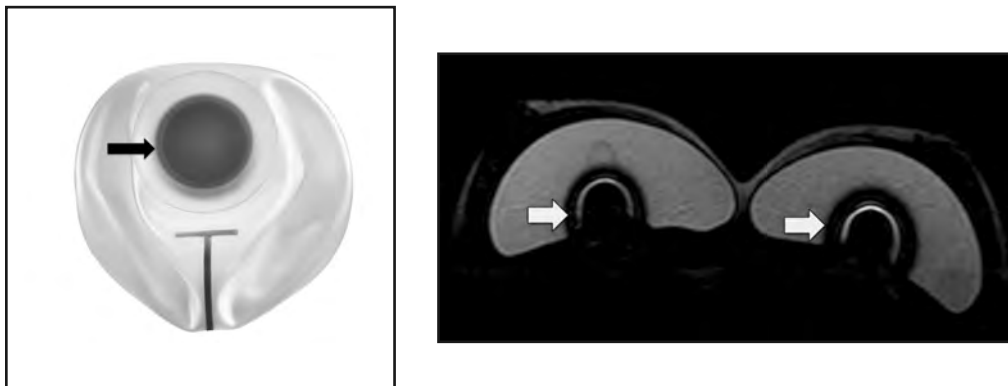
As part of the practice of medicine, MRI-trained radiologists may elect to override the labeling for implants, even if they are labeled MR Unsafe, by conducting a careful risk versus benefit analysis for individual cases. Therefore, in the event that a patient with a breast tissue expander with a magnetic port needs to undergo MRI for proper clinical management, the following procedural guidelines were proposed taking into consideration the clinical experience reported by Thimmappa, et al. (95) as well as additional, suitable precautions to prevent possible risks (55, 92, 93):

- (1) The supervising physician (i.e., usually the MRI-trained radiologist) must perform an assessment of the risks associated with the implant versus the benefit of the MRI exam. The theoretical risks or other possible problems include movement of the magnetic port component of the implant, potential MRI-related heating, possible polarity reversal of the magnet, and artifacts in the immediate area of the port (55). Notably, there is considerable evidence that MRI-related heating is a non-issue for breast implants with magnetic ports (55, 92, 93, 98), including a comprehensive study conducted by scientists from the FDA (94). Polarity reversal of the magnet rarely occurs and artifacts may be decreased by careful selection of pulse sequence parameters.
- (2) A physician must provide written and verbal informed consent to the patient, explaining the aforementioned possible problems.
- (3) The MRI exam should be performed using a scanner that does not exceed a static magnetic field strength of 1.5-Tesla.
- (4) The tissue expander with magnetic port should be stabilized by securely wrapping the area with an elastic compression wrap or by other suitable means (e.g., 6” Ace Bandage, elastic chest/rib belt, etc.).
- (5) If practical, the patient should be placed in a prone position to minimize or prevent movement of the magnetic port of the tissue expander.
- (6) The patient should be continuously monitored visually and verbally throughout MRI. If the patient reports any unusual sensation, immediately discontinue the MRI exam.

Breast Tissue Expander with an RFID Port. A new breast tissue expander was recently developed with a port that incorporates a radiofrequency identification device (RFID) that is used for needle localization for implant expansion. Bayasgalan, et al. (58) described the MRI testing conducted on this implant that resulted in it being designated MR Conditional at 1.5- and 3-Tesla. The relatively small artifact size associated with this tissue expander, which predominantly comes from the RFID, offers potential advantages for patients undergoing MRI compared to tissue expanders that have magnetic ports that create substantial signal losses and distortions on MR images (**Figure 3**).

476 MRI-Related Issues for Implants and Devices

Figure 3. (left) Breast tissue expander with RFID (black arrow). (right) MRI of the breasts in a patient with bilateral breast tissue expanders with RFID ports (white arrows). On this MR image obtained using a “silicone-only” pulse sequence, note the relatively small artifacts associated with the RFIDs and the fact that the artifact does not extend into the breast tissue. This breast tissue expander potentially offers advantages over tissue expanders that have magnetic ports that create substantial signal loss and distortion on MR images.



Coronary Artery Stents

MRI testing has been performed on the majority of the commercially available bare metal and drug eluting coronary artery stents. These tests included assessments of magnetic field interactions, heating, and the characterization of artifacts. The findings resulted in MRI labeling that indicates that patients may undergo MRI exams at 1.5- or 3-Tesla immediately after implantation of the coronary artery stents.

The standard policy that MRI labeling information is required to be reviewed before allowing scans in patients with coronary artery stents limits access to this essential diagnostic modality when labeling is unavailable. It should be noted that there has never been an adverse event reported in association with performing MRI in a patient with a coronary artery stent. Therefore, in consideration of the relevant peer-reviewed literature and other related documents (1, 2, 98-105), guidelines were developed indicating that it is acceptable to perform MRI exams in patients with all commercially available coronary artery stents, including patients with multiple coronary stents, by following specific guidelines. These guidelines were created by taking into consideration possible safety concerns, that is, magnetic field interactions and MRI-related heating for these implants. By following these admittedly conservative MRI conditions, every patient with a coronary artery stent can benefit from the diagnostic imaging information afforded by MRI (**Table 4**). Notably, the previous belief that it may be necessary to wait six weeks or longer after implantation of certain coronary artery stents to allow for endothelialization or other mechanism to prevent migration has been refuted because there are no coronary artery stents made from ferromagnetic materials (82, 98-105).

Table 4. Guidelines for the management of patients with coronary artery stents referred for MRI examinations.

The following guidelines apply to using MRI in patients with coronary artery stents (including patients with two or more stents or two or more overlapping stents):

- (1) Patients with all commercially available coronary artery stents (including drug-eluting and non-drug eluting or bare metal versions) can be scanned at 1.5-Tesla/64-MHz or 3-T/128-MHz, regardless of the value of the spatial gradient magnetic field.
- (2) Patients with all commercially available coronary artery stents can undergo MRI immediately after placement of these implants.
- (3) The MRI examination must be performed using the following parameters:
 - 1.5-Tesla or 3-Tesla, only
 - Whole body averaged specific absorption rate (SAR) of 2-W/kg (i.e., operating in the Normal Operating Mode for the MR system)
 - Maximum imaging time, 15 minutes per pulse sequence (multiple pulse sequences per patient are allowed)

Important Notes:

- This information does not apply to other stents such as peripheral vascular stents, abdominal aortic aneurysm (AAA) stent grafts, biliary stents, ureteral stents, or stents used for other applications (e.g., tracheobronchial stents, esophageal stents, etc.).
- Any deviation from the above MRI conditions requires prior approval by the Radiologist or supervising physician.
- These guidelines must be reviewed on an annual basis to confirm that no new coronary artery stent has become available that substantially deviates from the above MRI conditions or that is labeled, MR Unsafe.
- These guidelines should only be implemented for use after careful review by the supervising radiologist or other physician responsible for the MRI facility and with the adoption of the information as a written policy.

Figure 4. The continuous glucose monitor, CGM, Dexcom G6 (Dexcom, www.dexcom.com). This example shows the CGM attached by an adhesive disc to the individual's arm. The sensor in the CGM measures the individual's blood glucose level and can wirelessly transmit the information to a smart phone or other hand-held device.

478 MRI-Related Issues for Implants and Devices

Continuous Glucose Monitor

A continuous glucose monitor (CGM) is used to monitor blood glucose on a continual basis in individuals with insulin-dependent diabetes. A CGM uses a small needle-based sensor that is inserted subcutaneously and attached via an adhesive disc to the arm or abdomen (**Figure 4**). The CGM's sensor measures the individual's blood glucose level and can wirelessly transmit the information to a smart phone or other hand-held device. Because CGMs permit individuals to avoid needle sticks to determine their blood glucose level, these devices are extremely popular among diabetics.

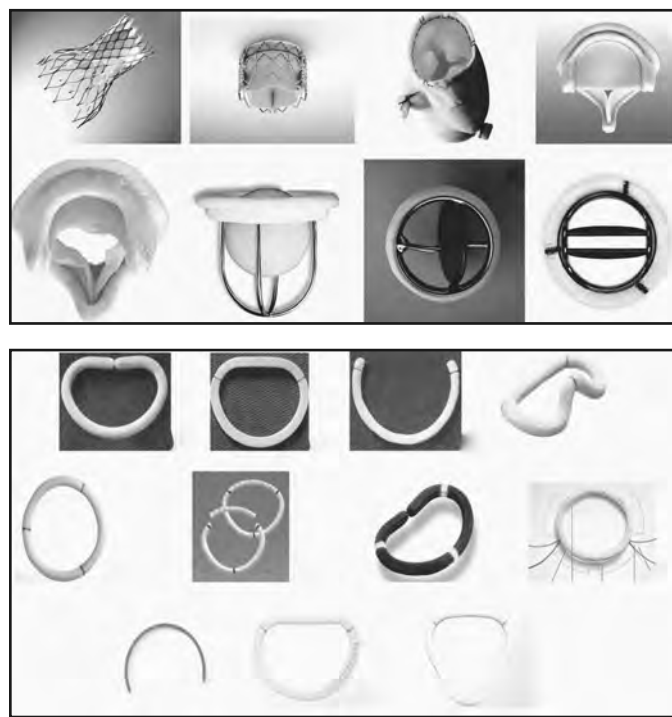
The most popular CGMs include the Dexcom G4 and Dexcom G6 (Dexcom, www.dexcom.com), the FreeStyle Libre products (Abbott, www.abbott.com), and the Guardian Connect (Medtronic, Inc., www.medtronic.com). Each of these CGMs is labeled MR Unsafe, requiring removal from the patient prior to permitting the individual to undergo an MRI exam.

Presently, there is one CGM that is labeled MR Conditional. This device is the Eversense CGM System (Ascensia Diabetes Care, www.eversensediabetes.com). This CGM has an implanted sensor and an external transmitter, which makes its design entirely different from the other CGMs. The MR Conditional labeling states that the external transmitter must be removed from the patient prior to MRI. MRI may be performed in patients at 1.5- or 3-Tesla, using a maximum spatial field gradient magnetic field of 2,000 gauss/cm, and a maximum MR system reported, whole body averaged specific absorption rate (SAR) of 4-W/kg (First Level Controlled Operating Mode) for 15 minutes of scanning per pulse sequence.

Heart Valve Prostheses and Annuloplasty Rings

In the clinical magnetic resonance imaging (MRI) setting, it is often necessary to manage patients with heart valve prostheses [including transcatheter aortic valve replacements (TAVR), transcatheter aortic valve implantation (TAVI) devices, percutaneous aortic valve replacement (PAVR) implants, transcatheter heart valves (THV), as well as other similar heart valve implants used in association with minimally invasive procedures] and annuloplasty rings (**Figure 5**). A large variety of heart valve prostheses and annuloplasty rings have been evaluated for MRI-related issues, especially with regard to the presence of magnetic field interactions and heating associated with exposure to clinical MR systems operating at field strengths of as high as 7-Tesla. Of these, certain ones exhibited measurable yet relatively minor magnetic field interactions. Because the actual attractive forces exerted on heart valve prostheses and annuloplasty rings are minimal compared to the force exerted by the beating heart (i.e., approximately 7.2-N), MRI will not pose a risk to patients with these implants. Furthermore, MRI-related heating has been reported to be relatively minor for all heart valve prostheses and annuloplasty rings that have undergone testing (1, 2, 82, 90, 103, 106-116).

Similar to the routine management of patients with coronary artery stents, the standard policy that MRI labeling information is required to be reviewed before allowing scans in patients with heart valve prostheses and annuloplasty rings limits access to this essential diagnostic modality when labeling is unavailable. Importantly, there has never been an adverse event reported in association with performing MRI in a patient with a heart valve

Figure 5. Examples of (top) heart valve prostheses and (bottom) annuloplasty rings.

prosthesis or annuloplasty ring. Therefore, in consideration of the relevant peer-reviewed literature and other related documents (1, 2, 82, 90, 103, 106-116), guidelines were developed indicating that it is acceptable to perform MRI exams in patients with all commercially available heart valve prostheses and annuloplasty rings by following specific guidelines. These guidelines were created by taking into consideration possible safety concerns, that is, magnetic field interactions and MRI-related heating for these implants. By following these admittedly conservative MRI conditions, every patient with a heart valve prosthesis or annuloplasty ring can benefit from the diagnostic imaging information afforded by MRI (**Table 5**).

Intrauterine Devices

An intrauterine device (IUD) is a relatively small implant that is placed inside the uterus to prevent pregnancy. IUDs may be made from nonmetallic materials (e.g., plastic or polyethylene) or a combination of nonmetallic and metallic materials (117-123) (**Figure 6**). Copper is typically the metal used in an IUD, however, stainless steel or other metals may also be utilized.

The IUDs made from nonmetallic materials are MR Safe. The ones that contain copper are MR Conditional (117-121). Common copper-based IUDs, such as the Copper T and Copper 7 IUD, have a fine copper coil wound around a portion of the implant. Accordingly, an artifact may be seen on MRI, however, the extent of the artifact is relatively small because of the low magnetic susceptibility of copper.

480 MRI-Related Issues for Implants and Devices

Table 5. Guidelines for the management of patients with heart valve prostheses and annuloplasty rings.

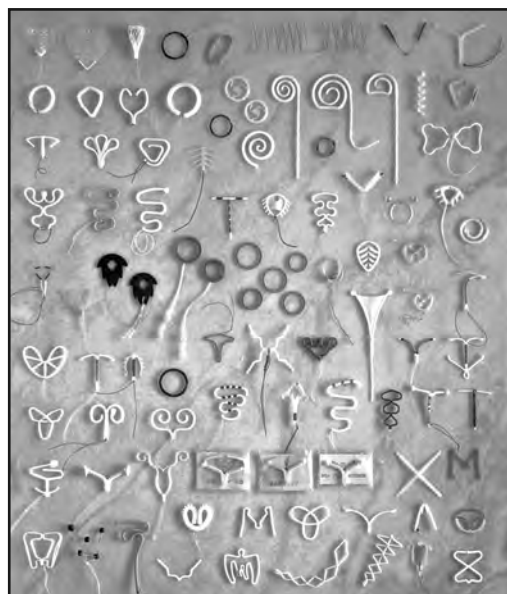
The following guidelines apply to using MRI in patients with heart valve prostheses and annuloplasty rings.

- (1) Patients with all commercially available heart valve prostheses and annuloplasty rings can be scanned at 1.5-Tesla/64-MHz or 3-T/128-MHz, regardless of the value of the spatial gradient magnetic field.
- (2) Patients with all commercially available heart valve prostheses and annuloplasty rings can undergo MRI immediately after placement of these implants.
- (3) The MRI examination must be performed using the following parameters:
 - 1.5-Tesla or 3-Tesla, only
 - Whole body averaged specific absorption rate (SAR) of 2-W/kg (i.e., operating in the Normal Operating Mode for the MR system)
 - Maximum imaging time, 15 minutes per pulse sequence (multiple pulse sequences per patient are allowed)

Important Notes:

- Any deviation from the above MRI conditions requires prior approval by the Radiologist or supervising physician.
- These guidelines must be reviewed on an annual basis to confirm that no new heart valve prosthesis or annuloplasty ring has become available that substantially deviates from the above MRI conditions or that is labeled, MR Unsafe.
- These guidelines should only be implemented for use after careful review by the supervising radiologist or other physician responsible for the MRI facility and with the adoption of the information as a written policy.

Figure 6. (left) Examples of IUDs. IUDs come in a wide variety of shapes and materials. **(right)** IUDs made from stainless steel.



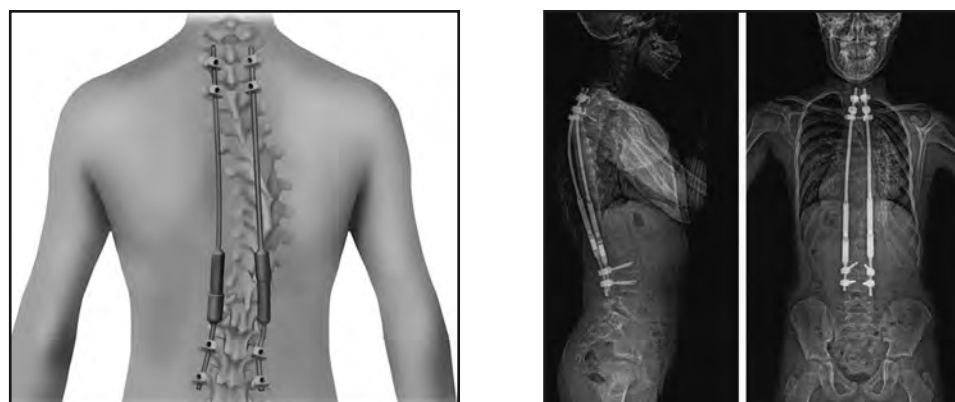
IUDs made from stainless steel may pose a hazard to a patient undergoing MRI depending on the type stainless steel that was used. Stainless steels used for implants, including IUDs, may be either austenitic, which is a nonferromagnetic form, or martensitic which is a ferromagnetic type of stainless steel. At least four different IUDs commonly used in Asia, especially China, are made from stainless steel. Of these, the only one tested to date which displayed high magnetic field interactions was the Chinese Ring (123). The other stainless steel IUDs (the Chinese Double Ring, the Ota Ring, and the Chongqing Uterine-Shaped IUD) have not undergone testing for magnetic field interactions or heating and, thus, should be considered unsafe for patients until information can be obtained to demonstrate that they are MR Conditional.

Magnetically-Activated Orthopedic Implants

Within the domain of orthopedic implants, certain products have magnetically-activated components that permit noninvasive adjustments of their lengths. For example, the Precice and Precice Stryde Systems (Nuvasive, www.nuvasive.com) are adjustable intramedullary rods that can be used for limb lengthening procedures involving the tibia or femur. These devices are lengthened using an external programmer, which eliminates the need for an external fixation system. The Precice System and Precice Stryde System are labeled MR Unsafe.

Another example of a magnetically-activated orthopedic implant is the MAGEC System (Nuvasive, www.nuvasive.com) which utilizes innovative magnetic technology that is incorporated within adjustable growing rods that are modulated by an external controller (**Figure 7**). The MAGEC system is designed to avoid multiple distraction surgeries for the treatment of early-onset scoliosis. As a result, the MAGEC System helps reduce associated complication risks from repetitive surgeries and simplifies the management of patients with early onset scoliosis.

Figure 7. (left) The MAGEC System which uses magnetically-adjustable growing rods that are modulated by an external controller. **(right)** X-rays showing a patient with the MAGEC System. Note the two distraction rods implanted to treat scoliosis in this adolescent patient. The external controller is used to lengthen the rods as the child grows.



482 MRI-Related Issues for Implants and Devices

The MRI safety information for this implant is, as follows:

Non-clinical testing demonstrated that the MAGEC System is MR Conditional. The following conditions must be followed:

A patient with this device can be scanned in an MR system meeting the following conditions:

- Static magnetic field of 1.5-Tesla (1.5-T)
- Maximum spatial field gradient of 3000-gauss/cm (30-T/m)
- Maximum MR system reported, whole-body averaged specific absorption rate (SAR) of 0.5-W/kg per pulse sequence

Under the scan conditions defined above, the MAGEC system is expected to produce a maximum temperature rise of no greater than 3.7° C after 15 minutes of continuous scanning. Additional considerations are listed on the following page.

Caution: The RF heating behavior does not scale with static field strength. Devices that do not exhibit detectable heating at one field strength may exhibit high values of localized heating at another field strength.

- The patient should not be permitted to roll on the table, as this motion may cause unintended lengthening/shortening of the implant.
- The External Remote Controller, Manual Distractor, and Wand Magnet Locator are MR Unsafe. Do not bring them into the MRI scan room.
- In non-clinical testing, the image artifact caused by the MAGEC system extends beyond the imaging field of view when imaged with a gradient-echo pulse sequence in a 1.5-T MR system. However, imaging in locations approximately 20-cm away from the actuator of the MAGEC System may produce images in which anatomical features may be discerned.

Notably, the MAGEC System represents an example of an implant with low SAR requirements insofar as the whole-body averaged SAR is limited to 0.5-W/kg. Adjusting pulse sequence parameters to achieve decreased SAR levels requires essential knowledge regarding which parameters may be suitably adjusted, while maintaining acceptable image quality. For example, increasing the repetition time, decreasing the echo train length, or reducing the phase encoding to lower the SAR can substantially impact image quality, as shown in **Table 6**. In consideration of this, it is often necessary to involve the radiologist whenever

Table 6. Adjusting pulse sequence parameters to lower SAR values.

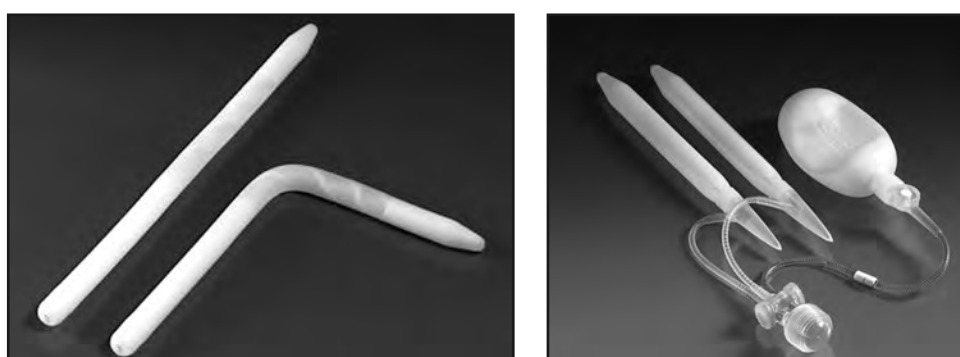
Adjustment	Tradeoff
Increase Repetition Time	Longer Acquisition Time
Decrease Echo Train Length	Longer Acquisition Time
Decrease Flip Angle	Signal-To-Noise and Contrast Changes
Decrease Number of Slices	Loss of Coverage and/or Resolution
Decrease Phase Encodes	Loss of Resolution
No Saturation Bands	Contrast Changes and/or Artifacts
No Fat Suppression	Contrast Changes and/or Artifacts
Change the transmit RF coil	Loss of Coverage and/or Uniformity

decreasing SAR values to make sure that the diagnostic aspects of the MRI exam will not be compromised.

Penile Implants

Various penile implants have been evaluated for MRI-related issues (1, 2, 125, 126) (**Figure 8**). Of these, two (i.e., the Duraphase and Omniphase models) demonstrated substantial ferromagnetic qualities when exposed to a 1.5- and 3-Tesla MR systems (1, 2, 125, 126). Fortunately, it is unlikely for a penile implant to cause an injury in a patient undergoing MRI because of magnetic field interactions. This is because of the manner in which such a device is utilized. With regard to scanning a patient with a penile implant made from ferromagnetic material, to avoid discomfort it is advisable to stabilize the implant by a suitable means such as an elastic bandage and to consider scanning the patient in a prone position. Findings for other penile implants reported that they either exhibited no translational attraction and torque, or relatively minor magnetic field interactions. To date, MRI-related heating has not been demonstrated to be substantial for any penile implant that has undergone testing.

Figure 8. Examples of penile implants. (**left**) Malleable penile implant. (**right**) Inflatable penile implant. For the inflatable implant, the pump and valve components are implanted in the patient's scrotum, while the fluid reservoir is implanted under the abdominal wall.



Vascular Access Ports

Vascular access ports are implants commonly used to provide long-term vascular administration of chemotherapeutic agents, antibiotics, analgesics, and other medications. A vascular access port is usually implanted in a subcutaneous pocket under the upper chest wall (i.e., subclavicular area) with the catheters inserted in the jugular, subclavian, or cephalic vein (**Figure 9**). These implants have a variety of similar features that include a reservoir, central septum, and catheters and may be constructed from different materials including stainless steel, titanium, silicone, and plastic. Because of the widespread use of vascular access ports and the high probability that patients with these devices may require MRI examinations, it has been important to characterize the MRI-related issues for these implants (1, 2, 31, 32, 127-129),

484 MRI-Related Issues for Implants and Devices

Figure 9. (left) Vascular access port implanted in a subclavicular position with its catheter inserted into the subclavian vein. **(right)** Examples of vascular access ports. These implants may be made from both metallic and nonmetallic materials.



Thus, over the years, MRI testing has been performed on the many commercially available vascular access ports (1, 2, 31, 32, 127-129). These tests included evaluations of magnetic field interactions, heating, and the characterization of artifacts. The findings resulted in MRI labeling that indicates that patients may undergo MRI exams at 1.5- or 3-Tesla immediately after implantation of the vascular access ports (1, 2, 31, 32, 127-129).

Similar to the information presented for coronary artery stents, heart valve prostheses, and annuloplasty rings, the standard policy that MRI labeling information is required to be reviewed before allowing scans in patients with vascular access ports limits access to this essential diagnostic modality when labeling is unavailable. It should be noted that there has never been an adverse event reported in association with performing MRI in a patient with a vascular access port. Therefore, in consideration of the relevant peer-reviewed literature and other related documents (1, 2, 31, 32, 127-129), guidelines were developed indicating that it is acceptable to perform MRI exams in patients with all commercially available vascular access ports. These guidelines were created by taking into consideration possible safety concerns, that is, magnetic field interactions and MRI-related heating for these implants. By following these admittedly conservative MRI conditions, every patient with a vascular access port can benefit from the diagnostic imaging information afforded by MRI (**Table 7**).

With respect to MRI and artifacts, vascular access ports that will produce the least amount of artifact are made entirely from nonmetallic materials such as plastic, silicon, Delrin polyethylene, or polyether ether ketone (commonly known as PEEK). The ones that produce the largest artifacts are composed of metals or have metallic components in an unusual shape (e.g., the OmegaPort Access Port). Even vascular access ports made entirely from nonmetallic materials are, in fact, seen on MR images because they contain silicone (i.e., the septum portion of the port). Using MRI, the Larmor precessional frequency of fat is close to that of silicone (i.e., 100-Hz at 1.5-Tesla). Therefore, silicone used in the construction of a vascular access port may be observed on MR images with varying degrees of signal intensity depending on the pulse sequence that is used.

If a radiologist did not know that a vascular access port was present in a patient, the MR signal produced by the silicone component of the implant could misinterpreted as an

Table 7. Guidelines for the management of patients with vascular access ports.

The following guidelines apply to using MRI in patients with vascular access ports.

- (1) Patients with all commercially available vascular access ports can be scanned at 1.5-Tesla/64-MHz or 3-T/128-MHz, regardless of the value of the spatial gradient magnetic field.
- (2) Patients with all commercially available vascular access ports can undergo MRI immediately after placement of these implants.
- (3) The MRI examination must be performed using the following parameters:
 - 1.5-Tesla or 3-Tesla, only
 - Whole body averaged specific absorption rate (SAR) of 2-W/kg (i.e., operating in the Normal Operating Mode for the MR system)
 - Maximum imaging time, 15 minutes per pulse sequence (multiple pulse sequences per patient are allowed)

Important Notes:

- Any deviation from the above MRI conditions requires prior approval by the Radiologist or supervising physician.
- These guidelines must be reviewed on an annual basis to confirm that no vascular access port has become available that substantially deviates from the above MRI conditions or that is labeled, MR Unsafe.
- These guidelines should only be implemented for use after careful review by the supervising radiologist or other physician responsible for the MRI facility and with the adoption of the information as a written policy.

abnormality, or at the very least, present a confusing image. For example, this may cause a diagnostic problem in a patient evaluated for a rupture of a silicone breast implant, because silicone from the vascular access port may be misread as an extracapsular silicone implant rupture.

7-TESLA MRI: INFORMATION FOR IMPLANTS AND DEVICES

The highest field strength MR system approved for clinical use is the 7-Tesla scanner. The unique research and clinical applications afforded by 7-Tesla MRI are predominantly due to the associated increase in the signal-to-noise ratio that can be exploited to achieve higher resolution images (4, 130-132). In addition, imaging at this ultra-high-field (UHF) enables the improved detection of functional and metabolic (i.e., using MR spectroscopy) abnormalities compared with lower-field-strength MR scanners (4, 130-132). Importantly, the UHF MR system presents unique safety issues, especially with respect to scanning patients with implants and devices (4, 130-132)(Figure 10). If 7-Tesla MRI is to reach its full potential as an imaging modality, scanning must become available to research subjects and patients with metallic implants.

486 MRI-Related Issues for Implants and Devices

Figure 10. 7-Tesla MR system (General Electric Healthcare, www.gehealthcare.com).



Magnetic Field Interactions

As previously described in this chapter, attractive translational and rotational forces acting on metallic objects, including medical implants and devices, depend on a myriad of factors including the composition of the material and its shape (1, 2, 4, 130-132). Translational forces are highly dependent on the field strength and the spatial gradient magnetic field, while rotational forces are directly proportional to the strength of the static magnetic field (1, 2, 4, 130-132). Of note is that, in comparison to a 3-Tesla MR system, a scanner operating at 7-Tesla has a fringe field that changes faster as a function of distance from the static magnetic field. That is, the fringe field has a “steeper” spatial gradient magnetic field. Because both the static magnetic and spatial gradient magnetic fields are greater at 7-Tesla than those at lower fields, translational attraction forces affect implants to a greater extent, which may pose higher risks for certain devices (4, 130-132).

MRI-Related Heating

The hydrogen proton resonance frequency at 7-Tesla is approximately 298-MHz and, therefore, the corresponding RF wavelength in tissue is substantially less than what exists at 64-MHz (i.e., for 1.5-Tesla) or 128-MHz (i.e., for 3-Tesla). This results in the potential to heat shorter metallic implants and cause thermal injuries at 7-Tesla compared to what might occur at 1.5- or 3-Tesla (4, 130-132). Importantly, MRI-related heating at 7-Tesla may be of considerable concern when utilizing “stronger” RF pulses (e.g., fast spin echo pulse sequences) because temperature has been demonstrated to increase with the square of the transmitted pulse power (133).

7-Tesla: Implants and Devices

To date, several hundred metallic implants and devices have been tested at 7-Tesla, which is a only a fraction of the more than 15,000 metallic items that have been tested at

1.5- and/or 3-Tesla (1, 2, 134-144). Only a small number of medical products have undergone proper testing and labeled with MRI-specific information (i.e., labeled MR Safe or MR Conditional). Test methods developed to assess translational attraction, torque, and RF field-induced heating at 1.5- and 3-Tesla have been adapted to test medical products at 7-Tesla. With regard to the heating test, this procedure was designed for a transmit body RF coil, however, at the present time, only transmit/receive head and knee RF coils exist for the 7-Tesla scanners approved for clinical use. Accordingly, the test procedure applied to implants had to be modified in consideration of the available RF coils. Once a transmit body RF coil becomes available for 7-T MR systems, re-testing will be necessary.

Untested Passive Implants. In 2019, Barisano, et al. (144) described a case involving 7-Tesla MRI of the brain in a subject with untested and unlabeled, total knee replacement implants. Because these orthopedic implants were made of materials that were nonmetallic or had low magnetic susceptibilities and were implanted in an anatomic area far removed from the transmitted RF energy (i.e., a transmit/receive head RF coil was used for imaging), there were no deleterious effects anticipated for the scan. The subject had an uneventful outcome. The investigators proposed that, by following a similar strategy that takes into consideration the materials for a given implant and the anatomic area receiving the transmitted RF energy, 7-Tesla MRI may be used safely in situations where there is an untested implant (144). Note that this information applies to passive implants, only.

Guidelines presented by Barisano, et al. (144) to manage patients or research subjects with untested implants were, as follows:

- (1) The supervising physician (e.g., the MRI-trained radiologist) must perform an assessment of the risks associated with the implant versus the benefits of the MRI exam.
- (2) Because of the lack of MRI-related testing for the implant, a physician must provide written and verbal informed consent to the individual and include a discussion of the potential benefits, risks, and alternative imaging procedure that may be appropriate.
- (3) The material used to make the implant must be identified in order to establish if there may be issues with respect to magnetic field interactions and heating. Typically, material information can be obtained by contacting the manufacturer. Some common low magnetic susceptibility, metallic materials that are used for implants include cobalt-chromium-molybdenum alloy, nitinol, austenitic stainless steel (e.g., 316L, 316LVM, etc.), platinum, platinum-iridium, titanium-aluminum-vanadium alloy, tantalum, commercially pure titanium, and titanium alloy.
- (4) Since all metals are conductors, the position of the implant relative to the transmitted RF energy must be considered with respect to the potential for excessive heating. Thus, to ensure minimal risk, the entire implant must be located outside of the RF coil and a suitable distance from the area of the transmitted RF energy. (Note, in consideration of the possibility of “traveling-wave” effects, a minimum distance of 30-cm is deemed acceptable. See section below.) As previously indicated, the 7-Tesla MR systems approved for clinical use currently have transmit/receive head and knee RF coils, only. As such, a relatively straightforward decision may be made with respect to possible hazards related to excessive implant heating for this scanner configuration. Once a transmit body or other transmit body part-specific RF coils becomes available, the prediction of implant heating will become a greater challenge.

488 MRI-Related Issues for Implants and Devices

- (5) Continuously monitor the individual visually and verbally throughout the MRI exam. If the individual reports any unusual sensation, the scan must be immediately discontinued.

Kraff and Quick (131) summarized additional information regarding scanning patients at 7-Tesla with untested passive implants, recognizing that because of the lack of tested and labeled implants, both research and clinical uses of 7-Tesla MRI may be limited because of the exclusion of individuals with metallic implants. They proposed that by using a well-considered, risk versus benefit analysis, the already known advantages of 7-Tesla MRI in neurological and musculoskeletal diagnostic imaging should not be denied to patients despite the presence of passive implants, particularly for those implants labeled MR Conditional at 3-Tesla (131).

In 2016, the national network German Ultrahigh Field Imaging (GUFI) published a consensus recommendation on the inclusion of study subjects imaged at 7-Tesla (145). The recommendation stated that the use of local transmit/receive RF coils (i.e., head and knee) has the advantage that the transmit RF exposure volume is considerably lower compared to the large exposure volume of transmit body RF coils that are on 1.5- and 3-Tesla scanners. As a result, the RF power density that exists outside of local transmit RF coils decreases rapidly. Therefore, for individuals with passive implants that are labeled MR Conditional at 3-Tesla, that do not contain magnetizable components, and that are located at a certain distance from the transmit RF coil, an overly conservative exclusion of individuals with implants would no longer be warranted, as previously required by many ethics committees.

Of note is that the minimum distance between the implant and the local transmit RF coil depends on both components and, thus, must always be considered on a case-by-case basis. At 7-Tesla, the phenomenon of the “traveling wave” effect (146) (Note, the traveling wave effect suggests that there is a possibility that the bore of the scanner can act as a hollow circular waveguide for traveling waves that could interact with an implant outside of the area of the transmitted RF) needs to be taken into account, primarily for implants that have a complex geometry or that form a conducting loop of a certain diameter, and/or with dimensions of integral multiples of half a wavelength, or in cases for partially implanted metallic objects (131, 145). Accordingly, to ensure patient safety, the minimum allowable distance between the edge of the transmit RF coil and the implant should be 30 cm. While this value has not been determined by numerical simulations of various exposure scenarios, it does represent a conservative guideline for passive implants in association with scanning at 7-Tesla. (131).

Untested Active Implants. As previously discussed, an active implant contains electrical circuits and/or a power supply. Presently, no active implant has been tested and labeled MR Conditional at 7-Tesla. The potential safety risks are considered to be extremely high and related to excessive magnetic field interactions, RF field-induced heating, induced currents, device malfunction, and other MRI-related issues.

GUIDELINES FOR THE MANAGEMENT OF THE POST-OPERATIVE PATIENT

There is often confusion regarding the issue of performing an MRI examination during the post-operative period in a patient with a metallic implant or device. Studies have sup-

ported that, if the metallic object is a “passive implant” and it is made from nonferromagnetic material, the patient may undergo an MRI exam *immediately* after implantation using an MR system operating at 3-Tesla or less (1, 2). In fact, there are reports that describe placement of vascular stents, coils, filters, and other metallic implants using MR-guided procedures that include the use of high-field-strength (1.5- and 3-Tesla) scanners (1, 147, 148). Additionally, a patient or individual with a nonferromagnetic, passive implant is allowed to enter the MRI environment associated with a scanner operating at 3-Tesla or less immediately after the implantation of the device.

Importantly, for a passive implant that does not state a “wait” period in the *Instructions for Use* (IFU) or MRI-related labeling, there is no need to delay the MRI examination for the patient. For patients with implants that are “weakly magnetic” but rigidly fixed or otherwise anchored in the body (e.g., orthopedic implants or other similar devices), these individuals may undergo MRI immediately after implantation of the device.

For an implant or device that exhibits ferromagnetic qualities, it may be necessary to wait a period of six weeks after implantation before performing MRI. For example, certain intravascular and intracavitary coils, stents, and filters designated as “magnetic” become firmly incorporated into tissue a minimum of six weeks following placement. In these cases, retentive or counter-forces provided by tissue ingrowth, scarring, granulation, or other mechanisms serve to prevent these objects from presenting risks or hazards to patients or individuals with respect to movement or dislodgement associated with magnetic field interactions (i.e., force and torque).

Of course, the information above pertains to magnetic field interactions (i.e., force and torque) and further consideration must be given to MRI-related heating for the implant or device.

If there is any concern regarding the integrity of the tissue with respect to its ability to retain the implant or object in place or the implant cannot be properly identified, the patient or individual should not be exposed to the MRI environment unless a radiologist gives careful consideration to the risk versus benefit aspects of the specific implant and the intended MRI conditions.

MANAGING PATIENTS WITH UNLABELED IMPLANTS

In the event that a patient referred for an MRI exam has a *passive implant* that does not have MRI labeling, the supervising physician may elect to clear the patient for MRI after a careful consideration of the risks versus the benefit, with attention to the factors that potentially pose a hazard for the particular implant (1, 4-12). These factors include magnetic field interactions (i.e, force and torque), MRI-related heating, and if the implant has a functional component, such as a programmable cerebral spinal fluid shunt valve, the impact of MRI on the operational aspects of the device must also be considered. It should be duly noted that the above information specifically pertains to scanning patients with *passive implants* and not to active implants because the inherent risks of AIMDs are particularly complicated and challenging to assess. Muhlenweg, et al. (11) and Kanal (12) provide thoughtfully de-

490 MRI-Related Issues for Implants and Devices

signed strategies to follow when considering various aspects of the MRI-related risks associated with passive implants.

CONCLUSIONS

This chapter provided an overview of MRI-related issues for implants and devices and presented MRI-related information for several passive medical products. Comprehensive information for active implants is presented elsewhere in this textbook. With the continued advances in MRI technology and the development of more sophisticated implants and devices, there is an increased potential for hazardous situations to occur in the MRI environment. To ensure safety for individual and patients, MRI healthcare professionals should follow the guideline whereby an MRI examination should only be performed in a patient with a medical product that has been previously tested and demonstrated to be safe. For implants and devices with MR Conditional labeling, the specific information must be carefully followed to prevent patient injuries.

REFERENCES

1. Shellock FG. Reference Manual for Magnetic Resonance Safety: 2020 Edition. Los Angeles: Biomedical Research Publishing Group; 2020.
2. www.MRIsafety.com, Accessed August, 2021.
3. Schenck JF. Safety of strong, static magnetic fields. *J Magn Reson Imaging* 2000;12:2-19.
4. ACR Manual on MR Safety. American College of Radiology 2020. Available via www.ACR.org. Accessed August, 2021.
5. ACR Committee on MR Safety: Greenberg TD, Hoff MN, Gilk TB, et al. ACR guidance document on MR safe practices: Updates. *J Magn Reson Imaging* 2020;51:331-338.
6. Shellock FG, Crues JV. MR procedures: Biologic effects, safety, and patient care. *Radiology* 2004;232:635-652.
7. Shellock FG, Spinazzi A. MRI safety update 2008: Part 2, screening patients for MRI. *AJR Am J Roentgenol* 2008;191:1140-9.
8. Panych LP, Madore B. The physics of MRI safety. *J Magn Reson Imaging* 2018;47:28-43.
9. Watson RE Jr, Edmonson HA. MR safety: Active implanted medical devices. *Magn Reson Imaging Clin N Am* 2020;28:549-558.
10. Stafford RJ. The physics of magnetic resonance imaging safety. *Magn Reson Imaging Clin N Am* 2020;28:517-536.
11. Muhlenweg M, Schaefers G, Trattnig S. Physical interactions in MRI: Some rules of thumb for their reduction. *Radiologe* 2015;55:638-648.
12. Kanal E. Standardized approaches to MR safety assessment of patients with implanted devices. *Magn Reson Imaging Clin N Am* 2020;28:537-548.
13. Davis P, Crooks L, Arakawa M, et al. Potential hazards in NMR imaging: Heating effects of changing magnetic fields and RF fields on small metallic implants. *Am J Roentgenol* 1981;137:857-860.
14. Winter L, Seifert F, Zilberti L, Murbach M, Ittermann B. MRI-related heating of implants and devices: A review. *J Magn Reson Imaging* 2021;53:1646-1665.
15. Nyenhuis JA, Sung-Min Park, Kamondetdacha R, et al. MRI and implanted medical devices: Basic interactions with an emphasis on heating. *IEEE Trans Device Mater Reliab* 2005;5:467-480.

MRI Bioeffects, Safety, and Patient Management 491

16. Bruhl R, Ihlenfeld A, Ittermann B. Gradient heating of bulk metallic implants can be a safety concern in MRI. *Magn Reson Med* 2017;77:1739–1740.
17. Schenck JF. The role of magnetic susceptibility in magnetic resonance imaging: MRI magnetic compatibility of the first and second kinds. *Med Phys* 1996;23:815–50.
18. Jungmann PM, Agten CA, Pfirrmann WF, et al. Advances in MR around metal. *J Magn Reson Imaging* 2017;46:972–991.
19. Lee EM, Ibrahim EH, Dudek N, et al. Improving image quality in patients with metallic implants. *Radiographics* 2021;41:E126–E137.
20. Delfino JG, Woods TO. New developments in standards for MRI safety testing of medical devices. *Current Radiology Reports* 2016;4:1–9.
21. U.S. Food and Drug Administration. Testing and Labeling Medical Devices for Safety in the Magnetic Resonance (MR) Environment. Guidance for Industry and Food and Drug Administration Staff, 2021. <https://www.fda.gov/regulatory-information/search-fda-guidance-documents/testing-and-labeling-medical-devices-safety-magnetic-resonance-mr-environment>. Accessed August, 2021.
22. International Organization for Standardization, Technical Standard, ISO/TS 10974:2018. Assessment of the safety of magnetic resonance imaging for patients with an active implantable medical device. International Organization for Standardization, 2018.
23. New PFJ, Rosen BR, Brady TJ, et al. Potential hazards and artifacts of ferromagnetic and nonferromagnetic surgical and dental materials and devices in nuclear magnetic resonance imaging. *Radiology* 1983;147:139–148.
24. Shellock FG, Crues JV. High-field MR imaging of metallic biomedical implants: An *ex vivo* evaluation of deflection forces. *AJR Am J Roentgenol* 1988;151:389–392.
25. Shellock FG. MR imaging of metallic implants and materials: A compilation of the literature. *AJR Am J Roentgenol* 1988;151: 811–814.
26. Shellock FG, Morisoli S, Kanal E. MR procedures and biomedical implants, materials, and devices: Update 1993. *Radiology* 1993;189:587–599.
27. Kanal E, Shellock FG. MR imaging of patients with intracranial aneurysm clips. *Radiology* 1993;187:612–614.
28. Kanal E, Shellock FG. Aneurysm clips: Effects of long-term and multiple exposures to a 1.5 Tesla MR system. *Radiology* 1999;210:563–5659.
29. Kangarlu A, Shellock FG. Aneurysm clips: Evaluation of magnetic field interactions with an 8.0-T MR system. *J Magn Reson Imaging* 2000;12:107–111.
30. Shellock FG, Tkach JA, Ruggieri PM, et al. Aneurysm clips: Evaluation of magnetic field interactions using “long-bore” and “short-bore” 3.0-Tesla MR systems. *AJNR Am J Neuroradiol* 2003;24:463–471.
31. Shellock FG. Biomedical implants and devices: Assessment of magnetic field interactions with a 3.0-Tesla MR system. *J Magn Reson Imaging* 2002;16:721–732.
32. Shellock FG. MR safety update 2002: Implants and devices. *J Magn Reson Imaging* 2002;16:485–496.
33. Shellock FG, Valencerina S. *In vitro* evaluation of MR imaging issues at 3T for aneurysm clips made from MP35N: Findings and information applied to 155 additional aneurysm clips. *AJNR Am J Neuroradiol* 2010;31:615–9.
34. Shellock FG, Schatz CJ. High field strength MRI and otologic implants. *AJNR Am J Neuroradiol* 1991;12:279–281.
35. Nogueira M, Shellock FG. Otologic biimplants: *Ex vivo* assessment of ferromagnetism and artifacts at 1.5 Tesla. *AJR Am J Roentgenol* 1995;163:1472–1473.
36. Shellock FG, Meepos LN, Stapleton MR, Valencerina S. *In vitro* magnetic resonance imaging evaluation of ossicular implants at 3 T. *Otol Neurotol* 2012;33:871–7.
37. Azadarmaki R, Tubbs R, Chen DA, Shellock FG. MRI information for commonly used otologic implants: Review and update. *Otolaryngology Head Neck Surg* 2014;150:512–519.

492 MRI-Related Issues for Implants and Devices

38. Shellock FG, Habibi R, Knebel J. Programmable CSF shunt valve: *In vitro* assessment of MR imaging safety at 3T. AJNR Am J Neuroradiol 2006;27:661-5.
39. Shellock FG, Wilson SF, Mauge CP. Magnetically programmable shunt valve: MRI at 3-Tesla. Magn Reson Imaging 2007;25:1116-21.
40. Shellock FG, Bedwinek A, Oliver-Allen M, Wilson SF. Assessment of MRI issues for a 3-T “immune” programmable CSF shunt valve. AJR Am J Roentgenol 2011;197:202-7.
41. Gill A, Shellock FG. Assessment of MRI issues at 3-Tesla for metallic surgical implants: Findings applied to 61 additional skin closure staples and vessel ligation clips. J Cardiovasc Magn Reson 2012;14:1-7.
42. Karacozoff AM, Shellock FG, Wakhloo AK. A next-generation, flow-diverting implant used to treat brain aneurysms: *In vitro* evaluation of magnetic field interactions, heating and artifacts at 3-T. Magn Reson Imaging 2013;31:145-9.
43. Escher KB, Shellock FG. An *in vitro* assessment of MRI issues at 3-Tesla for antimicrobial, silver-containing wound dressings. Ostomy Wound Manage 2012;58:22-7.
44. Shellock FG, Knebel J, Prat AD. Evaluation of MRI issues for a new neurological implant, the Sensor Reservoir. Magn Reson Imaging 2013;31:1245-50.
45. Karacozoff AM, Shellock FG. *In vitro* assessment of a fiducial marker for lung lesions: MRI issues at 3 T. AJR Am J Roentgenol 2013;200:1234-7.
46. Shellock FG, Giangarra CJ. Assessment of 3-Tesla MRI issues for a bioabsorbable, coronary artery scaffold with metallic markers. Magn Reson Imaging 2014;32:163-167.
47. Linnemeyer H, Shellock FG, Ahn CY. *In vitro* assessment of MRI issues at 3-Tesla for a breast tissue expander with a remote port. Magn Reson Imaging 2014;32:297-402.
48. Titterington B, Puschmann C, Shellock FG. A new vascular coupling device: Assessment of MRI issues at 3-Tesla. Magn Reson Imaging 2014;32:582-589.
49. Shellock FG, Audet-Griffin A. Evaluation of magnetic resonance imaging issues for a wirelessly-powered lead used for epidural, spinal cord stimulation. Neuromodulation 2014;17:334-339.
50. Audet-Griffin A, Pakbaz S, Shellock FG. Evaluation of MRI issues for a new, liquid embolic device. J Neurointerventional Surg 2014;6:624-629.
51. Shellock FG, Cronenweth C. Assessment of MRI issues at 3-Tesla for a new metallic tissue marker. International Journal of Breast Cancer 2015;2015:823759.
52. Moghtader D, Hans-Joachim Crawack HJ, Shellock FG. Assessment of MRI issues for a new cerebral spinal fluid shunt, gravity assisted valve (GAV). Magnetic Reson Imaging 2017;44:8-14.
53. Victoria T, Johnson AM, Adzick AS, Hedrick HL, Shellock FG. Evaluation of magnetic resonance imaging safety and imaging issues associated with the occlusion balloon used during Fetoscopic Endoluminal Tracheal Occlusion. Fetal Diagn Ther 2018;44:179-183.
54. Kraai TL, Loch RB, Shellock FG. Assessment of MRI safety issues for steel sutures used for microtia reconstruction. J Plast Reconstr Aesthet Surg 2018;71:1469-1475.
55. Dibbs R, Culo B, Tandon R, St. Hilair H, Shellock FG, Lau FH. Reconsidering the “MR Unsafe” breast tissue expander with magnetic infusion port: A case report and literature review. Arch Plast Surg 2019;46:375-380.
56. Vasquez L, Chen J, Shellock FG. Evaluation of MRI issues for a wirelessly-powered, spinal cord stimulation lead with receiver. AJR Am J Roentgen 2020;214;2:406-412.
57. Thompson RM, Fowler E, Culo B, Shellock FG. MRI safety and imaging artifacts evaluated for a cannulated screw used for guided growth. Magn Reson Imaging 2020;66:219-225.
58. Bayasgalan M, Munhoz AM, Shellock FG. Breast tissue expander with radiofrequency identification (RFID) port: Evaluation of MRI issues. AJR Am J Roentgen 2020;215:159-164.
59. Condon B, Hadley DM. Potential MR hazard to patients with metallic heart valves: The Lenz effect. J Magn Reson Imaging 2000;12:171-176.

MRI Bioeffects, Safety, and Patient Management 493

60. Golestanirad L, Dlala E, Wright JR, et al. Comprehensive analysis of Lenz effect on the artificial heart valves during magnetic resonance imaging. *Progress In Electromagnetics Research* 2012;128:1-17.
61. Edwards MB, et al. *In vitro* assessment of the Lenz effect on heart valve prostheses at 1.5 T. *J Magn Reson Imaging* 2015;41:74-82.
62. Greatbatch W, Miller V, Shellock FG. Magnetic resonance safety testing of a newly-developed, fiber-optic cardiac pacing lead. *J Magn Reson Imaging* 2002;16:97-103.
63. Rezai AR, Finelli D, Nyenhuis JA, et al. Neurostimulator for deep brain stimulation: *Ex vivo* evaluation of MRI-related heating at 1.5-Tesla. *J Magn Reson Imaging* 2002;15:241-250.
64. Sharan A, Rezai AR, Nyenhuis JA, et al. MR safety in patients with implanted deep brain stimulation systems (DBS). *Acta Neurochir* 2003;Suppl. 87:141-145.
65. Park SM, Nyenhuis JA, Smith CD, et al. Gelled vs. nongelled phantom material for measurement of MRI-induced temperature increases with bioimplants. *IEEE Transactions on Magnetics* 2003;39:3367-3371.
66. Martin TE, Coman JA, Shellock FG, et al. Magnetic resonance imaging and cardiac pacemaker safety at 1.5 Tesla. *J Amer Coll Cardiol* 2004;43:1315-1324.
67. Baker KB, Tkach JA, Nyenhuis JA, et al. Evaluation of specific absorption rate as a dosimeter of MRI-related implant heating. *J Magn Reson Imaging* 2004;20:315-320.
68. Shellock FG, Cosendai G, Park S-M, Nyenhuis JA. Implantable microstimulator: Magnetic resonance safety at 1.5-Tesla. *Invest Radiol* 2004;39:591-599.
69. Bhidayasiri R, Bronstein JM, et al. Bilateral neurostimulation systems used for deep brain stimulation: *In vitro* study of MRI-related heating at 1.5-Tesla and implications for clinical imaging of the brain. *Magn Reson Imaging* 2005;23:549-555.
70. Baker KB, Tkach J, Hall JD, et al. Reduction of MRI-related heating in deep brain stimulation leads using a lead management system. *Neurosurgery* 2005;57:392-397.
71. Shellock FG, Begnaud J, Inman DM. VNS Therapy System: *In vitro* evaluation of MRI-related heating and function at 1.5- and 3-Tesla. *Neuromodulation* 2006;9:204-213.
72. Shellock FG, Fischer L, Fieno DS. Cardiac pacemakers and implantable cardioverter defibrillators: *In vitro* evaluation of MRI safety at 1.5-Tesla. *J Cardiovasc Magn Reson* 2007;9:21-31.
73. Korb KS, Shellock FG, Cohen MS, Bystritsky A. Low-intensity focused ultrasound pulsation device used during MRI: Evaluation of MRI-related heating at 3-Tesla/128-MHz. *Neuromodulation* 2014;17:236-41.
74. Weiland JD, Faraji B, Greenberg RJ, Humayun MS, Shellock FG. Assessment of MRI issues for the Argus II retinal prosthesis. *Magn Reson Imaging* 2012;30:382-389.
75. Coffey RJ, Kalin R, Olsen JM. Magnetic resonance imaging conditionally safe neurostimulation leads: Investigation of the maximum safe lead tip temperature. *Neurosurgery* 2014;74:215-25.
76. Arduino A, Zanovello U, Hand J, et al. Heating of hip joint implants in MRI: The combined effect of RF and switched-gradient fields. *Magn Reson Med* 2021;85:3447-3462.
77. Bannan KE, Handler W, Chronik B, Salisbury SP. Heating of metallic rods induced by time-varying gradient fields in MRI. *J Magn Reson Imaging* 2013;38:411-416.
78. Graf H, Steidle G, Schick F. Heating of metallic implants and instruments induced by gradient switching in a 1.5-Tesla whole-body unit. *J Magn Reson Imaging* 2007;26:1328-1333.
79. Henderson J, Tkach J, Phillips M, Baker K, Shellock FG, Rezai A. Permanent neurological deficit related to magnetic resonance imaging in a patient with implanted deep brain stimulation electrodes for Parkinson's disease: Case report. *Neurosurgery* 2005;57:E1063.
80. Rezai AR, Baker K, Tkach J, et al. Is magnetic resonance imaging safe for patients with neurostimulation systems used for deep brain stimulation (DBS)? *Neurosurgery* 2005;57:1056-1062.

494 MRI-Related Issues for Implants and Devices

81. Manker, S. Shellock FG. Chapter 24. MRI Safety and Neuromodulation Systems. In: Krames ES, Peckham Hunter P, Rezai AR, Editors. Neuromodulation, Second Edition. New York: Academic Press/Elsevier; 2018. pp. 315-337.
82. Levine GN, Gomes AS, Arai AE, et al. Safety of magnetic resonance imaging in patients with cardiovascular devices: An American Heart Association Scientific Statement from the Committee on Diagnostic and Interventional Cardiac Catheterization. *Circulation*. 2007;116:2878-2891.
83. Shellock FG, Valencerina S, Fischer L. MRI-related heating of pacemaker at 1.5- and 3-Tesla: Evaluation with and without pulse generator attached to leads. *Circulation* 2005;112;Supplement II:561.
84. American Society for Testing and Materials International. ASTM F2052. Standard test method for measurement of magnetically induced displacement force on passive implants in the magnetic resonance environment. American Society for Testing and Materials International, West Conshohocken, PA.
85. American Society for Testing and Materials (ASTM) International. ASTM F2213-17. Standard test method for measurement of magnetically induced torque on passive implants in the magnetic resonance environment. American Society for Testing and Materials International, West Conshohocken, PA.
86. American Society for Testing and Materials International. ASTM F2182. Test method for Measurement of radio frequency induced heating near passive implants during magnetic resonance imaging. American Society for Testing and Materials International, West Conshohocken, PA.
87. American Society for Testing and Materials International. ASTM F2119. Standard test method for evaluation of MR image artifacts from passive Implants. American Society for Testing and Materials International, West Conshohocken, PA.
88. American Society for Testing and Materials International. ASTM F2503-20. Standard practice for marking medical devices and other items for safety in the magnetic resonance environment. American Society for Testing and Materials International, West Conshohocken, PA.
89. Shellock FG, Woods TO, Crues JV. MR labeling information for implants and devices: Explanation of terminology. *Radiology* 2009;253:26-30.
90. Kanal E, Froelich J, Barkovich AJ, et al. Standardized MR terminology and reporting of implants and devices as recommended by the American College of Radiology Subcommittee on MR Safety. *Radiology* 2015;274:866-870.
91. Woods TO. Standards for medical devices in MRI: Present and future. *J Magn Reson Imaging* 2007;26:1186-1189.
92. Marano AA, Henderson PW, Prince MR, et al. Effect of MRI on breast tissue expanders and recommendations for safe use. *J Plast Reconstr Aesthet Surg* 2017;70:1702-1707.
93. Nava MB, Bertoldi S, Forti M, et al. Effects of the magnetic resonance field on breast tissue expanders. *Aesthetic Plast Surg* 2012;36:901-7.
94. Park BS, Razjouyan A, Angelone LM, et al. RF safety evaluation of a breast tissue expander device for MRI: Numerical simulation and experiment. *IEEE Transactions on Electromagnetic Compatibility* 2017;59:1390-1399.
95. Thimmappa ND, Prince MR, Colen KL, et al. Breast tissue expanders with magnetic ports: Clinical experience at 1.5 T. *Plastic and Reconstructive Surgery* 2016;1171-78.
96. Zegzula HD, Lee WP. Infusion port dislodgement of bilateral breast tissue expanders after MRI. *Ann Plast Surg* 2001;46:46-8.
97. Duffy FJ Jr, May JW Jr. Tissue expanders and magnetic resonance imaging: The “hot” breast implant. *Ann Plast Surg* 1995;35:647-9.
98. Shellock FG, Forder JR. Drug eluting coronary stent: *In vitro* evaluation of magnetic resonance safety at 3 Tesla. *J Cardiovasc Magn Reson* 2005;7:415-9.
99. Ahmed S, Shellock FG. Magnetic resonance imaging safety: Implications for cardiovascular patients. *J Cardiovas Magn Reson* 2001;3:171-181.
100. Gerber TC, Fasseas P, Lennon RJ, et al. Clinical safety of magnetic resonance imaging early after coronary artery stent placement. *J Am Coll Cardiol* 2003;42:1295-8.

MRI Bioeffects, Safety, and Patient Management 495

101. Jehl J, Comte A, Aubry S, et al. Clinical safety of cardiac magnetic resonance imaging at 3 T early after stent placement for acute myocardial infarction. *Eur Radiol* 2009;19:2913-8.
102. Kaya MG, Okyay K, Yazici H, et al. Long-term clinical effects of magnetic resonance imaging in patients with coronary artery stent implantation. *Coron Artery Dis* 2009;20:138-42.
103. Karamitsos TD, Karvounis H. Magnetic resonance imaging is a safe technique in patients with prosthetic heart valves and coronary stents. *Hellenic J Cardiol* 2019;60:38-39.
104. Schenk CD, Gebker R, Berger A, et al. Review of safety reports of cardiac MR-imaging in patients with recently implanted coronary artery stents at various field strengths. *Expert Rev Med Devices* 2021;18:83-90.
105. Syed MA, Carlson K, Murphy M, et al. Long-term safety of cardiac magnetic resonance imaging performed in the first few days after bare-metal stent implantation. *J Magn Reson Imaging* 2006;24:1056-61.
106. Soulen RL. Magnetic resonance imaging of prosthetic heart valves [Letter]. *Radiology* 1986;158:279.
107. Soulen RL, Budinger TF, Higgins CB. Magnetic resonance imaging of prosthetic heart valves. *Radiology* 1985;154:705-707.
108. Randall PA, Kohman LJ, Scalzetti EM, et al. Magnetic resonance imaging of prosthetic cardiac valves *in vitro* and *in vivo*. *Am J Cardiol* 1988;62:973-976.
109. Frank H, Buxbaum P, Huber L, et al. *In vitro* behavior of mechanical heart valves in 1.5-T superconducting magnet. *Eur J Radiol* 1992;2:555-558.
110. Shellock FG, Morisoli SM. *Ex vivo* evaluation of ferromagnetism, heating, and artifacts for heart valve prostheses exposed to a 1.5-Tesla MR system. *J Magn Reson Imaging* 1994;4:756-758.
111. Edwards MB, Taylor KM, Shellock FG. Prosthetic heart valves: Evaluation of magnetic field interactions, heating, and artifacts at 1.5-Tesla. *J Magn Reson Imaging* 2000;12:363-369.
112. Shellock FG. Prosthetic heart valves and annuloplasty rings: Assessment of magnetic field interactions, heating, and artifacts at 1.5-Tesla. *Journal of Cardiovascular Magnetic Resonance* 2001;3:159-169.
113. Pruefer D, Kaldren P, Schreiber W, et al. *In vitro* investigation of prosthetic heart valves in magnetic resonance imaging: Evaluation of potential hazards. *J Heart Valve Disease* 2001;10:410-414.
114. Myers PO, Kalangos A, Panos A. Safety of magnetic resonance imaging in cardiac surgery patients: Annuloplasty rings, septal occluders, and transcatheter valves. *Ann Thorac Surg* 2012;93:1019.
115. Saeedi M, Thomas A, Shellock FG. Evaluation of MRI issues at 3-Tesla for a transcatheter aortic valve replacement (TAVR) bioprosthesis. *Magn Reson Imaging* 2015;33:497-501.
116. Hatamifar A, Vasquez LV, Chen J, Shellock FG, Chambers J. MRI evaluation of a new atrial- only anchored, transcatheter mitral valve replacement (TMVR) implant. *AJR Am J Roentgenol* 2020;214:524-528.
117. Mark AS, Hricak H. Intrauterine contraceptive devices: MR imaging. *Radiology* 1987;162:311-314.
118. Hess T, Stepanow B, Knopp MV. Safety of intrauterine contraceptive devices during MR imaging. *Eur Radiol* 1996;6:66-68.
119. Zieman M, Kanal E. Copper T 380A IUD and magnetic resonance imaging. *Contraception* 2007;75:93-5.
120. Correia L, Ramos AB, Machado AI, et al. Magnetic resonance imaging and gynecological devices. *Contraception* 2012;85:538-43.
121. Berger-Kulemann V, Einspieler H, Hachemian N, et al. Magnetic field interactions of copper-containing intrauterine devices in 3.0-Tesla magnetic resonance imaging: *In vivo* study. *Korean J Radiol* 2013;14:416-22.
122. Kido A, Togashi K, Kataoka ML, et al. Intrauterine devices and uterine peristalsis: Evaluation with MRI. *Magn Reson Imaging* 2008;26:54-8.

496 MRI-Related Issues for Implants and Devices

123. Bussman S, Luechinger R, Froehlich JM, et al. Safety of intrauterine devices in MRI. PLoS One 2018;13:e0204220.
124. Newmann W, Uhrig T, Malzacher M, et al. Risk assessment of copper-containing contraceptives: The impact for women with implanted intrauterine devices during clinical MRI and CT examinations. Eur Radiol 2019;29:2812-2820.
125. Shellock FG, Crues JV, Sacks SA. High-field magnetic resonance imaging of penile prostheses: *In vitro* evaluation of deflection forces and imaging artifacts. Society of Magnetic Resonance in Medicine, Book of Abstracts, pp. 915, 1987.
126. Lowe G, Smith RP, Cotabile RA. A catalog of magnetic resonance imaging compatibility of penile prostheses. J Sex Med 2012;9:1482-1487.
127. Shellock FG, Shellock VJ. Vascular access ports and catheters tested for ferromagnetism, heating, and artifacts associated with MR imaging. Magn Reson Imaging 1996;14:443-447.
128. Shellock FG, Meeks T. *Ex vivo* evaluation of ferromagnetism and artifacts for implantable vascular access ports exposed to a 1.5 T MR scanner. J Magn Reson Imaging 1991;1:243-247.
129. Titterington B, Shellock FG. Evaluation of MRI issues for an access port with a radiofrequency identification (RFID) tag. Magn Reson Imaging 2013;31:1439-44.
130. Hoff M, McKinney A, Shellock FG, et al. Safety concerns of 7-T MRI in clinical practice. Radiology 2019;292:509-518.
131. Kraff O, Quick HH. 7T: Physics, safety, and potential clinical applications. J Magn Reson Imaging 2017;46:1573-1589.
132. Okada T, Akasaka T, Thuy DHD, Isa. T. Safety for human MR scanners at 7T. Magn Reson Med Sci 2021 (In Press).
133. Roschmann P. Radiofrequency penetration and absorption in the human body: Limitations to high-field whole-body nuclear magnetic resonance imaging. Med Phys 1987;14:922-931.
134. Sammet CL, Yang X, Wassenaar PA, et al. RF-related heating assessment of extracranial neurosurgical implants at 7 T. Magn Reson Imaging 2013;31:1029-34.
135. Dula AN, Virostko J, Shellock FG. Assessment of MRI issues at 7-Tesla for twenty-eight implants and other objects. AJR Am J Roentgenol 2014;202:401-405.
136. Feng DX, McCauley JP, Morgan-Curtis FK, et al. Evaluation of 39 medical implants at 7.0 T. Br J Radiol 2015;88:20150633.
137. Oriso K, Kobayashi T, Sasaki M, et al. Impact of static and radiofrequency magnetic fields produced by a 7T MR imager on metallic dental materials. Magn Reson Med Sci 2016;15:26-33.
138. Chen B, Schoemberg T, Kraff O, et al. Cranial fixation plates in cerebral magnetic resonance imaging: A 3 and 7 Tesla *in vivo* image quality study. Magn Reson Mater Phy 2016;2:389-398.
139. Noureddine Y, Kraff O, Ladd ME, et al. Radiofrequency induced heating around aneurysm clips using a generic birdcage head coil at 7 Tesla under consideration of the minimum distance to decouple multiple aneurysm clips. Magn Reson Med 2019;82:1859-1875.
140. Santoro D, Winter L, Muller A, et al. Detailing radio frequency heating induced by coronary stents: A 7.0 Tesla magnetic resonance study. PloS One 2012;7:e49963.
141. Winter L, Oberacker E, Ozerdem C, et al. On the RF heating of coronary stents at 7.0 Tesla MRI. Magn Reson Med 2015;74:999-1010.
142. Tsukimura I, Murakami H, Sasaki M, et al. Assessment of magnetic field interactions and radiofrequency-radiation-induced heating of metallic spinal implants in 7 T field. J Orthop Res 2017;35:1831-1837.
143. Culo B, Valencerina S, Law M, Shellock FG. Assessment of metallic patient support devices and other items at 7-Tesla: Findings applied to 46 additional devices. Magn Reson Imaging 2019;57:250-253.
144. Barisano G, Culo B, Shellock FG, et al. 7-Tesla MRI of the brain in a patient with total knee replacement implants: Case report and proposed safety guidelines. Magn Reson Imaging 2019;57:313-316.

MRI Bioeffects, Safety, and Patient Management 497

145. German Ultrahigh Field Imaging (GUFI) Network, 2016. Approval of subjects for measurements at ultrahigh-field MRI. Available from http://www.mr-gufi.de/images/documents/Approval_of_subjects_for_measurements_at_UHF.pdf. Accessed August, 2021.
146. Brunner DO, De Zanche N, Frohlich J, Paska J, Pruessmann KP. Traveling-wave nuclear magnetic resonance. *Nature* 2009;457:994-998.
147. Campbell-Washburn AE, Tavallaei MA, Pop M, et al. Real-time MRI guidance of cardiac interventions. *J Magn Reson Imaging* 2017;46:935-950.
148. Reiter T, Gensler D, Ritter O, et al. Direct cooling of the catheter tip increases safety for CMR-guided electrophysiological procedures. *J Cardiovasc Magn Reson* 2012;14:12.

Chapter 19 Active Implanted Medical Devices: An Overview of MRI Safety Considerations

ROBERT E. WATSON, JR., M.D., PH.D.

Neuroradiologist

Division of Neuroradiology

Department of Radiology

Mayo Clinic

Rochester, MN

HEIDI A. EDMONSON, PH.D.

Medical Physicist

Department of Radiology

Mayo Clinic

Rochester, MN

INTRODUCTION

The number of active implanted medical devices available for treatment of medical conditions continues to increase rapidly. These devices are implanted frequently to address significant clinical conditions, and it is this group of patients that typically has need for clinical imaging, including magnetic resonance imaging (MRI). Since these implants contain metallic components, by definition they cannot be considered MR Safe; they can be considered only MR Conditional or MR Unsafe. An active implantable medical device (AIMD) is a “medical device relying for its function on a source of electrical energy or any source of power other than that directly generated by the human body or gravity”. In contrast, a passive medical device is one that serves its function without any source of power other than that generated by the human body or gravity (1). Notably, manufacturers are increasingly engineering their AIMDs to be MR Conditional, recognizing the commercial competitive advantage this can offer by permitting patients the ability to avail themselves of the diagnostic power of MRI.

Performing MRI examinations safely demands accurate identification of the precise make and model of any AIMD. Failure to identify an AIMD in a patient undergoing MRI can lead to severe risks. There is a well-known case in which a patient with a deep brain stimulation system suffered a severe radiofrequency (RF)-related burn to the thalamus, resulting in a permanent neurological deficit (2). Undisclosed cardiac pacemakers have been associated with patient deaths in associating with the use of MRI. In 2020, the Emergency Care Research Institute (ECRI) foundation declared incomplete AIMD information in MRI patients as one of the top ten patient safety risks (3). Also in 2020, a panel of ten radiologists with expertise in MRI safety from nine high-volume academic centers was formed, with the objective of providing clarity on safety issues for the ten most frequently questioned devices (4). This panel reviewed the relevant peer-reviewed literature that was focused on key MRI-related issues regarding screening and adverse event reports, in addition to the manufacturer's Instructions For Use for various products. Using a Delphi-inspired method, 36 practical recommendations were generated with 100% consensus that should aid the clinical MRI community with respect to screening patients with biomedical implants (4).

Sound, comprehensive screening processes are essential (5), and patients and/or their medical providers should be questioned at the time of ordering MRI exams about the presence of implanted devices. As an adjunct, electronic medical records are increasingly incorporating "implanted devices" modules that maintain important device-specific information (6). By identifying any device-specific MRI-related conditions prior to the patient's arrival at the facility, this can enhance efficiency by scheduling the patient on the proper 1.5-T or 3-T MR system, ensure timely availability of proper equipment such as transmit/receive RF head coils, and appropriate personnel (e.g., MR Safety Officers or MRSOs, specially-trained MRI technologists, MRI physicists, AIMD programming staff, etc). This device-specific information should be reconciled when the patient reports to the MRI facility. Frequently, the patient will have an implant identification card from the device manufacturer that identifies the particular device. If the device was implanted at another institution, surgical records should be provided by written means, frequently by fax or similar alternative, to obtain the relevant information including the particular type of AIMD that is present and its component parts (e.g., the models of the implantable pulse generator and leads). It should be noted that verbal relaying of important device-specific information should not be permitted due to potential errors in accurately conveying the information. As an example, three different types of Yasargil aneurysm clips (Aesculap, www.aesculap.com) exist. The model FD, FE, and FT - all of which rhyme, and if the information for the clip model were conveyed only by telephone, and it was misinterpreted, there could be severe safety consequences insofar as the FE and FT models are MR Conditional, while the FD is MR Unsafe. Similarly, blanket statements from an outside facility purporting to claim that all their implants are "MRI compatible" or "MRI Safe" is unacceptable. As part of the screening process at the MRI facility, a ferromagnetic detection system can assist in disclosing the presence of certain implanted devices (7, 8).

With positive identification of the device-specific make and model of the AIMD, several sources exist to identify whether a device is MR Unsafe or MR Conditional, with associated conditions. These include MRISafety.com, MagResource, Global Unique Device Identification Database (GUDID), and the specific device manufacturer's websites. The Food and Drug Administration (FDA) oversees the GUDID, which is a compilation of every device

500 Active Implanted Medical Devices: Safety

that has a unique device identifier (UDI). With the UDI number, the GUDID website provides the manufacturer, name of the device and, in some cases, the MRI safety information as to whether the device is MR Conditional, MR Unsafe, or MR Safe. Other possible sources can then be consulted regarding the necessary conditions for safe scanning. For example, the MagnetVision app is a tool that is designed to help MRI healthcare professionals assess anticipated risks for patients with implants prior to performing MRI examinations (9).

SAFETY CHALLENGES OF PERFORMING MRI IN PATIENTS WITH ACTIVE IMPLANTABLE MEDICAL DEVICES

Implant Movement

The MRI environment poses multiple challenges to safe scanning in a patient with an AIMD (**Table 1**). First, ferromagnetic content in the device is subject to translational attraction and torque from magnetic field interactions. Of note is that, typically, only limited ferromagnetic material remains in today's AIMDs, primarily associated with the power source (e.g., batteries). As the patient enters the MR system and moves through the spatial gradient magnetic field, nonferromagnetic metals are subjected to Lorentz forces that can produce slight displacement and vibration of the implanted metallic object. As such, it can be helpful for MRI staff members to alert the patient with an AIMD of this non-harmful possibility prior to entering the MR scanner to allay any concerns or fears if such minor movement is perceived. The potential mobility of the device is related to the degree to which it is encased by fibrous scar tissue or surgically fixed in place. Particularly for devices that are implanted off the central axis of the body, there is increasing tendency for these to be

Table 1. Potential implant risks associated with MRI and the test performed to characterize the problem.

Risk to Patient	Testing*
Force	B_0 -induced force
Torque	B_0 -induced torque
Heat	RF field-induced heating of the AIMD Gradient field-induced heating of the AIMD
Vibration	Gradient field-induced vibration
Extrinsic Electric Potential	Gradient field-induced lead voltage
Rectification	RF field-induced rectified lead voltage
Malfunction	B_0 -induced device malfunction RF field-induced device malfunction Gradient field-induced device malfunction

*Adapted from ISO/TS 10974:2018. Assessment of the safety of magnetic resonance imaging for patients with an active implantable medical device. 2018 (31).

affected by the spatial gradient magnetic field, for which MR Conditional limits are generally specified.

Heating of Device Components

Heating of device components primarily from the RF field is a major concern with respect to the leads associated with AIMDs. Conductive materials may act as resonant antennae, locally amplifying the RF energy used for MR image formation. Particularly in the context of neurostimulation systems, RF-related heating of leads in close proximity to sensitive tissues can potentially produce severe damage (2). In insulated leads where induced current is not dissipated over the length of the lead, heating is concentrated at the tip. Temperatures below 43°C are not associated with the long-term damage. However, at 60°C, there is instant protein denaturation and tissue coagulation. At temperatures between 44° and 60°C, tissue death is time-dependent.

Particularly in insulated leads, the lead length exposed to the RF field is an important variable because heating is associated with the resonant frequency, with maximal heating related to the one-half wavelength. MR systems operating at 1.5-T and 3-T detect the nuclear magnetic resonance signal of ¹H nuclei at 64-MHz (wavelength 52 cm, one-half wavelength - 26 cm) and 128-MHz (wavelength 26 cm, one-half wavelength - 13 cm) resonance frequency, respectively. It should be noted that in body tissue, the effective wavelength is affected also by tissue permittivity as well as other factors (10).

The physical length of the lead specified by the manufacturer may not correspond to the total length of the conductive material within the lead, making it difficult to predict which leads may create resonant conditions. Importantly, the attachment of a lead to an implantable pulse generator (IPG) can have a large influence on heating at the lead tip, with the possibility for temperatures being greatly elevated if the lead is unattached or abandoned. As result, there may be an increased risk of heating when scanning in the presence of abandoned leads, or when leads are unattached to an IPG (11).

Other factors that can influence RF energy-related current deposition and heat production include the type of transmit RF coil employed for imaging and the position of the metallic implant, as well as its “path” or configuration, relative to the transmitted RF. The majority of clinically utilized receive-only RF coils rely on an integrated body transmit RF coil for RF excitation, exposing the majority of the patient’s body to RF energy. Smaller transmit/receive (T/R) RF coils (e.g., the T/R head RF coil, T/R knee RF coil, etc.) that both broadcast RF and detect the emitted signals, are readily available on MR systems for head or extremity imaging. The smaller head or extremity transmit/receive RF coils typically deposit the majority of RF within the volume of the coil, only. Notably, the MRI-related conditions for AIMDs may specify eligible types of transmit RF coils and/or acceptable distances of the AIMD away from the transmit RF coil in order to limit or prevent exposure to RF energy during MRI.

It is important to emphasize that MRI-related conditions, particularly related to RF-induced heating, cannot be presumed at different static magnetic field strengths or for multi-nuclear (i.e., non-proton) imaging, because the frequency and the frequency and wavelengths of the RF pulses are field strength dependent. For example, conditional safety

502 Active Implanted Medical Devices: Safety

for an AIMD at 3-T/128-MHz at a specific SAR level does not imply conditional safety at 1.5-T/64-MHz (10). Induced currents, particularly within AIMDs, is also a possibility due to exposure to the rapidly switching gradient magnetic fields associated with MRI.

Device Malfunction

Time-varying gradient magnetic fields and RF can induce currents within the AIMD, which may interfere with the control electronics. Thus, when exposed to the RF and gradient fields, AIMDs may improperly function or “reset”. The static magnetic field can also interact with certain devices, especially those with moving metallic components. For example, implantable infusion pumps with rotor mechanisms can slow down or stop as a result of exposure to the static magnetic field of the MR system (see section on **Implantable Infusion Pumps**).

PERFORMING MRI IN PATIENTS WITH ACTIVE IMPLANTABLE MEDICAL DEVICES

Active implanted medical devices include cardiac devices (cardiac pacemakers, implantable cardioverter defibrillators, loop recorders and others) and neurostimulation systems (deep brain stimulation, spinal cord stimulation systems, vagus nerve stimulation systems, sacral nerve stimulation systems, hypoglossal nerve stimulation systems, peripheral nerve stimulation systems, auditory brainstem implants, cochlear implants, and others), implantable infusion pumps, ingestible video endoscopy capsules, and others devices. An exhaustive discussion of each of these is well beyond the scope of this chapter, however, other chapters in this textbook provide relevant information for AIMDs.

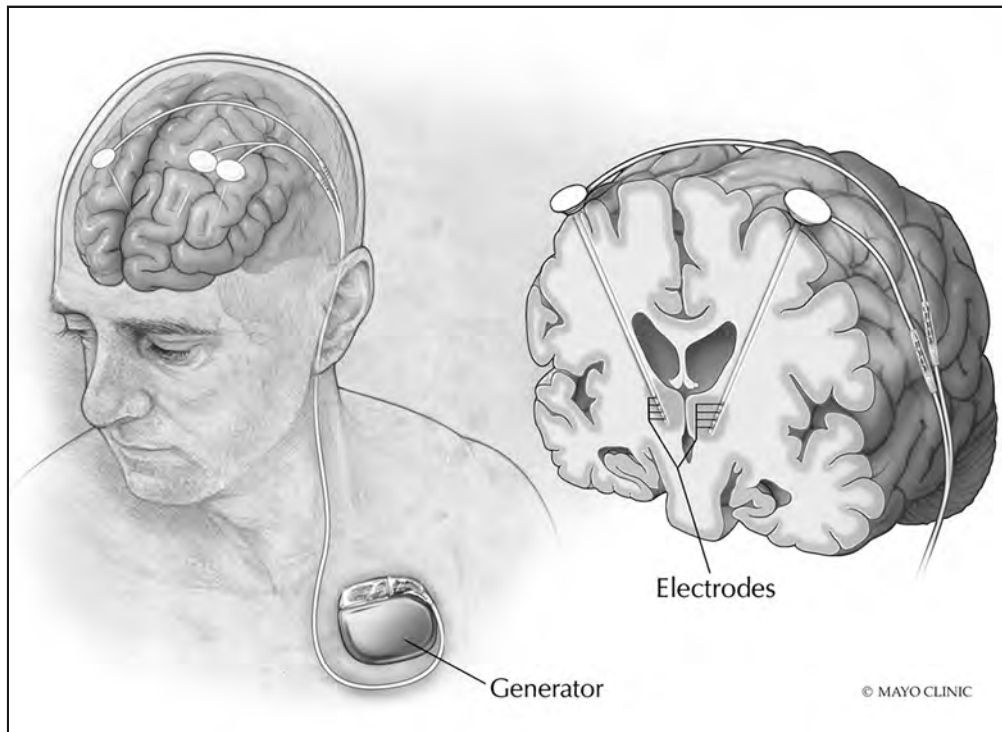
Because conditions for scanning frequently change and new devices are constantly becoming available, it is essential that MRI healthcare workers ensure that they are using the most up-to-date information that is available. As always, it is essential to not fall prey to “satisfied search” recognizing that patients may present with multiple implanted devices, any of which could be dangerous if not scanned with the appropriate MRI-related conditions.

It is also important to understand that, within a particular model of AIMD, there may be multiple configurations using various components or lead models. In general, the evaluation of an AIMD for MRI-related issues is highly specific to the complete system and particular to a given IPG and leads. As such, the MRI-related conditions to perform an MRI exam safely may have different limits, depending on which components are present in the patient. Each component of the AIMD must be carefully identified to ensure that the complete system is MR Conditional. In some cases, an AIMD may involve MR Conditional components from different manufacturers and, as a result, the safety of scanning the patient is unknown because that scenario was never tested.

Deep Brain Stimulation Systems

Deep brain stimulation (DBS) has been employed in the treatment of Parkinson’s disease, dystonia, essential tremor, epilepsy, and certain psychiatric conditions, including obsessive-compulsive disorder (12-14)(Figure 1). Because DBS electrodes are implanted in

Figure 1. Deep brain stimulation (DBS) system. The DBS system consists of a pulse generator, typically implanted in the infraclavicular region. Leads are tunneled subcutaneously cephalad and over the cranium, where the electrodes are implanted surgically into designated anatomic targets.

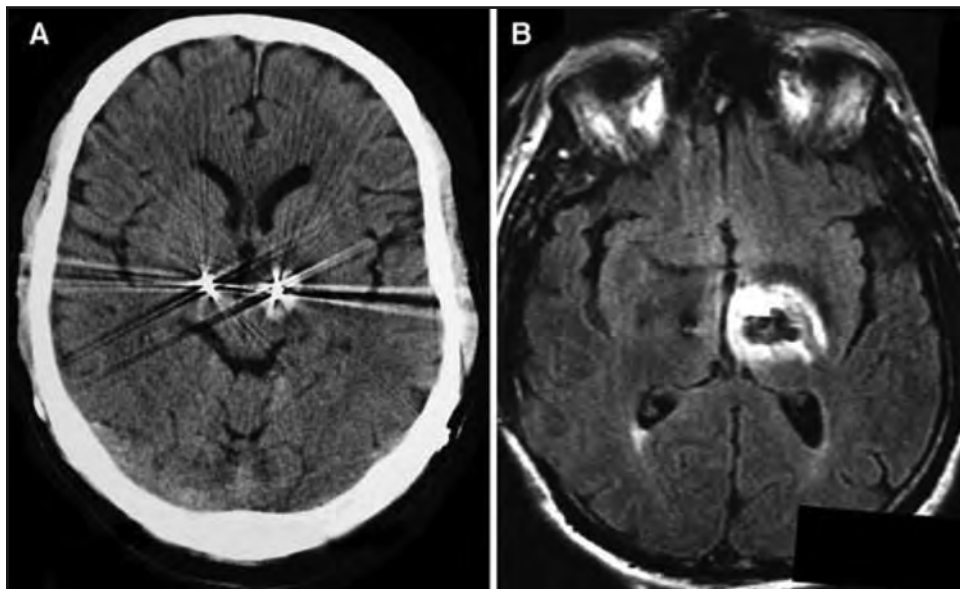


vital brain structures, MR-induced heating could have devastating clinical consequences, as reported by Henderson, et al. (2). A patient undergoing an MRI of the lumbar spine using a body transmit system suffered a significant lesion in the thalamus on the side ipsilateral to the relatively long lead connected to an IPG implanted in the abdomen area, resulting in a hemiparesis (2)(Figure 2). Whereas cardiac tissue is highly perfused and difficult to thermally injure in relation to MRI, neural tissues are extremely sensitive to even modest temperature elevations.

MRI safety conditions for scanning patients with certain DBS systems are generally associated with a strictly limited, whole-body averaged specific absorption rate (SAR) of 0.1 W/kg or a B_{1+} Root Mean Squared (B_{1+RMS}) value of 2.0 μT (13, 14). It is essential that, when performing MRI in patients with DBS systems, that the MRI safety conditions are followed in their entirety without deviations, and are considered with the entire system recognized (13, 14). Limiting the assessment of conditions for safe scanning only to those related, for example, to the IPG, without appreciating conditions associated with the implanted leads could pose substantial hazards for the patient. By way of example, for certain DBS systems from Medtronic, the presence of a pocket adapter associated with the IPG precludes the use of the transmit body RF coil, limiting the MRI exam to transmit/receive RF coils because pocket adaptors permit older style leads with low impedance (i.e., unsuitable for use of the

504 Active Implanted Medical Devices: Safety

Figure 2. MRI-related, radiofrequency burn centered at the left thalamus, seen in CT (**A**) and T2-weighted MR images (**B**) that resulted from the use of a transmit body RF coil to image the lumbar spine in a patient with a DBS system. This patient sustained a lesion on the left side of the brain, corresponding with the left-sided lead and the implantation of the left pulse generator in the abdominal area (i.e., which resulted in a longer length for the lead on the left side compared to the right side). No lesion was produced on the right side, where the pulse generator was in the standard infraclavicular position and the lead had a shorter, more commonly used length. (Figure used with permission: Henderson JM, Tkach J, Phillips M, Baker K, Shellock FG, Rezai AR. Permanent neurological deficit related to magnetic resonance imaging in a patient with implanted deep brain stimulation electrodes for Parkinson's disease: Case report. *Neurosurgery* 2005;57:E1063.)

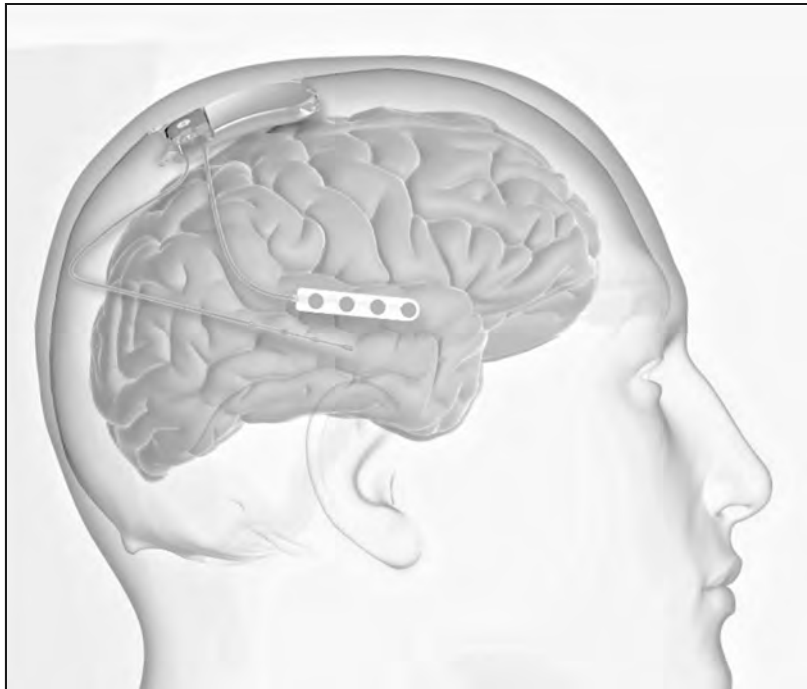


transmit body RF coil) to be connected to a more contemporary IPG. As previously indicated, untested component scenarios for AIMDs may pose risks to patients undergoing MRI.

Responsive Neurostimulation Systems

A responsive neurostimulation system (RNS) is used for the treatment of patients with drug resistant epilepsy. The RNS consists of a small neurostimulation device that is implanted in the skull that delivers stimulation to brain sites and is activated when sensing leads detect brain activity that is predictive of impending seizure activity (**Figure 3**). Earlier versions of this technology from NeuroPace Corporation (e.g., Model RNS-300M) were labeled MR Unsafe (13). The more recent version, Model RNS-320, is now 1.5-T, full-body eligible with defined conditions of scanning, thus, permitting patients to benefit from the diagnostic capabilities afforded by MRI. Similar to other devices, the associated device programmers and monitors are MR Unsafe and should not be allowed into the MR system room.

Figure 3. Responsive neurostimulation system (RNS). The RNS consists of a small neurostimulation device that is implanted in the skull that delivers stimulation to brain sites and is activated when sensing leads detect brain activity that is predictive of impending seizure activity (**A, top**). X-ray (lateral view) of a patient with an RNS (**B, bottom**). Note the IPG implanted in the skull and the leads associated with this device.



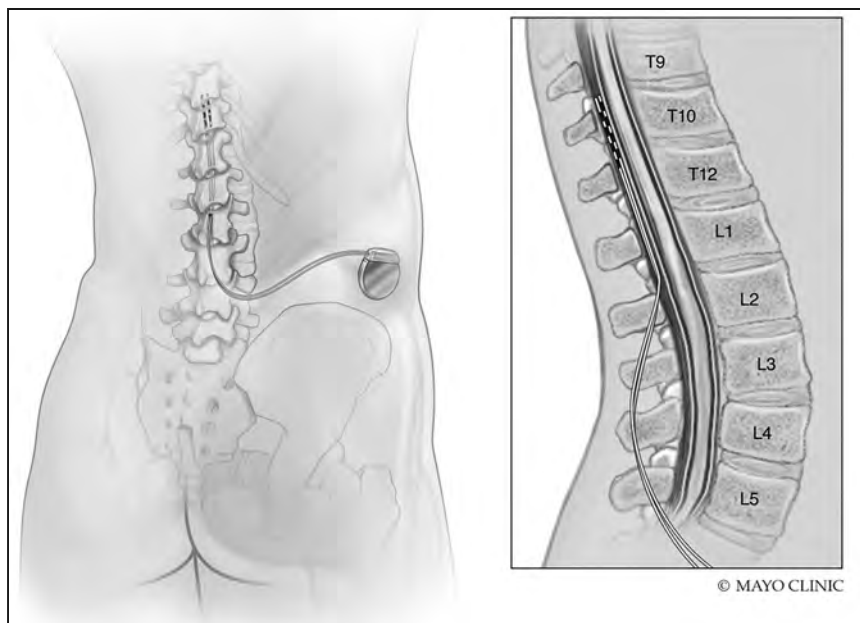
506 Active Implanted Medical Devices: Safety

Spinal Cord Stimulation Systems

Spinal cord stimulation (SCS) technology is increasingly providing therapeutic options particularly for patients suffering from chronic pain syndromes (13-16)(**Figure 4**). SCS systems are available from multiple manufacturers (13-16). Typically, older versions are MR Unsafe, while newer versions are MR Conditional. The MRI-related conditions for SCS systems may include important requirements related to the type of transmit RF coil that is allowed (e.g., transmit body RF coil combined with any type of receive-only RF coil or T/R head or extremity RF coils), as well as possible limitations for the whole-body averaged SAR or B_{1+RMS} values that are required to ensure patient safety (13). As with other AIMDs involving the combination of an IPG and leads, the entire “system” must exist in order to comprise its MR Conditional status. An MR Conditional IPG attached to non-MR Conditional leads renders the SCS device or any other AIMD for that matter, MR Unsafe.

Because the spinal cord level at which SCS electrodes are placed is variable and dependent on the patient’s clinical symptoms and the particular anatomic segment needing treatment, the “antenna-effect” of the lead system is similarly variable from patient-to-patient, posing additional challenges to safely performing MRI. Interestingly, some MR Conditional SCS systems have adopted technologies to “shield” their leads, such as the SureScan

Figure 4. Spinal cord stimulation (SCS) system. The SCS system consists of a pulse generator, typically implanted in the subcutaneous posterior soft tissues superior to the iliac bone. Leads are tunneled subcutaneously cephalad and enter the epidural space in the spinal canal. The leads can be advanced cephalad to the spinal level where there is maximal clinical benefit. Due to the variability of where the electrodes terminate, it is important to know their position prior to performing an MRI examination in a patient. Other conditions of scanning, including device programming and impedance checks are typically required.



devices from Medtronic. This important feature allows MRI exams to be performed with fewer limitations insofar because permits the use of the transmit body RF coil and higher RF exposure levels (13-16).

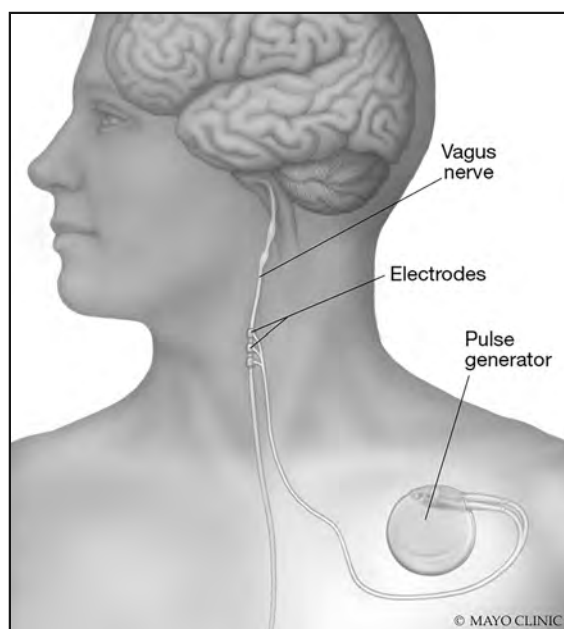
For example, the SureScan SCS devices incorporate a braided metallic shield around the leads, functioning as an RF shield, isolating the energy from the conductor leads, and dissipating the energy to adjacent tissues along the length of the lead. RF energy that is conveyed back towards the IPG is shunted to its case, where it is dispersed over the surrounding soft tissues. The Precision Montage SCS system which uses Avisa leads from Boston Scientific utilizes a technology termed, “billabong current suppression”, in which wires wound around the stimulation lead have short-reversed coil sections that suppress induced currents (13-15).

For certain MR Conditional AIMDs, it is essential for patients to bring their programmer to the MRI appointment so that the AIMD can be shut off or programmed into the MR Conditional mode. As with all MR Conditional AIMDs, it is crucial to follow the conditions stated in the labeling in order to safely conduct MRI in patients with SCS systems.

Vagus Nerve Stimulation Systems

Vagus nerve stimulation (VNS) systems are used primarily to increase seizure control in patients with epilepsy but are also being used in patients with treatment-resistant depression (13, 14, 17). A VNS system consists of an IPG typically implanted in the infraclavicular region, with a lead terminating around the left vagus nerve in the neck (**Figure 5**). VNS systems from LivaNova now permit scanning at 1.5-T and 3-T. Depending on the model, the use of a T/R head or extremity RF coil is permitted or the transmit body RF coil combine with any receive-only RF coil (13, 14, 17). As with other AIMDs, it is important to carefully

Figure 5. Vagus nerve stimulation (VNS) system. The VNS system consists of a pulse generator, typically implanted in the infraclavicular region. Leads are tunneled subcutaneously cephalad and then with deeper dissection, positive and negative helical electrodes are attached to the left vagus nerve, inferior to cardiac branches (23).



508 Active Implanted Medical Devices: Safety

identify all components of the patient's implanted system in order to correctly establish the specific conditions permissible to ensure safe scanning.

Prior to MRI, the stimulation parameters should be assessed for the VNS system, and several device outputs are set to 0 mA. VNS devices from LivaNova fall into either "Group A" or "Group B", with Group A permitting the use of the transmit body RF coil and scanning outside of the "exclusion zone" of C7 to L3, and Group B permitting the use of the T/R head or extremity RF coils and scanning outside of the "exclusion zone" of C7 to T8.

Not infrequently, VNS systems are explanted if that patient's epilepsy does not respond to VNS therapy. While explanation of the IPG is relatively simple, full explantation of the entire VNS lead is a complex procedure with the potential for causing considerable damage to the nerve due to scarring and tissue alterations associated with the distal end of the lead coiled around the vagus nerve. Damage to the vagus nerve can result in serious consequences that impact speech, cardiac, gastrointestinal, and other functions. Thus, in practice, the lead is cut, leaving a length of lead that is variable, along with the portion coiled around the vagus nerve. Fortunately, MR Conditional labeling exists for this situation. In these cases, it is important to obtain radiographs to determine the length of the retained lead because a length greater than 2 cm precludes the use of the transmit body RF coil for MRI.

Sacral Nerve Stimulation Systems

Sacral nerve stimulation (SNM) has been shown to be efficacious for urinary bladder and bowel control and, thus, this device is used to treat patients affected by overactive bladders, urinary urge incontinence, unobstructed urinary retention, and fecal incontinence. The SNM system consists of an IPG that is typically implanted subcutaneously, posterior to the upper margin of the buttocks (13, 14, 18-20). A lead is implanted adjacent to the sacral nerves (S2, S3, and S4). Previously, the available MR Conditional sacral nerve stimulation systems did not permit the use of the transmit body RF coil and, thus, were limited to the use of the T/R head or extremity RF coils. Those particular devices were the Interstim and the Interstim II neuromodulation systems used for SNM (Medtronic, www.medtronic.com) (13, 14). One manufacturer, Medtronic, now has attained FDA approval of its InterStim Micro System and its InterStim II System permitting full body MRI exams using the transmit body RF coil of the MR system. Verification of the model of the IPG and lead is imperative in order to determine the MR Conditional status of the device considering that the different models have different MRI-related conditions that must be followed to ensure patient safety.

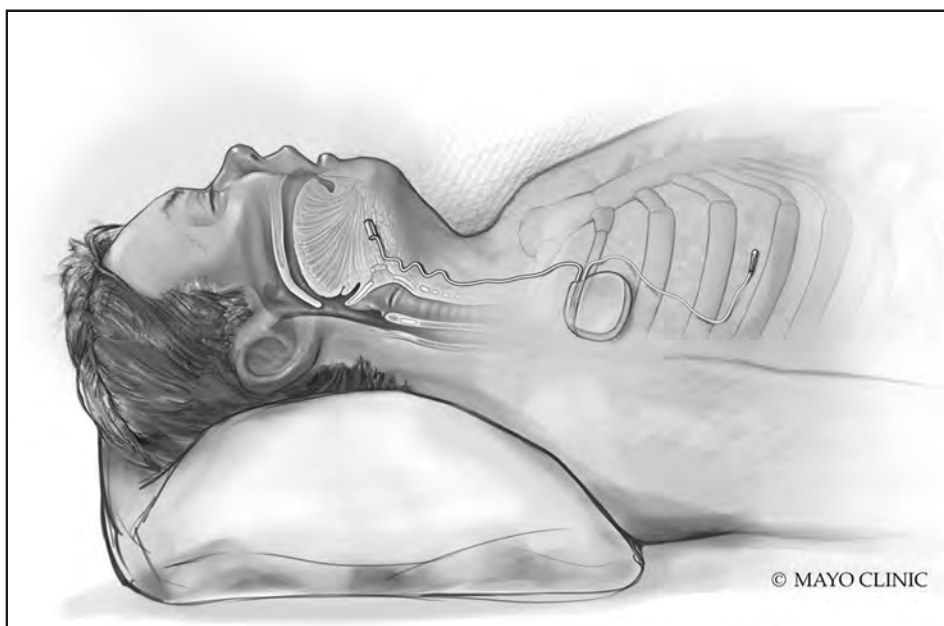
Hypoglossal Nerve Stimulation Systems

A new type of neuromodulation system has become available to treat patients with obstructive sleep apnea. This device called Inspire Upper Airway Stimulation (Inspire, Inc., www.inspiresleep.com), is used to treat a subset of patients with moderate to severe obstructive sleep apnea and is primarily used in patients that fail or cannot tolerate continuous positive airway pressure (CPAP) and that do not have a complete concentric collapse of the upper air at the soft palate level. The Inspire Upper Airway Stimulation system employs a lead directed at sensing the onset of a diaphragmatic inspiratory effort, with subsequent

stimulation of the hypoglossal nerve, pulling the soft tissues of the tongue anteriorly, and opening the oropharyngeal airway (**Figure 6**).

For the Inspire Upper Airway Stimulation device, one model is labeled MR Unsafe, Model 3024, while the other, Model 3028, is MR Conditional. The MR Conditional version requires the MRI examination to be performed at 1.5-T, operating in the Normal Operating Mode (i.e., limiting the whole-body averaged SAR to 2 W/kg or less or a particular B_{1+RMS} limits depending on the positioning of the T/R head RF coil), using the T/R head or extremity RF coils. Once again, this illustrates the need for absolute precision in terms of accurately identifying the make and model of the patient's AIMD, especially in instances when MR Unsafe and MR Conditional versions exist.

Figure 6. Hypoglossal nerve stimulation (HNS) system. The HNS system consists of a pulse generator, typically implanted in the infraclavicular region. The inferior lead is tunneled subcutaneously caudally, and senses onset of an inspiratory effort. The cephalad electrode attaches to hypoglossal nerve branches, and serves to contract the tongue's musculature at appropriate times in the breathing cycle, pulling the tongue anteriorly towards the genu of the mandible, and producing widening of the oropharyngeal airway.



Cochlear Implant Systems

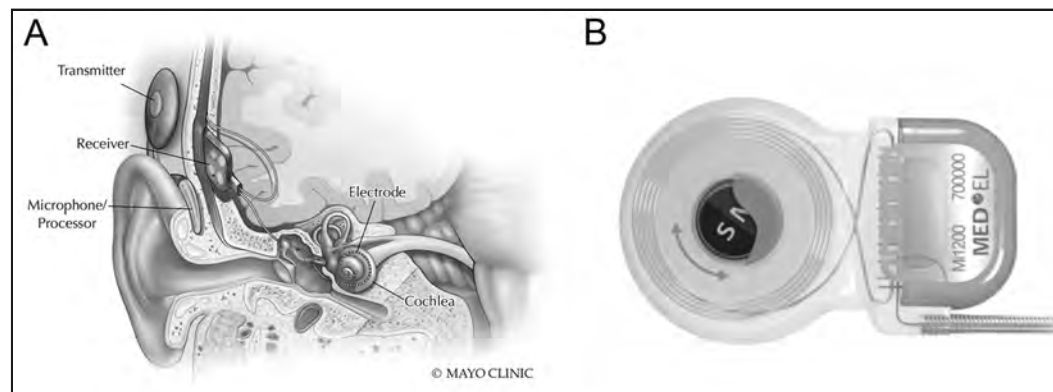
The internal components of a cochlear implant (CI) system consist of a receiver and stimulator, stimulation electrodes threaded into the cochlea, and an internal magnet that permits coupling with an externally-worn transmitter and sound processor (**Figure 7**) (21-23). These AIMDs are associated with scanning parameters permitting MRI examinations to be performed in patients under highly-specific conditions. An ongoing issue with most cochlear implants is the presence of the internal magnet and whether, in certain circum-

510 Active Implanted Medical Devices: Safety

stances, a risk versus benefit analysis and informed consent by the patient favors scanning with the magnet remaining in place (21, 22). While an option exists to surgically remove the internal magnet prior to MRI and then to replace it following the exam, as with any surgical procedure, there is a risk of infection or other complication. Particularly in CI patients that are in need of multiple MRIs, including those with neurofibromatosis 2 in which growth of multiple tumors must be constantly assessed, the repeated surgeries for magnet removal can pose a substantial risk.

When performing MRI in patients with cochlear implants, the alternative to magnet removal is to tightly wrap the patient's head using a special compression dressing in an effort to prevent magnet movement or displacement. Unfortunately, head wrapping is associated with patient discomfort, and despite this procedure, some magnets still dislodge (21-23). In addition, the presence of the magnet imparts significant susceptibility artifact, although techniques are available to mitigate these (23-25). Increasingly, efforts by CI manufacturers have addressed the aforementioned MRI-related issues, with at least three manufacturers that now have cochlear implants that incorporate magnetic components that self-align to the direction of the static magnetic field of the MR system: the MED-EL Synchrony (MED-EL, www.medel.com) (**Figure 7B**), the Advanced Bionics HiRes Ultra 3D (Advanced Bionics, www.advancedbionics.com), and the Cochlear Nucleus System (Cochlear, www.cochlear.com). This important design feature does away with the need for head wrapping because it reduces or eliminates the substantial force and torque experienced by older

Figure 7. Cochlear implant. Depiction of a typical cochlear implant system (A). This device consists of an externally-attached auditory microphone processor and transmitter system that is affixed transcranially to the implanted receiver that delivers stimulation through an electrode implanted into the cochlea to produce sound perception for the patient. The attachment of the cochlear implant is typically accomplished by metallic elements in the external component that couple with one or more magnets that are an inherent part of the internally implanted component. Newer generations of MR Conditional cochlear implants (B) feature rotating magnets that align with the direction of the MR system's static magnetic field, reducing or eliminating the substantial attractive force and torque that earlier generations of these devices typically experienced. (Diagram B used with permission from MED-EL. MRI & Cochlear Implants: Superior MRI Safety, 2018. Retrieved from <https://blog.medel.pro/mri-cochlear-implants-reliability/>.)



CI designs (26, 27). For additional information, the reader is referred to an excellent review by Erhardt, et al. (28), which discusses the MRI safety considerations related to cochlear implants and other intracranial implants.

Implantable Infusion Pumps

Implantable infusion pumps allow controlled delivery of medications into the subarachnoid space at the spinal canal. The most commonly infused medications are morphine, or its derivatives for pain control and baclofen, or its derivatives for control of spasticity. Implantable infusion pumps that have undergone proper testing are labeled MR Unsafe, while others, including several different versions from Medtronic, are labeled MR Conditional.

While the patient undergoes an MRI examination, drug infusion by the pump is typically suspended in order to prevent problems related to the dispensing of the medication. After MRI, it is essential to assess the operational aspects of the implantable infusion pump because the gears within the pump's motor may temporarily bind, and prevent the pump from restarting. This scenario could potentially lead to opioid withdrawal, or baclofen withdrawal syndrome, both of which are serious conditions (29).

Similar to other AIMDs, it is important to note the specific conditions for scanning associated with each type of implantable infusion pump, especially with respect to the name of the product and model number. Importantly, although labeled MR Conditional, conditions associated with safe scanning of the two different versions of the implantable infusion pumps from Flowonics Medical Inc. (www.flowonics.com), the Prometra and Prometra II, require that the drug reservoir be entirely emptied prior to permitting the patient entry into the MR system room. This is crucial because these devices can dispense medications in an uncontrolled manner during MRI. Notably, MRI-related safety issues for implantable infusion pumps were the subject of an FDA Safety Communication in 2017 (30).

Ingestible Video Capsule Endoscopy Devices

Ingestible, video capsule endoscopy devices are AIMDs that take images that are wirelessly conveyed as they pass through the gastrointestinal (GI) system. These devices include the various models of the PillCam (Medtronic, www.medtronic.com), the CapsoCam (CapsoVision, capsovission.com), the Mirocam (IntoMedic, www.intromedic.com), and the ENDOCAPSULE (Olympus, www.olympusamerica.com). Each one of these is MR Unsafe and exposure to MRI environment can corrupt or erase the data. Occasionally ingestible, video capsule endoscopy devices are not passed from the GI system in a timely manner, particularly when they enter a diverticulum pocket on the wall of the intestine, and are retained. The battery contains a small amount of ferromagnetic material that can experience translational attraction and torque in association with MRI. To date, no known clinically adverse events have been reported in association with inadvertent scanning of patients with these AIMDs, but they are associated with substantial susceptibility artifact.

SUMMARY AND CONCLUSIONS

AIMDs continue to proliferate and their overall benefit to clinical care is unquestioned. Increasingly, manufacturers are engineering MR Conditional systems such that patients

512 Active Implanted Medical Devices: Safety

with these AIMDs can have safe access to the diagnostic benefits afforded by MRI as long as the conditions are carefully followed. Diligent pre-MRI patient screening is essential to ensure that each and every AIMD is identified in its entirety, and conditions for scanning are strictly complied with because severe injury to the patient or substantial damage to the device can result if improper MRI-related conditions are applied.

In the coming years, a host of new innovative devices is likely. With the awareness of the concurrent needs of implant recipients to need access to MRI, the science behind designing and testing MR Conditional systems can be expected to rapidly advance. Because the MRI-related conditions of any particular AIMD may change or otherwise evolve over time, MRI healthcare professionals must be cognizant of the need to utilize the latest information prior to performing the MRI examinations. In this manner, patients will be protected from possible adverse events.

(This chapter is based, in part, on Watson RE Jr, Edmonson HA. MR safety: Active implanted medical devices. *Magn Reson Imaging Clin N Am* 2020;28:549-558.)

REFERENCES

1. Testing and Labeling Medical Devices for Safety in the Magnetic Resonance (MR) Environment. 2021. <https://www.fda.gov/regulatory-information/search-fda-guidance-documents/testing-and-labeling-medical-devices-safety-magnetic-resonance-mr-environment>. Accessed July, 2021.
2. Henderson JM, Tkach J, Phillips M, Baker K, Shellock FG, Rezai AR. Permanent neurological deficit related to magnetic resonance imaging in a patient with implanted deep brain stimulation electrodes for Parkinson's disease: Case report. *Neurosurgery* 2005;57:E1063.
3. Drees J. Top 10 health technology hazards for 2020: ECRI Institute. 2019; <https://www.ecri.org/landing-2020-top-ten-health-technology-hazards>. Accessed July, 2021.
4. Jabehdar Maralani P, Schieda N, Hecht EM, et al. MRI safety and devices: An update and expert consensus. *J Magn Reson Imaging* 2020;51:657-674.
5. Kimbrell V. Elements of effective patient screening to improve safety in MRI. *Magn Reson Imaging Clin N Am* 2020;28:489-496.
6. Watson RE, Cradick CM, Epps S, Mauck WD, Luetmer PH. Implementing an electronic health record medical device module-A critical patient safety enhancement. *J Am Coll Radiol* 2016;13:705-708.
7. Shellock FG, Karacozoff AM. Detection of implants and other objects using a ferromagnetic detection system: implications for patient screening before MRI. *AJR Am J Roentgenol* 2013;201:720-725.
8. Watson RE, Walsh SM, Felmlee JP, Friedman PA, Keene MN. Augmenting MRI safety screening processes: Reliable identification of cardiac implantable electronic devices by a ferromagnetic detector system. *J Magn Reson Imaging* 2019;49:e297-e299.
9. Kanal E. Standardized approaches to MR safety assessment of patients with implanted devices. *Magn Reson Imaging Clin N Am* 2020;28:537-548.
10. Stafford RJ. The physics of magnetic resonance imaging safety. *Magn Reson Imaging Clin N Am* 2020;28:517-536.
11. Langman DA, Goldberg IB, Finn JP, Ennis DB. Pacemaker lead tip heating in abandoned and pacemaker-attached leads at 1.5-Tesla MRI. *J Magn Reson Imaging* 2011;33:426-431.
12. Lozano AM, Lipsman N, Bergman H, et al. Deep brain stimulation: Current challenges and future directions. *Nat Rev Neurol* 2019;15:148-160.
13. Sayad D, Chakravarthy K, Amirdelfan K, et al. A comprehensive practice guideline for magnetic resonance imaging compatibility in implanted neuromodulation devices. *Neuromodulation* 2020;23:893-911.

MRI Bioeffects, Safety, and Patient Management 513

14. Manker, S. Shellock FG. Chapter 24. MRI Safety and Neuromodulation Systems. In: *Neurmodulation*. Second Edition. Krames ES, Peckham Hunter P, Rezai AR, Editors. Academic Press/Elsevier, New York, 2018; pp. 315-337.
15. Walsh KM, Machado AG, Krishnaney AA. Spinal cord stimulation: A review of the safety literature and proposal for perioperative evaluation and management. *Spine J* 2015;15:1864-9.
16. Rubino S, Adepoju A, Kumar V, et al. MRI conditionality in patients with spinal cord stimulation devices. *Stereotact Funct Neurosurg* 2016;94:254-258.
17. Yang J, Phi JH. The present and future of vagus nerve stimulation. *J Korean Neurosurg Soc* 2019;62:344-352.
18. Karrer-Warzinek E, Abt D, Kim OCH, et al. Safety of magnetic resonance imaging in patients under sacral neuromodulation with an InterStim Neuromodulator. *Urology* (In Press), 2021.
19. Chermansky CJ, Krlin RM, Holley TD, Woo HH, Winters JC. Magnetic resonance imaging following InterStim®: An institutional experience with imaging safety and patient satisfaction. *Neurourol Urodyn* 2011;30:1486-1488.
20. Heidler S, Ostermann S, Kuglitsch M, et al. Multiple magnetic resonance imaging in patients with implanted sacral nerve stimulator. *Neurourol Urodyn* 2020;39:2368-2372.
21. Srinivasan R, So CW, Amin N, et al. A review of the safety of MRI in cochlear implant patients with retained magnets. *Clin Radiol* 2019;74:972.e9-972.e16
22. Kim BG, Kim JW, Park JJ, Kim SH, Kim HN, Choi JY. Adverse events and discomfort during magnetic resonance imaging in cochlear implant recipients. *JAMA Otolaryngol Head Neck Surg* 2015;141:45-52.
23. Carlson ML, Neff BA, Link MJ, et al. Magnetic resonance imaging with cochlear implant magnet in place: Safety and imaging quality. *Otol Neurotol* 2015;36:965-971.
24. Edmonson HA, Carlson ML, Patton AC, Watson RE. MR imaging and cochlear implants with retained internal magnets: Reducing artifacts near highly inhomogeneous magnetic fields. *Radiographics* 2018;38:94-106.
25. Todt I, Guerkov R, Gehl HB, Sudhoff H. Comparison of cochlear implant magnets and their MRI artifact size. *Biomed Res Int* 2020;2020:5086291.
26. Cass ND, Honce JM, O'Dell AL, Gubbels SP. First MRI with new cochlear implant with rotatable internal magnet system and proposal for standardization of reporting magnet-related artifact size. *Otol Neurotol* 2019;40:883-891.
27. Todt I, Tittel A, Ernst A, et al. Pain free 3 T MRI scans in cochlear implant recipients. *Otol Neurotol* 2017;38:e401-e404.
28. Erhardt JB, Fuhrer E, Gruschke OG, et al. Should patients with brain implants undergo MRI? *J Neural Eng* 2018;15:041002.
29. Mohammed I, Hussain A. Intrathecal baclofen withdrawal syndrome- A life-threatening complication of baclofen pump: A case report. *BMC Clin Pharmacol* 2004;4:6.
30. Safety Concerns with Implantable Infusion Pumps in the Magnetic Resonance (MR) Environment: FDA Safety Communication. 2017; <https://www.fda.gov/medical-devices/safety-communications/safety-concerns-implantable-infusion-pumps-magnetic-resonance-mr-environment-fda-safety>. Accessed July, 2021.
31. ISO/TS 10974:2018. Assessment of the safety of magnetic resonance imaging for patients with an active implantable medical device. International Organization for Standardization, 2018.

Chapter 20 MRI-RELATED HEATING OF IMPLANTS AND DEVICES

LUKAS WINTER, PH.D.

Physikalisch-Technische Bundesanstalt (PTB)
Braunschweig und Berlin
Germany

FRANK SEIFERT, PH.D.

Physikalisch-Technische Bundesanstalt (PTB)
Braunschweig und Berlin
Germany

LUCA ZILBERTI, PH.D.

Istituto Nazionale di Ricerca Metrologica
Torino, Italy

MANUEL MURBACH, PH.D.

ZMT Zurich MedTech AG
Zurich, Switzerland

BERND ITTERMANN, PH.D.

Physikalisch-Technische Bundesanstalt (PTB)
Braunschweig und Berlin
Germany

INTRODUCTION

Magnetic resonance (MR) scanners utilize static magnetic, time-varying gradient magnetic, and radiofrequency (RF) fields to image human subjects. Even when interacting with purely biological tissues, these electromagnetic fields can pose a hazard for the patient by excessive tissue heating due to the transmitted RF field. While still an active area of research, a high level of understanding has been achieved for this phenomenon and mature safety provisions have emerged from this knowledge. The situation becomes more compli-

MRI Bioeffects, Safety, and Patient Management 515

cated when a patient has a metallic biomedical implant, especially if that device contains electrically conductive parts.

By the physical nature of their interactions, patient hazards related to magnetic resonance imaging (MRI) that are due to the presence of metallic implants can be grouped into four categories: (1) forces and torques acting on ferromagnetic objects due to the static magnetic field, B_0 ; (2) forces, sometimes referred to as Lenz forces, and related torques exerted by the static magnetic field on moving metallic objects, even if nonferromagnetic; (3) malfunction of an active implanted medical device (AIMD, i.e., an implant relying on an embedded energy source to function such as a cardiac pacemaker or a neuromodulation system) because of the strong electromagnetic fields used during MRI, which may impact the vital functions of the device or even damage it; and (4) localized heating and resulting tissue damage due to currents in the implant induced by the RF fields and the time-varying gradient magnetic fields (1-3).

Today's MR systems are built to image biological tissues but not to deal with implanted metallic objects and, thus, they have no means to automatically detect and adjust to them even though implemented safety measures are no longer adequate in the presence of metals (4). Ultimately, appropriate safety concepts for scanning patients with implants must be carried out at a *system level*. That is, MR scanners must be designed to detect an implant in the patient and respond accordingly by adjusting scan parameters or, in extreme cases, by rejecting the MRI exam if it cannot be conducted safely. However, this technology is not yet available and, until then, it will remain the responsibility of the MR system operators (i.e., the MRI technologists and radiographers) to ensure the safe scanning of patients with metallic implants.

Severe injuries and fatalities have occurred in patients with implants that underwent MRI (5-10). Most of these incidents were related to dislodgement of a ferromagnetic implant (e.g., an aneurysm clip) or the malfunction of a device, such as a cardiac pacemaker. Severe injuries solely because of excessive implant heating have been documented (8-12). In these instances, RF-induced heating of deep brain stimulation leads was believed to be responsible for the greatest risk during MRI (8-12). Of note is that, in phantom experiments, the temperature at the tip of a long wire may increase by as much as 75°C under certain RF exposure conditions (13).

The present chapter focuses on the state of knowledge on the important topic of MRI-related heating of implants and devices. This attention to this single subject is not because other MRI-related hazards would be less dangerous (the opposite is most certainly true) but because it is (1) omnipresent, and (2) scientifically and practically the most challenging case for a risk assessment (14). Within the limited space of this chapter, we will consider fully incorporated biomedical implants, while interventional and intraoperative devices will not be covered, despite plentiful conceptual similarities.

In the following sections, the underlying physics of implant heating will be presented and summarized. Additionally, the most relevant standardization documents in this field will be recapitulated since they define how both MR systems and implants are designed, built, and tested. Importantly, such standards inform MRI users as to what they can, or rather should not, expect from a device.

516 MRI-Related Heating of Implants and Devices

While this first part aims to provide a conceptual background at a level suited also for general readership, the subsequent sections address mostly the active researchers in the field. Methods to assess and emerging concepts to actively mitigate implant-related hazards in association with MRI technology will be reviewed, with a focus on recent developments. An extensive evaluation of past developments that brought the field to where it stands today is not possible within the present format. MR system users and operators seeking practical advice about scanning or not scanning a patient with implants or devices are kindly referred to the literature, continuously updated websites on this important subject (15, 16), and other chapters in this textbook.

PHYSICS OF IMPLANT HEATING

MRI relies on two time-varying magnetic fields, that is, the RF field and gradient magnetic field, which differ in frequency and amplitude. The sinusoidal RF field, B_1 , is required to excite the spins to be imaged. Usually, it is generated by a volume transmit RF coil like the scanner's body RF coil or a dedicated transmit/receive head RF coil. The design target is a homogeneous B_1 -field over most of the RF coil's geometrical volume. Amplitudes are in the $10 \mu\text{T}$ range and frequencies are in the 100 MHz regime. The gradient magnetic field, B_G , provides spatial encoding for image generation. The water-cooled gradient coils create $B_{(0,z)}$ gradients in three orthogonal directions. The design targets are linearly varying offset fields around the isocenter (where $B_G=0$). Radially, B_G fields are maximal at the MR system's bore; axially, they have maxima around the ends of the gradient coils (i.e., at $|z| \approx 30$ to 50 cm). In modern clinical MR scanners, amplitudes reach the 10 mT regime in those areas. Gradient magnetic fields have base frequencies in the kilohertz range, but higher harmonics up to several 10 kHz often exist.

Faraday's law requires that all time-varying magnetic fields $B(t)$ are accompanied by electric fields $E(t)$, where $E \propto fB$ for sinusoidal $B(t)$ with frequency f . In an electrically conductive metallic implant with conductivity σ , those E -fields drive so-called eddy currents with current densities $J = \sigma E$. This occurs also in biological tissue but is much more dramatic in metals (including "poorly conducting" alloys), which typically have $\sim 10^6$ times higher electrical conductivities. These induced currents have two effects: (1) due to ohmic losses, power $P \propto JE$ is locally deposited *inside* the implant, leading to a temperature increase with an initial slope of $dT/dt = P/C$, where C is the heat capacity of the exposed mass, and (2) secondary B - and E -fields are induced around the implant which superimpose the incident E -field and modify the power deposition. Both effects can lead to tissue heating but the mechanisms depend on frequency and, thus, are very different for gradients and RF fields.

RF-Induced Power Deposition in Tissues Around Implants

Under continuous RF exposure and without heat dissipation, the local tissue temperature in a patient undergoing MRI would rise linearly in time with the absorbed RF power P_{RF} per exposed mass Δm , the so-called specific absorption rate (SAR),

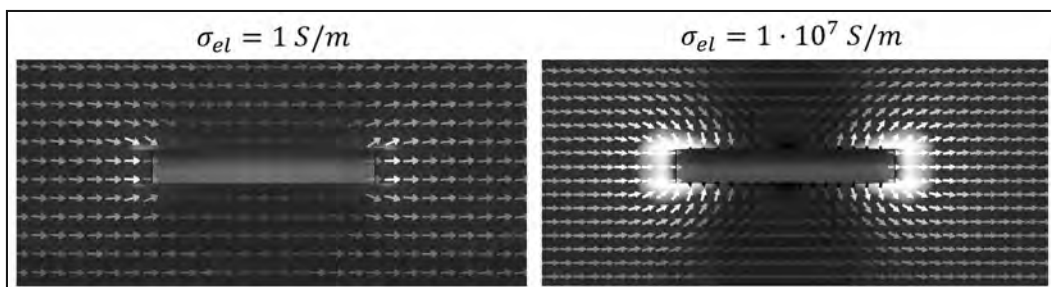
$$\text{SAR} \equiv \frac{\langle P_{RF} \rangle_t}{\Delta m} = \frac{\sigma \langle |E|^2 \rangle_t}{2\rho} , \quad (1)$$

where the angular brackets denote temporal averaging. Electrical conductivity σ and mass density ρ are tissue parameters; E depends on MRI hardware and software, the transmit RF coil, and pulse sequence. SAR is a local quantity since all parameters are position dependent and Equation (1) holds with or without an implant being present.

In a periodic MRI pulse sequence, $\langle P_{RF} \rangle_t$ in Equation (1) is given by the sum of all pulse energies $\int P_{RF} dt$ divided by the repetition time, TR. Consequently, sequences with a short repetition time (TR) and a high density of high-power pulses have increased SAR values. The time-averaged SAR can be modified and limited to safe exposure levels, for example, by reducing the flip angle and, thus, the power per RF pulse, and/or by extending the TR and, thus, the mean time between RF pulses.

RF currents at $f \sim 100$ MHz in metallic objects are restricted to a thin surface layer of about ~ 100 μm by the laws of electrodynamics (i.e., the skin effect). The mass of directly heated implant material remains too small, therefore, to affect the neighboring tissue noticeably. The current-induced secondary E -field (i.e., the “scattered field”) around the implant becomes highly relevant, however, as it can vastly exceed the primary “background” E -field in critical locations. RF currents induced directly in tissue by the scattered E -field are the dominant effect for RF-induced implant heating (**Figure 1**). In particular, a one-dimensional implant tends to exhibit the so-called “antenna effect” which is a pronounced maximum of the scattered E -field at the distal end, whose intensity peaks when the electrical length of the implant is in the range of one-quarter to one-half of the RF wavelength in tissue (17). The electromagnetic energy of the background field is then most effectively converted into implant current and corresponding scattered field.

Figure 1. Simulated electric-field distribution of a vascular stent with varying conductivity. For highly conductive materials such as metals, a scattered field is induced by the current in the stent that exceeds the incident electric field. This scattered field creates E -field (and SAR) hotspots at the ends of the stent. Adapted from color figure in Winter, et al. (1).



518 MRI-Related Heating of Implants and Devices

Gradient-Induced Power Deposition in Implants

In contrast to the RF energy case, secondary E -fields and the direct induction of currents *in tissue* are both negligible for gradient switching at kilohertz frequencies. Switched gradients can heat-up the metallic implant, itself, however, via eddy currents. These currents and the associated power deposition are confined to the metal, but thermal energy diffuses into adjacent tissues, subsequently. Such confined eddy-current loops are intrinsically limited in small or approximately one-dimensional implants (e.g., screws or leads) but are possibly substantial in implants with a large cross-sectional area (e.g., orthopedic prostheses such as total hip or knee replacement implants), where large, low-resistance closed current paths exist (18, 19).

Eddy currents inside a sphere (e.g., the femoral head of a total hip prosthesis) encircle the switched gradient field B_G . Their density is (19):

$$J = \frac{B_G}{\mu_0} \frac{3k^2 R}{2 \sin(kR)} \left[\frac{\sin(kr)}{(kr)^2} - \frac{\cos(kr)}{kr} \right] \sin\theta \quad (2)$$

in a generic radial position, r , with magnetic permeability of vacuum, μ_0 , colatitude θ with respect to the direction of B_G , assumed to be uniform, and $k^2 = -2 \pi i f \mu^0 \sigma$, where $i = \sqrt{-1}$. Equation (2) considers the skin effect and that eddy currents produce a secondary magnetic field perturbing the applied one. In the equatorial plane and for low k (i.e., low $f\sigma$), Equation (2) simplifies to

$$J = \sigma f B_G \pi r . \quad (3a)$$

Equations (2) and (3a) refer to the (complex) amplitudes of (rarely occurring) sinusoidal gradients with frequency f . For generic time-signals $B_G(t)$, Equation (3a) can be expressed as:

$$J(t) = \frac{1}{2} \sigma r \frac{dB_G(t)}{dt} . \quad (3b)$$

A broad variety of gradient waveforms exist but trapezoidal pulses with linear B_G ramps and flat tops are most common. Only the ramps create eddy currents, then, and the flat sections do not contribute. Under the simplifying assumptions of Equation (3b), the induced current density scales with implant conductivity, the change rate of B_G , and the radius, r , of the current loop. The total heating power of those currents depends on the square of the current density.

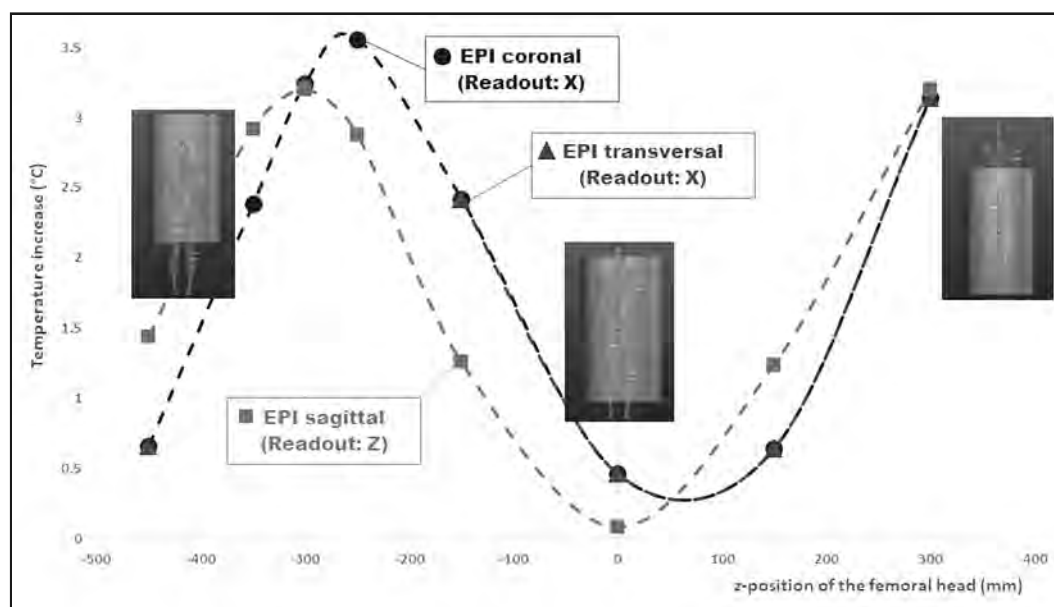
For a given implant, gradient heating is maximal, when the implant is positioned in the aforementioned locations of highest B_G , when the gradients are ramped at the highest available slew rate, and when pulse sequences are run with a high “slew percentage” (i.e., a high fraction of ramp time during the TR). The gradient strength itself is only indirectly a factor, insofar as higher gradients need longer ramp times to reach them.

Few studies on MRI-related gradient magnetic field-induced implant heating exist. Earlier reports did not find significant temperature elevations (20, 21), yet did not systematically investigate critical scenarios, as described in the previous paragraph. More recent work demonstrated that gradient magnetic field-induced heating of a hip prostheses (namely, the acetabular cup component) can increase the temperature in adjacent tissue by several degrees using a manufacturer-provided, “gradient aggressive” pulse sequence, in the aforementioned sense, on a clinical MR system (18, 22–24) (Figure 2). Very close agreement between experimental findings and computational results indicated that the effects are well understood (24).

From Power Deposition to Heating to Tissue Damage

So far, only implant-related changes in the power deposition were discussed, but the hazards are excessive tissue temperatures. As such, temperature is established by the balance between heating and cooling. Implant heating is a local phenomenon and the most widely used description in this context is Pennes Bioheat Equation (PBE) (25), as follows:

Figure 2. Maximum gradient field-induced heating of a total hip prosthesis made of CoCrMo alloy after 12 minutes of continuous exposure to an echo planar imaging pulse sequence performed by standard gradient coils for different readout directions and at different longitudinal positions of the body. The results refer to a gradient strength of 20 mT/m, a repetition time of TR = 43 ms and a readout slew rate of 168 (T/m)/s for a relatively short gradient-coil assembly. Adapted from color figure in Winter, et al. (1).



$$c_t \frac{dT_t}{dt} = \nabla \cdot \left(\frac{k_t}{\rho_t} \nabla T_t \right) + \rho_b c_b w_t (T_b - T_t) + Q_m + Q_{ext} . \quad (4)$$

Parameters are specific heat capacity, c ($\text{W s kg}^{-1} \text{ K}^{-1}$), thermal conductivity, k ($\text{W m}^{-1} \text{ K}^{-1}$), mass density, ρ (kg m^{-3}), and blood perfusion, w ($\text{m}^3 \text{ s}^{-1} \text{ kg}^{-1}$). Subscripts t and b refer to tissue and (arterial) blood, respectively. Tissue temperature change on the left is expressed as the balance of heat diffusion, perfusion cooling, metabolic heat Q_m (W kg^{-1}) and external heat, Q_{ext} (W kg^{-1}), such as SAR. Equilibrium ($d T_t / dt = 0$) is reached when the terms on the right-hand side compensate each other. PBE is not a fundamental law and makes a number of questionable assumptions (e.g., the blood pool as an infinite heat sink, isotropic thermal conduction, inadequate perfusion model, absence of thermoregulation, etc.). Still, it appears to work remarkably well in predicting tissue temperatures (see (26) for an extended discussion).

Thermal modeling is indispensable to assess hazards related to implant heating by gradient switching since the deposited power reaches the tissues only via thermal diffusion. But also for RF energy-induced heating it is highly advisable even though the existing regulations only impose limits on SAR. The tissue parameters k_t , w_t , and Q_m in Equation (4) can vary by orders of magnitude between tissue types (27). Therefore, even a uniform external power deposition would result in a non-uniform distribution of equilibrium temperatures in the human body. Equivalently, it can be said that for a non-uniform SAR distribution, the temperature hotspots will not normally coincide with the SAR hotspots (28). This discrepancy can be further enhanced by the high thermal conductivity of metallic implants. This reduces temperature differences along the implant and tends to “smear” out localized hotspots.

For a conclusive safety assessment, however, even a realistic temperature distribution is not yet sufficient, because tissue types vary not only in cooling properties but also in temperature resilience. For example, 10 minutes at a temperature of 45°C is not much of a problem for skin but it is for brain matter (29). *Thermal Dose* safety concepts, considering the applied temperature over time individually for each tissue type, account for this variation and arguably represent the best that can be done today. The best known example is the “*Cumulative Equivalent Minutes at 43°C* ” (CEM43) approach (29–32). This is beyond the scope of this chapter, however, the present standard is still the whole-body averaged SAR.

RF-Induced vs. Gradient-Induced Heating. As previously mentioned, RF-induced currents in metals are confined to a thin surface layer by the skin effect, while the low-frequency gradient currents fill almost the whole implant volume. Compared to RF fields, gradient switching has a lower frequency content ($<10^5$ Hz vs. $\sim 10^8$ Hz) but a higher magnitude (~ 10 mT vs. ~ 10 μT). The combined effect is that, in “bulky” (i.e., implants with a relatively larger surface area such as an implantable infusion pump or a total hip prosthesis) metallic objects, switched gradients can deposit much more power than RF energy (19). In a non-ferromagnetic sphere (radius $R = 2$ cm, $\sigma = 1$ MS/m, similar to the femoral head of a total hip prosthesis made of cobalt chromium alloy), the power deposition by a gradient magnetic

Table 1. Qualitative comparison of RF-induced and gradient field-induced heating in terms of the implant and pulse sequence parameters.

Parameter	RF-Induced Heating	Gradient-Induced Heating
Implant Size	Most critical: Lengths approximately one-quarter to one-half the RF wave-length in tissue.	Most critical: Bulky implants.
Implant Shape	Most critical: One-dimensional, pointed ends, multiple implants with short gaps between them.	Most critical: Large cross-sections.
Implant Material	Electrical conductivity is less relevant, higher thermal conductivity reduces temperature hotspots.	Higher electrical conductivity gives higher eddy currents. For example, CoCrMo alloy creates ~60% more gradient heating than the alloy, Ti-6Al-4V. Thermal conductivity is less relevant.
Implant Position	Most critical: Regions of highest background E -field. In a conventional transmit body RF coil, this field increases radially with distance from the RF coil axis (where it vanishes). Axially, the field is uniformly high within the footprint of the RF coil; substantial field tails beyond the end of the coil can exist.	Not critical: Isocenter. Critical: Locations in the MR system's bore where B_G -fields are highest, which is towards the ends of the gradient coil, that is, outside the imaging region (Figure 2). Radially, B_G increases monotonically with distance from the magnet axis; axially, a maximum is reached at $ z \approx 30$ to 50 cm from the isocenter (Table 2).
Implant Orientation	Most critical: Implant aligned with the background E -field vector (i.e., parallel to the magnet axis for conventional body RF coils).	Most critical: Large implant cross-section perpendicular to the direction of the switched B_G -fields with high amplitudes.
MRI Sequence Parameters	Most critical: Fast pulse sequences with high density of large flip-angle RF pulses, such as Turbo or Fast Spin Echo. Higher (local and whole-body averaged) SAR as indicated by the scanner corresponds to more critical pulse sequences, but the readings do not account for the implant and different exposure conditions (e.g., scanner, RF coil, subject, position, etc.) cannot be compared.	Most critical: Fast pulse sequences with high slew rates and high slew percentage, for example, echo planar imaging. Critical conditions are not indicated by the MR scanner.

Table 2. Maximum temperature elevation ΔT_{max} versus position z of a total hip prosthesis made of CoCrMo alloy in an MR system after 12 minutes of continuous exposure to a coronal plane, echo planar imaging pulse sequence with frequency encoding along the x -axis. Simulation data from Arduino A, et al. (24). For $z < 0$, $z = 0$, and $z > 0$, the upper body, pelvis, and lower limbs, respectively, are in the imaging position. See also **Figure 2**.

z (mm)	-450	-350	-300	-250	-150	0	150	300
ΔT_{max} (°C)	0.66	2.38	3.24	3.56	2.42	0.46	0.64	3.14

522 MRI-Related Heating of Implants and Devices

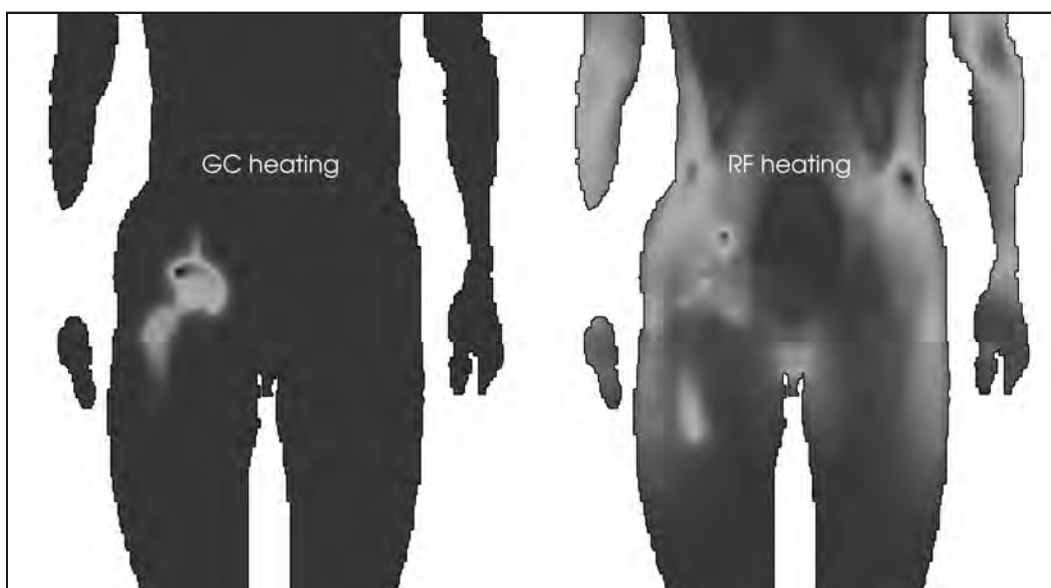
field of $B_G = 6 \text{ mT}$ at $f = 1 \text{ kHz}$ is about 900 mW, compared to 8 mW for an RF field of 10 μT at 64 MHz ($B_0 = 1.5 \text{ T}$) and 10 mW at 128 MHz ($B_0 = 3 \text{ T}$).

The effects of implant and pulse sequence parameters on RF-induced heating and gradient switching-related heating for an implant are compared in **Table 1**. A graphical illustration of the qualitative differences is presented in **Figure 3**. To date, only one study exists where the combined effect of RF energy and gradient heating on hip implants was investigated (33). This investigation demonstrated that either mechanism can prevail, depending on the pulse sequence and the subject's position in the MR system (33).

STANDARDS AND GUIDELINES

With respect to the safety of medical devices, the importance of standards cannot be overestimated. No product makes it to the market unless it conforms to the applicable standards. Therefore, these documents define how medical devices are designed, built, and tested. Furthermore, they inform users about what they can or should not expect from a given device.

Figure 3. Numerical simulations of the same voxel model (male adult with unilateral total hip prostheses) illustrating the different distributions of the temperature elevations resulting from gradient field-induced heating (**left**) versus RF-induced heating (**right**). Gradient field-induced heating is confined to the immediate vicinity of the implant and effective only in extended cross-sections (in this case, the acetabular cup of the total hip prosthesis). RF-induced heating can create hot spots everywhere in the body. The implant-related contribution of RF-induced heating is most prominent at pointed elements such as the tip of the femoral stem or the screw protruding from the acetabular cup. No absolute scales are shown since the exposure conditions cannot be compared. Adapted from color figure in Winter, et al. (1).



A set of international standards was established in recent decades covering implant safety in MRI (34), which was supplemented by recommendations from governmental agencies (35, 36). All refer to the international MRI safety standard from the International Electrotechnical Commission, IEC 60601-2-33, first established in 1995 (37). Below, we summarize the three most relevant standards concerning implant-related heating in the MRI environment, namely ASTM F2182 (38), IEC 60601-2-33 (37), and International Organization for Standardization/Technical Specification, ISO/TS 10974 (39). Note, however, that the instructions of use provided by the MR system manufacturer may be more restrictive than the currently applicable standard. These instructions are legally relevant, because not following them constitutes “off-label” use with potentially severe liability implications for the physician supervisor as well as the MR system operator.

All three standards adopt a scheme from ASTM F2503 (40) where implants are labeled as either *MR Unsafe* (“an item that is known to pose hazards in all MRI environments”), *MR Conditional* (“an item that has been demonstrated to pose no known hazards in a specified MRI environment with specified conditions of use”), or *MR Safe* (“an item that poses no known hazards in all MRI environments”). Note that metallic items can always exert Lenz forces and create image artifacts, which may present diagnostic hazards (41) and hence are never *MR Safe* in this terminology. This labeling is the responsibility of the implant manufacturer who defines the conditions for safe use in association with MRI technology.

ASTM F2182

The American Society for Testing and Materials (ASTM) International standard F2182 is fully designated to RF-induced implant heating (38). It provides the implant manufacturer with well-defined procedures and materials for *in vitro* heating tests of their devices. The standard itself defines no pass or fail criteria. The test results are sent to and evaluated by a competent authority, most notably the United States Food and Drug Administration (FDA), for a decision on the conditionality of the implant for MRI. There are other related ASTM International standards (i.e., ASTM F2052, F2119, F2213, and F2503) that are outside the scope of this chapter.

ASTM F2182 describes in detail a test procedure where the implant under test is embedded in gelled-saline filled phantom setup and exposed to a relatively high, whole-body averaged SAR value (i.e., 2 W/kg or higher) by using either a 1.5 T or 3 T MR scanner or a suitable benchtop system, reproducing the RF fields from a transmit body RF coil operating in a circularly-polarized (CP) mode. For 15 minutes, the temperature is monitored. By repeating the measurement with the implant removed, the background temperature rise is also measured, and the implant-related temperature rise can be determined.

The scope of ASTM F2182 is limited to passive implants that are completely inside the human body. However, similar methods described in ASTM F2182 can be applied for devices penetrating the body’s surface (e.g., external fixation systems, vascular catheters, etc.). Procedures described in ASTM F2182 are also appropriate to perform validation experiments as required by ISO/TS 10974.

524 MRI-Related Heating of Implants and Devices

IEC 60601-2-33

The IEC 60601-2-33 standard is the most relevant safety and performance standard for MRI (37). It provides manufacturers of MR systems with a comprehensive set of criteria and limits, thus allowing them to self-declare conformity if all requirements are met. This standard is generally all about the MR scanner and implant safety is only one of many topics presented in this document.

According to IEC 60601-2-33, the risk of RF field-induced heating of an MR Conditional device should be assessed in terms of the root-mean-square (RMS) averaged, B_{1+RMS}

$$B_{1,RMS}^+ = \sqrt{\int_0^{t_x} \frac{(B_1^+(t))^2 dt}{t_x}} \quad (5)$$

with an averaging period $t_x = 10$ s. From pre-scan flip-angle measurements, the absolute value of B_1^+ can be determined, making B_{1+RMS} a reliably calibrated quantity when averaged over a proper region of interest in a central axial slice. B_{1+RMS} is typically calibrated by the MR system, and its values should be displayed by the MR scanner's software. However, it is important to note that implant heating is related to the total B_1 (i.e., all three vector components), not just B_1^+ , and the standard gives some guidance to estimate the uncertainties when using B_{1+RMS} . This quantity is a much more consistent approach to assess RF-induced implant heating than the whole-body averaged SAR, which was previously the reference metric. In contrast to the whole-body averaged SAR, B_{1+RMS} is independent of the patient and calculated consistently by different MR system manufacturers.

In the latest version of IEC 60601-2-33, the so-called Fixed-Parameter Option (FPO) was introduced for 1.5 T MR scanners (FPO:B), which specifically addresses scanning patients with implants. In the FPO:B mode, both the RF and the gradient outputs are restricted, and the MR system manufacturer guarantees that specified maximum values are nowhere exceeded, within a defined volume in the bore of the MR scanner. Important FPO:B limit values are $B_{1+RMS} = 3.2 \mu\text{T}$ and $(dB_G)/dt|_{RMS} = 56 \text{ T/s}$ where

$$\left| \frac{dB_G}{dt} \right|_{RMS} = \sqrt{\int_0^{t_x} \frac{\left(\left| \frac{dB_G}{dt} \right| \right)^2 d\tau}{t_x}} \quad (6)$$

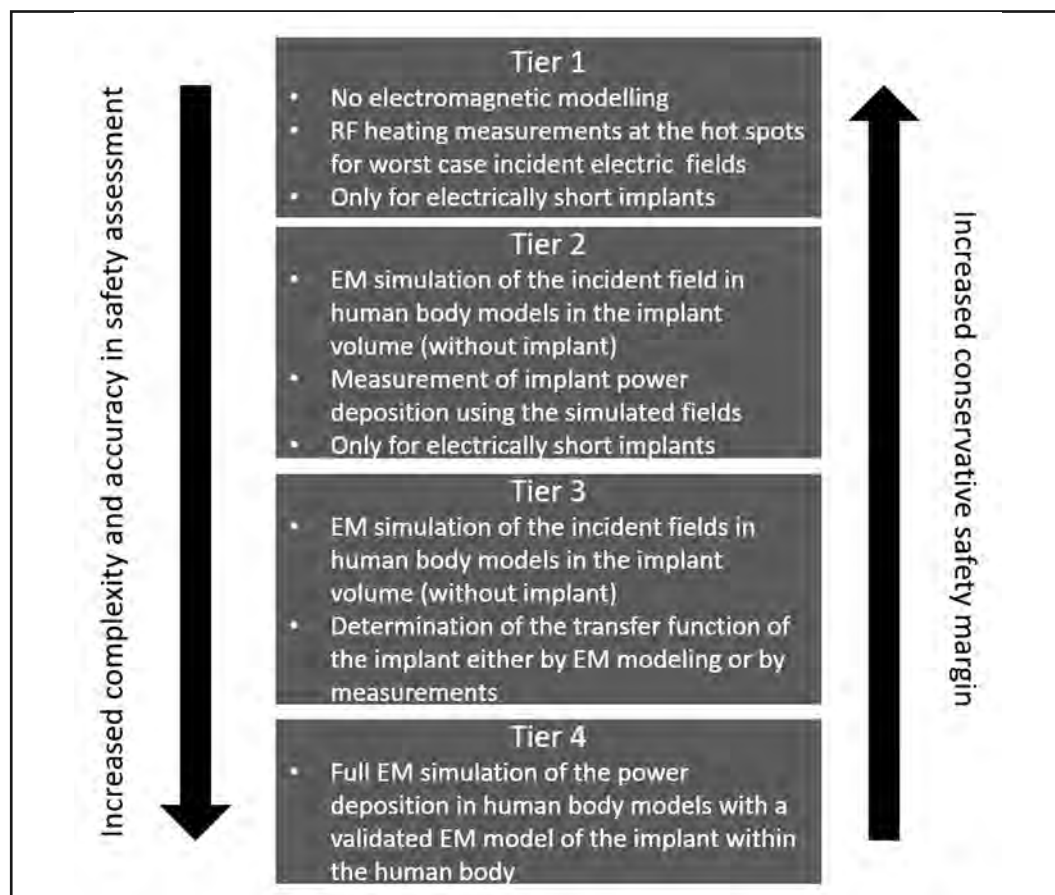
is the time-averaged temporal derivative of the gradient field. The latter limit relates to gradient-induced implant heating but was introduced primarily to protect the device from damage. Note that the FPO:B limits do not by themselves define "safe scan" conditions. The FPO rationale is that the MR system manufacturer guarantees that those field limits are kept, such that implant manufacturers can design and test their devices, accordingly. Only the combination, that is, a MR system operating in the FPO mode and an FPO-approved implant or device, would then establish a safe setting for the patient. The problem of the FPO is that a single set of field limits must suffice for a large variety of medical im-

plants. Up to now, medical implants labeled as MR Conditional with respect to FPO:B are very rare. The FPO approach is unlikely to reappear in future editions of the standard.

ISO/TS 10974:2018

The ISO/TS 10974:2018 is the first comprehensive standardization document on active implantable medical devices (AIMD) in an MRI context (39). The purpose of this document is to provide manufacturers of active implants with defined procedures and methods to assess the MRI safety aspects of their devices. Conceptually, it is the active implant's counterpart of ASTM F2182, which covers only passive implants. In its current version, the scope is restricted to 1.5 T scanners with cylindrical bore and body RF coil excitation. With respect to RF-induced heating, the standard deals with implant-related effects only, and not with possible background-SAR hotspots elsewhere in the body (which are covered by IEC 60601-2-33).

Figure 4. Schematic of the 4 Tier approach for implant-safety assessments in the ISO/TS 10974 standard (39). Each level increases the complexity of the simulations and/or testing methods, but at the same time increases the accuracy and decreases the overestimation of RF-induced heating, which allows for safe, but less conservative safety margins. Adapted from Winter, et al. (1).



526 MRI-Related Heating of Implants and Devices

To determine the RF power deposition, a four-tiered approach is prescribed (**Figure 4**). The tiers represent different levels of complexity and accuracy. Lower levels are synonymous with lower accuracy and larger safety margins that need to be applied. Tier 1 does not require electromagnetic modeling. Tier 2 uses simulated human RF exposures to “determine the electric field in the implant volume of interest”. Tiers 1 and 2 are restricted to “electrically short” AIMDs, since phase effects are not included. For Tier 3, an equivalent electromagnetic model of the AIMD is required to determine the transfer function (42). Tier 4 assesses the AIMD electromagnetic model within anatomical models for relevant RF field exposure conditions. Except for very simple implants, the Tier 4 approach is the most challenging, requiring state-of-the-art computational capabilities.

Detailed requirements are given on how measurements should be performed to validate the simulations. ISO/TS 10974 also deals with gradient-induced device heating in a tiered approach.

METHODS TO ASSESS IMPLANT SAFETY

Simplifications

Long, one-dimensional shaped implants (e.g., cardiac pacemaker leads) collect RF energy over their entire length which makes them potentially hazardous and simultaneously defies simplifying assumptions like a constant E -field, in magnitude and phase, over the entire implant. Their structural detail, for example, a finely wound helix or multiple electrodes, and steep field gradients near the implant call for a high mesh resolution but the simulation space, defined by the transmit body RF coil, remains large. To aggravate the problem, the trajectories for long leads are not well defined and, thus, a variety of different clinically relevant pathways needs to be investigated. Numerical simplification approaches exist and are widely used, such as the Huygens box concept where a high-resolution simulation of the implant region is embedded in a lower-resolution simulation of the rest of the body (43). For a discussion of the pros and cons of such procedures, the reader is referred to specialized reviews on numerical techniques including the work by Li, et al. (44).

To simplify the geometry, helices are often modeled as straight wires plus lumped elements to account for their inductance or stents as cylinders, ignoring their complex wire-mesh structure (45, 46). Despite these efforts, full Tier 4 simulations are not yet feasible with normal computational resources, and Tier 3 represents the actual state of the art. There, first the full-scale native problem, that is, a numerical body model without the implant in an MR scanner, is computed at an appropriate resolution providing the spatial distribution of the unperturbed background E -field. This part may be repeated for different body models, positions, postures, or transmit RF coils, resulting in a library of background fields. In a second step, the electrodynamic response of the metallic implant to that background field is computed. Frequently, this is expressed as the “scattered field,” that is, the difference between the total E -field with the implant and background field.

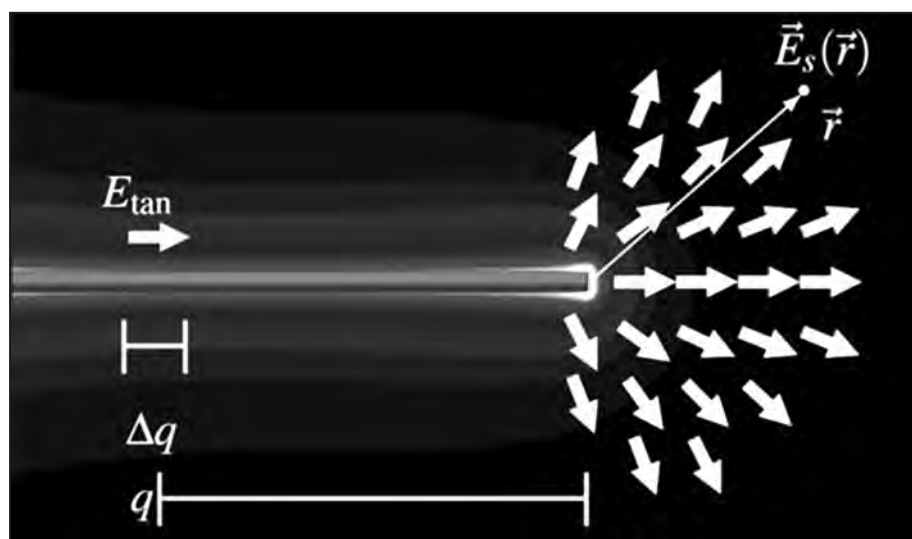
The critical spot of a wire-like implant is always at the distal tip and a frequent simplification, therefore, is to ignore all other locations. The scattered field at the tip can be derived from the background-field distribution along the implant trajectory. A first step in that di-

rection was the definition of a “safety index” as a metric to characterize one-dimensional implants (47). Later, this was succeeded by the introduction of the transfer function (TF) (42), the most widely-used approach to assess the MRI safety of one-dimensional implants today. To determine the scattered E -field at some reference \vec{r} in tissue, close to the tip, one needs to know the response $E_s(\vec{r})$ of the E -field at the reference point to a unit tangential E -field applied somewhere along the implant (**Figure 5**). The latter location is uniquely identified by a scalar coordinate, \hat{z} measuring its distance from the tip along the implant trajectory. This response can be expressed as a complex weight function $S(\hat{z}, \vec{r})$ and the desired ‘scattered’ field $E_s(\vec{r})$ can then be obtained by integrating the weighted tangential background field $E_{tan}(\hat{z})$ along the wire:

$$\vec{E}_s(\vec{r}) = \vec{F}_{tip}(\vec{r}) \int_0^L S(\hat{z}) E_{tan}(\hat{z}) d\hat{z} . \quad (7)$$

The normalized, dimensionless function $\vec{F}_{tip}(\vec{r})$ describes the spatial distribution of the scattered E -field around the tip and is assumed to be independent of how the implant was excited. Thus, the problem is broken down into two independent steps, namely to determine (1) the background E -field without implant, and (2) the transfer function $S(\hat{z})$ of the implant. The former means a state-of-the-art EMF simulation, the latter can be achieved either by simulations or experimentally. TF is a normalized, complex function, determining how various elementary RF currents induced along the length of the implant superimpose at the tip.

Figure 5. Graphical representation of the transfer function introduced by Park, et al. (42). A piece-wise excitation with an incident tangential electric field E_{tan} induces a scattered electric field $\vec{E}_s(\vec{r})$ at the tip of a one-dimensional implant. Adapted from color figure in Winter, et al. (1), original figure from Tokaya, et al. (48). The length coordinate q in this figure is denoted \hat{z} in the present chapter (**Equation 7**).



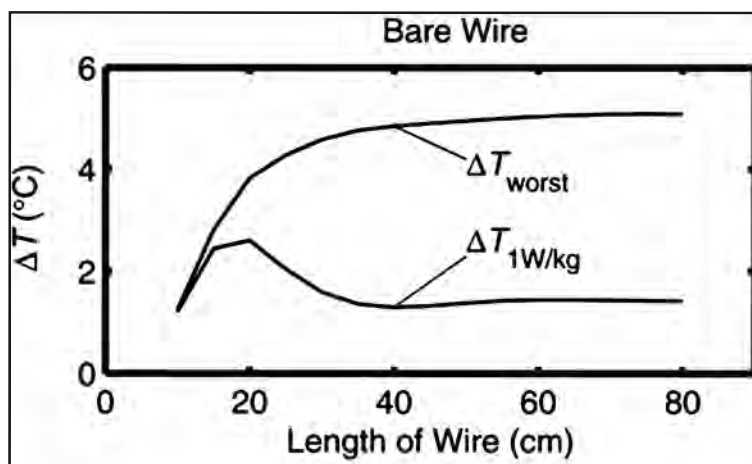
528 MRI-Related Heating of Implants and Devices

In this instance, the TF phase describes the propagation and the TF magnitude the attenuation of an RF current along the implant. In the simplest case, the TF phase would be a linear function of the distance from the tip. The E -field “collected” within a certain distance from the tip would then increase the scattered field around the tip while contributions from beyond that point would decrease it again (**Figure 6**). For longer distances, attenuation dampens the interference pattern, but a critical “resonance length” of one quarter to one half the RF current wavelength persists. This wavelength, and hence the TF, depend on the dielectric parameters of the tissue and possibly an insulation surrounding the implant. The TF of an implant depends on its environment, therefore, but for simplicity this fact is often ignored. For unfavorable phase distributions of the background E -field the tip heating can significantly exceed even the values for the resonant length (**Figure 6**).

The TF can be determined by measuring or calculating the scattered E -field at some reference point, \vec{r} close to the tip when the implant is exposed to a piece-wise excitation by a unity tangential E -field. In simulations, this can be approximated artificially by a short boxcar function (42) or as the E -field between two parallel metallic plates in close proximity to one another (48). Experimentally, for example, short toroid coils or coaxial cables with a few millimeters of bare inner conductor can be used (49, 50).

An important advancement to reduce the multitude of piece-wise excitations and measurements (and/or simulations) to a single excitation is based on the principle of reciprocity (51). Injecting a unit current at its tip, the TF is represented by the current distribution along the implant and several experimental strategies were proposed to determine this current (50, 52, 53).

Figure 6. Temperature increase at the tip of a bare wire as a function of wire length for RF exposure at 64 MHz. For a uniform phase distribution, the temperature increase ($\Delta T_{1W/kg}$) shows a maximum at a “resonance length” of roughly half the RF wavelength in the phantom medium. If the phase distribution is non-uniform over the implant (ΔT_{worst} = temperature increase for a worst-case phase distribution), which is often the case for relatively long implants, the tip temperature can increase even above the resonant length of the wire. Reproduced from Winter, et al. (1), original figure from Park, et al. (42).



Numerical Simulations. The numerical assessment of implant heating in the MR scanner involves a whole chain of exposure assessments, which can broadly be categorized into (1) three-dimensional (3D), computer aided design (CAD) models of RF or gradient coil, implant, and patient, (2) the electromagnetic simulation including dielectric properties of all involved tissues and electrical elements, and (3) the thermal simulation along with thermal and physiological tissue parameters.

Here, we focus on the implant-related aspects of simulations. A more detailed overview of electromagnetic-simulation techniques in an MRI safety context, in general, can be found, in the work by Fiedler, et al. (54).

Realistic Simulation and Body Models. If the 3D-CAD model of an implant cannot be obtained from the manufacturer, an electrically equivalent simulation model could be created from the actual implant, based on its geometry, composition, and size. Transmit RF and gradient coils are integral parts of the MR scanner and their actual design is more difficult to create. However, RF field measurements can be utilized to give a good estimate about the design, length, and diameter of commercial transmit body RF coils (55, 56). Regularly at 7 T but occasionally at lower field strengths, too, local transmit-receive RF coils are used (e.g., for head or knee MRI exams). In such a case, safety assessments of implants are only possible if the RF fields or the transmit RF coil model are known (57, 58). It is important to apply the correct transmit coil-driving conditions (e.g., circularly-polarized, CP, quadrature-driven). Transmit RF body coils of 1.5 T MR systems typically apply only the CP mode, whereas at 3 T and above, RF shimming is common to counteract B_{\perp}^+ inhomogeneities (59–61).

The distribution of the gradient magnetic field B_G can be derived from quasi-static field measurements or manufacture-provided field maps, if available.

Regarding numerical body models, a wide range is available with increasing resolution and quality (62–64). An extensive review on body models for electromagnetic simulations has been provided by Makarov, et al. (65).

The dielectric properties of human tissues can be assigned according to literature values. The publication by Gabriel, et al. (66) is the pioneering paper in this respect, while the wealth of today's knowledge in this field has been conveniently compiled in a comprehensive database of electromagnetic and thermal tissue parameters (27).

Electromagnetic Simulation Techniques – RF Fields and Currents. There are several simulation techniques in computational electromagnetics, each with advantages and weaknesses. For birdcage coils, the method of moments (MOM) also called the Boundary Element Method (BEM), or the finite elements method (FEM) may be the best choices, because they can treat curved geometrical objects more accurately than other techniques. However, when complex anatomical models or structures are involved, the simulation space can easily reach dimensions of 100 million voxels (three-dimensional pixels) or more, which is most efficiently handled by the finite-difference time-domain (FDTD) technique.

It has been shown that the common practice of simulating the metallic implant as a perfect electric conductor is sufficient for practical purposes (67). Thus, it is unnecessary to

530 MRI-Related Heating of Implants and Devices

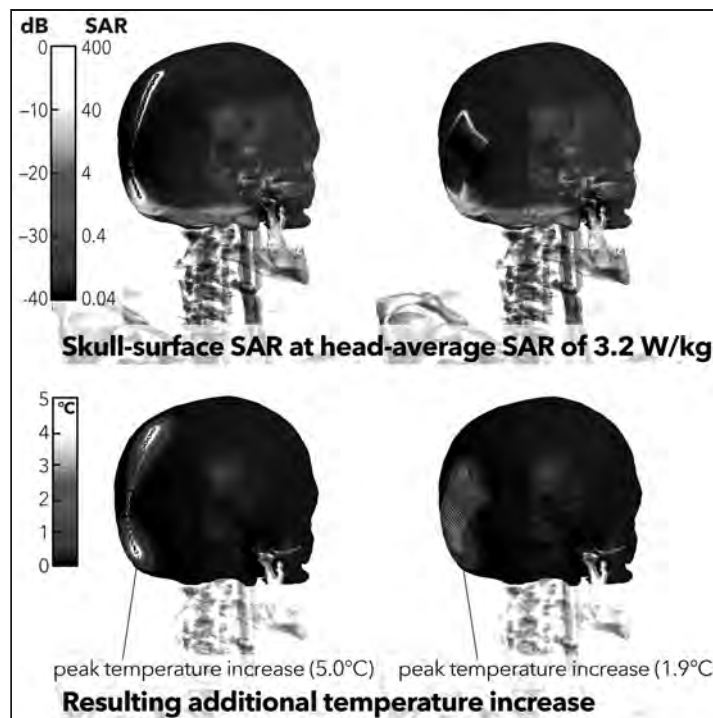
discretize the implant on the 10 μm scale of the RF penetration depth. Calculations can be parallelized on graphics processors, thus shortening simulation times by factors >100. The simulation output contains the induced E -field distribution in the patient for a given exposure scenario and can be expressed as SAR maps, which are subjected to different averaging volumes. The most important of which are the whole-body averaged SAR and the local SAR averaged over 10 g of tissue (37). For implants, there is an ongoing discussion whether smaller averaging masses should be used to assess temperature and thermal dose more correctly (45, 68, 69).

The exposure condition in the simulation model such as linearly-polarized, CP, or RF shimming, is important and needs to match reality since it determines the background E -field distribution responsible for the RF field-induced implant heating. With state-of-the-art electromagnetic modeling, satisfactory agreement (for the given purpose) with phantom measurements can be obtained and (standard) uncertainties in the range of 10 to 15% (70) should be achieved for local SAR values, because the dielectric properties of the tissues are only minimally affected by the physiological response.

Electromagnetic Simulation Techniques – Gradient Fields and Induced Currents. Most investigations dealing with the simulations of gradient-induced heating of bulky implants adopt the hybrid FEM/BEM frequency-domain formulation described by Zilberti, et al. (22). Such a formulation applies to non-magnetic metallic implants and, at the frequencies of interest, assumes that the current density induced inside bulky implants is much higher than in the surrounding tissues, thus limiting the electromagnetic problem to the implant volume. To simulate a gradient sequence realistically, the harmonic solutions are moved back to the time domain, where they are properly combined to follow the actual waveforms of the three gradient coils.

Electromagnetic Simulation Techniques – Thermal Simulations. The power-density distribution from electromagnetic simulations can be used as input for thermal simulations (**Figure 7**). For one-dimensional implants, RF power is absorbed along the whole length of the lead(s) but tissue heating occurs only around the tip or end and this fact can be exploited to reduce the total computational burden (71). Steady-state solvers can be used when only absolute equilibrium temperatures are of interest. To simulate temperature increase versus time, more complex transient time-domain solvers are required. As previously-stated, Pennes Bioheat Equation (PBE) (25) is presumably the most widely used formulation, and most commercial software to calculate tissue temperatures employs PBE or amended variants, for example, with thermoregulation included (i.e., temperature dependent tissue parameters). It performs well for the given exposure scenarios but is a heatsink model assuming stable core temperatures. If a patient's core temperature increase must be considered, the PBE can be enhanced by a variable blood temperature formulation. Other aspects remain neglected, however, such as anisotropic heat-flux or blood temperature variations along the vessel. For the latter, the impact of the thermal vasculature could be investigated based on a model which couples, one-dimensional convective vascular tree thermal simulations with 3D thermal modeling (72). While the PBE assumes that the arterial inflow to tissue is still at core temperature, such discrete vasculature (DIVA) models (73) acknowledge the flow directionality and the gradual thermalization of blood along the (arterial) vas-

Figure 7. Electromagnetic and temperature modeling and simulations of two different implant types positioned on the skull of a human body model. The SAR can be calculated based on the RF power deposition and used in the temperature simulations to determine the peak temperature increase at the implant for a given input power to the transmit RF coil. Adapted from color figure in Winter, et al. (1).



cular tree. Other formulations are also being used, such as the generic bioheat transfer model (74).

The total uncertainty for modeling the relatively high local temperature increase in MRI is about 20 to 30% (standard uncertainty) (32), with the largest contributions from tissue perfusion and thermoregulatory response.

Towards Subject Specific Models – Morphing and Image Registration. Sophisticated electromagnetic modeling can be performed on virtual body models, but these models never represent the true patient geometry. Personalized exposure evaluations might permit the reduction of the necessary safety margins for the majority of the patient population and, consequently, permit faster and safer MRI exams: for example, a dynamic adaptation of exposure limits based on the patient's body mass index (BMI) or body cross-section (70). We will briefly discuss two methods: a physics-based morphing and a three-dimensional image-registration approach.

A physics-based morphing technique can be applied on existing anatomical models via constrained biomechanical FEM simulations, where the body is treated as a hyper-elastic material (75, 76). The tissue deformation is constrained by the proximity of rigid bones and

532 MRI-Related Heating of Implants and Devices

regularized by the presence of surrounding soft tissue. This allows regional shrinkage or expansion of certain tissues (e.g., fat, muscle, etc.) to investigate the effect of different tissue distributions. A look-up table can be generated, where the actual patient would be matched to the closest morphing variant of an anatomical model. Pre-computed exposure data would serve as a coarse personalized estimate.

If a certain target anatomy of the actual patient is aimed for in higher detail, a 3D image registration is better suited to capture the actual skeletal anatomy and posture. Sparse (e.g., cross-sectional) pilot-scan images of the patient could be used as input for the non-rigid registration approach to map the numerical phantom to the patient-specific anatomy (77-79). The resulting 3D-registered derivative can then be used to compute the exposure estimation on-the-fly. Unfortunately, as of today, personalized electromagnetic simulations are not yet in widespread use.

Measurements

Measurement procedures for *in vitro* model validation are well described in ISO/TS 10974 (39). Assessments can be performed at points of interest near the implant, by measuring either (1) electromagnetic-field quantities using time-domain sensors, or (2) root-mean-square (RMS) quantities like voltage or temperature. Fiber-optic temperature probes are the most widely used sensors for safety assessments involving patients and metallic implants in MRI (11). They use a non-conducting transmission medium and are nonferromagnetic, preventing RF coupling and enabling a precise and accurate application to record temperatures in the harsh electromagnetic environment associated with the MR system. Importantly, in order to obtain an accurate assessment of temperatures, probe positioning relative to the implant is crucial. For example, for a peak temperature of 10°C, a 1°C change can be observed over less than 250 μm (80).

Time-domain probes yield information on amplitudes and phases of field quantities which is necessary, for example, for TF measurements (50, 81). For *in situ* applications in the MR scanner, the field probes must be nonferromagnetic and must not generate static magnetic fields by internal DC currents. Examples of *in situ* RF current measurements on implanted wires using optical fibers for signal transfer have been reported by Zanchi, et al. (13) and Weidemann, et al. (82). Recently, fully optical *E*-field measurements based on electro-optic field sensing have been used to assess the RF safety of different stent configurations (83). While this technique is promising, it is too premature for a final judgment with respect to its validity.

Another approach to perform *in situ* measurements especially in active devices is the use of already built-in sensors. Due to the lack of a phase reference, this appears to be limited to RMS measurements so far, but this issue may be resolved in the near future using state-of-the-art electronics. In a proof-of-principle investigation, it was shown that the temperature at the tip of an implanted pacemaker lead surrogate can be reliably measured during *in vivo* MRI using wireless data transfer (84).

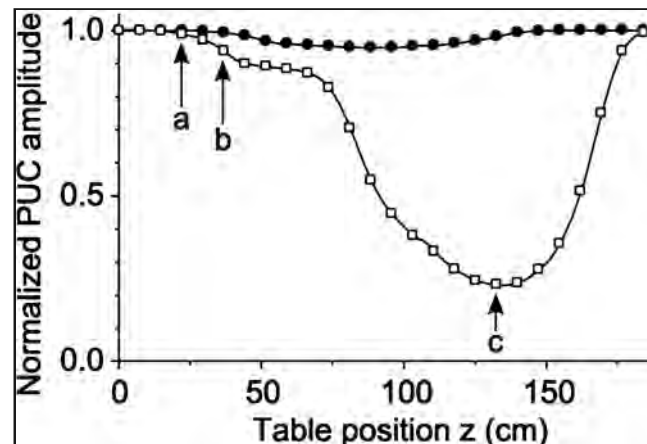
In Vivo Assessments of Implant Safety

Recently, methods have been investigated to assess implant safety *in vivo* by MR-based methods. This methodology, if further developed and validated, would enable patient-specific safety evaluations of implanted devices. Approaches to “put the implant patient in the scanner and see what happens” exist (85) and are not automatically unethical, if done with the necessary caution. Still, they are not discussed here as they do little to quantify the patient hazard.

Non-MR Based Methods. A metallic implant with strong coupling to the transmit RF coil causes substantial impedance changes. These can be measured via the RF coil’s current distribution or scattering (S) parameters and related to the induced current strengths and the location of the implant if a multichannel transmission system is used (86–88) (**Figure 8**). Such an “implant detector” at an MR system level would solve many problems, only it would be very difficult to ensure that every hazardous implant is detected.

Another method to determine potential RF field-induced heating *in vivo* independently of prior simulations is the use of integrated temperature sensors in the implant at locations where the maximum temperature increase is expected (84, 89). Alternatively, the thermo-acoustic effect can be utilized for external temperature monitoring (90, 91). The latter exploits the pressure waves that a sudden temperature increase inevitably generates and can be detected by sensitive acoustic receivers. It has been shown in a proof-of-concept study that this ultrasound signal can be used to detect RF field-induced heating of a lead tip and,

Figure 8. Normalized signal from a pick-up coil (PUC) as a measure of the current in one element of a parallel-transmit (pTx) coil array when a phantom with (open squares) and without (solid dots) a disconnected cardiac pacemaker lead inside is moved through the MR system. Decreased pick-up signal reflects increased coupling of the load (i.e., the phantom plus implant) to the RF coil element. Temperature measurements at patient table positions, **a** and **b**, showed no or negligible heating, respectively, while a temperature increase of 43.7 K within 30 seconds was observed at position **c**, indicating a strong correlation between the detected RF coil-implant coupling and the heating effect. Adapted from color figure in Winter, et al. (1), original figure from Graesslin, et al. (86).



534 MRI-Related Heating of Implants and Devices

therefore, could be utilized in a pre-scan MRI procedure (91). Translating such ultrasound-based systems to a robust clinical *in vivo* application is challenging, however (i.e., due to receiver size and positioning, movement, acoustic window, signal-to-noise constraints, quantified measurements etc.), and still needs to be demonstrated.

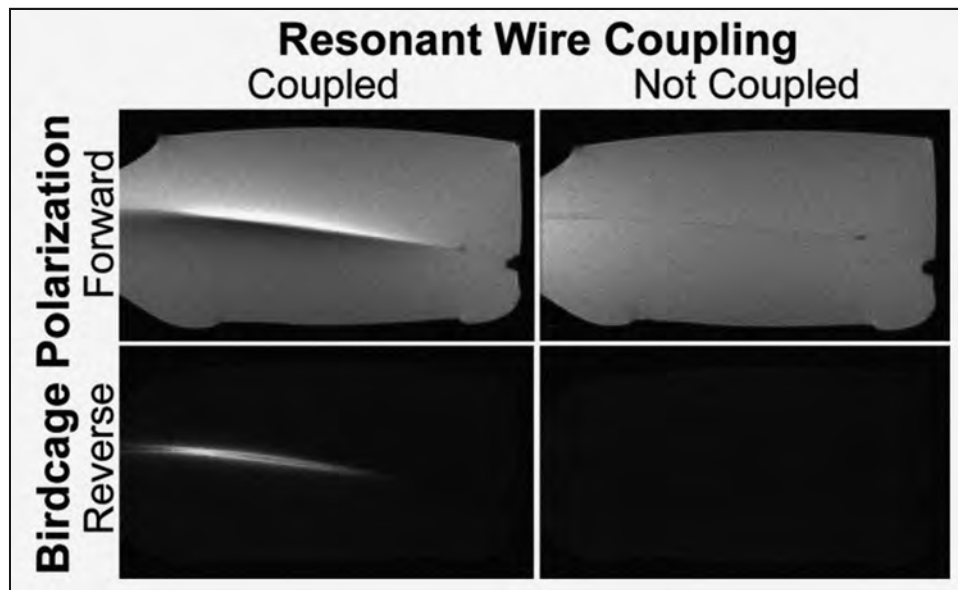
MR-Based Methods. The MR scanner itself is a versatile machine, and several publications demonstrated that it could be utilized for a noninvasive, implant safety assessment and monitoring, *in vivo*. However, this is ongoing research and not yet routinely available.

For elongated implants, tip heating is related to the induced RF currents in the implant (92), which then induce a new $B_{1,ind}$ -field altering the total B_1^+ . Consequently, tip heating can be estimated by MR-based measurements of B_1^+ around the implant (93, 94) (**Figure 9**). If $B_{1,ind}$ has a z -component, it will also shift the RF phase (95).

Implant-related image B_1 effects can also be translated to direct measurements of the induced RF current in the implant. This may appear as a detour because, ultimately, the quantity of interest is temperature, and implant current is only a surrogate. The advantage of current measurements is their sensitivity. In principle, relatively small and harmless implant currents are detectable *in vivo*, while a measurable temperature rise may be potentially hazardous for the patient. Frequently, model assumption like a perfect quadrature excitation or simplifications like a quasi-static treatment neglecting displacement currents are being used to facilitate direct current quantification without extensive numerical simulations. The measured B_1^+ magnitude at a certain radius from the conductor can be converted into the magnitude of the current by applying a simplified Ampere's circuit law (96–98). The background signal around the lead, which *in vivo* is often inhomogeneous, represents a source of error for magnitude-based methods. A way to suppress this background signal is by using reversed RF polarization on the transmitter and receiver (98) (**Figure 9**). In this manner, ideally only the implant coupling is visualized in the MR image and can be used to determine the current amplitude. On the receiver side, reverse polarization reconstruction is intrinsic to the acquired dataset, while on the transmit side, parallel RF transmission (pTx) systems with ≥ 2 channels would allow for reversed polarization during transmission.

Another method to quantify induced currents is based on analyzing the phase of an MR image around the implant (99). This way, RF field-induced implant currents can be detected with a low SAR, pre-scan sequence that poses no hazard in itself. Since the RMS-averaged RF current in the implant is proportional to B_{1+RMS} , the result from the pre-scan can easily be scaled to subsequent MR imaging sequences at higher SAR levels. Compared to magnitude-based methods, phase-based current measurements are potentially faster, independent of proton-density weighting and have lower SNR requirements. A disadvantage of phase-based methods is their sensitivity to gradient nonlinearities and phase variations of other origin, such as frequency shifts due to temperature variations, susceptibility jumps at interfaces, or blood flow. To reduce these influences, short echo times combined with a fast read-out using an ultra-short echo time (UTE) sequence was applied *in vivo* and demonstrated the ability to characterize RF currents within an accuracy of ~ 10 mA/ μ T (100). Based on these measurements and some simplifying assumptions, the corresponding RF-induced implant heating could be predicted accurately. Another relatively simple method to assess not only the current magnitude but also its phase *in vivo* is based on using multi-channel receive

Figure 9. MR image artifacts associated with induced current in a wire. If the wire is not coupled to the RF fields, only small signal changes indicate the location of the wire. If the wire is coupled to the transmitted RF energy, the current induced in the wire alters the B_{\perp}^+ distribution in its vicinity and leads to severe signal changes, resulting in bright and dark spots along the wire. Reversing the polarization of the birdcage RF coil shows only the wire currents, while the background signal disappears. Reproduced from Winter, et al. (1), original figure from Overall, et al. (98).

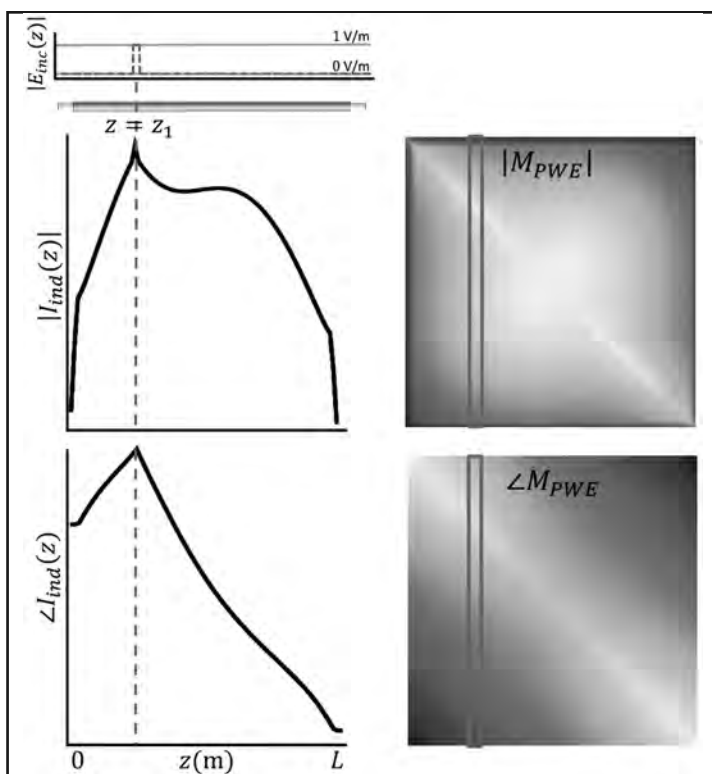


coils; it was applied for analyzing the image artifact around a deep brain stimulation (DBS) lead (101). Typically, two null-locations can be identified in the signal intensity emerging from the transmitter and receiver separately. Since the location of the receiver-null is independent of the transmitter and different for each receiver element, the receiver-null and transmitter-null locations can be identified independently by inspecting the MR images from each receive-coil element separately. The phase of the current can then be calculated from the geometric null location and is an important parameter to allow mitigation of RF field-induced currents on the DBS lead using pTx systems (101).

The MR-based determination of the transfer function represents another promising approach to measure implant currents (48, 102). This expands the TF approach beyond phantoms to more complex exposure scenarios with realistic tissue heterogeneity, implant geometry and location. The methodology uses the wire-like implant as a transceiver antenna. The implant is excited via a coaxial cable soldered to its tip and the resulting current distribution along its trajectory, reflecting the transfer function by virtue of the principle of reciprocity—can be measured by MRI (48, 51). The necessity to connect a cable to the implant modifies the TF, however, and prevents *in vivo* applications. This restriction was overcome by the introduction of the transfer matrix. This approach measures the RF field-induced currents in the implant directly and without the need of any galvanic contact from MR measurements alone (102–104) (**Figure 10**). The transfer matrix derived from this data contains

536 MRI-Related Heating of Implants and Devices

Figure 10. Simulation based construction of the transfer matrix by applying a localized incident electric field. The rows of the transfer matrix are the current distributions for the various excitations. The transfer function is the first column of the transfer matrix. The transfer matrix for an implant can be determined solely by MRI measurements, that is, B_1^+ , and transceiver phase distributions. Adapted from color figure in Winter, et al. (1), original figure from Tokaya, et al. (103).



not only the full TF, but additionally determines the total current along the implant for a given exposure situation. This allows not only the ability to fully evaluate tip heating based on an incident background field but also to assess other locations of potential RF-induced heating along the implant. Like its “ancestor” TF, the transfer matrix describes how the implant responds to a pre-existing background E -field. Therefore, the latter must be known, that is, simulations are still required while the aforementioned sensor-based methods are, in principle, independent of such prior knowledge. The techniques applied for transfer-matrix acquisition have similarities with electric-properties tomography (EPT) (105, 106) and consequently share some of its problems as well, most notably the transceive-phase approximation and assumptions on the vector orientation of B_1^+ and E .

Most of these described MR-based techniques to assess implant safety still need further investigations, in particular if more complex implant geometries or locations, multiple implants or complex lead trajectories come into play. Also, most of these MR-based current-measurement techniques assume a homogeneous or known B_1 transmit and/or receive field to work accurately (100, 101). These assumptions are increasingly difficult to attain at higher field strengths, which may limit the general applicability of such methods.

Current measurements are only an indirect measure of implant heating because they rely on thermal models that might be incomplete (e.g., neglecting perfusion or thermoregulation). Measuring temperatures around the implant is a more direct assessment of implant safety and a variety of temperature-dependent MR contrasts exists that can be exploited for that purpose (107, 108). As of today, however, MR thermometry could not replace RF-power monitoring in conjunction with dedicated SAR models as an MRI-related safety

monitor. One reason is its vulnerability to subject-specific error sources that may compromise temperature-reading accuracy *in vivo* beyond acceptable levels. In the presence of implants, accurate MR thermometry is even more challenging due to additional artifacts and signal voids around implants. Nevertheless, several studies have been performed showing the potential of MR thermometry around implants to assess heating with reasonable accuracies $<1^{\circ}\text{C}$ compared to fiber-optic thermometry (45, 109). Additional research is warranted to study the development and validation of robust, fast and accurate MR thermometry for *in vivo* applications around implants, which has an enormous potential impact on patient safety.

MITIGATION STRATEGIES

Mitigation strategies, that is, active countermeasures against implant heating, can target either the background *E*-field the implant is exposed to or the scattered *E*-field generated by the implant. The latter methods may require the implant manufacturer to modify the implant in terms of geometry, size, or materials, while the former addresses the MR system manufacturer because it requires variations in transmit RF coil design or transmission-field properties to reduce heating independently of the implant type. Mitigation of gradient field-induced heating is not yet supported by implant or scanner manufacturers. Therefore, to date, it is up to the MR system operator's common sense to avoid critical scenarios that may be injurious to patients.

Implant Geometry and Materials

Suppressing RF field-induced currents by replacing electrically conductive material is the ideal solution but not always feasible. Other alterations of the implant structure can be implemented, which at least reduce RF-induced currents and possibly allow them to shift their occurrence to less critical areas. These techniques can be grouped into the following approaches:

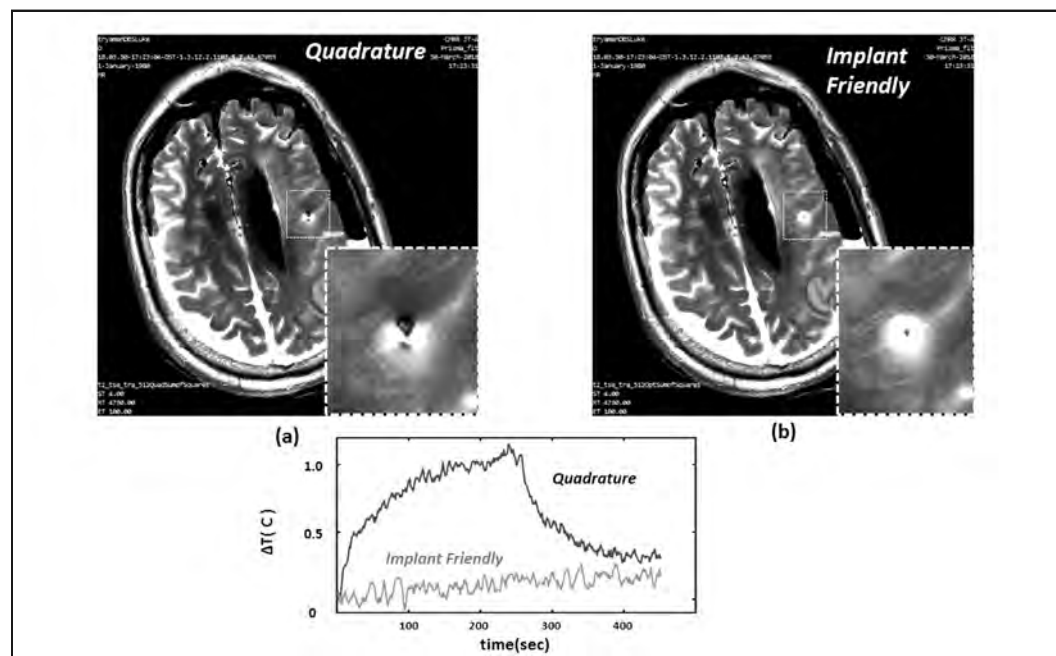
- 1) Increasing the resistivity of the implant reduces the induced currents (110–112).
- 2) Increasing the capacitance (permittivity and thickness) and conductivity of the insulation around the conductor attenuates the wave propagation along the conductor (113).
- 3) Implementing “RF chokes” or traps, that is, resonating circuits tuned to block RF currents at the Larmor frequency (112, 114, 115).
- 4) Adding inductances (e.g., by helical winding for one-dimensional implants) or capacitances (e.g., by adding dielectric materials) along the conductive lengths of the implant (116–119). This way, low-pass or high-pass filters are implemented, blocking or reducing RF-induced currents along the implant.
- 5) Cloaking the implant by using metamaterials (i.e., material engineered to have a property not found in naturally occurring materials) to reduce RF field interactions (120, 121).

While approaches (1), (2) and (5) focus on reducing the magnitude of the induced current, approaches (3) and (4) change the effective resonant length of the wire/implant. In the latter case, the result is frequency dependent, implying that the same configuration that safely reduces heating at 1.5 T/64 MHz might not be working effectively at 3 T/128 MHz, and vice versa.

Parallel Transmission

Each transmit RF coil produces a characteristic *E*-field distribution inside the human body. If a second coil element with another characteristic *E*-field distribution is added, the overall incident *E*-field is a coherent superposition of both *E*-field vectors. In particular, the phase difference, which allows the incident *E*-field vectors to be of opposite direction at a particular location, provides an opportunity to reduce the background *E*-field in dedicated regions. Most importantly, the relative pulse amplitudes and phases for different RF coil elements can be changed at the pulse sequence level without hardware modifications and, at least in principle, in real-time. A birdcage RF coil, the standard body RF coil design for many clinical MR systems, consists of two ports driven with a 90° phase difference to achieve the CP or quadrature-driven mode. However, if the two channels are driven individually as two independent linear polarization modes, the *E*-field distribution in the human body can change completely. Eryaman, et al. (122) have demonstrated that the linear mode has *E*-field null zones in which an implant would be exposed to highly reduced background *E*-field, hence strongly reduced RF field-induced heating. If the linear birdcage modes are combined, accordingly, to reduce the RF current on an implant such as a lead, this two-channel, pTx system effectively mitigates RF heating (101, 123–125) (**Figure 11**).

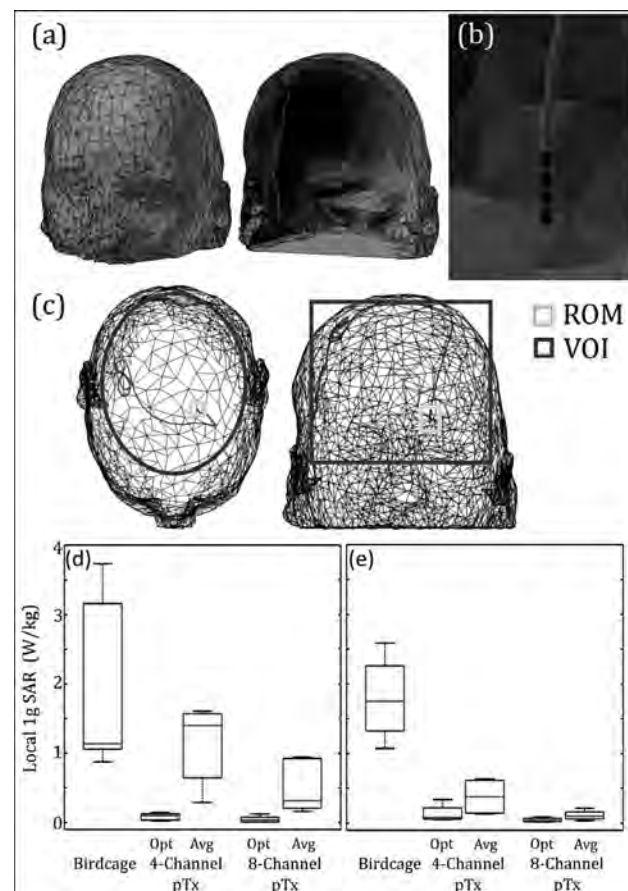
Figure 11. Detection and mitigation of RF-induced tip heating of a deep brain stimulation lead in a cadaver brain using an MR image-based method and a two-channel, parallel-transmission system. For the “implant friendly” mode, RF-induced tip heating (a, square box) was reduced substantially versus the quadrature transmission mode (b, square box), while at the same time image quality is improved. Adapted from color figure in Winter, et al. (1), original figure from Eryaman, et al. (101).



Increasing the number of pTx channels increases the degrees of freedom to reduce the E -field near the implant and, hence, suppresses unwanted hotspots with minimal loss of diagnostic image quality (126–130) (**Figure 12**). This is achieved in an optimization process that also reveals the worst-case and best-case RF heating scenario for a particular implant and transmit RF coil configuration, indicating the potential safety risk margins (131, 132). Investigators have demonstrated that an eight-channel pTx coil outperforms a four-channel pTx coil in suppressing unwanted SAR hotspots induced by DBS leads (130, 133, 134). Other constraints that can be embedded in the optimization of the RF pulse process are local SAR, whole-body averaged SAR, adaptive SAR (135), or the k-space trajectory for spokes pulses (127).

Interestingly, these pTx techniques are not restricted to proof-of-concept studies in phantoms on simplified implant geometries under controlled conditions; they could be an actual game changer for patients with implants that have complex geometries. This was recently demonstrated by two independent simulation studies investigating pTx mitigation of RF-induced heating of DBS leads with realistic trajectories extracted from CT-based patient data (130, 134) (**Figure 12**). Those studies showed that the local SAR could be decreased by more than 94% compared to body RF coil excitation at comparable B_1^+ homogeneity and global SAR. These results suggest that pTx systems could be a viable strategy to deal with the increasing complexity and number of medical implants in patients undergoing MRI

Figure 12. Simulation-based parallel-transmit (pTx) mitigation (a) of RF-induced tip heating of a deep brain stimulation lead (b) based on realistic trajectories and models obtained from patient data (c). A higher number of pTx channels reduces the absolute induced implant SAR values and decreases their standard deviation across the simulated patient population (d). Adapted from color figure in Winter, et al. (1), original figure from Mc Elcheran, et al. (134).



540 MRI-Related Heating of Implants and Devices

exams. However, more validation studies are needed to support this claim. Access to robust and flexible pTx system hardware is still very limited. Fortunately, efforts exist to attend to this need such as the ongoing development of an open-source, hardware-based pTx implant-safety testbed, which is adaptable to experiments with up to 32-channels at all relevant static magnetic field strengths (i.e., 1.5 to 7 Tesla) (136).

An interesting approach is to combine sensor measurements from on or around implants and use this information for pTx based mitigation. This has been demonstrated by using time-domain current (129, 132) and *E*-field sensors (136). More recently, even simple RMS sensors such as thermistors or diodes were utilized in proof-of-concept studies for real-time mitigation of RF-induced heating. In addition to being real-time capable, these sensor measurements also contain imaging information that can be used to maintain image quality, while at the same time RF field-induced heating is reduced substantially (136, 137). While still in its infancy, it is imaginable that in the future, sensor equipped “smart” medical implants could communicating with a pTx cable MRI device to guarantee safe scanning of implants even under varying conditions such as patient movement.

Other Techniques

If pTx hardware is not available, other methods can be applied to reduce implant heating by shaping the RF field. For example, the linear-polarization mode of the birdcage RF coil has regions of reduced *E*-field, and if these regions overlap with the implant, RF-induced currents are reduced (122). If a birdcage coil had multiple ports along its circumference, one could ‘rotate’ the linear-polarization mode by changing the feeding port. Similarly, a birdcage coil in the linear-polarization mode with a single transmit channel can be physically rotated to align the low *E*-field zone with the implant (138). This concept has been applied to DBS leads and showed significant improvement compared to the standard CP mode of the same birdcage coil (139). Another mitigation approach that does not rely on pTx technology or modified RF coil hardware is to put high-permittivity material pads on the subject at strategic locations. The high-permittivity dielectric modifies the background-field and it has been demonstrated that this can be efficiently used to reduce RF field-induced tip heating (140). A simple, but effective solution is using vertical MR scanners, where B_0 is directed perpendicular instead of parallel to the axis of the bore. Consequently, B^+_1 and the *E*-field directions change, and the same implant experiences a different background *E*-field. Simulations have shown that more than a ten-fold tip SAR reduction could be achieved for realistic DBS implants and lead geometries if scanned in a vertical MR system versus a horizontal one (141).

CONCLUSIONS

This chapter reviewed the existing literature on MRI-related heating of implants and devices. It should be noted that a number of topics had to be excluded because of space limitations (e.g., interventional tools and devices, low-power pulse sequences, etc.), but the crucial information for RF energy- and gradient field-induced heating of implants was presented.

Implant safety is an important field in MRI and much has been accomplished, but further work is needed. Three international standards are most relevant in this field: the MRI standard IEC 60601-2-33 and the implant standards that include ASTM F2182 and ISO/TS 10974. The latter set their scopes either on “passive” (ASTM) or “active” (ISO) implants. From the implant manufacturer’s point of view, this distinction is fundamental since active implants need electromagnetic compatibility (EMC) and other tests, while passive implants do not. From an MRI perspective, however, this distinction appears less relevant. Passive implant-related hazards are a subset of active implant-related hazards and are comprehensively covered by the document, ISO/TS 10974, as well. The document from the ASTM International, ASTM F2182, was a significant milestone and many of its procedural developments will prevail for the testing of passive implants. But no reasons exist, in these authors’ opinion, to maintain two implant standards in parallel. ISO/TS 10974 is in many respects more up-to-date and more general. Accordingly, all implants, active or passive, should be tested against it. Low-cost test procedures for low-risk implants would be on the wish list for future editions. For example, test strategies to easily translate an existing safety assessment from, say, one spinal fixation system to a similar one. The concept of an empirical parametrization of the implant-related hazard as demonstrated by Winter, et al. (45) may be helpful in this context (**Figure 13**).

It is important to note that the assessments of implant safety that are based on the current standards are always limited to a single, functional implant. Modifying this test scenario in any electromagnetically relevant way such as having multiple MR Conditional implants close to each other (83), multiple AIMD leads in close distance (142), or broken or abandoned AIMD leads of a previously MR Conditional implant (143) may pose potential safety hazards to the patient.

The paucity of peer-reviewed literature on gradient field-induced heating of implants suggests that excessive heating occurs only in unfavorable and potentially, unrecognized cases. Regardless, such cases are possible and, thus, it is unsatisfactory that presently, neither the manufacturer of the scanner nor the implant informs the MR system operator’s when a critical situation may arise and how to avoid it.

Accurate numerical simulations are the key to implant safety because they have reached a high level of maturity and can provide both insight and practical solutions. Future developments must be directed towards treating complex implants in realistic detail. To date, ISO/TS 10974’s Tier 4 is only of conceptual but not yet of any practical value. Simulations need validation, however, and measurements are often restricted to phantoms. This is acceptable as long as phantom measurements are not misunderstood as predictive for the *in vivo* case. Phantom experiments are a testbed to validate the simulation methodology, transmit RF coil models, and other situations that are then identically applied to anatomical voxel models.

Ex ante simulations of certain numerical models remain surrogates, however. Ultimately, any safety assessment must be specific to the given subject or patient, implant, and scan conditions. This means, that the scanner and implant must somehow “communicate”. For example, the implant must “inform” the MR system about its presence and condition, and the scanner must be able to “respond” to this input. The combination of real-time sensors

542 MRI-Related Heating of Implants and Devices

Figure 13. Simulated results for the RF-induced heating of a coronary artery stent as a function of different parameters (i.e., stent length, stent diameter, stent orientation, background local SAR) (a - f). The data can be fitted to empirical functions in an n -dimensional parameter space, which can then be used to estimate the maximum induced stent SAR values for a given background local SAR in a human-body model (g). This simulation-based parametrization approach for short implants gives a fast estimation of RF-induced heating and would enable a more generalized risk assessment of implant types instead of performing a full safety assessment for each new implant design. Adapted from color figure in Winter, et al. (1), original figure from Winter, et al. (45).

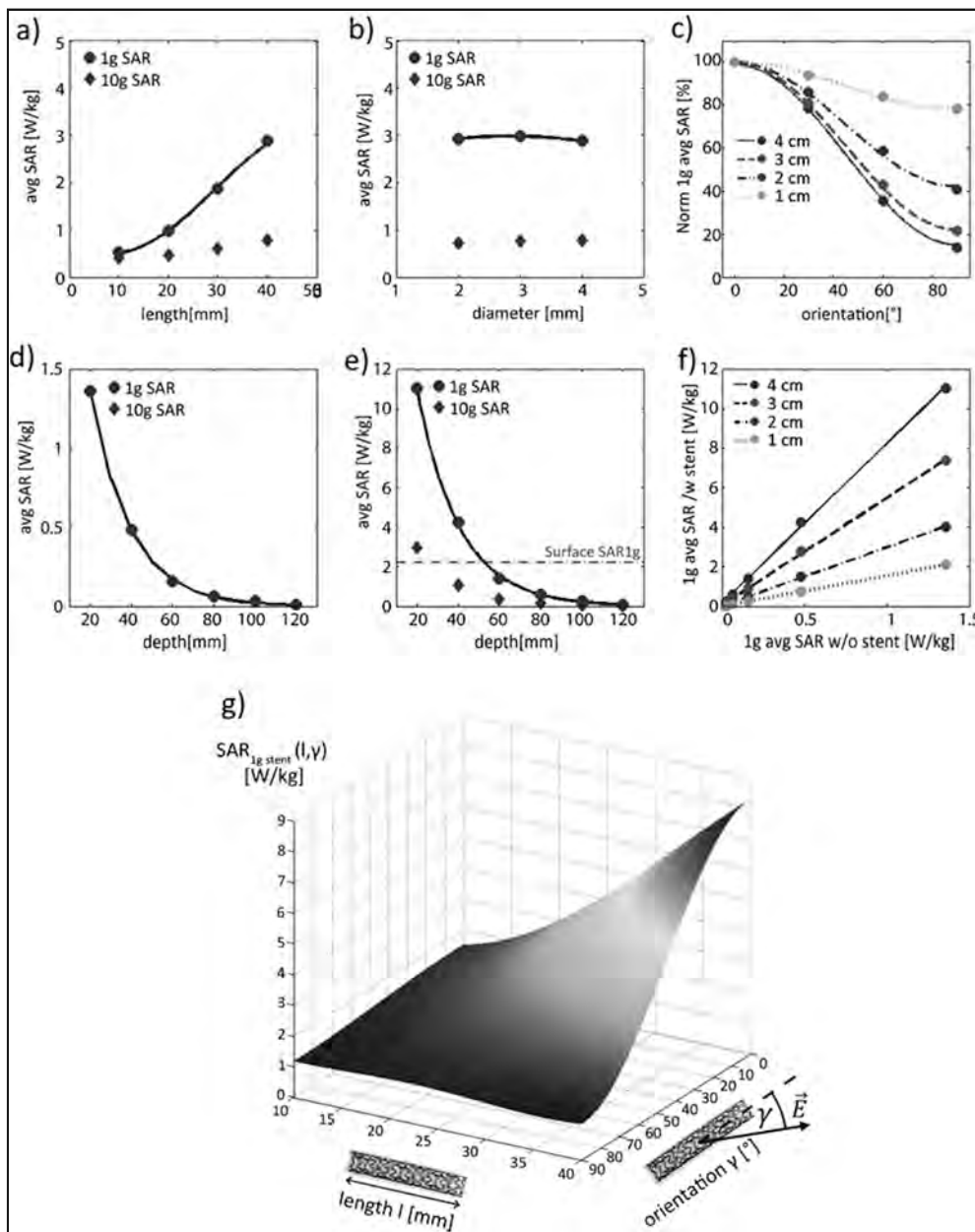
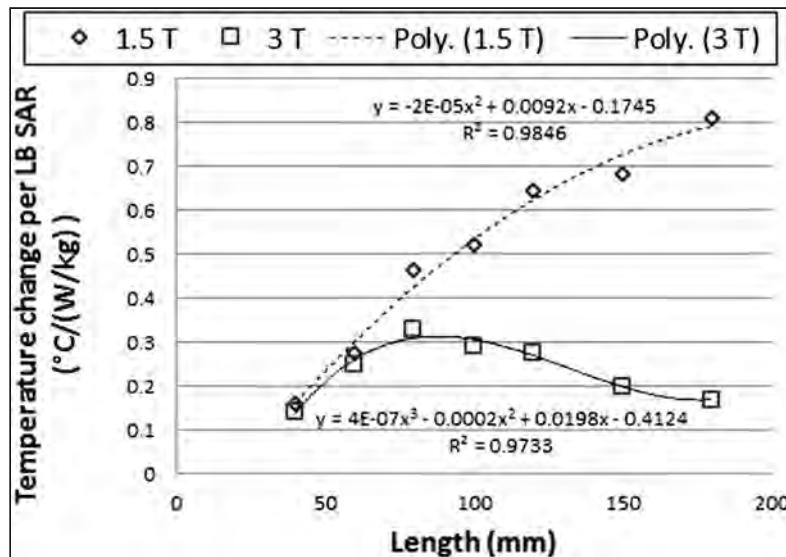


Figure 14. Temperature increase per local background SAR for different stent lengths. RF-induced heating experiments were performed in phantoms and conducted according to ASTM F2182. Adapted from color figure in Winter, et al. (1), original figure from Song, et al. (148).



(temperature, current, *E*-field, etc.) on the implant and a pTx system incorporated into the MR scanner would be most helpful to achieve this goal, but other approaches are certainly conceivable.

In implant safety-related discussions, it is often taken for granted that lower static magnetic field strengths automatically reduce the risk. ISO/TS 10974 or the Fixed-Parameter Option were initially conceived for 1.5 T but not for 3 T MR systems and, recently, the idea of dedicated or niche, low field strength scanners with fields less than 0.6 T (and as low as 0.05 T) is gaining new attention (144-147). Conceptually, the translation of B_{1+RMS} into implant SAR, for example, at the tip of a cardiac pacemaker lead, is a two-step process, however. First, B_{1+RMS} creates a background *E*-field. This effect scales with the frequency, hence B_0 , and the lower field strength may have the safety edge. In the second step, background *E*-field creates the tip *E*-field, and this conversion scales linearly with the RF wavelength in tissue (as long as half this wavelength is shorter than the implant and the transmit body RF coil). This time, the higher field strength has the advantage. Qualitatively, this effect can be seen in **Figure 14** (148). There is no universal answer to the question of a safest field strength, therefore, the individual implant, transmit RF coil, and scan parameters must be considered.

(This chapter is based on Winter L, Seifert F, Zilberti L, Murbach M, Ittermann B. MRI-related heating of implants and devices: A review. J Magn Reson Imaging 2021;53:1646-1665.)

544 MRI-Related Heating of Implants and Devices

ACKNOWLEDGMENTS

The authors wish to thank Alessandro Arduino, Oriano Bottauscio, Rüdiger Brühl, Mario Chiampi, Niels Kuster, Johannes Petzold, Berk Silemek, and Umberto Zanovello for many helpful discussions. This work was supported by funding from the EMPIR programme co-financed by the Participating States and from the European Union's Horizon 2020 research and innovation programme (grant 17IND01 – MIMAS).

REFERENCES

1. Winter L, Seifert F, Zilberti L, Murbach M, Ittermann B. MRI-related heating of implants and devices: A review. *J Magn Reson Imaging* 2021;53:1646–1665.
2. Davis P, Crooks L, Arakawa M, et al. Potential hazards in NMR imaging: Heating effects of changing magnetic fields and RF fields on small metallic implants. *Am J Roentgenol* 1981;137:857–860.
3. Nyenhuis JA, Sung-Min Park, Kamondetdacha R, et al. MRI and implanted medical devices: Basic interactions with an emphasis on heating. *IEEE Trans Device Mater Reliab* 2005;5:467–480.
4. Baker KB, Tkach JA, Nyenhuis JA, et al. Evaluation of specific absorption rate as a dosimeter of MRI-related implant heating. *J Magn Reson Imaging* 2004;20:315–320.
5. Irnich W, Irnich B, Bartsch C, et al. Do we need pacemakers resistant to magnetic resonance imaging? *EP Eur* 2005;7:353–365.
6. Ferris NJ, Kavoussi H, Thiel C, Stuckey S. The 2005 Australian MRI safety survey. *Am J Roentgenol* 2007;188:1388–1394.
7. Kanal E, Barkovich AJ, Bell C, et al. ACR guidance document on MR safe practices: 2013. *J Magn Reson Imaging* 2013;37:501–530.
8. Rezai AR, Baker KB, Tkach JA, et al. Is magnetic resonance imaging safe for patients with neurostimulation systems used for deep brain stimulation? *Neurosurgery* 2005;57:1056–62.
9. Spiegel J, Fuss G, Backens M, et al. Transient dystonia following magnetic resonance imaging in a patient with deep brain stimulation electrodes for the treatment of Parkinson disease: Case report. *J Neurosurg* 2003;99:772–774.
10. Henderson JM, Tkach J, Phillips M, et al. Permanent neurological deficit related to magnetic resonance imaging in a patient with implanted deep brain stimulation electrodes for Parkinson's disease: Case report. *Neurosurgery* 2005;57:E1063.
11. Shellock FG. Reference Manual for Magnetic Resonance Safety, Implants and Devices: 2020 Edition. Los Angeles: Biomedical Research Publishing Group; 2020.
12. Rezai AR, Phillips M, Baker KB, et al. Neurostimulation system used for deep brain stimulation (DBS): MR safety issues and implications of failing to follow safety recommendations. *Invest Radiol* 2004;39:300–303.
13. Zanchi MG, Venook R, Pauly JM, Scott GC. An optically coupled system for quantitative monitoring of MRI-induced RF currents into long conductors. *IEEE Trans Med Imaging* 2010;29:169–178.
14. Kraff O, Quick HH. Sicherheit von Implantaten im Hochfeld-und Ultrahochfeld-MRT. *Radiol* 2019;1–8.
15. MRI Safety Resources. International Society for Magnetic Resonance in Medicine (ISMRM) and Society for MR Radiographers & Technologists (SMRT). Available at <https://www.ismrm.org/mr-safety-links/>.
16. MRI Safety Resource. Available at <http://www.mrisafety.com/>.
17. Dempsey MF, Condon B, Hadley DM. Investigation of the factors responsible for burns during MRI. *J Magn Reson Imaging* 2001;13:627–631.

MRI Bioeffects, Safety, and Patient Management 545

18. Brühl R, Ihlenfeld A, Ittermann B. Gradient heating of bulk metallic implants can be a safety concern in MRI. *Magn Reson Med* 2017;77:1739–1740.
19. Zilberti L, Arduino A, Bottauscio O, Chiampi M. The underestimated role of gradient coils in MRI safety. *Magn Reson Med* 2017;77:13–15.
20. Graf H, Steidle G, Schick F. Heating of metallic implants and instruments induced by gradient switching in a 1.5-Tesla whole-body unit. *J Magn Reson Imaging* 2007;26:1328–1333.
21. Bannan KE, Handler W, Chronik B, Salisbury SP. Heating of metallic rods induced by time-varying gradient fields in MRI. *J Magn Reson Imaging* 2013;38:411–416.
22. Zilberti L, Bottauscio O, Chiampi M, et al. Collateral thermal effect of MRI-LINAC gradient coils on metallic hip prostheses. *IEEE Trans Magn* 2014;50:1–4.
23. Zilberti L, Bottauscio O, Chiampi M, et al. Numerical prediction of temperature elevation induced around metallic hip prostheses by traditional, split, and uniplanar gradient coils. *Magn Reson Med* 2015;74:272–279.
24. Arduino A, Bottauscio O, Brühl R, Chiampi M, Zilberti L. *In silico* evaluation of the thermal stress induced by MRI switched gradient fields in patients with metallic hip implant. *Phys Med Biol* 2019;64:245006.
25. Pennes HH. Analysis of tissue and arterial blood temperatures in the resting human forearm. *Appl Physiol* 1948;1:93–122.
26. Wissler EH. Pennes' 1948 paper revisited. *J Appl Physiol* 1998;85:35–41.
27. EM and thermal tissue parameter database. Available at <https://itis.swiss/virtual-population/tissue-properties/database/database-summary/>.
28. Collins CM, Liu W, Wang J, et al. Temperature and SAR calculations for a human head within volume and surface coils at 64 and 300 MHz. *J Magn Reson Imaging* 2004;19:650–656.
29. van Rhoon GC, Samaras T, Yarmolenko PS, et al. CEM43°C thermal dose thresholds: A potential guide for magnetic resonance radiofrequency exposure levels? *Eur Radiol* 2013;23:2215–2227.
30. Sapareto SA, Dewey WC. Thermal dose determination in cancer therapy. *Int J Radiat Oncol Biol Phys* 1984;10:787–800.
31. Yarmolenko PS, Moon EJ, Landon C, et al. Thresholds for thermal damage to normal tissues: An update. *Int J Hyperthermia* 2011;27:320–343.
32. Murbach M, Neufeld E, Capstick M, et al. Thermal tissue damage model analyzed for different whole-body SAR and scan durations for standard MR body coils: Thermal dose and tissue damage in MR RF heating. *Magn Reson Med* 2014;71:421–431.
33. Arduino A, Zanovello U, Hand J, et al. Heating of hip joint implants in MRI: The combined effect of RF and switched-gradient fields. *Magn Reson Med* 2021;85:3447–3462.
34. Delfino JG, Woods TO. New developments in standards for MRI safety testing of medical devices. *Current Radiology Reports* 2016;4:1–9.
35. Establishing Safety and Compatibility of Passive Implants in the Magnetic Resonance (MR) Environment - Guidance for Industry and Food and Drug Administration Staff. Food and Drug Administration, 2014.
36. Assessment of Radiofrequency-Induced Heating in the Magnetic Resonance (MR) Environment for Multi-Configuration Passive Medical Devices - Guidance for Industry and Food and Drug Administration Staff. Food and Drug Administration, 2016.
37. IEC 60601-2-33:2010+AMD1:2013+AMD2:2015 CSV: Medical electrical equipment - particular requirements for the basic safety and essential performance of magnetic resonance equipment for medical diagnosis. Edition 3.2. International Electrotechnical Commission (IEC). 2015.
38. ASTM F2182-19^{2c}. Standard test method for measurement of radio frequency induced heating on or near passive implants during magnetic resonance imaging. American Society of Testing and Materials International. 2019.

546 MRI-Related Heating of Implants and Devices

39. International Organization for Standardization (ISO), Technical Specification (TS) ISO/TS 10974:2018. Assessment of the safety of magnetic resonance imaging for patients with an active implantable medical device. Second Edition. 2018.
40. F2503-20. Standard practice for marking medical devices and other items for safety in the magnetic resonance environment. American Society of Testing and Materials International. 2020.
41. Food and Drug Administration (FDA). Testing and Labeling Medical Devices for Safety in the Magnetic Resonance (MR) Environment. Guidance for Industry and Food and Drug Administration Staff. Food and Drug Administration, 2021.
42. Park S-M, Kamondetdacha R, Nyenhuis JA. Calculation of MRI-induced heating of an implanted medical lead wire with an electric field transfer function. *J Magn Reson Imaging* 2007;26:1278-1285.
43. Umashankar K, Taflove A. A novel method to analyze electromagnetic scattering of complex objects. *IEEE Trans Electromagn Compat* 1982;EMC-24:397-405.
44. Li BK, Liu F, Weber E, Crozier S. Hybrid numerical techniques for the modelling of radiofrequency coils in MRI. *NMR Biomed* 2009;22:937-951.
45. Winter L, Oberacker E, Özerdem C, et al. On the RF heating of coronary stents at 7.0 Tesla MRI. *Magn Reson Med* 2015;74:999-1010.
46. Santoro D, Winter L, Müller A, et al. Detailing radio frequency heating induced by coronary stents: A 7.0 Tesla magnetic resonance study. *PLoS One* 2012;7:e49963.
47. Yeung CJ, Susil RC, Atalar E. RF safety of wires in interventional MRI: Using a safety index. *Magn Reson Med* 2002;47:187-193.
48. Tokaya JP, Raaijmakers AJE, Luijten PR, Bakker JF, van Den Berg CA. MRI-based transfer function determination for the assessment of implant safety. *Magn Reson Med* 2017;78:2449-2459.
49. Attaran A, Handler WB, Wawrzvn K, Chronik BA. Development of a transfer-function measurement procedure for the evaluation's of MRI-conditional medical devices at 3T. *IEEE Can Conf Electr Comput Eng (CCECE)*. 2018:1-4.
50. Missoffe A, Aissani S. Experimental setup for transfer function measurement to assess RF heating of medical leads in MRI: Validation in the case of a single wire. *Magn Reson Med* 2018;79:1766-1772.
51. Feng S, Qiang R, Kainz W, Chen J. A technique to evaluate MRI-induced electric fields at the ends of practical implanted lead. *IEEE Trans Microw Theory Tech* 2015;63:305-313.
52. Feng S, Wang Q, Wen C, et al. Simplified transfer function assessment of implantable leads for MRI safety evaluations. *IEEE Trans Electromagn Compat* 2019;61:1432-1437.
53. Mattei E, Censi F, Calcagnini G, Lucano E, Angelone LM. A combined computational and experimental approach to assess the transfer function of real pacemaker leads for MR radiofrequency-induced heating. *Magn Reson Mater Phys Biol Med* 2021.
54. Fiedler TM, Ladd ME, Bitz AK. SAR simulations and safety. *Neuroimage* 2018;s168:33-58.
55. Murbach MJ. EMF risk assessment: Exposure assessment and safety considerations in MRI and other environments. Doctoral Thesis. Research Collection. ETH Zürich; 2013.
56. Ittermann B, Bottauscio O, Hand J, et al. Metrology for MRI Safety. Seventeenth Int Congr Metrol. EDP Sciences 2015:09001.
57. Noureddine Y, Kraff O, Ladd ME, et al. *In vitro* and *in silico* assessment of RF-induced heating around intracranial aneurysm clips at 7 Tesla. *Magn Reson Med* 2018;79:568-581.
58. Noureddine Y, Kraff O, Ladd ME, et al. Radiofrequency induced heating around aneurysm clips using a generic birdcage head coil at 7 Tesla under consideration of the minimum distance to decouple multiple aneurysm clips. *Magn Reson Med* 2019;82:1859-1875.
59. Murbach M, Neufeld E, Cabot E, et al. Virtual population-based assessment of the impact of 3 Tesla radiofrequency shimming and thermoregulation on safety and B_1^+ uniformity: Safety and thermoregulation in 3T RF shimming. *Magn Reson Med* 2016;76:986-997.

60. Adriany G, Moortele P-FV de, Wiesinger F, et al. Transmit and receive transmission line arrays for 7 Tesla parallel imaging. *Magn Reson Med* 2005;53:434-445.
61. Vaughan JT, Adriany G, Snyder CJ, et al. Efficient high-frequency body coil for high-field MRI. *Magn Reson Med* 2004;52:851-859.
62. Gosselin M-C, Neufeld E, Moser H, et al. Development of a new generation of high-resolution anatomical models for medical device evaluation: The virtual population 3.0. *Phys Med Biol* 2014;59:5287-5303.
63. Saito K, Sato K, Kinase S, Nagaoka T. Japanese Computational Phantoms: Otoko, Onago, JM, JM2, JF, TARO, HANAKO, Pregnant Woman, and Deformable Child. In: *Handb Anat Models Radiat Dosim*. CRC Press; 2009. pp. 241-274.
64. Ackerman MJ. The visible human project. *Proc IEEE* 1998;86:504-511.
65. Makarov SN, Noetscher GM, Yanamadala J, et al. Virtual human models for electromagnetic studies and their applications. *IEEE Rev Biomed Eng* 2017;10:95-121.
66. Gabriel S, Lau RW, Gabriel C. The dielectric properties of biological tissues: II. Measurements in the frequency range 10 Hz to 20 GHz. *Phys Med Biol* 1996;41:2251-2269.
67. Zilberti L, Zanovello U, Arduino A, Bottauscio O, Chiampi M. RF-induced heating of metallic implants simulated as PEC: Is there something missing? *Magn Reson Med* 2021; 85:583-586.
68. Oberacker E, Paul K, Huelnhagen T, et al. Magnetic resonance safety and compatibility of tantalum markers used in proton beam therapy for intraocular tumors: A 7.0 Tesla study. *Magn Reson Med* 2017;78:1533-1546.
69. Destruel A, O'Brien K, Jin J, et al. Adaptive SAR mass-averaging framework to improve predictions of local RF heating near a hip implant for parallel transmit at 7 T. *Magn Reson Med* 2019;81:615-627.
70. Murbach M, Neufeld E, Kainz W, Pruessmann KP, Kuster N. Whole-body and local RF absorption in human models as a function of anatomy and position within 1.5T MR body coil: MR RF exposure as a function of large-scale anatomical properties. *Magn Reson Med* 2014;71:839-845.
71. Yao A, Zastrow E, Neufeld E, Kuster N. Efficient and reliable assessment of the maximum local tissue temperature increase at the electrodes of medical implants under MRI exposure. *Bioelectromagnetics* 2019;40:422-433.
72. Kotte A, Leeuwen G van, Bree J de, et al. A description of discrete vessel segments in thermal modelling of tissues. *Phys Med Biol* 1996;41:865-884.
73. Kok HP, Gellermann J, Berg CAT van den, et al. Thermal modelling using discrete vasculature for thermal therapy: A review. *Int J Hyperthermia* 2013;29:336-345.
74. Shrivastava D, Utecht L, Tian J, Hughes J, Vaughan JT. *In vivo* radiofrequency heating in swine in a 3T (123.2-MHz) birdcage whole body coil: *In vivo* RF heating in 3T. *Magn Reson Med* 2014;72:1141-1150.
75. Zienkiewicz OC, Taylor RL. *The Finite Element Method for Solid and Structural Mechanics*. Seventh Edition. Butterworth-Heinemann; 2013.
76. Szczzerba D, Neufeld E, Zefferer M, Buhlmann B, Kuster N. FEM Based Morphing of Whole Body Human Models. 2011 XXXth URSI Gen Assem Sci Symp. Istanbul: IEEE; 2011: pp.1-3.
77. Avants BB, Epstein CL, Grossman M, Gee JC. Symmetric diffeomorphic image registration with cross-correlation: Evaluating automated labeling of elderly and neurodegenerative brain. *Med Image Anal* 2008;12:26-41.
78. Akbarzadeh A, Gutierrez D, Baskin A, et al. Evaluation of whole-body MR to CT deformable image registration. *J Appl Clin Med Phys* 2013;14:4163.
79. Tward D, Ceritoglu C, Sturgeon G, et al. Generating patient-specific dosimetry phantoms with whole-body diffeomorphic image registration. Bioeng Conf NEBEC 2011 IEEE 37th Annu Northeast IEEE;2011:1-2.

548 MRI-Related Heating of Implants and Devices

80. International Organization for Standardization. Guidance for uncertainty analysis regarding the application of ISO/TS 10974. ISO/TR 21900. 2018.
81. Yao A, Zastrow E, Neufeld E, et al. Novel test field diversity method for demonstrating magnetic resonance imaging safety of active implantable medical devices. *Phys Med Biol* 2020;65:075004.
82. Weidemann G, Seifert F, Hoffmann W, Ittermann B. RF current measurements in implanted wires in phantoms by fiber optic current clamps. *Proc Intl Soc Magn Reson Med* 2015; 281.
83. Reiss S, Lottner T, Ozen A, et al. Analysis of the RF excitation of endovascular stents in small gap and overlap scenarios using an electro-optical *E-field* sensor. *IEEE Trans Biomed Eng* 2021;68:783-792.
84. Silemek B, Acikel V, Oto C, et al. A temperature sensor implant for active implantable medical devices for *in vivo* subacute heating tests under MRI. *Magn Reson Med* 2018;79:2824–2832.
85. Davidson B, Tam F, Yang B, et al. Three-tesla magnetic resonance imaging of patients with deep brain stimulators: Results from a phantom study and a pilot study in patients. *Neurosurgery* 2021;88:349-355.
86. Graesslin I, Krueger S, Vernickel P, et al. Detection of RF unsafe devices using a parallel transmission MR system. *Magn Reson Med* 2013;70:1440–1449.
87. Ellenor CW, Stang PP, Etezadi-Amoli M, Pauly JM, Scott GC. Offline impedance measurements for detection and mitigation of dangerous implant interactions: An RF safety prescreen. *Magn Reson Med* 2015;73:1328–1339.
88. Graesslin I, Vernickel P, Börnert P, et al. Comprehensive RF safety concept for parallel transmission MR. *Magn Reson Med* 2015;74:589–598.
89. Luechinger R, Zeijlemaker VA, Pedersen electromagnetic, et al. *In vivo* heating of pacemaker leads during magnetic resonance imaging. *Eur Heart J* 2005;26:376–383.
90. Winkler SA, Picot PA, Thornton MM, Rutt BK. Direct SAR mapping by thermoacoustic imaging: A feasibility study. *Magn Reson Med* 2017;78:1599–1606.
91. Dixit N, Stang PP, Pauly JM, Scott GC. Thermo-acoustic ultrasound for detection of RF-induced device lead heating in MRI. *IEEE Trans Med Imaging* 2018;37:536–546.
92. Acikel V, Uslubas A, Atalar E. Modeling of electrodes and implantable pulse generator cases for the analysis of implant tip heating under MR imaging. *Med Phys* 2015;42:3922–3931.
93. Camacho CR, Plewes DB, Henkelman RM. Nonsusceptibility artifacts due to metallic objects in MR imaging. *J Magn Reson Imaging* 1995;5:75–88.
94. Scott GC, Joy MLG, Armstrong RL, Henkelman RM. Electromagnetic considerations for RF current density imaging [MRI technique]. *IEEE Trans Med Imaging* 1995;14:515–524.
95. Graf H, Steidle G, Martirosian P, Lauer UA, Schick F. Effects on MRI due to altered rf polarization near conductive implants or instruments. *Med Phys* 2006;33:124–127.
96. Venook RD, Overall WR, Shultz K, et al. Monitoring induced currents on long conductive structures during MRI. *Proc Intl Soc Magn Reson Med* 2008:898.
97. van den Bosch MR, Moerland MA, Lagendijk JJ, Bartels LW, van den Berg CA. New method to monitor RF safety in MRI-guided interventions based on RF induced image artefacts. *Med Phys* 2010;37:814–821.
98. Overall WR, Pauly JM, Stang PP, Scott GC. Ensuring safety of implanted devices under MRI using reversed RF polarization. *Magn Reson Med* 2010;64:823–833.
99. Griffin GH, Anderson KJT, Celik H, Wright GA. Safely assessing radiofrequency heating potential of conductive devices using image-based current measurements. *Magn Reson Med* 2015;73:427–441.
100. Griffin GH, Ramanan V, Barry J, Wright GA. Toward *in vivo* quantification of induced RF currents on long thin conductors. *Magn Reson Med* 2018;80:1922–1934.
101. Eryaman Y, Kobayashi N, Moen S, et al. A simple geometric analysis method for measuring and mitigating RF induced currents on deep brain stimulation leads by multichannel transmission/reception. *NeuroImage* 2019;184:658–668.

102. Tokaya JP, Raaijmakers AJ, Luijten PR, van den Berg CAT. MRI-based, wireless determination of the transfer function of a linear implant: Introduction of the transfer matrix. *Magn Reson Med* 2018;80:2771–2784.
103. Tokaya JP, Raaijmakers AJE, Luijten PR, Sbrizzi A, van den Berg CAT. MRI-based transfer function determination through the transfer matrix by jointly fitting the incident and scattered B_1^+ field. *Magn Reson Med* 2020;83:1081–1095.
104. Tokaya JP, Berg CAT, Luijten PR, Raaijmakers AJE. Explaining RF induced current patterns on implantable medical devices during MRI using the transfer matrix. *Med Phys* 2021;48:132–141.
105. Katscher U, van den Berg CAT. Electric properties tomography: Biochemical, physical and technical background, evaluation and clinical applications. *NMR Biomed* 2017;30:e3729.
106. Katscher U, Voigt T, Findeklee C, et al. Determination of electric conductivity and local SAR via B_1 mapping. *IEEE Trans Med Imaging* 2009;8:1365–1374.
107. Rieke V, Butts Pauly K. MR thermometry. *J Magn Reson Imaging* 2008;27:376–390.
108. Winter L, Oberacker E, Paul K, et al. Magnetic resonance thermometry: Methodology, pitfalls and practical solutions. *Int J Hyperth* 2016;32:63–75.
109. Ehses P, Fidler F, Nordbeck P, et al. MRI thermometry: Fast mapping of RF field-induced heating along conductive wires. *Magn Reson Med* 2008;60:457–461.
110. Angelone LM, Ahveninen J, Belliveau JW, Bonmassar G. Analysis of the role of lead resistivity in specific absorption rate for deep brain stimulator leads at 3T MRI. *IEEE Trans Med Imaging* 2010;29:1029–1038.
111. Mattei E, Calcagnini G, Censi F, Triventi M, Bartolini P. Role of the lead structure in MRI-induced heating: *In vitro* measurements on 30 commercial pacemaker/defibrillator leads. *Magn Reson Med* 2012;67:925–935.
112. Bottomley PA, Kumar A, Edelstein WA, Allen JM, Karmarkar PV. Designing passive MRI-safe implantable conducting leads with electrodes. *Med Phys* 2010;37:3828–3843.
113. Golestanirad L, Angelone LM, Kirsch J, et al. Reducing RF field-induced heating near implanted leads through high-dielectric capacitive bleeding of current (CBLOC). *IEEE Trans Microw Theory Tech* 2019;67:1265–1273.
114. Griffin GH, Anderson KJT, Wright GA. Miniaturizing floating traps to increase RF safety of magnetic-resonance-guided percutaneous procedures. *IEEE Trans Biomed Eng* 2017;64:329–340.
115. Ladd ME, Quick HH. Reduction of resonant RF heating in intravascular catheters using coaxial chokes. *Magn Reson Med* 2000;43:615–619.
116. Ferhanoglu O, Eryaman Y, Atalar E. MRI compatible pacemaker leads. *Proc Intl Soc Magn Reson Med* 2005;13:963.
117. Baker KB, Tkach J, Hall JD, et al. Reduction of magnetic resonance imaging-related heating in deep brain stimulation leads using a lead management device. *Neurosurg* 2005;57:392–7.
118. Liu Y, Kainz W, Qian S, Wu W, Chen J. Effect of insulating layer material on RF field-induced heating for external fixation system in 1.5 T MRI system. *Electromagn Biol Med* 2014;33:223–227.
119. Nordbeck P, Weiss I, Ehses P, et al. Measuring RF field-induced currents inside implants: Impact of device configuration on MRI safety of cardiac pacemaker leads. *Magn Reson Med* 2009;61:570–578.
120. Zanovello U, Matekovits L, Zilberti L. An ideal dielectric coat to avoid prosthesis RF-artefacts in magnetic resonance imaging. *Sci Rep* 2017;7:326.
121. Zanovello U, Zilberti L, Matekovits L. A near-field cloaking study to reduce MRI RF-artefacts in presence of elongated prostheses. *IEEE J Electromagn RF Microw Med Biol* 2018;2:249–256.
122. Eryaman Y, Akin B, Atalar E. Reduction of implant RF heating through modification of transmit coil electric field. *Magn Reson Med* 2011;65:1305–1313.
123. Etezadi-Amoli M, Zanchi MG, Stang P, et al. Transmit array concepts for improved MRI safety in the presence of long conductors. *Proc Intl Soc Magn Reson Med* 2009;4801.

550 MRI-Related Heating of Implants and Devices

124. Eryaman Y, Turk EA, Oto C, Algin O, Atalar E. Reduction of the radiofrequency heating of metallic devices using a dual-drive birdcage coil. *Magn Reson Med* 2013;69:845–852.
125. Córcoles J, Yao A, Kuster N. Experimental and numerical optimization modelling to reduce radiofrequency-induced risks of magnetic resonance examinations on leaded implants. *Appl Math Model* 2021;96:177-188.
126. Gudino N, Sonmez M, Yao Z, et al. Parallel transmit excitation at 1.5 T based on the minimization of a driving function for device heating. *Med Phys* 2015;42:359–371.
127. Eryaman Y, Guerin B, Akgun C, et al. Parallel transmit pulse design for patients with deep brain stimulation implants. *Magn Reson Med* 2015;73:1896–1903.
128. Córcoles J, Zastrow E, Kuster N. Convex optimization of MRI exposure for mitigation of RF-heating from active medical implants. *Phys Med Biol* 2015;60:7293-7308.
129. Etezadi-Amoli M, Stang P, Kerr A, Pauly J, Scott G. Controlling radiofrequency-induced currents in guidewires using parallel transmit. *Magn Reson Med* 2015;74:1790–1802.
130. Guerin B, Angelone LM, Dougherty D, Wald LL. Parallel transmission to reduce absorbed power around deep brain stimulation devices in MRI: Impact of number and arrangement of transmit channels. *Magn Reson Med* 2020;83:299-311.
131. Seifert F, Weidemann G, Ittermann B. Q matrix approach to control implant heating by transmit array coils. *Proc Intl Soc Magn Reson Med* 2015:3212.
132. Godinez F, Scott G, Padorno F, Hajnal JV, Malik SJ. Safe guidewire visualization using the modes of a PTx transmit array MR system. *Magn Reson Med* 2020;83:2343–2355.
133. McElcheran CE, Yang B, Anderson KJ, Golestanirad L, Graham SJ. Parallel radiofrequency transmission at 3 tesla to improve safety in bilateral implanted wires in a heterogeneous model. *Magn Reson Med* 2017;78:2406–2415.
134. McElcheran CE, Golestanirad L, Iacono MI, et al. Numerical simulations of realistic lead trajectories and an experimental verification support the efficacy of parallel radiofrequency transmission to reduce heating of deep brain stimulation implants during MRI. *Sci Rep* 2019;9:2124.
135. Destruel A, Fuentes M, Weber E, et al. A numerical and experimental study of RF shimming in the presence of hip prostheses using adaptive SAR at 3 T. *Magn Reson Med* 2019;81:3826–3839.
136. Winter L, Silemek B, Petzold J, et al. Parallel transmission (pTx) medical implant safety testbed: Real-time mitigation of RF induced tip heating using time-domain *E-field* sensors. *Magn Reson Med* 2020;84:3468–3484.
137. Silemek B, Seifert F, Ittermann B, Winter L. Safe scanning of elongated implants with the sensor matrix Qs: Comparison of orthogonal projection and null mode based pTx mitigation. *Proc Intl Soc Magn Reson Med* 2021.
138. Golestanirad L, Keil B, Angelone LM, et al. Feasibility of using linearly polarized rotating birdcage transmitters and close-fitting receive arrays in MRI to reduce SAR in the vicinity of deep brain simulation implants. *Magn Reson Med* 2017;77:1701-1712.
139. Golestanirad L, Iacono MI, Keil B, et al. Construction and modeling of a reconfigurable MRI coil for lowering SAR in patients with deep brain stimulation implants. *NeuroImage* 2017;147:577-588.
140. Yu Z, Xin X, Collins CM. Potential for high-permittivity materials to reduce local SAR at a pacemaker lead tip during MRI of the head with a body transmit coil at 3 T. *Magn Reson Med* 2017;78:383-386.
141. Golestanirad L, Kazemivalipour E, Lampman D, et al. RF heating of deep brain stimulation implants in open-bore vertical MRI systems: A simulation study with realistic device configurations. *Magn Reson Med* 2020;83:2284–2292.
142. Kabil J, Felblinger J, Vuissoz P-A, Missoffe A. Coupled transfer function model for the evaluation of implanted cables safety in MRI. *Magn Reson Med* 2020;84:991-s999.
143. Yao A, Goren T, Samaras T, Kuster N, Kainz W. Radiofrequency-induced heating of broken and abandoned implant leads during magnetic resonance examinations. *Magn Reson Med* 2021;86:2156-2164.

MRI Bioeffects, Safety, and Patient Management 551

144. Campbell-Washburn AE, Ramasawmy R, Restivo MC, et al. Opportunities in interventional and diagnostic imaging by using high-performance low-field-strength MRI. *Radiology* 2019;293:384-393.
145. Sheth KN, Mazurek MH, Yuen MM, et al. Assessment of brain injury using portable, low-field magnetic resonance imaging at the bedside of critically ill patients. *JAMA Neurol* 2021 (In Press).
146. Van Speybroek CDE, O'Reilly T, Teeuwisse W, Arnold PM, Webb AG. Characterization of displacement forces and image artifacts in the presence of passive medical implants in low-field (<100 mT) permanent magnet-based MRI systems, and comparisons with clinical MRI systems. *Phys Med* 2021;84:116-124.
147. Turpin J, Unadkat P, Thomas J, et al. Portable magnetic resonance imaging for ICU patients. *Crit Care Explor* 2020;2:e0306.
148. Song T, Xu Z, Iacono MI, Angelone LM, Rajan S. Retrospective analysis of RF heating measurements of passive medical implants. *Magn Reson Med* 2018;80:2726-2730.
149. Steensma B. Effect of transmit frequency on RF heating of metallic implants. *Proceed Int Soc Magn Reson Med*, 2021.
150. Kazemivalipour E. Demystifying the effect of field strength on RF heating of conductive leads: A simulation study of SAR in DBS lead models during MRI at 1.5 T - 10.5 T. *Proc Intl Soc Magn Reson Med*, 2021.
151. Nordbeck P, Fidler F, Weiss I, et al. Spatial distribution of RF field-induced E-fields and implant heating in MRI. *Magn Reson Med* 2008;60:312-319.

Chapter 21 MRI Test Methods for MR Conditional Active Implantable Medical Devices

LOUAI AL-DAYEH, M.D., PH.D.

Research and Development Fellow
Boston Scientific Neuromodulation Corporation
Valencia, CA

MIZAN RAHMAN, PH.D.

Electrical Engineering Fellow
Boston Scientific Neuromodulation Corporation
Valencia, CA

ROSS VENOOK, PH.D.

Research and Development Fellow
Boston Scientific Neuromodulation Corporation
Valencia, CA

INTRODUCTION

Magnetic resonance imaging (MRI), through a well-orchestrated manipulation of electromagnetic fields, manages to create tomographic images of patients without exposure to ionizing radiation. However, MRI still exposes the patient inside the MR scanner to three different types of electromagnetic fields (a static magnetic field, time-varying gradients, and radiofrequency fields). Because these electromagnetic fields interact with the human body, MRI safety standards, such as the document from the International Electrotechnical Commission (IEC), IEC60601-2-33 (1), provide limits for field exposure levels and characteristics to reduce patient risks from hazards including: radiofrequency (RF)-induced burns, local and whole-body heating, peripheral nerve stimulation, and cardiac stimulation, among others. While these risks are mostly mitigated through the exposure limits, and MR systems have a strong history of safe use, there continues to be reports of adverse events, including in the Manufacturer and User Facility Device Experience (MAUDE) database from the Food and Drug Administration (2).

There are additional safety concerns related to implantable medical devices in patients undergoing MRI examinations due to the interactions of electromagnetic fields with the implants. These potential hazards, along with several unfortunate patient injuries related to interactions between MR scanners and implanted devices that occurred during the early days of the use of MRI technology historically led to conservative default consideration of implantable devices as being contraindicated for MRI (3-8). In the mid-1990s, passive medical devices (i.e., an implant without an internal power source), such as vascular stents and heart valve prostheses, began to undergo testing and received MR Conditional labeling following guidelines from the American Society for Testing and Materials (ASTM) International (9-13) and recommended MRI safety procedures presented in publications on this topic subject (14, 15).

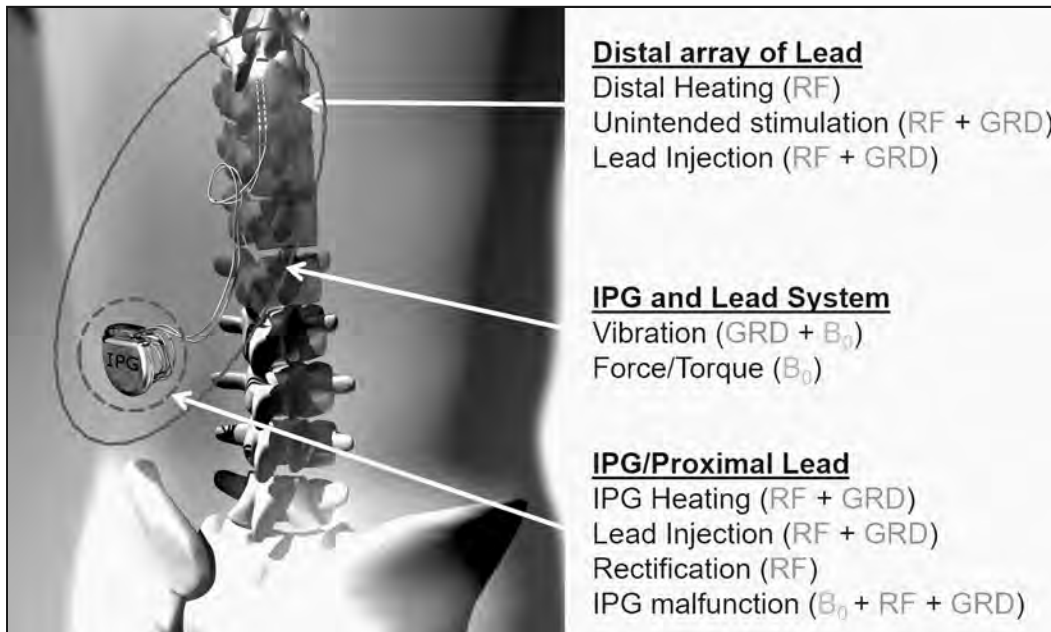
An active implantable medical device (AIMD), which is an implant relying on a source of electrical energy or any source of power other than that directly generated by the human body or gravity for its function (16), continued to be contraindicated for MRI throughout the 1990s and into the early 2000s due to the presence of the many different types of interactions and potential patient harms. In 2002, the neurosurgeon, Ali R. Rezai, and the group based at the Cleveland Clinic conducted multiple investigations focused on characterizing MRI-issues for deep brain stimulation (DBS) systems (17-20). This research contributed to the first successful MR Conditional labeling of an AIMD, the DBS system from Medtronic, Inc. nearly two decades ago. Despite the somewhat restrictive MRI operating conditions for this AIMD (i.e., 1.5 Tesla, only; use of a transmit/receive RF head coil was required; maximum whole body averaged specific absorption rate of 0.1 W/kg), patients were able to receive “on-label” MRI examinations for the first time.

AIMD manufacturers have come a long way in designing their implants with MRI-related issues in mind and with consideration given to what conditions of the MRI examination (e.g., level of the static magnetic field, limits of gradient fields and/or RF power level, etc.) permit the procedure to take place without compromising patient safety. In 2011, the first successful FDA labeling of an MR Conditional cardiac pacemaker (Medtronic, Inc.) occurred in the United States (21), which marked the beginning of the recent era in which many more patients with AIMDs from manufacturers across the industry can now have access to MRI through MR Conditional labeling.

The achievement of the current state of MR Conditional devices today, especially including the many industry-standard test methods that are the subject of this chapter, may not have been possible without an effort that started in 2006 across the MRI safety community, which included representatives from implanted device manufacturers, MR system manufacturers, safety test houses, and regulatory bodies. These experts came together as a Joint Working Group (JWG), convened under the International Standards Organization (ISO) and incorporated contributors to the existing MR system standards-making groups from the International Electrotechnical Commission (IEC) and ASTM International, with leadership from across the various stakeholders. A major outcome of this effort was the publication of an international Technical Specification (TS), ISO/TS 10974, documenting guidelines pertaining to the assessment of MRI safety for patients with AIMDs. The first version of this TS was published in 2012 (22) and the second updated version was published in 2018

554 MRI Test Methods for MR Conditional AIMDs

Figure 1. Illustration of a generic spinal cord stimulation system as an example of an AIMD with extended leads. Various potential MRI hazards are listed, with particular reference, shown in parentheses, to the causing fields: RF = radiofrequency; B_0 = static magnetic field, GRD = time-varying gradient fields. Note that understanding the induced fields for an AIMD for RF and the time-varying gradients includes surgical implantation variables, such as positioning or routing of the lead, as well as coiling of the lead in the IPG “pocket”. (Adapted from Reference 35.)



(23). Notably, this work is continuing and the group is presently updating and transitioning the TS into an International Standard.

The tests and methods presented in this chapter are directly related to those within the 2018 version of ISO/TS 10974 and they are generally consistent with the FDA guidance on the same topic (24). To have a specific focus, this chapter primarily addresses AIMDs with extended leads, for example, an implantable pulse generator (IPG) plus one or more leads (Figure 1).

Important Notes About MRI Safety Testing of AIMDs

The following notes address many common aspects of MRI safety testing of AIMDs and certain misconceptions that exist:

- There are many types of potential patient hazards, which require comprehensive testing. Notably, it is not simply about magnetic materials or RF energy-induced burns with respect to the MRI-related issues that exist for AIMDs.

MRI Bioeffects, Safety, and Patient Management 555

- The vast majority of implants that permit MRI examinations to be performed in patients are “MR Conditional” (i.e., a medical device with demonstrated safety in the MR environment with defined conditions including conditions for the static magnetic field, time-varying gradient magnetic fields, and radiofrequency fields) (24). Because all AIMDs contain metal, there is no, “MR Safe” (i.e., a medical device that poses no known hazards resulting from exposure to any MR environment) AIMD. Thus, if the implant has metallic components, it is either MR Conditional or MR Unsafe (i.e., a device which poses unacceptable risks to the patient, medical staff or other persons in the MR environment) (24).
- What can be considered MR Conditional is a specific device or system (e.g., a specific IPG plus a specific lead) according the device’s formal MRI safety labeling conditions listed in its Instructions for Use or Clinician’s Manual. These conditions, based on the field exposure conditions a device will experience within a patient in the MR scanner, are derived from the methods and results of the rigorous testing that was conducted by the device manufacturer or a test house.
 - According to this rule, the MR Conditional status is a “system tag” that is not practically applicable to one component of the system.
 - That is, for any MR Conditional system with a specific IPG and a specific lead, this specific IPG, by itself, does not carry the MR Conditional tag, because when it is combined with a lead not within the approved list of leads per this MR Conditional requirements, the “MR Conditionality” does not apply. A similar argument applies to leads. Note: Sterile packaging for such implants commonly includes a package for the IPG by itself, and a separate package for the lead by itself.
 - According to this rule, no generalizations of MRI safety can be made about any other device or system from the same manufacturer or from other manufacturers (e.g., lead extensions or lead-to-IPG adapter that are not included in the MRI-related label, and not MR Conditional).
- If mixing and matching an IPG from an MR Conditional device or system with lead(s) from another MR Conditional device or system, without the explicit labeling about this combination, one cannot assume that the new combination is MR Conditional or otherwise safe for a patient undergoing an MRI examination. Importantly, there is typically no testing or data available to assess or support the safety of such combinations.
- Fractured leads, abandoned leads, and other damaged or non-functional implants are typically not assessed for safety, although the test methods in ISO/TS 10974 could potentially be applied to such circumstances. Recent research suggests that excessive heating may occur under certain MRI conditions for these situations (25, 26).
- There are no generally accepted test methods or appropriate guidelines on how to safely scan a patient with multiple AIMDs (e.g., a cardiac pacemaker and a spinal cord stimulation system). Even if each device or system is MR Conditional by itself, the multi-system combination is not labeled for MR Conditional safety because of the lack of testing on such combinations. Of note is that there is a suggestion that lead electrode heating characteristics can change when another implant is present in close proximity (27).
- Almost all present safety testing and MR Conditional labeling of implants is for either 1.5 Tesla or 3 Tesla cylindrical bore, horizontal field MR systems, or both. Open-bore scanners that are either lower- or higher-field MR scanners typically are not yet included in testing standards or in MR Conditional labeling.

556 MRI Test Methods for MR Conditional AIMDs

- For testing related to RF field interactions, if an MR Conditional device or system is tested for safety in a specific static magnetic field strength and frequency (say 1.5 Tesla/64 MHz), there is no implication on MRI safety of the device within other field strengths and frequencies (e.g., lower fields such as 1 Tesla/42 MHz or higher field such as 3 Tesla/128 MHz or 7 Tesla/298 MHz)(15). No presumption of safety can be made at any field strength/frequency other than the specific ones at which the safety assessment was performed, because the RF fields-dependent properties of the system change substantially (e.g., RF field wavelength, current deposition in the leads, exposure fields in the patient due to scanner design differences, etc.) and could be either more safe or unsafe.
- In general, accessories of devices or systems (e.g., remote control, charger, etc.) are not MR Conditional, because they are neither designed nor tested for safety. Many such accessories are MR Unsafe and, therefore, cannot be brought safely into MR system rooms.

MRI AND AIMD INTERACTIONS: POTENTIAL SAFETY HAZARDS ACCORDING TO ISO/TS 10974

The demonstration of the MR Conditional status for an AIMD by device manufacturers, for example to achieve FDA labeling, involves testing in numerous (hundreds or thousands) different exposure conditions along with modeling of many thousands (or millions) of such potential exposure conditions. This includes exposure in realistic MRI environments, benchtop injection testing, and the development of appropriate risk assessments through physical experiments and modeling. This section of the chapter describes the full range of proper test methods according to established standards that collectively form the “testing package” regulatory bodies review for a given MR Conditional device label.

Importantly, while there are some abbreviated methods used by some researchers to preliminarily assess device safety through testing of a handful of configurations of a device within a phantom of tissue simulating medium (which was common in past decades, and still finds its way into the literature) such methods are simply insufficient for establishing the MR Conditional safety for AIMDs. While such tests can be a helpful first step, or potentially useful in demonstrating hazards, they unfortunately do not meaningfully evaluate safety in a comprehensive manner.

According to ISO/TS 10974:2018 (23), the potential safety hazards due to the MR system and the interactions with an AIMD are presented in **Table 1**. **Figure 2** also illustrates these possible risks. As indicated, each of the three different types of electromagnetic fields associated with an MR scanner (static magnetic field, time-varying gradient magnetic fields, and RF fields) generate specific interactions and potential safety hazards for patients, as do the different combinations of the fields (e.g., device vibration is a result of the combination of the static magnetic field and time-varying gradient fields).

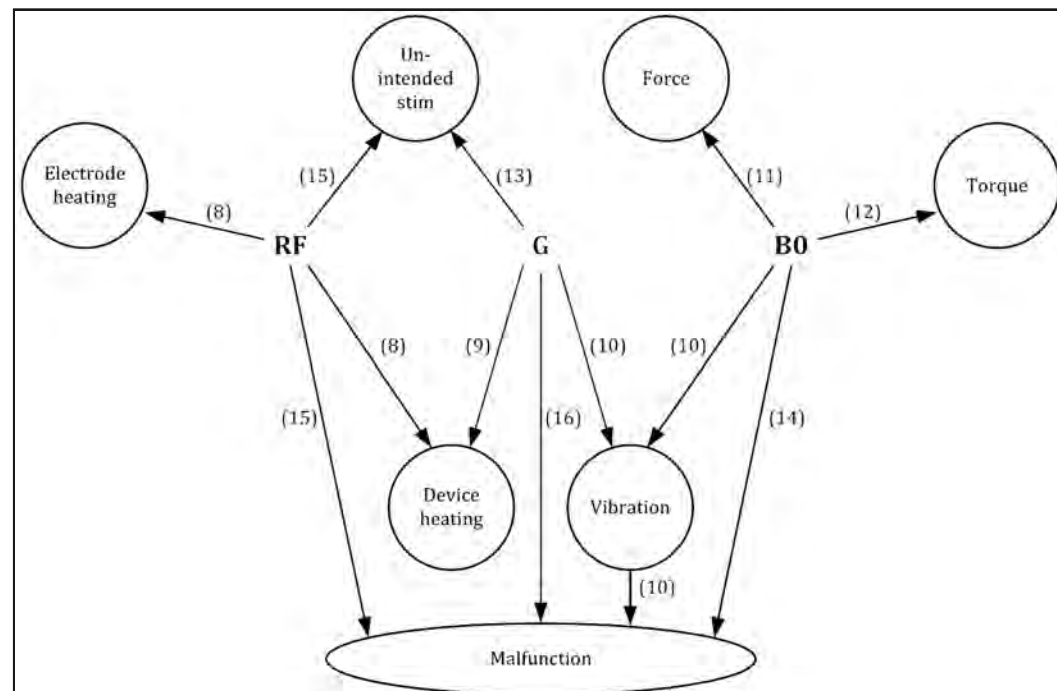
Acceptance Criteria

Most test methods described in the various standards do not include explicit acceptance criteria (e.g., how many degrees of temperature rise is acceptable for electrode heating). Since the risk level depends on the nature and location of the implant, as well as the tissues surrounding it, each device manufacturer must set and justify acceptance criteria for each potential hazard according to their internal risk management procedures, which is subject

Table 1. Potential patient hazards and corresponding test methods. Each “Clause” or chapter of the test method document defines the specific conditions for the testing to ensure proper coverage in the MRI environment (23).

Hazard	Test Method	ISO/TS 10974 Clause
Heat	RF field-induced heating of the AIMD	8
	Gradient magnetic field-induced device heating	9
Vibration	Gradient magnetic field-induced vibration	10
Force	Static magnetic field-induced force	11
Torque	Static magnetic field-induced torque	12
Unintended Stimulation	Gradient magnetic field-induced lead voltage (i.e., extrinsic electric potential) RF field-induced rectified lead voltage	13
Malfunction	Static magnetic field-induced device malfunction	14
	RF field-induced device malfunction	15
	RF field-induced device malfunction	16
	Combined fields test	17

Figure 2. The relationship between MR system’s output for the static magnetic field (B0), the time-varying gradient magnetic fields (G) and RF fields and the associated hazards (ISO/TS 10974 test method clause numbers are in parentheses). (Adapted from Reference 23.)



558 MRI Test Methods for MR Conditional AIMDs

to review by regulatory authorities. Typically, this includes using internal company data from a combination of relevant history of safe use, human trials, or animal studies, as well as accepted peer-reviewed literature. AIMD manufacturers are also working on creating vertical standards such as the document from the Association for the Advancement of Medical Instrumentation, AAMI PC76:2021 (36) and the one from the International Organization for Standardization, ISO 14708-3:2017 (37) focused on a specific type of implant with relevant acceptance criteria for these hazards. **Table 2** includes a detailed view on one way an AIMD manufacturer might consider and address the wide variety of potential safety hazards and acceptance criteria.

Notably, in May 2021, the FDA released a guidance document on Testing and Labeling Medical Devices for Safety in the Magnetic Resonance Environment (24). Among other guidances, this document includes recommendations on how acceptance criteria should be established based on the anatomical location of a medical device, using scientific rationale

Table 2. List of examples of MRI-related AIMD safety hazards, each of which generates requirements that an AIMD manufacturer must assess using appropriate test methods and rationale (35).

Requirement	ISO/TS 10974 Clause	Details of Meeting Requirement	Rationale/Source
RF-induced lead heating patient harm limit	8	When exposed to RF fields, heating of the lead shall not exceed XX CEM 43°C (28).	<ul style="list-style-type: none"> • ISO/TS 10974 • Tissue(s) around lead heating acceptance criteria • MRI environment exposure durations, levels.
Device (IPG) heating patient harm limit: • Gradient-induced • RF-induced	8 9	When exposed to combined RF and gradient fields, the thermal exposure of tissue surrounding the pocket shall not exceed XX CEM 43°C.	<ul style="list-style-type: none"> • ISO/TS 10974 • Tissue(s) around stimulator heating acceptance criteria • MRI environment exposure durations, levels. • MRI EMC acceptance criterion.
Gradient-induced vibration patient harm limit	10	When exposed to combined static magnetic and gradient magnetic fields, the pressure exerted by implanted IPG or lead(s) on the tissue shall not exceed XX PSI.	<ul style="list-style-type: none"> • ISO/TS 10974 • MRI vibration tissue damage acceptance criteria • MRI environment exposure durations, levels.
Static magnetic field-induced force patient harm limit	11	When exposed to the static magnetic field, <ul style="list-style-type: none"> • Translational force on the IPG shall not exceed XX N. • Translational force on any implantable system components shall not exceed the weight of the component. 	<ul style="list-style-type: none"> • ASTM F2052 • MRI force torque acceptance criterion. • MRI environment exposure durations, levels.

Table 2. (continued)

Requirement	ISO/TS 10974 Clause	Details of Meeting Requirement	Rationale/Source
Static magnetic field-induced torque patient harm limit	12	When exposed to the static magnetic field, <ul style="list-style-type: none"> • Torque on the IPG shall not exceed XX Nm. • Torque on all implanted system components shall not exceed the weight times the length of the longest side of the component. 	<ul style="list-style-type: none"> • ASTM F2213 • MRI force torque acceptance criterion. • MRI environment exposure durations, levels.
Electric potential patient harm limit <ul style="list-style-type: none"> • Gradient-induced, extrinsic • RF-induced and RF rectification 	13 15	When exposed to combined RF and gradient fields, <ul style="list-style-type: none"> • The current conducted by the IPG shall not exceed a Pulse Charge Limit of XX μC in each electrode. • Amplitude of the current pulse shall not exceed XX μA in IPG stimulation-off condition. And amplitude of the current pulse shall be within specified tolerances in IPG stimulation-on condition. 	<ul style="list-style-type: none"> • ISO/TS 10974 • MRI environment exposure durations, levels.
RF-induced device malfunction limit	15	When exposed to RF field, the IPG shall pass EMC criteria during and following exposure.	<ul style="list-style-type: none"> • ISO/TS 10974 • MRI environment exposure durations, levels. • MRI EMC acceptance criterion.
Static magnetic field-induced device malfunction limit	14	When exposed to static magnetic field, the IPG shall pass EMC criteria during and following exposure.	<ul style="list-style-type: none"> • ISO/TS 10974 • MRI environment exposure durations, levels. • MRI EMC acceptance criterion.
Gradient-induced device malfunction limit	16	When exposed to gradient magnetic fields, the IPG shall pass EMC criteria during and following exposure.	<ul style="list-style-type: none"> • ISO/TS 10974 • MRI environment exposure durations, levels. • MRI EMC acceptance criterion.
Combined fields - induced device malfunction limit	17	When exposed to combined static magnetic, RF, and gradient magnetic fields, the IPG shall: <ul style="list-style-type: none"> • Pass EMC criteria during and following exposure. • Retain its complete functionality during and following exposure. 	<ul style="list-style-type: none"> • ISO/TS 10974 • MRI environment exposure durations, levels. • MRI EMC acceptance criterion.
Combined fields – image artifacts or distortion.	N/A	Image artifacts due to the presence of IPG plus lead(s) shall be evaluated per ASTM F2219.	<ul style="list-style-type: none"> • ASTM F2119

[CEM 43°C, cumulative number of equivalent minutes at 43°C temperature; PSI, pound-force per square inch (pressure unit); N, Newton (force unit); Nm, Newton meter (torque unit); μ C: micro Coulomb (charge unit); μ A, micro Ampère (current unit).]

560 MRI Test Methods for MR Conditional AIMDs

or existing peer-reviewed literature. It also includes, for the first time, some specific tissue-specific temperature safety thresholds.

MRI AND AIMD TEST METHODS FOR DIFFERENT INTERACTIONS

One way to categorize potential safety evaluations for AIMDs is whether modeling is a part of the assessment or not. The following section lists these evaluations according to the two categories presented in **Table 3**.

Evaluation of the AIMDs for MRI Hazards Involves Bench-Top Testing, Modeling, MR Systems, or a Combination of These Approaches

1. Static Magnetic Field-Induced Force

A displacement force produced by the static magnetic field (B_0) on a device containing magnetic materials has the potential to cause unwanted movement of the implant. The force exerted on the device is a function of the spatial gradient of the static magnetic field (or the product of B_0 and the spatial gradient of B_0 , depending on whether the materials are below or above magnetic saturation) as well as the mass of magnetic material. This established test method described in ASTM F2052 (11). It is measurement-based and is typically conducted using an MR system.

The concept of testing is to measure the magnetically-induced displacement force of the implant where the “patient accessible” spatial gradient magnetic field is greatest (near the opening of the bore) and compare against value the gravitational force acting on the device (since all implanted devices are subjected to the force due to gravity without patient harm)(29). One version of this test is to suspend the device by a light-weight string at that location and measure the deflection angle. If the device deflects less than 45°, its magnetic force is less than that of gravity.

Implants with a displacement force less than the force of gravity are automatically deemed acceptable for patients undergoing MRI examinations. However, if the force is greater, it still could be acceptable with the justification of an appropriate acceptance crite-

Table 3. Categorization of MRI safety assessments based on whether or not electromagnetic modeling is involved.

Six MR Safety Assessments That Rely on Bench-Top Testing and/or MR Systems Without Modeling	Three MR Safety Assessments That Rely on Modeling In Addition to Measurement-Based Testing
<ol style="list-style-type: none"> 1. Static magnetic field-induced force 2. Static magnetic field-induced torque 3. Gradient magnetic field-induced vibration 4. Gradient magnetic field-induced device (e.g., IPG) heating 5. Device (IPG) malfunction (static magnetic field and/or gradient magnetic field-induced and/or RF field-induced) 6. Combined fields test 	<ol style="list-style-type: none"> 7. RF field-induced heating of the AIMD (i.e., the IPG and/or leads) 8. Unintended stimulation from RF field-induced lead voltage 9. Unintended stimulation from gradient magnetic field-induced lead voltage (i.e., extrinsic electric potential)

tion to maintain patient safety. For example, during the intended use of the device, counter-forces associated tissue ingrowth, scarring, granulation, or other mechanisms (i.e., fixation of the device by sutures or other means) can prevent the device from presenting a risk or hazard to a patient with regard to movement or dislodgement (30).

For most AIMDs with extended leads, since the main magnetic components that are implanted subcutaneously tend to be positioned far from vulnerable anatomical structures, static magnetic field-induced force is not considered a high-risk hazard.

2. *Static Magnetic Field-Induced Torque*

Magnetically-induced torque, produced by the static magnetic field (B_0), has the potential to cause unwanted movement of a device containing magnetic materials (i.e., rotating the implant to align it with the direction of the static magnetic field of the MR system). Torque is sensitive to field strength of the magnet and should be measured at a location where the static magnetic field is homogeneous (e.g., at the isocenter of an MR scanner). This established test method is described in ASTM F2213 (12). It is measurement-based and is typically conducted using an MR system.

Experimental approaches to conducting torque testing vary in complexity and applicability. Some methodologies are only applicable to devices that experience little or no torque, while others are appropriate for devices that experience substantial torque and must be more rigorously quantified to assess safety.

Most implantable devices, including AIMDs with extended leads, experience measurable torque but have no trouble passing a reasonable acceptance criterion. Similar to magnetically-induced force, the impact of torque acting on an implant may be mitigated by counter-forces that are present, *in situ* (30).

3. *Gradient Magnetic Field-Induced Vibration*

Time-varying gradient magnetic fields associated with an MR system induce eddy currents on the conductive surfaces of an AIMD. These eddy currents produce a time-varying magnetic moment that interacts with the static magnetic field, causing vibration of the conductive surfaces and, subsequently, the device. The primary potential for patient harm, since the vibration of the device is typically very low-amplitude due to the high frequency of oscillation, is related to possible breakage of internal components that may lead to malfunction of the device. As such, there could be compromised functionality or a lack of therapy from the device.

Vibration is sensitive to the static magnetic field and the time-varying gradient magnetic fields. This test is described in ISO/TS 10974:2018 (23). It is measurement-based and is conducted using an MR system or using a “shaker” table.

There are two methods for testing. One method requires the use of an MR scanner and provides higher accuracy with an increase in test burden, while the other method employs a shaker table and uses conservative approximations to reduce test burden after initial calibration testing utilizing an MR system. Because most conceived failures are due to fatigue fractures of internal components, the concept of testing is to expose the implant to extended periods of vibration and confirm full device functionality afterwards.

562 MRI Test Methods for MR Conditional AIMDs

The test duration represents the cumulative patient scan time over the lifetime of a typical AIMD. Guidelines in the standard establish, based on prior clinical experience, that conservative total MRI examination time exposure ranges from 2.5 hours to 7.5 hours, if considering at the top 0.8% of the population to the top 0.01% of the population, respectively.

For small- or medium-sized IPGs, and non-life-sustaining devices, vibration is not considered a high-risk hazard. Notably, larger devices (e.g., IPGs associated with implantable cardioverter defibrillators or implantable infusion pumps) typically vibrate more, with potentially greater likelihood of device damage.

4. Gradient Field-Induced Device (IPG) Heating

The time-varying gradient magnetic fields associated with MRI pulse sequences induce eddy currents on conductive AIMD enclosures (i.e., the IPG for an ICD) and other conductive internal surfaces such as battery components and circuit ground planes, which can result in device heating.

IPG heating is sensitive to the average or root-mean-square (RMS) gradient field amplitude $|\text{dB}/\text{dt}|$, with secondary dependence on the gradient waveform characteristics (i.e., the shape and frequency). It is greatest when the device is located where the gradient field $|\text{dB}/\text{dt}|$ RMS is maximum and when the device is oriented so that the gradient field vector is orthogonal to the AIMD surface(s) with the largest conductive area. Gradient magnetic field-induced heating also scales strongly with device radius (i.e., larger devices heat more).

This test is described in ISO/TS 10974:2018 (23). It is measurement-based, with preferential use of a laboratory gradient coil, amplifier, and function generator that can simulate clinical gradient field exposures. Alternatively, testing may be conducted using a clinical MR system.

Testing may be conducted using one of two tiers for the gradient waveform shape. Tier 1 uses a conservative waveform shape, and Tier 2 allows the characterization and use of a clinically relevant waveform. Tier 2 is most useful for AIMDs with larger conductive surfaces.

The standard calls for a test duration that is the maximum allowed for a clinical MRI examination as specified by the AIMD MR Conditional labeling, or 30 minutes. All other testing parameters are determined by the AIMD manufacturer to reflect conservative clinical use conditions for their device.

The key concern is local tissue heating due to radiant heat from the IPG. For most AIMDs with extended leads, this is not considered a high-risk hazard, though some MR Conditional labels have suggested applying an ice pack near a subcutaneously implanted device if the patient reports localized heating sensations near the device (IPG) during MRI.

5. Device (IPG) Malfunction: Static Magnetic Field, Gradient Magnetic Field, or RF Field-Induced

Exposure to the MR scanners static magnetic field and/or gradient magnetic field, and/or RF Field could have certain effects on an AIMD such as, but not limited to:

- Static Magnetic Field: Device reset, re-programming, magnetic remanence, premature battery discharge, and temporary or permanent damage.
- Gradient Magnetic Fields: Failure to deliver intended therapy, memory corruption, and temporary or permanent loss of device programmed settings.
- RF Field: Failure to deliver the intended therapy, re-programming, device reset, temporary or permanent damage, and tissue stimulation due to RF rectification.

These effects can be transient or permanent and might create a safety hazard that impacts the patient with the AIMD. Malfunction of an AIMD also has different implications based on the patient's dependence on the device (e.g., whether it is a life-sustaining therapy such as an implantable cardioverter defibrillator or not). The assessment is sensitive to or is a function of the field strength of the static magnetic field, the peak value for the time-varying gradient magnetic fields, and the peak RF field.

Three tests (i.e., one per MRI-related electromagnetic field) are described in elaborate details in ISO/TS 10974:2018 (23), including specifying a mixture of radiated and benchtop tests.

- For the static magnetic field: Implants are divided into three classes with various testing complexities. For many AIMDs that incorporate IPGs plus leads, it is sufficient for their class to meet the test requirement with no specific static magnetic field-related susceptibility orientations required, and for those, monitoring is done in accordance with a "combined field test" requirement (e.g., the test is performed using an MR system with all three electromagnetic fields active).
- For the gradient magnetic fields and RF field: The induced voltages and field level are found via a combination of computational modeling (see the later section on modeling) and exposure testing. Challenge testing of the device circuitry for malfunction includes benchtop injected voltage tests using sources of waveforms with appropriate shapes and magnitudes that reflect MRI-relevant pulse sequences.

The IPG should pass the acceptance criterion established by the device manufacturer based on the intended functionality (i.e., confirm expected device functionality) after the implant is exposed to each one of the three electromagnetic fields as described above.

6. Combined Fields Test

The Combined Fields Test provides field exposures typically encountered in clinical MRI examinations. It establishes an *in vitro* evaluation of the AIMD functioning under simultaneous exposure to the static magnetic field, gradient magnetic fields and RF field conditions. Unlike the maximal exposures required in the rest of measurement-based tests, this test exposes the AIMD to representative levels and temporal patterns of all three MRI-related electromagnetic fields, simultaneously.

This measurement-based assessment is conducted in an MR system and is sensitive to or is a function of the field strength of the static magnetic field, the peak value for the time-varying gradient magnetic fields, and the peak RF field. The test is described in ISO/TS 10974:2018 (23).

The Combined Fields Test is performed using an AIMD (i.e., the IPG and lead(s)) positioned in a tissue-simulating media phantom and placed inside of an MR scanner. The

564 MRI Test Methods for MR Conditional AIMDs

AIMD is exposed to a series of MRI pulse sequences that represent various common and clinically relevant protocols. Imaging is performed at different imaging landmarks or simulated patient positions within the MR system. The concept of testing is to expose the implant to the clinical combined fields and confirm expected device functionality during and after the exposure.

This test can be viewed as redundant to device (IPG) malfunction testing. However, it is required to make sure that the device is actually tested in a radiated environment under clinical conditions. In addition, bench-top exposure tests are typically more stringent, because they can apply higher-than-expected injection levels.

MRI Safety Assessments With Electromagnetic Modeling

ISO/TS 10974:2018 (23) has tiered approaches to modeling where the lower tier is easily implementable but overestimates the needed assessment, while the modeling in higher tiers is more complex but more accurate and with less overestimation. From a practical consideration, for AIMDs with extended leads, Tier 3 is the highest tier that is attainable with acceptable accuracy.

Tier 3 includes modeling the electromagnetic environment surrounding the AIMD to obtain the incident electric fields potentially picked up by the AIMD, together with measurements of how the AIMD handles such incident fields.

The process includes running a computer simulation that incorporates a hardware model of the scanner coil itself, whether its a gradient coil or an RF birdcage coil, as well as anatomical models of humans as representative samples per the device's patient characteristics. Electromagnetic simulations (gradient magnetic field or RF field) are run using these models in all relevant clinical imaging landmarks or patient positions to mimic the electromagnetic environment of the MR system. Modern-day simulations, across a range of human body models, and with a range of MR scanner coil models, can provide the electromagnetic field distribution everywhere inside the anatomical models across a range of potential clinical MRI examination scenarios.

The First Element Needed for Modeling, Tangential Electric fields (E-tan):

For the three assessments that rely heavily on modeling (**Table 3**), Tier 3 modeling requires that, along the lead path in every anatomical model, the tangential vector of the electrical component (E-tan) of the incident fields be extracted from the electromagnetic simulation. **Figure 3** shows the E-tan magnitude of example lead routings for deep brain stimulation (DBS) and spinal cord stimulation (SCS) device, for a specific landmark in an MR system with a transmit body RF coil.

The Second Element Needed for Modeling, the Transfer Function:

For RF energy, the first two of the three assessments shown in **Table 3**, the Transfer Function (31) is needed, which is really a characterization of how a particular AIMD (i.e., a specific IPG plus lead combination) behaves as an RF antenna in the MR scanner environment. For safety purposes benefiting the patient, the AIMD is favorable when it is a “bad antenna” in the electromagnetic environment of the MR scanner.

Figure 3. Left, Human model with one deep brain stimulation (DBS) and two spinal cord stimulation (SCS) lead routings (pathways). Upper right, RF field E-tan (tangential electrical field) magnitude of one DBS routing. Lower right, RF field E-tan magnitude of one SCS routing (Note, for both, the magnitude scale is not relevant to a specific RF energy level). (Adapted from Reference 35.)

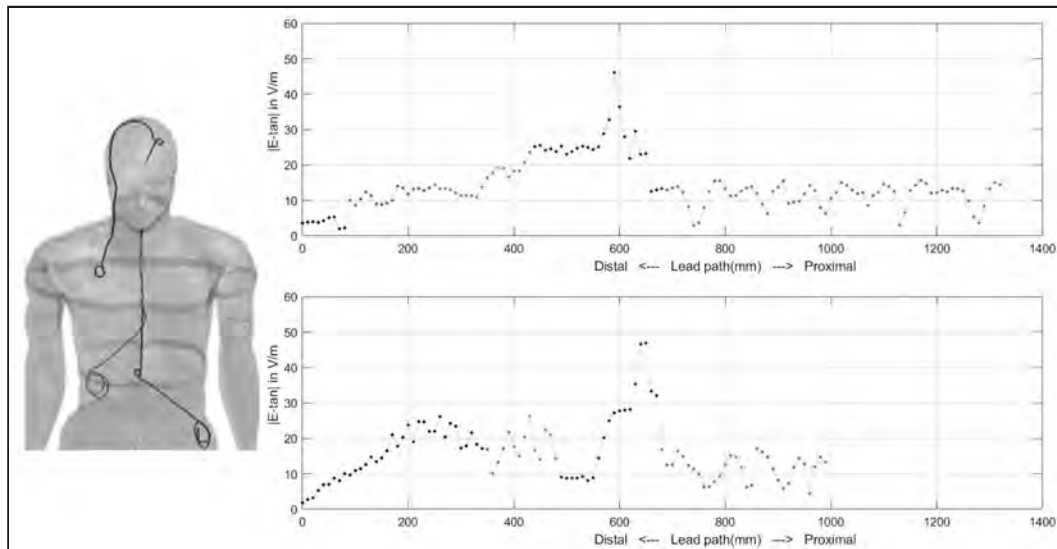
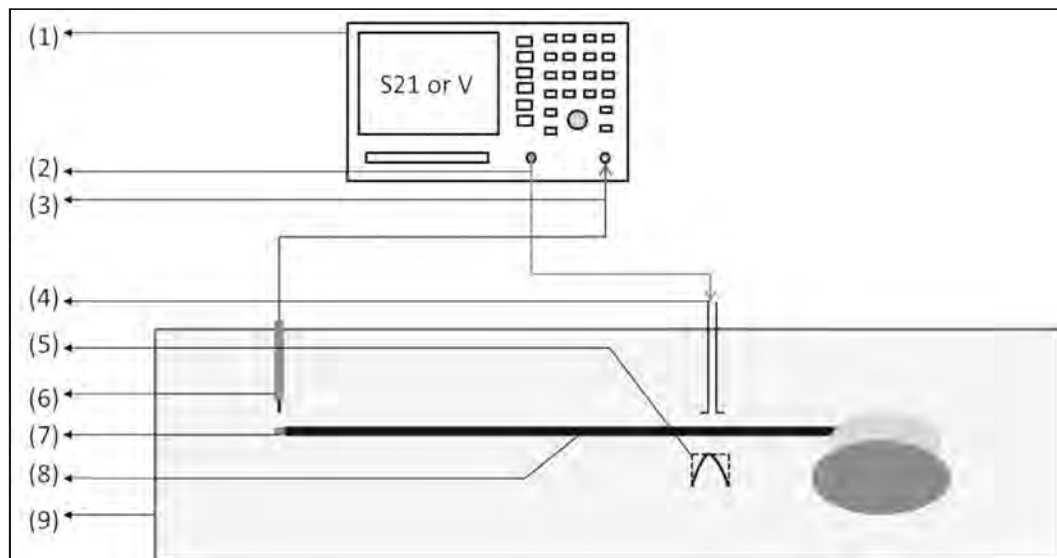


Figure 4. The Transfer Function benchtop RF injected setup: Vector Network Analyzer (VNA) (1), RF source (2), sense input (3), transmitting antenna (4), localized E-tan(z) (5), coaxial antenna (6), tip electrode (7), the AIMD (IPG plus lead) (8), tissue simulating phantom (9). (Adapted from Reference 34.)



566 MRI Test Methods for MR Conditional AIMDs

The Transfer Function of an AIMD, when exposed to a uniform E-tan excitation, can be measured using a benchtop RF injected setup (**Figure 4**) or simulated. The Transfer Function is a one-dimensional vector having the length of the lead undergoing the test with complex values (i.e., the term S in Equations 1 and 2), whose magnitude shows the resonance length(s) of the AIMD (**Figure 5**), which is the frequencies at which the AIMD is a “good” antenna.

Three MR safety assessments that rely on modeling are, as follows:

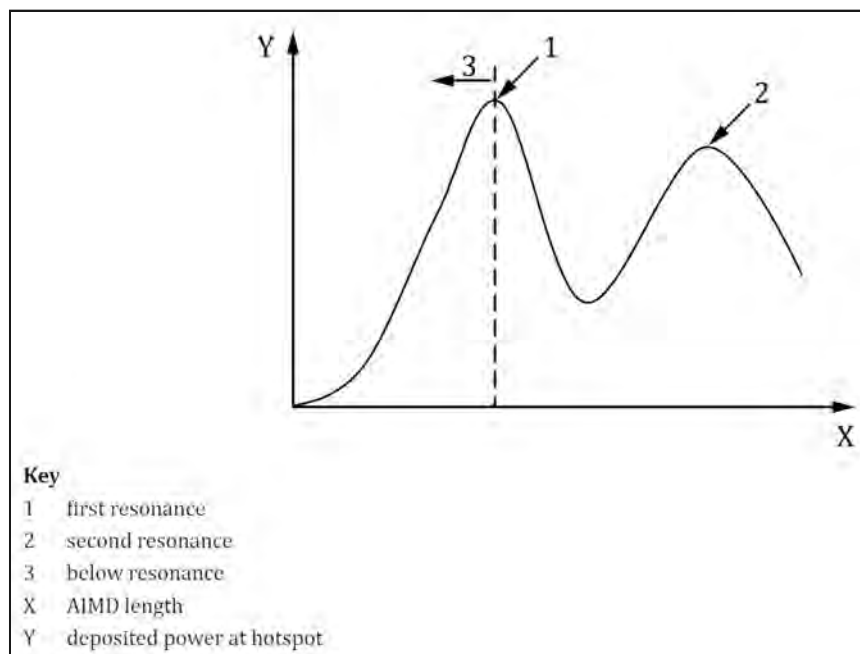
1. RF Field-Induced Heating of the AIMD (i.e., Lead Electrode Heating)

Patient harm due to RF-induced lead electrode heating is a function of absolute temperature, the duration of the temperature, and individual implant considerations. The assessment is sensitive to or is a function of the B_{1+RMS} . The test method is described in ISO/TS 10974:2018 (23).

The concept of this assessment is:

- Benchtop/MR system: The AIMD (i.e., the IPG and lead(s)) is positioned in a tissue-simulating media phantom and placed inside a of a transmit RF birdcage that is specifically-designed for testing or the transmit body RF coil of an MR scanner. The lead electrode heating is measured under various incident field conditions, including multiple lead pathways and/or RF exposures.

Figure 5. When the AIMD is exposed to a uniform E-tan excitation, the Transfer Function is obtained via measurements in benchtop RF injected setup or simulation. The peaks in its magnitude represent resonance lengths. This example shows two resonance lengths. (Adapted from Reference 23.)



- Simulation: Using simulation of this benchtop setup, *in vitro*, the E-tans are extracted for all clinically relevant lead pathways.
- Benchtop or simulation: The Transfer Function of the AIMD is measured using a benchtop injected setup or simulated.
- A predictive model of heating (and/or power) is established using the dot product of E-tans and Transfer Function according to the following formula (23, 31):

$$P = A \left| \int_0^l S_{\text{hotspot}}(z) \bullet E_{\tan}(z) dz \right|^2 \quad (1)$$

Where P is power (or heating), A is scalar imbedding the linear fit of the AIMD model and the incident field levels, S is the Transfer Function, E -tans are the *in vitro* tangential electrical incident fields, and dz is the spatial distance increment along the lead length.

- The formula above, which describes how the AIMD model is derived, is also applied to the extracted E-tans of the human using *in vivo* simulations. This often results in thousands to millions of heating predictions, accounting for all clinically relevant lead pathway scenarios and imaging conditions (i.e., human models, transmit RF coils, and imaging landmarks).
- Experimental exposure tests yield normalization factors that tie the heating results to specific $B_{1+\text{RMS}}$ levels, allowing prediction of heating under any desired $B_{1+\text{RMS}}$, as well as performing the MRI examination in the Normal Operating Mode (whole-body averaged specific absorption rate limited to 2 W/kg) or the First Level Controlled Operating Mode (whole-body averaged specific absorption rate limited to 4 W/kg).
- The heating acceptance criterion for the tissue surrounding the lead electrode dictates what RF limit is appropriate for the specific AIMD (i.e., the IPG plus lead(s)).
 - If the results of this assessment determine that this particular AIMD's lead electrode heats up tissue surrounding the electrode up to X degrees Celsius under MRI performed in the Normal Operating Mode, and if the acceptance criterion threshold for these tissue(s) heating is above this X level, then scanning under Normal Operating Mode is deemed safe for a patient implanted with this AIMD.
 - However, if the acceptance criterion for the tissue(s) heating is below this X level, then safe scanning requires selecting pulse sequence parameters that reduce the RF level on the MR system below the Normal Operating Mode limit to a level at which heating is below the acceptance criterion threshold. That RF exposure level will be considered acceptable and will be expressed in terms of a $B_{1+\text{RMS}}$ value, as well as its corresponding whole-body averaged SAR value as the RF limit in the MR Conditional information presented in the labeling for a given AIMD.

2. Unintended Stimulation from RF Field-Induced Rectified Lead Voltage

This assessment is very similar to the lead electrode heating. However, it is sensitive to or is a function of the peak RF field. And the test is described in ISO/TS 10974:2018 (23).

The concept of this assessment is:

568 MRI Test Methods for MR Conditional AIMDs

- Benchtop/MR system: The AIMD (i.e., the IPG and lead(s)) is positioned in a tissue-simulating media phantom and placed inside a transmit RF birdcage specially-designed for testing or of a transmit body RF coil of an MR scanner. The lead injection voltage towards the IPG is measured under various incident field conditions including, multiple lead pathways and/or RF exposures.
- Simulation: Using simulation of this benchtop setup *in vitro*, the E-tans are extracted for all clinically relevant lead pathways.
- Benchtop or simulation: The Transfer Function of the AIMD is measured using a benchtop injected setup or simulated.
- A predictive model of injection voltage is established using the dot product of E-tans and Transfer Function according to the following formula (23):

$$V = A \int_0^l S(z) \bullet E_{\tan}(z) dz \quad (2)$$

Where V is the voltage level, A is scalar imbedding the linear fit of the AIMD model and the incident field levels, S is the Transfer Function, E-tans are the *in vitro* tangential electrical incident fields and dz is the spatial distance increment along the lead length.

- The formula above, which describes how the AIMD model is derived, is also applied to the extracted E-tans of the human using *in vivo* simulations. That results in thousands to millions of RF level predictions accounting for all clinically relevant lead pathway scenarios and imaging conditions (i.e., human models, transmit RF coils, and imaging landmarks).
- The proper RF energy peak value(s) reflecting various transmit RF coil types in clinical MR systems are used in this assessment.
- The IPG should pass the acceptance criterion established by the device manufacturer based on the intended functionality when this voltage level is injected into the IPG.

3. Unintended Stimulation from Gradient Field-Induced Lead Voltage (Extrinsic Electric Potential)

Various scenarios of intra-lead, inter-lead or between electrodes and a conductive IPG enclosure can result in current flow through the IPG and could cause unintended stimulation of tissue in contact with the electrodes. This assessment is similar to the RF field-induced rectified lead voltage. However, because of the nature of gradient magnetic fields, it does not rely on a Transfer Function. The assessment is sensitive to or is a function of the peak gradient magnetic fields. The test is described in ISO/TS 10974:2018 (23).

The concept of this assessment is:

- The injection voltage assessment is established using the extracted E-tans of the human *in vivo* gradient simulations (23):

$$V = \int_0^l E_{\tan}(z) dz \quad (3)$$

Where V is the voltage level, E is the *in vivo* tangential electrical incident fields and dz is the spatial distance increment along the lead length.

- That results in thousands to millions of voltage predictions accounting for all clinically relevant lead pathway scenarios and imaging conditions (i.e., human models, gradient coils, and imaging landmarks).
- The IPG should pass the acceptance criterion established by the device manufacturer based on the intended functionality when this voltage is injected into the IPG.

LEARNING POINTS FOR MRI PROFESSIONALS WITH RESPECT TO PERFORMING MRI SAFELY IN PATIENTS - FOLLOWING THE LABELING:

- For an MR Conditional AIMD, the labeling conditions address the safety issues as long as clinical conditions stay within them according to the device's MRI-related, Instructions for Use.
 - That is, the MRI professionals (i.e., the MRI technologist/radiographer and radiologist) does not need to be concerned about specific AIMD-related, MRI-based risk versus benefit decisions, as long as the conditions are adhered to according to the MR Conditional labeling for the device.
- Certain implants allow scanning under the Normal Operating Mode, which does not usually pose a challenge to MRI technologists/radiographers with respect to performing safe and effective MRI examinations.
- Other implants may have limits on time-varying gradients (which is usually unlikely) and/or the RF energy levels (i.e., a low whole-body averaged SAR is required), which is the most common limit (typically expressed as B_{1+RMS} and/or SAR limits for AIMDs).
- Implants with a zonal (i.e., imaging landmark) or anatomical restriction typically have the restriction based on sensitivity to B_{1+RMS} , the whole-body average SAR, and/or the head SAR value.
- An implant with a transmit RF coil type restriction (e.g., a transmit/receive head RF coil only) requirement in the MR labeling, is also related to RF energy restriction based on sensitivity to the B_{1+RMS} (although, the peak RF energy is different for various transmit RF coils). Note: Transmit/receive head RF coils expose the patients to RF fields only within the confines of the head coil. When an AIMD is only cleared for use with a transmit/receive head RF coil, if the transmit body RF coil is activated for any reason with any receive-only RF coil, or if the transmit body RF coil and receive-only head RF coil is used, it could present a substantial patient hazard.
- For those implants with an RF limit of B_{1+RMS} (and its corresponding SAR limit), using the B_{1+RMS} -based limit is less restrictive, provided that the MR system provides the B_{1+RMS} value. This is because the SAR limit is the minimum value for the range of SAR values corresponding to this one particular B_{1+RMS} limit. That is, for each B_{1+RMS} value, the corresponding SAR is a range of values since SAR is a function of the patient's body weight and the imaging landmark.

570 MRI Test Methods for MR Conditional AIMDs

- Not adhering to the RF limits indicated in the MR Conditional label for an AIMD can lead to exceeding the acceptable limit and result in harm to the patient that are sensitive to B_{1+RMS}/SAR and/or RF coil type restrictions and/or zone landmark restrictions, which are the most important for electrode heating. The most prominent example, documented in 2005, is a patient with a DBS system who was scanned in violation of multiple labeling conditions, leading to a permanent neurological deficit (8).
- Malfunction of an AIMD can be related to the strength of the static magnetic field, the peak time-varying gradient magnetic fields, or the peak RF field. These are all electromagnetic field values that either cannot be changed or cannot readily be altered by the MRI technologist/radiographer. Thus, it is important to abide by the information in the MR Conditional labeling for the AIMD in order to ensure patient safety.
- For an AIMD requiring setting up or programming of the device in its “MRI mode” prior to scanning, it is important to do so to avoid potential device malfunction that can occur either during or following the MRI examination.
- For AIMDs requiring RF power levels lower than the Normal Operating Mode (i.e., whole body averaged SAR of 2 W/kg) when the intended pulse sequence to be used exceeds the implants B_{1+RMS} or SAR limit, the following may be done:
 - If the MR system is “implant friendly”, use the recommended option or software. For example, ScanWise Implant software (Philips Healthcare, Amsterdam, The Netherlands) may be used to place appropriate limits on the MRI parameters when scanning patients with MR Conditional implants (32). Importantly, this software provides step-by-step guidance to enter the acceptable field exposure values (e.g., B_{1+RMS}) for a given implant based on the Instructions for Use. Then, the MR system automatically applies these values for the entire examination, resulting in an easily implemented means of performing MRI in patients with implants and devices, especially when the conditions may be particularly restrictive. Otherwise, any parameter that affects RF power level can be adjusted to reduce the value according to the following suggestions (33).
 - Use the “Low SAR” option on the MR system. This feature is available on most MR scanners and helps to reduce the B_{1+RMS} or SAR, typically without impacting image quality. However, it is unlikely that this option, by itself, will suffice in certain instances. Therefore, use this option in combination with one or more options adjustments to the pulse sequence parameters: (1) increase the repetition time (TR), but not to the extent that it changes the image contrast, as in T1-weighted spin echo pulse sequences; and/or (2) reduce the number of section locations or the grouping of section locations; and/or (3) reduce the flip-angle used for the pulse sequence, or the refocusing flip-angle; and/or (4) use fewer RF saturation bands; and/or (5) decrease the number of phase encodes; and/or (6) reduce the number of echoes such as with respect to the echo train length or the turbo factor (34).

CONCLUSIONS

MR Conditional labels for AIMDs are developed through rigorous testing by implantable device manufacturers or test houses using methods and guidelines that were developed with contributions from experts in various fields including MR system manufacturers, implant manufacturers, test houses, MRI physicists and other scientists, and regulatory agencies. Formal Instructions for Use information for MR Conditional implants are the proper source for the MR scanning conditions and parameters that will ensure patient

safety because they derive directly from rigorous test methods. The MRI safety community is gaining expertise from the use of more MR Conditional AIMDs and reflecting these experiences with collaborations from experts in the field for the benefit and safety of scanning patients with implants and devices.

Patients and clinicians have also benefitted from efforts by MR system manufacturers to design more advanced software, including those with options for limiting exposure to MRI-related electromagnetic fields. These have already helped clinicians to provide access to MRI technology for patients with implanted devices. Furthermore, there are exciting opportunities for improving patient access to MRI examinations in a safe manner in the future through advancing technologies and continued collaboration in the development of safety testing methods and standards.

REFERENCES

1. International Electrotechnical Commission, IEC 60601-2-33:2010+AMD1:2013+AMD2:2015 CSV, Consolidated version. Medical electrical equipment - Part 2-33: Particular requirements for the basic safety and essential performance of magnetic resonance equipment for medical diagnosis.
2. Delfino JG, Krainak DM, Flesher SA, et al. MRI-related FDA adverse event reports: A 10-yr review. *Med Phys* 2019;46:5562-5571.
3. Erlebacher JA, Cahill PT, Pannizzo F, et al. Effect of magnetic resonance imaging on DDD pacemakers. *Am J Cardiol* 1986;57:437-40.
4. Becker RL, Norfray JF, Teitelbaum GP, et al. MR imaging in patients with intracranial aneurysm clips. *AJNR Am J Neuroradiol* 1988;9:885-889.
5. Klucznik RP, Carrier DA, Pyka R, et al. Placement of a ferromagnetic intracerebral aneurysm clip in a magnetic field with a fatal outcome. *Radiology*. 1993;187:855-856.
6. Shellock FG. MR imaging of metallic implants and materials: A compilation of the literature. *Am J Roentgenol* 1988;151:811-814.
7. Shellock FG, Slimp G. Severe burn of the finger caused by using a pulse oximeter during MRI. *AJR Am J Roentgenol* 1989;153:1105.
8. Henderson JM, Tkach J, Phillips M, et al. Permanent neurological deficit related to magnetic resonance imaging in a patient with implanted deep brain stimulation electrodes for Parkinson's disease: case report. *Neurosurgery* 2005;57:E1063.
9. American Society of Testing and Materials International, ASTM F2182-19e2. Standard Test Method for Measurement of Radio Frequency Induced Heating On or Near Passive Implants During Magnetic Resonance Imaging. 2019.
10. American Society of Testing and Materials International, ASTM F2503-20. Standard Practice for Marking Medical Devices and Other Items for Safety in the Magnetic Resonance Environment. 2020.
11. American Society of Testing and Materials International, ASTM F2052-15. Standard Test Method for Measurement of Magnetically Induced Displacement Force on Medical Devices in the Magnetic Resonance Environment, 2015.
12. American Society of Testing and Materials International, ASTM F2213-17. Standard Test Method for Measurement of Magnetically Induced Torque on Medical Devices in the Magnetic Resonance Environment.
13. American Society of Testing and Materials International, ASTM F2119-07 (2013). Standard Test Method for Evaluation of MR Image Artifacts from Passive Implants, 2013.
14. Shellock FG, Crues, JV. Editors. *MRI Bioeffects, Safety, and Patient Management*. Biomedical Research Publishing Group, Los Angeles, CA, 2014.

572 MRI Test Methods for MR Conditional AIMDs

15. Shellock FG. Reference Manual for Magnetic Resonance Safety, Implants, and Devices: 2020 Edition. Biomedical Research Publishing Group, Los Angeles, CA, 2020.
16. International Organization for Standardization, ISO 14708-1:2014. Implants for surgery — Active implantable medical devices — Part 1: General requirements for safety, marking and for information to be provided by the manufacturer.
17. Rezai AR, Finelli D, Nyenhuis JA, et al. Neurostimulator for deep brain stimulation: *Ex vivo* evaluation of MRI-related heating at 1.5-Tesla. *J Magn Reson Imaging* 2002;15:241-250.
18. Finelli DA, Rezai AR, Ruggieri P, et al. MR-related heating of deep brain stimulation electrodes: An *in vitro* study of clinical imaging sequences. *AJNR Am J Neuroradiol* 2002;23:1795-1802, 2002.
19. Finelli D, Rezai AR, Ruggieri P, Tkach J, Nyenhuis JA, Shellock FG. Neurostimulation systems used for deep brain stimulation: *In vitro* assessment of MRI-related heating at 1.5-Tesla. *Radiology* 2002;222:586.
20. Sharan A, Rezai AR, Nyenhuis JA, et al. MR safety in patients with implanted deep brain stimulation systems (DBS). *Acta Neurochir* 2003;Suppl. 87:141-145.
21. Mitka M. First MRI-safe pacemaker receives conditional approval from FDA. *JAMA*. 2011;305:985-986.
22. International Organization for Standardization, ISO/TS 10974:2012. Assessment of the safety of magnetic resonance imaging for patients with an active implantable medical device.
23. International Organization for Standardization, ISO/TS 10974:2018. Assessment of the safety of magnetic resonance imaging for patients with an active implantable medical device.
24. Testing and Labeling Medical Devices for Safety in the Magnetic Resonance (MR) Environment. Guidance for Industry and Food and Drug Administration Staff. Issued May, 2021.
25. Shellock FG, Zare A, Ilfeld BM, Chae J, Rauck RL, Strother R. *In vitro* MRI evaluation of fragmented, open-coil percutaneous peripheral nerve stimulation leads. *Neuromodulation* 2017;21:276-283.
26. Yao A, Goren T, Samaras T, et al. Radiofrequency-induced heating of broken, damaged, and abandoned leads. *Proceedings of the International Society of Magnetic Resonance in Medicine* 2021;29.
27. Aldayeh L, Rahman M, Venook R. Impact of a neighboring device on *in vitro* lead heating measurements. *Proceedings of the International Society of Magnetic Resonance in Medicine* 2020;28.
28. Kainz W. MR heating tests of MR critical implants. *J Magn Reson Imaging* 2007;26:450-451.
29. Shellock FG, Kanal E, Gilk T. Confusion regarding the value reported for the term “spatial gradient magnetic field” and how this information is applied to labeling of medical implants and devices. *AJR Am J Roentgenol* 2011;196:142-145.
30. Shellock FG, Crues JV. MR procedures: Biologic effects, safety, and patient care. *Radiology* 2004;232:635-652, 2004.
31. Park SM, Kamondetdacha R, Nyenhuis JA. Calculation of MRI-induced heating of an implanted medical lead wire with an electric field Transfer Function. *J Magn Reson Imaging* 2007;26:1278-85.
32. <https://www.usa.philips.com/healthcare/education-resources/technologies/mri/scanwise-implant>. Accessed June, 2020.
33. Franceschi AM, Wiggins GC, Mogilner AY, et al. Optimized, minimal specific absorption rate MRI for high-resolution imaging in patients with implanted deep brain stimulation electrodes. *AJNR Am J Neuroradiol* 2016;37:1996–2000.
34. International Organization for Standardization, ISO/TIR 21900:2018. Guidance for uncertainty analysis regarding the application of ISO/TS 10974.
35. Aldayeh L, Rahman M, Venook R. Practical Aspects of MR imaging safety test methods for MR Conditional active implantable medical devices. *Magn Reson Imaging Clin N Am* 2020;28:559-571.
36. Association for the Advancement of Medical Instrumentation, AAMI PC76:2021. Active implantable medical devices - Requirements and test protocols for safety of patients with pacemakers and ICDs exposed to magnetic resonance imaging.

MRI Bioeffects, Safety, and Patient Management 573

37. International Organization for Standardization, ISO 14708-3:2017. Implants for surgery - Active implantable medical devices - Part 3: Implantable neurostimulators

Chapter 22 Using MRI Simulations and Measurements to Evaluate Heating of Active Implants by Radiofrequency Fields and Gradient Magnetic Fields

JOHN NYENHUIS, PH.D.

Professor Emeritus of Electrical and Computer Engineering
Purdue University
School of Electrical and Computer Engineering
West Lafayette, IN

INTRODUCTION

Active implants may pose hazards to patients referred for magnetic resonance imaging (MRI) procedures. An active implant is defined as one that relies on its function from a source of electrical energy or any source of power other than that directly generated by the human body or gravity (1). In contrast, a passive implant, such as a coronary artery stent, hemostatic clip, or hip prosthesis, does not require electrical power or other external energy in its operation or during its intended use. Some active implants have external leads and electrodes for delivery of electric current for therapy and/or for physiologic sensing. Examples of active implants include cardiac pacemakers, implantable cardioverter defibrillators (ICDs), neurostimulation systems, bone growth stimulators, and cochlear implants. Other types of active implants, such as implantable drug infusion pumps, use electrical power for operation but may not have attached metallic leads and electrodes.

IN-VITRO TESTS OF HEATING

Implants with conducting leads have been referred to as “MR Critical” with respect to radiofrequency (RF) heating because of the length of the metallic materials (2). Testing in phantoms has demonstrated the potential for significant temperature rises at the electrodes of leads that are part of an active implant system (3). For example, Rezai, et al. (4) measured a temperature rise of 25.3°C on the tip of a deep brain stimulation (DBS) lead in a phantom

at 1.5-Tesla/64-MHz in association with an MR system reported, whole-body averaged SAR of 3.9-W/kg. Achenbach, et al. (5) reported a temperature increase of 63.1°C at the electrode tip for a cardiac pacing lead not connected to a pulse generator (PG) under 1.5-Tesla/64-MHz conditions. Luechinger (6) measured an RF-induced temperature rise in laboratory animals (pigs). A maximum temperature increase of 15°C was measured for a passive fixation lead and a temperature rise in excess of 30°C was measured for a “cork-screw” fixation lead (6). No significant threshold or impedance changes of the cardiac pacing leads were measured nor did pathology indicate any heat-related damage under the conditions used in this investigation.

CLINICAL RELEVANCE

An understanding of heating behavior for active implant-related leads is crucial to establishing patient safety in association with the use of MRI. Excessive heating at the electrode could damage the surrounding tissue, which may be particularly serious for neurological or cardiac tissue. Active implants with lead wires are mostly contraindicated for MRI primarily because of the large temperature rises that have been reported in laboratory testing. Before an implant manufacturer can receive regulatory approval for a given product relative to the use of MRI, tests and analyses must be undertaken to document that a patient with the implant can safely undergo an MRI procedure. This is particularly important for active implants.

Several active implants have labeling approved for patients needing MRI examinations including cardiac devices, neurostimulation systems, cochlear implants, and others. For example, the first cardiac pacemaker approved in the United States (U.S.) for MRI was the Revo MRI SureScan Pacing System (Medtronic, Minneapolis, MN) (7). Patients with the Vagus Nerve Stimulation (VNS), NeuroCybernetic Prosthesis (NCP) System (Cyberonics, Inc. and LivaNova) and the Activa Deep Brain Stimulation (DBS) System (Medtronic, Minneapolis, MN) may safely undergo MRI by following highly specific conditions (8, 9).

MRI-related heating of active implants without external leads is expected to be similar for a passive implant with similar geometry and materials (10). However, interactions of the electromagnetic fields with the device circuitry could result in heating or other issues. For example, magnetic saturation of a transformer core by the static magnetic field of the scanner may result in additional power delivery by a battery.

MECHANISM OF RADIOFREQUENCY FIELD-RELATED HEATING

The radiofrequency (RF) field used during MRI induces an electric field in the patient or the phantom (i.e., in the case of evaluating heating for implants and devices). The frequency of the RF electric field is the same as that of the RF magnetic field, 64-MHz for 1.5-T and 128-MHz for 3-T. The electric field results in power deposition from the ohmic heating of tissues. The specific absorption rate (SAR) with units of W/kg is the metric for the RF power.

The mechanism for heating of an implant during MRI is coupling of the metal with the electric fields. The tangential component of the electric field along the length of the lead

576 Using MRI Simulations and Measurements to Evaluate Active Implants

induces waves of electric current on the lead (11). These waves produce an electric field in the vicinity of the electrode, which produces heating of the tissue. There may also be measurable temperature rises due to ohmic heating by the induced RF current through the conducting wires in a lead.

Thus, the temperature rise at an electrode is due to the tangential electric field along the entire length of the lead. This concept was quantified by Park, et al. (12) using a transfer function (TF) method. The temperature rise may be expressed as

$$\Delta T = A \left| \int_0^L E_{tan}(\tau) S(\tau) d\tau \right|^2 \quad (1)$$

In Equation (1), A is a constant with units of $^{\circ}\text{C}/(\text{V}/\text{m})^2$, E_{tan} is the tangential electric field, distance $\tau = 0$ at the electrode and $\tau = L$ at the generator, and S is the transfer function (i.e., the lead model) between the incident E_{tan} and the scattered electric field near the electrode. The dimensions of S are inverse length. Both S and E_{tan} are complex, that is, they have magnitude and phase.

Due to phase effects, it is possible to have a high or low temperature rise for different lead paths in the phantom with similar magnitude of E_{tan} . This phenomenon was demonstrated by Mattei, et al. (13) who measured temperature rises for leads in a phantom for 374 different configurations. This group reported that the observed temperature rise at the tip of a pacemaker lead depended on the path in the phantom and whether or not the pulse generator was attached to the lead. In tests conducted in a circular phantom, Langman, et al. (14) also found that heating depended on the termination conditions at the generator end of the lead. Importantly, heating of a lead will also depend on how it is constructed. Nordbeck, et al. (15) measured RF heating of unipolar and bipolar pacing lead assemblies in a rectangular phantom. It was concluded that heating could be reduced by changes in the configuration of the lead. Mattei, et al. (16) tested the role of lead structure by *in vitro* measurements on 30 commercial cardiac pacemakers and implantable cardioverter defibrillator leads in a rectangular phantom. At a whole-body averaged exposure SAR of 1-W/kg, the recorded temperature rises ranged from 2.4°C to 15°C . These tests were conducted for straight-line placement of the lead in the phantom and, thus, it is possible that greater rises would be measured for other lead paths.

CALCULATION OF RADIOFREQUENCY FIELD-RELATED HEATING

The temperature rise of a passive implant in a phantom, such as a spine prosthesis or fixation device can be accurately calculated (17) and these types of simulations are described elsewhere in this textbook. Calculation of the transfer function and consequent temperature rise for an implanted lead is difficult because of the intricate and complicated geometry of the lead. The lead conductors have a minimum feature of the order of tens of microns, which is of the order of 10^5 greater than the length of the lead. Park, et al. (12) calculated S and RF-induced temperature rises for bare and insulated wires using method of moments. Neufeld, et al. (18) calculated heating for a straight insulated wire and for a helical wire

using the Finite Difference Time Domain (FDTD) method. Both groups reported agreement between calculations and measurements with a 17% uncertainty determined by Neufeld, et al. (18).

TECHNICAL SPECIFICATION ISO/TS 10974 FOR MRI AND ACTIVE IMPLANTS

A joint working group commissioned by the International Organization for Standardization (ISO) and International Electrotechnical Commission (IEC) developed a draft International Technical Specification ISO/TS 10974:2018 that provides test methods for MRI-related hazards associated with an active implantable medical device (AIMD) including RF-induced heating (1). The technical specification (TS) presents an approach with four tiers for assessment of RF heating of active implants. Tier 1 has the simplest test and computation requirements, but also requires the most conservative assumptions on incident RF energy. Tiers 2 and 3 progressively require more measurements and simulations, but are able to use successively less overestimation of test field magnitudes. Tier 4 requires the most stringent computational analysis and utilizes the least overestimation of test field magnitudes.

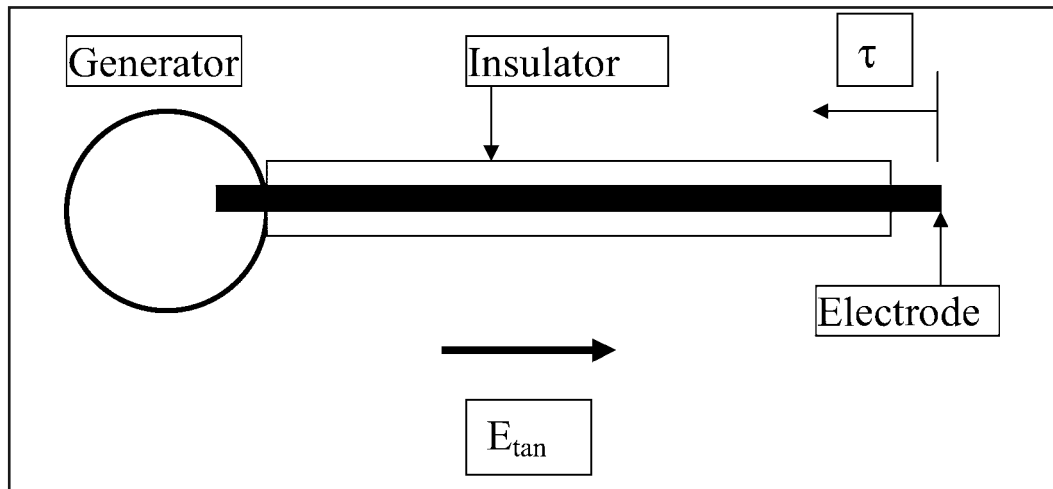
Cabot, et al. (19) evaluated RF heating of a generic deep brain stimulator in 1.5-T/64-MHz as a vehicle to test the four tiers of ISO/TS 10974. The model implant consisted of a stainless steel “can”, a dielectric header, and leads consisting of either an insulating helical copper lead or an insulated straight copper lead. Lead lengths of 50-, 100-, 150-, and 200-mm were evaluated. Simulations for this implant, which is much simpler than an actual DBS device, required as many as 500×10^6 mesh cells. Simulations were run on an accelerated cluster and it was projected that carrying out the estimated 12,000 simulations for a Tier 4 analysis would take several decades. Cabot, et al. (19) concluded with a suggestion for a procedure that follows a test strategy between Tier 3 and Tier 4.

In consideration of the above, the following information should be considered regarding MRI-related heating and active implants: (1) Heating at the electrode of an implanted lead used for a cardiac pacemaker, neurostimulation system, or other similar device that has an active lead may be significantly greater than the threshold rise of approximately 6 to 7°C for tissue injury (20). (2) Heating at the electrode is a complicated function of the magnitude and phase of the incident E_{tan} over the entire length of the lead. If only phantom tests are used to characterize lead heating behavior, a significant number of these tests may be required. (3) Current computational methods are not capable of accurately calculating the temperature rise for a clinically relevant lead wire. (4) A combined approach of innovative measurements and complementary computations will improve the accuracy and efficiency of determining the temperature rise of the lead over the clinically relevant range of incident E_{tan} .

A primary purpose of this chapter is to describe test methods and analyses to predict the heating that an active implant would undergo during MRI. The test case is a commercial neurostimulation system used for vagus nerve stimulation (Vagus Nerve Stimulation (VNS), NeuroCybernetic Prosthesis (NCP) System (Cyberonics, Inc. and LivaNova). First, the transfer function, S , is developed from electrical measurements of the response of the lead

578 Using MRI Simulations and Measurements to Evaluate Active Implants

Figure 1. Geometry of an active implant with lead wire in the presence of a tangential electric field, E_{tan} .



to a localized electric field and from selected phantom measurements. Second, the *in vivo* temperature rise is calculated based on the electric fields along the path of the lead in the patient during MRI and the transfer function. Thus, a focus of this chapter is on computer simulations and laboratory tests. More clinically oriented perspectives on performing MRI in patients with active implants are presented in other chapters of this textbook.

MECHANISM AND MODELING FOR HEATING OF AN ELECTRODE AT THE END OF A LEAD

Transfer Function Concept

Heating at the electrode of a lead for an active implant occurs from coupling of the RF electric field in the body to the lead. **Figure 1** illustrates this mechanism. The tangential electric field along the length of the lead induces waves of current on the metal of the lead. The current waves propagate along the lead and are partially reflected and partially transmitted at the pulse generator and at the electrode. The transmitted current at the electrode produces power deposition in the tissue surrounding the electrode and there is a consequent temperature rise.

The relationship between electric field \mathbf{E} and current density \mathbf{J} in the tissue at the electrode is

$$\mathbf{J} = \sigma \mathbf{E} \quad (2)$$

where σ is the electrical conductivity with units of S/m. The specific absorption rate (SAR) is the power deposition and is expressed as

$$SAR = \frac{\sigma E_{rms}^2}{\rho} \quad (3)$$

where E_{rms} is the root mean square (rms) value of the electric field and ρ is the mass density. For soft tissue, ρ is not too different from the value of 1000-kg/m^3 for water and conductivity generally ranges from $0.1\text{- to }1\text{-S/m}$. The temperature rise at the electrode will be proportional to the power deposition P in some fixed small fixed volume surrounding the electrode,

$$\Delta T = \zeta W \quad (4)$$

where power W is determined by the integration of the SAR around the electrode and the factor ζ between ΔT and W has units of $^{\circ}\text{C/W}$.

The background E_{tan} is the tangential electric field along the path of the lead that is present in the medium (phantom or patient) without the lead. The magnitude E_{rms} of the electric field at some location P near the electrode is due to the weighted integral E_{tan} along the length of the lead.

$$E_{rms}(P) = K(P) \left| \int_0^L E_{tan}(\tau) S(\tau) d\tau \right| \quad (5)$$

where K is a constant that is a function of location near the electrode and S is the transfer function that reflects the degree of coupling between the tangential electric field along the length of the lead.

At a fixed position surrounding the electrode, the temperature rise is proportional to E_{rms}^2 which is expressed by Equation (1), which is repeated here because of its importance.

$$\Delta T = A \left| \int_0^L E_{tan}(\tau) S(\tau) d\tau \right|^2 \quad (1)$$

Both E_{tan} and S are complex, that is, they have both magnitude and phase. By knowing S , the temperature rise at the electrode is known for any distribution of E_{tan} .

If incident electric field is uniform in magnitude and phase along the length of the lead, E_{tan} in Equation (1) can be taken outside the integral and temperature rise ΔT_U for uniform incident electric field is

580 Using MRI Simulations and Measurements to Evaluate Active Implants

$$\Delta T_U = A \left| \int_0^L S(\tau) d\tau \right|^2 |E_{tan}|^2 \equiv \gamma |E_{tan}|^2 \quad (6)$$

The γ factor in Equation (6) is generally what is measured in a phantom test conducted according to ASTM F2182 (21) on a relatively small implant that is inside a region of a uniform electric field.

The worst-case possible temperature rise ΔT_{max} is defined as the one that occurs when E_{tan} and S are conjugate in phase over the entire length of the lead. For this situation, the temperature rise depends on the magnitude of E_{tan} and S .

$$\Delta T_{max} \equiv A \left| \int_0^L |S(\tau)| |E_{tan}(\tau)| d\tau \right|^2 \quad (7)$$

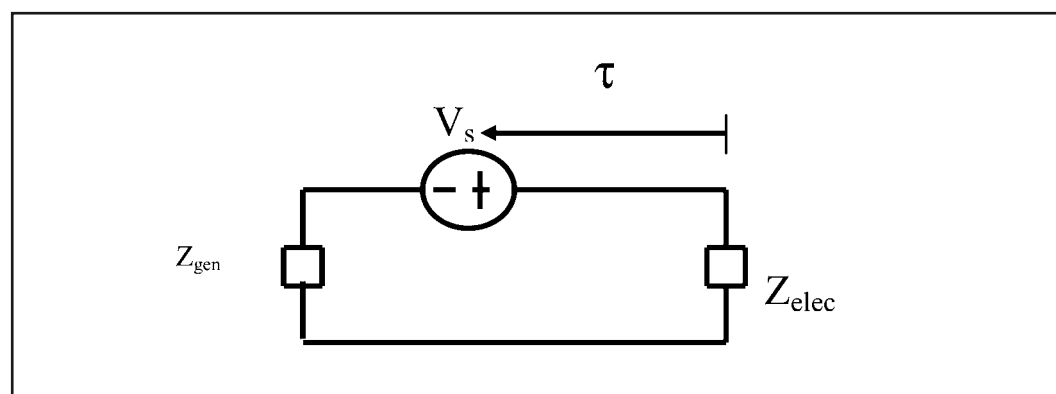
The rise ΔT_{max} is a calculated quantity that is not directly measured. It is a consequence of constructive contribution of E_{tan} over the length of the lead. The value for ΔT_{max} can be viewed as a metric of the total input power that is applied to the lead by the incident electric field.

Wave (Transmission Line) Model

A model incorporating propagation of electric current along the length of the lead and reflection of current from the pulse generator and the electrode is useful for understanding the behavior of the current waves on the lead. This model may also be useful for determination of an approximate transfer function through a spatial harmonic fit to temperature rises measured for different paths in a phantom.

Equations from transmission line theory are used to describe the behavior of the current waves on the lead. In **Figure 2**, a voltage $V_s = E_{tan} d\tau$ is applied at distance τ from the elec-

Figure 2. Transmission line circuit for analysis of current waves on a lead.



trode by the tangential component of the external electric field. The current induced by V_s is

$$I_{in} = \frac{V_s}{Z_{ingen} + Z_{inelec}} \quad (8)$$

where Z_{ingen} is the impedance from the excitation point to the generator and Z_{inelec} is the impedance to the electrode. Assume sinusoidal waves on a transmission line. Then the voltage, V , and current, I , may be written as

$$V(z) = V_+ [e^{-\gamma z} + \rho e^{\gamma z}] \quad (9)$$

$$I(z) = \frac{V_+}{Z_0} [e^{-\gamma z} - \rho e^{\gamma z}] \quad (10)$$

where $z = 0$ is at the electrode and $z = -L$ at the generator, V_+ is an amplitude factor, and ρ is the reflection coefficient at $z = 0$. The propagation constant γ is

$$\gamma = j\beta + \alpha = j\frac{2\pi}{\lambda} + \alpha \quad (11)$$

where λ is the wavelength and α is the damping constant that arises from energy loss in the medium in which the waves propagate. The reflection coefficient at the electrode is

$$\rho_{elec} = \frac{Z_{elec} - Z_L}{Z_{elec} + Z_L} \quad (12)$$

In Equation (12), Z_{elec} is the impedance at the electrode, and Z_L is the characteristic impedance for propagation of waves along the lead. Similarly, the reflection coefficient ρ_{gen} at the pulse generator is

$$\rho_{gen} = \frac{Z_{gen} - Z_L}{Z_{gen} + Z_L} \quad (13)$$

582 Using MRI Simulations and Measurements to Evaluate Active Implants

From transmission line theory

$$Z_{ingen} = Z_L \frac{e^{\gamma(L-\tau)} + \rho_{gen} e^{-\gamma(L-\tau)}}{e^{\gamma(L-\tau)} - \rho_{gen} e^{-\gamma(L-\tau)}} \quad (14)$$

$$Z_{inelec} = Z_L \frac{e^{\gamma\tau} + \rho_{elec} e^{-\gamma\tau}}{e^{\gamma\tau} - \rho_{elec} e^{-\gamma\tau}} \quad (15)$$

where L is the line length.

The electrode current due to the electric field applied over the differential length is then

$$dI_{electrode} = I_{in} \frac{1 - \rho_{elec}}{e^{\gamma\tau} - \rho_{elec} e^{-\gamma\tau}} \quad (16)$$

The voltage at the load is

$$dV_{electrode} = dI_{electrode} Z_L = I_{in} Z_L \frac{1 - \rho_{elec}}{e^{\gamma\tau} - \rho_{elec} e^{-\gamma\tau}} \quad (17)$$

The load voltage $dV_{electrode}$ is a function of position τ along the lead and is proportional to S .

TEST METHODS FOR MEASUREMENT OF ELECTRODE HEATING AND DETERMINATION OF THE TRANSFER FUNCTION

The objective of the tests and analysis described in this section is to determine the transfer function, S . Notably, all of the described analysis and measurement methods have been tested in this author's laboratory.

Heating Test Performed in a Rectangular Phantom (ASTM F2182)

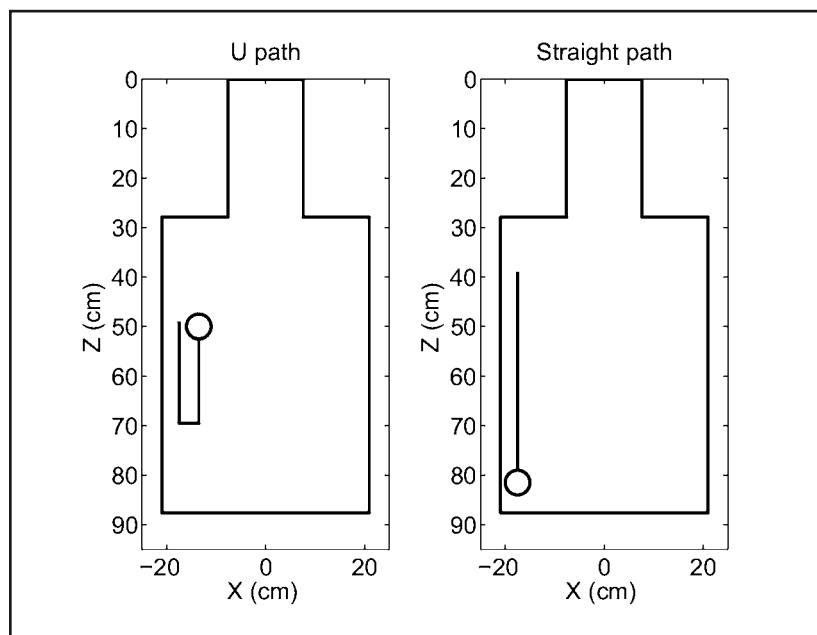
The standard from the American Society for Testing and Materials (ASTM) International, ASTM F2182 (21), specifies a method for testing RF-induced heating of a passive implant. It incorporates a rectangular phantom that is filled with gelled-saline and takes up much of the area of the bore of the MR system. One type of rectangular ASTM phantom is shown in **Figure 3**. The electric field induced in the phantom by the RF field used during MRI is non-uniform. Its distribution will depend on several factors including the position of the phantom in the bore, the RF frequency, and the polarization of the incident RF mag-

netic field. Plots of the calculated electric field for the phantom in **Figure 3** have been presented by Amjad, et al. (22). At the sides of the phantom and in the region of the landmark for MRI (i.e., the center of the body RF coil), the electric field in a vertical plane is parallel to the wall and is uniform in magnitude over a distance of approximately 20-cm. Passive implants are generally tested for heating in the region of a relatively uniform field, although the measurement accuracy may be impacted for larger implants by the variation of the electric field in the vertical direction of the phantom. The γ factor in Equation (6) may be derived from the phantom test. Since the standard specifies a fixed conductivity (i.e., 0.47-S/m) for the phantom filled with gelled-saline, the temperature rise normalized to the local background SAR will be proportional to γ .

The non-uniform distribution in magnitude and direction of electric field in the phantom can be useful for testing heating of active implants. **Figure 3** illustrates two paths for a heating test on a lead with a pulse generator. In the straight-line configuration, E_{tan} has somewhat uniform magnitude and phase over the entire lead length. The temperature rise for this configuration will be approximately proportional to γ . For the U-path, the magnitude of E_{tan} is approximately uniform along the lead, although the inner section of the loop will have lower $|E_{tan}|$ than the outer. However, the phase of E_{tan} will differ by about 180° between the two sections of the lead that are parallel to the wall. Notably, the temperature rise measured in the straight- and U-paths for the same incident RF power can be very different.

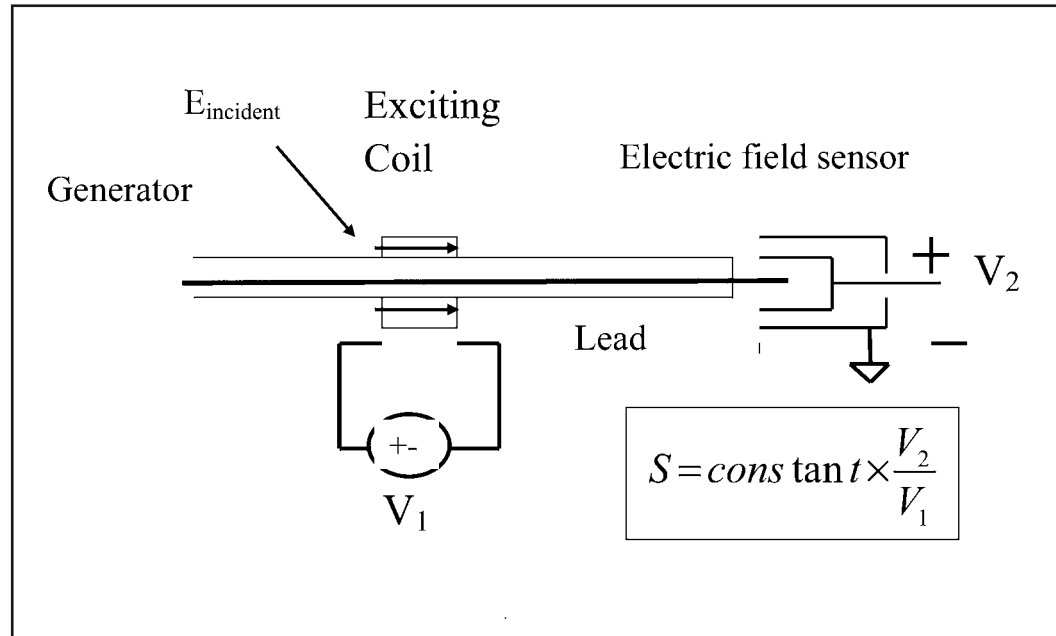
Temperature rises for a variety of E_{tan} distributions along the lead can be obtained by performing the heating tests with the lead arranged in more paths than the two that are de-

Figure 3. Top views of the ASTM phantom with sample paths for testing temperature rises at the electrode for a lead attached to a pulse generator. This figure illustrates a U-path (Left) and a straight-path (Right) for the lead.



584 Using MRI Simulations and Measurements to Evaluate Active Implants

Figure 4. Geometry for assessment of the transfer function. A tangential electric field is applied over a short length of the lead with a toroidal coil. The scattered electric field at the electrode of the lead is proportional to the voltage induced in an electric field sensor. The transfer function, S , is proportional to the ratio of the voltage, V_2 , at the sensor to the input voltage, V_1 , applied to the coil. The coil is translated along the lead to get the transfer function as function of the position relative to the lead.



picted in **Figure 3**. With sufficient heating information, it is in principle possible to obtain a good approximation for the transfer function, S . For leads with S that are well fit by the transmission line model, an accurate determination of S may be possible with just a small number of tests.

Electrical Measurement of the Transfer Function

Figure 4 illustrates the principle of the measurement of the transfer function, S . A tangential electric field is applied along a section of lead with a small toroidal coil, which may have a magnetic or an air core. Current applied to the coil produces an electric field on its axis that launches a current wave on the lead. The scattered electric field surrounding the electrode is measured with an electric field sensor.

A typical implementation for the transfer function measurement will be for V_1 to be the amplified output from port 1 of a network analyzer. The sensor voltage V_2 is applied to port 2 and the transfer function is proportional to the S_{21} that is measured by the vector network analyzer.

The apparatus in **Figure 4** will determine the network analyzer transfer function S_{NA} which is S multiplied by a constant.

$$S = K_S S_{NA} \quad (18)$$

The constant K_S depends on the several experimental factors, including coil geometry, coil RF response, sensor geometry and location of the electrode in the sensor. K_S is determined from the temperature rise ΔT_{test} , a heating test with a known distribution of electric field:

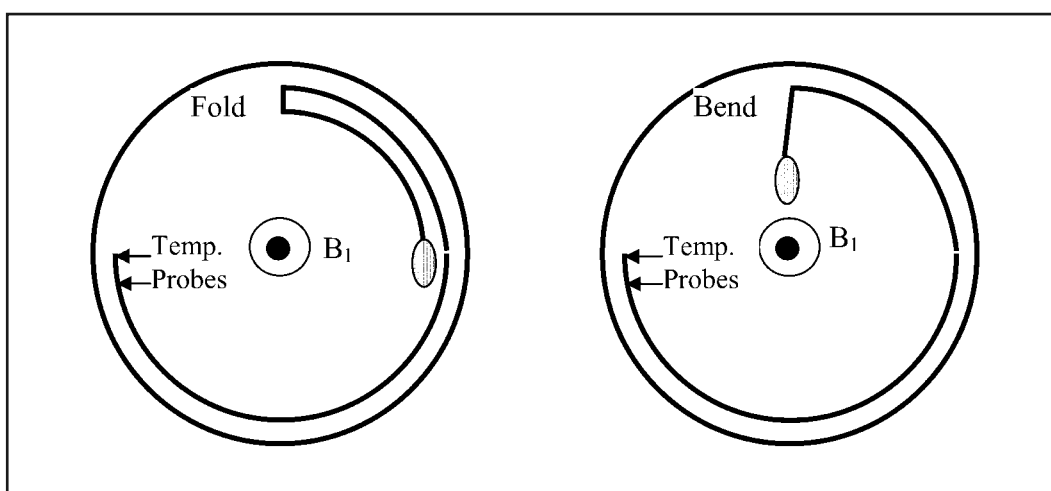
$$K_S^2 = \frac{1}{A} \frac{\Delta T_{test}}{\left| \int_0^L S_{NA}(\tau) E_{\tan}(\tau) d\tau \right|^2} \quad (19)$$

Note that K_S can be considered to be real, as adding a constant phase to the transfer function does not change the calculated temperature rise.

Foldback and Successive Length Tests in a Circular Phantom

Figure 5 shows two layouts for testing electrode heating in a circular phantom. In the foldback method, the lead with generator or other termination is placed in a circular phantom with gelled-saline of a composition that is the same or similar to that specified in ASTM F2182 (21). A representative phantom diameter is 33-cm. The entire length of the lead is about 2-cm from the wall of the phantom. A section of lead adjacent to the pulse generator is folded back toward the electrode. The overlapped sections of the lead should be arranged above each other, so that the entire length of the lead is at the same radial distance from the center of the phantom.

Figure 5. Geometry for the heating tests in a circular phantom. (Left) Fold back test. (Right) The progressive length (“spoke”) test.



586 Using MRI Simulations and Measurements to Evaluate Active Implants

It is desired that the tangential electric field E_{tan} (ϕ component) have uniform magnitude and phase around the circumference of the phantom. This is achieved by applying the RF magnetic field B_1 perpendicular to the plane of the phantom. B_1 should be either uniform over the phantom or be circularly symmetric with respect to the center of the phantom. This geometry of B_1 could be achieved using a vertical polarized birdcage coil, a single loop circular coil that surrounds the phantom, or other appropriate method.

Temperature probes are placed at the electrodes or other relevant locations. The temperature rise is measured as a function of the foldback distance (FBD) between the generator and the 180° turns in the lead. Let L_0 be the lead length. Then:

$FBD = 0$ means that the lead is in a straight line along the circumference.

$FBD = L_0/2$ means that the lead is in a “U” path.

$FBD = L_0$ means that the lead is a straight along the circumference, opposite the configuration for $FBD = 0$.

A possible procedure for the foldback test is as follows: (1) Measure the temperature rise for different values of FBD. A useful step size in FBD will be in the range of 3- to 5-cm. (2) Remove the lead and measure the background SAR along the path of the lead with one of the methods specified in ASTM F2182 (21) or other appropriate technique. (3) Determine $\Delta T_1(\max)$, which is the maximum rise for any of the foldback tests divided by the local background SAR. Units of $\Delta T_1(\max)$ are $^{\circ}\text{C}/(\text{W}/\text{kg})$.

In the foldback test, E_{tan} has uniform root mean square (rms) intensity of E_0 and a phase of either 0 or 180° . The temperature rise is then expressed as

$$\Delta T = A E_0^2 \left| \int_0^{L_0-FBD} S dz - \int_{L_0-FBD}^{L_0} S dz \right|^2 \quad (20)$$

Potential use of the measured temperature rises for different FBD is as follows: The measurements of ΔT can be used to validate S that was obtained by calculation or a separate measurement. If we can describe S in terms of parameters in an equation, such as for the transmission line model, then we can use an error minimization algorithm to determine the fitting parameters (such as $\alpha, \lambda, \rho_{elec}, \rho_{gen}$) based the measured temperature rises for different ΔT and FBD.

A variant on the foldback test is a progressive length (“spoke”) test in which part of the lead is parallel to the radial line of the phantom. This is the diagram on the right in **Figure 5**. A portion of the lead is exposed to uniform E_{tan} and the remainder of the lead has zero E_{tan} . The temperature rise for the spoke test with a bend a distance X from the electrode and the section between the generator and the bend radially directed is

$$\Delta T = AE_0^2 \left| \int_0^X S(\tau) d\tau \right|^2 \quad (21)$$

For calculation of SAR and electric field in the circular phantom, let R be the radial distance of the lead from the center of the phantom, E_0 the rms value of the electric field at radial distance R , and f the frequency. In the presence of uniform B_1 with rms value B_{10} , we then have approximately

$$E_0 = \pi f R B_1 \quad (22)$$

Measurement of Temperature Rise with a Locally Exciting RF Coil

The localized exciting RF coil in the TF apparatus of **Figure 4** will produce a temperature rise at the electrode. In the local coil test method, the temperature sensor in **Figure 4** is removed and the temperature rise at the electrode is measured with a temperature sensor. Assume the exciting coil is at a location τ away from the electrode. The temperature rise at the sensor is then

$$\Delta T = A |\Delta V|^2 |S(\tau)|^2 \quad (23)$$

where ΔV is the integrated E_{tan} over the length of the exciting coil.

CASE STUDY: DETERMINATION OF LEAD MODEL AND *IN VITRO* TEMPERATURE RISE FOR A LEAD USED WITH A NEURO-STIMULATION SYSTEM

In order to illustrate the test methods and analysis for heating of an active implant, this section describes the procedure for the determination of the lead model and *in vitro* temperature rise for a commercially available neurostimulation system, the Vagus Nerve Stimulator, VNS Therapy, NeuroCybernetic Prosthesis (NCP) System (Cyberonics, Inc. and LivaNova). The methodology makes use of the afore-mentioned test methods described in this chapter. The tests and analysis were made on a system used for VNS Therapy – the Model 303 lead and either the Model 102 or Model 103 pulse generator. Results of tests of MRI-related heating for physiologic paths in a rectangular phantom have been published for this system (23). The lead contains two filars and is 43-cm long. There are two electrodes made from platinum foil that are located at the end of the lead. The evaluation was made for a lead with the pulse generator, an isolated lead (uncapped), and a lead with an insulating cap at the pulse generator connector.

588 Using MRI Simulations and Measurements to Evaluate Active Implants

Heating Tests in a Rectangular Phantom

The temperature rises were measured in a rectangular phantom with the methods specified in ASTM F2182 (21). The tests were made using a transmit body RF coil at 64-MHz (Signa, General Electric Medical Systems, Milwaukee, WI). The conductivity of the gelled-saline used to fill the phantom was approximately 0.5-S/m. **Figure 3** shows diagrams of the phantom and the paths of the implant for the tests. **Figure 6** shows the Model 303 lead with the Model 102 pulse generator prior to immersion into the phantom liquid. **Figure 7** shows the intensity of E_{tan} along the two lead paths. In the tests, the local background SAR near the wall of the phantom was determined with the titanium rod technique that is described in F2182 (21). The distribution of E_{tan} was then determined from the SAR measurement at one location and the calculated distribution of electric field induced in the phantom by the RF magnetic field. **Figure 8** shows temperature rises for the lead with the pulse generator in the straight- and U-paths. The difference in temperature rise is very much dependent on the path. For the same input RF power, the U-path produces a temperature rise that is five times greater than the rise for the straight path.

Figure 6. Model 303 vagus nerve stimulation lead with the Model 102 pulse generator (Cyberonics, Inc. and LivaNova) used in U-path configuration for a heating test. Temperature rises at the electrodes were measured using Neoptix fiber-optic temperature probes with a 0.6-mm tip diameter.



In the measurements obtained in the rectangular and circular phantoms, there is an uncertainty of about 10% in the assessment of the background SAR. The measured SAR for each test was adjusted by a factor of less than this uncertainty in order to provide the best fit between the measured and calculated temperature rises.

Electrical Measurement of the Transfer Function

The Model 303 lead with the Model 103 pulse generator (Cyberonics, Inc. and LivaNova) was placed in the test apparatus depicted in **Figure 4**. The output of an HP 3577

Figure 7. Calculated rms tangential electric fields in the ASTM phantom along the lead paths shown in **Figure 3**. The RF power was 150-W and the phantom whole-body averaged SAR was approximately 2-W/kg.

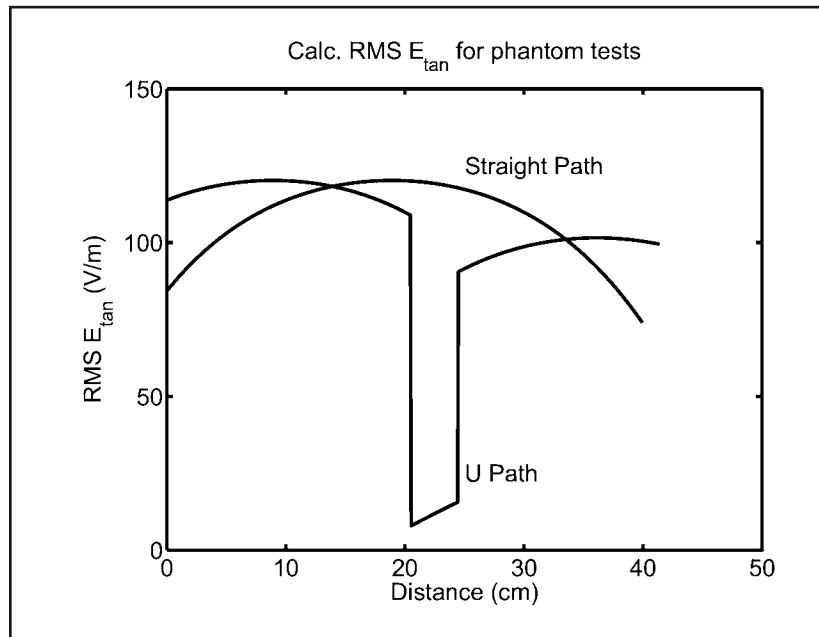
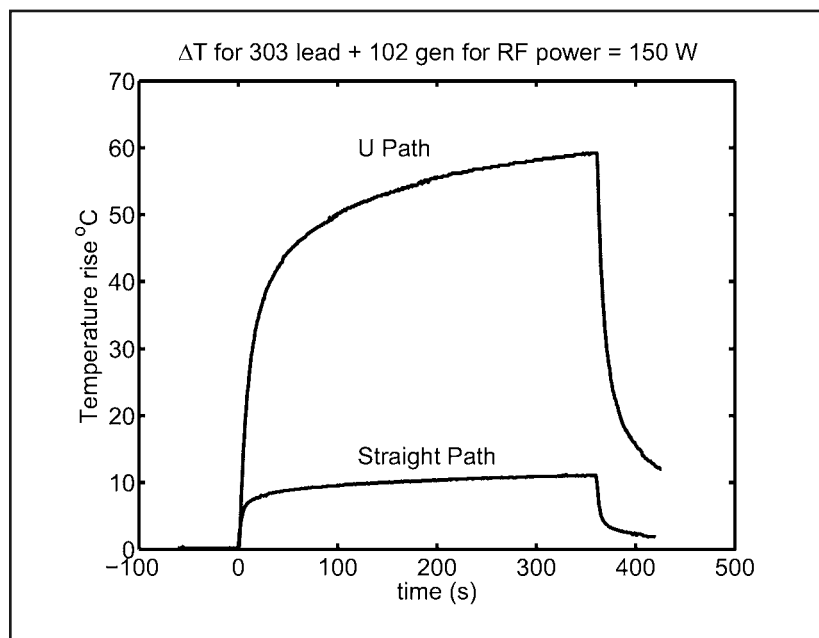


Figure 8. Temperature rises for two paths in a phantom for the Model 303 lead with Model 102 pulse generator (Cyberonics, Inc. and LivaNova). The temperature rises are scaled to the same input RF power.



590 Using MRI Simulations and Measurements to Evaluate Active Implants

network analyzer (Hewlett-Packard) was amplified with an ENI RF power amplifier whose output was connected to the exciting coil. The toroidal exciting coil had an inner diameter of approximately 1.5-cm, outer diameter 3-cm, and height of about 2-cm. The electric field sensor was connected to port 2 of the HP3577 network analyzer. The toroidal coil was moved along the length of the lead and magnitude and phase of S_{21} were measured as a function of the location of the coil.

Figure 9 shows the magnitude and phase of transfer function (TF) for the lead with an insulating cap [note, the normalizing factor $A = 1^\circ\text{C}/(\text{V}/\text{m})^2$ was applied for **Figure 9** and the other plots of transfer function shown in this chapter]. The points in **Figure 9** are from S_{21} measurements and the solid line is the calculation from transmission line equations presented in this chapter. There is essentially complete overlap between the measured and transmission line TF. At the capped end of the lead, the magnitude of the TF is small because the cap presents an open circuit. The TF has a maximum magnitude at about 20-cm from the cap. The maximum occurs because the impedance Z_{ingen} is small at this location because it is approximately 1/4 wavelength from the cap.

Figure 10 shows the transfer function for the lead with the pulse generator. The measured and transmission line fit TF are in reasonable overlap, but the match is not as good as for the capped lead. For this calculation, the generator impedance Z_{gen} was $-30 \text{ j}\Omega$, electrode impedance Z_{elec} was $500 - 350 \text{ j}\Omega$ and Z_L was 100Ω , $j = \sqrt{-1}$. A more comprehensive

Figure 9. Transfer function (TF) for a Model 303 lead with an insulating cap over the connector to the pulse generator. The points are measurements and the solid line is a transmission line fit for wavelength $\lambda = 80\text{-cm}$ and damping constant, $\alpha = 2$. The TF is scaled based on the temperature measurements in the ASTM phantom and circular phantom. $A=1$.

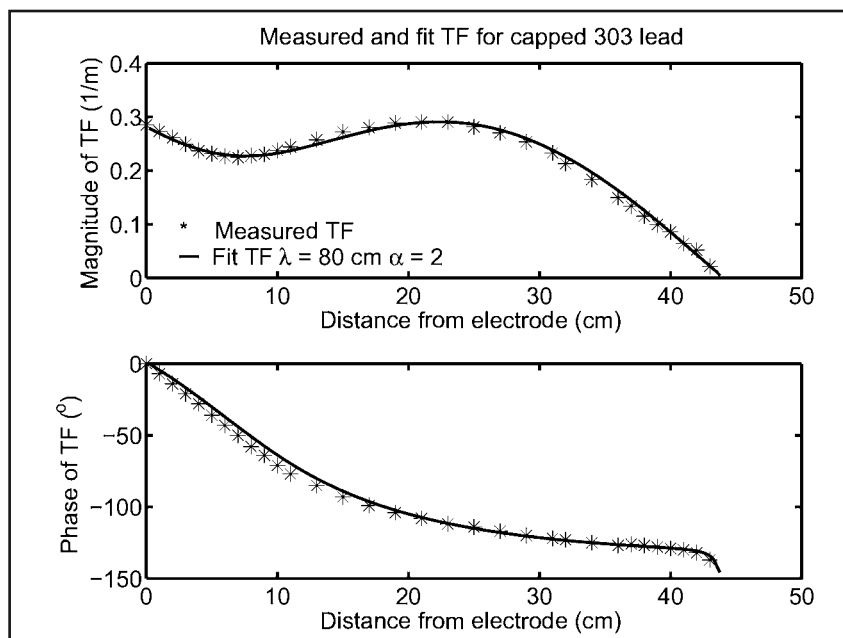
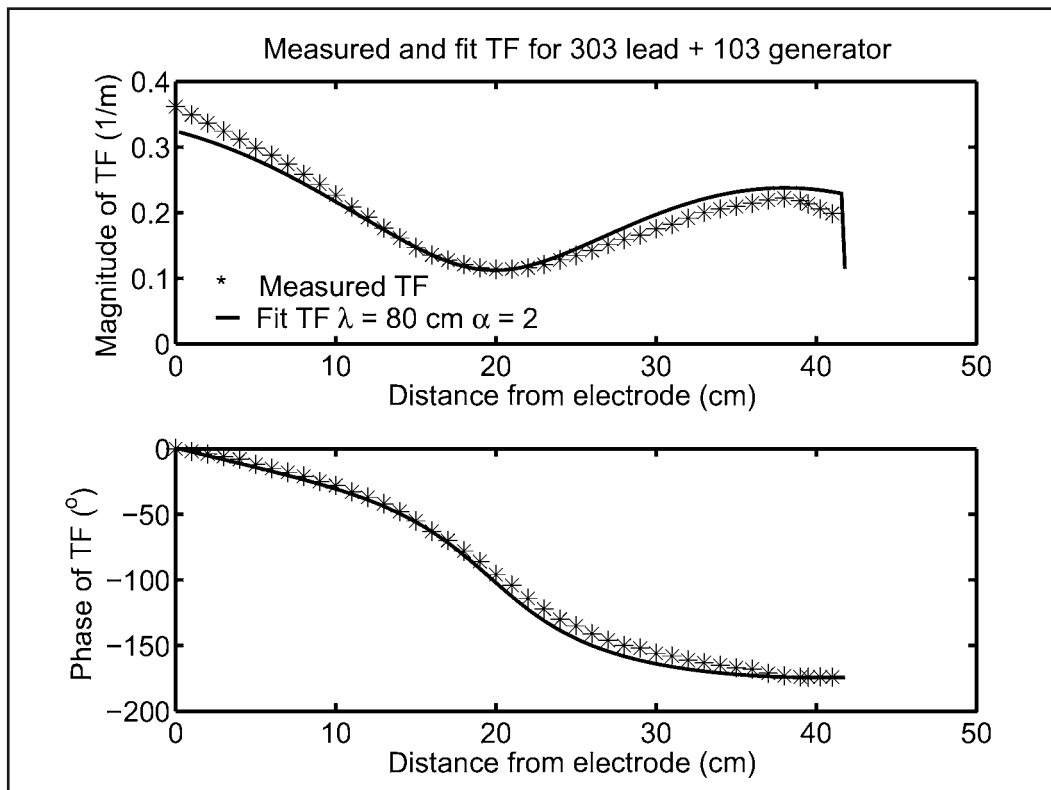


Figure 10. Transfer function for a Model 303 lead with Model 103 pulse generator (Cyberonics, Inc. and LivaNova). The points are measurements and the solid line is a transmission line fit for wavelength $\lambda = 80\text{-m}$ and damping constant $\alpha = 2$. The TF is scaled based on the temperature measurements in the ASTM phantom and circular phantom. A=1



analysis may result in determination of the appropriate parameters that provide a better fit to the measurements.

Foldback Tests in a Circular Phantom

Figure 11 shows the lead with the pulse generator the measured and calculated temperature rises, scaled to the local SAR versus the foldback distance. The measured rises track well with the calculated rises. The greatest rise occurs for a foldback of about half of the lead length and this configuration corresponds to the U-path in the rectangular ASTM phantom. As in the phantom tests, the temperature rise in the U-path is approximately 5 times the temperature rise in the straight path. **Figure 12** shows temperature rises measured in a foldback test on a capped lead. The measured temperature rises again track well with the calculated values. The greatest rise occurs for the lead in a straight line.

592 Using MRI Simulations and Measurements to Evaluate Active Implants

Figure 11. Temperature rises versus foldback for a Model 303 lead with Model 103 pulse generator (Cyberonics, Inc. and LivaNova). The points are the measurement and the line is calculation for the transfer function in **Figure 14**.

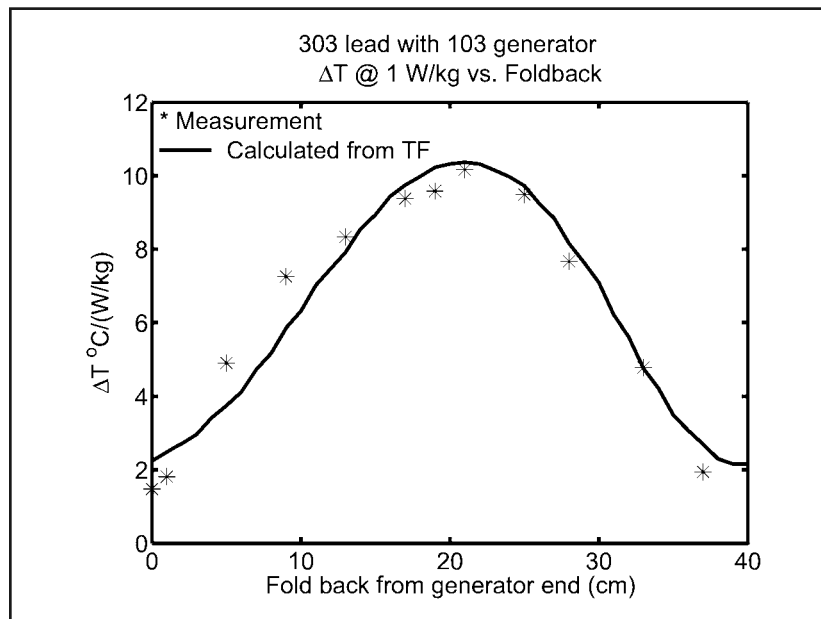
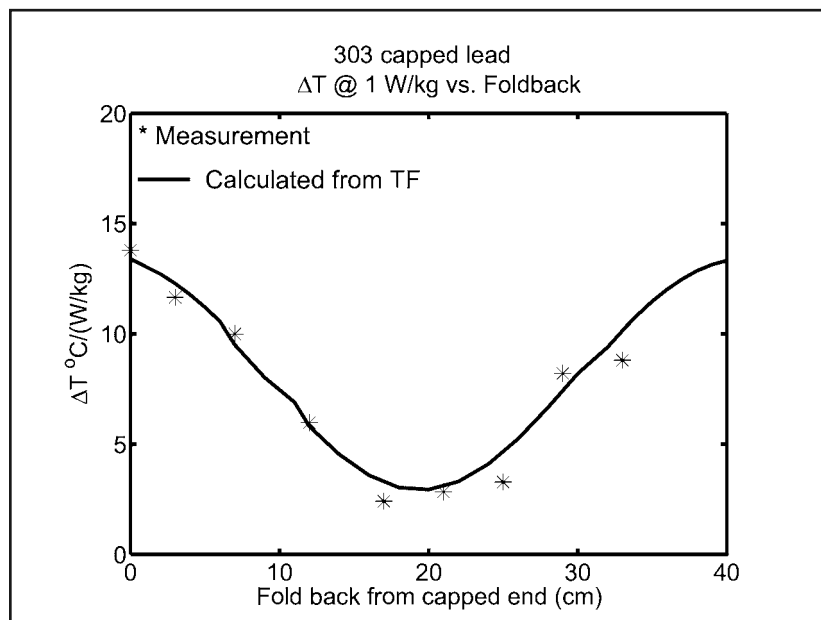


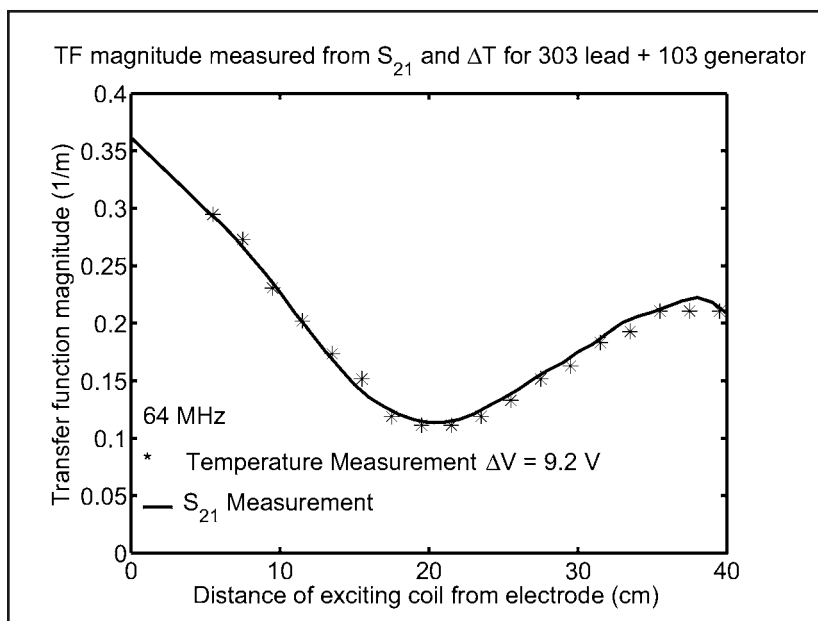
Figure 12. Temperature rises versus foldback for a Model 303 lead with Model 103 pulse generator (Cyberonics, Inc. and LivaNova). The points are measurements and the line is the calculation for the transfer function in **Figure 14**.



Measurement of Temperature Rise with a Local Exciting Coil

Figure 13 compares the magnitude of the transfer function obtained for the lead with the pulse generator with two different methods. The solid line is the transfer function measured by S_{21} and is normalized based on the temperature rise measurements in the circular and rectangular phantom. The points are proportional to the square root of the temperature rise at the electrode at different locations of the exciting coil, which is the same as the one used in the S_{21} measurements. For these tests, the integrated electric field over the length of the exciting coil, ΔV , is calculated to be 9.2-V. The magnitudes of the TF measured by the two different methods are in nearly complete overlap.

Figure 13. The solid line is the calculated magnitude of the transfer function from the S_{21} tests. The points are the transfer function magnitude measured from temperature rises at the electrodes of the lead (Cyberonics, Inc. and LivaNova).



Comparison of Calculated Rises in the Phantom Tests

Table 1 lists measured and calculated rises for the three leads in the straight-line path in the phantom. The calculated rises are based on the transfer functions in **Figure 14** and the E_{tan} along the lead that is shown in **Figure 7**. **Table 2** lists measured and calculated temperature rises for the leads in the U-path in the rectangular phantom. The difference between the calculated and measured rises is less than 5% of the rise ΔT_{max} that would occur if the transfer function and incident electric field were in phase conjugation.

Discussion on *In-vitro* Tests for Determination of the Transfer Function

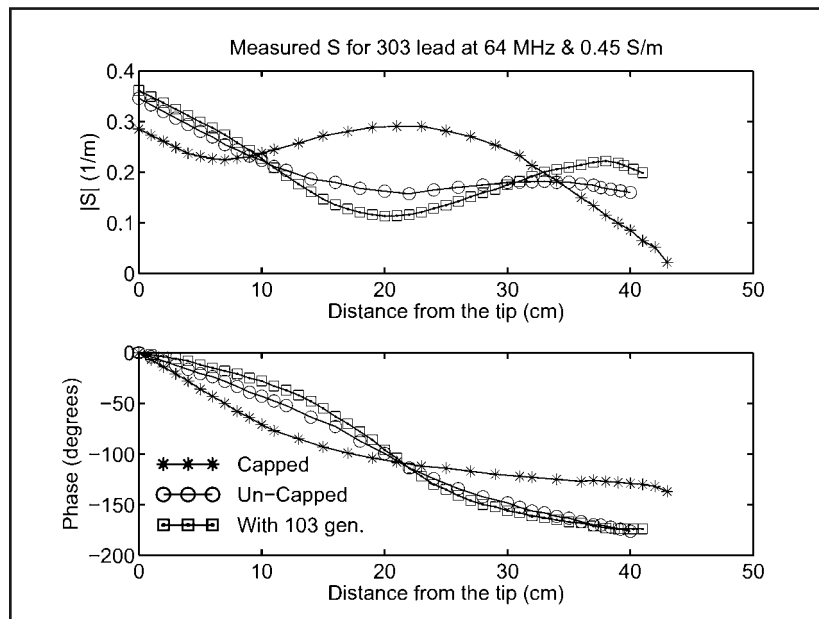
The tests described herein provide a robust assessment of the transfer function for the Model 303 lead and the three termination conditions. Three of the tests provide independent

594 Using MRI Simulations and Measurements to Evaluate Active Implants

Table 1. Measured and calculated temperature rises for the vagus nerve stimulation (VNS) lead (Model 303 lead, Cyberonics, Inc. and LivaNova) in the phantom with the lead in a straight-line path. *Note that this measurement was made with RF power reduced 50% so that the actual measured temperature rise is half of the listed value.

Termination	Measured ΔT Straight °C	Calculated ΔT Straight °C	Calculated ΔT_{max} °C	Measured vs. Calculated ΔT % of ΔT_{max}
Capped Lead	*77.0	76.3	109.3	0.6
Uncapped Lead	24.8	24.5	74.6	0.4
Pulse Generator	10.8	13.9	69.6	-4.4

Figure 14. Measured transfer function for the Model 303 lead with the Model 103 pulse generator (Vagus Nerve Stimulator, VNS Therapy, NeuroCybernetic Prosthesis (NCP) System, Cyberonics, Inc. and LivaNova). These transfer functions were used to calculate the *in vitro* and *in vivo* temperature rises. The normalizing factor A is unity.



outputs that depend on both the magnitude and the phase of the transfer function: (1) The S_{21} measurement; (2) The temperature rise measurement in the circular phantom with a large RF coil; and (3) The temperature rise measurement in a rectangular phantom for different paths of the lead. In addition, the heating test with the local exciting coil provides an independent measure of the magnitude of the TF.

Notably, the transfer function derived here is specific for the medium conductivity used in the tests. The TF will be different if the electrical properties of the surrounding medium

Table 2. Measured and calculated temperature rises for the vagus nerve stimulation lead (VNS) lead (Model 303 lead, Cyberonics, Inc. and LivaNova) in the phantom with the lead in a U-path. *Note that this measurement was made with RF power reduced 50% so that the actual measured rise is half of the listed value.

Termination	Measured ΔT U-Path °C	Calculated ΔT U-Path °C	Calculated ΔT_{max} °C	Measured vs. Calculated ΔT % of ΔT_{max}
Capped Lead	24.7	24.3	89.0	0.4
Uncapped Lead	47.0	47.0	69.3	0.0
Pulse Generator	*59.0	58.6	72.6	0.5

change. However, small changes to the TF over the range of electrical properties that characterize soft tissue are to be expected.

DETERMINATION OF *IN-VIVO* TEMPERATURE RISES DURING MRI AT 64-MHZ

The transfer functions presented in this chapter and the calculated electric field in the body during MRI are used to determine the *in vivo* temperature rises at the electrodes of the VNS lead studied here. **Figure 15** shows the path that was defined for the VNS lead in the Hugo human model, which is derived from the National Library of Medicine and has been used extensively in bio-electromagnetic calculations (24).

The Finite Difference Time Domain (FDTD) method was used to calculate E_{tan} along the lead at 64-MHz inside a high pass transmit body RF coil with a circularly polarized incident RF field. The intensity and phase of E_{tan} along the lead will depend on the location of the patient in the bore of the MR system.

Figure 16 shows a plot of magnitude and phase of E_{tan} along the VNS lead path at a landmark position of 30-cm (i.e., the plane of the patient 30-cm from the top of the head is at the center of the transmit body RF coil). Similarly, **Figure 17** plots E_{tan} along the VNS lead path for the transmit/receive head RF coil. For the transmit/receive head RF coil, only the section of lead near the electrode experiences a significant E_{tan} .

The *in vivo* temperature rises are calculated for RF intensity at the normal mode limit of 2-W/kg for whole-body averaged SAR and 3.2-W/kg for head SAR. **Figure 18** shows B_{1+} that will produce a whole-body averaged SAR of 2-W/kg and/or a head SAR of 3.2-W/kg. In **Figure 18** it is assumed that the transmit RF body coil will limit B_{1+} in the Normal Operating Mode for the MR system to an amplitude of 6- μ T.

Calculation of the *in vivo* temperature rises was done with Equation (1), the transfer functions in **Figure 14**, and the calculated E_{tan} . With the scaling of the TF, the temperature rises are based on the *in vitro* temperature rises after six minutes of RF power deposition. **Figure 8** shows that the *in vitro* temperature rises are effectively saturated after six minutes.

596 Using MRI Simulations and Measurements to Evaluate Active Implants

Figure 15. Path of Model 303 lead (Cyberonics, Inc. and LivaNova) in the Hugo model. The electrodes are wrapped around the vagus nerve at the top of the path and the pulse generator is located at the bottom of the path.

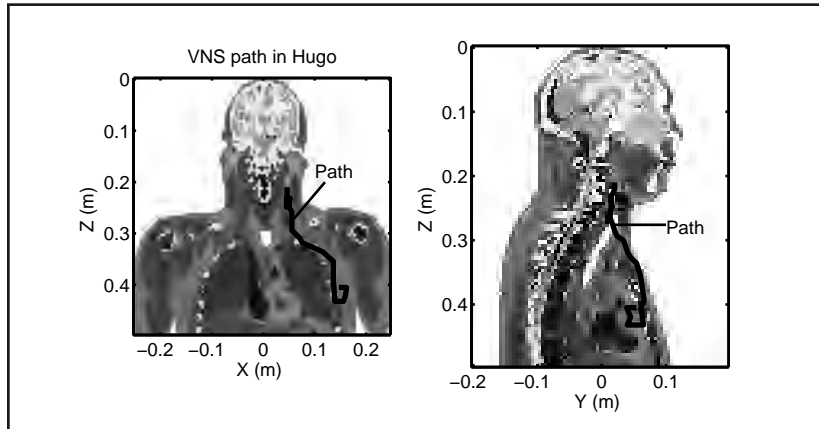
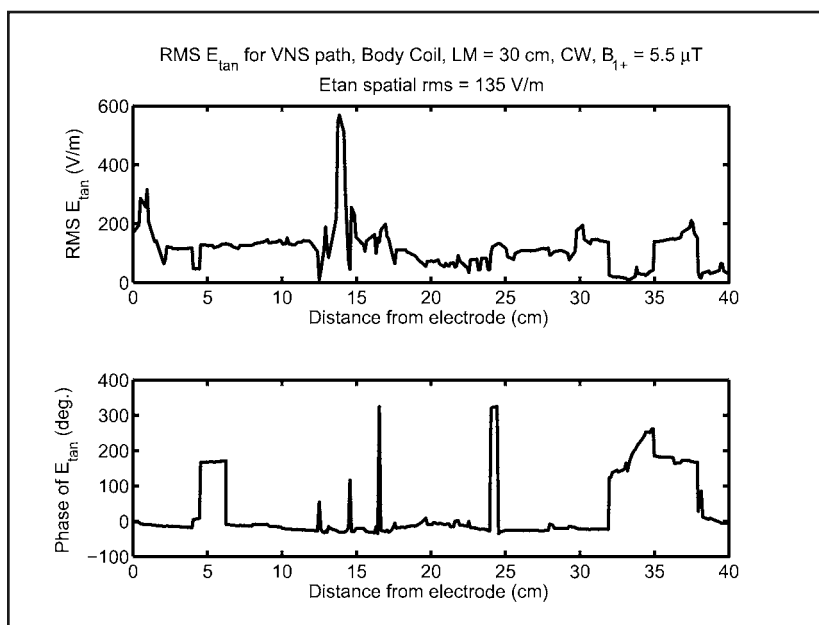


Figure 16. Magnitude and phase of the electric field along the path of the Model 303 lead (Cyberonics, Inc. and LivaNova) for the transmit RF body coil. The landmark (i.e., center of the transmit RF coil) is 30-cm from the top of the head and the whole-body averaged SAR is 2-W/kg.



Considering as well the cooling effect of blood perfusion (25), it is expected that the *in vivo* temperature rise will reach a saturation value within six minutes after the initiation of the delivery of RF energy.

Figure 19 plots the projected *in vivo* temperature rises at the electrode versus the landmark for the Hugo model for the three types of terminations at the proximal end. The tem-

Figure 17. Magnitude and phase of electric field along the path of the Model 303 lead (Cyberonics, Inc. and LivaNova) for the transmit/receive head RF coil. $B_{1+} = 8 \mu\text{T}$, which is expected to be the upper limit for the Normal Operating Mode of the MR system.

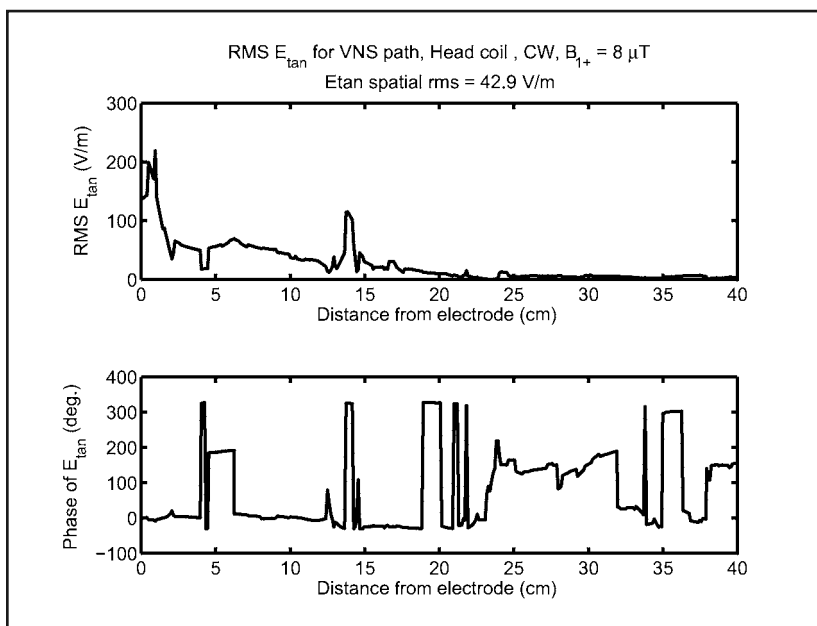
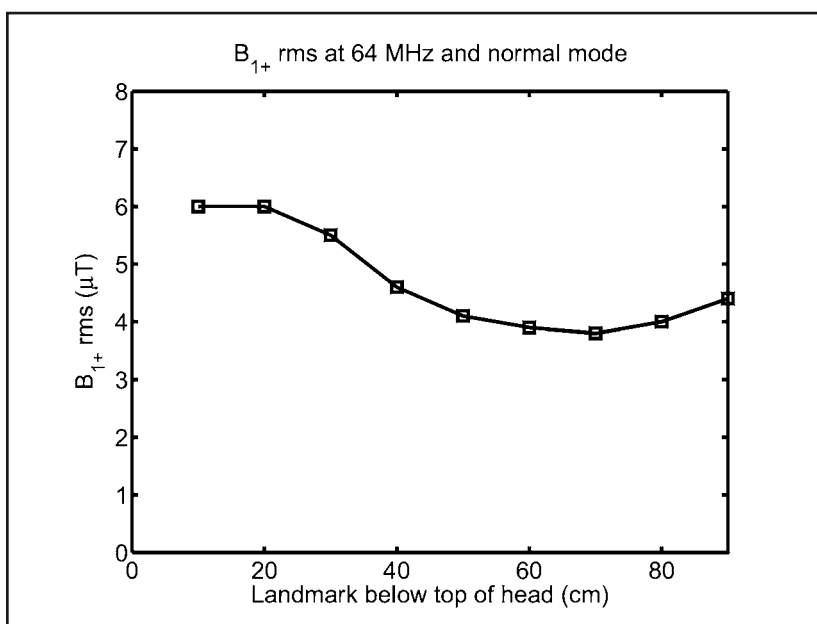


Figure 18. B_{1+} rms versus landmark used for calculation of the *in vivo* temperature rise. These values will produce SAR in the Hugo model at the limits for the Normal Operating Mode of the MR system that are specified in IEC 60601. It is assumed that the MR system will limit B_{1+} to 6- μT .



598 Using MRI Simulations and Measurements to Evaluate Active Implants

perature rises at each landmark are the greatest of the two values calculated for clockwise (CW) and counter-clockwise (CCW) rotation. The maximum temperature rises for the three leads all occur at the landmark of 30-cm, which is approximately at the level of the clavicle. At this landmark, the whole-body averaged SAR is 2-W/kg for the applied B_{1+} of 5.5- μ T. Maximum temperature rises for the capped, uncapped, and with the pulse generator leads are 45°C, 21°C, and 17°C, respectively.

Figure 19 also shows the calculated temperature rises with the RF field applied by the transmit/receive head RF coil. For this RF coil, the rise for B_{1+} of 8- μ T, which is expected to exceed the maximum RF intensity with the MR system in the Normal Operating Mode, is less than 4°C. Calculation of S for simple wire geometries is possible, as shown in **Figure 20** for a bare wire.

TRANSFER FUNCTION AT 64-MHz and 128-MHz

ISO/TS 10974 (1) focuses on implant interactions at 1.5-T. RF-induced heating and transfer function measurements described above were made at 1.5-T/64-MHz. It is of course relevant to evaluate implant interactions at 3-T, which corresponds to an RF frequency of either 123-MHz or 128-MHz, as some MR systems described as 3-T may have a static magnetic field of 2.9-T. It is planned that the upcoming International Standard version of 10974 will support information for both 1.5-T/64-MHz and 3-T/128-MHz.

Figure 19. Calculated *in vivo* temperature rise versus landmark in the Hugo model for the Normal Operating Mode of the MR system using the B_{1+} limits in **Figure 18**. The temperature rises plotted for the capped lead, uncapped lead, and lead with pulse generator (Cyberonics, Inc. and LivaNova) are the maximum values for clockwise (CW) and counter-clockwise (CCW) rotation for a high pass coil. The temperature rise for the transmit/receive head RF coil (TR HC) is calculated for $B_{1+}=8$ - μ T.

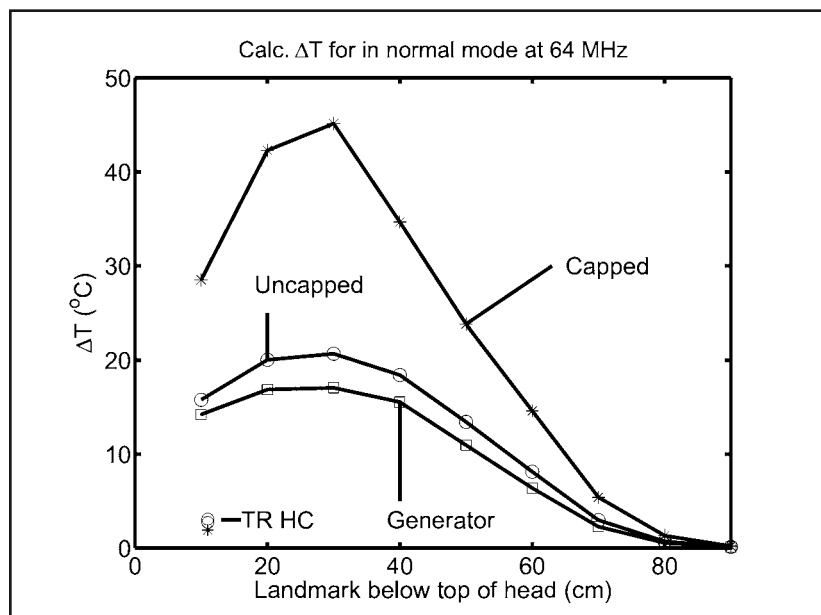


Figure 20. Measured and calculated transfer functions for a 40-cm long, 3-mm diameter aluminum rod. The transfer function was calculated with method of moments.

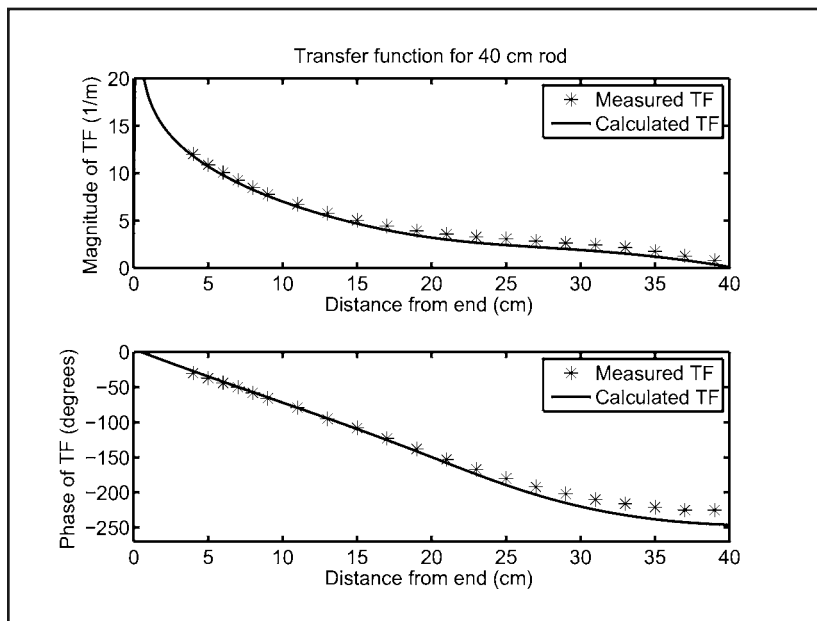


Figure 21. Measured electric field transfer functions at 64-MHz and 128-MHz for the Model 303 lead and pulse generator (Cyberonics, Inc. and LivaNova).

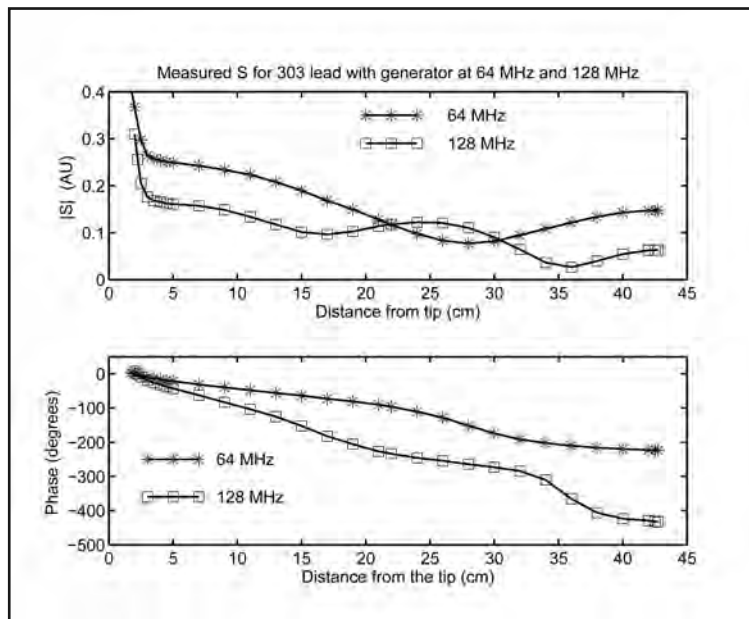


Figure 21 shows the measured transfer functions for the vagus nerve stimulation lead with pulse generator (Cyberonics, Inc. and LivaNova) at 64-MHz and 128-MHz. The

600 Using MRI Simulations and Measurements to Evaluate Active Implants

plots of magnitude and phase for 64-MHz are similar to those shown in **Figure 14**. The transfer function for 128-MHz compares to that for 64-MHz, as follows.

- (1) The minimum in the magnitude of the transfer function occurs at a distance of approximately 20 cm from the pulse generator at 64-MHz and at approximately a distance of 10 cm from the pulse generator at 128-MHz. This minimum occurs closer to the pulse generator at 128-MHz due to the fact that the wavelength is approximately 80 cm at 64-MHz and 40 cm at 128-MHz.
- (2) The difference in phase over the length of the lead at 128-MHz is approximately twice (~400°) compared to the corresponding phase difference at 64-MHz (~200°). The greater phase variation at 128-MHz is again due to the shorter wavelength.

For the determination of an *in-vivo* temperature rise at 3-T/128-MHz, the same procedure that is described above for 1.5-T/64-MHz would be used. As was done for 1.5-T/64-MHz, a physical heating test at 3-T/128-MHz would be needed to scale the magnitude of the measured transfer function.

RECENT DEVELOPMENTS IN THE MEASUREMENT OF THE ELECTRIC FIELD TRANSFER FUNCTION

The measurement of the electric field transfer function is now an established method in the process of determining RF-induced heating at the electrodes of the lead of an active implant system. Recent developments in the measurements of the transfer function are described in this section.

Feng, et al. (26) described a reciprocity approach for measurement of the transfer function. The apparatus in **Figure 4** depicts the use of the tangential electric field (E_{tan}) method along the length of the lead by application of current to the transmitter antenna from port 1 of the network analyzer and the signal from the electric field near the electrode is sensed by port 2. With the reciprocity method, current is induced in the lead by attaching the electrode to port 1 and port 2 is connected to a current sensor, such as a ferromagnetic toroid, that is translated along the length of the lead. Due to electromagnetic reciprocity, both methods yield the current electric field transfer function.

The advantages of the use of the reciprocal method for transfer function calculation and measurement include, the following:

- (1) Computation of the transfer function is simplified because the only source is the current applied to the electrode and it is necessary to make only one calculation of current along the lead. For the non-reciprocal method, the current source must be applied a number of locations along the length of the lead and the current distribution along lead must be calculated for each of the placements.
- (2) The reciprocal method may provide more flexibility on the type of sensor that is used to measure the current along the lead.

Missofe and Aisans (27) describe in detail the design of an apparatus for measurement of the transfer function, including details on the ferrite core that can serve as either the transmitter for induction of current into the lead or for the sensing of current in the lead wire. The apparatus was validated with insulated wires. The measured and calculated electric field transfer functions were in good agreement (27).

Tokaya, et al. (28) reported on a method in which the transfer function (TF) was measured in association with MRI. There was good agreement between measured and calculated transfer functions for linear and helical implants using relatively quick MRI acquisitions with millimeter spatial resolution. The authors concluded that the proposed MRI-based method allows for TF determination in more realistic exposure scenarios and solid media.

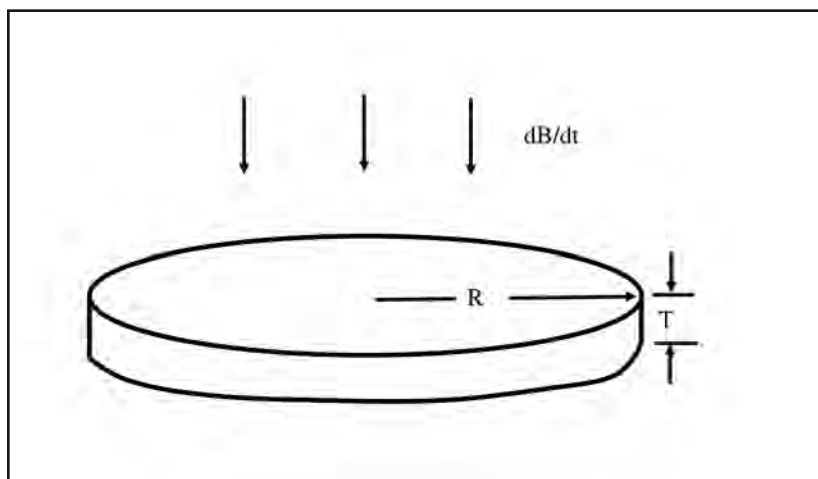
HEATING OF METALLIC IMPLANTS BY THE TIME-VARYING GRADIENT MAGNETIC FIELDS USED FOR MRI

Time-varying gradient magnetic fields used during MRI will induce eddy currents when incident on a planar surface of an implant or device. These eddy currents can produce a power dissipation that may produce a measurable temperature rise. Heating will tend to be greatest for implants that are relatively large, that have a geometry that provides easy pathways for flow of eddy currents, that have a high electrical conductivity, and that have a thickness that is approximately the same or greater than electrical skin depth. Examples of implants with the greatest potential for gradient magnetic field-induced heating include a large pulse generator associated with an active implant and the large acetabular shell of a hip prosthesis (i.e., a passive implant).

Note that the metal of the implant is directly heated by the time-varying gradient magnetic fields, which have frequencies in the range of a few hundred Hz to a few kHz. In contrast, in RF-induced heating, the tissue in the vicinity of an implant is heated and there is little direct heating of metal by the time-varying RF magnetic field (29). Calculation of gradient magnetic field induced-heating of model implants has been described in a Master's thesis by B. Stem (30).

Figure 22 illustrates a simple geometry in which time-varying gradient magnetic field, dB/dt , is normally incident on a metallic disk with radius R , thickness T , and conductivity σ . At low frequency, the time-varying gradient magnetic field induces an electric field, E , in the disk that is zero at the center and is proportional to the radial distance from the center.

Figure 22. Incident time-varying magnetic field, dB/dt , on a conducting disk with radius R and thickness T .



602 Using MRI Simulations and Measurements to Evaluate Active Implants

$$E(r) = \frac{r}{2} \frac{dB}{dt} \quad (24)$$

where r is radial distance from the center and $\frac{dB}{dt}$ is the time-varying gradient magnetic field due to the time-varying current in the gradient coils.

The average power per unit volume at a location in the implant is equal to the conductivity multiplied by the square of the electric field. The total average power deposition P_{ave} in the disk is

$$P_{ave} = \frac{\sigma T \pi R^4}{8} \left(\frac{dB_{rms}}{dt} \right)^2 \quad (25)$$

where σ is the electrical conductivity and $\frac{dB_{rms}}{dt}$ is the temporal root mean square (rms) of the incident time-varying magnetic field. Equation 25 is presented in ISO/IEC 10974:2018. The power deposition is proportional to the conductivity of the metal of the disk, the thickness, the 4th power of the radius and the square of rms dB/dt. Thus, gradient magnetic field-induced heating will be greatest for large and symmetric implants with higher electrical conductivity.

At sufficiently high frequency, the incident dB/dt does not completely penetrate the implant due to the induced reaction eddy currents in the implant. The depth of the penetration is of the order of the electrical skin depth, δ , a concept that is discussed in many standard textbooks on electromagnetism. The formula for the skin depth is

$$\delta = \frac{1}{\sqrt{\pi f \mu \sigma}} \quad (26)$$

where f is the frequency, μ is the magnetic permeability, and σ is the electrical conductivity. For paramagnetic medical grade implants, μ is essentially equal to the permeability of free space = $4 \pi \times 10^{-7} H/m$.

Figure 23 and **Table 3** provide information on electrical skin depths at different frequencies for alloys typically used for medical implants. Skin depth, δ , is generally comparable to or greater than implant dimensions at gradient frequencies but tends to be smaller than implant dimensions at the RF frequencies.

Figure 24 plots measured and calculated temperature rises for different diameter disks made from 0.6 mm thick commercial pure (CP) titanium. Agreement between calculated

Figure 23. Electrical skin depth versus frequency in the range of gradient frequencies for different metals typically used for medical implants.

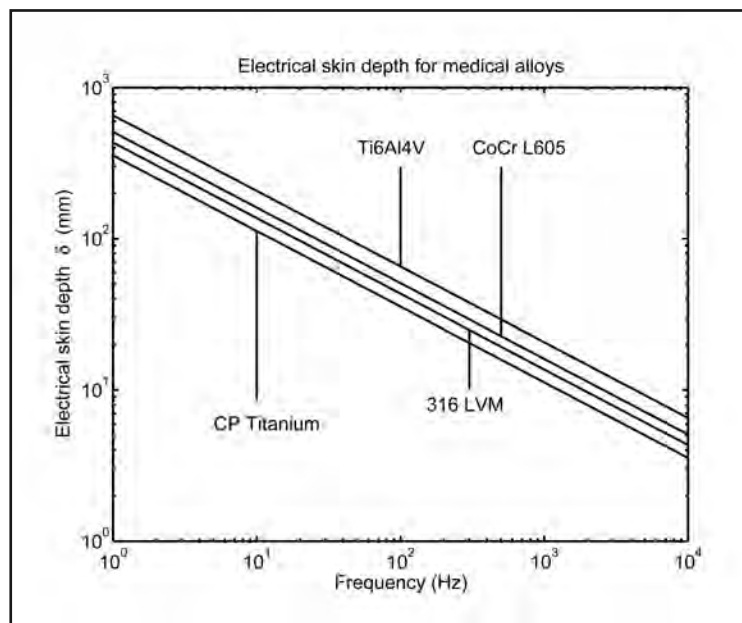
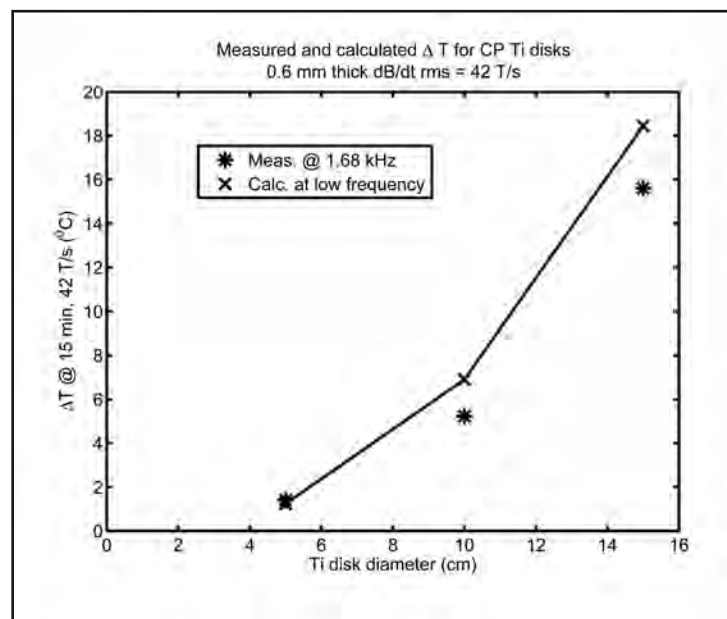


Figure 24. Measured and calculated dB/dt induced temperature rises versus diameter for commercially pure (CP) titanium disks. Disks were immersed in gelled saline that described in ASTM F2182. The calculation is for low frequency and the measurement was at 1.68 kHz. Time of power application was 15 minutes and dB/dt was 42 T/s rms. Note that the test sample has small holes whereas the calculation was for a solid disk.



604 Using MRI Simulations and Measurements to Evaluate Active Implants

Table 3. Electrical skin depths for medical alloys. 270-Hz is the default (Tier 1) frequency in Reference 1 for testing of gradient magnetic field-induced heating. 1750 Hz is the gradient magnetic field-induced test frequency that was proposed for the International Organization for Standardization (ISO) standard, 10974. 64-MHz and 128-MHz are RF frequencies at 1.5-T and 3-T, respectively.

Material	Electrical conductivity (S/m)	$\delta @ 270 \text{ Hz}$ (mm)	$\delta @ 1750 \text{ Hz}$ (mm)	$\delta @ 64 \text{ MHz}$ (mm)	$\delta @ 128 \text{ MHz}$ (mm)
Ti 6Al 4 V	5.9×10^5	39.9	15.7	0.082	0.058
CoCr L605	9.8×10^5	30.9	12.2	0.064	0.045
Stainless Steel 316 LVM	1.35×10^6	26.4	10.4	0.054	0.038
CP Ti	2.0×10^6	21.7	8.5	0.044	0.031

(Ti 6Al 4 V, aluminum alloy; CoCr L605, cobalt-chromium alloy; CP Ti, commercially pure titanium)

and measured temperature rise is good, even though the calculation is for low frequency and the measurement waveform was a 1.68 kHz sine wave. A simple computation was made by the author in which the concentric rings of current were used calculate the current distribution on a conducting disk with a small thickness compared to the skin depth. It was empirically observed that for a disk with radius-thickness product $RT < 0.4 \delta^2$, power deposition in the disk was within 3% of the low frequency value in Equation 25. For the CP titanium disks (**Figure 24**), with thickness of 0.6 mm, RT/δ^2 for disk diameters of 5, 10, and 15 cm was determined to be 0.21, 0.41, and 0.62, respectively. Even for the largest 15-cm diameter disk, the total power was within 5.8% of the low frequency value.

Brühl, et al. (31) presented a measurement of gradient magnetic field-induced heating in a clinical scenario. The *in-vitro* temperature rise for the acetabular shell of a hip prosthesis was measured in the presence of $(dB/dt)_{rms}$ of 49.7 T/s. The shell was made from titanium alloy (Ti-6Al-4V) and had a diameter of 54 mm and a mass of 70.7 gm. The phantom material used in the *in vitro* evaluation was a gelled-saline in order to prevent convection. After 10 minutes of applied gradient current using a 3-T MR system, the temperature rise was 3.8°C for the implant.

In summary, the gradient magnetic field-induced temperature rise ΔT for an implant can be approximately expressed as

$$\Delta T_{gradient} = K_{implant} \left(\frac{dB_{rms}}{dt} \right)^2 \quad (27)$$

where $K_{implant}$ is a factor that accounts for how the implant couples with the gradient magnetic fields. $K_{implant}$ is highest for an implant with symmetric and relatively large surface area (e.g., pulse generator used for an implantable cardioverter defibrillator, acetabular shell associated with a hip prosthesis, etc.) and smallest for an elongated implant with a small cross section (e.g., coronary artery stent). Note that $(dB/dt)_{rms}$ is the root mean square value of time-varying magnetic field from the gradients. $(dB/dt)_{rms}$ is proportional to the rms slew rate, which can be obtained from the pulse sequence parameters. $(dB/dt)_{rms}$ can also be measured with a search coil and a digitizing oscilloscope.

In the bore of an MR system, the dB/dt is the highest at an axial distance approximately 30 cm from iso-center and near the wall of the bore. Generally speaking, the maximum dB/dt (in T/s) on a bore axis is about 0.25 times the slew rate (in T/m/s). dB/dt is around 30 to 50% greater at $(z, r) = (0.3 \text{ m}, 0.2 \text{ m})$ compared to its value at $(z, r) = (0.3 \text{ m}, 0)$ (32, 33).

Notably, for gradient magnetic field-induced heating of an implant to be of clinical importance, all of the following conditions must be present.

- 1) The implant has a large, symmetric surface area. Heating also increases with increasing metal thickness and increasing metal conductivity.
- 2) The dB/dt is normally incident on the large surface of the implant.
- 3) There is a large sustained (> 5 minutes) rms gradient slew rate S_{rms} . Annex D of Reference 1 lists a most conservative (Tier 1) test (dB_{rms}/dt) of 42 T/s.
- 4) The implant is positioned in a region of the bore where dB/dt is most intense. (dB/dt is near zero at isocenter and maximum at $|z|$ approximately 30 cm and at a radial distance close to the wall of the bore.).

Considering the simultaneous requirements indicated above, it is not surprising that there have been few, if any, adverse event reports due to gradient magnetic field-induced heating of either active or passive implants. At this time, certain manufacturers of active implants may specify a maximum hardware slew rate in the *Instructions for Use* (IFU) for the implant with respect to MRI labeling. Notably, the IFUs for passive implants generally do not present maximum gradient magnetic field parameters, though regulatory guidance may require this information in the future for certain implants. In the absence of guidance from the manufacturer, a prudent precaution would appear to be not apply a long-duration and intense dB/dt sequence if the patient has a relatively large metallic implant.

The focus in this section was on heating due to interaction of a metallic implant with MRI-related, gradient magnetic fields. Both gradient magnetic field-induced heating and vibration arise from the eddy currents induced in the metal of the implant. Gradient vibration occurs from the torque induced on the implant due to the magnetic force exerted by the static magnetic field on the gradient current density. The same factors presented above that must be met for gradient magnetic field-induced heating of implants to be of clinical importance are also required for maximum gradient vibration. In addition, the maximum torque occurs when the static magnetic field is perpendicular to the gradient current density. Clause 10 of Reference 1 describes in some detail the mechanism and consequences of gradient-induced vibration.

606 Using MRI Simulations and Measurements to Evaluate Active Implants

SUMMARY AND CONCLUSIONS

A procedure is described in this chapter for the determination of *in vivo* temperature rises of an AIMD during MRI. Four complementary measurements for the determination of the transfer function, S , are presented. The overlapping results of the measurements provide confidence that the lead model presented herein has been accurately determined.

The analysis is focused on heating at 64-MHz (1.5-T). A similar methodology could be used for 3-T/128-MHz MRI conditions. The transfer function for 128-MHz is shown in **Figure 21**. Of note is that the characteristics of lead heating will be different at 3-T/128-MHz because the wavelengths associated with the current waves at 3-T (128-MHz) are approximately half of those at 1.5-T (64-MHz).

The transfer function for a lead incorporates the sensitivity of the lead to the magnitude and phase of the incident field along the length of the lead. After phase and relative magnitude measurements are made with a network analyzer, as few as one measurement of the temperature rise in a phantom is needed to determine the scaling factor, K_S . However, it will be appropriate to measure the temperature rise for more than one path in the phantom in order to demonstrate the validity of the transfer function, as Equation (1) should predict the temperature rise for any path in the phantom. The procedure outlined here does not require the calculation of S based on the construction of the lead. An accurate calculation of S for an actual clinical lead would be extremely challenging as the wire diameter, pitch, and insulation thickness of a typical lead are several orders of magnitude smaller than the length. Nonetheless, it would be interesting to compare measured and calculated S for such a lead.

The procedure presented in this chapter does require the knowledge of magnitude and phase of the electric field in the phantom and in the human placed in the transmit RF coil of the MR system. These calculations are straightforward, being performed with FDTD and have been previously described (34). These calculations may be conducted at a modest resolution such as 5-mm. If needed, a locally finer resolution could be achieved in the human model with variable gridding and the Huygens box method (18).

In-vivo temperature rises presented herein for the Vagus Nerve Stimulation (VNS), NeuroCybernetic Prosthesis (NCP) System (Cyberonics, Inc. and LivaNova) are shown to illustrate the overall procedure for determining RF heating. No recommendations have been made for acceptable MRI conditions. A more comprehensive assessment of the *in vivo* temperature rises would include: (1) An assessment to determine whether the electrical conductivity of the phantom materials are appropriate for the impedance conditions at the electrode; (2) An evaluation of the impact on temperature rises of the different tissue conductivities along the path of the VNS lead; (3) An assessment of the sensitivity of the temperature rises to variation in the path of the lead; and (4) A determination of *in vivo* temperature rises in additional human models, such as those in the virtual population from the IT'IS Foundation (35). Nevertheless the RF-induced temperature rises shown in **Figure 19** are consistent with the *Instructions for Use* for the Vagus Nerve Stimulation (VNS), NeuroCybernetic Prosthesis (NCP) System (Cyberonics, Inc. and LivaNova), which limit MRI procedures to those involving the use of a transmit/receive head RF coil and other similar RF coils (8).

The standard ISO/TS 10974 should be carefully studied when evaluating an active implant for MRI issues (1). In addition to RF heating, an assessment should be made whether other interactions associated with MRI, including magnetic field interactions, gradient stimulation, and electromagnetic interference are safe for the patient and the implant.

The calculation of the background electric field in the body during MRI and the measurement of local background SAR in the phantom are made with no implant. The calculation of temperature rise at the electrode is made assuming that the lead does not appreciably change the incident RF energy. This assumption should be fulfilled in MRI since the energy scattered by the lead should be at least two orders of magnitude less than the energy input to the RF coil. Experiments on model implants for which the measured temperature rises agree well with the calculated rises further demonstrate the validity of the computational procedure described herein (36).

Nyenhuis (37) has calculated the spatial distribution during MRI of the temperature rise surrounding the electrodes of a spinal cord stimulation system. It was determined that the region of greatest temperature rise was localized to approximately 2 mm around the electrodes. The approach was a computational extension to the transfer function approach, which is now possible due to improved computational software and hardware.

Informal tests that were made with the transfer function apparatus indicate that smooth curves in the path have minimal impact on S . This observation is supported by results in **Table 1** and **Table 2** where the same transfer function yields calculated temperature rises that agree well with measurements for both the straight- and U-paths of the lead. Nyenhuis, et al. (38) presented details on the influence of phantom boundaries and media parameters on the transfer function.

The measurements and calculations demonstrate that the temperature rise at the electrode of the VNS System (Cyberonics, Inc. and LivaNova) depends greatly on the termination state at the pulse generator. This suggests that heating of an active implant might be mitigated by optimizing the value of the termination impedance.

The methods presented in this chapter can be used to establish the SAR levels under which a patient with an active implant may undergo MRI. If the tests and analysis indicate the potential for harmful heating, then MRI may be safe only for SAR levels below the Normal Operating Mode limit of a whole-body averaged SAR of 2-W/kg or an SAR of 3.2-W/kg in the head (39). If the lead is found to heat excessively, then it may be deemed to be unsafe for a patient undergoing MRI. A summary of the results from the heating tests is typically presented in the MRI labeling information section of the device's *Instructions for Use* (8, 40).

In addition to safety with respect to RF heating, device and patient safety with respect to magnetic field interactions, pulsed gradient fields, and electromagnetic interference must be established before patients with the device may safely undergo MRI. Regulatory bodies such as the U.S. Food and Drug Administration review submissions by implant manufacturers prior to approval of the MRI-related labeling (40).

608 Using MRI Simulations and Measurements to Evaluate Active Implants

ACKNOWLEDGEMENTS

The author thanks graduate students J. Jallal, T. Mansheim, C. Miller, and N. Elder for their contributions to the measurement results presented in this chapter. In addition, the author is grateful to Dr. Sung-Min Park for his contributions to the development of the concept of the transfer function.

REFERENCES

1. International Organization for Standardization, ISO/TS 10974:2018, Second Edition. Assessment of the safety of magnetic resonance imaging for patients with an active implantable medical device, 2018.
2. Kainz W. MR Heating tests of MR critical implants. *J Magn Reson Imaging* 2007;26:450–451.
3. Nyenhuis JA, Park SM, Kamondetdacha R, et al. MRI and implanted medical devices: Basic interactions with an emphasis on heating. *IEEE Trans Dev Mater Reliability* 2005;5:467–480.
4. Rezai AR, Finelli D, Nyenhuis JA, et al. Neurostimulation systems for deep brain stimulation: *In vitro* evaluation of magnetic resonance imaging-related heating at 1.5 T. *J Magn Reson Imaging* 2002;5:241–250.
5. Achenbach S, Moshage W, Diem B, Schibgilla V, and Bachman K. Effects of magnetic resonance imaging on cardiac pacemakers and electrodes. *Am Heart J* 1997;134:467–474.
6. Luechinger RC. Safety aspects of cardiac pacemakers in magnetic resonance imaging, Ph.D. dissertation, Dept. Naturwissenschaften, Swiss Federal Inst Technol, Zurich, Switzerland, 2002.
7. Wilkoff BL, Bello D, Taborsky M, Vymazal J, et al. Magnetic resonance imaging in patients with a pacemaker system designed for the magnetic resonance environment. *Heart Rhythm* 2011; 6:65–73 and <http://www.medtronic.com/mrisurescan>
8. Vagus Nerve Stimulator, VNS Therapy, NeuroCybernetic Prosthesis (NCP) System, Cyberonics, Inc. and LivANova; MRI with the VNS Therapy System, Cyberonics 26-0006-4200/5, 2011. <https://vnstherapy.info/>.
9. MRI Guidelines for Medtronic Deep Brain Stimulation Systems – To the Physician. Medtronic, Minneapolis, MN; www.medtronic.com/mri
10. Nyenhuis JA, Kildishev AV, Bourland JD, et al. Heating near implanted medical devices by the MRI RF-magnetic field. *IEEE Trans Magn* 1999;35:4133–4135.
11. Konings MK, Bartels LW, Smits HFM, Bakker CJC. Heating around intravascular wires by resonating RF waves. *J Magn Reson Imaging* 2000;12:79–85.
12. Park SM, Kamondetdacha R, Nyenhuis JA. Calculation of MRI-induced heating of an implanted medical lead wire with an electric field transfer function. *J Magn Reson Imaging* 2007;26:1278–1285.
13. Mattei E, Triventi M, Calcagnini G, et al. Complexity of MRI induced heating on metallic leads: Experimental measurements of 374 configurations. *BioMedical Engineering OnLine* 2008;7:11.
14. Langman DA, Goldberg IB, Finn JP, Ennis DB. Pacemaker lead tip heating in abandoned and pacemaker-attached leads at 1.5 Tesla MRI. *J Magn Reson Imaging* 2011;33:426–431.
15. Nordbeck P, Fidler F, Friedrich MT, et al. Reducing RF related heating of cardiac pacemaker leads in MRI: Implementation and experimental verification of practical design changes. *Magn Reson Med* 2012;68:1963–1972.
16. Mattei E, Calcagnini G, Censi F, Triventi M, Bartolini P. Role of the lead structure in MRI induced heating: *In vitro* measurements on 30 commercial pacemaker/defibrillator leads. *Magn Reson Med* 2012;67:925–935.
17. Nyenhuis JA and Miller CR. Calculation of heating of passive implants by the RF electromagnetic field in MRI. General Assembly and Scientific Symposium, 30th International Union of Radio Science (URSI) Istanbul, 2011.
18. Neufeld E, Kuhn S, Szekely G, Kuster N. Measurement, simulation and uncertainty assessment of implant heating during MRI. *Phys Med Biol* 2009;54:4151–4169.

MRI Bioeffects, Safety, and Patient Management 609

19. Cabot E, Lloyd T, Christ A, et al. Evaluation of the RF heating of a generic deep brain stimulator exposed in 1.5 T magnetic resonance scanners. *Bioelectromagnetics* 2013;34:104-113.
20. Goldstein LS, Dewhirst MW, Repacholi M, et al. Summary, conclusions and recommendations: adverse temperature levels in the human body. *Int J Hyperthermia* 2003;19:373-384.
21. ASTM F2182. Standard test method for measurement of radio frequency induced heating on or near passive implants during magnetic resonance imaging, ASTM International.
22. Amjad A, Kamondetdacha R, Kildishev AV, Park SM, Nyenhuis JA. Power deposition inside a phantom for testing of MRI heating, *IEEE Trans Magn* 2005;41:4185-4187.
23. Shellock FG, Begnaud J, Inman DM. Vagus nerve stimulation therapy system: *In vitro* evaluation of magnetic resonance imaging-related heating and function at 1.5 and 3 Tesla. *Neuromodulation* 2006;9:204-213.
24. Kozlov M, Turner R. Fast MRI coil analysis based on 3-D electromagnetic and RF circuit co-simulation. *J Magn Reson Imaging* 2009;200:147-152.
25. Akca IB, Ferhanoglu O, Yeung CJ, et al. Measuring local RF heating in MRI: Simulating perfusion in a perfusionless phantom. *J Magn Reson Imaging* 2007;26:1228-1235.
26. Feng S, Qiang R, Kainz W, Chen J. A technique to evaluate MRI-induced electric fields at the ends of practical implanted lead, *IEEE Trans. Microwave Theory and Techniques* 2015;62:305:313.
27. Missoffe A, Aissani S. Experimental setup for transfer function measurement to assess RF-heating of medical leads in MRI: Validation in the case of a single wire. *Magn Reson Med* 2018;79:1766-1722.
28. Tokaya JP, Raaijmakers AJE, Luijten PR, Bakker JF, van den Berg CAT. MRI-based transfer function determination for the assessment of implant safety. *Magn Reson Med* 2017;78:2449-2459.
29. Zilberti L, Arduino A, Bottauscio O, Chiampi M. The underestimated role of gradient coils in MRI safety. *Magn Reson Med* 2017;77:13-15.
30. Stem B. Computer modeling and simulation of implants medical device heating due to MRI gradient coil fields. Master's Thesis, Purdue University, 2014.
31. Brühl R, Ihlenfeld A, Ittermann B. Gradient heating of bulk metallic implants can be a safety concern in MRI. *Magn Reson Med* 2017;77:1739-1740.
32. Nyenhuis JA, Bourland JD, Kildishev AV, Schaefer DJ. Chapter 2, Health Effects and Safety of Intense Gradient Fields. In, *Magnetic Resonance Procedures: Health Effects and Safety*. Shellock FG, Editor. CRC Press Boca Raton, FL. 2001.
33. Nyenhuis JA, Gross DC. Effect of Strong Time-Varying Magnetic Field Gradients on Humans. In, *Safety and Biological Aspects of MRI*. Handbook of Safety and Biological Aspects in MRI, Editors, Shrivastava D, Vaughan JT. John Wiley and Sons, New Jersey, 2019.
34. Liu W, Collins CM, Smith MB. Calculations of B_1 distribution, specific energy absorption rate, and intrinsic signal-to-noise ratio for a body-size birdcage coil loaded with different human subjects at 64 and 128 MHz. *Appl Magn Reson* 2005;9:5-18.
35. IT'IS Foundation. High-Resolution Human Models: Virtual Population. <http://www.itis.ethz.ch/itisfor-health/virtual-population/human-models>.
36. Nyenhuis JA. RF Device Safety and Compatibility. Encyclopedia of Magnetic Resonance, eMagRes. Editors, Harris RK, Wasylshen RL. John Wiley and Sons, New Jersey, 2010. doi:10.1002/9780470034590.emrstm1160
37. Nyenhuis JA. Electromagnetic Distribution in Tissue with Conductive Devices. In, *Theory and Applications of Heat Transfer in Humans*. Editor, Shrivastava D. John Wiley and Sons, New Jersey, 2018.
38. Nyenhuis JA, Jallal J, Min X, Sison S, Mouchawar G. Comparison of measurement and calculation of the electric field transfer function for an active implant lead in different media. *Computing in Cardiology* 2015;42:765-768.

610 Using MRI Simulations and Measurements to Evaluate Active Implants

39. International Electrotechnical Commission (IEC), Diagnostic imaging equipment, publication IEC 60601-2-33 Edition 3.0, Medical electrical equipment, Part 2. International Electrotechnology Commission International Electrotechnical Commission (IEC) 2015. Geneva, Switzerland.
40. Shellock FG, Woods TO, Crues JV III. MR labeling information for implants and devices: Explanation of terminology. Radiology 2009;253:26-30.

Chapter 23 The Role of Numerical Modeling and Simulations to Evaluate Implantable Leads: Implications for MRI Safety

EUGENIO MATTEI, PH.D., MEDENG.

Researcher

Department of Cardiovascular, Endocrine-metabolic Diseases and Aging
Italian National Institute of Health
Rome, Italy

FEDERICA CENSI, PH.D., EENG.

Lead Researcher

Department of Cardiovascular, Endocrine-metabolic Diseases and Aging
Italian National Institute of Health
Rome, Italy

GIOVANNI CALCAGNINI, PH.D., EENG.

Lead Researcher

Department of Cardiovascular, Endocrine-metabolic Diseases and Aging
Italian National Institute of Health
Rome, Italy

INTRODUCTION

The level of knowledge of a natural phenomenon has often been related to the ability to describe it through more or less complex mathematical relationships. Notably, physicists and engineers have always used mathematical tools and modeling to represent the real world. On the contrary, some biological disciplines, especially in the past, showed more skepticism to their use. It is argued that the biological reality is extremely complex and, therefore, not suitable to be represented by an oversimplified model. This objection implies that the description of a system through mathematical and physical models may produce a distortion of the phenomena under investigation. As such, it is difficult to refute this objection because, as a matter of fact, the construction of any mathematical model needs to formulate simplifying hypotheses. However, this is a characteristic of all cognitive phenomena,

612 The Role of Numerical Modeling and Simulations

which are always based on some form of schematization. What is interesting to see is whether the mathematical or physical model is indeed more distorting than other methods. The mere presentation of experimental results does not produce conceptual distortions, but cannot be considered free from defects on a practical level, because even the measurement, in itself, implies an alteration of the system. Moreover, and this is a point of great importance, it does not allow the interpretation of the phenomenon, since its function is purely descriptive. On the other hand, when it is possible to describe a complex phenomenon using the basic laws of physics, it is possible to provide an interpretative key to the results that are obtained (i.e., an interpretative model). On the basis of the model, it is then also possible to formulate predictions on the behavior of the same phenomenon over time, or even under conditions that differ from those observed when experimental data were collected (i.e., a predictive model).

It is useful to emphasize that the biomedical world has always been very familiar with the concept of model, although it is generally associated with *in vitro* studies or animal models. Indeed, experimental medical practice leads from clinical to laboratory experience to return to clinical experience, developing through abstraction and simplification steps, in order to understand the single aspects that contribute to complex natural phenomena. This approach is very similar to that of physical-mathematical modeling: the profound complexity that characterizes living organisms and the countless relationships existing between their different components, make it impossible to describe the system in its entirety and require the identification of specific sub-phenomena, with the introduction of drastically simplified models with respect to reality. However, keeping in mind these simplifications, the models can provide results and interpretations on the physical aspects of biological reality that could hardly be achieved by the observation of experimental evidence alone.

The definition of a model commonly accepted by methodologists of science is: given any system, S , where system means a set of elements connected to each other, it is said that a new system, M , represents a model of S when it is possible to establish a correspondence between the elements and relationships of S and the elements and relationships of M . Such definition implies that, to a certain extent, the study of the system S can be traced back to the study of the system M . When the elements of M are mathematical entities and the relationships between them are mathematical functions, M is called a mathematical model.

The definition of a physical model is more debated. In some cases, a physical model is defined as a mathematical model in which the relationships that bind the different elements of the model are borrowed from the language of physics. According to another interpretation, the physical model represents a simplification of the starting model that allows a simpler characterization and evaluation, but always in terms of experimental measurements and not through mathematical functions.

When it is possible to characterize the structure and properties of a system and write the relationships between the different variables, it is also possible to proceed to the construction of the mathematical model with interpretative function. However, it is evident that when choosing the structure of the model corresponding to the system under consideration, it is necessary to accept some simplification. Thus, the model is generally deduced through a process of abstraction and a series of simplifying hypotheses, which lead the real system

to be associated to an ideal or “abstract” system that is an image of the former but which it is not the exact replica.

The adoption of simplifying hypotheses poses the problem of the validation of the model, which is generally based on the comparison between the results obtained from the model, through logical deductions or numerical simulations, and the results obtained from the experimental analysis on the real system. Even when the comparison is successful, it is necessary to ask whether the model is valid only for the particular experiment carried out or has more general validity. In the first case, the model would lose all forecasting capacity. However, even in this case, the model would still have the merit of providing an interpretation of the experimental evidence, which goes far beyond the simple descriptive function.

When all the hypotheses underlying the model are demonstrated to be valid, the deductive nature of the modeling process reasonably allows the ability to recognize the interpretative (and predictive) capabilities of the model, for a various set of physiological conditions, not necessarily limited to those under which the validation was carried out. The possibility of modifying the structure of the physical/mathematical model that describes a particular biological phenomenon, undoubtedly represents a useful tool towards a form of predictive, preventive, and personal care, which is now becoming the paradigm of modern medicine.

The general concepts expressed so far fit well with the study of the interactions of electromagnetic fields with biological tissues. In particular, the modelistic approach has represented and continues to be an indispensable means of analysis for the evaluation, both in qualitative but also in quantitative terms, of human exposure to non-ionizing electromagnetic fields. The knowledge of the mechanisms underlying the propagation and the interactions of electromagnetic fields with the external world has always proceeded in parallel with the ability to describe them through mathematical laws. Beginning with the identification of simple relationships, valid only for particular cases and under strong simplifying hypotheses, with the progress of science, increasingly complex models of general validity have been formulated. In some cases, they have also permitted the capability to hypothesize the existence of particular phenomena before being able to have an experimental evidence of the same phenomena. Maxwell's equations constitute the fundamental mathematical model for the description of the electromagnetic phenomenon and give a complete description of the relationships between electromagnetic fields, charges, and current distributions.

$$\nabla \times E = -\frac{\delta B}{\delta t} \quad (1)$$

$$\nabla \times H = \frac{\delta D}{\delta t} + J \quad (2)$$

$$\nabla \cdot D = \rho \quad (3)$$

$$\nabla \cdot B = 0 \quad (4)$$

E = Electric Field (V/m)

H = Magnetic Field (A/m)

D = Electric induction (C/m²)

614 The Role of Numerical Modeling and Simulations

B = Magnetic induction (T)

J = Current density (A/m^2)

ρ = Charge density (C/m^3)

The resolution of these equations can be obtained, generally speaking, both through purely analytical methods and through numerical methods. In the first case, however, only relatively simple problems have so far been successfully addressed, such as the absorption of a plane wave by an infinite tissue surface, possibly consisting of several layers, or by spheres, and the absorbed electric field has been obtained in a closed form. Despite the major simplifications needed by the analytical approach, the latter has definitely helped in understanding the theoretical basis of the power absorption by a biological body, and in identifying the parameters that play a major role in this process.

In the case of numerical analysis, on the other hand, the electromagnetic equations are solved by algorithms that use numerical approximation. The rapid development of computational capacities during the last decades has made it possible to greatly reduce the impact of such approximation and to carry out studies on models that are very close to the actual system under investigation.

The numerical computation of the induced electromagnetic field inside the human body is the starting point for the study of the possible effects of electromagnetic fields on biological systems and the mechanisms underlying them. The parameter typically used to characterize the interactions between electromagnetic fields and tissues is the power absorbed per unit of mass or the specific absorption rate (SAR) measured in watts/kilograms (W/kg).

SAR is a function of the electric field and conductivity of biological tissues, according to the following:

$$SAR = \frac{\Delta P}{\rho \Delta V} = \frac{1}{2} \sigma \cdot \frac{|E|^2}{\rho} \quad (5)$$

P = total power (W);

ρ = tissue density (kg/m^3)

V = volume (m^3)

σ = electrical conductivity (S/m)

E = electric field (V/m)

The SAR is the typical parameter adopted by international regulations that address the protection from electromagnetic fields, as a basic parameter for the risk assessment. Such a choice derives from the consideration that the whole-body averaged SAR and local SAR are suitable quantities to compare the effects of electromagnetic exposure under different conditions. The SAR value resulting for a given exposure condition can also be related to the local induced temperature increase, thanks to the bioheat equation (1), which describes the heat exchange mechanisms within biological tissues:

$$c(r)\rho(r) \frac{\partial T(r,t)}{\partial t} = \nabla \cdot [K(r)\nabla T(r,t)] + A(r,T) - B(r,T)[(T(r,t) - T_b(t))] - S(r,t) + SAR(r)\rho(r) \quad (6)$$

r = spatial vector (m)

t = time (s)

c = specific heat capacity (W s/K kg)

ρ = tissue density (kg/m^3)

K = thermal conductivity (W/m K)

A = metabolic rate (W/ m^3)

S = heat loss at tissue/air interface (W/ m^3)

B = blood flow coefficient (W / K m^3)

SAR = absorbed energy rate (W/kg)

In parallel with the development of modeling/numerical techniques, the effects of the interactions between electromagnetic fields and biological tissues have also been investigated through experimental studies. In many cases, experimental measurements have represented the starting point for the definition of the numerical model, as well as the source of data necessary for the validation of the model itself.

However, by analyzing these experimental studies and the limitations necessarily related to them, the great importance of numerical models and simulations is even better highlighted. Generally speaking, experimental studies evaluate the electromagnetic field interactions with biological tissues by exposing a physical model of the human body, typically referred as a “phantom”, to the electromagnetic field. The strong simplification needed by the physical model compared to the case of actual biological tissues makes it difficult to immediately extend the results obtained to what can be expected in the real case in human subjects without any further analysis. In addition, the measurement of the electromagnetic quantities (e.g., electric field, induced currents, etc.) without perturbing the system is often a difficult challenge that must be adequately addressed. Therefore, an indirect measurement is often preferred, considering, for example, quantities, such as the temperature, that are

616 The Role of Numerical Modeling and Simulations

more easily accessible, but that, in any cases, must then be related to the electromagnetic quantities of interest always through mathematical models.

In consideration of the above, the modern computational capabilities and computing powers that have grown continuously in recent years have made the modelistic approach an excellent means to describe the interactions between electromagnetic fields and biological tissues, not only limited to the research field. Presently, numerical simulations are used as a predictive and design support tool in different contexts, from the industrial prototyping of new devices to the regulatory compliance evaluation in terms of electromagnetic compatibility issues.

NUMERICAL MODELS APPLIED TO MRI SIMULATIONS: A BRIEF HISTORY

The evaluation of the possible effects induced by magnetic resonance imaging (MRI)-related electromagnetic fields on a patient bearing a metallic implant is an excellent example to demonstrate the important role that computational modeling plays today. MR systems generate time-varying gradient magnetic fields and pulsed radiofrequency (RF) fields in the presence of a powerful static magnetic field to create an image of the body. Together, the three electromagnetic fields (static, time-varying gradient magnetic fields, and RF fields) create a hostile environment for any metallic device implanted in the patient, in particular for active implanted medical devices (i.e., medical devices relying on functioning by a source of electrical energy or any source of power other than that directly generated by the human body or gravity) such as a cardiac pacemaker, an implanted cardioverter defibrillator, a neurostimulation system or a cochlear implant.

The scientific community has been engaged in finding a practical solution to extend the unparalleled benefits of MRI to patients implanted with metallic devices since the early 1990s (2-8). Numerical analysis has been widely adopted for the design and optimization of MR systems: for the optimization of static magnetic field homogeneity and for shimming (9-14); for the design of gradient coils and their optimization (15-19); for the design of transmit RF coils and optimizing RF field homogeneity (20-26); and for the design of receiver coils and the assessment of the signal-to-noise ratio for MR images (27-33). Numerical tools were also adopted to model the human body's exposure to the three aforementioned components of the electromagnetic fields generated by the MR scanner. Electromagnetic modeling has been used to evaluate the biological effects related to the power static magnetic fields of MR systems (34-36), the peripheral nerve stimulation caused by the time-varying gradient magnetic fields (37-39), and safety aspects of RF power deposition and resultant tissue heating during MR signal excitation (40-50).

However, the modeling of the interactions with the human body in presence of a metallic implant, definitely suffered from the oversimplifications made necessary by the computational resources available at that time, and tools based on numerical simulations played, in this field, a secondary role compared to experimental measurements and *in vitro* studies.

Indeed, Maxwell equations have to be solved to simulate the interactions of the electromagnetic field with the implanted medical device. For a 1.5 Tesla MR scanner, the Lar-

mor frequency is 64 MHz, which corresponds to a wavelength in human tissues of approximately 40 cm. Therefore, the wavelength is about the size of the studied object, and full-wave simulations need to be run, meaning that no approximation on Maxwell equations can be made. This is true for MR systems that works at 3 T (Larmor frequency =128 MHz, wavelength in human tissues of about 20 cm) as well. Thus, in order to reduce the computational costs of the model, the human body was often represented as a homogeneous domain with a simple geometry (e.g., rectangular or ellipsoidal) (51-54), or only a part of the body, such as the head, could be modeled taking into account the different tissues properties (55-57). In addition, the model of the implant could not account for the actual structure and geometry of a real device (i.e., the insulation sheet and the arrangement of the inner wires of the lead were not considered) (58-62).

In vivo and *in vitro* experimental studies demonstrated the complexity of the interactions between the MR system, the human body, and the medical implant, and described multiple variables that may play an important role in such interactions, including the patient's size, anatomy, body composition, the patient's position in the MR system, the pulse sequence, (which included RF power level), lead routing, and lead design (63-66). The consequence of the great number of variables involved led to a substantial variability in the results presented in the peer-reviewed literature and indicated how the characterization of an implanted device in a patient undergoing MRI was an extremely complex problem.

While the experimental approach could demonstrate in a relatively easy way the hazards related to the exposure of a patient implanted with a device to the MRI-related electromagnetic fields, it was far more difficult to prove a solution to these hazards because of the complex and unpredictable nature of the MRI-implant interactions. The use of phantoms, which do not account for the anatomical details and differences in terms of dielectric properties of different tissues, does not allow the results to be immediately extended to what occurs in a human subject. In addition, the simple measurement of a parameter does not allow any interpretation of the mechanisms underlying the phenomenon and does little to identify any strategies to reduce the risks associated with the parameter of interest. Thus, it became evident early on that there was a need for a different approach that was able to provide an interpretative and predictive key to the phenomenon: the modeling and numerical analysis.

As the computational resources increased over the years, the reliance on numerical calculations increased as well. Such an increase was supported by the possibility of performing systematic analyses of the several variables affecting the interactions between the MRI electromagnetic fields and the implanted device, with decreased costs and increased reproducibility compared to performing experimental measurements. Computer-aided modeling demonstrated a practical and efficient method for exploring millions of variable combinations in a holistic manner. Additionally, computer modeling allowed the analysis of parameter extremes, outside the bounds of normal clinical practice, which permitted further assessment of safety margins and the sensitivity of influencing variables. The results of model simulations enabled predictions to be made about what would happen in the "real" system that was being studied in response to changing conditions, and to obtain information virtually impossible to obtain by experiments, like the electric fields inside a human body.

618 The Role of Numerical Modeling and Simulations

For all of these reasons, present-day numerical simulation has become an indispensable means of safety testing for metallic devices associated with MRI, not only for research purposes, but also for medical device manufacturers to affordably obtain MRI-related safety labeling for their products. As an example, the first cardiac pacemaker implant that obtain the FDA clearance as MR Conditional in 2009 used modeling data to support regulatory submissions for approval. In particular, the modeling data was, in fact, the primary vehicle to demonstrate safety for this active cardiac device (67).

Considering the complexity of the electromagnetic problem, most of the modelistic methods implement the numerical solution of the Maxwell's equations. The vast majority of numerical field calculations performed for MRI of the human subject, without or with a metallic implant, are related to the RF fields. Whereas perturbations associated with the static magnetic and time-varying gradient magnetic fields due to the presence of the human body in the MR system are only a few parts per million (on the order of 0.000001 times the applied field), perturbations in the RF field can easily be tens of a percentage (on the order of 0.1 times the applied field in free space). In addition, RF field-induced heating in tissue (concomitant with the maintenance of the RF field in a lossy medium) must be understood and monitored to avoid excess heating or a burn injury in a patient (68). This is also the major concern when assessing the MRI issues for a metallic implant that is present in a patient undergoing an MRI examination.

Several numerical methods exist, each of them solving the Maxwell's equations following a specific algorithm. However, every numerical method has the implicit limitation of not solving solutions in a linear continuum. Every physical system has to be discretized in finite domain, so that the numerical solution is computed based on partial differential equations. The geometry of the physical systems involved in the problem is partitioned into elements of space or cells, in which the differential equations can be computed. The entire net of elements discretized into the numerical system is typically named by the term, "mesh". Several meshes can be implemented based on the specific grid of elements defined. In general, a mesh can be classified based on the following factors:

- Domain dimension: One-, two-, or three-dimensional;
- Element type: Triangular, tetrahedral, quadrilateral, hexahedral, or a mix of more than one type;
- Element aspect ratio: Isotropic or anisotropic;
- Mesh density: Uniform or graded mesh; and
- Topology: Structured or unstructured mesh.

A structured mesh presents a regular topology with a well-known pattern. Conversely, an unstructured mesh has an irregular topology where the connectivity of the grid is part of the data structure. Once the mesh is defined, then the relation to the physical system within each element of the numerical space has to be found. What needs to be defined then is the algorithm that is able to solve the physical problem in the discretized space for the specific characteristics chosen. Several numerical methods exist to solve a physical system, however

each one is defined with respect to its numerical implementation. Thus, every method cannot be independently defined by the algorithm.

The methods used to solve Maxwell's equations in a physical system are based on differential or integral equation solvers, such that they discretize the differential or integral form of Maxwell's equations. Both methods can be solved in the time or frequency domain. In the time domain, the frequency range of interest is specified, and a gaussian signal with the frequency information is defined. Then, the signal is transformed into the time domain by using an inverse Fourier transformation, resulting in a time signal with a gaussian envelope. The system is then excited with this time pattern.

Conversely, in the frequency domain, the behavior of a physical system is usually relevant in a specified frequency range. Thus, no information can be concluded for a single frequency. Hence, several simulations in the frequency band of interest have to be performed, the number of which are defined by the software algorithms to achieve a predefined accuracy of results by interpolation of points.

The most favorable methods for this type of problem, in terms of memory requirements and simulation time are the Finite Difference Time Domain (FDTD) (69) or the Finite Integration Technique (FIT) solved in the time domain. These time domain solvers require reasonable memory and simulation time compared to the frequency domain solvers (FEM, Finite Element Method; MM, Method of Moments) (70). Moreover, these algorithms tend to be easily implemented on Graphic Processing Units (GPUs) allowing a tremendous acceleration of the simulations with a hardware cost way below the cost for a cluster of central processing units (CPUs).

One drawback of these time domain solvers is the hexahedral mesh, which is much less flexible than the tetrahedral mesh of a finite element solver. However, the possibility of using a conformal mesh permits the ability to follow the strong curvature of a geometry without having to dramatically refine the mesh. This is even more important because the smaller the mesh step, the smaller the time-step of the time domain solver.

The FDTD method is a related space-grid, time domain technique that involves the resolution of Maxwell's equations on their differential form. Since its introduction by Yee in 1966 (69), the FDTD method has been widely used for a broad range of electromagnetic applications including geophysical, bioelectromagnetic, and biophotonics (71) and this technique experienced an exponential growth starting from its first proposal. One of the major reasons for such growth is the increase of computational performances for a given cost of technological resources.

Because the FDTD algorithm is based on the solution of Maxwell's equations on their differential form, it is required to define the boundaries condition of the problem. In particular for wave-propagation problems in unbounded media, artificial boundary conditions have to be used to eliminate the reflections from the edge of the finite computational domain (72). A major turning point of the method for the study of wave propagation problems was the introduction of the perfectly matched layers (PML) by Berenger in 1992 (73). One of the characteristics of the FDTD method is that as the resolution of the sampled object is refined, the time required by the simulation to reach the Courant Friedrich Levy condition

620 The Role of Numerical Modeling and Simulations

grows. This is a direct consequence of the intrinsic definition of the time-step as directly proportional to the square root of space resolution (71). Thus, the smaller the resolution, the smaller the time-step, and the higher the number of time-step intervals required to perform a time-defined simulation. Presently, computers are able to simulate increasing simulation space with higher resolution steps within a reasonable amount of time for each simulation. As described by Taflove, et al. (71), there are several reasons for the popularity of this method, including its robustness and systematicity. On the other hand, one of the major disadvantages of the technique is due to the inability of modeling smooth curved and tilted profiles. Without the implementation of a specific algorithm, a curved or tilted profile implemented in FDTD will be affected by “staircasing”. Although the simplest and most frequently used approach is the staircasing approximation, it has been reported that there is a solution inaccuracy related with the staircasing effect (74, 75). Moreover, an error of up to 2% error can be committed in the evaluation of the resonance frequency of a resonant object with respect to the tilted angle of the object with Cartesian axes of the grid (74).

In addition to the staircasing approximation, in the past years several methods have been proposed to generate a conformal mesh for tilted and curved profiles. Among all, four categories can be highlighted: the contour path (CPFDTD) algorithm (76), the non-orthogonal FDTD (77), the hybrid methods using FDTD-FEM (78) or FDTD-MoM (79), and the sub-gridding method (80). Even though these methods have been extensively discussed and compared (81), the original FDTD Cartesian grid for the simulation of a radiofrequency (RF) coil for MRI has been, to date, the most commonly used methodology adopted in the peer-reviewed literature.

Other methods including the Method of Moments (MoM) and the Finite Element Method (FEM) are very good for creating accurate representations of good conductors of arbitrary geometry, but rely on methods such as matrix inversion that work best for sparsely-populated spaces. Finite element representations of the human body are used occasionally in MRI (82-84), but due to the computational requirements, the representations tend to have far more homogeneous representations of far fewer tissue types than FDTD methods can accommodate on a given system.

The FEM method is a near-neighbor, volume method for solving Maxwell's differential equations in the frequency domain. The physical space is divided into a non-structural grid, composed of meshes of small volumes or cells of tetrahedral elements, and this fact makes this method very suitable in modeling inhomogeneities and complex geometries. Once the volume has been subdivided, the unknown field within each element is approximated using linear extrapolation, starting from a sparse system equations matrix. The solution is given by the inversion of this matrix. The FEM can couple the electromagnetic solution with other physics, such as those associated with mechanical and thermal problems. However, it could be inefficient in the treatment of highly conductive radiators due to the requirement to have some mesh between the radiator and the absorber, and the mesh could be very complex, resulting in a meshing time that is longer than the solution time.

The MoM is a full wave solution of Maxwell's integral equations in the frequency domain. The radiating/scattering structure is replaced by equivalent currents (normally surface currents) that are discretized into wire segments. Then, a matrix equation is derived and

able to describe the interaction of every source segment on every other segment, computed with the Green's function. The strong points of this method are that: (1) it is unnecessary to discretize the "air space" around the antenna, leaving only the antenna and the region of interest to be considered; (2) only the surface is meshed; and (3) there is an efficient treatment of highly conducting surfaces. However, the MoM does not handle electromagnetically penetrable materials, especially if the material is inhomogeneous, and requires the surfaces to be closed, which is often impractical.

To represent both the transmit RF coils and human body accurately in the same simulation, some groups have devised hybrid methods combining more than one method and sharing results between them (85). After an electromagnetic simulation, the specific absorption rate (SAR) distribution that is obtained is then scaled for each real RF pulse of the sequence and can be given as an input to the transient heat equation solver.

For the magneto-static problem, to assess the interaction of the field with complex geometries, the most frequently used method is the FEM. For gradient magnetic fields for which the frequency is a few kHz, approximations can be made on the Maxwell equations and the most common method used is the FEM (86).

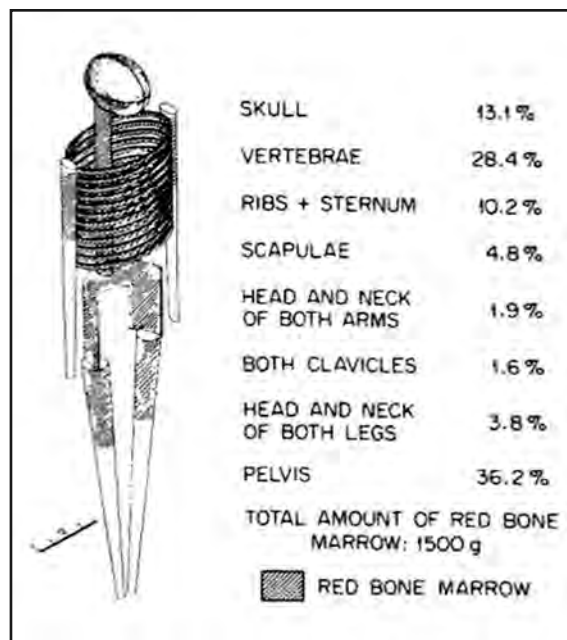
Today, the crucial role that the numerical simulations play in the evaluation of the electromagnetic field generation, propagation, and interaction with the human body, not only limited to research purposes but also for industrial design and manufacturing, is revealed by the several tools that are commercially available. The main commercial simulation software available on the market providing a time domain solver are CST Microwave Studio™ (CST GmbH, Germany), Sim4Life™ (Zurich MedTech AG, Switzerland), Xfdtd™ (REM-COM Inc., USA), and FEKOTM (Altair Development SA, South Africa). ANSYS™ (ANSYS Inc., USA) and COMSOL Multiphysics™ (COMSOL Inc., Sweden) are finite-element solvers that are mainly used in the frequency domain.

Parallel to the growth of the electromagnetic solver capability and computational efficiency, numerical human phantoms additionally evolved tremendously since the first need for these in the 1960s (87), from an approximate geometric model to the very detailed anatomical models existing today. The first numerical phantoms adopted in electromagnetic simulation were "stylized phantoms". These phantoms were the first generation of computational phantoms and were also called the mathematical phantoms (88, 89). They were implemented and used mainly between the 1960s and 2000s.

Stylized phantoms were introduced to assess the dose exposure in body organs and tissues that were described by mathematical expressions representing planes or cylindrical, conical, elliptical or spherical surfaces. All of the models developed over the years were representative of the "average or standard individual" as defined by International Commission on Radiological Protection (ICRP) data on the reference man (89). The most utilized stylized phantom model was the "MIRD" model. This phantom was named after the initials of the Medical Internal Radiation Dose (MIRD) Committee of the Society of Nuclear Medicine based in the United States (U.S.). The MIRD phantom was first introduced by Fisher and Snyder in 1967 and later refined (90, 91). The refined model shown in **Figure 1** was representative of an adult human model. In the following years, several other models that were part of the MIRD-type phantoms were released, representing infants and children of

622 The Role of Numerical Modeling and Simulations

Figure 1. The Medical Internal Radiation Dose (MIRD) model introduced by Fisher and Snyder in 1967 (91).



various ages, separate male and female adult models named Adam and Eva, and three phantoms representing the adult female in three stages of pregnancy (92-95).

The second generation of computational phantoms was the voxel phantoms. The voxel models were first presented as a “tomographic-type” and were introduced in 1984 by Gibbs, et al. (96) and in 1986 by Williams, et al. (97). These numerical models were generated from medical imaging data collected through MRI or computed tomographic (CT) scans. The voxel models were able to provide three-dimensional representations of the human body by volume elements of the same size (i.e., voxel) but representing the anatomical structures of the human body (e.g., white matter, muscle, bone, etc.).

Since their introduction in 1980s, the voxel models are still in use, and a large number of them are free to download or are commercially available. In the context of the MRI exposure assessment, one of the first studies on this important topic was performed by Dimbylow in 1996 (98). The exposure was computed on the NORMAN (i.e., NORmalized MAN) human voxel model with a weight of 73 kilograms (kg) and height of 1.76 meters (m). The model was implemented based on MRI data from a series of continuous, partial body scans of a single subject. Because the concept of the ICRP reference man was still strong, the final dimensions of the model were scaled so that the mass and height would agree with the new values for the reference man. Over the years, additional models were developed, including the Visible Human Man (VHM) and Visible Human Woman (VHW), which were completed in November 1994 and 1995, respectively. The VHM and VHW were the result of the visible human project led by the U.S. National Library of Medicine that started in 1956 and formed the basis for a large number of MRI safety assessments.

With the growth of computational power and imaging resolution, several other models were introduced. In particular, volumetric models were adjusted by using surface description methods, which allowed smoother surfaces that could be meshed at one’s convenience, with

a high-resolution that is essential when fine body structures were studied (99). Among all of the models available today, one of the more popular ones that are used for the assessment of electromagnetic exposures are the phantoms of the Virtual Family (100), which were expanded to the Virtual Population (101). The populations include models of males and females ranging from an infant to an older adult. Models of pregnant woman and obese human are also present.

Recently, a further improvement for computational phantoms is represented by the boundary representation (BREP) phantoms. The BREP phantoms are computational human models that contain exterior and interior anatomical features of a human body using the boundary representation method. With respect to the voxel models, the BREP phantoms are deformable phantom whose geometry can be conveniently transformed to fit particular physical organ shapes, volumes, or body postures. The operations that are possible to perform on BERP phantoms include extrusion, chamfering, blending, drafting, shelling, and tweaking (89). These features allow BREP models to include very complex anatomical features, as well as surface deformations. More details about the human phantoms adopted today in MRI numerical simulations, as part of complete model of interactions between the MR scanner and the patient, are provided in the next section.

THE COMPLETE MODEL OF INTERACTIONS BETWEEN MR SYSTEMS AND PATIENTS WITH IMPLANTED LEADS

Patients with active implants that incorporate one or more leads (e.g., cardiac pacemakers, neurostimulation systems, cochlear implants, etc.) are often referred for MRI examinations. Importantly, to ensure the safe use of MRI technology in these individuals, comprehensive *in vitro* testing is necessary to evaluate the various MRI issues that exist, especially MRI-related heating of the leads. As part of this assessment, modeling is often performed because of the above-mentioned reasons. Modeling of the interactions between the MR system and the patient implanted with metallic leads faces three major challenges:

First, there is inter-MRI examination-related variability. The initial studies that focused on the MRI safety of biomedical implants immediately highlighted that there are several factors that greatly impact the results and that justify the large variations of the findings reported in the peer-reviewed literature. For example, the type of MR scanner that is used and imaging conditions (e.g., the static magnetic field strength and frequency of the transmitted RF fields, the pulse sequence parameters, the duration of the scan, the body part undergoing imaging, etc.) vary between MRI procedures. Furthermore, other factors influence the level of lead heating that occurs during MRI such as the patient's position in the transmit RF coil, the position of the implant and the lead configuration inside the patient, and the patient's characteristics (e.g., size, morphology, and posture). In addition, variations exist in the length and design of the lead as well as in the type of implanted device that is present in the patient (i.e., cardiac pacemaker versus spinal cord stimulation system). Thus, the large number of different combinations of the factors mentioned above makes individual simulations of each combination a particularly challenging problem.

Second, there is body tissue heterogeneity. The different tissue types present in the human body are both geometrically complex and differ strongly in dielectric properties.

624 The Role of Numerical Modeling and Simulations

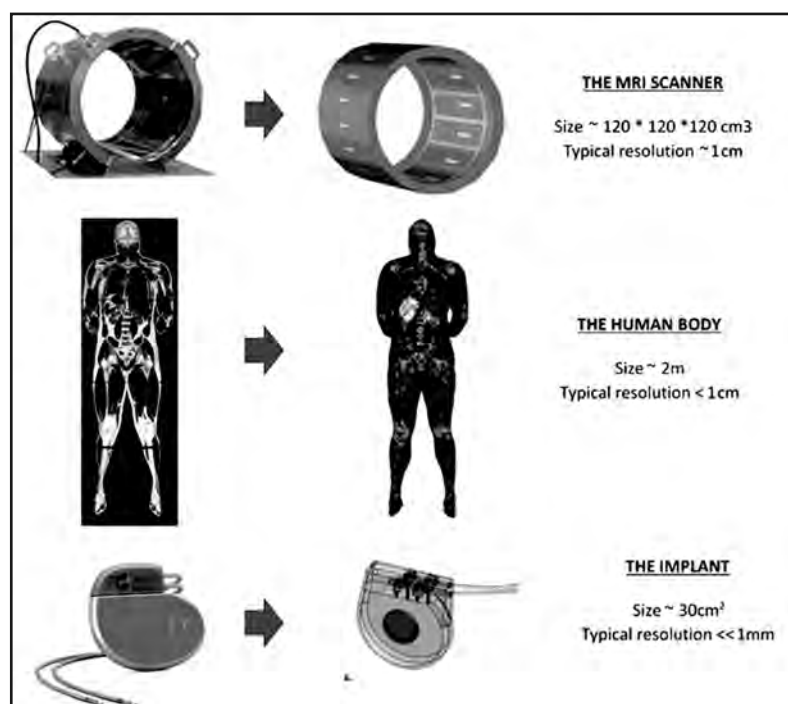
Just to get an idea, Liu, et al. (102) used conductivity values ranging from 0.02 S/m (yellow bone marrow) to 2.3 S/m (cerebrospinal fluid) and values for the relative permittivity ranging from 7 (fat and mammary tissue) to 128 (intestine/bowel content) in their simulations of an MR scanner operating at 64 MHz (1.5 T scanner).

Third, this is a multi-scale problem. Importantly, several length scales are present in the problem. At 64 MHz, the wavelength λ_0 of the RF field in free space is roughly five meters. Thus, the human body has a size of approximately $\lambda_0/3$. Inside the body, the wavelength is reduced to $\lambda = \lambda_0/\sqrt{\epsilon_r}$, where ϵ_r is the relative permittivity of the body tissue. Despite this reduction of the wavelength, in many cases the components of the implanted device (e.g., the insulation sheath of a cardiac pacemaker lead) have dimensions on a length scale of approximately $\lambda/1000$. Volume discretizing methods are able to resolve these length scales concurrently but are limited by overwhelming simulation times and memory requirements.

As shown in **Figure 2**, the three main components of the model of interactions between the MR scanner and the patient implanted with a device, that is, the MR scanner, the human body, and the implant. Each component varies in terms of size and the resolution needed for the respective model.

The implant extends typically over an area of approximately 30 cm² and must account for very small details, such as the thickness of the insulation sheath that cover the metallic lead and the geometry of the lead tip, that cannot be ignored in order to obtain reliable results and that entail the need to maintain a resolution of less than 1 mm. The human body has extremely complex geometry of weakly-conductive material that today is most readily represented on a high-resolution regular three-dimensional grid, with a minimum step of

Figure 2. The three main components of the model of interactions between the MR scanner and the patient implanted with a device: the MR scanner, the human body, and the implant. Each component varies in terms of size and the resolution needed for the respective model.



less than 1 cm. The MR scanner with its components (time-varying gradient magnetic field coils and transmit RF coil) covers a volume of about $120 * 120 * 120 \text{ cm}^3$, with a required resolution that generally does not exceed 1 cm. Running a simulation with such constraints is computationally expensive because it leads to a large number of discretization cells (up to 200 million cells) and a complex distribution of material of different electrical properties.

The Model of the MR System

The risks of MRI-related electromagnetic fields on implanted devices arise from three basic aspects of scanning (103-105). Magnetic resonance utilizes extremely powerful static magnetic forces (usually 30,000 to 60,000 times the Earth's magnetic field). This powerful magnetic field has the theoretical potential to move or dislodge an implanted metallic device. MRI also involves the use of time-varying gradient magnetic to image the scanned field of interest. These rapidly varying magnetic fields have the potential to induce electrical currents. Finally, MRI uses "pulsing" RF energy during the scanning process. If the implanted metallic device acts like an "antenna", this RF energy has the potential to cause substantial localized heating or to induce electrical currents.

Today, the materials typically used in implanted biomedical devices have physical properties that make mechanical effects (i.e., force and torque) negligible in association with static magnetic fields. As an example, reports confirm that, indeed, the forces for cardiac pacemaker pulse generators exposed to 1.5 T and 3T MR scanners tends to be lower than the gravitational force exerted by the Earth (106, 107). More dangerous are the effects related to the time-varying gradient magnetic fields and the RF fields, in particular when the implanted device is an active implanted medical device (105).

Devices such as cardiac pacemakers or ICDs have the ability to sense several physiological parameters of the patient and to modulate their activity, accordingly. The gradient magnetic fields and/or RF fields may affect the proper sensing activity, causing an inappropriate functionality of the device. In MR Conditional devices, this hazard has been mitigated by introducing a specific mode of operation, called the "MRI Safe Mode", "MRI Protection Mode" or other suitable term, that temporarily switches off the sensing ability of the active cardiac device, preventing any form of interference.

The heating generated at the tissue/device interface due to the electrical currents induced during the scanning process represents the most significant and potentially dangerous effect of the complex interactions between the implant and the MR system, in particular for those devices that used long metallic leads. Since the magnitude of the RF field is several times higher than the gradient magnetic fields, the induced heating is mainly due to the RF field. For this reason, the vast majority of numerical field calculations performed for MRI of the human subject implanted with metallic devices are related to the RF fields.

RF coils can be distinguished into surface coils, array coils, or volume coils. Volume coils (e.g., the transmit body RF coil) completely encompass the anatomy of interest and are mostly operated as transmit RF coils coupled with receive-only coils but are also capable of operating as transmit/receive RF coils. Volume coils are typically cylindrical and rely upon a sinusoidal distribution of currents arranged circumferentially around the tube and

626 The Role of Numerical Modeling and Simulations

running along the length of the coil to create a transverse magnetic field. Such RF coils, as the birdcage and the transverse electromagnetic (TEM) resonator, were designed to generate a very homogeneous RF excitation field B_1 across the entire covered volume.

A surface RF coil consists of a partial loop of wire having dimensions that match the area of interest and its inductance in resonance with the capacitance at the Larmor frequency. The inhomogeneous field profile of surface RF coils restricts their use primarily to the receive-only mode, except in the case where adiabatic pulses or trains of pulses are used to reshape the flip angle profile. However, they are, as their name suggests, good for detecting signals at a much higher SNR close to the surface of the patient. RF array coils are used to reduce imaging time by their ability to spatially localize signals.

Volume coils, and in particular birdcage coils, are the most common type of RF coils adopted as RF sources in the numerical field calculations performed for MRI of the human subject. The issue is to tune it properly to get the wanted homogeneous mode of the resonant structure. The birdcage body coils are implemented using two circular rings named end-rings connected by a certain number N of straight longitudinal connectors named rungs or legs. The RF field produced by the birdcage coil is the result of the currents flowing in the rungs. The currents flowing in the RF coil system is the result of the resonance of each network component of the coil structure.

In 1997 work, Leifer (108), accurately described the theory behind the birdcage resonator, through a simple LC (also called a resonant circuit) circuit. Leifer solved the birdcage coil using Kirchoff's mesh equations on the coil network. Leifer described the network as a generalized "band-pass" birdcage containing capacitors in both the end-rings and rungs. From the same structure "low pass" and "high pass" coils can be derived as special cases of the general band-pass coil. The three coil typologies are characterized by different resonant "modes". In fact, because of its geometry, the birdcage resonator shows a periodic or cycling nature. The periodic waves produced are named "modes" of resonance and their number is dependent on the number of coil rungs, such that the modes of resonance are those that show an integral number of wavelengths around the coil structure, each with a different field pattern and frequency of operation. Theory demonstrates that the number of resonant modes in a birdcage coil is strictly related to the number of rungs N , and equal to $N/2 - 1$. In addition to those, Leifer (108) showed that a mode of resonant can exist in which the currents flow in the same direction in each end ring. Because of co-rotating currents in the end rings, this mode was named Helmholtz or the co-rotational (CR) mode, and it cannot be constructed from any combination of currents in the LC network. This mode, however, doesn't produce any propagating wave around the RF coil, hence it doesn't generate a magnetic field in the sample region. With the addition of this last Helmholtz mode, a total of $N/2 + 2$ resonant mode exist in a birdcage coil of N rungs. Between the $N/2 + 2$:

- The mode of resonance with periodicity or order equal to 0 has equal and opposite ring currents and zero rung currents. It is called the anti-rotational (AR) ring mode.
- The 0 mode is followed by the CR mode that is not identified by a periodicity or order number.
- The mode of resonance with periodicity or order equal to 1 is the only one able to generate a homogeneous magnetic field. Thus, this is the typical mode used for imaging.

- All the other modes generate a magnetic field with a null at the center of the birdcage coil.

Low pass and high pass models present the same number of resonance modes, but they differ by showing a low or a high resonance spectrum, respectively. In particular for a low pass birdcage type, the AR and CR modes degenerate at zero frequency, with higher-order modes increasing in frequency. Conversely, in high pass birdcage type, the AR and CR modes form a doublet in high frequency, with higher-order modes decreasing in frequency.

Over the years, the RF birdcage coils have been proffered as the main implementation of RF coil for approximating the B_1 propagation in the patient. However, the presence of a patient can affect the B_1 homogeneity. As a result, there may be areas within the body of the patient in which the transmit RF field is substantially weaker than in other regions. Additionally, the loss of homogeneity increases with the static magnetic field strength and with the RF coil's dimensions. For this reason, other technologies have been implemented to overcome the loss of field homogeneity. The more relevant ones are the Transverse Electromagnetic (TEM) resonator coils, and the parallel multi-transmit RF coils. The TEM resonator was first introduced by Vaughan in 1999 (109). The structure of the TEM resonator differs from the one of a birdcage coil in two ways. First, longitudinal connectors of the birdcage coil are replaced in the TEM coil with microstrips that are affixed to the inner surface of a non-conducting cylinder. Second, in the birdcage coil the rungs current use the end-rings as a return path, whereas in the TEM resonator the microstrips are all connected to the outer thin metallic shield. Thus, inductance and self-resonance of the TEM coil are independent of RF coil's diameter, because the TEM coil return path follows the shield rather than the end rings. The main characteristic of the TEM resonator is that at high frequencies, it becomes a cavity resonator or longitudinal transmission line in which oscillating standing waves develop.

The increase of the SNR has always been the main target of improvement for RF birdcage body coils. To this aim, the use of multi elements excitation was adopted as a measure to improve the RF homogeneity in the excited volume. The simple birdcage coil was seen as a multi-element transmit coil array that could allow for an independent adjustment of amplitude and phase of the signal feeding each element of the coil. Starting from 2000s, this concept was evolved and made to take advantage of this method to reduce the RF inhomogeneities in the patients, particularly at high static magnetic fields (110). This new RF modality is also known as parallel multi-transmit or RF shimming. The degree of freedom given for each element of the coil to be fed with a specific waveform, permitted the ability to more carefully control and increase the homogeneity of the B_1 field generated by the RF excitation. Thus, the main concept of the multi-transmit coil is that the power is distributed to the feeding sources of the transmit RF coil (typically a TEM resonator) using two or more independent channels. A second advantage of these transmit RF coils is that they can be also used in a parallel receiving mode with a consequent reduction of the acquisition time.

The structure of the birdcage coils allows for multiple feeding conditions within the coil rings. Depending on the source number, and feeding phase and amplitude, different polarization of the produced magnetic field can occur. Historically in the 1980s, the birdcage coils were fed using a single port coil, such to achieve a linearly polarized field. However,

628 The Role of Numerical Modeling and Simulations

with such polarization, “quadrupole” artifacts were present in the resulting MR image (111). These artifacts manifested as “holes” or voids of decreased image intensity that could not be attributed to any anatomical feature of the patient scanned.

By running simulations with cylinders of different size and material, it was evident that the “holes” were caused by the asymmetric nature of induced eddy currents that derive from the finite conductivity of the medium. To overcome this artifact problem, it was suggested to implement the circularly polarized birdcage coil with two feeding ports. The two ports were fed with the same amplitude and differential phase of 90° in order to generate a purely rotating wave. With this new polarization, a 1.4 and 1.6 higher SNR was observed with respect to left/linear and right/linear polarization, respectively.

The linear polarization is then considered less efficient for MRI because half of the transmitted power is not used for the imaging process. The circularly polarized field is obtained by adding to the original linearly polarized field, a second field generated by sinusoidal current phase shifted by 90° . This is typically obtained by a quadrature transmission of signals in the RF birdcage coil.

This can be achieved by two or more feeding sources around the coil ring. When such a circularly polarized field is generated, the two counter-rotating components of the two generated fields (i.e., B_1^-) cancel each other, whereas the subfields effective at inducing MRI (i.e., B_1^+) add together. Hence all of the power is used for imaging and an overall higher efficiency is achieved. Presently, the RF coil implemented in a clinical MR system uses the highly efficient, quadrature excitation. Conversely, linearly polarized transmit RF coils are restricted for use in small animal imaging.

Beside the time-varying magnetic field (B_1) used for the excitation of the magnetization vector, when a conductive media, such as the human body, is present inside or in close proximity to the RF energy, an altering voltage or electromotive force is induced inside the conductive media by the variation of the magnetic flux. The electromotive force generates eddy currents inside the media that, in turns, generate a secondary magnetic field and a corresponding additional voltage. Overall, the induced internal fields are strongly dependent on both the incident field, and the size, shape, and dielectric properties of the exposed medium. The voltage induced by B_1 is much larger than the secondary one. However, within the human body it can be considerably high enough to perturb the primary field. This is due to the complexity of the body’s anatomy and to the inhomogeneity of the dielectric properties of the tissues.

Additionally, an electric field can be generated within the body by the distribution of electrical potential specific to a given resonant structure. In MRI, such an electric field is typically named “conservative” or “capacitive”. One possible situation in which the capacitive effect should be taken into account is when the medium is in close vicinity to the RF resonator. All these elements must be considered in the development of the model of the transmit RF coil used for MRI. For an ideal computation, the entire RF coil (with the actual power supply and the tuning capacitors able to produce the circularly polarized magnetic field), should be reproduced using a grid resolution fine enough to adequately account for the detail of the implanted device under investigation. As previously mentioned, the challenge is to combine a simulation of large dimensions (i.e., the length of the MRI’s transmit

RF coil > 1 m) and small structures (i.e., the thin wire $\ll 1$ mm). In order to decrease the computational effort required by the model, in many of the numerical studies, the birdcage coil is simplified with respect to its actual structure. In some investigations (112, 113), the birdcage coil is modeled removing all the lumped elements: the capacitors are replaced by current generators, with sinusoidal time behavior (i.e., at the frequency of 64 or 128 MHz) and a phase delay equal to the azimuthal angle in order to obtain circular polarization. In this case, the resonance mode is no longer achieved by tuning the capacitors, but by forcing the right current distribution inside the birdcage coil. This model is able to faithfully reproduce the electromagnetic field distribution of an unloaded birdcage coil, but, when adopted to simulate the interaction with an implanted device in the body, it becomes much less accurate, in particular when the implant is placed immediately underneath the skin (e.g., an implanted infusion pump), close to the transmit RF coil.

As already highlighted in the previous section, FDTD and related methods remain dominant in numerical field calculations that consider realistic human body models. However, it is not the ideal method in all situations, such as when dealing with fields near highly conductive surfaces in any arbitrary orientation, as with most RF coils. Generally, FDTD and related methods rely on a Cartesian grid (with regular or irregular grid spacing), so surfaces at oblique angles are represented in a ‘staircase’ fashion. Although there are some algorithms to help reduce the shortcomings of FDTD-type methods in these situations, other approaches include development of human body models for finite element methods (114) and hybrid approaches using one numerical method in regions containing the RF coils, and another in the region containing the human body are often adopted (115).

Modeling has also been applied to investigate the interactions between implants and the time-varying gradient magnetic fields. The gradient coils of an MR system generate time varying magnetic fields with a frequency in the kHz range. These varying magnetic fields generate induced electric fields on implanted metallic devices during the MRI process that results in the appearance of eddy currents which can generate induced voltages on the electronics of active implanted medical devices. In the frequency range of gradient fields, capacitive and electromagnetic propagation can be neglected, thus, it is possible to treat bioelectric currents and voltages in living tissues as stationary. This is known as the quasi-static approximation. Under quasi-static assumptions, the stimulus amplitude and the resulting voltage, electric field and current density are all in a linear relationship. Therefore, it is sufficient to employ a steady-state solver, which greatly simplifies the computational costs of the analysis required.

As for the static magnetic field, modeling and simulations were mainly adopted to address the problem of the disturbance of the static field owing to the presence of a metallic implant in the patient, resulting in imaging artifacts which may impact the diagnostic use of MRI, sometimes making it difficult or even impossible to interpret the images. To consider the implementation of correction techniques or magnetic susceptibility artifacts attenuation, it is essential to be able to calculate very accurately the disturbance of the local magnetic field generated by the implanted metallic object placed in MRI conditions. For this purpose, analytical models may be useful tools to perform design and optimization studies on metallic objects with simple geometries (116). For more complex geometries, however, an accurate computation of the local magnetic field is needed, using numerical

630 The Role of Numerical Modeling and Simulations

methods such as FEM. These numerical methods enable the modeling of magnetic field deformations in the diamagnetic and paramagnetic samples environment and they can be validated for simple implant geometries (117).

The Model of the Human Body

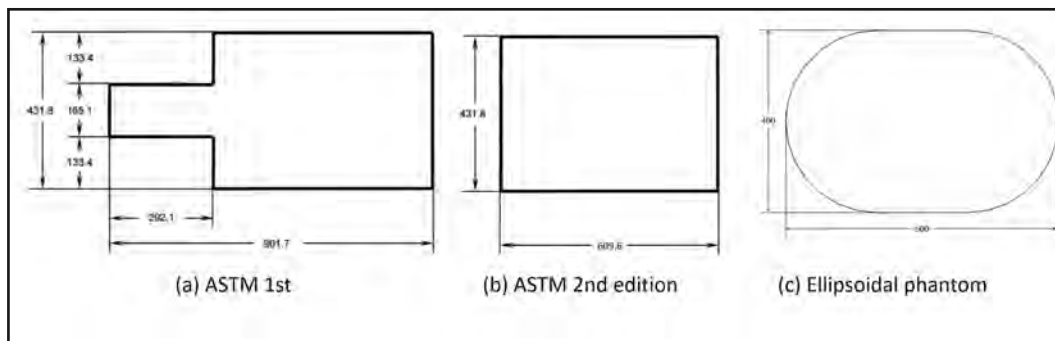
The success of computational modeling is due to the possibility of performing systematic analyses of the several variables affecting the interactions between the patient with a metallic implant and the MR system, with reduced costs and increased reproducibility compared to experimental measurements. If there are fundamental flaws or inaccuracies in the model that mask or modify the physics under examination, even if the simulation itself runs flawlessly, results might be erroneous and predictions based on that simulation will not accurately embody the intended aspects of the physical world. It is with this motivation in mind that developers of phantoms characterizing the human body and its corresponding physiological processes have continuously advanced the state-of-the-art and pursued ever more accurate representations of human anatomy at a variety of geometric scales.

Many MRI simulations that evaluated the safety of implanted devices, in particular the early studies conducted when the computational resources were still limited to account for the detailed representation of the human tissues, adopted numerical models of the body that were derived from the physical phantoms used in experimental studies. Physical phantoms are typically made of solid materials, which are approximately equivalent to human tissues in terms of electromagnetic properties. They can be based on simplified designs or they can be anthropomorphic phantoms.

Simplified phantoms have the advantage of being easily standardized. In the peer-reviewed literature, it is possible to find simplified phantoms made of different geometries such as: “oblong saline bath to simulate an endovascular intervention” (118), cylindrical phantom (119, 120), or spherical phantom (121). Because of their simplicity, simplified physical phantoms were also standardized. In the context of MRI exposures, the standardized phantom to assess MRI-related heating for a metallic implant is the American Society for Testing and Materials (ASTM) International phantom. In the first version of the standard, the phantom had a shape based on simplified human head and trunk regions (**Figure 3a**). In the 2011 edition of the standard (122), the phantom was revised to include only the trunk, suggesting a rectangular box shape (**Figure 3b**). The ASTM phantom of the standard is a container filled with a gelled-saline phantom material with electrical and thermal properties in the same range of the ones of the human body at the frequencies of interest (i.e., 64 to 128 MHz corresponding to 1.5 and 3 Tesla, respectively).

An additional phantom proposed for controlled exposure conditions is the ellipsoidal phantom, described in the Annex M-3 of the Technical Specification (TS), International Organization for Standardization (ISO), ISO/TS 10974:2018 (123) (**Figure 3c**). In addition to simplified phantoms, anthropomorphic phantoms have been also implemented for a more realistic representation of the human body heterogeneity. These phantoms typically consist of several tissue-equivalent materials that are molded into shapes of organs or bones to represent single part or all of the human body. Among all, the bottle manikin absorption (BOMAB) phantom represents the ICRP reference man and it consists of 10 high-density polyethylene containers (124). Each of these phantoms are representative of body sections,

Figure 3. ASTM phantoms (a) first edition and (b) second edition indicated in the ASTM F2182 standard (122). (c) Ellipsoidal phantom suggested in ISO/TS 10974:2018 (123).



such as the head phantom and human torso (125). However, even the most complex physical phantom cannot adequately represent the extremely complex morphological properties of the actual human body. On the other hand, numerical modeling allows for a much more realistic representation.

Currently, several voxel and surface human body models are available for downloading free of charge for non-commercial use. Among these, the most often used solution adopted not only for electromagnetic exposure evaluations but also in many other medical applications where the detailed human anatomy has to be reproduced, is the Virtual Family (VF) (100).

The VF is a set of four highly detailed, anatomically correct, whole-body models of an adult male, an adult female, and two children. The four models are based on high-resolution (MRI) data of healthy volunteers. Organs and tissues of the models are represented by three-dimensional, highly detailed computer-aided design (CAD) objects without self-intersections and gaps. The CAD objects allow the models to be meshed at arbitrary resolutions without loss of small features. As of the end of 2014, the VF was used in more than 120 medical device submissions to the Food and Drug Administration (FDA) and was cited more than 180 times in the peer-reviewed literature. The following two VF model versions are available free of charge:

- VF 1.0: The VF 1.0 models include segmentation of approximately 80 high-resolution organs and tissues. The Virtual Family Tool can be used to discretize and export the CAD objects in a generic voxel-based format. All four VF 1.0 models and the Virtual Family Tool are provided free of charge (except for shipping and handling fees) to the scientific community for academic purposes, only.
- VF 2.0: The VF 2.0 models consist of simplified CAD files optimized for finite-element modeling in any third-party platform. These models are based on a new, high-end generation of VF models that have been re-segmented at finer resolution to afford a higher degree of precision and anatomical refinement, as well as improved structural continuity of approximately 300 organs and tissues. For the purpose of simplification, these structures are combined into 22 high-resolution tissues. The VF 2.0 models are available free of charge (except for shipping and handling fees) to everyone.

632 The Role of Numerical Modeling and Simulations

Table 1. Main characteristics of the four models of the first generation of the Virtual Family (100).

Name	Sex	Age (years)	Height (m)	Weight (kg)	BMI (kg/m^2)
Duke	Male	34	1.77	70.3	22.4
Ella	Female	26	1.63	57.3	21.5
Billie	Female	11	1.49	34.0	15.4
Thelonius	Male	6	1.15	18.6	14.1

(BMI, Body Mass Index)

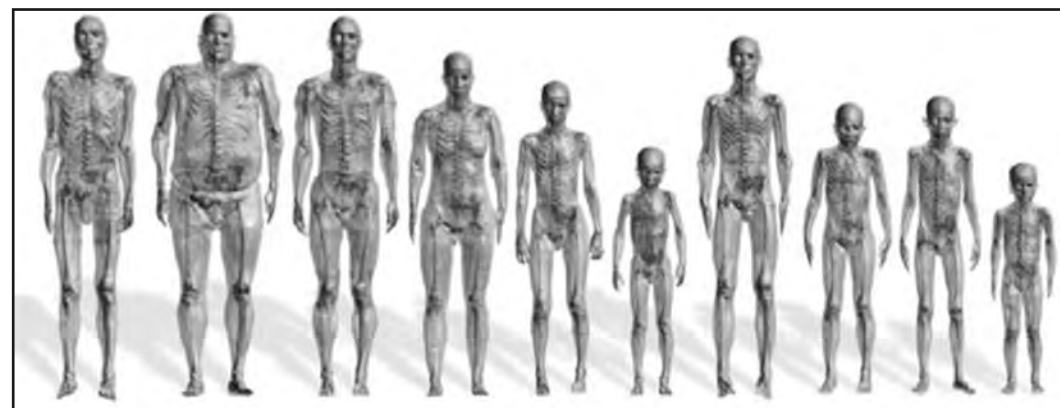
Table 1 summarizes the main characteristics of the four models of the VF.

In the VF models, individual tissues are composed of large numbers of triangles, and the whole-body triangle count ranges between 3.6 to 7.7 million. The models are distributed as surface meshes in STL (i.e., Standard Tessellation Language or STereoLithography) format. Each tissue is stored as a separate surface mesh, which is guaranteed to be closed, but may contain non-manifold edges or vertices.

In addition to the initial human body models, the VF has been then extended to increase the population coverage: the MR images of additional child volunteers (five and eight year old girls, and five and 14 year old boys) were segmented to create the Virtual Classroom. Increased coverage of anatomical variability was provided with obese (37 years old, 1.82 m, 120 kg) and elderly (84 years old, 1.73 m, 65 kg) male models, an eight week old baby model, and three pregnant women models at gestational stages of three, seven and nine months. Today, this widely used set of anatomical models is also known as the Virtual Population (ViP) (**Figure 4**).

The ViP 1.0 has been applied in a large variety of exposure studies, such as those involving mobile phones, wireless devices, MR systems, home appliances, and safety and efficacy assessments of medical treatments (e.g., hyperthermia therapy), implant safety,

Figure 4. Virtual Population voxel models (100, 101).



product development and optimization, and basic research, including mechanistic investigations).

However, while they have been employed in selected cases to the assessment of medical devices and therapies (e.g., the safety of implants during MRI), the first generation of the Virtual Population suffers from limitations related to limited local detail and accuracy, unsuitable tissue surface quality, missing fine structures and insufficient fine structure continuity, as well as inconsistent segmentation across the different models. Furthermore, current devices often combine complex interactions from multiple domains of physics and physiology sometimes in a coupled manner, which require models adapted to different solvers (e.g., a finite-element method, FEM), which typically requires high-quality unstructured meshes. In order to overcome these, a second generation of VF models (ViP3) was developed, reaching a level of detail and accuracy with more than 300 tissues and organs per model and a resolution of $0.5 \times 0.5 \times 0.5 \text{ mm}^3$ throughout the entire body. For these new-generation models, posing functionalities are available to parameterize the posture of the models. In addition, to further extend the population coverage, morphing functionality is also provided that allows, for example, the fat or muscle content to be increased or decreased to change the body-mass index (BMI) of the models while preserving realistic internal organ placement and tissue distributions.

The Virtual Population 3.0 models are integrated within the multiphysics simulation platform, Sim4Life, which includes only a time domain electromagnetic solver, or the SEMCAD time domain electromagnetic solver. The Virtual Population 3.0 models cannot be exported to any third-party software. The Virtual Family v1.x models are also compatible with Sim4Life or SEMCAD time domain electromagnetic solvers, or can be exported to other solvers only in voxel format, which is not suitable for import into solvers based on unstructured meshes.

Recent literature includes reports of the development of surface-based models obtained from the conversion of voxel-based data, and then used for electromagnetic simulation with solvers that need unstructured meshes (e.g., FEM), which could be more efficient in modeling in the frequency domain than other elements of the complete model, that is, the transmit RF coil and the implant. However, converting to high-quality, surface-based objects and correctly matching contact regions is not trivial and presents a significant challenge. Thus, only a few surface-based, full-body human models are available today, providing levels of detail of different human tissues that are not always adequate to be used as a realistic human model in MRI simulations for the assessment of the safety of implanted leads. However, these models have the advantage that can be obtained from the voxel models derived from the Visual Human Project Visible Man and Visible Woman data sets, which have formed the basis for a large number of MRI safety assessments (126). For inter-laboratory studies, in general, it is beneficial to use voxel- and surface-based models derived from the same dataset.

The anatomic accuracy of the human body model is not the only key element that guarantees the success of a numerical analysis. Depending on the physics to be applied in the simulation, the parameters of interest (e.g., electric and magnetic conductivity, permittivity and permeability for electromagnetic simulations, or thermal conductivity, heat generation

634 The Role of Numerical Modeling and Simulations

rate, heat transfer rate or perfusion, and heat capacity for thermal simulations) must be assigned to the different tissues. Such parameters can be derived from the studies available in literature that specifically investigated the properties of human tissues in the different frequency ranges (127) or from the databases available on-line (128) that, based on a comprehensive review of the aforementioned scientific papers, provide the modeling community with average and range-of-variation values of electromagnetic and thermal properties, as well as density and perfusion of biological tissues, as a function of the frequency of interest.

The Model of the Implant

The model of the lead represents the most critical aspect for MRI simulations that evaluates the safety of this implant. As such, it needs, at a minimum, a sub-millimeter discretization inside the comparatively large volume of the transmit body RF coil of the MR system and must account for a vast selection of realistic implant positions in numerous human body models in order to perform a statistical basis for a prediction of the expected worst-case condition. In addition, the inner structure of the lead is often difficult to be known in sufficient detail because each device manufacturer may adopt proprietary solutions that are rarely accessible by the general public. For these reasons, many MRI simulations directed toward comparing different exposure conditions (e.g., in terms of implant positioning inside the human body, the level of RF energy applied during MRI, the position of the body inside the transmit RF coil, etc.) or different implant basic characteristics (e.g., lead length, thickness of the insulation sheet, etc.), adopted as the implant model a simple insulated metallic wire with exposed conductive tips. It is obvious that such a simplified model does not produce realistic results and, thus, is not suitable to predict what can be expected during a “real” MRI examination involving a patient with actual implanted leads.

Typical leads used in implanted devices (e.g., cardiac pacemakers, implanted cardioverter defibrillators, neurostimulation systems, etc.) use coiled wire configurations. The coiling of the wire is essentially utilized to increase the flexibility and implanted lifetime of the lead. Coiled wires used in such devices may be single filar (single strand of wire) or have multi-filar windings (i.e., there may be more than one conductive strand coiled together to form the wire form). Such complex structures, arranged over realistic pathways compatible with the anatomy of the human body cannot be easily represented in the FDTD environment. Other techniques, such as the MoM, are more favorable, but then suffer from the already mentioned limitations, when the model of the implant has to be integrated inside an accurate model of the human body.

Studies that reproduced and investigated lead structures more complex than the simple insulated wire, mainly focused on developing and comparing the performance of implanted lead designs or strategies that could eliminate or ameliorate the hazards related to MRI (129, 130). Whereas these studies achieved a substantial significance with respect to the design of the MR Conditional implants, they were not suitable for adoption as an accurate implant model in the complete model of interactions between the MR scanner and the patient. The difficulties to numerically solve human and lead models simultaneously due to the complex structure of implanted lead systems prompted the researchers to find an alternative approach,

based on the concept that it may be advantageous to model the lead and the human separately and then combine the results to determine the heating.

In 2007 Park, et al. (131), introduced the concept the transfer function (TF) of a lead, that is a mathematical function that relates the incident electric field to the scattered electric field in the vicinity of the electrode. From knowledge of the TF, the heating at the lead's electrode and the resonant behavior of leads in phantom and human models can be predicted.

The TF concept comes directly from the formulation of the electromagnetic problem by the Method of Moments (MoM): the scattered field at the lead tip is considered to be the linear superposition of the effect of the tangential incident field all along the lead. Different methodologies have been proposed to measure the TF of an implanted lead.

Park, et al. (131) calculated the transfer function for simple wire geometries that simulated implanted leads using the MoM technique. First, the scattered electric field at a test point near the lead tip arising from a uniform incident electric field of 1 V/m was computed. Then, the radial component of scattered electric field at the same test point, P , was calculated for a step function of the tangential E-field that has unit value (1 V/m) over a specific segment of the lead and is zero over the remainder of the lead. The TF is finally obtained from these two contribute to the scattered electric field, considering the power dissipation around the lead tip as the linear superposition of the contribute obtained by the moving the step function of the tangential E-field all along the lead length.

By definition, the FT depends on the electrical properties of the surrounding tissue, the RF frequency, and on the structure and characteristics of the lead under test. Therefore, it is assumed to be independent from the particular lead path adopted. Thus, the electric field at the tip of the lead, placed in any possible configuration inside the human body model, can be easily estimated from the E-field distribution computed inside the body without the implant.

Even if such an approach allows the ability to “decouple” the model of the implanted lead and of the human body, the estimation of the TF obtained from numerical calculations is still rather demanding, since the actual detailed model of the lead has to be known and reproduced. The TF can be calculated also via experimental measurements, by exciting a small portion of the lead with an electric field that needs to be constant over the small section measured and then drastically reduced to zero in the nearby sections. The TF is then obtained by recording the E-field at the tip, while moving the excitation signal all along the lead. However, the generation of such an excitation signal is not immediate and requires specific and rather expensive systems (131, 132).

Due to the aforementioned limitations, alternative methods have been proposed in the peer-reviewed literature (133, 134). An interesting alternative approach is based on the reciprocity principle conjugated with the Huygens' principle (i.e., this principal shows how a wave field on a surface determines the wave field outside the surface) and demonstrates that, if one excites the electrode where the heating has to be evaluated, the current distribution along the lead is actually the transfer function. Thus, the current distribution can be obtained numerically, by exciting the lead with a known current source at the tip, or exper-

636 The Role of Numerical Modeling and Simulations

imentally, by injecting an RF signal (64 MHz or 128 MHz corresponding to 1.5 Tesla or 3 Tesla, respectively) into the lead and measuring the current along the lead itself. In the latter case, in order to obtain from the resulting current distribution a transfer function for the heating evaluation, a calibration factor has to be determined experimentally, by performing heating measurements under a known incident electric field.

Currently, the TF is widely adopted, not only for research purposes, but also by device manufacturers, in the design phase to test the safety of their products, and to produce evidence of the safety for the regulatory body in charge of issuing the marketing authorization. The TF is also described as one of the four-tiered approaches described in the Technical Standard (TS) from the International Organization for Standards, ISO/TS 10974:2018 (123), which will be discussed in detail in one of the following sections.

Model Verification, Validation, and Uncertainty Quantification

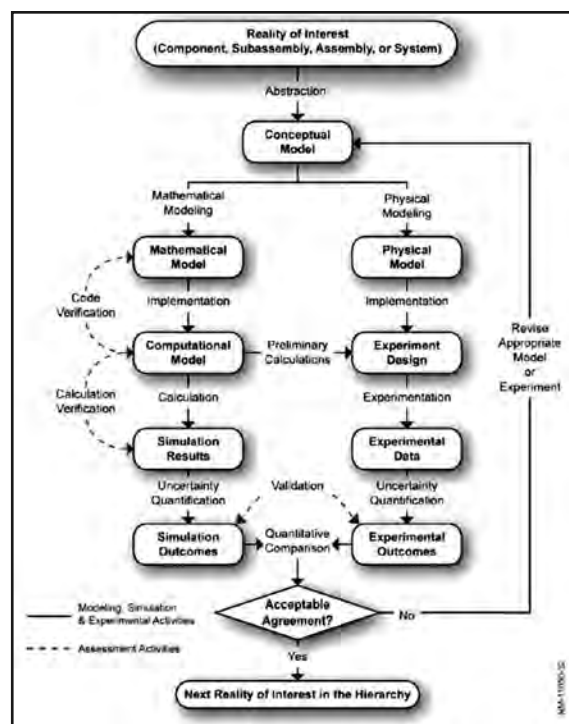
Although performing a numerical analysis has numerous benefits, experimental validation of the numerical model remains a complementary and fundamental step to determine the degree to which a model is an accurate representation of the real world from the perspective of the intended use of the model. Verification, Validation, and Uncertainty Quantification (VVUQ) is a complex set of procedures for the assessment of the overall quality of the physical system results that are obtained with numerical simulations. The process of determining the accuracy with which a computational model can produce results deliverable by the physical system on which it is based is a development process that follows several steps.

The flowchart presented in **Figure 5** from the American Society of Mechanical Engineers (ASME) guide on Standard for Verification and Validation in Computational Solid Mechanics (135) is a good outline of all the necessary steps that are required in the VVUQ process. The VVUQ can be essentially divided into three fundamental steps: (1) the verification of the numerical code implemented (2) the validation of the numerical results with experimental measurements, and (3) the quantification of the uncertainty of both numerical and experimental results. In accordance with this guidance from the ASME, these steps can be defined as:

- Verification: The process of determining that a computational model accurately represents the underlying mathematical model and its solution from the perspective of the intended uses of modeling and simulation.
- Validation: The process of determining the degree to which a model or a simulation is an accurate representation of the real world from the perspective of the intended uses of the model or the simulation.
- Uncertainty Quantification: The estimated amount or percentage by which an observed or calculated value may differ from the true value.

Ultimately, the numerical outcomes can be considered a good representation of the reality if the data are within the combined uncertainty of the numerical and experimental results. However, it is important to understand that a numerical code can never be fully verified for any conditions, but every code is verified against a set of numerical tests for the specific physical system of interest.

Figure 5. Flowchart describing the Verification, Validation, and Uncertainty Quantification, VVUQ (Adapted from ASME guide on Verification & Validation for Solid Mechanics) (135).



Over the years, the FDTD methods were thoroughly verified with respect to experimental results. Verification of the code is typically performed for simplified geometries and must be done for any algorithm implementing the numerical method. In the context of the RF fields associated with MRI, one of the first procedures was followed by Chen, et al. (136) in 1998. The main goal of their investigation was to analyze the SAR and electromagnetic fields in a realistic human head model excited by shielded RF coils. The researchers proposed a numerical method based on the combination of the FDTD with the MoM. To verify the numerical code, Chen, et al. (136) compared the numerical solutions of the magnetic field generated in a square waveguide excited by a current sheet with respect to the analytical calculation of the same distribution.

Similar approaches were also followed by Bowtell and Bowley for the magnetic fields generated by a gradient coil (137), and Collins, et al. (138) for the evaluation of the temperature rise and SAR in a human head exposed to electromagnetics field at 64 and 300 MHz. Once the implemented algorithm had been verified, the specific physical scenario modeled had to be validated with respect to the experimental measurements. In the context of the RF fields used for MRI, this step was not trivial, considering that it is not possible to measure the electromagnetic field distribution in a real-life situation, inside patient. However, over the years, several suggestions were made to validate the numerical results. Seifert, et al. (139) validated the numerical results with respect to the absolute value of the complex amplitude of the positively rotating component of the RF magnetic field, and the phase of the MRI signal. Those quantities were, indeed, part of the information included within the MR images obtained in a patient. The validation of results based on the B_1 maps was also followed by Homann, et al. (140) for different patient locations within the transmit RF coil, by Voigt, et al. (141), and by Van den Berg, et al. (142).

638 The Role of Numerical Modeling and Simulations

A good alternative for the validation of numerical results with experimental data is the use of phantoms. Because of their reproducibility in terms of geometric and physical characteristics (e.g., electrical properties, thermal properties), phantoms can be easily implemented in the numerical environment with a high physical accuracy. Furthermore, a second advantage of the use of phantoms is the possibility of measuring field values and distribution inside of the medium. Regarding imaging the human body, results obtained in a phantom can be validated as well with respect to B_1 maps. Ibrahim, et al. (143) validated FDTD results of three implementations of a transmit RF coil at 340 MHz, loading the numerical and physical coil with a plastic cylindrical phantom (diameter, 15.0 cm; length, 21.2 cm) filled with mineral oil. Cabot, et al. (144) extended the validation process measuring the electromagnetic field within a 64 MHz transmit RF coil, and Mattei, et al. (53) in terms of the return loss of the resonant coil and currents along the rungs.

Of note is that the uncertainty quantification comes both from experimental and numerical data. This can be due to several factors, such as instrumental, environmental, the operator, or the followed measurement process. Typically, experimental uncertainty is assessed by performing the measurement process more than one time and then estimated using statistical analysis of the set of measurements. Several investigations showed a high variability of results with respect to the mesh used, simulation setup (such as boundaries conditions), or computation convergence. Oberkampf, et al. (145) categorized the numerical uncertainty as:

- Aleatory uncertainty to describe the inherent variation associated with the physical system or the environment under consideration. Sources of aleatory uncertainty can commonly be singled out from other contributors to total modeling and simulation uncertainty by their representation as distributed quantities that can take on values in an established or known range, but for which the exact value will vary by chance from unit to unit or from time to time.
- Epistemic uncertainty as a potential inaccuracy in any phase or activity of the modeling process that is due to lack of knowledge.

The aleatory uncertainty is usually an irreducible uncertainty that is typically quantified by a probability distribution. Whereas the epistemic uncertainty is considered a reducible uncertainty. An important and thorough investigation including experimental and numerical uncertainty was performed by Neufeld, et al. (146). The goal of the study was to compare experimental setup and simulations of RF energy-induced heating at the tip of two generic implants for standardized testing. For each quantity of interest studied (e.g., electric field, SAR, and temperature), the uncertainty was calculated assuming a linear dependence of the measured values with respect to a varying parameter. Examples of parameters that were considered included: phantom position and electrical properties, positions of the temperature probe relative to the implant, lead geometry, and numerical resolution.

THE ROLE OF MRI SIMULATIONS IN THE RISK ASSESSMENT OF IMPLANTS EXPOSED TO MRI-RELATED, ELECTROMAGNETIC FIELDS: THE TECHNICAL STANDARD ISO/TS 10974:2018

As already mentioned in previous paragraphs, MRI simulations are today largely adopted, not only for research and design purposes, but they have also become the primary

means for device manufacturers to support regulatory submissions for approval of their MR Conditional products. Modeling data was the primary vehicle used to demonstrate safety for the first MR Conditional cardiac pacemaker (i.e., the EnRhythm™ in Europe and the Revo MRI™ in the U.S., Medtronic, Inc., www.medtronic.com), which was introduced into the market in 2008. (However, it should be noted that nearly twenty years ago, the first active implant that incorporated leads and implantable pulse generators to receive MR Conditional labeling was the deep brain stimulator system from Medtronic, Inc. The labeling for this device relied solely on physical testing of MRI-related issues that included force, torque, heating, induced currents, and artifacts.) These data were submitted only to competent regulatory authorities and, thus, were unavailable to the general public. Nevertheless, a general idea of the approach that was utilized to assess the MR Conditional cardiac pacemaker was presented in the work by Wilkoff, et al. (67): a comprehensive modeling framework was developed to predict the probability of a change in the pacing capture threshold (PCT) due to lead electrode heating associated with MRI. The effects of the MRI were numerically evaluated over approximately 2.4 million unique cases (i.e., equal to 19 body models * 9 positions in the transmit RF coil * 7 transmit RF coils * 2 electric field polarizations * 1,000 lead routes). At that time, comprehensive international standards or guidelines that the device manufacturers could adopt and follow to demonstrate the safety of active implants were unavailable, so that the first MR Conditional devices were essentially approved based on the evidence that each manufacturer produced following its own methodology.

Presently, what facilitated getting to the current state of MR Conditional devices today is a joint effort that started in 2006 across the MRI safety community, including representatives from device manufacturers, MR system manufacturers, and regulatory bodies. Experts in each area formed a Joint Working Group that participated in various technical venues helping to shape and update multiple standards. A major outcome of this effort was the publication of an international Technical Specification (TS), from the International Organization for Standardization (ISO), ISO/TS 10974:2018 (123), documenting guidelines on the assessment of MRI safety for patients with active implantable medical devices (AIMDs). The first version of this TS was published in 2012 and the second, updated version was published in 2018. The work is ongoing, and the group is updating and transitioning the TS into an international standard, with expected publication in 2021 or 2022.

The ISO/TS 10974:2018, entitled “Requirements for the safety of magnetic resonance imaging for patients with an active implanted medical device”, is today the only international technical specification that provides tests intended to be carried out on samples of a device to characterize interactions with the electromagnetic fields associated with an MR system. In particular, the technical specification is applicable to implanted parts of active implanted medical devices intended to be used in patients who might undergo an MRI examination using 1.5 Tesla, cylindrical bore, whole-body MR scanners for imaging hydrogen protons (i.e., the most widely used type of MR system in the world). Although, no requirements contained in the TS construe or imply any burden or obligation on the part of MR system manufacturers, it can be used to demonstrate device operation according to its MR Conditional labeling.

640 The Role of Numerical Modeling and Simulations

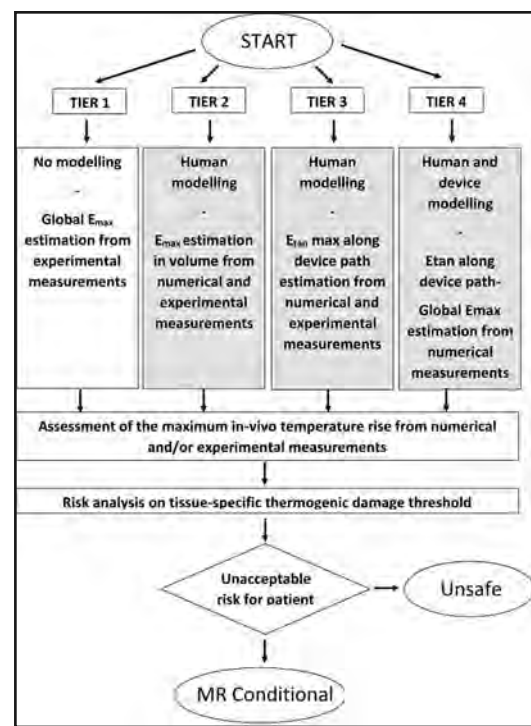
The requirements addressed in the TS were derived from seven known or foreseeable potential hazards to patients with an active implanted medical device undergoing an MRI examination. These general hazards give rise to specific test requirements as shown in **Table 2**. Evaluation of an AIMD for these hazards involves some combination of testing and modeling. In particular, modeling may be employed to determine appropriate test signal voltage levels or to estimate tissue heating.

In order to guarantee the protection from harm to the patient caused by RF energy-induced heating, the TS outlines a procedure that comprises as the first step the assessment of the energy deposition around the AIMD. To this aim, a four-tiered testing approach is described (**Figure 6**). Tier 1 is the most conservative and computationally simple and requires no additional electromagnetic modeling: the maximum energy deposition is assessed through experimental measurements, by exposing the AIMD inside a physical model of the human body to worst-case electromagnetic field levels, according to what specified in the TS. Tiers 2 and 3 provide successively less overestimation of test field magnitudes, justified by electromagnetic computational analysis. According to Tier 2, modeling is used to determine the incident field for testing the AIMD over any averaged 10 g tissue for the anatom-

Table 2. Potential patient hazards and corresponding test requirements, as described in ISO/TS 10974:2018 (123).

General Hazard to the Implant	Test Requirement	ISO/TS 10974:2018 Clause
Heat	RF field-induced heating	10
	Gradient magnetic field-induced heating	11
Vibration	Gradient magnetic field-induced vibration	12
Force	Static magnetic field-induced force	13
Torque	Static magnetic field-induced torque	14
Extrinsic electric potential	Gradient field-induced lead voltage	16
Rectification	RF field-induced rectified lead voltage	17
Malfunction	Static magnetic field-induced device malfunction	18
	RF field-induced device malfunction	19
	Gradient magnetic field-induced device malfunction (see note)	20
NOTE: Device malfunction due to eddy current heating of internal components is covered in Clause 11. Device malfunction due to vibration of internal components is covered in Clause 12.		

Figure 6. Four-tiered testing approach described in ISO/TS 10974:2018 to assess the protection from harm to the patient caused by RF field-induced heating (123).



ically relevant implant locations. Then, the RF power deposition is calculated by exposing the AIMD experimentally such field levels.

In Tier 3, the model of human body is used to determine the incident field in terms of the tangential electric field (i.e., magnitude and phase) and magnetic field, averaged over any 20 mm of anatomically relevant elongated AIMD path, for anatomically relevant implant locations. From the tangential electric field distribution, the deposited power can be assessed by experimental measurements or numerical analysis. In particular, the transfer function concept can be adopted, as described in the previous section.

Tier 4 requires the development of an electromagnetic model (i.e., full-wave or lumped element) of the AIMD being evaluated, placed in the anatomically relevant implant locations inside the human body model. The full electromagnetic model provides direct access to the evaluation of the deposited power in the human model around the implant, and it is associated with the least overestimation of test fields but requires the most stringent electromagnetic computational analysis.

Thus, Tier 2 through Tier 4 require electromagnetic simulation results using numerical human body models to identify the electric and magnetic field magnitudes used in the *in vitro* phantom test procedure. The TS provides a general overview of the requirements for the development, the assessment, and the validation of the numerical models. In particular, it is highlighted how the RF excitation of the AIMD is proportional to the B_1 field generated by the MR system's transmit RF coil and the relevant parameters that necessitates careful evaluation in the transformation of the B_1 field to the induced fields, as follows:

642 The Role of Numerical Modeling and Simulations

- RF frequency;
- body habitus or external anatomy;
- internal anatomy;
- location of the implant;
- design of the transmitting RF coil;
- position in the birdcage coil with respect to the isocenter of the MR scanner; and
- body posture in the RF coil.

As for the assessment procedure, the TS identifies three steps to be followed in order to obtain from the electromagnetic simulations conservative *in vitro* test conditions:

- (1) Identify the patient population and divide it into subgroups with respect to anatomical properties such as height, BMI, age, etc. and choose the 95th percentile of the patient population for each relevant property.
- (2) Compute the incident field distributions as defined in the applied tier and determine the 95th percentile incident field value for each subgroup in any of the clinically relevant postures and positions with respect to the isocenter of the MR system for the specified relevant transmitting RF coil designs.
- (3) Determine the largest 95th percentile incident field of all subgroups and RF coil designs for use as the incident field amplitude.

Validated electromagnetic simulation packages and human models must be used and an uncertainty budget of the incident field assessment is required and must be documented. In the uncertainty analysis, at least the following elements must be taken into consideration:

- transmitting RF coil design (including variations, for example, polarization, etc.);
- inner and outer anatomy (BMI, size, tissue distribution, dielectric, and thermal tissue parameters);
- position and posture in the birdcage coil (position in the birdcage coil with respect to the MR scanner's isocenter, body posture in the RF coil); and
- AIMD pathways in anatomy (i.e., the geometrical distribution of the AIMD's location inside the body).

Tier 3 and Tier 4 require (or may require for Tier 3) modeling the response of the AIMD to an incident electromagnetic field. The TS provides a possible *in vitro* approach that may be used to validate the AIMD model. The following steps are suggested:

- (1) Create a numerical model (e.g., full model or lumped element model) of the AIMD configuration to be tested that represents all of its relevant RF field characteristics and conduct a comprehensive uncertainty analysis for the AIMD model by a robust analysis (e.g., by Monte Carlo analysis).
- (2) Evaluate multiple conditions including high and low conductivity medium (if applicable), which provide differences in the maximum energy depositions larger than the relative uncertainty of the assessment techniques and that represent the AIMD's major electromagnetic properties. The test conditions shall be sufficiently large to validate the model prediction over the range of *in vivo* field conditions, one of which shall be the resonant

length. If no differences are larger than the uncertainty of the assessment techniques, then choose the worst cases with respect to performance.

- (3) Experimentally test the AIMD for all of the above test conditions.
- (4) Determine the relative differences of experimental and numerical assessments for each test condition.

If the relative differences between simulations and measurements for each of the test cases are within the combined relative uncertainties of measurement and simulation, the AIMD model can be considered validated and the combined relative uncertainties should be considered as the uncertainty of the AIMD model.

After completing the assessment of the RF energy deposition around the AIMD, the second step for the evaluation of the possible harm to the patient caused by RF field-induced heating is the assessment of the maximum *in vivo* temperature rise. According to the tier adopted, this can be achieved by performing the thermal modeling of the energy deposition into a temperature distribution or by performing experimental measurements. If numerical analysis is adopted, an uncertainty assessment of the thermal modeling must be performed and then combined to the uncertainty of the electromagnetic modeling to obtain the overall uncertainty.

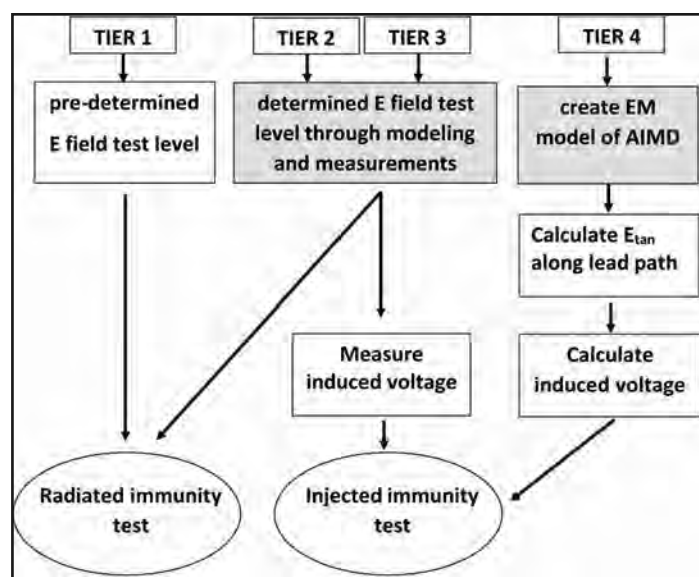
It should be noted that the TS does not provide tissue-specific thermogenic damage threshold values or guidance on how to determine specific risk factors for the determined temperature rise, which would inform the third and final step in a complete assessment. This final step is demanded to the risk analysis performed by the manufacturer.

A similar four-tiered approach is also applied to demonstrate the protection from harm to the patient caused by RF field-induced malfunction. The RF fields associated with the MR system could have certain effects on the AIMD such as, but not limited to, a failure to deliver the intended therapy, re-programming the device, resetting the device, and/or causing permanent damage to the device. These effects are caused by the unwanted induction of voltage on the leads or directly on internal circuits if RF fields penetrate the device's enclosure. The TS describes a series of functional tests that shall be performed, during which the device behavior and performance shall be monitored for proper functionality in accordance with the device's MR Conditional labeling. Either radiated or injected immunity tests are used, and the four-tiered approach is used to determine the field/signal levels to be adopted during the tests. An overview of the four-tiered testing approach is presented in **Figure 7**.

Beginning with Tier 1, each tier describes a progressively more rigorous analytic method for determining the electric field induced in the body by the B_1 field. The electric field is either used directly for radiated immunity testing or for determining injected voltage test levels. Although no electromagnetic modeling or computational analysis is required for Tier 1 because it uses pre-determined electric field levels, this tier utilizes the most conservative (highest) electric field test values. Tier 2 and Tier 3 require an electromagnetic computational analysis using numerical human body models. Tier 4 requires the most rigorous electromagnetic computational analysis and the development of AIMD models but has the potential to predict the lowest *in vivo* electric field and, hence, the lowest injected voltage test levels.

644 The Role of Numerical Modeling and Simulations

Figure 7. Four-tiered testing approach described in the ISO/TS 10974:2018 to demonstrate the protection from harm to the patient caused by RF field-induced malfunction (123).



Different from the approach adopted for the evaluation of the hazards caused by RF field-induced heating, the tiers are now used to calculate electric field and induced voltage exposure levels for assessing device behavior. The choice of tier requires, at a minimum, consideration of device type, implant location, lead configuration and orientation, immunity to radiated fields and signal levels, and the availability of test equipment, among other factors.

The more susceptible the device is, the higher the tier (i.e., four is higher than one) will be required, in all likelihood. The choice of tier can also influence the choice of test method, that is, radiated versus injected. For example, lower tiers, in particular Tier 1, will have electric field values (e.g., hundreds or thousands of V/m) that make radiated testing impractical. While Tier 4 is only applicable to the injected method since the intermediate analytic electric field values cannot be used for radiated testing. Injected testing is recommended in most cases, not only because of repeatability, but because the electric field can be scaled downwards to a practical level, and then the induced voltage can be measured at the ports of the device (e.g., the proximal end of a lead), and then the measured voltage scaled back up accordingly to use for the injected test level. The E-field cannot be scaled for radiated testing. The radiated method is also not appropriate for testing devices with attached leads. The *in vivo* induced electric fields associated with an MR system are non-uniform, and although the tiered approach described in this clause have steps in the method for multiplying the measured induced voltage with a resonant length weighting factor (also called the phase factor) to account for non-uniform fields, this factor cannot be applied to a uniform radiated electric field test.

Numerical modeling is also suggested for the test that the TS prescribes to evaluate the protection from harm to the patient caused by gradient magnetic field-induced malfunction. In a similar way to the case of RF field-induced malfunction, functional testing is based on tiered test levels and uses radiated and injected immunity tests. The radiated test shall be applied to all devices (with or without conductive leads) unless it can be shown that the de-

vice enclosure is completely shielded from electromagnetic fields, such that device behavior and functionality is not influenced. The test is normally performed without patient leads. The injected test shall be applied to all devices with conductive patient electrodes, leads, or other conductive elements such as external antennas or leadless electrode terminals.

Three tiers can be chosen, considering the device type, implant location, lead configuration and orientation, and immunity to injected signal levels, among other factors. Tier 1 is based on worst-case values for the rate of change of the incident magnetic field, dB/dt , on the surface of two different defined volumes. Test levels are derived from look-up tables, as a function of the implant lead length and location. This method results in very conservative test values without computational or modeling requirements. Less conservative results can be obtained with Tier 2 and 3. Tier 2 requires either electromagnetic computational analysis of the maximum incident magnetic field over the specific AIMD lead loop area or device area, or computational analysis of the maximum specific AIMD lead loop area. Tier 3 requires the most rigorous electromagnetic computational analysis, computing the induced tangential electric field over the lead path, and has the potential to predict the lowest injected voltage test levels.

In conclusion, the technical standard ISO/TS 10974:2018, that is today the only international technical specification that provides a consistent testing methodology for implant manufacturers on how to assess the potential risks for implanted medical devices arising from an MRI examination, explicitly recognizes the importance of numerical modeling. For many aspects, although pure experimental methodologies are allowed as well, the results obtained adopting a complete electromagnetic computational analysis are always less conservative than other approaches. Besides the primary purpose of the document, that is to provide a standard test methodology for manufacturers that want to demonstrate the MR Conditional status of their devices, the TS represents an extremely useful source of information. It can be used as guidance to properly account for all the crucial aspects (e.g., model validation, uncertainty analysis, etc.) that must be considered during the numerical modeling of the interactions between the MR system and an implanted device.

TOWARDS A PERSONALIZED TOOL FOR THE RISK ASSESSMENT OF PATIENTS WITH IMPLANTED LEADS UNDERGOING MRI

Starting from the late 1990s, the effort to make implanted devices less likely to cause harm to patients undergoing MRI examinations has resulted in the development of MR Conditional AIMDs including cardiac pacemakers, implantable cardioverter defibrillators, and various neurostimulation systems. Today, more than 10 years have passed since the first cardiac pacemaker received MR Conditional labeling, first in Europe and then in the U.S., extending to implanted patients the undisputed diagnostic imaging benefits of MRI. Most major cardiac device manufacturers (e.g., Abbott/St. Jude Medical, Biotronik, Boston Scientific, LivaNova, and Medtronic) now have MR Conditional products that include cardiac pacemakers, implantable cardioverter defibrillators, and loop records with labeling that permits MRI examinations to be performed in patients at 1.5 Tesla and, in some, cases even at 3 Tesla. The same scenario has occurred for manufacturers of neuromodulation systems, which have similar components, namely implanted pulse generators and leads (147-149). Accordingly, there are now a wide range of MR Conditional AIMDs used for neuromodu-

646 The Role of Numerical Modeling and Simulations

lation therapies that include deep brain stimulation systems, spinal cord stimulation systems, vagus nerve stimulation systems, and others. Reports and studies conducted in the following years on the performances of these AIMDs have not revealed any MRI-related complications or MRI-attributed device damage or malfunction (150-159). Thus, the enhancements in the device technology and the improved understanding of the interactions between device components and the electromagnetic fields generated by MR systems have finally allow more patients to receive the benefits of both these technologies. Numerical modeling and simulations played a crucial role for these achievements and, given the constant growth of the computational capability, which today can be easily accessed, will continue to be of fundamental importance for the future steps that still have to be made in this field.

The RF energy-induced heating is still the major concern for MRI simulations that are performed to evaluate implanted leads. To assess the RF field-related safety of an AIMD for all possible clinical scenarios, the incident electromagnetic field is typically characterized using the incident tangential electric field along the AIMD lead pathway (160). As already explained in the previous sections, the assumption that the RF field responses of an AIMD depends only on the tangential electric field (E_{tan}) allows splitting the RF-induced energy heating evaluation into two less complex sub-tasks: (1) analysis of human exposure to electromagnetic field generated by MRI RF-transmit coils, that is, calculation of a set of clinically relevant E_{tan} , and (2) estimation of the RF responses of an AIMD for this set of clinically relevant E_{tan} .

Experimental or numerical assessment of the RF field responses to the set of clinically relevant E_{tan} is still a sophisticated task, because: (1) the assessment must be performed in different inhomogeneous tissue environments that correspond to the AIMD lead surrounding tissues in a human, and (2) generating a set of clinically relevant E_{tan} requires the construction of a multichannel RF transmitter with properties that are difficult to implement. The lead TF can be used to obtain the analytical lead electromagnetic model, by which it is possible to evaluate an RF field response for an arbitrary E_{tan} . Different approaches such as piecewise excitation (161), reciprocity (133), transmission line model (162), and base function (163) can be adopted to assess the TF.

Even if the TF can be obtained for an inhomogeneous media, different AIMD lead pathways in the patient population result in a large variety of multi-tissue lead environments, leading to a quite complex assessment. To avoid this, ISO/TS10974:2018 Tier 3 (122) suggests using a homogeneous medium with electrical properties close to the tissue predominantly in contact with the AIMD lead. If the AIMD lead pathway spans more than 10% of its cumulative physical length in different tissues, the TF should also be evaluated in different media with appropriate electrical properties. Numerical simulation and realistic numerical models of the human tissues are unquestionably key players that can be utilized to achieve this goal.

Following the modern paradigm of medicine of the “four P” (predictive, preventive, personalized and participatory), the main aim for future years is to transform the generic model of interactions between the MR system and the patient implanted with a medical device into a patient-specific model, able to account for the contributions of realistic anatomical structures specific to each individual. High-resolution diagnostic images, such as those

obtainable with MRI or CT, have allowed the means of representing at a high-resolution the different anatomical districts of the human body in the form of discrete elements suitable to be imported into the most common simulation environment.

An extremely efficient semi-automatic processing pipeline to generate individualized surface-based models of the human body from the MR images of individual subjects has been recently described by Kalloch, et al. (164). This comprehensive workflow covers image acquisition, atlas-based segmentation of relevant structures, generation of segmentation masks, and surface mesh generation of the single, external boundary of each structure of interest. Similar processes can be adopted to customize the simulation on the specific positioning/lead path of the device inside the patient. High-resolution images can be used to identify and reproduce in the numerical model the patient-specific configuration of the implanted device, and the body tissues in direct contact with the device. This information, combined with the electromagnetic model of the lead, has to be considered in the development of a personalized tool for the risk assessment of patients with implanted lead undergoing MRI. It has been demonstrated, indeed, that the transfer function of a lead can vary as a function of its position inside the body (165) and consequently, for the same lead, the expected interaction with the MR system can be different even for the same value of E-field exposure (i.e., the same E_{tan}).

The role of the manufacturer of the medical device becomes critical, since in most cases, the electromagnetic model of the lead and its transfer function is known only to the manufacturer. Hopefully, this information can be explicated and made available to grant the proper implementation of the numerical analysis.

A patient-specific model able to account for the anatomical peculiarities of different individuals (e.g., gender, age, physical structure) and for the structural characteristic of the implanted device under evaluation could become an excellent tool to be used for design, forecasting, and optimization purposes. Simulations can be used as a virtual prototyping tool, to evaluate the performances of new design and solutions. It has obvious advantages in economic terms, including, before producing a real prototype, simulations can be carried out to better understand which of the possible solutions are worth investing more time and effort in.

Numerical models can also become a valuable tool to support the physician in his decisions and in the risk versus benefits evaluations (e.g., whether or not to perform an MRI examination in a patient with a non-MR Conditional device). That is, “try” in the virtual world of simulations what can be expected in real-life and, in case, test the different solutions that could be adopted, to choose the best one for the specific patient. Once the best solution is chosen, numerical simulation could still be used for optimization purposes, to minimize as much as possible the risks for the patient with an AIMD.

In order to adequately meet the objectives listed above, future studies and further efforts should be spent to increase the multi-physical and multi-scalar properties of the numerical model. Besides electromagnetic and thermal analysis, the overall model could also benefit from the integration of mechanical and biological aspects. As an example, electromagnetic and thermal models can be integrated with biological models of cellular dynamics capable of characterizing, on a microscopic scale, the effects of exposure to electromagnetic fields,

648 The Role of Numerical Modeling and Simulations

analyzing not only the interactions deriving from induced heating, but also evaluating any non-linear effects at the cellular level.

REFERENCES

1. Pennes HH. Analysis of tissue and arterial blood temperatures in the resting human forearm. *J Appl Physiol* 1948;9:3-122.
2. Moshage W, Achenbach S, Bolz A, et al. A non-magnetic, MR-compatible pacing catheter for clinical application in magnetocardiography. *Biomed Tech (Berl)* 1990;35:162-3.
3. Inbar S, Larson J, Burt T, Mafee M, Ezri MD. Case report: Nuclear magnetic resonance imaging in a patient with a pacemaker. *Am J Med Sci* 1993;305:174-5.
4. Lauck G, von Smekal A, Wolke S, et al. Effects of nuclear magnetic resonance imaging on cardiac pacemakers. *Pacing Clin Electrophysiol* 1995;18:1549-55.
5. Gimbel JR, Johnson D, Levine PA, Wilkoff BL. Safe performance of magnetic resonance imaging on five patients with permanent cardiac pacemakers. *Pacing Clin Electrophysiol*. 1996;19:913-9.
6. Hunyadi S Jr, Werning JW, Lewin JS, Maniglia AJ. Effect of magnetic resonance imaging on a new electromagnetic implanted middle ear hearing device. *Am J Otol* 1997;18:328-31.
7. Hofman MB. MRI-compatible cardiac pacing catheter. *J Magn Reson Imaging* 1997;7:612.
8. Achenbach S, Moshage W, Diem B, et al. Effects of magnetic resonance imaging on cardiac pacemakers and electrodes. *Am Heart J* 1997;134:467-73.
9. Kalafala AK. A design approach for actively shielded magnetic resonance imaging magnets. *IEEE Trans Magn* 1990;26:1181-1188.
10. Thompson MR, Brown RW, Srivastava VC. An inverse approach to the design of MRI main magnets. *Magn IEEE Trans* 1994;30:108-112.
11. Crozier S, Doddrell DM. Compact MRI magnet design by stochastic optimization. *J Magn Reson* 1997;127:233-237.
12. Zhao H, Crozier S, Doddrell DM. A hybrid, inverse approach to the design of magnetic resonance imaging magnets. *Med Phys* 2000;27:599-607.
13. Shaw NR, Ansorge RE. Genetic algorithms for MRI magnet design. *Appl Supercond IEEE Trans* 2002;12:733-736.
14. Cheng YN, Eagan TP, Brown RW, Shvartsman SM, Thompson MR. Design of actively shielded main magnets: An improved functional method. *Magn Reson Mater Phys, Biol Med* 2003;16:57-67.
15. Wong EC, Jesmanowicz A, Hyde JS. Coil optimization for MRI by conjugate gradient descent. *Magn Reson Med* 1991;21:39-48.
16. Crozier S, Doddrell DM. Gradient-coil design by simulated annealing. *J Magn Reson, Ser A* 1993;103:354-357.
17. Crozier S, Forbes LK, Doddrell DM. The design of transverse gradient coils of restricted length by simulated annealing. *J Magn Reson, Ser A* 1994;107:126-128.
18. Andrew ER, Szczesniak E. Low inductance transverse gradient system of restricted length. *Magn Reson Imaging* 1995;13:607-613.
19. Crozier S, Doddrell DM. A design methodology for short, whole-body, shielded gradient coils for MRI. *Magn Reson Imaging* 1995;13:615-620.
20. Ibrahim TS, Lee R, Baertlein BA, et al. Effect of RF coil excitation on field inhomogeneity at ultra high fields: A field optimized TEM resonator. *Magn Reson Imaging* 2001;19:1339-1347.
21. Vaughan JT, Garwood M, Collins CM, et al. 7T vs. 4T: RF power, homogeneity, and signal-to-noise comparison in head images. *Magn Reson Med* 2001;46:24-30.

22. Collins CM, Liu W, Swift BJ, Smith MB. Combination of optimized transmit arrays and some receive array reconstruction methods can yield homogeneous images at very high frequencies. *Magn Reson Med* 2005;54:1327–1332.
23. Mao W, Smith MB, Collins CM. Exploring the limits of RF shimming for high-field MRI of the human head. *Magn Reson Med* 2006;56:918–922.
24. Abraham R, Ibrahim TS. Proposed radiofrequency phased-array excitation scheme for homogenous and localized 7-Tesla whole-body imaging based on full-wave numerical simulations. *Magn Reson Med* 2007;57:235–242.
25. Van den Berg CA, Van den Bergen B, Kroeze H, Bartels LW, Lagendijk JJ. Simultaneous B_1^+ homogenisation and SAR hotspot suppression by a phased array MR transmit coil. Proceedings of the International Society for Magnetic Resonance in Medicine 2006;14.
26. Mueller A, Weisser-Thomas J, Naehe PC, et al. Clinical CMR at 3.0 Tesla using parallel RF transmission with patient-adaptive B_1 shimming: Initial experience. *J Cardiovasc Magn Reson* 2010;12:1–2.
27. Roemer PB, Edelstein WA, Hayes CE, Souza SP, Mueller OM. The NMR phased array. *Magn Reson Med* 1990;16:192–225.
28. Wright SM, Wald LL. Theory and application of array coils in MR spectroscopy. *NMR Biomed* 1997;10:394–410.
29. Pruessmann KP, Weiger M, Scheidegger MB, Boesiger P. SENSE: Sensitivity encoding for fast MRI. *Magn Reson Med* 1999;42:952–962.
30. Bulumulla S, Marinelli L, Hardy CJ. MRI-phased array evaluation using a human body model. Concepts Magn Reson, Part B: Magn Reson Eng 2010;37:20–28.
31. Ocali O, Atalar E. Ultimate intrinsic signal-to-noise ratio in MRI. *Magn Reson Med* 1998;39:462–473.
32. Ohliger MA, Grant AK, Sodickson DK. Ultimate intrinsic signal-to-noise ratio for parallel MRI: Electromagnetic field considerations. *Magn Reson Med* 2003;50:1018–1030.
33. Wiesinger F, Boesiger P, Pruessmann KP. Electrodynamics and ultimate SNR in parallel MR imaging. *Magn Reson Med* 2004;52:376–390.
34. Antunes A, Glover PM, Li Y, Mian OS, Day BL. Magnetic field effects on the vestibular system: Calculation of the pressure on the cupula due to ionic current-induced Lorentz force. *Phys Med Biol* 2012;57:4477.
35. Crozier S, Trakic A, Wang H, Liu F. Numerical study of currents in workers induced by body-motion around high-ultrahigh field MRI magnets. *J Magn Reson Imaging* 2007;26:1261–1277.
36. Wang H, Trakic A, Liu F and Crozier S. Numerical field evaluation of healthcare workers when bending towards high-field MRI magnets. *Magn Reson Med* 2008;59:410–422.
37. So PP, Stuchly MA, Nyenhuis JA. Peripheral nerve stimulation by gradient switching fields in magnetic resonance imaging. *Biomed Eng IEEE Trans* 2004;51:1907–1914.
38. Mao W, Chronik BA, Feldman RE, Smith MB, Collins CM. Consideration of magnetically-induced and conservative electric fields within a loaded gradient coil. *Magn Reson Med* 2006;55:1424–1432.
39. Bencsik M, Bowtell R, Bowley R. Electric fields induced in the human body by time-varying magnetic field gradients in MRI: Numerical calculations and correlation analysis. *Phys Med Biol* 2007;52:2337–2353.
40. Chen J, Feng Z, Jin J-M. Numerical simulation of SAR and B_1 field inhomogeneity of shielded RF coils loaded with the human head. *IEEE Trans Biomed Eng* 1998;45:650–659.
41. Collins CM, Li S, Smith MB. SAR and B_1 field distributions in a heterogeneous human head model within a birdcage coil. *Magn Reson Med* 1998;40:847–856.
42. Collins CM, Smith MB. Calculations of B_1 distribution, SNR, and SAR for a surface coil adjacent to an anatomically-accurate human body model. *Magn Reson Med* 2001;45:692–699.

650 The Role of Numerical Modeling and Simulations

43. Liu W, Collins CM, Smith MB. Calculations of B_1 distribution, specific energy absorption rate, and intrinsic signal-to-noise ratio for a body-size birdcage coil loaded with different human subjects at 64 and 128 MHz. *Appl Magn Reson* 2005;29:5–18.
44. Murbach M, Cabot E, Neufeld E, et al. Local SAR enhancements in anatomically correct children and adult models as a function of position within 1.5 T MR body coil. *Prog Biophys Mol Biol* 2011;107:428–433.
45. Yeo DT, Wang Z, Loew W, Vogel MW, Hancu I. Local specific absorption rate in high-pass birdcage and transverse electromagnetic body coils for multiple human body models in clinical landmark positions at 3T. *J Magn Reson Imaging* 2011;33:1209–1217.
46. Murbach M, Neufeld E, Kainz W, Pruessmann KP, Kuster N. Whole-body and local RF absorption in human models as a function of anatomy and position within 1.5 T MR body coil. *Magn Reson Med* 2014;71:839–845.
47. Pediaditis M, Leitgeb N, Cech R. RF-EMF exposure of fetus and mother during magnetic resonance imaging. *Phys Med Biol* 2008;53:7187–7195.
48. Hand JW, Li Y, Hajnal JV. Numerical study of RF exposure and the resulting temperature rise in the foetus during a magnetic resonance procedure. *Phys Med Biol* 2010;55:913–930.
49. Malik SJ, Begiri A, Price AN, et al. Specific absorption rate in neonates undergoing magnetic resonance procedures at 1.5 T and 3 T. *NMR Biomed* 2015;28:344–352.
50. Neufeld E, Gosselin MC, Murbach M, et al. Analysis of the local worst-case SAR exposure caused by an MRI multi-transmit body coil in anatomical models of the human body. *Phys Med Biol* 2011;56:4649–4659.
51. Thiele JP, Golombeck MA, Dössel O. Thermal heating of human tissue induced by electromagnetic fields of magnetic resonance imaging. *Biomed Tech* 2002;47:743–6.
52. Nordbeck P, Fidler F, Weiss I, et al. Spatial distribution of RF-induced E-fields and implant heating in MRI. *Magn Reson Med* 2008;60:312–9.
53. Mattei E, Calcagnini G, Censi F, Triventi M, Bartolini P. Numerical model for estimating RF-induced heating on a pacemaker implant during MRI: Experimental validation. *IEEE Trans Biomed Eng* 2010;57:2045–52.
54. Lucano E, Liberti M, Mendoza GG, et al. Assessing the electromagnetic fields generated by a radiofrequency MRI body coil at 64 MHz: Defeaturing versus accuracy. *IEEE Trans Biomed Eng* 2016;63:1591–1601.
55. Ibrahim TS, Lee R, Baertlein BA, Robitaille PM. B_1 field homogeneity and SAR calculations for the birdcage coil. *Phys Med Biol* 2001;46:609–19.
56. Hand JW, Li Y, Thomas EL, Rutherford MA, Hajnal JV. Prediction of specific absorption rate in mother and fetus associated with MRI examinations during pregnancy. *Magn Reson Med* 2006;55:883–93.
57. Ibrahim TS, Tang L, Kangarlu A, Abraham R. Electromagnetic and modeling analyses of an implanted device at 3 and 7 Tesla. *J Magn Reson Imaging* 2007;26:1362–7.
58. Nitz WR, Oppelt A, Renz W, et al. On the heating of linear conductive structures as guide wires and catheters in interventional MRI. *J Magn Reson Imaging* 2001;13:105–14.
59. Armenean C, Perrin E, Armenean M, et al. RF-induced temperature elevation along metallic wires in clinical magnetic resonance imaging: influence of diameter and length. *Magn Reson Med* 2004;52:1200–6.
60. Stuchly MA, Abrishamkar H, Strydom ML. Numerical evaluation of radio frequency power deposition in human models during MRI. *Conf Proc IEEE Eng Med Biol Soc* 2006;2006:272–5.
61. Pisa S, Calcagnini G, Cavagnaro M, et al. SAR temperature elevations in pacemaker holders exposed to electromagnetic fields produced by MRI apparatus. *IEEE MTT-S International Microwave Symposium Digest* 2006:1754–1757.

MRI Bioeffects, Safety, and Patient Management 651

62. Nordbeck P, Fidler F, Friedrich MT, et al. Reducing RF-related heating of cardiac pacemaker leads in MRI: Implementation and experimental verification of practical design changes. *Magn Reson Med* 2012;68:1963-72.
63. Mattei E, Triventi M, Calcagnini G, et al. Temperature and SAR measurement errors in the evaluation of metallic linear structures heating during MRI using fluoroptic probes. *Phys Med Biol* 2007;52:1633-46.
64. Calcagnini G, Triventi M, Censi F, et al. *In vitro* investigation of pacemaker lead heating induced by magnetic resonance imaging: Role of implant geometry. *J Magn Reson Imaging* 2008;28:879-86.
65. Mattei E, Triventi M, Calcagnini G, et al. Complexity of MRI induced heating on metallic leads: experimental measurements of 374 configurations. *Biomed Eng Online* 2008;7:11.
66. Mattei E, Calcagnini G, Censi F, Triventi M, Bartolini P. Role of the lead structure in MRI-induced heating: *In vitro* measurements on 30 commercial pacemaker/defibrillator leads. *Magn Reson Med* 2012;67:925-35.
67. Wilkoff BL, Albert T, Lazebnik M, et al. Safe magnetic resonance imaging scanning of patients with cardiac rhythm devices: A role for computer modeling. *Heart Rhythm* 2013;10:1815-21.
68. Collins CM. Numerical field calculations considering the human subject for engineering and safety assurance in MRI. *NMR Biomed* 2009;22:919-26.
69. Yee K. Numerical solution of initial boundary value problems involving Maxwell's equations in isotropic media. *IEEE Transactions on Antennas and Propagation* 1966;14:302-7.
70. Ibrahim TS. Modeling the electromagnetic wave interaction with the body and SAR. International Society for Magnetic Resonance in Medicine, Weekend Educational Course Syllabus, 2006.
71. Taflove A, Oskooi A, Johnson SG. Advances in FDTD computational electrodynamics: Photonics and nanotechnology. Artech House, Inc., Boston, 2013.
72. Liu Q. An FDTD algorithm with perfectly matched layers for conductive media. *Microwave and Optical Technology Letters* 1997;14:134-137.
73. Berenger JP. A perfectly matched layer for the absorption of electromagnetic waves. *Journal of computational physics*. 1994;114:185-200.
74. Cangellaris AC, Wright DB. Analysis of the numerical error caused by the stairstepped approximation of a conducting boundary in FDTD simulations of electromagnetic phenomena. *IEEE Transactions on Antennas and Propagation*. 1991;39:1518-1525.
75. Holland R. Pitfalls of staircase meshing. *IEEE Transactions on Electromagnetic Compatibility* 1993;35:434-439.
76. Jurgens T, Taflove A, Umashankar K, MOORE T. Finite-difference time domain modeling of curved surfaces. *IEEE Transactions on Antennas and Propagation* 1992;40:357-366.
77. Holland R. Finite-difference solution of Maxwell's equations in generalized nonorthogonal coordinates. *IEEE Transactions on Nuclear Science* 1983;6:4589-4591.
78. Monorchio A, Bretones AR, Mittra R, Manara G, Martín RG. A hybrid time-domain technique that combines the finite element, finite difference and method of moment techniques to solve complex electromagnetic problems. *IEEE Transactions on Antennas and Propagation* 2004;52:2666-2674.
79. Li BK, Ku B, Hui HT, Crozier S. A new approach for magnetic resonance RF head coil design. *Conf Proc IEEE Eng Med Biol Soc* 2005;2005:5100-3.
80. Bretones AR, Mittra R, Martín. A hybrid technique combining the method of moments in the time domain and FDTD. *IEEE Microwave and Guided Wave Letters* 1998;8:281-283.
81. White MJ, Iskander MF, Huang Z. Development of a multigrid FDTD code for three-dimensional applications. *IEEE Transactions on Antennas and Propagation* 1997;45:1512-1517.
82. Steeds MW, Broschat SL, Schneider JB. A comparison of two conformal methods for FDTD modeling. *IEEE Transactions on Electromagnetic Compatibility* 1996;38:181-187.

652 The Role of Numerical Modeling and Simulations

83. Cloos MA, Luong M, Ferrand G, et al. Local SAR reduction in parallel excitation based on channel-dependent Tikhonov parameters. *J Magn Reson Imaging* 2010;32:1209–1216.
84. Liu J, Zhu S, Yao Y, Zhang Z, He B. Finite element modeling of human head from MRI. *Conf Proc IEEE Eng Med Biol Soc* 2005;2005:2539-2542.
85. Kozlov M, Kalloch B, Horner M, et al. Chapter 13: Patient-Specific RF Safety Assessment in MRI: Progress in Creating Surface-Based Human Head and Shoulder Models. In: *Brain and Human Body Modeling: Computational Human Modeling at EMBC 2018*. Cham (CH): Springer; 2019. pp. 245-282.
86. Li BK, Liu F, Crozier S. Focused, eight-element transceive phased array coil for parallel magnetic resonance imaging of the chest - theoretical considerations. *Magn Reson Med* 2005;53:1251-7.
87. Büchler P, Simon A, Burger J, et al. Safety of active implanted devices during MRI examinations: A finite element analysis of an implanted pump. *IEEE Trans Biomed Eng* 2007;54:726-733.
88. Xu XG, Eckerman KF. *Handbook of Anatomical Models for Radiation Dosimetry*. Series in Medical Physics and Biomedical Engineering. CRC Press: Boca Raton, FL; 2009.
89. Xu XG. An exponential growth of computational phantom research in radiation protection, imaging, and radiotherapy: A review of the fifty-year history. *Phys Med Biol* 2014;59, R233–R302.
90. International Commission on Radiation Protection, ICRP, 1975. Report of the Task Group on Reference Man. ICRP Publication 23. Pergamon Press, Oxford.
91. Fisher HLJ, Snyder WS. Distribution of dose delivered in the body size from a source of gamma rays distributed uniformly in an organ. ORNL-4168, Oak Ridge National Laboratory 1967:245-256.
92. Cristy M, Eckerman K. Specific absorbed fractions of energy at various ages from internal photon sources. VI. Newborn, ORNL/TM-8381, Oak Ridge National Laboratory 1987.
93. Petoussi-Henss N, Zankl M, Fill U, Regulla D. The GSF family of voxel phantoms. *Phys Med Bio* 2001;47:89-106.
94. Kramer R, Vieira J, Khouri H, Lima F, Fuelle D. All about max: A male adult voxel phantom for Monte Carlo calculations in radiation protection dosimetry. *Phys Med Bio* 2003;48:1239-1262.
95. Stabin M, Tagesson M, Thomas S, Ljungberg M, Strand SE. Radiation dosimetry in nuclear medicine. *Appl Radiat Isot* 1999;50:73–87.
96. Gibbs SJ, Pujol A Jr, Chen TS, Malcolm AW, James AE Jr. Patient risk from interproximal radiography. *Oral Surg Oral Med Oral Pathol* 1984;58:347-54.
97. Williams G, Zankl M, Abmayr W, Veit R, Drexler G. The calculation of dose from external photon exposures using reference and realistic human phantoms and Monte Carlo methods. *Phys Med Biol* 1986;31:449-52.
98. Dimbylow P. FDTD calculations of the whole-body averaged SAR in an anatomically realistic voxel model of the human body from 1 MHz to 1 GHz. *Phys Med Bio* 1997;42:479-490.
99. Kim CH, Jeong JH, Yeom YS. Recent advances in computational human phantom for Monte Carlo dose calculation. *Prog Nucl Sci Technol* 2012;3:7-10.
100. Christ A, Kainz W, Hahn EG, Honegger K, Zefferer M, et al. The Virtual Family—Development of surface-based anatomical models of two adults and two children for dosimetric simulations. *Phys Med Bio* 2010;55:N23–38.
101. Gosselin MC, Neufeld E, Moser H, et al. Development of a new generation of high resolution anatomical models for medical device evaluation: The virtual population 3.0. *Phys Med Bio* 2014;59:5287-5303.
102. Liu W, Collins CM, Smith MB. Calculations of B_1 distribution, specific energy absorption rate, and intrinsic signal-to-noise ratio for a body-size birdcage coil loaded with different human subjects at 64 and 128 MHz. *Appl Magn Reson* 2005;29:5-18.
103. Pavlicek W, Geisinger M, Castle L, et al. The effects of nuclear magnetic resonance on patients with cardiac pacemakers. *Radiology* 1983;147:149-153.
104. Fetter J, Aram G, Holmes DR, Gray JE, Hayes DL. The effects of nuclear magnetic resonance imagers on external and implanted pulse generators. *Pacing Clin Electrophysiol* 1984;7:720-727.

MRI Bioeffects, Safety, and Patient Management 653

105. Shellock FG. Reference Manual for Magnetic Resonance Safety, Implants, and Devices: 2020 Edition. Los Angeles, CA: Biomedical Research Publishing Group; 2020.
106. Luechinger R, Duru F, Scheidegger MB, et al. Force and torque effects of a 1.5-Tesla MR system on cardiac pacemakers and ICDs. *Pacing Clin Electrophysiol* 2001;24:199–205.
107. Shellock FG, Tkach JA, Ruggieri PM, Masaryk TJ, Cardiac pacemakers, ICDs, and loop recorder: evaluation of translational attraction using conventional (“long-bore”) and “short-bore” 1.5- and 3.0-Tesla MR systems. *J Cardiovasc Magn Reson* 2003;5:387–397.
108. Leifer M. Resonant modes of the birdcage coil. *J Magn Reson* 1997;60:51–60.
109. Vaughn JT. Radio frequency volume coils for imaging and spectroscopy. U.S. Patent 5,557,247, 1996.
110. Katscher U, Börnert P. Parallel RF transmission in MRI. *NMR in Biomedicine* 2006;19:393–400.
111. Glover G, Hayes CE, Pelc N, et al. Comparison of linear and circular polarization for magnetic resonance imaging. *J Magn Reson* 1985;64:255–270.
112. Helfer JL, Gray RW, MacDonald SG, Bibens TW. Can pacemakers, neurostimulators, leads, or guide wires be MRI safe? Technological concerns and possible resolutions. *Minim Invasive Ther Allied Technol* 2006;15:114–20.
113. Ho H. Safety of metallic implants in magnetic resonance Imaging. *J Magn Reson Imaging* 2001;14:472–7.
114. Vogel MH, Kleihorst RP. Large-scale simulations including a human-body model for MRI. 2007 IEEE/MTT-S International Microwave Symposium 2007:1010.
115. Li BK, Liu F, Crozier S. Focused, eight-element transceive phased array coil for parallel magnetic resonance imaging of the chest: Theoretical considerations. *Magn Reson Med* 2005;53:1251–1257.
116. Balac S, Benoit-Cattin H, Lamotte T, Odet C. Analytic solution to boundary integral computation of susceptibility induced magnetic field inhomogeneities. *Mathematical and Computer Modeling* 2004;39:437–55.
117. Balac S, Caloz G. Mathematical modeling and numerical simulation of magnetic susceptibility artifacts in magnetic resonance imaging. *Comput Methods Biomed Engin* 2000;3:335–49.
118. Konings MK, Bartels LW, Smits HF, Bakker CJ. Heating around intravascular guidewires by resonating RF waves. *J Magn Reson Imaging* 2000;12:79–85.
119. Yeung CJ, Karmarkar P, McVeigh ER. Minimizing RF heating of conducting wires in MRI. *Magn Reson Med* 2007;58:1028–34.
120. Ibrahim TS, Lee R, Baertlein BA, Yu Y, Robitaille PM. Computational analysis of the high pass birdcage resonator: Finite difference time domain simulations for high-field MRI. *Magn Reson Imaging* 2000;18:835–43.
121. Nöth U, Laufs H, Stoermer R, Deichmann R. Simultaneous electroencephalography-functional MRI at 3 T: An analysis of safety risks imposed by performing anatomical reference scans with the EEG equipment in place. *J Magn Reson Imaging* 2012;35:561–71.
122. American Society for Testing and Materials International, ASTM F2052-15, Standard Test Method for Measurement of Magnetically Induced Displacement Force on Medical Devices in the Magnetic Resonance Environment, 2015.
123. ISO/TS 10974:2018. Assessment of the safety of magnetic resonance imaging for patients with an active implanted medical device, 2018.
124. Kramer GH, Burns L, Noel L. The BRMD BOMAB phantom family. *Health Phys* 1991;61:895–902.
125. Graedel NN, Polimeni JR, Guerin B, et al. An anatomically realistic temperature phantom for radiofrequency heating measurements. *Magn Reson Med* 2015;73:442–50.
126. Kozlov M, Bazin PL, Möller HE, Weiskopf N. Influence of cerebrospinal fluid on specific absorption rate generated by 300 MHz MRI transmit array. Proceedings of 10th European Conference on Antennas and Propagation (EuCA), Davos, Switzerland: 2016; pp. 2341–2345.

654 The Role of Numerical Modeling and Simulations

127. Gabriel S, Lau RW, Gabriel C. The dielectric properties of biological tissues: II. Measurements in the frequency range 10 Hz to 20 GHz. *Phys Med Biol* 1996;41:2251-69.
128. Hasgall PA, Di Gennaro F, Baumgartner C, et al. IT'IS Database for thermal and electromagnetic parameters of biological tissues. Version 4.0, 2018. Available via itis.swiss/database.
129. Gray RW, Bibens WT, Shellock FG. Simple design changes to wires to substantially reduce MRI-induced heating at 1.5 T: Implications for implanted leads. *Magn Reson Imaging* 2005;23:887-91.
130. Bottomley PA, Kumar A, Edelstein WA, Allen JM, Karmarkar PV. Designing passive MRI-safe implanted conducting leads with electrodes. *Med Phys* 2010;37:3828-43.
131. Park SM, Kamondetdacha R, Nyenhuis JA. Calculation of MRI-induced heating of an implanted medical lead wire with an electric field transfer function. *J Magn Reson Imaging* 2007;26:1278-85.
132. Zastrow E, Capstick M, Cabot E, Kuster N. Piece-wise excitation system for the characterization of local RF-induced heating of AIMD during MR exposure. International Symposium on Electromagnetic Compatibility Tokyo: 2014:241-244.
133. Feng S, Qiang R, Kainz W, Chen J. A technique to evaluate MRI-induced electric fields at the ends of practical implanted lead. *IEEE Transactions on Microwave Theory and Techniques* 2015;63:305-313.
134. Missoffe A, Aissani S. Experimental setup for transfer function measurement to assess RF heating of medical leads in MRI: Validation in the case of a single wire. *Magn Reson Med* 2018;79:1766-1772.
135. Schwer LE. An overview of the PTC 60/V&V 10: Guide for verification and validation in computational solid mechanics. *Engineering with Computers* 2007;23:245-252.
136. Chen J, Feng Z, Jin JM. Numerical simulation of SAR and Si-field inhomogeneity of shielded RF coils loaded with the human head. *IEEE Trans Biomed Eng* 1998;45:650-650.
137. Bowtell R, Bowley RM. Analytic calculations of the E-fields induced by time-varying magnetic fields generated by cylindrical gradient coils. *Magn Reson Med* 2000;44:782-90.
138. Collins CM, Liu W, Wang J, et al. Temperature and SAR calculations for a human head within volume and surface coils at 64 and 300 MHz. *J Magn Reson Imaging* 2004;19:650-6.
139. Seifert F, Wübbeler G, Junge S, Ittermann B, Rinneberg H. Patient safety concept for multichannel transmit coils. *J Magn Reson Imaging* 2007;26:1315-21.
140. Homann H, Börnert P, Eggers H, et al. Toward individualized SAR models and *in vivo* validation. *Magn Reson Med* 2011;66:1767-76.
141. Voigt T, Homann H, Katscher U, Doessel O. Patient-individual local SAR determination: *In vivo* measurements and numerical validation. *Magn Reson Med* 2012;68:1117-26.
142. Van den Berg CA, Bartels LW, van den Bergen B, et al. The use of MR B_1^+ imaging for validation of FDTD electromagnetic simulations of human anatomies. *Phys Med Biol* 2006;51:4735-46.
143. Ibrahim TS, Abduljalil AM, Baertlein BA, Lee R, Robitaill PM. Analysis of B_1 field profiles and SAR values for multi-strut transverse electromagnetic RF coils in high field MRI applications. *Phys Med Biol* 2001;46:2545-55.
144. Cabot E, Lloyd T, Christ A, et al. Evaluation of the RF heating of a generic deep brain stimulator exposed in 1.5 T magnetic resonance scanners. *Bioelectromagnetics* 2013;34:104-13.
145. Oberkampf L, DeLand SM, Rutherford BM, Diegert KV, Alvin KF. Error and uncertainty in modeling and simulation. *Reliability Engineering & System Safety* 2002;75:333-357.
146. Neufeld E, Kühn S, Szekely G, Kuster N. Measurement, simulation and uncertainty assessment of implant heating during MRI. *Phys Med Biol* 2009;54:4151-69.
147. Manker, S. Shellock FG. Chapter 24. MRI Safety and Neuromodulation Systems. In: Krames ES, Peckham Hunter P, Rezai AR, Editors. *Neurmodulation*, Second Edition. New York: Academic Press/Elsevier; 2018. pp. 315-337.
148. Sayad D, Chakravarthy K, Amirdelfan K, et al. A comprehensive practice guideline for magnetic resonance imaging compatibility in implanted neuromodulation devices. *Neuromodulation* 2020;23:893-911.

MRI Bioeffects, Safety, and Patient Management 655

149. Krauss JK, Lipsman N, Aziz T, et al. Technology of deep brain stimulation: Current status and future directions. *Nat Rev Neurol* 2021;17:75-87.
150. Wollmann CG, Steiner E, Vock P, Ndikung B, Mayr H, Monocenter feasibility study of the MRI compatibility of the Evia pacemaker in combination with Safio S pacemaker lead. *J Cardiovasc Magn Reson* 2012;14:67.
151. Wilkoff BL, Bello D, Taborsky M, et al. Magnetic resonance imaging in patients with a pacemaker system designed for the magnetic resonance environment. *Heart Rhythm* 2011;8:65-73.
152. Ferreira AM, Costa F, Tralhão A, et al. MRI-conditional pacemakers: Current perspectives. *Med Devices (Auckl)* 2014;7:115-124.
153. Boutet A, Hancu I, Saha U, et al. 3-Tesla MRI of deep brain stimulation patients: Safety assessment of coils and pulse sequences. *J Neurosurg* 2019;132:586-594.
154. Boutet A, Rashid T, Hancu I, Saha U, et al. 3-Tesla MRI of deep brain stimulation patients: Safety Functional MRI safety and artifacts during deep brain stimulation: Experience in 102 patients. *Radiology* 2019;293:174-183.
155. Boutet A, Elias GJB, Gramer R, et al. Safety assessment of spine MRI in deep brain stimulation patients. *J Spine Surg* 2020 ;1-11.
156. Davidson B, Tam F, Yang B, et al. Three-tesla magnetic resonance imaging of patients with deep brain stimulators: Results from a phantom study and a pilot study in patients. *Neurosurgery* 2021;88:349-355.
157. Franceschi AM, Wiggins GC, Mogilner AY, et al. Optimized, minimal specific absorption rate MRI for high-resolution imaging in patients with implanted deep brain stimulation electrodes. *AJNR Am J Neuroradiol* 2016;37:1996-2000.
158. Heidler S, Lusuardi L, Dieterdorfer F. First report of magnetic resonance imaging in patients with implanted InterStim Twin (model 7427T) sacral nerve stimulator. *Urol J (In Press)*.
159. Karrer-Warzinek E, Apt D, Kim O C-H, et al. Safety of magnetic resonance imaging in patients under sacral neuromodulation with an InterStim Neuromodulator. *Urology* 2021 (In Press).
160. Kozlov M, Kainz W. Comparison of different assessment quantities to evaluate lead electromagnetic model for radio frequency energy-induced heating. *IEEE Journal of Electromagnetics, RF and Microwaves in Medicine and Biology* 2020;4:157-163.
161. Yao A, Zastrow E, Kuster N. Data-driven experimental evaluation method for the safety assessment of implants with respect to RF-induced heating during MRI. *Radio Sci* 2018;53:700-709.
162. Liu J, Zheng J, Wang Q, Kainz W, Chen J. A transmission line model for the evaluation of MRI RF-induced fields on active implanted medical devices. *IEEE Transactions on Microwave Theory and Techniques* 2018;4271-4281.
163. Feng S, Wang Q, Wen C, et al. Simplified transfer function assessment of implanted leads for MRI safety evaluations. *IEEE Transactions on Electromagnetic Compatibility* 2019;61:1432-1437.
164. Kalloch B, Bode J, Kozlov M, et al. Semi-automated generation of individual computational models of the human head and torso from MR images. *Magn Reson Med* 2019;81:2090-2105.
165. Kozlov M, Angelone LM, Rajan S. Effect of multiple scattering on heating induced by radio frequency energy. *IEEE Transactions on Electromagnetic Compatibility* 2020;62:2311-2316.

Chapter 24 Performing MRI in Patients with Conventional (Non-MR Conditional) Cardiac Devices

EUNICE YANG, M.D.

Postdoctoral Clinical Fellow
Cardiac Electrophysiology
Johns Hopkins Hospital
Baltimore, MD

SAMAN NAZARIAN, M.D., PH.D., FHRS, FACC

Associate Professor of Medicine
Cardiac Electrophysiology
Perelman School of Medicine, University of Pennsylvania
Philadelphia, PA

HENRY R. HALPERIN, M.D., M.A., FHRA, FAHA

David J Carver Professor of Medicine
Professor of Biomedical Engineering and Radiology
Johns Hopkins Hospital
Baltimore, MD

INTRODUCTION

Magnetic resonance imaging (MRI) provides unparalleled soft tissue resolution utilizing multiple pulse sequences, each optimized for the evaluation of particular tissue attributes. Therefore, MRI is the modality of choice for visualizing numerous soft tissue conditions including various neurologic, musculoskeletal, thoracic, and abdominal abnormalities. Additionally, due to the absence of ionizing radiation, MRI is optimal for sequential imaging for disease follow-up and surveillance as well as diagnostic imaging in children and women of childbearing age. In parallel to an increase in the use of MRI, the number of patients with permanent cardiac pacemakers and implantable cardioverter defibrillators (ICD) continues to increase. As such, it is inevitable that healthcare providers will face the need to perform MRI in an implantable cardiac device recipient. The safety of using MRI in patients

with selected non-MR Conditional, cardiovascular implantable electronic devices (CIEDs) has been successfully demonstrated in a number of studies utilizing standardized protocols while under appropriate supervision. However, catastrophic complications have also been reported for patients with older (i.e., prior to 2000) CIEDs. In this chapter, we review potential interactions of MRI with CIEDs, prior investigations to assess safety, our institutional protocol for imaging patients with non-MR Conditional devices, and the potential effects of susceptibility artifacts.

Potential Interactions of MRI with Cardiovascular Implantable Electronic Devices (CIEDs)

The electromagnetic fields used with MRI are associated with several potential risks involving CIEDs. Therefore, prior to performing clinical studies of MRI in the setting of implanted cardiac devices, our group and others performed extensive *in vitro* and *in vivo* laboratory and animal studies to understand the extent of these interactions.

Magnetic Field Interactions: Force and Torque

Ferromagnetic materials in or near the MR system are exposed to a powerful static magnetic field involving induced force (i.e., translational attraction) and torque. Therefore, a common concern among practitioners is the potential for movement of device components relative to the scanner. However, current lead designs contain little or no ferromagnetic materials and, thus, are unlikely to experience force and torque (1). Although the amount of ferromagnetic materials in CIED pulse generators has substantially decreased over time and is relatively minor for modern-day systems, some ferromagnetic components remain vital to device function. The potential for movement of a pacemaker or ICD pulse generator in the MRI setting depends upon the field strength of the static magnetic field, ferromagnetic components of the device, implant stability (i.e., how it is retained in place, *in situ*), and the distance from the MR system (2). The maximal force acting upon modern permanent pacemakers (manufactured after 1996) and ICDs (manufactured after 2000) appears to be less than 0.98-Newton (equivalent to 100-grams) in association with a 1.5-Tesla MR scanner. The maximum torque in our studies was not found to be substantial and, thus, is unlikely to dislodge a chronically implanted device that is anchored to the surrounding tissue (3). These results are consistent with those of Luechinger, et al. (4) regarding modern pacemakers. However, Luechinger, et al. reported that some modern-day ICDs may still pose possible problems due to strong magnetic field interactions (4).

Current Induction

Current may be induced within wires that are present in patients undergoing MRI examinations. Therefore, the radiofrequency (RF) and time-varying gradient magnetic fields of the MR system may induce electrical currents in leads in association with an MRI exam. However, this is a possibility only if the lead is part of a current loop that is completed through the body (i.e., the pulse generator must complete the current path). For cardiac pacemakers, this condition is only satisfied during specific time points within the pacing cycle. Present-day designs have been developed to overcome this issue. The ratio of lead length versus the RF wavelength and lead configurations, such as loops of a certain diameter, are strongly associated with the extent of current induction (5-7).

658 Patients with Conventional (Non-MR Conditional) Cardiac Devices

We assessed the magnitude of MRI-induced current using a current recorder connected in series to single chamber permanent pacemakers programmed to sub-threshold asynchronous output during unipolar and bipolar pacing (8). Under conventional implant conditions (i.e., without additional lead loops), the magnitude of induced current was less than 0.5-milliampere (mA). Current induction at greater than 30-mA resulting in myocardial capture was possible with the addition of more than four lead loops that substantially increased the total circuit area. However, the presence of so many lead loops is never observed in the clinical setting (8). Bassen and Mendoza (9) have also investigated the possibility of current induction in association with MRI and reported that unintended stimulation may occur in the setting of abandoned leads as well as leads connected to a pulse generator with loss of the hermetic seal at the connector. Additionally, Bassen and Mendoza (9) noted that pacemaker-dependent patients could receive altered pacing pulses during MRI examinations.

MRI-Related Heating

Another potential MRI-related interaction with CIEDs is the possibility of heating and tissue damage where the lead tip contacts tissue. Metallic devices and leads can act as antennae, thus, amplifying local RF energy power deposition (10-12). In our studies utilizing clinical MRI protocols with whole body averaged, specific absorption rates (SAR) < 2.0 W/kg, temperature changes were limited to 1.0 °C in an *in vitro* model and to 0.2 °C in an *in vivo* model (3). However, it is important to note that due to poor correlation of heating profiles at different SARs associated with different pulse sequences across different scanner platforms, even for the same manufacturer, the reported SAR limits from one given study should not be directly applied to other MR systems. Fractured leads or lead loop configurations of a certain diameter may increase the potential for heating even further. The extent of heating also varies as a function of lead length and configuration, proximity to the edge of the gradient coils, proximity to the transmit RF coil, lead insulation thickness, lead design, and other factors (9-17).

Electromagnetic Interference and Other Issues

CIEDs may deliver unintended therapies or fail to provide necessary therapies in patients undergoing MRI. Cardiac pacemakers and ICDs have the potential to receive electromagnetic interference (EMI) during MRI, resulting in radiofrequency noise tracking, asynchronous pacing, inhibition of demand pacing, delivery of unintentional ICD therapies, programming changes, or loss of function. The static magnetic field of the MR system can also alter device function by inducing unexpected reed switch opening or closure. Additionally, temporary programming changes made to avoid device interaction with the scanner (such as disabling of tachycardia therapies) may lead to catastrophic results if a spontaneous arrhythmia occurs and is not recognized.

We implanted modern ICD systems (manufactured after 2000) from the three major manufacturers in the United States (U.S.) in 18 dogs, and after four weeks, performed 3- to 4-hour MRI examinations under worst-case scenario conditions (i.e., imaging over the region containing the pulse generator and using whole body averaged SARs that were greater than 3.5-W/kg) (3). No device dysfunction occurred. After eight weeks of follow up, pacing thresholds and intracardiac electrocardiogram amplitudes were unchanged, with the exception of one animal that experienced transient (less than 12 hours) capture failure. Due to

this observation, we initially did not perform MRI exams on pacemaker-dependent ICD patients. ICD leads are generally longer than pacemaker leads and, thus, may be more prone to possible heating at the lead tip. Pathological data of the scanned animals revealed very limited necrosis or fibrosis in the area around the tip of the lead, which was not different from controls that were not subjected to MRI (3). Similarly, Luechinger, et al. (17) found no clear evidence of heat-induced damage on histology despite observing lead parameter changes in their *in vitro* model. Recently, we relaxed the restriction on scanning pacemaker-dependent, ICD patients at our institution because of our experience with non-clinical scanning parameters that were used that did not result in problems, the lack of any histologic changes that were due to any potential heating, and observing no changes in pacing parameters in hundreds of patients with ICDs that underwent clinical MRI exams.

Clinical Studies of Safety

Implantable Cardiac Monitors and Loop Recorders

Implantable cardiac monitors and loop recorders have been evaluated for MRI-related issues. Gimbel, et al. (18) demonstrated the safety of MRI in the setting of implantable loop recorders in ten patients that underwent eleven examinations. No abnormalities were observed. Sensations of tugging or warmth at the implant site were not reported. We have also performed thoracic and non-thoracic MRI examinations on numerous implantable loop recorder recipients with similar findings of safety. Patients with implantable loop recorders can be safely scanned under specific conditions. However, the device may record MRI-related electromagnetic interference artifacts as an arrhythmia. Therefore, care should be taken to clear episodes recorded during MRI to prevent future misinterpretation of such artifacts as clinically significant arrhythmias. The Reveal implantable cardiac monitor (Medtronic, www.medtronic.com) was the first such device to receive MR Conditional labeling from the U.S. Food and Drug Administration (FDA) (19). Other similar devices from Medtronic as well as from other companies now have labeling stating that these systems are also MR Conditional (see the manufacturer's website or www.MRIsafety.com for specific information pertaining to MRI labeling for implantable cardiac monitors and loop recorders).

Temporary Cardiac Pacemakers

Temporary cardiac pacemakers (implanted outside of the electrophysiology laboratory) have leads that are longer and are potentially more susceptible to induction of lead currents and heating. An *in vitro* study of temporary transvenous pacing leads showed that lead-tip heating that exceeds 15° C is common and temperature rises up to 63.1° C are possible based on laboratory evidence (20). Additionally, the electronic platform of external temporary pacemakers is less sophisticated and has less filtering compared to modern permanent cardiac pacemakers. Therefore, such devices tend to be more susceptible to EMI during MRI procedures and, therefore, imaging of patients with temporary pacemakers is inadvisable. However, we have safely performed MRI in the setting of temporary cardiac pacing utilizing an active fixation, permanent lead, an externalized permanent pacemaker in contact with the patient's skin, and a non-conductive covering adhered to the patient's body with a pressure dressing.

660 Patients with Conventional (Non-MR Conditional) Cardiac Devices

Permanent Cardiac Pacemakers

Previous clinical MRI studies of permanent cardiac pacemakers are presented in **Table 1**. At our institution, the Johns Hopkins Hospital, we began the process of performing MRI on patients with permanent pacemakers based on findings from our *in vitro* and *in vivo* studies, which led to the development of a protocol including (a) device selection based on previous testing, (b) device programming to minimize inappropriate activation or inhibition of brady/tachyarrhythmia therapies, and (c) limitation of the whole body averaged SAR for the applied pulse sequences (less than 2.0-W/Kg) (21). The protocol is discussed in detail below. Using this protocol, we have now safely performed MRI on greater than 4,000 patients with implantable cardiac devices. Our latest report of safety included 880 patients with permanent cardiac pacemakers, 125 of whom were pacemaker-dependent (22). Pacing mode was changed to an asynchronous mode for pacemaker-dependent patients, and to demand mode for others. Blood pressure, electrocardiogram (ECG), pulse oximetry, and symptoms were monitored. The primary clinically significant event attributable to MRI was the occurrence of power-on-reset events in up to 1.5% of device recipients. Aside from transient episodes of asynchronous pacing induced by reed switch activation in certain pacemakers, no episodes of inappropriate inhibition or activation of pacing were observed. Statistically, both right ventricular and atrial sensing and right and left ventricular lead impedances were reduced immediately after MRI. At long-term follow-up, decreased right ventricular sensing, decreased right ventricular lead impedance, increased right ventricular capture threshold, and decreased battery voltage were noted. The observed changes did not require device revision or reprogramming and there were no significant differences between baseline and immediate or long-term sensing amplitudes, lead impedances, or pacing thresholds (22).

Leadless Cardiac Pacemakers

Leadless cardiac pacemakers received FDA approval in 2016, nearly 50 years after they were first conceived (23, 24). These devices carry great clinical utility, particularly for patients with a history of device infections as well as patients prone to thrombosis. In order to assess safety of cardiac MRI *in vivo* following leadless pacemaker implantation, a single-center, prospective non-randomized study was performed on 15 patients undergoing either a 1.5 T or 3.0 T cardiac MRI exam. Patients were followed at one and three months after the scan was completed. The study did not demonstrate any statistically significant changes in adverse clinical events and device parameters remained stable at both follow-up intervals (24). Furthermore, parameter changes were not statistically significant between patients undergoing imaging at 1.5 T or 3.0 T (24).

Implantable Cardioverter Defibrillators

A summary of previous studies of performing clinical MRI in the setting of ICDs is presented in **Table 2**. During our *in vitro* testing of ICDs, we found several pulse generators (manufactured before 2000) that were damaged by MRI. Therefore, in clinical studies, we restricted enrollment to patients with ICD systems manufactured after 2000. Based on our prior *in vitro* and *in vivo* testing, our safety protocol has now been used to safely scan more than 1,000 patients with ICDs. Our latest report of safety included 629 patients with ICD systems. All examinations were completed safely and no inappropriate tachycardia therapies

Table 1. Clinical studies of MRI in the setting of standard permanent cardiac pacemakers.

Source	Finding
Gimbel, et al. (41)	Five patients underwent MRI. No device abnormalities were noted after MRI (0.5 Tesla). A two second pause was noted on pulse oximetry in the pacemaker-dependent patient whose device (with unipolar leads) was programmed to dual chamber asynchronous pacing. Patients did not report pulse generator movement or warmth.
Sommer, et al. (42)	18 patients underwent MRI. Reed switch activation and continuous pacing at a fixed rate noted in the static field. Programming changes, damage of components, dislocation/torque of the generator and rapid pacing were not observed. Atrial and ventricular stimulation thresholds remained unchanged.
Sommer, et al. (43)	44 patients were enrolled. MRI performed at 0.5 Tesla did not inhibit pacing output or cause pacemaker malfunction.
Vahlhaus, et al. (44)	32 patients underwent MRI. Lead impedance and sensing and stimulation thresholds did not change immediately or three months after MRI at 0.5 Tesla. However, diminished battery voltage was noted immediately after MRI with recovery three months later. Reed switch temporary deactivation was seen in 12 of 32 patients when positioned in the center of the scanner's bore.
Martin, et al. (45)	54 patients underwent MRI. Cardiac, vascular and general 1.5 Tesla MRI studies were performed. Significant changes were reported in 9.4% of leads, however, only 1.9% required a change in programmed output.
Del Ojo, et al. (46)	13 patients underwent MRI at 2.0 Tesla. MRI was not associated with pacemaker inhibition, inappropriate rapid pacing, or significant changes in device parameters.
Gimbel, et al. (47)	Of 10 patients that underwent imaging, seven patients showed a rise or fall of 0.5 V in pacing threshold values between baseline and 3-month follow-up. More patients had a decrease than a rise in pacing capture threshold.
Sommer, et al. (48)	MRI was performed in 82 patients. MRI at 1.5 Tesla was not associated with inhibition of pacemaker output or induction of arrhythmias. However, increased capture threshold was noted post MRI. In four of 114 examinations, Troponin increased from a normal baseline value to above normal after MRI (one was associated with a significant increase in capture threshold).
Nazarian, et al. (21)	In 31 patients with pacemakers (55 total patients), MRI at 1.5 Tesla was not associated with any inappropriate inhibition or activation of pacing. There were no significant differences between baseline and immediate or long-term (median 99 days after MRI) sensing amplitudes, lead impedances, or pacing thresholds.
Naehle, et al. (49)	MRI was performed in 44 patients. MRI at 3 Tesla was unassociated with changes in lead impedance, pacing capture threshold or serum Troponin-I.
Mollerus, et al. (50)	In 32 patients with pacemakers (37 total patients), MRI at 1.5 Tesla was not associated with changes in Troponin-I levels or pacing capture thresholds.
Naehle, et al. (51)	Repetitive MRI at 1.5 Tesla (171 examinations on 47 patients) was associated with decreased pacing capture threshold and battery voltage.
Mollerus, et al. (52)	MRI was performed in 46 pacemaker recipients (52 total patients). Ectopy was observed but was unrelated to peak SAR, scan time duration, or landmark. Significant changes in pacing thresholds were not observed.

662 Patients with Conventional (Non-MR Conditional) Cardiac Devices

Table 1. (Continued)

Source	Finding
Mollerus, et al. (53)	MRI was performed in 105 pacemaker recipients (127 total patients). MRI at 1.5 Tesla was associated with decreased sensing amplitudes and pacing impedances. Other parameters were unchanged.
Halshtok, et al. (54)	MRI was performed in nine patients with pacemakers (18 total). MRI at 1.5 Tesla was associated with 5 power-on-reset events in 2 patients. No other effects were reported and device replacement was unnecessary.
Strach, et al. (55)	MRI at 0.2 Tesla in 114 pacemaker recipients was not associated with changes in lead impedance, capture threshold, or battery voltage.
Burke, et al. (56)	MRI was performed in 24 patients with pacemakers (38 total). MRI at 1.5 Tesla was not associated with device circuitry damage, programming alterations, inappropriate shocks, failure to pace, or changes in sensing, pacing, or defibrillator thresholds.
Buendia, et al. (57)	MRI was performed in 28 patients with pacemakers (33 total patients). Temporary communication failure in two cases, sensing errors during imaging in one case, and a safety signal in one pacemaker were noted.
Nazarian, et al. (22)	MRI was performed in 875 patients with pacemakers and 634 patients with ICDs (1,509 total patients, for a total of 2,103 MRI scans) MRI at 1.5-Tesla was associated with nine reset events, eight of which were transient. The most frequently noted finding was a change in device parameters (>50% change from baseline). Immediately after MRI, there was a decrease in P-wave amplitude, which occurred in 1% of the patients. No clinically nor statistically significant differences in lead parameters were noted at long-term follow-up.
Cohen, et al. (58)	MRI was performed in 69 patients with pacemakers (109 total). Decreases in battery voltage of ≥ 0.04 V in 4%, pacing threshold increases of ≥ 0.5 V in 3%, and pacing lead impedance changes of $\geq 50 \Omega$ in 6% were observed. Clinically important differences were not observed between the MRI group and an historic control group.
Russo, et al. (29)	MRI was performed in 1,000 patients with pacemakers and 500 patients with ICDs (1,500 total). One ICD generator was not programmed according to the pre-MRI protocol and required immediate replacement following the MRI acquisition. Six cases of self-terminating atrial fibrillation and 6 cases of partial electrical reset were observed. Repeat MRI was not associated with an increase in adverse events

were delivered (22, 25). We continue to track the safety of MRI with larger patient numbers and newer cardiac pacemaker and ICD systems.

Other investigators have also studied MRI safety in the setting of implanted pacemakers and ICD systems (**Table 1** and **Table 2**). A noteworthy study is the MagnaSafe Registry, a multicenter, prospective study reporting on the frequency of major adverse clinical events and device parameter changes for 1,500 patients with standard (i.e., non-MR Conditional) CIEDs who underwent clinically-indicated, non-thoracic MRI at 1.5 T (26-29). That registry-based investigation reported that there were no device or lead failures occurring in

Table 2. Clinical MRI studies in the setting of standard ICD systems.

Source	Finding
Coman, et al. (59)	MRI was performed in 11 patients with ICD systems. One patient felt mild heating near the pulse generator during spin echo sequences. One patient had a brief, but asymptomatic, pause in pacing during scanning. One patient with a device past the elective replacement interval had a power on reset and the device could not be interrogated after the scan. Normal device function and circuit integrity were noted at destructive testing.
Gimbel, et al. (60)	MRI was performed in seven patients with ICD systems. No changes in pacing, sensing, impedances, charge times, or battery status were observed with MRI at 1.5 Tesla. However, one implantable cardioverter defibrillator (Medtronic 7227Cx, lumbar spine MRI) experienced a “power on reset.”
Nazarian, et al. (21)	MRI was performed in 24 patients with ICD systems (55 total). MRI at 1.5 Tesla was not associated with any inappropriate inhibition or activation of pacing. There were no significant differences between baseline and immediate or long-term (median 99 days after MRI) sensing amplitudes, lead impedances, or pacing thresholds.
Mollerus, et al. (50)	MRI was performed in five patients with ICD systems (37 total). MRI at 1.5 Tesla was not associated with changes in Troponin-I levels or pacing capture thresholds.
Naehle, et al. (61)	MRI was performed in 18 patients with ICD systems. MRI at 1.5 Tesla was not associated with device circuitry damage, changes in lead parameters, or Troponin-I levels. However, battery voltage decreased post MRI, and over-sensing of EMI as ventricular fibrillation occurred in two devices, but therapies were not delivered.
Mollerus, et al. (52)	MRI was performed in six patients with ICD systems (52 total). Ectopy was observed but was unrelated to the peak SAR levels, scan time durations, or landmarks. Significant changes in pacing thresholds were not observed.
Pulver, et al. (62)	MRI was performed in eight patients with ICD systems. Inappropriate pacing or significant changes in generator or lead parameters were not observed.
Mollerus, et al. (53)	MRI was performed in 22 patients with ICD systems (127 total). MRI at 1.5 Tesla was associated with decreased sensing amplitudes and pace impedances. Other parameters were unchanged.
Halshtok, et al. (54)	MRI was performed in 9 patients with ICD systems (18 total). MRI at 1.5 Tesla was not associated with any untoward effects and device replacement was unnecessary.
Burke, et al. (56)	MRI was performed in 14 patients with ICD systems (38 total). MRI at 1.5 Tesla was not associated with device circuitry damage, programming alterations, inappropriate shocks, failure to pace, or changes in sensing, pacing, or defibrillator thresholds.
Buendia, et al. (57)	MRI was performed in five patients with ICD systems (33 total). Sensing errors during imaging in one case was noted.
Nazarian, et al. (22, 25)	MRI was performed in 634 patients with ICD systems. MRI at 1.5 Tesla was associated with one power-on-reset event. Statistically significant but clinically small (not requiring device revision or reprogramming) changes in lead parameters were observed.

664 Patients with Conventional (Non-MR Conditional) Cardiac Devices

Table 2. (Continued)

Source	Finding
Cohen, et al. (58)	MRI was performed in 40 patients with ICD systems (109 total). Decreases in battery voltage of ≥ 0.04 V in 4%, pacing threshold increases of ≥ 0.5 V in 3%, and pacing lead impedance changes of $\geq 50 \Omega$ in 6% were observed. Clinically important differences were not observed between the MRI group and an historic control group.
Russo, et al. (29)	MRI was performed in 500 patients with ICDs. One ICD generator was not programmed according to the pre-MRI protocol and required immediate replacement following the MRI acquisition. Six cases of self-terminating atrial fibrillation and 6 cases of partial electrical reset were observed. Repeat MRI was not associated with an increase in adverse events.

any patient with a non-MR Conditional pacemaker or ICD who underwent a nonthoracic 1.5 Tesla MRI exam and where a pre-specified protocol was carefully followed.

Retained Pacing Leads

Retained (capped and/or cut, and abandoned) leads are susceptible to the previously described risks of heating and current induction. Depending upon the lead length and configuration, retained segments may be prone to significantly higher temperature rises than those attached to pulse generators (14). We have performed at least 40 MRI examinations in the setting of absolute clinical necessity and retained cardiac lead segments. All of these studies were completed without safety issues. To further investigate the risks of cardiac MRI on patients with abandoned leads, Golestanirad, et al. (30) used electromagnetic simulations and bio-heat modeling utilizing numerical models of retained cardiac leads built using CT and X-ray images from six patients with retained cardiac leads. These simulations were performed considering the use of a transmit/receive RF body and transmit/receive head RF coils operating at 64 MHz and 128 MHz. Nine different imaging landmarks from the head to the lower limbs were studied. Their findings suggested that the amount of heating appeared to increase both with the field strength and frequency of the MR system (1.5 T/64 MHz versus 3.0 T/128 MHz) and with pulse sequence duration. However, all scans led to lead heating that did not exceed 6°C in all simulated models, which was considered to be clinically insignificant (30). Despite these interesting findings, clinical experience remains limited and, thus, additional investigations on this topic are warranted to accurately delineate the risks and benefits of using MRI in patients with abandoned pacing leads.

In 2021, Schaller, et al. (63) investigated the effect of MRI in 139 patients with CIEDs who also had abandoned leads (total, 243 leads). The findings indicated that there were no abnormal vital signs or sustained tachyarrhythmias in this patient group. Furthermore, there were no changes in battery voltage, power-on reset events, or changes of pacing rate. One patient with an abandoned subcutaneous array experienced sternal heating that subsided on premature cessation of the study. The investigators concluded that the risk of performing MRI in patients with abandoned CIED leads was low in their large observational study, including patients who underwent examinations involving the thorax (63). Thus, the growing aggregate of data challenge the absolute contraindication for performing MRI in patients with abandoned CIED leads.

Our Institutional Safety Protocol for MRI of Patients with CIEDs

With regard to performing MRI examinations in patients with non-MR Conditional CIEDs, the safety protocol followed at our institution is based on selection of device pulse generators previously tested under worst-case scenario (e.g., prolonged imaging over the region containing the device using whole body averaged SAR levels greater than 3.5-W/kg) MRI conditions (3). This protocol is summarized as a checklist in **Figure 1**.

To perform MRI on patients with CIEDs, we recommend that patients with device pulse generators prone to EMI (generally devices manufactured prior to 2000) be excluded. Reports of safe MRI immediately post-implantation exist in the literature (31), and the risk for lead and/or pulse generator movement is considered to be extremely low or nonexistent. However, we recommend conservative measures to exclude patients with leads that are susceptible to spontaneous (regardless of MRI) dislodgement or that do not have chronic stable lead parameters that would allow careful measurement of safety. Therefore, we advise avoiding MRI in patients with less than six weeks of time since the devices were implanted and those with acute parameter changes suggestive of lead malfunctions. In our experience, however, patients with mature active and passive fixation endocardial (and coronary sinus) leads of any diameter can safely undergo MRI exams. We recommend avoiding MRI when

Figure 1. The safety checklist utilized at our institution, Johns Hopkins Hospital, for performing MRI in the patients with non-MR Conditional cardiac pacemakers and implantable cardioverter defibrillators (ICDs).

When was the pacemaker or ICD pulse generator implanted?		<input type="checkbox"/> After the year 2000 <input type="checkbox"/> Before the year 2000 • If before the year 2000 → cancel MRI
When were the leads implanted?		<input type="checkbox"/> ≥ 6 weeks ago <input type="checkbox"/> < 6 weeks ago • If < 6 weeks, cancel MRI
Are surgically placed epicardial or abandoned leads present?		<input type="checkbox"/> Yes <input type="checkbox"/> No • If yes, cancel MRI
<input type="checkbox"/> Pacemaker <input type="checkbox"/> ICD Pacemaker Dependent?	<input type="checkbox"/> Yes • If yes, and the device is an ICD, cancel MRI • If yes, and the device is a pacemaker, program pacing to VOO/DDO • Deactivate magnet, rate response, noise response, and all tracking and triggered pacing features • Monitor blood pressure, ECG, oxygen saturation, and symptoms during MRI	<input type="checkbox"/> No • If no, program pacing to VVI/DDI and deactivate tachycardia detection and therapies
Device Manufacturer & model number:	Prior to MRI	After MRI
	Right Atrium Right Ventricle Left Ventricle	Right Atrium Right Ventricle Left Ventricle
Sensing		
Capture Threshold		
Impedance		
Battery Voltage		
• Keep patient ECG monitor after MRI until initial device programming has been restored • Advise follow-up in device clinic in 3-6 months after MRI		

666 Patients with Conventional (Non-MR Conditional) Cardiac Devices

device leads are present that are prone to heating, such as non-transvenous, epicardial and abandoned (capped) leads. We do, however, relax these restrictions if there is a compelling clinical need for the MRI exam, but require a higher level of monitoring. To reduce the risk of inappropriate inhibition of pacing due to detection of radiofrequency pulses, we program devices to an asynchronous, dedicated pacing mode in pacemaker-dependent patients.

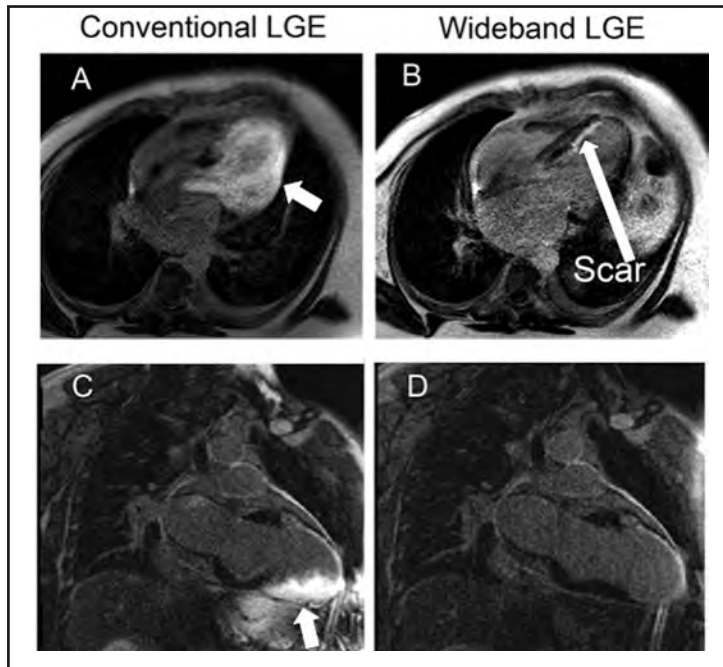
To avoid inappropriate activation of pacing due to tracking of radiofrequency pulses, we suggest device programming in patients without pacemaker-dependence to a non-tracking ventricular or dual chamber inhibited pacing mode. We also recommend deactivation of rate response, premature ventricular contraction response, ventricular sense response, and conducted atrial fibrillation response to ensure that sensing of vibrations or radiofrequency pulses does not lead to unwarranted pacing.

Although asynchronous pacing for short time periods is typically well tolerated, we prefer to reduce the already minimal chance of inducing arrhythmia or causing atrioventricular (AV) dyssynchrony by minimizing asynchronous pacing in patients without pacemaker dependence through deactivation of the magnet mode when possible. We typically deactivate tachyarrhythmia monitoring to avoid battery drainage that results from recording of multiple MRI-related, radiofrequency pulse sequences as arrhythmic episodes. Reed switch activation in ICD systems disables tachyarrhythmia therapies. However, reed switch function in the periphery of the scanner versus the bore of the MR system is unpredictable (21, 32, 33). Therefore, therapies should be disabled to avoid unwarranted anti-tachycardia pacing or shocks. Finally, blood pressure, ECG, pulse oximetry, and symptoms should be monitored in the patient for the duration of the MRI exam. We also favor the presence of a radiologist and cardiac electrophysiologist, or advanced cardiac life support (ACLS)-trained individual familiar with device programming and troubleshooting during all MRI examinations (21, 25, 34). At the end of the MRI procedure, all device parameters should be checked and programming should be restored to pre-MRI settings.

MRI-Related Susceptibility Artifacts in the Setting of Cardiac Pacemakers and ICD Systems

The quality of the MR image is not affected when the pacemaker or ICD is located outside the field of view or the area of interest. However, when performing thoracic imaging, the presence of a pacemaker or ICD can cause variations in the surrounding (i.e., local) magnetic field and other issues that result in issues including signal voids, bright areas, image distortion, or poor fat suppression. Typically, the artifacts associated with pacing and ICD leads are minimal in size. However, pulse generator-related artifacts, particularly with ICD systems, can be substantial (**Figure 2**) (35, 36). Such artifacts tend to be most pronounced on partial flip angle pulse sequences as well as others (e.g., inversion recovery and steady state sequences). Greater than 50% of cardiac sectors (primarily antero-apical segments) can be affected by pulse generator-related susceptibility artifacts in patients with left-sided ICD systems (37). Artifacts on inversion recovery images show high signal intensity and can mimic areas of delayed-enhancement, which would otherwise indicate myocardial scar. Correlation of artifact-related bright areas on different pulse sequences can help avoid misidentification of the artifact as pathology. Artifacts related to metal can be considerably reduced by using wideband pulse sequences (**Figure 2**) (35-37), even in pa-

Figure 2. (A, B): Late gadolinium-enhanced (LGE) MR images obtained for planning of a ventricular tachycardia ablation procedure in a patient with a transvenous ICD system. (C, D): LGE MR images obtained from a patient with a sub-cutaneous ICD system. (A, C): Note the large susceptibility artifacts (arrows) due to the presence of the ICD pulse generators in the conventional LGE images. With wideband imaging, the left ventricular septal scar due to a prior myocardial infarction is well seen (B, arrow). In addition, the susceptibility artifact is suppressed on the image of the patient with the subcutaneous ICD (D). Images adapted from Stevens S, et al. and Rahsepar A, et al. (35, 36).



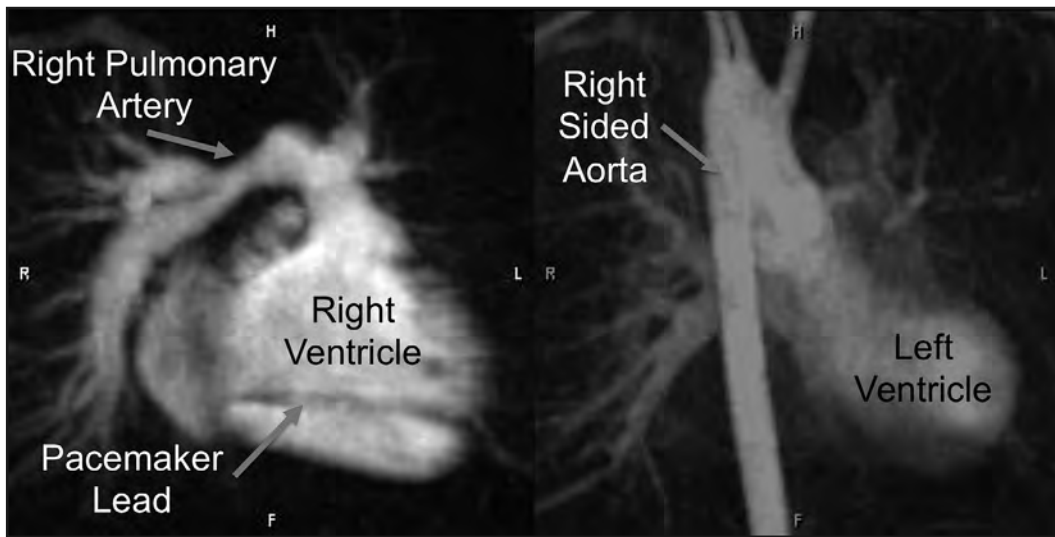
tients with subcutaneous ICDs (**Figure 2**). In addition, selecting imaging planes perpendicular to the plane of the device's pulse generator, shortening the echo time, and using spin echo and fast spin echo pulse sequences reduces the qualitative extent of the artifact (**Figure 3**). Using such techniques, images of sufficient quality to address diagnostic questions, as well as to guide therapeutic procedures, can be obtained in the majority of cases.

The Relationship Between MRI-Related Radiofrequency Energy and Device Function

Rahsepar, et al. (38) studied the relationship between MRI-related RF energy and device function in 2,028 MRI examinations performed in 1,464 study participants with 2,755 device leads. Clinical MRI protocols without SAR restrictions were used. Exclusion criteria were newly implanted leads, abandoned or epicardial leads, and dependence on a cardiac pacemaker with an ICD without asynchronous pacing capability. For each MRI pulse sequence, the calculated whole-body averaged values for SAR, levels of gradient magnetic fields, and scan duration were collected. Atrial and ventricular sensing, lead impedance,

668 Patients with Conventional (Non-MR Conditional) Cardiac Devices

Figure 3. MR images obtained using “TWIST” (time-resolved angiography with interleaved stochastic trajectories) angiography sequence in a patient with history of Tetralogy of Fallot status post repair and implantation of a cardiac pacemaker. The left panel shows an enlarged right ventricle, the right ventricular outflow tract status post patch repair and mild hypoplasia of the right pulmonary artery. Minimal susceptibility artifact from the right ventricular lead is visible. The right panel shows a right-sided aortic arch with mirror image branching.



and capture threshold were evaluated before and immediately after (i.e., within 10 minutes) completion of each MRI examination. There were some small, non-clinically significant changes in device parameters immediately after the MRI exams. However, there was no evidence of an association between MRI parameters that characterize patient exposure to radiofrequency energy and changes in device and lead parameters immediately after MRI. Importantly, the investigators indicated that cardiac device interrogation before and after MRI remains mandatory due to the potential for device reset and changes in lead or pulse generator parameters (38).

Center for Medicare & Medicaid Services Recommendations and Guidelines

In light of the growing body of evidence highlighting the safety profile of MRI for individuals with CIEDs, the Center for Medicare & Medicaid Services (CMS) recently approved national coverage of 1.5 Tesla scanning in individuals with legacy cardiac devices (39). In reviewing the literature, the CMS proposal indicated that performing 1.5 T MRI in patients with MR Conditional and non-MR Conditional CIEDs could be conducted with a similar, low clinical risk, as long as the exams followed a particular “checklist” of requirements. CMS further indicated that it would approve coverage of these types MRI exams for patients in all facilities that carefully adhered to the criteria shown in the checklist presented in **Table 3** (39).

Table 3. Center for Medicaid & Medicare Services (CMS) Guidelines for 1.5 T MRI facility checklist for performing MRI in patients with non-MR Conditional CIEDs (39).

<ul style="list-style-type: none"> Patient assessment must be performed to identify the presence of an implanted cardiac pacemaker, implantable cardioverter defibrillator, cardiac resynchronization therapy pacemaker, or cardiac resynchronization therapy defibrillator.
<ul style="list-style-type: none"> Prior to MRI, a risk versus benefit assessment must be performed by the supervising physicians (e.g., cardiologist and radiologist) and is communicated to the patient or the patient's delegated decision-maker.
<ul style="list-style-type: none"> Prior to MRI, the implanted cardiac pacemaker, implantable cardioverter defibrillator, cardiac resynchronization therapy pacemaker, or cardiac resynchronization therapy defibrillator must be interrogated and programmed into the appropriate MRI-related scanning mode.
<ul style="list-style-type: none"> A qualified physician, nurse practitioner, or physician assistant with expertise with an implanted cardiac pacemaker, implantable cardioverter defibrillator, cardiac resynchronization therapy pacemaker, or cardiac resynchronization therapy defibrillator must directly supervise the MRI exam (i.e., meaning that the individual is immediately available).
<ul style="list-style-type: none"> A discharge plan that includes before being discharged from the hospital/facility, the patient is evaluated and the implanted pacemaker, implantable cardioverter defibrillator, cardiac resynchronization therapy pacemaker, or cardiac resynchronization therapy defibrillator is re-interrogated to detect and correct any abnormalities that might have developed in association with the MRI exam.

CONCLUSIONS

MRI is the preferred imaging modality in many clinical scenarios. The decision to perform an MRI exam on a patient with a legacy cardiac pacemaker or ICD system is frequently made by considering the probable benefit of MRI relative to the potential risks. Therefore, it is important to conduct a systematic review of the patient's condition as well as the specific cardiac device that is present prior to proceeding with MRI. Notably, peer-reviewed literature involving patients with non-MR Conditional CIEDs continue to support the safe use of MRI (64, 65). As such, besides staying apprised of recently published information, the reader is encouraged to consult other resources such as the American Heart Association Scientific Statement (40), the practice guidelines from the American College of Radiology (66) and the International Society for Magnetic Resonance in Medicine (67), and websites (e.g., www.MRIsafety.com and CIED manufacturers' websites) that provide specific information regarding individual devices. Although there is a growing body of literature on safety of MRI for patients with CIEDs, it is critical that there is real-time monitoring of all patients undergoing MRI with CIEDs because the possibility of an adverse event, while very small, is still present.

670 Patients with Conventional (Non-MR Conditional) Cardiac Devices**REFERENCES**

1. Irnich W. Risks to pacemaker patients undergoing magnetic resonance imaging examinations. *Europace* 2010;12:918-920.
2. Shellock FG, Tkach JA, Ruggieri PM, Masaryk TJ. Cardiac pacemakers, ICDs, and loop recorder: Evaluation of translational attraction using conventional ("long-bore") and "short-bore" 1.5- and 3.0-Tesla MR systems. *J Cardiovasc Magn Reson* 2003;5:387-397.
3. Roguin A, Zviman MM, Meininger GR, et al. Modern pacemaker and implantable cardioverter/defibrillator systems can be magnetic resonance imaging safe: *In vitro* and *in vivo* assessment of safety and function at 1.5 T. *Circulation* 2004;110:475-482.
4. Luechinger R, Duru F, Scheidegger MB, Boesiger P, Candinas R. Force and torque effects of a 1.5-Tesla MRI scanner on cardiac pacemakers and ICDs. *Pacing Clin Electrophysiol Pacing Clin Electrophysiol* 2001;24:199-205.
5. Babouri A, Hedjeidj A. *In vitro* investigation of eddy current effect on pacemaker operation generated by low frequency magnetic field. *Conf Proc IEEE Eng Med Biol Soc* 2007;2007:5684-5687.
6. Nordbeck P, Weiss I, Ehses P, et al. Measuring RF-induced currents inside implants: Impact of device configuration on MRI safety of cardiac pacemaker leads. *Magn Reson Med* 2009;61:570-578.
7. Yeung CJ, Karmarkar P, McVeigh ER. Minimizing RF heating of conducting wires in MRI. *Magn Reson Med* 2007;58:1028-1034.
8. Tandri H, Zviman MM, Wedan SR, Lloyd T, Berger RD, Halperin H. Determinants of gradient field-induced current in a pacemaker lead system in a magnetic resonance imaging environment. *Heart Rhythm* 2008;5:462-468.
9. Bassen HI, Mendoza GG. In-vitro mapping of E-fields induced near pacemaker leads by simulated MR gradient fields. *Biomed Eng Online* 2009;8:39.
10. Calcagnini G, Triventi M, Censi F, et al. *In vitro* investigation of pacemaker lead heating induced by magnetic resonance imaging: Role of implant geometry. *J Magn Reson Imaging* 2008;28:879-886.
11. Mattei E, Triventi M, Calcagnini G, et al. Complexity of MRI induced heating on metallic leads: Experimental measurements of 374 configurations. *Biomed Eng Online* 2008;7:11.
12. Park SM, Kamondetdacha R, Nyenhuis JA. Calculation of MRI-induced heating of an implanted medical lead wire with an electric field transfer function. *J Magn Reson Imaging* 2007;26:1278-1285.
13. Nordbeck P, Bauer WR, Warmuth M, Hiller KH, Jakob PM, Ritter O. MRI-related heating at cardiac pacemaker leads *in vivo*. *Circulation* 2009;120:S371-S371.
14. Langman DA, Goldberg IB, Finn JP, Ennis DB. Pacemaker lead tip heating in abandoned and pacemaker-attached leads at 1.5 Tesla MRI. *J Magn Reson Imag* 2011;33:426-431.
15. Nordbeck P, Ritter O, Weiss I, et al. Impact of imaging landmark on the risk of MRI-related heating near implanted medical devices like cardiac pacemaker leads. *Magn Reson Med* 2011;65:44-50.
16. Bottomley PA, Kumar A, Edelstein WA, Allen JM, Karmarkar PV. Designing passive MRI-safe implantable conducting leads with electrodes. *Med Phys* 2010;37:3828-3843.
17. Luechinger R, Zeijlemaker VA, Pedersen EM, et al. *In vivo* heating of pacemaker leads during magnetic resonance imaging. *Eur Heart J* 2005;26:376-383.
18. Gimbel JR, Zarghami J, Machado C, Wilkoff BL. Safe scanning, but frequent artifacts mimicking bradycardia and tachycardia during magnetic resonance imaging (MRI) in patients with an implantable loop recorder (ILR). *Ann Noninvasive Electrocardiol* 2005;10:404-408.
19. Medtronic. Insertable Cardiac Monitor - Magnetic Resonance Imaging (MRI) and Reveal Implantable Cardiac Monitors. Medtronic, www.medtronic.com.
20. Achenbach S, Moshage W, Diem B, Bieberle T, Schibgilla V, Bachmann K. Effects of magnetic resonance imaging on cardiac pacemakers and electrodes. *Am Heart J* 1997;134:467-473.

MRI Bioeffects, Safety, and Patient Management 671

21. Nazarian S, Roguin A, Zviman MM, et al. Clinical utility and safety of a protocol for noncardiac and cardiac magnetic resonance imaging of patients with permanent pacemakers and implantable cardioverter defibrillators at 1.5 Tesla. *Circulation* 2006;114:1277-1284.
22. Nazarian S, Hansford R, Rahsepar AA, et al. Safety of magnetic resonance imaging in patients with cardiac devices. *N Engl J Med* 2017;377:2555-2564.
23. Spickler JW, Rasor NS, Kezdi P, Misra SN, Robins KE, LeBoeuf C. Totally self-contained intracardiac pacemaker. *J Electrocardiol* 1970;3(3-4):325-331.
24. Blessberger H, Kiblboeck D, Reiter C, et al. Monocenter investigation Micra(R) MRI study (MIMICRY): Feasibility study of the magnetic resonance imaging compatibility of a leadless pacemaker system. *Europace* 2019;21:137-141.
25. Nazarian S, Hansford R, Roguin A, et al. A prospective evaluation of a protocol for magnetic resonance imaging of patients with implanted cardiac devices. *Annals of Internal Medicine* 2011;155:415-424.
26. Cohen J, Costa H, Russo R. Pacemaker and implantable cardioverter defibrillator safety for patients undergoing magnetic resonance imaging (The MagnaSafe Registry). *J Am Coll Cardiol* 2009;53:A303-A304.
27. Cohen JD, Costa HS, Russo RJ. Pacemaker and implantable cardioverter defibrillator safety for patients undergoing magnetic resonance imaging (The MagnaSafe Registry). *Circulation* 2008;118:S778-S778.
28. Russo RJ, Costa H, Doud D, et al. Repeat MRI for patients with implanted cardiac devices does not increase the risk of clinical events or parameter changes: Preliminary results from The MagnaSafe Registry. *J Am Coll Cardiol* 2012;59:E649-E649.
29. Russo RJ, Costa HS, Silva PD, et al. Assessing the risks associated with MRI in patients with a pacemaker or defibrillator. *N Engl J Med* 2017;376:755-764.
30. Golestanirad L, Rahsepar AA, Kirsch JE, et al. Changes in the specific absorption rate (SAR) of radiofrequency energy in patients with retained cardiac leads during MRI at 1.5T and 3T. *Magn Reson Med* 2019;81:653-669.
31. Goldsher D, Jahshan S, Roguin A. Successful cervical MR scan in a patient several hours after pacemaker implantation. *Pacing and Clinical Electrophysiology* 2009;32:1355-1356.
32. Lauck G, von Smekal A, Wolke S, et al. Effects of nuclear magnetic resonance imaging on cardiac pacemakers. *Pacing Clin Electrophysiol* 1995;18:1549-1555.
33. Luechinger R, Duru F, Zeijlemaker VA, Scheidegger MB, Boesiger P, Candinas R. Pacemaker reed switch behavior in 0.5, 1.5, and 3.0 Tesla magnetic resonance imaging units: Are reed switches always closed in strong magnetic fields? *Pacing Clin Electrophysiol* 2002;25:1419-1423.
34. Nazarian S, Halperin HR. How to perform magnetic resonance imaging on patients with implantable cardiac arrhythmia devices. *Heart Rhythm* 2009;6:138-143.
35. Stevens SM, Tung R, Rashid S, et al. Device artifact reduction for magnetic resonance imaging of patients with implantable cardioverter-defibrillators and ventricular tachycardia: Late gadolinium enhancement correlation with electroanatomic mapping. *Heart Rhythm* 2014;11:289-298.
36. Rahsepar AA, Collins JD, Knight BP, Hong K, Carr JC, Kim D. Wideband LGE MRI permits unobstructed viewing of myocardial scarring in a patient with an MR-conditioned subcutaneous implantable cardioverter-defibrillator. *Clin Imaging* 2018;50:294-296.
37. Sasaki T, Hansford R, Zviman MM, et al. Quantitative assessment of artifacts on cardiac magnetic resonance imaging of patients with pacemakers and implantable cardioverter-defibrillators. *Circulation Cardiovascular Imaging* 2011;4:662-670.
38. Rahsepar AA, Zimmerman SL, Hansford R, et al. The relationship between MRI radiofrequency energy and function of nonconditional implanted cardiac devices: A prospective evaluation. *Radiology* 2020;295:307-313.
39. Decision memo for magnetic resonance imaging (MRI) (CAG-00399R3). Baltimore: Centers for Medicare & Medicaid Services, 2018 (<https://www.cms.gov/medicare-coverage-database/details/nca-decision-memo.aspx?NCAId=252%20&%20fromdb=true>) 2018.

672 Patients with Conventional (Non-MR Conditional) Cardiac Devices

40. Levine GN, Gomes AS, Arai AE, et al. Safety of magnetic resonance imaging in patients with cardiovascular devices: An American Heart Association scientific statement from the Committee on Diagnostic and Interventional Cardiac Catheterization, Council on Clinical Cardiology, and the Council on Cardiovascular Radiology and Intervention; endorsed by the American College of Cardiology Foundation, the North American Society for Cardiac Imaging, and the Society for Cardiovascular Magnetic Resonance. *Circulation* 2007;116:2878-2891.
41. Gimbel JR, Johnson D, Levine PA, Wilkoff BL. Safe performance of magnetic resonance imaging on five patients with permanent cardiac pacemakers. *Pacing Clin Electrophysiol* 1996;19:913-919.
42. Sommer T, Lauck G, Schimpf R, et al. MRI in patients with cardiac pacemakers: *In vitro* and *in vivo* evaluation at 0.5 tesla. *Rofo* 1998;168:36-43.
43. Sommer T, Vahlhaus C, Lauck G, et al. MR imaging and cardiac pacemakers: *In-vitro* evaluation and *in-vivo* studies in 51 patients at 0.5 T. *Radiology* 2000;215:869-879.
44. Vahlhaus C, Sommer T, Lewalter T, et al. Interference with cardiac pacemakers by magnetic resonance imaging: Are there irreversible changes at 0.5 Tesla? *Pacing Clin Electrophysiol* 2001;24(4 Pt 1):489-495.
45. Martin ET, Coman JA, Shellock FG, Pulling CC, Fair R, Jenkins K. Magnetic resonance imaging and cardiac pacemaker safety at 1.5-Tesla. *J Am Coll Cardiol* 2004;43:1315-1324.
46. Del Ojo JL, Moya F, Villalba J, et al. Is magnetic resonance imaging safe in cardiac pacemaker recipients? *Pacing Clin Electrophysiol* 2005;28:274-278.
47. Gimbel JR, Bailey SM, Tchou PJ, Ruggieri PM, Wilkoff BL. Strategies for the safe magnetic resonance imaging of pacemaker-dependent patients. *Pacing Clin Electrophysiol* 2005;28:1041-1046.
48. Sommer T, Naehle CP, Yang A, et al. Strategy for safe performance of extrathoracic magnetic resonance imaging at 1.5 tesla in the presence of cardiac pacemakers in non-pacemaker-dependent patients: A prospective study with 115 examinations. *Circulation* 2006;114:1285-1292.
49. Naehle CP, Meyer C, Thomas D, et al. Safety of brain 3-T MR imaging with transmit-receive head coil in patients with cardiac pacemakers: Pilot prospective study with 51 examinations. *Radiology* 2008;249:991-1001.
50. Mollerus M, Albin G, Lipinski M, Lucca J. Cardiac biomarkers in patients with permanent pacemakers and implantable cardioverter-defibrillators undergoing an MRI scan. *Pacing Clin Electrophysiol* 2008;31:1241-1245.
51. Naehle CP, Zeijlemaker V, Thomas D, et al. Evaluation of cumulative effects of MR imaging on pacemaker systems at 1.5 Tesla. *Pacing Clin Electrophysiol* 2009;32:1526-1535.
52. Mollerus M, Albin G, Lipinski M, Lucca J. Ectopy in patients with permanent pacemakers and implantable cardioverter-defibrillators undergoing an MRI scan. *Pacing Clin Electrophysiol* 2009;32:772-778.
53. Mollerus M, Albin G, Lipinski M, Lucca J. Magnetic resonance imaging of pacemakers and implantable cardioverter-defibrillators without specific absorption rate restrictions. *Europace* 2010;12:947-51.
54. Halshtok O, Goitein O, Abu Sham'a R, Granit H, Glikson M, Konen E. Pacemakers and magnetic resonance imaging: No longer an absolute contraindication when scanned correctly. *Isr Med Assoc J* 2010;12:391-5.
55. Strach K, Naehle CP, Muhlsteffen A, et al. Low-field magnetic resonance imaging: Increased safety for pacemaker patients? *Europace* 2010;12:952-960.
56. Burke PT, Ghanbari H, Alexander PB, Shaw MK, Daccarett M, Machado C. A protocol for patients with cardiovascular implantable devices undergoing magnetic resonance imaging (MRI): Should defibrillation threshold testing be performed post-(MRI). *J Interv Card Electrophysiol* 2010;28:59-66.
57. Buendia F, Sanchez-Gomez JM, Sancho-Tello MJ, et al. Nuclear magnetic resonance imaging in patients with cardiac pacing devices. *Rev Esp Cardiol* 2010;63:735-739.
58. Cohen JD, Costa HS, Russo RJ. Determining the risks of magnetic resonance imaging at 1.5 tesla for patients with pacemakers and implantable cardioverter defibrillators. *Am J Cardiol* 2012;110:1631-1636.
59. Coman JA, Martin ET, Sandler DA, Thomas JR. Implantable cardiac defibrillator interactions with magnetic resonance imaging at 1.5 Tesla. *J Am Coll Cardiol* 2004;4:138A-138A.

MRI Bioeffects, Safety, and Patient Management 673

60. Gimbel JR, Kanal E, Schwartz KM, Wilkoff BL. Outcome of magnetic resonance imaging (MRI) in selected patients with implantable cardioverter defibrillators (ICDs). *Pacing Clin Electrophysiol* 2005;28:270-273.
61. Naehle CP, Strach K, Thomas D, et al. Magnetic resonance imaging at 1.5-T in patients with implantable cardioverter-defibrillators. *J Am Coll Cardiol* 2009;54:549-555.
62. Pulver AF, Puchalski MD, Bradley DJ, et al. Safety and imaging quality of MRI in pediatric and adult congenital heart disease patients with pacemakers. *Pacing Clin Electrophysiol* 2009;32:450-456.
63. Schaller RD, Brunker T, Riley MP, Marchlinski FE, Nazarian S, Litt H. Magnetic resonance imaging in patients with cardiac implantable electronic devices with abandoned leads. *JAMA Cardiol* 2021 (Epub ahead of print).
64. Ning X, Li X, Fan X, et al. 3.0 T magnetic resonance imaging scanning on different body regions in patients with pacemakers. *J Interv Card Electrophysiol* 2020 (Epub ahead of print).
65. Padmanabhan D, Kella D, Isath A, et al. Prospective evaluation of the utility of magnetic resonance imaging in patients with non-MRI-conditional pacemakers and defibrillators. *J Cardiovasc Electrophysiol* 2020;31:2931-2939.
66. American College of Radiology, ACR Manual on MR Safety. <https://www.acr.org/Clinical-Resources/Radiology-Safety/MR-Safety>.
67. Vigen KK, Reeder SB, Hood MN, et al. ISMRM Safety Committee. Recommendations for imaging patients with cardiac implantable electronic devices (CIEDs). *J Magn Reson Imaging*. 2020 (Epub ahead of print).

Chapter 25 MRI and Patients with Cardiac Implantable Electronic Devices

SUMIT PATEL, M.D.

Cardiology Fellow

Division of Cardiovascular Medicine Cardiovascular and Thoracic Institute
Keck School of Medicine
University of Southern California
Los Angeles, CA

JOHN SUMMERS, M.D.

Medical Director, Cardiac Electrophysiology and Watchman Champion
SSM Health Saint Anthony Hospital
Oklahoma City, OK

JEROLD S. SHINBANE, M.D.

Professor of Clinical Medicine
Director, USC Arrhythmia Center
Director, Cardiovascular Computed Tomography/Division of Cardiovascular Medicine
Division of Cardiovascular Medicine
Cardiovascular and Thoracic Institute
Keck School of Medicine
University of Southern California
Los Angeles, CA

INTRODUCTION

The rapid technologic evolution of magnetic resonance imaging (MRI) has led to a broad spectrum of medical applications (1). In parallel, cardiac implantable electronic device (CIED) technologies have been developed for arrhythmia diagnosis as well as treatment of bradyarrhythmias, tachyarrhythmias, heart failure, and other conditions (2). The implementation of these two technologies has reached a crossroads, as increasingly, patients with CIEDs may require MRI exams, but are limited in performance by the presence of the cardiac device (3). The assessment of the potential interactions between CIEDs and the MRI

environment are important to the current and future designs of CIEDs in order to increase accessibility to MRI technology. Because there are now non-MR Conditional as well as MR Conditional CIEDs, the decisions and management of patients with these devices depend on the specific system that is present.

NON-MR CONDITIONAL CIEDS

The study of MRI and CIED interactions stems from known theoretical physics concerns related to the ferromagnetic content of cardiac devices, the effects of time-varying, gradient magnetic fields, and the impact of radiofrequency (RF) energy on the structure and function of CIEDs. In the era prior to the development of MR Conditional CIEDs, these MRI-related issues were studied through multiple means including: *in vitro* assessments, *in vivo* animal models, case reports, small retrospective series of patients inadvertently or intentionally exposed to the MRI environment, and prospective series of patients intentionally exposed to MRI procedures under specified conditions. Each of these lines of research provided data regarding MRI and CIED interactions but had inherent limitations. *In vitro* studies permit an assessment of the physics of MRI and CIED interactions but are limited because phantoms do not adequately reproduce the three-dimensional anatomy or physiology of the patient or *in vivo* device function. Animal models also have limited applicability to human subjects. Rare case reports of inadvertently scanned CIED patients with associated mortality lacked complete information on the patients, specific circumstances of the studies and, importantly, the fact that physiologic monitoring was not used (1-3). Notably, retrospective studies of patients with preexisting CIEDs do not serve as a true surrogate for properly performed MRI safety investigations.

Data from the pre-MR Conditional cardiac device era demonstrated that a small number of adverse events of variable clinical significance occurred in patients with CIEDs who underwent MRI (**Table 1**). In regard to permanent cardiac pacemakers, case series and prospective studies of patients intentionally exposed to MRI exams under specified conditions demonstrated various findings including: heating or discomfort at the implantable pulse generator (IPG) site (4), elevated cardiac biomarkers (5), MRI-related ectopy (4, 6-8), short pauses (9), asystole (10), pulse generator changed to the asynchronous mode due to activation of the reed switch (11), decreased battery voltage with subsequent recovery (12), clinically unimportant changes in sensing, pacing capture threshold, battery voltage, and lead impedance which did not require an increase in pacing output (13-20), significant change in the pacing threshold requiring an increase in programmed output (21), transient change to the elective replacement indicator (ERI) (22), ventricular lead impedance rise necessitating lead replacement (23), temporary, sensing errors and safety signal generation (24), pacing at maximum voltage at a fixed rate of 100-beats/minute (25), rapid pacing (26), communication failure (24, 27), power-on reset (4, 6, 17, 27-31), elective replacement indices reached after scanning (27), and other issues.

With respect to implantable cardioverter defibrillators (ICDs), reports of patients inadvertently subjected to MRI have shown inappropriate sensing, battery voltage transient or sustained change to End-of-Life (EOL) (32), inability to communicate with the device (33), noise detected as ventricular tachycardia and ventricular fibrillation, with no therapy presumably due to magnetic mode activation and asynchronous pacing as a result of a change

676 MRI and Cardiac Devices

Table 1. Summary of MRI case reports and studies involving patients with non-MR Conditional cardiac pacemakers and ICDs.

Author	Device Type	Study Year	Patient/Studies Report Type	MRI Conditions	Results
Iberer, et al. (174)	PPM	1987	1/1 Case Study	Unknown	No adverse effect.
Alagona, et al. (175)	PPM	1989	1/1 Case Intentional	1.5-T Brain	No adverse effect.
Inbar, et al. (176)	PPM	1993	1/1 Case Intentional	1.5-T Brain	No adverse effect.
Gimbel, et al. (9)	PPM	1996	5/5 Retrospective Intentional	0.35- to 1.5-T Cardiac, Brain, C-Spine	Two second pause.
Garcia-Boloa, et al. (177)	PPM	1998	1/2 Case Intentional	1-T Brain	No adverse effect.
Fontaine, et al. (26)	PPM	1998	1/1 Case Intentional	1.5-T Brain, C-Spine	Rapid pacing.
Sommer, et al. (11)	PPM	1998	18/18 Prospective	0.5-T Brain, Cardiac, Vascular	Asynchronous mode due to activation of the reed switch in all patients.
Sommer, et al. (178)	PPM	2000	45/51 Prospective	0.5-T, Multiple anatomic sites imaged	No adverse effect.
Vahlhaus, et al. (12)	PPM	2001	32/34 Prospective	0.5-T, Multiple anatomic sites imaged	Decrease in battery voltage recovered at three months.
Anfinsen, et al. (32)	ICD	2002	1/1 Case Inadvertent	0.5-T Brain	Inappropriate sensing, battery voltage transient change to EOL.
Martin, et al. (21)	PPM	2004	54/62 Prospective	1.5-T, Multiple anatomic sites imaged	Significant change in pacing threshold in 9.4% of leads, and 1.9% of leads requiring an increase in programmed output.
Fick, et al. (33)	ICD	2004	1/1 Case Inadvertent	0.5-T Brain	Unable to communicate with device.
Coman, et al. (37)	ICD	2004	11/11 Prospective	1.5-T Cardiac, Vascular, General	Brief asymptomatic pause in one patient. Unable to communicate with device in one patient.
Del Ojo, et al. (60)	PPM	2005	13/13 Prospective	2-T, Multiple anatomic sites imaged	No adverse effect.
Rozner, et al. (22)	PPM	2005	2/2 Case Intentional	1.5-T Thorax, Lumbar	Transient change to ERI in one patient.
Gimbel, et al. (14)	PPM	2005	10/11 Prospective	1.5-T Brain, C-Spine	Small variances in pacing threshold were seen in four patients.

MRI Bioeffects, Safety, and Patient Management 677

Table 1. (Continued) Summary of MRI examinations involving patients with cardiac pacemakers and ICDs.

Author	Device Type	Study Year	Patient/Studies Report Type	MRI Conditions	Results
Gimbel, et al. (38)	ICD	2005	7/8 Prospective	1.5-T Brain, L-Spine	“Power on reset” electrical reset requiring reprogramming in one patient.
Roguin, et al. (117)	ICD	2005	1/1 Case Intentional	1.5-T Cardiac	No adverse effect.
Wollmann, et al. (179)	ICD	2005	1/3 Case Intentional	1.5-T Brain	No adverse effect.
Sardanelli, et al. (180)	PPM	2006	1/1 Case Intentional	1.5-T Breast	No adverse effect.
Sommer, et al. (15)	PPM	2006	115/82 Prospective	1.5-T Extra-thoracic	Significant increase in pacing threshold, decreased lead impedance, and decrease in battery voltage. No inhibition of pacing or arrhythmias and no leads that required an increase in pacing output.
Naehele, et al. (107)	ICD	2006	1/1 Case Intentional	1.5-T Brain	No adverse effect.
Nazarian, et al. (118)	PPM 31 ICD 24	2006	55/68 Prospective	1.5-T	No adverse effect.
Nemec, et al. (34)	ICD	2006	1/1 Case Unintentional	Unknown Brain	Noise detected as ventricular tachycardia and ventricular fibrillation, with no therapy presumably due to magnetic mode activation. Asynchronous pacing due to noise-reversal mode.
Heatlie, et al. (25)	PPM	2007	5/6 Prospective	0.5-T Cardiac	Pacing at maximum voltage at a fixed rate of 100 beats/minute in one patient.
Mollerus, et al. (181)	PPM 32 ICD 5	2008	37/40 Prospective	1.5-T Trunk and other areas scanned	No adverse effect. No changes in cardiac troponin-I.
Naehele, et al. (109)	PPM	2008	44/51 Prospective	3-T Brain	No adverse effect. No changes in cardiac troponin-I. Use of transmit/receive RF head coil, only.

678 MRI and Cardiac Devices

Table 1. (Continued) Summary of MRI examinations involving patients with cardiac pacemakers and ICDs.

Author	Device Type	Study Year	Patient/Studies Report Type	MRI Conditions	Findings
Gimbel 2008 (110)	PPM 9 ICD 5	2008	13/15 Prospective	3-T Brain, Jaw, Lumbar spine, Thigh	One patient with a sensation of chest burning during the scan.
Gimbel, et al. (10)	PPM	2009	1/1 Case Intentional	1-T Brain	Asynchronous pacing mode (VOO) reversion to a back-up mode (VVI) with pacing inhibition from noise. Asystole, lack of pacing support for > 10 seconds with native escape rhythm.
Goldsher, et al. (182)	PPM	2009	1/1 Case Intentional	1.5-T Cervical	No adverse effect. Scan one day after implantation Pacemaker-dependent.
Mollerus, et al. (7)	PPM 46 ICD 6	2009	52/59 Prospective	1.5-T Trunk and other areas scanned	MRI-related ectopy in seven patients.
Naehle, et al. (16)	PPM	2009	47/171 Case Intentional	1.5-T General	Statistically significant but clinically irrelevant change in pacing capture threshold and battery voltage. Two or more serial scans.
Pulver, et al. (119)	PPM	2009	8/11 Prospective	1.5-T Cardiac, Non-cardiac	No adverse effect. Congenital heart disease with nine epicardial leads.
Strach, et al. (183)	PPM	2010	114/114 Prospective	0.2-T General	No adverse effect.
Millar, et al. (184)	PPM	2010	1/1 Case Study	1.5-T Brain C-spine	No adverse effects.
Burke, et al. (41)	PPM 24 ICD 10 CRT-ICD 4	2010	38/92 Prospective	1.5-T Brain, Spine, Pelvis, Extremity	No adverse effects No changes defibrillation threshold (ICD).
Buendia, et al. (24)	PPM 28 ICD 5	2010	33/33 Prospective	1.5-T Cardiac, Brain, Spine, Abdominal, Extremity	Temporary communication failure in two patients. Sensing errors during imaging in two patients. Safety signal generated in one pacemaker at the maximum magnetic resonance frequency and output level.
Naehle, et al. (121)	PPM 22 ICD 10	2011	32/32 Prospective	1.5-T Cardiac	No adverse effect. Diagnostic value greater for right-sided than left-sided implants.

MRI Bioeffects, Safety, and Patient Management 679

Table 1. (Continued) Summary of MRI examinations involving patients with cardiac pacemakers and ICDs.

Author	Device Type	Study Year	Patient/Studies Report Type	MRI Conditions	Results
Nazarian, et al. (17)	PPM 54% ICD 46% CRT 12%	2011	438/555 Prospective	1.5-T Thoracic, Non-thoracic.	Changes in right ventricular sensing, lead impedances, increased capture threshold and decreased battery voltage were noted at six month follow-up, but did not require device revision or reprogramming. In 1.5% of patients, transient reversions to back-up programming mode were noted (power-on-reset) without long-term sequelae.
Juntilla (129)	ICD	2011	10/30 Prospective	1.5-T Cardiac	Three serial studies in each patient. No adverse effect.
Baser, et al. (23)	PPM	2012	1/1 Prospective	Unknown Brain	Ventricular lead increased impedance and elevation of cardiac biomarkers. Ventricular lead was replaced.
Cohen, et al. (18)	PPM 85 ICD 40	2012	109/125 Retrospective Case Controlled	1.5-T Brain, Spine (All levels), Cardiac, Extremities	Decreases in battery voltage. Pacing threshold increases. Pacing lead impedance changes. Changes statistically significant but not clinically important and similar to control group.
Boilson, et al. (6)	PPM	2012	32/46 Prospective	Unknown Head, Spine	No clinically important adverse effects. “Power-on reset” in six scans, magnet-mode pacing in four scans, occasional ectopy in one patient .
Cohen, et al. (18)	PPM 85 ICD 40	2019	109/125 Prospective	1.5-T Multiple anatomic sites imaged	No clinically adverse effects. Battery voltage decrease \geq 0.04V in 4 cases, pacing threshold increase \geq 0.5V in 5 cases, pacing lead impedance change \geq 50 Ω in 13 cases

680 MRI and Cardiac Devices

Table 1. (Continued) Summary of MRI examinations involving patients with cardiac pacemakers and ICDs.

Author	Device Type	Study Year	Patient/Studies Report Type	MRI Conditions	Results
Friedman, et al. (8)	PPM 8 (\leq 42d old) PPM 211 (>42 d old)	2013	171/219 Prospective	1.5-T Head, Spine	No clinically important adverse effects. One patient had frequent ectopy requiring no treatment.
Brockmann, et al. (185)	CRT	2013	1/1 Case Inten-tional	1.5-T Head, Spine	No adverse effects.
Macfie, et al. (186)	PPM	2013	1/1 Case Inten-tional	Unknown Head, Neck	No adverse effects.
Muehling, et al. (187)	PPM	2014	356/356 Prospective	1.5-T Head	No adverse effects.
Keller, et al. (62)	scICD	2015	15/22 Prospective	1.5-T Multiple anatomic sites imaged	No adverse effects.
Shenthalar, et al. (188)	PPM	2015	159/159 Prospective	1.5-T Head, Chest	No adverse effects.
Higgins, et al. (28)	PPM 192 ICD 6	2015	198/256 Prospective	1.5-T Head, Chest	Nine studies with power-on reset with decrease in heart rate during scan (four) and transient anomalous battery life indication (one CRT-D). All devices with normal function after study.
Sheldon, et al. (189)	PPM 9 ICD 31	2015	42/40 Prospective CRT-P 7 CRT-D 31 CS, only ventricular lead 2	1.5-T Multiple anatomic sites imaged	No adverse effects.
Atar, et al. (35)	ICD 1	2016	1 Case Inadver-tent CRT-D	0.2-T Lumbar spine	ICD shock due to inappropriate sensing, battery depletion, “End of Life” (EOL) indicator requiring battery replacement
Dandamudi, et al. (190)	PPM 29 ICD 29	2016	58/62 Retro-spective 51 non-MR Conditional	1.5-T Cardiac, T-spine	No adverse effects.

MRI Bioeffects, Safety, and Patient Management 681

Table 1. (Continued) Summary of MRI examinations involving patients with cardiac pacemakers and ICDs.

Author	Device Type	Study Year	Patient/Studies Report Type	MRI Conditions	Results
Delve, et al. (191)	PPM	2016	1/1 Case International Single chamber PPM with atrial port plug (non-MR Conditional device)	1.5-T L-spine	No adverse effects.
Higgins, et al. (5)	PPM 283 ICD 65	2016	398/512 Prospective	1.5-T Multiple anatomic sites imaged	Twenty-two exams with troponin T change ≥ 0.002 ng/mL. No adverse effects.
Hussam-Ali, et al. (192)	PPM	2016	1/1 Case International	1.5-T Cardiac	No adverse effects.
Hwang, et al. (193)	PPM 38 ICD 2	2016	40/50 Retrospective 29 non-MR Conditional	1.5- and 3-T Multiple anatomic sites imaged	No adverse effects.
Horwood, et al. (99)	PPM 36 ICD 106	2017	142/160 Prospective	1.5-T Cardiac, Spine, Brain	No adverse effects. Minor device parameter changes, no reprogramming needed. Backup rate change from 90 to 50 in one case.
Okamura, et al. (27)	PPM 421 ICD 148	2017	442/569 Prospective	1.5-T Head, Chest	No adverse effects. Two scans in one patient close to ERI had “power-on reset” (pacemaker). One pacemaker reached ERI after scan.
Ono, et al. (194)	PPM 46 ICD 3	2017	49/58 Retrospective	1.5-T Multiple anatomic sites imaged	No adverse effects.
Russo, et al. (30)	PPM 1000 ICD 500	2017	1,246/1,500 Prospective All devices non-MR Conditional	1.5-T Non-thoracic	No adverse effects. Six cases had partial electrical reset (all pacemakers). 16.4% ICD leads with 3-ohm change in impedance. Unable to interrogate one ICD, electively replaced.

682 MRI and Cardiac Devices

Table 1. (Continued) Summary of MRI examinations involving patients with cardiac pacemakers and ICDs.

Author	Device Type	Study Year	Patient/Studies Report Type	MRI Conditions	Results
Shah, et al. (19)	PPM 74 ICD 39	2017	105/113 Prospective 97 scans non-MR Conditional 16 scans MR Conditional	1.5-T Multiple anatomic sites imaged	No adverse effects. Small, nonsignificant changes in lead characteristics.
Strom, et al. (4)	PPM 77 ICD 46	2017	123/189 Prospective non-MR Conditional devices	1.5-T Multiple anatomic sites imaged	One case of “power-on reset” leading to loss of pacing due to inhibition from electromagnetic interference (pacemaker). One case of self-limiting atrial arrhythmia (pacemaker). Two cases with heating/discomfort at the generator site (pacemaker).
van Dijk, et al. (108)	PPM	2017	32/32 Prospective	1.5- and 3-T Multiple anatomic sites imaged	No adverse effects.
Yadava, et al. (195)	PPM 170 ICD 71	2017	227/293 Prospective	1.5-T Multiple anatomic sites imaged	No adverse effects.
Bertelsen, et al. (13)	PPM	2017	184/207 Retrospective	1.5-T Multiple anatomic sites imaged	No adverse effects. Small, clinically insignificant increase in atrial sense.
Nazarian, et al. (31)	PPM 880 ICD 466 CRT-D 163	2017	1509/ 2103 Prospective	1.5-T Multiple anatomic sites imaged	No long-term clinically significant adverse events. were reported. 9 studies with device reset to a backup mode (8 transient) (1 pacemaker with less than 1 month left of battery life reset to ventricular inhibited pacing and could not be reprogrammed). Nonsignificant acute decrease in P-wave amplitude 1%; long-term decreased P-wave amplitude 4%, increased in right ventricular capture threshold (4%) and increased left ventricular capture threshold (3%).

MRI Bioeffects, Safety, and Patient Management 683

Table 1. (Continued) Summary of MRI examinations involving patients with cardiac pacemakers and ICDs.

Author	Device Type	Study Year	Patient/Studies Report Type	MRI Conditions	Results
Lupo, et al. (196)	PPM 71 ICD 71	2018	120/142 Prospective	1.5-T Multiple anatomic sites imaged	No adverse effects.
Nyotowidjojo, et al. (39)	PPM 111 ICD 89 CRT-P 2 CRT-D 36	2018	238/339 Prospective Non-MR Conditional devices	1.5-T Cardiac, chest, T-spine	No adverse effects. 1 case of “power-on reset,” re-programmed after scan without clinical event (CRT-D).
Shah, et al. (40)	PPM 3,692 ICD 1,440 LV lead 268	2018	5,099/5,908 Retrospective, meta-analysis Non-MR Conditional devices	1.5- and 3-T Multiple anatomic sites imaged	3 lead failures, 1 ICD shock, 94 “power-on reset” events in older devices (before 2007). Small, clinically insignificant changes in lead characteristics and battery voltages.
Xiong, et al. (20)	PPM	2018	86/86 Prospective	1.5-T Multiple anatomic sites imaged	Twelve patients with symptoms (anxiety, elevated BP, elevated HR). Ten pacemaker abnormalities (20% increase impedance, sensing abnormalities), but no significant intervention needed.
Seewöster, et al. (36)	PPM 46 ICD 105 scICD 1 ILR 49 BIV 22	2019	200/200 Retrospective 27 non-MR Conditional PPM 76 non-MR Conditional ICD	1.5-T Cardiac	One device premature end of service. Three cases of ventricular tachycardia unrelated to device or scanning, successfully treated. 10 ICD decreased battery capacity following scan.
Tanaka, et al. (197)	Unknown	2019	25/28 Retrospective	1.5-T Pelvic	No adverse events.
Padmanabhan, et al. (198)	PPM 45 ICD 54 CRT-D 17	2019	120/134 Prospective	1.5-T Thoracic	No adverse events.
Han, et al. (199)	PPM 28 ICD 7	2019	35/43 Retrospective 21 non-MR Conditional	1.5-T Multiple anatomic sites imaged	No adverse events.

684 MRI and Cardiac Devices

Table 1. (Continued) Summary of MRI examinations involving patients with cardiac pacemakers and ICDs.

Author	Device Type	Study Year	Patient/Studies Report Type	MRI Conditions	Results
Rahsepar, et al. (93)	PPM 853 ICD 454 CRT-D 157	2020	1,464/2,028 Prospective Inclusion of patient data from previous publications (17, 118, 132).	1.5-T Multiple anatomic sites imaged	No association between radiofrequency energy deposition, changes related to gradient magnetic fields, or scan duration and changes in device parameters. Thoracic MRI was associated with decreased battery voltage immediately after MRI. Longer right ventricular lead length was associated with decreased right ventricular sensing and capture threshold immediately after MRI.

Adapted and updated from Shinbane, et al. (54) with permission of Biomed Central. Case, case report; ICD, implantable cardioverter defibrillator; CRT, cardiac resynchronization therapy; CRT-P, cardiac resynchronization therapy pacemaker; CRT-D, cardiac resynchronization therapy defibrillator; scCRT, subcutaneous cardiac resynchronization therapy; EOL, end-of-life; ERI, elective replacement indicator; ICD, implantable cardioverter defibrillator; PPM, pacemaker; T, Tesla.

to the noise-reversal mode (34), and inappropriate shock with battery change to EOL (35). Case series and prospective study of patients intentionally exposed to the MRI examinations under specified conditions have demonstrated various findings including: MRI-related ectopy (7, 8), sensing errors (24), decreases in battery voltage, pacing threshold increases, changes in pacing and high-voltage lead impedance changes that were statistically significant but clinically unimportant (17, 18, 30, 31, 36), transient anomalous battery life indication (28), inability to communicate with a devices (30, 37) and power-on reset (17, 28, 29, 31, 38-40). In addition to issues related to performing MRI in patients with ICDs, investigators have raised the issue as to whether non-MR Conditional ICD defibrillation threshold testing should be performed after exposure to an MRI exam (41). This important matter warrants further study.

Prospective studies and registries have also been performed to assess for adverse effects associated with MRI in patients with non-MR Conditional CIEDs. In a large prospective study using MRI in patients with CIEDs, a total of 438 patients with cardiac devices (54% pacemakers and 46% ICDs) were enrolled between 2003 and 2010 (17). Of these patients, 53 (12%) had biventricular pacing systems. Patients with new devices (less than six weeks), abandoned or epicardial leads, and pacemaker-dependent patients were excluded from the study. In addition, pacemaker-dependent, ICD patients were excluded. Of a total of 555 MRI examinations performed at 1.5-Tesla/64-MHz, 18% of the scans were thoracic and 82% were non-thoracic. Although changes in right ventricular sensing, lead impedances, increased capture threshold and decreased battery voltage were noted at the six month follow

up interval, the observed changes did not require device revision or reprogramming. In three (1.5%) of the patients, transient reversions to back-up programming mode were noted (i.e., power-on reset) without long-term sequelae.

The MagnaSafe Registry was a prospective multicenter site registry of patients with non-MR Conditional pacemakers and ICDs that underwent clinically indicated, 1.5-Tesla/64-MHz non-thoracic scanning under specified conditions (30). Data was collected before, immediately after, and at 6 months following 1,000 MRI exams in patients with cardiac pacemakers ($n=818$) and 500 MRI exams in patients with ICDs ($n=428$) between April 2009 and April 2014. The results demonstrated no deaths, lead failures, or capture losses during non-thoracic MRI examinations. There were six cases of self-terminating atrial fibrillation or flutter, as well as six cases of partial electrical reset. There were no cases of full electrical reset. Of the pacemaker patients, 28% of the registry patients were pacemaker-dependent. Pacemaker-dependent ICD cases were excluded from the study. One ICD required replacement after it could not be interrogated following the MRI exam, however, this device had not been reprogrammed according to the study protocol beforehand. Sub-analysis suggested performing subsequent MRI exams for patients with implanted cardiac devices did not increase the risks of clinical events compared to patients who underwent a single scan.

A large prospective study reported safety data on 2,103 MRI exams (multiple 1,509 patients included 880 patients with cardiac pacemakers, 466 with ICDs, and 163 with cardiac resynchronization therapy defibrillator, CRT-D, devices studied at 1.5-Tesla/64-MHz at various anatomical positions) (31). Of this cohort, nine studies resulted in transient reset to a backup mode (seven pacemaker and one ICD). In one MRI exam, a pacemaker with less than one month left of battery life reset to ventricular inhibited pacing and could not be reprogrammed.

Non-significant, acute decrease in P-wave amplitude was present in 1% of cases. In the 63% of cases in which long-term data were available, decreased P-wave amplitude was present in 4% of patients, increased in right ventricular capture threshold in 4% of patients and increased left ventricular capture threshold in 3% of patients. These changes were not clinically significant and did not necessitate cardiac device reprogramming or revision. Of note is that there were no long-term clinically significant adverse events reported.

Meta-analysis of data related to performance of MRI in patients with non-MR Conditional devices has also been reported. The largest meta-analysis to date reviewed data from 5,099 patients with non-MR Conditional devices that underwent 5,908 scans between 1990-2017 (40). Of this group, 551 patients were pacemaker-dependent. There were no reported patient deaths and three lead failures. There were no clinically relevant changes in lead, battery, or pulse generator performance.

The evolving medical literature has led to an expert consensus statement from the Heart Rhythm Society (HRS) developed in collaboration with and endorsed by other multidisciplinary societies for the strategy to using MRI in patients with non-MR Conditional CIEDs (42). The societies included the Japanese Heart Rhythm Society, Brazilian Society of Cardiac Arrhythmia, Council of Affiliated Regional Radiation Oncology Societies, American College of Radiology, American Society for Radiation Oncology, European Heart Rhythm

686 MRI and Cardiac Devices

Association, Pediatric and Congenital Electrophysiology Society, American College of Cardiology, Asia Pacific Heart Rhythm Society, Latin American Society of Cardiac Stimulation and Electrophysiology, and the American Heart Association. These guidelines provide recommendations for the decision to perform an MRI and the management of patients with non-MR Conditional CIEDs undergoing MR imaging. The (HRS) document states: “It is reasonable for patients with non-MR Conditional CIEDs system to undergo MR imaging if there are no fractured, epicardial, or abandoned leads; the MRI is the best test for the condition; and there is an institutional protocol and a designated responsible MRI physician and CIED physician” (Recommendation: Class IIa, Level of Evidence: B-Nonrandomized) (42). This document provides recommendations delineating institutional workflow, personnel skill set and responsibilities, patient monitoring, equipment and location for potential resuscitative efforts and emergency treatments, CIED peri-scan evaluation, and programming. These recommendations should be followed in the context of the most up-to-date, overall MRI-related safe practices (43, 44).

MR CONDITIONAL CIEDS

The initial body of data related to use of MRI in patients with CIEDs raised questions such as (1) whether patients with important clinical issues to be resolved and no other adequate imaging options had absolute contraindications to MRI, (2) whether scanning had been performed based on the risk:benefit ratio, or (3) would this require the engineering of cardiac devices with MR Conditional labeling status (45-56). The limitations inherent in investigating and scanning patients with previous era devices led to the development of CIEDs designed for the MRI setting under highly specified conditions. Notably, a variety of MR Conditional CIEDs from several different manufacturers (i.e., Abbott/St. Jude Medical, Biotronik, Boston Scientific, LivaNova/Sorin, and Medtronic) have been released for use in the clinical setting. Each commercially available device has specified device and programming requirements as well as MRI parameters and conditions defined in the labeling, approved by the specific regulatory agency of the country where the device has been clinically released.

An expert consensus statement from the Heart Rhythm Society has been developed in collaboration with and endorsed by other multidisciplinary societies with recommendations and protocol for the management of patients with MR Conditional CIEDs undergoing MRI (42). The document states: “MR Conditional devices should be considered MR Conditional only when the product labeling is adhered to, which includes programming the appropriate “MR mode” and scanning with the prerequisites specified for the device” (Recommendation: Class I, Level of Evidence: A) (42). Similar to information for non-MR Conditional CIEDs, this document provides recommendations delineating institutional workflow, personnel skill set and responsibilities, patient monitoring, equipment and location for potential resuscitative efforts and emergency treatments, CIED peri-scan evaluation and programming. These recommendations should be followed in the context of the most up-to-date overall, MRI-related safe practices (43, 44).

MR CONDITIONAL DESIGN AND ENGINEERING

The precise use of nomenclature is extremely important to understanding and implementing technologies as it pertains to specific patient and scanning conditions in the MRI environment (57). The American Society for Testing Materials (ATSM) International designates implants and devices as being MR Safe, MR Conditional, or MR Unsafe (58). An MR Safe designated device would require nonmetallic, non-conducting materials and systems with no known hazards in all MRI environments. Thus, the engineering of an MR Safe designated pacemaker or ICD is not feasible. An MR Conditional designated device refers to an item that has been demonstrated to pose no known hazard in a specified MRI environment under defined conditions of use. These defined conditions may include the strength of the static magnetic field, spatial gradient magnetic field, time-varying, magnetic fields, RF fields (i.e., the specific absorption rate, SAR), and other factors. CIEDs designated as MR Conditional must be used in a specified MRI environment under defined programming parameters and with close attention to the patient specific clinical factors, such as the presence of abandoned or fractured leads. MR Conditional designs have sought to take into account both the theoretical and investigational concerns related to CIEDs and to create technological designs to minimize the possibility for interactions when implanted in patients undergoing MRI exams. Notably, the design and engineering of devices extends to all components including the implantable pulse generator, leads, and, programming software.

ELECTROMAGNETIC-RELATED ISSUES

Because MRI involves the use of static, gradient, and RF electromagnetic fields, these elements must be carefully considered because they can lead to substantial MRI/CIED interactions. Physical forces acting on ferromagnetic objects due to static and gradient magnetic fields can cause movement and/or vibration of these objects. Factors affecting these forces include the quantity and shape of the ferromagnetic content, proximity to the MR system's magnet, and the strength of the static magnetic field (59). Studies of non-MR Conditional and MR Conditional pacemakers at 1.5-Tesla/64-MHz have not demonstrated significant clinical effects (60-62). Conduction of electromagnetic energy through the cardiac device can occur due to the time-varying, gradient magnetic fields and/or the pulsed RF energy, leading to heating or interference with sensing or pacing. This potential energy transfer is dependent on factors including: the features of the time-varying, gradient magnetic fields (e.g., the slew rate, etc.), the type of RF pulse used in the MRI sequences, the whole body averaged and local SARs, the spatial relationship and orientation of the CIED relative to the transmit RF coil, the composition, length, geometry, configuration and orientation of the lead(s), and other factors (63-73).

IMPLANTABLE PULSE GENERATOR DESIGN

The reduction of ferromagnetic content of the pacemaker's or ICD's implantable pulse generator (IPG) can reduce magnetic field interactions. This requires the use of non-ferromagnetic materials with the appropriate characteristics including those related to conductivity, durability, and biocompatibility. The IPG's reed switch is susceptible to magnetic fields because this component allows the use of an external magnet to program continuous

688 MRI and Cardiac Devices

asynchronous pacing while in contact with the patient's skin overlying the IPG in order to avoid electromagnetic interactions with the use of electrocautery during surgical procedures (74). When present in the MR system, reed switch activity may be unpredictable, potentially varying with the orientation between the reed switch and direction of the magnetic field, as well as with the strength of the static magnetic field (3, 61, 75-77). One option is to replace the reed switch with a solid state, Hall sensor, which possesses a more predictable function in the presence of magnetic fields. Other design changes have been formulated such as a magnetic field detection sensor that prevents reed switch-related issues (78). Additional IPG design features include generator shielding and circuitry filters to inhibit or divert transference of particular electromagnetic frequencies. Importantly, IPGs used for ICDs tend to be larger and more complex than those used for cardiac pacemakers. They also have a greater ferromagnetic content, circuitry hardware related to arrhythmia detection and treatment, and capacitors for cardioversion and defibrillation (79-81). Therefore, MRI issues related to ICDs versus cardiac pacemakers tend to be more problematic. Device settings for an "MRI-mode" include pre-scan checklists, programming of pacing mode, disabling sensed activity, and inactivating tachycardia therapies during an MRI exam (42).

CIED LEADS

Pacemaker and ICD leads are composed of non-magnetic materials (e.g., platinum and iridium). With regard to MRI issues, leads may serve as antennas conducting electromagnetic energy impulses (26, 82). The effects of this energy transfer could potentially include pain, myocardial stimulation, heating with myocardial necrosis at the lead tip, and damage to the IPG. Adverse effects potentially include inappropriate sensing, increases in pacing threshold, and lead impedance changes. These factors could lead to inappropriate pacing function with associated bradyarrhythmias or tachyarrhythmias, as well as battery depletion (3, 7, 12, 14-16, 21, 22, 24-26, 83-89). These effects can be due to the transference of MRI-related electromagnetic energies at the resonant frequency of the lead. Importantly, a resonant lead length can be associated with a greater heating effect (90). Therefore, a focus of lead design and engineering is to avoid the resonant frequencies of the electromagnetic sources associated with MR systems through consideration of factors such as lead length, configuration, and morphology. In regard to heating, lead length, lead coiling, and the position of the lead in relation to the transmit RF coil can affect MRI-related heating (65, 69, 91, 92).

In a large prospective study assessing the relationship between SAR and non-MR Conditional CIED function, a longer right ventricular lead length was associated with decreased right ventricular sensing and capture threshold immediately after MRI (93). Lead wire coiling in a three-dimensional orientation is an important factor in transference or avoidance of the resonant frequency of electromagnetic energy (94). Decreasing the number of coiled filars, increasing the diameter of the filars and subsequent increases in the winding turns of the coils has resulted in a three-dimensional morphology for the lead that limits the conduction of MRI relevant frequencies in one design, while maintaining the strength of the lead (95). Furthermore, the use of a lead tip coating has decreased polarization. Because unipolar pacing is more susceptible to the environmental electromagnetic noise including that associated with the MR system, a bipolar lead configuration is also important in lead

design (88, 96).

The presence of abandoned leads can lead to conduction of electromagnetic energy and, therefore, may pose hazards when scanning a patient with an MR Conditional cardiac device. *In vitro* studies have suggested that abandoned pacemaker leads (40 to 60 cm lengths) experienced greater lead tip heating compared to attached leads (97). Small, predominantly retrospective studies in patients with abandoned leads have not demonstrated adverse effects (**Table 2**) (98-101). Considering the differences between *in vitro* and *in vivo* data, there is now controversy regarding how to proceed with MRI scans in patients with abandoned pacing leads. Retained epicardial wires cut short at the skin level from previous cardiothoracic surgical procedures have not been associated with substantial issues during MRI (102, 103). Furthermore, a study of MRI in orthotopic heart transplant recipients with retained CIED fragments was not associated with adverse events (104).

At the time of pacemaker or IPG replacement with pre-existing leads, cognizance of MR Conditional issues should play a role in decision-making. MR Conditional systems re-

Table 2. Summary of MRI examinations involving patients with abandoned pacing leads.

Author	Lead positions	Year	Patient/Studies Report Type	MRI Conditions	Findings
Higgins, et al. (98)	RA 15 RV 14 ICD 3	2014	19/35 Retro-spective Avg. 1.63 leads/scan	1.5-T Head, neck, spine, extremity, pelvis	No adverse effects.
Horwood, et al. (99)	SVC 1 RA 1 RV 1 LV 2 ICD 4 Epicardial 3	2017	10/10 Prospective	1.5-T Cardiac, spine, brain	No adverse effects.
Morris, et al. (100)	SVC 1 RA 1 RV 6 Epicardial 1	2018	9/12 Retrospective	1.5-T Brain, L-spine, C-spine, extremity, pelvis	No adverse effects.
Padmanabhan, et al. (101)	RA 13 RV 34 LV 9 ICD 18 Epicardial 10	2018	80/97 Retro-spective	1.5-T Unknown	No adverse effects.
Schaller RD, et al. (101)	RA 50 RV 70 LV 1 ICD 84 CS 6 Epicardial 30	2021	139/200 Retro-spective	1.5-T Multiple anatomic sites imaged	A low rate of arrhythmia, patient symptoms, and change in device settings was observed.

ICD, implantable cardioverter defibrillator; RA, right atrium; RV, right ventricle; LV, left ventricle; SVC, superior vena cava; CS, coronary sinus; ICD, implantable cardioverter defibrillator; T, Tesla.

quire manufacturer stated compatibility between MR Conditional leads and the respective IPGs. Therefore, at the time of pacemaker or IPG replacement, awareness of this compatibility may influence selection of specific devices to ensure that the entire system remains MR Conditional. If any existing leads have been retroactively labeled MR Conditional, they would need to be connected to a specific IPG that has been labeled as forming an MR Conditional system with those specific leads. Notably, capping an existing lead, even with newer a MR Conditional IPG connected to other MR Conditional leads would render the system non-MR Conditional.

DEVICE PROGRAMMING

The design of an MR Conditional device requires clearly demarcated MR Conditional programming modes for the time period when the patient undergoes MR imaging (42). If MRI is performed in patients with non-MR Conditional devices, specific decisions for programming must also be made (42). Programming of pacing in a sensing mode can lead to inappropriate inhibition of pacing due to lead noise caused by electromagnetic interference due to operation of the MR system (**Figure 1**). Programming decisions require knowledge of the patients underlying sinus rate, atrial-ventricular (AV) nodal conduction, ventricular rate and presence rate, and location of escape rhythms (**Figures 2 and 3**). These programming modes inactivate sensing and, therefore, the pacing function is either inactivated in a patient with a stable non-bradycardic rhythm or set to an asynchronous pacing mode in a pacemaker-dependent patient. Each mode possesses its own potential limitations. A patient

Figure 1. “Noise” in the cardiac pacing lead can result in inappropriate inhibition of ventricular pacing with ventricular pauses. Lead noise can be caused by electromagnetic interference due to operation of the MR system.

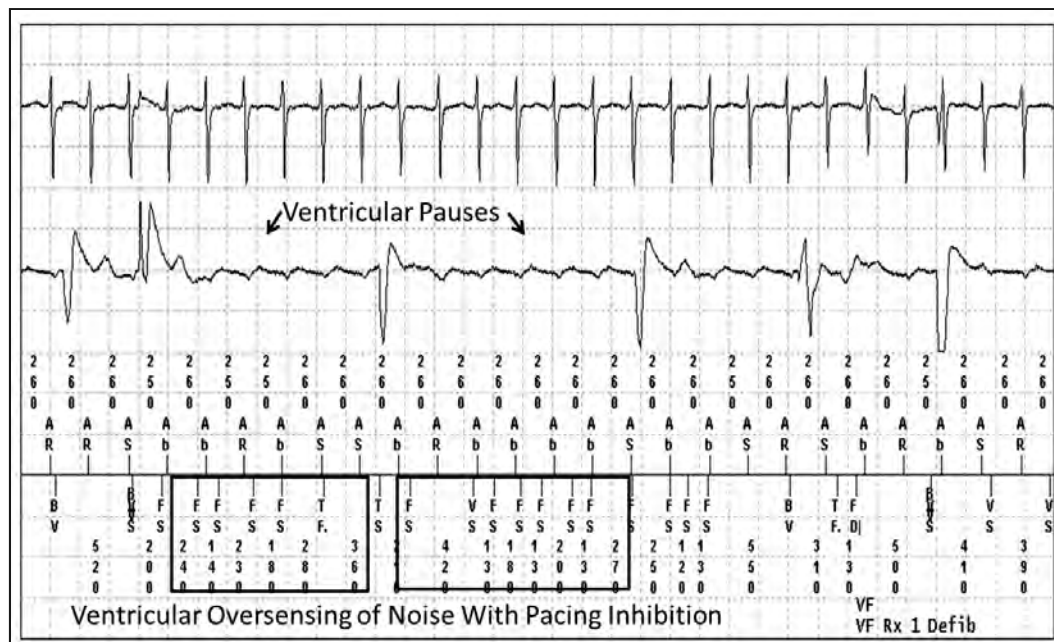
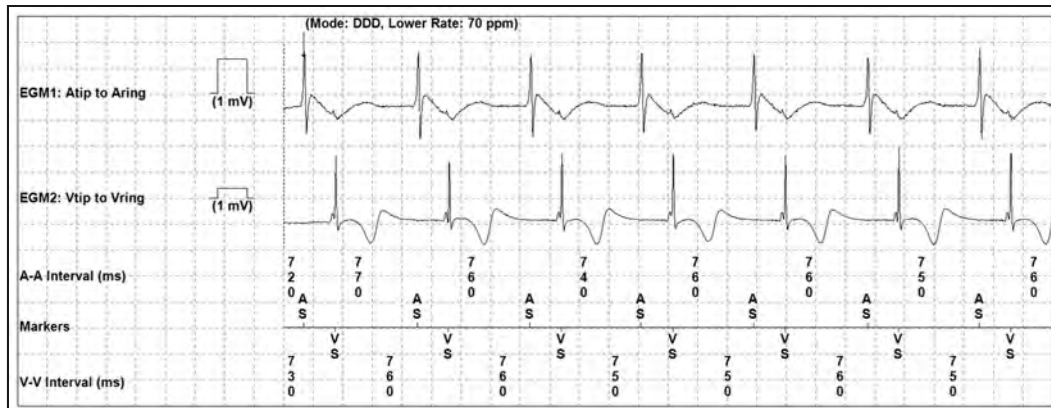


Figure 2. Pacemaker electrocardiograms in the setting of an intrinsic rhythm (non-pacemaker-dependent rhythm). There is an intrinsic sinus rhythm at 80-beats/min. with normal AV nodal conduction. This patient could potentially be programmed to the OOO-mode (non-functioning) for MRI. AS, atrial sensed rhythm; VS, ventricular sensed rhythm.



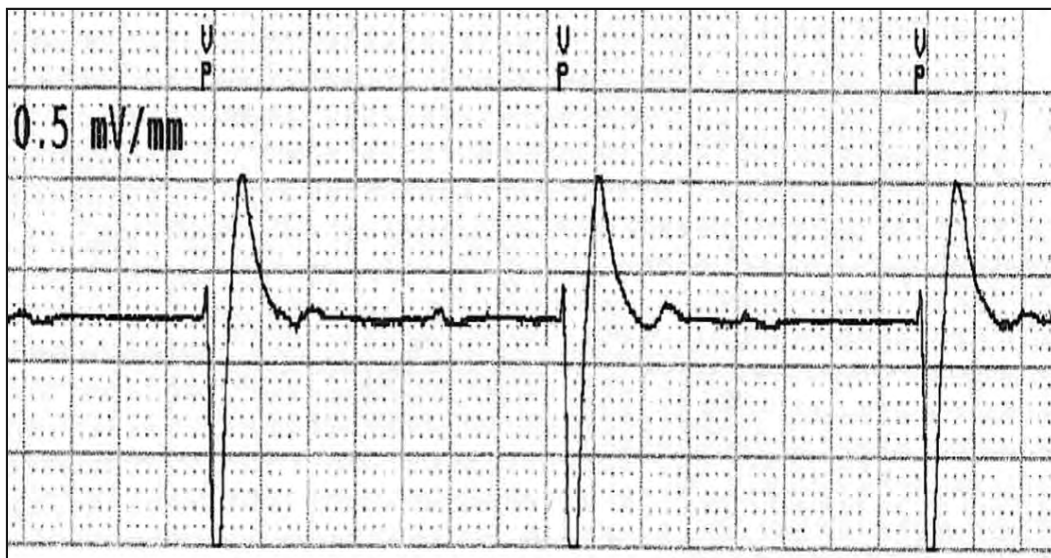
with a non-bradycardic rhythm at the time of programming could potentially have a bradyarrhythmia while in the scanner. If a patient programmed to an asynchronous pacing mode has a ventricular rate competing with asynchronous pacing, paced beats could occur during the vulnerable period of ventricular repolarization (i.e., the R-on-T phenomenon), potentially triggering ventricular tachycardia or ventricular fibrillation (3, 105, 106). In regard to ICDs, the same pacing function issues apply. In addition, antitachycardia therapies need to be inactivated during MRI. It remains unclear if ICD capacitors can properly charge in the MRI environment (107).

Older MR Conditional systems with nearly depleted batteries may result in unintended parameter changes during MRI. In a series of 442 patients, nine patients underwent 13 scans with devices at or near elective replacement indicator (ERI) (27). Two of these scans resulted in power-on reset events. One device programmed to asynchronous A and V pacing (DOO) converted to ERI during the scan and automatically reprogrammed to V only antibradycardia pacing (VVI) mode without any significant consequence. Another device close to ERI experienced an unintended mode change from DOO to VVI without any patient harm. Both devices were implanted before 2005. At the present time, most patients undergoing MRI will likely have newer generations of MR Conditional systems, which are less likely to have power-on reset events. However, caution and close monitoring with electrocardiogram (ECG) and pulse oximetry are recommended for patients that undergo MRI with devices close to ERI.

Considering the possibilities of bradyarrhythmias or tachyarrhythmias while the patient is in an MR Conditional mode or programmed for scanning for non-MR Conditional CIEDs, continuous monitoring of the patient's heart rate and rhythm as well as the ability to respond to an arrhythmia is required while the patient is programmed in the appropriate mode (42). Because artifacts related to the scanning can make electrocardiograms particularly challenging to interpret, the use of pulse oximetry is a necessity. Because the CIED programmer

692 MRI and Cardiac Devices

Figure 3. Pacemaker electrocardiogram in the setting of pacemaker-dependence. Note that there is no underlying intrinsic ventricular rhythm with ventricular pacing at 35-beats/min. A patient with this rhythm would need to be programmed to an asynchronous mode (DOO or VOO) for an MRI examination. VP, ventricular paced rhythm.



must stay outside of the MR system room, device programming immediately before entering the scanner room and reprogramming immediately after removal from the MRI setting can limit the amount of time that the patient is in the MR Conditional mode. Programming that permits storing of pre-MRI parameters for reprogramming the device after the MRI procedure is essential.

THE MR SYSTEM AND CIEDS

The first generation of MR Conditional cardiac pacemakers was approved by regulatory agencies for 1.5-Tesla/64-MHz scanners in 2008. Several, newer generation systems are now available with approval for 3-Tesla/128-MHz scanning. Additionally, there are ongoing investigations of MRI examinations using scanners greater than or less than 1.5-Tesla (108). One study evaluated the effect of 3-Tesla brain imaging in 41 patients undergoing MRI exams with non-MR Conditional pacemakers and found no safety events, elevations in troponin, or changes in lead parameters after scanning (109). Another single center study of non-MR Conditional pacemakers and ICDs followed 14 patients after 3-Tesla MRI exams without excluding pacemaker dependency, region scanned, or device type (110). Pacemaker-dependent patients were programmed to an asynchronous mode during the scans, while nondependent-pacemaker patients were set to the OOO mode, which essentially is turned off. Immediately after scanning and at one to three month follow-up periods, no patients suffered arrhythmias or changes in pacing parameters.

It is important to delineate pacemaker-dependent patients when undergoing higher Tesla MRI exams (i.e., 3-Tesla) with non-MR Conditional devices. The same investigator as the

previous study reported a case of brief asystole in a patient that had a 3-Tesla brain scan whose non-MR Conditional pacemaker in the asynchronous pacing mode (VOO) reverted to a back-up mode (VVI) and became inhibited due to “noise” during MRI (10). Regarding static magnetic field forces, a lower magnetic field strength and a greater distance of the CIED from the magnet of the MR system can decrease magnetic field interactions. The use of specialized dedicated-extremity or niche scanners used in patients with CIEDs has been previously reported and requires further assessment (111-113).

The first commercially released MR Conditional cardiac devices had limitations with respect to the transmit RF coil isocenter or landmarking position used for the patient, which effectively prohibited chest/thorax MRI examinations. Investigations have assessed the safety of performing cardiac MRI scans in the presence of CIEDs. A single center pilot study of 36 patients undergoing 1.5-Tesla cardiac MRI exams found no immediate adverse events during or after the MRI exams (114). Seven patients had significant increases in the ventricular pacing capture threshold, which spontaneously resolved in five patients and persisted in two patients at long-term follow-up. This difference in capture threshold was speculated to be due to MRI exam. This pilot study demonstrated the safety and feasibility of performing MR imaging with landmarks placed over the thorax in patients with cardiac pacemakers.

Further clinical applications and safety investigations of cardiac MRI in the setting of CIEDs have been conducted showing no significant harm (115, 116). Later regulatory-approved CIEDs allowed chest/thorax imaging. The investigation of the ability to image this anatomic area is obviously important to allow the greater implementation of MR Conditional cardiac devices. With respect to having CIEDs in the “field of view” or area of interesting, imaging artifacts related to signal loss and/or distortion caused by the device (i.e., the IPG and leads) are important factors that impact the diagnostic use of MRI, particularly for cardiac and thoracic examinations (87, 117-120). Research studies involving non-MR Conditional devices with cardiac imaging have demonstrated decreased artifact and improved imaging quality with CIEDs positioned in the right chest region (121, 122). Artifacts can also affect MRI when certain pulse sequences are used for image acquisition (122, 123). A multicenter study of 175 patients that had cardiac MRI with pacemakers and ICDs found that the probability for better image quality was greater for fast-gradient-echo (FGE) pulse sequences compared to steady-state-free-precession (SSFP) sequences (124). Because of the materials used for cardiac pacemaker leads, artifacts were significantly smaller than ICD lead artifacts. With the use of specific imaging sequences and wideband filtering algorithms that can dramatically reduce susceptibility artifacts, MRI remains interpretable in the presence of implanted cardiac pacemakers and ICDs (125-128).

The impact of multiple scans on patients with MR Conditional devices has been investigated in both small and large case series (17, 18, 129-131). The largest series to date followed 2,629 patients with MR Conditional pacemakers over a four year period (131). Five hundred twenty-six (28.5%) patients had MRI scans, of which 355 (67.5%) had one scan, 97 (18.4%) had two scans, and 74 (14.1%) had three or more scans. In one case, the patient had 11 scans. Of the 171 patients that had two or more scans, there were no MRI-related complications during or after scanning, as well as no cumulative increase in pacing capture threshold when followed long-term.

694 MRI and Cardiac Devices

MR Conditional systems have specific SAR limitations regarding the whole body averaged SAR and the SAR at the region of interest, such as the head SAR for brain MRI examinations. These specifications are available from individual device manufacturers to help guide imaging protocols during MRI exams. A prospective study evaluated the relationship between whole body averaged SAR values and the function of non-MR Conditional CIEDs. The study cohort of 1,464 patients underwent a total of 2,028 scans of multiple body regions. Of these patients, 853 had pacemakers, 454 ICDs, and 157 had CRT-D devices (93). The investigation included data from previous publications by the investigators (17, 118, 132). The authors reported that there was no association between radiofrequency energy power deposition, changes related to gradient magnetic fields, or scan duration and changes in CIED parameters. Thoracic MRI exams were associated with decreased battery voltage immediately after MRI in comparison to other imaging areas. Longer right ventricular lead length was association with decreased right ventricular sensing and capture threshold immediately after MRI. Research should continue regarding the evaluation of SAR limits, especially regarding clinically useful ranges of SARs for different types of MRI procedures.

MR CONDITIONAL CARDIAC DEVICE SYSTEMS

MR Conditional CIEDs are now readily available for clinical use and many newer systems are undergoing active investigation or planned for future studies (61, 77, 123, 133-140). For pacemakers and ICDs, the MR Conditional platforms consist of an MR Conditional IPGs, MR Conditional leads, and an MR Conditional programming device. A randomized, unblinded, two arm, multi-center study of MR Conditional pacemaker patients with standard criteria for dual chamber pacing (484 enrolled, 464 with successful implant, 258 randomized to a single non-medically indicated MRI examination and 206 randomized to a control group) reported no significant changes in pacing parameters (i.e., sensing, threshold, or impedance changes) compared to the control group (61). Both pacemaker-dependent and non-pacemaker-dependent patients were studied, with CIEDs in the asynchronous mode ($n = 158$) and no pacing ($n = 67$). The patients had continuous stable rhythms during MRI without complications reported through the one month visit including arrhythmias, electrical reset, inhibition of implantable pulse generator output, or adverse sensations.

A single-center, prospective, non-randomized study of MR Conditional pacemaker patients with standard pacemaker indications was performed in patients undergoing brain and lower lumbar spine MRI exams at 1.5-Tesla/64-MHz (123). Of the 30 patients scanned that were evaluated immediately pre-study, immediately after MRI, and at one and three month follow-up periods, there were no demonstrations of serious adverse device effects with respect to sensing, pacing, or lead impedance. In regard to the quality of the MRI examinations, there were imaging artifacts on brain diffusion-weighted pulse sequences. Power-on reset of an MR Conditional pacemaker in a pacing dependent patient has been reported during a 1.5-Tesla, brain MRI (29). There was subsequent malfunction of the device clock after the scan.

Since then FDA gave its first approval for an MR Conditional CIED (77), other MR Condition CIEDs including leadless pacemakers, ICDs, subcutaneous ICDs, and implantable loop recorders have been developed and studied for clinical use (19, 61, 108, 114, 116, 141-151). All major manufacturers have released FDA-approved MR Conditional de-

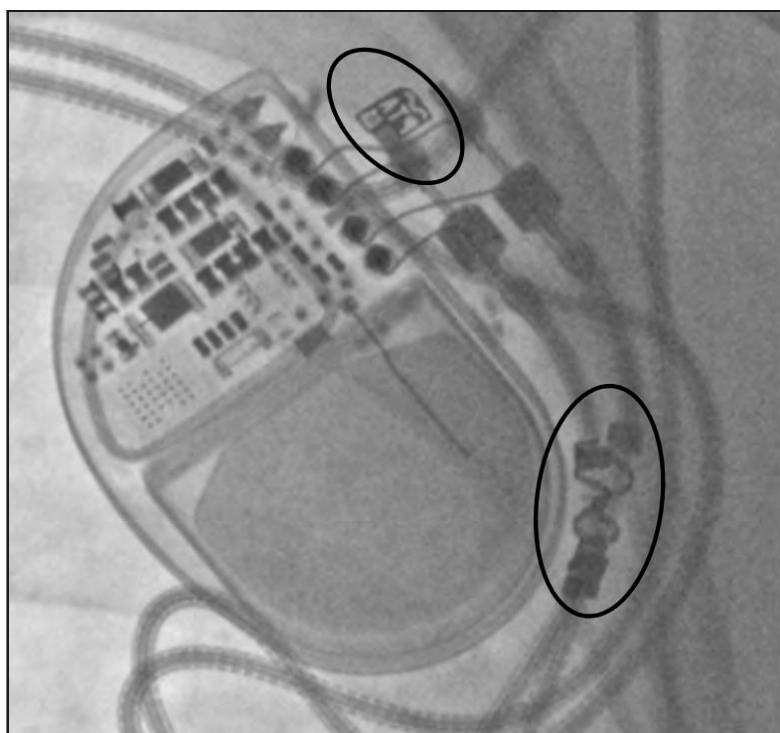
vices that are in clinical use. Importantly, in certain cases, the IPGs and leads of these CIEDs have specific markers to indicate that the components are MR Conditional (**Figure 4**). Each manufacturer has specific MR Conditional labeling as their products are released into market. Importantly, as previously mentioned, each MR Conditional device refers to the full system consisting of an MR Conditional IPG, MR Conditional leads, and MR Conditional programming device. Therefore, even though individual components may be marked as MR Conditional, information is still required to ensure that all components when connected are designated as an MR Conditional system.

Post-market data are important for the assessment of these CIEDs in larger populations and over longer periods of time (30, 42, 95, 114, 152, 153). A post-market study of 2,629 patients in 81 centers of an MR Conditional cardiac pacemaker demonstrated safety with MR imaging, including the ability to perform multiple scans (131).

Post-market labeling of CIEDs is subject to change as well. For instance, the Medtronic 5076 pacing lead was initially released as non-MR Conditional but was later relabeled as MR Conditional with concurrent use of a Medtronic MR Conditional pacemaker.

MR Conditional CIEDs have specific allowable, static magnetic field strengths or field strength ranges that can be used for MRI with some permitting scans at 3-Tesla. As MRI technology evolves and higher static magnetic field strengths are incorporated into clinical use (e.g., 7-Tesla is now approved for clinical use), and research use, further device studies will be necessary in association with new conditions.

Figure 4. Chest X-ray obtained in a patient with an MR Conditional cardiac pacemaker showing radiopaque markings identifying the pulse generator and leads as being MR Conditional components.



696 MRI and Cardiac Devices

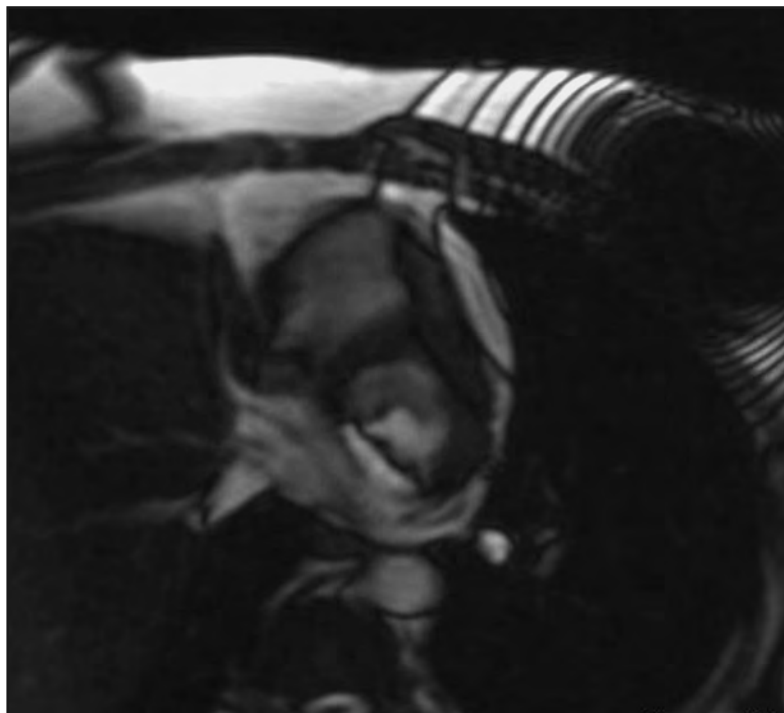
The number and type of CIEDs for diagnostic and therapeutic indications continues to increase which, in addition to standard cardiac pacemakers and ICDs, include resynchronization therapy devices, leadless pacing systems, implantable arrhythmia monitors, implantable physiologic measurement devices, and temporary pacing systems. There are published case reports of safe and successful MRI exams in patients with leadless pacemakers and MR Conditional leadless pacemakers are now commercially available (154-157).

Implantable loop recorders and other similar monitors have been studied and MR Conditional CIEDs used for arrhythmia monitoring have been clinically released. Regarding implantable loop recorders, a study reported a total of 24 patients who underwent 62, 3-Tesla brain MRI procedures without adverse events or loss of data (158). One MRI associated recording artifact occurred which simulated a narrow complex tachycardia. In another study of 1.5-Tesla scans, seven out of 11 MRI exams demonstrated artifacts mimicking bradyarrhythmias and/or tachyarrhythmias (159). A 3-Tesla brain study of one patient with an implantable loop recorder demonstrated prolonged artifactual asystole (110). An investigation of four patients with spine, brain, or hip 1.5-Tesla MRI exams all demonstrated artifacts with a spectrum including narrow and wide complex tachycardia, asystole, or complete heart block (160). A study of 27 cardiac MRI studies in patients with implantable loop recorders reported no adverse safety events or loss of data (161). Downloading data from the loop recorder or implanted cardiac monitor is recommended prior to MRI in order prevent loss of recorded information (42).

MRI EXAM ARTIFACTS AND IMAGE QUALITY IN PATIENTS WITH CIEDS

Ferromagnetic materials can affect local magnetic fields leading to image distortion, signal voids or bright areas, and poor fat suppression on MR images (**Figure 5**) (162). Variables associated with the presence and severity of artifacts include the type of CIED and location, patient body habitus, scanner type, field of view, imaging plane, and pulse sequence parameters. Because the CIED may be in or near the field of view or area of interest on an MRI exam, imaging artifacts related to signal loss and distortion caused by the CIED may impact the diagnostic use of MRI, particularly for cardiac and thoracic examinations (87, 117-120). An early case study with a single chamber subpectoral ICD placement demonstrated artifact overlying the heart, limiting a comprehensive evaluation of function (117). Investigations have reported image distortion can extend approximately 10 to 15 cm around the IPG, depending on the type of generator and the pulse sequence (87, 118). A study of 71 cardiac MR (CMR) exams found that those with right- or left-sided pacemaker implants and right-sided ICD implants had fewer artifacts compared to left-sided ICD implants (163). The same investigation reported that artifacts related to pacemaker and ICD leads were much smaller than those due to the IPG, which stands to reason considering the materials used to make each respective component. A study of 128 patients with a variety of CIEDs showed that device type and location were the primary indicators of image quality, with left-sided ICD systems being most problematic and, thus, recommended device-specific, tailored imaging protocols to reduce susceptibility artifacts (164). The distance between the IPG and the cardiac border on chest X-ray was inversely associated with artifact size. Additional studies of cardiac MR imaging demonstrated decreased artifact and im-

Figure 5. Cardiac MRI exam showing a substantial artifact over the left and right ventricles due to a left-sided, single chamber ICD.



proved imaging quality with CIEDs positioned in the right chest region as well (121, 122). As previously mentioned, cardiac pacemaker lead artifacts are significantly smaller than ICD lead artifacts regardless of the pulse sequence (124).

Leadless cardiac pacemakers can cause artifacts on MR images with two case reports demonstrating artifacts over small areas of the ventricular apex, which did not affect diagnostic interpretability (156, 157). In a study of 14 CMR examinations in patients with leadless right ventricular pacemakers, segmental ventricular analysis demonstrated artifacts in the mid-anteroseptal, inferoseptal, and apical septal left ventricle myocardial segments and mid- and apical right ventricular segments. The extent of the artifacts seen on MRI is greater when imaging 3-Tesla versus 1.5-Tesla (165). For implantable loop recorders, a study of 27 cardiac MRI exams found no clinically significant artifacts (161). Cardiovascular MRI exams performed at 1.5-T in two patients demonstrated no effect on the loop recorder but there were substantial imaging artifacts (166).

In regard to MRI pulse sequences, a multicenter study of 175 patients that underwent CMR with pacemakers and ICDs reported that the odds for better image quality were greater when using a fast-gradient-echo (FGRE) pulse sequence compared to a steady-state-free-precession (SSFP) sequence (124). However, use of FGRE sequences when imaging the area associated with the leads reduced the signal-to-noise ratio in the blood pool, making discrimination of the blood-myocardium interface more difficult compared to SSFP sequences (124). The same study found that ICD-related artifacts were smaller on horizontal,

698 MRI and Cardiac Devices

long axis orientation views compared to short axis orientation views. Another study reported greater image distortion with fast spin echo (FSE) and fast imaging employing steady-state acquisition (FIESTA) pulse sequences and improved image quality on FGRE, myocardial tagging (e.g., using spatial modulation of magnetization or SPAM), and FSPGR sequences (87).

Artifacts are generally more pronounced on inversion recovery (IR) and SSFP pulse sequences when performing CMR (118). Notably, artifacts on IR MR images show high signal intensity and can appear as areas of delayed enhancement, mimicking myocardial fibrosis. Comparison of images with bright areas on various pulse sequences can help avoid misinterpretation of artifacts. Imaging planes perpendicular to the IPG plane, shortening echo time, and using spin echo and fast spin echo pulse sequences can all reduce the qualitative degree of artifacts (118). Importantly, these pulse sequences can reduce the qualitative extent of artifacts associated with metallic implants. However, spin echo-based pulse sequences are less time efficient and are not designed to provide functional characteristics of the heart (124).

Metal artifact reduction strategies using a wideband, inversion pre-pulses has been reported to reduce imaging artifacts in ICD patients (125, 126, 167-169). With the use of various imaging sequences and wideband filtering algorithms, MRI remains interpretable in the presence of cardiac pacemakers and ICDs (127, 128). Artifacts can also affect MR images when certain pulse sequences are used with image acquisition in non-chest-related areas (122, 123). A study of 31 patients with an MR Conditional cardiac pacemaker demonstrated artifacts that affected brain images on diffusion-weighted images, but not when other imaging sequences were used (123). Regarding scanner type, further studies are needed to assess the degree of artifact with CIEDs with novel imaging sequences at various static magnetic field strengths.

CONCLUSIONS AND FUTURE DIRECTIONS

The overall impact of the implementation of MR Conditional CIEDs will depend on multiple factors including continued device development, demonstration of device safety and effectiveness, device approval by appropriate regulatory agencies, implant practices in different patient subgroups and geographies, device costs, cost effectiveness, and reimbursement. Even as MR Conditional CIEDs become the nominal platform of cardiac devices, a period of time will exist where a patient with a non-MR Conditional device will still need to undergo an MRI examination for diagnostic or therapeutic indications.

Expert consensus statements and multidisciplinary guidelines have been developed based on the current body of medical literature (42, 200-204). These guidelines provide recommendations for the decisions and management to perform MRI exams in patients with non-MR Conditional and MR Conditional CIEDs, as well as patients with abandoned pacing leads. Application of these guidelines requires education, cooperation, and collaboration of the medical professionals caring for patients whenever MRI is being utilized in patients with CIEDs. Naturally, these guidelines will require an update as technology advances and the medical literature continues to evolve. For example, MR systems are being created for real-time use during cardiovascular procedures and this important development needs to be

taken into consideration for applications in patients with MR Conditional, CIEDS (170-173). Thus, as MRI-based imaging modalities (e.g., PET/MRI) are further developed, they will require additional research to determine possible applications in patients with CIEDs.

REFERENCES

1. Kanal E, Borgstede JP, Barkovich AJ, et al. American College of Radiology white paper on MR safety: 2004 update and revisions. *AJR Am J Roentgenol* 2004;182:1111-4.
2. Avery JK. Loss Prevention case of the month. Not my responsibility! *J Tenn Med Assoc* 1988;81:523.
3. Irnich W, Irnich B, Bartsch C, et al. Do we need pacemakers resistant to magnetic resonance imaging? *Europace* 2005;7:353-65.
4. Strom JB, Whelan JB, Shen C, et al. Safety and utility of magnetic resonance imaging in patients with cardiac implantable electronic devices. *Heart Rhythm* 2017;14:1138-1144.
5. Higgins JV, Watson RE Jr, Jaffe AS, et al. Cardiac troponin T in patients with cardiac implantable electronic devices undergoing magnetic resonance imaging. *J Interv Card Electrophysiol* 2016;45:91-7.
6. Boilson BA, Wokhlu A, Acker NG, et al. Safety of magnetic resonance imaging in patients with permanent pacemakers: A collaborative clinical approach. *J Interv Card Electrophysiol* 2012;33:59-67.
7. Mollerus M, Albin G, Lipinski M, Lucca J. Ectopy in patients with permanent pacemakers and implantable cardioverter-defibrillators undergoing an MRI scan. *Pacing Clin Electrophysiol* 2009;32:772-8.
8. Friedman HL, Acker N, Dalzell C, et al. Magnetic resonance imaging in patients with recently implanted pacemakers. *Pacing Clin Electrophysiol* 2013;36:1090-5.
9. Gimbel JR, Johnson D, Levine PA, Wilkoff BL. Safe performance of magnetic resonance imaging on five patients with permanent cardiac pacemakers. *Pacing Clin Electrophysiol* 1996;19:913-9.
10. Gimbel JR. Unexpected asystole during 3T magnetic resonance imaging of a pacemaker-dependent patient with a 'modern' pacemaker. *Europace* 2009;11:1241-2.
11. Sommer T, Lauck G, Schimpf R, et al. MRI in patients with cardiac pacemakers: *In vitro* and *in vivo* evaluation at 0.5 tesla. *Rofo* 1998;168:36-43.
12. Vahlhaus C, Sommer T, Lewalter T, et al. Interference with cardiac pacemakers by magnetic resonance imaging: Are there irreversible changes at 0.5 Tesla? *Pacing Clin Electrophysiol* 2001;24:489-95.
13. Bertelsen L, Petersen HH, Philbert BT, et al. Safety of magnetic resonance scanning without monitoring of patients with pacemakers. *Europace* 2017;19:818-823.
14. Gimbel JR, Bailey SM, Tchou PJ, Ruggieri PM, Wilkoff BL. Strategies for the safe magnetic resonance imaging of pacemaker-dependent patients. *Pacing Clin Electrophysiol* 2005;28:1041-6.
15. Sommer T, Naehle CP, Yang A, et al. Strategy for safe performance of extrathoracic magnetic resonance imaging at 1.5 tesla in the presence of cardiac pacemakers in non-pacemaker-dependent patients: A prospective study with 115 examinations. *Circulation* 2006;114:1285-92.
16. Naehle CP, Zeijlemaker V, Thomas D, et al. Evaluation of cumulative effects of MR imaging on pacemaker systems at 1.5 Tesla. *Pacing Clin Electrophysiol* 2009;32:1526-35.
17. Nazarian S, Hansford R, Roguin A, et al. A prospective evaluation of a protocol for magnetic resonance imaging of patients with implanted cardiac devices. *Ann Intern Med* 2011;155:415-24.
18. Cohen JD, Costa HS, Russo RJ. Determining the risks of magnetic resonance imaging at 1.5 tesla for patients with pacemakers and implantable cardioverter defibrillators. *Am J Cardiol* 2012;110:1631-6.
19. Shah AD, Patel AU, Knezevic A, et al. Clinical performance of magnetic resonance imaging conditional and nonconditional cardiac implantable electronic devices. *Pacing Clin Electrophysiol* 2017;40:467-475.

700 MRI and Cardiac Devices

20. Xiong M, Zhao N, Qin Y, et al. Evaluation of the safety of MRI scans in patients undergoing dual-chamber pacemaker implantation. *Exp Ther Med* 2018;16:1593-1596.
21. Martin ET, Coman JA, Shellock FG, et al. Magnetic resonance imaging and cardiac pacemaker safety at 1.5-Tesla. *J Am Coll Cardiol* 2004;43:1315-24.
22. Rozner MA, Burton AW, Kumar A. Pacemaker complication during magnetic resonance imaging. *J Am Coll Cardiol* 2005;45:161-2.
23. Baser K, Guray U, Durukan M, Demirkiran B. High ventricular lead impedance of a DDD pacemaker after cranial magnetic resonance imaging. *Pacing Clin Electrophysiol* 2012;35:e251-3.
24. Buendia F, Sanchez-Gomez JM, Sancho-Tello MJ, et al. Nuclear magnetic resonance imaging in patients with cardiac pacing devices. *Rev Esp Cardiol* 2010;63:735-9.
25. Heatlie G, Pennell DJ. Cardiovascular magnetic resonance at 0.5T in five patients with permanent pacemakers. *J Cardiovasc Magn Reson* 2007;9:15-9.
26. Fontaine JM, Mohamed FB, Gottlieb C, Callans DJ, Marchlinski FE. Rapid ventricular pacing in a pacemaker patient undergoing magnetic resonance imaging. *Pacing Clin Electrophysiol* 1998;21:1336-9.
27. Okamura H, Padmanabhan D, Watson RE Jr, et al. Magnetic resonance imaging in nondependent pacemaker patients with pacemakers and defibrillators with a nearly depleted battery. *Pacing Clin Electrophysiol* 2017;40:476-481.
28. Higgins JV, Sheldon SH, Watson RE Jr, et al. "Power-on resets" in cardiac implantable electronic devices during magnetic resonance imaging. *Heart Rhythm* 2015;12:540-544.
29. Krebsbach A, Dewland TA, Henrikson CA. Malfunction of an MRI-conditional pacemaker following an MRI. *HeartRhythm Case Rep* 2017;3:148-150.
30. Russo RJ, Costa HS, Silva PD, et al. Assessing the risks associated with MRI in patients with a pacemaker or defibrillator. *N Engl J Med* 2017;376:755-764.
31. Nazarian S, Hansford R, Rahsepar AA, et al. Safety of magnetic resonance imaging in patients with cardiac devices. *N Engl J Med* 2017;377:2555-2564.
32. Anfinsen OG, Berntsen RF, Aass H, Kongsgaard E, Amlie JP. Implantable cardioverter defibrillator dysfunction during and after magnetic resonance imaging. *Pacing Clin Electrophysiol* 2002;25:1400-2.
33. Fiek M, Remp T, Reithmann C, Steinbeck G. Complete loss of ICD programmability after magnetic resonance imaging. *Pacing Clin Electrophysiol* 2004;27:1002-4.
34. Nemec J. Suppression of implantable cardioverter defibrillator therapy during magnetic resonance imaging. *J Cardiovasc Electrophysiol* 2006;17:444-5.
35. Atar I, Bal U, Ertan C, Ozin B, Muderrisoglu H. Inappropriate shock and battery switching to "End of Life" in a patient with biventricular ICD during magnetic resonance imaging. *Turk Kardiyol Dern Ars* 2016;44:79-81.
36. Seewoster T, Lobe S, Hilbert S, et al. Cardiovascular magnetic resonance imaging in patients with cardiac implantable electronic devices: Best practice and real-world experience. *Europace* 2019.
37. Coman JA, Martin ET, Sandler DA, Thomas RT. Implantable cardiac defibrillator interactions with magnetic resonance imaging at 1.5 Tesla. *J Am Coll Cardiol* 2004;43:138A.
38. Gimbel JR, Kanal E, Schwartz KM, Wilkoff BL. Outcome of magnetic resonance imaging (MRI) in selected patients with implantable cardioverter defibrillators (ICDs). *Pacing Clin Electrophysiol* 2005;28:270-3.
39. Nyotowidjojo IS, Skinner K, Shah AS, et al. Thoracic versus nonthoracic MR imaging for patients with an non-MR Conditional cardiac implantable electronic device. *Pacing Clin Electrophysiol* 2018;41:589-596.
40. Shah AD, Morris MA, Hirsh DS, et al. Magnetic resonance imaging safety in non-MR Conditional pacemaker and defibrillator recipients: A meta-analysis and systematic review. *Heart Rhythm* 2018;15:1001-1008.

MRI Bioeffects, Safety, and Patient Management 701

41. Burke PT, Ghanbari H, Alexander PB, et al. A protocol for patients with cardiovascular implantable devices undergoing magnetic resonance imaging (MRI): Should defibrillation threshold testing be performed post-(MRI). *J Interv Card Electrophysiol* 2010;28:59-66.
42. Indik JH, Gimbel JR, Abe H, et al. 2017 HRS expert consensus statement on magnetic resonance imaging and radiation exposure in patients with cardiovascular implantable electronic devices. *Heart Rhythm* 2017;14:e97-e153.
43. Safety ACR Committee, Greenberg TD, Hoff MN, et al. ACR guidance document on MR safe practices: Updates and critical information 2019. *J Magn Reson Imaging* 2020;51:331-338.
44. Jordan D, Gulani V. Editorial on “ACR guidance document on MR safe practices: Updates and critical information 2019”. *J Magn Reson Imaging* 2020;51:339-340.
45. Faris OP, Shein MJ. Government viewpoint: U.S. Food & Drug Administration: Pacemakers, ICDs and MRI. *Pacing Clin Electrophysiol* 2005;28:268-9.
46. Smith JM. Industry viewpoint: Guidant: Pacemakers, ICDs, and MRI. *Pacing Clin Electrophysiol* 2005;28:264.
47. Stanton MS. Industry viewpoint: Medtronic: Pacemakers, ICDs, and MRI. *Pacing Clin Electrophysiol* 2005;28:265.
48. Levine PA. Industry viewpoint: St. Jude Medical: Pacemakers, ICDs and MRI. *Pacing Clin Electrophysiol* 2005;28:266-7.
49. Fisher JD. MRI: Safety in patients with pacemakers or defibrillators: Is it prime time yet? *Pacing Clin Electrophysiol* 2005;28:263.
50. Martin ET. Can cardiac pacemakers and magnetic resonance imaging systems co-exist? *Eur Heart J* 2005;26:325-7.
51. Faris OP, Shein M. Food and Drug Administration perspective: Magnetic resonance imaging of pacemaker and implantable cardioverter-defibrillator patients. *Circulation* 2006;114:1232-3.
52. Wilkoff BL. Pacemaker and ICD malfunction--an incomplete picture. *JAMA* 2006;295:1944-6.
53. Shinbane JS, Colletti PM, Shellock FG. MR in patients with pacemakers and ICDs: Defining the issues. *J Cardiovasc Magn Reson* 2007;9:5-13.
54. Shinbane JS, Colletti PM, Shellock FG. Magnetic resonance imaging in patients with cardiac pacemakers: Era of “MR Conditional” designs. *J Cardiovasc Magn Reson* 2011;13:63.
55. Colletti PM, Shinbane JS, Shellock FG. “MR-conditional” pacemakers: The radiologist’s role in multidisciplinary management. *AJR Am J Roentgenol* 2011;197:W457-9.
56. Shinbane JS, Colletti PM, Shellock FG. MR imaging in patients with pacemakers and other devices: Engineering the future. *JACC Cardiovasc Imaging* 2012;5:332-3.
57. Shellock FG, Woods TO, Crues JV 3rd. MR labeling information for implants and devices: Explanation of terminology. *Radiology* 2009;253:26-30.
58. American Society for Testing and Materials (ASTM) International. F2503, Standard Practice for Marking Medical Devices and Other Items for Safety in the Magnetic Resonance Environment.
59. Shellock FG, Tkach JA, Ruggieri PM, Masaryk TJ. Cardiac pacemakers, ICDs, and loop recorder: Evaluation of translational attraction using conventional (“long-bore”) and “short-bore” 1.5- and 3.0-Tesla MR systems. *J Cardiovasc Magn Reson* 2003;5:387-97.
60. Del Ojo JL, Moya F, Villalba J, et al. Is magnetic resonance imaging safe in cardiac pacemaker recipients? *Pacing Clin Electrophysiol* 2005;28:274-8.
61. Wilkoff BL, Bello D, Taborsky M, et al. Magnetic resonance imaging in patients with a pacemaker system designed for the magnetic resonance environment. *Heart Rhythm* 2011;8:65-73.
62. Keller J, Neuzil P, Vymazal J, et al. Magnetic resonance imaging in patients with a subcutaneous implantable cardioverter-defibrillator. *Europace* 2015;17:761-6.

702 MRI and Cardiac Devices

63. Babouri A, Hedjeidj A. *In vitro* investigation of eddy current effect on pacemaker operation generated by low frequency magnetic field. Conf Proc IEEE Eng Med Biol Soc 2007;2007:5684-7.
64. Calcagnini G, Triventi M, Censi F, et al. *In vitro* investigation of pacemaker lead heating induced by magnetic resonance imaging: Role of implant geometry. J Magn Reson Imaging 2008;28:879-86.
65. Mattei E, Triventi M, Calcagnini G, et al. Complexity of MRI induced heating on metallic leads: Experimental measurements of 374 configurations. Biomed Eng Online 2008;7:11.
66. Nordbeck P, Weiss I, Ehses P, et al. Measuring RF-induced currents inside implants: Impact of device configuration on MRI safety of cardiac pacemaker leads. Magn Reson Med 2009;61:570-8.
67. Park SM, Kamondetdacha R, Nyenhuis JA. Calculation of MRI-induced heating of an implanted medical lead wire with an electric field transfer function. J Magn Reson Imaging 2007;26:1278-85.
68. Yeung CJ, Karmarkar P, McVeigh ER. Minimizing RF heating of conducting wires in MRI. Magn Reson Med 2007;58:1028-34.
69. Nordbeck P, Fidler F, Weiss I, et al. Spatial distribution of RF-induced E-fields and implant heating in MRI. Magn Reson Med 2008;60:312-9.
70. Nordbeck P, Ritter O, Weiss I, et al. Impact of imaging landmark on the risk of MRI-related heating near implanted medical devices like cardiac pacemaker leads. Magn Reson Med 2011;65:44-50.
71. Mattei E, Calcagnini G, Censi F, Triventi M, Bartolini P. Role of the lead structure in MRI-induced heating: *In vitro* measurements on 30 commercial pacemaker/defibrillator leads. Magn Reson Med 2012;67:925-35.
72. Nordbeck P, Fidler F, Friedrich MT, et al. Reducing RF-related heating of cardiac pacemaker leads in MRI: Implementation and experimental verification of practical design changes. Magn Reson Med 2012;68:1963-72.
73. Acikel V, Uslubas A, Atalar E. Modeling of electrodes and implantable pulse generator cases for the analysis of implant tip heating under MR imaging. Med Phys 2015;42:3922-31.
74. Driller J, Barold SS, Parsonnet V. Normal and abnormal function of the pacemaker magnetic reed switch. J Electrocardiol 1976;9:283-92.
75. Lauck G, von Smekal A, Wolke S, et al. Effects of nuclear magnetic resonance imaging on cardiac pacemakers. Pacing Clin Electrophysiol 1995;18:1549-55.
76. Luechinger R, Duru F, Zeijlemaker VA, et al. Pacemaker reed switch behavior in 0.5, 1.5, and 3.0 Tesla magnetic resonance imaging units: Are reed switches always closed in strong magnetic fields? Pacing Clin Electrophysiol 2002;25:1419-23.
77. Sutton R, Kanal E, Wilkoff BL, et al. Safety of magnetic resonance imaging of patients with a new Medtronic EnRhythm MRI SureScan pacing system: Clinical study design. Trials 2008;9:68.
78. Shellock FG, Fischer L, Fieno DS. Cardiac pacemakers and implantable cardioverter defibrillators: *In vitro* magnetic resonance imaging evaluation at 1.5-Tesla. J Cardiovasc Magn Reson 2007;9:21-31.
79. Neuzner J. Clinical experience with a new cardioverter defibrillator capable of biphasic waveform pulse and enhanced data storage: Results of a prospective multicenter study. European Ventak P2 Investigator Group. Pacing Clin Electrophysiol 1994;17:1243-55.
80. Brugada J, Herse B, Sandsted B, et al. Clinical evaluation of defibrillation efficacy with a new single-capacitor biphasic waveform in patients undergoing implantation of an implantable cardioverter defibrillator. Europace 2001;3:278-84.
81. Rinaldi CA, Simon RD, Geelen P, et al. A randomized prospective study of single coil versus dual coil defibrillation in patients with ventricular arrhythmias undergoing implantable cardioverter defibrillator therapy. Pacing Clin Electrophysiol 2003;26:1684-90.
82. Pictet J, Meuli R, Wicky S, van der Klink JJ. Radiofrequency heating effects around resonant lengths of wire in MRI. Phys Med Biol 2002;47:2973-85.
83. Pavlicek W, Geisinger M, Castle L, et al. The effects of nuclear magnetic resonance on patients with cardiac pacemakers. Radiology 1983;147:149-53.

MRI Bioeffects, Safety, and Patient Management 703

84. Erlebacher JA, Cahill PT, Pannizzo F, Knowles RJ. Effect of magnetic resonance imaging on DDD pacemakers. *Am J Cardiol* 1986;57:437-40.
85. Hayes DL, Holmes DR Jr, Gray JE. Effect of 1.5 tesla nuclear magnetic resonance imaging scanner on implanted permanent pacemakers. *J Am Coll Cardiol* 1987;10:782-6.
86. Holmes DR Jr, Hayes DL, Gray JE, Merideth J. The effects of magnetic resonance imaging on implantable pulse generators. *Pacing Clin Electrophysiol* 1986;9:360-70.
87. Roguin A, Zviman MM, Meininger GR, et al. Modern pacemaker and implantable cardioverter/defibrillator systems can be magnetic resonance imaging safe: *In vitro* and *in vivo* assessment of safety and function at 1.5 T. *Circulation* 2004;110:475-82.
88. Trigano A, Blandau O, Souques M, Gernez JP, Magne I. Clinical study of interference with cardiac pacemakers by a magnetic field at power line frequencies. *J Am Coll Cardiol* 2005;45:896-900.
89. Achenbach S, Moshage W, Diem B, et al. Effects of magnetic resonance imaging on cardiac pacemakers and electrodes. *Am Heart J* 1997;134:467-73.
90. Yeung CJ, Susil RC, Atalar E. RF heating due to conductive wires during MRI depends on the phase distribution of the transmit field. *Magn Reson Med* 2002;48:1096-8.
91. Mattei E, Calcagnini G, Censi F, Triventi M, Bartolini P. Numerical model for estimating RF-induced heating on a pacemaker implant during MRI: Experimental validation. *IEEE Trans Biomed Eng* 2010;57:2045-52.
92. Bottomley PA, Kumar A, Edelstein WA, Allen JM, Karmarkar PV. Designing passive MRI-safe implantable conducting leads with electrodes. *Med Phys* 2010;37:3828-43.
93. Rahsepar AA, Zimmerman SL, Hansford R, et al. The relationship between MRI radiofrequency energy and function of nonconditional implanted cardiac devices: A prospective evaluation. *Radiology* 2020;191132.
94. Gray RW, Bibens WT, Shellock FG. Simple design changes to wires to substantially reduce MRI-induced heating at 1.5 T: Implications for implanted leads. *Magn Reson Imaging* 2005;23:887-91.
95. United States of America, Department of Health And Human Services Food and Drug Administration Center For Devices and Radiological Health Medical Devices Advisory Committee Circulatory System Devices Panel. 2020.
96. Scholten A, Silny J. The interference threshold of unipolar cardiac pacemakers in extremely low frequency magnetic fields. *J Med Eng Technol* 2001;25:185-94.
97. Langman DA, Goldberg IB, Finn JP, Ennis DB. Pacemaker lead tip heating in abandoned and pacemaker-attached leads at 1.5 Tesla MRI. *J Magn Reson Imaging* 2011;33:426-31.
98. Higgins JV, Gard JJ, Sheldon SH, et al. Safety and outcomes of magnetic resonance imaging in patients with abandoned pacemaker and defibrillator leads. *Pacing Clin Electrophysiol* 2014;37:1284-90.
99. Horwood L, Attili A, Luba F, et al. Magnetic resonance imaging in patients with cardiac implanted electronic devices: Focus on contraindications to magnetic resonance imaging protocols. *Europace* 2017;19:812-817.
100. Morris MF, Verma DR, Sheikh H, Su W, Pershad A. Outcomes after magnetic resonance imaging in patients with pacemakers and defibrillators and abandoned leads. *Cardiovasc Revasc Med* 2018;19:685-688.
101. Padmanabhan D, Kella DK, Mehta R, et al. Safety of magnetic resonance imaging in patients with legacy pacemakers and defibrillators and abandoned leads. *Heart Rhythm* 2018;15:228-233.
102. Hartnell GG, Spence L, Hughes LA, et al. Safety of MR imaging in patients who have retained metallic materials after cardiac surgery. *AJR Am J Roentgenol* 1997;168:1157-9.
103. Kanal E. Safety of MR imaging in patients with retained epicardial pacer wires. *AJR Am J Roentgenol* 1998;170:213-4.

704 MRI and Cardiac Devices

104. Austin CO, Landolfo K, Parikh PP, et al. Retained cardiac implantable electronic device fragments are not associated with magnetic resonance imaging safety issues, morbidity, or mortality after orthotopic heart transplant. *Am Heart J* 2017;190:46-53.
105. Fries R, Steuer M, Schafers HJ, Bohm M. The R-on-T phenomenon in patients with implantable cardioverter-defibrillators. *Am J Cardiol* 2003;91:752-5.
106. Chilidakis JA, Karapanos G, Davlouros P, et al. Significance of R-on-T phenomenon in early ventricular tachyarrhythmia susceptibility after acute myocardial infarction in the thrombolytic era. *Am J Cardiol* 2000;85:289-93.
107. Naehle CP, Sommer T, Meyer C, et al. Strategy for safe performance of magnetic resonance imaging on a patient with implantable cardioverter defibrillator. *Pacing Clin Electrophysiol* 2006;29:113-6.
108. van Dijk VF, Delnoy P, Smit JJJ, et al. Preliminary findings on the safety of 1.5 and 3 Tesla magnetic resonance imaging in cardiac pacemaker patients. *J Cardiovasc Electrophysiol* 2017;28:806-810.
109. Naehle CP, Meyer C, Thomas D, et al. Safety of brain 3-T MR imaging with transmit-receive head coil in patients with cardiac pacemakers: Pilot prospective study with 51 examinations. *Radiology* 2008;249:991-1001.
110. Gimbel JR. Magnetic resonance imaging of implantable cardiac rhythm devices at 3.0 tesla. *Pacing Clin Electrophysiol* 2008;31:795-801.
111. Shellock FG, O'Neil M, Ivans V, et al. Cardiac pacemakers and implantable cardioverter defibrillators are unaffected by operation of an extremity MR imaging system. *AJR Am J Roentgenol* 1999;172:165-70.
112. Shellock FG, Bert JM, Fritts HM, et al. Evaluation of the rotator cuff and glenoid labrum using a 0.2-Tesla extremity magnetic resonance (MR) system: MR results compared to surgical findings. *J Magn Reson Imaging* 2001;14:763-70.
113. Zlatkin MB, Hoffman C, Shellock FG. Assessment of the rotator cuff and glenoid labrum using an extremity MR system: MR results compared to surgical findings from a multi-center study. *J Magn Reson Imaging* 2004;19:623-31.
114. Wollmann CG, Thudt K, Kaiser B, et al. Safe performance of magnetic resonance of the heart in patients with magnetic resonance conditional pacemaker systems: The safety issue of the ESTIMATE study. *J Cardiovasc Magn Reson* 2014;16:30.
115. Kono T, Ogimoto A, Saito M, et al. Cardiac magnetic resonance imaging for assessment of steroid therapy in a patient with cardiac sarcoidosis and a magnetic resonance-conditional pacemaker. *Int J Cardiol* 2014;176:e89-91.
116. Klein-Wiele O, Garmer M, Urbien R, et al. Feasibility and safety of adenosine cardiovascular magnetic resonance in patients with MR Conditional pacemaker systems at 1.5 Tesla. *J Cardiovasc Magn Reson* 2015;17:112.
117. Roguin A, Donahue JK, Bomma CS, Bluemke DA, Halperin HR. Cardiac magnetic resonance imaging in a patient with implantable cardioverter-defibrillator. *Pacing Clin Electrophysiol* 2005;28:336-8.
118. Nazarian S, Roguin A, Zviman MM, et al. Clinical utility and safety of a protocol for noncardiac and cardiac magnetic resonance imaging of patients with permanent pacemakers and implantable-cardioverter defibrillators at 1.5 tesla. *Circulation* 2006;114:1277-84.
119. Pulver AF, Puchalski MD, Bradley DJ, et al. Safety and imaging quality of MRI in pediatric and adult congenital heart disease patients with pacemakers. *Pacing Clin Electrophysiol* 2009;32:450-6.
120. Quarta G, Holdright DR, Plant GT, et al. Cardiovascular magnetic resonance in cardiac sarcoidosis with MR conditional pacemaker *in situ*. *J Cardiovasc Magn Reson* 2011;13:26.
121. Naehle CP, Kreuz J, Strach K, et al. Safety, feasibility, and diagnostic value of cardiac magnetic resonance imaging in patients with cardiac pacemakers and implantable cardioverters/defibrillators at 1.5 T. *Am Heart J* 2011;161:1096-105.

MRI Bioeffects, Safety, and Patient Management 705

122. Klein-Wiele O, Garmer M, Busch M, et al. Cardiovascular magnetic resonance in patients with magnetic resonance conditional pacemaker systems at 1.5 T: Influence of pacemaker related artifacts on image quality including first pass perfusion, aortic and mitral valve assessment, flow measurement, short tau inversion recovery and T1-weighted imaging. *Int J Cardiovasc Imaging* 2017;33:383-394.
123. Wollmann CG, Steiner E, Vock P, Ndikung B, Mayr H. Monocenter feasibility study of the MRI compatibility of the Evia pacemaker in combination with Safio S pacemaker lead. *J Cardiovasc Magn Reson* 2012;14:67.
124. Schwitter J, Gold MR, Al Fagih A, et al. Image quality of cardiac magnetic resonance imaging in patients with an implantable cardioverter defibrillator system designed for the magnetic resonance imaging environment. *Circ Cardiovasc Imaging* 2016;9.
125. Ranjan R, McGann CJ, Jeong EK, et al. Wideband late gadolinium enhanced magnetic resonance imaging for imaging myocardial scar without image artefacts induced by implantable cardioverter-defibrillator: A feasibility study at 3 T. *Europace* 2015;17:483-8.
126. Rahsepar AA, Collins JD, Knight BP, et al. Wideband LGE MRI permits unobstructed viewing of myocardial scarring in a patient with an MR-conditional subcutaneous implantable cardioverter-defibrillator. *Clin Imaging* 2018;50:294-296.
127. Do DH, Eyvazian V, Bayoneta AJ, et al. Cardiac magnetic resonance imaging using wideband sequences in patients with nonconditional cardiac implanted electronic devices. *Heart Rhythm* 2018;15:218-225.
128. Singh A, Kawaji K, Goyal N, et al. Feasibility of cardiac magnetic resonance wideband protocol in patients with implantable cardioverter defibrillators and its utility for defining scar. *Am J Cardiol* 2019;123:1329-1335.
129. Junntila MJ, Fishman JE, Lopera GA, et al. Safety of serial MRI in patients with implantable cardioverter defibrillators. *Heart* 2011;97:1852-6.
130. Russo RJ. Determining the risks of clinically indicated nonthoracic magnetic resonance imaging at 1.5 T for patients with pacemakers and implantable cardioverter-defibrillators: Rationale and design of the MagnaSafe Registry. *Am Heart J* 2013;165:266-72.
131. Williamson BD, Gohn DC, Ramza BM, et al. Real-world evaluation of magnetic resonance imaging in patients with a magnetic resonance imaging conditional pacemaker system: Results of 4-year prospective follow-up in 2,629 patients. *JACC Clin Electrophysiol* 2017;3:1231-1239.
132. Nazarian S. Cardiac electrophysiology procedures, known unknowns, and unknown unknowns: The potential of magnetic resonance guidance. *JACC Clin Electrophysiol* 2017;3:104-106.
133. Advisa MRI Clinical Study. (NCT01110915). <http://clinicaltrials.gov>.
134. Clinical Evaluation of the Sorin Group's Reply MR-Conditional Pacing System. (NCT01341522). <http://clinicaltrials.gov>.
135. Accent MRI Pacemaker and Tendril MRI Lead New Technology Assesment. (NCT01258218). <http://clinicaltrials.gov>.
136. Safety and Efficacy of the Accent Magnetic Resonance Imaging (MRI) Pacemaker and Tendril MRI Lead. (NCT01576016). <http://clinicaltrials.gov>.
137. Safety and Performance Study of the INGEVITY Lead. (NCT01688843). <http://clinicaltrials.gov>.
138. ProMRI AFFIRM Study of the EVIA/ENTOVIS Pacemaker With Safio S Pacemaker Leads. (NCT01460992). <http://clinicaltrials.gov>.
139. ProMRI Study of the Entovis Pacemaker System. (NCT01761162). <http://clinicaltrials.gov>.
140. Lobodzinski SS. Recent innovations in the development of magnetic resonance imaging conditional pacemakers and implantable cardioverter-defibrillators. *Cardiol J* 2012;19:98-104.
141. Al-Wakeel N, O H-Ici D, Schmitt KR, et al. Cardiac MRI in patients with complex CHD following primary or secondary implantation of MRI-conditional pacemaker system. *Cardiol Young* 2016;26:306-14.

706 MRI and Cardiac Devices

142. Bailey WM, Mazur A, McCotter C, et al. Clinical safety of the ProMRI pacemaker system in patients subjected to thoracic spine and cardiac 1.5-T magnetic resonance imaging scanning conditions. *Heart Rhythm* 2016;13:464-71.
143. Nielsen JC, Giudici M, Tolasana Viu JM, et al. Safety and effectiveness of a 6-French MRI Conditional pacemaker lead: The INGEVITY(TM) clinical investigation study results. *Pacing Clin Electrophysiol* 2017;40:1121-1128.
144. Florian A, Ludwig A, Rosch S, Sechtem U, Yilmaz A. Magnetic resonance of the heart in a muscular dystrophy patient with an MR conditional ICD: Assessment of safety, diagnostic value and technical limitations. *J Cardiovasc Magn Reson* 2013;15:49.
145. Awad K, Griffin J, Crawford TC, et al. Clinical safety of the Iforia implantable cardioverter-defibrillator system in patients subjected to thoracic spine and cardiac 1.5-T magnetic resonance imaging scanning conditions. *Heart Rhythm* 2015;12:2155-61.
146. Gold MR, Sommer T, Schwitter J, et al. Full-body MRI in patients with an implantable cardioverter-defibrillator: Primary results of a randomized study. *J Am Coll Cardiol* 2015;65:2581-2588.
147. Kawakami H, Nagai T, Matsuyama TA, et al. Benefit of magnetic resonance-conditional cardiac resynchronization therapy defibrillator: A case of cardiac sarcoidosis-involved cervical extradural lesion. *HeartRhythm Case Rep* 2016;2:88-91.
148. Kypta A, Blessberger H, Hoenig S, et al. Clinical safety of an MRI conditional implantable cardioverter defibrillator system: A prospective Monocenter ICD-Magnetic resonance Imaging feasibility study (MIMI). *J Magn Reson Imaging* 2016;43:574-84.
149. Zbinden R, Wollmann C, Brachmann J, et al. Clinical safety of the ProMRI implantable cardioverter-defibrillator systems during head and lower lumbar magnetic resonance imaging at 3 T: Results of the ProMRI 3T ENHANCED Master study. *Europace* 2019;21:1678-1685.
150. Nazarian S, Cantillon DJ, Woodard PK, et al. MRI safety for patients implanted with the MRI Ready ICD System: MRI Ready study results. *JACC Clin Electrophysiol* 2019;5:935-943.
151. Blessberger H, Kiblboeck D, Reiter C, et al. Monocenter Investigation Micra MRI study (MIMICRY): Feasibility study of the magnetic resonance imaging compatibility of a leadless pacemaker system. *Europace* 2019;21:137-141.
152. Mitka M. First MRI-safe pacemaker receives conditional approval from FDA. *JAMA* 2011;305:985-6.
153. Bailey WM, Rosenthal L, Fananapazir L, et al. Clinical safety of the ProMRI pacemaker system in patients subjected to head and lower lumbar 1.5-T magnetic resonance imaging scanning conditions. *Heart Rhythm* 2015;12:1183-91.
154. Ubrich R, Kreiser K, Sinnecker D, Schneider S. Magnetic resonance imaging at 1.5-T in a patient with implantable leadless pacemaker. *Eur Heart J* 2016;37:2441.
155. Soejima K, Edmonson J, Ellingson ML, et al. Safety evaluation of a leadless transcatheter pacemaker for magnetic resonance imaging use. *Heart Rhythm* 2016;13:2056-63.
156. Kypta A, Blessberger H, Kiblboeck D, Steinwender C. Three Tesla cardiac magnetic resonance imaging in a patient with a leadless cardiac pacemaker system. *Eur Heart J* 2017;38:2628.
157. Lobe S, Hilbert S, Hindricks G, Jahnke C, Paetsch I. Cardiovascular magnetic resonance imaging in a patient with implanted leadless pacemaker. *JACC Clin Electrophysiol* 2018;4:149-150.
158. Haeusler KG, Koch L, Ueberreiter J, et al. Safety and reliability of the insertable Reveal XT recorder in patients undergoing 3 Tesla brain magnetic resonance imaging. *Heart Rhythm* 2011;8:373-6.
159. Gimbel JR, Zarghami J, Machado C, Wilkoff BL. Safe scanning, but frequent artifacts mimicking bradycardia and tachycardia during magnetic resonance imaging (MRI) in patients with an implantable loop recorder (ILR). *Ann Noninvasive Electrocardiol* 2005;10:404-8.
160. Wong JA, Yee R, Gula LJ, et al. Feasibility of magnetic resonance imaging in patients with an implantable loop recorder. *Pacing Clin Electrophysiol* 2008;31:333-7.

MRI Bioeffects, Safety, and Patient Management 707

161. Wiles BM, Illingworth CA, Couzins ML, Roberts PR, Harden SP. A tertiary centre experience of thoracic CT and cardiac MRI scanning in the presence of a reveal LINQ insertable cardiac monitoring system: A case series review of artefact, patient safety and data preservation. *Br J Radiol* 2018;91:20170615.
162. Peh WC, Chan JH. Artifacts in musculoskeletal magnetic resonance imaging: Identification and correction. *Skeletal Radiol* 2001;30:179-91.
163. Sasaki T, Hansford R, Zviman MM, et al. Quantitative assessment of artifacts on cardiac magnetic resonance imaging of patients with pacemakers and implantable cardioverter-defibrillators. *Circ Cardiovasc Imaging* 2011;4:662-70.
164. Hilbert S, Jahnke C, Loebe S, et al. Cardiovascular magnetic resonance imaging in patients with cardiac implantable electronic devices: A device-dependent imaging strategy for improved image quality. *Eur Heart J Cardiovasc Imaging* 2018;19:1051-1061.
165. Kiblboeck D, Reiter C, Kammler J, et al. Artefacts in 1.5 Tesla and 3 Tesla cardiovascular magnetic resonance imaging in patients with leadless cardiac pacemakers. *J Cardiovasc Magn Reson* 2018;20:47.
166. Blaschke F, Lacour P, Walter T, et al. Cardiovascular magnetic resonance imaging in patients with an implantable loop recorder. *Ann Noninvasive Electrocardiol* 2016;21:319-324.
167. Stevens SM, Tung R, Rashid S, et al. Device artifact reduction for magnetic resonance imaging of patients with implantable cardioverter-defibrillators and ventricular tachycardia: Late gadolinium enhancement correlation with electroanatomic mapping. *Heart Rhythm* 2014;11:289-98.
168. Ibrahim EH, Runge M, Stojanovska J, et al. Optimized cardiac magnetic resonance imaging inversion recovery sequence for metal artifact reduction and accurate myocardial scar assessment in patients with cardiac implantable electronic devices. *World J Radiol* 2018;10:100-107.
169. Bhuva AN, Kellman P, Graham A, et al. Clinical impact of cardiovascular magnetic resonance with optimized myocardial scar detection in patients with cardiac implantable devices. *Int J Cardiol* 2019;279:72-78.
170. Weller D, Salamon JM, Frolich A, et al. Combining direct 3D volume rendering and magnetic particle imaging to advance radiation-free real-time 3D guidance of vascular interventions. *Cardiovasc Intervent Radiol* 2020;43:322-330.
171. Heidt T, Reiss S, Krafft AJ, et al. Real-time magnetic resonance imaging - guided coronary intervention in a porcine model. *Sci Rep* 2019;9:8663.
172. Nordbeck P, Bauer WR. Real-time magnetic resonance imaging-guided cardiac electrophysiology: The long road to clinical routine. *Eur Heart J Cardiovasc Imaging* 2019;20:136-137.
173. Rogers T, Ratnayaka K, Karmarkar P, et al. Real-time magnetic resonance imaging guidance improves the diagnostic yield of endomyocardial biopsy. *JACC Basic Transl Sci* 2016;1:376-383.
174. Iberer F, Justich E, Stenzl W, Tscheliessnig KH, Kapeller J. Nuclear magnetic resonance imaging of a patient with implanted transvenous pacemaker. *Herz* 1987;7:196-9.
175. Alagona P Jr, Toole JC, Maniscalco BS, et al. Nuclear magnetic resonance imaging in a patient with a DDD Pacemaker. *Pacing Clin Electrophysiol* 1989;12:619.
176. Inbar S, Larson J, Burt T, Mafee M, Ezri MD. Case report: Nuclear magnetic resonance imaging in a patient with a pacemaker. *Am J Med Sci* 1993;305:174-5.
177. Garcia-Bolao I, Albaladejo V, Benito A, Alegria E, Zubietta JL. Magnetic resonance imaging in a patient with a dual-chamber pacemaker. *Acta Cardiol* 1998;53:33-5.
178. Sommer T, Vahlhaus C, Lauck G, et al. MR imaging and cardiac pacemakers: In-vitro evaluation and in-vivo studies in 51 patients at 0.5 T. *Radiology* 2000;215:869-79.
179. Wollmann C, Grude M, Tombach B, et al. Safe performance of magnetic resonance imaging on a patient with an ICD. *Pacing Clin Electrophysiol* 2005;28:339-42.
180. Sardanelli F, Lupo P, Esseridou A, Fausto A, Quarenghi M. Dynamic breast magnetic resonance imaging without complications in a patient with dual-chamber demand pacemaker. *Acta Radiol* 2006;47:24-7.

708 MRI and Cardiac Devices

181. Mollerus M, Albin G, Lipinski M, Lucca J. Cardiac biomarkers in patients with permanent pacemakers and implantable cardioverter-defibrillators undergoing an MRI scan. *Pacing Clin Electrophysiol* 2008;31:1241-5.
182. Goldsher D, Jahshan S, Roguin A. Successful cervical MR scan in a patient several hours after pacemaker implantation. *Pacing Clin Electrophysiol* 2009;32:1355-6.
183. Strach K, Naehle CP, Muhlsteffen A, et al. Low-field magnetic resonance imaging: Increased safety for pacemaker patients? *Europace* 2010;12:952-60.
184. Millar LM, Robinson AG, O'Flaherty MT, et al. Magnetic resonance imaging in a patient with a dual chamber pacemaker. *Case Rep Med* 2010;2010:292071.
185. Brockmann C, Sommer T, Pirzer R, et al. Repeated MRI of a patient with an intramedullary tumour and implanted cardiac resynchronization therapy defibrillator (CRT-D). *Clin Neuroradiol* 2013;23:237-41.
186. Macfie CC, Laws PG. Planned magnetic resonance imaging for a patient with a permanent pacemaker *in situ* with suspected spontaneous intracranial hypotension. *Br J Anaesth* 2013;111:1033-4.
187. Muehling OM, Wakili R, Greif M, et al. Immediate and 12 months follow up of function and lead integrity after cranial MRI in 356 patients with conventional cardiac pacemakers. *J Cardiovasc Magn Reson* 2014;16:39.
188. Shenthal J, Milasinovic G, Al Fagih A, et al. MRI scanning in patients with new and existing CapSureFix Novus 5076 pacemaker leads: Randomized trial results. *Heart Rhythm* 2015;12:759-65.
189. Sheldon SH, Bunch TJ, Cogert GA, et al. Multicenter study of the safety and effects of magnetic resonance imaging in patients with coronary sinus left ventricular pacing leads. *Heart Rhythm* 2015;12:345-9.
190. Dandamudi S, Collins JD, Carr JC, et al. The safety of cardiac and thoracic magnetic resonance imaging in patients with cardiac implantable electronic devices. *Acad Radiol* 2016;23:1498-1505.
191. Delve J, Wright P, Patwala A, Patel D, Stevenson M. Off-label MRI examination of an MR conditional pacemaker. *BJR Case Rep* 2016;2:20150219.
192. Hussam A, Epicoco E, Sorgente A, Lupo P, Cappato R. Safety and utility of cardiac MRI in a patient with pericardial effusion and a recently implanted conventional pacemaker. *J Atr Fibrillation* 2016;9:1419.
193. Hwang YM, Kim J, Lee JH, et al. Cardiac implantable electronic device safety during magnetic resonance imaging. *Korean Circ J* 2016;46:804-810.
194. Ono M, Suzuki M, Isobe M. Feasibility, safety, and potential demand of emergent brain magnetic resonance imaging of patients with cardiac implantable electronic devices. *J Arrhythm* 2017;33:455-458.
195. Yadava M, Nugent M, Krebsbach A, et al. Magnetic resonance imaging in patients with cardiac implantable electronic devices: A single-center prospective study. *J Interv Card Electrophysiol* 2017;50:95-104.
196. Lupo P, Cappato R, Di Leo G, et al. An eight-year prospective controlled study about the safety and diagnostic value of cardiac and non-cardiac 1.5-T MRI in patients with a conventional pacemaker or a conventional implantable cardioverter defibrillator. *Eur Radiol* 2018;28:2406-2416.
197. Tanaka T, Froemming AT, Panda A, et al. Safety and image quality of 1.5-T endorectal coil multiparametric MRI of the prostate or prostatectomy fossa for patients with pacemaker or implantable cardioverter-defibrillator. *AJR Am J Roentgenol* 2019;212:815-822.
198. Padmanabhan D, Kella DK, Deshmukh AJ, et al. Safety of thoracic magnetic resonance imaging for patients with pacemakers and defibrillators. *Heart Rhythm* 2019;16:1645-1651.
199. Han D, Kang SH, Cho Y, Oh IY. Experiences of magnetic resonance imaging scanning in patients with pacemakers or implantable cardioverter-defibrillators. *Korean J Intern Med* 2019;34:99-107.
200. Schaller RD, Brunker T, Riley MP, Marchlinski FE, Nazarian S, Litt H. Magnetic resonance imaging in patients with cardiac implantable electronic devices with abandoned leads. *JAMA Cardiol* 2021;6:549-556.

MRI Bioeffects, Safety, and Patient Management 709

201. Ning X, Li X, Fan X, et al. 3.0 T magnetic resonance imaging scanning on different body regions in patients with pacemakers. *J Interv Card Electrophysiol* 2020 (Epub ahead of print).
202. Padmanabhan D, Kella D, Isath A, et al. Prospective evaluation of the utility of magnetic resonance imaging in patients with non-MRI-conditional pacemakers and defibrillators. *J Cardiovasc Electrophysiol* 2020;31:2931-2939.
203. American College of Radiology, ACR Manual on MR Safety. <https://www.acr.org/Clinical-Resources/Radiology-Safety/MR-Safety>.
204. Vigen KK, Reeder SB, Hood MN, et al. ISMRM Safety Committee. Recommendations for imaging patients with cardiac implantable electronic devices (CIEDs). *J Magn Reson Imaging*. 2021;53:1311-1317.

Chapter 26 MRI Safety Issues for Neuromodulation Systems

MIZAN RAHMAN, PH.D.

Electrical Engineering Fellow
Research & Development
Boston Scientific Neuromodulation Corporation
Valencia, CA

FRANK G. SHELLOCK, PH.D.

Director of MRI Safety
USC Stevens Neuroimaging and Informatics Institute

Adjunct Clinical Professor of Radiology and Medicine
Keck School of Medicine
University of Southern California
Los Angeles, CA

INTRODUCTION

Magnetic resonance imaging (MRI) has been utilized in the clinical setting for more than 35 years. During this time, the technology has continued to evolve to improve image quality, acquisition time, and patient comfort. These changes resulted in MR systems with more powerful static magnetic fields, faster and stronger time-varying gradient magnetic fields, and improved radiofrequency (RF) transmission coils. The short-term exposures to the electromagnetic fields used for MRI at the levels recommended in the governing MRI standard from the International Electrotechnical Commission, IEC 60601-2-33 and by the United States (U.S.) Food and Drug Administration have resulted in relatively few problems for the hundreds of millions of MRI examinations performed to date (1-7). MRI-related injuries and the few fatalities that have occurred in patients without and with implants have been mostly due to not following recommended user guidelines related to the safety aspects of the MR scanners and medical implants.

Accordingly, the preservation of a safe MRI environment requires the utmost vigilance with respect to the management of patients with implants and devices because the variety and complexity of these items constantly changes (3, 6-9). This is particularly important when managing patients with active implantable medical devices (AIMDs) because of the elaborate nature of these implants (3, 6, 9). In consideration of the above, this chapter discusses MRI safety issues for neuromodulation systems, which are widely used and clinically important AIMDs.

WHAT IS NEUROMODULATION?

Neuromodulation utilizes a medical device to relieve symptoms through alteration or modulation of nerve system function via the targeted delivery of a stimulus, such as electrical stimulation or a chemical agent, to a specific neurological site in the body (7-12). Neuromodulation therapies have been available since the 1960s and are an essential tool for healthcare professionals. The field of neuromodulation encompasses a wide range of therapeutic applications from chronic pain to neurological conditions, such as epilepsy, dystonia, and Parkinson's disease, with the goal of supporting the recovery of abilities such as hearing, vision, and mobility, as well as the control of bladder or bowel function (7-12). In many instances, neuromodulation therapies improve the lives of patients because they provide an alternative to long-term drug therapy for the symptomatic relief of persistent or chronic conditions, which is especially important when existing medications are ineffective or become problematic for chronic use due to development of tolerance, addiction, adverse side-effects, or toxicity (10).

Technological advances in neuroscience combined with neuromodulation systems that were miniaturized to feasibly permit implantation contributed to the exponential growth of neuromodulation applications, including those used for deep brain stimulation, peripheral nerve stimulation, spinal cord stimulation, sacral nerve stimulation, vagus nerve stimulation, as well as the administration of drugs for pain management (7-12). Notably, neuromodulation systems are the fastest growing segment of the overall medical device industry.

MRI SAFETY ISSUES FOR NEUROMODULATION SYSTEMS

Static Magnetic Field-Related Issues

Static magnetic field-related issues are known to present hazards to patients with certain implants or devices primarily due to movement or dislodgment of objects made from ferromagnetic materials (3-9, 12, 13). Thus, neuromodulation systems with ferromagnetic materials, which are usually related to the power supply in the implantable pulse generator (IPG), will be attracted to (i.e., force) and aligned (i.e., torque) with the strong static magnetic field of the MR system (**Figure 1**). This movement could result in patient injury (e.g., torn sutures, internal bleeding, etc.) or require surgical revision to reposition the device (i.e., to restore therapy or for patient comfort). Exposure to the scanner's powerful static magnetic field may also alter the neuromodulation system's settings, requiring reprogramming, or permanently damage the device, necessitating replacement surgery (8, 9).

712 MRI Safety Issues for Neuromodulation Systems

Figure 1. High ferromagnetic material content of a neuromodulation system, which is usually related to the power supply in the implantable pulse generator, will increase magnetic field interactions (i.e., force and torque), resulting in issues including patient injury or device damage.



Numerous studies have assessed magnetic field interactions for implants and devices by measuring translational attraction and torque associated with the static magnetic fields of MR systems (3, 6). These investigations demonstrated that, for certain items, MRI exams may be performed safely if the items are nonferromagnetic or “weakly” ferromagnetic (i.e., the object minimally interacts with the magnetic field in relation to its *in vivo* application), such that the associated magnetic field interactions are insufficient to move or dislodge the items, *in situ*. Furthermore, the “intended use” of the implant must be taken into consideration, because this can greatly impact whether or not a particular item is acceptable for a patient undergoing MRI from a magnetic field interaction consideration. Sufficient *in situ*-related forces (e.g., fibrous encapsulation of an IPG) can exist to retain even a ferromagnetic device once it is implanted in the patient (3, 6).

Time-Varying Gradient Magnetic Field-Related Issues

MRI may be unsafe for patients with certain implants or devices due to induced energy and/or eddy currents related to the time-varying gradient magnetic fields. According to Faraday’s Law of Induction, any circuit located within the rapidly changing magnetic fields is subject to induced currents (9, 13, 14). With typical neuromodulation systems that utilize a lead and electrode, the circuit can be formed between the implanted electrode and the IPG, on a metallic structure (i.e., the IPG), or on individual components (e.g., coiled structures like antennas or energy transfer coils) (**Figure 2**). A variety of interactions can occur if current flows. For AIMDs, like neuromodulation systems, there is the risk of unintentional stimulation at the switching rate of the MR system’s gradient coils. Unintentional stimulation can be relatively benign as is the case with most neurostimulation scenarios, since neurostimulation pulse frequencies are much higher than the gradient switching frequencies associated with clinical MRI exams.

It should be noted that the gradient-induced voltages acting on the antennae and recharge coils of AIMDs, such as neuromodulation systems, can be extremely high, due to the number of coils within the associated components. If the circuitry is not robust enough to shield against high voltages, the device may sustain damage to its communication or recharge sys-

Figure 2. Time-varying gradient magnetic fields used during MRI can induce voltages that impact neuromodulation systems, resulting in unintended stimulation.



tem, memory, or output channels in association with MRI. If the device is damaged, it may require reprogramming or surgical replacement.

An additional concern from the time-varying gradient fields is the heating of the metallic surfaces of AIMDs caused by eddy currents. Large metallic surfaces with poor conductivity such as those associated with IPGs and implantable infusion pumps, may heat excessively resulting in possible burns.

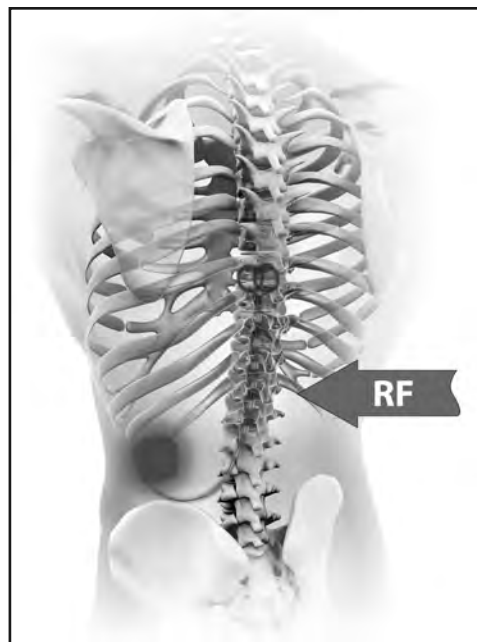
Radiofrequency Field-Related Issues

The use of AIMDs, physiological monitors, external accessories and similar objects made from conductive materials has caused excessive heating, resulting in serious burn injuries to patients undergoing MRI (3, 6, 7). The heating of implants and devices tends to be problematic primarily for objects made from conductive materials that have an elongated shape such as electrodes, leads, guidewire, and certain types of catheters (e.g., thermodilution catheters with thermistors, intracranial pressure monitoring catheters, etc.)(3, 6, 7, 14, 15).

Relatively long conductive structures can act as antennas during MRI, collecting RF energy and dissipating it along the path of least resistance. For leads associated with neuromodulation systems, this typically occurs at the electrodes of the leads, which are commonly found at the distal end and in contact with the organ receiving stimulation (e.g., brain, occipital nerve, vagus nerve, sacral nerve, etc.)(**Figure 3**). Since the electrodes used with neuromodulation systems are relatively small, the dissipated energy is concentrated very close to their surface. Excessive heating can be generated in neuromodulation systems under certain MRI conditions and there have been reports of serious patient injuries (16-18). A variety of factors contribute to the potential heating of a neuromodulation system. The important variables that impact MRI-related heating of an implanted medical device are presented in **Table 1** (3-7, 9, 14-28). Importantly, each of these variables must be taken into consideration to create safe MRI operating conditions for patients with neuromodulation

714 MRI Safety Issues for Neuromodulation Systems

Figure 3. The coupling of RF energy associated with MRI and a spinal cord stimulation system. Note that excessive heating typically occurs at the electrodes located at the distal end of the lead.



systems. It is particularly important to appreciate the complex interactions between the variables related to RF heating. For example, each RF frequency used for MRI (i.e., 64-MHz associated with 1.5-Tesla, 128-MHz associated with 3-Tesla, etc.) needs to be evaluated and considered individually for a given neuromodulation system because the resulting temperature rises may actually be lower at higher frequencies compared with lower frequencies (3, 6, 9, 14, 15-28)(**Figure 4**).

Over the years, different RF field-induced heating mitigation strategies have been employed and presented in the MR Conditional labeling for neuromodulation products. For example, for certain neuromodulation systems that did not incorporate design changes in consideration of the electromagnetic fields used for MRI, the strategy was to exclude the RF exposure entirely by utilizing a transmit RF head or extremity coil if the neuromodulation system was implanted outside of that particular transmit coil. In those instances, the transmitted RF energy did not subject any part of the implant to heating, resulting in a safe MRI exam (3, 6, 8, 9). Other neuromodulation systems used a reduced whole-body averaged SAR or B_{1+RMS} limit to minimize exposure to RF energy, while still other neuromodulation products have been specially designed to safely manage the RF energy so that the MR system can be operated under normal RF power levels (i.e., the Normal Operating Mode or First Level Controlled Operating Mode)(3, 6, 8, 9).

With respect to the whole-body averaged SAR value reported by the MR system, it should be realized that this metric is especially problematic with regard to MRI-related implant heating, as reported by Baker, et al. (29, 30) and Nitz, et al. (31). The scanner reported SAR values can be considered to be “not to exceed” values, such that each MR system manufacturer may have a different safety margin (i.e., comparing one manufacturer to another) to ensure that the displayed SAR values are not exceeded. Because there is no direct way to measure SAR prior to or during an MRI exam, scanner manufacturers rely on numerical

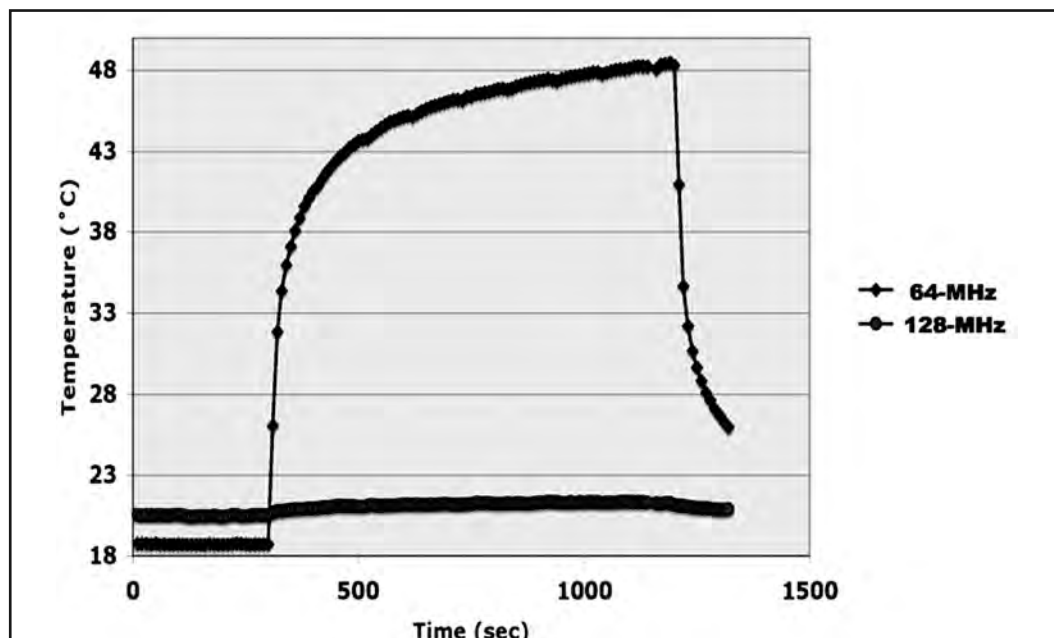
MRI Bioeffects, Safety, and Patient Management 715

Table 1. Important variables that impact MRI-related heating of a medical implant.

Area	Variable	Comments
MRI Related Variables	Static Field Strength and RF Frequency	The RF frequency is related to the static magnetic field strength of the MR system.
	RF Power Level, Whole-Body Averaged Specific Absorption Rate (SAR), or B_{1+RMS}	In the Normal Operating Mode, the RF power is limited to 2.0-W/kg whole-body averaged SAR and 3.2-W/kg averaged head SAR. In the First Level Controlled Operating Mode, the RF power is limited to 4.0-W/kg whole-body averaged body SAR and 3.2-W/kg averaged head SAR.
	Landmark (Area of Body Exposed to RF Energy)	Depending on which area of the patient's body is being imaged, more or less of the implanted medical device may be exposed to the RF energy.
	Transmit RF Coil Size	Transmitting RF energy with an extremity or head RF coil exposes less of the patient's body and, therefore, potentially less or none of the implanted medical device.
	Scan Duration	Thermal injuries are based on thermal doses to tissue. Thermal dose is a function of time and temperature. Thus, it takes a shorter time to damage tissue at higher temperatures.
Medical Device Variables	Conductive Structure Design	Some design structures may be better or worse antennas, resulting in greater or less RF field-induced heating.
	Conductive Structure Length	Structures may have a worst-case length depending on the resonant frequency. In general, relatively short structures may not be long enough to act as a good antenna.
	Implant Location	The amount of RF energy incident on a device depends on the device's location including lead or catheter routings.
	Loops/Coils of the Leads	Crossover points of the leads provided by strain relief or "slack" loops can alter the distribution of RF energy, possibly resulting in localized RF energy dissipation at the cross-over point and a decrease in the amount dissipated at the electrodes.
Patient Variables	Size	Larger patients have more tissue and, therefore, higher RF power is needed to excite the tissue for MRI.
	Body Composition	Fat is more permeable to RF energy so less energy is required to penetrate it.

716 MRI Safety Issues for Neuromodulation Systems

Figure 4. MRI-related heating at 1.5-Tesla/64-MHz (diamond) versus 3-Tesla/128-MHz (circle) for a lead not connected to a pulse generator. The MR system reported, whole-body averaged SAR used at 1.5-Tesla was 1.4-W/kg and at 3-Tesla it was 3-W/kg. Note the substantial differences in the temperature profiles during MRI-related heating of the lead (i.e., 1.5-T/64-MHz showing substantially higher temperatures), which illustrates that different resonant effects impact temperature rises for elongated implants. For an implant of a given length, different RF wavelengths will yield different heating effects (i.e., 64-MHz versus 128-MHz).



models to conservatively estimate the SAR for a particular scan sequence and each manufacturer uses certain assumptions for their SAR models. Importantly, the estimates of SAR did not consider situations when metallic implants were present in patients. Therefore, it is important to understand that implant heating may differ significantly when using different MR systems of the same static magnetic field strength and frequency for a given pulse sequence.

Significant variations in heating for a deep brain stimulation lead in association with different 1.5-Tesla scanners (notably from the same manufacturer) was first reported by Baker, et al. (29) and further examined in a later investigation (30). The specific concern is when MRI safety labeling for an implant is based on data generated using a particular MR system that has a high SAR safety margin, which ultimately equates to a lower transmitted RF power. In the clinical setting, the device's safety conditions may be followed using a different scanner that has a lower SAR safety margin, resulting in a higher transmitted RF power level. The end result could be a substantially higher temperature rise for the implant, potentially resulting in a patient injury.

In consideration of the myriad of issues of using SAR to ensure safety for patients with implants, the Food and Drug Administration along with other entities recommended that a different metric for RF energy should be utilized to characterize MRI-related heating specifically for AIMDs. This metric, the B_{1+RMS} , is the root-mean-square value of the MRI-effective component of the RF magnetic field (B_1 field). That is, it is the time-averaged RF magnetic field component relevant for creating an MR image.

The MR scanner measures the B_1^+ field (i.e., the positively rotating RF magnetic field) needed for an imaging sequence and uses the time-averaged B_1^+ field, or B_{1+RMS} , that is associated with a particular imaging sequence. Thus, the B_{1+RMS} value is calibrated by the MR system's software during the "prep" or "pre-scan" phase of an MRI exam. An important characteristic of B_{1+RMS} is that it is not an estimated value but it is a known quantity based on the pulse sequence and the associated parameters. Notably, B_{1+RMS} is not patient-dependent nor is it calculated differently based on a given MR system manufacturer.

Understanding the importance of B_{1+RMS} as a metric for RF energy that is presented in MR Conditional labeling of AIMDs necessitates an appreciation of basic MRI physics. When a patient enters the MR scanner, protons in the body align in the direction of the static magnetic field (B_0), similar to a compass aligning with the Earth's magnetic field. An MR imaging sequence is composed of a series of RF pulses that produce a magnetic field that interacts with these magnetically-aligned protons and rotates them through a specific angle commonly referred to as the "flip angle". The RF magnetic field (B_1 field) of which only one part, known as the positively rotating or "+" component, is useful for "flipping" the magnetically-aligned protons, allowing MR images to be created. The maximum 10-second, time-averaged B_1^+ field strength of the RF pulses in the imaging sequence is the root-mean-square or "RMS" B_1^+ value of the imaging sequence.

In 2013, the (International Electrotechnical Commission (IEC) mandated that all MR systems manufactured going forward must display the B_{1+RMS} . Therefore, it is unlikely to see B_{1+RMS} information presented on older scanners or those with software that has not been updated. B_{1+RMS} is measured and reported by the MR system in units of micro-Tesla (μT).

Considering that B_{1+RMS} is a more precise RF exposure metric than SAR, AIMD manufacturers typically present values for B_{1+RMS} that must not be exceeded when scanning patients in the *Instructions for Use* (IFU) for their implants. When following B_{1+RMS} as a condition of use, the SAR value is irrelevant, unless, of course, a particular operating mode of the MR system is specified. Using B_{1+RMS} tends to provide better performance for the MRI exam because it has fewer limitations versus using SAR values for patients with AIMDs.

Because B_{1+RMS} is being used by manufacturers in their MR Conditional labeling for AIMDs, it is vital to understand how to adjust protocols to achieve an acceptable B_{1+RMS} value to ensure patient safety. The parameters that an MR system operator uses to modify B_{1+RMS} will vary with the particular MR system. By way of example, parameters and options that can be adjusted to reduce B_{1+RMS} include, the following: (1) increase the RF pulse duration, (2) utilize a "Low SAR" mode or other similar option, (3) increase the repetition time (TR), (4) reduce the number of slices for a given TR, (5) reduce the echo train length

718 MRI Safety Issues for Neuromodulation Systems

(ETL) in a fast spin echo (FSE) pulse sequence, (6) reduce the refocusing angle (i.e., for FSE sequences), (7) reduce the flip angle (i.e., for gradient echo, GRE, pulse sequences) and (8) use a GRE sequence instead of a spin echo or fast spin echo pulse sequence (3, 6).

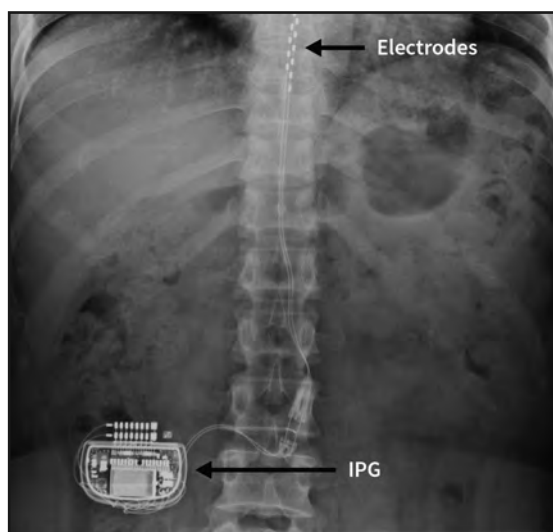
In addition to being a more precise metric for controlling RF power deposition, another advantage to using B_{1+RMS} as opposed to SAR is that, once the adjustment is made to a desired B_{1+RMS} value for a given sequence, that information can be saved in scanner's protocol library for future use. The B_{1+RMS} will then remain at that value for the next patient unless the imaging parameters are changed.

As previously stated, patients with neuromodulation systems are exposed to the risks associated with the RF energy collected in undesirable antennas in the leads, resulting in excessive heating. Because RF energy can also travel in the opposite direction towards the IPG, device components or memory can be damaged and, thus, may require replacement surgery in the event that the electronics are compromised (3, 6, 8, 9, 14). The RF energy entering into the IPG can impact the internal electronics causing rectification (i.e., rectification is the process of turning an alternating current waveform into a direct current waveform, thus, creating a new signal that has only a single polarity) and the resultant signal can be delivered to the patient through the lead contacts creating unintended stimulation.

MRI EXAMINATIONS AND NEUROMODULATION SYSTEMS

As previously indicated, neuromodulation systems have been employed for a variety of neurological disorders as well as for many other conditions (8, 9, 11, 12). A typical neuromodulation system used for stimulation consists of an IPG (i.e., similar to a cardiac pacemaker) and one or more leads that conduct the electrical pulses to the therapeutic target via one or more electrodes (3, 6, 8, 9)(Figure 5). The IPG contains electronics and a single-use or rechargeable battery. The size of the IPG and the therapeutic target dictate the potential implant locations and lead routings through the patient's body.

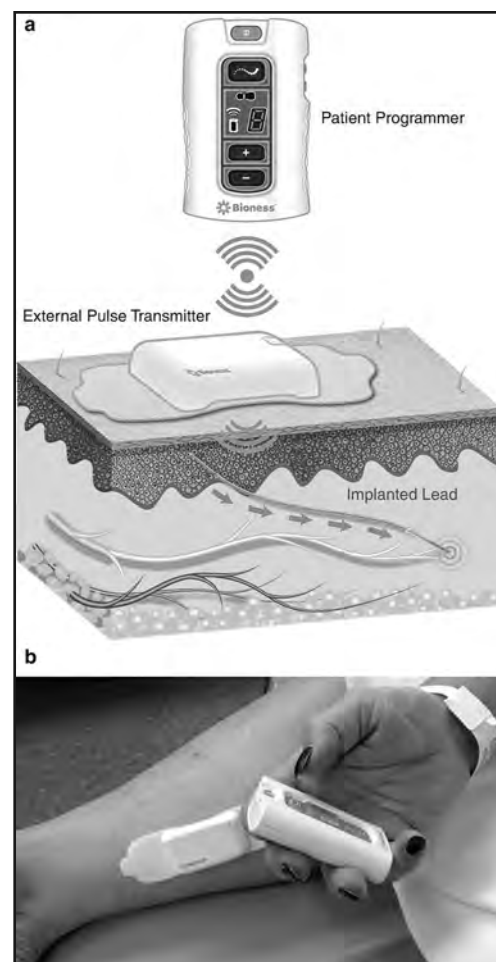
Figure 5. X-ray showing a typical neuromodulation system used for stimulation that consists of an IPG and a set of leads that conduct the electrical pulses to the therapeutic target via one or more electrodes. This example shows a spinal cord stimulation system. Note the positions of the IPG, leads, and electrodes.



There is a newer type of neuromodulation system that is predominantly used for spinal cord stimulation (SCS) or peripheral nerve stimulation (32-34). This device utilizes an implanted lead and has an external battery and stimulator. The external component communicates with the implanted lead using wireless technology (3, 6, 8, 9)(Figure 6). This platform was developed for neuromodulation for various reasons. Traditional neuromodulation systems require surgical implantation of multiple components: the IPG, lead extensions, and lead with stimulating electrodes. The IPG used with a conventional neuromodulation system is somewhat bulky and, thus, may cause tissue damage or other problems (32-34). Because of possible complications and hardware-related issues, the standard neuromodulation system platform is suggested to pose a higher risk for certain adverse events (32-34).

By comparison, wirelessly-powered leads used for SCS or peripheral nerve stimulation represent a practical option for patients with respect to their clinical utilization. Importantly, a clear advantage of using a wirelessly-powered lead system is the elimination of components that are required by traditional systems, namely the pulse generators, lead extensions, and longer leads (32-34). Thus, the proposed benefits of a wirelessly-powered lead system include decreased implantation procedural time, lower risk of infection (i.e., because fewer components are implanted), reduced overall costs compared with conventional neuromod-

Figure 6. Example of a neuromodulation system used for spinal cord or peripheral nerve stimulation that utilizes an implanted lead and an external battery and stimulator. The external component communicates with the implanted lead using wireless technology. (a) This example shows the Patient Programmer, the External Pulse Transmitter, and the implanted StimRouter Lead (Bioness, www.stimrouter.com). (b) The Patient Programmer can be used by the patient to self-administer stimulation.



720 MRI Safety Issues for Neuromodulation Systems

ulation systems and, because of its unique design (i.e., an external simulation component and power supply), diminished limitations for patients undergoing MRI (32-34).

Current neuromodulation therapies approved by the FDA and other notified bodies include deep brain stimulation (DBS) for essential tremor, Parkinsonian tremor, dystonia, and obsessive-compulsive disorder and other conditions; SCS for chronic pain; peripheral nerve stimulation for chronic pain; sacral nerve stimulation for urinary and fecal incontinence; gastric stimulation for gastroparesis; vagus nerve stimulation (VNS) and responsive neurostimulation (RNS) for epilepsy; VNS for depression; auditory nerve stimulation for hearing impaired patients; administration of Baclofen or other medications for chronic pain via implantable infusion pumps; as well as many others (8, 9, 11, 12, 33, 34).

During the early days of MRI technology, because of the inherent risks associated with neuromodulation systems relative to the MRI environment, the presence of these AIMDs and others was considered a strict contraindication for patients. However, over the years, various studies were performed that supported the safety of scanning patients with neuromodulation systems under highly specific MRI conditions (9, 11, 12, 20, 22, 24, 29, 30, 33-61). Because of concerted efforts of device manufacturers and biomedical investigators, a large number of neuromodulation systems now have MR Conditional labeling, allowing patients to benefit from the diagnostic capabilities of MRI (8, 9, 11, 12, 62, 63). As such, if specific guidelines are followed, MRI examinations may be conducted safely in patients with certain neuromodulation systems.

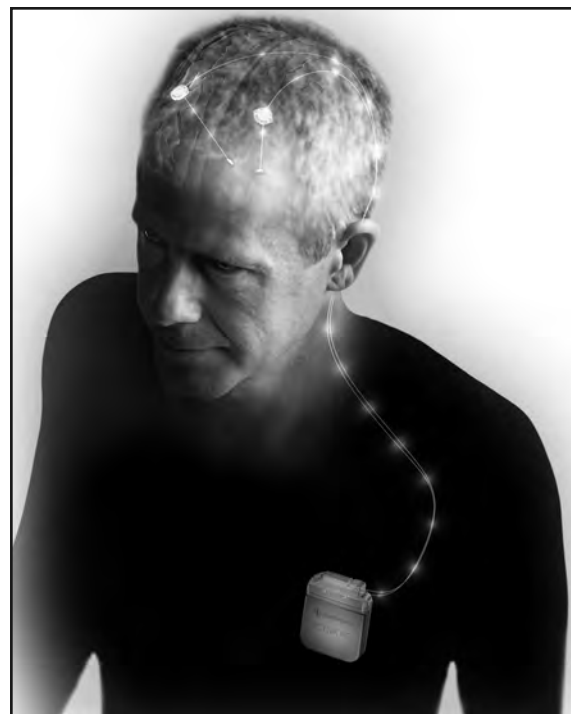
Various representative examples of neuromodulation systems that have criteria defined to permit safe MRI examinations are presented in the following sections of this chapter, with the acknowledgment that many other devices exist with approved MR Conditional labeling. It should be noted that certain neuromodulation systems are labeled MR Unsafe in the United States but MR Conditional outside the United States. Therefore, it is always important to obtain country-specific labeling information for a given neuromodulation system. In addition, because the labeling for implants may change based on new information, health-care professionals are advised to contact the manufacturer of the neuromodulation system to obtain the latest information to ensure patient safety relative to the use of MRI.

Deep Brain Stimulation Systems

Deep brain stimulation is one of the most rapidly growing areas in neuromodulation. Since 1997, there have been well over 160,000 patients implanted with DBS systems worldwide. As previously mentioned, DBS is currently approved for the treatment of essential tremor, Parkinsonian tremor, dystonia, and obsessive-compulsive disorder. In addition, clinical trials are underway assessing the role of DBS to treat epilepsy, chronic pain, cluster headaches, major depression, post-traumatic stress syndrome, morbid obesity, and other conditions (11, 35-40).

A typical DBS device includes an IPG, which is usually implanted in a subclavicular position but may also be placed in an abdominal site. The IPG is connected to one or two lead extensions, and one or two leads that run through the torso, chest, and neck region to the brain (**Figure 7**). This neuromodulation device delivers high frequency electrical stim-

Figure 7. Example of a DBS system (Activa PC Model 37601 IPG, Model 37085 lead extension, and Model 3389 lead, Medtronic, Inc.). Note the positions of the IPG, lead extensions, leads, and electrodes implanted in the brain.



ulation to multiple contact electrodes placed in the ventral intermediate nucleus of the thalamus or other anatomic sites.

The necessity of using MRI is essential to the use of DBS therapy in patients. MRI is important for the diagnosis of hemorrhage, stroke, and intracranial lesions, as well as for assessing the progression of neurodegenerative disorders. Additionally, MRI-guided procedures are used to optimally position the DBS electrodes, resulting in a substantial decrease in the time required for implantation (58, 59). MRI is used post-operatively to determine the location of the DBS leads and electrodes, which is critical information for the evaluation of patients with sub-optimal results or side effects, as well as for targeting during revision, or other cranial surgeries. Furthermore, functional MRI (fMRI) has been demonstrated to be beneficial for understanding the mechanisms of DBS (47, 60).

The inherent desire to use MRI in DBS patients prompted several groups to systematically study MRI-related issues for these AIMDs (8, 9, 29, 30, 41-57, 61). Approximately 20 years ago, the earliest research contributed to the first AIMD to receive MR Conditional labeling, the DBS system from Medtronic. Despite the limitations for MRI that included scanning at 1.5 Tesla, only, using a transmit/receive RF head coil, and a maximum head SAR of 0.1 W/kg, patients were allowed to undergo MRI for the first time. Importantly, these studies along with those conducted by device manufacturers resulted in MR Conditional labeling for several DBS systems, including those that are “full-body eligible”, enabling a wide range of MRI exams to be performed in patients (8, 9). Because manufacturers of DBS systems have strict safety criteria for MRI examinations, healthcare professionals must only scan patients according to the specific information indicated in the *Instructions*

722 MRI Safety Issues for Neuromodulation Systems

for Use documents for these products. Otherwise, serious injuries can occur, like the catastrophic injury reported by Henderson, et al. (17) (**Figure 8**).

In this case report, Henderson, et al. (17) described a patient with Parkinson's disease that sustained a serious permanent neurological injury secondary to an RF lesion caused by excessive heating of the electrode of a DBS system associated with MRI of the lumbar spine. Because the patient was an avid hunter, the IPG for the DBS system was placed in his abdomen rather than in the typical subclavicular region to avoid interference with the butt of his rifle. Seven months after placement of the IPG, the patient underwent an MRI of the lumbar spine for the evaluation of back and left leg pain. Multiple scan sequences were performed at 1.0-Tesla/42-MHz with a transmit body RF coil and a receive-only spine coil. Following the MRI examination, the patient experienced hemiparesis.

The patient was subsequently evaluated by his neurologist, who noted that he exhibited "obtunded aphasia with right hemiplegia, bilateral extensor plantar responses, and skew deviation, right eye below left." A computed tomography scan performed immediately following the MRI revealed hemorrhage surrounding the left DBS electrode. An MRI of the brain conducted using a 1.5-Tesla MR system two days after the lumbar scan found "subacute hemorrhage with methemoglobin in the left thalamus, posterior limb of the left internal capsule, and left cerebral peduncle." The hemorrhage was adjacent to the DBS electrode, with surrounding edema seen on T2-weighted pulse sequences (**Figure 8**).

Figure 8. (A) A computed tomography scan performed immediately after a lumbar spine MRI exam was performed in a symptomatic patient with a DBS system, which revealed evidence of a hemorrhage surrounding the left DBS electrode. (B) Axial plane, T2-weighted MR image of the patient's brain showing edema around the left DBS electrode. In this case, the patient underwent MRI of the lumbar spine at 1.0-Tesla, using a transmit body RF coil, substantially deviating from the safety labeling for the DBS system, resulting in a permanent neurological deficit.

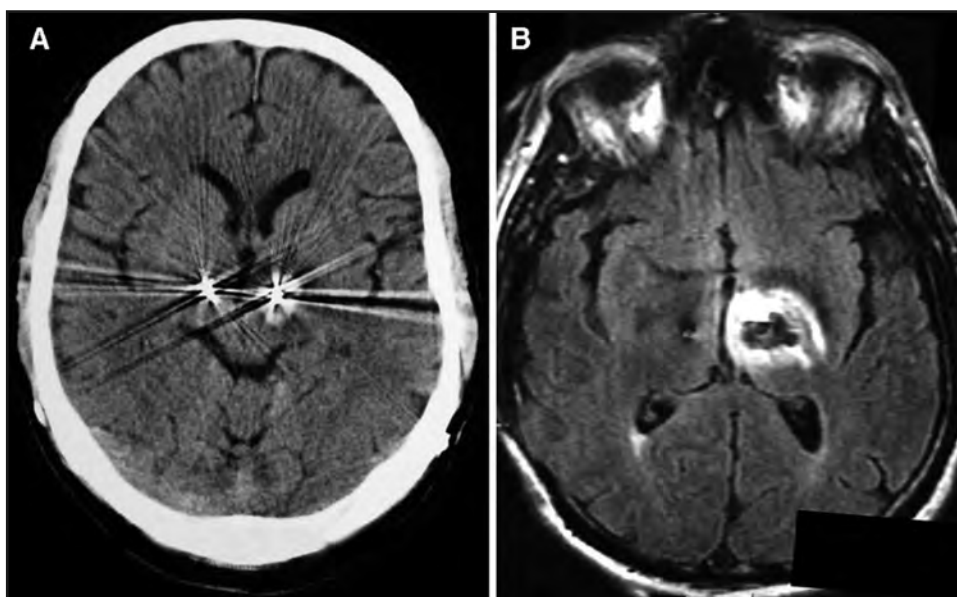


Table 2. Head-Only Deep Brain Stimulation (DBS) System, Activa SC Model 37602, Medtronic, Inc.

Implant System	Head-Only Deep Brain Stimulation (DBS) System, Activa SC Model 37602
Scan Region	Head-Only
Scan Requirements	IPG implanted in pectoral or abdomen area Impedance test to determine open or short circuits No abandoned leads within transmit/receive head RF coil If programmer cannot communicate with IPG or if IPG is end of life (EOS), MRI safety is unknown
System Settings During Scan	Therapy On with special Bipolar program only with Pocket Adaptor
MRI Scan Conditions	1.5 T horizontal cylindrical bore Max. spatial gradient magnetic field, 19 T/m Max. gradient slew rate, 200 T/m/s Transmit/receive head RF coil, only Head SAR \leq 0.1 W/kg
Active Scan Time	No restrictions
Patient Positioning	Supine or Prone
Post Scan	Program back to original settings, turn Therapy On
Website	https://manuals.medtronic.com/manuals/main/region

(IPG, implantable pulse generator; WBA, whole-body averaged; SAR, specific absorption rate)

The patient was evaluated seven months following the MRI exam and determined to have severe dysarthria that made his speech nearly impossible to understand. He had persistent right hemiparesis with falling toward the right and clumsiness of his right hand. Notably, this patient's neurological deficits were identified immediately after his lumbar MRI exam, implicating a direct relationship between the imaging procedure and associated brain lesion. In addition, the hemorrhage and edema demonstrated on subsequent brain imaging surrounded the DBS electrode circumferentially, as would be expected of a lesion generated by RF heating (17). Of further note is that this patient suffered from a lesion on the left side of the brain, corresponding with the left-sided lead and the IPG implanted in his abdomen. No lesion was produced on the right side, where the IPG was implanted in the standard subclavicular position. This serious accident clearly emphasizes that, while MRI may be performed safely in patients with DBS systems with close adherence to specific safety guidelines (i.e., in this case, the labeling required imaging at 1.5-Tesla using a transmit/receive RF head coil and not exceeding a head SAR of 0.1-W/kg), any deviation from the stated MRI requirements can result in serious consequences for the patient.

While the findings from numerous investigators helped the medical community understand the safety and risks associated with MRI of patients with DBS systems, because of the complicated and expensive nature of the testing procedures (9, 13, 14), device manufacturers decided to conduct their own evaluations based on guidelines outlined in the In-

724 MRI Safety Issues for Neuromodulation Systems

Table 3. Full-Body Deep Brain Stimulation (DBS) System, Model B35200, Medtronic, Inc.

Implant System	Full-Body Deep Brain Stimulation (DBS) System, Model B35200
Scan Region	Full-Body
Scan Requirements	IPG implanted in pectoral or abdomen area Impedance test to determine open or short circuits No elevated body temperature If programmer cannot communicate with IPG or if IPG is end of life (EOS), MRI safety is unknown
System Settings During Scan	Set IPG to MRI Mode, Therapy Off
MRI Scan Conditions	1.5 T or 3 T horizontal cylindrical bore Max. spatial gradient magnetic field, 19 T/m, 1.5 T Max. spatial gradient magnetic field, 19 T/m, 3 T Max. gradient slew rate 200 T/m/s, 1.5 T or 3 T Transmit body RF coil with any receive-only coil Transmit/receive head RF coil Transmit/receive extremity RF coil transmit 1.5 T, $B_{1+RMS} \leq 2.0 \mu\text{T}^*$ 3 T, $B_{1+RMS} \leq 2.5 \mu\text{T}^*$ *If B_{1+RMS} is unavailable, then max. WBA SAR or Head SAR < 0.1 W/kg
Active Scan Time	30 min. in a 90 min. window
Patient Positioning	Supine or Prone
Post Scan	Program back to original settings, turn Therapy On
Website	https://manuals.medtronic.com/manuals/main/region

(IPG, implantable pulse generator; WBA, whole-body averaged; SAR, specific absorption rate)

International Organization for Standardization/Technical Standard (ISO/TS) 10974:2018 and other pertinent documents (25–28), resulting in approval for MR Conditional labeling from various regulatory bodies, including the FDA. **Tables 2, 3 and 4** present examples of MRI-related labeling information for DBS systems, including head-only and full-body eligible versions. For complete and up-to-date information, readers are advised to visit the manufacturer's websites.

Responsive Neurostimulation Systems

Responsive neurostimulation (RNS) is a recent breakthrough surgical approach for treating seizures that cannot be managed by medication (64, 73). A relatively small neurostimulator is implanted in the skull and connected to two leads that have electrodes implanted either on the surface of the brain, into the brain, or both (**Figure 9**). The RNS device is programmed to detect seizures by continuously monitoring brain activity. When it detects

MRI Bioeffects, Safety, and Patient Management 725

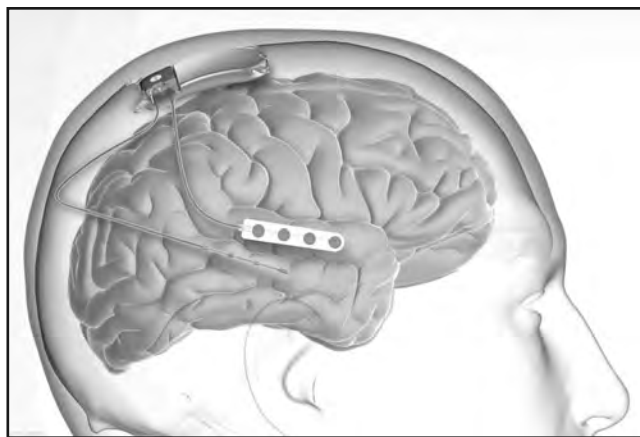
Table 4. Full-Body Vercise Gevia Deep Brain Stimulation (DBS) System, Boston Scientific Corporation.

Implant System	Vercise Gevia Deep Brain Stimulation (DBS) System
Scan Region	Full-Body or Head Using Transmit/Receive Head RF Coil
Scan Requirements	<p><i>Leads Only Version, DB-2201 or DB-2202 Leads</i></p> <p>Patient is implanted with a booted lead system comprised of Leads, Lead Boots, and Burr Hole Cover</p> <p>Leads are capped with Lead Boots on proximal ends and excess Lead is coiled and implanted under the scalp of the skull</p> <p>No fractured Leads</p> <p>No Extensions are present</p> <p>No Stimulator is present</p> <p>Externalized portion of Lead is not contacting the patient and is positioned in a straight configuration without loops, and centered with reference to the transmit/receive RF coil</p> <p><i>Fully Implanted Version</i></p> <p>Patient implanted with full DBS system comprised of Leads, Extensions, Stimulator, and Burr Hole Cover</p> <p>No fractured leads</p> <p>No elevated body temperature</p>
System Settings During Scan	<p>IPG fully charged</p> <p>Set IPG to MRI Mode, Therapy Off</p> <p>Impedance check automatically performed. If no error messages, proceed with MRI</p>
MRI Scan Conditions	<p>1.5 T horizontal cylindrical bore</p> <p>Max. spatial gradient magnetic field, 40 T/m</p> <p>Max. gradient slew rate, 200 T/m/s</p> <p><i>Lead Only Version, DB-2201 or DB-2202 Leads</i></p> <p>Transmit body RF coil and any receive-only coil</p> <p>Transmit/receive head RF coil</p> <p>$B_{1+RMS} \leq 2.0 \mu\text{T}^*$</p> <p><i>Fully Implanted Version, DB-2201 or DB-2202 Leads</i></p> <p>Transmit body RF coil and any receive-only coil</p> <p>Transmit/receive head RF coil</p> <p>Transmit/receive head RF coil</p> <p>$B_{1+RMS} \leq 2.0 \mu\text{T}^*$</p> <p>Transmit body RF coil and any receive-only coil with DB-2201 Leads:</p> <p>Isocenter above vertebra T5: $B_{1+RMS} \leq 1.5 \mu\text{T}^*$</p> <p>At or below vertebra T5: $B_{1+RMS} \leq 2.0 \mu\text{T}^*$</p> <p>Transmit body RF coil and any receive-only coil with DB-2202 Leads:</p> <p>Isocenter above vertebra T12: $B_{1+RMS} \leq 1.2 \mu\text{T}^*$</p> <p>At or below vertebra T12: $B_{1+RMS} \leq 2.0 \mu\text{T}^*$</p> <p>*If B_{1+RMS} is unavailable, then max. WBA SAR or Head SAR < 0.1 W/kg</p>
Active Scan Time	30 min. in a 60 min. window
Patient Positioning	Supine or Prone
Post Scan	Disable MRI Mode and turn Therapy On
Website	https://www.bostonscientific.com/imageready/image-ready/gateway.html

(IPG, implantable pulse generator; WBA, whole-body averaged; SAR, specific absorption rate)

726 MRI Safety Issues for Neuromodulation Systems

Figure 9. Responsive neurostimulation (RNS) device (RNS-320, NeuroPace, Inc.). Note the relatively small neurostimulator that is implanted in the skull and connected to two leads that have electrodes implanted on the surface of the brain and into the brain.



seizure or seizure-like activity, the RNS device delivers an electrical current to the brain to stop or shorten the seizure, or possibly prevent it altogether. In 2013, the first commercially available RNS system received FDA approval for the treatment of drug-resistant focal epilepsy. The first generation of this neuromodulation system (RNS-300M, NeuroPace, Inc.) was labeled MR Unsafe. A newer version (RNS-320) is labeled MR Conditional. The MRI-related information for both of these systems is presented in **Table 5**.

Spinal Cord Stimulation Systems

Spinal cord stimulation (SCS) is commonly used to treat chronic pain of neurologic origin, as well as other conditions that are undergoing clinical investigations (8, 9, 12). Several types of IPGs and many different types of leads with different electrode arrays are used to administer SCS. **Figure 10** shows an example of a SCS device. Equipment-related factors associated with standard SCS devices substantially complicate MRI-related issues for these devices (8, 9, 65-72). Importantly, the lead used for SCS varies in length depending on the spinal location targeted for stimulation, presenting particular challenges for the evaluation of MRI-related heating (i.e., because the length of an implant is a major determinant of heating)(3, 9, 13-15, 74). There are several different manufacturers of SCS products, many of which have MR Conditional labeling.

Figure 10. A typical spinal cord stimulation (SCS) system consists of an IPG, which is implanted near the buttocks or abdomen, attached to leads. The electrodes associated with the leads are typically implanted in the epidural space (i.e., the area between the dura mater and the vertebral wall).

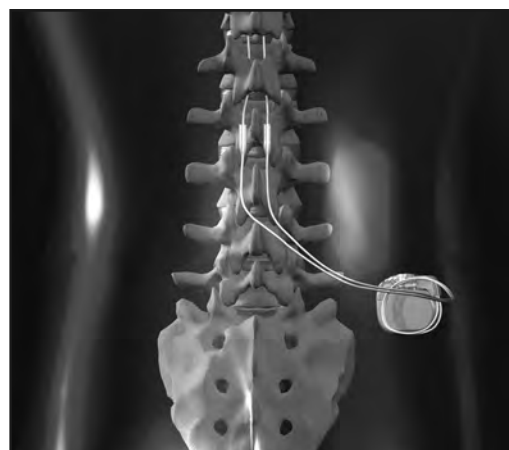


Table 5. Responsive Neurostimulation System, RNS, NeuroPace, Inc.

Implant System	Responsive Neurostimulation System, RNS-320	RNS-300M
MRI Eligibility	MR Conditional	MR Unsafe
Scan Region	Full-Body	NA
Scan Requirements	IPG is not end of service, EOS 10 days has passed since implant procedure Patient has no other implant system No elevated body temperature Enable MRI Mode	NA
System Settings During Scan	Set IPG to MRI Mode, Therapy Off	NA
MRI Scan Conditions	1.5 T horizontal cylindrical bore Max. spatial gradient magnetic field, 30 T/m Max. gradient slew rate, 200 T/m/s Transmit body RF coil with any receive-only coil No transmit head or extremity RF coil (untested) -Isocenter above T2 vertebra: B _{1+RMS} ≤ 2.95 µT, Max. Head SAR: 0.6 W/kg -Isocenter between vertebrae T8 to T2: B _{1+RMS} 4.67 µT, Max. WBA SAR: 1.0 W/kg -Isocenter below vertebra T8: B _{1+RMS} 4.67 µT, Max WBA SAR: 2.0 W/kg	NA
Active Scan Time	30 min. per session, 30 min. wait period between sessions	NA
Patient Positioning	Supine	NA
Post Scan	Disable MRI Mode, turn Therapy On	NA
Website	https://www.neuropace.com/providers/rns-system-mri-guidelines/	

(IPG, implantable pulse generator; WBA, whole-body averaged; SAR, specific absorption rate)

Initially, SCS systems approved for patients undergoing MRI were limited to the use of 1.5-Tesla/64-MHz scanners to image the head using a transmit/receive RF head coil, only. In 2013, the first “full-body” MR Conditional SCS systems from Medtronic were approved for scanning at 1.5-Tesla/64-MHz. These AIMDs utilized “MRI SureScan” technology, which involved substantial modifications of the IPGs, leads, and electrodes and still have conditions that must be complied with in order to perform risk-free MRI exams (8, 9). Other device manufacturers such as Boston Scientific, Abbott, Nevro, and others now have MR Conditional SCS systems that are full-body eligible. Patients with these particular SCS systems are now afforded the benefit of the diagnostic capabilities of MRI since other body parts can be examined in addition to the head. **Tables 6 and 7** present MRI-related information for two SCS devices from Abbott and Boston Scientific, respectively.

728 MRI Safety Issues for Neuromodulation Systems

Table 6. Proclaim XR Recharge-Free Spinal Cord Stimulation (SCS) System, Abbott.

Implant System	Proclaim XR Recharge-Free SCS System
Scan Region	Full-Body
Scan Requirements	IPG in upper buttock, low back, midline, flank, or abdomen Lead tip in the epidural space between vertebrae T7 and T12 No broken or nonfunctional leads No abandoned devices, extensions or leads Components fully implanted No elevated body temperature Enable MRI Mode
System Settings During Scan	Set IPG to MRI mode, Therapy Off
MRI Scan Conditions	1.5 T horizontal cylindrical bore Max. spatial gradient magnetic field, 30 T/m Max. gradient slew rate, 200 T/m/s With Octrode 3186 Leads: Transmit body RF coil with any receive-only coil WBA SAR ≤ 0.8 W/kg With Penta 3228 Leads: Transmit body RF coil with any receive-only coil WBA SAR ≤ 0.1 W/kg
Active Scan Time	30 min. per session, 30 min. wait between sessions
Patient Positioning	Supine
Post Scan	Disable MRI Mode, Therapy On
Website	https://www.neuromodulation.abbott/us/en/hcp/provider-resources/mri-support.html

(IPG, implantable pulse generator; WBA, whole-body averaged; SAR, specific absorption rate)

Spinal Cord Stimulation Systems with Implanted Leads and External Components

As previously mentioned, standard SCS systems have an IPG that contains the stimulator along with a power source that connects with leads to deliver electrical pulses via electrodes into the spinal column (8, 9, 12). The other platform used for SCS has an implanted lead (which may incorporate pulse generating electronic components) and an external battery and stimulator that wirelessly communicates with the lead (33, 34). Using this type of SCS system, the patient must wear the external components when therapy is needed for pain management. Because of the inherent shorter lead lengths and fewer metallic components, it is less challenging to meet the MRI safety requirements for these SCS systems compared to traditional SCS systems (33, 34). In all instances, the external components are MR Unsafe and must be removed from the patient prior to entering the MR system room. Various manufacturers make SCS devices with implanted leads and external components. **Table 8** describes the MRI-related information for one such system, the Freedom-8A (FR8A) Stimulator Receiver for Spinal Cord Stimulator (SCS) from Stimwave Technologies.

Table 7. Precision Montage MRI Spinal Cord Stimulator (SCS) System, Model SC-1200, Boston Scientific Corporation.

Implant System	Precision Montage MRI Spinal Cord Stimulator (SCS) System, Model SC-1200
Scan Region	Full-Body
Scan Requirements	IPG in upper buttock or lower flank Leads in epidural space No abandoned leads of IPGs No fractured leads or compromised system integrity No elevated body temperature No external devices allowed in MR system room Enable MRI Mode
System Settings During Scan	Set IPG to MRI mode, Therapy off
MRI Scan Conditions	1.5 T horizontal cylindrical bore Max. spatial gradient magnetic field, 40 T/m Max. gradient slew rate, 200 T/m/s Transmit body RF coil and any receive-only coil Transmit/receive head RF coil or transmit/receive extremity RF coil With Avista leads: Normal Operating Mode WBA SAR ≤ 2.0 W/kg Head SAR ≤ 3.2 W/kg All other leads: Normal Operating Mode WBA SAR ≤ 0.1 W/kg; $B_{1+RMS} \leq 2.0 \mu\text{T}$ or Head SAR ≤ 0.2 W/kg
Active Scan Time	30 min. per session, 60 min. wait period between sessions
Patient Positioning	Supine or Prone
Post Scan	Disable MRI Mode, turn Therapy On
Website	https://www.bostonscientific.com/imageready/image-ready/gateway.html

(IPG, implantable pulse generator; WBA, whole-body averaged; SAR, specific absorption rate)

Peripheral Nerve Stimulation System

The use of peripheral nerve stimulation (PNS) to treat chronic pain conditions has become an increasingly important field in the area of neuromodulation (8, 9, 12). Pain in the extremities may occur due to a variety of central and peripheral neuropathic and nociceptive syndromes. Accordingly, peripheral nerve stimulation may be particularly effective when the pain is localized to a part of a single extremity or when the source of the pain is related to the malfunction of a known peripheral nerve. The ongoing advances in electrical neuromodulation technology since 1999 led to the miniaturization of the implantable electronics

730 MRI Safety Issues for Neuromodulation Systems

Table 8. Freedom-8A (FR8A) Stimulator Receiver for Spinal Cord Stimulator (SCS), Stimwave Technologies.

Implant System	Freedom-8A (FR8A) Stimulator Receiver for Spinal Cord Stimulator (SCS)
Scan Region	Full-Body
Scan Requirements	No external component of the Freedom-8A (FR8A) (e.g., Wearable Antenna Assembly, WAA) is allowed in the MR system room
System Settings During Scan	None
MRI Scan Conditions	1.5 T or 3 T horizontal cylindrical bore Max. spatial gradient magnetic field, 10 T/m Max. gradient slew rate, 200 T/m/s Transmit body RF coil with any receive-only coil Normal Operating Mode Head and Extremity: Max. WBA SAR: 2.0 W/kg (3 T) Torso: Max. SAR: 2.0 W/kg (1.5 T), Max. SAR: 0.3 W/kg (3 T)
Active Scan Time	None
Patient Positioning	Supine and Prone
Post Scan	None
Website	https://stimwavefreedom.com/about-us/mri-information

(WBA, whole-body averaged; SAR, specific absorption rate)

and that paved the way for using a minimally invasive percutaneous approach to target those peripheral nerves directly as opposed to using standard SCS systems.

Despite the advances in the PNS technologies, there are only a handful of neuromodulation devices designed specifically for the periphery. However, similar to SCS devices with implanted leads and external components, because of the miniaturization of the implantable PNS devices, there are fewer limitations for the use of MRI in patients with these implants (**Figure 11**). **Table 9** summarizes the MRI-related information for the Nalu Neurostimulation System (Nalu Medical, Inc.) used for PNS.

Figure 11. The Nalu Neurostimulation System (Nalu Medical, Inc.) is approved for peripheral nerve stimulation and spinal cord stimulation, as shown in this figure. Note the miniaturized implantable electronics.



Table 9. Nalu Neurostimulation System for Peripheral Nerve Stimulation (PNS), Nalu Medical, Inc.

Implant System	Nalu Neurostimulation System for Peripheral Nerve Stimulation (PNS)
Scan Region	Head and Extremity
Scan Requirements	Impedance check of $10\text{k}\Omega$ within prior 7 days of scan Do not sedate the patient No external part allowed in the MR system room
System Settings During Scan	None
MRI Scan Conditions	1.5 T or 3 T horizontal cylindrical bore Max. spatial gradient magnetic field, 20 T/m Max. gradient slew rate, 200 T/m/s Normal Operating Mode Max. WBA SAR: 2.0 W/kg No parts of the implanted system are allowed within any transmit/receive RF coil
Active Scan Time	15 min.
Patient Positioning	Supine or Prone
Post Scan	None
Website	https://nalumed.com/physician-resources-content/

(WBA, whole-body averaged; SAR, specific absorption rate)

Sacral Nerve Stimulation System

The sacral nerve stimulation (SNS) system is a neuromodulation system that is indicated for the treatment of urinary retention and the symptoms of overactive bladder, including urinary urge incontinence and significant symptoms of urgency-frequency alone or in combination, in patients who have failed or could not tolerate more conservative treatments. SNS devices may also be used for bowel control and, thus, are indicated for the treatment of chronic fecal incontinence in patients who have failed or who are not candidates for more conservative treatments.

Medtronic pioneered the first SNS systems, the InterStim and InterStim II Neuromodulation Systems) for clinical applications (**Figure 12**), both of which have MR Conditional labeling (75-78). Recently, Axonics Modulation Technologies, received FDA approval and MR Conditional labeling for their device, the Axonics Sacral Nerve Stimulation (SNM) Neurostimulator (**Figure 13**). The MRI-related information for the Interstim II Sacral Nerve Stimulation System and the Axonics Sacral Nerve Stimulation Neurostimulator is shown in **Tables 10** and **11**.

Vagus Nerve Stimulation Systems

Vagus nerve stimulation (VNS) therapy is a technique that uses a pulse generator to deliver intermittent electrical pulses via a lead that has helical cuff electrodes that are used to securely attach them to the vagus nerve at the cervical level (9, 79-88). In the U.S., VNS

732 MRI Safety Issues for Neuromodulation Systems

Figure 12. The Interstim II Sacral Nerve Stimulation System, Medtronic, Inc. Note the IPG implanted near the buttocks and the positions of the lead and electrodes.

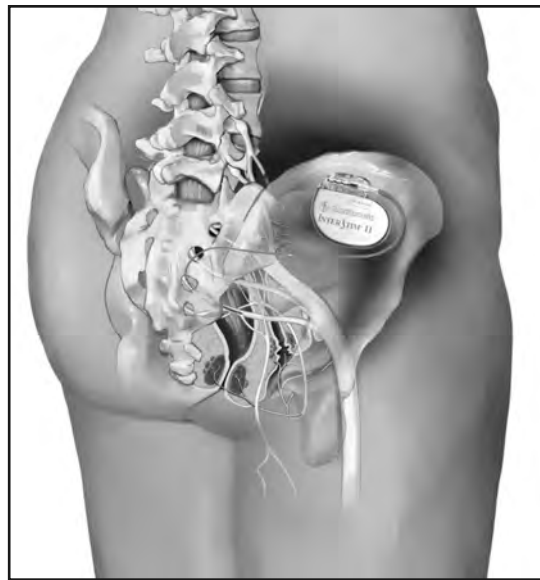
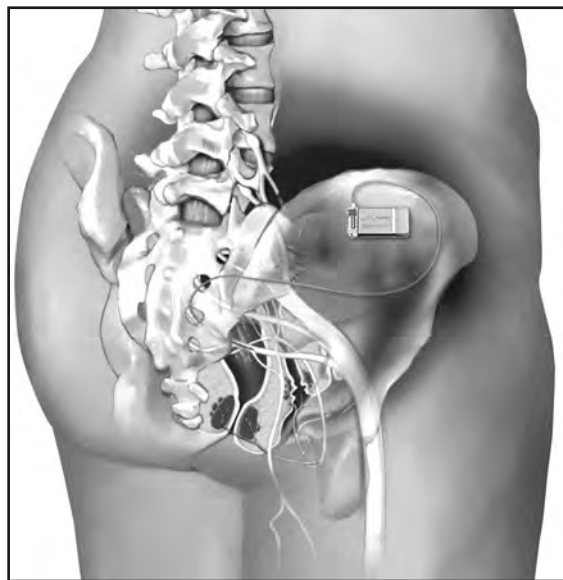


Figure 13. Axonics Sacral Nerve Stimulation (SNM) Neurostimulator, Axonics Modulation Technologies, Inc.

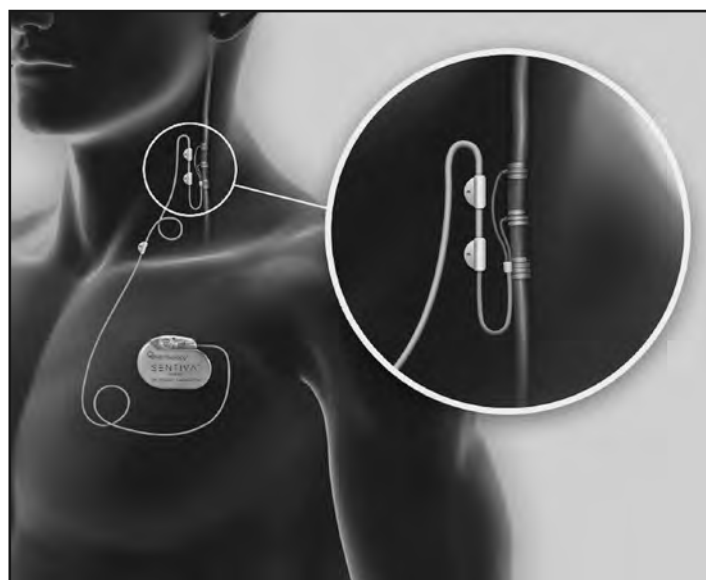


therapy is approved for treatment of epilepsy and medication-resistant depression and is under investigation as a therapy for other disorders, including anxiety, Alzheimer's disease, morbid obesity, and migraine headaches. Currently, a few AIMDs are available from LivaNova (previously Cyberonics) and Enteromedics that are FDA approved for vagus nerve stimulation, but only the devices from LivaNova have MR Conditional labeling, such as the SenTiva Vagus Nerve Stimulation System, Model 1000 (LivaNova, Inc.) (Figure 14). MRI is often needed to evaluate patients with the VNS devices, including for the purpose of elucidating the mechanisms responsible for the success or failure of this therapy (9, 79-88). The MRI-related information for the SenTiva Vagus Nerve Stimulation System, Model 1000 is presented in Table 12.

Table 10. Interstim II Sacral Nerve Stimulation System, Medtronic, Inc.

Implant System	Interstim II Sacral Nerve Stimulation System
Scan Region	Full-Body
Scan Requirements	No elevated body temperature
System Settings During Scan	MRI readiness check, enable MRI Mode, Therapy Off
MRI Scan Conditions	<p>1.5 T or 3 T horizontal cylindrical bore Max. spatial gradient magnetic field, 20 T/m Max. gradient slew rate, 200 T/m/s</p> <p>Transmit body RF coil with any receive-only coil -Isocenter at or above vertebra T7: Normal Operating Mode or First Level Controlled Operating Mode (1.5 T and 3 T)</p> <p>-Isocenter below vertebra T7: $B_{1+RMS} \leq 4.0 \mu\text{T}$ or WBA SAR $\leq 2.0 \text{ W/Kg}$ (1.5 T)</p> <p>-Isocenter below T7 vertebra: $B_{1+RMS} \leq 2.0 \mu\text{T}$ or WBA SAR $\leq 1.4 \text{ W/Kg}$ (3 T)</p>
Active Scan Time	30 min. with 5 min. wait period between sessions
Patient Positioning	Supine or Prone
Post Scan	Disable MRI Mode and turn Therapy On
Website	https://manuals.medtronic.com/manuals/main/region

(WBA, whole-body averaged; SAR, specific absorption rate)

Figure 14. The SenTiva Vagus Nerve Stimulation System, Model 1000, LivaNova, Inc. Note the lead with helical cuff electrodes that are used to securely attach them to the vagus nerve at the cervical level.

734 MRI Safety Issues for Neuromodulation Systems

Table 11. Axonics Sacral Nerve Stimulation (SNM) Neurostimulator, Axonics Modulation Technologies, Inc.

Implant System	Axonics Sacral Nerve Stimulation (SNM) Neurostimulator, Model 1101 With Tined Lead, Model 1201 or 2201
Scan Region	Full-Body
Scan Requirements	IPG must be implanted in the posterior hip area or upper buttock area No other implanted device No external components permitted in the MR system room
System Settings During Scan	Turn Therapy Off
MRI Scan Conditions	1.5 T or 3 T horizontal cylindrical bore Max. spatial gradient magnetic field, 25 T/m Max. gradient slew rate, 200 T/m/s Transmit body RF coil with any receive-only coil Normal Operating Mode 1.5 T, Max. WBA SAR 0.85 W/Kg, Max. B_{1+RMS} 3 μ T 3 T, Max. WBA SAR 0.6 W/Kg, Max. B_{1+RMS} 1 μ T
Active Scan Time	Max. 30 min.
Patient Positioning	Supine or Prone
Post Scan	Turn Therapy On
Website	https://www.axonics.com/

(IPG, implantable pulse generator; WBA, whole-body averaged; SAR, specific absorption rate)

Cochlear Implants

A cochlear implant (CI) is a neuromodulation system designed to help severely-to-profoundly deaf adults and children who get little or no benefit from external hearing aids (89–106). Notably, even individuals with severe or profound “nerve deafness” may benefit from these AIMDs. A cochlear implant has two main parts: an external part that hooks over the ear or that is worn on the head, and a surgically implanted internal part (**Figure 15**). The two components are coupled together using powerful magnets, one or more of which are implanted. With respect to the external part of the CI, this component contains a transmitter, microphone, and speech or sound processor. The microphone detects acoustic sounds and sends it to the speech processor. The processor then analyzes and digitizes the signal before sending it to the transmitter. The transmitter “codes” the signals and sends them to the implanted receiver via the magnetic coupling. With respect to the internal part, this component includes one or more magnets, a receiver, which is located under the skin on the temporal bone, and one or more electrode arrays (**Figure 16**). The receiver collects signals from the transmitter and converts them to electrical pulses, which are then dispatched to the electrodes that have been inserted into the inner ear. The electrodes directly stimulate the auditory nerve throughout a portion of the cochlea, resulting in the brain interpreting the signals as sound.

Table 12. SenTiva Vagus Nerve Stimulation (VNS) System, Model 1000, LivaNova, Inc.

Implant System	SenTiva Vagus Nerve Stimulation (VNS) System, Model 1000
Scan Region	Full-Body
Scan Requirements	IPG implanted in upper chest or above armpit
System Settings During Scan	MRI readiness check, enable MRI Mode, Therapy Off, Sensing Off
MRI Scan Conditions	1.5 T or 3 T horizontal cylindrical bore Max. spatial gradient magnetic field, 30 T/m Max. gradient slew rate, 200 T/m/s Body RF transmit coil w/ any receive coil only Transmit-Receive head coil or extremity coil Exclusion Zones: Vertebra C7 to L3 (transmit body RF coil), Vertebra C7 to T8 (transmit head or extremity RF coil) Max. SAR: 3.2 W/kg (head or extremity RF coil) Max. SAR: 2.0 W/kg (transmit body RF coil)
Active Scan Time	No time restrictions for transmit/receive head RF coil Transmit body RF coil, 15 min. with 30 min. wait period between sessions
Patient Positioning	Supine or Prone
Post Scan	Disable MRI Mode, turn Therapy On.
Website	www.vnstherapy.com

(IPG, implantable pulse generator; WBA, whole-body averaged; SAR, specific absorption rate)

The technology used for cochlear implants has made tremendous advancements since the earliest version used in the 1960s, which was relatively large and had a single electrode (106). Presently, sophisticated CI devices exist and are available from three major manufacturers: Cochlear Limited, Advanced Bionics, and MED-EL. Similar to other AIMDs, CI systems were not originally designed in consideration of the electromagnetic fields used during MRI. Not surprisingly, the implanted magnets, which are integral parts of these devices, along with the presence of other ferromagnetic materials used in the internal components of cochlear implants, present particular challenges for MRI safety (89, 93, 98, 99, 101-105).

MRI-related labeling for the first CI devices required removal of the magnets prior to performing MRI exams, meaning that the patient had to undergo two separate surgical procedures: one to remove the magnet and another to replace it after undergoing MRI (**Figure 17**). One of the major issues related to removal and replacement of the magnet is that the patient with a CI needed to endure a period without sound to allow the surgical wound to heal. Obviously, this was undesirable for most patients, resulting in many individuals refusing to have MRI exams, undergoing less favorable diagnostic imaging procedures, which usually involved exposure to ionizing radiation.

736 MRI Safety Issues for Neuromodulation Systems

Figure 15. Diagram showing a typical cochlear implant (CI). A CI has two main components: an external part that hooks over the ear or that is worn on the head, and a surgically implanted internal part. The two components are coupled together using a magnet. The external part contains a transmitter, microphone, and speech or sound processor. The internal part includes the magnet, a receiver, which is located under the skin on the temporal bone, and one or more electrode arrays.

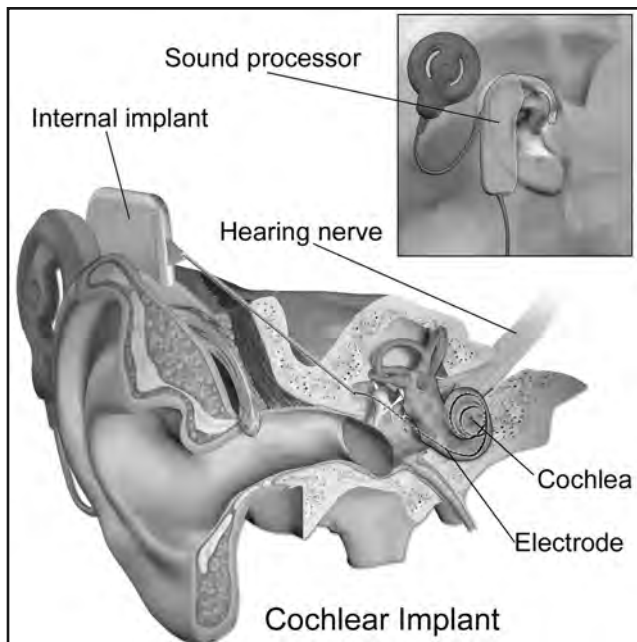
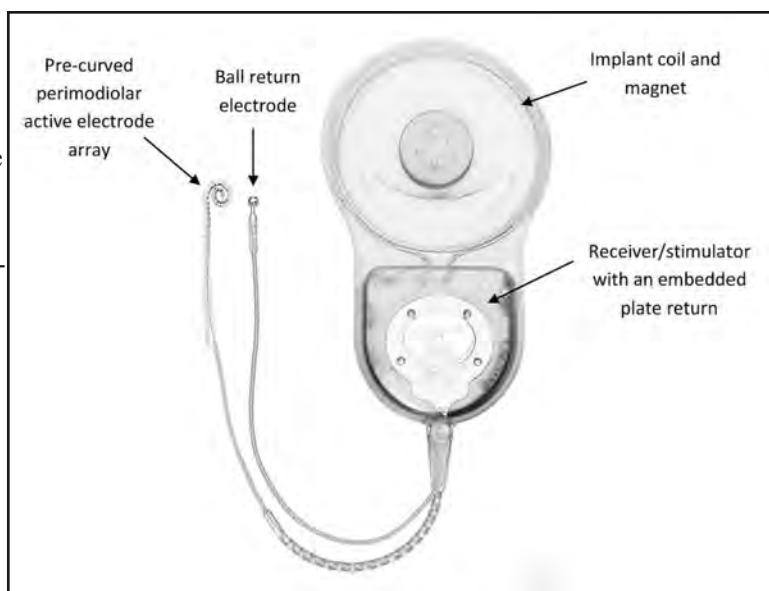


Figure 16. Diagram showing the internal parts of one type of cochlear implant: active electrode array; ball return electrode; implant coil and magnet; and receiver/stimulator.



In order to avoid magnet removal and replacement surgery, an alternative approach was utilized, whereby a “compression bandage and splint kit” was used to immobilize the cochlear implant’s magnet and control its orientation with respect to the direction of the static magnetic field (98, 101-104). This MRI safety strategy was suboptimal because patients could experience unintended acoustic stimulation because of the implant’s interactions with the electromagnetic fields that are applied during scanning (89). Notably, clinical imaging of the patient’s head was still impacted by substantial signal loss and distortion caused by the implant (this occurred even with the magnet removed due to the ferromagnetic materials used in cochlear implants)(89, 94, 97-99). Furthermore, there was still a tendency

Figure 17. Schematic showing removal of the internal magnet used with a cochlear implant. The first MR Conditional cochlear implants required removal of the magnets prior to performing an MRI exam.



Figure 18. Modified Stenver's view X-rays before (left panel) and after (right panel) magnet displacement associated with exposure to an MRI system. Before MRI and displacement, the magnet (2) was located in the geometrical center of the antenna coil (3). After MRI and magnet dislocation (right panel), the magnet is clearly shifted outwards in relation to the antenna coil (white arrow).

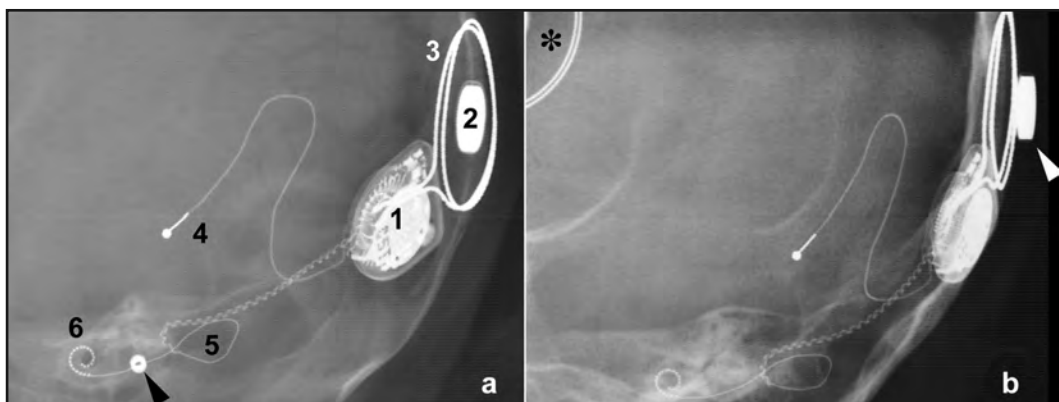


Figure 19. The HiRes Ultra 3D Cochlear Implant, Advanced Bionics, LLC. Note the magnetic component (3D). This device has multiple magnets that rotate to align to the direction of the static magnetic field of the MR system.

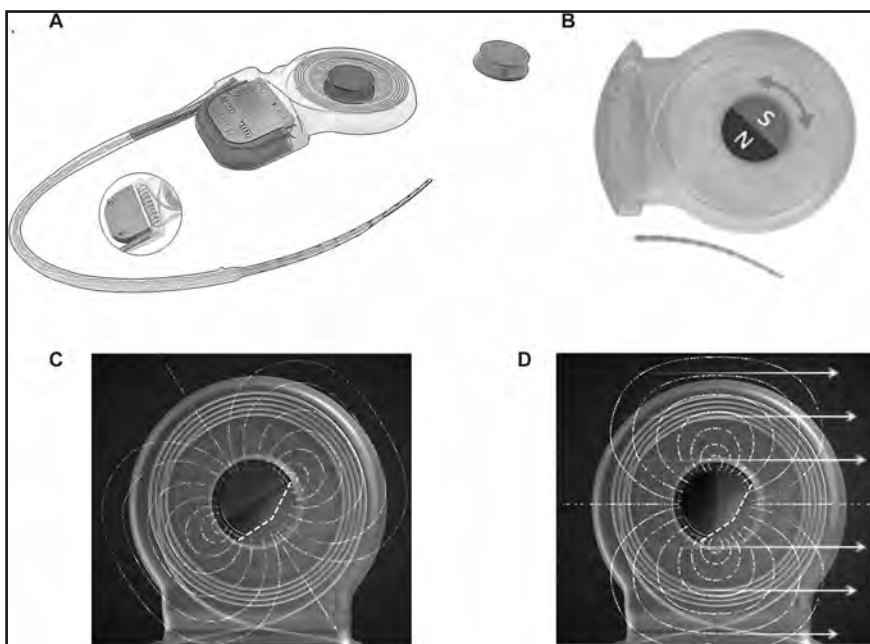


738 MRI Safety Issues for Neuromodulation Systems

Figure 20. The HiRes Ultra 3D Cochlear Implant, Advanced Bionics, LLC has a unique multi-magnet assembly that is composed of four rotatable magnets encased in a revolving disc, permitting the magnets to align with the direction of the static magnetic field of an MR system.



Figure 21. The Mi1200 SYNCHRONY Cochlear Implant, MED-EL Corporation has diamagnetic poles that rotate within the device to align with the direction of the static magnetic field of the MR system. (A) This cochlear implant has the possibility of removing the internal magnet, if that is desired for the MRI exam. (B) The magnet is freely rotating. (C) The magnet is in a random position, when no external magnetic field is applied. (D) The magnet is aligned to the direction of the static magnetic field of the MR scanner.



for the implanted magnets to be dislocated (**Figure 18**), causing pain and other problematic symptoms in patients, and/or to be demagnetized, especially when patients were imaged at 3-Tesla (90-96, 98-105)

A new generation of cochlear implants has been specifically-designed for patients undergoing MRI. These cochlear implants have multiple “rotating” magnets that align to the direction of the MR scanner’s static magnetic field (**Figures 19, 20, and 21**). This unique feature was implemented with the intent of preventing the painful symptoms frequently ex-

perienced by patients, along with avoiding dislocated magnets, which tends to occur with standard cochlear implants (89-96, 98-105). Unfortunately, patients with these cochlear implants continue to experience injury, explantation, and device malfunction despite the substantial efforts made to prevent such issues. **Tables 13 and 14** lists the MRI-related information for cochlear implants that have rotating magnets, the HiRes Ultra 3D Cochlear Implant (Advanced Bionics, LLC) and the Mi1200 SYNCHRONY Cochlear Implant (MED-EL Corporation), both of which have MR Conditional labeling at 1.5- and 3-Tesla.

Implantable Infusion Pumps

Implantable infusion pumps systems are used for intrathecal or intravascular administration of various medications, especially those used for pain management (8, 9, 107-114) (**Figure 22**). Targeted drug delivery with these AIMDs provides several advantages including the fact that significantly decreased dosages may be used in patients (which appears to reduce drug-related adverse events) and, importantly, these devices permit patient mobility (8, 107, 108).

An infusion pump operates by having the drug enter the pump through the reservoir fill port, where it passes through the reservoir valve and the pump's reservoir. At normal body temperatures, pressurized gas that is stored below the reservoir expands, exerting pressure on the reservoir. The pressure helps advance the drug into the pump's tubing. The peristaltic action of the pump moves the drug from the pump's reservoir, through the pump's tubing, check valve, catheter access port, through the implanted catheter, to the infusion site. **Figure 23** shows a schematic of the critical components of an implantable infusion pump.

Table 13. HiRes Ultra 3D Cochlear Implant, Advanced Bionics, LLC.

Implant System	HiRes Ultra 3D Cochlear Implant
Scan Region	Full-Body
Scan Requirements	External sound processor and headpiece must be removed No elevated body temperature 2 to 4 weeks has passed since surgery
System Settings During Scan	None
MRI Scan Conditions	1.5 T or 3 T horizontal cylindrical bore Max. spatial gradient magnetic field, 20 T/m Max. gradient slew rate, 200 T/m/s Transmit body RF coil with any receive-only coil Max. WBA SAR: 2.0 W/kg (1.5 T & 3 T) Max. Head SAR: 3.2 W/kg (1.5 T), 2.6 W/kg (3 T)
Active Scan Time	15 min. continuous scanning
Patient Positioning	Supine or Prone
Post Scan	None
Website	www.advancedbionics.com/mri

(WBA, whole-body averaged; SAR, specific absorption rate)

740 MRI Safety Issues for Neuromodulation Systems

Table 14. Mi1200 SYNCHRONY Cochlear Implant, MED-EL Corporation.

Implant System	Mi1200 SYNCHRONY Cochlear Implant
Scan Region	Full-Body
Scan Requirements	Electrically and mechanically intact Surgically remove the magnet External sound processor and headpiece must be removed No elevated body temperature
System Settings During Scan	None
MRI Scan Conditions	1.5 T or 3 T horizontal cylindrical bore Max. spatial gradient magnetic field, 29 T/m Max. gradient slew rate, 200 T/m/s Transmit body RF coil with any receive-coil Normal Operating Mode Max. WBA SAR: 2.0 W/kg (1.5 T & 3 T) Max. Head SAR: 3.2 W/kg (1.5 T), 1.6 W/kg (3 T)
Active Scan Time	No restrictions
Patient Positioning	Supine, Prone, or Lateral Decubitus Positions With Head Kept Straight
Post Scan	None
Website	www.medel.com/isi/

(WBA, whole-body averaged; SAR, specific absorption rate)

Figure 22. Example of a typical infusion pump used for intrathecal or intravascular administration of medication. The infusion pump is implanted subcutaneously in the area of the abdomen and the end of catheter is placed at a desired delivery site.

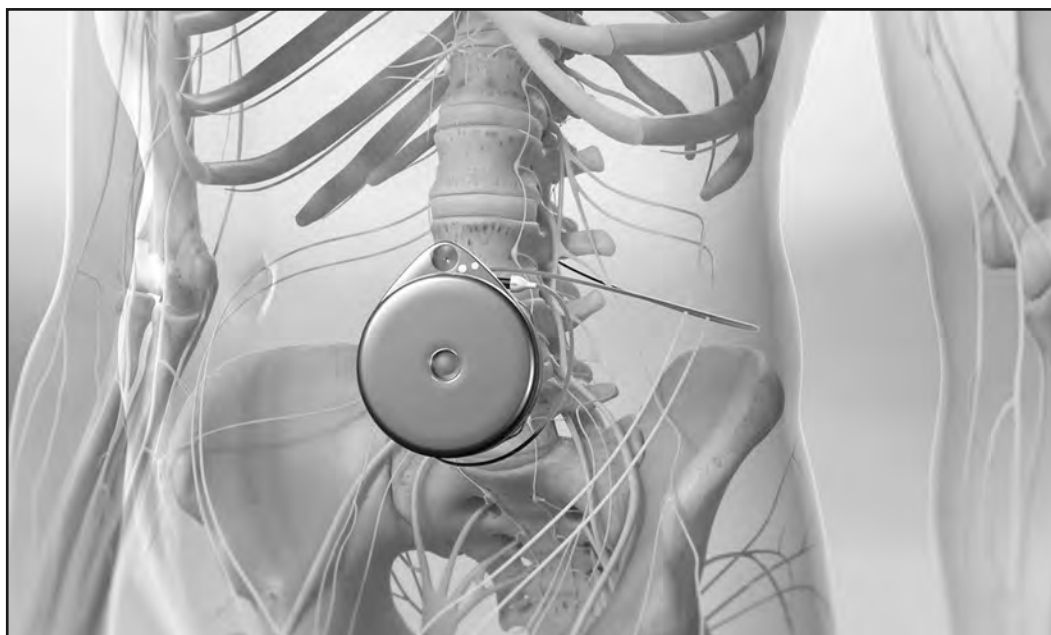
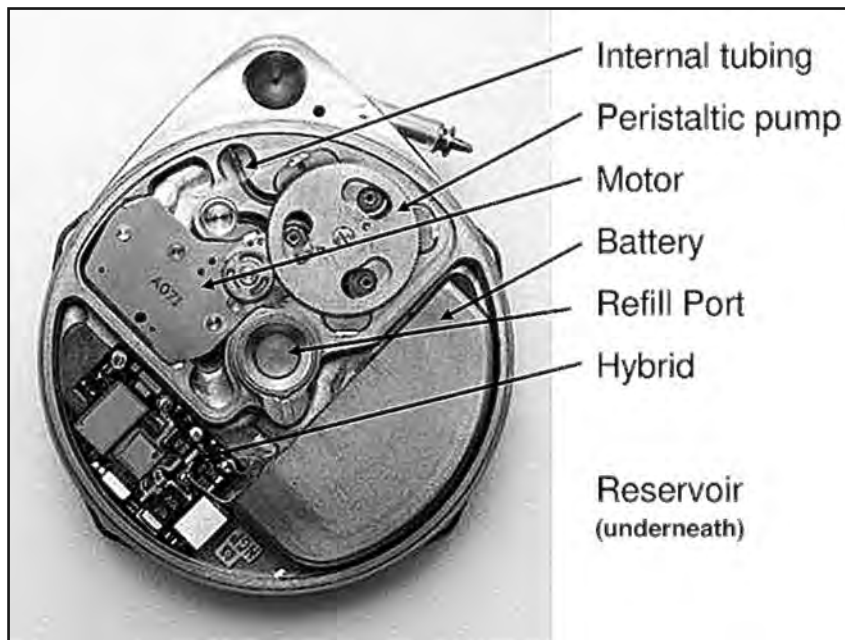


Figure 23. Schematic of the SynchroMed II Implantable Drug Infusion Pump, Medtronic, Inc. showing the various critical components including the peristaltic pump, motor, battery, refill port, and reservoir.



Infusion pumps and associated catheters typically contain metallic parts and, thus, can be impacted by MRI-related electromagnetic fields (3, 9, 100-114). For example, the electromagnetic fields (static magnetic, time-varying gradient magnetic, and radio frequency fields) may displace the infusion pump, generate excessive heating, alter the programmed settings, damage the device, and create substantial artifacts. Several programmable pumps have undergone comprehensive MRI testing and certain ones have FDA approved, MR Conditional labeling. **Tables 15 and 16** present the MRI-related information for two of the more popular implantable infusion pumps: the Prometra II Programmable Pump (Flowonix Medical) and the SynchroMed II Implantable Drug Infusion Pump (Medtronic, Inc.).

CONCLUSIONS

With the continued advancements in MRI technology and the development of more sophisticated AIMDs, there is an increased potential for hazardous situations to occur in the MRI environment. Therefore, to prevent incidents and accidents, it is essential to be cognizant of the latest information pertaining to MRI safety and to adhere to current labeling for AIMDs, particularly for neuromodulation systems. Unfortunately, there is still reluctance by MRI facilities to scan patients with neuromodulation systems. Thus, further interaction is needed by the device manufacturers to provide educational resources and technical support, so that MRI healthcare professionals feel competent when performing MRI in patients with AIMDs.

742 MRI Safety Issues for Neuromodulation Systems

Table 15. Prometra II Programmable Pump, Flowonix Medical.

Implant System	Prometra II Programmable Pump
Scan Region	Full-Body
Scan Requirements	Surgical site must be fully healed Make sure the patient can be deprived of drug delivery for the duration of the MRI exam
System Settings During Scan	Confirm the pump operations and settings Empty the pump prior to MRI
MRI Scan Conditions	1.5 T horizontal cylindrical bore Max. spatial gradient magnetic field, 19 T/m Max. gradient slew rate, 200 T/m/s Circularly polarized drive RF coil Transmit body RF coil with any receive-only coil Normal Operating Mode Max. WBA SAR: 2.0 W/kg
Active Scan Time	10 min. per pulse sequence
Patient Positioning	Supine, Prone, or Lateral Decubitus
Post Scan	Confirm the pump operations and settings.
Website	www.flowonix.com

(WBA, whole-body averaged; SAR, specific absorption rate)

Table 16. SynchroMed II Implantable Drug Infusion Pump, Model 8637, Medtronic, Inc.

Implant System	SynchroMed II Implantable Drug Infusion Pump, Model 8637
Scan Region	Full-Body
Scan Requirements	Make sure that the patient can be deprived of drug delivery for the duration of the MRI exam
System Settings During Scan	Confirm that the pump is not oriented 90° with respect to the Z-axis of the static magnetic field of the MR system
MRI Scan Conditions	1.5 T or 3 T horizontal cylindrical bore Max. spatial gradient magnetic field, 19 T/m Max. gradient slew rate, 200 T/m/s Transmit body RF coil with any receive-only coil First Level Controlled Operating Mode Max. SAR: Not Specified
Active Scan Time	30 min. continuous scanning
Patient Positioning	Supine or Prone
Post Scan	Motor of the pump may stall and delay the infusion up to 24 hrs. Wait for 20 min. and confirm that therapy has resumed.
Website	https://manuals.medtronic.com/manuals/main/region

(SAR, specific absorption rate)

REFERENCES

1. International Electrotechnical Commission, IEC 60601-2-33: Particular requirements for the basic safety and essential performance of magnetic resonance equipment for medical diagnosis. 2015.
2. U.S. Department of Health and Human Services, Food and Drug Administration, Center for Devices and Radiological Health, Guidance for Industry and FDA Staff: Criteria for Significant Risk Investigations of Magnetic Resonance Diagnostic Devices. 2014.
3. Shellock FG. Reference Manual for Magnetic Resonance Safety, Implants and Devices: 2020 Edition. Los Angeles: Biomedical Research Publishing Group; 2020.
4. Stafford RJ. The physics of magnetic resonance imaging safety. *Magn Reson Imaging Clin N Am* 2020;28:517-536.
5. Panych LP, Madore B. The physics of MRI safety. *J Magn Reson Imaging* 2018;47:28-43.
6. www.MRIsafety.com, Accessed September, 2021.
7. ACR Manual on MR Safety. American College of Radiology 2020. Available via www.ACR.org. Accessed September, 2021
8. Sayad D, Chakravarthy K, Amirdelfan K, et al. A comprehensive practice guideline for magnetic resonance imaging compatibility in implanted neuromodulation devices. *Neuromodulation* 2020;23:893–911.
9. Manker, S. Shellock FG. Chapter 24. MRI Safety and Neuromodulation Systems. In: Krames ES, Peckham Hunter P, Rezai AR, Editors. *Neuromodulation*. Second Edition. New York: Academic Press/Elsevier; 2018. pp. 315-337.
10. International Neuromodulation Society. Ten Things to Know About Neuromodulation. www.neuromodulation.com. Accessed September, 2021
11. Krauss JK, Lipsman N, Aziz T, et al. Technology of deep brain stimulation: Current status and future directions. *Nat Rev Neurol* 2021;17:75-87.
12. Walsh KM, Machado AG, Krishnaney AA. Spinal cord stimulation: A review of the safety literature and proposal for perioperative evaluation and management. *Spine J* 2015;15:1864-9.
13. Aldayeh L, Rahman M, Venook R. Practical aspects of MR imaging safety test methods for MR Conditional active implantable medical devices. *Magn Reson Imaging Clin N Am* 2020;28:559-571.
14. Watson RE Jr, Edmonson HA. MR safety: Active implanted medical devices. *Magn Reson Imaging Clin N Am*. 2020 Nov;28:549-558.
15. Shellock FG. Radiofrequency energy-induced heating during MR procedures: A review. *J Magn Reson Imaging* 2000;12:30-36.
16. Spiegel J, Fuss G, Backens M, et al. Transient dystonia following magnetic resonance imaging in a patient with deep brain stimulation electrodes for the treatment of Parkinson disease. *J Neurosurg* 2003;99:772-774.
17. Henderson J, Tkach J, Phillips M, et al. Permanent neurological deficit related to magnetic resonance imaging in a patient with implanted deep brain stimulation electrodes for Parkinson's disease: Case report. *Neurosurgery* 2005;57:E1063.
18. Rezai AR, Baker K, Tkach J, et al. Is magnetic resonance imaging safe for patients with neurostimulation systems used for deep brain stimulation (DBS)? *Neurosurgery* 2005;57:1056-1062.
19. Mattei E, Triventi M, Calcagnini G, et al. Temperature and SAR measurement errors in the evaluation of metallic linear structures heating during MRI using fluoroptic probes. *Phys Med Biol* 2007;21;52:1633-46.
20. Coffey RJ, Kalin R, Olsen JM. Magnetic resonance imaging conditionally safe neurostimulation leads: Investigation of the maximum safe lead tip temperature. *Neurosurgery* 2014;74:215-25.
21. Winter L, Seifert F, Zilberti L, Murbach M, Ittermann B. MRI-related heating of implants and devices: A review. *J Magn Reson Imaging* 2021;53:1646-1665.

744 MRI Safety Issues for Neuromodulation Systems

22. Gupte AA, Shrivastava D, Spaniol MA, Abosch A. MRI-related heating near deep brain stimulation electrodes: More data are needed. *Stereotact Funct Neurosurg* 2011;89:131-40.
23. Shrivastava D, Abosch A, Hughes J, et al. Heating induced near deep brain stimulation lead electrodes during magnetic resonance imaging with a 3 T transceive volume head coil. *Phys Med Biol* 2012;57:5651-65.
24. Cabot E, Lloyd T, Christ A, Kainz W, et al. Evaluation of the RF heating of a generic deep brain stimulator exposed in 1.5-T magnetic resonance scanners. *Bioelectromagnetics*. 2013;34:104-113.
25. Woods TO. Standards for medical devices in MRI: Present and future. *J Magn Reson Imaging* 2007;26:1186-1189.
26. Delfino JG, Woods TO. New developments in standards for MRI safety testing of medical devices. *Current Radiology Reports* 2016;4:1-9.
27. International Organization for Standardization/Technical Standard, ISO/TS 10974:2018. Assessment of the safety of magnetic resonance imaging for patients with an active implantable medical device. International Organization for Standardization. 2018.
28. U.S. Food and Drug Administration. Testing and Labeling Medical Devices for Safety in the Magnetic Resonance (MR) Environment. Guidance for Industry and Food and Drug Administration Staff, 2021. <https://www.fda.gov/regulatory-information/search-fda-guidance-documents/testing-and-labeling-medical-devices-safety-magnetic-resonance-mr-environment>. Accessed September, 2021.
29. Baker KB, Tkach JA, Nyenhuis JA, et al. Evaluation of specific absorption rate as a dosimeter of MRI-Related implant heating. *J Magn Reson Imaging* 2004;20:315-320.
30. Baker KB, Tkach JA, Phillips MD, Rezai AR. Variability in RF-induced heating of a deep brain stimulation implant across MR systems. *J Magn Reson Imaging* 2006;24:1236-42.
31. Nitz WR, Brinker G, Diehl D, Frese G. Specific absorption rate as a poor indicator of magnetic resonance-related implant heating. *Invest Radiol* 2005;40:773-6.
32. Speck B. Complications and risks associated with implantable pulse generators (IPGs): White paper. London, UK: Stimwave Technologies, Inc., 2016.
33. Shellock FG, Audet-Griffin AJ. Evaluation of magnetic resonance imaging issues for a wirelessly powered lead used for epidural, spinal cord stimulation. *Neuromodulation* 2014;17:334-349.
34. Vasquez LP, Chen J, Shellock FG. Evaluation of MRI issues for a new wirelessly powered, spinal cord stimulation lead with receiver. *AJR Am J Roentgenol* 2020;214:406-412.
35. Oluigbo CO, Salma A, Rezai AR. Deep brain stimulation for neurological disorders. *IEEE Rev Biomed Eng* 2012;5:88-99.
36. Taghva A, Corrigan JD, Rezai AR. Obesity and brain addiction circuitry: Implications for deep brain stimulation. *Neurosurgery* 2012;71:224-38.
37. Taghva A, Oluigbo C, Corrigan J, Rezai AR. Posttraumatic stress disorder: Neurocircuitry and implications for potential deep brain stimulation. *Stereotact Funct Neurosurg* 2013;91:207-219.
38. Ho AL, Sussman ES, Pendharkar AV, et al. Deep brain stimulation for obesity: Rationale and approach to trial design. *Neurosurg Focus* 2015;38:E8.
39. Kundu B, Brock AA, Englot DJ, et al. Deep brain stimulation for the treatment of disorders of consciousness and cognition in traumatic brain injury patients: A review. *Neurosurg Focus* 2018;45:E14.
40. Holtzheimer PE, Husain MM, Lisanby SH, et al. Subcallosal cingulate deep brain stimulation for treatment-resistant depression: A multisite, randomised, sham-controlled trial. *Lancet Psychiatry*, 2017;4:839-849.
41. Rezai AR, Phillips M, Baker K, et al. Neurostimulation system used for deep brain stimulation (DBS): MR safety issues and implications of failing to follow guidelines. *Invest Radiology* 2004;39:300-303.
42. Baker KB, Tkach J, Hall JD, Nyenhuis JA, Shellock FG, Rezai AR. Reduction of MRI-related heating in deep brain stimulation leads using a lead management system. *Neurosurgery* 2005;57:392-397.

MRI Bioeffects, Safety, and Patient Management 745

43. Bhidayasiri R, Bronstein JM, Sinha S, et al. Bilateral neurostimulation systems used for deep brain stimulation: *In vitro* study of MRI-related heating at 1.5-Tesla and implications for clinical imaging of the brain. *Magn Reson Imaging* 2005;23:549-555.
44. Finelli DA, Rezai AR, Ruggieri P, et al. MR-related heating of deep brain stimulation electrodes: An *in vitro* study of clinical imaging sequences. *Am J Neurorad* 2002;23:1795-1802.
45. Rezai AR, Finelli D, Nyenhuis JA, et al. Neurostimulator for deep brain stimulation: *Ex vivo* evaluation of MRI-related heating at 1.5-Tesla. *J Magn Reson Imaging* 2002;15:241-250.
46. Rezai AR, Finelli D, Ruggieri P, et al. Neurostimulators: Potential for excessive heating of deep brain stimulation electrodes during MR imaging. *J Magn Reson Imaging* 2001;14:488-489.
47. Carmichael DW, Pinto S, Limousin-Dowsey P, et al. Functional MRI with active, fully implanted, deep brain stimulation systems: Safety and experimental confounds. *Neuroimage* 2007;37:508-17.
48. Kazemivalipour E, Keil B, Vali A, et al. Reconfigurable MRI technology for low-SAR imaging of deep brain stimulation at 3T: Application in bilateral leads, fully-implanted systems, and surgically modified lead trajectories. *Neuroimage* 2019;199:18-29.
49. Falowski S, Safriel Y, Ryan MP, Hargens L. The rate of magnetic resonance imaging in patients with deep brain stimulation. *Sterotact Funct Neurosurg* 2016;94:147-153.
50. Franceschi AM, Wiggins GC, Mogilner AY, et al. Optimized, minimal specific absorption rate MRI for high-resolution imaging in patients with implanted deep brain stimulation electrodes. *AJNR Am J Neuroradiol* 2016;37:1996-2000.
51. Golestanirad L, Angelone LM, Iacono MI, et al. Local SAR near deep brain stimulation (DBS) electrodes at 64 and 127 MHz: A simulation study of the effect of extracranial loops. *Magn Reson Med* 2017;78:1558-1565
52. Boutet A, Hancu I, Saha U, et al. 3-Tesla MRI of deep brain stimulation patients: Safety assessment of coils and pulse sequences. *J Neurosurg* 2019;132:586-594.
53. Boutet A, Hancu I, Saha U, et al. 3-Tesla MRI of deep brain stimulation patients: Safety assessment of coils and pulse sequences. *J Neurosurg* 2019;132:586-594
54. Boutet A, Rashid T, Hancu I, Saha U, et al. Functional MRI safety and artifacts during deep brain stimulation: Experience in 102 patients. *Radiology* 2019;293:174-183.
55. Boutet A, Elias GJB, Gramer R, et al. Safety assessment of spine MRI in deep brain stimulation patients. *J Spine Surg* 2020;32:973-983.
56. Davidson B, Tam F, Yang B, et al. Three-tesla magnetic resonance imaging of patients with deep brain stimulators: Results from a phantom study and a pilot study in patients. *Neurosurgery* 2021;88:349-355.
57. Eross L, Riley J, Levy EI, Vakharia K. Neuroimaging of deep brain stimulation. *Neurol Clin* 2020;38:201-214.
58. Starr PA, Christine CW, Theodosopoulos PV, et al. Implantation of deep brain stimulators into the subthalamic nucleus: Technical approach and magnetic resonance imaging-verified lead locations. *J Neurosurg* 2002;97:370-387.
59. Starr PA, Martin AJ, Ostrem JL, et al. Subthalamic nucleus deep brain stimulator placement using high-field interventional magnetic resonance imaging and a skull-mounted aiming device: Technique and application accuracy. *J Neurosurg* 2010;112:479-90.
60. Phillips MD, Baker KB, Lowe MJ, et al. Parkinson disease: Pattern of functional MR imaging activation during deep brain stimulation of subthalamic nucleus- initial experience. *Radiology* 2006;239:209-216.
61. Zrinzo L, Yoshida F, Hariz MI, et al. Clinical safety of brain magnetic resonance imaging with implanted deep brain stimulation hardware: Large case series and review of the literature. *World Neurosurg* 2011;76:164-72.
62. Shellock FG, Woods TO, Crues JV. MR labeling information for implants and devices: Explanation of terminology. *Radiology* 2006;253:26-30.

746 MRI Safety Issues for Neuromodulation Systems

63. Kanal E, Froelich J, Barkovich AJ, et al. Standardized MR terminology and reporting of implants and devices as recommended by the American College of Radiology Subcommittee on MR Safety. *Radiology* 2015;274:866-870.
64. Razavi B, Rao VR, Lin C, et al. Real-world experience with direct brain-responsive neurostimulation for focal onset seizures. *Epilepsia* 2020;61:1749-1757.
65. Liem LA, van Dongen VC. Magnetic resonance imaging and spinal cord stimulation systems. *Pain* 1997;70:95-97.
66. De Andres J, Valía JC, Cerdá-Olmedo G, et al. Magnetic resonance imaging in patients with spinal neurostimulation systems. *Anesthesiology* 2007;106:779-86.
67. De Andres J, Martinez-Sanjuan VV, Fabregat-Cid G, et al. MRI-compatible spinal cord stimulator device and related changes in patient safety and imaging artifacts. *Pain Med* 2014;15:1815-9.
68. Desai MJ, Hargens LM, Breitenfeldt MD, et al. The rate of magnetic resonance imaging in patients with spinal cord stimulation. *Spine* 2015;40:E531-7.
69. Rubino S, Adepoju A, Kumar V, et al. MRI conditionality in patients with spinal cord stimulation devices. *Stereotact Funct Neurosurg* 2016;94:254-258
70. Manfield J, Bartlett R, Park N. Safety and utility of spinal magnetic resonance imaging in patients with high-frequency spinal cord stimulators: A prospective single-centre study. *Stereotact Funct Neurosurg* 2019;97:272-277.
71. Jotwani R, Abd-Elsayed A, Villegas K, et al. Failure of SCS MR-Conditional modes due to high impedance: A review of literature and case series. *Pain Ther* 2021;10:729-737.
72. Hagedorn JM, Parmele JB, Wolff JS, Bendel MA, et al. The prevalence of elevated impedances and magnetic resonance imaging ineligibility following implantation of 10 kHz spinal cord stimulation devices: A retrospective review. *Neuromodulation* 2021 (In Press)
73. Razavi B, Rao VR, Lin C, et al. Real-world experience with direct brain-responsive neurostimulation for focal onset seizures. *Epilepsia* 2020;61:1749-1757.
74. Winter L, Seifert F, Zilberti L, Murbach M, Ittermann B. MRI-related heating of implants and devices: A review. *J Magn Reson Imaging* 2021;53:1646-1665.
75. Elkelini MS, Hassouna MM. Safety of MRI at 1.5-Tesla in patients with implanted sacral nerve neuromodulator. *Eur Urol* 2006;50:311-6.
76. Guzman-Negrón JM, et al. Can lumbosacral magnetic resonance imaging be performed safely in patients with a sacral neuromodulation device? An *in vivo* prospective study. *J Urol* 2018;200:1088-1092.
77. Heidler S, Lusuardi L, Dieterdorfer F. First report of magnetic resonance imaging in patients with implanted InterStim Twin (model 7427T) sacral nerve stimulator. *Urol J* (In Press)
78. Karrer-Warzinek E, Apt D, Kim O C-H, et al. Safety of magnetic resonance imaging in patients under sacral neuromodulation with an InterStim Neuromodulator. *Urology* 2021;154:115-119.
79. Binnie CD. Vagus nerve stimulation for epilepsy: A review. *Seizure* 2000;9:161-169.
80. Kosel M, Schlaepfer TE. Beyond the treatment of epilepsy: New applications of vagus nerve stimulation in psychiatry. *CNS Spect* 2003;8:515-521.
81. Panebianco M, Zavanone C, Dupont S, et al. Vagus nerve stimulation therapy in partial epilepsy: A review. *Acta Neurol Belg* 2016;116:241-248.
82. Benbadis SR, Nyenhuis J, Tatum WO, et al. MRI of the brain is safe in patients implanted with the vagus nerve stimulator. *Seizure* 2001;10:512-515.
83. Narayanan JT, Watts R, Haddad N, et al. Cerebral activation during vagus nerve stimulation: A functional MR study. *Epilepsia* 2002;43:1509-1514.
84. Groves DA, Brown VJ. Vagal nerve stimulation: A review of its applications and potential mechanisms that mediate its clinical effects. *Neurosci Biobehav Rev* 2005;29:493-500.

MRI Bioeffects, Safety, and Patient Management 747

85. Shellock FG, Begnaud J, Inman DM. VNS Therapy System: *In vitro* evaluation of MRI-related heating and function at 1.5- and 3-Tesla. Neuromodulation 2006;9:204-213.
86. Gorny KR, Bernstein MA, Watson RE Jr. 3 Tesla MRI of patients with a vagus nerve stimulator: Initial experience using a T/R head coil under controlled conditions. J Magn Reson Imaging 2010;31:475-81.
87. de Jonge JC, Melis GI, Gebbink TA, et al. Safety of a dedicated brain MRI protocol in patients with a vagus nerve stimulator. Epilepsia 2014;55:e112-115.
88. Fetzer S, Dibue M, Nagel AM, Trollmann R. A systematic review of magnetic resonance imaging in patients with an implanted vagus nerve stimulator. Neuroradiology 2021;63:1407-1417.
89. Azadarmaki R, Tubbs R, Chen DA, Shellock FG. MRI information for commonly used otologic implants: Review and update. Otolaryngology Head Neck Surg 2014;150:512-519.
90. Majdani O, Lenung M, Rau T, et al. Demagnetization of cochlear implants and temperature changes in 3.0T MRI environment. Otolaryngol Head Neck Surg 2008;139:833-839.
91. Cuda D, Murri A, Succo G, Hospital SL. Focused tight dressing does not prevent cochlear implant magnet migration under 1.5 Tesla MRI. Acta Otorhinolaryngol Ital. 2013;33:133-136.
92. Hassepass F, Hassepass F, Stabenau V, et al. Magnet dislocation: An increasing serious complication following MRI in patients with cochlear implants. Rofo 2014;186:680-5.
93. Kim BG, Kim J, Park JJ, et al. Adverse events and discomfort during magnetic resonance imaging in cochlear implant recipients, JAMA Otolaryngology - Head and Neck Surgery 2015;141:45-52.
94. Carlson ML, Neff BA, Link MJ, et al. Magnetic resonance imaging with cochlear implant magnet in place: Safety and imaging quality. Otol Neurotol 2015;36:965-971.
95. Leong WJC, Yuen HW. Dislocation of cochlear implant magnet during 1.5 Tesla magnetic resonance imaging despite head bandaging and its repositioning using an endoscopic approach. J Laryngol Otol 2018;132:943-945.
96. Leinung M, Loth A, Groger M, et al. Cochlear implant magnet dislocation after MRI: Surgical management and outcome. Eur Arch Otorhinolaryngol. 2020;277:1297-1304.
97. Edmonson HA, Carlson ML, Patton AC, Watson RE. MR imaging and cochlear implants with retained internal magnets: Reducing artifacts near highly inhomogeneous magnetic fields. Radiographics 2018;38:94-106.
98. Srinivasan R, So CW, Amin N, et al. A review of the safety of MRI in cochlear implant patients with retained magnets. Clin Radiol 2019;74:972.e9-972.e16.
99. Shew M, Wichova H, Lin J, et al. Magnetic resonance imaging with cochlear implants and auditory brainstem implants: Are we truly practicing MRI safety? Laryngoscope 2019;129:482-489.
100. Cass ND, Honce JM, O'Dell AL, Gubbel SP. First MRI with new cochlear implant with rotatable internal magnet system and proposal for standardization of reporting magnet-related artifact size. Otol Neurotol 2019;40:883-891.
101. Fussell WL, Patel NS, Carlson ML, et al. Cochlear implants and magnetic resonance imaging: Experience with over 100 studies performed with magnets in place. Otol Neurotol 2021;42:51-58.
102. Fierens G, Standaert N, Peeters R, et al. Safety of active auditory implants in magnetic resonance imaging. J Otol 2021;16:185-198.
103. Gallant SC, Danehy AR, Licameli GR. Adverse events in pediatric cochlear implant patients undergoing magnetic resonance imaging. Int J Pediatr Otorhinolaryngol 2021 (In Press).
104. Bestourous DE, Davidson L, Reilly BK. A review of reported adverse events in MRI-Safe and MRI-Conditional cochlear implants. Otol Neurotol 2021 (In Press)
105. Holtmann L, Hans S, Kaster F, et al. Magnet dislocation following magnetic resonance imaging in cochlear implant users: Diagnostic pathways and management. Cochlear Implants Int 2021;22:195-202.
106. Eshraghi AA, Nazarian R, Telishchi FF, et al. The cochlear implant: Historical aspects and future prospects. Anat Rec 2012;295:1967-1980.

748 MRI Safety Issues for Neuromodulation Systems

107. Smith T, Swainey C, Coyne P. Pain management, including intrathecal pumps. *Cur Pain Headache Rep* 2005;9:243-248.
108. Turner M. Intrathecal drug delivery 2002. *Acta Neurachir* 2003;87:29-35.
109. von Roemeling R, Lanning RM, Eames FA. MR imaging of patients with implanted drug infusion pumps. *J Magn Reson Imaging* 1991;1:77-81.
110. Shellock FG, Crivelli R, Venugopalan R. Programmable infusion pump and catheter: Evaluation using 3-Tesla magnetic resonance imaging. *Neuromodulation* 2008;11:163-70.
111. De Andres J, Villanueva V, Palmisani S, et al. The safety of magnetic resonance imaging in patients with programmable implanted intrathecal drug delivery systems: A 3-year prospective study. *Anesth Analg*. 2011;112:1124-119.
112. Diehn FE, Wood CP, Watson RE Jr, Mauck WD, et al. Clinical safety of magnetic resonance imaging in patients with implanted SynchroMed EL infusion pumps. *Neuroradiology* 2011;53:117-22.
113. Kosturakis A, Gebhardt R. SynchroMed II intrathecal pump memory errors due to repeated magnetic resonance imaging. *Pain Physician* 2012;15:475-477.
114. Huh B, Roldan CJ. Magnetic fields and intrathecal pump malfunction. *Am J Emerg Med* 2016;34:115.e5-6.

Chapter 27 MRI Safety Policies and Procedures for a Hospital or Medical Center Setting

JOHN POSH, R.T., (R)(MR)

Lead MRI Technologist
Robert Wood Johnson University Hospital
New Brunswick, NJ

INTRODUCTION

No matter what the structure of the facility, be it an academic medical center, a community hospital, or a small rural hospital, the overriding mandate is to maintain a safe environment for the patients and employees. To this end, with specific regard to magnetic resonance imaging (MRI), facilities must “establish, implement, and maintain current MRI safety policies and procedures,” often referred to as a “Safety Manual”, to ensure the safety of patients, visitors, and staff members (1). These policies and procedures dictate the desires of the organization and how they are to be implemented. In consideration of the above, the objective of this chapter is to focus on policies and procedures, the nature of how these are developed, implemented, reviewed and distributed, and the legal implications with an emphasis on MRI safety in the setting of a hospital or medical center.

GENERAL INFORMATION

Policies and procedures are written for a variety of reasons. Some are designed to be the institution’s response to regulatory and governing body requirements (2). This is less true with MRI than it is for modalities that use ionizing radiation (e.g., X-ray and nuclear medicine) due to differing levels of governmental oversight and regulation. Some policies and procedures are written as a means of ensuring consistency across similar entities within a larger organization, as is the case with larger academic and regional institutions with small satellite campuses and diagnostic imaging centers. Policies and procedures can also be written in response to events. For example, before 2001, few facilities had a formal policy on the use of portable oxygen cylinders or other tanks used for gases utilized in the MRI envi-

750 MRI Safety Policies and Procedures - Hospital / Medical Center

ronment (3, 4). By far, the most common reason policies and procedures are written is to ensure compliance with industry best practices. Some believe that the current *de facto*, best practice standard for MRI is the American College of Radiology (ACR) Guidance Document on MR Safe Practices: 2013 (1). The ACR document rapidly changed the manner in which the clinical MRI setting operated. The MRI industry, self-governed since the beginning, suddenly had a written document to use as a template to guide MRI safety procedures. As far as written documentation was concerned, while this document had no enforceability, it almost overnight prompted significant changes.

One key concept of the ACR document, and the only element to be detailed in this chapter, is the concept of dividing the imaging facility into four discrete zones with increasingly restricted access as the zones progress from Zones I to IV. The zone model is intended to help control access to the MRI environment and, thus, facilitate safety in this setting. Zone I represents the public space and is essentially unregulated. Zone II represents the public interface and can be defined as the public space within the MRI department such as the waiting, changing, and interview areas as well as the areas for the restrooms and similar spaces. Zone III represents the limited access, technical workspace between Zone II and the MR system room and as such is under the constant supervision of trained MR personnel. Zone IV is the scanner room and is the most tightly controlled space. In Zone IV, the potential problems exist whereby ferromagnetic implants, foreign bodies, and external devices will be affected. Failure to restrict access to those personnel without proper training and the use of support equipment specifically designed for use in the MRI setting can result in significant injury or death to patients, visitors, and staff members. The only other published standard, and one which dovetails nicely with the ACR guidance document, is the Sentinel Event Alert #38, published by The Joint Commission (5, 6).

When creating policies and procedures based on industry best practices, it is important to carefully search the published literature on the topic. Drafting a policy and procedure with outdated information or improper terminology (e.g., using “MRI compatible” versus “MR Conditional” for MRI labeling purposes) offers little in the way of guidance or protection for any of the parties involved. It is also important when formulating policies based on best practices, to create a comprehensive manual of policies and procedures to ensure that all aspects of operations are covered. A sample outline for a comprehensive MRI Safety Manual presented in Appendix I.

Some MRI facilities in the hospital or medical center setting use the ACR guidance document as single blanket policy covering all general operations within the department or as a road map to drafting individual policies. Other facilities use the guidance document as a starting point and draft additional policies and procedures to narrow the focus of operational issues in key areas, as needed, or if there are persistent concerns, such as a pattern of MRI-safety related events that occur during the preparation of patients for the MRI examinations.

The scope with which policies and procedures are written can be very broad and applicable to everyone within the organization or narrowly focused to apply to a very limited target audience. Whatever the reason for writing the policy and procedure, it is vital that the policy works toward the goals of the organization without placing undue burden on op-

erations. The global scope and application of policies and procedures is beyond the boundaries of this chapter, which will instead focus on the basics as they pertain to MRI.

In general terms, the hospital or medical center policy and procedure manuals operate on a “trickle down” approach whereby the top institutional policies and procedures apply to all those lower down the organizational and operational chain. The lower you go, the more narrow the scope of the policy. For example, an institutional policy and procedure on Infant Safe Haven Laws applies to everyone in the institution regardless of department or position, while a policy and procedure pertaining to screening patients prior to entering the MRI environment applies only to those individuals employed in and empowered to enter the MRI setting. With this in mind, the policies and procedures used in MRI are generally quite specific and require a basic understanding of the safe operation of the MR systems in use today.

POLICIES AND PROCEDURES

Policy and Procedure: Definitions

Policy and procedure manuals are an essential component of all institutions. They convey the desires of senior leadership with respect to common departmental operations. Additionally, they instruct the staff on how issues are to be handled during routine operations and unexpected events. Policy and procedure manuals also set the cultural tone of the department and allow the vision of the organization’s leadership to manifest itself in daily operations while protecting the institution from undue risk (7). In the broadest terms, the policy and procedure manual is the “owner’s manual” for the hospital or medical center and the standard to which the facility holds itself and to which it will be held by others.

Policy and Procedure: Essential Elements

There are many formats that policies and procedures can follow. Some take the form of detailed memos, position statements, or papers that narrate how specific situations or comprehensive operations are to be handled within the department. Others utilize a formalized layout specifically optimized for hospital policies. Lastly, policies can take on the form of a MRI Safety Manual that governs all relevant operational items and activities within the department. Regardless of which format is selected there are a few basic needs that each should have in some form.

Policy

The “policy” is the name of the document or file pertaining to a specific situation, condition, or scenario. The following is an example:

Example 1. MRI Screening Policy – This document or file pertains to the issue of screening in MRI. This is very straightforward and names the policy precisely. This format allows no room for interpretation or debate about the information that it will contain.

Purpose: The purpose is a brief narrative of why the policy is needed. It can be as simple as “to ensure patient safety,” or it can be a comprehensive rationalization of why one particular policy was written. For example, the stated purpose the MRI Screening Policy is to

752 MRI Safety Policies and Procedures - Hospital / Medical Center

Table 1. Basic policies and procedures for a hospital or medical center. This table provides a list of the basic policies and procedures needed for an MRI department, the rationale behind them, and the elements that they should contain.

Policy and Procedure	Rationale	Basic Elements
Access Control	The MRI department represents specialized space that necessitates limiting access to specially-trained individuals, only.	This policy should detail the establishment and demarcation of a four zone system as described by the American College of Radiology, with details regarding who has access to the zones and the process for entering and leaving the area of the MR system room (Zone IV).
Personnel	The unique MRI environment requires personnel to receive specialized training.	This policy should detail the establishment of defined Level 1 and Level 2 MR Personnel based on responsibilities and training. The type, amount, timing, and frequency of the training should be clearly defined.
Patient, Visitor, and Personnel Screening	All individuals entering the MRI environment need to be properly screened to ensure the safety of the patients, visitors, and personnel.	This policy should detail who performs the screening, how the screening is conducted, what tools are to be used, how the results are documented, and how to proceed when unsafe materials or situations are discovered. This policy should be inclusive of all individuals and patients including emergency patients, first responders, prisoners and parolees, and Level 1 and Level 2 MR Personnel.
Device and Object Screening	Any device or equipment entering the MRI environment for use with a patient must be established as MR Safe or MR Conditional with the specific conditions clearly defined.	This policy is where the facility should describe how devices, equipment, and objects are to be screened, what tools should be used during the screening process, and how devices should be properly labeled.
MRI Department Staffing	The MRI department requires specialized staff with proper significant training in order to safely operate the equipment and to ensure safety.	This policy should describe and detail who is allowed to operate the MR system, what training and licensure is needed, and how the department is to be staffed during normal operational hours, off-hours, and emergency situations.
Pregnant Patients and Healthcare Workers	Pregnancy represents a possible risk scenario in the MRI setting.	This policy should cover pregnant patients and healthcare workers. For patients, the MRI approval process needs to be clearly defined as well as any limitation on the use of techniques and MRI contrast agents. For healthcare workers, duties should be clearly established as well as possible limitations.
Pediatric Patients	Children are not small adults. Therefore, they require the use of specialized techniques.	This policy should detail how pediatric patients are screened, scheduled, and, if needed, sedated during the MRI examination. Patient monitoring must be clearly defined as well as the role of all personnel in the process. Emergency procedures also need to be clearly defined.

MRI Bioeffects, Safety, and Patient Management 753**Table 1. Continued**

Policy and Procedure	Rationale	Basic Elements
Cryogens	Cryogens pose a unique danger in the event of a quench in the MRI environment.	This policy should detail what cryogens are, their possible risks, and what to do in the event of a quench as well as a quench that involves a ventilation pipe failure.
Sedation, Anesthesia, and Pain Control	MRI facilities utilizing medications for sedation, anesthesia, and pain management need special policies regarding these medications.	This policy should detail how patients are assessed for the need for sedation, anesthesia, and pain management medications. Patient monitoring must be clearly defined as well as the role of all personnel in the process. Emergency procedures also need to be clearly defined.
MRI Contrast Agents	MRI contrast agents are drugs and their usage needs to be clearly defined.	This policy should detail the clinical indications for MRI contrast agents, who can administer them, and what conditions prevent patients from receiving contrast agents. Any distinction between classes of agents should be covered as well and any required laboratory testing prior to use.
Intracranial Aneurysm Clips	A patient with a ferromagnetic intracranial aneurysm clip will experience a significant risk if allowed in the MR system room.	This policy should clearly state that the pedigree for all implanted intracranial clips be established and the procedure to follow if the required information cannot be obtained.
Cardiac Pacemakers and Implantable Cardioversion Defibrillators (ICDs)	Patients with standard (i.e., non-MR Conditional) cardiac pacemakers or ICDs may experience a significant risk in association with MRI.	This policy should detail the specific devices that can be scanned and the specific procedure to be followed in order to safely do so. This policy needs to be very detailed and the role of all support personnel needs to be clearly defined. Special directions are necessary for MR Conditional cardiac devices.
Emergency Preparedness	Emergencies may occur and impact the MRI setting. All MRI facilities must have pre-planned responses in place to properly handle emergency situations.	This is a critical policy because it needs to address patient issues such as contrast reactions, cardiac situations, and seizures, etc. It also needs to cover facility issues such as water leaks, power failures, and fires both in the MRI setting and in close proximity. Lastly, this policy and procedure needs to cover natural disasters such as flooding, earthquake, tornado, and fire. This policy and procedure will reference and be directly linked to many other policies within the hospital or medical center.

754 MRI Safety Policies and Procedures - Hospital / Medical Center

ensure that all patients, visitors, and non-MRI employees undergo comprehensive screening for the presence of contraindicated materials on or in the body that could result in injury to self or others if taken into the MR system room (i.e., Zone IV).

Scope: The section of the policy referred to as the “scope” defines the policy’s intended audience. Some policies are very limited to a specific piece of equipment, room, or department, while others are all encompassing and apply to an entire organization. Accurately defining the scope helps to ensure that the policy will be followed by those who need it and not lost in the realm of non-applicable policies. If properly worded, the scope of the policy will not need to be revised when capabilities are changed, hardware is upgraded, or scanners are added unless they involve entirely new departments.

Procedure

While the policy dictates the desires of the institution, the procedure details the methods by which the policy is carried out. Using Example 1 above, the MRI Screening Policy, the procedure would detail the necessary steps to be taken to screen patients, visitors, or non-MRI personnel so that they may safely enter the scanner room. The procedure will vary in detail depending on facility type, patient mix, and level of complexity of the MRI examinations that are performed. The procedure for all MRI facilities should include the core elements of what is to be done, how it is to be done, who is responsible for performing the procedure, and what, if any, resources should be utilized.

Additionally, the procedure should contain sufficient detail so that it can be easily understood by those covered in the “scope” section of the document. It should not contain excessive details that do not provide clinical relevance. For example, a venipuncture policy that specifies the size of catheter to be used includes a detail that serves no purpose except to limit the type of departmental flexibility needed for efficient operations, since the size of catheter can vary depending on the status of the patient, size of the patient, and examination to be performed. An effective venipuncture policy should instead specify that a suitable sized catheter should be inserted based on the examination to be performed. The choice of catheter size should be at the discretion of the hospital or medical center personnel establishing the venous access. While this type of attention to detail may seem trivial and lead to frustration, we must remember that overly detailed policies make compliance difficult and lead to routine deviations. Deviations from policy are to be expected occasionally and, if clinically justifiable, do not pose a problem. On the other hand, regular deviations suggest a poorly conceived and worded policy and should be avoided.

Implementation and Revision Date for Policies and Procedures

MRI safety policies and procedures developed for MRI facilities in hospitals and medical centers should contain a minimum of two dates, one for the date of creation and/or implementation and the other indicating the date of the last revision. The implementation date can be a single date for all policies that commence on the day a new facility begins operations or the dates can vary if policies are added over time in established facilities. The implementation date should not be edited in later revisions.

The revision date indicates the date the policy was last reviewed. The preferred method for documenting revision history is with multiple date lines progressing chronologically. While this is a slightly more “busy” effect visually, it allows the full revision history to be established. A single date that changes at subsequent revisions, while satisfying the basic need to keep policies and procedures current, does not indicate any temporal frequency or periodicity with respect to the review process. This is, of course, academic with a fully digital manual that can take advantage of revision history and version control features of the software. In general, the frequency of review and revision should be annually. Additionally, if there is a substantial change in operations such as the addition of a new scanner, new operating locations, or a major upgrade with respect to the equipment (e.g., software or hardware), this also warrants a review of the policies and procedures that specifically apply to MRI safety (1, 13).

Signatures

All policies and procedures should be signed. The signature can be a line item on all policy and procedure documents in facilities that have numerous individual documents or a single signature on the revision page of a comprehensive MRI Safety Manual. Exactly who signs the policies is up to each individual facility operating within a hospital or medical center. At the very least, the signature should be that of the modality, section, or department chief. Ideally, the document would claim multiple signatures from an administration representative, the MRI Safety Officer or Chairperson of the MRI Safety Committee, and the party responsible for daily operations within the department, usually the MRI Manager. The use of electronic signatures for electronic policy and procedure manuals is well established and is acceptable as long as it complies with established hospital security protocols.

Managing the Policy and Procedure Manual

The need for a comprehensive policy and procedure manual is evident. There are situations though, in which the responsibility for the manual becomes less obvious. For most hospitals and medical centers, the lines are well defined. The departmental policy and procedure manual is created and maintained by the departmental leadership. In certain cases, this is not always possible, such as when MRI examinations are provided as a contracted service through a third-party company. These arrangements are overall quite common, though the service delivery model can vary considerably. Sometimes MRI service is provided one or more days per week via a visiting mobile MRI unit or the unit can be parked full-time as a lower-cost “imaging center”. It is also possible to have a fully functional, fixed MRI center within the confines of the hospital that is operationalized and managed by a third-party who provides staff and operational support. Regardless of the arrangement, the policy and procedure manual needs to be agreed upon by all parties and should be discussed as a matter of course during any negotiations for provided services. Adherence to policy and procedure standards by contracted personnel should also be considered an integral part of the contracted service and any violation should be treated as a material breach of the contracted terms. It is critical to remember that the hospital or medical center is responsible for the care of their patients even if a component of the care is outsourced to a third-party.

756 MRI Safety Policies and Procedures - Hospital / Medical Center

When MRI procedures are provided via a contracted mobile service, there are additional safety policies and procedures that need to be considered. In a mobile arrangement, the zone model described by the ACR (1), while not mandatory, is less easily achieved and, therefore, it may be necessary to build docking structures, temporary shelters, or other adaptable spaces. The regulations governing the use of these spaces varies greatly from state to state with some municipalities requiring electricity, plumbing, HVAC (i.e., heating, ventilation, and air conditioning) and even fire suppression. Whatever the type of structure, it is important that the policy and procedure manual matches the delivery model.

The policy and procedure manual is also only as good as the data it contains and it is important to keep the information as current as possible, as previously stated regardless of MRI facility type, it is essential that the policy and procedure documents be maintained as a “living document” (1, 2). The old policies should be compared with any departmental changes and equipment upgrades to see if it still satisfies the original purpose. All facilities should be familiar with governmental, agency, or regulatory mandated review requirements, though at present few, if any exist with particular regard to MRI safety. As an example, the State of Pennsylvania mandates that all radiology policies be reviewed annually (8). Other states recommend a two-year review while still others have no formal provision for reviewing policies and procedures (9-11). On the agency side, The Joint Commission (TJC) has no formal standard, but a policy review date older than three years would raise concerns and lead the inspector to question what other areas of operations have not been reviewed or revised in greater than a three-year period (Personal Communication, The Joint Commission Standards Interpretation Group, December 27, 2012).

Policy and procedure review on an annual basis can be time consuming but the time is well spent. There are different strategies for managing the manual. Some hospitals and medical centers use a formal committee to review, revise, and manage the policy and procedure manual. Others delegate management of specific sections of the manual (e.g., MRI, computed tomography, ultrasound, etc.) to the department managers and/or modality chiefs. Whichever technique a hospital or medical center chooses to follow, it is essential that they follow a regimented schedule of review and document the process with updated signatures and dates.

Implementing New Policies and Procedures

When developing and implementing new policies and procedures for MRI safety, it is essential that the process be based on careful research and deliberate thought as well as a focused review of industry best practices in order to be the most effective (2, 6-7). The proposed policy and procedure should be initiated as a preliminary document with an implementation date and proposed review date. The preliminary document should be revisited after the third month of implementation to assess the clinical impact and to revise, as needed. When initially written, policies and procedures tend to be either too specific or too vague. Therefore, implementing them as preliminary for a period of three months allows the department to better assess the impact of the policy and procedure on the overall operation of the department and to correct problems with the wording of the policy or the “mechanics” of the procedure. Once final and fully operationalized, there is usually no need for further revision unless mandated by departmental changes.

DISTRIBUTION OF THE POLICY AND PROCEDURE MANUAL

Once a hospital or medical center has a workable version of the policy and procedure manual, it needs to be available to all entities within the organization. For a small hospital with a single scanner this is a relatively simple task. A university-level hospital with several departments and affiliated smaller centers faces a greater challenge. Irrespective of facility type, there are two basic choices for the distribution method of the policy and procedure manual. Both have benefits and complications and the ultimate distribution choice depends on the needs of the hospital or medical center.

Hard copy distribution of the policy and procedure manual has been the standard for many years. It is basic and, once the manual is written, quite effective. The policy and procedure manual is copied and a copy is then provided to key locations where it can be accessed, such as the MRI center. Typically, there is one copy of the MRI safety policies and procedures manual provided to the MRI department and another maintained in the administrative area where it resides in a larger manual of global radiology documents covering the other imaging or therapeutic modalities. Manual distribution is low cost and requires very little time commitment. For a larger hospital or medical center with more entities and locations, or even when a few locations are geographically distant from the main facility, the manual distribution method becomes much less desirable. A major disadvantage of hard copy manuals is the intricacies of the revision process. A change in a policy and procedure, regardless of the magnitude of the change, requires that the old version be physically replaced with the newer version in all manuals. This process requires diligence and attention to detail and, thus, it is a frequent weak link in the process.

Many modern-day hospitals and medical centers and certainly most facilities with multiple clinical areas, campuses, and affiliated centers opt instead for an electronic policy manual distribution. Maintaining an electronic manual of policies and procedures offers significant benefits over hard copy manuals. For example, the master manual can be updated, as needed, and the changes applied to all subordinate documents immediately and universally. The same applies to updates for signatures and revision dates. A single source policy and procedure manual, once edited, passes through to all locations and entities ensuring consistency and minimizes the chances that an outdated document will remain in a forgotten manual. Another feature of electronic manuals is that there are few limits on what can be included. Some hospitals and medical centers include photographs that serve as visual aids for the policy and procedure or even links to videos that reinforce certain elements of the document. Notably, the greatest benefit of an electronic policy and procedure manual is the ability of it to be linked together with other documents. In an electronic manual, it is easy to include a hyperlink to another policy and procedure in the same department or any department in the organization. This is extremely important when dealing with complex policies and procedures that may contain important elements that not only directly impact the safety of the MRI department but are also associated with nursing policies and those involved in safety.

Examples of policies and procedures that have a high degree of commonality with other departments include any such document that discusses the administration of non-contrast medications, which relate very closely to nursing policies, or any document that discusses

758 MRI Safety Policies and Procedures - Hospital / Medical Center

conscious sedation or anesthesia in the MRI department, which ties in heavily to anesthesia policies. With electronic-based policies and procedures, the referenced nursing or anesthesia policy is instantly available, making the manual far more effective overall. The drawback of this increased effectiveness is that the manual requires an increased level of commitment in terms of time and resources. While it is preferred to have references to other departments, it is imperative that the reference links be maintained and that the referenced policies are current and accurate. This increased complexity requires a high-level commitment at the administrative level to devote the time and resources necessary to create and maintain the electronic manual. It is also imperative to maintain the electronic policies and procedure manual in a way that is accessible in the event of a connectivity failure, since patient care continues even in the absence of the hospital's or medical center's intranet. If the manual is copied to local computer hard drives as part of the update process, it should be readily available at all times as long as there is electrical power to the department. If the facility relies heavily on cloud-based technology the situation becomes more complicated as access to data could be compromised in the event of a connectivity failure. Generally, Information Technology departments have systems in place for maintaining data and allowing for continuation of care during a communication blackout or emergency. With respect to an electronic policy and procedure manual, it can be as simple as a periodic hard disk backup of the manual that is available in the command center or on strategically placed hard drives. The details can vary but what is important is the need to have all relevant departments involved from the beginning.

LEGAL IMPLICATIONS OF POLICIES

The rule of law is that everyone must obey the law. If people violate the law, they are subject to the consequences depending on the nature and severity of the violation. The content of the policy and procedure manual can be viewed as the "law" of the department. All employees must follow the law and no employee is exempt. As such, policy and procedure manuals are designed to clearly define the responsibilities of the healthcare professional and set the standards to which employees are held (12). Ideally, each hospital and medical center will have an up-to-date, comprehensive manual covering all aspects of departmental operations for both routine and non-routine situations. A facility without a policy and procedure manual is declaring, "I cannot meet the standard of care so I have no policy for it" and, unfortunately, that facility starts on the defensive in any legal action (Personal communication, Emanuel Kanal, M.D., November 06, 2012).

In the broadest general terms, the key to any policy and procedure is its ability to be defended. The range of variation in a policy and procedure from one facility to another within the same industry may be significant. Where any facility falls within the range from conservative to liberal is based primarily on the culture of the organization. Therefore, especially with respect to MRI safety matters, it is critical that the facility constructs the policies and procedures with sound judgment and that they meet the basic standard of care set forth in the industry (1). For example, a small community hospital typically does not possess the infrastructure to scan patients with MR Conditional pacemakers and, therefore, it should have a policy stating that these devices are not to be scanned at the MRI center. As the hospital grows and the level of sophistication of the department increases, the policy and procedure needs to grow as well to reflect any changes it desires. If the policy is that

pacemakers are still absolute contraindications, then an exclusion policy will suffice. If the hospital or medical center decides to allow scanning of patients with MR Conditional pacemakers only, then the policy and procedure needs to be amended to reflect specifically which pacemakers can be scanned, which cannot, and the exact procedure to be followed to safely do so. This is a key point in that whatever policy and procedure the department chooses, it will remain as the standard they are held to until the document is changed.

Consider the following fictionalized example. In this example, there will be two patients with cardiac pacemakers who undergo MRI examinations at two separate but equally capable, hospitals (Facility A and Facility B). Both MRI facilities in these hospitals are prepared to scan these complicated patients with all of the necessary collateral support from nursing and cardiology. Unfortunately, both patients experience negative consequences that require the cardiac pacemakers be replaced after the MRI examinations. Facility A has a policy and procedure detailing how pacemaker patients are to be scanned and follows that information to the letter. Therefore, Facility A's liability is limited with respect to the damaged pacemaker. Facility B performs exactly as Facility A, but their policy and procedure is outdated and states than cardiac pacemakers are an absolute contraindication to MRI and patients with these devices are not allowed into the MR system room (Zone IV). Facility B's liability is greater because, although they had the same negative outcome as Facility A, Facility B violated their own policy. This example is exaggerated to illustrate the point that each facility dictates the standards to which it will be held within the range of common practice. It is important that those standards be appropriate for the protection of patients, staff, and visitors without limiting the functionality of the department. Failing to keep policies current and accurate is like announcing, "I did not know the problem existed and, therefore, I have not thought about it" (Personal communication, Emanuel Kanal, M.D., November 06, 2012).

There is also a delicate balance between a policy and procedure that is too restrictive and one that is too vague. A policy and procedure that contains too many details can negatively impact the department on several levels. The policy will ultimately be difficult to follow, as flexibility is lost in the presence of overly tedious details. Additionally, any issues arising from failure to follow the policy and procedure place the department in a defensive posture. An overly restrictive policy and procedure, particularly in the realm of MRI safety, slows the delivery of care and will surely be violated on a regular basis, neither of which is good news for the patient, department, or facility in general.

There are times when extremely specific details are necessary for patient safety. For example, implanted devices approved for use in patients referred for MRI examinations under specific conditions are labeled MR Conditional and the specific conditions under which these devices can be safely scanned are specified in writing by the manufacturer, usually presented in the *Instructions for Use*. The difference between scanning the patient safely and risking injury relies squarely on the details, which are clearly spelled out in the product literature. Accordingly, any policy and procedure concerning the device must clearly state what needs to be done in step-by-step fashion with all possible details intact.

When drafting policies and procedures, the choice of language is also a factor. Words like "shall," "must", and "will" should be avoided as they suggest absolutes. The policy

760 MRI Safety Policies and Procedures - Hospital / Medical Center

should opt for “should” instead as it allows for a bit more flexibility. Improper language, poor choice of words, absolutes, and colloquialisms are all potential problems when the policy is viewed by non-imaging professionals, opposing counsel, and in the worst case, a jury.

In the event of a legal case there are a few things to be considered. First, the policies and procedures manual will be requested by opposing counsel as part of the discovery process. A good attorney knows that the manual contains the type of details that can be used to validate or discredit a witness. Second, the contents of the policy and procedure manual will be used by opposing counsel to assess fundamental knowledge during depositions and not knowing that the policy and procedure existed or what information it contains will not make the situation better. All staff members are held to the standards contained within the manual and, thus, need to know the entire content, where to find it, and what information it contains. Lastly, policies and procedures may be used during a trial. If the legal case involves a loss suffered as a result of a violation of a policy and procedure, it will certainly feature prominently in the trial process.

In the end, violating a policy and procedure of a hospital or medical center by itself is not going to result in legal action. Depending on the violation, it could result in disciplinary action as defined in the employee handbook but it is not, in and of itself, a legal issue. If the violation of the policy and procedure is determined to be the proximate cause of an injury, illness, or negative outcome for a patient, visitor, or co-worker then the situation has changed and is more likely to involve the legal system.

CONCLUSIONS

Healthcare providers must make patient, visitor, and employee safety a prime concern and take the necessary steps to create a comprehensive culture of safety within the organization. Policies and procedures serve as a sound foundation for any safety program, especially with regard to MRI safety. A policy and procedure manual can be a single document detailing that an industry standard or guideline (e.g., the ACR guidance document) is utilized as the *de facto* operational policy for the department, a collection of individual documents tailored to specific operational issues in the department, or a comprehensive Safety Manual for MRI. As long as the policies and procedures are based on industry best practices and understood by all involved parties to be the standard to which they are held, they will be an effective tool for improving safety without limiting operational agility.

REFERENCES

1. Kanal E, Barkovich AJ, Bell C, et al. ACR guidance document on MR safe practices: 2013. *J Magn Reson Imaging* 2013;37:501-530.
2. Page SB. Establishing a System of Policies and Procedures. Westerville, OH: Process Improvement Publishing; 2009.
3. Chaljub G, Kramer L, Johnson R, et al. Projectile cylinder accidents resulting from the presence of ferrous nitrous oxide of oxygen tanks in the MR suite. *AJR Am J Roentgenol* 2001;177:27-30.
4. Chen D. Small town reels from boy's MRI death. The New York Times [online] August 1, 2001 Available at: <http://www.nytimes.com/2001/08/01/nyregion/small-town-reels-from-boy-s-mri-death.html?src=pm>. Accessed March 2020.

MRI Bioeffects, Safety, and Patient Management 761

5. Issue 38: Preventing accidents and injuries in the MRI suite (2008). Available at: www.jointcommission.org/assets/1/18/sea_38.PDF Accessed March 2020.
6. Gilk T, Kanal E. Interrelating sentinel event alert #38 With the ACR guidance document on MR safe practices: 2013. An MRI safety review tool. *J Magn Reson Imaging* 2013;37:531-543.
7. McQuate, C. Penning Effective Policies, Digital Booklet. American Society for Industrial Security: 2005
8. Pennsylvania Code Chapter 127. Radiology Services. Available at: www.pacode.com/secure/data/28/chapter127/chap127toc.html Accessed March 2020.
9. Unannotated Code of Maryland and Rules. Available at: www.lexisnexis.com/hottopics/mdcode/ Accessed March 2020.
10. State of Delaware Title 16, Health and Safety. Available at: <http://delcode.delaware.gov/title16/c074/index.shtml> Accessed October 2012.
11. Missouri Code of State Regulations: Title 19. Department of Health and Senior Services. Available at: www.sos.mo.gov/adrules/csr/csr.asp Accessed March 2020.
12. Judson K, Harrison C. Law and Ethics for the Health Professions, Sixth Edition. New York: McGraw Hill; 2010.
13. ACR Committee on MR Safety, Greenberg TD, Hoff MN, et al. ACR guidance document on MR safe practices: Updates and critical information 2019. *J Magn Reson Imaging*. 2020;51:331-338.

Appendix A. Example of MRI Safety Manual Outline.

1. **MRI Safety Committee**
 - 1.1. Mission Statement
 - 1.2. Members
 - 1.3. Operational Parameters
2. **Overview**
 - 2.1. Objectives
 - 2.2. MR System and Associated Risks
3. **Physical Environment**
 - 3.1. Access Restrictions
 - 3.1.1. MR Personnel
 - 3.1.2. ACR Recommended
 - 3.1.3. MRI Zone Chart
 - 3.2. Contingency Preparations
 - 3.2.1. Medical Gases
 - 3.2.2. Emergency Power
 - 3.2.3. Procedure Lighting / Equipment
 - 3.3. Infection Control Provisions
 - 3.3.1. Hand Washing
 - 3.3.2. Surface Cleaning
 - 3.3.3. Device Cleaning
4. **MRI Safety Training and Orientation**
 - 4.1. MRI Safety Resources
 - 4.2. Reporting Critical Findings
 - 4.3. Adverse Event Reporting
 - 4.3.1. Near Miss
 - 4.3.2. Serious Injury
 - 4.3.3. Death
 - 4.4. Staff Training and Competency Documentation
 - 4.5. Level 1 MR Personnel
 - 4.6. Level 2 MR Personnel
 - 4.7. MR Medical Director, MR Safety Officer, MR Safety Expert
 - 4.8. Other Personnel (Transporters, Nurses, Anesthesia Personnel, Respiratory Therapists, etc.)

762 MRI Safety Policies and Procedures - Hospital / Medical Center

- 4.9. Public Safety Training (Fire, Police, Other First Responders)
- 5. **MRI Environmental Safety**
 - 5.1. Static Magnetic Field
 - 5.1.1. Signage
 - 5.1.2. Fringe Field
 - 5.1.3. Spatial Gradient Magnetic Field
 - 5.2. Bioeffects
 - 5.2.1. Magnetohydrodynamic Effect
 - 5.3. Effects on Implants and Foreign Bodies
 - 5.3.1. Translational Forces
 - 5.3.2. Spatial Gradient Magnetic Field
 - 5.3.3. Rotational Forces
 - 5.3.4. Lenz Forces
 - 5.4. Radiofrequency Magnetic Field
 - 5.4.1. Patient Positioning to Prevent Burns
 - 5.4.2. Transmit RF Coil Precautions
 - 5.4.3. Specific Absorption Rate (SAR)
 - 5.4.4. B₁+RMS
 - 5.4.5. Specific Energy Dose (SED)
 - 5.4.6. Bioeffects
 - 5.4.6.1. Tissue Heating
 - 5.4.6.2. Radiofrequency-Related Burns
 - 5.4.7. Implants, Devices, and Other Items
 - 5.4.7.1. Tattoos
 - 5.4.7.2. Permanent Cosmetics / Makeup
 - 5.4.7.3. Jewelry, Body Piercing Jewelry, and Body Modification Implants
 - 5.4.7.4. Electrically Conductive Leads, Wires, and Other Items
 - 5.4.7.5. Transdermal Medication Delivery Patches
 - 5.4.7.6. Electrically Conductive Clothing
 - 5.4.7.7. Electrically Conductive Implants and Devices
 - 5.5. Time Varying Magnetic Fields
 - 5.5.1. Bioeffects
 - 5.5.1.1. Peripheral Nerve Stimulation
 - 5.5.1.2. Induced Voltages
 - 5.5.1.3. Magnetophosphenes
 - 5.5.1.4. Acoustic Noise
 - 5.5.2. Implants, Devices, and Other Items
 - 5.5.2.1. Device Malfunction or Damage
 - 5.5.2.2. False Bio-feedback
 - 5.6. Electrical Safety
 - 5.7. Cryogen Safety
 - 5.8. Infection Control Laser Safety (Hybrid Systems)
 - 5.9. Cryoablation Safety (Hybrid Systems)
 - 5.10. Radiation Safety (Hybrid Systems)
- 6. **Emergency Procedures**
 - 6.1. Cardiac Arrest (i.e., Code Blue)
 - 6.1.1. Zone IV (i.e., MR System Room)
 - 6.1.2. Zones I to III
 - 6.2. Quench
 - 6.2.1. Definition
 - 6.2.2. When to Quench
 - 6.2.3. Who Is Permitted to Quench
 - 6.2.4. How To Quench
 - 6.2.4.1. Photo of Quench Button
 - 6.3. Emergency Shutdown
 - 6.4. Power Failure

MRI Bioeffects, Safety, and Patient Management 763

- 6.5. Fire Emergency (i.e., Code Red)
 - 6.5.1. Fire in Zone IV (i.e., MR System Room)
 - 6.5.2. Fire in Zone III
 - 6.5.3. Fire in Zones I and II
 - 6.6. Environmental or Natural Disaster (Flood, Earthquake, Tornado, etc.)
 - 6.7. Violent Patient, Prisoner, Staff Member
 - 6.8. Emergency Personnel
 - 6.8.1. Local Fire Department
 - 6.8.2. Local Police Department
 - 6.8.3. Other Emergency Personnel or First Responders
- 7. MRI Screening / Preparation for Patients and Others**
- 7.1. MRI Exam Ordering
 - 7.2. Routine Patient Screening
 - 7.3. Inpatient Screening
 - 7.4. Emergent Patient Screening
 - 7.5. Altered / Unconscious Patient Screening
 - 7.6. Pediatric Patient Screening
 - 7.7. Orbital Screening for Metallic Foreign Body
 - 7.8. Use of Ferromagnetic Detection System
 - 7.9. Patient and Visitor Clothing
 - 7.10. Patient Preparation
 - 7.11. Managing Claustrophobia and Anxiety
 - 7.12. Time-out Prior to Entering MRI
- 8. MRI Screening for MR Personnel**
- 8.1. Annual Screening for MR Personnel
 - 8.1.1. Workplace Safety vs. Health Insurance Portability and Accountability Act Health Insurance Portability and Accountability Act (HIPAA) Concerns
 - 8.2. Employee Pregnancy
 - 8.3. Employee Dress Code
 - 8.3.1. All Types of Ferromagnetic Items Permitted (i.e., No Restrictions on Watches, Underwire Bras, Shoes, etc.)
 - 8.3.2. Essential Ferromagnetic Items, Only
 - 8.3.3. Ferrous Free (No Ferromagnetic Items Permitted)
- 9. MRI Screening for Implants, Devices, and Equipment**
- 9.1. Old Terminology (Pre-2005)
 - 9.2. New Terminology, MR Safe, MR Conditional, MR Unsafe (Post-2005)
 - 9.3. Risks of Implants and Devices
 - 9.4. Identifying Unanticipated Ferromagnetic Implants During Scanning
 - 9.5. Aneurysm Clips
 - 9.6. Hemostatic Clips
 - 9.7. Heart Valve Prostheses and Annuloplasty Rings
 - 9.8. Intravascular Stents, Coils, and Filters
 - 9.9. Joint Replacement Prostheses
 - 9.10. Foreign Bodies
 - 9.11. Cerebral Spinal Fluid (CSF) Shunts and Valves
 - 9.12. Implantable Active Cardiac Devices
 - 9.13. Implantable Medication Pumps
 - 9.14. Neurostimulation Systems
 - 9.15. Cochlear Implants
- 10. MRI Contrast Agents**
- 10.1. ACR Position Statement on the Use of MRI Contrast Materials
 - 10.2. Contrast Agent Instructions for Use, IFU
 - 10.3. Classification of Agents, Relaxivity and Structure
 - 10.4. Pre-Contrast Lab Values and Guidelines
 - 10.5. Special Patients

764 MRI Safety Policies and Procedures - Hospital / Medical Center

- 10.5.1. Pregnant Patients
- 10.5.2. Nursing Mothers
- 10.5.3. Dialysis, End Stage Kidney Disease
- 10.6. Contrast Sensitivity
 - 10.6.1. Reaction Risk Factors
 - 10.6.2. Premedication Guidelines
- 10.7. MRI Contrast Agent Retention
- 10.8. Patient Gadolinium-Based Contrast Agent (GBCA) Medication Guide Distribution
- 10.9. Documentation of GBCA Administration
- 10.10. Documentation of post GBCA Assessment
- 11. Patient Monitoring, Sedation, and Anesthesia**
 - 11.1. Equipment Restrictions
 - 11.2. Prevention of Thermal Injuries
 - 11.3. Electrocardiogram
 - 11.4. Pulse Oximetry
 - 11.5. Non-invasive blood pressure
 - 11.6. Oxygen Saturation
 - 11.7. Temperature monitoring
- 12. Infection Control Processes**
 - 12.1. Isolation Patients
 - 12.2. Room Cleaning
- 13. Appendices**
 - 13.1. American College of Radiology, Guidance Documents
 - 13.2. American College of Radiology, Contrast Agent Manual

Chapter 28 MRI Safety Policies and Procedures for an Outpatient Facility

LAURA FOSTER, J.D., M.P.H.

Senior Vice President, Compliance and Regulatory Affairs
Radnet, Inc.
Los Angeles, CA

LAWRENCE N. TANENBAUM, M.D., FACR

Chief Technology Officer
Radnet, Inc.
New York, NY

JOHN V. CRUES, III, M.D., FACR

Medical Director
Radnet, Inc.
Los Angeles, CA

INTRODUCTION

A well-designed safety program to protect medical personnel and patients is mandatory for all centers performing clinical medical imaging. However, due to unique inherent risks, specific requirements must be stipulated for the outpatient magnetic resonance imaging (MRI) facility (1, 2). **Table 1** lists safety concerns relevant to all medical imaging procedures. All outpatient imaging departments must have a written safety program, properly implemented and maintained by management, technologists, and radiologists.

This chapter provides the requirements for a safety program to help ensure protection of employees, patients, and others while complying with regulatory obligations. Thus, this chapter should assist new and existing facilities in developing and/or revising safety, health, environment, and loss control programs while establishing consistency in operations and medical delivery with particular attention focused on proper policies and procedures.

766 MRI Safety Policies and Procedures for an Outpatient Facility

Table 1. Safety requirements shared by all diagnostic imaging modalities.

Equipment	
MRI, CT, PET, NM, US, MM	A performance evaluation is performed annually by a medical physicist and includes all required testing.
All modalities	Quality control and maintenance activities are identified and time frames are established for how often they are to be performed and documented.
CT	The radiation dose, CTDI, is measured annually for commonly used protocols and verified by a medical physicist to be within 20% of the displayed dose.
CT	Incidents where radiation dose indices are exceeded are reviewed and analyzed and compared to external benchmarks.
All modalities	Data is collected on all equipment related injuries and sentinel events are reported, as required.
MRI	Adequate patient padding is provided and regularly inspected for integrity and burn protection techniques are implemented for all patients.
MRI	Hearing protection is provided to all patients.
All radiation modalities	Lead shielding is readily available and tested no less than annually for integrity.
All modalities	Emergency response equipment is readily available and routinely checked for integrity and expiration dates.
Facility	
All radiation facilities	A structural radiation shielding design assessment is conducted prior to imaging equipment installation or room modification.
All radiation facilities	A radiation protection survey is conducted after installation of imaging equipment or construction, prior to clinical use of the room.
MRI	Access to the MRI suite is restricted by screening, warning signage, barrier controls.
CMS sites	ACR Consumer Complaint Notice is posted in view of patients.
All facilities	Disaster protocols are in place and evacuation drills are conducted.

PERSONNEL: RESPONSIBILITIES AND DUTIES

Staffing of the outpatient MRI facility should be carefully considered and maintained. Appropriate experience and training of the management team (e.g., the MR medical director, imaging center manager, MR modality specialist, MR team leader, and MR safety officer) is crucial to operating an efficient and safe imaging department. The key personnel in outpatient imaging safety include the management team, members of the MRI Safety Committee, the MR medical director (MRMD), MR Safety Officer, and other involved employees, because employees are one of the key elements that help ensure a safe outpatient MRI center.

The management team should establish an MRI Safety Committee. The Safety Committee should then designate an MR Safety Officer if one has not already been established.

Table 1. (Continued) Safety requirements shared by all diagnostic imaging modalities.

Personnel	
Interpreting physicians	Documentation of primary education, state license, board certification, continuing education and continuing experience is available for each interpreting physician.
Medical physicists	Documentation of primary education, board certification or alternate pathway, continuing education and continuing experience is available for each medical physicist.
Technologists	Documentation of primary education, state license, modality certification, continuing education and continuing experience is available for each technologist.
CMS sites	Source verification is conducted to confirm licensure and OIG exclusion status.
Radiation modalities	Staff dosimetry results are reviewed by a Radiation Safety Officer, medical physicist or health physicist no less than quarterly.
Radiation modalities	Policies are in place to manage pregnant radiation workers.
Policies and Procedures	
All modalities	Patient identification protocols are available and followed.
All modalities	Processes are in place to identify and manage pregnant or potentially pregnant patients.
All modalities	Imaging protocols are established based on current standards of practice and are reviewed per established timeframes.
Radiation modalities	Imaging protocols are tailored to minimize exposure to pediatric patients.
All modalities	Patient positioning guidance is available and followed.
All modalities	Processes are in place to document patient consent for exams that carry risk.
All modalities	Processes are in place to address patients with medical emergencies, anxiety or emotional distress.
All modalities	Infection control protocols are available and followed.
All modalities	Processes are in place to protect patient privacy.
MRI, CT, XR	Contrast agent administration protocols are available and followed.
All modalities	Systems are in place to expedite report delivery of critical findings.
Mammography	A patient medical outcomes audit program is in place.

(MRI, magnetic resonance imaging; CT, computed tomography; PET, positron emission tomography; NM, nuclear medicine; US, ultrasound; MM, mammography; CMS, Centers for Medicare & Medicaid Services; ACR, American College of Radiology; XR, x-ray)

The MR Safety Officer, or appropriately designated physician, shall chair the MRI Safety Committee. Responsibilities of the management team, the MRI Safety Committee, the MR Safety Officer and the employees are outlined in **Tables 2 to 5**, respectively.

Encouraging active communication between the different elements of the safety team is critical to long-term success. This can be facilitated by establishing a center hotline, sched-

768 MRI Safety Policies and Procedures for an Outpatient Facility

Table 2. Responsibilities of the management team.

Management Team Responsibilities
<ol style="list-style-type: none"> 1. Implementation of the Safety Program, including the policies and procedures, through motivation, training, counseling, and enforcement. 2. Initiating and ensuring compliance for all safety program elements. 3. Identifying hazards through safety inspections and developing timely countermeasures. 4. Training personnel in accident prevention and safe work habits. 5. Performing timely accident investigations and reporting, including appropriate documentation and corrective actions.

Table 3. Responsibilities of the MRI Safety Committee.

MRI Safety Committee Responsibilities
<ol style="list-style-type: none"> 1. Meet on a regular schedule. 2. Review and approve safety programs designed to meet the goals of the MRI facility. 3. Review incident reports, self-inspection results, and employee safety recommendations. 4. Recommend and assist in establishing additional general safety rules as needs are identified. 5. Develop and monitor a safety improvement plan. 6. Prepare a written Safety Committee Report of its activities.

Table 4. Responsibilities of the MR Safety Officer.

MRI Safety Officer Responsibilities
<ol style="list-style-type: none"> 1. Maintaining current safety policies. 2. Monitoring safety training to ensure that all new personnel are properly trained and all employees receive annual safety training. 3. Reviewing incident reports and determining if appropriate corrective actions are implemented by site management. 4. Conducting regularly scheduled facility safety inspections. 5. Reviewing and recommending changes as safety program needs are identified. 6. Designating the appropriate maintenance of safety records for each facility. 7. Establishing a system for providing first aid, medical emergency equipment, and personal protective equipment. 8. Serving as the Chairperson for the MRI Safety Committee.

Table 5. Responsibilities of employees.

Employee Responsibilities
<ol style="list-style-type: none"> 1. Learn and comply with safety and health rules and regulations established by the center. 2. Report all safety and health hazards to a supervisor and take all necessary actions to establish immediate or temporary control of the hazard until permanent control can be established. 3. Immediately report all accidents or incidents on the job to their supervisor. 4. Cooperate and assist in all investigations. 5. Use all appropriate personal protective equipment provided.

uling regular meetings to discuss safety, establishing training programs, posting key responsibilities in easily accessed employee areas, and providing newsletters with relevant information.

MRI SAFETY PROGRAM

Outpatient MRI facilities should be accredited by either the American College of Radiology (ACR), the Intersocietal Commission for the Accreditation of Magnetic Resonance Imaging Laboratories, RadSite or The Joint Commission. Services should be performed under the direct supervision of a physician certified by the American Board of Radiology or other equivalent national medical imaging certifying body and licensed to practice medicine in the state where the center is located. Some state and local governments require additional certification. The MRI technologists should be active participants in the continuing compliance and quality assurance standards of the facility's accreditation certification. These individuals are key members of the safety team discussed above.

Patient Safety

A key component of the MRI safety program is to protect patients. This requires a comprehensive system that includes appropriate policies and procedures and begins with the patient's first interaction with the MRI facility. Scheduling of MRI studies requires an order from a licensed medical professional. The order must be provided to the facility as one of the following:

- A written document signed by the treating physician/practitioner that is hand-delivered, mailed, or faxed to the facility;
- A telephone call by the treating practitioner, with written documentation of the order by both the practitioner's office and the center; or
- An electronic communication.

Telephone orders for outpatients without a written order should be verified by a return call to the referring physician's office and the call should be documented in the medical record. The written order must be permanently maintained in the patient's record. A complete order should include all of the elements listed in **Table 6**.

Table 6. Examination ordering requirements for outpatient MRI services.

Requirements for All MRI Exam Orders
<ul style="list-style-type: none"> • Learn and comply with safety and health rules and regulations established by the center. • Report all safety and health hazards to a supervisor and take all necessary actions to establish immediate or temporary control of the hazard until permanent control can be established. • Immediately report all accidents or incidents on the job to their supervisor. • Cooperate and assist in all investigations. • Use all appropriate personal protective equipment provided.
Additional Items, as Applicable
<ul style="list-style-type: none"> • Date and time of scheduled surgery • Indication of "STAT" if requested

Determination of the appropriateness of the requested examination should be performed before the patient is exposed to the MRI environment, preferably at the time of scheduling.

770 MRI Safety Policies and Procedures for an Outpatient Facility

Appropriateness Criteria from the American College of Radiology can assist in this process (please see <http://www.acr.org/Quality-Safety/Appropriateness-Criteria>).

If the patient is determined to be pregnant and the referring physician is not aware at the time of the imaging request, then the referring physician must be notified and approval obtained before allowing the patient into the magnetic resonance (MR) system room. The radiologist must also approve MRI examinations on pregnant patients. The risk versus benefits of MRI must be considered and explained to the patient by a trained healthcare professional before proceeding with the study and documented in the patient's medical record.

The MRI technologist should carefully review the examination order and confer with the radiologist if the order is incomplete, unclear or needs amending. The MRI technologist cannot change the requested order without approval by the radiologist or authorization from the requesting physician. Any change in the original order requires documentation of an amended order including:

- Names, titles and other identifying information for both parties involved in the amendment;
- Date and time of the amendment; and
- Specific information describing the changes made.

Importantly, Independent Diagnostic Testing Facilities (IDTFs) are required to obtain all referring physician orders and modifications in writing.

Implants

Screening patients for the presence of implants and devices that may pose hazards in the MRI environment must begin with the scheduling process. Notably, the Safety Committee should provide scheduling personnel with guidelines so that implants and devices inappropriate for MRI are detected and exams not scheduled. Patients should be asked at the time of scheduling to bring their implant device card or information in writing from their physician. The physician or surgical center can be contacted when the patient cannot provide the necessary information. The presence, nature and MRI information for implants and devices (i.e., the labeling for MRI which is usually found in the Instructions for Use, IFU, for the item) should be re-verified by the MRI technologist when reviewing the patient's history just prior to the patient entering the MR system room.

All employees should be familiar with current MRI labeling terminology, as follows: MR Safe, MR Conditional, or MR Unsafe (3, 4). The MRI-specific restriction information for each MR Conditional-designated implant should be carefully evaluated before the patient is allowed into the scanner to ensure compliance (e.g., strength of the static magnetic field, level of the spatial gradient magnetic field, type of transmit radiofrequency coil, specific absorption rate limitation, etc.) (3-7). Scheduling personnel must have access to an MRI technologist and/or a radiologist in case questions concerning safety of specific devices cannot be resolved. A detailed list of this information can be found on the website, www.MRIsafety.com, in an annually updated textbook (4), or from the implant manufacturer. In addition to the above, policies and procedures must be in place to ensure that pa-

tients are properly identified and the correct patient information is entered into the MR system and medical record.

Access Zones

Because of the potential risk inherent in the MRI environment, the American College of Radiology (ACR) recommends segmenting the area into four different zones (5, 7). In new construction, these zones should be physically separated by barriers or other appropriate means. In certain outpatient MRI centers, physical separation may not be practicable and, in general, has been found to be unnecessary.

Areas that are restricted, that is, the immediate areas outside the MR system room (Zone III) and the scanner room (Zone IV) where the static magnetic field exceeds 5-Gauss should be clearly marked and designated as being potentially hazardous. Danger signs should be prominently displayed at the entry of hallways and rooms that are adjacent to the MR system room and should also be prominently displayed on the door of the scanner room (5, 7).

Where locking mechanisms are available, the MR system room should be physically restricted from general access by key locks whenever MRI personnel are not in the immediate vicinity and cannot control access (e.g., lunch break and evening closing). Only MRI personnel should be provided with the access keys to the scanner room. The ACR recommends that physical barriers be maintained across doorways when the MR system room must remain open for cleaning or maintenance (5-7).

Patients are screened for risk factors before being escorted into the Restricted Zones III (hallways or rooms adjacent to the scanner room) and IV (the MR system room). This topic is covered in great detail elsewhere in this textbook. Patients (or their family, guardian, or designate) must complete a written screening form. Special diligence is required for incommunicative and critical patients. The facility can create its own screening form approved by the Safety Committee or a form can be obtained from other sources, such as the ACR (5, 7) or downloaded from www.MRIsafety.com. A completed and signed screening form should be obtained each time a patient presents for an MRI examination. Screening of unconscious or incommunicative patients who are unable to provide a history for surgery, trauma, metal exposure, or prior MRI contrast reactions should be performed by the MRI technologist in conjunction with the patient's spouse, closest relative, guardian, or personal physician. This individual should complete and sign the screening form designated for this purpose.

The MRI technologist performing the examination must review the completed screening form and verbally review the answers with the patient or other individual before witnessing (i.e., signing) the form. The screening form is placed in the patient's medical record. Any implants, devices, or metallic foreign bodies raising concerns relative to MRI safety should be checked with published sources or by other means (1-6), before allowing entry into the MR system room. Consultation with the supervising radiologist or MR Safety Officer is recommended if any safety concerns cannot be resolved. The MRI technologist should perform a final visual and verbal safety check prior to entering the MR system room with the patient.

772 MRI Safety Policies and Procedures for an Outpatient Facility

Sedated, anesthetized, incommunicative or high-risk patients should undergo appropriate physiologic monitoring throughout the MRI examination. This may include checking the patient's vital signs, such as respiratory rate, heart rate, electrocardiogram, blood pressure, and oxygen saturation as clinically indicated and as deemed appropriate by the MRI facility and supervising physician (5).

A critical component of the outpatient MRI facility's safety program is planning for attending to patients who may have medical emergencies in the MR system room. Appropriately trained personnel and supervisory physician shall be available at all times to provide emergency medical treatment to patients with cardiac and respiratory arrest. Mock emergency or "code blue" drills are recommended to ensure that the emergency team can efficiently manage medical emergencies. In the setting of a serious emergency such as a cardiopulmonary arrest, the patient should be rapidly and safely removed from the scanning room and immediate basic or advanced life support or other appropriate treatment should be initiated. Emergency medical equipment and medications should be readily available and accessible to emergency personnel.

Pregnant Patients

Pregnant patients warrant special consideration. MRI may be performed at any stage of pregnancy if the patient's physician and radiologist determine that the risk versus benefit warrants performing the exam. This topic is covered in detail in another chapter in this textbook.

The indications and other information for scanning during pregnancy must be documented in the patient's medical record and should include that the MRI study cannot be acquired via other non-ionizing means such as ultrasound, the diagnostic information is medically necessary to diagnose the mother or fetus during pregnancy, the referring physician does not believe it is prudent to wait until a later stage of pregnancy or after pregnancy, and the patient agrees to have the examination during pregnancy. Importantly, the prior requirement for written and verbal informed consent is no longer a requirement from the American College of Radiology (7). **Table 7** outlines the indications for performing MRI in pregnant patients.

Table 7. Documentation required when managing pregnant patients referred for MRI.

The following indications for scanning during pregnancy must be documented in the patient's medical record:
<ol style="list-style-type: none"> 1. The information from the MRI exam cannot be acquired via other non-ionizing diagnostic imaging such as ultrasound. 2. The diagnostic imaging information is medically indicated to diagnose either the mother or fetus during pregnancy. 3. The referring physician does not believe that it is prudent to wait to obtain the information until a later stage of pregnancy or after pregnancy.

MRI contrast agents should only be administered to pregnant patients after risk versus benefit consideration and approval by an MRI-trained radiologist (7-9). Notably, the fetus

has a higher exposure to gadolinium in the first few weeks of pregnancy when the mother may not know she is pregnant (8). Ray, et al. (9) reported that gadolinium exposure at any time during pregnancy may be associated with an increased risk of inflammatory conditions, stillbirth, and neonatal death.

Fetal MRI

Fetal MRI is indicated for use if diagnostic ultrasound is inadequate or the examination provides important information about the fetus that would otherwise require exposure to ionizing radiation (4, 5, 7-9). Fetal MRI is conducted only on the recommendation of a radiologist after consultation with the referring physician (4, 7-9). The radiologist should document in the radiology report the fact that: (1) the diagnostic study could not be acquired via other non-ionizing diagnostic imaging means, (2) the information was needed to potentially affect the care of the fetus during the pregnancy, and (3) the referring physician did not feel that it was prudent to wait until the fetus was born to obtain the information. Of note is that recent investigation reported that MRI exposure to the fetus during the first trimester of pregnancy was not associated with increased risks (9).

Specific MR System-Related Patient Risks

The time-varying magnetic fields applied during image acquisition induce currents in conductors in the field's influence and, when applied in the presence of a high static magnetic field, create torque on the gradient coils, producing acoustic noise. Because of the intensity of the noise induced by gradient switching in high field strength MR systems, patients should wear hearing protection when undergoing MRI (4, 7, 10-12). Typical hearing protection devices include earplugs, headphones, or headphones with noise reduction technology. Certain MR scanners provide active noise control (noise cancellation) systems that attenuate acoustic noise and/or have an option of using quiet pulse sequences (11). Despite these features being available, patients should still utilize passive noise control (earplugs or headphones) during all MRI exams performed on high field strength scanners.

The radiofrequency (RF) fields used during MRI can generate heat in conductors (4, 7, 12-16) resulting in temperature increases. Therefore, all unnecessary electrically conductive materials should be removed from the patient and the bore of the MR system before initiating scanning to prevent patients from experiencing excessive heating or burns (4, 7). All electrical connections, such as on surface RF coils, electrocardiogram leads, and other similar items should be checked by the MRI technologist prior to each use to ensure integrity, and that the thermal and electrical insulation is intact. Damaged cables and exposed wires should be immediately reported to the service engineer and the equipment taken out of service until it is repaired.

For electrically conductive materials, such as wires, that are required to remain in the bore of the MR system during MRI, the wires must be oriented so that no loops are formed (4, 7). Adequate thermal insulation (i.e., using air, padding, etc.) should separate the patient's skin from all conducting materials, as well as the transmit RF coil (e.g., the body RF coil) during MRI. Procedures to prevent excessive heating and burns in patients during MRI have been previously presented and should be closely followed as part of preparing patients for MRI examinations (4, 5, 7).

774 MRI Safety Policies and Procedures for an Outpatient Facility

Before undergoing an MRI examination, patients should be asked if they have ever had a permanent coloring technique (i.e., tattoos or permanent cosmetics) applied to the body. This includes cosmetic applications such as eyeliner, lip liner, lip coloring, as well as decorative designs. Screening is necessary because of associated imaging artifacts and, more importantly, because a small number of patients have experienced transient skin irritation, cutaneous swelling, or heating sensations at the site of the permanent coloring in association with MRI (4). These issues do not represent a contraindication to MRI but precautionary measures should be in place, such as application of a dry, cold compress (ice pack wrapped in a towel) to the tattoo site during the exam. Patients should be advised to immediately notify the MRI technologist regarding any unusual sensation felt at the site of the tattoo during scanning (4, 5, 7).

Patients with metallic body piercing jewelry must be evaluated on a case-by-case basis and cleared in the same manner as other implanted devices that have no labeling information. Accordingly, the supervising physician must make a careful assessment of risk associated with the MRI versus the benefit of the diagnostic information.

Some drug delivery or medication patches may contain metallic foil or other similar conducting material. Subjecting the area of the medication patch to RF energy may result in thermal injury to the patient (4). Since removal or repositioning can result in altering the medication dose, consultation with the patient's prescribing physician is recommended. If the medication patch is removed, a nursing staff member should be given the responsibility for ensuring that it is replaced or repositioned (4).

Sedation

Certain outpatients may require sedation in order to complete a successful MRI examination (17-19). The Safety Committee must have written policies and procedures detailing how adult and pediatric patients should be medicated in the MRI setting. For pediatric patients, these policies and procedures should be based on national standards, facility-specific policies defined by the referring pediatrician and the pediatric radiologist, the age of the patient, the mental capacity of the patient, the time duration of the MRI examination, and the depth of sedation needed. Written guidelines for adult sedation are also needed. Facility-specific policies developed in conjunction with anesthesiologists should determine the type of sedation that is utilized. Sedation should always be administered in accordance with national guidelines and state and local laws (4, 7, 17-19). Separate sedation consent forms must be approved by the Safety Committee and explained to the patient by an appropriate healthcare professional before the patient or designate signs the document.

Gadolinium-Based MRI Contrast Issues

The most common adverse event leading to emergency room visits from outpatient MRI facilities is an adverse reaction to intravenous administered MRI contrast agents. No patient should be given an intravenous contrast agent without the written prescription of a licensed physician in accordance with state laws. Depending on state regulations, a physician, registered nurse, or IV-qualified MRI technologist may start and attend to the peripheral intravenous access line and administer the MRI contrast agent as a bolus or continuous injection.

Before administering an intravenous MRI contrast agent, preferably at the time of scheduling the study, a history must be obtained from the patient or patient's guardian concerning prior contrast injections and possible adverse reactions (20-23). A history of asthma or allergic-type respiratory reaction not associated with MRI contrast agents is a risk factor for adverse reactions, but does not require premedication in most circumstances. Monitoring the cardiovascular and/or respiratory status (i.e., via the use of an MR Conditional pulse oximeter) is prudent during and following administration of intravenous gadolinium-based MRI contrast agents in high-risk patients. According to recommendations by the ACR, if the patient has a history of an adverse reaction to a gadolinium-based contrast agent, then the patient should be considered for premedication prior to receiving the contrast dosage (20). The patient's cardiovascular and respiratory status should also be carefully monitored using appropriate techniques during MRI and for 30 minutes following contrast administration. While serious reactions are rare (21, 23), patients who have had a severe anaphylactoid reaction to prior gadolinium-based contrast media should be given careful consideration before use in future MRI exams.

According to recent recommendations in the ACR Manual on Contrast Media (20), outpatients do not need to be screened for renal function status before administration of a Group II agent at standard or lower doses unless they have the known risk factors. In other instances, screening questions designed to determine the patient's risk for nephrogenic systemic fibrosis (NSF) should be asked at the time of scheduling and when the MRI technologist obtains the patient's history prior to MRI (24-34). **Table 8** lists screening questions that we recommend to ask patients relative to the issue of NSF. A positive answer to any of these questions requires calculation of the patient's glomerular filtration rate (GFR) to determine risk for NSF before administering gadolinium-based contrast agents in the outpatient setting.

Table 8. Screening questions for determining risk for nephrogenic systemic fibrosis (NSF).

Screening Question For All MRI Patients Regarding Dialysis
Are you currently on renal dialysis?
If Yes, Screen With Additional Questions
Do you have a history of kidney disease, including:
<ul style="list-style-type: none"> • Kidney surgery or a kidney transplant? • Single kidney? • Kidney tumor or renal cancer?
Do you have hypertension that requires medication?
Are you diabetic?

If the patient is on dialysis, has an estimated GFR less than 30 mL/min/1.73-m² (stage 4 or stage 5 renal disease), or has acute renal injury, then injection of a gadolinium-based contrast agent should be given cautiously only after the following information is documented:

776 MRI Safety Policies and Procedures for an Outpatient Facility

- The referring physician and radiologist or attending physician must confer and decide that use of the gadolinium-based contrast agent is essential for diagnosis and no other reasonable means is available;
- Written orders from the referring physician and the supervising radiologist must be obtained, which include the name of the patient, the name and brand of the MRI contrast agent used, dose, route and rate of administration, the date and signature of the radiologist;
- The lowest effective dose of a lower-risk Group II gadolinium-based contrast agent should be used unless there is a specific indication for another agent.

Although the benefits of hemodialysis have not been definitively established if the patient is on dialysis, the patient should undergo a hemodialysis session as soon as possible after the administration of the gadolinium-based contrast agent, preferably within a few hours of the study. The ACR no longer recommends that dialysis be repeated 24 hours later (20). Of note is that peritoneal dialysis provides less NSF risk reduction compared to hemodialysis.

Visitor Screening

All visitors entering the Restricted Zones (III and IV) must be screened for MRI risk factors and fill out a specific screening form designed for those not undergoing an MRI examination (4) while still in the Patient Preparation Zone and undergo screening by the MRI technologist. If deemed safe to enter the Restricted Zones by the MRI technologist, then the visitor may be allowed access to these areas under direct supervision by an MRI safety-trained healthcare worker. Prior to entering the MR system room, it is recommended that the visitor change into a gown or scrubs provided by the MRI facility. However, if the visitor is allowed to remain in street clothes, pockets must be emptied of all metallic objects, external hearing aids, jewelry and analog watches, and any other objects that are ferromagnetic or could be damaged in the presence of a high static magnetic field must be removed.

Emergency Personnel

Emergency responders (e.g., first responders), firefighters, police, and security personnel must be fully screened as a visitor and cleared by an MRI technologist before being allowed access to the scanner room. Furthermore, it is prudent for outpatient MRI facilities to periodically inform their local police and firefighter organizations of the risks of the powerful static magnetic field of the MR system and the 24-hour presence of the magnetic field for superconducting magnets before emergencies arise so that emergency personnel will be cognizant of the risks when responding to emergencies. Security personnel must remove all metallic objects from their possession including guns and ammunition, electronically-activated restraint devices, radios, cell phones, badges, name tags, jewelry, coins, wallets, keys, pocket knives, and similar items before entering the MR system room. If the patient is a detainee and requires a restraining device, a plastic restraint device must be used (7).

Employee Safety

The outpatient MRI facility is a dynamic and often stressful environment. Therefore, it is important to establish policies and procedures for professional behavior and etiquette to

avoid unnecessary patient stress on top of an anxiety-provoking examination. Center personnel who interact with patients should properly identify themselves and explain their roles.

All employees of an outpatient MRI facility must be screened for MRI risk factors and any employee who is deemed to be unsafe for the MRI setting (e.g., as a result of having an unsafe implant) must be kept from the Patient Preparation and the MR system room. Employees with access to the scanner room must complete and pass an MRI safety training course, which should be repeated on an annual basis (5, 7).

If an equipment malfunction occurs, then the chief or lead MRI technologist, facility manager, or radiologist should be informed in a timely manner. Only certified and qualified MRI technologists and MRI safety-trained radiologists should be permitted to operate an MR system and have unrestricted access to the scanner room. These individuals must be extensively trained and educated in the broader aspects of MRI safety, including issues related to the potential for attraction of ferromagnetic implants and devices, burns, peripheral nerve stimulation, acoustic noise, and other potential risk factors (4-7).

In order to minimize errors, it is recommended that the MRI technologist indicated in the patient's medical record should be responsible for screening the patient and performing the MRI examination. Only safety-trained MRI technologists should be authorized to conduct MRI screening. Non-MRI personnel should be accompanied by and/or under the immediate supervision of an MRI technologist while they are in the immediate area prior to the MR system room and the scanner room, itself.

Pregnant Personnel

Pregnant healthcare workers can work in and around the MRI environment throughout all stages of their pregnancy (4, 5, 7). This includes, but is not limited to, positioning patients, scanning, archiving, injecting MRI contrast agents, entering the scanner room in an emergency, and performing similar tasks. However, if pregnant workers are uncomfortable with the concept of exposure to the static magnetic field of the MR system, they should not be required to work in the MR system room. Pregnant healthcare workers should not remain within the bore of the scanner during the operation of the scanner (4, 5, 7).

Equipment

Proper installation and maintenance is necessary for the safe operation of an MR system. All equipment used in the scanner room must be deemed safe for use in the MRI environment. Oxygen tanks must be nonferromagnetic throughout the imaging facility. Fire extinguishers must be MR Conditional versions and must be placed in a conspicuous place in or near the scanner. Monitoring equipment such as pulse oximeters and anesthesia equipment must be MR Conditional in order to be used in the MR system room. All other equipment such as IV poles, step stools, stretchers, and other patient support items must also be MR Safe or MR Conditional.

There are risk factors unique to the powerful magnet associated with an MR scanner. For example, if an individual is "trapped" against the MR system by a large ferromagnetic object, then the static magnetic field will likely need to be shut down immediately. If the

778 MRI Safety Policies and Procedures for an Outpatient Facility

magnet is resistive, then the power can be shut off. If the magnet is superconducting, then the field must be reduced using the “quench button”, which should be located in a conspicuous place. Special training and education are important for all staff members working in the outpatient MRI facility with regard to specific procedures to follow involving a quench (4, 7).

Preventive maintenance is mandatory to ensure high performance of the scanner in order to minimize down time and to maximize image quality and should be performed according to the manufacturer’s recommendations and properly documented.

CONCLUSIONS

Optimal MRI safety in outpatient imaging centers requires a well-organized plan that includes the facility’s management, employees, an MRI Safety Committee and committed MR Medical Director, and MR Safety Officer. A written safety plan that includes policies and procedures that address the risks uniquely associated with the MRI environment must be developed and explained to all employees, along with the assignment of specific responsibilities for execution of the plan. Since few lay people understand the risks associated with high static magnetic fields and other potential hazards associated with MRI, screening must begin at scheduling and continue prior to scanning. Strict adherence to patient safety management must be practiced before and during the MRI exam. Visitors, emergency personnel, and others must be screened and prohibited from entering the MR system room with unsafe devices to ensure both their safety as well as that of patients and staff members. Fortunately, extensive experience with MRI technology in outpatient facilities worldwide during more than thirty years has demonstrated that outpatient MRI is extremely safe if proper policies and procedures are in place and the precautions discussed herein are rigorously enforced.

REFERENCES

1. Beam AS, Ketchum JM, Wilson A, et al. Safety resources and processes in MR imaging departments. Radiol Technol 2019;90:225-236
2. Cross NM, Hoff MN, Kanal KM Avoiding MRI-related accidents: A practical approach to implementing MR safety. J Am Coll Radiol 2018;15:1738-1744.
3. Shellock FG, Woods, Crues JV. MR labeling information for implants and devices: Explanation of terminology. Radiology 2009;253:26-30.
4. Shellock FG. Reference Manual for Magnetic Resonance Safety, Implants, and Devices: 2020 Edition. Los Angeles, CA: Biomedical Research Publishing Group, Los Angeles, CA, 2020.
5. Kanal E, Barkovich AJ, Bell C, et al. ACR guidance document on MR safe practices: 2013. J Magn Reson Imaging 2013;37:501-530.
6. ACR Committee on MR Safety, Greenberg TD, Hoff MN, et al. ACR guidance document on MR safe practices: Updates and critical information 2019. J Magn Reson Imaging 2020;51:331-338.
7. ACR Manual on MR Safety, ACR Committee on MR Safety, Version 1.0, 2020 <https://www.acr.org/Clinical-Resources/Radiology-Safety/MR-Safety>.
8. American College of Radiology. ACR-SPR Practice Parameter for the Safe and Optimal Performance of Fetal Magnetic Resonance Imaging (MRI), www.acr.org.

MRI Bioeffects, Safety, and Patient Management 779

9. Ray JG, Vermeulen MJ, Bharatha A, Montanera WJ, Park AL. Association between MRI exposure during pregnancy and fetal and childhood outcomes. *JAMA* 2016;316:952-996.
10. Shellock FG, Crues JV, Editors. *MRI Bioeffects, Safety, and Patient Management*. Los Angeles, CA: Biomedical Research Publishing Group, Los Angeles, CA, 2014.
11. Lauer AM, El-Sharkawy AM, Kraitchman DL, Edelstein WA. MRI acoustic noise can harm experimental and companion animals. *J Magn Res Imaging* 2012;36:743-747.
12. Shellock FG, Crues JV. MR procedures: Biologic effects, safety, and patient care. *Radiology* 2004;232:635-652.
13. Shellock FG, Spinazzi A. MRI safety update 2008: Part 2, screening patients for MRI. *AJR Am J Roentgenol* 2008;191:1140-1149.
14. Zikria JF, Machnicki S, Rhim E, Bhatti T, Graham RE. MRI of patients with cardiac pacemakers: A review of the medical literature. *AJR Am J Roentgenol*. 2011;196:390-401.
15. Jacob ZC, Tito MF, Dagum AB. MR imaging-related electrical thermal injury complicated by acute carpal tunnel and compartment syndrome: Case report. *Radiology* 2010;254:846-50.
16. Shellock, FG. Radiofrequency energy-induced heating during MR procedures: A review. *J Magn Reson Imaging* 2000;12:30-36.
17. Berlin L. Sedation and analgesia in MR imaging. *AJR Am J Roentgenol* 2001;177:293-299.
18. Bluemke DA, Breiter SN. Sedation procedures in MR imaging: Safety, effectiveness, and nursing effect on examinations. *Radiology* 2000;216:645-652.
19. Finn JP. Sedation in MR imaging: What price safety? *Radiology* 2000;216:633-634.
20. American College of Radiology. *ACR Manual on Contrast Media*, 2020. American College of Radiology, www.acr.org
21. Jung J, Kang H, Kim, M, et al. Immediate hypersensitivity reaction to gadolinium-based MR contrast media. *Radiology* 2012;264:414-22.
22. Bird ST, Gelperin K, Sahin L et al. First-trimester exposure to gadolinium-based contrast agents: A utilization study of 4.6 million U. S. pregnancies. *Radiology* 2019;293:193-200.
23. Prince MR, Zhang H, Zou Z, et al. Incidence of immediate gadolinium contrast media reactions. *AJR Am J Roentgenol* 2011;196:138-143.
24. Sena, BF, Stern JP, Pandharipande PV, et al. Screening patients to assess renal function before administering gadolinium chelates: Assessment of the Choyke questionnaire. *AJR Am J Roentgenol* 2012;195:424-428.
25. Altun E, Martin DR, Wertman R, et al. Nephrogenic systemic fibrosis: Change in incidence following a switch in gadolinium agents and adoption of a gadolinium policy – Report from two U.S. universities. *Radiology* 2009;253:689-696.
26. Juluru K, Vogel-Claussen J, Macura KJ, et al. Nephrogenic systemic fibrosis: Protocols, practices, and imaging techniques to maximize patient safety. *Radiographics* 2009;29:9-22.
27. Wang Y, Alkasab TK, Narin O, et al. Incidence of nephrogenic systemic fibrosis after adoption of restrictive gadolinium-based contrast agent guidelines. *Radiology* 2011;260:105-111.
28. Leiner T, Kucharczyk W. Special issue: Nephrogenic systemic fibrosis. *J Magn Res Imaging* 2009;30:1233-5.
29. Perez-Rodriguez J, Lai S, Ehst BD, Fine DM, Bluemke DA. Nephrogenic systemic fibrosis: Incidence, associations, and effect of risk factor assessment – Report of 33 cases. *Radiology* 2009;250:371-377.
30. Sieber MA, Lengsfeld, P, Walter J, et al. Gadolinium-based contrast agents and their potential role in the pathogenesis of nephrogenic systemic fibrosis: The role of excess ligand. *J Magn Res Imaging* 2008;27:955-969.
31. Wang Y, Alkasab TK, Narin O, et al. Incidence of nephrogenic systemic fibrosis after adoption of restrictive gadolinium-based contrast agent guidelines. *Radiology* 2011;260:105-111.

780 MRI Safety Policies and Procedures for an Outpatient Facility

32. Wertman R, Altun E, Martin DR, et al. Risk of nephrogenic systemic fibrosis: Evaluation of gadolinium chelate contrast agents at four American universities. *Radiology* 2008;248:799-806.
33. Wiginton CD, Kelly B, Oto B, et al. Gadolinium-based contrast exposure, nephrogenic systemic fibrosis, and gadolinium detection in tissues. *AJR Am J Roentgenol* 2008;190:1060-1068.
34. Shellock FG, Spinazzi A. MRI safety update 2008: Part I, MRI contrast agents and nephrogenic systemic fibrosis. *AJR Am J Roentgenol* 2008;191:1129-1139.

Chapter 29 MRI Policies and Procedures for a Children's Hospital Setting

CHRISTINE HARRIS, R.T., (R) (MR), MRSO

Corporate Director, Medical Imaging
Jefferson Health System, New Jersey
Cherry Hill, New Jersey

INTRODUCTION

In all aspects of life, children are provided with a different set of rules and regulations than adults to help keep them safe, and this is no different in the medical field, particularly in radiology. In fact, a major initiative in radiology is to reduce exposure to ionizing radiation in the pediatric population. In 2008, the *Image Gently* campaign was created by the Alliance for Radiation Safety in Pediatric Imaging to help the medical community change their practice by increasing awareness of the opportunities to promote radiation protection in the diagnostic imaging of children. While there is presently no similar group leading the effort with regard to the use of magnetic resonance imaging (MRI) in the pediatric population, it is this author's hope that we will continue to share best practices within the MRI community which will help ensure safety in pediatric patients relative to the utilization of MRI technology.

The objective of this chapter is to provide an overview of information pertaining to best practices as well as to present policies and procedures related to MRI safety for pediatric patients. Notably, in the MRI environment, children can present many challenges in imaging and safety (1-4). Trying to establish safety policies and guidelines in the use of equipment (e.g., radiofrequency coils, monitoring systems, anesthesia equipment, etc.) and the development of MRI techniques can be extremely challenging. To help guide us through these issues, it is essential for the facility to establish an MRI Safety Committee and safety enhancement program.

THE MRI SAFETY COMMITTEE

It can be challenging to impose the concept of MRI safety upon those not directly involved with it on a daily or otherwise routine basis. Without an MRI Safety Committee, the

782 MRI Policies and Procedures for a Children's Hospital Setting

involvement from ancillary teams (e.g., nursing, anesthesia, transportation, etc.) can be difficult to establish. As such, a collaborative approach allows for the development of rules and regulations that impact the workflow of all individuals involved in the care of patients who undergo MRI exams. By seeking the advice or input from the other healthcare professionals, the implementation of new policies and procedures becomes a synergistic effort. Developing an MRI Safety Committee composed of vital representatives from ancillary departments such as the anesthesia department, the intensive care unit (ICU), respiratory care, and nursing staff members is beneficial because it provides a path by which the members of the committee become the liaison between radiology/MRI and the individual disciplines and departments.

FUNCTION OF THE MRI SAFETY COMMITTEE

Before developing an MRI Safety Committee, careful thought should be given as to how the committee will function, as well as to the development of the roles and responsibilities of the various committee members (5-8). There are several avenues the group can take when forming an MRI Safety Committee. The committee can be one of three basic types: (1) Advisory, (2) Policy Making, or (3) a combination of the two.

- (1) The Advisory Committee investigates MRI safety issues within the department and hospital, offering guidelines, as needed. This committee does not make policies, but rather, offers opinions to those individuals responsible for developing rules that impact the MRI facility.
- (2) The Policy Making Committee is entrusted with the power to make or change policies and procedures based on their safety findings or in response to a need to address an accident or incident. Similar to the Advisory Committee, the Policy Making Committee may have to investigate or research topics and issues, but this committee is also granted the further discretion to formulate new policies and procedures.
- (3) The Combination Committee takes into account recommendations from both the Advisory Committee and the Policy Making Committee. This committee should be given specific guidelines on its authority. In some instances, its authority may be advisory, while other issues may require the latitude to develop and implement new policies and procedures

The goal of the MRI Safety Committee should be to promote awareness and understanding of MRI safety issues by collaborating and actively soliciting information that will provide a safer and more secure MRI setting. Membership in the MRI Safety Committee may include the following:

- (1) Radiology Leadership including the Radiologist-in-Chief or designate, Radiology Patient Safety Officer/MRI Safety Committee Medical Director, Radiology Administrative Director, Radiology Manager and the MR Safety Officer (MRSO)
- (2) Anesthesia, including personnel from Cardiac Anesthesia and General Anesthesia and/or those providers overseeing sedation such as the Medical Director of Sedation Services (as appropriate)
- (3) Environmental Health and Safety, Director of Environmental Health and Safety
- (4) MRI Technologists, MRI Team Leader, Quality and Safety, and Cardiac MRI Technologists (if applicable)

MRI Bioeffects, Safety, and Patient Management 783

- (5) Cardiology including the MRI Cardiologist and Cardiac Nursing Director (i.e., if the department has a cardiac imaging program)
- (6) Imaging Nurses
- (7) Biomedical Engineering personnel
- (8) Respiratory Medicine personnel

MRI SAFETY ENHANCEMENT PROGRAM

MRI safety should be continuously enhanced because every year, new biomedical equipment and medical implants are deployed that can create possible unsafe situations in the MRI setting and for patients. Additionally, every year new personnel join medical centers, many of which may need to visit the MRI facility. These new employees require specialized training and need to be kept informed regarding new developments that impact MRI safety. An enhancement program may include the following:

- An education and communication plan to address topics such as The Joint Commission requirements for MRI or new information from the American College of Radiology.
- Environmental enhancement needs or other similar needs such as incorporating a ferromagnetic detection system to supplement screening for patients and other individuals.
- Budgeting for new safety equipment, devices, and software.

Essentially, an MRI enhancement program may adopt a similar philosophy as the Institute for Magnetic Resonance Safety, Education and Research (IMRSER.org) which is, as follows (9):

- To promote awareness and understanding of MRI safety
- To disseminate information regarding current and emerging MRI safety issues
- To develop and provide materials and resources to facilitate MRI safety-related education training
- To respond to critical MRI safety issues with a sense of urgency

MRI EDUCATION

Education of the team members increases their knowledge about critical aspects of the MRI environment, the special challenges with MRI safety, and the how's and why's of new policies and procedures. There should be the opportunity for initial learning, annual refresher courses, Just In Time (JIT) education and other related educational endeavors. At a minimum, educational courses should include the following content:

- Basic MRI principles
- MRI safety concerns
- Screening processes and the importance of completing the screening forms
- Images showing examples of accidents
- The history of why MRI safety matters
- Policies and procedures of the MRI facility

This education can be provided or reinforced by any one or combination of the following means:

784 MRI Policies and Procedures for a Children's Hospital Setting

- (1) "Field trips" to nursing units that discuss basic MRI information and safety concerns, the purpose and importance of family members filling out the MRI screening forms for pediatric patients, and images of accidents that highlight the importance of MRI safety.
- (2) Online courses and presentations that encompass a basic understanding of MRI-related issues, as well as an advanced level of MRI safety education (e.g., see www.appliedradiology.org/mrisafety).
- (3) One-on-one education with an MRI technologist that includes all personnel who need access to the MRI environment in order to discuss the policies and procedures for MRI safety.
- (4) Annual education that is provided to all MRI staff members and ancillary teams who frequent the MRI setting including: security officers and first responders, members of the Pediatric Intensive Care Unit (PICU) and Neonatal Intensive Care Unit (NICU), and anesthesia personnel who are involved in the management of patients in the MRI setting on a regular basis.
- (5) Just in Time (JIT) education is typically used to teach and re-teach known medical techniques and is a great resource for staff members that may have a limited rotation to the MRI facility (10). This particular type of education should be kept simple and relatively brief, while touching on key items. **Figure 1** presents an example of a flyer that can be used as a tool for JIT. Note that it covers the key points directed towards the hospital's nursing staff that they must review before entry to the MRI area. JIT may also be used as screen savers on computers at the nursing stations to remind staff members of key items related to MRI safety.

MRI safety is usually misunderstood by individuals that do not work in the MRI setting. Using techniques such as formalized educational programs provide an opportunity to remind all hospital personnel of the dangers inherent in the MRI area, making sure that ancillary staff members obtain the necessary knowledge to keep pediatric patients safe. Importantly, the pursuit of MRI safety should be an integral part of an overall institutional safety program.

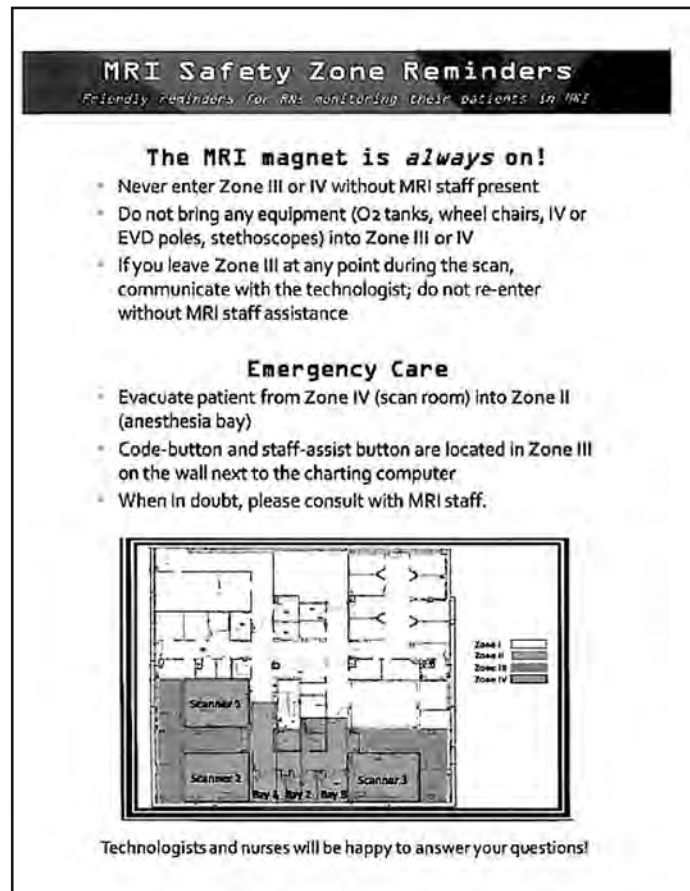
SIMULATION AND ITS ROLE IN MRI SAFETY

Hospitals and medical centers now offer variations of simulation-based training whereby medical and other personnel have the opportunity to develop skill sets on mannequins and to use other tools in specific settings before actually performing the skills involving patients, such as venipuncture and responses to various types of emergencies. Similarly, an MRI simulation center can be a useful tool to improve the culture of safety relative to the MRI environment. Additionally, an MRI simulation center can help facilitate the review of policies and procedures by simulating real life situations. The objectives of these simulations should be to ensure that the policies and procedures are clear and that all involved can effectively perform the critical tasks, as needed.

QUALITY MEASURES OF THE MRI SAFETY PROGRAM

Evaluation of an MRI safety program can help to determine whether the strategies, policies and procedures, and the implementation of new technology are effective in improving MRI safety (11-17). Methods of evaluation may consist of the following:

Figure 1. Example of a “Just In Time” education tool. (Image provided courtesy of Children’s National Hospital.)



- Consultation
- Transparency and Awareness
- Monitoring and Data Collection

Consultation

Review by an MRI Safety Leader, MRI Safety Officer (MRSO), MRI Safety Expert (MRSE) or other appropriate individual may be useful to:

- Review current policies and procedures
- Provide suggestions for new policies
- Give advice on additional policies and procedures that are needed
- Tour the various MRI facilities to evaluate current safety equipment and suggest additional enhancements that may be needed
- Provide comprehensive presentations to hospital staff about current MRI safety topics
- Meet with members of the MRI Safety Committee to present findings on the current safety status and provide suggestions

786 MRI Policies and Procedures for a Children's Hospital Setting

Transparency and Awareness

To ensure that staff members are aware of all policies, procedures, and job aids or tools for MRI safety, all documents should be reviewed and updated annually and kept readily available to staff members (e.g., on the institution's intranet).

Monitoring and Data Collection

To verify that policies and procedures are understood and followed, members of the MRI Safety Committee should monitor, collect, and evaluate data pertaining to MRI safety issues on a monthly basis. The following are representative data that could be collected:

Time Out and Visual Check of the Patient and Equipment

- (1) Properly identify the patient and the MRI Exam
 - Two patient identifiers
 - Confirm type of MRI exam and body part undergoing the MRI procedure
 - Two-way communication with registered nurse, nurse practitioner, physician, and/or parent
 - Ancillary staff members should remove outer clothing such as jackets or sweaters, squeeze pockets to identify items, etc.
 - Review the MRI screening form
- (2) Visual check of patient and equipment
 - Confirm that the stretcher or wheelchair that is intended to enter the MR system room is MR Safe or MR Conditional
 - A staff member should lift blankets, sheets, and gowns to inspect the patient for possible unwanted items, especially if the patient is in a wheelchair or on a stretcher
 - Confirm that a patient support device (e.g., oxygen tank) is acceptable for use in the MR system room
- (3) All staff members entering the MR system room must remove all unsafe items
- (4) All doors with access to the MR system room should be locked when not being supervised by an MRI safety-trained staff member

POLICIES, PROCEDURES, AND JOB AIDS

A “policy” is a non-negotiable requirement of a regulatory agency or a self-imposed governing rule to ensure safety, quality, compliance, or cost-effectiveness (14-17). In general, policies should be written clearly and concisely. Language in the policy statement should mirror the language of the regulation itself. Policies should be fewer in number in the “Focus and Simplify” format. A key point is that, if procedures and job aids are well-written, a policy may only need to be accessed infrequently because the associated documents would help one to adhere to the policy (14-17).

- Purpose - Defines a governing rule or a non-negotiable requirement
- Volume - Few in number
- Source - Regulatory agency or self-imposed to ensure safety, quality, compliance or cost effectiveness
- Structure - Written clearly and concisely in a few sentences
- References - Included in the document
- Use - Accessed only when needed and for informational purposes

A “procedure” outlines a step-by-step process to carry out a work process, much like a recipe. It outlines the steps an employee needs to follow, in order, from start to finish. A procedure may be related to a policy, or it may be a stand-alone procedure. Accordingly, there should be many more procedures than policies (15-17).

- Purpose - Provides step-by-step actions to carry out a work process or to achieve an outcome, usually based on a policy
- Volume - Many
- Source - May be related to a policy or may stand-alone
- Structure - Includes steps in a process (i.e., similar to a recipe). Two-column or three-column format. Minimum level of detail for the experienced person and supplementary.
- References - Not usually included in the document
- Use - Can be a reference document or a continuous use document

It is important to note that when writing policies and procedures, make sure that they are evidence-based and not simply based on the way things have always been done.

A “job aid” is any informational tool or supplement used to carry out a policy or procedure. It is important to note that a single policy or procedure may have multiple job aids associated with it. Information contained in job aids is guidance-oriented, rather than action-oriented. Examples of job aids include, but are not limited to, the following: checklists, flowcharts, pictures or diagrams, and lists. In the proper format, there should be many more job aids and procedures than policies (16,17).

- Purpose - Any informational tool or supplementary information used to carry out a policy or procedure
- Volume - Many
- Source - May be related to a policy or procedure or may stand-alone
- Structure - Not specifically defined but may be in the form of a checklist, decision aid, reference guide, list, and/or a visual sign
- References - Not usually included
- Use - Can be reference or a continuous use document

EXAMPLES OF POLICIES AND PROCEDURES

Let’s now consider the special issues that the management of pediatric patients bring to the formulation of the policies and procedures for MRI safety.

Screening Policies

Most pediatric patients are usually unable to speak for themselves and, thus, rely on parents and guardians to provide and convey information for them and to ensure their safety. If you are a parent, you know that when you take your child to the hospital for an examination or procedure, you are focused on the child getting diagnosed or treated and may not always remember the answers to all the questions being asked. Parental anxiety plays a major role in how screening questions for MRI are answered and, therefore, having multiple tools and/or interviewing sessions provide parents with the opportunity to remember something they may have forgotten.

788 MRI Policies and Procedures for a Children's Hospital Setting

MRI Screening Process for In-Patients. Pediatric in-patients rely heavily on ancillary personnel to support them during MRI exams. Monitoring the ancillary staff, allowing a family member into the MR system room, performing the scan, answering telephones, and other tasks can be overwhelming for the MRI technologist due to the variety and vast number of support staff members that may be involved and the duties that are required. As such, to help monitor the large number of staff members in the MRI environment, there is a great dependence on screening policies and procedures.

The MRI Screening Form. MRI facilities should have screening forms readily available for every individual that needs to enter the MR system room (**Figures 2 to 4**). When screening pediatric patients, a family member or responsible guardian should fill out the screening form. In the event that there is not a parent or guardian available before the MRI exam, then a knowledgeable nurse or physician can fill out the form. Notably, the MRI screening form should include the parent or guardian's cell phone number in the event that it is necessary to ask questions so that these individuals can be reached directly and not delay their child's MRI exam. Once the screening form has been completed, the MRI technologist must review the content for the following information:

- Any implant or device that may be of concern
- Follow up on any question on the form answered "yes" or "unknown"
- A list of prior diagnostic imaging procedures

The MRI technologist then signs the screening form, which verifies that the form was reviewed and that the information was verified. In addition, if the pediatric patient has an

Figure 2. Children's National Hospital's MRI safety screening form used for patients.
(Image provided courtesy of Children's National Hospital.)

MRI HAZARD PATIENT CHECKLIST/SCREENING	
A New Checklist is REQUIRED FOR EVERY visit to MRI	
<p>Children's National</p> <p>The following items may be harmful to you during your MRI scan or may interfere with your MRI Examination You must provide a Yes, No or NA for EVERY item.</p>	
PATIENT LABEL	
<p>OBJECTS TO BE REMOVED PRIOR TO MRI SCAN:</p> <p><input type="checkbox"/> Y <input type="checkbox"/> N All Jewelry (including body piercings) <input type="checkbox"/> Y <input type="checkbox"/> N All hair pins, bobby pins, barrettes, clips etc. <input type="checkbox"/> Y <input type="checkbox"/> N All dentures, partial dental plates, etc. <input type="checkbox"/> Y <input type="checkbox"/> N Pocket knife, firearm <input type="checkbox"/> Y <input type="checkbox"/> N Watch, pager, cell phone, credit/bank cards <input type="checkbox"/> Y <input type="checkbox"/> N Metal cards with a magnetic strip <input type="checkbox"/> Y <input type="checkbox"/> N Eyeglasses / eyeglass case <input type="checkbox"/> Y <input type="checkbox"/> N Wigs <input type="checkbox"/> Y <input type="checkbox"/> N Accessories with metallic components including zippers, buttons, belts, shoes <input type="checkbox"/> Y <input type="checkbox"/> N Bra, any type <input type="checkbox"/> Y <input type="checkbox"/> N Metallic objects from your pockets <input type="checkbox"/> Y <input type="checkbox"/> N Any other type of metallic items <input type="checkbox"/> Y <input type="checkbox"/> N In gown/scrubs and all clothing removed except underwear</p>	
<p>VASCULAR:</p> <p><input type="checkbox"/> Y <input type="checkbox"/> N Any type of clip, coil, filter, stent <input type="checkbox"/> Y <input type="checkbox"/> N Artificial heart valve <input type="checkbox"/> Y <input type="checkbox"/> N Brain or Spine clips</p>	
<p>SURGICAL:</p> <p><input type="checkbox"/> Y <input type="checkbox"/> N Artificial limb or joint <input type="checkbox"/> Y <input type="checkbox"/> N Rods, plates, pins, screws, nails, wires <input type="checkbox"/> Y <input type="checkbox"/> N Metal mesh, clip or staple <input type="checkbox"/> Y <input type="checkbox"/> N IV access port, Broviac, PICC, Port-a-cath <input type="checkbox"/> Y <input type="checkbox"/> N Penile implants <input type="checkbox"/> Y <input type="checkbox"/> N Artificial eye / eyelid spring / eye prosthesis <input type="checkbox"/> Y <input type="checkbox"/> N Any other type of implanted item <input type="checkbox"/> Y <input type="checkbox"/> N Trach - any wire in shaft <input type="checkbox"/> Y <input type="checkbox"/> N Dental Braces <input type="checkbox"/> Y <input type="checkbox"/> N Pregnant LMP: _____</p>	
<p>DEVICES:</p> <p><input type="checkbox"/> Y <input type="checkbox"/> N Cardiac pacemaker/defibrillator <input type="checkbox"/> Y <input type="checkbox"/> N Neurostimulator (Tens Unit) <input type="checkbox"/> Y <input type="checkbox"/> N Implanted drug pump (Insulin, Baclofen) <input type="checkbox"/> Y <input type="checkbox"/> N Internal/External electrodes or wires <input type="checkbox"/> Y <input type="checkbox"/> N Hearing aids/ Inner ear prostheses/implants <input type="checkbox"/> Y <input type="checkbox"/> N Ventricular (VP) Shunt <input type="checkbox"/> Y <input type="checkbox"/> N Ingestibles (PiCari, SmartPhl, etc)</p>	
<p>Attest that the above information is correct to the best of my knowledge.</p> <p>Patient/Parent/Guardian signature _____ Date: _____</p> <p>Staff signature _____ Date: _____</p> <p>Staff print name _____</p> <p>Staff signature _____ Date: _____</p> <p>Staff print name _____</p>	
<p>Pre-Scan - Visual Patient Check:</p> <p><input type="checkbox"/> Y <input type="checkbox"/> N Arm board replaced with non-metal <input type="checkbox"/> Y <input type="checkbox"/> N All wires removed <input type="checkbox"/> Y <input type="checkbox"/> N Metal clips and twists are removed <input type="checkbox"/> Y <input type="checkbox"/> N Medication patch</p>	
<p>FINAL RAD CHECK "TIME OUT/ALL SAFE"</p> <p>Staff, Patient & Equipment have been inspected for safety and checked for loose metal objects, ECG wires, tubing, cables and MR safety designation etc.</p> <p>MD/AA: _____</p> <p>RN: _____</p> <p>Res. Therapist: _____</p> <p>Resp. Equip. Battery Setting _____</p>	
<p>"Pt. prepared to enter Zone 3"</p> <p>MRI RT: _____</p> <p>"I have verified ALL circled items"</p>	
<p>Ht: _____ cm Wt: _____ kg</p> <p>Rev: 2/20/2019</p>	

MRI Bioeffects, Safety, and Patient Management 789

Figure 3. Children's National Hospital MRI safety screening form used for visitors. (Image provided courtesy of Children's National Hospital.)

<p style="text-align: center;"><i>Children's National</i></p> <p style="text-align: center;">MRI HAZARD</p> <p style="text-align: center;">CHECKLIST/SCREENING FOR ALL NON-MR STAFF ENTERING ZONES 3 and 4.</p> <p>1) CN Staff visiting MRI 2) Parent / Guardian 3) Visitors to MRI</p> <p>Please consult the MR staff if you have any questions or concerns BEFORE you enter ZONE 3.</p> <p>I attest that the responses are correct to the best of my knowledge. I have read and understand the entire contents of this form, and I have had the opportunity to ask questions regarding the information on this form.</p>	<p>Certain metallic, electronic, magnetic or mechanical implants, devices or objects may be hazardous to you in the MR environment. Do not enter the MR environment if you have questions or concerns regarding implants or any other device or medical equipment.</p> <p>You must provide a Yes or No response for every item.</p> <p>DEVICES:</p> <p><input type="checkbox"/> Yes <input type="checkbox"/> No Cardiac pacemaker <input type="checkbox"/> Yes <input type="checkbox"/> No Defibrillator (ICD) <input type="checkbox"/> Yes <input type="checkbox"/> No Neurostimulator <input type="checkbox"/> Yes <input type="checkbox"/> No Programmable shunt <input type="checkbox"/> Yes <input type="checkbox"/> No Insulin or Infusion pump <input type="checkbox"/> Yes <input type="checkbox"/> No Hearing aids <input type="checkbox"/> Yes <input type="checkbox"/> No Inner ear prosthesis, aids <input type="checkbox"/> Yes <input type="checkbox"/> No Any other type of implant <input type="checkbox"/> Yes <input type="checkbox"/> No Any other device: Specify type: _____</p> <p>SURGICAL:</p> <p><input type="checkbox"/> Yes <input type="checkbox"/> No Joint replacements / prosthesis <input type="checkbox"/> Yes <input type="checkbox"/> No Aneurysm clip <input type="checkbox"/> Yes <input type="checkbox"/> No Pacing Wires <input type="checkbox"/> Yes <input type="checkbox"/> No Heart Valve</p> <p>OTHER/Ingestibles:</p> <p><input type="checkbox"/> Yes <input type="checkbox"/> No Pregnant <input type="checkbox"/> Yes <input type="checkbox"/> No Shrapnel/eye sliver <input type="checkbox"/> Yes <input type="checkbox"/> No Any other metals: Specify type: _____</p> <p>The following items have been removed: <input type="checkbox"/> Yes <input type="checkbox"/> No Bobby pins / hairpins / barrettes <input type="checkbox"/> Yes <input type="checkbox"/> No Penis, watch <input type="checkbox"/> Yes <input type="checkbox"/> No Keys, firearm <input type="checkbox"/> Yes <input type="checkbox"/> No Wallet / money clip / coins credit cards, bank cards <input type="checkbox"/> Yes <input type="checkbox"/> No Jewelry (necklace, earrings) <input type="checkbox"/> Yes <input type="checkbox"/> No Eyeglasses / eyeglass case <input type="checkbox"/> Yes <input type="checkbox"/> No Belt, clip on suspenders <input type="checkbox"/> Yes <input type="checkbox"/> No Stethoscope <input type="checkbox"/> Yes <input type="checkbox"/> No Pager <input type="checkbox"/> Yes <input type="checkbox"/> No Mobile / cell phone <input type="checkbox"/> Yes <input type="checkbox"/> No Scissors / Clamps <input type="checkbox"/> Yes <input type="checkbox"/> No Safety pins <input type="checkbox"/> Yes <input type="checkbox"/> No ID Badge (with metal clips) <input type="checkbox"/> Yes <input type="checkbox"/> No ASCOM Phone <input type="checkbox"/> Yes <input type="checkbox"/> No Any other magnetic item Specify type: _____</p> <p>Please print: Parent or Guardian signature: _____ Date: _____ / _____ / _____ CNStaff / Visitors signature: _____ Date: _____ / _____ / _____ MR Staff signature: _____ Date: _____ / _____ / _____</p> <p style="text-align: right;">REV: 2/20/2019</p>
---	---

Figure 4. Children's National Hospital's MRI safety screening form used for Neonatal Intensive Care Unit patients. (Image provided courtesy of Children's National Hospital.)

<p style="text-align: center;"> Children's National</p> <p>MRI HAZARD RESEARCH INCUBATOR / "Onesies" PATIENT CHECKLIST / SCREENING</p> <p><input type="checkbox"/> Yes Any surgeries If Yes, contact Deena Brooks, MR Lead Tech at 202-476-3865 Or MR Bearisation Tech at 202-476-2927 And Fax to this form to 202-476-2532</p> <p>DEVICES: <input type="checkbox"/> Yes <input type="checkbox"/> No Cardiac pacemaker / Defibrillator <input type="checkbox"/> Yes <input type="checkbox"/> No Neurostimulator (Tens-Unit) <input type="checkbox"/> Yes <input type="checkbox"/> No Implanted drug pump (Insulin, Radofen) <input type="checkbox"/> Yes <input type="checkbox"/> No Internal / External electrodes or wires <input type="checkbox"/> Yes <input type="checkbox"/> No Hearing aids / Inner ear prosthesis / implants <input type="checkbox"/> Yes <input type="checkbox"/> No Ventricular (VP) Shunt If yes: <input type="checkbox"/> Yes Programmable <input type="checkbox"/> No Non-Programmable</p> <p>SURGICAL: <input type="checkbox"/> Yes <input type="checkbox"/> No Rods, plates, pins, screws, nails, wires <input type="checkbox"/> Yes <input type="checkbox"/> No Metal mesh, clip or staple <input type="checkbox"/> Yes <input type="checkbox"/> No Silver wound dressing <input type="checkbox"/> Yes <input type="checkbox"/> No IV access port: Brovatec, PICC, Port-a-Cath <input type="checkbox"/> Yes <input type="checkbox"/> No Feeding Tubes, Any type <input type="checkbox"/> Yes <input type="checkbox"/> No Any other type of implanted item <input type="checkbox"/> Yes <input type="checkbox"/> No Trach – any wire shaft</p> <p>VASCULAR: <input type="checkbox"/> Yes <input type="checkbox"/> No Any type of clip, coil, filter, stent <input type="checkbox"/> Yes <input type="checkbox"/> No Artificial Heart Valve <input type="checkbox"/> Yes <input type="checkbox"/> No Brain or Spine clips <input type="checkbox"/> Yes <input type="checkbox"/> No Other Specify: _____</p> <p>I have been made aware that some items can be harmful to the patient during their MR scan and may interfere with a MR examination. I have reviewed and attest that the above information is correct to the best of my knowledge.</p> <p>Physician's signature / Print : _____ Date: _____ Time: _____ Bedside RN / Print : _____ Date: _____ Time: _____</p> <p style="text-align: center;"></p>	<p>FINAL RAD CHECK Staff, Patient & Equipment have been inspected for safety and checked for loose metal objects, ECG wires, tubing, cables and MR safety designation etc.</p> <p>Research Coordinator: _____ RN: _____ Resp. Therapist: _____ Resp. Equip. Battery Setting: _____</p> <p>Once signed, I acknowledge that the patient checklist screening form has been completed and signed by a physician and registered nurse. I verified with the research team that all patient checkpoints have been completed.</p> <p>MR RT: _____</p> <p>Patient Checkpoints VERIFIED:</p> <table border="1" style="width: 100%; border-collapse: collapse;"> <tr> <td>Neotrode leads and wires are removed</td> <td>_____</td> </tr> <tr> <td>All jewelry, hair accessories, and clothing with metallic components removed</td> <td>_____</td> </tr> <tr> <td>Pulse Ox on foot with ID band in place with foot exposed</td> <td>_____</td> </tr> <tr> <td>Ear wax and Ear muffs in place</td> <td>_____</td> </tr> <tr> <td>Medication patches are removed</td> <td>_____</td> </tr> <tr> <td>Arm board replaced with non-metal armboard</td> <td>_____</td> </tr> <tr> <td>Blanket roll or pads in place to prevent skin to skin contact</td> <td>_____</td> </tr> <tr> <td>Any type of metal clamps, clips are removed</td> <td>_____</td> </tr> <tr> <td>RN: _____ Date: _____</td> <td>_____</td> </tr> <tr> <td>RN: _____ Date: _____</td> <td>_____</td> </tr> </table> <p style="text-align: center;">PATIENT LABEL</p>	Neotrode leads and wires are removed	_____	All jewelry, hair accessories, and clothing with metallic components removed	_____	Pulse Ox on foot with ID band in place with foot exposed	_____	Ear wax and Ear muffs in place	_____	Medication patches are removed	_____	Arm board replaced with non-metal armboard	_____	Blanket roll or pads in place to prevent skin to skin contact	_____	Any type of metal clamps, clips are removed	_____	RN: _____ Date: _____	_____	RN: _____ Date: _____	_____
Neotrode leads and wires are removed	_____																				
All jewelry, hair accessories, and clothing with metallic components removed	_____																				
Pulse Ox on foot with ID band in place with foot exposed	_____																				
Ear wax and Ear muffs in place	_____																				
Medication patches are removed	_____																				
Arm board replaced with non-metal armboard	_____																				
Blanket roll or pads in place to prevent skin to skin contact	_____																				
Any type of metal clamps, clips are removed	_____																				
RN: _____ Date: _____	_____																				
RN: _____ Date: _____	_____																				

790 MRI Policies and Procedures for a Children's Hospital Setting

implant or device, this information should be documented with respect to the name, model, and any warnings that may exist. Ideally, information for an implant or device should be entered in the departmental or Hospital Information System. The patient should then be approved to be scheduled for the MRI examination. Upon arrival to the MRI department, the patient should be screened again by an MRI technologist - once in the department and then again at the final "Time Out and Visual Check" procedure, described below. This is a four-step process that includes:

- (1) Proper identification of the patient and the MRI examination
 - a. Verify that the correct patient information is present, utilizing two patient identifiers as suggested in The Joint Commission's goals (i.e., name, date of birth, medical record number, etc.).
 - b. Verify that the correct examination will be performed and that the correct body part will undergo the MRI exam.
- (2) Review of the MRI screening form
 - a. Review the screening form to ensure that all questions and concerns have been addressed.
- (3) Visual inspection of ancillary staff
 - a. Ensure that staff members remove jackets and other clothing articles that may conceal ferromagnetic or other potentially problematic objects (e.g., cell phones, beepers, etc.).
 - b. All pockets are to be squeezed, not simply patted down, to identify unwanted objects.
- (4) Visual check of equipment and patient
 - a. For the patient, lift blankets, sheets, and gowns to look for ferromagnetic items or other unsafe objects.
 - b. Confirm that the wheelchair or stretcher is MR Safe or MR Conditional and labeled, accordingly.
 - c. Confirm that oxygen tanks, IV poles, and all similar patient support devices are acceptable for use in the MR system room.

MRI Screening Process for Out-Patients. The MRI screening process is different for the out-patient population. At the time of scheduling, the parent (or patient, as appropriate) should be questioned in regards to potential MRI safety issues. If there is a concern, the MRI safety group member (i.e., a designated MRI technologist whose responsibility it is to investigate implants, devices, or safety issues before the patient arrives to the MRI facility) should be contacted via phone or email. All details of the investigation should be documented as part of the scheduled visit.

A preliminary MRI screening procedure is ideally performed before the patient arrives for the appointment, but if this does not occur during this time, then it can be conducted on the day the patient arrives and before the next screening step is performed. In order to facilitate this process, the MRI technologist may evaluate the following:

- Review the most recent X-rays and report for implants or devices.
- Review medical documentation in the institution's Information System for the presence of implants or devices.

On the day the appointment is scheduled, the patient should be prescreened and, upon arrival, a more in-depth documented screening process should be conducted to ensure that

the patient is safe to have the MRI exam. Once the patient is ready for the MRI procedure, an official “Time Out and Visual Check” procedure should be performed prior to entry into the MR system room.

PROTECTION FROM ACOUSTIC NOISE

Acoustic noise can pose a threat to a child’s psychological and physical health. Therefore, the use of proper hearing protection in pediatric patients is an important part of ensuring safety. Modern-day MR systems can generate acoustic noise from 78- to 130-decibels or higher depending on the pulse sequence and other factors. While certain scanners may have reduced the maximal acoustic noise levels to 90-decibels, it is still recommended that all patients utilize hearing protection. In addition, healthcare workers who remain in the MR system room during the MRI exam should likewise wear hearing protection.

Hearing protection is utilized to minimize the risk of hearing impairment in association with MRI. Special noise attenuation devices may be used (e.g., MiniMuffs (Natus Medical, Seattle, WA) for neonates and young infants (**Figure 5**). These devices may be used in conjunction with soft ear putty (silicone-based and/or beeswax). Additional protection such as using positioning sponges (i.e., the ones provided with the MR system’s head RF coil) will help prevent acoustic noise-related problems for pediatric patients. The combination of MiniMuffs and ear putty is advantageous over other types of earplugs because they provide the best type of noise reduction and help to avoid the difficulty of inserting earplugs into relatively small ear canals. This strategy also prevents the possibility of small children swallowing or choking on tiny earplugs.

Figure 5. MiniMuffs (Natus Medical, Seattle, WA) noise attenuation devices that are used to protect hearing in pediatric patients undergoing MRI examinations.



792 MRI Policies and Procedures for a Children's Hospital Setting

MRI SAFETY ISSUES RELATED TO THERMOREGULATION IN PEDIATRIC PATIENTS

Thermoregulation is the ability to maintain body temperature independent of the outside environment. Infants rely on their mothers to regulate their temperatures *in utero*. Once born, the infant has a somewhat limited ability to regulate body temperature in response to exposure to cold environments primarily due to the inability to shiver. While an infant can sweat, only the glands in the head, neck, hands and feet are active (i.e., approximately 25 to 30% of their total body size) (18-25). To keep warm, a baby may try to curl up into the fetal position, move, or cry. However, a baby's main source of heat production is the special type body fat, known as brown adipose tissue (BAT). BAT starts developing at 26 to 30 weeks of gestation and makes up about 2 to 7% of the baby's total body weight at birth. BAT is similar to the fat tissue found in hibernating animals.

BAT plays an important role in providing body heat for the infant. Unfortunately, a disadvantage of using BAT to stay warm is that the metabolism associated with utilizing this type of fat to produce heat requires extra oxygen and glucose. This can result in the newborn becoming physically stressed, as the infant attempts to maintain a proper body temperature. If allowed to become too cold (the baby's temperature should be never be lower than 36°C), the infant may be reluctant to feed in an effort to conserve energy, thus, compounding the problem (21-25).

Importantly, procedures should be in place to ensure that a newborn's temperature is maintained at an acceptable level throughout the MRI examination. Once a patient from the neonatal intensive care unit (NICU) is ready to travel to the MRI facility, a checklist composed of three sections should be used for: (1) Pre-Study, (2) Arrival at the MRI facility, and (3) Post-Scan Instructions.

Pre-Study

This checklist is followed in the NICU and before arrival to the MRI facility:

- A decision is made regarding how to keep the patient still and comfortable during the MRI exam. The choices are sedation or feeding combined with an immobilization technique.
- A pre-study body temperature should be recorded to determine if it is safe to take the infant out of the NICU environment.
- If the infant's temperature is less than 36.5°C axially, the MRI exam must be approved by the attending physician.

If the baby is approved to travel to the MRI facility, certain items must come with the patient, including those items required for traveling (e.g., items needed to care for the patient outside of the NICU) as well as the items specific to the MRI environment. The following must be considered:

- Confirmation that the MRI screening form has been appropriately completed and sent to the MRI facility.
- The infant should be placed in clothing with no snaps (hospital issued clothing only).
- Confirmation that there is a need for extra intravenous tubing for patients on IV infusion pumps.

- If patient has a metal-based tracheostomy tube in place, it must be changed to a silicone or other MR Conditional tube before going to the MRI facility.

Arrival at MRI

- Hand-off care from the NICU staff to the MRI nursing staff
- Body temperature recorded again. If less than 36.5°C axially, the NICU attending physician should be informed to discuss sedation versus immobilization technique or cancellation of the MRI examination.
- MRI nursing staff should check for the following:
 - The hard copy of MRI screening form is available,
 - Clothing has no metallic parts (e.g., snaps, zipper, etc.),
 - Necessity for “cozy bunting” or other immobilization device,
 - Hearing protection is in place,
 - Change over or remove unsafe items such as electrodes, monitoring devices, etc., and
 - Placement of an acceptable (i.e., MR Conditional) temperature probe.

Note: If the temperature recorded using an MR Conditional temperature probe does not correlate with the axially acquired temperature, document both readings and leave the temperature probe in place for trending purposes. Furthermore, if the body temperature appears to begin a downward trend, add extra blankets and/or hot packs. If the temperature drops by 1°C during the MRI examination, the procedure should be discontinued and rescheduled. The infant must be returned to a warmed environment (Isolette and/or warming bed such as a Transwarmer) as soon as possible.

Post-Scan Instructions

- Documentation of post-scan body temperature
 - If less than 36.5°C axially, it is necessary to determine the need to transport the infant in a Transwarmer or Isolette.
 - If the infant is on oxygen delivered by a source in the MR system room, the infant should be taken off of oxygen and then transferred to oxygen delivered via an oxygen tank.
 - The infant should travel with a checklist of the above information and this checklist should be maintained at the MRI facility.

While it is important to maintain the infant’s temperature during MRI, it is equally important to review the relevant MRI procedure when utilizing an MR Conditional incubator for that purpose of ensuring that there will be no issues (**Figure 6**). Fortunately, several types of MR Conditional incubators from various manufacturers are available for use in the MRI setting. These incubators offer thermal regulation with air warming, which allows the infant’s skin temperature to be monitored at all times during transport to and from the MRI facility and throughout the MRI examination (26-28).

CONCLUSIONS

The physiology of children and adults differ and these differences can greatly impact MRI safety issues. The safety of the MRI environment for a pediatric patient relies on the proper training and education of healthcare professionals, ancillary staff, family members,

794 MRI Policies and Procedures for a Children's Hospital Setting

Figure 6. Example of an MR Conditional incubator. (Image provided courtesy of Sree Medical.)



and others (29). One component of this process involves developing and implementing specialized policies and procedures specifically for pediatric patients that are collaborative, evidence-based, and supported by the MRI Safety Committee.

ACKNOWLEDGEMENTS

I would like to thank the following individuals for their sharing of information and continuous support: Dr. Gilbert Vezina, Marjean Cefaratti, Jillian Forst, Katarina Harvey, Maggie Johnson, and Stan Frickle, Children's National Hospital; Jen McAndrews, Ralph Magee, and Phyllis K. Hendy, Children's Hospital of Philadelphia.

REFERENCES

1. SMRT Educational Seminars. MR Safety in the Pediatric MR Environment. <http://www.ismrm.org/smrt/homestudy/0803.htm>. Accessed March 2021.
2. Goske MJ, Applegate KE, Bulas D, et al. Image gently: Progress and challenges in CT education and advocacy. *Pediatric Radiology* 2011;41 Supplement 2:461-466.
3. Erondu OF. Challenges and peculiarities of paediatric imaging. *Medical Imaging in Clinical Practice*. 2012. Open access. <https://www.intechopen.com/books/medical-imaging-in-clinical-practice/challenges-and-peculiarities-of-paediatric-imaging>. Accessed March 2021.
4. Watson T. Considerations and challenges for pediatric patients in the imaging department. <https://www.tractmanager.com/resource/considerations-and-challenges-for-pediatric-patients-in-the-imaging-department>. Accessed March 2021.

MRI Bioeffects, Safety, and Patient Management 795

5. Advisory Committee. In: The Office of the United States Trade Representative. <http://www.usrt.gov/about-us/intergovernmental-affairs/advisory-committees>. Accessed March 2021.
6. Committee Types and Roles The Congressional Research Service. <http://www.judiciary.senate.gov/legislation/upload/CRS-CommitteeTypes.pdf>. Accessed March 2021.
7. The Mentoring Resource Center. Building an Effective Advisory Committee. http://educationnorthwest.org/webfm_send/232. Accessed March 2021.
8. Masaoka, J. What is an Advisory Board and Should We Have One? <https://blueavocado.org/>. Accessed March 2021.
9. Institute for Magnetic Resonance Safety, Education, and Research (IMRSER.org), MRI Safety Guidelines. <http://www.imrsr.org/PaperPDFlist.asp?pgname=Guidelines> 2012. Accessed March 2021.
10. Soriano RD. Just-in-Time Education for Intensive Care Nurses. Paper 34. https://fisherpub.sjfc.edu/nursing_etd_masters/34/. Accessed March 2021.
11. Centers for Medicaid and Medicaid Services. Quality Measures. <https://www.cms.gov/Medicare/Quality-Initiatives-Patient-Assessment-Instruments/QualityMeasures/index.html>. Accessed March 2021.
12. Baker DW, Qaseem A. Evidence-based performance measures: Preventing unintended consequences of quality measurement. Ann Intern Med 2011;155: 638–640.
13. Firbank, MJ. Quality assurance for MRI: Practical experience. Br J Radiol 2000;73:376-83.
14. Focus and Simplify. Office of Patient Safety and Quality. http://intranet.chop.edu/sites/patient_safety/focus-and-simplify/index.html. Accessed March 2021.
15. Wyer LA. Preventing error in POCT with effective policies and procedures. <https://acute caretesting.org/en/articles/preventing-error-in-poct-with-effective-policies-and-procedures>. Accessed March 2021.
16. Power DM. Writing policies and procedures best practices for law enforcement: A step by step guide. <https://www.powerdms.com/blog/writing-policies-and-procedures/> Accessed March 2021.
17. Stone DA. How to prepare a radiology policy and procedure manual. Radiol Manage 1980;2:16-20.
18. Labour and Birth. From Bellies to Babies and Beyond. <http://www.birth.com.au/Your-baby-soon-after-birth-what-you-need-to-know/Body-temperature-regulation?view=full>. Accessed March 2021.
19. Hallowell LM, Stewart SE, de Amorim e Silva CT, et al. Reviewing the process of preparing children for MRI. Pediatr Radiol 2008;38:271–79.
20. ACR Manual on MR Safety. [www.ACR.org](http://www.acr.org). Accessed March 2021.
21. Emergency Nursing World. Temperature Measurement in Acute Care: The Who, What, Where, When, Why, and How? <http://enw.org/Research-Thermometry.htm>. Accessed March 2021.
22. Healthline. Brown fat: What you should know. <https://www.healthline.com/health/brown-fat#1>. Accessed March 2021.
23. Brazier Y. Brown fat: What is it and can it help reduce obesity? <https://www.medicalnewstoday.com/articles/240989>. Accessed March 2021
24. Stephens JM. The fat controller: Adipocyte development. PLoS Biology 2012;10:e1001436.
25. Thought Co. The Purpose and Composition of Adipose Tissue. <https://www.thoughtco.com/adipose-tissue-373191>. Accessed March 2021.
26. Sree Medical Systems. Neonatal MRI Transport Incubator. <https://www.advimg.com/product/neonatal-mri-transport-incubator/>. Accessed March 2021.
27. Lane A, Chuk L, Colditz PB, Coulthard A. The MRI-compatible neonatal incubator in practice. J Paediatr Child Health 2013;49:E377-80.
28. Whitby E, Griffiths PD, Lonneker-Lammers T, et al. MRI-compatible incubator allow high-quality neonatal imaging. Ultrafast Magnetic resonance imaging of the neonate in a magnetic resonance-compatible incubator with a built-in coil. Pediatrics 2004;113:e150-e152.

796 MRI Policies and Procedures for a Children's Hospital Setting

29. Chandra T, Chavhan GB, Sze RW, et al. Practical considerations for establishing and maintaining a magnetic resonance imaging safety program in a pediatric practice. *Pediatr Radiol* 2019;49:458-468.

Chapter 30 MRI Safety Policies and Procedures for a Research Facility

ANNE MARIE SAWYER, B.S., R.T.(R)(MR), FSMRT

Instructor

Magnetic Resonance Imaging Department
Health & Wellness Division
Greenville Technical College
Charleston, SC

INTRODUCTION

Maintaining safety in the magnetic resonance imaging (MRI) environment is a never-ending challenge, whether it is part of a clinical facility or one that is restricted to research studies. There are, however, specific concerns that may only be encountered in a research facility due to the variety of individuals allowed to access the MRI environment, including those present for the development of software, hardware, and ancillary equipment. This calls for specific policies and procedures that are vigilantly maintained by those managing and supporting MRI laboratories in the research setting.

Over the years, there appears that the number of reported MRI safety incidents is increasing. There are many theories as to why this is happening including an increase in the number of MR systems worldwide, the increase in the number of scanners with higher static magnetic fields being installed especially at research facilities, the improvement in the reporting of such incidents, the increase in the number of MR systems being installed in departments and facilities outside of the traditional radiology department, an increase in the overall number of MRI examinations performed, or possibly more incidents are actually occurring.

In consideration of the above, an investment is required to ensure that the utmost is being done to maintain safety for patients and volunteer subjects, researchers, faculty and staff members. Understanding this investment requires both time and money, paving the way for a successful MRI safety program. Importantly, it takes only one mistake for the freedom that an MRI research facility currently enjoys to be revoked. Therefore, we must act responsibly and out of concern for study subjects, patients, and staff members.

798 MRI Safety Policies and Procedures for a Research Facility

DESIGN AND ACCESS OF THE MRI ENVIRONMENT

Zones of the MRI Environment

Since the early developments of interventional or intra-operative MR systems, the areas associated with the MRI department have been divided into specific sections as a method to clearly identify which individuals and equipment are given access, and under which conditions. This was further reinforced by the American College of Radiology (ACR) document on MRI safety, first published in 2002 and updated in later years, thus, identifying and demarcating the four “zones” of an MRI department (1-6).

Basically, the four zones described by the ACR include as follows, the area typically accessed by the general public (Zone 1); the dressing room, bathroom and patient preparation room (Zone 2); control room used for MR system operation (Zone 3); and the scanner room (Zone 4). The MRI suite of rooms should include specific areas separated by locked doors using card key access or other means to control access, but not combination locks. The codes for combination locks can be easily communicated to many individuals, requiring multiple changes to maintain security.

The initial design of the MRI suite includes critical details, as follows: card key locked access from the hallway, lobby, or reception area into the MRI suite; easy visual access from the control room of the MR system room door and the path leading from the dressing room and patient preparation room towards the scanner room door; visual access from the control room into the MR system room; emergency exhaust fan controls located inside and outside of the scanner room; quench button for a superconducting magnet located immediately inside or outside of the scanner room door; and video observation of the inside of the bore of the MR system.

It may be problematic to move walls due to cost and space issues when planning to renovate an MRI suite for enhanced safety. Therefore, it is critical to focus on what can be done to ensure maximum safety through reduced and controlled access to the various areas of the MRI environment (1-6). Doors with locked access should be in place between general access areas such as main hallways, waiting rooms and reception areas (i.e., Zone 1) and Zones 2, 3, and 4. Only individuals appropriately screened and accompanied by trained MRI staff members are allowed to access the dressing room and patient preparation room (Zone 2) and the MR system room (Zone 4). Patients and volunteer subjects should never be allowed unaccompanied access past Zone 1 into Zones 2, 3 or 4, and should never be left unattended in Zones 2, 3 or 4 at any time.

Access

Policies and procedures must be in place that clearly identify which kind of access is given to each of the MRI staff members as well as MRI physicians, other healthcare professionals supporting patients or volunteers undergoing the MRI examination, clinicians, and family members. For example, technologist aides may be allowed to initially review the completed screening form with patients or volunteer subjects, and accompany them to the dressing room and give initial preparation instructions. The MRI technologist or radiographer conducts the final review of the completed screening form and accompanies the

Figure 1. An example of signs, rugs, placards, and stanchions used to warn individuals of the dangerous environment associated with the MR system room. Signs on the wall next to the MR system room door are important in the event that someone leaves the door leading into the room open because the signs on the door would then not be visible.



patient or volunteer subject into the MR system room, positions and immobilizes, and gives instructions immediately before and during the examination.

Signage

Current and appropriate signage, especially immediately before entering the MR system room (Zone 4) is an absolute requirement (1-4). Other forms of warning to individuals entering the area of the dangers of the MRI environment are also recommended. These include MRI warning rugs, stanchions, placards, or gates placed in front of the door leading into the scanner room (**Figure 1**). Frequently, something more three-dimensional or that provides a tactile experience is extremely helpful in reminding all individuals about the potential danger of entering the MR system room.

PERSONNEL

Assigned Responsibilities, Education, and Training

Depending upon the number and type of scanners present in the research facility, an adequate number of appropriate staff should be present to support the various research stud-

800 MRI Safety Policies and Procedures for a Research Facility

ies and patient examinations (1-5). This includes but is not limited to: MRI technologists/radiographers, nurses, receptionists, assistants and/or technologist aides, radiologists and/or clinicians, administrative support, and/or research associates (e.g., doctoral, Ph.D., scientists). Current policies and procedures must include the assigned level of responsibility for each staff member. This will determine the level of education and hands-on training required for each. In addition to the staff previously listed, limited but appropriate training will also need to be provided to other individuals including: housekeeping and maintenance personnel, ancillary staff (nursing, respiratory therapy, etc.), physicians, firefighters, police and security officers, and first responders. Of particular importance is for firefighting personnel that may respond to a fire or other emergency at the facility to undergo MRI safety training in order to acquaint them with the dangers of the MRI environment.

In order to properly support scientific research studies, the MRI technologists/radiographers must possess a thorough working knowledge of MRI. Using research software, hardware, radiofrequency (RF) coils, and prototype accessory devices can result in a variety of artifacts and other imaging challenges including safety. Possessing a clear understanding of the principles and physics of MRI allows the technologists/radiographers to quickly address MR system difficulties resulting in the successful completion of research studies. Competency lists are excellent tools to determine the educational needs of each staff member. At a minimum, these lists should include: anatomy and physiology; MRI physics and principles; scan parameters and imaging options; safe and appropriate use of RF coils and other ancillary equipment including physiologic monitoring systems; patient and volunteer subject preparation, instruction and communication; positioning and immobilization; sterile technique; and emergency procedures.

Ongoing education is a must in the rapidly changing world of MRI especially in the research facility. Time and financial support must be provided to ensure that all staff members maintain a comprehensive knowledge in order to competently support the research MRI studies being conducted. Continuing education can be obtained through attendance at educational seminars, completion of online webinars, and video training. Subscription to the MRI technologist society, the Section for Magnetic Resonance Radiographers and Technologists, (www.ismrm.org/smrt/) provides educational support with current knowledge shared by peers and other experts in the field. The investment in continuing education for MRI technologists/radiographers results in knowledgeable, productive healthcare professionals. Understanding MRI physics and principles are necessary to comprehend the issues in MRI safety and screening. It also clearly communicates to the staff that they are a valued part of the team resulting in responsible, interested individuals. In addition, enlisting the faculty at the research facility to use their specific expertise to provide training to the MRI technologists/radiographers provide the foundation for successful teamwork. This results in the successful completion of research studies because the staff comprehends the faculty's priorities. Both didactic and hands-on training are equally valuable in this comprehensive training program.

MRI Safety Committee

A most critical asset for a research MRI facility is that of a Safety Committee (1-5). The safety officers who sit on this committee are responsible for setting MRI safety and

screening policies and procedures. They must be afforded time and resources to maintain their MRI safety and screening expertise. The safety officers are selected from those with an advanced knowledge in MRI and MRI safety. To ensure comprehensive safety support, the committee should include an MRI technologist/radiographer, a radiologist or MRI clinician, and an MRI scientist (e.g., typically a doctoral level person, Ph.D.). The MRI technologist/radiographer and radiologist/MRI clinician are primarily responsible for making all decisions concerning MRI pre-procedure screening of patients, volunteer subjects and researchers. The MRI scientist provides the expert understanding of hardware and software necessary for comprehensive decision-making.

Research MRI Procedures Conducted by MRI Technologists

MRI research examinations that involve the administration of contrast agents, interventional procedures, the introduction of intra-cavitory coils, and patients or volunteer subjects with special concerns such as paralysis require the presence of an MRI research technologist/radiographer (2, 3, 5). Proficiency in sterile technique and intravenous (IV) set up procedures is part of the competency required by the MRI technologist/radiographer. As healthcare professionals are trained in the skills of medical procedures and patient communication, this background is extremely valuable to ensure patient comfort and safety during IV placement, positioning of the patient or volunteer subject with the IV line in place, resuscitation procedures in the event of a reaction to the IV placement or injection, extravasation issues, and/or insertion of an endo-rectal RF coil.

The IV administration of contrast media requires the presence of a minimum of two healthcare professionals. In addition to the MRI technologist, either a nurse, physician or tech aide is required to ensure safety for the patient or volunteer subject during IV placement. If the patient should suddenly lose consciousness, it will require two trained healthcare professionals to safely and successfully address the situation (i.e., to slowly lower the subject's head to the same level as the body while maintaining control over the IV site). A physician trained in emergent care is required to be present in the MRI suite during the injection of the contrast media and for a short period thereafter (approximately 15 minutes) to ensure there are no resulting reactions or complications (1, 2).

It is also extremely beneficial that an MRI technologist/radiographer be present for more complex animal model research studies. In addition to the operation of the MR system, this individual's responsibility includes maintaining a safe environment for people and equipment. Research studies commonly involve multiple individuals (researchers, clinicians, surgeons, veterinarians, and veterinary technicians) who are present in the MRI environment but engaged in their specific roles, focusing on their particular research needs and outcomes of the research study. In addition to protecting the many individuals working in the research study, the MRI technologist/radiographer is responsible for preventing expensive damage to the MR system and maintaining cleanliness standards required for human MRI examinations (patients and volunteer subjects) following the animal model study.

MRI Procedures Conducted by Researchers

Researchers may be allowed to conduct research studies on phantoms and human subjects without an MRI technologist/radiographer present. The researchers must first complete

802 MRI Safety Policies and Procedures for a Research Facility

their requirements for MR system access and use, including MRI safety and policy and procedure training, hands-on scanner training, RF coil training, and Health Insurance Portability and Accountability Act (HIPAA) training (3, 4, 7). In addition, it is policy that any scanner equipment or accessory issues, or human subject screening question issues be reported immediately to the appropriate support staff or the MRI Safety Committee for resolution.

During weekdays (e.g., 7:00 am to 6:00 pm), a minimum of two safety-trained researchers should be present for all scans on human subjects including normal, healthy volunteers, as well as patients. To ensure safety and fulfill the ability to manage any emergent situation involving a human subject such as a loss of consciousness, seizure, or other serious event, a minimum of two safety-trained researchers should be required to be present for all evening, night and weekend scans being conducted (5). This is further discussed below in emergent cradle/table operation.

All new MRI accessories, equipment, devices, RF coils, furniture, and patient support equipment are required to be reviewed by the MRI Manager (MRI technologist/radiographer on the Safety Committee) before being taken into the MR system room. If the device has an electronic component, then it must undergo comprehensive testing to ensure that it does not contribute noise (i.e., electromagnetic interference) to the images or other data being acquired (8).

Imaging accessories, devices, and RF coils are often designed and developed as a prototype for use during research MRI examinations. In addition, these same prototype components may be purchased from third party vendors. If an investigational device is a “non-significant risk device”, an investigator does not need to submit an investigational device exemption (IDE), the IDE will be “considered approved” under Food and Drug Administration (FDA) regulations. Such devices do not have to comply with FDA premarket approval and performance standards prior to use in research studies (9). To ensure safety for the patients and volunteer subjects as well as the MR system, and to ensure that it will function properly with the scanner in use, early contact with the members of the MRI Safety Committee is recommended to prevent inappropriate designs that could result in costly mistakes, wasted resources, and/or potential safety issues.

Other Personnel Responsibilities

It is recommended that an MRI technologist/radiographer or technologist aide complete stocking responsibilities in the MR system suite to ensure the medical supplies present are not only correct, but also not expired when they are needed. This is not something that should be delegated to an individual (e.g. student, etc.) who is not a health care professional. Along with sterile technique, the importance of cleanliness in the medical imaging environment is stressed during didactic and hands-on training to ensure human subject safety as long-term consequences can prevail without this. Maintenance and stocking of the crash cart located in the MRI suite is required to be conducted by a healthcare professional, either MRI technologist/radiographer or nurse due to the presence of drugs.

An important part in maintaining patient and volunteer subject safety is routine monthly preventative maintenance conducted by the MR system manufacturer field service engineer. In addition to poor image quality, poorly maintained scanners can result in serious patient

injuries (e.g., burns). Frayed cables of RF coils or monitoring equipment cables and/or fractured housing on RF coils or connector boxes are just a few potentially dangerous scenarios if left unrepaired.

In addition, routine preventative maintenance of all ancillary equipment directly involved with human MRI examinations must be performed annually, at a minimum. This includes automatic injectors, infusion devices, and physiologic monitoring equipment to ensure that compromised function of any equipment does not affect the patient or volunteer subject.

MRI SAFETY: POLICY AND PROCEDURE TRAINING

To access and/or use any of the research MR system, completion of an initial MRI Safety Policy and Procedure Training conducted by the MRI Manager (e.g., MRI technologist/radiographer member of Safety Committee) is required. All researchers are required to complete this training despite any previous experience working on or around scanners at other facilities, either clinical or research. Typically, this review is a 90-minute comprehensive yet interactive presentation that includes all aspects of MRI safety and human subject screening, in addition to covering the research facility's policies and procedures. Annually, each of the approved researchers is required to complete an online renewal that is similar to the initial training but includes quizzes spaced throughout the tutorial. It also includes completion of the MRI pre-procedure screening form. The results of each completed quiz are automatically emailed to the members of the MRI Safety Committee and registered in a database.

A commitment for a minimum of six months use of the research MR system is required by researchers to attend the initial MRI Safety Policy and Procedure Training and to subsequently be given access to the scanners. If a researcher has completed this training and then is absent from conducting or participating in research scans for a period of three months or longer, completion of the online version of the MRI Safety and Policy and Procedure Training is required prior to accessing the MR systems. A database should be maintained with all of the trained researchers' names and contact information that allows automatic reminders to be sent instructing them to take the required annual training, and automatic removal from accessing the scanners if the training is not completed within a designated time period. Other databases are maintained for the purpose of distribution of information to researchers.

The presence of a whole body 7 Tesla (T) scanner highlights the need for an additional and highly specific MRI safety training (6). This focuses on the challenges present in working around such a high static magnetic field and spatial gradient magnetic field (dB/dx) in Zone 4 (the scanner room), the fringe fields present in Zones 2 and 3, and increased specific absorption rate (SAR) associated with MRI-related heating for researchers, patients, and volunteer subjects. Currently, at most facilities housing high field strength MR systems such as 1.5 T or 3 T, the five-Gauss line is contained within the scanner room. However, the fringe field present in the control room, equipment room, or other nearby rooms of a research 7 T scanner may exceed 100 Gauss. Thus, careful thought must be given to the type of access allowed to each individual and specifically where the MRI pre-procedure screen-

804 MRI Safety Policies and Procedures for a Research Facility

ing form is completed by a patient or volunteer subject in order to prevent any inappropriate access.

All researchers are provided cards to carry that contain the names and phone numbers of the individuals who support their research studies being conducted at the scanners. This includes the MRI Safety Committee members, MRI research technologists/radiographers, and the building manager. The cards also include the phone numbers for each of the MR system suite, security services, and the local law enforcement agencies.

MR SYSTEM TRAINING

After completion of the initial MRI Safety Policy and Procedure Training, each researcher undergoes additional required training at the scanner with an MRI research technologist/radiographer. This hands-on training includes emergent MR system cradle and table removal, location and operation of the quench button and exhaust fan, safe and appropriate use of RF coils, presence and operation of research devices, insulation and separation of the human subject using positioning pads and sponges (to prevent excessive heating and possible burns), room temperature and operation of the scanner's bore fan, research support equipment and accessories, scanner software, and support information (3, 5, 7). An important policy for all those accessing the MRI suites is to keep the scanner room (Zone 4) door closed at all times. A scanner room door should only be allowed to remain open if an MRI safety-trained individual is actively monitoring all equipment and persons attempting to pass through.

Emergent MR System Cradle and Table Removal

In the event of a suddenly unconscious or unresponsive patient or volunteer subject, researchers must be fully trained in the safe removal of the individual from the MR system and the room (Zone 4), into the patient preparation room (Zone 2) prior to the arrival of paramedics or other resuscitation (code blue) team members. Emergent care of the patient or volunteer subject must never be conducted within the scanner room due to the unmonitored devices carried and used by first responders to revive the subject and the time required to properly complete screening procedures for those individuals (3, 5, 7). This requires the utmost preparation and speed to complete certain procedures prior to the arrival of the resuscitation team or first responders. Practice sessions should be conducted on a regular basis (e.g., bi-annually) by all MRI technologists/radiographers to ensure their proficiency in the procedures.

The number of researchers required to be present for MRI examinations conducted on human subjects, whether patients or normal volunteers, is determined by the day and time of the examination. MRI studies conducted in the evening (after 6:00 pm), early morning (12:00 am to 7:00 am), and weekends require a minimum of two researchers to be present (5). This is to ensure the necessary emergent procedures can be completed successfully in the event of a safety issue with the patient or volunteer subject. Even if only "normal, healthy" volunteer subjects are being scanned, there is always a risk, albeit small, that these individuals could experience a stroke, heart attack or syncope. Being thoroughly prepared for this type of situation demonstrates to university officials that the researchers conducting

MRI examinations are as prepared as any clinical facility to adequately deal with any human frailties. Importantly, these training and preparation procedures can successfully prevent liability for the academic institution.

Quench Button and Exhaust Fan

The location and operation of the quench button and exhaust fans are also part of the comprehensive MR system training for researchers. In the event an individual would be pinned against the scanner requiring release of the magnetic field of a superconducting magnet to prevent further injury or death, researchers must be fully trained as to when quenching is necessary and when it is not (5). In addition, all of the potential resulting issues from a quench should be addressed in proper training including the formation of a helium cloud in the MR system room, failure of an exhaust fan that may prevent the opening of the door to the scanner room, and liquid helium dripping from the cryogen exhaust pipe. Training in the operation of the quench button should only be given to appropriate researchers, never to housekeeping or maintenance personnel. Instructions that clearly and quickly direct researchers on quench procedures are posted in convenient locations in the MRI suite.

Safe and Appropriate Use of RF Coils

Instruction in the safe and appropriate use of RF coils specific to each research study is given to all researchers. This instruction in the prevention of potential risks associated with RF coils includes the operation and safe utilization of these devices, and correct RF coil selection in the MR system software. Basic knowledge is reviewed in the appropriate use for specific anatomy, positioning of the RF coil as well as the associated cable and connector box, and immobilization of the coil relative to the human subject. Additionally, training should encompass the prevention of cables coiling upon themselves and preventing the cables coming into contact with other cables, devices, human subjects and/or the bore of the scanner (1-3, 5-7, 10). First-time use of any RF coil at the research facility requires training by the MRI Manager (MRI technologist on Safety Committee), MRI research technologist/radiographer, or Scientific Center Director (Ph.D. on the MRI Safety Committee).

All RF coils and devices should be thoroughly checked before use in any MRI examination for signs of damage including fraying cables, cracked housing and/or loose contents in the coils or connector boxes in order to prevent risk of burns to the patient or volunteer subject, or damage to the scanner. RF coils used to image anatomy other than its designated use must be referred to the MRI Manager or MRI research technologist/radiographer for approval. For example, wrapping a cardiac RF coil around an elbow and positioning it next to the MR system's bore is a mistake that could easily result in injury to the patient and/or hardware. Imaging pediatric brains using a knee coil may be an acceptable alternative to the indicated anatomy for that coil, and should not result in any potential dangers for the patient or scanners as long as proper padding (insulation) is provided to prevent contact between skin and the coil housing.

Presence of Research Devices

Research MRI examinations may involve additional devices to be placed in the magnet with the patient or volunteer subject, or in the MR system room. This is especially true of

806 MRI Safety Policies and Procedures for a Research Facility

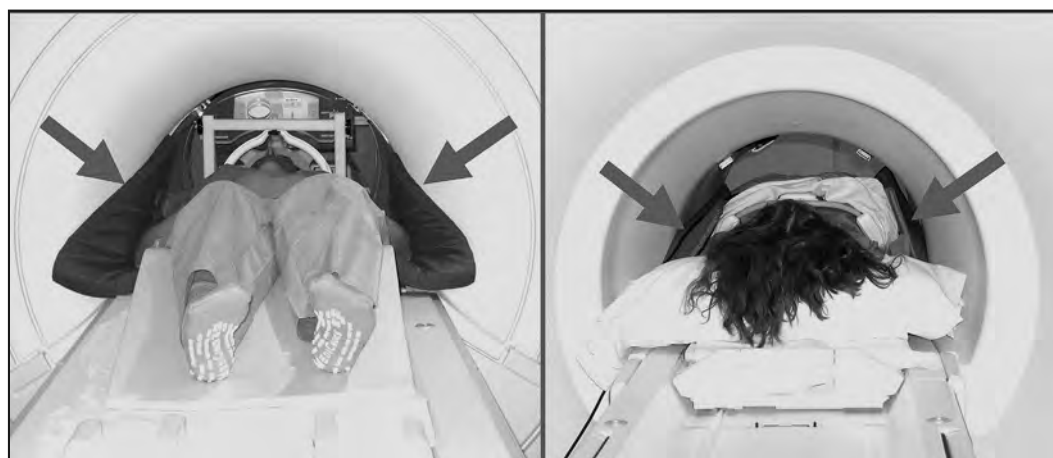
functional MRI (fMRI) research studies, motion tracking studies, and focused ultrasound (FUS) treatments guided by MRI. Some of these devices include response boxes and cables, electroencephalography (EEG) cap and cables, transmagnetic stimulation (TMS) coils and cables, eye tracker video camera and cables, thermode (provides heat for pain stimulation) and cables, plethysmograph sensor (or pulse oximetry) and cable, galvanic skin response (GSR/EDA), and electrocardiography (ECG) electrodes and cables. Many of these items may not have been FDA approved for use within the confines of the scanner. All prototype designs must be used with equal care as product devices to prevent loops in their cables, prevent loops with other devices present and their cables, and prevent secondary interaction with the human subject and the MR system's bore (1-3, 5, 7, 10).

Insulation and Separation using Positioning Pads and Sponges

Positioning sponges and pads in multiple sizes and shapes should be available in the MR system room for immobilization and to provide comfort to the patient or volunteer subject. In addition, the sponges and pads provide the necessary separation and insulation for all cables and devices to prevent areas of excessive heating to the patient or volunteer subject and/or damage to the scanner (1-3, 5, 7, 10, 11). This includes critical insulation between human anatomy and the bore walls and ceiling of the MR system. The necessary insulation space between cables and devices, between cables, devices and the human subject, and between cables, devices and the MR system's bore must be a minimum of 1 cm (11).

In any scan in which the RF is transmitted by the body coil that is housed within the cover (shroud) of the scanner, the risk for inducing a substantial current is greater as a larger area is exposed versus that of a much smaller transmit-receive head RF coil or knee RF coil (1-3, 5, 7, 10). Many RF coils in use are receive-only in which the body RF coil is used for the transmission part of the MRI scans. These receive-only RF coils are not only used to image large anatomical areas such as the chest, abdomen and pelvis, they may also be

Figure 2. An example of placement of sponges or pads between the volunteer subject and the bore of the MR system to prevent possible heating issues related to direct contact between the subject's tissue and the transmit RF body coil.



smaller coils designed to image the brain, knee, or wrist but still utilize the much larger RF body coil to perform the RF transmission. Therefore, it is critically important for the researchers to clearly understand how the RF coil they are using operates to ensure necessary insulation is provided for the human volunteer subject or patient, coils, cables and devices present in the bore of the MR system.

If there is not 1 cm of insulation guaranteed and maintained using pads and sponges between the subject's arms, chest or abdomen and the bore of the scanner, the patient or volunteer should not be scanned because the risk of heating and subsequent burns is far too great due to the electrical fields present. Faulty RF coils including the body RF coil can also be the cause of burns. Positioning sponges or pads between the subject's arms and other body parts that come into close proximity to the bore walls is, therefore, a requirement for all imaging that utilizes the body coil to transmit the RF energy (**Figure 2**). The cost of positioning sponges and pads for use in the MRI environment is expensive, especially those that are durable, and maintain their position without slipping. However, the issues surrounding the burn of a patient or volunteer subject in the MRI environment results in a far greater financial liability.

Room Temperature and Bore Fan Operation

Understanding the potential issues with ambient room temperature is another topic to be reviewed with all researchers. The MR system room temperature should not exceed 68°F (20° C) given the speed in which the temperature may increase in the MR system's bore and subsequently, the scanner room, due to rapid imaging sequences with multiple RF pulses.

The operation of the scanner's fan is to be used to prevent an increase of temperature inside the bore and to maintain patient and volunteer subject comfort during the procedure (1-3, 5, 7, 10). It is recommended that patients and volunteer subjects not be exposed to extreme heat or any situation that challenges their innate ability to regulate their body temperature during MRI examinations. This is especially important for patients compromised by disease or those receiving medications known to impact thermoregulatory function.

Research Support Equipment and Accessories

Non-magnetic carts are available in all of the MRI suites to allow easy transport of the larger RF coils, IV and contrast media supplies, and various supplies and equipment employed in the research MRI examinations. Before moving any non-magnetic carts into the MR system room, the researchers are required to check all shelves for any potential metallic projectiles. These carts or shelves do not have drawers or cupboard doors in order to prevent the accidental introduction of hidden projectiles.

A wide variety of support equipment and accessories are available in the MRI setting and MR system room, and all must be verified to be "conditionally safe" (i.e., MR Conditional) to use. Audio systems, projectors, mirror systems, and screen-mirror combinations for RF coils are available for fMRI studies. MR Conditional physiologic monitoring systems are available that provide a variety of data including heart rate, electrocardiography (ECG or EKG), oxygen saturation, end tidal carbon dioxide (i.e., to assess respiratory rate), body

808 MRI Safety Policies and Procedures for a Research Facility

temperature, non-invasive blood pressure, invasive blood pressure, and automatic identification of anesthesia agent(s). Water blankets for body temperature maintenance are also available for animal model MRI examinations.

MR Safe or MR Conditional plastic chairs, step stools, aluminum IV poles, aluminum ladders, and plastic containers are available for use by researchers in the MR system room. In addition, a wide variety of accessories are available, including earplugs, earphones, disposable earphone covers, table pads and immobilization straps for human subjects and RF coils, and phantoms of various sizes and contents (water, saline, agar, peanut oil, copper sulfate, etc.).

MR System Software

Hands-on training is provided to all researchers using the scanner to ensure maximum efficiency and ultimately successful studies. Training should be tailored specifically to the type of study each individual researcher will be conducting. This will include selection of imaging sequences (research and product), scan parameters and options, graphic scan prescription, high order shimming, advanced scan control variables, post-processing, monitoring of the raw data directory, accessing the service error log, trouble-shooting system errors and artifacts, transfer and/or archival of raw and image data, completion of the online scanner problem reports, and requests for immediate support.

The researchers, technologists and radiographers operating the MR system must clearly understand the operating modes available to them in the MR system software. These modes include Normal Operating Mode, First Level Controlled Operating Mode, and Second Level Controlled Operating Mode (5). These modes typically control outputs including RF (SAR) and slew rates for time-varying, gradient magnetic fields. Other outputs may be included dependent upon the scanner's manufacturer. The Normal Operating Mode is the recommended selection for all human subject especially patients compromised by disease to ensure that none of the outputs would cause physiologic stress to the subject (5). The First Level Controlled Operating Mode should only be used in normal, healthy control subjects as the outputs may result in some physiologic stress. The Second Level Controlled Operating Mode may require a password to access and should only be used when scanning phantoms due to the potential for excess physiologic stress due to the level of outputs. Conducting MRI examinations in human subjects with the scanner operating in the Second Level Controlled Operating Mode requires approval by the Institutional Review Board (IRB).

Support for Researchers Using MR Systems

Support is provided to all researchers using the MR systems during operational hours, which, at a research MRI facility, is twenty-four hours a day, seven days a week (24/7). This support includes all aspects of MRI safety and other relevant areas including screening volunteer subjects and assisting with questions that are answered by the MRI Manager, MRI technologist, or radiologist (clinician) from the Safety Committee. The MRI Manager is on call 24/7. The radiologist/MRI clinician and research scientist (Ph.D.) from the MRI Safety Committee provide additional support 24/7.

MRI PRE-PROCEDURE SCREENING

Each research MRI facility should configure a list of basic MRI safety rules on which all researchers are encouraged to focus every time they are working in the MRI environment. These should be simple, thereby, making them easy to remember. For example:

- 1 - Make no assumptions
- 2 - Trust no one
- 3 - Ask questions
- 4 - Screen four times
- 5 - Know your RF coils
- 6 - No loops in cables or humans
- 7 - Keep the MR system room door closed and/or control access to the area
- 8 - Remain vigilant at all times (watchful and alert)

Patients and Volunteer Subjects

All patients and volunteer subjects undergoing research scans must be ambulatory (i.e., possess the ability to walk into the MR system room unassisted and climb up on to the table). If they are not fully ambulatory, the MRI Manager must be consulted to provide procedures that ensure safety for the patients and volunteer subjects, as well as for the researchers conducting the scans.

If the research facility is not licensed by the state, in-patients from any healthcare facility cannot undergo an MRI examination at that location. In addition, no scans can be conducted in which patients or volunteer subjects pay for the scans or their insurance pays for the scans.

Injection of drugs or the administration of gases to patients and volunteer subjects is not allowed at any time unless approved by the Institutional Review Board (IRB) and the members of the MRI Safety Committee at the research facility. Sedatives, sedation (full, moderate, or conscious) is not allowed unless an anesthesiologist is present for the entire examination.

Scans of human subjects are never to be conducted for health issues that are not part of an IRB-approved research study. In addition, patients and volunteer subjects are not allowed to receive complete or incomplete sets of their image data from the researchers conducting the studies. If the image data has been transferred to the picture archiving and communication system (PACS) of the affiliated medical center and an interpretation by a radiologist has been conducted, then the patient or volunteer subject can obtain their report and images through the radiology department at the medical center.

810 MRI Safety Policies and Procedures for a Research Facility

MRI Pre-Procedure Screening

Safety screening of patients and human subjects is conducted routinely before each and every MRI examination (1-5, 7). Screening is done to ensure safety upon entering the MR system room (Zone 4), entering the scanner and residing in the scanner during the examination. Potential dangers are due to the presence of the static main magnetic field (B_0), radiofrequency (RF) electromagnetic fields (B_1), and the varying gradient magnetic fields ($G_{x,y,z}$).

Metals and conductors are the main concerns as well as the sound levels attributed to the time-varying magnetic fields. Metal can exhibit one or more behaviors when exposed to an MR system. It can exhibit translational attraction, becoming a projectile (missile) by being pulled into the magnet due to the change in static main magnetic field (B_0) over distance (dB/dz); exhibit torque or rotational alignment (attempt to align with the main static magnetic field lines; heat resulting in burns to the patient or damage to the scanner; and/or generate artifacts in the images and/or raw data (1-5, 7). Translational attraction is strongest at the ends of the MR system and zero at the center, whereas torque is strongest at the center of the scanner. Due to the additional magnetic shielding added to an MR system allowing it to have a reduced fringe field, the compressed field lines of the magnet result in projectiles experiencing attraction to the sides of the scanner's bore as well as to the center of the bore in the Z-direction.

In 2005, the American Society for Testing and Materials (ASTM) International published new terminology for use in describing and labeling biomedical implants and devices as well as equipment to determine under which specific conditions that they can safely enter the MR system room and be present in the scanner during the examination. The labeling terms are MR Unsafe, MR Safe, and MR Conditional (8).

MR Unsafe describes an item that poses hazards in all MRI environments. MR Safe describes an item that poses no known hazards in all MRI environments. MR Conditional describes an item that has been demonstrated to pose no known hazards in a specified MRI environment with specified conditions of use. Field conditions that define the specified MRI environment include field strength, spatial magnetic field gradient (SFG, MSG), dB/dt or slew rate (time rate of change of the time varying gradient magnetic fields), radio frequency (RF) fields, specific absorption rate (SAR), and B_{1+RMS} . Additional conditions, including specific configurations of the implant or device, may be required (8). Implants, devices, and other items should be labeled with proper terminology and researchers engaged in performing investigations using MRI technology should carefully consider this information in the realm of MRI screening policies and procedures.

Researchers are required to screen each patient and volunteer subject four times including: conducting a telephone interview or email screening, completing the screening form on site at the MRI facility on the day of the scheduled examination (followed by a review of the completed form by the researcher with the patient or volunteer subject), a visual and verbal screening at dressing room, and a visual and verbal screening immediately before entering the MR system room (Zone 4).

MRI Pre-Procedure Screening Forms

Two MRI screening forms should be available (**Figures 3a and 3b**). One form is completed by patients and volunteer subjects undergoing the MRI examination prior to entering the MR system room (1-5, 7). A shorter version is completed by individuals who wish to enter the MRI environment but that will not be scanned. This second form is used for family members when it is necessary or useful for them to be present in the MR system room with the patient or volunteer subject. This same form is also used for maintenance and house-keeping personnel, visiting researchers, clinicians, nurses, and others. It is important to routinely check with all researchers to ensure that they are using the most current MRI pre-procedure screening forms. This is especially important for researchers from departments other than the one in which the scanner is located.

The screening process is an interactive one between the researcher and the patient or volunteer subject. The researcher conducting the screening must be trained and, therefore, qualified to perform the required screening procedures (1-5, 7). They must have completed the required MRI Safety Policy and Procedure Training and be current with their online safety training. All screening questions regarding biomedical devices and implants, and/or any other condition which may prevent the patient or volunteer subject from undergoing the MRI examination is forwarded to the MRI Manager or radiologist/MRI clinician from the MRI Safety Committee. A good rule to always follow in MRI safety is that “a previous MRI procedure does not guarantee safety” for any subsequent MRI examination. In addition, researchers are required to consult with the MRI Manager, or radiologist/MRI clinician from the MRI Safety Committee if the patient or volunteer subject mentions any previous surgeries. Further investigation is necessary to obtain additional information in order to make the decision for the patient or volunteer subject to undergo the research MRI examination. This includes the date of the surgery, city, state and country in which surgery was conducted, the physician's and/or surgeon's name, name of hospital, anatomical location, surgical procedures conducted, reason for surgery, and devices or implants present (1-5, 7).

Researchers are required to complete the patient and volunteer subject MRI pre-procedure screening form once a year when they complete their MRI Safety Policy and Procedure Training tutorial online. If a researcher undergoes surgical procedures or acquires a biomedical device or implant then they are required to report to the MRI Manager to determine if it is safe for them to enter the MR system room, to work around the scanner and/or be scanned as a volunteer subject. Pregnant patients and volunteer subjects may undergo research MRI examinations if approved by the Institutional Review Board (IRB) and the MRI Safety Committee. The decision to allow pregnant researchers to enter the MR system room is made by the MRI Safety Committee for that particular research facility.

In research studies, more than one MRI examination may take place during the course of the investigation. The participant undergoes the informed consent process typically once and signs the consent form. However, the MRI pre-procedure screening form should be completed each and every time the participant is scanned, even if the scans are only one day apart (1-5, 7). Much can happen in twenty-four hours that might not be noticeable to the researcher conducting the study (e.g., having a pacemaker implanted). Importantly, the screening form should be completed on-site at the research facility on the day of the MRI

812 MRI Safety Policies and Procedures for a Research Facility

Figure 3. (a) Example of an MRI Pre-Examination Screening Form that is used for volunteer subjects and patients.

MRI PRE-EXAMINATION SCREENING FORM																																																																																																																							
Center for Research Imaging																																																																																																																							
Phone <u>xxxxxxx-xxxx</u>																																																																																																																							
Date _____	<input checked="" type="checkbox"/> Magnet <input type="checkbox"/> 0.5T <input type="checkbox"/> 1.5T <input type="checkbox"/> 3.0T <input type="checkbox"/> 7.0T																																																																																																																						
Name _____ Last name _____ First name _____ M.I. _____	Height _____	Weight _____																																																																																																																					
Date of Birth _____	<input type="checkbox"/> Female	<input type="checkbox"/> Male	Ethnic Origin _____																																																																																																																				
Address _____	City _____																																																																																																																						
State _____ Zip Code _____	Phone (H) (_____) (W) (_____)																																																																																																																						
Physician's name & address _____																																																																																																																							
1. Have you ever had surgery or other invasive procedures? <input type="checkbox"/> Yes <input type="checkbox"/> No If yes, please list below. Type: _____ Date: ____ / ____ / ____ Type: _____ Date: ____ / ____ / ____																																																																																																																							
2. Have you had any previous MR studies? <input type="checkbox"/> Yes <input type="checkbox"/> No If yes, please list most recent below. <table style="width: 100%;"><tr><td style="width: 25%;">Area of Body</td><td style="width: 25%;">Date</td><td style="width: 25%;">Facility Name & Location</td><td style="width: 25%;"></td></tr><tr><td>_____</td><td>_____ / _____</td><td>_____</td><td>_____</td></tr><tr><td>_____</td><td>_____ / _____</td><td>_____</td><td>_____</td></tr></table>						Area of Body	Date	Facility Name & Location		_____	_____ / _____	_____	_____	_____	_____ / _____	_____	_____																																																																																																						
Area of Body	Date	Facility Name & Location																																																																																																																					
_____	_____ / _____	_____	_____																																																																																																																				
_____	_____ / _____	_____	_____																																																																																																																				
3. Have you ever had an injury to the eye(s) by a metallic object (metallic slivers, shavings, or foreign body)? <input type="checkbox"/> Yes <input type="checkbox"/> No 4. Are you or think you may be pregnant, experiencing late menstrual period, or having fertility treatments? <input type="checkbox"/> Yes <input type="checkbox"/> No 5. Are you currently taking or have recently taken any medication? <input type="checkbox"/> Yes <input type="checkbox"/> No Please list: _____ 6. Do you have drug allergies or have you had an allergic reaction? <input type="checkbox"/> Yes <input type="checkbox"/> No Please list: _____ 7. Have you ever had an allergic reaction to a MR/CT/X-Ray contrast media injection? <input type="checkbox"/> Yes <input type="checkbox"/> No 8. Do you have or previously had kidney problems and/or diabetes? <input type="checkbox"/> Yes <input type="checkbox"/> No Please list: _____																																																																																																																							
Some of the following items may be HAZARDOUS to your safety & some may interfere with the MRI exam. Do you have any of the following:																																																																																																																							
<table style="width: 100%; border-collapse: collapse;"> <tr> <td style="width: 5%;"><input type="checkbox"/> Yes</td> <td style="width: 5%;"><input type="checkbox"/> No</td> <td>Cardiac pacemaker or defibrillator</td> <td style="width: 5%;"><input type="checkbox"/> Yes</td> <td style="width: 5%;"><input type="checkbox"/> No</td> <td>Pessary or bladder ring</td> </tr> <tr> <td><input type="checkbox"/> Yes</td> <td><input type="checkbox"/> No</td> <td>Internal cardiac pacing wires</td> <td><input type="checkbox"/> Yes</td> <td><input type="checkbox"/> No</td> <td>Transdermal drug delivery patch</td> </tr> <tr> <td><input type="checkbox"/> Yes</td> <td><input type="checkbox"/> No</td> <td>Heart valve prosthesis</td> <td><input type="checkbox"/> Yes</td> <td><input type="checkbox"/> No</td> <td>Prosthesis (eye, penile, etc.)</td> </tr> <tr> <td><input type="checkbox"/> Yes</td> <td><input type="checkbox"/> No</td> <td>Aneurysm clip or brain clip</td> <td><input type="checkbox"/> Yes</td> <td><input type="checkbox"/> No</td> <td>Artificial limb or joint</td> </tr> <tr> <td><input type="checkbox"/> Yes</td> <td><input type="checkbox"/> No</td> <td>Carotid artery vascular clamp</td> <td><input type="checkbox"/> Yes</td> <td><input type="checkbox"/> No</td> <td>Electrodes (on body, head or brain)</td> </tr> <tr> <td><input type="checkbox"/> Yes</td> <td><input type="checkbox"/> No</td> <td>Neurostimulator or DBS</td> <td><input type="checkbox"/> Yes</td> <td><input type="checkbox"/> No</td> <td>Shrapnel, buckshot, or bullets</td> </tr> <tr> <td><input type="checkbox"/> Yes</td> <td><input type="checkbox"/> No</td> <td>Spinal fusion stimulator</td> <td><input type="checkbox"/> Yes</td> <td><input type="checkbox"/> No</td> <td>Metal fragments (eye, head, ear, skin)</td> </tr> <tr> <td><input type="checkbox"/> Yes</td> <td><input type="checkbox"/> No</td> <td>Implanted drug infusion device</td> <td><input type="checkbox"/> Yes</td> <td><input type="checkbox"/> No</td> <td>Metal or wire staples, sutures, mesh implants</td> </tr> <tr> <td><input type="checkbox"/> Yes</td> <td><input type="checkbox"/> No</td> <td>Insulin pump</td> <td><input type="checkbox"/> Yes</td> <td><input type="checkbox"/> No</td> <td>Metal rods in bones; joint replacements</td> </tr> <tr> <td><input type="checkbox"/> Yes</td> <td><input type="checkbox"/> No</td> <td>Venous umbrella</td> <td><input type="checkbox"/> Yes</td> <td><input type="checkbox"/> No</td> <td>Implant or dentures held in place by a magnet</td> </tr> <tr> <td><input type="checkbox"/> Yes</td> <td><input type="checkbox"/> No</td> <td>Tissue expander (breast, etc.)</td> <td><input type="checkbox"/> Yes</td> <td><input type="checkbox"/> No</td> <td>Bone or joint pin, screw, nail, wire, plate</td> </tr> <tr> <td><input type="checkbox"/> Yes</td> <td><input type="checkbox"/> No</td> <td>Aortic or vascular clips</td> <td><input type="checkbox"/> Yes</td> <td><input type="checkbox"/> No</td> <td>Wig, toupee, or hair implants, extensions</td> </tr> <tr> <td><input type="checkbox"/> Yes</td> <td><input type="checkbox"/> No</td> <td>Cochlear, otologic or ear implant</td> <td><input type="checkbox"/> Yes</td> <td><input type="checkbox"/> No</td> <td>Circle/Big Eye or Triggerfish Contact Lenses</td> </tr> <tr> <td><input type="checkbox"/> Yes</td> <td><input type="checkbox"/> No</td> <td>Stents, filters, or coils (vascular or other)</td> <td><input type="checkbox"/> Yes</td> <td><input type="checkbox"/> No</td> <td>Tattoos: body, eyeliner, eyebrows or lips</td> </tr> <tr> <td><input type="checkbox"/> Yes</td> <td><input type="checkbox"/> No</td> <td>Shunt (spine or ventricles)</td> <td><input type="checkbox"/> Yes</td> <td><input type="checkbox"/> No</td> <td>Acupuncture beads or needles (<i>Remove</i>)</td> </tr> <tr> <td><input type="checkbox"/> Yes</td> <td><input type="checkbox"/> No</td> <td>Vascular access port or catheters</td> <td><input type="checkbox"/> Yes</td> <td><input type="checkbox"/> No</td> <td>Body/head piercing(s) (<i>Remove before scan</i>)</td> </tr> <tr> <td><input type="checkbox"/> Yes</td> <td><input type="checkbox"/> No</td> <td>Swan-Ganz catheter</td> <td><input type="checkbox"/> Yes</td> <td><input type="checkbox"/> No</td> <td>Hearing aid (<i>Remove before scan</i>)</td> </tr> <tr> <td><input type="checkbox"/> Yes</td> <td><input type="checkbox"/> No</td> <td>Harrington rods (spine)</td> <td><input type="checkbox"/> Yes</td> <td><input type="checkbox"/> No</td> <td>Dentures (<i>Remove before scan</i>)</td> </tr> <tr> <td><input type="checkbox"/> Yes</td> <td><input type="checkbox"/> No</td> <td>Intrauterine Device (IUD)</td> <td><input type="checkbox"/> Yes</td> <td><input type="checkbox"/> No</td> <td>Seizures or motion disorders</td> </tr> </table>						<input type="checkbox"/> Yes	<input type="checkbox"/> No	Cardiac pacemaker or defibrillator	<input type="checkbox"/> Yes	<input type="checkbox"/> No	Pessary or bladder ring	<input type="checkbox"/> Yes	<input type="checkbox"/> No	Internal cardiac pacing wires	<input type="checkbox"/> Yes	<input type="checkbox"/> No	Transdermal drug delivery patch	<input type="checkbox"/> Yes	<input type="checkbox"/> No	Heart valve prosthesis	<input type="checkbox"/> Yes	<input type="checkbox"/> No	Prosthesis (eye, penile, etc.)	<input type="checkbox"/> Yes	<input type="checkbox"/> No	Aneurysm clip or brain clip	<input type="checkbox"/> Yes	<input type="checkbox"/> No	Artificial limb or joint	<input type="checkbox"/> Yes	<input type="checkbox"/> No	Carotid artery vascular clamp	<input type="checkbox"/> Yes	<input type="checkbox"/> No	Electrodes (on body, head or brain)	<input type="checkbox"/> Yes	<input type="checkbox"/> No	Neurostimulator or DBS	<input type="checkbox"/> Yes	<input type="checkbox"/> No	Shrapnel, buckshot, or bullets	<input type="checkbox"/> Yes	<input type="checkbox"/> No	Spinal fusion stimulator	<input type="checkbox"/> Yes	<input type="checkbox"/> No	Metal fragments (eye, head, ear, skin)	<input type="checkbox"/> Yes	<input type="checkbox"/> No	Implanted drug infusion device	<input type="checkbox"/> Yes	<input type="checkbox"/> No	Metal or wire staples, sutures, mesh implants	<input type="checkbox"/> Yes	<input type="checkbox"/> No	Insulin pump	<input type="checkbox"/> Yes	<input type="checkbox"/> No	Metal rods in bones; joint replacements	<input type="checkbox"/> Yes	<input type="checkbox"/> No	Venous umbrella	<input type="checkbox"/> Yes	<input type="checkbox"/> No	Implant or dentures held in place by a magnet	<input type="checkbox"/> Yes	<input type="checkbox"/> No	Tissue expander (breast, etc.)	<input type="checkbox"/> Yes	<input type="checkbox"/> No	Bone or joint pin, screw, nail, wire, plate	<input type="checkbox"/> Yes	<input type="checkbox"/> No	Aortic or vascular clips	<input type="checkbox"/> Yes	<input type="checkbox"/> No	Wig, toupee, or hair implants, extensions	<input type="checkbox"/> Yes	<input type="checkbox"/> No	Cochlear, otologic or ear implant	<input type="checkbox"/> Yes	<input type="checkbox"/> No	Circle/Big Eye or Triggerfish Contact Lenses	<input type="checkbox"/> Yes	<input type="checkbox"/> No	Stents, filters, or coils (vascular or other)	<input type="checkbox"/> Yes	<input type="checkbox"/> No	Tattoos: body, eyeliner, eyebrows or lips	<input type="checkbox"/> Yes	<input type="checkbox"/> No	Shunt (spine or ventricles)	<input type="checkbox"/> Yes	<input type="checkbox"/> No	Acupuncture beads or needles (<i>Remove</i>)	<input type="checkbox"/> Yes	<input type="checkbox"/> No	Vascular access port or catheters	<input type="checkbox"/> Yes	<input type="checkbox"/> No	Body/head piercing(s) (<i>Remove before scan</i>)	<input type="checkbox"/> Yes	<input type="checkbox"/> No	Swan-Ganz catheter	<input type="checkbox"/> Yes	<input type="checkbox"/> No	Hearing aid (<i>Remove before scan</i>)	<input type="checkbox"/> Yes	<input type="checkbox"/> No	Harrington rods (spine)	<input type="checkbox"/> Yes	<input type="checkbox"/> No	Dentures (<i>Remove before scan</i>)	<input type="checkbox"/> Yes	<input type="checkbox"/> No	Intrauterine Device (IUD)	<input type="checkbox"/> Yes	<input type="checkbox"/> No	Seizures or motion disorders
<input type="checkbox"/> Yes	<input type="checkbox"/> No	Cardiac pacemaker or defibrillator	<input type="checkbox"/> Yes	<input type="checkbox"/> No	Pessary or bladder ring																																																																																																																		
<input type="checkbox"/> Yes	<input type="checkbox"/> No	Internal cardiac pacing wires	<input type="checkbox"/> Yes	<input type="checkbox"/> No	Transdermal drug delivery patch																																																																																																																		
<input type="checkbox"/> Yes	<input type="checkbox"/> No	Heart valve prosthesis	<input type="checkbox"/> Yes	<input type="checkbox"/> No	Prosthesis (eye, penile, etc.)																																																																																																																		
<input type="checkbox"/> Yes	<input type="checkbox"/> No	Aneurysm clip or brain clip	<input type="checkbox"/> Yes	<input type="checkbox"/> No	Artificial limb or joint																																																																																																																		
<input type="checkbox"/> Yes	<input type="checkbox"/> No	Carotid artery vascular clamp	<input type="checkbox"/> Yes	<input type="checkbox"/> No	Electrodes (on body, head or brain)																																																																																																																		
<input type="checkbox"/> Yes	<input type="checkbox"/> No	Neurostimulator or DBS	<input type="checkbox"/> Yes	<input type="checkbox"/> No	Shrapnel, buckshot, or bullets																																																																																																																		
<input type="checkbox"/> Yes	<input type="checkbox"/> No	Spinal fusion stimulator	<input type="checkbox"/> Yes	<input type="checkbox"/> No	Metal fragments (eye, head, ear, skin)																																																																																																																		
<input type="checkbox"/> Yes	<input type="checkbox"/> No	Implanted drug infusion device	<input type="checkbox"/> Yes	<input type="checkbox"/> No	Metal or wire staples, sutures, mesh implants																																																																																																																		
<input type="checkbox"/> Yes	<input type="checkbox"/> No	Insulin pump	<input type="checkbox"/> Yes	<input type="checkbox"/> No	Metal rods in bones; joint replacements																																																																																																																		
<input type="checkbox"/> Yes	<input type="checkbox"/> No	Venous umbrella	<input type="checkbox"/> Yes	<input type="checkbox"/> No	Implant or dentures held in place by a magnet																																																																																																																		
<input type="checkbox"/> Yes	<input type="checkbox"/> No	Tissue expander (breast, etc.)	<input type="checkbox"/> Yes	<input type="checkbox"/> No	Bone or joint pin, screw, nail, wire, plate																																																																																																																		
<input type="checkbox"/> Yes	<input type="checkbox"/> No	Aortic or vascular clips	<input type="checkbox"/> Yes	<input type="checkbox"/> No	Wig, toupee, or hair implants, extensions																																																																																																																		
<input type="checkbox"/> Yes	<input type="checkbox"/> No	Cochlear, otologic or ear implant	<input type="checkbox"/> Yes	<input type="checkbox"/> No	Circle/Big Eye or Triggerfish Contact Lenses																																																																																																																		
<input type="checkbox"/> Yes	<input type="checkbox"/> No	Stents, filters, or coils (vascular or other)	<input type="checkbox"/> Yes	<input type="checkbox"/> No	Tattoos: body, eyeliner, eyebrows or lips																																																																																																																		
<input type="checkbox"/> Yes	<input type="checkbox"/> No	Shunt (spine or ventricles)	<input type="checkbox"/> Yes	<input type="checkbox"/> No	Acupuncture beads or needles (<i>Remove</i>)																																																																																																																		
<input type="checkbox"/> Yes	<input type="checkbox"/> No	Vascular access port or catheters	<input type="checkbox"/> Yes	<input type="checkbox"/> No	Body/head piercing(s) (<i>Remove before scan</i>)																																																																																																																		
<input type="checkbox"/> Yes	<input type="checkbox"/> No	Swan-Ganz catheter	<input type="checkbox"/> Yes	<input type="checkbox"/> No	Hearing aid (<i>Remove before scan</i>)																																																																																																																		
<input type="checkbox"/> Yes	<input type="checkbox"/> No	Harrington rods (spine)	<input type="checkbox"/> Yes	<input type="checkbox"/> No	Dentures (<i>Remove before scan</i>)																																																																																																																		
<input type="checkbox"/> Yes	<input type="checkbox"/> No	Intrauterine Device (IUD)	<input type="checkbox"/> Yes	<input type="checkbox"/> No	Seizures or motion disorders																																																																																																																		
PLEASE REMOVE ALL athletic clothing and undergarments with antimicrobial solution in the material. *PLEASE REMOVE ALL METAL OBJECTS* before MR exam including: Bra, Cell Phone, Keys, Hair Pins & Barrettes, Jewelry, Watch, Safety Pins, Paperclips, Money Clip, Coins, Pens, Pencils, Belt, Pocket Knife, Clothing with Metal or Metal Buttons. *HEARING PROTECTION* is required during the MRI exam.																																																																																																																							
Signature of Person Completing Form			/ / Date																																																																																																																				
Form Completed by: <input type="checkbox"/> Patient / Volunteer		<input type="checkbox"/> Relative: _____																																																																																																																					
<input type="checkbox"/> Physician: _____		<input type="checkbox"/> Other: _____																																																																																																																					
Form Reviewed by (please PRINT NAME clearly & attach to consent form): _____																																																																																																																							

MRI Bioeffects, Safety, and Patient Management 813

Figure 3. (b) Example of a Visitors MRI Screening Form that is used for individuals who are not going to be scanned but will enter the MR system room including family members, physicians, healthcare professionals, maintenance personnel, housekeeping staff members, and others individuals.

VISITORS MR SCREENING FORM (0.5T, 1.5T, 3.0T & 7.0T)																																																					
Center for Research Imaging Department Street Address, City, State XXXX-XXX-XXX																																																					
WARNING: THE MAGNET IS ALWAYS ON																																																					
Note: If you are going to be scanned, you are required to complete a different form.																																																					
Date _____ / _____ / _____	Magnet <input type="checkbox"/> 0.5T <input type="checkbox"/> 1.5T <input type="checkbox"/> 3.0T <input type="checkbox"/> 7.0T																																																				
Name _____	Last name	First name	M.I.																																																		
Age _____	Telephone (H) (_____)	(W) (_____)																																																			
Address _____	City _____																																																				
State _____	Zip Code _____																																																				
1. Have you ever had surgery or other invasive procedures? <input type="checkbox"/> Yes <input type="checkbox"/> No If yes, please list: Type: _____ Date: _____ / _____ / _____ Type: _____ Date: _____ / _____ / _____																																																					
2. Are you pregnant, experiencing a late menstrual period, or having fertility treatments? <input type="checkbox"/> Yes <input type="checkbox"/> No																																																					
Some of the following items may be hazardous to your safety due to the proximity of the MR system and the strong magnetic field. Do you have any of the following:																																																					
<table style="width: 100%; border-collapse: collapse;"> <tbody> <tr> <td style="width: 15%;"><input type="checkbox"/> Yes</td> <td style="width: 15%;"><input type="checkbox"/> No</td> <td>Cardiac pacemaker or defibrillator</td> </tr> <tr> <td><input type="checkbox"/> Yes</td> <td><input type="checkbox"/> No</td> <td>Aneurysm clip or brain clip</td> </tr> <tr> <td><input type="checkbox"/> Yes</td> <td><input type="checkbox"/> No</td> <td>Neurostimulator or Deep Brain Stimulator (DBS)</td> </tr> <tr> <td><input type="checkbox"/> Yes</td> <td><input type="checkbox"/> No</td> <td>Insulin or infusion pump</td> </tr> <tr> <td><input type="checkbox"/> Yes</td> <td><input type="checkbox"/> No</td> <td>Implanted drug infusion device</td> </tr> <tr> <td><input type="checkbox"/> Yes</td> <td><input type="checkbox"/> No</td> <td>Spinal fusion stimulator or spinal cord stimulator</td> </tr> <tr> <td><input type="checkbox"/> Yes</td> <td><input type="checkbox"/> No</td> <td>Cochlear, otologic or ear implant</td> </tr> <tr> <td><input type="checkbox"/> Yes</td> <td><input type="checkbox"/> No</td> <td>Implant held in place by a magnet</td> </tr> <tr> <td><input type="checkbox"/> Yes</td> <td><input type="checkbox"/> No</td> <td>Artificial or prosthetic limb or prosthesis</td> </tr> <tr> <td><input type="checkbox"/> Yes</td> <td><input type="checkbox"/> No</td> <td>Heart valve prosthesis</td> </tr> <tr> <td><input type="checkbox"/> Yes</td> <td><input type="checkbox"/> No</td> <td>Aortic or vascular clips</td> </tr> <tr> <td><input type="checkbox"/> Yes</td> <td><input type="checkbox"/> No</td> <td>Stents, filters or coils (vascular or other)</td> </tr> <tr> <td><input type="checkbox"/> Yes</td> <td><input type="checkbox"/> No</td> <td>Shunt (spine or ventricles)</td> </tr> <tr> <td><input type="checkbox"/> Yes</td> <td><input type="checkbox"/> No</td> <td>Metal fragments (eye, head, ear or skin)</td> </tr> <tr> <td><input type="checkbox"/> Yes</td> <td><input type="checkbox"/> No</td> <td>Hearing aid</td> </tr> <tr> <td><input type="checkbox"/> Yes</td> <td><input type="checkbox"/> No</td> <td>Other implants in body or head</td> </tr> </tbody> </table>						<input type="checkbox"/> Yes	<input type="checkbox"/> No	Cardiac pacemaker or defibrillator	<input type="checkbox"/> Yes	<input type="checkbox"/> No	Aneurysm clip or brain clip	<input type="checkbox"/> Yes	<input type="checkbox"/> No	Neurostimulator or Deep Brain Stimulator (DBS)	<input type="checkbox"/> Yes	<input type="checkbox"/> No	Insulin or infusion pump	<input type="checkbox"/> Yes	<input type="checkbox"/> No	Implanted drug infusion device	<input type="checkbox"/> Yes	<input type="checkbox"/> No	Spinal fusion stimulator or spinal cord stimulator	<input type="checkbox"/> Yes	<input type="checkbox"/> No	Cochlear, otologic or ear implant	<input type="checkbox"/> Yes	<input type="checkbox"/> No	Implant held in place by a magnet	<input type="checkbox"/> Yes	<input type="checkbox"/> No	Artificial or prosthetic limb or prosthesis	<input type="checkbox"/> Yes	<input type="checkbox"/> No	Heart valve prosthesis	<input type="checkbox"/> Yes	<input type="checkbox"/> No	Aortic or vascular clips	<input type="checkbox"/> Yes	<input type="checkbox"/> No	Stents, filters or coils (vascular or other)	<input type="checkbox"/> Yes	<input type="checkbox"/> No	Shunt (spine or ventricles)	<input type="checkbox"/> Yes	<input type="checkbox"/> No	Metal fragments (eye, head, ear or skin)	<input type="checkbox"/> Yes	<input type="checkbox"/> No	Hearing aid	<input type="checkbox"/> Yes	<input type="checkbox"/> No	Other implants in body or head
<input type="checkbox"/> Yes	<input type="checkbox"/> No	Cardiac pacemaker or defibrillator																																																			
<input type="checkbox"/> Yes	<input type="checkbox"/> No	Aneurysm clip or brain clip																																																			
<input type="checkbox"/> Yes	<input type="checkbox"/> No	Neurostimulator or Deep Brain Stimulator (DBS)																																																			
<input type="checkbox"/> Yes	<input type="checkbox"/> No	Insulin or infusion pump																																																			
<input type="checkbox"/> Yes	<input type="checkbox"/> No	Implanted drug infusion device																																																			
<input type="checkbox"/> Yes	<input type="checkbox"/> No	Spinal fusion stimulator or spinal cord stimulator																																																			
<input type="checkbox"/> Yes	<input type="checkbox"/> No	Cochlear, otologic or ear implant																																																			
<input type="checkbox"/> Yes	<input type="checkbox"/> No	Implant held in place by a magnet																																																			
<input type="checkbox"/> Yes	<input type="checkbox"/> No	Artificial or prosthetic limb or prosthesis																																																			
<input type="checkbox"/> Yes	<input type="checkbox"/> No	Heart valve prosthesis																																																			
<input type="checkbox"/> Yes	<input type="checkbox"/> No	Aortic or vascular clips																																																			
<input type="checkbox"/> Yes	<input type="checkbox"/> No	Stents, filters or coils (vascular or other)																																																			
<input type="checkbox"/> Yes	<input type="checkbox"/> No	Shunt (spine or ventricles)																																																			
<input type="checkbox"/> Yes	<input type="checkbox"/> No	Metal fragments (eye, head, ear or skin)																																																			
<input type="checkbox"/> Yes	<input type="checkbox"/> No	Hearing aid																																																			
<input type="checkbox"/> Yes	<input type="checkbox"/> No	Other implants in body or head																																																			
PLEASE REMOVE ALL METALLIC OBJECTS before entering the magnet room: keys, pager, cell phone, paperclips, coins, hair pins, barrettes, safety pins, money clip, computer jump drive, credit cards, hearing aid, pocket knives, tools & analog watches.																																																					
_____ Signature of Person Completing Form			_____ Date																																																		
Form Completed by: <input type="checkbox"/> Researcher / Scientist <input type="checkbox"/> Visitor Form Reviewed by (please print clearly): _____																																																					

814 MRI Safety Policies and Procedures for a Research Facility

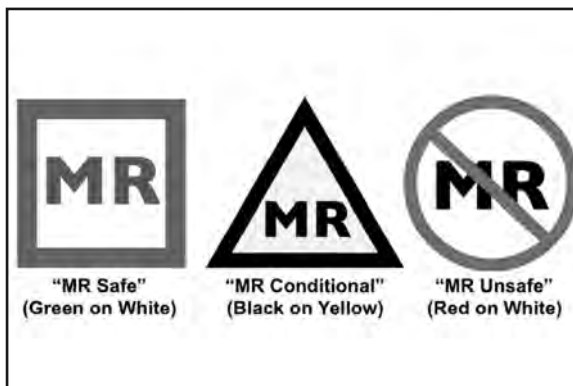
examination. Researchers are required to conduct an earlier telephone interview or email pre-screening for major issues such as the presence of biomedical devices or implants, pregnancy, presence of acupuncture needles, body piercing, etc. These are issues that would need to be resolved by those responsible on the MRI Safety Committee before the patient or volunteer subject would be allowed to undergo the MRI examination.

It is critical that the researcher conveys to the patient or volunteer subject the seriousness of the screening form and how important it is to provide accurate, complete answers to ensure their safety. After the patient or volunteer subject completes the MRI pre-procedure screening form, the researcher sits down with the individual to review their responses on the form. This is to ensure that the patient or volunteer subject has not misunderstood or forgotten any information, surgeries, or conditions that might prevent them from undergoing the MRI examination. After the review is complete, the researcher prints his or her first and last name at the bottom of the completed form. This ensures that a record is kept of which individual reviewed the completed screening form with the patient or volunteer subject before taking this individual into the MR system room. The completed screening form goes in a secured file with the completed consent form in the office of the principal investigator (PI) as evidence that everything was done to ensure safety for the patient or volunteer subject during the MRI examination.

As with a clinical MRI department, it should be clearly documented in the research facility's policies and procedures, to which the responsibility falls to make the decision for the patient or volunteer subject to undergo the MRI examination if there is a potential safety issue present such as a biomedical device or implant. As the patients and volunteer subjects undergoing MRI research scans are enrolled in a research study, there is typically no benefit versus risk evaluation conducted as is done in a clinical facility. In addition, frequently there is not a formal image or data interpretation by a board-certified radiologist with a report entered into the radiology department database (Radiology Information System or RIS). Research studies are conducted on groups of people (to prove a hypothesis), typically not done to provide diagnoses on individual patients. Because of this, pre-procedure screening becomes much more conservative than what is practiced in the clinical MRI department. Pregnant women and volunteer subjects with pacemakers, even MR Conditional pacemakers, are not scanned unless approved by the IRB and the MRI Safety Committee. If there is any risk at all, the radiologist/MRI clinician makes the final decision (1-5, 7, 12). If neither the MRI Manager nor the radiologist/MRI clinician can be contacted for approval, the patient or volunteer subject is not to enter the MR system room nor undergo the research MRI examination.

Most biomedical devices and implants are considered "MR Conditional" unless they are made completely from nonmetallic and non-conducting components such as plastic or nylon (1, 3-5, 7). Each manufacturer of a biomedical device or implant determines the specific conditions under which their product can safely undergo an MRI examination. In research studies, the scan parameters are selected and typically maintained across all scans of all individuals participating in that particular research study. Therefore modification of scan parameters in order to adhere to safety conditions may not be acceptable for the aim of the research study. Any alterations to previously set scan parameters may result in the exclusion of certain participants' data in the study.

Figure 4. MRI labeling system showing the icons as defined by the ASTM International that is used to mark implants, devices, and equipment.



Only one family member (i.e., parent, spouse, adult child, etc.) is allowed to accompany the patient or volunteer subject into the scanner room. The shorter screening form for visitors and other similar individuals is completed first and reviewed by the researcher. All metals and potential projectiles including jewelry, watches, hair accessories, external hearing aids, and other related items are removed and secured in a locker. If the family member is going to remain in the MR system room with the patient or volunteer subject, then hearing protection is required.

MRI pre-procedure screening forms should be comprehensive but the information contained should be easily understood, therefore, not too technical nor should it contain too much medical jargon. The MRI Safety Committee reviews and updates these forms on a regular basis, typically every six months. Any new changes due to information from the FDA, ASTM International, manufacturers of medical implants and devices, and other entities should be reviewed by the MRI Safety Committee which subsequently determines if changes or additions should be made to the screening forms.

Examples of MRI pre-procedure screening forms can be obtained at: <http://www.mrisafety.com> and at the website for the Institute for Magnetic Resonance Safety, Education, and Research, <http://www.imrser.org> (both sites created and maintained by Frank G. Shellock, Ph.D.) (13, 14).

Static Magnetic Field

Metallic items that are attracted to a magnet are referred to as ferromagnetic (1-9, 15). Examples of ferromagnetic materials include iron and certain types of steel. Some examples of nonferromagnetic materials include aluminum, copper, brass, lead, nickel, titanium, cobalt, mercury, chromium, platinum, and gold. It is important to remember that often metals are a mixture (alloy) that makes it difficult to easily determine if a given item is ferromagnetic even if the percentage of each element present is known. Testing by very strong handheld magnet is typically the only way to determine if a specific item will be attracted to the magnet of the MR system, remembering that handheld magnets are generally never as strong as the MRI, such as 1.5 T or 3 T (1-5).

816 MRI Safety Policies and Procedures for a Research Facility

Every precaution must be taken to ensure that ferromagnetic items are not taken into the MR system room. Given the shielding present in most scanners, the spatial magnetic field gradient of the static magnetic field (B_0) can be quite short and steep. Therefore, the distance traversed between a ferromagnetic item feeling no attraction, to quickly being pulled into the MR system can be quite small. This translational attraction is dependent upon several conditions including the strength and spatial gradient of the static magnetic field, magnet design (e.g., long-bore versus short-bore), the degree of attraction due to mass and geometry of the object, the type of retention, location, orientation, time in place (i.e., for implants), and other factors.

Items in the patient preparation room or any rooms located close (Zones 2 and 3) to the MR system room (Zone 4) must be clearly identified with labels indicating that they may not be taken into the scanner room at any time for any reason (1-4, 6, 7). Some of these items may include emergency (i.e., crash) carts, laundry carts, storage cabinets, and chairs. Recommended items that reside in the patient preparation room should be identified and labeled as MR Safe, MR Conditional, or MR Unsafe. In a MRI research facility, it is realistic to expect that some items that reside in the control room as well as the volunteer subject/patient preparation room will be MR Unsafe. This is especially true because in the research setting there is often hardware and devices that are under development (prototypes). Therefore, labels indicating MR Unsafe are absolutely necessary for such items. The labels used for this purpose should be those defined by the ASTM International (1-4, 6, 9). **Figure 4** shows the proper labels for marking purposes related to MR Safe, MR Conditional, and MR Unsafe.

RF Electromagnetic Fields

Heating of the patient and potential subsequent burns are serious concerns in the MRI examination. Because patients are not well, it is imperative that everything is done to ensure that precautions are put into place prior to scans beginning, and also that communication with the patient is ongoing during the examination. Concerns range from an increased sensation of overall warmth adding to the already present feeling of discomfort due to their condition to local (focal) thermal injury. Three different values are currently reported in the scanner's software to the operators including SAR, B_{1+RMS} , and SAE (specific absorbed energy) or SED (specific energy dose).

The specific absorption rate (SAR) is a means of characterizing the absorption of radiofrequency (RF) energy in human tissue and is typically reported in watts per kilogram (W/kg) (1-6, 10, 16). SAR is primarily dependent on the following parameters: imaging frequency, type and number per repetition time (TR) of RF pulses, type of transmit RF coil, anatomy exposed to the transmitting RF coil, and patient weight (and height on some MR systems). The measurement of SAR is typically reported on MR systems as whole body averaged and peak values. In general, as SAR increases, the number of slices available in a given imaging sequence is reduced in order to decrease the whole body averaged SAR level. Realistically, the only modifiable parameters available to the MRI operator to reduce SAR are the repetition time, degree of flip angle(s), number of flip angles per TR (echo train or turbo factor) including presaturation bands and chemical presaturation, and/or number of slices, unless the researcher can change the transmit RF coil or move to a lower static

magnetic field (B_0) MR system. Entering the incorrect weight of the patient or volunteer subject is risky and could result in increased RF energy being deposited into the patient, potentially resulting in a burn (10).

B_{1+RMS} values have recently been added to the RF and heating parameters being reported in the MR system software and also to the list of conditions for biomedical implants and devices. “ B_{1+} ” (B_1 plus) is the part of the applied RF that is used in imaging as opposed to “ B_{1-} ” (B_1 negative) that is not used in imaging but contributes to heating. “RMS” (root mean squared) is an averaging technique. B_{1+RMS} is part of the equation determining the SAR for a given scan but it is also a potentially more accurate means of reporting the RF power that is being transferred by the RF transmit coil. For that reason, it may be more important as an indicator of heating in the presence of biomedical devices and implants. SAR, however, should always be monitored to minimize discomfort for patients especially in those individuals who cannot properly regulate their heating due to disease conditions present and any pharmaceutical therapies they may be undergoing (4).

SAE (specific absorbed dose) or SED (specific energy dose) have historically been set to a limit of 60 minutes for a maximum of 14.4 kilojoules per kilogram (kJ/kg). These RF limitations are in place due to longer MRI examination times. The maximum is calculated by 4 watts per kilogram (W/kg) multiplied by one hour (3600 seconds) (6).

Risks surrounding the RF electromagnetic fields (B_1) include the heating of metallic objects or devices, associated components, and/or the surrounding tissues. The increased heating can result in burns to the patient or volunteer subject, and/or damage to the MR system and RF coils. Burn scenarios include the exposure (close proximity) to a transmit RF coil, focus of RF energy in a specific area (i.e., the antenna effect), currents being induced in conductors (e.g., cables, metallic devices of certain lengths and human beings), reflected power (using RF shields, mylar/space blankets or aluminum foil), and an inappropriate use of an RF coil (1-7, 10).

Procedures to prevent currents being induced in conductors, and the proper positioning and insulation of cables, RF coils, devices and human subjects must be utilized for all MRI examinations especially those using the RF body coil to transmit RF energy (Figure 5). In addition, all loop formation must be prevented including cables forming loops, cables forming loops with other cables, and cables forming loops with human subjects (1-7, 10). Loops can be defined as crossing and/or touching, or changing direction within the scanner (e.g., a cable runs through the bore, then turns and runs back through the bore a second time) (1-7, 10, 11). Loops in cables present in the MR system bore become a greater risk as the loop becomes larger. For example, if an ECG cable is attached to a patient or volunteer subject via electrodes, the cable runs then out the back of the magnet, turns and returns through the scanner’s bore to its electrical connection at the front of the scanner. This forms a very large and potentially dangerous loop. Cables on RF coils are sometimes too long. Placing a sponge or pad to separate the smaller unpreventable loops of the cable should prevent induced currents.

Attention must be given to the potential for patient burns occurring due to the human body acting as a conductor. A gap 1-cm of air must be guaranteed between anatomy within the confines of the transmitting RF coil using sponges and pads to separate and insulate (1-

818 MRI Safety Policies and Procedures for a Research Facility

7, 10, 11). For example, during any scan in which the RF body coil is used as the transmit RF coil, hands should not be clasped together, hands should not rest on forehead during breast MRI examinations, hands should not rest against hips, and calves (lower leg) should not touch. Pads or sponges may need to be positioned between the legs from upper thigh to feet to ensure no loops are formed. In addition to the potential for peripheral nerve stimulation due to time-varying gradient magnetic fields, these types of contact or any other combinations should be avoided due to the risk of providing a route for induced currents to flow.

In the research environment, many prototype devices are designed and constructed to be used while imaging patients and volunteer subjects. These are either used alone or simultaneously with other product or prototype devices. Individuals possessing the appropriate expertise must complete extensive testing to ensure these prototype devices can be used safely within the magnetic environment. The device design and safety risks, if present, are described in the human study protocol to be approved by the IRB prior to use. In addition, consultation with the MRI Manager is required before use in the scanner room.

Utilizing different static magnetic field strengths within the same research facility necessitates the possession of knowledge regarding RF bandwidth, its dependence upon the static magnetic field, and interaction with certain lead lengths (as applicable) as well as the human body. This is critical in the prevention of not only image artifacts but also potential risks for burns. For example, imaging the brain at 3-T versus that of 1.5-T means the RF frequency is 128-MHz versus 64-MHz. The brain then encounters more “half wavelengths” at 3-T resulting in a B_1 inhomogeneity (dielectric resonance) that is seen as brightness in the center of the axial brain images (1-10, 17, 18). While SAR (RF energy deposited into the human body) increases by the square root of 2 at 3-T versus that at 1.5-T resulting in increased patient heating. However, increased SAR is not always present in the event of a patient burn due to induced currents. For example, dependent upon a given lead length, there may be less resultant heating due to standing waves at 3-T (128-MHz) versus 1.5-T (64-MHz), as reported by Shellock, et al. (19).

Due to the many different designs of RF coils from major MR system manufacturers and third-party vendors, it is critical that specific instructions be followed when utilizing these coils. This is especially true of the so-called “array” coils available as product versions since the early 1990s. Various designs of RF array coils include coupled, isolated, or phased. Some of these designed to image large areas of the body (e.g., cardiac, torso and abdomen) are manufactured as two parts, one to be positioned anteriorly and the other, posteriorly. Preventing these particular RF coils from overlapping at the sides of the patient or volunteer subject may be a requirement to prevent interactions resulting in excessive heating and possible burns. Sponges or pads must always be present or placed between the RF coil and the anatomy being imaged, some of which are provided by the manufacturer. This is to prevent inappropriate loading that can potentially result in malfunction of the RF coil and subsequent disproportionate heating.

Positioning one RF coil inside of another for MR imaging is generally something that should never be done unless the coils are specifically designed by the manufacturer to do so safely. For example, an earlier version of the endorectal coil was used to image the prostate in conjunction with a pelvic phased array coil. To proceed safely, researchers must

first consult the MRI Manager, MRI research technologist, or lab director (MRI scientist or Ph.D.) of the research facility. Finally, an RF coil should never be left unplugged and in the bore of the scanner during an MRI examination which may result in heating of the unplugged RF coil and resulting in a burn to the subject or patient and/or damage to the hardware and scanner.

Time-Varying Gradient Magnetic Fields

Risks associated with the time-varying gradient magnetic fields are due to the rapid switching to spatially localize during MR imaging (1-5, 7, 19, 20). This rapid switching is made up of two parts, the size [maximum amplitude measured in milliTesla per meter (mT/m)] and the speed [slew rate measured in milliTesla per meter per millisecond (mT/m/msec)]. As a current is made to flow in a conductor moving through a static magnetic field, a flowing current can also be induced in a static conductor when exposed to a rapidly changing magnetic field.

Other risks include peripheral nerve stimulation and auditory effects that are associated with the time-varying gradient magnetic fields (1-5, 7, 19, 20). While peripheral nerve stimulation due to the slew rate is a reality, it is subjective and, therefore, difficult to determine exactly which patients and volunteer subjects will experience this sensation. While it can be perceived as painful or extreme pressure, it has not been reported to result in residual effects. Some of the MR systems offer options to image under reduced slew rates, thereby minimizing the risk.

Manufacturers of MR systems continue to devise methods to reduce the acoustic noise generated by gradient magnetic fields and this topic is covered in detail in another chapter in this textbook. New imaging sequences, especially those being designed in research facilities are often rapid, increasing the noise level. Therefore, it is essential to use earplugs or other hearing protection accessories and devices rated appropriately by the noise reduction ratings (NRR). In addition, it is of equal importance that the earplugs be placed correctly within the ear canal. Researchers are to check the placement of the earplugs before moving the patient or volunteer into the scanner's bore. Headphones (earmuffs) are recommended for use in conjunction with earplugs to provide maximum protection during scans of the body and extremities. Researchers are required to instruct their patients and volunteer subjects to notify them using the squeeze bulb or verbally through the intercom system if the earplugs become loose, fall out, or if the noise of the scanner is bothersome or painful so that the examination can be immediately stopped. Posters demonstrating the procedure for correct placement of earplugs should be posted within each of the research MR system rooms for easy referral for researchers and their patients and volunteer subjects. If earplugs cannot be positioned appropriately, the patient or volunteer subject should not be scanned. If headphones are used alone, the NRR should be at least 30-dB of protection that is provided including any earplugs that fit inside of the headphones, some of which deliver audio instructions during research studies.

Presence of Biomedical Implants or Devices

The risks of allowing human subjects with MR Unsafe or MR Conditional (when conditions have not been met) biomedical implants or devices into the MRI environment to

820 MRI Safety Policies and Procedures for a Research Facility

Figure 5. To proactively prevent RF heating incidents, it is important to position all MR system-related RF coil cables and monitoring system cables away from the bore of the scanner along with padding to prevent direct contact with a volunteer subject or patient. Note that ECG (EKG) cables should not be looped and must exit the bore of the MR system directly away from the patient.



undergo an MRI examination include the objects being moved or dislodged, induction of a current in the device or associated lead wires, excessive heating and subsequent burns, altered function of the device, de-magnetization of the device, temporary or permanent damage to the device, and other problems (1-4, 7, 9, 10, 12, 16, 21-23).

Having general policies for managing individuals with biomedical devices and implants are never a good idea because testing has not been conducted on all implants, there tend to be exceptions, new devices are being developed on an ongoing basis, and implants and devices are approved for safe scanning under different MR conditions (4, 5).

Risks are dependent upon many criteria including the static magnetic field strength, spatial gradient of the static magnetic field, ferromagnetic properties of the implant or device [composition, mass and geometry, passive versus active, and method of activation (electrically, magnetically, or mechanically)], and/or location and orientation of the implant or device [type of tissue, retention means (scarring, sutures, cement, etc.)], adjacent vital anatomic structures, and other factors (1-4, 7, 9, 10, 12, 16, 21-23).

To accurately evaluate the conditions under which a patient or volunteer subject with an implant or device can safely undergo an MRI examination, specific information must be

obtained including the name of the manufacturer of the device or implant, composition of the material, date surgically placed, anatomical location, name of surgeon and hospital, and/or reason for placement of implant or device (1-4, 7, 9, 10, 12, 16, 21-23). The more information that can be obtained about the implant or device, the easier it will be to make a knowledgeable and accurate decision. Patients are sometimes given cards to carry with information from the manufacturer about the implant or device. In addition, contacting manufacturers or reviewing their website can provide the necessary information. The decision to undergo the MRI examination, however, should never be made from a verbal reply only (e.g., "The surgeon said it was ok to scan."). Dependent upon the type of implant or device, the MRI Manager or the radiologist/MRI clinician from the MRI Safety Committee should make the decision for the patient or volunteer subject to undergo the MRI procedure. For more complex devices such as cardiac pacemakers and neurostimulation systems, it is the radiologist/MRI clinician who must make the final decision not the MRI Manager or MRI facility manager (1-4, 7, 9, 10, 12, 16, 19, 21-23). As stated earlier, the patients and volunteer subjects undergoing MRI procedures are enrolled in a research study, therefore, they are considered "volunteers" for the research study. Thus, there is typically no benefit versus risk evaluation conducted as is done in a clinical facility.

If the implant or device is identified to be MR Conditional, then the set of MRI scan parameters as set down in the research protocol must be reviewed to ensure it is capable of being modified to ensure that the specific conditions are met for safe scanning without affecting the outcome of the research study. These modifications to the scan parameters and protocol must be accepted and approved by the principal investigator (PI) of the research study.

Body piercing jewelry and cosmetic jewelry may pose a hazard to a study subject or patient undergoing MRI (24-26). Therefore, in general, all individuals must remove metallic body piercing and cosmetic jewelry before being involved in research MRI examinations (24-26). Because there is no benefit versus risk evaluation conducted for research scans, even the smallest amount of risk must be removed. Patients and volunteer subjects with body piercing jewelry and cosmetic jewelry that cannot be removed are not permitted to undergo research MRI examinations.

Screening Tools

A list of common projectiles that have made their way into MR systems should be provided to researchers to ensure that they remember what items could be problematic. For example, paper clips, staples, hairpins, barrettes and other hair accessories, jewelry and watches, keys, hearing aids, scissors, pocketknives, tools, flashlights, metal pens, clipboards, notebooks, money clips, cell phones, and other similar objects.

Quality handheld magnets are another valuable investment to be made for checking equipment, imaging accessories, and hair accessories and jewelry (worn by researchers) (1-4, 7). To check any of these items, they must be removed from the body and placed on a hard surface over which the handheld magnet is placed. Handheld magnets should never be used to detect the presence of ferrous metal in or on the body (1-4, 7). Strong handheld magnets are available in several forms. The most valuable is a neodymium magnet (1200-Gauss or higher). The use of a handheld magnet of a lower strength is discouraged.

822 MRI Safety Policies and Procedures for a Research Facility

Reference materials including books and websites can be very helpful in the gathering of current information concerning many aspects of MRI safety and screening. Publications from the American College of Radiology (ACR) are comprehensive documents that should be carefully reviewed by the MRI Safety Committee members (1). Utilizing reference materials and websites are especially helpful for the evaluation of biomedical devices and implants. It should be remembered, however, that these are for reference only and should never be used as the sole piece of evidence to decide whether the patient or volunteer subject should undergo the MRI examination. This decision is made by the radiologist or MRI clinician.

Websites to consult are those from the manufacturer of the biomedical device or implant which provide information and conditions under which a particular device can safely be exposed to all parts of the MRI examination involving the respective electromagnetic fields. Websites such as www.mrisafety.com (created and maintained by Frank G. Shellock, Ph.D.) provide educational documents and testing results for thousands of biomedical devices and implants (13). In addition, other websites such as www.imrser.org, provide a wealth of information about safety and pre-procedure screening in the MRI environment that can be used by those on the MRI Safety Committee to keep their knowledge of MRI safety current (14). A textbook entitled, "Reference Manual for Magnetic Resonance Safety, Implants, and Devices", is an information resource that is fully updated on an annual basis (3). This is an extremely valuable yet inexpensive investment for all MRI departments, both research and clinical.

Participation in a worldwide MRI technologist automatic email list server is also helpful in adding to one's arsenal of knowledge in MRI safety and screening (**Figure 6**). Questions are answered, suggestions made, and issues discussed on a daily basis. In this manner, a wealth of information is being shared freely without cost to the participants. However, time is required to triage the emails and read the ones particularly valuable to a given research facility.

Ferromagnetic detections systems (FMDS), devices that identify ferromagnetic materials, have recently replaced the metal detectors initially thought to be an important part of the fully equipped MRI department in the 1980s. Conventional metal detectors quickly became viewed as a waste of funds given the many issues surrounding them including over-dependence by users, the generation of false-positives and false-negatives, the function-related dependence upon size and mass of the metallic object, the sensitivity setting of the device, and other issues. Currently there are several different companies manufacturing a variety of designs for FMDS and a chapter is devoted to this topic in this textbook. These devices can be very helpful in preventing injuries from larger ferromagnetic objects such as oxygen tanks, IV poles, infusion machines, gurneys, hospital beds, and many other items that have found their way into MRI environments over the years. Most of these situations resulted in expensive damage to the MR systems and RF coils. Others resulted in injuries to healthcare workers and patients and at least one death involving a patient. A report by Shellock and Karacozoff (27) indicated that a FMDS may also be used to identify ferromagnetic implants and foreign bodies.

Visitors, Tours, Classes, and Videotaping

Visitors to the MRI suite are allowed if an individual who has completed the required MRI Safety Policy and Procedure Training accompanies them. Visitors are not allowed to enter the MR system room (Zone 4) except when absolutely necessary and then approval must be obtained from the MRI Manager (the MRI technologist from the MRI Safety Committee). If approved to enter the scanner room, the visitor completes the appropriate screening form that is then reviewed by an MRI safety-trained individual. The visitor then checks all pockets by placing their hands inside of each and removes all potential projectiles in addition to jewelry, watches, hair accessories and hearing aids.

Due to the extremely high fringe field associated with a 7-Tesla MR system, the control and scanner room are treated the same with regards to screening visitors and other individuals. Thus, the screening form is completed in the lobby or in the patient preparation room, reviewed, and approved before the visitor may enter the control and/or scanner room of the 7-Tesla scanner.

To conduct tours, classes, and videotaping sessions in the MRI suite must be approved by the MRI Manager prior to scheduling. Classes and videotaping sessions are scheduled through the MRI Manager to ensure the availability of an MRI research technologist. This has proven to be valuable as the technologist scans while the faculty member (i.e., scientist or physician) delivers instruction to the class. Having an MRI technologist present not only ensures safety for individuals present and the MR systems, it prevents modifications from being made to the MRI suite and its contained equipment. It also ensures that the MRI suite that appears in a video shown on TV or in media pictures will be represented appropriately and that any scanning of human subjects that are participating are filmed according to departmental policy.

Housekeeping and Maintenance Staff

The MRI Manager and building manager are responsible for training the housekeeping and maintenance staff in the basic aspects of MRI safety (1-4). Specifically, this includes in which rooms they can access and which they are never allowed entry. Complete agreement and support must be obtained from housekeeping management to ensure that, in the event of sick leave or vacation, the MRI Manager and/or building manager is notified immediately and that replacement housekeeping staff is fully trained before entering any of the MRI suites. Housekeeping and maintenance staff are never to enter the MR system rooms (Zone 4) at any time. Dependent upon the location of the fringe field in the scanner control room (Zone 3), housekeeping and maintenance may not be given automatic access to that area. Cleaning and maintenance are scheduled for each of the MRI suites when the MRI Manager, building manager, or MRI technologist is available to provide full time monitoring.

PREPARATION OF PATIENTS AND VOLUNTEER SUBJECTS

During the scheduling process for patients and volunteer subjects, it should be communicated clearly that specific items should be left at home including all jewelry, body piercing jewelry, hair accessories, and undergarments with metallic fibers or components. Facial

824 MRI Safety Policies and Procedures for a Research Facility

makeup should not be worn because some can result in an irritation to the skin from tiny metallic particles and/or cause an imaging artifact. Hair products can also contain components of metallic glitter or other compounds that pose a problem for MRI (e.g., hair concealment spray). Artificial hair extensions have proven to be problematic for imaging of the brain due to the resulting lack of homogeneity and failure of magnetic field shimming due to the presence of the synthetic material that is present. Wigs and hairpieces should be removed or closely checked underneath for any hairpins that may be in place.

Having all patients and volunteer subjects change out of street clothes into scrubs or gowns that do not have pockets is required for all MR examinations (1-6). This policy takes pockets out of the equation and allows easier visual access to ensure that items that may be problematic have been removed. Street clothing that contains antimicrobial solutions can act as a conductor in the bore of the MR system resulting in patient heating and subsequent burns. It is also a way to remind the patients and volunteer subjects that preparation for entering the MRI environment is a serious issue and that their safety is considered paramount by the researchers conducting the MRI examinations. Compare the costs associated with the purchase of disposable scrubs and those provided by a laundry service. It can be the case that disposable scrubs are less expensive over time. Disposable foot covers are also a requirement for patients and volunteer subjects. Whether placed over bare feet or socks, it ensures some additional cleanliness in the MRI area but, more importantly, the dots on the bottom of the foot covers assist in the prevention of slipping and possible injuries.

All personal items belonging to patients and volunteer subjects must be secured in a locker within the MRI suite. This process facilitates a conversation between the researchers and the patient or volunteer subject to ensure that items will not be taken into the scanner

Figure 6. Participation in a worldwide MRI technologist and radiographer email list server is helpful in increasing knowledge and awareness of MRI safety by observing discussions and sharing information.

The screenshot shows the homepage of the SMRT (Society of Magnetic Resonance Technologists) website. At the top, there is a navigation bar with links for HOME, ABOUT, MEMBERS, RESOURCES, EDUCATION, SCHOLARSHIP FUND, and CAREER CENTER. The logo for "A WORLD OF KNOWLEDGE FOR MRI TECHNOLOGISTS PROFESSIONALS" is visible. A search bar and a "Select Language" dropdown are also at the top. On the right side of the header, there is a "ISMRM ONE" logo. The main content area is titled "MR TECHNOLOGISTS EMAIL COMMUNITY". Below this, a section titled "SMRT's MR Technologists Email Community" is described. It states that the SMRT manages an email-based discussion group for all members of the MR community called "SMRT MR Technologists Community". It explains that the purpose of this group is to foster open discussion of professional and scientific issues related to the field of MRI. A detailed description of the membership requirements follows, mentioning that while primarily intended for MR technologists/radiographers, others in related fields can join. The text emphasizes that the SMRT is a professional society with a diverse membership including educators, trainers, and other individuals working with MRI.

MRI Bioeffects, Safety, and Patient Management 825

room or the MR system. Leaving personal items of any kind out on counters, especially jewelry or wallets, can be problematic. This can lead to a patient or volunteer subject making a claim that “something is missing”. Glasses can be worn into the scanner room but should never be worn by the patient or volunteer subject into the bore of the MR system due to the metallic components (e.g. small screws) that will result in artifacts in images and data acquired. Pillows or toys from home should never be allowed in the scanner room nor scanner bore unless fully checked with a strong handheld magnet first. Items such as these can easily hide the presence of a piece of ferromagnetic material.

It is valuable to have a checklist present and a “stop, look, and feel” policy and procedure before entering the MR system room with the patient or volunteer subject (1-4, 6). This is especially important in research facilities that may have patients and volunteer subjects arriving by wheelchair or gurney, and/or with IV poles and/or infusion devices. If the MR system table does not undock to be moved to the patient preparation room for transfer of the patient or volunteer subject, an acceptable (i.e., MR Safe or MR Conditional) wheelchair and/or gurney should also be available. All of these items should be included on the checklist to ensure no unsafe items from the outside make their way into the scanner room and that all conditions are met. In addition, checking under sheets and blankets is also a requirement before entering the scanner room.

Policies and procedures must also be in place for patient and volunteer subject transfers from wheelchairs and gurneys to the MR system table. Only those individuals trained in the proper techniques should perform lifts and transfer of human subjects in order to prevent injuries. Depending on the number of patient/volunteer transfers necessary, purchasing a patient lift sling may prove to be indispensable.

Patients and volunteer subjects participating in a research study that requires the administration of a contrast media intravenously undergoes the intra-catheter placement in the patient preparation room immediately prior to the MRI examination. This prevents using valuable MR system time for this type of preparation that can be time consuming in the event that veins are not easily accessed. It also allows for safe intervention in the event the patient experiences syncope (fainting) or other difficulties with the placement of the intra-catheter or needle.

As previously mentioned, specific instruction for the preparation and placement of earplugs or other hearing protection must be given as well as checking to ensure necessary hearing protection is positioned effectively (1-5). If the MRI examination includes audio delivery via headphones (e.g., fMRI), sanitary covers are required. As hearing damage from exposure to loud noise is cumulative and typically irreversible, this procedure should be given adequate time to complete successfully.

Research MRI studies may involve more than one individual in a family. There may be times when an entire family is present for the MRI examination. If there are small children being imaged, the entire family may be waiting in the patient preparation room or control room in the MRI suite. Therefore, researchers must be on constant alert, monitoring the whereabouts of each of the family members, especially the children. It is helpful to point out to each family member the areas they can and cannot access. For example, “that is the door into the MR system room, so no one enters that room without one of the researchers

826 MRI Safety Policies and Procedures for a Research Facility

taking you in." Additionally, it is a good idea to remind parents and spouses who are not going into the scanner room that they cannot enter the area without being properly screened and prepared even if their child or spouse calls out for them. Keeping the scanner room door closed during these studies is always important to ensure that family members are not accidentally "lured" in by the sight of their child or spouse on the table of the MR system. They should be reminded they are to wait in the patient preparation room or in the control room and not wander about the MRI suite.

POSITIONING AND IMMOBILIZING OF PATIENTS AND VOLUNTEER SUBJECTS

An explanation pertaining to the MR system and the planned examination is highly recommended for all patients and volunteer subjects. This is the critical first step in securing their trust and compliance. This should include a brief explanation describing the scanner, the room, lighting, fan control, intercom system, and use of the emergency squeeze ball.

Instructions should also include the value of maintaining position of the anatomy plus control of breathing and swallowing, if pertinent to the anatomy being imaged. Patients and volunteer subjects should be reminded not to rearrange any of the devices or accessories placed in the MR system (**Figure 7**). If modifications are necessary, the researchers should be immediately notified via the intercom system or squeeze ball to make the requested changes for the patient or volunteer subject. This is especially important for many items including cables and RF coils, mirrors and/or screens used in fMRI studies, GSR (galvanic skin response) or EDA (electrodermal activity) cables, eye trackers, EEG caps and cables, and TMS (transcranial magnetic stimulation) coils.

Pads and sponges are strategically placed to immobilize and comfort the patient or volunteer subject. They are also used to provide safety and prevent burns as previously described (1-6). These procedures are especially critical if the RF body coil is being used to transmit RF energy.

Whenever the patient or volunteer subject is moving into or out of the MR system, the researchers are to closely observe the process to ensure it is completed without injury to the person being scanned or damage to the equipment or accessories. Furthermore, the patients and volunteer subjects should be instructed to notify the researchers via the intercom system and/or squeeze ball if they feel or experience anything uncomfortable or painful. They should be reminded that the fan can be turned on or the speed increased if they become too warm, or blankets can be added if they become too cold.

After leaving the MR system room and returning to the control room, the researcher is to immediately check in with the patient or volunteer subject using the intercom system to inquire about their present state. Continually notifying the patient or volunteer of the upcoming scan time, table (cradle) motion, and pre-scan (tuning) procedure is very important as part of maintaining communication. This will reassure the individual that he or she has not been left alone or abandoned. This communication should take place at the end of each scan to inquire about the patient's or volunteer subject's condition as well as immediately before each subsequent scan, coaching the individual to remain still, breathe quietly, and to

Figure 7. To prevent unwanted interactions and possible excessive heating, volunteer subjects and patients should be reminded that they should not rearrange any devices or accessories placed in the MR system's bore with these individuals. This includes all monitoring devices, visual aids, and RF coils.



relax. The human subjects should be encouraged to alert the operators (researchers or technologists/radiographers) of any discomfort they experience or concerns they may have during the MR examination (5).

During the scanning, visual monitoring of the subject should be constantly maintained in addition to the ongoing verbal communication. This includes the use of remote video cameras inside the scanner room and/or the bore. The human subject (normal, healthy volunteers and patients) should never be left unattended visually to ensure their continued safety (5).

EMERGENCY PROCEDURES

Instruction in emergency procedures is provided to researchers as part of the training for the MRI Safety Policies and Procedures (5). This includes fire and earthquake training but is particularly focused on emergent removal of the patient or volunteer subject from the MR system and the room, itself (e.g., in the event of a magnet quench or patient failure to respond).

The researchers are instructed in the proper evacuation techniques to follow if the patient or volunteer subject should become unresponsive. This includes removing the cradle (table top) from the scanner using the emergency handle that releases it from the “trolley unit” that pulls and pushes the cradle in and out of the scanner. Importantly, for some MR systems

828 MRI Safety Policies and Procedures for a Research Facility

with detachable tables, the cradle must be in the “home” position (moved out of the bore to the end of the table) before the table can be undocked from the front of the MR system and moved out of the room. If the research scanner does not have a patient table that undocks and rolls away from the scanner, an appropriate gurney (i.e., MR Safe or MR Conditional) must be readily available in the MRI suite as well as an appropriate transport board or roller system. The transport board or roller system allows the researchers to safely and quickly move the patient or volunteer subject from the table onto the gurney without experiencing possible injuries.

Selecting the appropriate pedal at the foot end of the table undocks the MRI patient table. On some MR systems, there exists a backup release handle typically located under or near the docking unit at the housing of the scanner. Arm rails should be raised to prevent the patient or volunteer subject from falling off of the table during the transport out of the room to the patient preparation room.

In the case of a serious emergency, one researcher is responsible for calling first responders (e.g., 911) if the MRI research facility is a stand-alone building and not attached to a hospital. This researcher then promptly goes to the front door of the MRI research facility to receive the paramedics and quickly direct them to the appropriate MRI area. The second researcher is responsible for moving the patient or volunteer subject out of the MR system, undocking the table and moving the table into the patient preparation room, closing the scanner room door, and monitoring the individual until the paramedics arrive. Emergent care must never be conducted in the scanner room due to the increased risk of metal objects being brought into the MRI environment, as previously stated. The MRI pre-procedure screening form that was completed by the subject should be made available to the paramedics when they arrive as they will need information regarding current conditions and medications.

For a quench, the procedures include information for a deliberate (controlled) quench (e.g., in a ‘life or death’ situation) and a spontaneous quench (e.g., in the event of an earthquake or substantial problem with the magnet of the MR system) (1-5). Researchers would be responsible to deliberately activate a quench if an individual, for example, is pinned to the magnet by a large metal object and is unable to get loose, and/or has experienced life-threatening injuries. A comprehensive set of instructions with easy-to-follow bullets is posted in the MRI suites for a quench. During hands-on training, the location and function of the quench button is reviewed with researchers. In the event of a spontaneous quench, researchers are instructed to quickly remove the patient or volunteer subject from the scanner and turn on the emergency exhaust fan in the room to remove any collection of helium gas that may form.

INCIDENTAL FINDINGS (POTENTIAL ABNORMALITIES)

Researchers are required to evaluate all MR images reconstructed at the MR system during the examination and those reconstructed off-line as soon as possible to identify motion artifacts, artifacts from other sources, and incidental findings (potential abnormalities). If images acquired during MRI research studies are not routinely transferred to PACS for an interpretation by a radiologist, then specific procedures must be in place for researchers

Figure 8. An example of an Exit Form that is designed to be completed by a patient or volunteer subject immediately after the MRI examination. This information provides a conduit to provide feedback to researchers and those individuals managing the MRI research facility. Additionally, these completed forms provide evidence for the level of safety that is being maintained at the MRI research facility.

EXIT FORM for SCAN SUBJECTS																													
Center MR Research Studies																													
>>PLEASE PRINT CLEARLY & COMPLETE ALL SECTIONS<<																													
Researcher completes this section																													
Magnet:	<input type="checkbox"/> 0.5T	<input type="checkbox"/> 1.5T	<input type="checkbox"/> 3.0T	<input type="checkbox"/> 7.0T																									
Date _____	Researcher name _____	PI name _____																											
Anatomy scanned:	<input type="checkbox"/> Brain	<input type="checkbox"/> Chest	<input type="checkbox"/> Abdomen	<input type="checkbox"/> DC Spine	<input type="checkbox"/> DT Spine																								
	<input type="checkbox"/> Neck	<input type="checkbox"/> Breast	<input type="checkbox"/> Pelvis	<input type="checkbox"/> Shoulder	<input type="checkbox"/> Knee																								
	<input type="checkbox"/> Other: _____																												
Coil:	<input type="checkbox"/> 8 ch Head	<input type="checkbox"/> 32 ch Nova Head	<input type="checkbox"/> 32 ch GE Head	<input type="checkbox"/> 48 ch GE Head																									
	<input type="checkbox"/> 8 ch NeuroVascular	<input type="checkbox"/> 8ch Cardiac Array	<input type="checkbox"/> 16 ch Flex Array	<input type="checkbox"/> 32 ch Torso Array																									
	<input type="checkbox"/> Other: _____																												
Scan subject name: _____	Date of Birth: _____																												
Gender: <input type="checkbox"/> Female	<input type="checkbox"/> Male	Phone # _____																											
Scan subject completes this section																													
On a scale from ☺ (most comfortable) to ☹ (least comfortable):																													
<table border="0"> <thead> <tr> <th colspan="2"></th> <th style="text-align: center;">most</th> <th colspan="2"></th> <th style="text-align: center;">least</th> </tr> </thead> <tbody> <tr> <td colspan="2">How comfortable were you before the scan?</td> <td><input type="checkbox"/> ☺</td> <td><input type="checkbox"/></td> <td><input type="checkbox"/> ☹</td> <td><input type="checkbox"/></td> </tr> <tr> <td colspan="2">How comfortable were you during the scan?</td> <td><input type="checkbox"/> ☺</td> <td><input type="checkbox"/></td> <td><input type="checkbox"/> ☹</td> <td><input type="checkbox"/></td> </tr> <tr> <td colspan="2">How comfortable were you after the scan?</td> <td><input type="checkbox"/> ☺</td> <td><input type="checkbox"/></td> <td><input type="checkbox"/> ☹</td> <td><input type="checkbox"/></td> </tr> </tbody> </table>								most			least	How comfortable were you before the scan?		<input type="checkbox"/> ☺	<input type="checkbox"/>	<input type="checkbox"/> ☹	<input type="checkbox"/>	How comfortable were you during the scan?		<input type="checkbox"/> ☺	<input type="checkbox"/>	<input type="checkbox"/> ☹	<input type="checkbox"/>	How comfortable were you after the scan?		<input type="checkbox"/> ☺	<input type="checkbox"/>	<input type="checkbox"/> ☹	<input type="checkbox"/>
		most			least																								
How comfortable were you before the scan?		<input type="checkbox"/> ☺	<input type="checkbox"/>	<input type="checkbox"/> ☹	<input type="checkbox"/>																								
How comfortable were you during the scan?		<input type="checkbox"/> ☺	<input type="checkbox"/>	<input type="checkbox"/> ☹	<input type="checkbox"/>																								
How comfortable were you after the scan?		<input type="checkbox"/> ☺	<input type="checkbox"/>	<input type="checkbox"/> ☹	<input type="checkbox"/>																								
During the MRI exam did you experience any of the following:																													
Nervousness	<input type="checkbox"/> Yes	<input type="checkbox"/> No	Sleepiness	<input type="checkbox"/> Yes	<input type="checkbox"/> No																								
Muscle Stimulation	<input type="checkbox"/> Yes	<input type="checkbox"/> No	Dizziness	<input type="checkbox"/> Yes	<input type="checkbox"/> No																								
Heat Sensation	<input type="checkbox"/> Yes	<input type="checkbox"/> No	Headache	<input type="checkbox"/> Yes	<input type="checkbox"/> No																								
Changes in vision	<input type="checkbox"/> Yes	<input type="checkbox"/> No	Nausea	<input type="checkbox"/> Yes	<input type="checkbox"/> No																								
Unusual Taste	<input type="checkbox"/> Yes	<input type="checkbox"/> No	Pain	<input type="checkbox"/> Yes	<input type="checkbox"/> No																								
Other _____																													
<hr/> <hr/> <hr/>																													
Signature of Scan Subject: _____																													

830 MRI Safety Policies and Procedures for a Research Facility

to follow in the event of an incidental finding (possible abnormality). Anything that is observed in the images that is suspected of being an incidental finding is reported to the MRI research technologists. A medical record number and accession number are generated, the exam modified, and forwarded to PACS. Results are forwarded to the PI and researcher who conducted the scan. The PI or representative then discusses the report with the patient or volunteer subject and forwards the results to the individual's physician.

The researchers are also required to report to the MRI Manager, MRI research technologists, or lab director any suspicious artifacts present in the images. It is then determined if these fall under potential abnormalities, presence of metal in the body or biomedical implants, system software or hardware issues, or subject-generated (motion) artifacts.

EXIT FORM

All patients and volunteer subjects are required to complete an Exit Form immediately after the MRI examination concludes and before leaving the MRI research facility (**Figure 8**). This form is designed so that the researcher completes the top half of the form while the subject is being scanned, and then the patient or volunteer completes the bottom half. The top half of the form includes the MR system at which they were scanned, RF coil used and anatomy scanned, date, researcher and PI name, and patient/study subject information. The bottom half includes questions regarding medical conditions, medications and treatments, a comfort scale for before, during, and after the MRI examination, and questions regarding nervousness, muscle stimulation, vision changes, unusual taste, dizziness, headache, nausea and pain.

The Exit Form provides the patient and volunteer subject with a conduit to provide feedback to the researchers and those individuals managing the MRI research facility. Importantly, this is valuable information concerning many aspects of the research examinations and the respective scanners. All completed forms are entered into a secure database. This database also provides evidence to the level of safety that is being maintained at a specific MRI research facility.

CONCLUSIONS

Potential risks exist in the MRI environment for, not only the patient or volunteer subject, but also for MRI technologists, healthcare professionals, physicians, and others who only intermittently access the MR system room. This becomes a more complex issue in the research setting because there is often more freedom for a wide variety of individuals present in the facility including researchers and scientists, research assistants, students and post-docs, physicians, visiting scholars, and research and administrative staff. Intermittent but routine visitors to the research MRI facility include manufacturer representatives and scientists from various companies developing products, camera and photography personnel taping for television programs and documentaries, and other specialized healthcare professionals from nursing, anesthesia and respiratory therapy. Insofar as many of these individuals may not be healthcare professionals but investigators engaging in a systematic activity to acquire knowledge, it is often difficult to successfully manage all MRI safety policies and procedures that are set down by the MRI Safety Committee. This requires ongoing moni-

toring of all those using the research scanners including regular verbal and written reminders. This continued one-on-one communication should convey to the researchers a genuine interest in their safety, as well as the patients and volunteer subjects, and the MR system, ancillary equipment, and ultimately, an interest in the successful completion of the research study.

Continuing communication, both facilitated and offered, is a critical tool in maintaining safety in the MRI environment. In addition, any and all assumptions must be entirely removed, as they are certainly the beginning of a dangerous and risky path for all present. As George Bernard Shaw (Irish playwright and a co-founder of the London School of Economics, 1856 to 1950) said, “The single biggest problem in communication is the illusion that it has taken place”.

REFERENCES

1. Kanal E, Barkovich AJ, Bell C, et al. ACR guidance document on MR safe practices: 2013. *J Magn Reson Imaging* 2013;37:501-530.
2. Kanal E, Barkovich AJ, Bell C, et al. ACR guidance document for safe MR practices: 2007. *Am J Roentgenol* 2007;188:1447-74.
3. Shellock FG, Spinazzi A. MRI safety update 2008: Part 2, screening patients for MRI. *Am J Roentgenol* 2008;191:1-10.
4. Shellock FG. Reference Manual for Magnetic Resonance Safety, Implants, and Devices: 2020 Edition. Los Angeles, CA: Biomedical Research Publishing Group; 2020.
5. Calamante F, Faulkner WH Jr, Ittermann B, et al. MR system operator: Recommended minimum requirements for performing MRI in human subjects in a research setting. *J Magn Reson Imaging* 2015;41:899-902.
6. ACR Committee on MR Safety: Greenberg TD, Hoff MN, et al. ACR guidance document on MR safe practices: Updates and critical information 2019. *J Magn Reson Imaging* 2020;51:331-338.
7. Shellock FG, Crues JV. MR procedures: Biologic effects, safety, and patient care. *Radiology* 2004;232:635-652.
8. American Society for Testing and Materials (ASTM) International, Designation: F2503. Standard Practice for Marking Medical Devices and Other Items for Safety in the Magnetic Resonance Environment. ASTM International, West Conshohocken, PA.
9. Woods TO. Standards for medical devices in MRI: Present and future. *J Magn Reson Imaging* 2007;26:1186-1189.
10. Shellock FG. Radiofrequency energy-induced heating during MR procedures: A review. *J Magn Reson Imaging* 2000;12:30-36.
11. Schaefer DJ. Safety aspects of radiofrequency power deposition in magnetic resonance. *Magn Reson Imaging Clin N Am* 1998;6:775-89.
12. Shellock FG. Guest Editorial. Comments on MRI heating tests of critical implants. *J Magn Reson Imaging* 2007;26:1182-1185.
13. <http://www.mrisafety.com>
14. <http://www.IMRSER.org>, website for the Institute for Magnetic Resonance Safety, Education, and Research.
15. Schenck JF. Safety of strong, static magnetic fields. *J Magn Reson Imaging* 2000;12:2-19.
16. Baker KB, Tkach JA, Nyenhuis JA, et al. Evaluation of specific absorption rate as a dosimeter of MRI-Related implant heating. *J Magn Reson Imaging* 2004;20:315-320.

832 MRI Safety Policies and Procedures for a Research Facility

17. Kuhl CK, Träber F, Schild HH. Whole-body high-field-strength (3.0-T) MR imaging in clinical practice. Part I. Technical considerations and clinical applications. *Radiology* 2008;246:675-96.
18. Kuhl CK, Träber F, Gieseke J, et al. Whole-body high-field-strength (3.0-T) MR imaging in clinical practice. Part II. Technical considerations and clinical applications. *Radiology* 2008;247:16-35.
19. Manker, S. Shellock FG. Chapter 24. MRI Safety and Neuromodulation Systems. In: Neuromodulation. E, Peckham P, Hunter P, Rezai, AR, Editors. Academic Press/Elsevier, New York, 2018; pp. 315-337.
20. Schaefer DJ, Bourland JD, Nyenhuis JA. Review of patient safety in time-varying gradient fields. *J Magn Reson Imaging* 2000;12:20-29.
21. Shellock FG. Biomedical implants and devices: Assessment of magnetic field interactions with a 3.0-Tesla MR system. *J Magn Reson Imaging* 2002;16:721-732.
22. Levine GN, Gomes AS, Arai AE, et al. Safety of magnetic resonance imaging in patients with cardiovascular devices: An American Heart Association scientific statement from the Committee on Diagnostic and Interventional Cardiac Catheterization. *Circulation* 2007;116:2878-91.
23. Shinbane J, Colletti P, Shellock FG. MR in patients with pacemakers and ICDs: Defining the Issues. *J Cardiovascular Magnetic Resonance* 2007;9:5-13.
24. Armstrong ML, Elkins L. Body art and MRI. *Am J Nurs* 2005;105:65-6.
25. DeBoer S, Fishman D, Chwals W, Straus C, Amundson T. Body piercing/tattooing and trauma diagnostic imaging: Medical myths vs. realities. *J Trauma Nurs* 2007;14:35-8.
26. Muensterer OJ. Temporary removal of navel piercing jewelry for surgery and imaging studies. *Pediatrics* 2004;114:e384-6.
27. Shellock FG, Karacozoff AM. Detection of implants and other objects using a ferromagnetic detection system: Implications for patient screening prior to MRI. *Am J Roentgenol*. 2013;201:720-5.

Chapter 31 Safety Issues for Interventional MR Systems

DANIEL F. KACHER, M.S.

Biomedical Engineering Department
Brigham and Women's Hospital
Harvard Medical School
Boston, MA

JANICE M. FAIRHURST, B.S., R.T. (R)(MR)

Radiology Department
Brigham and Women's Hospital
Harvard Medical School
Boston, MA

JOSHUA C. VACANTI, M.D.

Anesthesiology Department
Brigham and Women's Hospital
Harvard Medical School
Boston, MA

CLARE M. TEMPANY-AFDHAL, M.D.

Radiology Department
Brigham and Women's Hospital
Harvard Medical School
Boston, MA

SRINIVASAN MUKUNDAN JR, M.D., PH.D.

Radiology Department
Brigham and Women's Hospital
Harvard Medical School
Boston, MA

834 Safety Issues for Interventional MR Systems

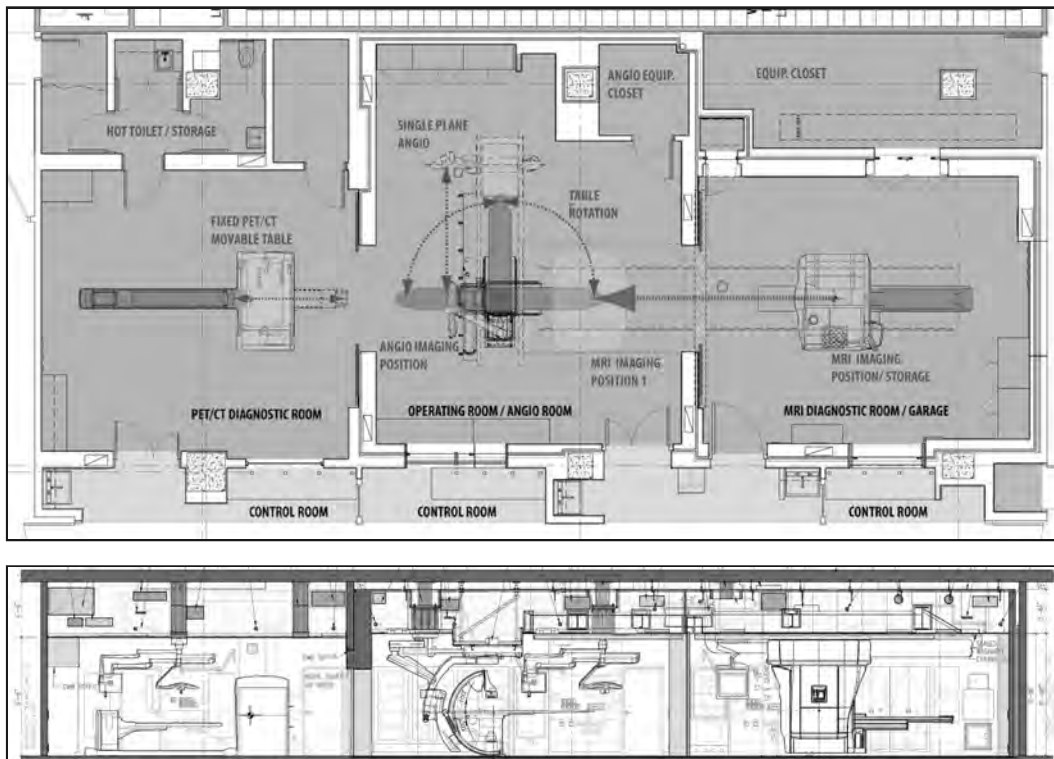
INTRODUCTION

During the last three decades, interventional and intraoperative uses of magnetic resonance imaging (MRI) have evolved into important applications for image-guided therapy and surgical procedures (1, 2). These two unique uses of MRI technology will be referred to as interventional MRI or “iMRI” in this chapter. Because iMRI involves toolsets unlike those used in diagnostic MRI, it presents multiple challenges in designing a safe work environment (3). The complex and unique workflow of therapeutic and surgical procedures performed in the iMRI suite may involve anesthesia and new approaches for perioperative and intraoperative care. These departures from standard uses of MRI requires the safe translation of clinical applications from the interventional suite and the operating room (OR) into the iMRI setting. For example, percutaneous needle-based procedures and thermal ablations (4-6), catheter-based intravascular interventions (7, 8), endoscopies (9, 10), and “open” surgeries (11-14) have special instrumentation and access requirements. The therapy-related armamentarium for each type of procedure can introduce challenges for effective integration into the iMRI environment (15, 16), but also for safe operation. In this active and potentially chaotic setting, assuring safety for patients and staff members is paramount. This chapter presents the most important aspects of safety in the iMRI environment which is based on more than twenty years of experience with multiple types of iMR systems spanning a large number of clinical applications at the Brigham and Women’s Hospital (BWH).

The design of interventional suites and operating rooms requires consideration of various workflow paradigms related to the procedures. If image-guidance is involved, the imaging systems should be closely integrated with the procedural workflow (17). However, since many imaging systems can potentially injure or harm the patient and staff, careful consideration of the unique safety issues are central to the design of safe and effective paradigms. This concern is particularly true in the iMRI environment. Several unique factors must be considered when an iMRI suite is designed and built. Furthermore, when an MR system is located in an OR environment, the requirements are even more complex, since MRI safety must be combined with other patient safety measures (18). If an MR system is co-located with an X-ray system (XMRI), positron emission tomography (PET) system, or computed tomography (CT) system, then MRI safety issues are compounded with concerns regarding system interactions and the use of ionizing radiation (19).

The Advanced Multimodality Image Guided Operating (AMIGO) Suite at the BWH consists of three procedure rooms: (1) the central OR housing the operating table, a ceiling-mounted single-plane X-ray system, a surgical navigation system, surgical microscope, and an ultrasound system, flanked by (2) a positron emission tomography/computed tomography (PET/CT) room on one side, and (3) an MR system room on the other side with integrated cryotherapy, ablative laser, and targeting systems. The 3-T Siemens Verio MR scanner was modified by IMRIS (Minnetonka, MN) to move into the OR via ceiling rails. Sliding “barn” doors separate the PET/CT and MR system rooms from the central OR (20). Each procedure room has a separate entrance to the control corridor and support spaces (**Figure 1**). The complexity of this space results in the inclusion of nearly every safety challenge experienced by other iMRI facilities.

Figure 1. (A) Floor plan showing the size of each procedure room and its respective control room, as well as the equipment in each room and its maneuverability. (B) Cutaway view.



Minimally invasive procedures performed entirely in the MR system room are conducted iteratively, with the patient scanned at isocenter in the scanner, then withdrawn partially from the bore of the MR system in order to undergo the intervention with an “in-and-out” approach. All devices and instruments used in this setting must be MR Safe or MR Conditional.

In contradistinction, a combination of conventional MR Unsafe, ferromagnetic surgical instruments and devices are used in the central OR. Prior to translation of the mobile 3-Tesla iMR system into the central OR for the imaging portion of the procedure, these tools and devices are moved outside of the 5-gauss line or removed from the room, entirely.

To acquire a PET/CT scan during an OR procedure, the patient is shuttled along a removable bridge that connects the OR table with the PET/CT table, through the sliding doors that adjoin the rooms, and into the adjacent stationary PET/CT scanner. Although the MRI risks are absent, the hazards associated with moving an intubated patient with intravenous access are present.

The AMIGO Suite will be used in this chapter as an example to illustrate the safety issues for iMR systems and to propose solutions. The valuable perspectives of other groups related to this topic have been previously published (21-27), and various competing para-

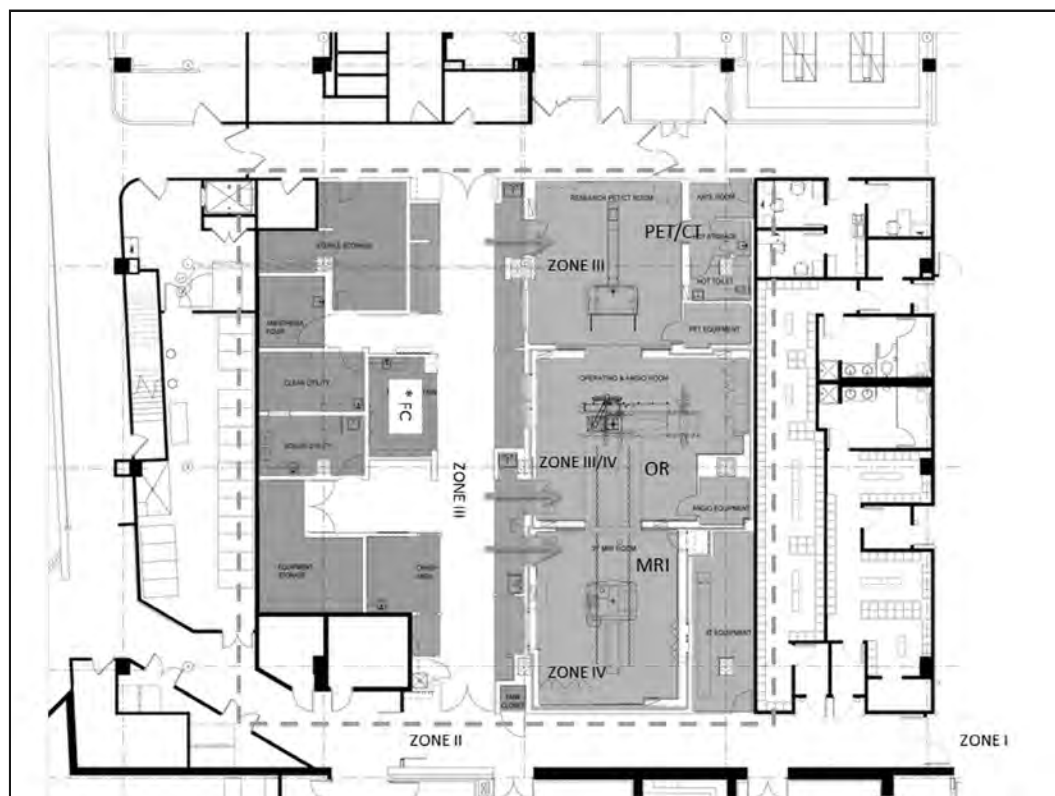
836 Safety Issues for Interventional MR Systems

digms have emerged for suite design and procedural workflow (28). Notably, the scope of iMRI procedures are expanding (29). The facilities built to support iMRI are often unique, reflecting design elements required by the specific purpose of the space. Although safety issues related to iMRI can be challenging, they can be minimized and managed through effective policies, procedures, staff training, access controls, and facility design to promote best practices and the correction of safety lapses.

DESIGNING FOR SAFETY

Architectural design is one useful means of facilitating desired behaviors for MRI safety. Selecting a space remote from the main OR enables the staff to enter the mindset that they are not in their usual working environment and, thus, they must adapt their habits to the iMRI setting. A remote location further limits the flow of staff members, not involved with the procedure, into this particular space. In emergency situations such as codes, the location has both positive and negative attributes. The advantage is that it affords the opportunity to post an MRI Safety Screener at the entrance to ensure that members of the responding team do not enter into the space unless they have undergone screening and determined that they can safely enter the area. The disadvantage of a remote location is the potential delay in the

Figure 2. The floor plan for the AMIGO Suite. (A) Procedure space is to the right of the central corridor and support space is to the left. The ACR designated zones are labeled. The position of the flow coordinator (* FC) is central to the suite. The dashed lines show the boundary of the suite. The arrows indicate the doors into the three procedure rooms.

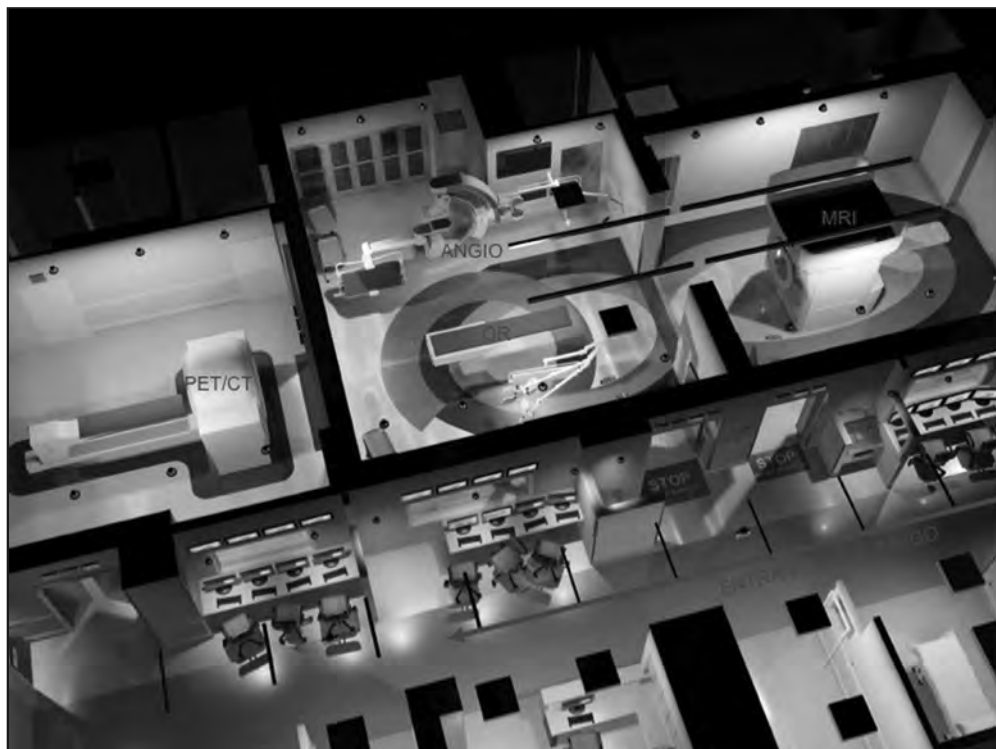


arrival time of the first responders. This can be overcome by local policies such as in the AMIGO Suite, which is located near a cardiology recovery room, where anesthesia staff members from that space, rather than from the more remote hospital OR, are assigned as first responders.

The AMIGO Suite was laid out in accordance with recommendations from the American College of Radiology (ACR) document (30) pertaining to the MRI environment by which the first layer of swipe-card access enables staff members to enter from Zone I (public space) into Zone II (a restricted staff members, gowning area) (**Figure 2**). A second swipe-card access point (**Figure 3A**) is located at the entrance to Zone III (the control room corridor). Access points into Zone II and III are monitored by security cameras connected to the Flow Coordinator's desk and to the hospital's security department.

The MR system room is classified as Zone IV, mandating that MR Unsafe equipment is not allowed to enter the area. Depending on the current location of the MR scanner, the central OR shifts between Zone III (MRI sequestered), where ferromagnetic objects are permitted, and Zone IV (MR system deployed). Before the MR scanner is moved into the central OR, the sliding door that separates the OR from the MR system room is opened to create a single, large radiofrequency (RF) shielded space. Conjoining the spaces enables the MR scanner to move along the ceiling-mounted rails from the MR system room into the central OR. Upon opening the sliding doors, the door between the control corridor and the MR system room automatically locks to prevent staff members from entering the scanner

Figure 2. (B) Perspective rendering of the three procedure rooms (Image provided courtesy of Balazs Lengyel, M.D.).



838 Safety Issues for Interventional MR Systems

Figure 3. (A) Threshold between Zone II and Zone III with lockers for personal belongings.



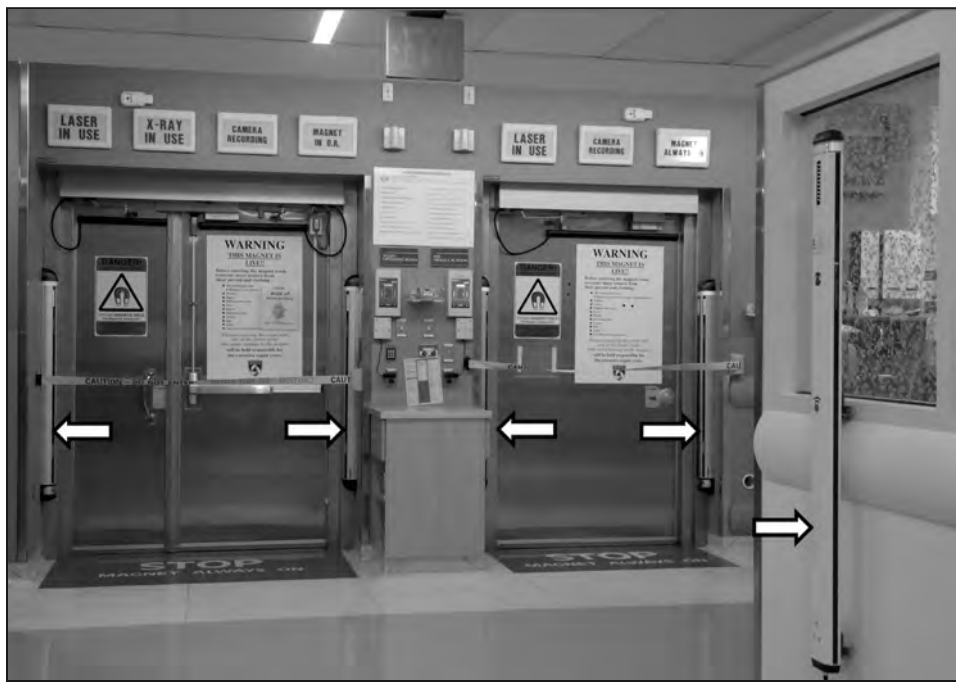
room, resulting in a single entry pathway from the control corridor into the conjoined OR/MR system room.

Additional oversight of this space due to this design results from patients transiting into the appropriate procedure room via the control corridor. This practice is different from typical interventional spaces, such as angiography labs, in which a second doorway into the procedure spaces allows the control rooms to be free of patient traffic. A second entry point in an iMRI suite represents a potential vulnerability, especially if proper line-of-site from the control corridor to the door is obscured and, thus, the desired restriction of staff members' access would be compromised. The complexity of controlling access into the MR system room (Zone IV) is increased at sites (i.e., unlike the AMIGO Suite), where a single scanner services more than one OR.

The doors into the procedure rooms have two operating modes: (1) activation by a push plate, or (2) activation by a keypad code entry. The keypad code is held by only a few core staff members. Controlling or eliminating pathways for the flow of staff members helps to ensure that no MR Unsafe devices or instruments are brought into the room with the MR system, particularly during off hours.

With regard to the AMIGO Suite, a dual-stage ferromagnetic detection (FMD) system was added to the the Zone III control corridor (**Figure 3B**). Although not standard at the time of initial design and construction, the use of such systems has become a standard Facilities Guideline Institute requirement for all future MRI installations. A screening FMD system is located near the flow coordinator's desk that is used for first-stage screening. The second stage screening is accomplished via FMD gates placed near the doors to the procedure spaces.

Figure 3. (B) Ferromagnetic detection systems are positioned at the doors to the procedure rooms and freestanding for screening. Illuminated signage is above the entrances and safety mats are embedded into the floor.



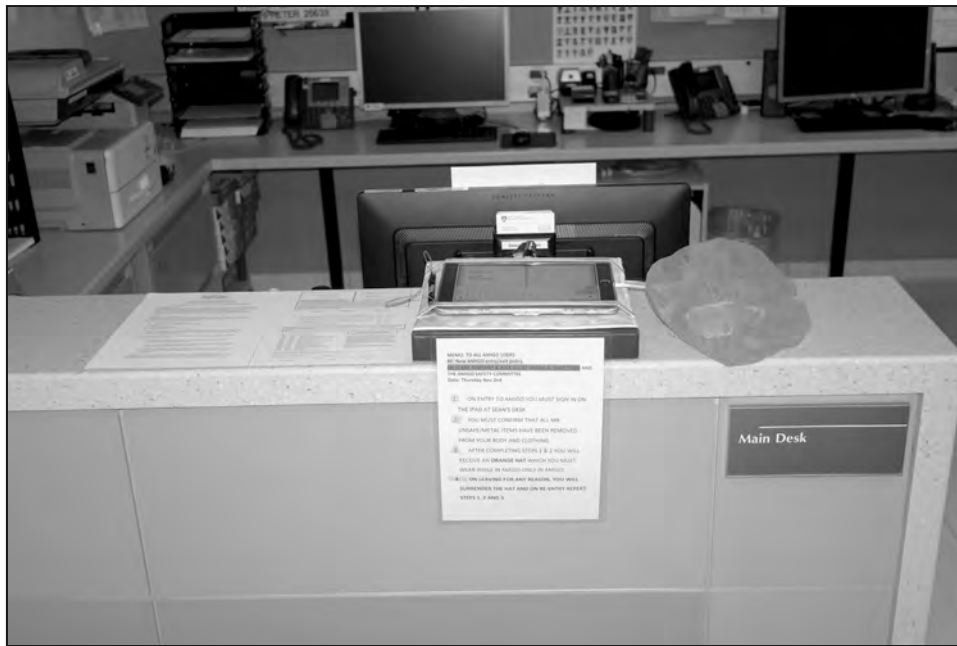
MRI danger signs are posted on doors, along with conspicuous mats that read “Stop! Magnet Always On” are embedded in the flooring. Indicator lights above the doors inform staff members regarding which room the MR system is “parked” in, and when the X-ray machine or the laser is in use (**Figure 3B**). Retractable yellow caution belts bar the door when the respective room is not being utilized. While signage is necessary, in reality, it is seldom effective. Physical barriers such as locked doors and limiting entrances are crucial to mitigate risk in the iMRI environment.

SAFETY POLICIES AND PROCEDURES

Policies and procedures, which can be difficult to standardize, are tailored for site appropriateness. An issue all facilities have in common is the daunting risk inherent to combining medical procedures and iMRI. It has now been many years since the patient fatality (31, 32) that galvanized the MRI community to deal with safety issues centered on diagnostic MRI. Despite policy recommendations and raised awareness since that event (33), there has been an increase in the number of reported accidents related to the MRI environment (34). Recent accidents highlight the continued risk. For example, an experienced staff member was injured at one site (35) and a visitor was fatally wounded at another (36). Risks tend to be greater in the iMRI environment, where ferromagnetic materials such as interventional devices and surgical support equipment are purposely introduced into the environment to facilitate mission critical tasks. In addition to projectile risks, the improper use of necessary equipment can increase the risk of patient burns in association with MRI.

840 Safety Issues for Interventional MR Systems

Figure 3. (C) Immediately following entry to Zone III, staff members must sign in with the Flow Coordinator. Once it is deemed that the staff member is “ferromagnetic free”, an orange bouffant hat is placed over his or her existing head cover to visually indicate a completed screening process.



Whereas suite design can help facilitate safety by limiting or directing the flow within the suite, design alone is incapable of eliminating all hazards. Thus, safety policies and ongoing safety training are required to establish a desired set of acceptable behaviors. As with all policy-based approaches, they are subject to the fallibility of the individual. A clear and effective safety policy is a valuable tool to reduce risk. Establishing a dedicated multidisciplinary core team assigned daily to the iMRI environment is an important factor to formalize, promulgate, and enforce policies and procedures that help to ensure safety within the suite. Primary issues that should be addressed by all iMRI sites include training, access, and safety checklists. Policy governing site-specific issues such as the shared use of space for clinical and research purposes as well as the management of tour groups and vendors should be considered. Other centers have site-specific issues such as the shared use of the installation for interventional and/or intraoperative use and diagnostic imaging (26).

Training and Accreditation

All staff members who work in or have duties that require them to have access to the AMIGO Suite must complete highly specific safety training prior to receiving access to the area. Training and testing ensure that all staff members and vendors working in the suite have a clear understanding of policy and procedures and fully comprehend the potential risks associated with MRI, as well as ionizing radiation hazards in the AMIGO Suite environment. Training modules include a general suite orientation, MRI safety, and general radiation safety. Staff members must pass a written exam on MRI safety and have no contraindications to working in the MRI environment, as documented on an MRI safety

screening form that is reviewed by the MRI Technologist or Flow Coordinator. Upon successful completion of training, a visual indicator is added to the hospital badge. On-line refresher courses are administered on an annual basis.

Staff Member Flow

An accredited staff member will have badge access to gain entry to Zone II. In this area, cell phones, pagers, and other ferromagnetic objects are placed in a day locker. A non-ferromagnetic key to the locker remains with the staff member. Badge access is then used to gain entry into Zone III, at which point it is required to sign in at the Flow Coordinator desk and use the FMD system for screening. After substantiating that no ferromagnetic objects are in their possession, the staff members are provided with orange bouffant hats to wear over their existing OR hat, to indicate that they have been screened and may enter Zone IV (**Figure 3C**). This hat is discarded upon leaving the suite.

Tailored Checklists and Tailored Roles

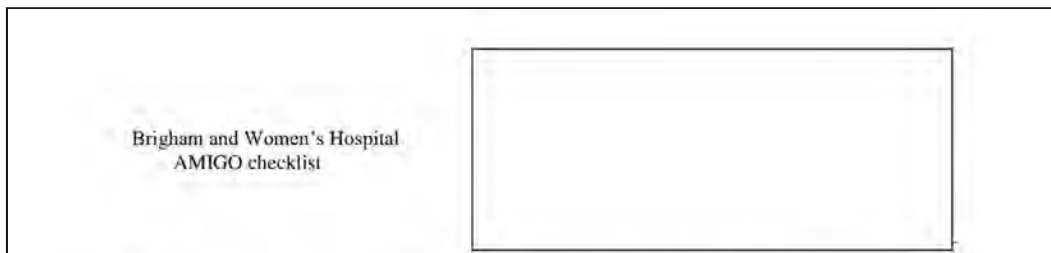
In a typical diagnostic MRI environment, the MRI technologists are the primary staff members tasked with ensuring safety. In the iMRI setting, safety challenges require the inclusion and expertise of a larger, more diverse group. In addition to our core team members who have specific roles for each procedure, it has been necessary to create two new roles whose focus is entirely on safety and compliance within the suite during a procedure.

The first new role is a Safety Screener, stationed at the entrance to the suite between Zone II and Zone III. This team member's job is to ensure that entering staff have complied with requirements to place ferromagnetic items in the day locker. The Flow Coordinator sits at a central location in the suite, and has camera views of the Zone I to Zone II transition, as well as the Zone II to Zone III transition. The Flow Coordinator is responsible for maintaining a sign-in list of all staff members present for a procedure and verifies that individuals entering the AMIGO Suite have undergone all necessary training (by cross-reference to a training database), are properly attired, have removed ferromagnetic items from their person, and have undergone screening using the ferromagnetic detection system. This team member also screens vendors and visitors for contraindications to be in the MRI environment. Another core staff member is stationed facing the entrance into Zone IV to ensure the approved workflow is not broken and no non-approved items are brought into the OR or MR system rooms. The Safety Nurse is responsible for knowing the roles and background of all staff members in the procedure and adjoining space. The Safety Nurse is charged with tracking when and why each device and instrument kit is introduced into the procedure, and ensuring that unneeded equipment is not admitted into the area. He or she administers the safety checklists in conjunction with the MRI Technologist.

In addition to the World Health Organization Surgical Safety Pause performed at intervals in all surgeries (37), an MRI Safety Pause has been instituted to mitigate risks prior to bringing the patient into the MR system room or the adjoining OR, as well as prior to transferring the MR scanner into the OR. **Figure 4** shows the respective checklists. Each procedure has a checklist tailored to the attending equipment and instruments and is modified to adapt to changes in the procedure as it evolves. The MRI status of each device is noted and

842 Safety Issues for Interventional MR Systems

Figure 4. (A) Checklist used during “pause” before the patient is brought into iMR system room or the adjoining OR.

 Brigham and Women's Hospital AMIGO checklist	
<u>Pre-Procedure MRI Safety Checklist – Before Entering OR or MRI Room</u>	
ACTION	Verified
Patient screened at Metrasens stand up screener in CVRR	MR Tech/RN
Confirm patient is on MR safe stretcher	MR Tech/RN
MR patient screening form completed	MR Tech/RN
Jewelry & ferrous items removed	MR Tech/RN
Eyeglasses <input type="checkbox"/> Dentures <input type="checkbox"/> Hearing-aid <input type="checkbox"/> Medication Patch <input type="checkbox"/> removed	MR Tech/RN
Shaving completed	MR Tech/RN
All staples/paperclips removed from chart/forms that will enter room	MR Tech/RN
OR Staff have signed in to front desk: All ferrous items have been removed (pager, phone etc) and obtained orange hat; Self pat-down completed	MR Tech/RN
Signature: _____ RN circulator	
Signature: _____ MRI Tech	
Date: _____ MM/DD/YYYY	

appropriate actions are taken to ensure safety and artifact free imaging, such as de-activating electrical outlets powering certain devices.

Before moving the MR scanner into the OR, ceiling-mounted booms, lights, and monitors are pivoted outside the 5-gauss line towards the walls where rails have been installed as tether points. Large, MR Unsafe devices are removed from the room (e.g., surgical mi-

MRI Bioeffects, Safety, and Patient Management 843

Figure 4. (B) Checklist used during “pause” prior to bringing the ceiling mounted mobile 3-T MR system into the OR.

<u>NEURO Checklist for Moving Magnet into OR</u>			
	Surgical Planning Image	Intra-op Image	Post-op Image
SELF PAT DOWN PERFORMED BY EACH TEAM MEMBER			
Patient Safety Check			
<ul style="list-style-type: none"> • MRI coil is not touching patient • No direct skin to skin contact • Foley catheter is draining; metal clamp removed • Surgical clipper/head is removed from room • Confirm ear plugs in place • Remove ESU return electrode (grounding pad) • Bair Hugger hose removed • SCD sleeves disconnected 			
Confirm Surgical Counts are done			
<ul style="list-style-type: none"> • Remove all instruments, needles, sharps, small accessories/countables from surgical field • Perform counts of above ferrous items & verbally report and document that counts correct • Neuro Wire and Lead counts correct • Patient cleared by RN/MRI tech 			
Move ALL equipment outside 5 gauss line			
<ul style="list-style-type: none"> • All equip microscope, US, workstation out of room • All Booms • All Lights moved • Brain lab moved • Angio foot pedal TIED down *** bed base cleared 			
Anesthesia safety check			
<ul style="list-style-type: none"> • MRidium infusion system safe outside 10,000 Gauss line • Anesthesia Doppler out of room • Twitch monitor in holder outside 5 Gauss line • Laryngoscope blade and hand pieces and needles accounted for and on anesthesia cart • Arterial transducer secured • Check wave guide for cords 			
Self pat-down performed by each team member			
Final Safety Check completed: RN & MRI Tech Verbal OK & Initials RN Signature _____ <ul style="list-style-type: none"> • MRI Tech Signature _____ • _____ 			

croscope, ultrasound system, navigation system). Additional safety activities include confirming that the patient’s hearing protection is in place and that the monopolar electrosurgical unit return electrode is removed, which may be a risk for an MRI-induced patient burn

844 Safety Issues for Interventional MR Systems

due to the conductive foil backing. The checklist mandates an accurate instrument count, since consequences of an inaccurate count are increased in the iMRI environment. A ferromagnetic tool left in the surgical field can become a projectile when the patient enters the bore of the scanner. If a metallic tool is touching the patient, an image artifact or even a burn can occur. Although not implemented at our facility, technology is evolving for automated counting of instruments that can help identify errors (38, 39).

The MRI Technologist is also tasked with screening the patient prior to the procedure, with the help of nurses and the surgical team. The MRI technologist may reference literature and established criteria to confirm that an implant can be safely imaged. He or she may consult the institutional MRI Safety Team, including the MR Medical Director (Physician), MR Safety Expert (Physicist), and MR Safety Officer (Technologist), as needed. Another role of the MRI technologist is to collect MRI data, sometimes in conjunction with an MRI physicist, and to gather vendor claims about a new device for review by an internal committee before it is used in proximity to the MR system.

The watchful eyes and constant communication involving the Safety Screener, Flow Coordinator, MRI Technologist, Safety Nurse and other staff members associated with the procedure have prevented many potential errors in the ten years of operation of the AMIGO Suite to build on the successful twenty-six year iMRI history at BWH.

Emergency Response

Staff members including anesthesiologists, nurses, surgeons, interventionalists, radiologists, and MRI technologists should be trained to respond to cardiopulmonary emergencies that may occur either in the MR scanner room or in the OR when the MR system is present. Mock emergency code drills (e.g., code blue) are important for refining the processes and to gain comfort levels surrounding the different situations. Policy and education should exist to prevent responders from other areas from bringing ferromagnetic materials and equipment into any space in which the MR scanner is deployed. Conversely, first responders should not be delayed from assisting the medical team if the MR system is safely sequestered.

In the AMIGO Suite, the emergency code button has a different meaning from the code button in other areas of the hospital. A special MRI-trained team with swipe-card access responds to the emergency. Although there are devices in development for resuscitation in the MR system room, none are yet commercially available (40, 41). Therefore, the patient undergoing an intervention in the MR system room (Zone IV) is immediately removed from the room and brought to a designated resuscitation area within the suite in Zone III. Some scanners have break-away tables that can serve as a transport table. Scanners with fixed tables require that the patient is transferred to an MR Safe or MR Conditional stretcher. A designated team member should be responsible for shutting and locking the door to the MR system room and maintaining access restrictions, while other staff members expeditiously move the patient to the resuscitation area. The area should have adequate space, monitoring equipment, oxygen, suction, and electrical outlets to facilitate resuscitation and management of the patient.

If the MR system is in the OR when an emergency occurs, the scanner must be expeditiously removed from the OR, and the doors to the MR system room must be closed and locked. Once the scanner has been removed from the OR, the crash cart, defibrillator, and other resuscitation equipment can then enter the OR area.

Although known difficult intubation or prior history of allergic reaction to medication or a contrast agent can be addressed prior to entering the MR system room (Zone IV), unanticipated difficult intubation or an anaphylactic reaction that the patient may experience requires rapid action and exit from this area.

The oxygen used in the OR setting as well as therapeutic heat sources (e.g., laser) increase the risk of fire. Non-ferromagnetic fire extinguishers are available for management of small fires. In the rare event of a magnet quench, out gassing of cryogens (helium) can displace the oxygen in the adjacent spaces. Sites should have a plan for rapid removal of patients in these life-threatening situations, even when there is no time to close a surgical wound. To minimize this risk, inspection of the quench line should be performed at intervals, similar to diagnostic MR systems.

Screening

Patient screening must be conducted by a Level 2 MR Personnel, MRI safety-trained staff member (42, 43), and potential contraindications should be reviewed by the institution's MRI safety team. The screening form combined with a verbal interview will help to rule out contraindications for MRI procedures such as certain electronically-activated implants and ferromagnetic aneurysm clips. Staff members who work in the iMRI suite should be subjected to the same screening procedure. However, since the staff members will not be imaged, some contraindications (e.g., body piercing jewelry, joint replacement, etc.) do not need to be considered. Screening forms designed for patients and other individuals (i.e., staff members, visitors, etc.) may be obtained from the website, www.MRIsafety.com. Patients should change into a hospital gown as per surgical standard of care. External hearing aids, hairpins, barrettes, jewelry (including body piercings), analog watches, metal-based medication patches, MR Unsafe electrocardiogram (ECG) electrodes from previous inpatient examinations, and similar items should be removed prior to entering the MR system room or central OR.

Procedure Vetting Process

All procedures in the AMIGO Suite are performed under Institutional Review Board (IRB) approval. An application describing the procedure, focusing on the impact that image guidance is likely to have on patient outcomes, is required. An internal and external panel reviews the application and refines the proposed procedure. This process forces clinicians to invest their time learning about the MRI environment.

The next step in preparation for a new iMRI procedure is to conduct multiple mock procedures to refine workflow, decrease procedure time, and to do a gap analysis on devices and instruments. All staff members who will be involved in the case must be present for these sessions. Failure Mode and Effects Analysis can be applied to identify and address areas of concern. Volunteer imaging and MRI protocol development is typically done out-

846 Safety Issues for Interventional MR Systems

side of these sessions for the sake of brevity. Team building and cohesion as well as the creation of a culture of safety occur during this crucial period. In these mock sessions, procedure specific MRI safety checklists are developed and tailored to include both equipment and work flow. These safety checklists are reviewed in the OR before the MR system enters the room.

Patient Positioning

There is often a compromise between the ideal imaging position and the ideal surgical or interventional position for the patient. The ideal positioning centers the anatomy in the “sweet spot” of the magnet to enable imaging without distortion artifacts related to off-isocenter positioning. Sweet spot dimensions vary across MR systems but are typically 30- to 50-cm ellipsoids.

In many iMRI cases, the patient will be under general anesthesia and unable to move. Therefore, it is essential that the patient be positioned properly and placed in a suitable alignment. All pressure points should be appropriately padded to maintain good circulation for the patient. Padding must be used to eliminate closed loops created by skin-to-skin contact areas or contact between the skin and an ECG lead or the cable used with the RF coil (43). The integrity of the insulation and/or housing of all components, including RF coils, leads, cables, and wires need to be regularly checked.

SAFETY STANDARDS AND TESTING

Labeling

The American Society for Testing and Materials (ASTM) International has designated definitions (i.e., terminology) for labeling devices, as follows MR Safe, MR Conditional, and MR Unsafe (44). At our institution, candidate instruments for a procedure are tested with a powerful handheld magnet by the nurse, MRI technologist, or MRI physicist before being added to the instrument kit. Instruments used in the OR can be ferromagnetic since they can be safely positioned before the MR scanner is transferred into the OR. In the AMIGO Suite, instruments used in the MR system room must pass ASTM International standard F2052 testing (45), which determines if a handheld instrument or device has the potential to become a projectile in the presence of the magnetic field and involves testing for translational attraction (**Figure 5**). While the worst-case location is specific to the model of the MR system, even for scanners operating at the same field strength (e.g., Siemens 3-Tesla Skyra versus Siemens 3-Tesla Prisma), this position tends to be in the proximity of the opening of the bore of the MR system.

Many of the devices used in the OR are MR Unsafe but are appropriately managed before the MR system enters the room. In the scanner room, an RF enclosure recessed in the wall was designed into the architecture to house MR Unsafe equipment. Waveguides in this enclosure provide an opening for intravenous (IV) tubing, a patient temperature control, hot air hose, and pneumatic tubing for deep vein thrombosis prevention boots. Devices in proximity to the scanner’s bore must be MR Safe or MR Conditional. Sites that perform procedures in the periphery of the MR system room on a second table using MR Unsafe in-

Figure 5. MRI testing conducted to determine if a ferromagnetic object will become a projectile in the presence of the static magnetic field of the MR system. A deflection angle above 45 degrees indicates that the magnetic force is greater than the force of gravity, resulting in a “fail” for this test.

- (A) An RFID tag attached to a surgical sponge, passing the deflection angle criteria.
 (B) The same RFID tag without the added mass of the sponge, failed the test.



struments and devices must enact strict guidelines to specify the zones where such items must remain (46).

Other international standards are used to test biomedical implants for torque (47), radiofrequency (RF)-induced heating (48), image artifact (49), and safety for active implants such cardiac pacemakers and neuromodulation systems (50). Although these standards are useful for implants, specific standards and procedures are needed for the task of evaluating items used in iMRI (e.g., robotic actuators, head fixation systems, infusion pumps, AC/DC power adaptors, biopsy trajectory devices, patient positioning devices, etc.) but, at the present time, they do not exist. The MR system manufacturers have their own tests for device evaluation. Accordingly, the end-user is largely reliant on the vendor for providing information for a given device. This information may be distributed by various means including the device user manual, vendor-issued bulletins, and labels on the device, itself. As always, the term MR Conditional has specific meaning on a per device basis, requiring the user to be sophisticated enough to understand the meanings.

In the AMIGO Suite, a dedicated anesthesia technologist manages and appropriately positions MR Conditional and MR Unsafe anesthesia equipment and devices. As an example of the complexity, a device console may have a different maximum permissible field strength where it can be safely used, which is different from the limit for the AC/DC adaptor that powers it. It is the nature of some surgeries that the anesthesia set-up may be at the patient’s left or right based on the surgical approach. As such, equipment is regularly moved. Human vigilance is essential for preventing error. If this process were managed by a larger non-dedicated group of staff members, the likelihood of error would increase.

848 Safety Issues for Interventional MR Systems

Labeling claims are frequently specific to tested conditions, such as the strength of the static magnetic field, the spatial gradient of the magnetic field, imaging gradient slew rate and amplitude, specific absorption rate (SAR), and configuration or position of the device (e.g., parallel or perpendicular to the bore, proximity to the wall of the bore, routing for cables, etc.). Notably, after an equipment upgrade or change to the environment, testing results may no longer be applicable. Kugal (51) has reviewed the risks inherent to the static magnetic field, gradient fields, RF field, and cryogens through the lens of iMRI safety.

The American College of Radiology (ACR) takes the position that, "... users need to recognize that one should never assume MR compatibility or safety information about a device if it is not clearly documented in writing" (30). Practices at the AMIGO Suite reflect an amplification of this recommendation but verify even written vendor claims, because some claims are inaccurate or do not apply to a given MRI setting. If in-house expertise exists, a set of tests can be performed to confirm vendor claims or establish the level of safety of an instrument or device (52).

Static Magnetic Field-Related Issues

Although the adverse events associated with diagnostic MRI that are most frequently reported in the Food and Drug Administration's (FDA) Manufacturer and User Facility Device Experience (MAUDE) database and in the United Kingdom (53) are due to burns, the greatest safety concern in environments where MRI-guided open surgeries (e.g., breast, brain, and spine) are performed is the static magnetic field. Such procedures may require the use of MR Unsafe items such as surgical microscopes, electrosurgical units, and light sources. The effect of the static magnetic field drastically increases with proximity to the bore of the MR system. This sudden change in translational attraction gives little warning to a staff member holding a ferromagnetic object as he or she approaches the scanner. Lines indicating the fringe field levels associated with the MR system can be marked on the floor around the scanner to serve as a visual reminder to staff members. In the AMIGO Suite, the 5-gauss fringe field is marked on the floor. The 400-gauss field line is also shown to indicate the limit for the particular anesthesia machine utilized in this setting. The MR system used in the AMIGO Suite can be offset and rotated 180-degrees to enable additional procedural workflows in the scanner room. Therefore, the fringe field markings on the floor are a worst-case superposition of the lines for the two different imaging locations. A second set of lines is present in the OR to depict the fringe field when the scanner is at its third imaging location (**Figure 5A**). The relationship between the isogauss lines and the force exerted on an object has been carefully studied at our institution (54).

Translational attraction and torque constitute the greatest risks in the MRI setting. An object may become a projectile as it accelerates in the direction of the spatial gradient of the static magnetic field. Large objects can generate incredible force as they are rapidly drawn into the magnet. As previously stated, our practice is to test all devices, even with MR Safe labels, using a powerful handheld magnet. Additionally, we cautiously introduce larger items into the MR system room with a tether, if necessary, and follow other appropriate procedures to conduct a proper evaluation of magnetic field interactions.

For facilities performing surgery very close to the MR system or with the patient's head protruding from the rear of the scanner, MR Safe or MR Conditional instruments are nec-

essary. Titanium alloy and ceramic materials are not subjected to magnetic field interactions and cause relatively small artifacts that are the direct result of their negligible magnetic susceptibilities. Various vendors at points in time have produced instruments for the iMRI market (15). Understandably, costs and lead times for these instruments are higher than for conventional instruments. Fortunately, some conventional off-the-shelf instruments are constructed from titanium due to the material's inherent advantage of being lower in weight compared to steel.

Image Artifacts Caused by a Device

Electromagnetic interference (EMI) emanating from an active device can manifest in the MR image as a zipper artifact or increased noise across the entire image, depending on the bandwidth of the noise and of the MR system's receiver bandwidth. Vendors may erroneously assume that because their device passes EMI tests at a higher field strength/frequency, their test results can be extended to lower field strengths/frequencies. However, EMI harmonics may be present in the imaging bandwidth at one field strength, but not another. The user may learn this when a patient is undergoing MRI and a zipper artifact obscures the critical anatomy of interest.

EMI testing may be performed by running the MR system manufacturer's quality assurance scans for noise with and without the device present. The device can be activated, in a stand-by mode, or "off" but plugged in, depending on its state in the clinical setting during imaging. The frequency of the zipper can be identified and can be useful in tracing the source in the electronics. A zipper drifting in frequency usually indicates the source of EMI is the electronics associated with a digital clock in the device. The EMI revealed by such scans may have low enough energy as to not be clinically relevant, so scans from a clinical protocol should also be tested. At our institution, variations in shielding of MR Conditional devices has yielded one instance of a device that did not emit EMI and another that was problematic. A complicated issue, however, is the interactivity of multiple devices. EMI from one device can be carried or amplified by another device resulting in image artifacts when the devices used individually are not problematic. Moreover, EMI from a device may be a function of position within the room. The device may pick up and amplify EMI from a leaky penetration panel, window, or other vulnerable point in the RF shielding. A device placed in the line-of-site of the receive RF coil may induce a zipper artifact, whereas the same device placed on the side of the scanner may not be problematic. A spectrum analyzer with a sniffer loop is a valuable tool in identifying EMI sources. These analyzers are not MR Safe, so long cables are required.

Image artifacts can be assessed in phantoms by imaging with and without the device under test present. Distortion or signal void due to susceptibility mismatch between the object and the surrounding medium can be evaluated (55). An artifact observed on an MR image is a function of field strength/frequency, pulse sequence parameters (mainly receiver bandwidth and echo time), and the orientation of the object to the static magnetic field of the MR system. Artifacts can change the apparent location of the device, which for example can give rise to inaccurate or unsafe needle targeting associated with a biopsy procedure (56). In open surgery, the susceptibility mismatch between air and tissue can appear as a region of hyperintensity that can mimic contrast-enhanced tissue (57).

850 Safety Issues for Interventional MR Systems

Currents induced by the imaging gradients can interact with the static magnetic field and cause vibrations in a device, which can create ghosting in the image. The coupling of electrically conductive structures with the electromagnetic field can result in signal shielding. Such RF-related artifacts can compromise visualization of the lumen in the presence of a vascular stent (58).

Artifacts can lead to image misinterpretation due to distortion of geometry, or regionally obscuring or obliterating the signal from tissue. The degree of acceptable artifact is subject to the judgment of the physician performing the procedure and the radiologist interpreting the images. If contrast administration during brain tumor resection is repeated, images may be difficult to interpret due to the continued spread of contrast throughout the edematous brain. This problem is not experienced in a comparatively brief diagnostic MRI session. To avoid this problem, some centers reserve the administration of an intravenous contrast agent until the tumor has been resected and then use imaging to assess the completeness of the surgery (59).

Unintentional Output and Operational Inhibition of Devices

It should be confirmed that the static magnetic field, imaging gradients, and RF pulses do not impact the function of the device. For example, one model of an MR Conditional physiological monitor had design issues with the motor that inflates the blood pressure cuff. Long-term exposure to the static magnetic field impacted the motor's performance and resulted in the feature being unusable.

The imaging gradients can create a field switching at about 100-Hz to several kilohertz. For the time-varying, gradient magnetic fields, the worst-case scenario location for testing is not at isocenter of the MR system. The fields due to the imaging gradients increase proportional to the distance from isocenter and then fall off outside of the field of view. The peak field is about 30-cm from isocenter and varies across different scanners depending on the features of the gradient coils. The time-varying, gradient magnetic fields can induce eddy currents in the patient and in conducting materials, but is generally not a concern for substantial heating. However, the induced currents in devices can interact with the static magnetic field, creating forces and torques on the device. If the device vibrates and is in contact with the patient, image artifacts can occur. If the device is a part of a positioning stage for needle targeting and the gradients cause vibrations in a component of the device, inaccuracies may occur.

Heating

Devices and instruments that are left in contact with the patient during scanning must be tested for MRI-induced heating. Current safety guidelines for patients that do not consider the presence of devices limit temperature increases in the torso to 2°C or a peak specific absorption rate (SAR) of 8- to 10-W/kg. The whole-body-averaged SAR is limited to 4-W/kg in the body, and 3.2-W/kg in the head over a 15-minute period (60, 61). RF energy associated with MRI is a concern for heating due to ohmic heating. As previously indicated, most MRI-related adverse events are due to RF-induced patient burns (62).

The transmit RF body coil runs almost the entire length of the bore of the MR system. The worst-case locations occur where the electric field (as opposed to the magnetic field used to create the MR image) is highest. This field tends to be highest closest to the conductors and is impacted by RF coil geometry. Any conductor in or near the transmit RF coil, including the patient, has the potential to be involved in RF-induced heating.

Cables should be padded to eliminate contact with the patient's skin or, if possible, removed during scanning. As a preventive measure, a cold compress or ice pack can be applied to areas potentially affected by heating. While rare, skin-to-skin contact points should be avoided, since these have been reported to be associated with burns (63). Precautions to prevent excessive heating are of particular importance for patients under sedation or general anesthesia who are unable to notice or report pain. Heating may be minimized with the use of a local transmit RF coil (e.g., quadrature head coil) instead of the body RF coil and judicious selection of pulse sequences and parameters to limit the SAR (65).

A fiber-optic temperature measurement device with multiple probes is necessary to accurately test for heating. When evaluating MRI-related heated for an implant or device, probes should be placed on or near corners and tips, as well as other discontinuities where the electric field tends to be the highest (66). The design that is used for the phantom to simulate the patient for a proper heating assessment is critical. Importantly, a device in free space will behave differently than a device that is in contact with the patient. For example, our team assessed a carbon-fiber, Jackson table used for positioning patients undergoing spine surgery. No heating was measured with the square piece of material in isolation. When a tissue equivalent load was placed at the corner, a notable temperature elevation was observed.

Temperature elevations that occur in long conducting wires of a certain length can be sudden and extreme, especially at the tip of the wire. Our team observed a 50°C temperature elevation after five seconds of MR imaging in the cable of a non-MR Conditional RF ablation probe. Obviously, solutions to this problem are needed to enable the use of devices for vascular interventions and other procedures (67-69).

Occupational Considerations

Some staff members have reported that, while moving their heads close to the bore of the scanner or having their heads in the bore of the scanner during activation of the gradients, they experience reversible side effects such as nausea, vertigo, magnetophosphenes (flashes of light), or metallic taste. Therefore, clinicians planning to perform iMRI procedures should be assessed for these possible issues to determine if such sensations will be problematic. Legislation in the European Union initially placed constraints that would prohibit real-time intervention close to the bore of the MR scanner. Fortunately, after an appeal by the MRI community (70, 71), it was replaced by legislation providing a provision for iMRI (72).

SAFETY IMPLICATIONS FOR ROOM CONFIGURATION

Approaches for the iMRI suite layout include a dual room environment in which the MR system room and procedure room are separated and a single room where the imaging and procedural environments are co-located. The advantage of the dual room solution is

852 Safety Issues for Interventional MR Systems

Figure 6. (A) The fringe field lines of the MR system depicted on the floor of the OR. **(B) to E)** The AMIGO staff transforming the environment to prepare for the entry of the IMRIS MR system on the ceiling-track.

Figure 6 (A)

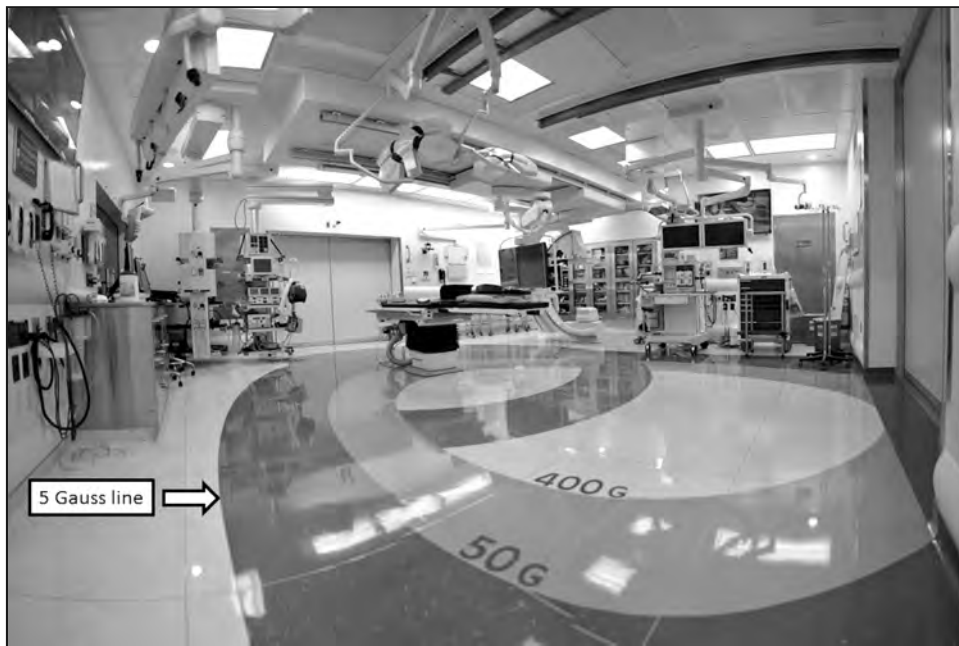


Figure 6 (B)



Figure 6 (C)



Figure 6 (D)



854 Safety Issues for Interventional MR Systems

Figure 6 (E)



that the procedure room is a more familiar setting to the surgeon or interventionalist. In the absence of the static magnetic field, conventional MR Unsafe equipment like a surgical microscope, ultrasound system, and steel instruments can be used. Great care must be taken to manage all devices and instruments before performing MR imaging. As in the AMIGO Suite, before the mobile MR system is translated on ceiling rails into the procedure room, MR Unsafe ceiling-mounted booms, lights, and monitors are pivoted to the walls and other MR Unsafe items are either brought out of the room or moved outside the 5-gauss line (**Figure 6**).

Alternatively, with other approaches, the patient can be moved from the OR into the MR system room. The same time out and procedure-specific checklists must be completed prior to moving the patient from the OR into the MR scanner room. In addition to the risk of unaccounted for items becoming projectiles when the patient is moved, there is a risk of extubation or extravasation due to tension on the breathing circuit or intravenous lines, respectively. The anesthesia machine and physiological monitor are tethered by interfaces to the patient and, therefore, these devices must move as a unit with the patient table. A solution to mount the cable connection point for the physiological monitor to the patient table is available. Efforts have also been made to couple a defeatured anesthesia machine to the table to avoid cable tension during transfer (73).

A commonality across original equipment manufacturers is that the patient stays on a rigid transfer board for the entire procedure. The transfer board is MR Safe and is integrated with both the MR system platform and the surgical table platform. Multiple vendors have variants on the transfer approach. In one case, a manually moved transfer table end-docks with the surgical table, collects the transfer board/patient, then moves into the MR system

room where it docks with the scanner for imaging (**Figure 7**). In another variant, the surgical table moves along a floor track to dock with the MRI table before transferring the patient from one table to the other with the transfer board (26) (**Figure 8**). Single room approaches use a similar transfer concept or have a table that pivots out of the scanner into an area with a relatively low fringe field, where surgery is performed (46, 74) (**Figure 9**).

The advantage of the single room solution is the rapid turn around between imaging and intervention. This gain comes at the expense of using MR Safe or MR Conditional equipment and regaining needed functionality through ingenuity, or omitting the functionality, potentially compromising the procedure. Alternatively, MR Unsafe devices can be used while managing risk. To minimize patient movement, neurosurgical procedures can be performed with the in-and-out paradigm, in which the patient's head extends from the back of the bore of the scanner to permit the surgical procedure and then back into the MR system for imaging. MR imaging can be achieved by moving the patient approximately one-meter to isocenter (75) (**Figure 10**). Similarly, abdominal interventions can be performed with this same in-and-out paradigm.

Figure 7. Patient transfer solution in which the MR system table end-docks to the OR table, collects the transfer board and patient, and delivers the patient to the MR system. In some variants, a third trolley serves as the transport mechanism between tables.



Figure 8. Patient transfer solution in which the OR table travels to the MR system on floor tracks. The table top and patient move into the scanner as a unit.

856 Safety Issues for Interventional MR Systems

Figure 9. A single room solution in which the patient table pivots to receive the transfer board. The navigation system is ceiling mounted on the ceiling to avoid magnetic attraction. A solid marking and a striped marking on the floor depict the 5-gauss (0.5mT) and 50-gauss (5mT) isogauss lines, respectively (Adapted from Reference 46.)



Procedures can also take place in the horizontal gap of a standard “open” scanner (**Figure 11**). A 0.5-Tesla vertically-open MR system (Signa SP, General Electric Medical Systems) has been able to support a multitude of procedures without moving the patient (3, 4). A head only 0.15-Tesla was also produced to support neurosurgeries (76). However, both of these products were discontinued. The different scanner architectures of MR systems have been compared and contrasted for applicability in iMRI (28, 77).

Multi-modality environments are emerging in which the MR system is coupled with other imaging modalities in the vicinity to complement capabilities (19). The AMIGO Suite is flanked by an MR system room and a PET/CT scanner (**Figure 12**). MR Conditional electrocardiogram (ECG) electrodes, physiological monitoring equipment, and the anesthesia machine are used in the PET/CT room to avoid MR Unsafe devices from entering the area, as well as to obviate logistics regarding which devices can be used if the operating physician calls for an MRI exam.

ANESTHESIA DELIVERY IN THE MRI ENVIRONMENT

All of the anesthesia concerns in the diagnostic MRI environment are present in the interventional/intraoperative environment. A patient receiving anesthesia in the iMRI environment is at a higher risk than a patient undergoing anesthesia in a conventional setting (78-82). Therefore, a facility planning member from the Department of Anesthesia is critical for identifying and minimizing risks in the iMRI setting.

The electromagnetic fields used with MRI necessitates that all monitors and devices be MR Conditional. Not all available devices used in the conventional setting are mirrored in the iMRI environment. It is critical that anesthesia staff members cycle through the area frequently enough to maintain competency on these devices which are not encountered elsewhere in the institution, as well as to maintain awareness of MRI safe practices. Backup

Figure 10. Neurosurgery being performed with the patient's head extended from the rear of the MR system's bore.



Figure 11. Interventional procedure being performed in a standard horizontal gap, open MR system.

Figure 12. Bridge and transfer board solution used between the AMIGO Suite OR table and the PET/CT scanner.



858 Safety Issues for Interventional MR Systems

devices should be available in the event that the primary equipment fails, which increases costs.

MR Conditional Equipment

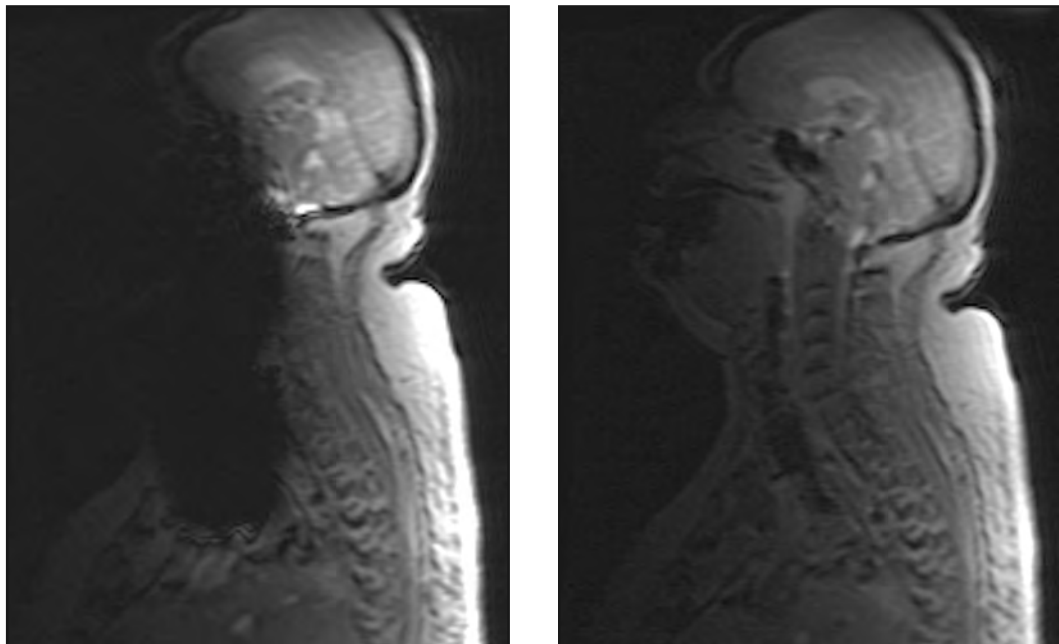
Although MR Conditional anesthesia machines, ventilators, drug infusion pumps, and physiological monitors are available, the development of MR Conditional anesthesia support equipment is not keeping pace with the development of new procedure enabling devices. While simultaneous electroencephalography (EEG) monitoring during functional MRI (fMRI) is now common (83), there is no commercially available MR Conditional bi-spectral index device nor peripheral nerve stimulator for assessing the depth of anesthesia. If MR Unsafe devices are used, they must be removed before the MR system is transported into the OR. Furthermore, at the present time, there is no commercially-available, external defibrillator that is MR Conditional. If either cardiac arrhythmias or cardiac instability is noted during an iMRI procedure, the patient must be removed from the MR system room (i.e., Zone IV) before using an external defibrillator. In situations where there is the likelihood of cardiac instability or arrhythmia in non-MRI environments, external defibrillator/pacing pads may be placed on the patient before the induction of anesthesia. This precaution cannot be done in the MR system room because the metallic foil backing on the pads increases the potential for skin burns, where the pads contact the patient. In this case, the risk of instability or arrhythmia may outweigh the potential benefit of proceeding with the procedure. Although MR Conditional, core body temperature measurement devices are now available, there are no MR Conditional temperature control devices for patients. For example, at BWH, the air blower is removed prior to the MR scanner entering the OR. In the MR system room, a blower is positioned in an RF shielded closet built into the room. An MR Safe extension hose is used to replace the MR Unsafe hose packaged with the device. Although there is some loss due to heat transfer through the hose, it is still possible to warm or cool the patient.

Intubation near the MR scanner is enabled by laryngoscope designs with MR Conditional batteries. To our knowledge, to date, no video laryngoscopes are marketed for use in the MRI setting. However, we have tested devices that show promise for use outside the bore of the scanner. MR Conditional steerable endoscopes have been constructed by several research groups (84, 85). The inadvertent placement of a certain type of endotracheal tube (Fastrach ETT, LMA/Teleflex) at our institution during a diagnostic MRI examination of a patient with a difficult airway resulted in images with substantial signal losses (**Figure 13**). No injury occurred to the patient. The packaging for this particular ETT had no indication of its level of MRI-related issues. This endotracheal tube has a reinforcing metallic coil running the length of the device, which is magnetic. This incident led to an appraisal of this and other items in the conventional armamentarium for anesthesia delivery, some of which are listed in the *Reference Manual for Magnetic Resonance Safety, Implants, and Devices* and posted online at www.MRIsafety.com.

Cardiac Issues

Patients that are candidates for intervention and intraoperative procedures often have cardiac comorbidities. The poor quality of continuous electrocardiogram (ECG) tracings when the patient is in the MR system is the most serious limitation in monitoring an anesthetized patient. Imaging gradients can induce characteristic field frequency-based artifacts

Figure 13. (A, Left) MR image depicting signal void created by an MR Unsafe endotracheal tube in the patient and (B, Right) an MR image from a patient with an MR Conditional endotracheal tube.



in the ECG that can mimic malignant arrhythmia. Additionally, the static magnetic field can induce apparent ST-segment abnormalities, as well as other alterations in the waveform (87). The benefit of image-guidance, therefore, should be weighed against the risk of anesthetizing a patient at risk of further cardiac injury during ischemic stress.

There are efforts to improve ECG monitoring. Adaptive filters have been shown to be successful in removing noise induced by the imaging gradients, which are present only during scanning (89). ECG monitoring in the static magnetic field, however, is problematic even when images are not being acquired. A dominant QRS complex and undistorted S-T segment are important for both cardiac-gated MRI examinations and to permit physiological monitoring for cardiac ischemia, especially during cardiac interventions (90). The magnetohydrodynamic (MHD) effect arises when blood, which is conductive, flows in the presence of a static magnetic field. The MHD effect generates a voltage that distorts the “real” electrocardiogram, especially with respect to the S-T segment when blood flow occurs from the left ventricle into the aorta (91). It is possible to remove the MHD artifact by processing ECG signals using a baseline ECG collected outside the bore of the MR system in conjunction with an adaptive filter (92).

There are multiple efforts underway to develop an iMRI treatment for arrhythmias using RF ablation (93, 94) and cryoablation catheters (95). This procedure, and others, will benefit from enabling developments to overcome current limitations in cardiac monitoring. Treatment of members of the patient population with cardiac implantable electronic devices (CIED), are also a hurdle in iMRI.

860 Safety Issues for Interventional MR Systems

Historically, CIEDs (e.g., cardiac pacemakers and implantable cardioverter defibrillator, ICD) have been considered contraindications for MRI (96, 97). For more than 15 years, a variety of reports have supported the safety of scanning patients with “standard” cardiac pacemakers and ICDs. With appropriate screening and device programming, many investigations have demonstrated patients with non-MR Conditional CIEDs can be scanned without significant clinical risks (98-113). Based upon the guidelines published in the peer-reviewed literature, institutions have developed programs for performing MR imaging in patients with non-MR Conditional CIEDs. These programs are typically administered under combined leadership of both cardiology and radiology departments with participation from the vendors.

Fortunately, five major vendors (LivaNova/Sorin, Boston Scientific, Abbott/St.Jude Medical, Medtronic, and Biotronic) now offer FDA or CE mark approved, MR Conditional CIEDs that include cardiac pacemakers, ICDs, and recorder devices. Patients implanted with these devices can safely undergo MRI at 1.5 Tesla and, with certain MR Conditional CIEDs, 3 Tesla scanning is also allowed (112).

Remote Monitoring

Acoustic noise from the gradient magnetic fields, especially at 3-Tesla, can prohibit the anesthesiologist from hearing the physiological monitor’s alarms and ECG tones when more than a few feet from the equipment. Although developing technologies with active noise cancellation will allow transmission of monitoring equipment alarms and tones into the anesthesiologist’s headphones, this technology is not widely available. As an alternative, remote monitoring is routinely performed at our institution.

Primarily because of the acoustic noise associated with MRI, the anesthesiologist in the AMIGO Suite remotely monitors the patient after the onset of anesthesia and the patient is stable. Remote monitoring is accomplished with another physiological monitor placed in the control corridor that displays information for the patient’s vital signs and end tidal gases; a view of the anesthesia machine’s ventilator and its settings by either direct line-of-site or remote camera; and a camera view of the patient in the bore of the MR system. Line-of-site to the patient is limited when the patient is inside the scanner’s bore, even when the anesthesiologist is at the bedside. If an intervention by the anesthesiologist is needed during imaging, the scan is halted until the issue is resolved. MR Conditional volume infusion pumps are available with remote consoles outside the room. Alternatively, conventional infusion pumps can be stationed outside the MR system room with an extension set of IV tubing penetrating the room via the waveguide. The disadvantage of this setup is that pump alarms are not audible when the care provider is at the bedside. Recently, a commercially available MR Conditional caddy has been developed to house ferrous pumps in the MR system room. This device has an alarm to indicate when the gauss limit is exceeded. The caddy’s alarm indicator is more readily visible than the alarms on each pump, permitting visualization by MRI users outside the scanner room.

SAFE USE OF MRI PULSE SEQUENCES FOR iMRI

The type of pulse sequence that is used during iMRI is generally more constrained than it is for diagnostic imaging. Real-time, interactive imaging can be employed, which demands high acquisition rates, while sacrificing some contrast and resolution. Special fast-imaging pulse sequences used in iMRI are more likely to make use of fast gradient switching and/or may employ RF pulsing rates that are substantially greater than those used in routine clinical MR imaging and, thus, are more likely to push the limits of safe use. Safety concerns related to pulse sequence choice are also heightened in iMRI because of the possibility of interaction with implants or interventional devices that are in place during the MRI procedure, resulting in a greater potential for dangerous levels of heating from RF fields or induction of currents from gradient magnetic field switching.

The primary biological effects in MRI are tissue heating due to RF exposure, nerve stimulation due to currents induced by gradient switching and sensations such as vertigo caused by rapid movement in the static magnetic field (43, 113). Pulse sequences that tend to cause the greatest heating due to RF exposure are those with a high temporal density of RF pulsing, such as fast (or turbo) spin echo sequences, which employ multiple high-flip-angle refocusing pulses as well as steady-state sequences such as FIESTA (or True FISP), which have very short repetition times (114). These pulse sequence types are commonly used in iMRI and may be referred to as “high-SAR” pulse sequences. Pulse sequences that involve rapid gradient switching, such as echo planar imaging sequences, may induce currents that can cause peripheral nerve stimulation or interfere with implantable device operation, may be referred to as “high-dB/dt” sequences. Safety concerns in iMRI, as with standard MR imaging, involve the use of high-SAR and/or high-dB/dt pulse sequences. Artifacts such as signal loss and distortion caused by imaging in the presence of metallic objects such as biopsy needles can also be considered a safety issue because they diminish or confuse MR-guidance capabilities during interventional procedures. Gradient echo pulse sequences, especially multi-echo sequences such as echo planar imaging, are especially subject to exhibit artifacts caused by the susceptibility effects due to the presence of metallic objects in tissues (115, 116). High bandwidth spin echo sequences and special sequence adaptations may be employed to minimize such artifacts (114, 115).

Regulatory bodies such as the FDA have placed limits on the allowable exposures for patients to RF energy and gradient magnetic fields. MR system manufacturers include monitoring software and hardware to ensure that these exposures are not exceeded when their MR scanners are running in routine operating modes. In the absence of metallic implants, devices, or foreign objects present during the scanning, MR systems that are set in routine operating modes (i.e., the Normal Operating Mode or First Level Controlled Operating Mode) should not be of concern for safety. Even when high-SAR or high-dB/dt sequences are used, limitations by the MR system on the setting of parameters such as the number of slices or the repetition time will ensure that exposures remain within the defined limits. It may be possible to supersede the limits as set by regulatory bodies, although Institutional Review Board approval and informed patient consent is required in such cases. As long as system SAR and dB/dt monitoring remains in place, the degree of exposure can be assessed and a decision whether or not to proceed based on risk versus benefit assessment can be

862 Safety Issues for Interventional MR Systems

made for the patient. Involving an MRI physicist to assess these risks is advisable in such cases.

Of greater concern when using high-SAR or high-dB/dt sequences is when implants catheters, needles or other foreign objects are present during scanning because heating can be enhanced by the presence of the device, and it is much more difficult to predict the degree of the effects. Ideally, information is available from the manufacturer of the device in terms of specifying conditions of use. For example, perhaps a given device is limited with respect to the strength of the static magnetic field and the Normal Operating Mode must be used.

Workflows can be developed that are designed to enable safe guidance. For example, non-metallic stylets are first placed with MRI-guidance prior to deploying a deep brain stimulating electrodes, which are at risk of MRI-induced heating. Post-operative CT can be performed instead of MRI to evaluate for complications such as hematoma.

CONCLUSIONS

The need to use strong magnets, high spatial gradients, RF energy and cryogens for performing diagnostic MRI results in an inherent level of risk, and the possibility of accidents should not be underestimated. In the iMRI environment, the potential risk is exacerbated by the introduction of additional tools and devices required to perform the intervention. Moreover, the presence of individuals less experienced with the MRI environment could lead to additional risk. However, through the appropriate facility design, education and safety policies, risk can be managed such that it is outweighed by the benefit of performing the procedure in the MRI environment. Furthermore, a culture of teamwork and safety can be engrained in staff members by ongoing training, and policy enforcement and iterative improvement. Together, these approaches act in concert to ensure safety.

Since the early 1990s when iMRI was first introduced, it has rapidly developed and the number of users and procedures have increased. iMRI expanded through the introduction of new surgical approaches and/or techniques in open surgery, vascular and cardiac applications, and minimally-invasive endoscopies. Efforts now focus on the development of new, more advanced imaging methods, navigational techniques, surgical instruments and devices, the more efficient use of computing technologies, and the integration of diagnostic and therapy devices with navigational tools to expand iMRI applications.

Safety measures must keep pace with this increasingly complex environment as the number of installations also increases. Patient and staff member safety is the concern of a large multimodality and multidisciplinary infrastructure like that which exists in the BWH AMIGO Suite, where iMRI is complimented with newly developed, multiple molecular probes (e.g., nuclear, optical, mass spectrometer, etc.) that also must be used safely. A primary concern for the operation of the suite is how to provide a safe environment for clinical and research activity in iMRI that incorporates multimodal imaging. The workflows in the suite should be designed to suit the way that multidisciplinary teams work while understanding and mitigating safety risks.

Most of the centers involved in iMRI report no serious adverse incidents. In our more than 25 years of experience with a 0.5-Tesla iMRI (23) and, more recently with 3-Tesla, we

also have a major incident-free operation. The occurrence of near misses and the ensuing safety reviews have demonstrated that ongoing review of safety policies and continuous training should be a hallmark of any safety program, similar to any other place within the medical environment. With appropriate control, a strong safety record can be maintained. The main reason for this successful and safe operation is continuous vigilance, policy enforcement, and a serious attitude towards safety.

REFERENCES

1. Jolesz FA. Interventional and intraoperative MRI: A general overview of the field. *J Magn Reson Imaging* 1998;8:3-7.
2. Jolesz FA. Introduction. In: *Intraoperative Imaging and Image-Guided Therapy*. Jolesz FA, Editor. Springer Science and Business Media, New York, NY. pp. 1-23, 2014.
3. Kettenbach J, Silverman SG, Schwartz RB, et al. Design, clinical suitability and future aspects of a 0.5 T MRI special system for interventional use. *Radiologe* 1997;37:825-34.
4. Silverman SG, Collick BD, Figueira MR, et al. Interactive MR-guided biopsy in an open-configuration MR imaging system. *Radiology* 1995;197:175-81.
5. McDannold NJ, Jolesz FA. Magnetic resonance image-guided thermal ablations. *Top Magn Reson Imaging* 2000;11:191-202.
6. Bhagavatula SK, Lane J, Shyn P. A radiologist's view of tumor ablation in the radiology suite. *Anesthesiol Clin* 2017;35:617-626.
7. Kandarpa K, Jakab P, Patz S, Schoen FJ, Jolesz FA. Prototype miniature endoluminal MR imaging catheter. *J Vasc Interv Radiol* 1993;4:419-27.
8. Campbell-Washburn AE, Tavallaei MA, Pop M, et al. Real-time MRI guidance of cardiac interventions. *J Magn Reson Imaging*. 2017;46:935-950.
9. Hsu L, Fried MP, Jolesz FA. MR-guided endoscopic sinus surgery. *AJNR Am J Neuroradiol* 1998;19:1235-40.
10. Thomas TT, Teitelbaum DH, Smith EA, et al. Magnetic resonance imaging (MRI)-assisted laparoscopic anorectoplasty for imperforate anus: A single center experience. *Pediatr Surg Int*. 2017;33:15-21.
11. Schwartz RB, Hsu L, Wong TZ, et al. Intraoperative MR imaging guidance for intracranial neurosurgery: Experience with the first 200 cases. *Radiology* 1999;211:477-88.
12. Golby AJ, and Orringerpp DA. Magnetic Resonance Image-Guided Neurosurgery. In: *Intraoperative Imaging and Image-Guided Therapy*. Jolesz FA, Editor. Springer Science and Business Media, New York, NY. pp. 451-462, 2014.
13. Gombos EC, Jagadeesan J, Richman DM, Kacher DF. Magnetic resonance imaging-guided breast interventions: Role in biopsy targeting and lumpectomies. *Magn Reson Imaging Clin N Am* 2015;23:547-61.
14. Schmidt EJ, Kacher DF, Wang W, et al. MRI-monitored anterior cervical discectomy and fusion (ACDF) surgery: Observation of intra-procedural nerve decompression during surgery. 25th Annual Meeting of the International Society for Magnetic Resonance in Medicine, Honolulu, HI. 2017.
15. Jolesz FA, Morrison PR, Koran SJ, et al. Compatible instrumentation for intraoperative MRI: Expanding resources. *J Magn Reson Imaging* 1998;8:8-11.
16. Quick HH. MR-compatible instruments for interventional MRI. In: *Interventional Magnetic Resonance Imaging (Medical Radiology/Diagnostic Imaging)*. Kahn T, Busse H, Editors. Springer-Verlag, Berlin Heidelberg, pp. 35-51, 2012.
17. Jolesz FA. Designing a safe work environment. 1996 RSNA Eugene P. Pendergrass New Horizons Lecture. Image-guided procedures and the operating room of the future. *Radiology* 1997;204:601-12.

864 Safety Issues for Interventional MR Systems

18. Silverman SG, Jolesz FA, Newman RW, et al. Design and implementation of an interventional MR imaging suite. *AJR Am J Roentgenol* 1997;168:1465-71.
19. Colen RR, Kekhia H, Jolesz FA. Multimodality intraoperative MRI for brain tumor surgery. *Expert Rev Neurother* 2010;10:1545-58.
20. Kacher DF, Whalen B, Handa A, Jolesz FA. The Advanced Multi-Modality Image Guided Operating (AMIGO) Suite. In: *Intraoperative Imaging and Image Guided Therapy*. Jolesz FA, Editor. Springer Science, New York, NY, pp 339-368, 2014.
21. Sutherland GR, Kaibara T, Louw D, et al. A mobile high-field magnetic resonance system for neurosurgery. *J Neurosurg* 1999;91:804-813.
22. Hushek SG. Safety protocols for interventional MRI. *Acad Radiol* 2005;12:1143-8.
23. Kettenbach J, Kacher DF, Kanan AR, et al. Intraoperative and interventional MRI: Recommendations for a safe environment. *Minim Invasive Ther Allied Technol* 2006;15:53-64.
24. Johnston T, Moser R, Moeller K, Moriarty TM. Intraoperative MRI: Safety. *Neurosurg Clin N Am* 2009; 20:147-153.
25. White MJ, Thornton JS, Hawkes DJ. Design, operation, and safety of single-room interventional MRI suites: Practical experience from two centers. *J Magn Reson* 2015; 41:34-43.
26. Jankovski A, Francotte F, Vaz G. Intraoperative magnetic resonance imaging at 3 T using a dual independent operating room-magnetic resonance imaging suite: development, feasibility, safety, and preliminary experience. *Neurosurgery* 2008;63:412-24.
27. Rahmathulla G, Recinos PF, Traul DE. Surgical briefings, checklists, and the creation of an environment of safety in the neurosurgical intraoperative magnetic resonance imaging suite. *Neurosurg Focus* 2012; 33:E12.
28. Hushek SG. Systems for Interventional MRI. *Interventional Magnetic Resonance Imaging*. In: *Interventional Magnetic Resonance Imaging*. Kahn T, Busse H, Editors. Springer-Verlag, Berlin Heidelberg, pp. 3-15, 2012.
29. Hata N. Image-Guided Robotics in Minimally Invasive Therapies. In: Jolesz FA, Editor. *Intraoperative Imaging and Image Guided Therapy*. Springer Science, New York, NY, pp. 439-447, 2014.
30. ACR Manual on MR Safety. American College of Radiology, www.ACR.org.
31. Chaljub G, Kramer LA, Johnson RF III, et al. Projectile cylinder accidents resulting from the presence of ferromagnetic nitrous oxide or oxygen tanks in the MR suite. *AJR Am J Roentgenol* 2001;177:27-30.
32. MRI Safety 10 Years Later: What can we learn from the accident that killed Michael Colombini? In: Patient Safety and Quality Healthcare. November, December 2011. Available at: <http://www.psqh.com/component/content/article/137-november-december-2011/992-mri-safety-10-years-later.html>. Accessed March, 2021.
33. Joint Commission. Preventing accidents and injuries in the MRI suite. *Sentinel Event Alert*, 38, 2008.
34. Gilk T. Effectiveness of existing MR safety regulatory, licensure, and accreditation standards. In: Proceedings of the Magnetic Resonance Imaging (MRI) Safety Public Workshop. October 25-26, 2011, Silver Spring, MD.
35. Ward P. Details emerge of MRI accident in Sweden. Aunt Minnie (11/4/2019). <https://www.auntninnie.com/index.aspx?sec=sup&sub=mri&pag=dis&ItemID=126979> Accessed March, 2021.
36. Musumeci N. Man dies after being sucked into MRI chamber. New York Post (1/29/2018). <https://nypost.com/2018/01/29/man-dies-after-being-sucked-into-mri-chamber/>. Accessed March, 2021
37. Surgical Safety Checklist. First Edition. In: World Health Organization Patient Safety Tools and Resources. <https://www.who.int/patientsafety/safesurgery/checklist/en/>. Accessed March, 2021.
38. JD Breen, FA Jolesz, DF Kacher. Radiofrequency identification for tracking of surgical instruments in the intra-operative MRI setting. Proceedings of the 7th Interventional MRI Symposium. Baltimore, MD. 2008.

MRI Bioeffects, Safety, and Patient Management 865

39. Yamashita K, Kusuda K, Ito Y. Evaluation of surgical instruments with radiofrequency identification tags in the operating room. *Surg Innov* 2018;25:374-379.
40. Schmidt EJ, Watkins RD, Zviman MM. A magnetic resonance imaging-conditional external cardiac defibrillator for resuscitation within the magnetic resonance imaging scanner bore. *Circ Cardiovasc Imaging* 2016;9:e005091.
41. Shusterman V, Hodgson-Zingman D, Thedens D. High-energy external defibrillation and transcutaneous pacing during MRI: Feasibility and safety. *J Cardiovasc Magn Reson* 2019;21:47.
42. Price RR. The AAPM/RSNA physics tutorial for residents: MR imaging safety considerations. *Radiographics* 1999;19:1641-51.
43. Shellock FG and Crues JV. *MRI: Bioeffects, Safety, and Patient Management*. Los Angeles, CA. Biomedical Research Publishing Group. 2014.
44. ASTM International, F2503. Standard practice for marking medical devices and other items for safety in the magnetic resonance environment. ASTM International, West Conshohocken, PA.
45. ASTM International, F2052. Standard test method for measurement of magnetically induced displacement force on medical devices in the magnetic resonance environment. ASTM International, West Conshohocken, PA.
46. White MJ, Thornton JS, Hawkes DJ, et al. Design, operation, and safety of single-room interventional MRI suites: Practical experience from two centers. *J Magn Reson Imag* 2015;41:34-43.
47. ASTM F2213. Standard test method for measurement of magnetically induced torque on medical devices in the magnetic resonance environment. ASTM International, West Conshohocken, PA.
48. ASTM F2182. Standard test method for measurement of radio frequency induced heating on and near passive implants during magnetic resonance imaging. ASTM International, West Conshohocken, PA.
49. ASTM F2119. Standard test method for evaluation of MR image artifacts from passive implants. ASTM International, West Conshohocken, PA.
50. ISO/TS 10974. Assessment of the safety of magnetic resonance imaging for patients with an active implantable medical device. American National Standards Institute.
51. Kugel H. Safety Considerations in Interventional MRI. In: *Interventional Magnetic Resonance Imaging*. Kahn T, Busse H. Editors. Springer-Verlag, Berlin Heidelberg, 2012.
52. Schaefers G and Melzer A. Testing methods for MR safety and compatibility of medical devices. *Minimally Invasive Therapy & Allied Technologies* 2006;15:71-75.
53. De Wilde JP, Grainger D, Price DL, Renaud C. Magnetic resonance imaging safety issues including an analysis of recorded incidents within the UK. *Prog Nucl Magn Reson Spectrosc* 2007;51:37-48.
54. Panych LP, Kimbrell VK, Mukundan S Jr, Madore B. Relative magnetic force measures and their potential role in MRI safety practice. *J Magn Reson Imaging* 2020;51:1260-1271
55. Schenck J. The role of magnetic susceptibility in magnetic resonance imaging: MRI magnetic compatibility of the first and second kinds. *Med Phys* 1996; 23:815-850.
56. DiMaio SP, Kacher DF, Ellis RE, et al. Needle artifact localization in 3-T MR images. *Stud Health Technol Inform* 2006;119:120-5.
57. Hirose M, Kacher DF, Smith DN, Kaelin CM, Jolesz FA. Feasibility of MR imaging-guided breast lumpectomy for malignant tumors in a 0.5-T open-configuration MR imaging system. *Acad Radiol* 2002;9:933-41.
58. Bartels LW, Bakker CJ, Viergever MA. Improved lumen visualization in metallic vascular implants by reducing RF artifacts. *Magn Reson Med* 2002;47:171-180.
59. Hall WA, Truwit CL. Intraoperative MR-guided neurosurgery. *J Magn Reson Imaging* 2008;27:368-75.
60. U.S. Department of Health and Human Services. Food and Drug Administration, Center for Devices and Radiological Health. Guidance for the submission of premarket notifications for magnetic resonance diagnostic devices. Rockville, MD: US DHHS FDA; 2016.

866 Safety Issues for Interventional MR Systems

61. International Electrotechnical Commission (IEC). Medical electrical equipment. In: Particular Requirements for the Safety of Magnetic Resonance Equipment for Medical Diagnosis. International Standard IEC 60601-2-33, IEC, Geneva, Switzerland, 2015.
62. Delfino JG, Krainak DM, Flesher SA, Miller DL. MRI-related FDA adverse event reports: A 10-yr review. *Med Phys* 2019;46:5562-5571.
63. Knopp MV, Essig M, et al. Unusual burns of the lower extremities caused by a closed conduction loop in a patient at MR imaging. *Radiology* 1996;200:772-75.
64. Mandel NS, Ramdial JL, and Marcus, EN. A second-degree burn after MRI. *Cleveland Clinic Journal of Medicine* 2017;84:348-349.
65. Rezai AR, Phillips M, Baker KB, et al. Neurostimulation system used for deep brain stimulation (DBS): MR safety issues and implications of failing to follow safety recommendations. *Investigative Radiology* 2004;39:300-303.
66. Jackson JD. Classical Electrodynamics, Second Edition. John Wiley & Sons, New York, NY, 1975.
67. Yeung CJ, Karmarkar P, McVeigh ER. Minimizing RF heating of conducting wires in MRI. *Magn Reson Med* 2007;58:1028-34.
68. Van den Bosch MR, Moerland MA, et al. New method to monitor RF safety in MRI-guided interventions based on RF induced image artifacts. *Med Phys* 2010;37:814-21.
69. Reiter T, Gensler D, Ritter O, et al. Direct cooling of the catheter tip increases safety for CMR-guided electrophysiological procedures. *J Cardiovasc Magn Reson* 2012;14:12.
70. Hill DL, McLeish K, Keevil SF. Impact of electromagnetic field exposure limits in Europe: is the future of interventional MRI safe? *Acad Radiol* 2005;12:1135-42.
71. Keevil SF, Gedroyc W, Gowland P, et al. Electromagnetic field exposure limitation and the future of MRI. *Br J Radiol* 2005;78:973.
72. Directive 2013/35/EU of the European Parliament and of the Council of 26 June 2013 on the minimum health and safety requirements regarding the exposure of workers to the risks arising from physical agents (electromagnetic fields) (20th individual Directive within the meaning of Article 16(1) of Directive 89/391/EEC) and repealing Directive 2004/40/EC. <https://eur-lex.europa.eu/legal-content/EN/TXT/?qid=1567898600092&uri=CELEX:32013L0035>. Accessed March, 2021.
73. Philip JH, Smith CB, Martin RF, Kacher DF. MR-compatible portable anesthesia machine with ventilator moves with patient through the magnet bore. In: Proceedings of the American Society of Anesthesiologists, 2008.
74. Martin AJ, Hall WA, Liu H, et al. Brain tumor resection: intraoperative monitoring with high-field-strength MR imaging-initial results. *Radiology* 2000;215:221-8.
75. Hall WA, Galicich W, Bergman T, Truwit CL. 3-Tesla intraoperative MR imaging for neurosurgery. *J Neurooncol* 2006;77:297-303.
76. Hadani M. Development and design of low field compact intraoperative MRI for standard operating room. *Acta Neurochir Suppl* 2011;109:29-33.
77. Morrison PR, Silverman SG, Tuncali K, Tatli S. MRI-guided cryotherapy. *J Magn Reson Imaging* 2008;27:410-420.
78. Martin R. Anesthetic Concerns in the Magnetic Resonance (MR) Environment. In: Interventional Magnetic Resonance Imaging. Kahn T, Busse H, Editors. Springer-Verlag, Berlin Heidelberg. pp. 89-93, 2012.
79. Henrichs B, Walsh RP. Intraoperative magnetic resonance imaging for neurosurgical procedures: Anesthetic implications. *AANA J* 2011;79:71-77.
80. Smith JA. Hazards, safety, and anesthetic considerations for magnetic resonance imaging. *Top Companion Anim Med* 2010;25:98-106.
81. Tan TK, Goh J. The anaesthetist's role in the setting up of an intraoperative MR imaging facility. *Singapore Med J* 2009;50:4-10.

MRI Bioeffects, Safety, and Patient Management 867

82. Thimmappa ND, Shellock FG. Chapter 14. Patient Monitoring in the MRI Environment. Shellock FG and Crues JV, Editors. In: *MRI: Bioeffects, Safety, and Patient Management*. Los Angeles, CA. Biomedical Research Publishing Group. 2014.
83. Mele G, Cavaliere C, Alfano V, et al. Simultaneous EEG-fMRI for functional neurological assessment. *Front Neurol* 2019;10:848.
84. North OJ, Ristic M, Wadsworth CA, Young IR, Taylor-Robinson SD. Design and evaluation of endoscope remote actuator for MRI-guided endoscopic retrograde cholangio-pancreatography (ERCP). In: Proceedings of the International Conference on Biomedical Robotics and Biomechatronics (BioRob). Fourth IEEE RAS & EMBS; pp. 787–792, 2012.
85. Zuo S, Ymanaka N, Masamune K, et al. MRI compatible rigid-flexible outer sheath device using pneumatic locking mechanism for endoscopic treatment. *IFMBE Proceedings* 2008;19:741–744.
86. Shellock, FG. Reference Manual for Magnetic Resonance Safety, Implants and Devices, 2020 Edition. Los Angeles: Biomedical Research Publishing Group. Los Angeles, CA. 2020.
87. Birkholz T, Schmid M, Nimsky C, Schuttler J, Schmitz B. ECG artifacts during intraoperative high-field MRI scanning. *J Neurosurg Anesthesiol* 2004;16:271-6.
88. Dabaghyan M, Zhang SH, Ward J, et al. 3T cardiac imaging with on-line 12-lead ECG monitoring. *J Cardiovasc Magn Reson* 2016;18(Suppl 1): P212.
89. Wu V, Benbash IM, Ratnayaha K, et al. Adaptive noise cancellation to suppress electrocardiography artifacts during real-time interventional MRI. *J Mag Reson Imaging* 2011;33:1184-93.
90. Haberl R. *ECG Pocket*. Second Edition. Borm Bruckmeier Publishing LLC, El Segundo, CA, 2006.
91. Gupta A, Weeks AR, Richie SM. Simulation of elevated T-waves of an ECG inside a static magnetic field (MRI). *IEEE Trans Biomed Eng*. 2008;55:1890-6.
92. Tse ZTH, Dumoulin CL, Clifford G, et al. 12-lead ECG in a 1.5 Tesla MRI: Separation of real ECG and MHD voltages with adaptive filtering for gating and non-invasive cardiac output. In: Proceedings of the Society for Cardiac Magnetic Resonance; Phoenix: Arizona; 2010.
93. Mukherjee RK, Chubb H, Roujol S, et al. Advances in real-time MRI-guided electrophysiology. *Curr Cardiovasc Imaging Rep* 2019;12:6.
94. Chubb H, Harrison JL, Weiss S, et al. Development, preclinical validation, and clinical translation of a cardiac magnetic resonance - Electrophysiology system with active catheter tracking for ablation of cardiac arrhythmia. *JACC Clin Electrophysiol* 2017;3:89-103.
95. Lichter J, Kholmovski EG, Coulombe N, et al. Real-time magnetic resonance imaging-guided cryoablation of the pulmonary veins with acute freeze-zone and chronic lesion assessment. *Europace* 2019;21:154-162.
96. Faris OP, Shein MJ. Government viewpoint: U.S. Food & Drug Administration: Pacemakers, ICDs and MRI. *Pacing Clin Electrophysiol* 2005;28:268-9.
97. Shinbane J, Summers J. Chapter 18. MRI and Cardiac Devices: MR Conditional Pacemakers and Implantable Defibrillators. Shellock FG, Crues JV, Editors. In: *MRI: Bioeffects, Safety, and Patient Management*. Biomedical Research Publishing Group, Los Angeles, CA. 2014
98. Martin ET, Coman JA, Shellock FG, Pulling CC, Fair R, Jenkins K. Magnetic resonance imaging and cardiac pacemaker safety at 1.5-Tesla. *J Am Coll Cardiol* 2004;43:1315-1324.
99. Sommer T, Naehle CP, Yang A, et al. Strategy for safe performance of extrathoracic magnetic resonance imaging at 1.5 tesla in the presence of cardiac pacemakers in non-pacemaker-dependent patients: A prospective study with 115 examinations. *Circulation* 2006;114:1285-1292.
100. Nazarian S, Roguin A, Zviman MM, et al. Clinical utility and safety of a protocol for noncardiac and cardiac magnetic resonance imaging of patients with permanent pacemakers and implantable cardioverter defibrillators at 1.5 Tesla. *Circulation* 2006;114:1277-1284.
101. Cohen J, Costa H, Russo R. Pacemaker and implantable cardioverter defibrillator safety for patients undergoing magnetic resonance imaging (The MagnaSafe Registry). *J Am Coll Cardiol* 2009;53:A303-A304.

868 Safety Issues for Interventional MR Systems

102. Nazarian S, Hansford R, Roguin A, et al. A prospective evaluation of a protocol for magnetic resonance imaging of patients with implanted cardiac devices. *Annals of Internal Medicine* 2011;155:415-424.
103. Russo RJ, Costa H, Doud D, et al. Repeat MRI for patients with implanted cardiac devices does not increase the risk of clinical events or parameter changes: Preliminary results from The MagnaSafe Registry. *J Am Coll Cardiol* 2012;59:E649-E649.
104. Nazarian S, Hansford R, Rahsepar AA, et al. Safety of magnetic resonance imaging in patients with cardiac devices. *N Engl J Med* 2017;377:2555-2564.
105. Rahsepar AA, Zimmerman SL, Hansford R, et al. The relationship between MRI radiofrequency energy and function of nonconditional implanted cardiac devices: A prospective evaluation. *Radiology* 2020;295:307-313.
106. Ning X, Li X, Fan X, et al. 3.0 T magnetic resonance imaging scanning on different body regions in patients with pacemakers. *J Interv Card Electrophysiol* 2020 (Epub ahead of print).
107. Vigen KK, Reeder SB, Hood MN, et al. ISMRM Safety Committee. Recommendations for imaging patients with cardiac implantable electronic devices (CIEDs). *J Magn Reson Imaging*. 2020 (Epub ahead of print).
108. Schaller RD, Brunker T, Riley MP, Marchlinski FE, Nazarian S, Litt H. Magnetic resonance imaging in patients with cardiac implantable electronic devices with abandoned leads. *JAMA Cardiol* 2021 (Epub ahead of print).
109. Russo RJ, Costa HS, Silva PD, et al. Assessing the risks associated with MRI in patients with a pacemaker or defibrillator. *N Engl J Med* 2017;376:755-764.
110. Rajiah P, Kay F, Bolen M, et al. Cardiac magnetic resonance in patients with cardiac implantable electronic devices: Challenges and solutions. *J Thorac Imaging* 2020;35:W1-W17.
111. Padmanabhan D, Farwati M, Izath A, et al. Safety of magnetic resonance imaging in patients with non-conditional cardiac implantable electronic devices: A systematic review and meta-analysis. *European Heart Journal* 2020;22:288-298.
112. Indik JH, Gimmel JR, Haruhiko A, et al. 2017 HRS expert consensus statement on magnetic resonance imaging and radiation exposure in patients with cardiovascular implantable electronic devices. *Heart Rhythm* 2017;14:e97-e153.
113. Cunqueiro A, Lipton ML, Dym RJ, et al. Performing MRI on patients with MRI-conditional and non-conditional cardiac implantable electronic devices: An update for radiologists. *Clin Radiol* 2019;74:912-917.
114. Chopra SS, Rump J, Schmidt SC, et al. Imaging sequences for intraoperative MR-guided laparoscopic liver resection in 1.0-T high field open MRI. *Eur Radiol* 2009;19:2191-6.
115. Yutzy SR, Duerk JL. Pulse sequences and system interfaces for interventional and real-time MRI. *J Magn Reson Imaging* 2008;27:267-75.
116. Cernicanu A, Lepetit-Coiffe M, Roland J, et al. Validation of fast MR thermometry at 1.5 T with gradient-echo echo planar imaging sequences: Phantom and clinical feasibility studies. *NMR Biomed* 2008;21:849-58.

Chapter 32 Occupational Exposure During MRI

DONALD W. MCROBBIE, PH.D.

Associate Professor, Discipline of Medical Physics
School of Physical Sciences
University of Adelaide
Adelaide, Australia

INTRODUCTION

With the growth of magnetic resonance imaging (MRI), large cohorts of patients and staff members are now routinely exposed to the static, time-varying, and radiofrequency (RF) fields integral to the imaging procedure. For the millions of MRI examinations performed each year, the majority are conducted on 1.5-Tesla or 3-Tesla scanners with a smaller number of 7-Tesla scanners installed in research or clinical, academic health centers around the world. Increasing technical advances have resulted in the magnitude of exposures to electromagnetic fields (EMF) to steadily grow during the use of clinical MRI, which began in the early 1980s.

Many voluntary international (1-4) and national (5-7) standards or guidelines for occupational and public exposure to EMF are in existence and reviewed elsewhere in this textbook. In the European Union (EU) and United Kingdom (UK) the Physical Agents (electromagnetic fields) Directive 2013/35/EC regulates occupational exposure limits for EMF through national laws (8). Although patient safety in MRI has always been paramount within the MRI community (9, 10), with exposure guidelines (11-14) and operational safety standards (1, 14-16), the EU regulations brought a renewed focus on MRI healthcare worker exposures (17).

Staff exposures mainly involve the static magnetic field and its associated spatial gradient magnetic field that are responsible for the projectile force acting on ferromagnetic objects. The time-varying magnetic fields from the imaging gradients and the radiofrequency (RF) excitation field are substantially confined to within the bore of the MR system and, thus, only become significant for staff members if they remain close to or enter the bore during the scan acquisition (17).

870 Occupational Exposure During MRI

DEFINITIONS AND OCCUPATIONAL LIMITS

Biological effects of electromagnetic fields and their underlying physical and physiological mechanisms are described elsewhere in this textbook. In occupational exposure or hygiene it is commonplace to consider the *incident* and *induced* EMFs: the former are those generated directly from the scanner (e.g., static magnetic, B_0 ; gradient magnetic, dB/dt ; and RF fields, B_1), the latter are those generated in tissue as a consequence of the incident exposure (e.g., induced electric fields, current densities or specific absorption rate, SAR) and that are considered to be responsible for acute effects, such as vertigo, metallic taste sensations, peripheral nerve stimulation (PNS), and tissue heating. Accurate dosimetry for both incident and induced EMF is an essential prerequisite in occupational exposure studies.

Incident Fields

In occupational hygiene, static magnetic fields are sometimes denoted by the abbreviation SMF, and time-varying magnetic fields by TVMF. The magnetic field intensity, \mathbf{H} , is indicated in units of amperes per meter (A/m). However, in MRI it is more usual to consider magnetic induction or flux density, commonly called “magnetic field strength”, B_0 , measured in Tesla (T). In a linear, isotropic medium the magnetic flux density \mathbf{B} is:

$$\mathbf{B} = \mu_0 (1 + \chi) \mathbf{H} \quad (1)$$

where μ_0 , the permeability of vacuum, has a value $4\pi \times 10^{-7}$ henry/m and χ is the dimensionless magnetic susceptibility. Beyond the bore of the MR system, the fringe field of B_0 varies spatially with a gradient dB/dz in Tesla per meter (T/m). A time-weighted average (TWA) SMF over a duration T is defined as:

$$B_{\text{TWA}} = \frac{1}{T} \int_0^T B(t) dt \quad (2)$$

The gradient magnetic fields are defined as linear spatial variations in B_z :

$$G_x = \frac{dB_z}{dx}; \quad G_y = \frac{dB_z}{dy}; \quad G_z = \frac{dB_z}{dz} \quad (3)$$

and are specified in milli-Tesla per meter (mT/m). The gradient slew rate (SR), or maximum switching speed is defined in Tesla per meter per second (T/m/s). The rate of change of B (dB/dt) or the step change in B (ΔB) is physiologically significant for acute sensory effects.

The RF field, B_1 , is measured in micro-Tesla (μT) but is also specified as H_1 [Equation (1)] and has an electric field component E_1 . Electric fields (E) are measured in volts per meter (V/m). For a plane wave in the far field, the ratio of E/H has a constant value of 337-ohms and the power density is:

$$P = E B / \mu_0 = E^2 / 337 \quad (4)$$

measured in watts per square meter (W/m^2). The specific absorption rate (SAR) is the RF power absorbed per unit body mass (W/kg). An SAR value may apply for the whole or as a partial body (e.g., head or extremities) exposure. For more information please refer to the relevant chapters in this textbook.

The incident fields (B , H , and their time derivatives) are vectors and may have directional components which are not utilized in the image formation process but which, nevertheless, contribute to occupational exposures. For both patient and occupational exposures, it is important to consider the magnitude of these vector fields, e.g., for B :

$$|B| = \sqrt{(B_x^2 + B_y^2 + B_z^2)} \quad (5)$$

Exposure limits are often expressed as root mean square (RMS) values. The RMS value of a time-varying function (e.g., B_1 and the imaging gradients) is:

$$B_{\text{RMS}} = \lim_{T \rightarrow \infty} \sqrt{\left(\frac{1}{T} \int_0^T B(t)^2 dt \right)} \quad (6)$$

For a sinusoidal waveform, the peak value is $\sqrt{2}$ times the RMS value.

Induced Fields

The generation of the induced fields in tissue is determined by Faraday's law of Induction:

$$\oint \mathbf{E}_i \cdot d\mathbf{l} = - \frac{d}{dt} \int_s \mathbf{B} \cdot d\mathbf{S} \quad (7)$$

where \mathbf{E}_i is the induced electric field around a closed path and $d\mathbf{S}$ is the differential area vector normal to the applied field. For a circular loop of radius, r , in a uniform medium normal to the applied field this simplifies to (18):

872 Occupational Exposure During MRI

$$E_i = \frac{r}{2} \frac{dB}{dt} \quad (8)$$

The induced electric field generates a current density J_i (A/m^2) in tissue:

$$J_i = \sigma E_i \quad (9)$$

where σ is the electrical conductivity of the tissue in siemens per meter (S/m). Both induced E_i and J_i vary linearly with the loop radius, and therefore increase with body size. For an elliptical body cross section perpendicular to the magnetic field, the maximum current density is (19):

$$J_{max} = \frac{a^2 b}{a^2 + b^2} \sigma \frac{dB}{dt} \quad (10)$$

where a is the semi-major axial length and b the semi-minor. The choice of axes will depend upon the orientation of the subject within the field. For a person standing close to the bore of the MR system, a would be in the head-foot direction, and b left-right, and with typical values of 0.4-m and 0.2-m, the geometric multiplier would be 0.16.

Movement through the gradient of the static field (i.e., through the fringe field spatial gradient) effectively acts as a time-varying magnetic field. In the simplest case of a uniform body moving with a constant velocity v (m/s):

$$E_i = v \frac{r}{2} \frac{dB}{dz} \quad (11)$$

and, therefore, moving more slowly will result in lower induced fields in tissues. The elliptical geometric term [Equation (10)] may also be used in place of r , with appropriate values of a and b .

Concerning the RF field, B_1 , for a spatially uniform rectangular RF pulse with duty cycle D and a uniform spherical medium of density ρ (kg/m^3) the maximum SAR is (20):

$$SAR = 0.5 \sigma \pi^2 r^2 f^2 B_1^2 D / \rho \quad (12)$$

and, thus, SAR has a square dependence upon Larmor frequency or B_0 , B_1 , patient ‘radius’ and a linear dependence upon duty cycle or reciprocal repetition time, 1/TR.

Occupational Exposure Standards and Limits

The numerous occupational exposure guidelines for electromagnetic fields in the frequency range 0-Hz to 300-GHz cover all aspects of work-related exposures, not just those related to MRI. Most guidelines operate under two regimes: Basic Restrictions, also known as “Exposure Limit Values” (ELV), “Exposure Reference Values” (ERV), or “Dosimetric Reference Values” (DRL), are set to avoid short term acute adverse effects and are defined in terms of RMS induced electric field, E_i , in tissue. As the induced fields are not directly measurable, compliance can be demonstrated using derived Reference Levels (RL), also known as “Dosimetric Reference Levels” (DRL), “Action Levels” (AL), “Exposure Reference Levels” (ERL) or “Action Values” (AV), specified in terms of the incident fields. Some standards include higher limits for “controlled” or “restricted” situations. These apply in highly organized settings with appropriately trained staff and would, therefore, be applicable in the MRI environment.

For situations where an incident field limit (e.g., RL) is not exceeded, it can be assumed that the induced field limit (e.g., BR) will not be exceeded. Compliance with a Reference Level ensures compliance with the underlying Basic Restriction or equivalent limit. However, when an incident limit is exceeded, it is necessary for the employer to establish that the relevant induced field limit is not exceeded. This would normally entail modeling of the induced fields. The derivation of the incident field limits is often based upon algebraic calculations, that is, from Equations (7) to (12) using idealized body geometries with homogeneous electrical properties.

Within the EU and UK, Directive 2013/35/EC contains a derogation for MRI from the limits defined in the Directive: ELVs *may* be exceeded for the exposures related to the installation, testing, use, development, maintenance of, or research related to MRI for patients in the health sector, subject to a number of conditions. EU Directive limits are based upon current International Commission on Non-Ionizing Radiation Protection (ICNIRP) values.

MR system manufacturers follow the International Electrotechnical Commission (IEC) standard 60601-2-33 that includes limits for occupational exposure specifically for MRI workers (1). Other chapters in this textbook review patient exposure guidelines in greater detail.

Table 1. Static magnetic field limits for occupational exposure. All values are peak levels.

	Trunk & Head Instantaneous Ceiling (T)	Limbs (T)
IEC (1)	8	8
ICNIRP (2)	2	8
IEEE (5)	0.5	0.5

874 Occupational Exposure During MRI

Static Magnetic Fields

Occupational limits for static fields are shown in **Table 1**. The ICNIRP has a 2-T limit for static magnetic field exposure but allows for peak exposures of up to 8-T in controlled situations (2). The Institute of Electrical and Electronics Engineers (IEEE) limit applies for slowly varying sinusoidal fields of less than 0.153-Hz defined as RMS (5), but as shown in **Table 1**, converted to a peak value for comparison. The IEC 60601-2-33 limit for workers is 8-T (1).

Movement within the static field gradient is experienced as a slowly time-varying magnetic field, which will induce an electric field in tissues. ICNIRP has developed limits for movement within the static magnetic field (21), shown in **Table 2a** and **2b**.

Time-Varying Fields up to 100-kHz

The ICNIRP and IEEE Basic Restrictions for time-varying magnetic fields up to 100-kHz are shown in **Figure 1**, along with the IEC First Level limit for peripheral nerve stimulation. The IEEE limits are specific to the body part: brain, heart and other, while ICNIRP's are for central nervous system (CNS) tissues in the head or for any tissue in a controlled situation. IEC 60601-2-33 stipulates that the MRI worker should not experience PNS and,

Table 2a. ICNIRP Basic Restrictions for movement within the static magnetic field (21).

Frequency (Hz)	Uncontrolled			Controlled
	ΔB^1 (T)	B_{pk-pk}^2 (T)	Induced E ³ (V m ⁻¹)	Induced E ⁴ (V m ⁻¹)
0	2	-	-	-
0 - 1	-	2	-	-
0 - 0.66	-	-	1.1	1.1
0.66 - 1	-	-	0.7 / f	1.1

Critical effects are stated to be: ¹ “Vertigo due to motion in B-field”; ² “Vertigo due to time-varying B-field;

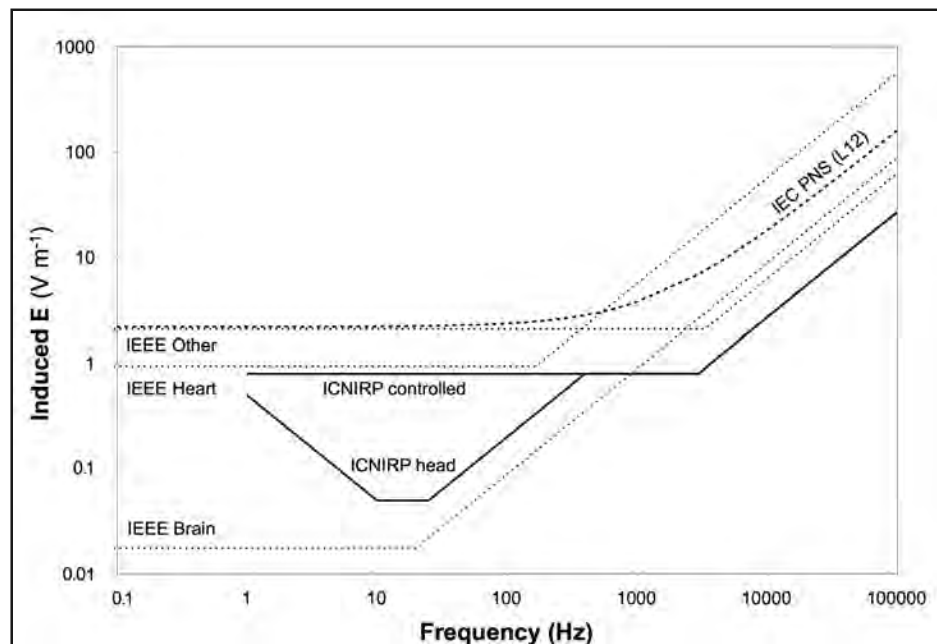
³ “PNS effects due to movement in the B-field or time-varying B field; and ⁴ “Phosphenes due to movement in the B-field or time-varying B-field”.

Table 2b. ICNIRP Reference Levels for movement within the static magnetic field (21).

Frequency (Hz)	Uncontrolled	Controlled
	$(dB/dt)_{pk}$ (T/s)	
0 - 0.66	2.7	2.7
0.66 - 1	1.8 / f	2.7

Critical effects are stated to be: “Phosphenes due to movement in the B field or time-varying B field”.

Figure 1. Induced field limits (Basic Restrictions) up to 100 kHz. ICNIRP (3) and IEEE (5). Values are root mean square (RMS). The IEC limit (1) is the 100% median PNS threshold.



in the absence of experimental data from a specific MR system, proposes a rheobase of 2.2-V/m or 20-T/s and chronaxie of 0.36-ms (see Chapter 3).

These limits pertain to single frequency sinusoidal fields. For non-sinusoidal pulses, in the region 1 to 100-kHz, one can apply the limits to each frequency component present in the waveform (22):

$$\sum_{f_{\min}}^{f_{\max}} \frac{B_i}{L_i} \leq 1 \quad (13)$$

where, B_i , is each individual frequency component of the field, L_i , the appropriate limit value and f_{\min} and f_{\max} define the frequency range. This approach may result in overly conservative limits because it assumes coherent phase between the spectral components (23). For frequency ranges where the incident field limit, B_L , has an inverse relationship to frequency, its time derivative, dB/dt , is constant and may be used to test compliance even for complex waveforms (22, 23):

$$(dB/dt)_{pk} = \sqrt{2} \cdot 2\pi f B_L \quad (14)$$

876 Occupational Exposure During MRI

Applying this approach, the ICNIRP Reference Level becomes 2.6-T/s over the frequency range 300 to 3000-Hz. Similarly, the IEEE head and trunk MPEs below 20-Hz become 0.48-T/s and, for the heart, 18.4-T/s below 3.325-kHz. This methodology is particularly useful for MRI where gradient waveforms are usually of trapezoidal form with multiple harmonics but a single peak dB/dt. **Figure 2** shows Reference Levels up to 100-kHz.

Radiofrequency Fields

Occupational limits relevant to MRI for RF exposures are shown in **Table 3**. Induced field limits are specified as SAR, with a whole-body limit of 0.4-W/kg time averaged over six minutes, chosen to restrict a core body temperature rise to not more than 0.1°C. This is one tenth of the upper limit for patients. The IEEE incident field limits have a frequency and, therefore, a dependence on the strength of the static magnetic field of the scanner. The IEC uses the same limit both for workers and patients, that is, a whole-body SAR of up to 4-W/kg (1). Also specified are local (surface) RF transmit coil SAR limits of 10-W/kg for the head and trunk and 20-W/kg for the limbs.

STUDIES OF INCIDENT FIELDS

Studies of occupational exposures have utilized a number of approaches. The most direct is to issue magnetic dosimeters to staff members and to record their exposures to static and time-varying magnetic fields during the working day (24-30). The second approach is to record the movements of staff members during real activities and correlate these with field maps, either from the manufacturers' data sheets, theoretical calculations, or environmental electromagnetic field (EMF) measurements (31-32). The third approach is to simulate staff member activities while measuring the magnetic field exposure. This has the advantage of being predictive, such that worst-case movements can be investigated and peak exposures may be estimated (33-37). In a more generalized approach to occupational exposure in MRI, one can identify specific tasks and their temporal and magnitude exposures to formulate a Job Evaluation Matrix (38). This can then be used predictively to estimate occupational exposures for different staff groups over a prolonged period of time.

Personal Dosimeter Studies

Personal magnetic dosimeters utilize a combination of three-axis Hall effect probes (B) and search coils (dB/dt), sometimes in conjunction with an integrator to give B readings. **Figure 3** shows typical readings of instantaneous B and dB/dt over a whole shift on a 1.5-T clinical system. **Table 4** summarizes the results from various studies. The average instantaneous exposure from all studies combined (excluding nurse only data from reference (27)) is 39% of B_0 . The combined TWA B is 7.6-mT over all 721 shifts. The average instantaneous dB/dt is 0.93 T/s. **Figure 4a** shows mean static magnetic field and gradient magnetic field exposures from the Netherlands study (28) by professional role. **Figure 4b** shows shift TWA exposures by profession.

De Vocht, et al. (30) monitored occupational exposure for MR system engineering staff performing various tasks, including shimming, body coil adjustment, magnet ramping and system tests. In general, magnet shimming produced the highest exposures with TWA static

Figure 2. Incident field limits: ICNIRP Reference Levels (3) and IEEE Exposure Reference Levels (5).

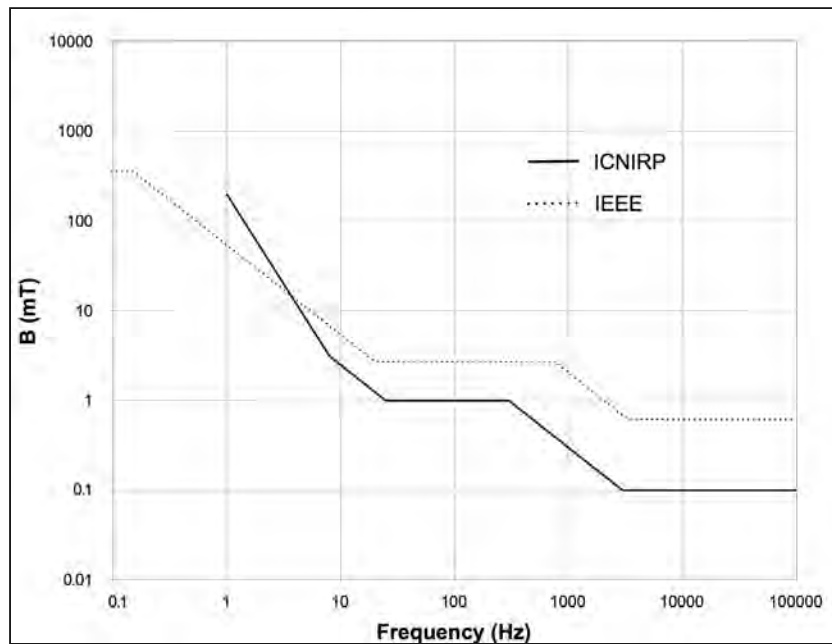


Table 3. RF limits for occupational exposure as applicable to MRI. All time-averaged over 6-minutes.

	Scanner B_0	Frequency (MHz)	Basic Restriction	Reference Level, Limit or Exposure Reference Level*				
				SAR (W/kg)	E (V/m)	H (A/m)	B (μ T)	Power density (W/m ²)
IEC (1)	Any	All	4	N/A	N/A	N/A	N/A	N/A
ICNIRP (4)	Any	10 to 400	0.4	61	0.16	0.2	10	
IEEE (5) ¹	1-T	42.57	0.4	61.4	0.383	N/A	10	
	1.5-T	63.9	N/A	61.4	0.255	N/A	10	
	3-T	127.7	N/A	61.4	0.163	N/A	10	
	7-T	298.0	N/A	61.4	0.163	N/A	10	

(N/A, not applicable, *Exposure Reference Levels for whole-body exposure of persons permitted in restricted environments.)

magnetic field values of 17-, 25- and 86-mT for 1-, 1.5- and 3-T scanners, respectively, showing a strong correlation with the strength of the static magnetic field. Peak exposures occurred in the range of 54- to 1094-mT with a mean of $549\text{-mT} \pm 303\text{-mT}$. The dB/dt values were up to 3.97-T/s and were associated with movement within the static field gradient. The peak dB/dt did not correlate well with B_0 .

878 Occupational Exposure During MRI

Figure 3. Staff dosimeter readings over one work shift from a 1.5 T clinical system. Top: Instantaneous B; Bottom: Instantaneous dB/dt. Reproduced with permission from Reference 24.

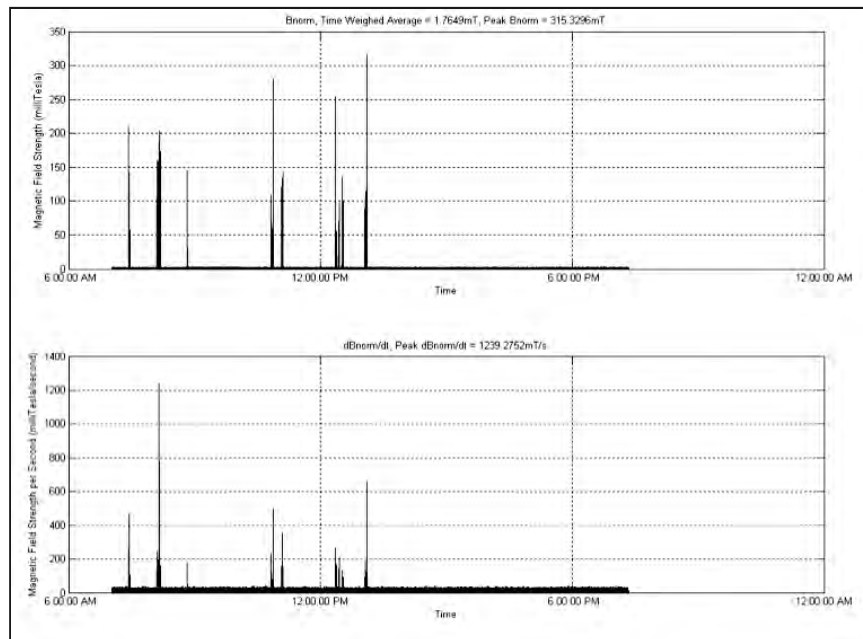


Table 4. Personal dosimetry measurements from MRI workers.

B ₀ (T)	No. of Scanners	No. of Shifts	Average ¹ Peak B (mT)	TWA B ^{1,2} (mT)	Maximum B (mT)	Average Peak dB/dt (T/s)	Maximum dB/dt (T/s)	Ref.
0.6	1	19	380	5.7 ± 3.0	380	N/A	N/A	(24)
1.5	4	103	467 ± 103	5.1 ± 2.8	518	N/A	N/A	(24)
1.5	3	23	601 ± 240	5.1 ± 3.1	1281	2.2 ± 1.5	5.98	(25, 26)
1.5	>7	138	594 (2.38)	18 (1.3)	2981	1.05 (3.01)	12.46	(29)
1.5 ³	1	5	67 ± 49	-	120	-	-	(27)
2.0	1	2	561 ± 33	6.9 ± 1.2	584	1.5 ± 0.4	1.75	(25, 26)
3.0	1	12	822	4.8 ± 2.4	822	N/A	N/A	(24)
3.0	1	6	1261 (1.13)	24 (2.2)	1588	1.56 (1.23)	1.90	(29)
4.0	1	5	513 ± 67	6.4 ± 2.9	616	1.7 ± 0.4	2.04	(25, 26)
0.5 - 7.0	>15	413	595 (2.39)	4.8 (3.67)	2661	0.95 (3.13)	5.02	(28)

(TWA, time-weighted average; N/A, not applicable)

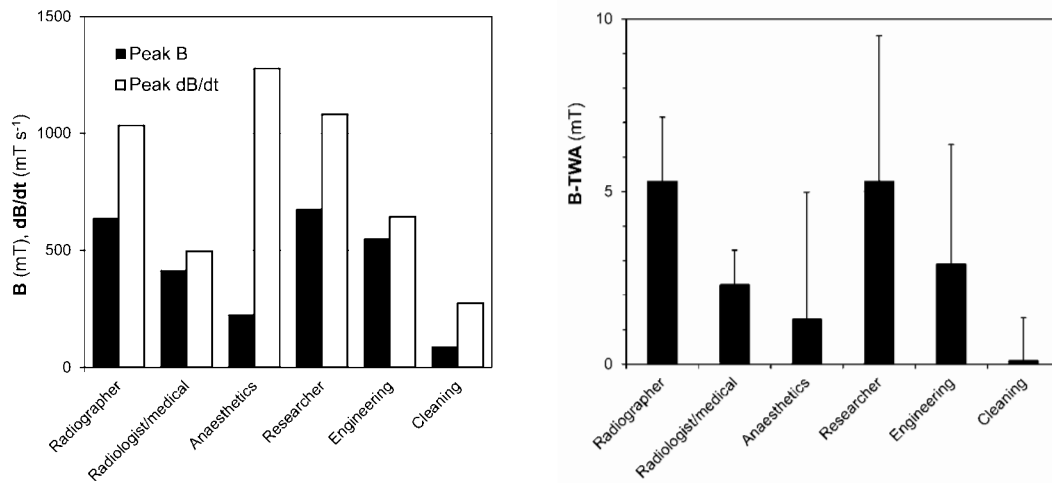
Mean values ± standard deviation

1 - Arithmetic mean values; ± denotes standard deviation; (x) denotes geometric standard deviation.

2 - Averaged over shift.

3 - Nurses only.

Figure 4. Staff dosimetry study in the Netherlands (28) for different staff groups: **(a)** Peak B and dB/dt; **(b)** Time-weighted average (over a shift) B. Data adapted from Reference 28.



Environmental EMF Studies

Static Magnetic Field

Static magnetic field surveys (31, 33) show that 200-mT (the ICNIRP RMS reference level for 1-Hz) is exceeded at about 0.5-m from the bore opening for most 1.5-T and 3-T MR systems. The 500-mT contour (IEEE ERL for <0.153-Hz) lies in the region 0.2 to 0.3-m from the bore entrance. **Figure 5** shows measured field plots in one-quadrant outside the bore for a 1-T open, 1.5-T, 3-T and 7-T (unshielded) closed bore scanners.

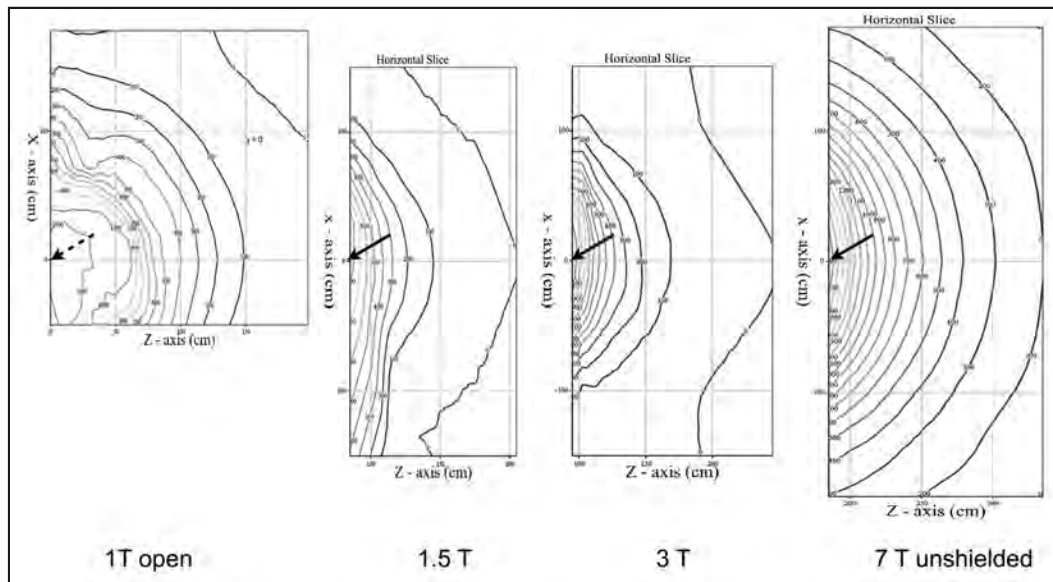
Time-Varying Magnetic Fields

Measurements of gradient fringe fields beyond the bore of the scanner have been made using 3-axis calibrated meters (31, 33, 34, 36, 37). **Table 5** shows peak B, dB/dt and percentage of the ICNIRP reference levels measured outside the bore of the magnet for the worst-case sequences from the available data. The ICNIRP RLs are rarely exceeded outside the bore of the MR system, rendering a staff exclusion zone unnecessary (19).

In general, the faster pulse sequences (e.g., EPI, b-TFE, b-FFE, TruFISP) had higher peak dB/dt, although some MR systems are programmed to utilize the highest possible slew rate, making the peak dB/dt more independent of the sequence type. Greater exposures may occur for open scanners (39), although the data of **Table 5** does not support this assertion. For the other MR systems, the length of the bore is important. For example, the very long

880 Occupational Exposure During MRI

Figure 5. Single quadrant static field plots for 1-T open, 1.5-, 3- and 7-T MR systems. The dotted arrow indicates the isocenter, the solid arrow indicates the center of the bore opening. Reproduced with permission from Reference 31.



bore of the 7-T scanner ensures that the fringe field of the gradients is negligible outside this MR system's bore. The exposure values scale with various factors including pixel size, field-of-view (31), slice thickness and orientation, bandwidth, echo time and acoustic noise reduction (37). **Figure 6** shows the instantaneous $|dB/dt|$ (vector sum for all gradients) for various pulse sequences from one scanner measured at the entrance to the bore.

The fundamental frequency of the sequences ranged from as low as 80-Hz (turbo spin echo) to 1-kHz (echo planar imaging, EPI). Most of the fast pulse sequences relevant to interventional MRI (b-TFE, b-FFE, TruFISP) had fundamental frequencies in the range of 300- to 500-Hz, appropriate to the application of the ICNIRP dB/dt limit of 2.6-T/s. **Figure 6** also shows the frequency components for an EPI sequence.

Radiofrequency Field

Studies of the fringe field associated with the RF B_1 -field for a turbo spin echo (TSE) pulse sequence used for magnetic resonance cholangiopancreatography (MRCP) examinations and a bespoke test sequence on a range of MR systems showed that Reference Levels can be exceeded close to the bore of the MR system (31), within 0.45-m for an open scanner and 0.2-m for a short-bore, closed MR system (34).

Time-Motion Studies

In a study commissioned by the European Commission, under the auspices of the European Society of Radiology and specifically designed to investigate the impact on MRI of an earlier version of the EU Directive, Capstick, et al. (31) observed staff members during typical clinical procedures in an open 1-T scanner and closed bore 1.5-, 3- and 7-T MR sys-

Table 5. Static magnetic field (B_0) and magnetic fringe field values and percent (%) limit exposures from the imaging gradients for worst-case sequences. Negative distance indicates distance into the bore of the MR system. <<RL indicates measurement substantially less than the Reference Level.

B_0 (T)	MR System	$ B _{rms}$ (μ T)	Peak dB/dt (T/s)	% ICNIRP RL	Distance from Bore Entrance (m)	Sequence	Fundamental Frequency	Reference
0.6	Fonar	N/A	0.22	9	0.30	FSE	Unknown	24
1.0	Philips Panorama	N/A	0.32	12	0.0	b-TFE	260-Hz	31
1.0	Philips Panorama	N/A	0.1	4	0.0	EPI	Unknown	36
1.5	GE Signa Twin	N/A	1.14	44	0.0	EPI	Unknown	24
1.5	Philips Achieva	114	N/A	11	0.2	EPI	Unknown	26
1.5	Philips Achieva	118	N/A	12	0.45	Q-flow	Unknown	26
1.5	Unspecified A	1500	N/A	150	0.0	b-FFE	300-Hz	33
1.5	Unspecified B	700	N/A	84	0.0	b-FFE	360-Hz	33
1.5	Philips Intera	650	N/A	108	0.0	FFE	500-Hz	34
1.5	Siemens Avanto	N/A	1.99	77	0.15	TruFISP	670-Hz	31
1.5	Siemens Espree	100	0.77	29	0.3	TruFISP	Unknown	37
3.0	Philips Achieva	N/A	1.69	65	0.11	EPI	1-kHz	31
3.0	Philips Achieva	N/A	1.6	62	0.0	EPI	Unknown	36
7.0	Philips Intera	662	1.78	<<RL	-0.85	Perfusion	770-Hz	31

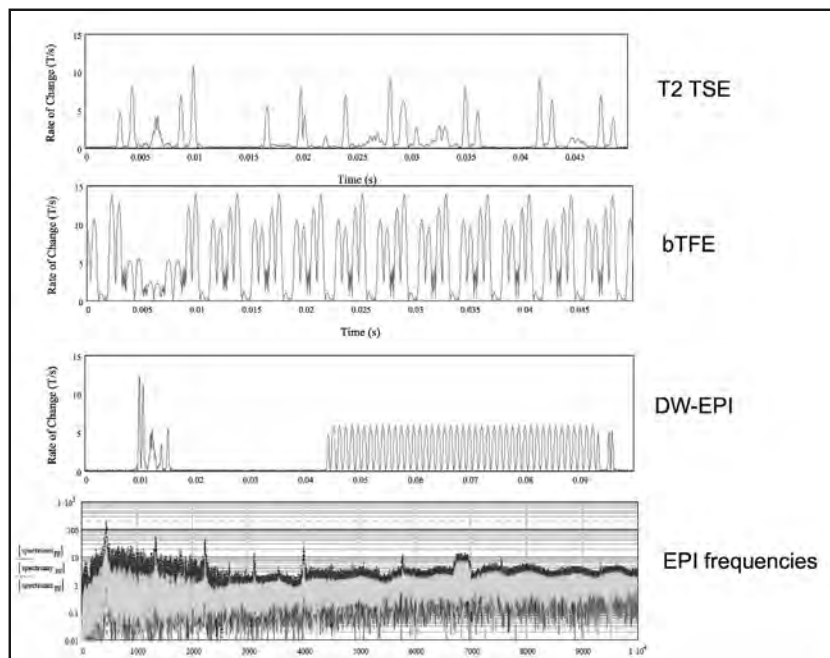
(RL, Reference Level; N/A, not applicable)

tems (**Figure 7**). Staff movements were recorded by a two-camera video system and their position, velocity and exposure times were determined for each procedure. The staff groups investigated included radiographers, anesthetists, interventional radiologists, cleaners, researchers and parent/care givers. By combining these observations with three-dimensional volumetric environmental EMF measurements, the staff exposures were estimated in terms of maximum and mean B, maximum static field gradient ($|dB/dr|$), maximum dB/dt and fundamental frequency from the imaging gradients, and TWA B_1 , H_1 and E_1 (time-averaged over 6-min.).

Figure 8 and **Table 6** summarize these results and those from other studies (24-28, 30, 31) for B, both from the static magnetic field and the gradients, shown with respect to the

882 Occupational Exposure During MRI

Figure 6. Instantaneous dB/dt from the imaging gradients (vector sum of all gradients) measured outside the bore 95-cm from the isocenter. Top three tracings: Turbo spin echo, balanced Turbo-Field Echo, Diffusion imaging. Lowest trace: Spectral content of the DW-EPI sequence. Reproduced with permission from Reference 31.



ICNIRP incident field limits (RL). Some movement-related exposures exceeded the ICNIRP movement-related limits. Imaging gradient dB/dt exceeded the ICNIRP Reference Level (RL) (300 to 3000-Hz) for the clip insertion by 1.9 times. The ICNIRP Reference Levels for exposure from the imaging gradients were exceeded for breast biopsy clip insertion (by 7% with a sequence fundamental frequency of 260-Hz) and monitoring patients under general anesthesia (by 16% for a fundamental frequency of 670-Hz). In no instance was a RF field Reference Level exceeded, although for the breast interventional procedure this was largely due to the time averaging (i.e., the procedure only lasted 42-s).

Other studies have investigated exposures and induced fields from specific movements by volunteer subjects chosen to mimic actual movements performed by staff members carrying out their duties close to the MR system (33, 35, 36). The observed dB/dt values in the range of 1- to 3-T/sec. are in good agreement with the dosimetric studies. Using a unique dosimeter Glover, et al. (35) directly measured induced electric fields E_i in the range of 0.042- to 0.17-V/m for movements, compared with 2.4- to 3.8-mV/m from the gradients for a person standing next to the opening of the bore of the MR system and a gradient slew rate of 10-T/m/s.

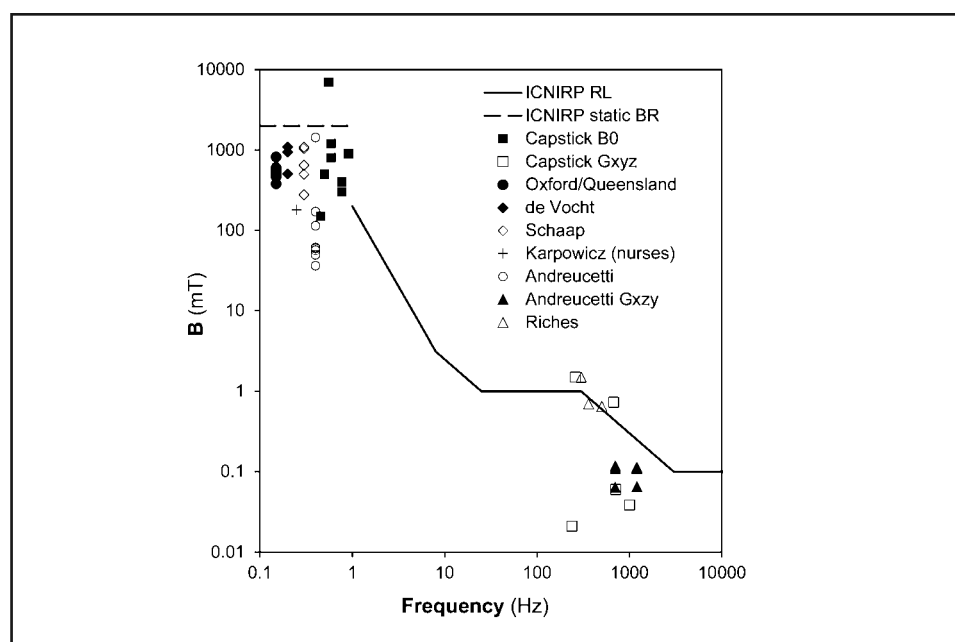
STUDIES OF INDUCED FIELDS IN TISSUES

As the Basic Restrictions are given in terms of induced fields or SAR, numerical simulations may be required to demonstrate compliance. Both quasi-static finite difference or

Figure 7. Various activities from the EU study (31). Top left: Biopsy clip insertion on a 1-T open MR system. Top Right: Pediatric general anesthesia monitoring on a 1.5-T system. Bottom Left: Tactile fMRI on a 3-T system. Bottom Right: Manual contrast administration on a 7-T MR system. Reproduced with permission from Reference 31.



Figure 8. Static field and gradient field exposures from various studies (References 24-28, 30, and 31) plotted against the ICNIRP Reference Level (3).



884 Occupational Exposure During MRI

Table 6. Peak static magnetic field (B), dB/dt and average RF field (B_1) for various activities and staff groups observed in the EU study. The ICNIRP reference level for dB/dt from movement is from a draft document. Reproduced with permission from Reference 31.

			Peak B (mT)	Peak dB/dt movement	Peak dB/dt gradients	TWA- B_1 (6-min. RMS)	Complies with ICNIRP Reference Levels?
			(mT)	(T/s)	(T/s)	(μ T)	
ICNIRP Reference Level			280	1.8	2.6	0.2	
B_0	Activity	Occupation					
1-T	Breast biopsy	Radiologist	150	0	0	0	Yes
	Breast clip insertion	Radiologist	800	1.94	5	0.08	No
	General anesthesia child	Care giver	50	0	<<RL	<<RL	Yes
	Emergency	Radiographer	50	0.21	0	0	Yes
1.5-T	General anesthesia child	Anesthetist	500	0.13	1.89	0	No
	Manual contrast	Radiographer	200	0.13	0	0	Yes
	Emergency	Radiographer	200	0.19	0	0	Yes
	Cleaning	Cleaner	1500	0.36	0	0	No
3-T	Tactile fMRI	Radiographer	400	0.5	0.32	<<RL	No
	Cardiac stress	Cardiologist	150	0.6	0.05	<<RL	Yes
	General anesthesia	Anesthetist	300	0.72	0.39	<<RL	No
	Emergency	Radiographer	100	0.5	0	0	Yes
	Cleaning	Radiographer	3000	0.9	0	0	No
7-T	Manual contrast	Radiologist	1200	0.73	<<RL	<<RL	No
	EEG	Researcher	7000	3.7	0	0	No
	Emergency	Radiographer	900	2.5	0	0	No

(TWA, time-weighted average)

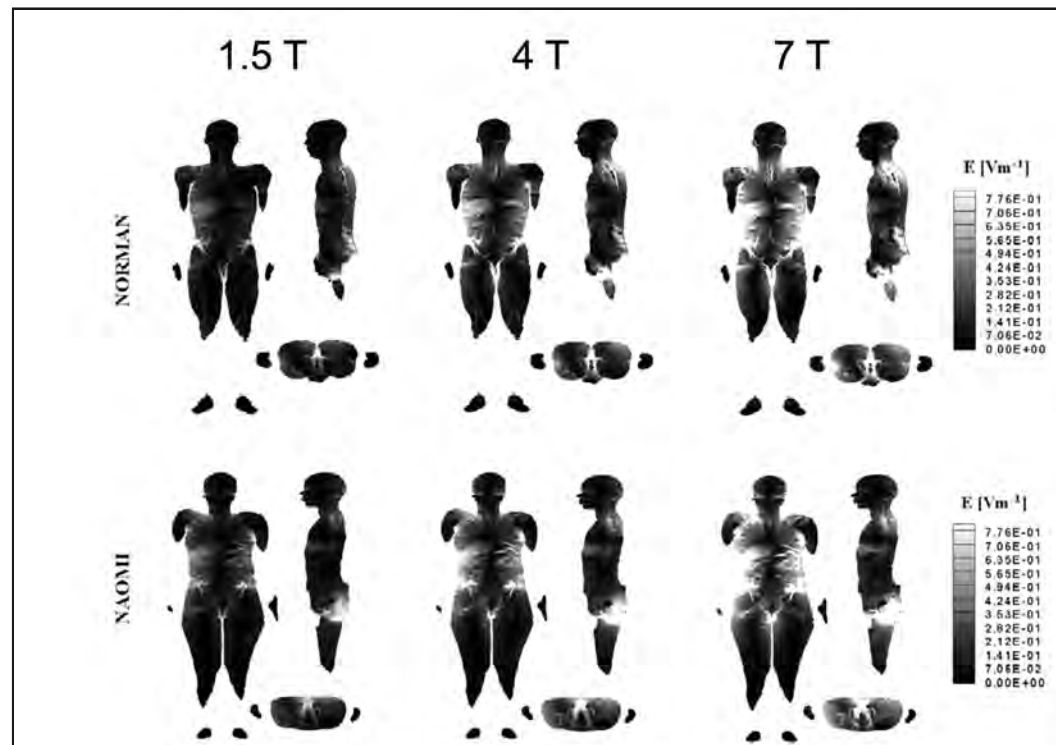
finite integration numerical techniques of the field interactions for anatomically realistic models have been employed (40-47).

Motion in the Static Magnetic Field

Studies of linear motion of workers around MR system magnets (1.5- to 7-T) have confirmed that induced field limits may be exceeded for motion at 1-m/s within 0.5- to 1-m of the MR system (42, 43). The induced electric field and current density scaled with B_0 (**Figure 9**). The worst-case situations associated with these occurred for motion parallel to the z-axis towards the magnet. The ICNIRP 1-Hz Basic Restrictions was exceeded in the spine and brain for 4-T and 7-T, and the IEEE basic restriction for brain was exceeded in every case. A further study of bending towards high field strength scanners revealed similar E_i in CSF with 0.16 to 0.56-V/m in the brain but much less in the spine (44).

In the study of Capstick, et al. (31) emergency evacuation which had the greatest velocities (mean 1.5 ± 0.5 -m/s) gave a maximum J_{RMS} in the range of 9.1 for 1-T to 24.6-mA/m² for 7-T with the maximum induced current in neural tissue approximately 60% less. RMS current densities from movement during other activities (e.g., tactile fMRI, general anesthesia monitoring, cardiac stress test, manual contrast injection) were in the range of 5.7- to 32.9-mA/m². Cleaning the bore of the MR system gave values up to 16.7-mA/m². It is hard to estimate the maximum E_i in neural tissue from movement in these instances but using a maximum conductivity of neural tissue of 0.10-S/m, most of these activities exceed

Figure 9. Induced E_i fields from movement towards 1.5-, 4- and 7-T MR systems at 1-m/sec. Reproduced with permission from Reference 43.



886 Occupational Exposure During MRI

the IEEE Basic Restriction of 0.0177-V/m RMS. The only activity investigated that may exceed the ICNIRP Basic Restriction of 0.5-V/m RMS (0.8-V/m controlled situation) was the interventional breast biopsy clip insertion in the open 1-T MR system which gave maximum J_{RMS} of 84-mA/m² (estimated 0.85-V/m) averaged over 1-cm² in neural tissue.

Induced Fields from the Gradient Magnetic Fields

Crozier, et al. (45) considered a 1-kHz trapezoidal gradient similar to that used in an EPI sequence normalized to 1-mT/m with a 0.1-ms rise time. Care is required when scaling up to higher levels because the full gradient strength assumed in this study of 40-mT/m is not typical for most clinical scans and would result in an unrealistically high slew rate. However, assuming this as a worst-case, peak E_i greater than 2.2-V/m ($J_{max} = 815\text{-mA/m}^2$) in the spinal cord was calculated on axis close to the end of the coil for combined G_x , G_y and G_z . For a more realistic gradient amplitude of 20-mT/m the ICNIRP head central nervous tissues Basic Restriction was only exceeded within 0.01-m of the end of the coil. However, other tissues also exceeded tissue limits: skin up to 0.4-m, fat 0.3-m, muscle 0.25-m and heart 0.1-m.

In a more realistically representative model, with the subject positioned 0.35-m off-axis laterally, 0.19-m from the end of the coil and exposed to a G_z of 10-mT/m at 1-kHz, Li, et al. (46), estimated E_i of 32-mV/m RMS in CNS tissue ($J_i = 20.6\text{-mA/m}^2$, 1-cm² average) with a maximum J_i of 59-mA/m² in muscle tissue and maximum E_i of 4.1-V/m in skin.

The European study (31, 47) calculated induced current densities of 60-mA/m² RMS for any tissue and 10-mA/m² RMS for neural tissue for real clinical tasks such as performing tactile fMRI and general anesthesia monitoring near closed bore 1.5- and 3-T scanners. The maximum E_i of 1.05-V/m RMS from the x-gradient occurred in the skin of the head (**Figure 10**).

The exposure to the interventional radiologist within the bore of a 1-T open MR system (**Figure 11**) produced up to 220-mA/m² RMS averaged over 1-cm² in any tissue, with 140-mA/m² RMS in neural tissue. The peak E_i was 0.74-V/m RMS in the skin of the head. As tissue conductivities vary considerably the maximum J_i does not necessarily coincide with the maximum E_i , nevertheless, these simulations suggest compliance with both the IEEE and ICNIRP Basic Restrictions.

Radiofrequency Exposure and SAR

The European study investigated two instances when a member of staff may exceed an RF reference level (31, 47). From their numerical simulations, a bystander standing close to the bore entrance would receive a 0.9-mW/kg whole body SAR and a 14-mW/kg peak in 10-g SAR (**Figure 12**). The second situation was an interventional radiologist within the bore of an open system, receiving 0.053-W/kg whole body SAR and 0.44-W/kg in 10-g of tissue. These are well below any occupational SAR limit.

Figure 10. Induced current densities and electric fields from the gradients in a person standing adjacent to bore opening of a closed MR system from 40-mT/m x-gradient at 1-kHz. The maximum single voxel J_i is 69-mA/m² (41-mA m² averaged over 1-cm²). J_i greyscale bars are normalized to the maximum value. Reproduced with permission from Reference 31.

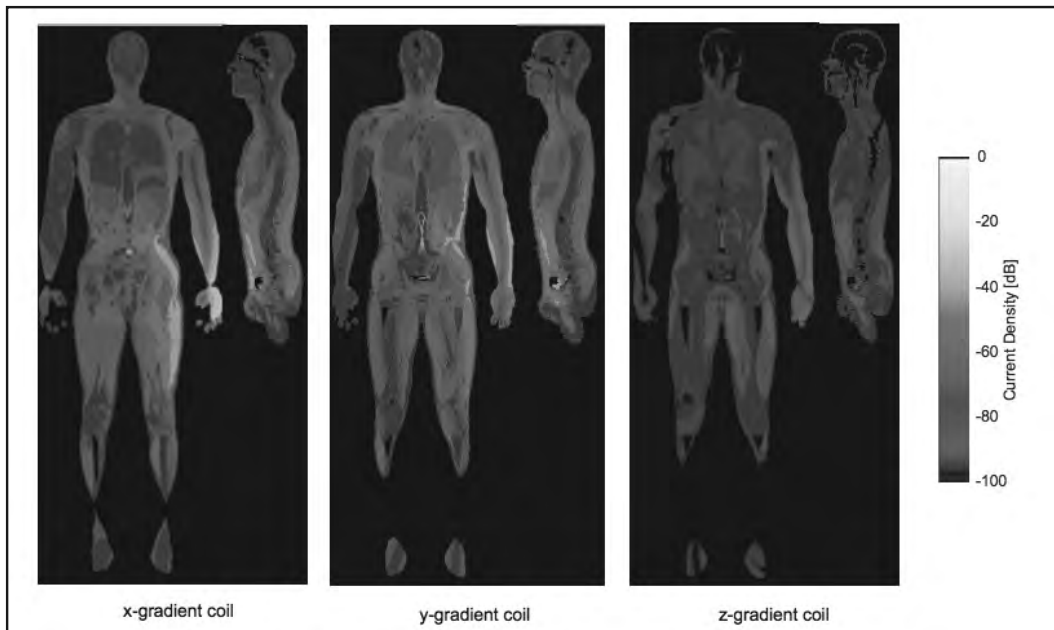
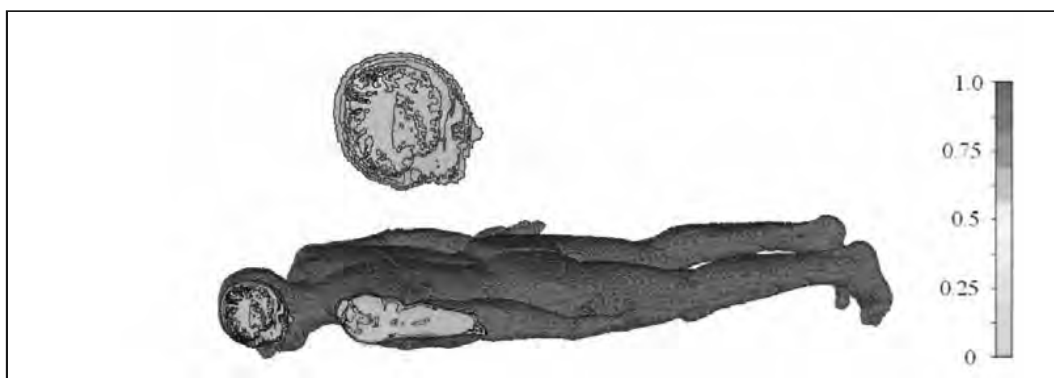
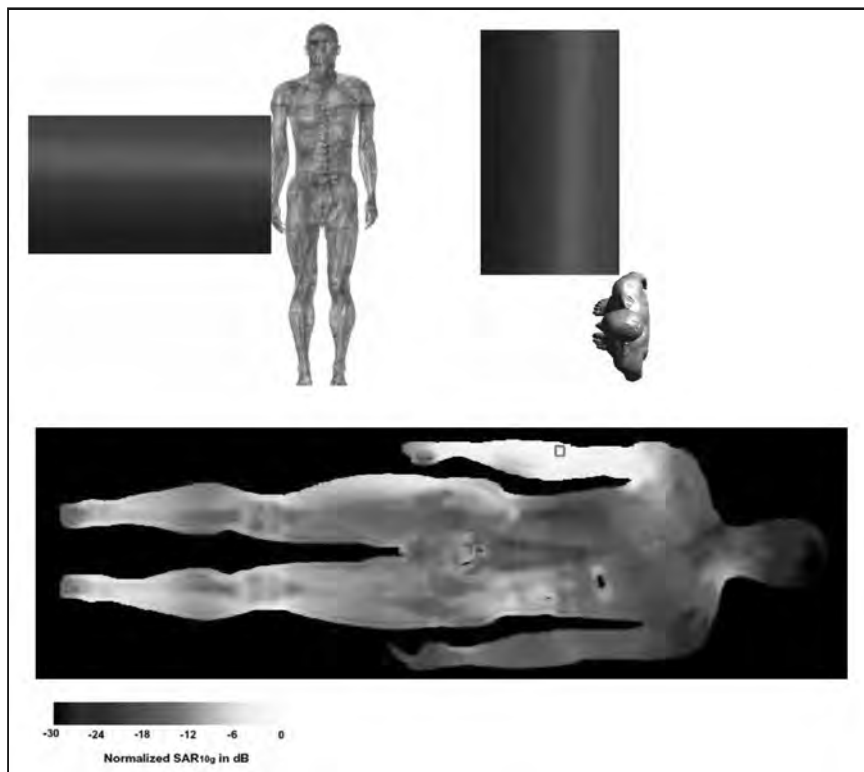


Figure 11. Induced fields in an interventional radiologist within the bore of a 1-T open MR system, z-gradient, 26-mT/m. The maximum single voxel J_i is 1.2-A/m² (510-mA/m² averaged over 1-cm²) and occurs in the CNS. Reproduced with permission from Reference 31.



888 Occupational Exposure During MRI

Figure 12. SAR distribution for a person standing adjacent to the opening of the bore of an MR system. The SAR 10-g is normalized to the peak value. The maximum is in the arm and has a value 10-g SAR = 0.87-mW/kg for a B_1 in the isocenter of 1- μ T. The whole-body SAR is 0.057-mW/kg for a B_1 in the isocenter of 1- μ T. Reproduced with permission from Reference 31.



BIOEFFECTS RESULTING FROM OCCUPATIONAL EXPOSURE

Some studies have specifically concentrated on detecting bioeffects amongst MR and magnet factory workers as a consequence of their work activities. De Vocht, et al. (48) noted light dizziness, slight or mild headache, and eye strain occurring during 4% of the measured shifts from 104 MR workers in the UK. Schaap, et al. (49) reported incidences of vertigo amongst Netherlands MR workers at 1.5, 3, and 7T as 3.5%, 7.6%, and 22.6%, and with nausea incidences of 1.2, 1.5 and 3.2%. Minor changes in hearing threshold (1-5 decibels) amongst MRI factory workers who have undergone up to 60 scans as volunteers has been reported (50), but were only significant for the right ear. Cognitive testing on MR system engineers showed that the speed of movement for particular actions correlated with the occurrence of sensory effects (51). A study of 538 workers in a MRI manufacturing facility reported a cautious possible link of prolonged cumulative exposure to SMF with hypertension; however, dosimetry data was unavailable and the conclusions were tentative (52). These results warrant further research.

PREGNANT STAFF

The current advice for pregnant staff members is to avoid being in the MR system room during scan acquisition, principally because of the potential risk to fetal hearing from acoustic noise (15, 16, 53). Specific dosimetric studies for pregnant staff have not been carried out, although incident field exposures are expected to be similar to those for other staff members. Kanal, et al. (54) conducted a limited epidemiological study of pregnant MRI healthcare workers, concluding that there was no adverse effect on pregnancy outcome. Studies of pregnancy outcomes from patients who have undergone first trimester MRI have shown no adverse effect on neonatal and infant hearing function, birthweight, nor increased incidence of stillbirth, neonatal death, congenital anomalies, neoplasms, or vision loss (55, 56).

SUMMARY AND CONCLUSIONS

Outside the bore of the MR system, exposure from the imaging gradients and RF is generally well below most incident and induced field limits. Careful consideration needs to be given to movement around high field strength magnets for MR systems. Most activities that occur during clinical MRI will only result in significant occupational exposure in association with the static field. Special cases of particular importance include pregnant staff members, and those who must remain close to the bore of the MR system during scanning (e.g., anesthesiologists, intervention radiologists, nurses and researchers).

Time-averaged static field exposures to clinical staff are relatively low, in the region of 5- to 7-mT, with peak static magnetic field exposures of about 40% of B_0 . These figures may be higher for engineering staff and researchers. Dosimetric surveys of dB/dt for clinical and research staff indicate that they receive peak dB/dt of around 1- to 3-T/s arising from movement in the static magnetic field gradient.

For higher static magnetic field strengths, induced fields due to movement may exceed those generated by the gradients and, because of the lower limits in the low frequency range, routine activity around scanners will frequently result in the exceeding of one or more limits. For high field strength MR systems, the occurrence of sensory effects (e.g., nausea, vertigo, metallic taste, etc.) is evidence that limits are being exceeded. These induced field exposures can be minimized through staff training and appropriate control measures, such as moving slowly.

Definitive proof that EMF exposures associated with MRI to staff members are biologically safe remains elusive, although there is no evidence to the contrary. The occurrence of some acute effects confirms the validity and importance of occupational exposure limits, staff education and training, and the conducting of appropriate risk assessments relating to EMF exposure. Whether national regulatory requirements intensify or reduce, occupational exposure is a topic that the MR community needs to continually review.

890 Occupational Exposure During MRI

REFERENCES

1. International Electrotechnical Commission. Medical Electrical Equipment – Part 2-33: Particular Requirements for the Safety of Magnetic Resonance Equipment for Medical Diagnosis. IEC 60601-2-33, Third Edition. Geneva: IEC;2015.
2. International Commission on Non-Ionizing Radiation Protection. Guidelines on limits to exposure from static magnetic field. *Health Physics* 2009;96:504-514.
3. International Commission on Non-Ionizing Radiation Protection. Guidelines for limiting exposure to time-varying electric, magnetic, and electromagnetic fields (up to 100 kHz). *Health Physics* 2010; 99:818-836 and Erratum *Health Physics* 2011;100:112.
4. International Commission on Non-Ionizing Radiation Protection. ICNIRP statement on the “Guidelines for limiting exposure to time-varying electric, magnetic, and electromagnetic fields (up to 300 GHz)”. *Health Physics* 2009;93:257-258.
5. Institute of Electrical and Electronics Engineers. IEEE Standard for Safety Levels with Respect to Human Exposure to Radio Frequency Electromagnetic Fields. 0 Hz to 300 GHz, C95.1-2019. New York, USA: IEEE; 2019.
6. National Radiological Protection Board. Advice on Limiting Exposure to Electromagnetic Fields (0-300 GHz). Documents of the NRPB 2004;15,2.
7. Australian Radiation Protection and Nuclear Safety Agency. RPS-3 Maximum Exposure levels to Radiofrequency Fields 3 kHz-300 GHz. Yallambie, Vic: ARPANSA; 2002.
8. Directive 2013/35/EC of the European Parliament and of the Council, Official Journal of the Union, L 179/1;2013.
9. Shellock FG, Crues JV III, Editors. *MRI Bioeffects, Safety, and Patient Management*. Boca Raton; CRC Press; 2014.
10. Partain CL, Editor. *Journal of MRI* special edition: MRI safety. *J Magn Reson Imag* 2007;26:1175-1344.
11. Food and Drugs Administration. Criteria for significant risk investigations of magnetic resonance diagnostic devices. Rockville, MD: Center for Devices and Radiological Health, US Food and Drug Administration; 2014.
12. Health Protection Agency. Protection of patients and volunteers undergoing MRI procedures, Documents of the Health Protection Agency RCE-7, Chilton, United Kingdom: Health Protection Agency; 2008.
13. International Commission on Non-Ionizing Radiation Protection. Medical magnetic resonance (MR) procedures: Protection of patients. *Health Phys* 2004;87:197-216.
14. International Commission on Non-Ionizing Radiation Protection. Amendment to the ICNIRP “Statement on medical magnetic resonance procedures: Protection of patients.” *Health Physics* 2009;97:259-261.
15. Medicines and Healthcare Products Regulatory Agency. Safety guidelines for magnetic resonance imaging equipment in clinical use. MHRA DB2007. London, United Kingdom: Medicines and Healthcare Products Regulatory Agency; 2015.
16. Kanal E, Barkovich JA, Bell CM, et al. Expert Panel on MR Safety: ACR guidance document on MR safe practices: 2013. *J Magn Reson Imag* 2013;37:501-530.
17. McRobbie DW. Occupational exposure in MRI. *Br J Radiol* 2012;85:293-312.
18. Budinger TF. Thresholds for physiological effects due to RF and magnetic fields used in NMR imaging. *IEEE Trans Nucl Sci* 1979; NS-26:2821-2825.
19. McRobbie D, Foster MA. Pulsed magnetic field exposure during pregnancy and implications for NMR foetal imaging: A study with mice. *Magn Reson Imag* 1985;3:231-234.
20. Schaefer DJ. Bioeffects of radiofrequency power deposition. In: Shellock FG, Crues JV III, Editors. *MRI Bioeffects, Safety, and Patient Management*. Los Angeles: Biomedical Research Publishing Group; 2014. pp. 256-281.

MRI Bioeffects, Safety, and Patient Management 891

21. International Commission on Non-Ionizing Radiation Protection. ICNIRP guidelines for limiting exposure to electric fields induced by movement of the human body in a static magnetic field and by time-varying magnetic fields below 1Hz. *Health Physics* 2014;106:418-425.
22. International Commission on Non-Ionizing Radiation Protection. Guidance on determining compliance of exposure to pulsed and complex non-sinusoidal waveforms below 100 kHz with ICNIRP guidelines. *Health Physics* 2003;84:383-387.
23. Jokela K. Assessment of complex EMF exposure situations including inhomogeneous field distribution. *Health Physics* 2007;92:531-540.
24. Bradley JK, Nyekiova M, Price DL, et al. Occupational exposure to static and time-varying gradient magnetic fields in MR units. *J Magn Reson Imag* 2007;26:1204-1209.
25. Fuentes MA, Trakic A, Wilson SJ, Crozier S. Analysis and measurements of magnetic field exposures for healthcare workers in selected MR environments. *IEEE Trans Biomed Eng* 2008;55:1355-1364.
26. Andreuccetti D, Contessa GM, Falsaperla R, et al. Weighted-peak assessment of occupational exposure due to MRI gradient fields and movements in a nonhomogeneous static magnetic field. *Medical Physics* 2013;40:011910.
27. Karpowicz J, Gryz K. The pattern of exposure to static magnetic field of nurses involved in activities related to contrast administration into patients diagnosed in 1.5 T MRI scanners. *Electromagn Biol Med* 2013;32:182-191.
28. Schaap K, Christopher-de Vries Y, Crozier S, et al. Exposure to static and time-varying magnetic fields from working in the static magnetic stray fields of MR scanners: A comprehensive survey in the Netherlands. *Ann Occup Hygiene* 2014;5:1094-1110.
29. Batistatou E, Möller A, Kromhout H, et al. Personal exposure to static and time-varying magnetic fields during MRI procedures in clinical practice in the UK. *Occup Environ Med* 2016;73:779-786.
30. de Vocht F, Muller F, Engels H, et al. Personal exposure to static and time-varying magnetic fields during MRI system test procedures. *J Magn Reson Imag* 2009;30:1223-1228.
31. Capstick M, McRobbie D, Hand J, et al. An investigation into occupational exposure to electro-magnetic fields for personnel working with and around medical magnetic resonance imaging equipment. Report on Project VT/2007/017 of the European Commission Employment, Social Affairs and Equal Opportunities DG; 2008. <https://itis.swiss/assets/Downloads/Papers-Reports/Reports/VT2007017FinalReportv04.pdf> Accessed September 2019.
32. Hartwig V, Vanello N, Giovannetti G, et al. A novel tool for estimation of magnetic resonance occupational exposure to spatially varying magnetic fields. *MAGMA* 2011;24:323-330.
33. Riches SF, Charles-Edwards GD, Shafford JC, et al. Measurements of occupational exposure to switched gradient and spatially-varying magnetic fields in areas adjacent to 1.5T clinical MRI systems. *J Magn Reson Imag* 2007;26:1346-1352.
34. Riches SF, Collins DJ, Scuffham JW, Leach MO. EU Directive 2004/40: Field measurements of a 1.5 T clinical MR scanner. *Br J Radiol* 2007;80:483-487.
35. Glover PM, Bowtell R. Measurement of electric fields induced in a human subject due to natural movements in static magnetic fields or exposure to alternating gradient fields. *Phys Med Biol* 2008;53:361-373.
36. Kannala S, Toivo T, Alanko T, Jokela K. Occupational exposure measurements of static and pulsed gradient magnetic fields in the vicinity of MRI scanners. *Phys Med Biol* 2009; 54:2243-2257.
37. Wilen J, Hauksson J, Hansson Mild K. Modification of pulse sequences reduces occupational exposure from MRI switched gradient fields: Preliminary results. *Bioelectromagnetics* 2010;31:85-87.
38. Christopher-de Vries Y, Bongers S, Engels H, et al. A generic model for estimating exposure to MRI-related static magnetic fields and its use in reconstructing historical occupational exposure. Proc. British Occupational Hygiene Society X2012 Conference Edinburgh, 4 July 2012.
39. Bassen H, Shafer DJ, Zaremba L, et al. IEEE committee on man and radiation (COMAR) technical information statement. Exposure of medical personnel to electromagnetic fields from open magnetic resonance imaging systems. *Health Physics* 2005;89:684-689.

892 Occupational Exposure During MRI

40. Hand JW. Modelling the interaction of electromagnetic fields (10 MHz-10 GHz) with the human body: Methods and applications. *Phys Med Biol* 2008;53:R243-286.
41. Liu F, Crozier S. A distributed equivalent magnetic current based FDTD method for the calculation of E-fields induced by gradient coils. *J Magn Reson Imag* 2004;169:323-327.
42. Liu F, Zhao H, Crozier S. Calculation of electric fields induced by body and head motion in high-field MRI. *J Magn Reson Imag* 2003;161:99-107.
43. Crozier S, Trakic A, Wang H, Liu F. Numerical study of currents in workers induced by body-motion around high-ultrahigh field MRI magnets. *J Magn Reson Imag* 2007;26:1261-1277.
44. Wang H, Trakic A, Lui F, Crozier S. Numerical field evaluation of healthcare workers when bending towards high-field MRI magnets. *Magn Reson Med* 2008;59:410-422.
45. Crozier S, Wang H, Trakic A, Lui F. Exposure of workers to pulsed gradients in MRI. *J Magn Reson Imag* 2007;26:1236-1254.
46. Li Y, Hand JW, Wills T, Hajnal JV. Numerically simulated induced electric field and current density within a human model located close to a z-gradient coil. *J Magn Reson Imag* 2007;26:1286-1295.
47. Li Y, Hand J, Christ A, et al. Modelling occupational exposure to RF and gradient fields associated with an interventional procedure in an open 1 T MR system. In: Proceedings of the International Society for Magnetic Resonance in Medicine, 17th Annual Meeting, Honolulu, HI. Berkeley, USA: International Society for Magnetic Resonance in Medicine (ISMRM), 2009; pp. 3042.
48. De Vocht F, Batistatou E, Möller A, et al. Transient health symptoms of MRI staff working with 1.5 and 3.0 Tesla scanners in the UK. *Eur Radiol* 2015;25:2718-2726.
49. Schaap K, Christopher-DeVries Y, Mason CK, et al. Occupational exposure of healthcare and research staff to static magnetic stray fields from 1.5-7 tesla MRI scanners is associated with reporting of transient symptoms. *Occ Environ Med* 2014;71:423-439.
50. Bongers S, Slottje P, Kromhout H. Hearing loss associated with repeated MRI acquisition procedure-related acoustic noise exposure: an occupational cohort study. *Occ Environ Med* 2017;74:776-784.
51. de Vocht F, van Drooge H, Engels H, et al. Exposure, health complaints and cognitive performance among employees of an MRI scanners manufacturing department. *J Magn Reson Imag* 2006;23:197-204.
52. Bongers S, Slottje P, Kromhout H. Development of hypertension after long-term exposure to static magnetic fields among workers from a magnetic resonance imaging device manufacturing facility. *Environ Res* 2018;164:565-573.
53. Temperton DH. Pregnancy and work in diagnostic imaging departments. 2nd Edition London: British Institute of Radiology; 2009.
54. Kanal E, Gillen J, Evans, JA, et al. Survey of reproductive health among female MR workers. *Radiology* 1993;187:395-399.
55. Strizek B, Jani JC, Mucyo E, et al. Safety of MR imaging at 1.5 T in fetuses: A retrospective case-control study of birth weights and the effects of acoustic noise. *Radiology* 2015;275:530-537.
56. Ray JG, Vermeulen MJ, Bharatha A, et al. Association between MRI exposure during pregnancy and fetal and childhood outcomes. *JAMA* 2016;316:952-961.

Chapter 33 MRI Standards and Guidance Documents from the United States, Food and Drug Administration

WOLFGANG KAINZ, PH.D.

Research Biomedical Engineer
Division of Biomedical Physics
Office of Science and Engineering Laboratories
Center for Devices and Radiological Health
Food and Drug Administration
Silver Spring, MD

INTRODUCTION

In 1976, the United States (U.S.) Food and Drug Administration (FDA) was given the authority to regulate medical devices through the Medical Device Amendments to the U.S. Food, Drug, and Cosmetic (FD&C) Act. The FDA's regulation of medical devices roughly coincided with the first experimental uses of nuclear magnetic resonance (MR) systems in 1979. The FDA develops guidance documents to communicate its current thinking on medical device review and policy and participates in the development of voluntary consensus standards by national and international standards development organizations (SDOs) to promote methods important to the evaluation of medical devices. Following the publication of consensus standards, the FDA's Center for Devices and Radiological Health (CDRH) utilizes a process to publicly recognize all, or parts, of a consensus standard that is helpful to assess the safety and effectiveness of medical devices. CDRH updates the list of FDA-recognized consensus standards periodically, adding newly recognized consensus standards for medical devices and radiation-emitting electronic products, while replacing certain recognized consensus standards with newly approved revisions. The FDA believes that conformance with recognized consensus standards can provide sound performance characteristics, testing methodologies, manufacturing practices, scientific protocols, compliance criteria, and labeling as part of the data used to establish a reasonable assurance of safety and effectiveness of a medical device. However, conformance with recognized consensus standards may not always provide enough information to establish safety and effectiveness and, thus, additional data or information may be necessary. Conformance with

894 MRI Standards and Guidance Documents from FDA

recognized consensus standards is strictly voluntary for a medical device manufacturer. Therefore, a manufacturer may choose to conform to applicable consensus standards or may choose to obtain evidence about safety and effectiveness in another manner. It should be noted that relevant and up-to-date information for medical device and radiation-emitting product standards can be found at CDRH's Standard website (1).

This chapter provides an overview of FDA's statutory authority, and subsequent regulatory interpretations, over magnetic resonance imaging (MRI) devices in the United States. Furthermore, it describes the procedures that have been developed to facilitate the medical device review mechanisms, followed by a discussion of current FDA guidance documents related to MRI (2), current international consensus standards for MRI equipment safety (also referred to as the "MR system" or "scanner"), and consensus standards for the safety of medical devices in the MRI environment, including some discussion of possible future developments in the field of MRI safety.

Importantly, the content of this chapter does not establish new FDA policies or make changes to existing policies. Furthermore, the content in this chapter is valid only at the time of publication and subject to change. The reader is referred to pertinent FDA and SDO websites to obtain comprehensive and up-to-date information regarding FDA policies, guidance documents, submissions of medical devices, and consensus standards updates.

FDA AUTHORITY AND REGULATORY MECHANISMS

The Medical Device Amendments of 1976 to the FD&C Act provide the statutory authority for FDA regulation of medical devices, including those involving MRI equipment. The Medical Device Amendments established three classes of devices, which are differentiated by the degree of risk and the amount of regulatory control needed to ensure safety and effectiveness. The three classifications are, as follows: (1) Class I devices, which are generally low risk and require only general controls; (2) Class II devices, which are devices for which general controls alone are insufficient for reasonable assurance of safety and effectiveness, but for which there is sufficient information to establish special controls to provide such assurance; and (3) Class III devices, which are the highest risk and are those devices for which insufficient information exists to assure safety and effectiveness solely through general or special controls.

Most Class II devices require premarket notification, that is, a 510(k) submission (3), prior to marketing. A 510(k) is a premarket submission to demonstrate that the device is at least as safe and effective or "substantially equivalent (SE)", to a legally marketed device (21 CFR 807.92(a)(3)). A legally marketed device (also known as a predicate device) is a device that was (1) legally marketed prior to May 28, 1976 (preamendments device), (2) a device which has been reclassified from Class III to Class II or I, (3) a device which has been found to be SE through the 510(k) process, or (4) a device that was granted marketing authorization via the *de novo* classification process under section 513(f)(2) of the Federal FD&C Act. Although devices recently cleared under 510(k) are often selected as the predicate to which equivalence is claimed, any legally marketed device may be used as a predicate.

MRI Bioeffects, Safety, and Patient Management 895

Class III devices are those that (1) support or sustain human life, (2) are of substantial importance in preventing impairment of human health, or (3) which present a potential, unreasonable risk of illness or injury. Manufacturers of Class III devices must submit a pre-market approval (PMA) application demonstrating that the device is safe and effective. Clinical data is generally needed to support a PMA. If a study for an investigational device involves a significant risk to patients, the manufacturer must submit an Investigational Device Exemption (IDE) to the FDA prior to beginning clinical trials in the U.S.

A Humanitarian Use Device (HUD) designation may be requested for devices that are intended for use in treatment or diagnosis of a disease or condition that affect 8,000 or less individuals per year in the United States. A HUD designation must be obtained prior to submitting a Humanitarian Device Exemption (HDE) application.

Since the 1976 Medical Device Amendments, new mechanisms have been developed to facilitate the introduction of medical devices into the marketplace. These mechanisms include alternatives to the traditional 510(k) pathway: (1) the Special 510(k) Program, (2) the Abbreviated 510(k) Program, and (3) the Third-Party Review. The Special 510(k) Program is used for devices with modifications or changes and utilizes design controls to show substantial equivalence of the modified device to the manufacturer's own legally marketed predicate device. (3). If a new 510(k) is needed for the modification, then summary information that results from the design control process can serve as the basis for clearing the application. Under the Special 510(k) review, 510(k) holders who intend to modify their own legally marketed devices shall conduct a risk analysis and the necessary verification and validation activities to demonstrate that the design outputs of the modified device meet the design input requirements. The Abbreviated 510(k) Program is an alternative approach that uses guidance documents, special controls and voluntary consensus standards to aid FDA's premarket review of 510(k) submissions. An Abbreviated 510(k) submission must include the required elements identified in 21 CFR 807.87 (information required in a pre-market notification submission). However, in an Abbreviated 510(k) submission, device manufacturers elect to provide summary reports on the use of guidance documents, special controls, or declarations of conformity to FDA-recognized consensus standards. Effective February 1, 1989 MRDDs were reclassified by the FDA from Class III to Class II as described in the Code of Federal Regulations (CFR) Title 21 (4). As Class II devices MRDDs are granted marketing authorization in the U.S. using a regular premarket notification (510(k)). However, an Abbreviated 510(k) can be appropriate for an MR system because there are several applicable consensus standards, such as IEC 60601-2-33 Edition 3.2 (5) and the standards developed by the National Electrical Manufacturers Association (NEMA) (6).

The FDA's regulatory authority applies to medical device manufacturers, including medical device distributors. For example, the FDA can ask MR system manufacturers to provide information regarding the spatial distribution of the static magnetic field associated with the MR system and to establish a controlled access zone at the 5-Gauss line in the instruction manuals provided with the scanner. However, the FDA does not inspect MRI facilities and cannot require end-users to establish a controlled access zone. Authority for such activities resides with state governmental agencies or other similar entities. Another common misconception is that the FDA premarket approval or marketing clearance of a

896 MRI Standards and Guidance Documents from FDA

device ensures insurance reimbursement. The FDA's authority does not extend to reimbursement decisions, which are made by private or public insurance providers.

FDA GUIDANCE DOCUMENTS REGARDING MAGNETIC RESONANCE IMAGING

Over the last decade, CDRH has developed and published five guidance documents related to MRI for industry and the FDA's staff members: two related to Magnetic Resonance Diagnostic Devices (MRDDs) and three related to the safety and compatibility of passive implants in the MRI environment. The following two sections provide summaries regarding the purpose and content of these guidance documents. The FDA guidance documents do not establish legally enforceable responsibilities. Instead, guidance documents describe the Agency's current thinking on a topic and should be viewed only as recommendations, unless specific regulatory or statutory requirements are cited.

Guidance Documents Regarding Magnetic Resonance Diagnostic Devices (MRDD)

CDRH published two guidance documents related to the safety of MRDDs:

Submission of Premarket Notifications for Magnetic Resonance Diagnostic Devices

The purpose of this guidance is to provide a detailed description of the information needed in a premarket notification, or 510(k) submission, for a MRDD submitted to the FDA. This guidance is applicable to premarket notifications not only for MRI, but also for magnetic resonance spectroscopy (MRS) systems, MR system components of dual-modality devices, for example positron emission tomography (PET)/MR systems, components, and accessories, which could significantly affect the safety or effectiveness of the MRDD. It describes FDA-recognized consensus standards which can be used to help demonstrate substantial equivalence and defines the information needed to adequately describe the MRDD in the submission. Related to electrical, mechanical, structural, and system safety it guides the user to specific FDA-recognized consensus standards to be used to evaluate these safety aspects. Furthermore, it defines the physical laboratory testing related to safety and performance to demonstrate substantial equivalence. It describes the details needed for sample clinical images to support the ability of the MRDD to generate diagnostic quality images. Finally, it provides examples to better understand possible changes in a previously-cleared MRDD which would trigger the requirement for a new 510(k) and gives detailed instructions of what information the labeling should include.

Criteria for Significant Risk Investigations of Magnetic Resonance Diagnostic Devices

This guidance describes MRDD operations that the FDA considers significant risk for the purposes of determining whether a clinical study requires the FDA approval of an IDE. The FDA believes that an MRDD used under specific conditions and exposure limits of the operating conditions is a significant risk and, therefore, studies involving such a device do not qualify for the abbreviated IDE. A sponsor should consider the following operating conditions when assessing whether a clinical study may be considered significant risk: (1) the main static magnetic field; (2) the specific absorption rate (SAR), (3) the gradient, time-varying fields, rate of change; and (4) the sound level, that is, the acoustic noise. For each

for the four conditions, the guidance document defines specific conditions and exposure limits for when the clinical study is considered a significant risk and, therefore, requires an IDE approval.

There are many other FDA guidance documents containing information regarding to MRDDs including *The Guidance for Industry, FDA Reviewers and Compliance on Off-The-Shelf Software Use in Medical Devices* issued September 9, 1999 or *The Guidance for the Content of Premarket Submissions for Software Contained in Medical Devices* issued May 11, 2005 (2).

Guidance Documents Regarding Passive Implants in the MRI Environment

CDRH published three guidance documents related to the safety and compatibility of passive implants:

Establishing Safety and Compatibility of Passive Implants in the MR Environment

This guidance addresses testing and labeling of passive implants for MRI safety, that is, “MR Safe” or “MR Conditional” labeling, in the MRI environment. More information about labeling of implants can be found in (7). This guidance document gives recommendations for MRI-related language to be included in the labeling of passive implants only, which are implants without the supply of electronic power or electronic circuits, that are submitted through PMA, IDE, or 510(k). Active implants, or devices that are not implants, do not fall within the scope of this guidance. The main safety concerns affecting the “MR Safe” or “MR Conditional” labeling of a passive implant in the MRI environment are magnetically induced displacement force and torque, radiofrequency (RF) heating, and image artifacts. The static magnetic field induces displacement forces and torque on magnetic materials. The RF fields may induce substantial heating in tissues near metallic implants. The presence of an implant may also produce image artifacts that can appear as region or signal loss, or as a geometric distortion of the MR image. If the image artifact is near the area of interest, the artifact could render the MR image non-diagnostic or may lead to an erroneous clinical diagnosis, potentially leading to inappropriate medical action.

The guidance recommends non-clinical testing for PMA, IDE, or 510(k) submissions to establish the MR status of the passive implant in the MRI environment. Testing should encompass the entire range of sizes of the implant or device, particularly the size or implant combinations that represent a worst-case scenario. The guidance further recommends the marking terminology defined in ASTM F2503, *Standard Practice for Marking Medical Devices and Other Items for Safety in the Magnetic Resonance Environment* (8), for defining the safety of items in the MRI environment: “MR Safe”, “MR Conditional”, and “MR Unsafe”. If a passive implant is labeled as “MR Safe”, the premarket submission should include a scientific rationale or adequate test results supporting the “MR Safe” labeling. For “MR Conditional” labeling of passive implants, the premarket submission should include MRI test results indicating the safety and efficacy of the implant under the proposed labeling conditions. For “MR Unsafe” labeling of passive implants, a scientific rationale or MRI test results should be provided to support the implant as “MR Unsafe”.

898 MRI Standards and Guidance Documents from FDA

For all passive implants, the guidance recommends the following consensus standards to be used: ASTM F2052, ASTM F2213, ASTM F2182, and ASTM F2119 (9-12). All ASTM consensus standards will be discussed in detail below. Importantly, if a medical device which is deemed “MR Safe” or “MR Conditional” in a 1.5-Tesla/64-MHz MR system, it may not be “MR Safe” or “MR Conditional” in an MR system with a higher or lower static magnetic field/RF frequency.

Assessment of Radiofrequency-Induced Heating in the Magnetic Resonance (MR) Environment for Multi-Configuration Passive Medical Devices

This guidance provides an assessment paradigm for RF-induced heating for multi-configuration passive medical devices in the MRI environment (2). Certain passive devices are not single-configuration devices, but rather multi-configuration devices, such as orthopedic implants. Multi-configuration implants are either multi-component devices or single-component devices with various dimensions and shapes. Multi-component passive devices, such as orthopedic external or internal fixation devices, may result in a very large number of possible device configurations and combinations of individual components. Single-component devices, such as cardiovascular stents, are also frequently available in multiple sizes or shapes. For these multi-configuration passive devices, it can be challenging to leverage RF-induced heating test results from one device configuration or combination to other device configurations or combinations, because the geometry or configuration of the device can affect the heating in an unknown manner. As a result, the total number of possible configurations or combinations that need to be assessed for RF-induced heating can be very large. Importantly, the paradigm presented in this guidance provides an approach to reduce the total number of possible device configurations or combinations to a manageable number for testing the RF-induced heating in the MRI environment. Additionally, this guidance document provides recommendations on how to assess RF-induced device heating for multi-configuration passive medical devices.

Testing and Labeling Medical Devices for Safety in the Magnetic Resonance (MR) Environment

This guidance document which is entitled, The Standard Practice for Marking Medical Devices and Other Items for Safety in the Magnetic Resonance Environment, applies to all implanted medical devices, external medical devices that are fastened to or carried by (i.e., implanted) a patient, and all medical devices that are intended to enter the MRI environment. This guidance document does not apply to the MR system itself. It provides recommendations on MR safety assessments and labeling information, that should be included in all pre-market submissions. Specifically, the document covers terminology, relevant consensus standards and guidance documents, addressing hazards for medical devices in the MRI environment, reporting results, and MRI safety labeling.

NEMA STANDARDS FOR MR SYSTEMS – MS 1 TO MS 12

Standardized tests for demonstrating safety and effectiveness that have been recognized by the FDA facilitate the premarket review process for MR system manufacturers and the FDA. Without recognition by the FDA, measurement techniques submitted to the FDA need

to be independently justified by each medical device manufacturer. The National Electrical Manufacturers Association (NEMA) formed the Magnetic Resonance Section and then the Magnetic Resonance Technical Committee (under the MR Section) to develop standards for MR Systems. The MR Technical Committee currently has published various MRI standards that are readily available at NEMA's website (5). According to NEMA mandates, these standards must be reviewed every five years and either re-approved, updated and re-approved, or withdrawn. NEMA provides standardized methods for measuring performance and safety parameters for MRDDs which can be utilized in Traditional, as well as, Abbreviated 510(k)s. The following information provides an overview of currently published NEMA Standards (5):

NEMA MS 1-2008 (Revision 2014), Determination of Signal-to-Noise Ratio (SNR) in Diagnostic Magnetic Resonance Imaging

NEMA MS 1-2008 (R2014) defines four test methods for measuring the signal-to-noise ratio (SNR) under a specific set of conditions, using head and body radiofrequency (RF) coils. NEMA MS 1-2008 (R2014) does not address the use of surface RF coils, chemical shift imaging, or spectroscopy.

The major feature of the first method is that the SNR performance of the MR system is evaluated using a standard clinical scan sequence. However, this method involves the subtraction of two images, and therefore it can be very sensitive to MR system instabilities that may occur during the data acquisition process. If the results are highly variable, the MS 1 recommends performing the alternative calculation of the standard deviation, described in the first method, or using one of the other methods. These alternative methods have been designed to be less susceptible to MR system instabilities and can be used to determine if any variability in the SNR is due to the scanner instability or genuinely poor SNR. All methods are intended to measure thermal and other broadband noise, and specifically do not address low frequency variations in an image or artifacts.

NEMA MS 2-2008 (Revision 2014), Determination of Two-Dimensional Geometric Distortion in Diagnostic Magnetic Resonance Images

NEMA MS 2-2008 (R2014) defines a method for determining the maximum percent difference between the measured distances in an image and the actual phantom dimensions. This standard evaluates the geometric distortion in three orthogonal planes passing through the center of the specification volume. The purpose of the defined procedure is to provide a standardized method of measuring and reporting two-dimensional geometric distortion in an MR system (i.e., the maximum percent difference between the measured distances in an image and the actual corresponding phantom dimensions). Radial measurements, those that are between points spanning the geometric center of the test object, are used to characterize the geometric distortion. Measurements should be evenly spaced with an angular separation less than 45-degrees to sample sufficiently the angular variation of the geometric distortion.

900 MRI Standards and Guidance Documents from FDA

NEMA MS 3-2008 (Revision 2014), Determination of Image Uniformity in Diagnostic Magnetic Resonance Images

NEMA MS 3-2008 (R2014) defines a test method for measuring image-uniformity performance of MRDDs using head and body RF coils. NEMA MS 3-2008 (R2014) does not address the use of surface RF coils, chemical shift imaging, or spectroscopy. Image uniformity can be characterized in different ways. The choice of a measurement and reporting method was guided by a desire for simplicity, accuracy, and ease of implementation on all MR systems. The peak deviation method represents a single image test that can quickly determine and report uniformity with a single number. It works best with very high SNR images. The gray-scale uniformity map image represents a single image test that can visually describe image uniformity. Both the American College of Radiology (ACR) MR Accreditation Procedure method and the Normalized Absolute Average Deviation method resolve some of the image SNR issues of the peak deviation method. Measurements are made over a volume that is representative of the region used for typical clinical studies. Due to the difficulty in handling large phantoms, it is permitted to use a test phantom that only covers 85% of the specification area. This document does not address the use of special purpose RF coils (see MS 6) or RF coils that require multiple receiver channels for operation (see MS 9).

NEMA MS 4-2010, Acoustic Noise Measurement Procedure for Diagnostic Magnetic Resonance Imaging (MRI) Devices

NEMA MS 4-2010 defines test conditions and parameters that approximate the worst-case acoustic noise levels that a particular magnet/gradient system combination produces when using pulsed gradient waveforms. NEMA MS 4-2010 also describes how the acoustic noise levels should be measured. In the absence of specific guidelines for sound level exposure associated with the operation of MRI equipment, this procedure references the OSHA (Occupational Safety and Health Administration) guidelines for acoustic noise exposure and the IEC standards for sound level meters.

NEMA MS 5-2010, Determination of Slice Thickness in Diagnostic Magnetic Resonance Imaging

NEMA MS 5-2010 defines two methods for determining slice or section thickness in diagnostic MRI. The methods presented are essentially numerical in character and, consequently, will require the preparation and use of supplementary dedicated computer software to perform the computations. The methods are based on determining the slice profile, from which the slice thickness is obtained as the full width at half maximum. The slice profile is obtained either by direct measurement with a thin inclined slab of signal-producing material, or by numerical differentiation of the measured edge response function from an inclined surface of a wedge immersed in signal producing material. A correction technique is provided to compensate for errors caused by tilting the phantom. With the inclined slab approach, better SNR can be realized. However, the extremely thin slabs required for measurement of very thin slices are not practical to fabricate. Differentiation of the edge response function degrades the SNR that is obtained for the slice profile and usually requires the averaging of several measurements. Slices of any thickness, which can provide adequate

signal, may be evaluated with the wedge procedure, whereas the slab method is suitable for thicker slices.

NEMA MS 6-2008 (Revision 2014), Determination of Signal-to-Noise Ratio and Image Uniformity for Single-Channel, Non-Volume Coils in Diagnostic Magnetic Resonance Imaging (MRI)

NEMA MS 6-2008 (R2014) defines methods for evaluating single-channel non-volume coils or a single channel of an array RF coil. Both receive-only and transmit-receive RF coils are included. Head and body RF coils, and single-channel volume specialty RF coils, are excluded (see NEMA MS 1 and NEMA MS 3), as are RF coils requiring multiple receiver channels for operation (i.e., array RF coils, see NEMA MS 9) (5). R2014 presently permits the analysis of one channel of a multi-channel coil. These RF coils are used to receive signals from a limited region of interest and include linear or quadrature combined surface RF coils, flexible coils, pairs of coils such as Helmholtz coils, or RF coils that partially surround a specific tissue such as the calf or other extremity. NEMA MS 6-2008 (R2014) refers to these coils as “surface coils.” These RF coils achieve good SNR performance because of their increased filling factor. The purpose of the defined test procedure is to provide a standard means for measuring and reporting the SNR and uniformity of signal intensity in images acquired with surface RF coils. These quantities are helpful in evaluating RF coil performance and effectiveness. Evaluations are performed on phantom images generated using standard clinical MRI sequences.

NEMA MS 7-1993 (Revision 1998, Rescinded), Measurement Procedure for Time Varying Gradient Fields (dB/dt) for Magnetic Resonance Imaging Systems

NEMA MS 7-1993 defined two independent characterization methods including test conditions and parameters that ensure that worst-case dB/dt values of time-varying gradient fields used for patient exposure regions associated with MRI are measured or calculated (5). Both methods were based on the maximum peak dB/dt that the gradient system can produce, when using pulsed waveforms. If the static magnetic field is oriented along the z-axis, then time-varying gradient fields necessary for an MRI procedure are the dB_z/dt components produced by the x-, y, and z-gradients.

NEMA MS 8-2016, Characterization of the Specific Absorption Rate (SAR) for Magnetic Resonance Imaging Systems

NEMA MS 8-2016 defines two measurement procedures to assess the whole-body average, specific absorption rate (WB-SAR). This standard does not define a relationship between the SAR and the body temperature increase. Two procedures for WB-SAR measurements, the calorimetric method and the pulse-energy method are defined. The document does not apply to gradient (low-frequency time-varying magnetic fields) safety where nerve and possible cardiac excitation are the primary safety issues. It is also not intended to apply to spatial peak or local average SAR, nor does it address other factors involved with patient heating. The tests are specifically developed for volume RF transmit coils that produce relatively homogeneous RF fields. In 2016 NEMA MS 8 has been significantly revised. Changes were made to clarify the measurement methods and to make them easier for use by those who are not MR manufacturers. Specifically, the methods to consider the

902 MRI Standards and Guidance Documents from FDA

impact of uniformity for the static magnetic field were revised, a new method was added using power meters, and details on experimental methods, clarification of existing definitions, clarifying to the phantom requirements, and additional details on error analysis were made.

NEMA MS 9-2008 (Revision 2014), Characterization of Phased Array Coils for Diagnostic Magnetic Resonance Images (MRI)

NEMA MS 9-2008 (R2014) defines a test method for measuring the SNR and image uniformity of MR images produced using receive-only phased array coils. These quantities are helpful in evaluating the impact of MR system changes on performance or in demonstrating effectiveness for FDA applications. Other RF coil configurations have been addressed in MS 1, MS 3, and MS 6. Phased array RF coils consist of multiple receive-only coils that are used to detect signals from a limited portion of the patient's anatomy. The output of each RF coil element, or combined set of elements, is connected to the input of an independent receiver chain. Phased array RF coils may be composed of surface coils, flexible coils, pairs of coils such as Helmholtz coils, or RF coils that surround a specific anatomical region as well as combinations of these coils. Phased array RF coils achieve good SNR performance because of their increased filling factor and the use of smaller, higher SNR, receive coils. Major changes to R2014 are additional information related to noise statistics for coils with more than one channel and a table with the channel count dependent noise statistics.

NEMA MS 10-2010, Determination of Local Specific Absorption Rate (SAR) in Diagnostic Magnetic Resonance Imaging (MRI)

NEMA MS 10-2010 defines a measurement method for local specific absorption rate (SAR). The measurement method requires construction of a radiofrequency phantom for a given frequency and the use of radiofrequency transparent thermometry. The procedure is intended for local SAR measurements only and specifically does not address whole-body SAR. Local SAR is a parameter that relates to the safety of MRI scanners. The primary safety concern with transmit surface coils involves local SAR which may be highest near electrical conductors. This standard does not attempt to establish relationships between SAR and body temperature.

NEMA MS 11-2010 (Rescinded), Determination of Gradient-Induced Electric Fields in Diagnostic Magnetic Resonance Imaging

NEMA MS 11-2010 defined measurement methods for determining the gradient-induced electric fields for each gradient axis at a radius of 20-cm off the patient axis. The measurement method requires construction of electric field dipoles, spacers, a phantom, and the use of a high impedance device for measuring voltages. The electric field measurements are done in a solution with a conductivity value similar to that of the human body. Numerical methods of estimating the electric field are discussed in an appendix to NEMA MS 11-2010. Gradient-induced electric fields may affect the safety and comfort of patients. Typically, stimulation requires a gradient induced electric field of more than 2 V/m. The method described in this standard makes electric field measurements inside a phantom loaded with electrically conductive material. NEMA MS 11-2010 defines methods for de-

terminating the gradient-induced electric fields of diagnostic MRI gradient coils (head and body) under specific conditions. However, it does not address the effect of electrical inhomogeneities in the body on internal, gradient-induced, electrical fields.

NEMA MS 12-2016, Quantification and Mapping of Geometric Distortion for Special Applications

MS 12-2016 defines test methods for measuring the absolute spatial variation of geometric accuracy within MR images. The methods present an absolute geometric accuracy as a map, graph, or table throughout the imaging region rather than as simple figures of merit such as average or worst-case error. This standard deals exclusively with absolute error measurements, because it is assumed the end user will need geometric distortion error measurements in absolute terms. While the intent of this standard is to quantify equipment induced geometric errors only, the phantom used for these measurements will also introduce some geometric errors. It is not possible to remove the phantom-induced errors within the scope of this standard, and this standard assumes that the measured errors are exclusively equipment errors. Therefore, it is necessary for the user of this standard to be able to differentiate between geometric errors due to the MR system and errors that arise from measuring geometric distortion with a test object. The user should attempt to estimate the error the phantom introduces for the specific test conditions used.

This standard also recognizes that the measurements are ideally performed with three-dimensional acquisitions and large volume phantoms, but the cost, weight, and size of the required phantom may be prohibitive in certain situations. Therefore, this standard permits the use of a substantially two-dimensional phantom in conjunction with a set of two-dimensional image acquisitions in different orientations. These procedures could also be helpful in evaluating the impact of system changes on performance, for quality control programs that seek to continually reaffirm system performance, or in demonstrating effectiveness for FDA applications. However, this standard does not supersede NEMA MS 2 Determination of Two-Dimensional Geometric Distortion in Diagnostic Magnetic Resonance Images. MS 2 is designed to produce simple figures of merit that describe basic geometric distortions, or image field of view errors, that could arise from imaging gradient amplitude scaling errors. The revision in 2016 includes various changes to the spherical harmonic analysis-based methods.

ASTM INTERNATIONAL MRI STANDARDS FOR MEDICAL DEVICES AND IMPLANTS

In 1997, CDRH requested that the American Society for Testing and Materials (ASTM) (now known as the “ASTM International”) develop test methods to address safety and effectiveness issues for medical devices in the MRI environment. Based on this request, the ASTM formed the task group F04.15.11 on the safety and compatibility of implant materials and medical devices in the MRI environment. Task group F04.15.11 developed test methods for evaluating magnetically induced displacement force and torque, radiofrequency (RF) heating, image artifacts, and MR labeling. The first ASTM MRI test method was published in 2000 as the consensus standard, F2052-00, *Standard Test Method for Measurement of Magnetically Induced Displacement Force on Passive Implants in the Magnetic Resonance*

904 MRI Standards and Guidance Documents from FDA

Environment. Presently, ASTM International has five different consensus standards for MRI evaluation of passive implants and devices, including, the following:

(1) *ASTM F2052 Standard test method for measurement of magnetically induced displacement force on medical devices in the magnetic resonance environment* (9) defines a method for determining the displacement force or translational attraction. The spatial gradient of the magnetic field of the MR system produces a displacement force on magnetic objects placed in the magnetic field. This displacement force is responsible for the projectile effect that continues to cause injuries in the MRI environment.

ASTM F2052 requires the test object to be suspended by a thin string, less than 1% of the weight of the tested device and moved to the position in the magnetic field that produces the greatest displacement. The angular deflection of the device from the vertical is measured and the deflection force is calculated. If the angular deflection is less than 45°, and the magnetic force is in the horizontal direction, then the deflection force is less than the device's weight and it is assumed that the risk imposed by the magnetically-induced deflection force is no greater than the risk due to the gravitational force. However, counter-forces may also need to be considered, because these can act on an implant and prevent movement or displacement of the object. ASTM F2052 was revised in 2015 to require the test be performed in a MR system and change the test location to a location along the axis of the scanner's bore where the static magnetic field and spatial gradient of the magnetic field have components in the z direction only. A method was added to Appendix X3 for calculating the maximum allowable spatial gradient of the magnetic field for an implant or device.

(2) *ASTM F2213 Standard test method for measurement of magnetically induced torque on medical devices in the magnetic resonance environment* (10) defines a method for measuring the torque on a medical device in the MRI environment. The static magnetic field produces a torque on an object and forces it to align the long-axis of the object with the magnetic field. For this test procedure, the medical device with one principal axis aligned in the vertical direction is placed on a holder suspended on a torsional spring. The test fixture is then placed in the center of the MR system where the effect of torque is at a maximum. The angular deflection of the holder from its equilibrium position is recorded and the torque is calculated. The frame supporting the spring and holder is rotated through 360-degrees, and the torque, as a function of the angle of the device is determined. This measurement is repeated for the other two principal axes of the device to determine the maximum torque. According to ASTM F2213, the torque is acceptable if the maximum torque induced by the MR system is less than the product of the longest dimension of the implant and its weight. For medical devices within the acceptance criteria, the magnetically induced torque is less than the worst-case torque on the implant due to gravity. Again, counter-forces may also need to be considered because these can act on an implant and prevent movement or displacement of the object associated with torque. ASTM F2213 was revised in 2017 to add the Low Friction Surface Method, the Pulley Method, the Suspension Method, and the Calculation Based on Measured Displacement Force Method.

(3) *ASTM F2182 Standard test method for measurement of radio frequency induced heating on or near passive implants during magnetic resonance imaging* defines a test method for measuring RF-induced heating of passive implants (11). The RF field associated

with an MR system induces electrical currents in the body, which generate heat. The specific absorption rate (SAR), reported in Watts per kilogram (W/kg), is the mass normalized rate at which RF energy is coupled to biological tissue, which, if a metallic implant is present, is an important parameter to prevent excessive heating that may result in patient injury. According to ASTM F2182, the implant to be tested is placed in a phantom filled with a medium that simulates the electrical and thermal properties of the human body. The implant is placed at a location with well-characterized exposure conditions. The phantom material is a gelled-saline consisting of a saline solution and a gelling agent. Temperature probes, which are typically fluoroptic thermometry probes, are placed at locations where the induced implant heating is expected to be the greatest (this may require pilot experiments to determine the proper placement of the temperature probes). The phantom is then placed in an MR system or an apparatus that reproduces just the RF field. ASTM F2182 recommends using an RF field producing a whole-body averaged SAR of about 2 W/kg applied for approximately 15-minutes (or other time sufficient to characterize the temperature rise and the local SAR). The test procedure is divided into two steps: (1) the temperature rise on or near the implant at several locations is measured using the temperature probes during approximately 15-minutes of RF application. The temperature rise is also measured at a reference location during Step 1. (2) The implant is removed, and the same RF application is repeated while the temperature measurements are obtained at the same probe locations as in Step 1 (i.e., at the positions applied to the implant that is undergoing evaluation). From these measurements, the local SAR is calculated for each probe, including the reference location. The local SAR at the temperature reference probe is used to verify that the same RF exposure conditions are applied during Steps 1 and 2 of the test procedure.

ASTM F2182 underwent a major revision and ASTM published a new version end of 2019 (11). This new version has less emphasis on scaling the measured temperature rise to the average whole-body (WB) SAR. Instead of WB-SAR scaling, which is no longer required, the heating results are scaled to the local RF background exposure. The local RF background exposure can be characterized with either temperature probes (as it was done before) or with electric field measurements. The phantom shape changed by removing the “head” section from the phantom. The head section of the phantom was confusing because it suggested the idea that the phantom was an acceptable replica of the human anatomy. The new version emphasizes that the shape of the phantom is not specifically required. One example of phantom size and shape is provided in the document, but other types of phantoms are also allowed, as long as the local exposure is well characterized and that there is at least 2 cm distance between the implant and the phantom surface. Further changes included removing the requirement for intermediate conductivity measurements when building the phantom and revising certain sections regarding the implant holder and multi-configuration devices. The ASTM International committee agreed that a future revision should include computational modeling for passive implants. Notably, such modeling is already performed by many companies and MRI testing experts. This type of modeling uses computer-aided design (CAD) models of the implant to compute the *in vitro* heating with respect to local SAR, and then calculates the *in vivo* heating by scaling the *in vitro* results to the computationally assessed *in vivo* electric fields.

(4) *ASTM F2119 Standard test method for evaluation of MR image artifacts from passive implants* (12) defines a protocol for determining image artifacts associated with im-

906 MRI Standards and Guidance Documents from FDA

plants and devices using standardized pulse sequences (10). Although image artifacts do not generally affect the safety of a device in the MRI setting, physicians may need information about the size and location of image artifacts with respect to the location of the portion of the body that is to be imaged. The test defines pairs of spin echo and gradient echo MR images generated both with and without the implant in the field of view. The image artifacts are assessed by computing the differences between the reference and implant images.

(5) *ASTM F2503 Standard practice for marking medical devices and other items for safety in the magnetic resonance environment* (8) defines the terms, “MR Safe”, “MR Conditional”, and “MR Unsafe”, as follows: “MR Safe” — an item that poses no known hazards in all MRI environments; “MR Unsafe” — an item that is known to pose hazards in all MRI environments; and “MR Conditional” — an item that has been demonstrated to pose no known hazards in a specified MRI environment with specified conditions of use. The particular conditions that define the specified MRI environment include the static magnetic field strength, spatial gradient magnetic field, time-varying magnetic fields, radiofrequency fields, and the specific absorption rate (SAR). Additional conditions, including specific configurations or operational conditions of the implants or device, may also be defined.

In addition to these definitions, ASTM F2503 defines icons for the three definitions. The icons are intended for use on implants, devices, and other items that may be brought into, or near, the MRI environment, as well as in product labeling. The icons can be in color or in black and white. The MR Safe icon consists of the letters “MR” in green in a white square with a green border, or the letters “MR” in white within a green square. The MR Conditional icon consists of the letters “MR” in black inside a yellow triangle with a black border and the MR Unsafe icon consists of the letters “MR” in black on a white field inside a red circle with a diagonal red stripe. The MR Conditional item labeling must include information for the acceptable conditions that are sufficient to characterize the behavior of the item in the MRI setting. This additional information should address magnetic field interactions (i.e., magnetically-induced displacement force and torque) and RF-induced heating. Other possible safety issues may include induced currents/voltages, electromagnetic field-related issues, thermal injury, nerve stimulation, possible acoustic noise issues, interaction among different devices, the safe functioning of the device, and the safe operation of the MR system. Any parameter that affects the safety of the item should be listed and any condition that is known to produce an unsafe condition must be described in the MR Conditional labeling for the item. F2503 was revised in 2013 to create an ASTM International and an IEC standard with identical content.

THE ISO TECHNICAL SPECIFICATION (TS) 10974 FOR ACTIVE IMPLANTABLE MEDICAL DEVICES

For many years, scanning a patient with an Active Implantable Medical Device (AIMD) was contraindicated by the MR system and AIMD manufacturers. Because performing MRI procedures in patients with AIMDs, such as cardiac pacemakers, neurostimulation systems, cochlear implants, implantable infusion pumps, and other similar devices, is increasingly necessary for proper patient management, CDRH is faced with increasingly more marketing submissions requesting MR Conditional labeling for AIMDs. The issue of AIMDs in patients referred for MRI examinations became even more apparent because of anecdotal re-

ports of off-label scanning and the possible perception that the risk is not as significant as believed by AIMD manufacturers, MR system manufacturers, and regulatory bodies. Interestingly, FDA's Manufacturer and User Facility Device Experience (MAUDE) (13) database for adverse event reporting still indicates instances of device failures and patient injuries associated with MRI examinations performed on patients with AIMDs. Because of the harsh electromagnetic environment associated with MRI, the testing of AIMDs in these fields is especially challenging. The development of appropriate test methods required detailed technical knowledge of the electromagnetic fields emitted by the MR system.

In 2005, CDRH held meetings with representatives from both MR system and AIMD manufacturers that led to an International Organization for Standardization (ISO) recommendation to form a liaison with the International Electrotechnical Commission (IEC/SC 62B/MT 40, responsible for the safety standard for MRI equipment, IEC 60601-2-33, *Particular requirements for the basic safety and essential performance of magnetic resonance equipment for medical diagnosis*) (5), to consider recommendations that could be used to write MRI-related safety requirements for AIMDs. In April 2018, the joint ISO/IEC working group (JWG) published the second edition of the dual logo Technical Specification (TS) 10974 entitled, "*Assessment of the safety of magnetic resonance imaging for patients with an active implantable medical device*" (14). This second edition incorporated experience gained from the first edition of its use in practice and the current understanding of relevant issues and concerns at 1.5 T. Based on information received from the committee the JWG is currently working on converting the TS into an International Standard. By mutual agreement between the JWG and MT 40, all MR scanner-related requirements will be considered by MT 40 and will be released through future amendments and editions of IEC 60601-2-33. It is important to mention that no requirements contained within 60601-2-33, including the use of clinical scanners, construe or imply any obligation for compliance on the part of MR scanner manufacturers. The test methods contained in TS 10974 for evaluating device operation against several hazards are applicable to a broad class of AIMDs. Specific compliance criteria and the determination of risk resulting from device responses during these tests are outside the scope of TS 10974. The test methods in TS 10974 were derived from six known potential hazards to patients with an AIMD undergoing an MR scan. These potential hazards are: device heating due to the RF field and the gradient magnetic fields, vibration due to the gradient magnetic fields, force and torque due to the static magnetic field, unintended stimulation due to the gradient magnetic field-induced lead voltage and the RF field-induced rectified lead voltage, and device malfunction due to the static magnetic field, the RF field, and the gradient magnetic fields. Evaluation of the AIMD for these hazards involves some combination of testing and modeling. Tests may use bench-top testing, modeling, MR scanners, or a combination of these approaches. Implants and devices are subjected to radiated fields or injected voltages in order to elicit device responses. Modeling may be employed to determine appropriate test signal voltage levels or to estimate tissue heating. Major changes planned to be incorporated in the new International Standard (IS) 10974 is the addition of 3 T test methods, enhancement of the combined field test method, and eliminating what is referred to as a Tier 1 approach for RF-induced heating testing. The JWG is attempting to maintain the requirements for IS 10974 backwards compatible with the second edition of TS 10947 so that regulators don't require re-testing legacy devices. The JWG plans to develop the draft for IS 10974 in the near future.

908 MRI Standards and Guidance Documents from FDA

THE IEC STANDARD 60601-2-33 FOR MR SYSTEMS

As outlined in detail above the National Electrical Manufacturers Association (NEMA) has developed standards for the measurement of performance and safety parameters in MRI. Another international standard setting organization, the International Electrotechnical Commission (IEC) has developed IEC 60601-2-33 that addresses many of the safety issues associated with MRI examinations. In the early 1990s, work began on IEC 60601-2-33, *Particular Requirements for the Safety of Magnetic Resonance Equipment for Medical Diagnosis*, and the first edition was finalized in 1995. The FDA participated in the development of this document, which had a significant influence on current FDA policies and guidance documents relating to MRI. This is particularly important because the FDA has the responsibility of ensuring both the safety and effectiveness of medical devices.

The latest version of IEC 60601-2-33 Edition 3.2, *Particular Requirements for the Basic Safety and Essential Performance of Magnetic Resonance Equipment for Medical Diagnosis*, was published in 2015 (5). Although the title mentions “essential performance”, no such requirements have been identified within the scope of the standard. The third edition mainly establishes particular basic safety to provide protection for the patient and the MRI health-care worker. Because IEC 60601-2-33 does not address performance issues, such as the signal-to-noise ratio, image uniformity, geometric distortion, and slice thickness, the FDA has specified in the guidance titled *Submission of Premarket Notifications for Magnetic Resonance Diagnostic Devices* (2) from November 2016, performance tests for MR imaging and spectroscopy.

Before working on the Fourth Edition of 60601-2-33 the Committee (IEC 62/62B/MT40) released two Amendments to the Third Edition. The first amendment (AMD1) was released in 2013 with formal updates to the latest general and collateral standards, whereas the second amendment (AMD2) was released in 2015. AMD1 was published to adapt IEC 60601-2-33:2010 to the technical corrections introduced to IEC 60601-1:2005. AMD2 was developed to increase the First Level Controlled Operating Mode limit for the static magnetic field from 4 T to 8 T considering the FDA, the ICNIRP (15), and the peer reviewed scientific literature. In addition, a non-compulsory option, called the Fixed Parameter Option B (Basic) (FPO:B) (16), was introduced to limit RF and gradient field outputs (peak and the root mean square, RMS) for scanning patients with MR Conditional implants and devices. Consequently, text was proposed for the Instructions For Use (IFU) to guide users in scanning patients with MR Conditional implants and devices. Plans for the Fourth Edition of 60601-2-33 include the single fault safety of the emergency rundown button, to reestablish acoustic protection, to include reference to the Medical Imaging & Technology Alliance (MITA) RF coil/cable heating test standard, and to reestablish systemic and local RF protection without introducing the CEM43 concept (17, 18).

CONCLUSIONS

In the past thirty-five years, MRI technology has developed into a major radiological modality to the point where it has become the gold standard or technique of choice for the diagnosis of a number of disorders, conditions, and abnormalities. During this period, there have been major changes in safety standards and guidance documents, particularly in the

field of AIMD safety, where the TS 10974 was developed and is widely used to assess the safety of AIMDs in relative to the use of MRI technology. In general, recommended patient exposure limits have risen as a result of increased knowledge regarding the biological effects of the static, time-varying magnetic, and RF fields associated with MRI. One of the most important lessons learned is that safety standards and guidance documents, although subject to change over time, provide the most current and generally accepted guidance towards safe use of MRI technology and should be followed, if applicable, to address safety concerns. Any deviations from recommended guidance documents should be accompanied by a detailed and scientifically sound rationale.

Disclaimer

The findings and conclusions in this chapter have not been formally disseminated by the Food and Drug Administration and should not be construed to represent any Agency determination or policy.

Acknowledgements

I wish to acknowledge the valuable contributions of the CDRH reviewers regarding the improvement of quality, coherence, and content of this chapter. My sincere thanks goes to Jismi Johnson (CDRH/OPEQ), Dr. Randall Brockman (CDRH/OPEQ), Dr. Zane Arp (CDRH/OSEL), and Dr. Sunder Rajan (CDRH/OSEL) for their valuable input, guidance, and thorough review of this chapter.

REFERENCES

1. Standards and Conformity Assessment Program. In: Medical Devices / Device Advice: Comprehensive Regulatory Assistance. Food and Drug Administration. Available at www.fda.gov/medical-devices/device-advice-comprehensive-regulatory-assistance/standards-and-conformity-assessment-program. Accessed March, 2020.
2. Guidance Documents (Medical Devices and Radiation-Emitting Products). In: Medical Devices / Device Advice: Comprehensive Regulatory Assistance. Food and Drug Administration. Available at www.fda.gov/medical-devices/device-advice-comprehensive-regulatory-assistance/guidance-documents-medical-devices-and-radiation-emitting-products. Accessed March, 2020.
3. Premarket Notification 510(k). In: Medical Devices / Device Advice: Comprehensive Regulatory Assistance / How to Study and Market Your Device / Premarket Submissions. Food and Drug Administration. Available at www.fda.gov/medical-devices/premarket-submissions/premarket-notification-510k. Accessed March, 2020.
4. Magnetic resonance diagnostic device. In: Code of Federal Regulations, Title 21 Food and Drugs, Part 892 Radiology Devices, Subpart B Diagnostic Devices, §892.1000. Electronic Code of Federal Regulations (e-CFR). Available at www.ecfr.gov. Accessed March, 2020.
5. International Electrotechnical Committee (IEC). 60601-2-33 Edition 3.2, Medical electrical equipment - Part 2-33: Particular requirements for the basic safety and essential performance of magnetic resonance equipment for medical diagnostic. 2015.
6. National Electrical Manufacturers Association (NEMA). In: The Association of Electrical Equipment and Medical Imaging Manufacturers. Available at www.nema.org. Accessed March, 2020.
7. Shellock FG, Woods TO, Crues JV. MR labeling information for implants and devices: explanation of terminology. Radiology 2009;253:26-30.

910 MRI Standards and Guidance Documents from FDA

8. American Society for Testing and Materials (ASTM) International. ASTM F2503 Standard practice for marking medical devices and other items for safety in the magnetic resonance environment.
9. American Society for Testing and Materials (ASTM) International. ASTM F2052 Standard test method for measurement of magnetically induced displacement force on medical devices in the magnetic resonance environment.
10. American Society for Testing and Materials (ASTM) International. ASTM F2213 Standard test method for measurement of magnetically induced torque on medical devices in the magnetic resonance environment.
11. American Society for Testing and Materials (ASTM) International. F2182, Standard test method for measurement of radio frequency induced heating on or near passive implants during magnetic resonance imaging.
12. American Society for Testing and Materials (ASTM) International. ASTM F2119 Standard test method for evaluation of MR image artifacts from passive implants.
13. FDA/CDRH. MAUDE - Manufacturer and User Facility Device Experience Available via www.accessdata.fda.gov/scripts/cdrh/cfdocs/cfmaude/search.cfm. Accessed Nov. 2019.
14. ISO TS 10974/Ed.2, Assessment of the safety of magnetic resonance imaging for patients with an active implantable medical device. 2018.
15. International Commission on Non-Ionizing Radiation Protection (ICNIRP). Guidelines for limiting exposure to time-varying electric, magnetic, and electromagnetic fields (up to 300 GHz). Health Phys 1998;74:494–522.
16. Steckner M, et al. Proposed fixed parameter option: Limiting MRI scanner outputs for patients with MR conditional active implantable medical devices. Proceedings of the International Society for Magnetic Resonance Imaging, Scientific Workshop. MR Safety in Practice: Now and In the Future. Sweden 2012;5-7.
17. Murbach M, Neufeld E, Capstick M, et al. Thermal damage tissue models analyzed for different whole-body SAR and scan duration for standard MR body coils. Magn Reson Med 2014;71:421–431.
18. Murbach M, Neufeld E, Kainz W, Pruessmann KP, Kuster N. Whole-body and local RF absorption in human models as a function of anatomy and position within 1.5T MR body coil. Magn Reson Med 2014;71:839–845.

Chapter 34 MRI Standards and Safety Guidelines in Europe

STEPHEN F. KEEVIL, PH.D.

Head of Medical Physics

Department of Medical Physics

Guy's and St Thomas' NHS Foundation Trust

London, England

United Kingdom

and

Professor of Medical Physics

School of Biomedical Engineering and Imaging Sciences

King's College London

London, England

United Kingdom

INTRODUCTION

In the period from 2003 to 2013, the magnetic resonance imaging (MRI) community in Europe was engaged in a campaign related to a portion of the European Union (EU) occupational health and safety legislation, the Physical Agents (Electromagnetic Fields, EMF) Directive (1), which appeared to pose a substantial threat to the use of MRI in clinical practice and research (2, 3, 4). This contentious debate served to highlight the question of how MRI safety issues are currently regulated in Europe. Although there is no single piece of European legislation concerned expressly with MRI safety, there are a number of sets of regulations and official guidance that are relevant in this area and which staff members working with MRI should be aware of to ensure they remain legally compliant and, importantly, to promote a safe environment for both patients and staff members.

In this chapter, the body of the EU safety legislation, international standards and guidelines that impact the use of MRI in Europe are discussed. Although Europe and the European Union are neither synonymous nor coterminous, this chapter will be concerned mainly with the situation in the EU. Notably, in some policy areas, including occupational health and safety, EU legislation also applies in the wider European Economic Area (EEA) (encompassing Iceland, Liechtenstein, and Norway), often also in Switzerland, and in some in-

912 MRI Standards and Safety Guidelines in Europe

stances even more widely (e.g., the legislation of medical devices as it is applied in Turkey, see below). Since there will be considerable discussion of EU legislation in this chapter, background information is needed for readers outside the EU (and for many within it).

NATIONAL AND SUPRANATIONAL LEGISLATION IN THE EUROPEAN UNION

Currently, the EU is a partnership of 27 sovereign countries¹, each with its own independent government, legislature, and body of law. However, under the treaties establishing the EU, these “member states” have conferred certain powers on the EU collectively, including the power to make laws that are binding on all of them in order to advance the objectives of the treaties. The mechanism by which EU law is made varies between different policy areas but, in general, it involves the European Commission, the European Parliament, and the Council of the EU. The Commission is composed of permanent officials and provides the EU’s “civil service”. It is headed by the College of Commissioners, a group of politicians forming the “cabinet” of the EU. There is one Commissioner from each member state, each having different policy responsibilities. Only the Commission has the power to propose new legislation, which is then passed to the Parliament and Council for amendment and approval. The European Parliament is composed of members (MEPs) directly elected by citizens of EU member states for terms of five years. Like most national legislatures, it contains a variety of political groupings and carries out much of its work through a system of committees focusing on different policy areas. The Council of the EU is made up of government ministers from each member state, with the attending minister changing depending on the area of policy under discussion. In practice, much of its work is carried out in committees and working parties made up of civil servants and diplomats. The overall political direction of the EU is set by a separate body, rather confusingly called the European Council, made up of member state heads of government. (Even more confusingly, there is also an international organization called the Council of Europe, which is entirely distinct from the EU.)

Most EU legislation (for our purposes) takes the form of *directives* and *regulations*, which become law in member states in different ways. Once the Parliament and Council have adopted a directive, all member state governments are required to implement its provisions in their domestic law (a process known as “transposition”) by a fixed date. If a member state fails to meet the transposition deadline, the Commission may take “infraction proceedings” against that country in the Court of Justice of the EU. A regulation, by contrast, is legally binding in all member states as soon as it comes into force, without the need for transposition. EU law takes priority over individual national law, although member states are able to introduce more stringent laws in some policy areas, including worker protection.

Several EU directives have implications for MRI safety. The most significant of these are discussed below, but others that may need to be taken into account in the context of MRI include the Physical Agents (Noise) Directive (2003/10/EC) and the Pressure Equipment Directive (97/23/EC), as well as more general legislation dealing with issues such as electrical and mechanical safety, manual handling, use of display screens, and others. Most of these issues will not be discussed further in this chapter, where the focus is primarily on

the management of hazards arising from electromagnetic fields (EMF) with an emphasis on MRI.

THE PURPOSE OF STANDARDS AND GUIDELINES: DIRECT AND INDIRECT HAZARDS ASSOCIATED WITH MRI

The hazards of MRI are discussed in detail elsewhere in this textbook. Briefly, MRI safety discussions often focus on direct and indirect hazards of EMF. *Direct hazards* are those arising directly from exposure of the human body to EMF (the static magnetic field, time-varying magnetic fields and radiofrequency radiation), primarily peripheral nerve stimulation (PNS) and radiofrequency (RF) heating. There are also transient sensory effects such as magnetic field-induced vertigo and (rarely in MRI) magnetophosphenes. There has been some debate as to whether or not these phenomena should be regarded as adverse health effects. Most in the MRI community would take the view that they should not, but some commentators argue that the World Health Organization (WHO) definition of health as “complete physical, mental and social well-being...” (5) implies that transient disturbances of this kind do constitute adverse effects. Direct hazards are often addressed by setting exposure limits in order to avoid or to minimize the effect in question. These limits may be specific to MRI, or may apply to all sources of EMF exposure.

Indirect hazards arise when electromagnetic fields interact with an object or device in such a way that it then poses a hazard to patients or workers. Examples are ferromagnetic projectiles attracted by the strong static magnetic field and effects on biomedical implants. By far, these are the more serious type of hazards associated with MRI that are best prevented through the adoption of rules for safe working, worker training, and by other means rather than by imposing exposure limits. This may be an entirely local matter, but in some countries there are national guidelines on MRI safety to provide more effective and uniform protection. Both types of hazard may also be minimized through proper equipment and facility design.

THE EU HEALTH AND SAFETY FRAMEWORK DIRECTIVE: RULES AND RESPONSIBILITIES

Most European countries do not have specific laws addressing MRI safety. However, generic legislation to protect worker health and safety exists in each EU member state, based on the health and safety framework directive (89/391/EEC) (6). Under this legislation, employers (which in this context would encompass hospitals, private clinics and universities) have a duty to ensure the safety and health of workers in every aspect related to the work. For example, they must conduct risk assessments of each work process, adopt appropriate protective measures, and provide workers with adequate training. There are also requirements placed on workers to take care of their own health and safety, and that of other persons, and to make correct use of work equipment. However, this is explicitly dependent on the training and instructions received so, again, the primary responsibility rests with the employer. These provisions apply to MRI just as much as to any other occupational setting. In the United Kingdom (UK), the Health and Safety Executive (HSE), the government agency responsible for occupational health and safety, has in recent years conducted in-

914 MRI Standards and Safety Guidelines in Europe

Table 1. A simple risk assessment matrix. Performance of risk assessments in all workplaces, including MRI facilities, is a requirement of the EU health and safety framework directive (89/391/EEC).

		Consequences (severity of injury / financial loss / reputational damage)				
Likelihood (within a year)		Minimal	Minor	Moderate	Major	Catastrophic
	Almost certain	Moderate risk	Significant risk	High risk	Extreme risk	Extreme risk
	Likely	Low risk	Moderate risk	Significant risk	High risk	Extreme risk
	Possible	Low risk	Low risk	Moderate risk	Significant risk	High risk
	Unlikely	Low risk	Low risk	Low risk	Moderate risk	Significant risk
	Rare	Low risk	Low risk	Low risk	Low risk	Moderate risk

spections of MRI facilities, requiring risk assessment documentation and other evidence of safe working practices.

Risk assessment is an important aspect of compliance with the framework directive. A variety of approaches exist for assessing and quantifying risk and the impact of risk mitigation, often taking the form of a matrix in which the risk of an event is categorized (and sometimes quantified) according to its likelihood and the potential severity of its outcome (**Table 1**). In the case of MRI, a projectile incident, for example, might be categorized as an “extreme risk” event in the absence of appropriate safety procedures and training, but with that mitigation in place might then be downgraded to a “moderate risk”.

THE MEDICAL DEVICES REGULATION

EU legislation relating to “medical devices” (a broad term that encompasses everything from bandages to MR systems) also creates health and safety responsibilities for both manufacturers and users of MR scanners. Many classes of product require a “CE mark” before they can be placed on the market in the EU. These include products as diverse as gas appliances, refrigerators, weighing instruments, fireworks, and toys. The process of obtaining a CE mark requires the manufacturer to ensure that the product conforms to the requirements of applicable EU regulations and directives. In the case of medical devices, regulation has hitherto taken the form of a series of medical device directives, requiring transposition in each member state and hence providing scope for a degree of nuancing to meet local circumstances. However, in 2017 the EU adopted the Medical Devices Regulation (Regulation (EU) No 2017/745) (MDR) (7) in order to create a more robust and uniform regulatory environment across the Union. This regulation was due to come fully into force in May 2020, but has now been delayed until May 2021 due to the Covid-19 pandemic.

One of the most important of the “general safety and performance requirements” set out in the MDR is that “Devices...shall not compromise the clinical condition or the safety of patients, or the safety and health of users or, where applicable, other persons”. Demonstrating safety is therefore a key aspect of the CE marking process and, hence, a prerequisite for marketing a medical device in Europe.

Previous medical device directives contained a provision whereby manufacture or modification of devices within the same health institution in which they were to be used was exempt from all requirements of the directive (known as the health institution exemption, HIE). The term “health institution” in this context includes research laboratories “that support the healthcare system” (e.g., university laboratories). This situation has changed under the new MDR, and such devices will now be required to comply with the general safety and performance requirements of the MDR. In practice, this should not be a major issue, since quite apart from medical device legislation there is already a more general legal requirement for institutions to ensure that devices they manufacture are safe and fit for purpose. However, the MDR also creates a requirement for manufacture *and use* of such devices to take place within “appropriate quality management systems”. At the time of writing, regulators in member states are still drawing up guidelines as to how this should be interpreted. The new HIE requirements clearly apply to development of new MR systems or components (e.g., RF coils) in research laboratories, but they also affect modification of commercial systems, potentially including pulse programming if this takes the system outside the scope of its original CE mark.

THE IEC/EN 60601 STANDARD SERIES

The International Electrotechnical Commission (IEC) 60601 standard series provides the usual means whereby medical device manufacturers demonstrate compliance with previous medical device directives and with the new MDR. The European Commission recognizes these standards as harmonized standards for this purpose, so that satisfying their requirements gives a “presumption of conformity” with relevant legislative requirements. These are global standards, not specific to Europe. They underpin the design and manufacture of MR systems sold throughout the world and are recognized by many national medical device regulatory agencies, including the United States (U.S.) Food and Drug Administration (FDA). However, they have a particular importance in Europe because of their close relationship to the MDR and, therefore, are discussed in some detail here. Strictly speaking, it is the version of the IEC standard adopted by the European Committee for Electrotechnical Standardization (CENELEC), known as an EN standard, that is harmonized to the MDD but this is practically identical to the IEC original.

The IEC/EN 60601 series consists of a general medical device safety standard (60601-1) (8), “collateral standards” covering specific aspects of device performance, some of which are relevant to MRI such as electromagnetic compatibility (60601-1-2) and usability (60601-1-6), and “particular standards” in the 60601-2 series dealing with specific device types. Standard 60601-2-33 is the particular standard for MR systems (9) and is maintained by a group of MRI experts drawn from industry, clinical users, regulators and the academic community.

IEC/EC 60601-2-33 sets out criteria for equipment safety and details of measurement procedures for manufacturers to demonstrate compliance. Importantly, it also describes the “Instructions for Use” that manufacturers must provide to purchasers of scanners. These include mandatory safety information and create obligations for the end user in areas such as safe system operation, worker training, control of access to the scanner, and patient handling. Much of this material is intended to manage indirect hazards.

916 MRI Standards and Safety Guidelines in Europe

Table 2. Exposure limits for patients and MRI workers according to the IEC standard 60601-2-33.

	Static magnetic field	Switched gradients*	Radiofrequency field**		
			Gradient output as a percentage of directly determined mean PNS threshold level	Maximum core temperature (°C)	Maximum local tissue temperature (°C)
Normal Operating Mode	≤ 3-T	≥ 80%	39	39	0.5
First Level Controlled Operating Mode	> 3-T, ≤ 8-T	≥ 100%	40	40	1
Second Level Controlled Operating Mode	> 8-T	> 100%	> 40	> 40	>1

*Default limits are also defined, in terms of induced electric field strength and gradient switching rate, as an alternative to direct determination.

**Various specific absorption rate (SAR) limits are also defined to ensure compliance with these temperature limits.

Unusually for a standard of this type, 60601-2-33 also contains EMF exposure limit values, addressing direct hazards. These limits are summarized in **Table 2**. They apply equally to patients and to MRI workers, with the rationale that the intention to avoid adverse effects in patients ensures that workers are also protected. The standard adopts a tiered approach to EMF exposure limitation, with three operating modes defined by exposure thresholds. In the *Normal Operating Mode*, there is considered to be no risk of “physiological stress” to patients. In the *First Level Controlled Operating Mode*, the threshold for physiological effects may be approached, and medical supervision is recommended. In the *Second Level Controlled Operating Mode*, there may be significant risk and local regulatory approval is required (e.g., from a research ethics committee or institutional review board, IRB), which should explicitly state the permitted levels of exposure. The instructions for use passed to the end user must refer to the hazards associated with EMF and to these exposure limits. They must also give advice on worker training to mitigate transient effects, such as vertigo, that may occur at higher exposure levels, and explain that national laws may set lower exposure limits for workers in some countries, as is discussed later in this chapter.

One point worthy of particular note is that the main approach to limiting exposures to time-varying magnetic fields focuses on direct determination of the physiological threshold for peripheral nerve stimulation (PNS) (which is merely a tactile sensation at the onset level) in a group of healthy volunteers, with the *Normal Operating Mode* limit set at 80% of this threshold. This differs from most other guidelines in avoiding the unwanted physiological

effect directly, rather than by means of an exposure limit expressed in terms of physical quantities that is inevitably a conservative proxy. There are also default limits on induced electric field and gradient switching rates for use when direct determination has not been employed, but these are also derived from an empirical equation describing PNS thresholds.

ICNIRP GUIDELINES ON EMF EXPOSURE

The EMF exposure limits contained in IEC/EN standard 60601-2-33 are designed specifically for use in MRI and, as far as possible, they are incorporated into MR scanners in the form of hardware and software interlocks and other safety features. There are also international guidelines on EMF exposure of more generally applicability. The International Commission on Non-Ionizing Radiation Protection (ICNIRP) is the main organization active in this area and its guidelines have significant influence in Europe.

The ICNIRP develops guidelines and exposure limits to address adverse health effects of exposure to all forms of non-ionizing radiation, including EMF. The ICNIRP issued guidance on static magnetic field exposure in 1994 (10), which was updated in 2009 (11). Guidance on time-varying magnetic fields in the frequency range up to 300-GHz was published in 1998 (12), and updated in 2010 for the frequency range 1-Hz to 100-kHz (13), and in 2020 for the frequency range 100-kHz to 300-GHz (14). In 2014 ICNIRP issued new guidance on exposure to time-varying magnetic fields with frequencies below 1-Hz (primarily to prevent sensory effects associated with movement in and around static magnetic fields associated with MRI) (15). With the exception of (15), all of these guidelines contain exposure limits for workers, and also lower limits for members of the general public, which do not concern us directly here. There is also a specific statement from the ICNIRP on protection of patients in MRI, published in 2004 (16) and revised in 2009 (17).

The ICNIRP bases its exposure limits, known as “basic restrictions”, on the thresholds for “established adverse effects”, determined by critical review of the literature (18). The biological effects of EMF on the human body vary dramatically with frequency. In the low frequency range relevant to the switched gradients in MRI (around 1-kHz), the relevant effect is stimulation of nervous tissue. The obvious manifestation of this is PNS, but historically there has been a tendency to regard magnetophosphenes (which only occur over a narrow frequency range around 10- to 50-Hz) as a possible indication of EMF interactions with the central nervous system over a much wider frequency range (19), resulting in much lower exposure limits than are justified by the desire to avoid PNS alone. This is more of an issue with the 1998 guidelines than with those issued in 2010, where a helpful distinction has been drawn between adverse effects (PNS) and transient disturbances (magnetophosphenes). In the radiofrequency range the critical effect is tissue heating and setting a limit is simply a matter of deciding how much heating is acceptable. Basic restrictions are often expressed in terms of quantities that cannot be readily determined, such as the electric field or current density induced in the body by a time-varying magnetic field, so the ICNIRP also defines “reference levels” in terms of quantities that are easier to measure, such as static magnetic field strength. These are derived from the basic restrictions using conservative models, so that complying with the reference level ensures that the relevant basic restriction is satisfied.

918 MRI Standards and Safety Guidelines in Europe

Table 3. ICNIRP basic restrictions for occupational exposure to electromagnetic fields relevant to MRI.

Static magnetic field	Movement in static magnetic field (< 1-Hz representative frequency)	Switched gradients (1-kHz representative frequency)	Radiofrequency field
<u>1994</u> - Time average: 200-mT - Head and trunk: 2-T - Limbs: 5-T	<u>1998</u> Induced current density (RMS) - Head and trunk: 40-mA m ⁻² (≈ 200-mV m ⁻¹)	<u>1998</u> Induced current density (RMS) - Head and trunk: 10-mA m ⁻² (≈ 50-mV m ⁻¹)	<u>1998 and 2020</u> SAR* - Whole body: 0.4-W kg ⁻¹ - Localized, head and trunk: 10-W kg ⁻¹ - Localized, limbs: 20-W kg ⁻¹
<u>2009</u> - Controlled environment: 8-T	<u>2014</u> Maximum change in magnetic flux density over any 3 s period: 2-T Induced electric field (controlled environment): 1.1 Vm ⁻¹	<u>2010</u> Induced electric field - Head and body: 800-mV m ⁻¹	

*SAR values averaged over 6-minutes, except whole body SAR in 2020 guidance averaged over 30-minutes;
Localized SAR values averaged over 10-g of tissue.

The ICNIRP's basic restrictions on occupational exposure are often more restrictive than the exposure limits contained in the IEC standard. This is mainly because the ICNIRP applies reduction factors to adverse effect thresholds in order to arrive at the basic restrictions. The rationale is that this reflects uncertainties in scientific knowledge about adverse effects and their thresholds, and also accounts for biological variations in effect thresholds that may exist between individuals. Also, the ICNIRP adopts a broad definition of health, based on that of the WHO (5), so that effects resulting in annoyance or discomfort, affecting a person's wellbeing but otherwise harmless, may be regarded as potential health hazards (18). To add to this, because it is often impractical to demonstrate compliance with the basic restrictions, there is a tendency to treat the more conservative reference levels as default exposure limits.

Table 3 summarizes the ICNIRP basic restrictions for workers, insofar as they are relevant to MRI. For clarity, reference levels, general public limits and the complexities of frequency dependence have been omitted. Where guidelines allow, it has been assumed that MRI is a "controlled environment" in which workers have been adequately trained. In some instances higher limits apply in such circumstances. In the case of switched gradients, which have complex non-sinusoidal waveforms, the ICNIRP limits at a representative frequency of 1-kHz have been used. Values from the superseded 1994 and 1998 guidelines are included, for reasons that will become clear later.

Table 4 summarizes the ICNIRP guidance on exposure limits for MRI patients. In its MRI statements, the ICNIRP takes a similar approach to that adopted in IEC 60601-2-33. Three tiers of exposure are defined: *Normal Operating Mode*, *Controlled Operating Mode* (requiring medical supervision) and *Experimental Operating Mode* (requiring institutional review board, IRB, approval). The gradient exposure limits are based on PNS perception

Table 4. ICNIRP recommended limits for patient exposures during MRI.

	Static magnetic field	Switched gradients	Radiofrequency field				
			Gradient switching rate (dB/dt) as a percentage of mean perception threshold for PNS*	Maximum core temperature rise (°C)	Maximum local tissue temperature (°C)		
					Head	Trunk	Extremities
Normal Operating Mode	≤ 4-T	≥ 80%	0.5	38	39	40	
Controlled Operating Mode	> 4-T, ≤ 8-T	≥ 100%	1	38	39	40	
Experimental Operating Mode	> 8-T	> 100%	>1	>38	>39	>40	

*The peripheral nerve stimulation (PNS) mean perception threshold is derived from an empirical equation.

thresholds derived from the same equation as is used to generate the IEC default limit values. Thus, they are based on actual effect thresholds, although direct determination is not embraced. RF heating limitations are also similar to those in the IEC standard and, again, there are a number of derived SAR limits. However, crucially, these limits apply only to patients undergoing MRI. MRI workers remain subject to the ICNIRP occupational basic restrictions shown in Table 3.

THE EU EMF DIRECTIVE

Article 16 (1) of the framework directive (6) envisages adoption of additional individual directives to address specific health and safety hazards. In this context, the Physical Agents (EMF) Directive (2004/40/EC) (1) was adopted by the European Parliament and Council on 29th April 2004, with a deadline of 30th April 2008 for member state transposition. Its objective was to protect workers from the “known short-term adverse effects in the human body” of exposure to EMF. This document was concerned only with occupational exposure, not exposure of MRI patients or of the general public.

920 MRI Standards and Safety Guidelines in Europe

The directive incorporated the 1998 ICNIRP exposure limits for time-varying magnetic fields, with the intention of making the ICNIRP basic restrictions into legally binding limits throughout the EU.

Members of the European MRI community became aware of the directive shortly before it was adopted. It was quickly realized that the proposed exposure limits are exceeded in a number of situations in MRI and that the directive would have serious consequences for both clinical and research activity. A lengthy lobbying campaign followed, led by the European Society of Radiology (ESR). There were also campaigns in individual member states and a parliamentary inquiry in the United Kingdom (UK) (20). After considerable effort and the publication of research showing that the limits are indeed exceeded by MRI workers (21, 22), the community's argument about the impact of the directive was accepted. Specifically, research showed that the limit for frequencies below 1-Hz was exceeded by a factor of up to 10 for workers moving through the static magnetic field near the MR system (21), and the ELV in the gradient frequency range by a factor of 20 or more for workers standing close to the scanner during imaging (22) (note, RF exposure is rarely, if ever, a problem). Thus, providing clinical care to a patient during MRI, all forms of interventional MRI, certain research activities, or even walking at a normal speed close to an MR system, would have become illegal throughout the EU following transposition of the directive.

Of course, this does not mean that workers in these situations are placing themselves at risk of direct EMF effects: IEC 60601-2-33 ensures that this is not the case. The problem is the large safety factors built into the ICNIRP basic restrictions, particularly in the gradient frequency range. These may have a place in industrial settings with highly variable EMF outputs, but are unnecessary and highly problematic in the context of MRI, where EMF outputs are precisely controlled and adverse effects are already addressed under the more specific IEC standard.

The deadline for transposition of the directive was delayed in 2007 and again in 2012. In 2011, the European Commission proposed a new directive, based on the new 2009 and 2010 ICNIRP recommendations but also incorporating a “derogation” to exclude MRI workers from the exposure limits, subject to certain conditions. After further lengthy negotiations, this proposal was adopted, and the 2004 directive was repealed (23).

The MRI derogation in the 2013 directive allows workers to exceed the exposure limit values, when this can be justified, during work related to “installation, testing, use, development, maintenance of or research related to magnetic resonance imaging (MRI) equipment for patients in the health sector”. This rather cumbersome wording was arrived at during negotiation in order to encompass as wide a range of activities as possible. There is a requirement for a risk assessment (already necessary under the framework directive), and for a range of other factors to be taken into account. It must be shown that workers' health and safety is still protected by other means (such as the IEC standards, safe working practices and appropriate training). There is also a provision for member state governments to introduce additional derogations on a time-limited (but renewable) basis where this can be justified.

Even in this modified form the directive remains controversial. A report produced for the European Commission in 2015 (prior to the 2016 deadline for national transposition)

recommended that the rationale for retaining the directive should be reconsidered, and that it might be repealed in its entirety (24).

EXPOSURE LIMITS AND GUIDELINES IN INDIVIDUAL COUNTRIES

The transposition deadline for the 2013 EMF directive was July 2016. The aim of the directive was that from that date onwards there should be a uniform approach to EMF exposure limitation across the EU. However, historically individual European countries have taken a variety of approaches to EMF exposure limitations. In some cases, 1994 and/or 1998 ICNIRP limits were enforced legally, or there were even more restrictive limits. Whilst no definitive summary of current legislation exists, there was no requirement for these countries to relax their more stringent regulations following adoption of the new directive. To add to the confusion, some EU member states transposed the 2004 directive before it was repealed, although by 2015 some had reversed this process or were simply not enforcing the legislation (24). Other countries had introduced additional requirements in relation to risk assessment or health surveillance, going beyond the requirements of the directive (24). On the other hand, in the UK the HSE adopted as flexible and helpful an approach as possible, with the MRI derogation and associated conditions re-worded in a simplified way in national legislation (25), and the power of derogation at national level exercised to include any MRI activities that were not already encompassed. A commentary on implementation of the UK regulations in the context of MRI has been published (26), and at the time of writing more extensive professional body guidance is awaited.

In addition to implementing the new EU legislation, some countries have adopted specific guidance on MRI safety. The UK Medicines and Healthcare Products Regulatory Agency (MHRA) guidance covers issues such as safety infrastructure, safe working practices, worker training, and control of access to MRI facilities (27). In the Netherlands, safe working guidance was issued in 2008 with the support of the relevant professional bodies and government agencies (28). The prospect of harmonized EU-wide MRI safety guidelines in the wake of the amended EMF directive has triggered initiatives such as development of standards on the role and training of MRI safety officers in Austria (29, 30).

SUMMARY AND CONCLUSIONS

Protection of patients and workers from hazards associated with EMF related to MRI requires both appropriate equipment design and use to ensure that the thresholds for direct effects are not exceeded and appropriate working practices and training to minimize the probability of indirect effects. The combination of the Medical Devices Regulation, supported by the IEC 60601 series standards, and the framework health and safety directive should be sufficient to ensure that these conditions are met in Europe. In practice, however, it is unclear how uniformly the obligations created by the framework directive are applied in MRI facilities. The ICNIRP occupational exposure guidelines are a blunt instrument in our context, designed to apply across very wide frequency ranges and incorporating safety factors that are both unnecessary and problematic. A critical difference between the IEC and ICNIRP approaches is that the IEC standard recognizes that MR systems designed to ensure patient safety are also safe for workers at the same exposure levels, whereas the IC-

922 MRI Standards and Safety Guidelines in Europe

NIRP applies different exposure limits for patients and workers. After a lengthy lobbying campaign, the derogation for MRI in the revised EMF directive ensures that MRI activities can continue in Europe, while workers remain protected by the IEC standard and by guidelines on safe working and training.

[¹In June 2016, an advisory referendum was held in which citizens of the United Kingdom (UK) voted by a narrow margin that the country should leave the European Union. The government decided to implement this and Brexit took place on 31st January 2020. EU laws remain in place during a ‘transition period’ lasting until the end of 2020. After that, existing legislation means that there will at least initially be a high degree of regulatory alignment between the United Kingdom and the European Union.]

REFERENCES

1. Directive 2004/40/EC of the European Parliament and of the council of 29 April 2004 on the minimum health and safety requirements regarding the exposure of workers to the risks arising from physical agents (electromagnetic fields). Official Journal of the European Union. Available at: <http://eur-lex.europa.eu/LexUriServ/LexUriServ.do?uri=OJ:L:2004:159:0001:0026:EN:PDF>. Accessed March 2020.
2. Keevil SF, Gedroyc W, Gowland P, et al. Electromagnetic field exposure limitation and the future of MRI. Br J Radiol 2005;78:973-975.
3. Keevil SF, Krestin GP. EMF directive still poses a risk to MRI research in Europe. Lancet 2010;376:1124-1125.
4. Keevil SF. The European union EMF directive and MRI: Is a solution in sight at last? Diagnostic Imaging Europe 2012;28:8-12.
5. Preamble to the Constitution of the World Health Organization as adopted by the International Health Conference. New York: 1946.
6. Council Directive 89/391/EEC of 12th June 1989 on the introduction of measures to encourage improvements in the safety and health of workers at work. Official Journal of the European Communities. Available at: <http://eur-lex.europa.eu/LexUriServ/LexUriServ.do?uri=OJ:L:1989:183:0001:0008:EN:PDF>. Accessed December 2012.
7. Regulation (EU) 2017/745 of 5th April 2017 on medical devices, amending Directive 2001/83/EC, Regulation (EC) No 178/2002 and Regulation (EC) No 1223/2009 and repealing Council Directives 90/385/EEC and 93/42/EEC Official Journal of the European Union. Available at: <https://eur-lex.europa.eu/legal-content/EN/TXT/PDF/?uri=CELEX:32017R0745>. Accessed March 2020.
8. International Electrotechnical Commission (IEC). Medical electrical equipment – Part 1: general requirements for basic safety and essential performance, IEC 60601-1:2005, Edition 3.1 Geneva: IEC, 2012.
9. International Electrotechnical Commission. Medical electrical equipment – Part 2-33: particular requirements for the safety of magnetic resonance equipment for medical diagnosis, IEC 60601-2-33:2010, Edition 3.2. Geneva: IEC, 2015.
10. International Commission on Non-Ionizing Radiation Protection. Guidelines on limits of exposure to static magnetic fields. Health Physics 1994;66:100-106.
11. International Commission on Non-Ionizing Radiation Protection. Guidelines on limits of exposure to static magnetic fields. Health Physics 2009;96:504-514.
12. International Commission on Non-Ionizing Radiation Protection. Guidelines for limiting exposure to time-varying electric, magnetic, and electromagnetic fields (up to 300 GHz). Health Physics 1998;74:494-522.
13. International Commission on Non-Ionizing Radiation Protection. Guidelines for limiting exposure to time-varying electric and magnetic fields (1 Hz - 100 kHz). Health Physics 2010;99:818-836.

MRI Bioeffects, Safety, and Patient Management 923

14. International Commission on Non-Ionizing Radiation Protection. Guidelines for limiting exposure to electromagnetic fields (100 kHz to 300 GHz). *Health Physics* 2020;118:483–524.
15. International Commission on Non-Ionizing Radiation Protection. Guidelines for limiting exposure to electric fields induced by movement of the human body in a static magnetic field and by time-varying magnetic fields below 1 Hz. *Health Physics* 2014;106:418-425.
16. International Commission on Non-Ionizing Radiation Protection. Statement on medical magnetic resonance (MR) procedures: protection of patients. *Health Physics* 2004;87:197-216.
17. International Commission on Non-Ionizing Radiation Protection. Amendment to the ICNIRP “Statement on medical magnetic resonance (MR) procedures: protection of patients”. *Health Physics* 2009;97:259-261.
18. International Commission on Non-Ionizing Radiation Protection. General approach to protection against non-ionizing radiation. *Health Physics* 2002;82:545-548.
19. Attwell D. Interaction of low frequency electric fields with the nervous system: The retina as a model system. *Radiat Protect Dosimetr* 2003;106:341-348.
20. House of Commons Science and Technology Committee. Watching the directives: scientific advice on the EU Physical Agents (Electromagnetic Fields) Directive. London: The Stationery Office Limited; 2006. pp.140. Available at: <http://www.publications.parliament.uk/pa/cm200506/cmselect/cmsctech/1030/1030.pdf>. Accessed March 2020.
21. Crozier S, Trakic A, Wang H, Liu F. Numerical study of currents in workers induced by body-motion around high-ultrahigh field MRI magnets. *J Magn Reson Imaging* 2007;26:1261-1277.
22. Crozier S, Wang H, Trakic A, Liu F. Exposure of workers to pulsed gradients in MRI. *J Magn Reson Imaging* 2007;26:1236-1254.
23. Directive 2013/35/EU of the European Parliament and of the Council of 26 June 2013 on the minimum health and safety requirements regarding the exposure of workers to the risks arising from physical agents (electromagnetic fields). Official Journal of the European Union. Available at https://eur-lex.europa.eu/legal-content/EN/TXT/?uri=uriserv:OJ.L_.2013.179.01.0001.01.ENG&toc=OJ:L:2013:179:TOC <https://eur-lex.europa.eu/legal-content/EN/TXT/PDF/?uri=CELEX:32013L0035&from=EN>. Accessed March 2020.
24. Evaluation of the Practical Implementation of the EU Occupational Safety and Health (OSH) Directives in EU Member States. Report by Directive: Directive 2004/40/EC on the Minimum Health and Safety Requirements Regarding the Exposure of Workers to the Risks Arising from Physical Agents (Electromagnetic Fields). Kongens Lyngby: COWI A/S, 2015. Available at: <https://ec.europa.eu/social/keyDocuments.jsp?advSearchKey=electromagnetic+fields&policyArea=&subCategory=&year=&country=&type=&mode=advancedSubmit&langId=en&searchType=&search=Search>. Accessed March 2020.
25. The Control of Electromagnetic Fields at Work Regulations 2016. London: The Stationery Office, 2016. Available at: http://www.legislation.gov.uk/uksi/2016/588/pdfs/uksi_20160588_en.pdf. Accessed March 2020.
26. Keevil SF, Lomas DJ. The control of electromagnetic fields at work regulations 2016 and medical MRI. *Br J Radiol* 2017;90:20160813.
27. Medicines and Healthcare Products Regulatory Agency. Device bulletin DB2007(03). Safety guidelines for magnetic resonance imaging equipment in clinical use, version 4.2. London: MHRA, 2015. Available at: https://assets.publishing.service.gov.uk/government/uploads/system/uploads/attachment_data/file/476931/MRI_guidance_2015_-_4-02d1.pdf. Accessed March 2020.
28. MRI Working Group. Using MRI safely: Practical rules for employees. Available at: Ministerie van Sociale Zaken en Werkgelegenheid. Available at: http://www.ismrm.org/smrt/files/20081210_Dutch_Guidelines_on_MR_Safety.pdf. Accessed March 2020.
29. Austrian Standards Institute. ÖNORM S 1125-1: Safety officer for magnetic resonance equipment for medical diagnosis - part 1: Responsibilities and competences. Vienna: Austrian Standards Institute, 2009. Available at: <https://www.astandis.at/shopV5/Preview.action;jsessionid=5411938848EBC85559C0D51F240F6DDE?preview=&dokkey=305935&selectedLocale=de>. Accessed March 2020.

924 MRI Standards and Safety Guidelines in Europe

30. Austrian Standards Institute. ÖNORM S 1125-2: Safety officer for magnetic resonance equipment for medical diagnosis - part 2: Requirements on training. Vienna: Austrian Standards Institute, 2009. Available at: <https://www.astandis.at/shopV5/Preview.action;jsessionid=5164FB96391EEFCEA351D097601A8EE1?prview=&dokkey=305936&selectedLocale=de>. Accessed March 2020.

Chapter 35 MRI Safety Practices, Guidelines, and Standards in Canada

TRINA GULAY, R.T. (R) (MR)

MRI Supervisor
Nanaimo Regional General Hospital
Vancouver Island Health Authority
Vancouver, British Columbia
Canada

INTRODUCTION

Safety is paramount when considering that both demand and utilization rates for magnetic resonance imaging (MRI) have increased dramatically in the past decade. As such, effective safety training and education are essential, particularly because MRI has increasingly become the modality of choice for a number of medical indications and scanners with higher static magnetic fields, faster gradient magnetic fields, and more intense radiofrequency (RF) fields are frequently being used. Canadian MRI facilities strive to align with relevant standards and with guidelines developed by leading organizations and experts to ensure that policies and procedures function to protect patients, staff members, and others working in and around the MRI environment.

HEALTHCARE IN CANADA

Canada has publicly funded healthcare where the federal government provides money to the ten provinces and three territories as described under the Canada Health Act. Each province and territory then manages and delivers healthcare to all citizens. The high cost of providing healthcare means that MRI programs receive a great deal of attention from politicians, senior administrators, and the media. In particular, the time that patients must wait for MRI scans is a politically sensitive issue. Consequently, the number of scanners installed across Canada has steadily increased.

926 MRI Safety Practices, Guidelines, and Standards in Canada

MRI in Canada

The Canadian Agency for Drugs & Technologies in Health (CADTH) confirms a national trend of increased examination volumes in *The Canadian Medical Imaging Inventory, 2017* that estimated that 1.86 million MRI scans were performed in 2017, up from 1 million in 2007 (1). CADTH reports that between 2007 and 2017 the number of MR systems in Canada increased from 222 to 366 (1). In Canada, the vast majority of MR systems are hospital-based; although some provinces offer MRI services in private clinics. The Organization for Economic Cooperation and Development (OECD) finds that as of 2018 there are 10.2 MRI scanners per 1,000,000 inhabitants in Canada, compared to 39.1 MRI scanners per million inhabitants in the United States and 55.2 MRI scanners per million people in Japan (2). Since MRI access is less readily available in Canada compared to other countries, such as the United States and Japan, management of MRI service is critical and receives a great deal of attention.

As MRI technology has progressed over the past 30 years, it has become apparent that higher exposure levels than those contained within *Safety Code – 26, Guidelines on Exposure to Electromagnetic Fields from Magnetic Resonance Clinical Systems* (3) are now considered to be safe, depending on a variety of factors. Increasingly, stronger systems are being installed at facilities throughout the country. As of 2017, CADTH reports that 83.2% of the units installed in Canada are 1.5 T units, although there has been a proliferation of 3 T units (13.7%) in MRI facilities across Canada (1). In total, 1.5 T and 3 T MR systems account for 97% of the scanners in the nation. Therefore, the most common scanners transmit and receive radiofrequency in the range of 64 to 128 megahertz (MHz). The range of frequency used in MR systems is in the particular range where the primary concern from RF deposition is tissue heating and resultant tissue temperature increases.

EXPOSURE LIMITS AND EQUIPMENT OPERATION IN CANADA

In 1987, shortly after the arrival of the innovative new technology, Health Canada published Safety Code 26 that set limits for human exposure to static magnetic fields, time-varying magnetic fields, and radiofrequency (RF) fields (3). Safety Code 26 set the early exposure limits, but many of the guidelines are out of date given the MR systems available now. The major concerns and potential risks to the patient and operator relate to the bioeffects and the combination of the three fields. Health Canada has published guidelines relating to RF exposure, but the guidelines are not meant to apply to operation of medical imaging equipment in Canada. Currently MR system manufacturers apply limits for MRI equipment in alignment with the International Electrotechnical Commission (IEC).

HEALTH CANADA'S SAFETY CODE 26

Safety Code 26, one of the first foundational safety MRI publications in Canada, arrived at a time when both MRI and magnetic resonance spectroscopy (MRS) were just beginning to gain clinical acceptance and application. As with any technology, even when beneficial in medical applications, the potential health hazards and safety precautions are managed to mitigate risks. There are several safety factors that must be considered with respect to the clinical use of MRI in human subjects. The fields produced by MR systems (i.e., static mag-

netic, time-varying gradient magnetic, and RF fields) can potentially create detrimental biological effects. Thus, questions have been raised regarding the safety of these electromagnetic fields generated by MR systems.

Static Magnetic Field, Gradient Magnetic Field, and RF Field Exposure Limits

The amount of RF energy deposited in the body by the RF pulse is termed the specific absorption rate (SAR). Exposure to RF fields at certain SARs leads to local and whole-body temperature increases in the body (3). SAR is the dosimetric term, expressed in units of watts per kilogram (W/kg), related to the rate of RF energy deposition per unit mass of exposed body tissue (3, 4). SAR provides a quantifiable means to estimate the thermal effects of the applied RF pulses used in MRI scanners. SAR is used by regulatory agencies, including Health Canada, to establish safety guidelines relevant to RF exposure (3, 4). RF pulses at certain SAR levels and extended exposure durations must be managed appropriately to reduce the amount of temperature rise in human tissues. SAR is not spatially uniform within the human body and the spatial distribution depends on the design of the transmitter coils, the frequency, the shape, the size and the type of tissue in the coil (3).

Safety Code 26 briefly reviews the biological effects of the electromagnetic fields used in MR devices and provides general guidance on acceptable exposure levels for the patient and for the operator. Health Canada's Safety Code 26 (3) recommended limits for patient exposure can be found in **Table 1**. The levels cited in the safety code were never meant to be considered as strict limits. Rather, if the limits were to be exceeded, an individual evaluation was required in each scenario. The intent of the guidance document was to set an established level. Below the established level there are minimal potential hazards, and if the level is exceeded there may not be a dangerous situation depending on the risk benefit analysis. Additionally, the limits outlined in the safety code have not been updated in nearly 32 years and the document serves as an early MRI exposure document.

Safety Code 26 contains additional information related to operator exposure and recommends, “operators should not be continuously exposed to a magnetic flux density exceeding 0.01 T during the working day and exposures to higher flux densities are permitted for short-time durations” (3). The number and duration of exposures are to be minimized (3). There is outdated guidance on management of those who are pregnant, those with cardiac pacemakers, and those with other metallic implants and devices. Other safety issues not directly related to human subject exposure to electromagnetic fields (EMF) that exist in the MRI environment are not addressed in the safety code. These safety issues include possible injury by projectiles (e.g., due to the forces from the static magnetic field acting on ferromagnetic objects), injury due to the quench of a cryogenic magnet, acoustic noise and hearing protection, and electromagnetic interference by MRI-related electromagnetic fields with other medical devices such as patient monitoring systems, automatic injectors, and ventilation systems (3).

HEALTH CANADA'S SAFETY CODE 6

Health Canada's *Safety Code 6, Limits of Human Exposure to Radiofrequency Electromagnetic Energy in the Frequency Range from 3 kHz to 300 GHz*, was updated in 2015 and

928 MRI Safety Practices, Guidelines, and Standards in Canada

Table 1. 1987 Health Canada safety code 26 patient exposure limits.

Exposure Source	Limit
Static magnetic field	2 T
Rate of time change of the magnetic field	3 T/s
Radiofrequency limits*	
• Core body temperature rise of no more than	0.5°C
• Temperature rise in any part of the body no more than	1°C
RF averaged over 25% of whole-body mass, SAR does not exceed:	
• RF exposures >15 minutes	1 W/kg
• RF exposures <= 15 min	2 W/kg

*RF limits defined as temperature increase in degrees Celsius (°C) or as RF averaged over 25% of whole-body mass in watts/kilogram (W/kg)

RF limits that exceed the specifications are not necessarily hazardous, if the benefits of the MRI examination outweigh the risks.

Source: Health Canada Safety Code 26

is available online (5). Safety Code 6 is not applicable to deliberate exposure under the direction of qualified medical practitioners (5). The limits outlined in Safety Code 6 are intended to harmonize with other recommendations from leading international organizations, such as those of the International Commission on Non-Ionizing Radiation Protection (IC-NIRP) (6). The limits are stated to be fairly consistent with those in the United States, Japan, Europe, Australia, and New Zealand (7). The general public exposure limits cover a very wide range of frequencies and err on the side of abundant caution to incorporate wide safety margins that are far below the threshold for adverse health effects (6, 7). In the MRI equipment setting, the IEC standard 60601-2-33 (8) sets equipment operation limits for the patient and operator that balance the risks and benefits of MRI technology.

There is also a companion document, *Safety Code 6 Technical Guide for Interpretation and Compliance Assessment of Health Canada's Radiofrequency Exposure Guidelines* (9) to aid in the interpretation of Safety Code 6. Although these documents apply to the frequency range used by MRI RF pulses, the safety code states, "Safety Code 6 does not apply to the deliberate exposure for treatment of patients by, or under the direction of, medical practitioners" (9). As an interpretation of this statement, the 2015 Revisions to Safety Code 6: Summary of Consultation Feedback (6) states, "Safety Code 6 does not cover deliberate exposure of RF energy to medical patients or persons operating magnetic resonance imaging (MRI) or other RF-emitting medical equipment." Instead, other international standards and guidelines published by the provincial health ministry cover protection for RF exposure by medical equipment and MR systems are regulated under the Food and Drugs Act (6).

IEC 60601-2-33 STANDARDS

In order to sell an MR system in Canada, the manufacturer must obtain a medical device license from Health Canada. This is a complex process and Health Canada has published a *List of Recognized Standards for Medical Devices* (10) that the manufacturer is encouraged to conform with. Of particular interest to this chapter is that Health Canada has endorsed the IEC 60601-2-33 standards for use in medical electrical equipment in the list. Although the IEC standards are intended for manufacturers and regulators, many requirements affect how the scanners are used and inform the development of MR system guidelines. For example, the IEC standards are used to define patient, worker, and visitor safe work practices in the MRI environment and these are commonly followed in Canada.

The IEC standards define levels of equipment operation for the patient and the MR worker who are exposed to the MRI environment. These three levels apply to the fields encountered in the MRI environment – the static magnetic field, the time varying magnetic field, and the radiofrequency field. *Normal Operating Mode* is defined as equipment operation where none of the fields have a value that can cause physiological stress to patients (8). *First Level Controlled Operating Mode* is defined as equipment operation where one or more fields reach a value that can cause physiological stress to patients and medical supervision becomes a requirement (8). To enter *First Level Controlled Operating Mode*, the user must actively and deliberately choose to accept the setting. The mechanism to enter the *First Level Controlled Operating Mode* (whether a window pop up or toggle button) is different for each system manufacturer. It is not unusual to enter this mode, however the requirement for medical supervision while operating in the controlled modes is not optional. *Second Level Controlled Operating Mode* is defined as equipment operation where one or more fields reach a value that can produce significant risk for patients. This mode is typically only seen in research applications and explicit ethics approval is required (8). *Second Level Controlled Operating Mode* must have security measures such as a password in effect to prevent unauthorized operation. There are no specific upper limits in *Second Level Controlled Operating Mode* as each protocol is required to be individually approved by a review board. The local approval by the review board shall include limits for static magnetic field, SAR, and gradient output (8). For research applications, the informed consent of the patient prior to the procedure is required.

IEC Static Magnetic Field Limits

IEC sets currently accepted limits for exposure to the static magnetic field for patients. The static magnetic field limit for *Normal Operating Mode* is 3-T or less (8). The *First Level Controlled Operating Mode* static magnetic field limit is greater than 3-T but less than 8-T (8). The *Second Level Controlled Operating Mode* limit for static magnetic field is greater than 8-T (8). No long-lasting harmful effects can be attributed to short-term exposure to strong static magnetic fields because the physiologic effects are small and it is difficult to estimate the level where strong magnetic fields become a hazard (11). The most commonly reported sensory effects noticed above the *Normal Operating Mode* by patients and MR system operators include vertigo and nausea that are related to the rate of movement in the static magnetic field. This is known as movement through the spatial gradient magnetic field and has units of Tesla per second (T/s). The IEC limit for moving a patient into

930 MRI Safety Practices, Guidelines, and Standards in Canada

the bore is 3-T/s. Interestingly, this is also the value that Health Canada set in Safety Code 26 in 1987. Other effects of moving through the static field include a metallic taste in the mouth and even magnetophosphenes when rapidly moving the eyes in high field systems (8).

IEC Time-Varying Gradient Magnetic Field Limits

Exposure to the time-varying gradient magnetic fields can cause peripheral nerve stimulation (PNS) and the onset of PNS is the threshold level (8). Uncomfortable PNS can be tolerable to the informed patient, however intolerable PNS is the level where the scan procedure must be terminated (8). When the gradient reaches a level that is capable of causing PNS, the equipment must display a warning to the operator that the gradient output exceeds the limits. Gradient exposure values in clinical systems are not enough to induce cardiac stimulation, defined as an ectopic beat (8, 12). The MR system minimizes intolerable PNS. *Normal Operating Mode* is not to exceed 80% of the PNS threshold level and *First Level Controlled Operating Mode* is not to exceed 100% of the PNS threshold level (8). These gradient limits are complicated and based on direct observational studies of human volunteers, or as a default expressed as maximum values of an induced electric field, E (V/m) or as the time rate of change of the gradient magnetic field, dB/dt (8). IEC defines conditions on how to conduct human studies to determine PNS output limits.

IEC Acoustic Noise Level Limits and Hearing Protection

The IEC 60601-2-33 standard states that manufacturers shall make a statement in the instructions for use outlining, “for all equipment capable of producing more than an A-weighted root mean square (RMS) sound pressure level of 99 dB (A), hearing protection shall be used for the safety of the patient and that this hearing protection shall be sufficient to reduce the A-weighted RMS sound pressure level to below 99 dB (A)” (8). Patients are typically given low-cost disposable earplugs.

IEC Radiofrequency Limits

Volume Transmit RF Coil SAR Limits. Radiofrequency power deposition is dependent on the type of transmit RF coil used for the MRI examination. The whole-body transmit RF coil is built into the scanner and, when using this coil for RF transmission, the SAR limits are defined by different means than when using a local transmit RF coil, such as a head, knee, or wrist transmit RF coil. The patient mass that is input as a parameter in the MR system console is used to calculate the whole body averaged SAR. The head SAR is averaged over the mass of the head and averaged over a specified time. The partial body SAR is averaged over the mass of the body exposed to the radiofrequency from the volume transmit RF coil and averaged over a specified time. **Table 2** shows the SAR limits for volume transmit RF coils in Canada (8).

Local Transmit RF Coil SAR Limits. Local transmit RF coils are smaller than the built-in body coil and deposit RF power to smaller areas of tissue. Calculation of local RF power deposition in the volume transmit RF coils is easier than the estimation of spatial peak SAR for planar transmit surface coils (13). Local SAR is averaged over 10 grams of tissue in a localized area of the body over a specified time. **Table 3** shows the SAR limits for local

Table 2. SAR limits for volume transmit RF coils.

Parameter	Limit	Limit	Limit
Body Part →	Whole body	Exposed body part	Head
Operation Mode ↓	Units (W/kg)		
Normal	2	2 - 10 a	3.2
First Level Controlled	4	4 - 10 a	3.2
Second Level (Research)	>4	>(4 - 10) a	>3.2
Averaging time	6 min		
Short Term SAR	SAR over any 10 second period will not exceed two times the stated values		
Specific Absorbed Energy	The maximum energy dose (SAR * exam time) will be limited		

^a The limit scales dynamically with the ratio “exposed patient mass/patient mass”:

Normal Operation Mode:

- Partial body SAR = 10 W/kg – (8 W/kg * exposed patient mass/patient mass)

First Level Controlled Operation Mode:

- Partial body SAR = 10 W/kg – (6 W/kg * exposed patient mass/patient mass)

Source: IEC standard 60601-2-33

Table 3. Canadian SAR limits for local transmit RF coils.

Operation Mode	Head*	Trunk/Torso	Extremities
Normal Mode	10 W/kg	10 W/kg	20 W/kg
First Level Mode	20 W/kg	20 W/kg	40 W/kg
Second Level (Research)	>20 W/kg	>20 W/kg	>40 W/kg
Averaging time	6 min		
Short Term SAR	SAR over any 10 second period shall not exceed two times the stated values		

*If the patient's orbits are in the field of view for the MRI examination, the temperature rise is limited to 1°C.
Source: IEC standard 60601-2-33

transmit RF coils in Canada (8). When an orbit is in the field of view, care must be taken to ensure that the temperature rise is limited to 1°C.

RF Power Deposition Temperature Limits. In Canada, MR systems are programmed to operate according to the IEC standards for equipment operation, given scanner room temperature of less than 25°C. At higher temperatures, the values for whole-body SAR are reduced by 0.25 W/kg per degree of room temperature over 25°C until the SAR is adjusted to 2 W/kg or the *Normal Operating Mode* (8). The limits in **Table 4** outline the temperature limits for RF energy deposition and are viewed as conservative limits. IEC states that higher temperatures may be permitted if there is no unacceptable risk for the patient. For this reason, operation in the *Second Level Controlled Operating Mode* does not have an upper limit, and, is based on the approval of a review board for research studies.

932 MRI Safety Practices, Guidelines, and Standards in Canada

Table 4. Canadian temperature limits for different operation modes of the MR system.

Operation Mode	Maximum Core Temperature Rise	Maximum Local Tissue Temperature	Maximum Core Temperature
Normal Operating Mode	0.5°C	39°C	39°C
First Level Controlled Operating Mode	1°C	40°C	40°C
Second Level Controlled Operating Mode (Research)*	>1°C	>40°C	>40°C

* *Second Level Controlled Operating Mode* requires Institutional Review Board (IRB) approval

10 grams is the mass used to determine local SAR

Source: IEC standard 60601-2-33

Operator Exposure to EMF

IEC limits also apply to the MRI worker. Due to the varying nature of work in the MRI environment, safe work procedures are followed in accordance with national and provincial regulations. For workers who stay in the room operation of the scanner, such as in the case of surgical or interventional scanners, simply increasing distance from the MR system minimizes exposure to the time-varying and radiofrequency fields.

Additional IEC Requirements

IEC standards require all equipment manufacturers of MR systems to include basic safety guidance for facilities in their instructions for use (IFU). This guidance is an excellent resource and can form the basis for the development of site-specific policy and procedures regarding MRI department operations in Canada. More specifically, the instructions for use from the manufacturer, found in the system owner manual, include information on the MR system regarding (8):

- Where to find details and technical specifications about the scanner and environment, such as:
 - Controlled access area
 - Electromagnetic field (EMF) radiation and signage
 - Bore dimensions, including weight and size restrictions
 - System frequency
 - Static magnetic field strength (B_0)
 - Maximum spatial gradient magnetic field (T/m or Gauss/cm)
 - Contour lines of the stray fringe field plotted in three axes
 - Labeling of auxiliary equipment required to go into the MR scanner room
 - Controlled access and demarcation of the 0.5 milliTesla (mT) line
 - Time-varying (gradient) performance, including:
 - Maximum spatial encoding gradient amplitude (mT/m)
 - Minimum rise times in milliseconds (ms)
 - Maximum slew rate (mT/m/ms or T/m/s) per axis
 - Maximum combined gradient output (dB/dt in T/s)
 - Acoustic noise and hearing protection requirements for patients, operators, or individuals within the MRI environment during equipment operation
 - RF system
 - Shielding
 - Coils

MRI Bioeffects, Safety, and Patient Management 933

- Peak RF power deposition limits
- B_{1+RMS}
- Scan protocols and pulse sequences
- Handling of system, fault, and error messages
- Patient and MRI worker pre-screening for classes of patients who may:
 - Be contraindicated for imaging (e.g., those with unsafe medical devices or foreign metallic objects in their body)
 - Require emergency treatment and resuscitation
 - Be contraindicated where controlled operation modes are possible (e.g., those with implants or limited thermoregulatory capabilities)
- Patient comfort and coil positioning
- Operating modes (*Normal Operating Mode, First Level Controlled Operating Mode, Second Level Controlled Operating Mode*)
- Exposure to static magnetic fields
- Exposure to gradient magnetic fields
- Exposure to radiofrequency fields
- Occupational exposures, such as:
 - Limiting exposure to the 3 fields for staff and other individuals
 - Limiting exposure of the fetus during scanning in pregnancy
- Medical supervision, visual contact, patient comfort, and patient monitoring especially when scanning in:
 - Febrile or unconscious patients
 - Pregnancy
 - Controlled operating modes
 - Patients with active or passive implants, including fixed parameter options (FPOs) if available
 - Research studies with predefined parameter limits when in second level controlled operating mode
- Emergency procedures for:
 - Medical emergencies and resuscitation
 - Fire (including education of local fire departments)
 - Emergency power off (EPO)
 - Emergency field shutdown (quench)
- Cryogens
 - Hazards
 - Quench pipe documentation and design
 - Monitoring cryogen levels
- Training for operators and local facility education
- Quality assurance (in accordance with MRI physicist)
 - QC procedures and phantoms
 - Artifacts
 - Maintenance of scanner and quench pipe

Consequently, local site policy can define appropriate patient, operator, and staff safety in the MRI environment. Up to date standards and guidelines must be developed and followed in each facility to mitigate risks or hazards associated with access to the area. In Canada, the manufacturer provides signage for each MRI facility and the lead technologist will develop other required signage. At a provincial level, the MANQAP and BC DAP standards seem to be fairly closely related to the broader IEC requirements, and will be discussed

934 MRI Safety Practices, Guidelines, and Standards in Canada

further under “Accreditation”. There are currently a wide variety of resources that amalgamate to define the current state of MRI safety practices that form the foundations of quality and customer service excellence in Canada.

MRI SAFETY RESOURCES PROVIDING STANDARDS AND GUIDELINES

The implementation of standards, policies, and procedures are the foundation upon which an MRI safety culture is built. Updated and relevant resources, protocols, and safety documents for staff are indispensable and enable technologists to manage individuals and other personnel in the MRI department. Canadian sites refer to a variety of resources to develop MRI safety guidelines and standards for clinical practice. At the federal level, the *Canada Occupational Health and Safety Regulations SOR/86-304* (14) enabled by the *Canada Labour Code* (15) set limits for occupational exposure to noise and hazardous substances, such as cryogens, in the workplace. Each province also has its own regulations regarding safety of the workplace. Patient safety is covered by an assortment of policies, bylaws, and provincial regulations. Patient safety concerns are related to screening, implant safety, and the use of contrast agents, sedatives, and anaesthetics. Regarding staff, the Canadian Centre for Occupational Health and Safety (CCOHS) explains the 14 jurisdictions in Canada: one federal, ten provincial and three territorial (16). These jurisdictions each have legislation and guidelines that outline safety standards for workers, supervisors, and employers. In Canada, the resources commonly used by an MRI facility include the following:

Recognized MRI Safety Resources and Guidelines

- The American College of Radiology (ACR), Guidance Document on MR Safe Practices: 2013 (17).
- The latest document from the American College of Radiology (ACR), ACR Guidance Document on MR Safe Practices: Updates and Critical Information 2019 (18).
- The Reference Manual for Magnetic Resonance Safety, Implants, and Devices annual edition by Dr. Frank G. Shellock (19). This medical textbook provides a comprehensive resource that includes guidelines and recommendations for MRI safety based on peer-reviewed literature, labeling information on devices from manufacturers, and documents developed by International Society for Magnetic Resonance in Medicine (ISMRM), American College of Radiology (ACR), the Food and Drug Administration (FDA), the National Electrical Manufacturers Association (NEMA), the International Electrotechnical Commission (IEC), the Medical Devices Agency (MDA) and the International Commission on Non-Ionizing Radiation Protection (ICNIRP), and other agencies (19).
- The website, www.MRIsafety.com that was developed and is maintained by Dr. Frank G. Shellock (20). This website is updated on a regular basis.

Canadian National MRI Safety Regulations, Standards, and Guidelines

- Canadian Association of Radiologists (CAR) Standard for Magnetic Resonance Imaging, approved April 2011 (21)
- Canadian Association of Radiologists (CAR) on Gadolinium Deposition in the Brain: A Systematic Review of Existing Guidelines and Policy Statement issued by the Canadian Association of Radiologists, published in Canadian Association of Radiologists Journal, 2018 (22)

MRI Bioeffects, Safety, and Patient Management 935

- Canadian Association of Radiologists (CAR) updated guideline Gadolinium-Based Contrast Agents in Kidney Disease, published 2019 (23)
- Canadian Association of Medical Radiation Technologists (CAMRT) Best Practice Guidelines (BPGs) (24)
- Canada Occupational Health and Safety Regulations SOR/86-304 (14) and the Enabling Act: Canada Labour Code (15)
- Canadian Centre for Occupational Health and Safety (CCOHS) (16)
- Health Canada acceptance testing of the MRI facility and approval of the MR system, RF coils, and peripheral equipment as safe medical devices
- Justice Canada's Medical Devices Regulations SOR/98-282 (25) and the enabling act: Food and Drugs Act (26)

Provincial MRI Regulations, Local Policies, and Procedures

- Workplace Safety and Health Act and Regulations (in each province or territory)
- Regulated Health Professions Act (RHPA) in the applicable province
- Professional regulatory bodies
- Existing local MRI safety, guidelines, procedures, and policies
- Accreditation requirements for the MRI facility
- Careful screening and preparation of individuals before entering the MRI environment
- MRI contrast agent administration
- Appropriate qualified medical personnel and continuing medical education
- Quality control programs
- Quality improvement programs

DEVELOPMENT OF MRI SAFETY GUIDELINES, PROCEDURES, AND POLICIES

MRI safety practices, that empower staff and providers who are experts in the field, form the foundational building blocks of a safety culture. The list above is very helpful when formulating guidelines, SOPs, and policies for departmental operations of MRI facilities. When drafting safety documents, the standards must be in alignment with any applicable national or provincial legislation and regulations. The main resources that inform guidelines and standards are the CAR standards (21-23) and the CAMRT BPGs (24). The provincial Workplace Safety and Health Regulations, the Regulated Health Professions Act (RHPA), the site administration, the MRI staff, and the regulatory colleges ensure that work in the MRI environment is safe for operators, patients, and the public. Other recognized resources that help shape the policies and procedures in Canadian MRI to be more safety-oriented are the annually updated *Reference Manual for Magnetic Resonance Safety, Implants, and Devices*, the MRISafety.com website, the *ACR Guidance Document on MR Safe Practices: 2013*, and the *ACR Guidance Document on MR Safe Practices: 2019 update* (17, 18, 19, 20).

Protocol and Procedure Manuals

Developing clinical standards, in addition to regularly maintaining and reviewing them, is important in diagnostic imaging to ensure the best image quality, a timely diagnosis, and the best outcomes for the patient. Standards and adherence to guidelines prevent adverse

936 MRI Safety Practices, Guidelines, and Standards in Canada

MRI safety incidents and negative clinical outcomes. Canadian imaging techniques may vary from site to site, but many similarities can be seen in clinical indications, applications, and safety practices. The radiologist/clinician collaboration determines the appropriateness of a given examination for a particular patient. CAR has worked extensively to develop standards and referral guidelines for each diagnostic discipline. In Canada, Medical Radiation Technologists (MRTs) in collaboration with radiologists develop procedures, using clinical experience and judgment, to provide diagnostic imaging that is in the patient's best interest (24). Canadian Association of Radiologists (CAR) recommends that safety policies and procedures can be reviewed annually by the supervising diagnostic radiologist, the lead MRI technologist, and the other team members for feedback, clarification, discussion, and review. Collaborative development of safety guidelines with frontline staff contributes to a culture of safety for staff, patients, and visitors to the MRI department. The recommendations point to the importance of incident reporting in quality improvement initiatives in order to build on professional development and optimize learning.

CLINICAL STANDARDS FOR MRI

The *CAR Standard for Magnetic Resonance Imaging*, published in 2011 is the most current version detailing the guidelines recommended for clinical MRI service provision. This document is freely available on the CAR website. These standards offer a very basic overview of MRI safety considerations in MRI departments. The section on MRI safety points correctly to commonly accepted reference material, but discusses practices at a rudimentary level. The clinical standards avoid being overly prescriptive and focus largely on the recognized clinical applications of MRI for neurological, abdominal, pelvic, musculoskeletal, cardiovascular, thoracic, breast, and fetal imaging (21). Other items of interest that are discussed briefly include MR system specifications, equipment, quality control, acceptance testing, quality improvement, qualifications of personnel, contrast usage, sedation, and general anesthesia recommendations. Unfortunately, discussion of labeling and implants uses outdated terminology and glosses over the many safety considerations encountered in modern MRI facilities.

CONTROLLED ACCESS, LABELING, AND SAFETY PRACTICES

MRI technologists are responsible for policy development, screening, patient advocacy, preparation, safe work procedures, in addition to safe operation of the equipment. MRI technologists are primarily responsible for controlling access and the safety of patients, visitors, and staff. The CAR MRI standards provide advice on how to mitigate risks related to the strong static magnetic field with respect to implants, ferromagnetic objects, and cryogenic requirements. Canadians follow strict guidelines related to supervised and controlled access in MRI departments. The CAMRT supports the principle of controlled access in preventing accidents, reducing the risk of fatal injury, ensuring expensive medical devices and systems are not damaged, mitigating downtime, and maintaining a safe and effective working environment (24).

Facility Design, Controlled Access, and Safety Zones

CAMRT endorses the four zone approach as described by the American College of Radiology to MRI facility design with the aim of minimizing safety risks (24). A four zone design approach controls access to the MRI environment and keeps other healthcare personnel away from areas of danger (17, 24). To ensure controlled access and restrictions within the MRI environment, many sites develop a map showing the zones and designate a Magnetic Resonance Safety Officer (MRSO) or a lead technologist to enforce safety principles. Controlling access is an important safety mechanism to prevent accidents and reduce risks due to projectile hazards, ensure that expensive medical equipment is not damaged, mitigate downtime, and maintain a safe work environment for staff (24). For safety, it is common to break an MR imaging department into four distinct zones. Zone I is defined as any area that is freely accessible to the general public. Zone II is where patients and visitors enter the MRI department, typically the reception and registration area where there is public access. Zone II is where unscreened individuals complete the safety questionnaire and MRI screening checklist. Zone III is a restricted access, controlled area (ideally with a physical barrier in newer departments) with key or swipe card access for Level 2 Personnel. Zone III and IV are locked down when not under direct supervision of Level 2 Personnel for the safety of staff, patients, visitors and the facility (24). All persons entering Zone III must be under direct supervision of Level 2 MR personnel (24). Zone IV is the MR scanner room and any area where the fringe field exceeds 0.5 mT. Some sites choose to mark the fringe field of the static magnetic field at the 0.5 mT (or 5 Gauss) line, as a safety mechanism and exclusion zone for implants and other electronic devices. Design components in MRI departments can physically restrict access in Zone III and IV due to the risks of the MRI environment. Multiple entrances to the MR scanner room are not generally advised.

The IEC standards also define the reasoning behind the controlled environment in the technical description of the MRI equipment in Section 201.7.9.3.101 (8). The *controlled environment* is required when the 0.5 mT fringe field extends outside of the equipment cover. The manufacturer shall give markings on the floor to control access by unauthorized persons, labeled at all entries by warning signs indicating the presence of static magnetic fields, and warn about the attractive and torqueing forces of the MR system (8). MR personnel are aware of the potential hazards of static magnetic and RF fields and must relay this information to other healthcare professionals and maintenance staff. MRI facilities meet the conditions for a *controlled environment* due to RF emissions. The MR system room shall not be freely accessible to the general public. IEC requires that there will be RF shielding and warning signs indicating that occupancy is “restricted to authorized personnel only” at all viewing distances and angles where access to the controlled environment is possible (8). The placement of signage is required prior to entry to the department and at the entrance to the controlled environment to clearly identify the presence of RF emissions in the area (8, 9).

The CAMRT best practice guidelines define Level 2 MR Personnel as those who control and authorize access to the MRI environment and maintain a presence at all times during the performance of MRI exams (24). Entry into controlled access areas can only be authorized by Level 2 MR Personnel (17, 24). Level 2 MR Personnel in Canada are CAMRT registered MRI technologists (RTMRs) that have passed a national certification examination

938 MRI Safety Practices, Guidelines, and Standards in Canada

in the discipline of MRI (24). Other Level 2 MR Personnel include MRI physicists, scientists, radiologists, and physicians who have undergone extensive MRI safety training. Level 1 MR Personnel are defined as those who are minimally educated on MRI safety issues with enough training to ensure their own safety. Access to the MR system room is restricted to only screened patients, Level 2 MR Personnel, and other screened facility or Level 1 MR Personnel that are educated on MRI safety procedures.

Signage and Labeling of MRI Devices

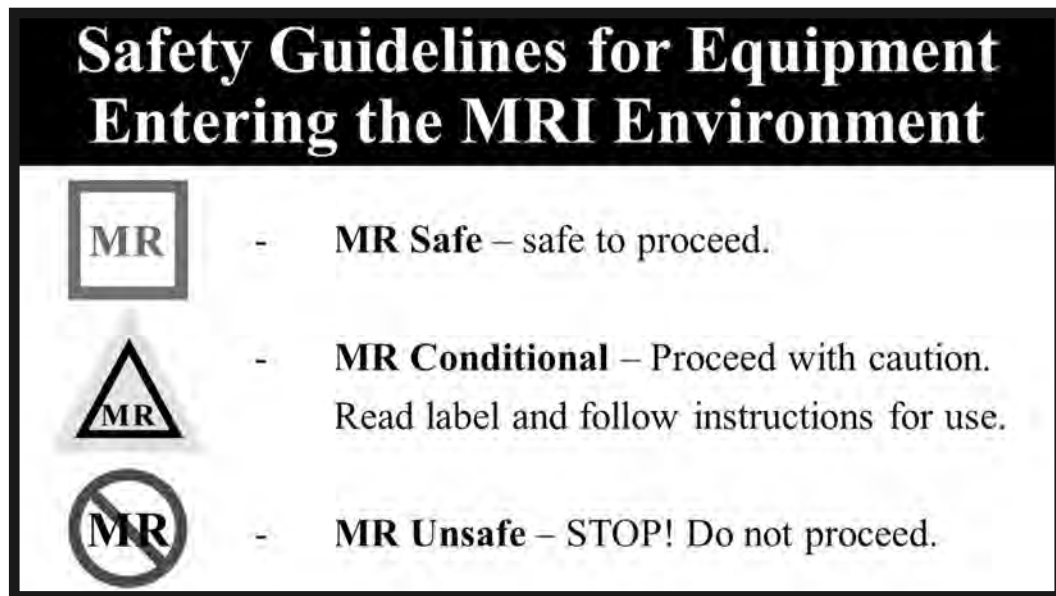
Recommendations from the CAMRT outline the need for “clear and explicit signage” to reinforce the four zone safety concept (24). These signs are normally placed when a new scanner is installed. Examples of signage, as recommended by the CAMRT (24) are:

- Permanent demarcation of the 0.5-mT (5 Gauss) line
- Prominent “Do Not Enter” danger signs on the MR system room door
- “Magnet Always On” lighted signs running on back-up power
- “Magnet Always On” signage above or beside the MR system room door
- MRI departmental zone signs indicating restricted access in Zones III and IV

All equipment used in Zones III or IV, such as IV poles, wheelchairs, and stretchers should be labeled to indicate the conditions of use. MRI labeling guidelines are in accordance with the American Society for Testing and Materials (ASTM) F2503 standards that are referenced by the ACR guidance document, the IEC, and the most current Reference Manual for Magnetic Resonance Safety, Implants, and Devices (8, 17, 19, 27). The CAR and the CAMRT follow the standards used for labeling, although the definitions in the standards and on the CAMRT website need to be updated to reference current information sources and accepted terminology. The accepted international criterion breaks down all objects into *MR Safe*, *MR Conditional*, and *MR Unsafe* statuses. The *MR Safe* designation refers to an object that poses no known hazards in all MRI environments and is non-metallic, non-conducting, and nonmagnetic. The icon is a green square or box with “MR” written on or inside the box. *MR Conditional* is an object that may or may not be safe depending on specific and well-defined conditions. The icon is a yellow triangle with “MR” in black letters incorporated into the triangle. The specific conditions are variable and include limits on static and maximum spatial gradient of the magnetic field, dB/dt (gradient output) limits, RF field limits, and SAR limits. Finally, the *MR Unsafe* designation and status applies to an item that is known to pose a hazard in all MRI environments. The icon is a red circle with a diagonal line through the letters “MR.”

One role of the lead technologist or MRSO is to create safety policies in conjunction with the medical director. Other roles of the lead technologist include categorizing staff, labeling items in Zones III and IV, and ensuring appropriate signage exists. These individuals also educate facility staff, code team members, security officers, and support staff in MRI environment safety. The lead technologist or MRSO is responsible for education of local fire and police teams to ensure a safe informed response for emergency situations in the MRI setting. Other education, such as refresher training and practice runs of mock emergency situations are useful to ensure that MRI department safety practices are understood by all emergency responders or those who routinely enter the MRI environment.

Figure 1. Equipment and device labeling standards.



Source: Adapted from ASTM International F2503.

MRI Safety Practices and Education

To ensure that MR Unsafe devices are not brought into the MR system room, strict safety protocols can be developed to label all items in the department and prevent unauthorized access to the MR system room. Recommended safety guidelines for preventing missile effect accidents are widely accepted in Canada and can be found in the current Reference Manual for Magnetic Resonance Safety, Implants, and Devices (19). The recommended safety practices that are endorsed by both CAR and the CAMRT include:

- Appointing an MRI Safety Officer (MRSO)
- Establishing and reviewing safety procedures regularly
- Providing formal MRI safety education and refresher training
- Emphasizing the “Magnet is Always On” principle (including appropriate signage)
- Keeping MR Unsafe equipment out of the MR system room
- Following conditions for MR Safe and MR Conditional devices
- Maintaining a list or equipment log of MR Safe and MR Conditional equipment with relevant restrictions in the facility and updating the list regularly
- Testing and labeling all items and affixing an appropriate safety label to the device (especially those items that are permanently housed in the MR system room, control room, and preparation areas) with internationally recognized labeling as shown in **Figure 1** (27)
- Bringing non-ambulatory patients into the MR system room with tested MR Conditional gurneys, wheelchairs, and assistive devices
- Performing safety “full-stop and final checks” for foreign metallic objects (such as oxygen tanks hidden under blankets) prior to room entry (18)
- Having patients change into gowns and pants free of metallic thread or objects (24)
- Using ferromagnetic detection systems

940 MRI Safety Practices, Guidelines, and Standards in Canada

- Ensuring effective ferromagnetic screening procedures for all individuals (outlined further below)

MRI SCREENING PROCEDURES AND IMPLANT SAFETY

Canadian MRI technologists are certified with the CAMRT and responsible for the safety of the patient, including conducting highly effective screening procedures, ensuring appropriate preparation of the patient for the MRI procedure, maintaining departmental safety, and operating the equipment. Many sites choose to have hard copy and online access to current MRI safety resources, including the Reference Manual for Magnetic Resonance Safety, Implants, and Devices (19) and the MRI safety website, mrisafety.com (20). There must be site policy outlining what documents are required to ensure accurate and effective screening of the patient and/or any individuals required to go into Zone IV. The development of effective screening procedures ensures that preventable injuries to patients, visitors, staff members, and Level 2 MR Personnel do not occur.

The screening procedures in Canada follow a multi-step process, without exception, prior to the MRI examination. The initial step is pre-screening performed by the referring physician, but frequently this step is missed and relevant information is often missing on the requisition or referral. The second step occurs upon receipt of the paperwork where the clerical staff, the technologists, and the radiologists pre-screen the requisition for any contraindicated devices or conditions that may complicate imaging. Some sites opt to complete a quick confirmation checklist (extra step) over the phone during the scheduling process with the patient using an abbreviated series of questions to pick up major issues prior to patient arrival. Additionally, an information sheet may be sent out in the mailed appointment letter directing the patient to phone the department if they have any contraindicated devices or pre-existing medical conditions prior to arrival.

Once the patient is in the department, the MR staff will greet and provide the patient with screening forms to complete prior to commencing the procedure. The third step in the screening process is completion of the MRI screening forms. Patients and other persons entering the MRI scanner room must complete the screening forms. The forms in Canada can be from international resources, such as the PDF forms on the MRI safety website and in the Reference Manual for Magnetic Resonance Safety, Implants, and Devices (19). There are example forms available on the International Society for Magnetic Resonance in Medicine (ISMRM) website (28). There are examples of screening forms in other languages on both ISMRM website and www.MRIsafety.com. In Canada, the two official languages are English and French. When language and fluency pose issues to screening, the help of a family member or translator can assist with the screening process. In the case of patients who are hearing or visually impaired, the technologist can use other methods of communicating with the patient prior to and during the examination, including the services of an ASL translator.

The fourth step in the screening process is a verbal screening review of the form with the patient by Level 2 MR Personnel. The MRI technologist greets the patient and introduces themselves by name and occupation, then provides a description of the test to be performed. The use of the name, occupation, duty (commonly called a “NOD” in Canada) increases

patient satisfaction and builds trust into healthcare interactions. The screening process is one of the most important patient safety components that technologists assume in their daily routine to reduce the risk of harm and minimize potential hazards to the patient (24). Technologists must explain the importance of obtaining relevant and accurate safety information to ensure patients and their escorts understand the implications of withholding relevant information. The technologist will attempt to answer relevant questions posed by the patient, family, guardian, public trustee, or escort.

The MRI technologist performs diagnostic services that deliver benefits and minimize risks (24). The use of checklists enhances information exchange between two parties. Any questions or concerns the patient or technologist has regarding contrast, sedation, claustrophobia, implanted devices, or past surgery can be discussed prior to the examination. Technologists with experience clue in when patients have not filled out the checklist adequately or accurately prior to the examination. The MRI technologist and the patient (or a family member, guardian, or public trustee who knows the pertinent medical history) signs off the screening form to ensure both parties are in full understanding of the procedure. Typically, there is a reminder discussing the safety risks associated with not accurately divulging information. The patient completes the screening form prior to each MR imaging study to ensure current information about the patient's medical history. Effective screening includes asking the patient about all prior surgeries, medical conditions, pregnancy, and claustrophobia. Prior to contrast administration, the technologist screens for additional information such as medications, medical conditions, drug allergies, and a history of liver or kidney failure. If necessary, the patient and technologist complete and sign the contrast forms prior to the initiation of venipuncture.

Screening of Visitors and Staff Entering the MRI Environment

Visitors to the MRI department may be nurses, healthcare aids, physicians, maintenance, support and trades staff, fire department members, prison guards, paramedics, and other escorts. All staff members or escorts required to enter the scanner room must fill out the screening form and be verbally screened prior to being granted access to the MR system room. For visitors who assist in the department regularly, completed forms may be kept in a secure location for ease of reference.

Screening of High Risk Patients

In the case of patients who cannot fill out the screening form, other mechanisms can be used to ensure safety. High-risk patients tend to be those where screening or communication is a challenge and may be:

- Unconscious
- Hospitalized and non-ambulatory
- Unable to communicate
- Sedated or heavily medicated
- Exhibiting psychiatric disturbances (including dementia or confusion)
- Exhibiting violent behaviour
- Infants or neonates

942 MRI Safety Practices, Guidelines, and Standards in Canada

These individuals may be screened with the assistance of a family member, guardian, or public trustee who knows their entire medical history and condition. If the information is not adequate, prior imaging studies that are recent can be reviewed. Alternately, radiographs can be obtained of the chest, abdomen, skull, pelvis, and other areas as per discussion with the radiologist. The patient can be inspected for scars related to surgical procedures or bumps that may indicate implanted devices. In all occasions, implanted devices or foreign object clearance must be obtained prior to the scan. If the information is not available, the radiologist and referring clinician may do a risk vs. benefit assessment on whether or not to proceed with the scan. In the case of emergency scans where verbal screening cannot be performed and no reliable medical history can be provided, the patient may undergo radiographic imaging of the skull, orbits, chest, abdomen, and pelvis to exclude metallic foreign objects or implanted devices (24).

Implanted Devices

The Canadian *Medical Devices Regulations* requires that manufacturers shall provide patients with 2 implant registration cards, specifically the manufacturer information, a notice regarding the purpose of the card, and up-to-date address information for the purpose of information exchange (29). The card is to be designed for recording the name of the device including the control number, the name of the healthcare professional who implanted the device, the date of implantation, the healthcare facility where the device was implanted, and the patient's name (29). This legislation is covered by the *Food and Drugs Act* (30). Section 67 indicates that a staff member at the healthcare facility where the implantation takes place will fill out the implant registration card and give one to the patient and the manufacturer. Despite this being a legal requirement, often the patient misplaces this information or the physician may not provide the relevant implant information.

In the screening process the technologist often identifies the presence of medical implants and/or devices, and is tasked with obtaining the device or implant information, including the model, reference, and/or serial number from the surgical or operative reports. In certain situations, the manufacturer may need to be contacted for MR-specific information regarding safety of the device in the MRI setting. The *Reference Manual for Magnetic Resonance Safety, Implants, and Devices* and the MRI safety website are often consulted in Canada to determine safety and exposure conditions prior to the scan (19, 20). Implants and safe scanning practices are classified separately for passive and active implants. The relevant information that the technologist must gather includes the type of implant, the location of the surgery, the surgeon, the date of the surgery, the operative and perioperative documentation, and any product stickers or ID cards related to the implant.

Common implants such as stents, aneurysm clips, heart valves, joint replacements, screws, rods, and fixation devices are considered to be passive implants. Active implants include electronically active devices such as cardiac pacemakers, implantable cardioverter defibrillators (ICDs), infusion pumps, cochlear implants, and spinal cord or deep brain stimulation (DBS) systems. Sites ought to have local policies and procedures for scanning implants and devices. In the case of active implants, the MRI physicist may be consulted to ensure the safety of scanning these devices. Additionally, the manufacturer information for scan conditions must be available for consultation. In some cases, a representative from the

MRI Bioeffects, Safety, and Patient Management 943

manufacturer may assist or require paperwork to be completed. In the case of scanning pacemakers and defibrillators, commonly called Cardiac Implanted Electronic Devices (CIEDs) the CAR has official guidance (31). Often, the presence of support staff from cardiology or neurology is required to ensure functionality of the device, and may be required to test or reset the device post MRI examination. In all cases, adequate documentation and follow through with post examination care is essential.

Conditions to consider when scanning implants are magnetic field strength, spatial gradients, torqueing, heating and SAR or B_{1+RMS} restrictions, artifacts, induced currents in conductors, the physical properties and dimensions of the object or device, the location of the object near vital structures, and the amount of counter forces on the object from normal physiology, encapsulation, or scarring (19, 24). For further information on these types of issues, Canadian MRI technologists consult the most recent edition of the *Reference Manual for Magnetic Resonance Safety, Implants, and Devices*. In the case of electronically active devices, the MR professionals will contact the manufacturer for the most recent and updated labeling information prior to performing an MRI examination on the patient (19).

In 2019, CADTH issued a rapid response report entitled *Magnetic Resonance Imaging for Patients with Implantable Cardiac Devices: A Review of Safety and Guidelines*. The report explores reported adverse safety events occurring in literature when patients with conventional and *MR Conditional* CIEDs are scanned. The document includes loop recorders in the discussion, however *MR Conditional* loop recorders have been scanned in Canada for many years following specific conditions. The report does not appear to be written by a person with a great deal of MR experience. The report assessed literature from outside of Canada, mostly in the United States, regarding the use of MRI in patients with *MR Conditional* or non-*MR Conditional*, conventional or “standard” cardiac devices. The report acknowledged the lack of primary studies with high quality evidence for scanning patients with conventional cardiac devices and the lack of information from Canada, where medically implanted devices might be different from those implanted in the United States (32). The available evidence did suggest few adverse events in the 13 relevant publications that were identified, but could not provide evidence-based guidelines because of the small sample size and might fail to detect adverse outcomes (32).

Canada has been slow to adopt scanning patients with CIEDs outside of large, specialized centers. For this reason, CAR and the Canadian Heart Rhythm Society published a consensus statement with recommendations on MR imaging of those with CIEDs. Of particular note, the document uses the correct terminology of device and implant labeling and discusses the challenges of identifying patients with *MR Conditional* systems (31). The document discusses the risks, considerations, consent, abbreviated scan protocols, coils, and monitoring requirements. The recommended field strength to scan CIED is 1.5 T, with a SAR of less than or equal to 2 W/kg for each sequence, and a slew rate of less than 200 T/m/s (33). CAR advises against scanning patients with abandoned leads. The recommended process is a collaborative approach between the cardiac clinic, cardiologists, MRI radiologists, MRI technologists, MRI physicists, and nurses (31). The development of a working SOP is essential. Larger tertiary care centers in Canada, with the aid of cardiologists and radiologists working collaboratively, do scan patients with *MR Conditional* pacemakers and defibrillators. The “off label” decision to scan a patient with a non-*MR Conditional* pace-

944 MRI Safety Practices, Guidelines, and Standards in Canada

maker is not advised by Health Canada, manufacturers, or joint cardiovascular and radiology societies and is not considered to be a standard of practice (31).

Foreign Metallic Object Screening

Effective screening procedures pick up any potential internal foreign metallic objects in the patient that may prove to be a contraindication to MR imaging. If there is concern regarding the possibility of an orbital or other foreign metallic object such as a bullet, shrapnel, BB, pellet, or other penetrating or retained metallic object in the patient, radiographs may be obtained. The technologist will then ask the radiologist to interpret the radiographs. In the particular case of a possible orbital foreign body where the patient has sought medical attention, radiographs are recommended. The ACR advises that radiographs can be used in screening the orbits with one or two radiographic views and that a previous MRI examination without incident after the orbital trauma does not prove the safety to subsequently scan the patient (18). Clinical history and timelines of the injury must be accurately recorded by the technologist upon verbal clarification of the injury with the patient.

In clinical practice, CT and radiographic imaging of the area in question that is recent or performed after the injury or surgical procedure is required to screen for the presence of contraindicated objects. The technologist keeps the patient informed of the situation and any delays encountered prior to imaging. Information is presented in clear and simple language to ensure that the patient or caregivers understand the reasons for the delay (24). If the technologist cannot answer the patient's question, and the issue falls outside of their scope of practice, they will involve the radiologist in the discussion. The radiologist becomes involved with approval to proceed with the scan after a review of any additional imaging.

On very rare occasions, the patient neglects to disclose a metallic foreign body or implanted device. This may be due to cognitive issues or out of fear that the examination might be cancelled. When the technologist becomes aware of an undisclosed foreign metallic object and visualizes an artifact on scouts or MR images, they must notify the radiologist immediately and slowly remove the patient from the MR system (24). The patient ideally remains parallel to the scanner and as far out of the fringe field as possible in a supine position (24). When out of the room, the technologist will explain to the patient why the examination is being aborted. The patient may be questioned further and sent for imaging upon the radiologist's request. Attempts may be made to obtain medical records that indicate what object is located in the patient.

Detection of Ferromagnetic Metallic Objects

Detection methods to identify any ferromagnetic objects prior to MR system room entry must be employed at all times. The Level 2 MR Personnel will visually screen the patient for any metallic objects, quarantine any foreign metallic objects, and lock up the patient's valuables. Patients who are deemed safe to enter the MRI environment are often required to change into MR Safe clothing provided by the imaging department prior to entry into the MR system room (18, 19). MRI technologists then direct the patient to the entrance to Zone IV and perform a final screening and "*full-stop and final check*" at the doorway to ensure no objects, such as dental work, hearing aids, or assistive devices get into the room (18, 19). Some sites employ ferromagnetic detection systems in the doorway to identify

any hazards that may have been missed for those patients who can walk through the entrance to Zone IV unassisted. Other sites may use a handheld wand.

At times, additional information is needed by the radiologist for interpretation prior to authorization of the MRI examination. Mechanisms to ensure safety of those who are deemed high risk patients, those with implanted devices, and those who may not be able to fill out the screening questionnaire accurately are essential. MRI technologists understand when it is necessary to request further imaging as required by the radiologist to “clear” the patient. Radiologist assistance is often required for clearance prior to the MRI examination and to review other previously acquired diagnostic information, such as radiographic or CT studies. The supervising radiologist has the final approval on making an informed decision to scan the patient, recommend an alternate modality, or determine if there are further considerations to be made regarding the safety of the MRI examination. The radiologist may require additional information upon collaboration with the MRI technologist, who must assist in obtaining all pertinent information while advocating in the best interest of the patient.

Patients who are non-ambulatory and arrive in by stretcher, wheelchair, or with assistive devices pose another challenge, especially on older MR systems without detachable tables. The MRI department has a variety of MR Safe or MR Conditional equipment available for non-ambulatory patients. Thorough preparation, in addition to collaboratively working with intensive care unit staff and surgeons (in the case of intraoperative MR), prior to transporting the patient into the scanner room is mandatory. Often, a final team “*full-stop and final check*” prior to room entry to look for oxygen tanks, monitoring devices and equipment, extraneous objects on or in the non-MRI staff member’s clothing, is an excellent mechanism to pick up metallic objects that may have previously gone undetected. All individuals entering the MR system room must be re-educated and re-screened each time they assist in the MRI environment.

TIME-VARYING MAGNETIC FIELD ISSUES

The major issues related to time varying (gradient) magnetic fields are related to induced currents, peripheral nerve stimulation, and acoustic noise. There does not appear to be a great deal of information on induced currents and PNS in the Canadian guidance documents. For safety limits related to PNS, technologists may wish to consult the IEC standards. The limits the IEC outlines for peripheral nerve stimulation set the exposure level below the threshold of painful nerve stimulation on the MR system. Induced currents related to the rapidly switching gradients are of particular importance to medical implants that are conductive and electrically active.

Acoustic Noise and Hearing Protection

Acoustic noise is a serious safety concern and degrades verbal communication between the technologist and the patient. The gradient magnetic fields, when activated, can generate a wide variety of intermittent noises, such as clicks, knocks and taps, depending on the pulse sequence used (24). Noise is a hazard inherent to MRI environments for both patients and others who are required to remain in the MRI scanner room and each person has a dif-

946 MRI Safety Practices, Guidelines, and Standards in Canada

ferent threshold for noise tolerance. Biological responses and effects such as annoyance, anxiety, communication interference, and transient or permanent hearing loss in extreme situations are related to noise exposure (19). The average noise levels generated in the MRI scanner can vary greatly, but are typically in the range of 82 to 93 decibels (dB) on the A-weighted scale (20). Other worst-case scenarios report noise levels of up to 115 dBA for EPI protocols on 1.5 T (19). Studies conducted at 3 T have shown levels in the range of 126 to 131 dB where the recommendation is to provide the patient with properly fitting earplugs and headphones (19). Thin slice acquisitions, small field of view (FOV) scans, three-dimensional scans, fast GRE pulse sequences, and EPI pulse sequences are well known to generate the highest sound pressure levels. IEC standards state that every person required to be in the scanner room during MR image acquisition is required to wear hearing protection such as earplugs, plastic noise-reducing headphones, or ear muffs if the sound pressures are expected to exceed 99 dB (A), but Canada has different guidelines for environments where workers are exposed to noise.

Health Canada stipulates levels of sound permissible for workers. Occupational exposure limits (OELs) for noise in the *Canada Occupational Safety and Health Regulations*, (e,SOR/86-304) take into account different noise levels and sound pressure levels using the A-weighted sound pressure levels in dBA (14). CCOHS outlines that the noise exposure assessment is to be conducted in accordance with CSA standard Z107.56-13 *Measurement of Noise Exposure* (14, 33). The CSA Group (formerly known as the Canadian Standards Association) is an independent, impartial organization that develops standards and codes in Canada, similar to ANSI in the United States. The organization tests and certifies brands to ensure they comply with U.S. standards such as those written by ANSI, ASME, ASSE, ASTM, ASFE, UL, CSA, NSF, and more (34). The CSA seal is affixed to all objects in Canada that are deemed CSA approved, such as hearing protection that conforms to the CSA Standard Z94.2-14 *Hearing Protection Devices – Performance, Selection, Care and Use* (14, 34).

The employer is required to appoint qualified personnel to carry out an investigation if an employee's hearing is endangered by noise levels and must provide hearing protection for noise exposures for 8 hours of exposure to noise levels above 87 dBA (14, 35). Noise level regulations are permissible to noise exposure levels for 8 hours of continuous noise and/or impulse/impact noise levels that are defined in peak pressure levels (35). The noise exposure levels for an 8-hour continuous exposure (L_{ex8}) are lower than peak pressure levels. Additionally, there are exchange rates that mean that as the sound level increases, the exposure time must be decreased. For instance, if the sound level is doubled, exposure duration is halved (35).

The provinces and territories have lower noise exposure limits of 85 dBA. These regulations are commonly outlined in the *Workplace Safety and Health Act and Regulations* (36). For instance, in Manitoba, there is the *Workplace Safety and Health Act and Regulations* (Man. Reg. 217/2006) and the employer is required to make regulations available to staff. Clear and visible warning signs must be located at all entrances into the workplace where noise levels are greater than 85 dBA (36). The warning sign shall include a pictogram, according to CSA Standard CAN/CSA-Z321-96, *Signs and Symbols for the Workplace* (36). Further, employers are required to make hearing protection available to employees that are

exposed to higher than permissible limits with a hearing protector that complies with CSA Standards Z94.2 *Hearing Protection Devices – Performance, Selection, Care, and Use* (14, 35, 36).

MRI staff members must explain and educate the patient on expected noise levels and the options for hearing protection prior to commencing the scan. Hearing protection is usually provided in the form of disposable earplugs that are non-latex containing and that have noise reduction rates (NRR) of up to 30 dB. Earplugs have an effective rating of 50% and can abate noise by 10 – 30 dB when used properly (19, 37). MRI personnel will instruct or assist the subject on the proper usage of earplugs to ensure conformance and adequate fitting. There are system headphones that can be used in addition to earplugs to play music and improve the overall MRI experience. MRI departments can purchase earmuffs that are MR Safe and reduce noise levels in the room with an effective rating of 70% (37). Hearing protection alternatives known as “mini-muffs” work well for pediatric and neonatal patients. Newer variations of common pulse sequences have also been developed by manufacturers specifically to reduce noise levels for a wide range of applications, such as pediatric imaging.

PATIENT MANAGEMENT AND MONITORING

Preparation of the patient prior to the MRI is critical to a successful examination. Through proper preparation, the quality and safety of the examination are improved. Instructions are often given the patient prior to the procedure regarding fasting, the reasons behind preparations, and other important information related to the procedure (24). Simply asking the patient if they need to use the washroom prior to imaging, can mean the difference between a complete and incomplete MRI examination. Monitoring of the patient is an important safety measure taken to reduce the potential for heating or adverse outcomes of the test. Discussions regarding the emergency call systems, contrast usage, or often the use of sedation or other medications leads up to a successful scan without unwanted delays. Other design elements that allow the MR staff to supervise patient care areas from the console are useful, such as closed-circuit video surveillance systems. System manufacturers must provide a means to monitor the patient in the MR system. Ideally this is a camera to monitor the patient during a scan directed into the end of the bore.

RF Power Deposition Limits

Tissue heating is the primary established bioeffect of RF field exposure. Thermal injuries related to MR system burns are one of the most common adverse events encountered in the MRI department (24). The National Electrical Manufacturers Association (NEMA) publishes standards for the medical diagnostic device industry and has stated that when “an insulated slab of tissue at thermal equilibrium with the environment is exposed to SAR of 1 W/kg, the temperature will increase at a rate of 1°C per hour” (38). NEMA considers RF heating to be within safe levels if exposures to RF fields during scanning are insufficient to produce a core temperature rise of 1°C and localized heating of 38°C in the head, 39°C in the trunk, and 40°C in the extremities (38). NEMA and device manufacturers are required to ensure that medical equipment operates within the levels recommended by the IEC 60601-2-33 standards.

948 MRI Safety Practices, Guidelines, and Standards in Canada

The SAR determination is done by either the calorimetric or the pulse energy methods (38). Calorimetric methodology calculates the absorbed RF power directly (38). The pulse energy method measures the net power delivered to the transmitter, minus the losses, to measure the absorbed power (38). SAR is defined as either maximum whole-body SAR or peak spatially-averaged SAR. Restrictions exist for both whole-body averaged SAR and peak spatially-averaged SAR. Maximum whole-body averaged SAR is the term applicable to RF exposure that is averaged over the entire body. SAR is limited to avoid RF field induced thermal responses and the resultant alterations of core body temperature in humans (5).

In an adult human body weighing 62 kg, there are 62,000 discrete one-gram tissue parcels in an unending variety of configurations, each with complex compositions and different heat dispersal characteristics. Peak spatially-averaged SAR is the term applicable to RF exposure that is averaged over a small cubical volume (typically 1 to 10 grams) over a specified time (5, 19, 38). Thermoregulation in these discrete volumes can most often efficiently dissipate heat and avoid body temperature changes greater than 1°C (5). SAR calculations are difficult to calculate during MRI and measure in the human body (19, 38). The main factors to consider (19, 39) related to SAR and RF power deposition, include:

- MRI scanning parameters
 - Resonant frequency of the MR system
 - TR, number images/TR
 - RF pulses (bandwidth, flip angle, waveform, duty cycle)
 - Saturation pulses (water excitation, fat suppression, magnetization, spatial, IR)
 - Pulse sequences
 - Type of transmit RF coils (local RF coils minimize RF exposure)
- Patient anatomy and physiology
 - Larger diameter structures absorb more power (38),
 - Orientation of the body
 - Shape of the anatomy
 - Particular volume of tissue in the coil
 - Physiological processes (blood flow, perspiration)
- Environmental conditions (blankets, clothing, air flow, ambient room temperature)

Prevention of Thermal Injuries

Prevention is imperative to avoid excessive RF power deposition that may result in high tissue temperature increases. MRI technologists understand how the RF coils work and the differences between local and volume coil SAR deposition limits. Communication with patients throughout the examinations ensures the patient is not having any unusual experiences. For example, if the patient feels any heating, this must be addressed immediately by checking to make sure contributing factors are minimized. Preparation of the patient must include an explanation by the technologist regarding the potential for heating, and the normal heating to be expected with the MRI examination. This is especially critical if the patient has tattoos or medical implants. Patients will ideally change into hospital gowns and clothing to prevent burns that may be caused from metallic threads in the clothing (17, 19, 24). In patients who are unable to communicate, further care must be taken to ensure that no potential for excessive heating exists, including keeping the scanner in the *Normal Operating*

Mode when possible. Sites adhere to established guidelines and local policy to ensure that RF power deposition limits are not exceeded. *Normal Operating Mode* is advisable in those with limited thermoregulation. Scanning in the *First Level Controlled Operating Mode* requires constant medical supervision (and a communicative patient) if employed. Burns can occur even when operating in the *Normal Operating Mode*.

Each MRI facility establishes local policy to ensure radiofrequency power deposition limits are within recommended limits. The IEC regulates the settings in the scanner, depending on input variables, such as weight, height, position of the patient, in addition to the type of transmit RF coil used. The MR system vendor, field service engineer, and the MRI physicist ensure that the equipment is operating within the limits specified by the IEC. Outlining ideal conditions for imaging ensures that operators know how to mitigate burn risks and manage alerts that may pop up on the system. Prevention of adverse events due to excessive thermal heating can be achieved through a variety of mechanisms. The recommended practices to avoid burns can be grouped into categories and include (17, 19, 21, 24, 39):

- Environmental Conditions
 - Maintain scanner room temperatures between 18 – 22°C
 - Maintain scanner room humidity between 40 to 60%
 - Increase air flow
- Screening and Patient Preparation
 - Change patients into MR Safe clothing
 - Remove unnecessary metallic objects from within the scanner bore and on the patient
 - Remove foil medication patches
 - Scan tattoos and permanent cosmetics with care
 - Visually inspect for metallic objects on skin and under sheets
 - Remove thermal heating blankets
- Patient Monitoring
 - Monitor patients closely
 - Educate patients on call bell use
 - Warn patients to report heating or uncomfortable sensations
 - Remove blankets
 - Stop the scan if the patient is sweating profusely or reports warming
 - Scan in *Normal Operating Mode* if the patient is febrile or has a condition that compromises thermoregulation
- Patient Positioning
 - Avoid bore contact points
 - Use insulation pads of at least 1 cm thickness between bore, transmitter, and contact points
 - Avoid “cross points” and conductive loops
- Implant Precautions
 - Use caution when scanning implants with resonant lengths
 - Use caution when scanning skin staples and metallic sutures
 - Scan only MR Conditional active implants according to manufacturer conditions
 - Consult the MR medical director if there are scan concerns for implanted devices
 - Scan active implants with extreme caution according to current manufacturer conditions
- Device/Coil Positioning
 - Avoid cable loops
 - Remove unnecessary coils from the bore
 - Inspect coils for damage regularly

950 MRI Safety Practices, Guidelines, and Standards in Canada

- Route cables and wires down the center of the bore
- Avoid patient skin contact with coils, cables, leads, and monitoring devices
- Use only approved MR Conditional leads and electrodes
- Operator Controls
 - Enter height and weight accurately
 - Maintain contact with the patient at regular intervals
 - Provide medical supervision if scanning in *First Level Controlled Operating Mode*
 - Use care when accepting popups to enter *First Level Controlled Operating Mode*
 - If the *First Level Controlled Operating Mode* is entered, the operator ideally changes the system back to normal mode prior to commencing the next pulse sequence
 - Stop the scan if the patient reports heating or burning
 - Decrease the refocusing flip angle, echo train length, flip angle, number of slices per repetition time
 - Use low SAR mode or increase the repetition time
 - Use strategies to lower SAR and the RF duty cycle
 - Consider the use of different coils, if appropriate, to limit SAR
 - Adhere to medical device conditions for SAR or B₁+RMS for implants

CAMRT and CAR recommend that MRI departments can focus on reducing SAR in alignment with the strategies outlined above (21, 24). MRI technologists who are uncertain on how to meet the SAR or other heating guidelines will consult with an individual such as a lead MRI technologist or MRI physicist. MRI-related burns must be reported to the MR supervising technologist and MR radiologist (24). In the event of a burn, a cool compress will be placed on the patient's skin. A non-conformance or incident report must be completed outlining the specifics of the situation, in addition to a technologist comment in the Radiology Information System (RIS) and final MR report (24). SAR information may be included in the image DICOM header for each pulse sequence.

Specific Absorbed Energy and Specific Energy Dose

The estimated rate of temperature rise related to SAR matters, but there are other metrics that capture the total accumulated amount of energy that is deposited in the patient (18). Manufacturers have come up with calculations of RF dose known as Specific Absorbed Energy (SAE) or Specific Energy Dose (SED) on the newer MR systems to limit thermal increases (18). The SED is represented in J/kg and prevents excessive temperature increases in patients where imaging is performed for long intervals, for example entire spine imaging (18). SED = SAR multiplied by time. Factors that affect the amount of power deposited in the patient are related to selection of pulse sequence parameters and these factors are important for the technologist to understand. If SED limits are expected to be encountered on the MR system, the technologist should know how to reduce the thermal load of pulse sequences on long examinations (18). Additionally, the SED warnings and lockouts do exist on MR systems in Canada. On some systems, a SED warning will pop up at 6,000 J/kg, and if the limit of 14,400 J/kg is reached, it is no longer possible to scan the patient (8).

Fixed Parameter Options (FPOs) and B₁+RMS

Fixed parameter options limit the gradient and RF outputs of the scanner when scanning those with implanted devices and MR Conditional labeling. SAR calculations are estimated

differently by each vendor and are conservative which can limit imaging possibilities in those with implanted devices (40). A metric now required to be displayed on MR systems by manufacturers is called the B_{1+RMS} . B_{1+RMS} is not an estimated value but a known value based on the pulse sequence and parameters and it is calculated the same from system to system (40). IEC requires manufacturers to display the value on newer scanners (40). Device manufacturers have started to label devices with a given B_{1+RMS} value not to be exceeded, and this information can be found where the SAR information is found on the newer MR systems in Canada (40).

Claustrophobia

Claustrophobia is commonly encountered in the MRI environment and occurs for a variety of reasons. Claustrophobia is thought to occur in approximately 4% of the population due to fear of suffocation and fear of restriction (24). Fear of the MR system can prevent an essential step in the diagnosis and treatment of patients. Those with claustrophobia can successfully be coached and managed with a variety of techniques, but early identification can help in preparing the patient for an exam (19). Strategies to manage claustrophobia are well-defined (19, 21, 24) and include:

- Maintaining communication with the patient
- Reassurance and coaching
- Having a family member or friend remain in the MRI environment
- Reminding the patient that they have control over the situation and instructing the patient in call bell usage
- Mirrors and prism glasses
- Virtual reality system distraction
- Modified positioning (feet first or prone scanning if possible)
- Placing a blindfold or washcloth over the eyes
- Bright lights
- Increasing air flow in the scanner's bore
- Relaxation, meditation, hypnosis
- Music or scent therapy
- Sedative or anxiolytic administration
- Anaesthesia

Emergency Call Systems

Emergency call systems are a necessity to communicate with the patient and used to alert the operator to any change in patient condition when the patient is in the MR scanner. The call bell function should be tested each day to ensure the system is fully functional. The test results are kept in an equipment log. Each patient must be provided with an explanation of the emergency call bell system and instructed on how to use the device prior to the scan in the event they need to alert the operator to stop the scan. Call bell usage ensures the safety of the patient in the event they experience any unusual sensations, burning, discomfort, distress or claustrophobia in the scanner. Patients who understand that they are in control of the test know they can stop the scan if the need arises. Staff must immediately respond and acknowledge the activation of the emergency call system. In the event of an emergency, staff will initiate the appropriate emergency response procedure.

952 MRI Safety Practices, Guidelines, and Standards in Canada

Sedation and Anaesthesia Procedures

In mild to moderate cases of claustrophobia, the patient may obtain a prescription for a mild, oral sedative from their physician. Technologists are trained to identify and manage patients with a high degree of anxiety. The role of the technologist requires monitoring the patient for a verbal response, operating the equipment, ensuring quality vital signs monitoring, recognizing complications that may be encountered with sedative usage, and preparing in the event of an emergency. In some cases, other healthcare providers may be present to monitor the patient, and is often the case with neonatal and pediatric patients. The patient must bring a driver after taking sedative medication and the MRI technologist should confirm that the patient does not drive post procedure (24).

For patients with claustrophobia that is severe, other measures such as IV sedative administration and conscious sedation may be indicated in the absence of any contraindicated medical conditions. If the site is to offer sedation, there must be policy and procedures in place to allow for trained staff, such as nurses, to monitor the patient and administer the IV sedation (21). The technologist and nurse have a collaborative role to ensure the patient can be aroused by verbal stimulation during the scan (24). Departments that administer sedation will keep a Compendium for Pharmaceuticals and Specialties (CPS) on site for ease of reference and must ensure the appropriate monitoring of the patient. Often site pharmacists can assist radiologists by providing educational materials, developing guidelines and procedures that aid in recognizing and treating complications such as desaturation, hypotension, excessive sedation, and nausea or vomiting (24).

The use of general anaesthesia for deep sedation can be used to successfully complete the MRI examination for severely claustrophobic and pediatric patients (24). Anaesthesia procedures are most often reserved for pediatric settings and in the case of interventional or surgical MR-guided imaging. An anaesthesiologist or intensive care physician provides care for patients who require anaesthesia (21). The patient requires vital signs monitoring (in the case of deep sedation or anaesthesia) that is monitored by the person administering the sedation or anaesthesia. The use of monitoring devices and ventilators that are MR Conditional are available to the intensive care staff. When the patient arrives, baseline vitals are recorded by the nurse or physician, in addition to during the scan with MR Safe or MR Conditional monitoring equipment, and during post procedural care in recovery (24). The pharmacologic measures to conduct scans pose greater risk to the patient and require more in depth medical information and adequate preparation prior to the scan.

Patient and Vital Signs Monitoring

In Canada, MRI technologists monitor their patients at all times for a change in condition and to prevent adverse events (24). The patient is monitored during the entire MRI procedure visually and verbally to ensure their physical and emotional state and to respond to any signs of distress. If the status of the patient changes and they lose consciousness or appear to be in a state of respiratory or cardiac distress, emergency procedures are initiated. Site procedures for emergency response must be in place to address different types of medical emergencies. In the event of any emergency, the patient will be immediately removed from the MRI environment and the technologist will respond and seek out appropriate assistance.

Communication is critically important for patients who have or are at risk of developing cardiovascular collapse, anaphylactic reactions, seizure disorders, cardiac problems, claustrophobia or other anxiety disorders, and those whose thermoregulation abilities are impaired (8). Emergency call systems can only be relied upon in an alert and cooperative individual who is physically able to communicate. In the event of an unconscious patient, the vital signs may be monitored with approved *MR Safe* or *MR Conditional* ancillary equipment that is designed for use in the MRI environment. Communication may not be reliable when high risk individuals are being scanned. In the situation that communication is not possible; the patient must be monitored by MR Conditional vital signs monitoring devices.

PEDIATRIC MRI CONSIDERATIONS

Pediatric patients undergoing MRI procedures pose different challenges than adults. Neonates, infants, and children from intensive care units (ICU) may also require MRI procedures frequently. With older children, simulation procedures may be helpful for families to prepare for the scan. Policies and procedures can be developed in alignment with other healthcare professions (such as nursing, intensive care staff, respiratory therapists, and anaesthesia specialists) to support the needs of children. Special equipment and immobilization devices are often needed in order to deliver appropriate clinical care to pediatric patients. Screening policies govern more people than simply the patient. Adequate preparation involves caregivers and other healthcare providers, especially if they are required to stay in Zone III and IV with the patient. Contrast administration is carefully considered as pediatric patients may be exposed to more GBCAs during their lives than adults. Caregivers may be more stressed and ask more questions, and even worry about the choices relating to consent for procedures such as venipuncture, contrast media, and the scan.

The limits in the IEC guidelines for pediatric patients are reduced for magnetic field strength. Hearing protection requirements are different due to the small anatomy of infants and children. Additionally, neonatal patients have different thermoregulatory requirements than adults. Finally, sedation and anaesthesia procedures are required frequently when performing MRI on pediatric patients in order to obtain quality images.

MRI IN PREGNANT PATIENTS

Many studies provide evidence suggesting that MRI exposure during the first trimester (as compared to no MRI exposure during pregnancy) is not associated with increased harm to the fetus or in early childhood (19). Nonetheless, MRI facilities in Canada are cautious and screen females of reproductive age (11 to 55 years) for pregnancy before permitting them access to MRI environment (24). If pregnancy is established, consideration is given to whether the requested MRI examination could safely wait to the end of the pregnancy, in consultation with the radiologist and referring clinician. When other methods of imaging are inadequate, the patient is advised that, “to date there have been no deleterious effects related to the use of clinical MR imaging during pregnancy” (17, 19, 24). CAR guidelines suggest that safety of MRI scanning during pregnancy has not been established. The decision to scan must be made on a case-by-case basis, after a consideration of medical necessity and alternate imaging methods have been explored (21). Therefore, no special consideration

954 MRI Safety Practices, Guidelines, and Standards in Canada

is recommended for the first, versus any other, trimester in pregnancy but attention can be paid to limiting SAR and scanning with radiologist supervision.

Pregnant Patient Management

CAR guidelines do offer indications for fetal imaging in select circumstances (21). Regardless of trimester, MRI use for certain indications is the standard of care (19). The recommended assessment prior to initiating imaging (19, 24) includes asking the following questions:

- Can ultrasound be used?
- Will the MRI exam address the clinical question?
- Is early delivery a possibility?
- Is termination of the pregnancy a possibility?

CAMRT suggests that informed consent be obtained by the radiologist prior to the examination. The Reference Manual for Magnetic Resonance Safety, Implants, and Devices (19) indicates that MRI examinations are not to be denied in the following circumstances, when a pregnant patient presents with:

- Active brain or spine signs and symptoms requiring diagnosis
- Cancer requiring staging or diagnosis
- Chest, abdominal, or pelvic signs and symptoms of active disease where sonography is non-diagnostic
- Patients with fetal anomalies

Pregnant Healthcare Workers

Pregnant MRI workers must notify their employer when they become aware of pregnancy (24). MRI healthcare professionals are allowed to work around the MR system when the RF and gradient fields of the equipment are not operating during all stages of the pregnancy (24). The recommendations regarding a policy for pregnant workers include allowing pregnant technologists and healthcare workers to perform MRI procedures, enter the room to position patients, and otherwise attend to the patient during all trimesters of pregnancy (19). The pregnant healthcare worker should not remain in the room during equipment operation when scans are underway (8, 19).

MRI CONTRAST AGENT ADMINISTRATION AND SAFETY

The decision to administer contrast is approved by the radiologist and indicated on the protocol sheet or the requisition. Conspicuity of certain pathology is enhanced with the use of contrast agents. CAR outlines specific indications for contrast agent usage and safety (21). MRI technologists and nurses in Canada can be delegated the specialized function of peripheral IV access. To become certified in venipuncture, the technologist will successfully complete an educational program as deemed appropriate by the medical director and receive advanced training on IV starts under the supervision of other professionals skilled in the task. The education will consist of theory, an examination, observation, and demonstration

of the skill. Each technologist must be closely supervised and evaluated to ensure they are competent to perform venipuncture and signed off on by the supervising radiologist and trainer. The demonstration of skills will be documented in a training document, with the skills and competence reassessed annually.

The MR medical director will keep a register of all technologists who are authorized to perform venipuncture in the department. All venipuncture procedures are charted on a consent form and in the radiology information system (RIS) by the technologist including date, site or route of injection, name of technologist, the size of cannula, and the amount and type of contrast administered. Additionally, any reactions to the contrast or complications arising from the venipuncture procedures must be documented. For in patients, this information will be noted in the patient's chart. Technologists will only administer contrast that is approved by Health Canada and as directed by the ordering radiologist, if the practice is in compliance with the regulations governing their profession.

Screening prior to the administration of contrast begins upon receipt of the requisition. Information requested prior to a contrast enhanced examination is required to be completed by the referring physician. Any history of prior allergies, contrast reactions, asthma, hypertension requiring medication, diabetes, or other related concerns are important factors to consider prior to contrast administration. Questions related to contrast administration will include whether the patient has a history of kidney disease, kidney transplant, single kidney, kidney surgery, dialysis, or a history of kidney cancer. The patient needs to be informed of the risks and involved in the decision to administer contrast (24). Patients have the right to decline a contrast agent injection at any point in time.

GBCA Administration in Pregnancy

The decision to administer contrast to a pregnant patient depends on a variety of variables and a more complete discussion can be found in the current Reference Manual for Magnetic Resonance Safety, Implants, and Devices (19). The choice to administer a GBCA to a pregnant patient is left to the referring clinician and the supervising radiologist. This decision is only considered if there is a significant benefit to the patient that outweighs the risk of free gadolinium to the fetus (19). CAR does not offer any public guidance on this issue, but often aligns with recommendations and ACR guidance for such issues. CAMRT advises that the use of a GBCA should be avoided in pregnant patients because there is insufficient evidence to prove that gadolinium poses no risk to the fetus (24). If it is necessary to use a GBCA, the radiologist must provide informed consent for the procedures.

Adverse Contrast Reactions

Technologists are trained to recognize any adverse reactions related to contrast administration. Injections are administered in alignment with local site policy that requires oversight by a licensed physician. In 2017, CAR published a Canadian update on management of adverse contrast reactions. In the update, there is a discussion of acute reactions that may be considered mild, moderate and severe (41). Reactions are defined as either anaphylactoid or non-anaphylactoid. The predisposing risk factors to consider include a prior reaction to a GBCA, certain medical conditions, infants and seniors, women, and those on certain nephrotoxic medications (41). The risks of an adverse reaction to GBCAs are overall lower

956 MRI Safety Practices, Guidelines, and Standards in Canada

as compared to iodinated contrast agents, at 0.4 per 1000 doses, but the chances of a severe reaction in those few cases is often double (41). The update offers a recommended treatment protocol for adverse reactions for Canadian clinicians based on symptoms. The treatment protocols include urticaria, facial/laryngeal edema, bronchospasm, hypotension with bradycardia, hypotension with tachycardia, hypertension, seizures, and pulmonary edema (41). There is also a recommended prophylactic pre-treatment protocol (41). While GBCAs are thought to carry a lower risk for adverse reaction than iodinated contrast agents and they are not considered to be nephrotoxic, the potential for nephrogenic systemic fibrosis (NSF) exists. NSF poses a risk for those on dialysis, those with low eGFR, and those with acute kidney injury (AKI).

Gadolinium-Based Contrast Agents in Kidney Disease

In 2017, a panel of radiologists and nephrologists developed clinical practice guidelines (CPGs) on management of patients with AKI, severe chronic kidney disease (CKD), and those on dialysis. The rationale was to assess the evidence regarding the usage of macrocyclic and newer linear GBCAs. Screening for renal function on outpatients was recommended by CAR in specific settings in the initial CPG in alignment with the European Society of Urogenital Radiology. The guideline was not aligned with the ACR Contrast Manual, Version 10.3, but the intent was to reissue guidance in 2 years after a literature review.

In 2019, the CAR updated the CPG on the use of GBCAs in kidney disease. A literature review was conducted to see if there were any unconfounded cases of NSF related to Group II and Group III GBCAs. Only a single case was reported in a patient with Stage 2 CKD after the patient received gadobenate dimeglumine and no other cases were found between 2017 and 2019 (23). The recommendations remained mostly the same from the 2017 CPG, with the change that, “screening for renal disease in the outpatient setting is no longer justifiable, cost-effective or recommended” when using Group II and Group III agent, gadoteric acid (23).

The document provides guidance on how to manage patients requiring contrast. These guidelines apply to use of GBCAs in adult and pediatric patients in the following circumstances:

- Mild renal impairment (eGFR between 60 – 90 mL/min/1.73 m²)
- Moderate renal impairment (eGFR between 30 – 60 mL/min/1.73 m²)
- Severe CKD (eGFR between <30 mL/min/1.73 m²)
- Dialysis
- Acute Kidney Injury (AKI)

Gadolinium Retention in the Brain

The United States Food and Drug Administration (FDA) issued warnings regarding brain accumulation of GBCAs beginning in July 2015 (42). The safety announcements were issued due to new findings that found retained gadolinium deposits in the brains of patients who had repeat contrast-enhanced MRI (22, 42, 43, 44). The findings were described primarily in the dentate nucleus and globus pallidus, and to a lesser extent in the cerebellar

white matter, the frontal lobes, pons, and thalamus (22). Gadolinium retention has been found on routine unenhanced T1-weighted imaging and upon autopsy in those with normal renal function with both linear and macrocyclic agents (22). Deep brain deposition was found to have a positive correlation with increasing number of doses of gadolinium-based contrast agents (GBCAs) (22, 45). Gadolinium has also been found in the skin, bone, liver, and other organs (45). In September 2017, the FDA issued warnings that there was a greater risk with linear as compared to macrocyclic agents (43).

Health Canada, the Canadian FDA equivalent, followed suit and issued a safety alert in 2017 after an initial investigation in 2016 (46). Health Canada issued *New Safety Information on Injectable Gadolinium-Based Contrast Agents Used in MRI Scans*, an information update in 2017, advising Canadians of the findings. Another alert was issued in May 2018. Both alerts explain that no adverse effects, and more importantly no health consequences, have been identified with gadolinium accumulation in the brain (46, 47). The safety review also considers that pregnant women and children are more at risk of gadolinium build-up and to use macrocyclic agents in those cases, however the majority of facilities in Canada already use macrocyclic agents (47). Health Canada, as of 2017, now requires manufacturers to update product labels to include the information (46, 47). Drug manufacturers of GBCAs updated product monographs to outline the finding of gadolinium accumulation in the brain within the last 2 years.

In 2018, the CAR issued a position statement entitled, *Gadolinium Deposition in the Brain: A Systematic Review of Existing Guidelines and Policy Statement Issued by the Canadian Association of Radiologists* (22). The objectives of the CAR working group were to review evidence, position statements, and existing guidelines from other organizations and to formulate an evidence-based position statement from CAR (22). The CAR position statement states that GBCA administration should be considered carefully with respect to potential risks and benefits, standard dosing should be used, repeat administrations should be avoided unless deemed necessary, and use of GBCAs should be limited to only when required (22). CAR arranges GBCAs as follows: macrocyclic agents, linear ionic agents, and linear non-ionic agents (in order of decreasing stability) and they conclude that there is insufficient evidence to recommend one class of GBCA over another at this point in time (22). The issue is currently being watched closely.

CANADIAN EDUCATIONAL PROGRAMS

Canadian medical and healthcare educational programs are accredited through national non-profit independent organizations, such as Accreditation Canada and the Canadian Medical Association (CMA). Accreditation standards ensure the educational curriculums offered through Canadian colleges and universities are rigorous and high quality and developed by professionals in the field. The competency profiles are vetted through experienced healthcare professionals and build skills in new learners. The curriculum prepares the candidate to take national certification exams that test knowledge in key concepts and fundamental elements of the training.

958 MRI Safety Practices, Guidelines, and Standards in Canada

MRI Technology Training

Nationally, the Canadian Association of Medical Radiation Technologists (CAMRT) develops the competency profiles that guide educational programs on appropriate course content and prepares the student Medical Radiation Technologist (MRT). The CAMRT is the national professional association and certification body for medical radiation technologists and set the competency profiles for the eight MRI technology programs in the country. Canadian technologists are commonly referred to as MRTs. MRI technologists who successfully complete the CAMRT national MRI certification examination become Registered Technologists, Magnetic Resonance or RTMRs. Upon completion of the didactic and clinical training, entry-level technologists are expected to be competent in a wide variety of MRI procedures at a general duty level. The competency profiles are developed by working groups of CAMRT-certified MRI technologists and educational professionals who set the learning outcomes and nationally-accepted standards of competency, defined as a practice tasks that can be performed with entry-level proficiency (48). The CAMRT encourages professional development activities, develops best practice guidelines (BPGs), descriptions of practice, a code of ethics, job scopes, and standards of practice for members.

In Canada, the CAMRT enlists voluntary professionals in each of the imaging disciplines to set the curriculum to ensure high quality, rigorously prepared candidates. Candidates who have successfully completed a course of study at one of the recognized and accredited Canadian educational facilities become eligible to write the national certification exams. The CAMRT MRI competency profile is broken into modules on professional practice, patient management, health and safety, equipment operation, and procedure management. The profiles are updated regularly (5 year intervals) to reflect current practice. The MRI technology educational programs are offered in British Columbia, Alberta, Manitoba, Nova Scotia, and Ontario. The current accredited list of MRI technologist educational programs and the curriculum guidelines can be found on the CAMRT website (48).

Diagnostic Radiology Training

In Canada, the Royal College of Physicians and Surgeons of Canada and the Collège des médecins du Québec ensure that Diagnostic Radiologists have fellowship and documented training through a recognized Canadian University. The Diagnostic Radiology residency program is a 5-year Royal College-accredited program that is completed after a medicine degree program. The Specialty Training Requirements in Diagnostic Radiology are available online and require program completion, a relevant research project, and successful completion of the certification exam (49, 50). The Specific Standards of Accreditation for Residency Programs in Diagnostic Radiology can be found on the Royal College of Physicians and Surgeons website (50). The document has nine standards (50) related to programs that include:

- An appropriate organizational structure, leadership, and administration to support a residency program, teacher, and residents
- A program director and residency program committee
- Preparation for independent practice
- Resources to support the program
- Safety and wellness promotion for learners, teachers, and administrators

- Respectful conduct and support for residents
- Teachers that support the residency program in full
- Administrative personnel who are valued and supported in program delivery
- Continuous improvement and education

The university develops the curriculum and a recognized third-party organization regularly accredits the program. A Diagnostic Radiologist who chooses to specialize further within the MRI subspecialty usually requires fellowship training with at least 6 months spent reading MR studies with experienced MR-trained radiologists.

QUALIFIED MEDICAL PERSONNEL

In order to have a high-quality MRI facility, a team of appropriately trained medical personnel is essential. This team will consist of radiologists, a physicist, nurses, and MRI technologists. As CAR outlines in their standards, a Diagnostic Radiologist with subspecialty training in MRI is required to supervise and interpret MRI exams in addition to supporting clinical MRI service provision. Canada requires that physicians interpreting MR images are board-certified radiologists with the Royal College of Radiology. Foreign-trained specialists are acceptable as long as they have a fellowship that is approved by the provincial college and they have an appointment in a Canadian University as a Radiologist (21). Each province has a regulatory professional college that supports the continued professional practice, development, and education of each Diagnostic Radiologist. The local College of Physicians and Surgeons in each province usually has a licensing committee that oversees the regulation and scope of interpretation for radiologists in the province.

The newest *ACR Guidance Document on MR Safe Practices: Updates and Critical Information 2019* states that the physician responsible for MRI safety, known as the MR medical director, “is required to ensure continued appropriate evaluation and screening of patients, implants or devices, and equipment (e.g., patient support equipment and surgical, radiation, and anesthesia devices) that are brought into the MRI environment” (18). Many of these functions can be delegated, under appropriate oversight in a clinical setting, to an experienced MRI technologist. In a research setting, there may be other non-technologist Level 2 Personnel designated individuals who have undergone advanced training and education in MRI safety principles, such as imaging physicists, physicians, and research scientists.

MRI technologists are MRTs who have been certified by the CAMRT in the discipline of magnetic resonance (RTMR). Additionally, in at least 6 of the 10 Canadian provinces the technologist must be registered with the provincial regulatory body. Technologists must maintain current certification in CPR (according to the employer) and the CAMRT BPGs recommend that technologists receive annual retraining (24). At most Canadian facilities, MRI technologists will be certified in CPR if they are delegated the responsibility of venipuncture. Technologists are responsible for equipment operation, patient care, and safety of the equipment, staff, visitors, and patients in the MRI department. Technologists prepare and screen patients, in addition to supporting them through the exam, to produce images that are diagnostic. Assessment of the image for quality and artifacts is the responsibility of the technologist. MRI technologists are the frontline staff responsible for delivering edu-

960 MRI Safety Practices, Guidelines, and Standards in Canada

tion and training regarding the specific risks of the scanner and the environment. MRI technologists ensure restricted and controlled access in the department in Zones III and IV to minimize the chance of MRI safety-related accidents.

In Canada, qualified medical physicists have certification from the Canadian College of Physicists in Medicine (CCPM) and are also members of the Canadian Organization of Medical Physicists (COMP). Alternatively, certification by the American Board of Radiology (ABR) is often recognized. Ideally, the medical physicist will have certification in the subfield of magnetic resonance imaging, but this is not usually required. The physicist is skilled in MRI physics, acceptance testing, system performance, troubleshooting, and quality control activities. In Canada, it is very common for the physicist to be affiliated with a university, have academic responsibilities, and be involved in research. The MRI physicist collaborates with administrators, technologists, radiologists, and field service engineers (FSEs) from the vendor. The role the MR physicist plays in medical imaging departments is important to ensure the safety of the equipment and in the safety of patients with complex implants. The physicist develops scan protocols and parameters in collaboration with the MRI technologist to optimize sequences and ensure safe scan methods. Additionally, the medical physicist oversees the quality assurance program along with the diagnostic medical director and the lead MRI technologist. The physicist provides feedback and assistance regarding preventative maintenance and any issues relating to faulty coils or phantoms in the department in collaboration with the FSE.

The FSE is usually employed by the vendor and manufacturer of the MR system (21). The role of the FSE is installation, calibration, and preventative maintenance at regular intervals. FSEs have usually completed electronic engineering technologist training programs. The lead technologist maintains communication with the FSE for troubleshooting and routine maintenance. The MRI technologists keep a record of troubleshooting, errors, faults, artifacts and other system deficiencies in a logbook and equipment manual. The information is part of the annual quality report submitted to the physicist.

PROFESSIONAL REGULATION AND PROVINCIAL LEGISLATION

In Canada, the provinces regulate qualified medical practitioners under the *Regulated Health Professions Act*. Most provinces and some territories have regulatory colleges that oversee conduct and development of members. At the provincial level, there are regulations in the Regulated Health Professions Act legislation that function to promote the safety of the public. Most provinces have a provincial College of Physicians and Surgeons that governs the practice of Diagnostic Radiologists. Regulatory colleges investigate the conduct of members if a public complaint is registered with the professional body. In the case of medical physicists, the CCPM governs members on a national basis. The current state of regulation for Canadian MRTs is progressing towards each province having a regulatory college for MRTs. The CAMRT and provincial associations only function to certify members, while regulatory bodies focus on public protection, safety, and patient care. The provinces who have regulatory colleges for MRTs are Alberta, Saskatchewan, Ontario, Quebec, Nova Scotia and New Brunswick. British Columbia and Manitoba have been moving towards the formation of a regulatory body and professional self-regulation for RTMRs with the assistance of the CAMRT and the Alliance of Medical Radiation and Imaging Tech-

nologists Regulators of Canada (AMRTRC) (51). Regulation of imaging professionals is done at the provincial level and ensures professionals follow specific practice, conduct, competence, professional development, and ethical standards. More information can be found online.

ACCREDITATION OF MRI FACILITIES

Accreditation of MRI facilities across Canada is conducted by a variety of organizations to assess and ensure provision of high-quality diagnostic MRI services. The Canadian territories are Northwest, Nunavut and Yukon. There is currently only one scanner located in the entire Arctic in Whitehorse, Yukon. Western Canada is formed by four provinces: British Columbia, Alberta, Saskatchewan, and Manitoba. Eastern Canada is formed by six provinces: Ontario, Quebec, New Brunswick, Nova Scotia, Prince Edward Island, and Newfoundland/ Labrador. MRI accreditation in Canada is conducted by either Accreditation Canada or provincially through the College of Physicians and Surgeons. The arctic territories and eastern Canada are usually accredited along with the healthcare organization they belong to by Accreditation Canada; however, the DI standards used by Accreditation Canada were not available at the time of publication. Most of the western provinces are accredited provincially by The College of Physicians and Surgeons through a facility medical director. Medical directors must be qualified to make decisions and establish standards that benefit patient care. Medical directors in MRI programs are usually specialized in magnetic resonance and involved in the development and review of policy and procedures.

In British Columbia (BC), Alberta, and Manitoba there are specialty diagnostic accreditation programs that function as part of the College of Physicians and Surgeons in each province. In BC, the discipline-specific standards are published by the Diagnostic Accreditation Program (DAP) and the program is given authority under the *Health Professions Act*. The *Accreditation Standards 2014*, appear to be updated regularly, are effective as of 2018, and are available online (52). In Alberta, the College of Physicians and Surgeons of Alberta inspects MRI facilities and issues accreditation certificates. The College of Physicians & Surgeons of Manitoba has a provincial accreditation body for diagnostic imaging, known as the Manitoba Quality Assurance Program, or MANQAP. The *Manitoba Diagnostic Imaging Standards* are regularly updated and revised with the current version effective January 2019 and available online (53). The provincial MRI standards provide an excellent resource that enable sites to prepare policy, guidelines, and standard operating procedures (SOPs) that serve to improve MRI service quality and enhance departmental safety. Annual signoff of documents is a requirement, although the mechanism, in electronic or hard copy, is currently different depending on the site and individual facility director. The trend in some provinces, such as Alberta, Manitoba, Saskatchewan, Nova Scotia, and PEI, seems that diagnostic and health services are starting to amalgamate and become provincially managed and centralized.

The frequency of inspection by the accrediting bodies varies slightly across the Canadian provinces. New MRI facilities are inspected prior to clinical and research operations commencing. If the new site meets all standards, they are granted a conditional certificate of accreditation. In general, existing MRI sites are inspected at least once every 5 years. Regular inspection allows for facilities to review policy and procedures and improve quality

962 MRI Safety Practices, Guidelines, and Standards in Canada

at the provincial level. Sites are encouraged to collaborate and share policies and procedures that are deemed effective.

ACCEPTANCE TESTING FOR MR SYSTEMS

For accreditation purposes, most facilities require an acceptance testing report prior to offering clinical MRI services. In Canada, MRI acceptance testing of new MR systems is conducted by a qualified medical physicist. In rare cases the installation report from the equipment manufacturer is adequate provided it is reviewed by a qualified medical physicist. One copy of the acceptance report is usually kept onsite in the department in an equipment manual and one is shared with management. The CAR recommends following the ACR guidelines (21). However, this is not a requirement and many sites perform their own tests. The BC DAP program requires magnetic field homogeneity, RF shield integrity, ambient RF noise, uniformity of the body coil, gradient performance, and table positioning accuracy (52).

It is common to use tests built-in to the scanner as a negative result is easily verified by the vendor. The actual tests performed will vary somewhat depending on the make and model of scanner. Ideally the shim will be verified and the slice position and thickness measured. All coils should be checked to confirm signal level and signal-to-noise ratio are within specifications. It is preferred that each coil element be independently verified. Given the large number of coils ordered with a scanner, this can be a lengthy process. All images should be free of unexpected artifacts. Coils that are faulty in construction, damaged, or fail to meet image quality baselines must be replaced and not used for patient imaging. Measurements of system stability and geometric distortion are often helpful. When the system is used for spectroscopy, a special phantom is often used to verify accuracy of the corresponding sequences. Medical physicists often conduct an analysis of various pulse sequences to ensure there are no artefacts or ghosts. All sequences are tested and reviewed by the MRI technologists and radiologists after the system is handed over. The physicist and technologist work together to perform a full inspection of the site, the MR system, the peripheral equipment, monitoring devices, and the RF coils. This includes verifying pulse oximeters, respiratory bellows, and ECG functionality.

For a new facility, the MRI team should be involved during the design phase of the project. If possible, the team should visit during construction to confirm the locations of medical gasses, light switches, and other important design elements. After construction is completed, the inspection of the site is ideally conducted collaboratively with the MRI physicist, the MR medical director, and the MRI technologist to review the patient and staff flow through the area. Further, a review of the departmental safety features and the final acceptance report are completed. All areas in the department are inspected for construction irregularities or flaws. The MRI team can ensure that signage, access restrictions, and labeling of devices are adequate prior to accreditation. CAR specifically recommends a review of the locations and functionality of the lighting and safety switches, MRI conditional fire extinguishers, the emergency power off (EPO) and quench switches, the patient monitoring devices, and the emergency call systems (21).

Demarcation of the 5 Gauss line in the MRI environment is highly recommended. The MANQAP and BC DAP accreditation standards outline this as a requirement (52, 53). The vendor is required to provide maps of the fringe field as per the IEC requirements to ensure the safe usage of peripheral equipment in the room and for exclusion zone purposes. The physicist can also measure the fringe field using a Gauss meter. It is also useful to mark the 100 Gauss line as this is about the maximum field that peripheral equipment can tolerate. Other elements to consider are a review of the quench line documentation, the quench pipe outlet, and regular quality control program requirements.

QUALITY CONTROL PROGRAM

The quality control (QC) program at the MRI facility is overseen by a medical director and medical physicist. QC programs monitor equipment performance and are an important requirement for accreditation. Trends in these measurements can indicate equipment failure or other issues such as interference from external sources. Considering that very few sites have a dedicated medical physicist, it is important that the measurements be straightforward to perform. Ideally the signal and signal-to-noise values for the head or knee RF coil are measured and the results recorded. It is fine to use software on the scanner to do this as long as numerical results are provided (i.e., a simple pass or fail result is unacceptable). The measurements are typically repeated at regular intervals, e.g., once per month, to fit into the departmental workflow. In addition, it is important that all coils be separately tested once per year. The MR system manufacturer provides a variety of phantoms for regular testing of all coils. It is a good idea for the physicist to annually review the QC measurements and test results and provide recommendations in writing. It may be a requirement of accreditation to remediate any non-conformances or deficiencies. Some sites in Canada elect to follow the recommendation of CAR and use the ACR guidelines and an ACR phantom. However, this is not necessarily a good fit from many Canadian sites given the resources available.

The MRI technologists in the department have knowledge and experience in running the routine quality assurance activities. The technologists are also familiar with recognizing a variety of image artifacts and notifying the lead technologist if artifacts become apparent. Often the lead MRI technologist is delegated the responsibility to ensure conformance to the quality control program according to a schedule developed by the MRI physicist. The lead technologist is responsible to maintain the written logs, procedures, and record results in order to report on the QC program to the MRI physicist. Many sites choose to keep a QC and equipment manual to maintain a log of system errors, artifacts, and system downtime relating to equipment failure. If remediation is required, documentation and service records related to preventative maintenance or parts replacement are maintained by the lead technologist. Another part of the regular system maintenance will include inspection of the RF coils for signs of wear and tear or damage. Regular preventative maintenance schedules and analysis of QC results serve to detect major systems issues before they result in coil failure, equipment malfunction, or system downtime. In Canada, equipment downtime can result in the diversion of patients requiring emergent imaging to alternate imaging centers.

The MR system manufacturer provides a variety of phantoms for regular testing of all system coils and these phantoms can be used, although some sites choose to follow other

964 MRI Safety Practices, Guidelines, and Standards in Canada

guidelines. Some sites in Canada may follow the ACR guidelines with the use of an ACR phantom, in conjunction with an MRI physicist knowledgeable in the application of the program. The physicist will annually review the quality control measurements and test results and provide recommendations in writing with a timeline to remediate any non-conformances or deficiencies.

QUALITY IMPROVEMENT PROGRAM FOR MRI

Given the financial limitations in the Canadian healthcare system, a great deal of focus is on improving access to MRI, triaging patients, and developing appropriateness criteria for imaging. Unfortunately, lengthy queues exist in Canada, due to the relative lack of MR systems available. The Choosing Wisely campaign has been endorsed by the CAR as an improvement initiative to reduce the amount of unnecessary imaging. Unnecessary and repeat imaging that does not alter treatment plans, introduces the potential for harm. In Canada, with limited resources and increased scrutiny of how healthcare dollars are spent appropriateness is a big deal and the CAR has developed referral guidelines.

Other processes, including peer review and imaging audits are important for quality improvement initiatives. Most facilities conduct regular image audits for technologists to identify safety and image quality issues. Radiologist peer review processes are conducted on the provincial level through the College of Physicians and Surgeons that licenses, regulates, and gives privileges to radiologists (and on occasion cardiologists) to interpret MRI examinations.

The quality improvement program allows the radiologist to supervise and sign off on policy and procedures relating to contrast administration, patient management, emergency procedures, sedation, and monitor safety concerns in the department that put patients or staff at risk. Adverse events and critical incidents or occurrences must be reported in alignment with local site policies and procedures and reviewed with the medical director.

MEDICAL DEVICES IN CANADA

All medical devices in Canada are subject to the *Food and Drugs Act* and the associated regulations (54). The MR system specifications and performance must meet all provincial and federal guidelines, including Health Canada guidelines. Health Canada ensures that medical devices used for diagnosis are regulated according to the standards set forth by the Medical Devices Bureau of the Therapeutic Products Directorate (TPD). According to the Health Canada website, the TPD applies both the *Food and Drug Regulations* (C.R.C., c. 870) and the *Medical Devices Regulations* (SOR/98-282) under the authority of the *Food and Drugs Act* to regulate pharmaceutical drugs and medical equipment to ensure those devices and products are safe, effective, and high quality (25, 26, 54). The terms and conditions of medical device licensure minimize any potential harm and achieve two end goals; manufacturer compliance and a high level of public health and safety. Health Canada's regulations for licensing medical devices are some of the most stringent regulations in the world but improvements are being made through Health Canada's *Action Plan on Medical Devices* (55).

MRI Bioeffects, Safety, and Patient Management 965

To ensure that a medical device is safe and effective the manufacturer is required to balance the risks associated with the usage medical device with the benefits offered to the patient. The manufacturer must identify the inherent risks in the device and eliminate those risks if possible. If it is not possible to eliminate the risks in the device, the manufacturer must reduce the risks and provide protection appropriate to the risks (such as alarms). Instructions for use and other important information must be provided with the device to outline and mitigate any risks that remain. The obligation of the manufacturer is to minimize any hazards from potential failures of the device during the useful life of the device. Manufacturers must ensure that there exists a high level of protection in the devices they wish to obtain licensing approval for and in turn sell to healthcare institutions in Canada.

A medical device must function and perform as intended for the purposes and uses that the device has been sold and manufactured. Manufacturers are required to ensure that the device will maintain performance during the projected life of the device so that the device does not become a risk to the health and safety of a patient, user, or other person. The design and manufacture of the device must minimize all risks and hazards to the patient and user related to (25):

- Flammability or explosion
- Contamination
- Radiation
- Electrical, mechanical or thermal hazards
- Fluid leaks

Further, the device must perform and pass measurements within certain tolerance limits. Software must perform as intended by the manufacturer. Mandatory quality control according to CSA and ISO standards, testing, and quality assurance in manufacturing ensures compliance with the medical devices regulations. Additionally, there exists labeling requirements for all medical devices dependent on the class of the device.

In Canada, medical devices are categorized into four classes based on the level of risk associated with their use. Class I devices present the lowest potential risk (e.g., oral thermometers, hospital beds, wheelchairs, leg prostheses) and Class IV devices present the greatest potential risk (e.g., cardiac pacemakers, defibrillators, breast implants, bone grafts). Class II devices include infusion sets, syringes, tracheostomy tubes, urethral catheters. An MR system is classified as a Class II medical device by these regulations (25). Class III devices are infusion pumps, anesthesia gas machines, and IUDs. Class II, III, and IV devices receive increasingly rigorous reviews, and must be licensed before being sold in Canada. By comparison, Class I devices do not require medical device licences, but they are monitored through establishment licences.

Establishment licences ensure that TPD knows of the manufacturers, importers, and distributors of the devices that are being sold in Canada. Health Canada issues Medical Device Establishment Licences (MDEL) and Medical Device Licences (MDL). Medical device licences can be suspended and devices can be recalled if they are found to no longer be safe and effective and pose a safety risk to Canadians. In order to determine if a particular MR system is approved for use in Canada, a searchable database called Medical Devices Active Licence Listing (MDALL) is available that lists Class II, III, and IV medical devices cur-

966 MRI Safety Practices, Guidelines, and Standards in Canada

rently licensed in Canada. Both active and archived licenses can be viewed at the MDALL website (56).

The *Medical Devices Regulations* were last amended June 2019. Sections 26 to 32 in the regulations are applied to MR systems and these are summarized from the Government of Canada's website, as follows (25):

Class II, III, and IV Medical Device Prohibitions (Sections 26, 27)

In Canada, Class II, III, and IV medical devices without a valid Canadian device license cannot be sold or imported. If the device has been changed, an amended medical device license must be obtained. Devices cannot be advertised for sale in Canada unless they have a medical device license. In the case that the device has been changed, an amended medical device license must be obtained prior to sale. If the device in question is advertised in print, the device must have a warning indicating that it may not have been licensed in accordance with Canadian Law.

Medical Devices Considered Licensed (Sections 28, 30 – 31)

If a system is licensed, all of the components that are manufactured by the manufacturer are deemed licensed for sale, import, or advertisement. If a medical device or medical device group is licensed and forms a medical device family or a medical device group family, all the other medical devices or medical device groups in the family are deemed to be licensed. If all of the medical devices forming part of a medical device group are licensed, the medical device group is deemed licensed and can be imported, sold, and advertised.

Application for a Medical Device License

The manufacturer must submit an application for a Canadian medical device license to the health ministry. In Canada, this is a rigorous process with medical imaging equipment. The application must be in the format established by the Minister and include:

- The name of the device
- The class of the device
- The device identifier of the system, medical device group, medical device family, or medical device group family
- The name and address of the manufacturer on the device label
- The name and address of the establishment where the device is being manufactured if different than the preceding statement

An application for a Class II medical device license will contain:

- A description of medical conditions, purposes and uses for that the device is manufactured, sold, and represented
- A list of standards the manufacturer has complied with to satisfy the safety and effectiveness requirements
- A senior official of the manufacturer attesting that the vendor has objective evidence to prove that the device meets the safety and effectiveness requirements
- A senior official of the manufacturer attesting that the device label meets the labeling requirements in the Medical Devices Regulations

- A senior official of the manufacturer attesting that the investigational testing of the device has been conducted on human subjects who are representative of the intended use and conditions of use
- A copy of a quality management certificate that the device is manufactured and complies with the National Standard of Canada CAN/CSA-ISO 13485:03, *Medical devices — Quality management systems — Requirements for regulatory purposes*

REPORTING ON ADVERSE EVENTS AND INCIDENTS

Health Canada publishes new regulations and amendments to laws in the Canada Gazette. A major amendment to the *Food and Drugs Act*, called *Protecting Canadians from Unsafe Drugs Act* (Vanessa's Law) was passed and updates the law that applies to medical devices and drugs in 2014 (57). This amendment is the biggest change within the past 50 years and the changes will come into force as the *Medical Device Regulations* and the *Food and Drug Regulations* are updated (57). There are now harsh financial penalties for the marketing of unsafe products, better mechanisms to recall products, and the law will compel drug companies to test and revise labels to reflect health risk information (57).

Health Canada's *Action Plan on Medical Devices* was developed as a strategic move to improve the oversight of medical devices (55). The main goal is to increase patient protection. The action plan has three goals that include:

- Improving how devices get on the market (increase protection and research)
- Strengthening monitoring and follow up (mandatory hospital reporting)
- Providing more information on medical devices to Canadians

The action plan and new regulations encourage healthcare practitioners and those in the healthcare system to improve the reporting of serious adverse drug reactions (ADRs) and medical device incidents (MDIs) to Health Canada (55, 57, 58). The plan aims to strengthen the knowledge base on product safety to improve patient safety, outcomes, and public health. Mandatory reporting by hospitals *within 30 calendar days* to adverse events will now apply (58). The change is primarily due to under reporting and poor reporting on ADRs and MDIs (55). Health Canada will also launch a searchable database that contains medical device incident reports (55). It is unclear if the action plan applies to all classes of medical devices (55), however the *Mandatory Reporting of Serious Adverse Drug Reactions and Medical Device Incidents by Hospitals* guidance document gives a definition of what medical devices and pharmaceuticals are covered (58). The guidance document indicates that the term "medical device covers a wide range of health and/or medical instruments used in the treatment, mitigation, diagnosis or prevention of a disease" and that mandatory reporting includes all classes of medical devices (58).

The Health Canada webpage *Reporting an Adverse Reaction or Medical Device Problem* has links to MedEffect Canada, the Canada Vigilance Program, the Canadian Medical Devices Sentinel Network, and other related resources (59). The new mandatory reporting requirements will apply to all hospitals beginning December 16, 2019 (59). Healthcare workers can report directly online at Canada.ca/medeffect beginning in the fall of 2019 (59). The regulations will supplement adverse reporting that has traditionally been received largely from the manufacturer. This new mechanism will expand the Canadian Medical De-

968 MRI Safety Practices, Guidelines, and Standards in Canada

vices Sentinel Network (CMDSNet). The expansion of the safety and effectiveness of medical devices and products will allow evidence to “compel manufacturers to reassess their product in light of the new information and to provide the report to Health Canada (59).”

CONCLUSIONS

There are numerous governing bodies that issue guidelines and standards regarding MRI safety in Canada. The challenge is assimilating all of the resources together to come up with best safety practices, guidelines, and standards that are current and relevant. The lack of one Canadian governing document covering the safety, bioeffects, and management of MRI operations could create gaps in clinical service standards. Canadian MRI departments that clearly develop and stipulate which policies and procedures they operate under offer clarity in service provision. A local departmental policy manual with specific guidance for staff safeguards patient and staff safety. Preventative practices are in alignment with other international standards and put in place to mitigate the risk of adverse events and outcomes in the MRI environment. MRI healthcare professionals work collaboratively to ensure that all safety guidelines, quality management programs, policies, and standard operating procedures (SOPs) function to enhance safety, minimize adverse events, and optimize patient outcomes.

DISCLAIMER

The content of this chapter reflects the opinions of the author and not of her places of employment. The information contained in this chapter is publicly available on the Health Canada, Government of Canada Justice Laws, Canadian Association of Radiologists, and Canadian Association of Medical Radiation Technologists websites. Importantly, this information is valid only at the time of publication and is subject to change. Therefore, reader is referred to the pertinent Health Canada, Government of Canada, Canadian Association of Radiologists, and Canadian Association of Medical Radiation Technologists websites to obtain comprehensive and up-to-date information regarding Health Canada policies, submissions of medical devices in Canada, and other information related to Canadian standards.

REFERENCES

1. The Canadian medical imaging inventory, 2017. In: CADTH optimal use report. Canadian Agency for Drugs & Technologies in Health. Available at: https://www.cadth.ca/sites/default/files/pdf/canadian_medical_imaging_inventory_2017.pdf Accessed May, 2020.
2. Magnetic resonance imaging (MRI) exams. In: OECD data. Organization for Economic Cooperation and Development. Available at: <https://data.oecd.org/healthcare/magnetic-resonance-imaging-mri-exams.htm>. Accessed May, 2020.
3. Guidelines on Exposure to Electromagnetic Fields from Magnetic Resonance Clinical Systems, 1987. In: Safety code 26. Health Canada. Available at: <http://www.hc-sc.gc.ca/ewh-semt/pubs/radiation/87ehd-dhm127/index-eng.php#a51>. Accessed May, 2020.
4. Shellock FG. Radiofrequency–Energy Induced Heating During MRI: Laboratory and Clinical Experiences. In: Shellock FG, Crues JV, Editors. MRI Bioeffects, Safety, and Patient Management. 1st edition. Los Angeles: Biomedical Research Publishing Group; 2014. pp.155-170.

MRI Bioeffects, Safety, and Patient Management 969

5. Limits of human exposure to radiofrequency electromagnetic energy in the frequency range from 3 kHz to 300 GHz - 2015. In: Health Canada. Government of Canada. Available at: https://www.canada.ca/content/dam/hc-sc/migration/hc-sc/ewh-semt/alt_formats/pdf/consult/_2014/safety_code_6-code_securite_6/final-finale-eng.pdf. Accessed May, 2020.
6. 2015 revisions to safety code 6: Summary of consultation feedback. In: Health Canada. Government of Canada. Available at: <https://www.canada.ca/en/health-canada/services/environmental-workplace-health/consultations/2015-revisions-safety-code-6-summary-consultation-feedback.html>. Accessed May, 2020.
7. Understanding safety code 6, 2015. In: Health Canada. Government of Canada. Available at: <https://www.canada.ca/en/health-canada/services/environmental-workplace-health/reports-publications/radiation/understanding-safety-code-6.html>. Accessed May, 2020.
8. IEC 60601-2-33. Medical electrical equipment – part 2-33: Particular requirements for the basic safety and essential performance of magnetic resonance equipment for medical diagnosis. International Electrotechnical Commission (IEC), Geneva, Switzerland.
9. Technical guide for interpretation and compliance assessment of health Canada's radiofrequency exposure guidelines. In: Health Canada. Government of Canada. Available upon request at: <https://www.canada.ca/en/health-canada/services/environmental-workplace-health/reports-publications/radiation/safety-code-6-health-canada-radiofrequency-exposure-guidelines-environmental-workplace-health-health-canada.html>.
10. List of recognized standards for medical devices. In: Health Canada. Government of Canada. Available at: <https://www.canada.ca/content/dam/hc-sc/documents/services/drugs-health-products/medical-devices/standards/list-recognized-standards-medical-devices-guidance/list-recognized-standards-medical-devices-guidance.pdf>. Accessed May, 2020.
11. Kangarlu A. Bioeffects of Static Magnetic Fields. In: Shellock FG, Crues JV, Editors. MRI Bioeffects, Safety, and Patient Management. 1st Edition. Los Angeles: Biomedical Research Publishing Group; 2014. pp.29-63.
12. McRobbie DW. Bioeffects of Gradient Magnetic Fields. In: Shellock FG, Crues JV, Editors. MRI Bioeffects, Safety, and Patient Management. 1st Edition. Los Angeles: Biomedical Research Publishing Group; 2014. pp.64-87.
13. Schaefer DJ. Bioeffects of Radiofrequency Power Deposition Associated with MRI. In: Shellock FG, Crues JV, Editors. MRI Bioeffects, Safety, and Patient Management. 1st Edition. Los Angeles: Biomedical Research Publishing Group; 2014. pp. 131-154.
14. Canada Occupational Health and Safety Regulations. In: Justice laws website. Government of Canada. Available at: <https://laws-lois.justice.gc.ca/eng/regulations/sor-86-304/index.html>. Accessed May, 2020
15. Canada Labour Code. In: Justice laws website. Government of Canada. Available at: <https://laws-lois.justice.gc.ca/eng/acts/L-2/>. Accessed May, 2020.
16. Acts and Regulations. In: Canadian centre for occupational health and safety (CCOHS). Government of Canada. Available at: <https://www.ccohs.ca/topics/legislation/acts/>. Accessed May, 2020.
17. Kanal E, Barkovich AJ, Bell C, et al. ACR guidance document on MR Safe practices: 2013. J Magn Reson Imaging 2013;37:501-530.
18. ACR Committee on MR Safety: Greenberg TD, Hoff MN, et al. ACR guidance document on MR Safe practices: Updates and critical information 2019. J Magn Reson Imaging. 2020; 51:331-338.
19. Shellock FG. Reference Manual for Magnetic Resonance Safety, Implants, and Devices: 2020 Edition. Biomedical Research Publishing Group, Los Angeles, CA, 2020.
20. www.MRIsafety.com. Accessed May, 2020.
21. CAR Standard for Magnetic Resonance Imaging, 2011. In: Practice guidelines. Canadian Association of Radiologists. Available at: <https://car.ca/wp-content/uploads/Magnetic-Resonance-Imaging-2011.pdf>. Accessed May, 2020.

970 MRI Safety Practices, Guidelines, and Standards in Canada

22. Costa AF, van der Pol CB, et al. Gadolinium deposition in the brain: A systematic review of existing guidelines and policy statement issued by the Canadian association of radiologists. *Canadian Association of Radiologists Journal* 2018;69:373-382.
23. Schieda N, Maralani PJ, Hurrell C, Tsampalieros AK, Hiremath SH. Updated clinical practice guideline on use of gadolinium-based contrast agents in kidney disease issued by the Canadian association of radiologists. *Canadian Association of Radiologists Journal* 2019; 70:226-232.
24. Best practice guidelines. In: BPG home. Canadian Association of Medical Radiation Technologists (CAMRT). <https://camrt-bpg.ca>. Accessed February, 2020.
25. Medical devices regulations. In: Justice laws website. Government of Canada. Available at: <http://laws-lois.justice.gc.ca/eng/regulations/SOR-98-282/page-5.html#docCont>. Accessed February, 2020.
26. Food and Drugs Act. In: Justice laws website. Government of Canada. Available at: <https://laws-lois.justice.gc.ca/eng/acts/F-27/>. Accessed February, 2020.
27. American Society for Testing and Materials International. F2503. Standard practice for marking medical devices and other items for safety in the magnetic resonance environment. American Society for Testing and Materials International, West Conshohocken, PA.
28. http://www.ismrm.org/smrt/safety_page/PreScrnF.pdf. Accessed May, 2020.
29. Medical devices regulations. In: Justice laws website. Government of Canada. Available at: <https://laws-lois.justice.gc.ca/eng/regulations/SOR-98-282/>. Accessed May, 2020.
30. Food and drugs act. In: Justice laws website. Government of Canada. Available at: <https://laws-lois.justice.gc.ca/eng/acts/F-27/>. Accessed May, 2020.
31. Verma A, Ha ACT, Dennie C, et al. Canadian heart rhythm society and Canadian association of radiologists consensus statement on magnetic resonance imaging with cardiac implantable electronic devices. *Can Assoc Radiol J* 2014;65:290-300.
32. Yeung SST, Clark M, Loshak H. Magnetic resonance imaging for patients with implantable cardiac devices: A review of safety and guidelines. CADTH; 2019 April. (CADTH rapid response report: Summary with critical appraisal).
33. Noise – measurement of workplace noise. In: CCOHS – OSH Answers Fact Sheets. Government of Canada. Available at: https://www.ccohs.ca/oshanswers/phys_agents/noise_measurement.html. Accessed May, 2020.
34. Marks and labels for North America. In: Testing and Certification. CSA Group. Available at: <https://www.csagroup.org/testing-certification/marks-labels/csa-marks-labels-north-america/>. Accessed May, 2020.
35. Noise – Occupational exposure limits in Canada. In: CCOHS - OSH answers fact sheets. Government of Canada. Available at: https://www.ccohs.ca/oshanswers/phys_agents/exposure_can.html. Accessed May, 2020.
36. Manitoba workplace safety and health act and regulation. In: Labour & Regulatory Services – workplace, safety & health. Government of Manitoba. Available at: <https://www.gov.mb.ca/labour/safety/wshl.html>. Accessed May, 2020.
37. Hearing protectors. In: CCOHS - OSH answers fact sheets. Government of Canada. Available at: https://www.ccohs.ca/oshanswers/prevention/ppe/ear_prot.html. Accessed May, 2020.
38. National Electrical Manufacturers Association. MS 8-2016. Characterization of the specific absorption rate (SAR) for magnetic resonance imaging systems. National Electrical Manufacturers Association, Rosslyn, VA.
39. Guidelines to prevent excessive heating and burns associated with magnetic resonance procedures. In: MRI safety guidelines. Institute for Magnetic Resonance Safety, Education, and Research. Available at: http://www.imrser.org/PaperPDFRecord.asp?WebRecID=85&PgName=Guidelines&WebRecID=&sb_SummaryTitle=&. Accessed May, 2020.

MRI Bioeffects, Safety, and Patient Management 971

40. Faulkner W. B_{1+RMS} as a condition of use. In: SMRT-Signals. International Society for Magnetic Resonance in Medicine (ISMRM). Available at: https://www.ismrm.org/smrt/E-Signals/2016FEBRUARY/eSig_5_1_hot_2.htm. Accessed May, 2020.
41. Morzycki A, Bhatia A, Murphy KJ. Adverse reactions to contrast material: A Canadian update. *Can Assoc Radiol J* 2017;68: 187-193.
42. FDA drug safety communication: FDA evaluating the risk of brain deposits with repeated use of gadolinium-based contrast agents for magnetic resonance imaging (MRI). In: Drugs. Food and Drug Administration (FDA). Available at: <https://www.fda.gov/drugs/drug-safety-and-availability/fda-drug-safety-communication-fda-evaluating-risk-brain-deposits-repeated-use-gadolinium-based>. Accessed May, 2020.
43. FDA drug safety communication: FDA identifies no harmful effects to date with brain retention of gadolinium-based contrast agents for MRIs; review to continue. In: Drugs. Food and Drug Administration (FDA). Available at: <https://www.fda.gov/drugs/drug-safety-and-availability/fda-drug-safety-communication-fda-identifies-no-harmful-effects-date-brain-retention-gadolinium>. Accessed May, 2020.
44. FDA drug safety communication: FDA warns that gadolinium-based contrast agents (GBCAs) are retained in the body; requires new class warnings. In: Drugs. Food and Drug Administration (FDA). Available at: <https://www.fda.gov/drugs/drug-safety-and-availability/fda-drug-safety-communication-fda-warns-gadolinium-based-contrast-agents-gbcas-are-retained-body>. Accessed May, 2020.
45. Guo, BJ, Yang, ZL, Zhang, LJ. Gadolinium deposition in brain: Current scientific evidence and future perspectives. *Frontiers in Molecular Neuroscience* 2018; 11:1-12.
46. Information update – new safety information on injectable gadolinium-based contrast agents used in MRI scans. In: Recalls and alerts. Government of Canada. Available at: <http://healthycanadians.gc.ca/recall-alert-rappel-avis/hc-sc/2017/61676a-eng.php>. Accessed May, 2020.
47. Summary safety review – gadolinium based contrast agents – assessing the risk of gadolinium build-up in the brain and potential brain and nervous system (neurological) side effects. In: Drugs and Health Products. Government of Canada. Available at: <https://www.canada.ca/en/health-canada/services/drugs-health-products/medeffect-canada/safety-reviews/gadolinium-based-contrast-agents-assessing-risk-build-up-in-brain-and-potential-brain-nervous-system-side-effects.html>. Accessed May, 2020.
48. Magnetic Resonance Competency Profile. www.camrt.ca. Accessed May, 2020.
49. Specialty training requirements in diagnostic radiology. In: Information by discipline – diagnostic radiology. Royal College of Physicians and Surgeons of Canada. Available at: <http://www.royalcollege.ca/rcsite/ibd-search-e>. Accessed May, 2020.
50. Specialty standards of accreditation for residency programs. In: Information by discipline – diagnostic radiology. Royal College of Physicians and Surgeons of Canada. Available at: <http://www.royalcollege.ca/rcsite/ibd-search-e>. Accessed May, 2020.
51. Medical radiation and imaging technologist regulation – public focus, public protection, patient care. In: Why regulation matters. Alliance of Medical Radiation and Imaging Technologists Regulators of Canada (AMRITRC). Available at: <https://www.amritrc.ca/why-regulation-matters.html>. Accessed May, 2020.
52. Diagnostic accreditation program (DAP) accreditation standards. In: Diagnostic Imaging. College of Physicians and Surgeons of British Columbia. Available at: <https://www.cpsbc.ca/files/pdf/DAP-AS-Diagnostic-Imaging.pdf>. Accessed May, 2020.
53. Manitoba diagnostic imaging standards. In: Manitoba diagnostic imaging standards. College of Physicians and Surgeons of Manitoba. Available at: <https://cpsm.mb.ca/cjj39alckF30a/wp-content/uploads/MAN-QAP/DI%20Standards%20%20January%202019.pdf>. Accessed May, 2020.
54. Medical devices. In: Drugs and health products. Government of Canada. Available at: <https://www.canada.ca/en/health-canada/services/drugs-health-products/legislation-guidelines/medical-devices-legislation-guidelines.html>. Accessed May, 2020.

972 MRI Safety Practices, Guidelines, and Standards in Canada

55. Health Canada's action plan on medical devices: Continuously improving safety, effectiveness and quality. In: Drugs and health products. Government of Canada. Available at: <https://www.canada.ca/en/health-canada/services/publications/drugs-health-products/medical-devices-action-plan.html#a3>. Accessed May, 2020.
56. Medical devices active licence listing (MDALL). In: Drug and health products. Government of Canada. Available at: <https://www.canada.ca/en/health-canada/services/drugs-health-products/medical-devices/licences/medical-devices-active-liscence-listing.html>. Accessed May, 2020.
57. Protecting Canadians from unsafe drugs act (Vanessa's Law) amendments to the food and drugs act (bill C-17). In: Drugs and health products. Government of Canada. Available at: <https://www.canada.ca/en/health-canada/services/drugs-health-products/legislation-guidelines/protecting-canadians-unsafe-drugs-act-vanessa-law-amendments-food-drugs-act.html>. Accessed May, 2020.
58. Mandatory reporting of serious adverse drug reactions and medical device incidents by hospitals – Guidance document. In: Drugs and health products. Government of Canada. Available at: <https://www.canada.ca/en/health-canada/services/drugs-health-products/medeffect-canada/adverse-reaction-reporting/mandatory-hospital-reporting/drugs-devices.html>. Accessed May, 2020.
59. Report an adverse reaction or medical device problem. In: Drugs and health. Government of Canada. Available at: <https://www.canada.ca/en/health-canada/services/drugs-health-products/medeffect-canada/adverse-reaction-reporting.html#a5>. Accessed May, 2020.

Chapter 36 MRI Safety Standards and Guidelines in Australia

GREGORY BROWN, PH.D., A. DIP. RAD. TECH. (DIAG.), A. DIP. ADMIN. (HEALTH), FSMRT

Lecturer in Medical Radiations
Allied Health & Human Performance
University of South Australia
Adelaide, Australia

INTRODUCTION

The use of magnetic resonance imaging (MRI) technology must deliver a practical level of protection for patients and staff by avoiding harm and balancing all risks against the benefits of the examination. While the technology and the potential hazards of the MRI environment are essentially common to the practice of MRI globally, there are jurisdictional and regional differences that impact local differences in practice. These stem from variations in regulatory structures, professional standards and education for radiologists and radiographers, levels of participation in international professional and scientific communities, the implants and devices found in the respective marketplace, legal structures, and local public expectations regarding medical risks. This chapter describes and reviews the relevant documented material underpinning the patterns of clinical MRI safety practices in Australia.

MRI in Australia

Australia is an island nation covering an area of land similar to that of the continental United States (U.S.) but with a population of approximately 25.4 million people. The population is predominately urban and residing mainly on the east coast. There are also population clusters in the middle of the southern coast (2 million), at the southern and northern extent of the west coast (4 million), as well as a small population center on the northern coast, and on a large island state (Tasmania). Capital cities and regional centers are well serviced by MRI facilities that operate within a modern western healthcare system. The Organization for Economic Co-operation and Development (OECD) reported that, in 2011, Australia had 14.1 MR systems per million people (377 scanners) performing approximately 1.2 million examinations per year (1).

974 MRI Safety Standards and Guidelines in Australia

The exact size of the Australian MRI installed base is difficult to determine because reporting is influenced by funding arrangements. An Australian Government 2019 report confirmed the OECD figures by listing 356 fully and partially funded scanners (2). Industry groups estimate that there are an additional 250 MR scanners providing medical examinations outside of the Australian universal health funding arrangements. By comparison, the OECD country average is 12.5 MR systems per million people, while the U.S. is equipped with approximately 39 scanners per million individuals (1).

The majority of the installed scanners are less than 10 years old, generally operating with high-performance gradient systems, comprehensive phased-array radiofrequency (RF) coils, and advanced applications software. Medicare does not fund services performed on MR systems more than 20 years old. Most MRI examinations are performed for clinical indications in hospitals or stand-alone radiology practices using MR systems operating at 1.5-Tesla, but about 40% of scanners operate at 3-Tesla, a substantial increase in proportion since 2012. There are only a few lower field strength and/or vertical-field scanners, none of which are covered by the federal funding arrangements in Australia. There are three clinical and one research driven custom designed MR guided linear accelerators (MR-LINAC) operational, with more installations planned in the future by a private provider. Several clinical centers and research facilities operate human positron emission tomography (PET) MR systems and several have intra-operative MR scanners. Two research centers operate 7-Tesla, whole-body MR systems equipped with high order, parallel transmit RF systems, neither currently provides clinical imaging services.

MRI Funding

Australia operates a “fee for service” healthcare model supported by a universal health insurance system called Medicare. The Australian Federal Department of Health, through Medicare, is the major source of all medical service funding, including MRI examinations performed in public and privately owned facilities. Under the Commonwealth Medical Benefits Schedule (MBS) scheme, a fixed fee is paid for a defined range of MRI procedures, carried out by specifically licensed sites, for specified clinical indications. Virtually all of the 345 Medicare funded sites also perform variable numbers of MRI examinations for indications that are not eligible for Medicare payments. Some of those examinations are billed to the patient while others are performed at no charge, depending on local contractual and commercial factors. Currently the MBS fees for MRI examinations are between \$201.00 and \$1,440.00 Australian dollars, with small additional rebates paid for the use of MR spectroscopy, contrast media, sedation, and general anesthesia support during MRI (3). Many private MRI facilities charge the patient more than the MBS fee and require so-called “gap” payments from the patient. Gap payments are not covered by any private insurance systems in Australia. At many sites, the terms of their Medicare contract prohibits gap billing. MRI exams certain motor vehicle, workers compensation or veterans affairs funded claims fall outside of the Medicare MBS arrangements, but there are similar administrative and legal limitations on examination fees charged for these situations and they generally approximate the MBS fees and typically do not involve gap payments by the patient.

MRI Facility Ownership

Clinical MRI facilities are almost exclusively operated within radiology departments and practices. The Royal Australian and New Zealand College of Radiologists (RANZCR) has established accreditation of Radiologists performing MRI and operates the Quality Assurance Accreditation program. Each of these elements will be explored in detail later in this chapter. Independent cardiologist-owned MR systems are rare in Australia, although many sites offer time for cardiology-directed examinations on scanners owned by radiology practices. Thus, cardiologists may be the responsible healthcare group for MRI facility and patient safety at certain times. Radiation Therapy providers operate a growing number of MR simulator systems external to Radiology providers. The current numbers are unknown. A small number of commercial veterinary scanners are also operated by the private sector. Arrangements at human research centers associated with universities fall outside clinical arrangements. These particular scanners maybe operated by graduate or undergraduate students with limited training, in conjunction with specialist support staff, such as radiographers. Universities generally follow the recommendations for operating their MRI facilities developed by the International Society for Magnetic Resonance in Medicine (ISMRM) (4).

MRI Staffing and Radiographer Training

In Australia, radiographers are the most engaged healthcare professionals on matters of MRI safety. While there is currently no Australian legal requirement for MRI services to be provided by specifically qualified staff, the majority of clinical MRI exams are performed by radiographers who are nationally registered as Medical Radiation Practitioners (MRP) under a board, the Medical Radiation Practice Board of Australia (MRPBA), and the Australian Health Practitioner Registration Agency (AHPRA) authorized by the Health Practitioner Regulation National Law Act (2009) (5). The educational requirements for registration are determined by an independent accreditation committee. The original 2013 MRPBA professional capabilities intentionally omitted professional capabilities for ultrasound (US) and MRI (6). In 2019, the MRPBA acknowledged that basic registrants could not be assumed to have the understanding to deliver safe and competent MRI services without the supervision of an undefined “more experienced practitioner” (7).

New professional capabilities came into effect in 2020 with specific capabilities indicated for ultrasound and MRI (7). Entry-level registrants will need to understand how MRI is employed in clinical situations for diagnosis and radiation therapy planning (7), but are not expected to deliver MRI (or ultrasound, for that matter) services. Practitioners who provide MRI services must demonstrate certain additional capabilities. These include requiring the radiographer to operate the MR system safely by applying knowledge of the principles, equipment, and the clients that they manage during MRI exams. Safety considerations specifically include those associated with contrast agents and other pharmaceuticals used in procedures, site management and the integrity of safety “zones” (i.e., as specified by the American College of Radiology), minimizing MRI-related heating as well as peripheral nerve stimulation, and actively managing risks related to acoustic noise and implant interactions (7). These aforementioned topics form the minimum capabilities the public can expect from any registered Medical Radiation Practitioner who is providing MRI services.

976 MRI Safety Standards and Guidelines in Australia

To date, the MRPBA Accreditation Committee, which provides the board with advice on educational programs deemed sufficient to develop the required professional capabilities, has not described or endorsed educational requirements for practitioners performing MRI. In the Australian implementation, this may not occur because, unlike the arrangements in New Zealand, providing MRI services does not require a specific class of registration. The obligation to perform competently arises when the practitioner includes MRI in their activities. A challenge to the competence of a practitioner may only occur following a complaint to the MRPBA by a patient or other individual. Considering the lack of previous enforceable standards in MRI capabilities and the range of practices that may have developed expediently, the capabilities of individual practitioners around MRI safety may come under scrutiny from mandatory notifications to the MRPBA or the Medical Board under the AHPRA system. Registrants are obliged to notify the Board when they believe the public is placed at risk where the practice is a significant departure from accepted professional standards (i.e., section 140(d) of the National Law) (8).

The degree courses for Medical Radiation Practitioner registration teach MRI principles, safety, and clinical applications at an introductory level, which is obviously insufficient for independently practicing MRI. Therefore, to achieve appropriate MRI competency, radiographers undertake site-based “on the job” training, the basic Australian Society for Medical Imaging & Radiation Therapy (ASMIRT) Level 1 accreditation, or pursue post-graduate education. Unlike graduate level radiography courses, the site and post-graduate training curricula are not standardized or specified by the registration authority. The adequacy of a practitioner’s safety skills and competency may initially be decided administratively by the MRI practice following a complaint or incident as the practitioner and carries the responsibility to show competence relative to the new professional capabilities statement.

At least three Australian universities offer post-graduate courses in MRI technology and clinical practice. The courses are self-funded and students may exit with a post-graduate diploma, up to a Master’s degree level. MRI safety is typically addressed in the first year of study along with physics and imaging principles.

The national radiographic professional body, the Australian Society for Medical Imaging & Radiation Therapy was formerly known as the Australian Institute of Radiography (A.I.R.). ASMIRT operates a two-level MRI certification program amongst a range of modality specific accreditations. Currently, the certification is only open to diagnostic and therapy radiographers at this time and does not specifically offer certification of professional capabilities required by the new document (7).

Level 1 MRI certification is achieved by passing an online exam and the completion of three hundred MRI examinations in a twelve-month period. Certification is maintained by performing nine hundred MRI examinations in a three-year period. ASMIRT Level 2 MRI certification, intended for MRI supervisors, is granted on presentation of a portfolio of professional development activities and this certification is maintained with continuing evidence of professional activities and a larger number of clinical examinations that must be performed. Details of the program and fees are available at the ASMIRT website and in a recently revised MRI certification manual (9).

The MRI safety module of the Level 1 accreditation curriculum requires knowledge of MRI bioeffects and the potential hazards associated with the static, time-varying, and radiofrequency (RF) electromagnetic fields. In combination with general patient care topics, it accounts for 15% of the examination's content and score. However, this is not to say that knowledge of MRI safety topics is examined in depth by the Level 1 certification process. Issues of motion through the static magnetic field, the spatial gradient magnetic field and interactions between medical implants and the scanner are not included. Many experienced MRI radiographers recognize that the ASMIRT Level 1 accreditation represents a relatively low standard of knowledge. Not surprisingly, the ASMIRT currently recommends that radiographers undertaking MRI should undergo further education and certification. Their certification is also supported by the national radiology professional guidelines (10).

As previously mentioned, Australian MRI radiographers tend to take the lead role in understanding MRI technology, pulse sequences, and imaging principles as well as the comprehensive issues of MRI safety. To a degree, radiographers have attempted to informally fill the gap left by less involved radiologists. A potential pitfall to this is that staff members may be functioning clinically above their knowledge base and beyond their delegated professional roles, resulting in possible risks to themselves and patients.

There is a high level of membership in the International Society for Magnetic Resonance in Medicine's (ISMRM) and the Society for MR Radiographers and Technologists (SMRT) amongst Australian radiographers performing MRI. The International and Australia & New Zealand (ANZ) chapter of the SMRT provides a continuing stream of high quality MRI safety educational programs through annual national and international meetings, and via online educational materials. This provides a core of several hundred highly aware radiographers operating in connection with international sources, although industry mechanisms and practice do not presently appear to value the resource these members represent. Of note is that very few Australian clinical MRI facilities employ medical physicists. The Australian College of Physical Scientists and Engineers in Medicine (ACPSEM) commenced a program of lectures, practical assignments and examination in 2020 to offer professional body certification scientists the role of an MR Safety Expert. First completions are expected in mid to late 2021.

MRI SAFETY PRACTICES IN AUSTRALIA

Australia has few absolute requirements regarding MRI safety practices. The legal and clinical responsibilities to keep public, staff, patients and other individuals free from harm are supported by equipment and device standards, professional and regulatory body guidelines, and publications from government departments and authorities. This section will explain and review the key documents applicable to MRI safety.

Australian Standards for MRI Equipment and Patient Exposure

The Australia/Standards New Zealand (AS/NZS) document, AS/NZS 3200.2.3.2005 (11) is essentially equivalent to the International Electrotechnical Commission (IEC) document, IEC 60601-2-33. Australian MR systems have therefore been programmed to observe the global limits for the static magnetic field strength, RF, specific absorption rate

978 MRI Safety Standards and Guidelines in Australia

(SAR), and time-varying, magnetic field limits (TVMF) related to patient exposures rather than old FDA requirements that were replaced by IEC limits in 2014 (12).

Key MRI Safety Points From AS/NZS 3200.2.33:2005. The IEC model of three-tiered operating modes for the MR system is employed in Australian standards and in clinical practice. The standards specify thresholds for the static magnetic field strength, RF power deposition, and time-varying magnetic fields at each operating mode (**Table 1**). In the Normal Operating Mode, none of the scanner outputs may cause physiological stress to patients. In the First Level Controlled Operating Mode, one or more of the scanner outputs are at values that may cause physiological stress to patients. Before employing the First Level Controlled Operating Mode, a decision must be made on medical grounds to confirm that the patient can handle the increased exposure level. Medical supervision is required to control any physiological stress caused by the scanner. The standards require scanners operate in a way that needs a deliberate action by the MR system operator before enabling the First Level Controlled Operating Mode. A Second Level Controlled Operating Mode also exists, where one or more of the scanner outputs reach levels that may cause significant risk for patients. Operation of the MR system in this mode requires explicit local ethical approvals. Notably, most clinical MR systems cannot be easily switched to the Second Level Controlled Operating Mode.

MR system manufacturers bear the primary responsibility of implementing many requirements of the IEC and AS/NZS standards in these regards (13). The AS/NZS 3200.2.33:2005 has not been revised since 2005 and is now out of step with the parent standard (third edition, 2013). Most notably, the Australian and New Zealand standards classify all MRI use above 2-Tesla as the *First Level Controlled Operating Mode* (i.e., requiring a medical decision and supervision). The current European standard IEC60601-2-33:2013 3.1 (9) sets 3-Tesla as the upper limit of the *Normal Operating Mode*, with 8 Tesla as the upper limit of the *First Level Controlled Operating Mode* compared to 4 Tesla in the older standards.

The AS/NZS and IEC standards can be purchased on-line or accessed through academic libraries. However, because of its age, it is not a useful document in practice. The current IEC standard is a wiser investment. Libraries may offer access to the equivalent document under the British Standards (15). Despite their technically dry language, the international standards contain substantial appendices and discussions addressing the rationale of the selected patient exposure limits. They also provide insights into occupational exposure issues, specific requirements for the documentation provided with scanners, patient screening, acoustic noise levels, and several test methodologies that make them important reading material for advanced MRI practitioners.

Therapeutic Goods Administration

Compliance with an Australian standard is not compulsory unless enforced by law or regulation. Compliance with AS/NZS 3200.2.33:2005 is required indirectly by the regulations and processes of the Therapeutic Goods Administration (TGA). The TGA is empowered by federal law (The Therapeutic Goods Administration Act 1989) to control the import, export, manufacture, and supply of all therapeutic goods in Australia including medical devices, medicines, and biological products.

Table 1. Key Australian exposure limits for MRI. *

Parameter	Normal Operating Mode	First Level Controlled Operating Mode	Second Level Controlled Operating Mode
RF Power	Averaged over 6-min.	Averaged over 6-min.	Averaged over 6-min.
Whole Body SAR	2-W/kg	4-W/kg	Above 4-W/kg
Head SAR	3.2-W/kg	3.2-W/kg	> 3.2-W/kg
Local SAR Head	10-W/kg	10-W/kg	>10-W/kg
Local SAR Trunk	10-W/kg	10-W/kg	>10-W/kg
Local SAR Extremities	20-W/kg	20-W/kg	>20-W/kg
Static Magnetic Field Strength	≤ 3-Tesla	≥ 3-Tesla, ≤ 8-Tesla	≤ 8-Tesla

(SAR, specific absorption rate; W/kg, Watts per kilogram)

*Via TGA approval of IEC 60601-2-33:2015 compliance.

All MR systems must obtain registration on the TGA's Australian Registry of Therapeutic Goods (ARTG) before they can be imported or sold in Australia. Certified conformance with the IEC60601-2-33:2013 or AS/NZS 3200.2.33.2005 can be accepted as evidence to place an MR scanner on the ARTG. The harmonization of FDA MR equipment safety standards with the IEC in 2014 has removed the potential for the differences from scanners built to comply with older FDA standards.

The ARTG system also approves all implanted medical devices used in Australia. The registration process assesses information provided by a device sponsor against a set of defined “essential principles”. The essential principles require that use of the sponsored device does not compromise health and safety, that it has been designed and constructed to comply with safety principles, that the device remains safe throughout its useful life, and that the benefits of the device outweigh any undesirable effects. There are also additional “essential principles” regarding design and construction that include specific information to be supplied by the manufacturer. These requirements define the content of Australian Information for Use, (IFU) documents for implants and medical devices, requiring them to include “Any warnings, restrictions on use, or precautions that should be taken in relation to the device.” The TGA regulations are similar to those of the European Union (EU). The TGA will accept conformity assessments issued by specific EU Notified Bodies or other evidence of compliance with Australian or international standards, as evidence of compliance with many of the essential principles. The ARTG requirements to provide warnings, restrictions on use, and precautions, includes exposure to MR systems, but the TGA does not prescribe a format for information regarding MRI and device interactions in the way that the U.S. Food and Drug Administration (FDA) has done since 2005. As a result, the information concerning interactions between implants or devices and MR systems is variable but most “Instructions for Use” for a medical product include FDA-style statements of the MRI conditions for safe scanning, utilizing the American Society for Testing and Materials International (ASTM)/IEC symbols for MR Safe, MR Conditional, and MR Unsafe.

980 MRI Safety Standards and Guidelines in Australia

The TGA relies upon the Advisory Committee on Medical Devices (ACMD) to consider the information for an implant or device. Most of the 15 members of the advisory committee are surgeons, with one eminent biomedical engineer, but no medical physicists or members familiar with MRI safety. In 2017, the ACMD assumed the responsibilities of the Advisory Committee on the Safety of Medical Devices. The ACMD is reactive, collaborating closely with industry on problems that have been identified through complaints and incidents. Notably, a review of the guidelines commenced in 2016 but has not been completed at the time of writing. Several submissions regarding standardizing information for MRI-related interactions were received. Early reports suggest that the scope of the MRI section will be reduced in length (16). In the initial responses to professional and industry submissions contained some concerning signs (17, 18). The ACMD decided to disregard the International Organization for Standardization Technical Standard (ISO TS) 10974 and to remove requirements for MRI-specific labeling as well as patient identification cards for implants, although they recognized that such information would be helpful to the TGA to grant device approval (16). New guidelines will need close review to determine if they decrease rather than increase the information provided about devices in the MRI environment.

PROFESSIONAL STANDARDS

Radiologists are medical practitioners registered by the Medical Board of Australia. Active assurance of safe practice is one of the five elements of a 2017 “Professional Performance Framework” designed by the Medical Board to ensure that medical practitioners deliver services competently and ethically (19). This document requires all medical practitioners to actively assure safety as a central pillar of their professional activities.

The Royal Australian and New Zealand College of Radiologists (RANZCR) Standards of Practice for Clinical Radiology details the professional standards expected for participation in their Medical Imaging Accreditation Program (20). Members of the RANZCR are expected to respect the Standards of Practice. Non-observance can lead to professional consequences or may open a practice to censure by, or complaint to the Medical Practitioners Board. Medicare funding is conditional on the observance of these professional standards through the RANZCR Quality Assurance Program. For these reasons, the Standards of Practice arguably define the Australian minimum acceptable position on MRI safety, although the level of legal liability is unclear.

Section 13 of the document includes several specific standards and indicators regarding MRI safety. A practice must ensure that all sedation, anesthesia, and monitoring equipment used in the MR system room is certified “MRI-compatible” (sic) by the manufacturer. Despite the error in terminology, this suggests that such equipment must be used in accordance with specific MR Conditional labeling in order to ensure safety use monitoring devices. Safety training for staff members is not specifically addressed in this document. The reporting radiologist must be credentialed as an “MR Radiologist”, usually by virtue of the general registration or education processes in RANZCR since January 1995.

RANZCR requires that the radiographers who conduct MRI exams have appropriate training. In the absence of stipulations by the radiographer registration board (MRPBA), the Level 1 ASMIRT MR accreditation is represented by RANZCR as the standard level for

MRI radiographers. The RANZCR clinical standards require that Level 1 staff performing MR scanning are supervised by a Level 2 ASMIRT MR accredited radiographer. The new professional capabilities required for registered radiographers providing MRI services, issued by the Medical Radiation Practitioner Board (7) take legal superiority as of March 2020, and the RANZCR standards are likely to require revision.

Specific MRI safety standards are listed in section 13.4 of the RANZCR standards. The primary requirement is that “MRI safety practices and policies must be documented, enforced and periodically reviewed by the supervising radiologist(s)”. The MR Radiologist is primarily responsible for the safe operation and administration of MRI service. The use of several titles (MR Radiologist, supervising radiologist, Liason MRI Radiologist, etc.) clouds the identification of this healthcare professional, but could be clarified, along with delegations, in site-specific MR safety policies. Reviews of policies are required at least annually. Additionally, policies must protect patients and personnel in the MRI area from potential hazardous interactions, but the standard only focusses on ferromagnetic interactions associated with the static magnetic field of the scanner. Furthermore, the standard identifies the document from the IEC, (IEC 60601-2-33), as the main MRI safety standard while endorsing the American College of Radiology (ACR) guidance document as well as the United Kingdom’s Medicines and Healthcare products Regulatory Agency’s (MHRA) MRI safety guidelines as recommended resources. Previous standards on the availability of an MRI radiologist for consultation on safety questions and the maintenance of a registry of unauthorized objects entering the MR system room have been removed since the 2012 version. Beyond these general points, the Standards of Practice refer to the RANZCR Guidelines on MRI Safety.

Anecdotally, these requirements are not universally observed, with reports of non-radiographers preparing and positioning patients and solo operation of scanners by non-accredited radiographers. Whether these practices remain defensible or tolerated under new practitioner registration requirements remains to be seen. The RANZCR document is intended to apply in New Zealand and Australia, yet there is no mention of the specific registration category and the post-graduate educational requirements required for a registered radiographer under the New Zealand Medical Radiation Technologists Registration Board (21).

RANZCR MRI SAFETY GUIDELINES

The RANZCR MRI Safety Guidelines support the RANZCR Standards of Practice by offering a broad range of guidance material regarding MRI safety (20). Beyond the obligations created by the Standards of Practice that were detailed above, there are no enforced consequences for non-adherence with the guidelines.

The 2017 RANZCR guideline is a substantial improvement over the 2007 document. Input was sought from medical physicists, the Society for Magnetic Resonance Radiographers and Technologists (SMRT), Australian MR safety experts and the ASMIRT before completion by an RANZCR panel. The document has a strong blend of current international opinion and practice models. It retains some similarities with the 2013 ACR Guidance document on MRI safe practice (22), but offers a less didactic text covering a wider range of

982 MRI Safety Standards and Guidelines in Australia

physical and administrative topics. The structure appears to be modeled after the UK MHRA guidelines (23). The College describes the guidelines as an advisory document, but given the Standards for Clinical Practice, and the requirements for Medical Board registration, it is a key document representing appropriate professional practice with respect to MRI safety.

Section 3: Administrative Aspects and Roles

Important administrative aspects of MRI safety open the guidelines, stressing the importance of planning for the delivery safe practices as a fundamental element of the MRI examination. The three tiers of MRI safety personnel described in international consensus is interpreted for the Australian clinical model (24). A radiologist must be explicitly designated for each MRI facility making the suggested title of “Medical Director of MRI” analogous to the consensus title of MR Medical Director or MRMD. An MRI Safety Officer (MRSO) with the responsibilities for day-to-day implementation of MRI safety policies works with the MRMD to develop a consistent approach to ensure the safety of the site, patients, and staff members. This MRSO is described as a designated position, which implies greater knowledge and responsibility than the operational MRI radiographers. Notably, there is no suggestion in the document that the term “MRSO” is prescriptive of the MRSO designation registered by the American Board of Magnetic Resonance Safety, or that a specific MRI safety training curriculum or accreditation is supported by the guidelines. The RANZCR guidelines recommend that MRI sites have access to an “expert third party” who would be invited to offer advice on specific matters such as reviewing facility policies, procedures, and planning. The MR Safety Expert (MRSE) may simply be an MRMD or an MRSO from another site, but these individuals are expected to possess in-depth knowledge of the technical and engineering aspects of MRI equipment and interactions of MRI-related electromagnetic fields with human subjects. Diagnostic imaging physicists (or medical physicists) with specific MRI training are likely to be the best fit for the role of MRSE.

It is suggested that larger facilities establish MRI safety committees to manage policies and to review and examine incidents. A site-specific MRI safety manual is specifically required, along with an incident reporting system. Incidents must be reported internally within 24 hours, with a documented review and response that analyze root causes, providing recommendations for improvement. An active review and monitoring process is central to active provision of safe practices. The clear documentation of annual training of staff working within the MRI facility is another key administrative tool relied upon by the guidelines.

RANZCR has opted for the terms Junior and Senior MRI personnel, instead of Level 1 and 2 MR Personnel as indicated by the ACR, but the patterns of responsibility are similar. Junior personnel have basic training on-site security and rules involving MRI technology, as well as emergency procedures, screening, and hearing protection. These staff members can work within the ACR designated Zones 3 and 4 (i.e., the MR system room) in order to perform initial patient screening. The senior staff members are additionally trained in the physical principles of MRI safety including exposure limits, cryogen hazards, and management of patients with implants and devices. Furthermore, Senior MRI personnel are responsible for signing off the final MRI safety screening procedure and for supervising the other staff members, including non-MRI trained personnel.

Sections 4 & 5: MRI Equipment

In this section of the document, there are certain departures from the TGA position that place the RANZCR guidelines closer to current international standards. Equipment output limits and the MR system's operating modes are drawn directly from the IEC 60601-2-33 2013 edition, appropriately sidelining the relevance of the AS/NZ standard. Some details that conflict with the current IEC standard seem to have been retained from earlier versions, including interest in room humidity (no longer a controlled element relevant to SAR limits specified by the IEC), the identification of 7 Tesla scanners as research devices (now considered First Level Controlled Operating Mode MR systems; notably, these very high field strength scanners have been approved for clinical use in Europe and the U.S.), and the limit on specific absorbed energy of 14.4KJ/kg (replaced by manufacturer specific risk guidelines in the IEC standard).

Section 6: Site Design

The physical zones developed by the ACR and now adopted within IEC 60601-2-33 are dealt with in a mixed manner. The RANZCR guidance has a clear preference for ACR's four-zone strategy and requires all new construction of MRI facilities to implement this means of controlling access of the MRI environment on the basis that zones are stipulated in the Australian Health Facility Guidelines 2016 (25). Designated areas outside the MR system room are required for resuscitation activity, anesthetic induction and recovery, and cryogen storage. Access to all areas with a static magnetic field above 0.5 mT must be controlled by MRI personnel. The guideline also contains specific requirements limiting access to areas of the quench pipe discharge. MRI facilities are required to supply MR appropriate fire extinguishers, room temperature and humidity monitors, patient stretchers and wheelchairs, scanner room oxygen monitors, patients call buttons, and to have direct vision of patients and all MR system room access doors from the control desk.

Sections 9 & 10: Patient/Individual Screening and Scan Room Access

Screening patients and other individuals for implants and foreign bodies is required for all individuals entering the MR system room. Those entering zone 3 must have basic checks for cardiac pacemakers (interestingly, without mention of other implanted "active" devices), plus appropriate restrictions on their access to zone 4, the scanner room. Patient screening is expected on three occasions in addition to statements from the referrer on the MRI request form regarding implants and the suitability for an MRI exam. The first screening by MRI staff can be carried out remotely during scheduling, while the second and third screenings must be conducted on-site by MRI personnel, directly. At least one screening should involve the use of a written screening form and one should involve review of the information on the form along with a verbal screening by Senior MRI personnel who must confirm and identify themselves on the screening form. Section 9 of the guidelines provides a strong discussion of how to document and to make scanning decisions.

If implants are identified during the screening process, further investigation is performed which involves a review of case notes, past imaging studies, a physical examination, an assessment of the implant information provided by the manufacturer (e.g., a review of the Instructions for Use), and possibly additional imaging to help determine the conditions for

984 MRI Safety Standards and Guidelines in Australia

safe scanning. Concerns regarding safety must be resolved carefully, in consultation with an MR safety expert, as needed. The final decision to proceed with an MRI exam is a clinical one and, thus, is made by the radiologist. Scanning a patient with an implant using conditions that are outside those specified by the manufacturer must be covered by a written policy from the facility and be approved by the MRI Medical Director. Furthermore, this action requires written and verbal informed consent of the patient. These afore-mentioned requirements obviously limit the potential for site-specific, policies for implants and devices.

Scan room access during scanning operations is considered specifically by section 10. The door to the MR system room must be kept closed unless individuals are walking through it and, when the entryway is open, it must be visually monitored. All objects entering the scanner room must be labeled with appropriate ASTM F2503 icons: MR Safe or MR Conditional). Only essential non-patients (e.g., support personnel such as nurses, respiratory therapists, or anesthesiologists) are allowed into the MR system room during examinations.

Section 11: Patient Handling

Some points distinguishing practice in Australia from guidelines elsewhere are presented in this section. All patients must be visually monitored during the procedure and provided with a button to alert scanning staff or any issue or concern that occurs during the MRI exam. A patient who cannot verbally communicate or initiate contact during MRI requires monitoring using pulse oximetry at a minimum, while a sedated patient must be monitored using pulse oximetry and blood pressure recording equipment. Under those circumstances, the supervising medical practitioner must be present and immediately available in accordance with professional anesthesia guidelines.

Section 12: Contrast Agents

The gadolinium-based contrast agents (GBCA) section of the guidelines opens with the clear statement that “an MRI Radiologist shall be responsible for assessing in each case whether contrast administration is appropriate”, and for reviewing initial non-contrast views (20). Therefore, the guidelines reinforce the responsibility of the MRI radiologist and the need to a patient-specific, examination-specific prescription of GBCA use. This statement is additional to the 2017 RANZCR statement on gadolinium retention, supported by the TGA (26), in which they noted that routine use of GBCA in some patients “where there is not a specific indication” should be reviewed by a medical professional (27).

GBCA safety measures are summarized but the primary code of practice is the RANZCR 2013 GBCA guideline (28) Gadolinium retention is also addressed in the MRI safety document by recommending that macrocyclic contrast agents should be used unless there is a clear clinical benefit for using a linear contrast agent. The management of the use of a GBCA in a pregnant patient is discussed in section 15.2 of the guidelines with an uncited opinion and the statement that no adverse effects have been convincingly demonstrated. Notably, the RANZCR position is in conflict with a large-scale Canadian study that identified GBCA as a potential significant source of health effects in the fetus, but not with respect to exposures to MRI-related, electromagnetic fields during gestation (29), despite this investigation being explicitly referred to for other conclusions.

Section 13: Noise Protection

The guidelines are explicit and prescriptive regarding the matter of hearing protection in the MRI setting. All MR patients in Australia and New Zealand must wear hearing protection unless it can be clearly documented that the sound pressure levels will stay below 85 dBA during the MRI exam. If a patient refuses to use hearing protection, the MRI radiographer must use pulse sequences with documented sound pressure levels that are less than 85 dBA. Furthermore, all individuals remaining in the MR system room during the imaging procedure must wear hearing protection.

Section 14: Thermal injury

The cause and control of thermal-induced injuries associated with is described in great detail. Certain aspects of the material conflict with the current IEC standard, such as consideration of an assumed maximum relative humidity and the statement that specific absorption rate (SAR) levels may not be corrected for ambient temperature in excess of 24°C. Patients at risk and the heating of internal metal are well-described for information purposes. The conventional measures to reduce the potential for MRI-related burns, removal of conductive leads, padding to the bore, not crossing the patient's limbs, and using padding between skin surfaces are included. The document relies on patient feedback related to heating. It does not discuss possible "deep" burns from RF hotspots related to modified and parallel transmit RF systems, or nonstandard transmit RF coil designs. Of note is that there is no discussion of follow up care in the event that the patient experiences localized heating or skin reddening.

Note 15.1 places additional conditions on research and voluntary scans beyond those applicable for medically requested procedures. They require human research ethics approval, screening and a medical assessment, the exclusion of pregnant volunteers, informed consent, and a limit (presumably site determined) on the number of research scans per person per year. The RANZCR requires that all images acquired shall be reported (by an MR Radiologist) and appropriate clinical follow up provided.

AUSTRALIAN GOVERNMENT SCIENTIFIC AUTHORITIES

Patient, Public, and Occupational Exposure Limits

Exposure limits for static magnetic, time-varying magnetic fields, and RF fields have been defined in Australian standards for the patient undergoing an MRI procedure, where the patient receives some benefit from undergoing the examination. Exposure limits for the general public or occupational exposures are often set lower than a patient limit to reflect the lack of benefit from that exposure.

In the early period of MRI use in Australia, prior to adoption of the IEC standards, the primary Australian scientific body, the National Health and Medical Research Council (NHMRC) commissioned production of the "Safety guidelines for magnetic resonance diagnostic facilities" (30). Such publications were in line with the NHMRC objective to "advise the Australian community on the achievement and maintenance of the highest practicable standards of individual and public health" (30). The NHMRC guidelines were

986 MRI Safety Standards and Guidelines in Australia

published in a radiation health series and placed the responsibility for MRI safety in the hands of the Australian Radiation Protection and Nuclear Safety Agency (ARPANSA). ARPANSA is the body responsible for monitoring ionizing radiation from medical exposure, solar radiation exposure, environmental non-ionizing radiation (such as microwaves and low frequency electromagnetic fields), the uranium mining industry, and Australian nuclear reactors. This delegation mirrors similar decisions in the United Kingdom and Europe.

The 1991 document drew its material largely from early publications and international scientific bodies of the period. It recognized a paucity of information regarding repeated exposure to the electromagnetic fields used by MR systems and, thus, established somewhat conservative recommendations. After a period of public comment, it was published and then seemed to be largely ignored or to go unnoticed by the clinical MRI community.

In 2004, the document was withdrawn by ARPANSA and replaced with a “trusted international document”, the 2004 International Commission on Non-Ionizing Radiation Protection (ICNIRP) statement on medical magnetic resonance procedures (31). The creation of the AS/NZS 3200.2.33 standard released ARPANSA from direct responsibility for setting MRI exposure limits.

The ARPANSA returned obliquely to matters that impacted MRI exposures with its work to establish an Australian radiation protection standard establishing maximum exposure levels for electric and magnetic fields 0 Hz (static) to 3 Hz. This work was initially intended to address public concerns regarding the safety of proximity to electrical power lines and was to replace a 1989 statement on 50/60 Hz field exposures (32). The working group responsible for drafting the radiation protection standard was dominated by representatives of the power generation and distribution industry. A draft was released for public comment in late 2006 (33). The document was focused on power line field exposure, but also set out to establish mandatory restrictions for the general public and occupational exposure over the full range of activities that produce extremely low frequency (ELF) fields. In another chapter in this textbook which pertains to MRI safety in Europe, Dr. Stephen Keevil illustrates how efforts to address safety concerns public concerns over exposure to extremely low frequency (ELF) time-varying electrical and magnetic fields (EMF) from sources such as power transmission lines, and specific industrial exposures can impact the practice of MRI. Scientific consideration of an extensive literature review in the draft focused on certain information on peripheral nerve stimulation (PNS).

The 2006 consultation document did not recognize any potential impact on the practice of MRI (even though it included an occupational limit of 2 Tesla at a time when 3 Tesla MR systems were being installed) and the committee responsible for the proposed exposure limits failed to make any connection with the European Union (EU) debate raging at that time. MRI professional organizations including the ISMRM, SMRT, and RANZCR (34) were mobilized and approximately one-third of all submissions made to the ARPANSA working group came from MRI professionals and MRI equipment suppliers concerned that the proposed exposure limits would interfere with important diagnostic technology and practice. By February 2008, the ARPANSA was taking note of the concerns regarding MRI (35) and apparently considered increasing the static magnetic field limits and adopting the

International Commission on Non-Ionizing Radiation Protection (ICNIRP) approach of exempting certain professional activities (35).

The release of a final radiation protection standard was expected by the middle of 2010 but with public consultation and the release of international reviews of the scientific literature, the ARPANSA stepped away from producing a radiation protection standard in the ELF range. The ARPANSA moved to adopt the ICNIRP 2010 statement on limiting ELF exposures (36) in line with a policy of adopting international best practices. In 2017, the ICNIRP published a paper describing existing regulations on diagnostic devices using non-ionizing radiations, suggesting incorrectly that the 1991 document remains in use in Australia with regulatory strength. ARPANSA has confirmed that this is not the case (37).

Reporting MRI Safety Incidents

Incident Reporting and Investigation Scheme (IRIS). The TGA operates the medical devices Incident Reporting and Investigation Scheme (IRIS). Reports of adverse events associated with MRI can be made on-line. The reports receive a thorough risk assessment procedure and are reviewed by a panel of scientific, engineering, and clinical experts who may recommend further investigation. The event reports and findings recorded in the IRIS database can be used by the TGA to initiate a range of responses such as recalls, user education, or compliance testing. The system is well described on its website (38). The IRIS database does not facilitate public or researcher access to reports, but final details of the reports appear on the Database of Adverse Events Notifications (DAEN), Medical Devices database described below. IRIS is the primary place to report MRI-related safety incidents because it is managed by the government agency responsible for medical device registration and safety.

Database of Adverse Events Notifications – Medicines

The TGA manages the Database of Adverse Events Notifications (DAEN) - medicines. Initially DAEN-medicines collated adverse events surrounding the use of medications drawn from reports to the Australian Adverse Drug Reaction Reporting Scheme (ADRRS) (39). Adverse events related to gadolinium-based contrast agents or medications administered during MRI should be reported using this system. The DAEN system is relatively transparent and provides for public searches by product name. Approximately 700 DAEN - medicines notifications have been made for gadolinium-based contrast agents since 1986, including seven deaths, with one attributed to gadolinium associated systemic fibrosis, also known as nephrogenic systemic fibrosis.

Database of Adverse Events Notifications – Medical Devices

In July 2012 the “DAEN – Medical Devices” database was initiated to collate adverse event reports in relation to medical devices from Australian reports from consumers or device sponsors (39). Reporting adverse events with medical devices can be performed via an on-line form. Reporting is voluntary for healthcare professionals, but under the federal Therapeutic Goods Act 1989 it is mandatory for manufacturers and sponsors to report serious or potentially serious events associated with a medical device. Some reports received prior to July 2012 may not be included if the levels of information and evidence are not to

988 MRI Safety Standards and Guidelines in Australia

the required standard. DAEN - Medical Devices offers a public search function for events involving one or a number of specific devices from the ARTG. Devices in the search term are cross-referenced to the ARTG meaning that the searches are highly specific and take some additional work to be sensitive to a particular type of event or events with a class of devices such as MR systems. While the report indicates there was an association between a reported adverse event and a device, causality may not be certain. Care is needed to cross-check the report incident numbers before coming to a conclusion regarding the event.

Twenty-two incidents attributed to the use of MRI technology have been reported since July 2013 including burns related to skin-to-skin contact, contact with the scanner's bore, RF coils or other conductors, an RF coil covering, patient clothing (presumably containing metallic threads). There were two cases of patients that had finger entrapment by the patient table (i.e., when moving into or out of the scanner). Another eighteen incidents have been reported in which the magnets used with cochlear implants were involved, confirming that MRI-related incidents may be reported in association with an implant or device, or the scanner, itself, but not cross-referenced. Interestingly, several prominent MRI safety events shared anecdotally on social media sites do not appear in the DAEN-Medical Devices searches, reflecting a culture of incomplete or under reporting.

Radiology Event Registry

In 2006, the Radiology Event Register (RaER) was established and operated for approximately one decade. The RaER was initially managed under a Federal Government grant by the Royal Australian and New Zealand College of Radiologists within a quality assurance program and then maintained independently by the Australian Patient Safety Foundation at the University of South Australia. Radiologists, radiographers, and those involved in medical imaging were invited to report incidents (www.raer.org). Trainee radiologists were instructed in the use of the system and required to demonstrate experience with it as a component of their training. By 2012, there were nearly 4,000 incidents reported.

The information held in the reports was maintained under statutory immunity in Australia and New Zealand meaning that material cannot be used in legal proceedings in those countries. The RaER was intended to be adjunctive and not a replacement for the obligations to report within institutions, or to report to the TGA. Reports made to the RaER were analyzed by a team of radiologists focused on quality improvement, but their activity was transparent. Reporting was limited to a few conference papers and one publication (41). None of the reports to the RaER identified incidents by modality. The RaER ceased operation sometime between 2015 and 2019. The author's enquiries to the academic management team about access to the records have not been answered. The current location of the RaER data is not known.

Electromagnetic Radiation Health (EMR) Health Complaint Register

ARPANSA provides an online mechanism for making submissions to its Electromagnetic Radiation Health (EMR) Complaint Register (42). The register was opened in 2003 to provide a vehicle for Australians to report any health issues they believe they may have suffered from exposure to electromagnetic radiation (EMR) from 0 to 300-GHz. The register was initiated by an Australian Senate inquiry into EMR exposure held in late 2000. This

inquiry considered that the collection of data from the public may provide insight on the issue and indicate future research needs. The register is poorly subscribed with only 163 complaints lodged in fifteen years. Only one complaint mentioned exposure to MRI.

AUSTRALIAN MRI SAFETY RESEARCH AND EDUCATION

Research Regarding Australian MRI Safety Practice

There have only been two published attempts to research the practice of MRI safety in Australia. Ferris, et al. (43) published a survey of Australian MRI safety practices following the release of the first RANZCR MRI Safety Guidelines in 2004. A series of questions was sent to supervising MRI radiologists at all known MRI facilities in Australia seeking to examine general and difficult aspects of MRI safe practices in the field through anonymous or attributed responses. Ninety-two of 115 sites (80%) responded after diligent follow up. The study reported selected results including the observation that the new RANZCR and ACR guidelines were considered equally influential (38% each) and ten sites reported using external consultation to review their MRI safety procedures (34).

Seven sites reported inadvertent scanning of eight cardiac pacemaker patients. One of these events resulted in a death in 2000. Eight MRI facilities were willing to accept requests to scan patients with non-MR Conditional cardiac pacemakers but did not specify their precautions. Four sites had intentionally imaged cardiac pacemaker patients with undisclosed precautions. There was a general refusal to scan patients with retained pacemaker leads (77 sites) and twenty MRI facilities refused to scan patients with any type of intracranial aneurysm clip. Of the seventy-one MRI facilities that would scan patients with intracranial aneurysm clips, virtually all (70/71) relied on documented evidence of the clip's identity. Additionally, ten sites insisted that the aneurysm clip was in its original packaging before insertion, and four MRI facilities reported that they did their own testing on clips prior to implantation. With regard to patients with metallic implants, the manufacturer's product information and third-party sources were used equally to justify the decision to perform an MRI examination (34).

The variations in MRI safety practices prompted discussions between the radiology and neurosurgical professional bodies, as well as with the TGA, but there were no concrete results from these interactions. The study method did not probe the site's understanding or use of ASTM F2503 and FDA-style statements of conditions for performing safe MRI examinations in patients with implants and devices. Eighty-six percent of the sites reported procedural delays while MRI safety issues were resolved and these situations occurred frequently and on a constant basis. The investigators concluded that dealing with MRI safety questions continues to be difficult and increased vigilance including requiring the referring physician to supply critical MRI safety information at the time of the examination request is required to prevent the inadvertent scanning of cardiac pacemaker patients (34). Ferris, et al. (43) also indicated there may be a role for an MRI safety advisor providing an external audit of site policies and procedures.

In 2007, Burwell and Davidson (44) offered another insight into MRI safety policy and procedures in Australia. Their qualitative questionnaire explored who established site safety

990 MRI Safety Standards and Guidelines in Australia

policies, who was considered the local final authority, requested details pertaining to pre-scan screening, and determined how often policies were reviewed. This study also asked about safety breaches, although many participants chose not to respond to that section. A total of 110 surveys were sent out and 46 were returned. Considering the growth of MRI in Australia and the similarity in the number of sites identified by these two studies, it is quite likely that data for the Burwell and Davidson report was collected in 2005, about the time of the survey by Ferris, et al. (43).

The Burwell and Davidson survey reported that experienced MRI radiographers and radiologists created site safety policies independently or collaboratively. In contrast to Ferris, et al. (43), this survey indicated that the ACR white paper on MRI safety and the various peer-reviewed and other published works by Dr. Frank G. Shellock were most commonly used when creating a site policy. Screening, which RANZCR requires to be conducted at four points before the examination, was typically performed only two or three times. Only 62% of the sites reported using written processes to follow up questions raised by the patient screening questionnaire.

In general, safety policies were reviewed “as required” rather than on a regular schedule. Eighty percent of respondents claimed to maintain the required log of safety violations and near misses, but few were prepared to respond to a question that asked if there had been an incident during which a patient was harmed. The undisclosed number who did respond reported that ten contrast reactions occurred, eight MRI-related burns, two problems related to “incompatible” or otherwise unsafe medical implants, and there was one projectile injury. This report concluded, without clear justification, that a large number of sites did not meet the simple RANZCR safety standards of the time.

MRI Safety Education for Radiologists

Australian radiologists who completed their training after January 2005 are automatically certified as MRI radiologists for as long as they maintained MRI-specific continuing professional development (CPD) credits. The standards of their profession, and elements of their registration mean that the MRI radiologist has the primary responsibility for the safety of patients, and others at their facilities.

MRI safety is addressed in the Applied Imaging Technology (AIT) syllabus of the RANZCR radio-diagnosis curriculum (45), the training program for radiologists. Patient and staff safety are considered “special knowledge” relevant to the radiologist’s status as “an expert in the field”. An understanding of MRI safety issues, specifically missile effects and heating issues relating to implants or devices are described in the highest category of the curriculum and given the same importance as that of radiation exposure minimization to decrease cancer risk (i.e., Category 1, Must Know). The AIT curriculum also covers MRI hardware and imaging principles.

There is no indication that radiology trainees receive structured education on MRI safety-related clinical decision-making taught by radiologists. These matters would only be observed in the MRI section of a trainees’ clinical work. This lack of didactic instruction from the available body of literature and practice has resulted in a prolonged weakness in the central professional group. MRI safety practice relies upon informed radiologists dele-

gating appropriately to educated staff members, but the training of radiologists is not addressing this need with any great urgency.

Evidence suggests that the radiology trainee's understanding of MRI safety is not closely tested. Review of the twenty-eight AIT exam papers since 2004 demonstrated that questions probing MRI safety knowledge had been used only five times and that candidates had been tested on safety far less than on basic knowledge of image production. MRI safety questions may appear in the multiple-choice AIT exams, but these are not publicly accessible. Post qualification MRI safety education available from the College is also sparse. There are no MRI safety resources in the RANZCR public presentation archive (46), but members may have access to a wide selection from those that are readily available (e.g., peer-reviewed journals, websites, etc.). Interestingly, the programs of RANZCR Annual Scientific meetings from 2007 to 2019 have only included two presentations on MRI safety issues - one international expert reviewing implant and MRI interactions and a local expert providing a review of nephrogenic systemic fibrosis (NSF) literature in 2007. These points combined make it difficult to determine where and Australian radiologists obtain their knowledge of MRI safety.

CONCLUSIONS

Australia has an MRI safety system, standards, and regulatory strategy that are aligned more closely with European models than those of the United States. A change in approach is slowly developing with a generation of experienced clinical MRI physicists from the United Kingdom influencing the radiology and medical physics training curricula.

Australian MRI facilities make regular use of the statements of conditions for safe scanning of implants and devices required by the U.S. Food and Drug Administration. Limited research on the practice of MRI safety in Australia confirmed that the ACR guidance documents on MRI safe practice and the resources published by an independent, U.S.-based expert and his website (i.e., Frank G. Shellock, Ph.D., www.MRIsafety.com) were apparently more influential on MRI practitioners than the local professional guidelines. However, specific research has not reflected the strong anecdotal experience that, at many MRI facilities, radiologists are only marginally involved in MRI safety decisions and that the radiographers strongly influence the assimilation of evolving knowledge.

Radiologists and radiographers accessing information at international conferences, in print, and online appear to have the greatest impact on appropriate MRI safety practices. By comparison, a local active MRI safety discussion seems absent apart from regular sessions at the annual meeting of the ANZ Chapter of the Society for Magnetic Resonance Technologists (SMRT). Hopefully, the foundation of an ANZ Chapter of the ISMRM will ultimately provide another vehicle to generate cross-disciplinary education and discussion.

The imminent changes the professional capabilities of radiographers will increase the expected level of knowledge providing the public with greater protection against underperforming staff members. Alignment of the RANZCR guidelines and standards are needed to recognize this new legislative backed reality. At the same time, opening MRI services to nuclear medicine and radiation therapy radiographers and the expansion of services into

992 MRI Safety Standards and Guidelines in Australia

rural areas will result in a growth in the number of practitioners who will need to manage MRI safety issues effectively. New professional capability standards place a direct obligation on the radiographer to provide the public with a safe and effective imaging service, while the radiologists consider themselves experts in the field and retain the medical responsibility for the examination. Mobilization and training of the medical physicists could provide an extra dimension to the MRI safety dialogue by introducing better scientific perspectives and a departure from the power imbalance of the employer/employee relationship between radiologists and radiographers.

The RANZCR could consider the use of MRI facility policies that produce consistent decisions on commonly encountered implants and devices in the Australian market place. MRI practitioners should also urgently consider delegating common MRI safety decisions to appropriately experienced and educated MRI personnel such as advanced MRI radiographers and medical physicists, working in conjunction with the clinical aims expressed by radiologists, and working with appropriate recognition and remuneration for their skills and responsibilities. This last initiative will require that MRI facilities develop much clearer statements of reasoned decision-making than are currently found. The specific training needs for radiologists, radiographers, or physicists should also be revisited, with improvements made at all levels.

In this author's view, the need to clarify roles, improve education and more significantly improve daily practice has been chronic and must be openly addressed. This needs far greater engagement from radiologists than has been observed in the field, to date.

Radiographers at all MRI sites will need to improve their technical knowledge and strategic thinking skills to help guide a structured approach to facility's policies and decisions. Above all, professionals need to deliver on the existing guidelines. Folklore, hearsay, and hero worship must be replaced by factual clear reasoning for practices to improve as MRI moves from first-generation enthusiasts to second-generation learners. MRI safety is a scientific and clinical endeavor that requires knowledge and literacy in both domains. Educated specialist voices need to be valued over those without qualifications or experience. The ultimate goal of the MRI community is to reasonably maintain the extremely high safety record of MRI while maximizing the benefit of the technology to patients.

REFERENCES

1. OECD Data. MRI units by country: Organization for 2018 (updated 21 March 2018; cited 2018). Available at <https://data.oecd.org/healtheqt/magnetic-resonance-imaging-mri-units.htm>. Accessed June, 2020.
2. MRI (Magnetic Resonance Imaging). The Department of Health. Australian Government; 2019. Available at <https://www1.health.gov.au/internet/main/publishing.nsf/Content/mri-index>. Accessed June, 2020.
3. Medicare Benefits Schedule Book Category 5. Department of Health. Australian Government; 2019. Available at [http://www.mbsonline.gov.au/internet/mbsonline/publishing.nsf/Content/797BE31AE62DB6F4CA258489000B715A/\\$File/201911-Cat5.pdf](http://www.mbsonline.gov.au/internet/mbsonline/publishing.nsf/Content/797BE31AE62DB6F4CA258489000B715A/$File/201911-Cat5.pdf). Accessed June, 2020.
4. Calamante F, Faulkner WH, Jr., Ittermann B, et al. MR system operator: Recommended minimum requirements for performing MRI in human subjects in a research setting. *J Magn Reson Imaging* 2015;41:899-902.
5. Health Practitioner Regulation National Law Act, (2009). Australian Government Canberra. Available at https://www.legislation.act.gov.au/View/a/db_39269/current/PDF/db_39269.PDF. Accessed June, 2020.

MRI Bioeffects, Safety, and Patient Management 993

6. Professional capabilities in medical radiation practice, 2013. Medical Radiation Practice Board of Australia. Australian Registered Health Practitioners Authority. Available at <https://www.medicalradiationpractice-board.gov.au/documents/default.aspx?record=WD13%2f12534&dbid=AP&checksum=OJuB81d6eQCqo%2bewP9PHOA%3d%3d>. Accessed June, 2020.
7. Professional capabilities for medical radiation practice, 2020 Medical Radiation Practice Board of Australia. Australian Registered Health Practitioners Authority. Available at <https://www.medicalradiationpractice-board.gov.au/Registration/Professional-Capabilities.aspx>. Accessed June, 2020.
8. Guidelines for mandatory notifications for registered health practitioners. 2014. Australian Health Practitioner Regulation Agency. Available at <https://www.medicalboard.gov.au/documents/default.aspx?record=WD14%2f13326&dbid=AP&checksum=6PgV3lDTI0fwe%2bSb0D342g%3d%3d>. Accessed June, 2020.
9. MIAP 1 Policy and procedures manual - Magnetic Resonance Imaging (MRI). Version 2: Australian Society of Medical Imaging and Radiation Therapy. 2019. Available at <https://www.asmirt.org/media/1127/1127.pdf>. Accessed June, 2020.
10. Standards of Practice for Clinical Radiology. V 11. 2019 The Royal Australian and New Zealand College of Radiologists. Sydney Available at <https://www.ranzcr.com/documents/510-ranzcr-standards-of-practice-for-diagnostic-and-interventional-radiology/file>. Accessed June, 2020.
11. Australian/New Zealand Standard. AS/NZS 3200.2.33 2005 Medical electrical equipment Particular requirements for safety- Magnetic resonance equipment for medical diagnosis. Sydney, Wellington: Standards Australia/Standards New Zealand, 2005.
12. Submission of premarket notifications for magnetic resonance diagnostic devices. 2016 Center for Devices and Radiological Health, FDA. Available at <https://www.fda.gov/media/92921/download>. Accessed June, 2020.
13. Bottomley PA. Turning up the heat on MRI. J Am Coll Radiol 2008;5:853-855.
14. International Electrotechnical Commission. Amendments to Edition 3.1 IEC 60601-2-33 3.1. 2014. Medical electrical equipment. Particular requirements for the basic safety and essential performance of magnetic resonance equipment for medical diagnosis.
15. British Standards Institute. BS EN 60601-2-33-2010+A12-2016. Medical electrical equipment. Particular requirements for the basic safety and essential performance of magnetic resonance equipment for medical diagnosis. London: BSI; 2016.
16. Clinical Evidence Guidelines: Medical devices - Action on submissions. Therapeutic Goods Administration. Canberra 2017. Available at <https://www.tga.gov.au/clinical-evidence-guidelines-medical-devices-actions-submissions>. Accessed June, 2020.
17. RANZCR submission to TGA on the draft clinical evidence guidelines - Medical Devices, The Royal Australian and New Zealand College of Radiologists. 2016. Available at <https://www.tga.gov.au/sites/default/files/submissions-received-draft-clinical-evidence-guidelines-medical-devices-ranzcr.pdf>. Accessed June, 2020.
18. MTAA Submissions to TGA draft clinical evidence guidelines- Medical devices. Medical Technology Association of Australia, 2016. Available at <https://www.tga.gov.au/sites/default/files/submissions-received-draft-clinical-evidence-guidelines-medical-devices-mtaa.pdf>. Accessed June, 2020.
19. Building a professional performance framework. Medical Board of Australia, 2017. Available at <https://www.medicalboard.gov.au/Registration/Professional-Performance-Framework.aspx>. Accessed June, 2020. Accessed June, 2020.
20. RANZCR MRI Safety Guidelines. The Royal Australian and New Zealand College of Radiologists. Melbourne Australia: 2017. Available at <https://www.ranzcr.com/documents/512-mri-safety-guidelines/file>. Accessed June, 2020.
21. Competence standards for medical imaging and radiation therapy practice in New Zealand. New Zealand Medical Radiation Technologists Board. Auckland 2018. Available at https://www.mrtboard.org.nz/assets_mrtb/Uploads/RP-MRT002-V2-Competence-Standards-2018Jul.pdf. Accessed June, 2020.
22. Expert Panel on MR Safety, Kanal E, Barkovich AJ, Bell C, et al. ACR guidance document on MR safe practices: 2013. J Magn Reson Imaging 2013;37:501-30.

994 MRI Safety Standards and Guidelines in Australia

23. Safety Guidelines for Magnetic Resonance Imaging Equipment in Clinical Use 2016. Medicine and Healthcare Products Regulatory Agency, London, U.K. Available at <https://www.gov.uk/government/publications/safety-guidelines-for-magnetic-resonance-imaging-equipment-in-clinical-use>. Accessed June, 2020.
24. Calamante F, Ittermann B, Kanal E, et al. Recommended responsibilities for management of MR safety. *J Magn Reson Imaging* 2016;44:1067-1069.
25. Part B Health Facility Briefing and Planning 0440 - Medical Imaging Unit. Australian Health Infrastructure Alliance. 2018. Available at https://aushfg-prod-com-au.s3.amazonaws.com/HPU_B.0440_7.pdf. Accessed June, 2020.
26. Safety Advisory - gadolinium based contrast agents for MRI scans. Therapeutic Goods Administration. Available at <https://www.tga.gov.au/alert/gadolinium-based-contrast-agents-mri-scans> Accessed June, 2020.
27. RANZCR statement on Gadolinium Retention, 2017. The Royal Australian and New Zealand College of Radiologists. Available at <https://www.ranzcr.com/whats-on/news-media/171-ranzcr-statement-on-gadolinium-retention>. Accessed June, 2020.
28. Guidelines on the use of gadolinium containing MRI contrast agents in patients with renal impairment. The Royal Australian and New Zealand College of Radiologists. 2013. Available at <https://www.ranzcr.com/college/document-library/gadolinium-containing-mri-contrast-agents-guidelines>. Accessed June, 2020.
29. Ray JG, Vermeulen MJ, Bharatha A, et al. Association between MRI exposure during pregnancy and fetal and childhood outcomes. *JAMA* 2016;316:952-961.
30. National Health and Medical Research Council. Safety guidelines for magnetic resonance imaging facilities. Radiation Health Series. Canberra Australia: Australian Radiation Protection and Nuclear Safety Agency - Radiation Health Section. 1991.
31. International Commission on Non-Ionizing Radiation Protection. ICNIRP statement on medical magnetic resonance (MR) procedures: Protection of patients. *Health Phys* 2004;87:197-216.
32. National Health and Medical Research Council. Interim guidelines on limits of exposure to 50/60 Hz electric and magnetic fields (1989). RHS No.30 Australian Radiation Laboratory, Yallambie Victoria, Australia.
33. Radiation Protections Standard. Exposure limits for Electric & Magnetic Fields - 0 Hz to 3 kHz Public Consultation draft. Australian Radiation Protection and Nuclear Safety Agency, 2006. Available at http://www.arpansa.gov.au/pubs/comment/dr_elf_ris.pdf. Accessed June, 2020.
34. Ferris NJ. RANZCR submission to ARPANSA regarding draft ELF exposure. 2007.
35. Martin L. Limits & precautionary measures for reducing exposure to electric & magnetic fields - 0khz to 3 khz. Magnetic Resonance Imaging Issues. 2008. Available at http://www.arpansa.gov.au/pubs/events/lm_mri.pdf. Accessed June, 2020.
36. International Commission on Non-Ionizing Radiation Protection. Guidelines for Limiting Exposure to Time-Varying Electric and Magnetic Fields (1 Hz TO 100 kHz). *Health Phys* 2010;99:818-836.
37. ICNIRP Statement on Diagnostic Devices Using Non-Ionizing Radiation: Existing Regulations and Potential Health Risks. Australian Radiation Protection and Nuclear Safety Agency. 2018 Available at <https://www.arpansa.gov.au/icnirp-statement-diagnostic-devices-using-non-ionizing-radiation-existing-regulations-and-potential>. Accessed June, 2020.
38. Medical device incident reporting & investigation scheme (IRIS): Therapeutic Goods Administration. Australian Government Department of Health and Ageing; 2013 (updated 30 Oct 2019). Available at <http://www.tga.gov.au/safety/problem-device-iris.htm>. Accessed June, 2020.
39. Database of Adverse Events Notification (DAEN). Therapeutic Goods Administration. Department of Health. Australian Government. 2013. Available at <http://www.tga.gov.au/safety/daen.htm>. Accessed June, 2020.
40. Report a problem or side effect. Therapeutic Goods Administration. Department of Health. Australian Government. Available at <https://www.tga.gov.au/reporting-problems> Accessed June, 2020.

MRI Bioeffects, Safety, and Patient Management 995

41. Hannaford N, Mandel C, Crock C, et al. Learning from incident reports in the Australian medical imaging setting: Handover and communication errors. *Br J Radiol* 2013;86:20120336.
42. Australian Radiation Protection and Nuclear Safety Agency. Electromagnetic Radiation Health Complaint Register 2013. Australian Radiation Protection and Nuclear Safety Agency Available at <https://www.arpansa.gov.au/research/surveys/electromagnetic-radiation-health-complaints-register>. Accessed June, 2020.
43. Ferris NJ, Kavoudias H, Thiel C, Stuckey S. The 2005 Australian MRI safety survey. *AJR Am J Roentgenol* 2007;188:1388-1394.
44. Burwell J, Davidson R. An evaluation of safety policies and procedures in Australian magnetic resonance imaging departments. *Radiographer* 2007;54:4-7.
45. Applied Imaging Technology Syllabus in Radiodiagnosis Curriculum. V22. The Royal Australia and New Zealand College of Radiologists 2014. Available at <https://www.ranzcr.com/college/document-library/applied-imaging-technology-syllabus-in-radiodiagnosis-curriculum>. Accessed June, 2020.
46. Media Site, The Royal Australian and New Zealand College of Radiologists. 2019. Available at <https://webcast.ranzcr.com/Mediasite>Showcase>. Accessed June, 2020.

Index

A

- A-weighted, 160–161, 930, 946
- Abandoned leads, 66, 501, 555, 572, 658, 664, 673, 686, 689, 703, 708, 723, 729, 868, 943
- Acoustic noise, 18–19, 26, 31–32, 59–61, 68, 70, 75, 82, 132, 157–178, 180–192, 194–207, 287–288, 291–293, 296–297, 308–309, 328, 448, 762, 773, 777, 779, 791, 819, 860, 880, 889, 892, 896, 900, 906, 927, 930, 932, 945, 975, 978
- Active implant, 60, 90, 154, 429, 463, 468, 472, 488–490, 525, 541, 574–578, 580, 582–584, 586–588, 590, 592, 594, 596, 598, 600–602, 604–610, 623, 639, 847, 897, 942, 949
- Active implantable medical device, 69, 93, 230, 463, 491, 498, 500, 502, 513, 525, 546, 548, 552–553, 572–573, 577, 608, 639, 711, 743–744, 865, 906–907, 910
- Active noise control, 70, 176, 197, 203, 773
- Active shielding, 15, 43, 74
- Acute reactions, 333–336, 338, 340–344, 346–350, 955
- American College of Cardiology, 672, 686
- American College of Radiology, 92, 172, 202, 211, 306–307, 326, 340, 342, 344, 348, 354, 364, 379–380, 399, 401, 431–432, 437, 458, 490, 494, 669, 673, 685, 699, 709, 743, 746, 750, 752, 764, 767, 769–772, 778–779, 783, 798, 822, 837, 848, 864, 900, 934, 937, 975, 981
- AMIGO Suite, 835–838, 840–841, 844–848, 854, 856–857, 860, 862
- Anaphylactic, 334, 336, 340, 344–346, 348–350, 388, 845, 953
- Anaphylactoid, 342, 344, 349, 775, 955
- Anaphylaxis, 336, 346, 348–350
- Aneurysm clips, 56, 67, 84–86, 90, 94–95, 110, 114, 123, 127, 230, 391, 467, 472–474, 491, 496, 499, 546, 571, 763, 845, 942, 989
- Annuloplasty ring, 478–480, 484, 495, 763
- Anti-phase noise, 176–177, 192
- Anxiety, 157, 198, 284–288, 290–294, 296, 298, 300–305, 335–336, 340, 345–346, 397, 683, 732, 763, 767, 777, 787, 946, 952–953
- Apnea, 438, 448, 508

ASTM International, 64, 74, 85–86, 211, 471, 523, 541, 553, 609, 815–816, 831, 846, 865, 903–906, 939

Asynchronous pacing, 658, 660–661, 666–667, 675, 677–678, 688, 691, 693

Athermal effects, 233

Auditory perception, 196

Australian Radiation Protection and Nuclear Safety Agency, 890, 986, 994–995

B

Birdcage coils, 221, 529, 626–627

Body temperature, 119–120, 130, 208, 226, 236, 239–243, 249, 251, 266, 272, 275, 278–279, 283, 450–453, 460, 724–725, 727–729, 733, 739–740, 792–793, 807–808, 858, 876, 901–902, 928, 948

Breastfeeding, 388, 390

Bronchospasm, 334, 340–341, 343, 956

Bullets, 395, 828

Burn, 35, 55–56, 66, 208, 230, 256, 271, 275, 282, 391, 442–444, 447, 450, 452, 459–460, 499, 504, 544, 552, 554, 571, 618, 653, 713, 762, 766, 773, 777, 803–805, 807, 810, 816–820, 824, 826, 839, 843–844, 848, 850–851, 858, 866, 947–950, 970, 985, 988, 990

C

Canadian Association of Radiologists, 354, 364, 934–936, 957, 968–970

Capnometer, 448–449

Cardiac excitation, 155, 901

Cardiac implantable electronic device, 70, 433, 512, 673–674, 699–701, 704, 707–709, 859, 868, 970

- Cardiac pacemaker, 56, 60, 66, 68, 90, 95, 127, 389, 391, 400, 402, 428, 463, 468, 493, 499, 502, 515, 526, 533, 543, 549, 553, 555, 574–577, 608, 616, 618, 623–625, 634, 639, 645, 648, 651–653, 656–662, 665–672, 675–685, 688, 692–693, 695–704, 706–708, 718, 753, 759, 779, 821, 847, 860, 867, 906, 927, 942, 965, 983, 989
- Cardiac stimulation, 60, 145, 153–154, 552, 686, 930
- Cataract, 236, 245, 267–268
- Catheters, 67, 69, 86, 338, 442, 448, 468, 483, 496, 523, 549, 650, 713, 741, 859, 862, 965
- Center for Devices and Radiological Health, 123, 156, 201, 229, 251, 703, 743, 865, 890, 893, 993
- Checklist, 123, 665, 668–669, 688, 787, 792–793, 825, 840–844, 846, 854, 864, 937, 940–941
- Children’s hospital, 324, 379, 781–782, 784, 786, 788, 790, 792, 794, 796
- Circularly polarized waves, 215
- Class I devices, 894, 965
- Class II devices, 894–895, 965
- Class III devices, 894–895, 965
- Claustrophobia, 195, 284–292, 294–296, 298, 300–305, 391, 397, 763, 941, 951–953
- Cochlear implant, 90, 389, 444, 465–466, 502, 509–511, 513, 574–575, 616, 623, 734–740, 747, 763, 906, 942, 988
- Coronary artery stents, 86–87, 476–478, 484, 495
- Counterforce, 405, 421, 464–465, 561
- Cryogens, 196, 753, 845, 848, 862, 933–934
- Current induction, 69, 657–658, 664
- D**
- Deep brain stimulation, 56, 66, 68–70, 493, 499, 502–504, 512, 515, 535, 538–539, 544, 548–550, 553, 564–565, 571–572, 574–575, 608, 646, 655, 711, 716, 720, 723–725, 743–745, 866, 942
- Deflection angle, 74, 85, 87, 560, 847
- Demagnetize, 466
- Dephase, 6, 12–13
- Diamagnetic, 36–37, 41, 45, 98–99, 101, 103, 106–110, 114–115, 117–119, 122, 129, 630
- Diamagnetic susceptibility anisotropy, 101, 115
- Direct hazards, 913, 916
- E**
- Earplugs, 157, 159, 162, 167, 171, 173–176, 197, 391, 773, 791, 808, 819, 825, 930, 946–947
- Electric fields, 59, 68, 74, 102, 124, 129, 132, 149–150, 156, 212, 218, 220, 222, 225, 237, 255, 516, 546, 564, 575, 578, 589, 609, 617, 629, 644, 649, 654, 870–871, 882, 887, 891–892, 902–903, 905, 923
- Electrocardiogram, 46, 64, 102, 125, 145, 217, 338, 341–344, 445–446, 658, 660, 691–692, 764, 772–773, 845, 856, 858–859
- Electromagnetic interference, 238, 442, 452, 470, 607, 658–659, 690, 802, 849, 927
- Electromotive force, 48, 102, 628
- Electrophysiology, 656, 659, 671, 674, 686, 705, 707, 867
- Emergency procedures, 752, 762, 800, 827, 933, 952, 964, 982
- Emotional distress, 284, 286–288, 290, 292, 294, 296, 298, 300–302, 304
- Excessive heating, 244–245, 442, 444, 447–448, 467, 487, 541, 555, 575, 713–714, 718, 722, 741, 745, 773, 804, 806, 818, 820, 827, 851, 905, 948, 970
- Exclusion, 85, 88, 230, 369, 455–456, 488, 508, 667, 735, 759, 767, 814, 879, 937, 963, 985
- Exposure limit values, 171, 260, 873, 916, 920
- F**
- Faraday’s Law, 46, 48, 60, 96, 136, 233, 395, 404, 516, 712, 871
- Fast spin echo, 21, 26, 30, 169, 200, 204, 246, 308, 320, 469, 486, 521, 667, 698, 718
- Fatality, 98, 345–346, 350, 379, 408, 436, 440, 462, 464, 472, 515, 710, 839
- Ferromagnetic, 1, 14–16, 26, 36–37, 39, 41–44, 59–61, 70, 73–74, 85, 97, 101, 103, 105–108, 110, 114–115, 121–122, 125, 127–128, 238, 380, 394–396, 399–416, 418–434, 440, 446, 454–455, 457, 459, 463–466, 470, 473–474, 476, 481, 483, 489, 491, 499–500, 511–512, 515, 571, 600, 657, 675, 687–688, 696, 711–712, 735–736, 750, 753, 763, 776–777, 783, 790, 815–816, 820, 822, 825, 832, 835, 837–841, 844–848, 864, 869, 913, 927, 936, 939–940, 944, 981
- Ferromagnetic detection system, 70, 380, 394–395, 399–400, 402, 404, 406, 408–410, 412–414, 416, 418, 420, 422, 424–426, 428, 430, 432–434, 457, 499, 512, 763, 783, 832, 839, 841, 939, 944
- Ferromagnetism, 105, 125, 129, 474, 491, 495–496
- Fetus, 162, 172–173, 199, 202, 257, 268–269, 281, 307–309, 313–314, 317, 320–321, 326–328, 330–332, 367, 390, 650, 772–773, 933, 953, 955, 984
- Finite-Difference Time-Domain, 63, 529

998 Index

First Level Controlled Operating Mode, 25, 151, 153, 209–210, 240, 255, 262–263, 267, 271, 478, 567, 714–715, 733, 742, 808, 861, 908, 916, 929–930, 932–933, 949–950, 978, 983
Fixed parameter option, 908, 910, 933, 950
Fluoroptic thermometry, 120, 241, 251, 452, 905
Food and Drug Administration (FDA), 72, 97, 120, 152, 171, 209, 255, 306, 313, 367, 379, 395, 469, 499, 523, 546, 631, 659, 802, 893, 915, 934, 956, 971, 979
Foreign bodies, 101, 388, 395, 399, 401, 428, 432–433, 750, 762–763, 771, 822, 983
Free induction decay (FID), 11
Frequency encoding, 20, 134, 165, 469, 521
Frequency response function, 168, 182, 186
Fringe field, 14–15, 43, 74, 101, 121, 401–403, 406–407, 409, 417–418, 430, 454, 486, 762, 803, 810, 823, 848, 852, 855, 870, 872, 879–881, 932, 937, 944, 963
Functional MRI (fMRI), 23, 25, 82, 110, 157, 286, 721, 806, 858

G

Gadolinium accumulation, 957
Gadolinium retention, 365–366, 368, 370, 372, 374–376, 378, 956–957, 984, 994
Gadolinium-based contrast agent, 93, 311, 313–314, 328, 333–334, 336–338, 340–344, 346, 348–350, 364–365, 370, 375–378, 388, 764, 775–776, 779, 935, 956–957, 970–971, 984, 987
GBCA, 308, 313, 333–339, 345, 347–348, 353–354, 357–358, 360–362, 365–374, 388, 390, 764, 953, 955–957, 971, 984
Glomerular filtration rate, 351–352, 359, 364, 367–368, 388, 775
Gradient amplitude, 18, 31, 60, 148, 153, 156, 164, 185, 197, 308, 886, 903, 932
Gradient coils, 16–17, 19, 35, 58–59, 68–69, 73–75, 149, 156, 163–165, 170, 191–195, 197, 200–201, 206–207, 516, 519, 529–530, 545, 569, 602, 609, 616, 629, 648, 654, 658, 712, 773, 850, 892, 903
Gradient echo, 20, 27, 29, 75, 79–81, 86, 90, 145, 153, 164, 174, 179–183, 204–205, 308, 314, 320, 469, 472, 718, 861, 906
Gradient magnetic fields, 16, 18–19, 22–23, 26–27, 35, 61, 68, 74, 96–97, 101, 120, 132, 134, 136, 138, 140, 142, 144–146, 148, 150–152, 154–156, 196, 240, 296, 308, 325, 381, 463, 468, 470, 486, 502, 515–516, 555–558, 561–563, 568, 570, 574, 601, 605, 616, 618, 621, 625, 629, 657, 667, 675, 684, 687, 694, 710, 712–713, 808, 810, 818–819, 850, 860–861, 870, 886, 891, 907, 925, 930, 933, 945, 969

Gradient slew rate, 23, 133, 145, 185, 189, 605, 723–725, 727–731, 733–735, 739–740, 742, 848, 870, 882
Gradient waveform, 134, 137, 149, 152, 181–182, 184–186, 189, 518, 562, 876, 900
Gradient-induced heating, 75, 520–521, 530

H

Hall effect, 104, 876
Headphones, 173, 175–178, 292, 295–297, 773, 819, 825, 860, 946–947

Health and Safety Executive, 202, 913
Health Canada's Safety Code, 926–927
Hearing loss, 60, 68, 158, 161–162, 172–175, 198–199, 203, 304, 310–311, 892, 946

Hearing protection, 18, 60, 159, 162, 164, 167, 170–176, 180, 188, 192, 203, 293, 391, 766, 773, 791, 793, 815, 819, 825, 843, 927, 930, 932, 945–947, 953, 982, 985

Heart rate, 239–242, 248, 251, 259–260, 278, 293, 310, 328, 340, 345, 439, 445, 447, 449–451, 453, 458, 460, 680, 691, 772, 807

Heart valve prosthesis, 463, 465–466, 478–480, 484, 493, 495, 553, 763

Helium, 14, 99, 805, 828, 845

Hemostatic clip, 467, 574, 763

Hugo model, 596–598

I

Implantable cardioverter defibrillator, 90, 95, 493, 502, 562–563, 574, 576, 605, 645, 656, 660, 663, 665, 669, 671–673, 675, 684, 689, 700, 702, 704–706, 708, 860, 867, 942

Implantable infusion pump, 466, 468, 502, 511, 513, 520, 562, 713, 720, 739, 741, 906

Implantable pulse generator, 499, 501, 548, 554, 639, 675, 687, 694, 702–703, 711–712, 723–725, 727–729, 734–735, 744

Indirect hazards, 913, 915

Induced currents, 19, 46, 57, 59–61, 67–69, 75, 82, 90, 219, 468–470, 488, 502, 507, 516, 520, 530, 534–535, 537, 540, 548–550, 615, 639, 670, 702, 712, 817–818, 850, 906, 943, 945

Induced electric field, 102, 132, 136–137, 139, 145, 149–150, 152, 156, 546, 609, 629, 644, 654, 870–873, 882, 885, 892, 902–903, 916–918, 930

Induced EMF, 102, 870

Induction coils, 411

- Injury, 56, 66, 93, 108, 114, 117–118, 121, 124, 157, 230, 238, 267, 278, 280, 282, 325, 352, 366, 379, 381, 389, 391, 398–399, 408–409, 432–433, 436–437, 440, 442, 448, 452, 458–459, 462–465, 467–468, 470–473, 483, 486, 490, 512, 515, 551, 553, 577, 618, 710–713, 715–716, 722, 739, 744, 750, 754, 759–761, 764, 766, 774–775, 779, 803, 805, 816, 822, 824–826, 828, 858–859, 864, 895, 904–907, 914, 927, 936, 940, 944, 947–948, 956, 985, 990
- International Commission on Non-ionizing Radiation Protection, 64, 73, 91, 120, 130, 151, 156, 171, 247, 250, 255, 276, 309, 873, 890–891, 910, 917, 922–923, 928, 934, 986, 994
- International Electrotechnical Commission, 25, 73, 91, 120, 130, 145, 151, 156, 171, 202, 209, 229–230, 251, 254, 276, 523, 545, 552–553, 571, 577, 610, 710, 717, 743, 866, 873, 890, 907–908, 915, 922, 926, 934, 969, 977, 993
- International Organization for Standardization, 470, 491, 513, 523, 546, 548, 558, 572–573, 577, 604, 608, 630, 639, 744, 907, 980
- Interventional MRI, 65–67, 185, 204, 325, 546, 650, 834, 863–867, 880, 920
- Intracranial pressure monitoring, 442, 713
- Intraoperative MRI, 459–460, 863–864, 866
- Iso-center, 605
- ISO/TS 10974, 211, 230, 491, 500, 513, 523, 525–526, 532, 541, 543, 546, 548, 553–559, 561–564, 566–568, 572, 577, 598, 607–608, 630–631, 636, 638–641, 644–645, 653, 744, 865

L

- Larmor equation, 5
- Larmor frequency, 47, 49–50, 52, 58, 72, 107, 122, 133, 537, 617, 626, 873
- Leads, 47, 60, 66–69, 71, 79, 81, 187, 217, 256–257, 300, 376, 429, 442, 444, 446–448, 467–468, 470, 493–494, 499, 501–507, 512, 515, 518, 526, 535, 539–541, 546, 548–551, 554–556, 560–564, 572, 574–577, 584, 593, 598, 608–609, 611–612, 623, 625, 633–635, 639, 643–646, 651, 653–655, 657–659, 661, 664–667, 670–671, 673, 676–678, 681, 684, 686–690, 693–696, 698–699, 702–703, 705, 708, 713, 715, 718–721, 723–730, 743–745, 762, 773, 846, 868, 927, 943, 947, 950, 985, 989
- Lenz's Law, 220, 395, 404
- Linearly polarized waves, 214
- Loop recorder, 90, 502, 653, 659, 670, 695–697, 701, 706–707, 943
- Lorentz force, 26, 35, 38, 46, 59–60, 75, 82, 132, 163, 170, 191–194, 206, 500, 649

M

- MagnaSafe Registry, 662, 671, 685, 705, 867–868
- Magnetic moment, 31, 61, 101, 108, 214, 417, 561
- Magnetic sensors, 409, 411–412, 415, 425, 433
- Magnetic susceptibility, 11, 36–37, 63, 101, 103, 105, 107, 110, 112, 116, 127, 415–416, 425, 464, 469, 473, 479, 487, 491, 629, 653, 849, 865, 870
- Magnetically-induced stimulation, 132
- Magnetite, 103, 129
- Magnetization effects, 402, 404
- Magnetohydrodynamic, 46, 64, 104, 126, 129, 762, 859
- Magnetophosphenes, 119, 122, 129–130, 141, 154, 762, 851, 913, 917, 930
- Magnetoresistance, 104
- Magnetostriction, 105
- Medical Device Amendments, 893–895
- Medicines and Healthcare Products Regulatory Agency, 173, 431, 890, 921, 923, 981
- Missile effect, 97, 401, 404–405, 408, 435, 939, 990
- Monitoring patients, 436–438, 882
- Monitoring temperature, 452
- Motion damping, 402, 404
- MR Conditional, 74, 84–85, 87–91, 211, 238, 292, 295–297, 339, 381, 397, 405–408, 419–420, 422, 428, 430–431, 435, 437, 439–440, 444–457, 461, 470–471, 473, 475, 478–479, 481–482, 487–488, 490, 498–502, 506–512, 523–525, 541, 552–556, 558, 560, 562, 564, 566–572, 618, 625, 634, 639, 643, 645, 647, 656–660, 662, 664–666, 668–670, 672, 675–676, 681–682, 684–696, 698–699, 701, 704, 706, 708, 714, 717, 720–721, 724, 726–727, 731–732, 737, 739, 741, 743, 750, 752–753, 758–759, 763, 770, 775, 777, 786, 790, 793–794, 807–808, 810, 814, 816, 818, 821, 825, 828, 835, 844, 846–851, 855–856, 858–860, 867, 897–898, 906, 908, 910, 938–939, 943, 945, 949–950, 952–953, 979–980, 984, 989
- MR Medical Director (MRMD), 766
- MR Safe, 74, 202, 230, 326, 349, 381, 399, 405, 408, 431–432, 435, 444, 449, 455, 457, 470–471, 479, 487, 490, 498, 500, 523, 544, 555, 687, 701, 750, 752, 760–761, 763, 770, 777–778, 786, 790, 808, 810, 816, 825, 828, 831, 835, 844, 846, 848–849, 854–855, 858, 890, 897–898, 906, 934–935, 938–939, 944–945, 947, 949, 952–953, 959, 969, 979, 984, 993
- MR Safety Expert (MRSE), 982
- MR safety officer, 423, 499, 761, 766–768, 771, 778, 782, 844

1000 Index

MR Unsafe, 87, 90, 381, 397, 405, 419, 440, 443, 457, 470–471, 474–475, 477–478, 480–482, 485, 492, 498–500, 504, 506, 509, 511, 523, 555–556, 687, 720, 726–728, 763, 770, 810, 816, 819, 835, 837–838, 842, 845–848, 854–856, 858–859, 897, 906, 938–939, 979
MRI contrast agent, 287, 311–315, 325, 351–352, 354, 356, 358, 360–364, 377, 388, 397, 436–437, 753, 763–764, 772, 774–777, 780, 935, 954, 994
MRI contrast agents in pregnancy, 312–313
MRI labeling, 19, 408, 432, 470–472, 476, 478, 484, 489, 605, 607, 659, 750, 770, 815, 938
MRI of the fetus, 314, 320
MRI safety committee, 755, 761, 766–768, 778, 781–782, 785–786, 794, 800, 802–805, 808–809, 811, 814–815, 821–823, 830, 982
MRI screening procedures, 380, 940
MRI simulations, 574, 576, 578, 580, 582, 584, 586, 588, 590, 592, 594, 596, 598, 600, 602, 604, 606, 608, 610, 616, 630, 633–634, 638, 646

N

National Electrical Manufacturers Association, 223, 231, 895, 899, 908–909, 934, 947, 970
Nephrogenic systemic fibrosis, 80, 351–352, 354, 356, 358, 360, 362–365, 370, 374, 377, 388, 775, 779–780, 956, 987, 991
Neuromodulation system, 90, 391, 463, 467–468, 472, 494, 508, 513, 515, 645, 654, 710–714, 716, 718–720, 722, 724, 726, 728, 730–732, 734, 736, 738, 740–744, 746, 748, 832, 847
Neurostimulation, 19, 66, 97, 389, 444, 470, 493, 501–502, 504–505, 544, 572, 574–575, 577, 587, 608, 616, 623, 634, 645, 712, 720, 724, 726–727, 730–731, 743–746, 763, 821, 866, 906
Non-significant risk criteria, 209

Normal Operating Mode, 25, 85, 151, 153, 209–210, 255, 259, 262, 265, 267–269, 271, 308, 471, 477, 480, 485, 509, 567, 569–570, 595, 597–598, 607, 714–715, 729–731, 733–734, 740, 742, 808, 861–862, 916, 918, 929–933, 949, 978

Numerical modeling, 87, 269, 271, 611–612, 614, 616, 618, 620, 622, 624, 626, 628, 630–632, 634, 636, 638, 640, 642, 644–646, 648, 650, 652, 654

O

Occupational exposure, 64, 82, 121, 123, 170, 200, 250, 326, 432, 869–874, 876–878, 880, 882, 884, 886, 888–892, 918–919, 921, 933–934, 946, 970, 978, 985–986

Occupational Safety and Health Administration (OSHA), 201
Octave band spectra, 165, 175
Outpatient MRI facility, 439, 766, 769, 772, 774, 776–778
Oxygen saturation, 239, 241–242, 251, 438–439, 449–451, 458, 764, 772, 807

P

Pacemaker, 56, 60, 66, 68, 70, 90, 95, 127, 389, 391, 400, 402, 428, 463, 468, 493–494, 499, 502, 512, 515, 526, 532–533, 543–544, 546, 548–550, 553, 555, 571–572, 574–577, 608, 616, 618, 623–625, 634, 639, 645, 648, 650–653, 655–662, 664–673, 675–685, 687–709, 718, 753, 758–759, 779, 811, 814, 821, 832, 847, 860, 867–868, 906, 927, 942–943, 965, 983, 989
Pacemaker leads, 66, 68, 526, 546, 548–549, 608, 651, 659, 670, 689, 693, 702, 705, 708, 989
Panic attack, 284–285, 287, 298, 302, 336, 345
Parallel transmission, 70, 92, 94, 252, 276, 280, 282, 538, 548, 550
Paramagnetic, 37, 41, 45, 73–74, 98, 101–103, 106, 108, 110, 114, 117, 602, 630
Passive implant, 84, 86, 88–89, 94–95, 230, 463, 467–469, 472, 487–490, 494, 523, 525, 541, 545, 571, 574–576, 582–583, 601, 605, 608–609, 865, 896–898, 903–905, 910, 933, 942
Passive noise control, 179, 773
Pediatrics, 202, 231, 280, 458, 795, 832
Penile implants, 483
Peripheral nerve stimulation, 19, 23, 31, 60, 68, 74, 119, 132, 141, 145, 149, 153–156, 502, 552, 572, 616, 649, 711, 719–720, 729–731, 762, 777, 818–819, 861, 870, 874, 913, 916, 919, 930, 945, 975, 986
Permanent magnet, 14, 18, 35–36, 85, 87, 105–106, 428, 551

Permanent threshold shifts, 174
Phase effects, 194, 526, 576
Phase encoding, 20, 24, 482
Phased-array, 23, 649, 974
Planck's constant, 4
PNS perception thresholds, 147–148
PNS strength-duration curve, 140
Post-operative, 488, 862
Pre-procedure screening, 801, 803, 809–811, 814–815, 822, 828
Precession, 5, 98, 103, 153, 215, 693
Pregnancy, 154, 162, 172–173, 202, 265, 268–269, 280–281, 306–310, 312–332, 367, 388, 392–393, 479, 622, 650, 752, 763, 772–773, 777, 779, 814, 889–890, 892, 933, 941, 953–955, 994

- Pregnant healthcare worker, 325–326, 752, 777, 954
 Pregnant patient, 172–173, 269, 306–308, 314–315,
 317–319, 323, 325–326, 329–330, 390, 752,
 764, 767, 770, 772, 811, 953–955, 984
 Projectile effect, 83, 403, 904
 Psychological distress, 284–285, 293
 Pulse generator, 468, 494, 499, 501, 503–504, 506–
 507, 509, 548, 554, 575–576, 578, 580–581,
 583, 585, 587–596, 598–601, 605, 607, 625,
 639, 645, 652, 657–658, 660–661, 663–668,
 675, 685, 687, 694–695, 702–703, 711–712,
 716, 719, 723–725, 727–729, 731, 734–735,
 744
 Pulse oximeter, 251, 338, 341–342, 440, 442–443,
 447, 449–451, 458–459, 571, 775, 777, 962
- ## Q
- Quadrature coil, 220
 Quadrature excitation, 209, 211, 218, 534, 628
 Quench, 408, 440, 753, 762, 778, 798, 804–805,
 827–828, 845, 927, 933, 962–963, 983
 Quiet gradient coils, 194, 206
 Quiet MRI sequence, 188
- ## R
- Radiofrequency energy, 63, 94, 251, 280–281, 667–
 668, 671, 684, 694, 703, 743, 779, 831, 868
 Radiofrequency field, 32, 96–97, 247, 276, 467, 470,
 552, 555, 574–576, 713, 876, 880, 890, 906,
 916, 918–919, 929, 932–933
 Radiofrequency power deposition, 63, 66, 94, 120,
 208, 210, 212, 214, 216, 218, 220, 222, 224,
 226, 228, 230, 232, 248, 327, 831, 890, 930,
 949, 969
 Receive-only RF coil, 220, 501, 506–507, 569, 806
 Relaxation, 6–8, 10, 12, 25, 78–79, 81, 129, 247,
 290, 292, 296, 365, 369–370, 951
 Relaxivity, 79, 81, 763
 Repetition time, 18, 20–22, 79, 83, 134–135, 163,
 165, 187–189, 199, 234, 469, 482, 517, 519,
 570, 717, 816, 861, 873, 950
 Rephase, 12
 Resistive magnets, 14
 Resonant, 53, 56, 67, 69, 90, 208–209, 220, 225,
 234, 282, 467, 501, 528, 537, 549, 620, 626,
 628, 635, 638, 642, 644, 653, 688, 703, 715–
 716, 948–949
 Resonant frequency, 53, 209, 234, 501, 688, 715,
 948
 RF energy-induced heating, 214, 234–240, 244,
 246–247, 520, 638, 640, 646
 RF hearing, 196
 Root mean square, 141, 194, 579, 586, 602, 605,
 871, 875, 908, 930
 Rotating frame, 5–6, 12
 Royal Australian and New Zealand College of Radiologists, 975, 980, 988, 993–995
- ## S
- Sacral nerve stimulation, 502, 508, 711, 720, 731–
 734
 Screening form, 380–394, 397–398, 427, 771, 776,
 783–784, 786, 788–790, 792–793, 798, 803,
 810–815, 823, 828, 841, 845, 940–941, 983
 Screening patients, 70, 398–399, 401, 438, 490, 499,
 751, 770, 779, 831, 983
 Second Level Controlled Operating Mode, 25, 151,
 209–210, 808, 916, 929, 931–933, 978
 SEMCAD, 633
 Shrapnel, 388–389, 392, 944
 Signage, 762, 766, 799, 839, 932–933, 937–939, 962
 Signal decay, 10–11
 Signal-to-noise, 22, 24, 31–32, 71, 91, 94, 110, 219,
 482, 485, 534, 609, 616, 648–650, 652, 698,
 899, 901, 908, 962–963
 Slew rate, 18–19, 23, 26, 58, 74, 96, 133–134, 141,
 145, 147–148, 150, 164, 173, 185, 188–190,
 308, 519, 521, 605, 687, 723–725, 727–731,
 733–735, 739–740, 742, 808, 810, 819, 848,
 870, 879, 882, 886, 932, 943
 Sound pressure level, 75, 159, 161, 165, 194, 196,
 200, 930, 946, 985
 Specific absorption rate, 19, 22, 25, 32, 49, 65, 70,
 73, 90, 93, 97, 208, 212–214, 223–224, 227,
 231, 234, 245, 248, 250, 252, 254, 271, 278,
 281–282, 308, 327, 381, 467–468, 470–471,
 477–478, 480, 482, 485, 493, 503, 516, 544,
 549, 553, 567, 572, 575, 578, 614, 621, 650,
 653, 655, 658, 671–672, 687, 715, 723–725,
 727–731, 733–735, 739–740, 742, 744–745,
 762, 770, 803, 810, 816, 831, 848, 850, 870–
 871, 896, 901–902, 905–906, 916, 927, 970,
 977, 979, 985
 Specific energy dose, 762, 816–817, 950
 Spin echo pulse sequence, 21, 135, 179, 246, 486,
 570, 667, 698, 718
 Spin-lattice relaxation, 7–8
 Spin-spin relaxation, 10
 Spinal cord stimulation, 19, 389, 492, 502, 506, 513,
 554–555, 564–565, 607, 623, 646, 711, 714,
 718–719, 726, 728, 730, 743–744, 746
 Superconducting magnet, 14, 73, 119, 127, 196, 401,
 440, 495, 776, 798, 805
 Susceptibility artifacts, 27, 80–81, 122, 396, 629,
 653, 657, 666–667, 693, 697
 Systematic desensitization, 292, 296, 298, 302

1002 Index

T

- T1 recovery, 6, 10, 30
- T1 relaxation, 6, 8, 10, 78–79
- T1-weighted, 20–21, 30, 78–80, 86, 167, 201, 204–205, 319, 365, 367, 370, 375–376, 442, 570, 705, 957
- T2 decay, 10–11, 13, 30
- T2 relaxation, 10, 12, 78, 247
- T2-weighted, 21, 78, 318, 320, 504, 722
- Tattoos, 89, 94, 103, 126, 379, 762, 774, 948–949
- Temperature monitoring, 66, 453, 458–460, 533, 764
- Temporary threshold shifts, 174
- Testes, 242, 244–245, 322
- Therapeutic Goods Administration, 978, 993–994
- Thermal homeostasis, 237
- Thermal simulation, 66, 252, 280–281, 529–530, 634
- Time-varying magnetic field, 60, 65, 68, 132, 143, 154–156, 470, 516, 601–602, 605, 609, 628, 649, 654, 773, 810, 869–870, 872, 874, 876, 879, 891, 901, 906, 913, 916–917, 920, 923, 945, 978, 985
- Tissue conductivity, 138, 606, 886
- Torque, 37, 44–45, 63–64, 98, 101, 104–106, 108–117, 119, 127, 230, 395, 402, 404, 407, 463–465, 471, 483, 487, 489, 494, 500, 510–511, 515, 557–561, 571, 605, 625, 639–640, 653, 657, 661, 670, 711–712, 773, 810, 847–848, 850, 865, 897, 903–904, 906–907, 910
- Transfer function, 57, 67, 163, 168–169, 201, 526–527, 535–536, 546, 549–550, 564–568, 572, 576–580, 582, 584–585, 588, 590–595, 598–601, 606–609, 635–636, 641, 647, 654–655, 670, 702
- Translational attraction, 108–109, 114, 395, 402, 463–465, 471, 483, 486–487, 500, 511, 653, 657, 670, 701, 712, 810, 816, 846, 848, 904
- Transmetallated gadolinium, 313
- Transmission line theory, 580, 582
- Transmit RF coil, 19, 27, 30, 73, 76–77, 80, 83, 86–91, 96, 173, 192, 208–210, 215, 218, 224–226, 234, 247, 255, 258, 271–272, 275–276, 308, 444–445, 468, 482, 488, 501, 506, 516–517, 526, 529, 531, 533, 537–539, 541, 543, 567–569, 606, 616, 621, 623, 625, 627–629, 633–634, 637–639, 641, 658, 687–688, 693, 715, 762, 773, 816–818, 851, 930–931, 948–949, 985

U

- Urticaria, 334, 340–341, 343, 345, 956

V

- Vagal reaction, 340, 342, 344–345
- Vagus nerve stimulation, 56, 66, 502, 507, 513, 575, 577, 588, 594–595, 599, 606, 609, 646, 711, 720, 731–733, 735, 746
- Vascular access port, 467, 483–485, 496
- Vascular clip, 463
- Ventilator, 409, 440, 454–456, 458, 461, 858, 860, 866, 952
- Verbal interview, 303, 391, 393, 398, 845
- Verbal screening, 393, 810, 940, 942, 983
- Vertigo, 45, 82, 93, 104, 119, 122, 141, 285, 325, 332, 388, 851, 861, 870, 874, 888–889, 913, 916, 929
- Vibration, 18, 26, 61, 69, 75, 159, 161, 163, 170, 176, 179–180, 190–192, 197, 200–201, 203, 206, 463, 500, 556–558, 560–562, 605, 640, 666, 687, 850, 907

W

- World Health Organization, 120, 130, 199, 255, 841, 864, 913, 922
- www.MRISafety.com, 380–381, 490, 544, 659, 669, 743, 770–771, 815, 822, 831, 845, 858, 934, 940, 969, 991

X

- X-axis, 133, 521

Y

- Y-axis, 110, 146

Z

- Z-axis, 5–6, 110–112, 114, 133–134, 136, 222, 742, 885
- Z-magnetization, 7
- Zipper artifact, 849
- Zones, 538, 735, 750, 752, 762–763, 771, 776, 798, 803, 816, 836, 847, 937–938, 960, 975, 982–983